Cranfield University

J.I. ULIZAR ÁLVAREZ

SIMULATION OF MULTI FLUID GAS TURBINES

School of Mechanical Engineering
Thermal Power

Ph.D. Thesis

CRANFIELD UNIVERSITY

SCHOOL OF MECHANICAL ENGINEERING
THERMAL POWER

Ph.D. THESIS

J.I. ULIZAR ÁLVAREZ

SIMULATION OF MULTI FLUID GAS TURBINES

Supervisor: **Dr. P. PILIDIS**

January 1998

This thesis is submitted in partial fulfilment for the degree of Philosophy Doctor

ABSTRACT

This work focuses on two main subjects: first, the development and validation of a robust generic performance code for industrial gas turbines (GTSI) and, second, the study of an innovative carbon dioxide/argon semi-closed cycle burning low calorific gas coming from coal gasification. GTSI will be able to simulate open, closed and semi-closed cycles at design and off-design conditions.

A comprehensive thermodynamic study of the properties of the most common working fluids has been carried out, introducing the results in GTSI for a wide range of temperatures and pressures, being easy to add other gases.

To make the code very general, in addition to gas turbines conventional components, such as inlet, compressor, intercooler, regenerator, combustor, turbine and exhaust system, GTSI can model evaporative intercooler, steam injection and reheat. The possibility of variable geometry was introduced in the compressor, steam injector and turbine modules. Given the high temperatures in modern and future turbines, a detailed cooling system modeling has been developed, being able to predict cooling flow requirements according to different technology levels. The control of the complete power plant has also been considered in detail, allowing the user to select among different options. The code incorporates a simple steam turbine bottoming cycle for a preliminary analysis of the combined cycle arrangement. In addition to the conventional off-design simulations it is possible to carry out studies involving engine deterioration and modification, or substitution, of components.

A validation process was carried out using different gas turbine arrangements. The result has been satisfactory, although additional configurations should be examined when more data is available.

As a direct application of GTSI, the conceptual design of the carbon dioxide/argon semi-closed cycle was conducted. Several key performance factors were considered in this study, such as the working fluid composition, the gas turbine arrangement and the cooling technology. Other main parameters were selected according to the state-of-the-art technology. Advanced concepts such as cryogenic precooling and turbine stator internal cooling, together with improved component efficiencies and higher temperatures were contemplated for a mid-long term future design. The results obtained for the conventional cycles have not been very promising, with slightly better values for the advanced cycles. Five of the most interesting cycles were selected for off-design studies, evaluating the part-power behaviour, the variable geometry requirement, etc. To complete the investigation, the starting sequence of one of them was performed. Also, considering the possibility of using existing turbomachinery, designed for air, in a semi-closed cycle pilot plant, the operation of several gas turbine configurations was analysed.

ACKNOWLEDGEMENT

The author is grateful to Dr. Pericles Pilidis for his inspired suggestions and assistance during this research; and to Prof. Riti Singh for his generous advice.

The EEC financial support through the JOULE II programme is also greatly appreciated.

Finally, but not less important, the author would like to take this opportunity to thank my family, friends and colleagues in Cranfield and ITP.

TABLE OF CONTENTS

TABLE OF CONTENTS

TABLE OF CONTENTS

TABLE OF CONTENTS

TABLE OF CONTENTS

TABLE OF CONTENTS

TABLE OF CONTENTS

TABLE OF CONTENTS

TABLE OF SYMBOLS

A:	Area
a:	Coefficient for thermodynamic properties equations (chapter 2)
ABB:	Asea Brown Boveri
AIAA:	American Institute of Aeronautics and Astronautics
ASME:	American Society of Mechanical Engineers
b:	Combustor efficiency constant (eq. [3.125]-[3.128])
BMT:	Blade Metal Temperature
CC:	Closed Cycle
	Combustor Casing (eq. [3.125]-[3.128])
CCPP:	Combined Cycle Power Plant
C_D:	Cold losses drag coefficient
CDP:	Compressor Discharge Pressure
CDT:	Compressor Discharge Temperature
CFD:	Computational Fluid Dynamics
CHP:	Combined Heat and Power
C_P:	Constant pressure specific heat (based on total temperature)
c_p:	Constant pressure specific heat (based on static temperature)
d:	Differential
DLE:	Dry Low Emission
FAR:	Fuel to Air Ratio
FCFC:	Full Coverage Film Cooling
FPT:	Free Power Turbine
GE:	General Electric
GT:	Gas Turbine
GTSI:	Gas Turbine Simulation - Industrial
H:	Total enthalpy
h:	Static enthalpy
HAT:	Humid Air Turbine
HP:	Horse power
HPC:	High Pressure Compressor
HPS:	High Pressure Shaft
HPT:	High Pressure Turbine
HRSG:	Heat Recovery Steam Generator
ISA:	International Standard Atmosphere
K':	Duct cold pressure loss factor (eq. [3.16])
k_1:	Combustor cold pressure loss factor (eq. [3.105])
k_2:	Combustor hot pressure loss factor (eq. [3.114])
K_1:	High pressure turbine capacity (eq. [5.22])
K_2:	Low pressure turbine capacity (eq. [5.23])

TABLE OF SYMBOLS

L:	Length
LHV:	Low heating value
LPC:	Low pressure compressor
LPS:	Low Pressure Shaft
LPT:	Low pressure turbine
M:	Mach number
N:	Rotational speed
NASA:	National Aeronautics and Space Administration
NGV:	Nozzle Guide Vane (stator)
NIC:	Nitrogen Internal Cooling
NO_x:	Oxides of nitrogen
N_{stg}:	Number of stages
P:	Total pressure
p:	Static pressure
PLF:	Pressure Loss Factor
ppm:	Parts Per Million
PT:	Power Turbine
PW:	Power
P&W:	Pratt & Whitney
PZ:	Primary Zone
RNI:	Reynolds Number Index
RR:	Rolls Royce
SM:	Surge Margin
SPO:	Specific Power Output
q:	Dynamic head
Q:	Heat flow
R:	Gas constant
r:	Radius
Re:	Reynolds number
Rn:	Degree of reaction
RH:	Relative Humidity
	Reheat
S:	Total entropy
s:	Static entropy
sf:	Scaling factor
SL:	Sea Level
SOT:	Stator Outlet Temperature
ST:	Steam Turbine
T:	Total temperature
t:	Static temperature
TET:	Turbine Entry Temperature

TABLE OF SYMBOLS

U:	Blade speed
UHC:	Unburnt Hydrocarbons
V:	Velocity
Vol:	Volume
vppm:	Parts Per Million (in volume)
W:	Mass flow
WAR:	Water to Air Ratio
x^i:	Mass fraction of component i
XN:	Shaft speed
XNRT:	Corrected speed
1:	Inlet
2:	Outlet
1-9:	Engine stations according to SAE ARP-755B (when appropriate)
α:	Variable stators angle
β:	Compressor map parameter
Δ:	Delta (increment of)
δ:	Corrected pressure (P/P_{std})
	Delta (differential)
ε:	Cooling effectiveness
Φ:	Total phi
ϕ:	Static phi, equivalence ratio (combustor efficiency equations)
γ:	Ratio of constant specific heats
η:	Efficiency
φ:	Flow swirl (whirl) angle
λ_i:	Increase in enthalpy from compressor inlet to bleed i position relative to the total increase in enthalpy across the compressor (eq. [3.34])
μ:	Viscosity (static)
ν:	Viscosity (dynamic)
π:	Pressure ratio
θ:	Corrected temperature (T/T_{std})
	Circumferential direction
ρ:	Density
Σ:	Sum of
Ψ:	Loading factor
	Function of gamma, Mach number and injection angle (eq. [3.87])
ζ:	Air system pressure loss coefficient (eq. [5.27])

SUBSCRIPTS AND SUPERSCRIPTS

amb:	Ambient
ax:	Axial
b:	Bleed
c:	Compressor
cc:	Combustion chamber
ds:	Design
f:	Fuel
in:	Inlet
is:	Isentropic
N:	Number of variables
n:	number of iteration
out:	Outlet
poly:	Polytropic
pz:	Primary Zone
ref:	Reference
reg:	Regenerator
sat:	Saturation
ss:	Steady state
stoic:	Stoichiometric
t:	Turbine
th:	Thermal
tr:	Transient
vap:	Vapour

CHAPTER 1

INTRODUCTION TO THE INDUSTRIAL GAS TURBINE

1.1. INDUSTRIAL GAS TURBINES

The gas turbines, developed in the late 30s and early 40s as aircraft propulsion systems, have contributed largely to the rapid growth of aviation. However, aircraft propulsion is not the only application of the gas turbines, and the industrial market constitutes one of the most interesting and profitable areas where these power plants can be employed. Thousands of units in service and hundreds of millions of hours of reliable and safe operation constitute the best credential for this well established technology, that entered into production in 1939 with the first successful industrial gas turbine, a 4 MW open cycle machine, designed by Adolf Meyer and built by Brown Boveri. The same year Jacob Ackeret and Curt Keller designed a closed cycle using air as working fluid. That machine, rated at 2 MW, produced electricity for over 6000 hours, with a thermal efficiency of 32.6% and a turbine entry temperature (TET) of 650°C. However, prior to these successful engines, there is a long and, sometimes, frustrating path.

1.1.1. THE EARLY YEARS

The first patents for a gas turbine engine by John Barber in 1791 did not materialise into a working device. At the end of the XVIII century, J.F. Stolze designed a hot air turbine, built eventually in the period 1900-1904. However, this was an unsuccessful project, and no net power was obtained. Several other experiments took place in the same period, with the same results. However, in 1903 the Norwegian Aegidius Elling developed the first engine that produced real net work. It had a six stage centrifugal compressor, with variable angle diffuser vanes and water injection between stages, followed by a combustion chamber and a heat exchanger to produce steam, that was mixed with the combustion products prior to the expansion, and finally an axial impulse turbine. The TET was around 400°C and the net power 11 HP. One year later Elling built a regenerative gas turbine, with a TET 100°C higher than the first one, and a net power of 44 HP. The door for a new technology was open.

In 1905 the company formed two years before by the French Charles Lemale contracted Brown Boveri for the design of a centrifugal compressor with an overall pressure ratio of three, in...25 stages!!. The isentropic efficiency of this component was about 65-70%. The net power should have been negative with the TETs employed then. However, the TET achieved was exceptionally high, 1800°C,[1] with a

---

[1] Even at the present time this temperature has not been reported in any production gas turbine, and perhaps only the most advanced demonstrator engines have achieved peak temperatures of this order during tests.

carborundum lined combustor and a steam cooled turbine.[2] The thermal efficiency of the machine was a poor 3.5%.

Important efforts were made during the first decades of the XX century by Hans Holzwarth, Sanford Moss, Glenn B. Warren, Adolph Vogt, Barbezat, Karavodine, Hugo Junkers, Aurel Stodola, etc.

From the end of the Second World War a huge investment, in terms of economic and human resources, has been made in the industrial gas turbines. The results are evident: combined cycle power plants (CCPP) with thermal efficiencies higher than 55% and output of 2500 MW or more can be found in many countries. The development of larger, more efficient and *cleaner* aero engines has also contributed to the industrial market. Simple cycle aeroderivative gas turbines with efficiencies over 40% are already in operation. The future of the gas turbine is, apparently, exceptional, although in most areas there are technological details that can be improved considerably.

1.1.2. CHARACTERISTICS OF THE GAS TURBINE POWER PLANTS

Industrial gas turbines can be classified in many ways:

- **Type of gas turbine cycle:**

1. Open cycle: the working fluid is air taken from the atmosphere and rejected after the completion of the cycle. The air can be heated either in a combustor (in most cases) or in a heat exchanger (not very frequent).
2. Closed cycle: the working fluid can be whatever substance appropriate for the Brayton cycle. The heat is added employing a heat exchanger. Hence, after the necessary precooling, the fluid can be recirculated. Only a few have been operated, despite the large variety of possible applications: submarine propulsion, space power, etc.
3. Semi-closed cycle: the working fluid must be one that the combustion products of the fuel with the required oxidizer are the same as the working fluid, plus other that can be removed from the cycle before its completion. Like the closed cycle, this one also requires precooling to return the working fluid to its initial condition. As the heat addition is done using a combustor, there is always an excess in mass flow that must be continuously removed. This concept is still in its early stages and, from the knowledge of the author, no operative machine has been built.

---

[2] The idea of steam cooled turbines was revived in the 60s, although the enormous problems found delayed the entry into service of this concept until the mid-end of this decade with the General Electric Frame 9H (S-109H & S-107H).

- **Power plant arrangement:**

  1. Simple cycle: The gas turbine is the only power system of the plant. In addition to the conventional configuration (compressor, combustor and turbine) it is possible to have also intercoolers, evaporative coolers and regenerators. In some advanced concepts reheat has also been introduced.

  2. Combined cycle: there are two or more cycles that generate net power. The most common one has the gas turbine as the topping cycle and the steam turbine as bottoming cycle. The criterion for the cycle selection is the operational temperature: the exit temperature of the topping cycle must be the highest temperature of the bottoming cycle. For example, the gas turbine could act as the bottoming cycle of a magnetohydrodynamic machine operating at very large temperatures (3000$^+$ K), provided that the heat exchanger can resist them.

  3. Steam injection gas turbine: the exit heat is employed to produce high pressure - high temperature steam, that can be introduced in the gas turbine either at the exit of the compressor, in the primary zone of the combustor or after a partial expansion in the turbine. It is difficult to classify the steam injection machines either as a simple or a combined cycle, because they have common characteristics with both.

- **Gas turbine general arrangement:**

  1. Single spool (one spool - one shaft): the compressor/s, turbine/s are in the same shaft. The power is extracted from this shaft.

  2. Single spool with free power turbine (one spool - two shaft): the compressor/s and the turbine/s that produce the power for the compressor/s are in one shaft. The turbine that drives the load is located in other shaft.

  3. Two or more spools (two spool - two shaft,.): the compressors and turbines are in more than one spool. The load is usually driven with the low pressure spool, although there are exceptions.

  4. Two or more spools with free power turbine (two spool - three shaft,..): the compressors and turbines are in more than one spool, and the power is extracted from a free turbine located, typically, at the low pressure end of the machine.

- **Origin of the machine:**

  1. Heavy duty: the machine has been specifically designed for industrial purposes

2. Aeroderivative: the engine was initially designed for aircraft propulsion and, later, with the necessary modifications, was converted for industrial applications.

- **Frequency of use:**
  1. Peak load: with 1000 hours of operation per year or less
  2. Intermediate load: with 1000 to 4000 hours of operation per year
  3. Base load: with over 4000 hours of operation per year. Typically the base load gas turbines operate for over 8000 hours, driving electricity generators, compressors, etc. These machines must have high reliability, availability and maintainability, with very low fuel consumption.

- **Application:**
  1. Power only: including electricity generation and compressor drive. The gas turbine exit gases are either rejected to the atmosphere or employed to produce steam for a bottoming cycle or for injection in the gas turbine.
  2. Combined heat and power (CHP): the exit gases are typically used to generate steam for district heating or processes.

- **Fuel employed:**
  1. Natural gas (mainly methane)
  2. Clean distillate liquid fuels (Diesel Fuel No.2, etc.)
  3. Residual fuels
  4. Coal derivative fuels (low calorific value synthetic gas)
  5. Other fuels (hydrogen is proposed frequently for future machines)

1.1.3. THE EMISSIONS ISSUE

Emissions regulations are becoming more and more strict. The EPA Standards for Stack Gas Emissions constitute the most common laws, although several countries or states have their own, and sometimes more severe, regulations.

The EPA specifies that the NO_x emissions must be kept below 75 ppm, with special allowances for amount of N_2 in fuel and gas turbine efficiency, which may total as much as 65 ppm. In the case of oil field and pipeline service the emissions can be as high as 150 ppm. The SO_2 emissions must be under 150 ppm or 0.8% of the maximum sulphur in fuel, with no CO or opacity allowed.

The efforts to abate NO_x and CO emissions over the whole operating range involve an extremely important budget for gas turbine manufacturers. Since the early

80s, when rich burn/rapid quench was introduced, the environmental impact of industrial gas turbines has been continuously reduced, as shown in figure 1.1 for NO_x emissions.

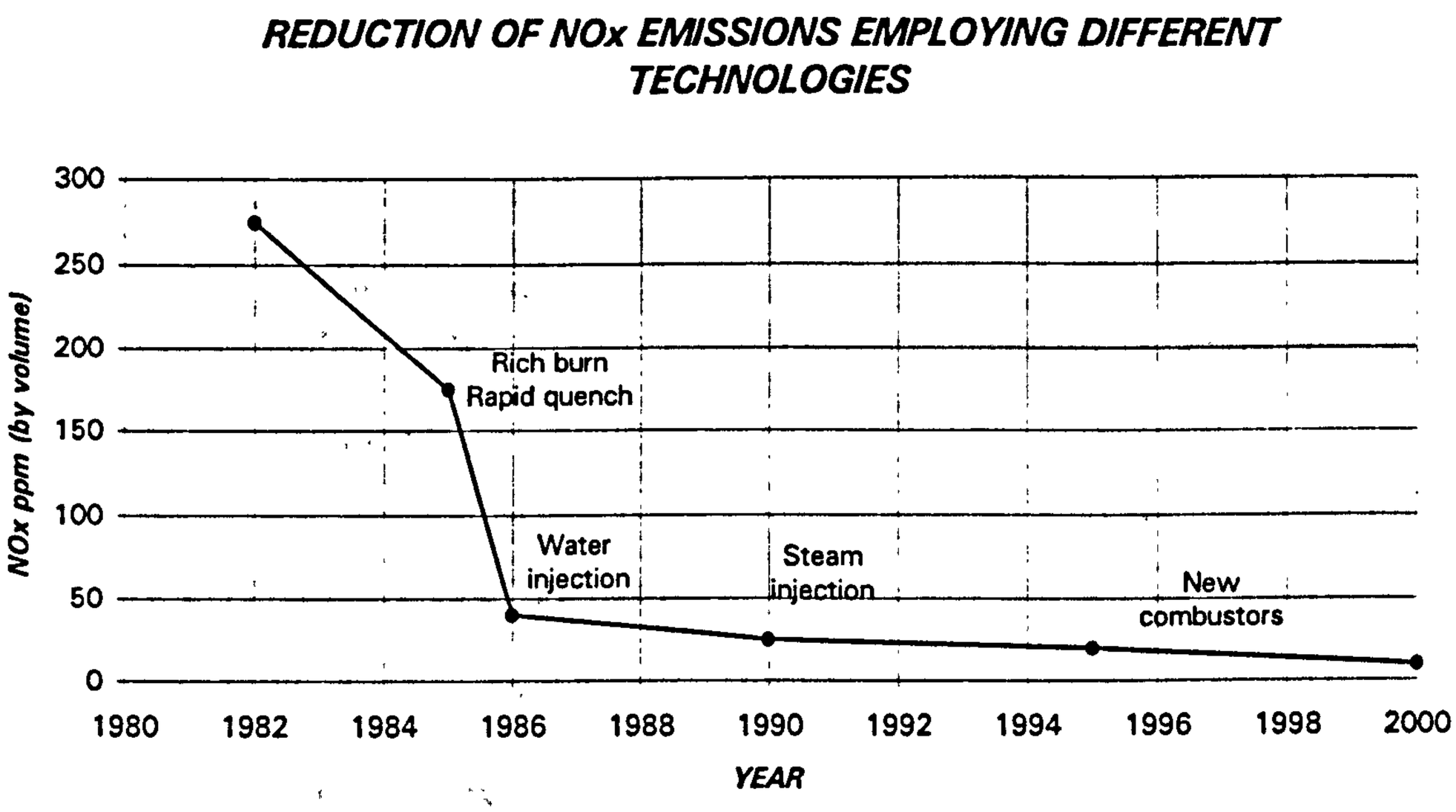

Figure 1.1. Reduction of NO_x emissions over several different technologies

Water and steam injection started to be employed in the mid 80s as a mean of reducing NO_x emissions, caused, basically, by the high combustion temperatures [29], [128]. However, water injection has the disadvantage of thermal efficiency reduction and increase in CO and unburnt hydrocarbons (UHC) emissions. Steam injection increases the efficiency and power output, but still carries the same problems with CO and UHC. In addition to these deficiencies, both concepts need additional pipework and plant size, as well as a continuous supply of clean distillate water.

The latest combustor development works involve, in most cases, fuel staging, both in parallel and series. With these concepts levels of NO_x below 25 vppm have been demonstrated, with similar figures for CO [29], [80] and [142].

In series fuel staging, at full load, a portion of the fuel pre-mixed with air is injected into the primary combustion zone. Additional fuel pre-mixed with air is injected downstream of the primary zone, into the secondary zone, and some may be burned in tertiary or quaternary zones. Rolls Royce (RR) selected this solution for the new Dry Low Emission combustor (DLE) [29].

In parallel fuel staging, a large number of lean pre-mix burners are used. As load is reduced a certain number of injectors are shut off, while the others remain at full fuel flow. Lean pre-mixed technology is generally fitted to this type of combustors.

In the case of an experimental General Electric (GE) combustor [80], the variable geometry closes the air flow into the regions where the fuel flow has been shut off.

A common concept in both, parallel and series fuel staging, is the lean premixed combustion. This technology has demonstrated that NO_x can be independent of gas pressure, combustor inlet temperature and residence time [80]. In conventional combustors NO_x increases with these three parameters. The only factor is then the flame temperature, with an exponential influence. Therefore, high pressure ratio machines, with a high combustor inlet temperature, such as the aeroderivative gas turbines, can be employed without any disadvantage in terms of pollutant emissions. At the same time, combustors with large residence time can be designed to achieve low CO and UHC figures.

1.1.4. THE FUTURE OF GAS TURBINES

The advantages of the gas turbine over the competitors, specially oil or coal fired steam turbine or nuclear power plants, are clear, and cover the most important areas for both, operators and clients. It is important to note that before the mid-late 80s all the large power plants were based on steam turbines,[3] with the gas turbine systems used for emergency or peak load. Since those dates most of the new base load plants are based on gas and steam turbine combined cycles.

- The **size** of the power plants has been reduced, as well as the **period of construction** and delivery of the complete system, and **economic investment**, in comparison with the old coal and oil fired steam turbines and nuclear reactors. Less than two years for a simple cycle gas turbine, around three for a combined cycle plant, five or six for a large coal/oil fired and ten to twelve years for a nuclear plant, are typical figures.

- **Reliability, availability and maintainability** offered by gas turbines are better than any other system. The outage periods are lower and less frequent and, in some cases, failures are solved in less than a day. The use of natural gas has helped to the increase in the availability.

- Safety of the system is also better than in nuclear or oil/coal fired steam turbines.

---

[3] The other system, not included here, is the hydroelectric. The main reason for the exclusion is the difficulty in building new dams. Not only the most suitable locations already have dams, but also the public response to new ones is always a factor of concern.

- **Performance**, based mainly in thermal efficiency, is larger than in nuclear reactors (typically around 30%), and steam turbine cycles (up to 49% in the most advanced cases). For combined cycles figures around 55% are not difficult to find, with 42% for simple cycles. In the case of CHP it is possible to obtain a global efficiency of 80-85%.

- **Environmental aspects** are clearly against the nuclear reactors, with the programmes stopped in most of the countries, and plants being shut down. The emissions of oil/coal boilers are also worse than in gas turbine combustors.

- **Operational and transient response**. A decade ago, over 300-400 people were required to run an oil/coal fired or nuclear plant, while now under 30 people are needed for a 2000 MW CCPP. In terms of response, and just as an example, the Steam Plant Recommended Performance establish a rate up to 2% per minute over a 2 hours period from 100% to 50% of the power and vice versa. In the case of a simple cycle heavy duty gas turbine times around 5 minutes can be achieved between the starting, acceleration to synchronous idle and loading up to full load. Considerably shorter periods can be obtained for the aeroderivative machines (of the order of 30 sec.).

As described in the first pages, water and steam injection, new advanced combustors, reheat systems, steam cooling, new materials and manufacturing processes have been introduced in the last generations of industrial gas turbines. A key issue for the success is that all of these advanced technologies have been implemented in the gas turbine without decreasing the reliability and availability of the machines. In some cases, the aero engines have performed as test beds for their industrial derivatives while, in other cases, thousands of severe test hours before a component enters service ensure its satisfactory behaviour.

The forecast for industrial gas turbines is now excellent. Even in the early and mid 90s, when the recession affected the aircraft industry, and consequently the aero gas turbine world, its effect over the industrial gas turbines was relatively low.

1.2. NEED FOR ACCURATE PERFORMANCE SIMULATION PROGRAMMES

Given the considerations made in the first section, the need for accurate simulation programmes for existing machines, for possible improvements and modifications of gas turbines already in operation, fault diagnostic analysis and future advanced cycles is evident.

Improvements and modifications, such as the introduction of steam injection in new and also in existing machines, new closed cycles operating with different gases

and mixtures of gases, semi-closed cycles, industrialisation of aeroengines, etc., need to be simulated to be able to make a clear performance assessment that, together with other operating considerations, must be understood.

For these purposes two new programmes were developed by the author. The first is an optimisation code and the second is a design, off-design and transient performance code, called GTSI. Both were validated using different existing gas turbines and other data available to the author, although only for steady-state. For the transient case, where almost no validation data was available, future development will be needed, specially for configurations where heat exchangers, regenerators, bottoming cycles and, in general, components with a very large heat storage capacity are present. However, due to this characteristic, the transient behaviour of these systems is frequently considered, from the gas turbine point of view, as a sequence of steady-state simulations .

During the development of the codes five features were considered very important:

- The first one was to built **robust programmes** capable of simulating most of the existing industrial gas turbines, with minimum modifications accounting for different efficiency correlations, control laws, etc. Combined cycles have been also included, although the steam turbine has been modeled in a simplified way.

- The second point is the **growth capability** of the programme. If the study requires, for example, a detailed steam turbine simulation, not included in the available code, it should be possible to link the adequate steam power plant simulation programme with minimum effort.

- The third one was to give special attention to the **turbine cooling bleed** calculations, to be able to make an accurate assessment of the performance impact employing different technologies, evaluating the losses inherent to the cooling system.

- The fourth is to have a code able to simulate **closed and semi-closed cycles**. Very little attention has been paid to closed cycles, although the possibilities for actual and future applications are very interesting, as mentioned in 1.1.2. In the case of the semi-closed cycle, a study sponsored by the EEC, under the JOULE II programme, has been carried out, and very promising results have been obtained for a completely new cycle, where the author has focused the attention in the performance studies for both, design and off-design simulations.

- Finally, the possibility of **modifying an existing gas turbine,** adding new elements and maintaining some others. Examples of this feature could be the industrialisation of an aero engine, the introduction of steam injection, mass flow and power growth by changing the compressor and/or turbine, etc.

1.3. THE INDUSTRIAL GAS TURBINE MARKET

The industrial gas turbine market is, probably, among the most competitive ones, with several machines in the different power ranges offering each one different advantages and, apparently, very small differences. After a lengthy period of low activity, focused mainly in the peak & emergency power, in the late 80s and early 90s the activity started a slow recovery, and, for example, in 1992/93 one of the largest aero engine companies had 40% of the revenues coming from its industrial branch.

Forecasts for the market predict revenues of around $45,000 million (in 1995 US dollars) in the next decade. Almost 75% of this $45 billion will be for the electric power generation, and the rest from mechanical drives and marine propulsion, as indicated in figure 1.2. Figures 1.3 and 1.4 show the break down of power range for the electric power generation and mechanical drive machines respectively.

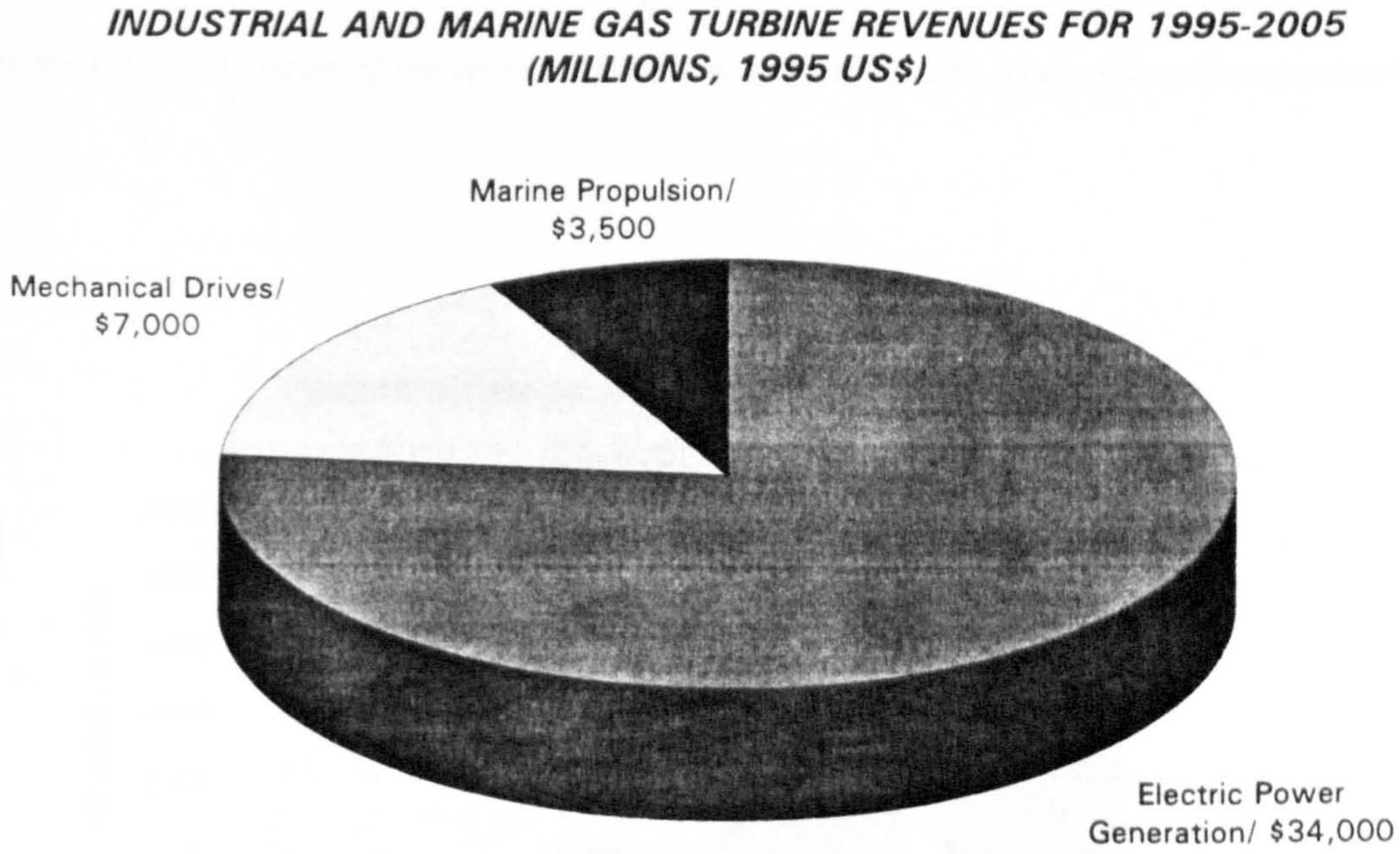

Figure 1.2. Forecast of revenues in the industrial and marine gas turbines for the next decade

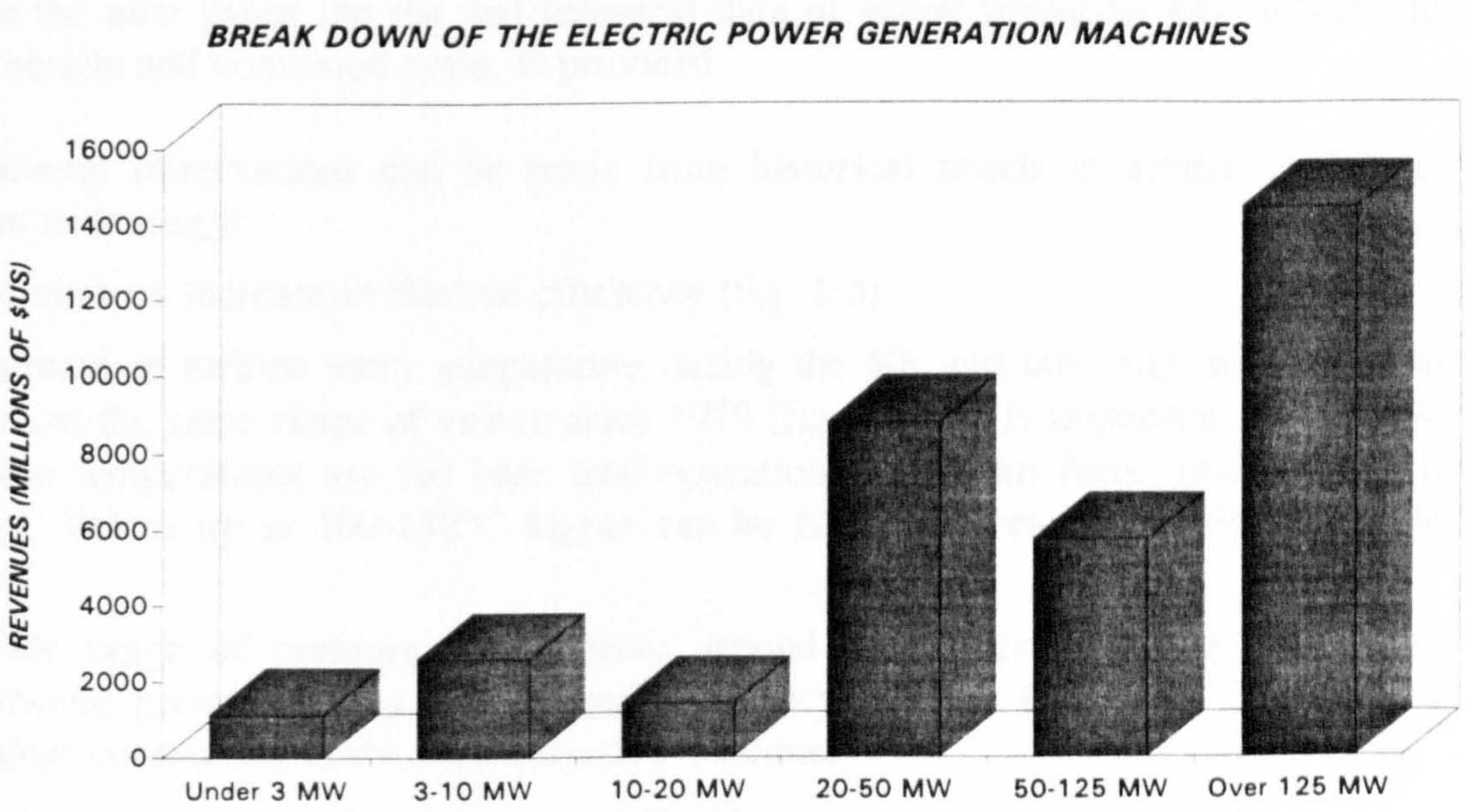

Figure 1.3. Break down of the revenues for the next decade in the power generation gas turbines

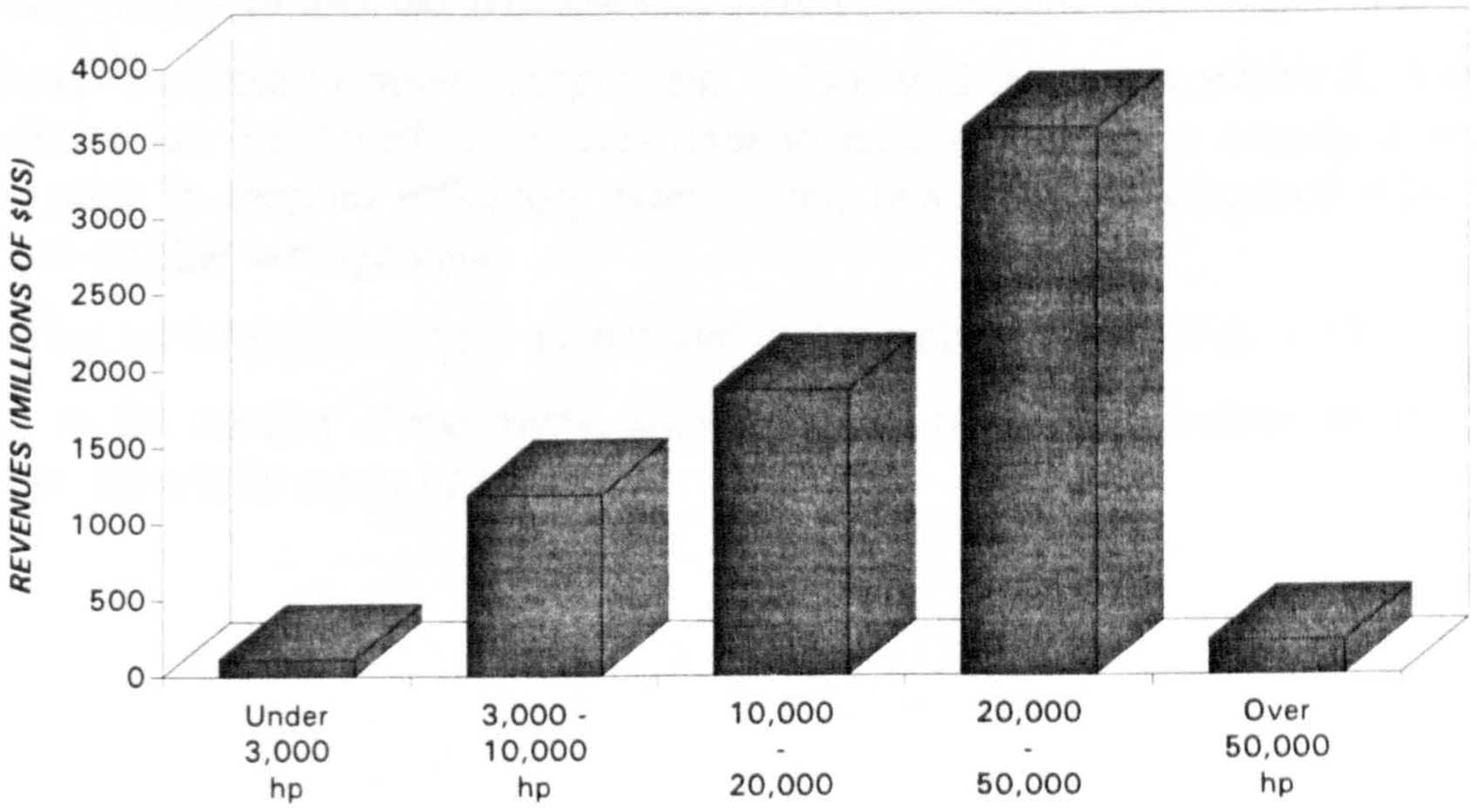

Figure 1.4. Break down of the revenues for the next decade in the mechanical drives gas turbines

In the next pages the list and technical data of actual industrial gas turbines in both, simple and combined cycle, is provided.

Several observations can be made from historical trends in simple cycle gas turbine technology:

- Continuous increase in thermal efficiency (fig. 1.5).
- Increase in turbine entry temperature during the 50s and 60s, and maintained in almost the same range of values since 1970 (fig. 1.6). It is important to note that these temperatures are for base load operation with clean fuels, mainly natural gas. Values up to 100-150°C higher can be found for peak load with the same fuel.
- Wide range of pressure ratios (from around 5 to over 30). The correlation between pressure ratios and thermal efficiency is clear (fig. 1.7). The largest values correspond to the aeroderivative machines.
- Continuous increase in power output (fig. 1.8).
- Correlation between thermal efficiency and specific power output (fig. 1.9).
- Important increase in the number of machines, showing a favorable market trend for the gas turbines in the whole range of powers.

Similar observations can be made for combined cycles:

- Continuous increase in thermal efficiency (fig. 1.10a and 1.10b).
- Important growth in thermal efficiency relative to the simple cycle (fig. 1.11)
- Continuous increase in power output (fig. 1.12), with packages where 2, 3 or 4 gas turbines are employed. It is important to note that there is usually a small improvement in thermal efficiency when using this strategy compared with the single gas turbine arrangement.
- Correlation between gas turbine power and steam turbine power (fig. 1.13).
- Increase in the number of machines, showing a favorable market trend for the gas turbine in the whole range of powers.

TABLE 1.1: SIMPLE, REGENERATIVE, INTERCOOLED AND STEAM INJECTED GAS TURBINE CYCLES

		Year	Power (MW)	Heat Rate (BTU/MW-h)	Press. Ratio	Mass flow (kg/s)	EGT (K)	TET (K)	Efficiency (%)	SPO (kW/kg/s)
ABB										
	MARS (HD)	1977	8.840	10.990	16.0	37.19	739	1330	31.04	237.7
	GT 35 (HD)	1968	16.900	10.670	12.0	92.08	647	1092	31.98	183.5
	GT 35 (cogen) (HD)	1986	18.950	10.500	13.0	92.08	682	1171	32.49	205.8
	GT 10 (HD)	1981	21.850	10.470	13.6	78.02	790	1371	32.59	280.1
	GT 8 (HD)	1984	47.100	10.800	16.3	176.90	796	1438	31.59	266.3
	GT8C (HD)	1995	52.800	9.920	15.7	179.00	790	1415	34.39	295.0
	GT 11 (HD)	1971	71.900	10.970	11.0	284.85	793	1312	31.10	252.4
	GT 11N (HD)	1987	81.600	10.660	12.4	310.26	788	1339	32.01	263.0
	GT11N2 (HD)	1994	115.500	9.780	15.0	375.00	797	1413	34.89	308.0
	GT 200 (HD)	1977	93.000	9.800	16.0	347.00			34.81	268.0
	GT 13 (HD)	1970	98.900	10.660	12.5	405.96	762	1298	32.01	243.6
	GT 13E (HD)	1983	147.900	9.850	13.9	491.24	789	1376	34.64	301.1
	GT13E2 (HD)	1996	165.100	9.550	14.6	532.00	797	1405	35.73	310.3
	GT24 (HD)	1996	166.000	9.000	30.0	378.00	883		37.91	439.2
	GT26 (HD)	1996	241.000	8.930	30.0	545.00	883		38.21	442.2
ALLIED SIGNAL (former TEXTRON LYCOMING)										
	IM831-800 (AE)	1972	0.505	16.400	11.0	3.58	772	1236	20.80	140.9
	IM831-800 (AE)	1972	0.520	16.150	11.0	3.58	772	1236	21.13	145.1
	AS1042 (AE)	1996	9.000	9.800	21.1	32.40	788	1584	34.81	277.8
	AS4055 (AE)	1993	3.999	8.960	8.4	12.76	844	1316	38.08	313.4
	TF-15 (rec) (HD)	1985	1.491		14 5					
	TF-25 (AE)	1970	1.864	15.070	6.5	9.98	872	1241	22.64	186.8
	TF-35 (AE)	1975	2.610	13.160	7.0	11.80	878	1298	25.93	221.2
	TF-40 (AE)	1975	2.950	12 880	8.4	12.70	883	1333	26.49	232.3
	TF50 (AE)	1998	3.872	11.256	11.0	14.56	895	1481	30.31	265.9
ALLISON GT										
	501-KB3 (AE)	1977	2.840	13.136	9.3	12.90	839	1338	25.97	220.2
	501-KB4 (standby) (AE)	1980	4.330	11.697	9.3	15.60	896	1429	29.17	277.6
	501- KB5 (AE)	1982	3.924	11.304	10.1	15.47	835	1308	30.18	253.7
	570-KA (AE)	1979	4.877	11.528	12.1	18.60	836	1413	29.60	262.2
	571-KA (HD)	1986	5.910	10.067	12.7	19.64	806	1378	33.89	300.9
	501-KH (steam inj) (AE)	1986	5.940	8.645	11.8	17.92	798	1255	39.47	331.5
	501-KB5S (AE)	1992	4.100	11.570	10.1	15.60	852	1312	29.49	262.8
	501-KB7 (AE)	1996	5.220	10.826	13.4	20.20	811	1322	31.51	258.4
	ALLISON 601-KB-9 (HD)	1998	6.700	10.124	15.0	23.60	802	1466	33.70	283.9
	ALLISON 601-KB-11 (HD)	1999	8.200	10.035	20.0	30.10	777	1494	34.00	272.4
ALSTHOM GT										
	PG 5371 (HD)	1987	26.300	11.820	10.2	122.47	756	1230	28.86	214.7
	PG 6541 (HD)	1978	38.340	10.860	11.8	136.53	813	1377	31.42	280.8
	PG 9161 (HD)	1978	116.900	10.310	12.1	403.24	802	1377	33.09	289.9
	PG 9281 (HD)	1991	212.200	9.995	13.5	600.10	856	1533	34.14	353.6
ANSALDO										
	V64.3 (HD)	1988	63.000	9.665	16.1	192.00	804	1449	35.30	328.1
	V64.3A (HD)	1994	70.000	9.270	16.6	194.00	838	1520	36.80	360.8
	V84.2 (HD)	1988	103.200	10.220	10.7	349.26	813	1337	33.38	295.5
	V84.3 (HD)	1991	139.000	9.555	15.6	412.77	807	1444	35.71	336.8
	V94.2 (HD)	1974	159.000	9.890	11.0	519.00	813	1346	34.50	306.4
	V94.3A (HD)	1996	240.000	8.980	16.6	640.00	835	1515	37.99	375.0
CENTRAX GT										
	CX62 (AE)	1983	3.731	12.264	9.3	15.42	806	1308	27.82	241.9
	CX 350-KB5 (AE)	1980	4.617	12.184	12.1	19.05	878	1484	28.00	242.4
	CX571 (AE)	1985	5.620	10.591	12.7	19.50	827	1413	32.21	288.1
COOPER ROLLS										
	COBERRA 2000 (AE)	1964	14.620	11.850	9.2	77.56	703	1149	28.79	188.5
	COBERRA 6000 (AE)	1974	24 940	9.575	20.0	89.81	739	1437	35.63	277.7
DEUTZ MWM										
	TA 216 (HD)	1955	0.080	30.925	2.8	0.91	923	1133	11.03	88.2
	KA 215 (HD)	1978	0.220	18.672	9.0	1.81	791	1252	18.27	121.3
	KT 215 (HD)	1978	0.427	19.144	9.0	3.54	791	1252	17.82	120.7
	KA 123 (HD)	1979	0.700	15.888	9.0	4.90	766	1213	21.47	142.9
	KA 134 (HD)	1978	1.177	15.697	8.0	7.85	778	1200	21.74	150.0
	KA 334 (HD)	1982	1.470	16.961	9.2	9.07	818	1301	20.12	162.0
	LA 136 (HD)	1976	1.812	15.200	6.5	9.62	873	1287	22.45	188.4
	KT 134 (HD)	1979	2.260	16.187	8.0	15.69	778	1200	21.08	144.0
	KT 334 (HD)	1982	2.824	17.484	9.2	17.96	818	1301	19.51	157.2
	LA 237 (HD)	1976	2.900	12.911	8.4	12.47	883	1377	26.43	232.5
	CA 135 (HD)	1979	3.050	13.108	8.3	15.42	823	1310	26.03	197.8
	CA 139 (HD)	1983	3.650	12.050	9.3	15.56	806	1285	28.31	234.6
	CA 149 (HD)	1980	4.400	12.424	11.2	19 05	878	1459	27.46	231.0
	CA 159 (HD)	1985	5.450	10.602	12.0	19.50	827	1395	32.18	279.4
DRESSER-RAND										
	KG2-3C (HD)	1968	1.475	21.620	3.9	12.88	838	1098	15.78	114.5
	KG2-3E (HD)	1989	1.850	20.650	4.6	14.92	819	1103	16.52	124.0
	KG2-3R (recup) (HD)	1981	1.330	13.190	3.9	12.61	573	1098	25.87	105.5
	KG5 (HD)	1976	3.000	16.100	6.5	21.09	773	1143	21.19	142.2
	DR-990 (HD)	1986	4.220	11.780	12.6	20.41	754	1323	28.96	206.7
	DR-60G (AE)	1973	13.400	9.570	21.5	45.81	755	1491	35.65	292.5
	DR-160 (HD)	1969	15.000	11.830	8.7	77.11	703	1148	28 84	194.5
	DR-61 (AE)	1969	21.900	9.515	18.1	68.04	805	1504	35.86	321.9
	DR-300 (AE)	1979	22.100	9.406	18.1	68.04	801	1504	36.27	324.8
	DR-290 (AE)	1976	25.000	9.538	19.3	89.81	737	1435	35.77	278.4
	DR-460 (AE)	1984	33.700	9.335	26.8	122.47	718	1428	36.55	275.2
	DR-600 (AE)	1990	40.914	8.523	29.0	125.19	725	1491	40.03	326.8

		Year	Power (MW)	Heat Rate (BTU/MW-h)	Press. Ratio	Mass flow (kg/s)	EGT (K)	TET (K)	Efficiency (%)	SPO (kW/kg/s)
EBARA										
	PW-6E (AE)	1990	0.570	16.300	7.0	3.18	873	1219	20.93	179.5
	PW-7E (AE)	1990	0.700	15.535	8.5	3.81	850	1219	21.96	183.7
	FT8 (AE)	1990	25.420	8.950	20.3	85.27	716	1359	38.12	298.1
	FT8-TWIN (AE)	1990	51.100	8.905	20.3	170.55	716	1359	38.31	299.6
EUROPEAN GAS TURBINES (former ROUSTON GT)										
	HURRICANE (HD)	1991	1.600	13.400	9.2	6.99	873	1407	25.46	229.1
	TB5000 (HD)	1977	3.809	13.310	6.8	21.32	761	1183	25.63	178.7
	TYPHOON (HD)	1989	3.903	11.314	12.8	16.78	773	1327	30.16	232.6
	TORNADO (HD)	1981	6.249	11.265	12.1	27 67	741	1273	30.29	225.8
	RLM1600 (AE)	1989	13.404	9.617	21.5	44.91	756		35.46	298.5
	RLM2500-PE (AE)	1979	21.437	9.703	18.8	68.04	802	1499	35.16	315.1
	RLM2500-PE (AE)	1979	22.106	9.453	18.4	67.13	801	1505	36.09	329.3
	RLM5000-PC (AE)	1984	33.723	9.484	26.1	126.55	717	1443	35.97	266.5
	RLM5000-PC (AE)	1984	33.766	9.348	25.4	122.92	719	1446	36.50	274.7
	RLM6000	1994	43.000	8.216	28.0	126.50	722	1473	41.53	339.9
	G3142	1975	10.400	13.320	7.1	53.00	809	1216	25.61	196.2
	G3142 (recup)	1975	10.000	10.370	7.3	53.00		1227	32.90	188.7
	PG5371 (PA)	1987	26.300	11.820	10.2	122.47	756	1230	28.86	214.7
	PG6551 (B)	1988	39.200	10.730	11.8	138.00	814	1377	31.80	284.1
	PG6101 (FA)	1989	70.100	9.980	15.0	196.00	860	1561	34.19	357.7
	PG 9171 (E)	1987	123.400	10.100	12.5	402.33	810	1397	33.78	306.7
	PG 9331 (FA)	1994	226.500	9.570	15.0	614.40	862	1561	35.65	368.7
	TEMPEST (HD)	1996	7.500	10.339	14.0	27.20	809	1403	33.00	275.7
FIAT AVIO										
	LM500 (AE)	1980	3.850	11.120	14 0	15.42	789	1378	30.68	249.6
	LM2500 (AE)	1979	21.100	9.435	18.0	66.22	769	1420	36.16	318.6
	TG 20 (HD)	1971	37.850	11.590	11.0	159.21	793	1312	29.44	237.7
	TG 20 (HD)	1984	42.500	10.600	14.0	156.94	775	1353	32.19	270.8
	TG 50 (HD)	1975	103.000	10.990	12.0	386.01	808	1363	31.04	266.8
	TG 50 (HD)	1985	128.340	10.080	14.0	443.16	767	1340	33.85	289.6
GE MARINE&INDUSTRIAL										
	LM1600-PA (AE)	1989	13.400	9 476	22.0	44 91	755	1459	36.00	298.4
	LM1600-PB-STIG (AE)	1991	16.100	8 615	25.0	47.63	722	1322	39.60	338.0
	LM2500-PE (AE)	1973	22.200	9.404	18.4	67.13	801	1487	36.28	330.7
	LM2500-PE (AE)	1973	21.550	9.650	18 6	68.04	802	1493	35.36	316.7
	LM2500-PH-STIG (AE)	1986	29.950	8.529	20.0	68.49	777	1361	40.00	437.3
	LM2500-PH-STIG (AE)	1986	25.050	8.770	20.0	68.49	767	1344	38.90	365.7
	LM5000-PC (AE)	1984	33.750	9.346	25.3	122.92	719	1433	36.51	274.6
	LM5000-PC (AE)	1984	33.750	9 483	26.0	126.10	716	1437	35.98	267.6
	LM5000-PD-STIG (AE)	1986	52.700	7.731	32.3	141.52	680	1311	44.13	372.4
	LM5000-PD-STIG (AE)	1986	48.950	8.019	32.0	141.97	677	1303	42.55	344.8
	LM6000-PA (AE)	1992	42.200	8.430	29.8	102.96	721	1491	40.47	409.8
	LM6000-PA (AE)	1992	41.550	8.467	29.8	102.96	721	1491	40.30	403.5
GE POWER GENERATION										
	PG5371 (PA) (HD)	1987	26.300	11.820	10.2	122.47	756	1230	28.86	214.7
	PG6541 (B) (HD)	1978	38.340	10.860	11.8	136.53	812	1377	31.42	280.8
	PG7111 (EA) (HD)	1976	83.500	10.480	12.4	290.75	803	1377	32.56	287.2
	PG7191 (F) (HD)	1987	150.000	9.880	13.5	416.40	856	1533	34.53	360.2
	PG9171 (E) (HD)	1987	123.400	10.100	12.5	402.33	810	1397	33.78	306.7
	PG9281 (F) (HD)	1987	212.200	9.995	13.5	600.10	856	1533	34.14	353.6
	PGLM2500-PE (AE)	1979	21.790	9.780	18.7	66.22	804	1497	34.89	329.0
	PGLM2500-PE (AE)	1979	21.160	10.030	18.7	66.22	805	1499	34.02	319.5
	PGLM5000-PC (AE)	1986	33.060	9.730	30.0	122.92	721	1494	35.06	268.9
	PGLM5000-PC (AE)	1986	33.090	9.860	30.0	126.10	719	1489	34.60	262.4
	PGLM6000 (AE)	1992	41.500	8 650	29.5	125.19	725	1497	39.44	331.5
HITACHI										
	G3142 (J) (HD)	1975	10.450	13.320	7.1	52.16	799	1201	25.61	200.3
	PG5371 (PA) (HD)	1987	26.300	11.820	10.2	122.47	756	1230	28.86	214.7
	PG6541 (B) (HD)	1987	38 340	10.860	11.8	136.53	812	1366	31.42	280.8
	PG7111 (EA) (HD)	1987	83.500	10.480	12.4	290.75	803	1398	32.56	287.2
	PG7191 (F) (HD)	1988	150.000	9.880		416.40	856		34.53	360.2
	PG9171 (E) (HD)	1987	123.400	10.100	12.3	403.70	811	1377	33.78	305.7
	H-15 (Intercooled) (HD)	1990	13.800	11.044		49.44	823		30.89	279.1
	H-25 (HD)	1988	23.500	10.560		88.00	803		32.31	267.1
	H-25 (Intercooled) (HD)	1988	26.770	10.465		88.00	823		32.60	304.2
HITACHI ZOSEN										
	GT10-5 (HD)	1982	3.660	11.300	9.3	15.56	806	1308	30.19	235.2
	GT15A (HD)	1979	4.590	11.530	12.1	18.60	819	1385	29.59	246.8
	GT15B (HD)	1986	5.560	10.070	12.7	19.64	806	1378	33.88	283.1
	CCS7	1986	4.850	8.710	17.1	17.15	802	1464	39.17	282.9
	GT151 (HD)	1982	14.760	11.707	9.1	77.11	709	1144	29.14	191.4
	GT201 (AE)	1982	23.520	10.025	19.8	88 45	751	1434	34.03	265.9
INTERNATIONAL POWER TECHNOLOGY										
	SERIES 7 (HD)	1981	5.500	8.911						
	SERIES 5 (HD)	1987	1.900	12.000						
ISHIKAWAJIMA-HARIMA HEAVY INDUSTRIES										
	IM400-6 (HD)	1983	3.610	12.040	9.3	15.42	806	1308	28.34	234.1
	IM600 (HD)	1980	4.500	12.150	11.2	18.60	856	1422	28.08	242.0
	IM610 (HD)	1987	5.330	10.940	12.7	19.50	808	1381	31.19	273.3
	LM1600 (AE)	1988	12.820	9.310	14.8	45.36	770	1361	36.65	282.6
	LM2500 (AE)	1976	21.560	9.470	18.1	67.58	796	1472	36.03	319.0
	IM5000 (AE)	1978	34.700	9.220	28.8	127.01	706	1450	37.00	273.2
	TWIN IM5000 (AE)	1978	69.400	9.220	28.8	254.01	706	1450	37.00	273.2
	STIG-LM2500 (AE)	1986	25.400	9.000					37.91	
	STIG-LM5000 (AE)	1986	49.100	8.180					41.71	
	STIG-IM5000 (AE)	1986	50.900	7.850					43.46	

	Year	Power (MW)	Heat Rate (BTU/MW-h)	Press. Ratio	Mass flow (kg/s)	EGT (K)	TET (K)	Efficiency (%)	SPO (kW/kg/s)
JOHN BROWN ENGINEERING									
PG3002J (HD)	1949	10.200	13.500	7.2	52.16	799	1216	25.27	195.5
PG5001PA (HD)	1958	26.300	11.820	10.2	122.47	756	1230	28.86	214.7
PG6001B (HD)	1978	38.340	10.860	11.8	136.53	812	1377	31.42	280.8
PG7001EA (HD)	1976	83.340	10.500	12.4	290.75	803	1377	32.49	286.6
PG9001EA (HD)	1979	123.400	10.350	12.1	403.24	802	1377	32.96	306.0
PG7001F (HD)	1988	150.000	9.880	13.5	416.40	856	1533	34.53	360.2
PG9001F (HD)	1991	212.000	9.995	13.5	600.10	856	1533	34.14	353.3
LM2500PE (AE)	1978	21.100	9.790	18.7	66.68	789	1470	34.85	316.4
LM2500PE (AE)	1978	20.510	10.090	18.7	66.68	789	1470	33.81	307.6
LM5000PC (AE)	1983	33.100	9.720	30.0	122.92	722	1496	35.10	269.3
LM5000PC (AE)	1983	33.090	9 860	30.0	122.92	722	1496	34.60	269.2
LM6000-PA	1992	42.200	8.430	29.8	102.96	721	1491	40.47	409.8
PGLM6000	1992	41.500	8.650	29.5	125.19	725	1497	39.44	331.5
SB60 (HD)	1986	15.290	11.400	13.7	61.69	797	1373	29.93	247.9
KANIS ENERGIE									
G3142 (J) (HD)	1952	10.450	13.320	7.1	52.16	799	1216	25.61	200.3
G3142R (J) (recup) (HD)	1952	10.000	10.370	7.3	52.16	626	1227	32.90	191.7
PG5371 (PA) (HD)	1987	26.300	11.820	10.2	122.47	756	1230	28.86	214.7
PG6541 (B) (HD)	1987	38.340	10.860	11.8	136.53	812	1377	31.42	280.8
PG9171 (E) (HD)	1990	123.400	10.100	12.3	404.60	811	1377	33.78	305.0
KAWASAKI HEAVY INDUSTRIES									
S1A-02 (HD)	1978	0.200	21.840	9.0	1.77	793	1203	15.62	113.1
S1T-02 (HD)	1978	0.390	22.220	9.0	3.49	793	1203	15.35	111.7
S2A-01 (HD)	1979	0.660	16.370	9.0	4.72	768	1203	20.84	139.8
M1A-01 (HD)	1978	1.110	17.150	8.0	7.89	788	1173	19.89	140.6
M1A-03 (HD)	1982	1.390	16.450	9.0	9.12	818	1233	20.74	152.5
M1T-01 (HD)	1979	2.150	17.570	8.0	15.92	783	1173	19.42	135.0
M1T-03 (HD)	1982	2.680	16.810	9.0	18.10	813	1233	20.30	148.1
M1A-11 (HD)	1989	1.210	14.250	8.8	7.48	738	1173	23.94	161.7
M1A-13 (HD)	1989	1.490	13.870	8.7	7.39	828	1303	24 60	201.5
M1T-11 (HD)	1989	2.337	14.720	8.8	15.01	738	1173	23.18	155.7
M1T-13 (HD)	1989	2.898	14.320	8.7	14.79	828	1303	23.83	196.0
M1A-13CC (HD)	1989	1.277	16.480	7.8	7.12	838	1283	20.70	179.3
M1A-13CC (STIG) (HD)	1989	2.364	10.450	9.2	7.53	843	1283	32.65	314.0
KVAERNER EUREKA									
PG5371 (PA) (HD)	1987	26.300	11.820	10.2	122.47	756	1230	28.86	214.7
PG6541 (B) (HD)	1978	38.340	10.860	11.8	138.80	812	1377	31.42	276.2
PG9161 (E) (HD)	1987	116.900	10.310	12.1	409.14	802	1377	33.09	285.7
LM2500PE (AE)	1988	21.160	10.030	18.0	68.04	805	1487	34.02	311.0
LM5000 (AE)	1986	33.090	9.860	30.0	124.28	719	1490	34.60	266.2
LM6000-PA	1992	41.550	8.467	29.8	102.96	721	1491	40.30	403.5
MAN-GHH									
THM1203 (HD)	1971	5.348	14.883	7.6	34.47	793	1178	22.92	155.1
THM1304-9 (HD)	1980	8.899	12.229	10.0	44.91		1248	27.90	198.2
THM1304R-10 (recup) (HD)	1983	9 055	9.991	10.0	44.91		1273	34.15	201.6
FT8 (AE)	1990	25.420	8.950	20.1	84.37			38.12	301.3
FT8 TWIN (AE)	1990	51.100	8.905	20.1	168.74			38.31	302.8
MITSUBISHI HEAVY INDUSTRIES									
MF-61 (HD)	1989	5.925	11.915	15.0	27.22	769	1364	28.63	217.7
MF-111A (HD)	1985	12.610	11.250	13.0	47.63	820	1409	30.33	264.8
MF-111B (HD)	1985	14.570	10.020	15.0	53.52	803	1424	34.05	272.2
MF-221A (HD)	1992	26.000	10.905	13.0	97.98	817	1403	31.29	265.4
MF-221B (HD)	1992	30.000	10.665	15.0	113.40	799	1417	31.99	264.6
FM-451 (HD)	1992	46 410	10.360	14.0	146.06	827	1444	32.93	317.8
MW-251 (HD)	1964	36.860	11.790	12.0	156.94	790	1333	28.94	234.9
MW-501 (HD)	1980	104.570	10.260	14.0	359.24	794	1387	33.25	291.1
MW-701 (HD)	1981	130.550	10.070	14.0	444.52	786	1372	33.88	293.7
MW-701DA (HD)	1992	136.900	10.040	14.1	444.52	809	1415	33.98	308.0
501F (HD)	1989	153.200	9.670	14.0	427.74	851	1487	35.28	358.2
701F (HD)	1994	221.100	9.440	15.6	616.43	836	1495	36.14	358.7
701F2 (HD)	1995	253.700	9.200	17.0	667.00	852	1554	37.08	380.4
701G1 (HD)	1996	271.000	8.820	19.0	645.00	861	1585	38.68	420.2
701G2 (HD)	1996	308.000	8.750	21.0	741.00	847	1594	38.99	415.7
MITSUI ENGINEERING & SHIPBUILDING									
SB5 (HD)	1987	1.080	13.390	10.0	4.99	765	1240	25.48	216.5
SB15 (HD)	1986	2.630	13.160	10.6	14.06	755	1239	25.93	187.0
SB30 (HD)	1973	5.260	13.860	6.7	27.67	786	1200	24.62	190.1
SB60 (HD)	1981	12.490	11.530	12.1	55.34	729	1273	29.59	225.7
SB60 (HD)	1988	13.570	11.490	13.2	59.42	765	1319	29.69	228.4
SB90 (HD)	1969	14.610	13.820	6.2	77.56	783	1200	24.69	188.4
SB120 (HD)	1985	23.000	11.190	11.7	102.06	748	1273	30.49	225.4
NUOVO PIGNONE-TURBOTECNIA									
PGT2 (HD)	1989	2.000	13.650	12.0	9.98	811	1368	24.99	200.4
MS1002 (HD)	1972	4.820	13.640	8.2	24.49	801	1216	25.01	196.8
MS1002R (recup) (HD)	1972	4.610	10.495	8.3	24.49		1227	32.51	188.2
PGT10 (HD)	1986	9.980	10.665	14.0	41.28	735	1336	31.99	241.8
PGT10R (recup) (HD)	1986	9.620	10.040	14.2	41.28		1336	33.98	233.1
MS3002 (HD)	1952	10.450	13.330	7.1	52.16	800	1216	25.59	200.3
MS3002R (recup) (HD)	1952	10.000	10.370	7.5	52.16		1227	32.90	191.7
PGT16 (AE)	1989	13.170	9.727	21.5	45.36	766	1473	35.08	290.4
PGT25 (AE)	1981	21.640	9.648	18.7	68.04	801	1492	35.36	318.1
LM2500/30 (AE)	1988	22.360	9.685	18.7	68.04	801	1492	35.23	328.6
MS5001 (HD)	1958	26 830	11.700	10.2	123.83	755	1230	29.16	216.7
LM5000 (AE)	1988	33.760	9.543	30.0	122.02	719	1444	35.75	276.7
MS6001 (HD)	1978	38.980	10.790	11.5	137.89	810	1377	31.62	282.7
MS7001 (HD)	1988	83.500	10.475	12.4	291.20	803	1372	32.57	286.7
MS9001 (HD)	1976	123.400	10.240	11.6	410.05	811	1377	33.32	300.9

		Year	Power (MW)	Heat Rate (BTU/MW-h)	Press. Ratio	Mass flow (kg/s)	EGT (K)	TET (K)	Efficiency (%)	SPO (kW/kg/s)
OPRA BV										
	OP16 (HD)	1996	1.500	13.850	6.5	7.60	863	1272	24.63	197.4
PRATT & WHITNEY CANADA										
	ST6L-795 (AE)	1986	0.643	14.459	7.5	3.18	874	1277	23.60	202.5
	ST6L-813 (AE)	1976	0.782	13.892	8.5	3.81	851	1277	24.56	205.2
	SPW124-2 (AE)	1993	1.584	12.460	13.8	7.71	805	1423	27.38	205.4
	FT8 (AE)	1990	25.420	8.950	20.3	85.27	716	1359	38.12	298.1
	FT8 TWIN (AE)	1990	51.100	8.905	20.3	170.55	716	1359	38.31	299.6
	V84.2 (HD)	1988	103.200	10.220	10.7	349.26	813	1337	33.38	295.5
	V64.3 (HD)	1990	60.500	9.705	15.6	183.70	807	1444	35.16	329.3
	V84.4 (HD)	1993	150.300	9.535	16.1	416.40	836	1508	35.78	361.0
PRVNI BRNENSKA STROJIRNA										
	GTG-250C (HD)	1993	2.850	11.750	12.0	12.70	703	1206	29.04	224.4
	GT6.5-C (recup) (HD)	1988	6.500	10.970	4.6	52.62	542	1073	31.10	123.5
	GTG8 (recup) (HD)	1993	9.160	10.150	5.2	51.71	784	1122	33.61	177.1
ROLLS-ROYCE										
	AVON (AE)	1964	14.420	12.030	9.2	77.56	714	1149	28.36	185.9
	RB211 (AE)	1974	24.940	9 575	20.0	89.81	739	1437	35.63	277.7
	Trent	1997	51.190	8.210	35.0	158.90	701	1504	41.56	322.2
SIEMENS KWU										
	V64.3 (HD)	1988	60.500	9.705	15.6	183.70	807	1444	35.16	329.3
	V84.2 (HD)	1985	103.200	10.220	10.7	349.26	813	1337	33.38	295.5
	V84.3 (HD)	1991	139.000	9.555	15.6	412.77	807	1444	35.71	336.8
	V94.2 (HD)	1974	150.200	10.210	10.7	498 95	818	1346	33.42	301.0
	V94.3 (HD)	1992	200.000	9 555	15.6	594.20	807	1444	35.71	336.6
	V94.3A (HD)	1996	240.000	8.980	16.6	640.00	835	1515		
SOLAR GT										
	SATURN T1500 (HD)	1960	1.080	14.785	6.7	6.40	772	1146	23.08	168.9
	SATURN (recup) (HD)	1984	0.890	11.310	6.5	6.30	569		30.17	141.2
	CENTAUR (recup) (HD)	1984	2.550	11.515	8.3	17.64	586		29.63	144.5
	CENTAUR T-4500 (HD)	1985	3.130	12.945	.9.4	17.55	722	1154	26.36	178.3
	CENTAUR TYPE H (HD)	1985	3.880	12.200	9.3	17.46	789	1257	27.97	222.2
	CENTAUR TAURUS (HD)	1989	4.370	12.200	11.0	20.87	772	1278	27.97	209.4
	MARS (HD)	1977	8.840	10.980	15.7	37.47	739	1323	31.07	235.9
	TAURUS 70 (HD)	1995	6.300	10.900	15.0	25.50	761	1350	31.30	247.1
	MARS 90 (HD)	1995	9.290	10.765	16.2	39.20	737	1330	31.69	237.0
	MARS 100 (HD)	1996	10.690	10.515	17.1	41.60	761	1390	32.45	257.0
SOVIET UNION										
	GTNR-10 (recup) (HD)	1975	11.000	10.500	4.8	84.82		1103	32.49	129.7
	GTNR-12 (recup) (HD)	1991	12.500	10.470	5.3	90.26		1123	32.59	138.5
	GTN-16	1983	16.800	11.570	11.5	84 82	703	1193	29.49	198.1
	GTE-32	1990	30.000	11.770	12.5	169.64	673	1173	28.99	176.8
	GTN-25	1982	29.300	11.770	12.5	161.48	733	1248	28.99	181.4
	GTN-25A	1990	25 500	9.750	25.0	95.71	696	1473	34.99	266.4
	GTE-45	1993	45 000	11.380	17.0	247.66		1263	29.98	181.7
	GTE-60	1995	60.000	10.340	18.0	247.66		1423	33.00	242.3
	GTG-35 (HD)	1969	32.000	13.760	7.8	219.54	673	1043	24.80	145.8
	GTG-45 (HD)	1989	54.000	12.190	7.8	270.34	738	1173	27.99	199.7
	GTE-115 (HD)	1993	114.000	10.340	12.3	394.17	788	1413	33.00	289.2
	GTE-100 (HD)	1969	105.000	11.975	13.0	469.01	673	1190	28.49	223.9
	GTE-150 (HD)	1989	128.000	11.190	13.0	634 57	696	1223	30.49	201.7
	GTE-150 (HD)	1990	157.000	11.010	13.0	628.68	803	1355	30.99	249.7
	GTE-200 (HD)	1995	185.000	10.470	15.6	628.68	818	1523	32.59	294.3
STEWART & STEVENSON										
	TG-831	1967	0.515	16.216	11.0	3.58	772	1236	21.04	143.7
	TG-501 KB (AE)	1962	3.224	12.628	9.3	15.65	797	1255	27.02	206.0
	TG-501-KB5 (AE)	1981	3.693	12.018	9.3	15.65	806	1308	28.39	236.0
	TG-571 K (AE)	1985	5.588	10.650	12.7	20.05	806	1378	32.04	278.7
	TG-1600 (AE)	1987	13.427	9.554	22.5	45.81	755	1467	35.71	293.1
	TG-1600 STIG 50 (AE)	1990	16.900	8.472	22.5	53.52	710	1273	40.27	315.7
	TG-2500-33 (AE)	1973	22.236	9.401	18.7	68.04	801	1492	36.29	326.8
	TG-2500 STIG (AE)	1986	26.466	8.532	18.7	73.94	777	1343	39.99	358.0
	TG-5000 PC (AE)	1987	33.762	9.348	28.8	122.02	719	1477	36.50	276.7
	TG-6000 PA (AE)	1991	42.400	8.300	29.5	126.55	723	1493	41.11	335.0
	TG-5000 STIG 80 (AE)	1986	46.890	8.174	28.8	149.23	686	1292	41.74	314.2
	TG-5000 STIG 120 (AE)	1986	51.620	7.907	28.8	157.40	680	1281	43.15	328.0
SULZER-ESCHER WYSS										
	3, (HD)	1976	6.500	12.055	10.0	33.11	740	1243	28.30	196.3
	R3 (recup) (HD)	1976	6.040	10.264	9.9	33.11	638	1243	33.24	182.4
	7, (HD)	1970	11.000	13.650	7.5	63.50	758	1198	24.99	173.2
	R7 (recup) (HD)	1970	10.600	10.800	7.7	63.50	609	1198	31.59	166.9
THOMASSEN INTERNATIONAL										
	PG3142 (J) (HD)	1949	10.230	13.480	7.1	51.71	801	1216	25.31	197.8
	G3142 (J) (recup) (HD)	1951	10.000	10.370	7.3	52.16	626	1227	32.90	191.7
	G5261 (R) (HD)	1958	19.400	13.260	8.1	96.61	786	1211	25.73	200.8
	PG5371 (PA) (HD)	1961	26.300	11.820	10.2	122.47	756	1230	28.86	214.7
	PG6541 (B) (HD)	1981	38.340	10.860	11.5	136.53	816	1377	31.42	280.8
	PG9171 (E) (HD)	1979	123 400	10.100	12.1	410.05	811	1393	33.78	300.9

	Year	Power (MW)	Heat Rate (BTU/MW-h)	Press. Ratio	Mass flow (kg/s)	EGT (K)	TET (K)	Efficiency (%)	SPO (kW/kg/s)
THOMASSEN STEWART & STEVENSON INT									
LM1600 (AE)	1988	13.420	9.563	22.5	45.36	760	1476	35.68	295.9
LM1600 STIG 30 (AE)	1991	17.600	8.338	22.5	45.36			40.92	388.0
LM2500 PE (AE)	1973	21.450	9.700	18.7	68.49	802	1494	35.17	313.2
LM2500 PE (AE)	1973	22.235	9.400	18.7	68.04	801	1492	36.30	326.8
LM2500 STIG 40 (AE)	1986	24.920	9 003	18.7	74.39	767	1326	37.90	335.0
LM2500 STIG 40 (AE)	1986	26.835	8.573	18.7	74.39	777	1343	39.80	360.7
LM5000 PC (AE)	1984	33.555	9.530	28.8	125.64	717	1472	35.80	267.1
LM5000 PC (AE)	1984	33.760	9.347	28.8	122.02	719	1476	36.50	276.7
LM5000 STIG 80 (AE)	1986	44.595	8.510	28.8	149.68	687	1294	40.09	297.9
LM5000 STIG 80 (AE)	1986	46.890	8.173	28.8	149.23	686	1292	41.74	314.2
LM5000 STIG 120 (AE)	1986	48.105	8.215	28.8	157.40	676	1273	41.53	305.6
LM5000 STIG 120 (AE)	1986	51.620	7.907	28.8	157.40	680	1281	43.15	328.0
LM6000 (AE)	1991	41.370	8.510	28.0	126.55	723	1475	40.09	326.9
LM6000 (AE)	1991	42.230	8.335	28 0	126.55	723	1475	40.93	333.7
TOSHIBA CORP									
PG9151 (HD)	1982	112.000	10.600	11.8	401.43	801	1366	32.19	279.0
TURBOMECA									
ASTAZOU (AE)	1972	0.300	18.940	5.6	2.54	763	1088	18.01	118.1
BASTAN VI (AE)	1968	0.560	17.870	5.5	4.35	773	1098	19.09	128.6
BASTAN VII (AE)	1972	0.800	15.980	7.2	5.99	723	1090	21.35	133.6
MAKILA TI (AE)	1988	1.050	13.410	9.6	5.44	778	1249	25.44	192.9
TURBO POWER									
FT8 (AE)	1990	25.420	8.950	20.3	85.27	716	1433	38.12	298.1
FT8 TWIN (AE)	1990	51.100	8.905	20.3	170.55	716	1433	38.31	299.6
V64.3 (HD)	1990	60.500	9.705	15.6	183.70	807	1444	35.16	329.3
V84.2 (HD)	1988	103.200	10.220	10.7	349.26	813	1337	33.38	295.5
V84.4 (HD)	1993	150.300	9.535	16.1	416.40	836	1506	35.78	361.0
US TURBINE CORP									
UST700 (HD)	1979	0.661	16.490	9.0	4.63	772	1213	20.69	142.9
UST1100 (HD)	1978	1.112	17.176	8.0	7.89	788	1183	19.86	140.9
UST1200 (recup) (HD)	1989	1.206	14.262	8.0	7.44	738	1283	23.92	162.1
UST1400 (HD)	1982	1.392	16.451	9.0	8.98	822	1243	20.74	155.0
UST1500 (HD)	1989	1.491	13.883	8.7	7.35	828	1283	24.58	202.9
UST2200 (HD)	1979	2.148	17.598	8.0	15.78	782	1183	19.39	136.1
UST2400 (HD)	1989	2.337	14.720	8 8	14.92	738	1283	23.18	156.6
UST2700 (HD)	1982	2.680	16.828	9.0	18.01	814	1233	20.27	148.8
UST3000 (HD)	1989	2.898	14.320	8.7	14.74	828	1283	23.83	196.6
UST3400 (HD)	1962	3.307	12.668	9.3	15.47	798	1255	26.93	213.8
UST3800 (HD)	1982	3.923	12.161	9.3	15.69	835	1330	28.06	250.0
UST4600 (HD)	1979	4.612	12.195	12.1	18.60	837	1415	27.98	248.0
UST5700 (HD)	1986	5.588	10.650	12.7	19.64	807	1379	32.04	284.5
UST2500CC (steam inj) (HD)	1988	2.365	10.450	9.4	7.12	842	1283	32.65	332.1
UST5600CC (steam inj) (HD)	1986	5.554	8.944	17.1	15.78	769	1255	38.15	351.9
UST12000 (HD)	1986	12.760	11.210	12.8	48.08	818	1523	30.44	265.4
UST15000 (HD)	1987	14.730	10.980	14.7	55.79	801	1523	31.07	264.0
UST18000 (steam inj) (HD)	1988	16 880	9.955	16.1	48.08	826	1523	34.27	351.1
WESTINGHOUSE ELECTRIC									
RB211	1984	27.240	9.575	21.0	91.90	765	1463	35.63	296.4
Trent	1997	51.190	8.210	35.0	158.90	701	1504	41.56	322.2
CW251B12 (HD)	1982	46.500	10.550	15.3	173.27	783	1395	32.34	268.4
W501D5 (HD)	1975	104.400	10.290	14.2	358.79	794	1391	33.16	291.0
501F (HD)	1989	152.800	9.700	14.0	427.74	851	1487	35.17	357.2
701D (HD)	1992	144.210	10.064	14.0	474.50	770	1345	33.90	303.9
501G (HD)	1994	235.250	8.740	19.2	553.40	863	1617	39.04	425.1
701F (HD)	1994	251.100	9.212	16.2	658.90	931	1680	37.04	381.1

TABLE 1.2: COMBINED AND STEAM INJECTED GAS TURBINE CYCLES

		Year	Power (MW)	Heat Rate (BTU/MW hr)	ress. Ratio	EGT (K)	TET (K)	SC Efficiency (%)	CC Efficiency (%)	GT Power (MW)	ST Power (MW)	TURBINE
ABB												
	KA M-1 (HD)	1989	12.600	7.668	16.0	739	1330	31.04	44.49	8.600	4.000	One MARS
	KAM-2 (HD)	1989	25.300	7.633	16.0	739	1330	31.04	44.70	17.200	8.100	Two MARS
	KA 35-1 (HD)	1989	25.300	7.737	12.0	647	1171	31.98	44.10	17.800	7.500	One GT 35
	KA 35-2 (HD)	1989	51.000	7.685	12.0	647	1171	31.98	44.40	35.600	15.400	Two GT 35
	KA 10-1 (HD)	1989	31.300	7.183	13.6	790	1371	32.59	47.50	20.800	10.500	One GT 10
	KA 10-2 (HD)	1989	63.300	7.094	13.6	790	1371	32.59	48.09	41.600	21.700	Two GT 10
	KA 8-1 (HD)	1983	70.100	7.183	16.3	796	1438	31.59	47.50	45.300	24.800	One GT 8
	KA 8-2 (HD)	1983	141.300	7.123	16.3	796	1438	31.59	47.90	90.600	50.700	Two GT 8
	KA 8-3 (HD)	1983	212.800	7.094	16.3	796	1438	31.59	48.09	135.900	76.900	Three GT 8
	KA 8-4 (HD)	1983	284.200	7.079	16.3	796	1438	31.59	48.20	181.200	103.000	Four GT 8
	KA 11N-1 (HD)	1987	121.100	7.035	12.4	788	1339	32.01	48.50	78.100	43.000	One GT11-N
	KA 11N-2 (HD)	1987	244.500	6.978	12.4	788	1339	32.01	48.89	156.200	88.300	Two GT11-N
	KA 11N-3 (HD)	1987	367.800	6.949	12.4	788	1339	32.01	49.10	234.300	133.500	Three GT11-N
	KA 11N-4 (HD)	1987	491.400	6.935	12.4	788	1339	32.01	49.20	312.400	179.000	Four GT11-N
	KA 13-1 (HD)	1981	144.200	7.094	12.5	762	1298	32.01	48.09	94.000	50.200	One GT13
	KA 13-2 (HD)	1981	289.900	7.064	12.5	762	1298	32.01	48.30	188.000	101.900	Two GT13
	KA 13-3 (HD)	1981	434.900	7.064	12.5	762	1298	32.01	48.30	282.000	152.900	Three GT13
	KA 13-4 (HD)	1981	581.100	7.050	12.5	762	1298	32.01	48.39	376.000	205.100	Four GT13
	KA 13E-1 (HD)	1983	213.800	6.743	13.9	789	1376	34.64	50.60	142.100	71.700	One GT 13E
	KA 13E-2 (HD)	1983	429.300	6.717	13.9	789	1376	34.64	50.79	284.200	145.100	Two GT 13E
	KA 26-1 SS (HD)	1996	366.000	5.830	30.0	883		38.21	58.52	232.600	133.400	One GT26
	KA 26-2 (HD)	1996	732.000	5.830	30.0	883		38.21	58.52	465.200	266.800	Two GT26
	KA 24-1 SS (HD)	1996	248.300	5.940	30.0	883		37.91	57.44	159.500	88.800	One GT24
	KA 24-2 (HD)	1996	498.500	5.940	30.0	883		37.91	57.44	319.000	179.500	Two GT24
ALSTHOM TURBINES A GAZ												
	VEGA 105PA (HD)	1976	38.200	8.140	10.2	756	1230	28.86	41.91	25.700	12.500	One PG5371PA
	VEGA 205PA (HD)	1976	77.100	8.066	10.2	756	1230	28.86	42.30	50.600	26.500	Two PG5371PA
	VEGA 106B (HD)	1978	56.500	7.370	11.8	813	1377	31.42	46.29	37.500	19.000	One PG6541B
	VEGA 206B (HD)	1978	116.000	7.185	11.8	813	1377	31.42	47.49	75.000	41.000	Two PG6541B
	VEGA 109E (HD)	1978	174.000	6.910	12.5	802	1377	33.09	49.37	114.900	59.100	One PG9161E
	VEGA 209E (HD)	1978	352.400	6.825	12.5	802	1377	33.09	49.99	229.800	122.600	Two PG9161E
	VEGA 109F (HD)	1987	319 000	6.640	13.5	856	1533	34.14	51.38	208.400	111.100	One PG9281F
	VEGA 209F (HD)	1987	641.500	6.615	13.5	856	1533	34.14	51.58	416.800	224.700	Two PG9281F
	VEGA 109FA (HD)	1995	355.800	6.514	15.0	862	1561	35.65	52.38	224.400	131.400	One PG9331FA
	VEGA 209FA (HD)	1995	714.100	6.489	15.0	862	1561	35.65	52.58	448.800	265.700	Two PG9331FA
ANSALDO												
	COBRA 1.64.3 (HD)	1989	92.666	6.613	16.1	804	1449	35.30	51.59	60.666	32.000	One V64.3
	COBRA 2.64.3 (HD)	1989	186.000	6.545	16.1	804	1449	35.30	52.13	122.000	64.000	Two V64.3
	COBRA 1.64.3A (HD)	1995	103.500	6.331	16 6	838	1520	36.80	53.89	67.500	36.000	One V64.3A
	COBRA 2.64.3A (HD)	1995	211.000	6.183	16.6	838	1520	36.80	55.18	135.000	76.000	Two V64.3A
	COBRA 1.94.2 (HD)	1977	243.000	6.525	11.0	813	1346	34.50	52.29	154.000	89.000	One V94.2
	COBRA 2.94.2 (HD)	1977	486 000	6.505	11.0	813	1346	34.50	52.45	308.000	178.000	Two V94.2
	COBRA 3.94.2 (HD)	1977	731.480	6.490	11.0	813	1346	34.50	52.57	462.000	269.000	Three V94.2
	COBRA 1.94.3A (HD)	1996	358.000	5.965	16.6	835	1515	37.99	57.20	233.000	125.000	One V94.3A
	COBRA 2.94.3A (HD)	1996	715.000	5.985	16.6	835	1515	37.99	57.01	466.000	249.000	Two V94.3A
EBARA												
	FT8 (AE)	1990	32.280	7.010	20.3	716	1359	38.12	48.67	24.700	7.580	One FT8
	FT8 Twin (AE)	1990	65.310	6 930	20.3	716	1359	38.12	49.23	49.660	15.650	Two FT8
	FT8TPx2 (AE)	1993	130 620	6.930	20.3	716	1359	38.12	49.23	99.400	31.220	Four FT8
FIAT												
	CC 100 (HD)	1985	120.000	7.370	14.0	775	1353	32.19	46.29	82.000	38.000	Two TG 20
	CC 200 (HD)	1985	364.000	7.055	14.0	767	1340	33.85	48.36	248.000	116.000	Two TG 50
	CC30 (AE)	1987	31.670	6.561	18.0	805	1487	34.02	52.00	21.210	10.460	One LM2500
	CC50 (AE)	1992	53.800	6.467	29.8	721	1491	40.30	52.76	39.200	14.600	One LM6000
	CC130 (HD)	1992	127.290	6.985	14.0	775	1353	32.19	48.84	77.220	50.070	Two TG.20B7/8
	CC140 (HD)	1989	152.140	6.697	14.5	784	1368	32.97	50.95	97.090	55.050	Two TG.20B11/12
	CC400 (HD)	1989	406.890	6.782	14.0	767	1340	33.85	50.31	272.020	134.850	Two TG.50D5
	CC430 (HD)	1993	428.680	6.753	14.5	778	1357	34.71	50.52	285.540	143.140	Two TG.50D5S
	CC760 (HD)	1996	765.200	6.005	15.6	836	1495	36.14	56.82	497.530	267.670	Two 701F
GE POWER GENERATION												
	S-106B (HD)	1987	56.500	7.370	11.8	812	1377	31.42	46.29			One MS6001B
	S-206B (HD)	1979	115.900	7.190	11.8	812	1377	31.42	47.45			Two MS6001B
	S-406B (HD)	1979	233.500	7.130	11.8	812	1377	31.42	47.85			Four MS6001B
	S-107EA (HD)	1977	123.500	7.090	12.4	803	1377	32.49	48.12			One MS7001EA
	S-207EA (HD)	1979	249.000	7.030	12.4	803	1377	32.49	48.53			Two MS7001EA
	S-109E (HD)	1979	180 300	6.910	12.1	802	1377	32.96	49.37			One MS9001E
	S-209E (HD)	1979	363.100	6.860	12.1	802	1377	32.96	49.73			Two MS9001E
	S-107F (HD)	1987	222.000	6.670	13.5	856	1533	34.53	51.15			One MS7001F
	S-207F (HD)	1987	445.700	6.650	13.5	856	1533	34.53	51.31			Two MS7001F
	S-109F (HD)	1987	318.600	6.660	13.5	856	1533	34.14	51.23			One MS9001F
	S-109G (HD)	1996	420.000	5.885	13.7	860	1540	35.60	57.97			One MS9001G
	S-109H (HD)	1997	480.000	5.690	14.2	882	1560	37.30	59.96			One MS9001H
	S-107G (HD)	1996	350.000	5.885	13.7	860	1540	35.50	57.97			One MS7001G
	S-107H (HD)	1997	400.000	5.690	14.2	882	1560	37.20	59.96			One MS7001H
	S-225 (HD)	1979	58.400	7.140	18.4	801	1487	36.28	47.78			Two LM2500PE
	S-225 (HD)	1979	57.700	7.210	18.6	802	1493	35.36	47.32			Two LM2500PE
	S-425 (HD)	1979	117.800	7.070	18.4	801	1487	36.28	48.26			Four LM2500PE
	S-425 (HD)	1979	115.700	7.140	18.6	802	1493	35.36	47.78			Four LM2500PE
	S-160 (HD)	1992	53.300	6.721	29.8	721	1491	40.47	50.76			One LM6000
	S-250 (HD)	1983	88.400	7.270	25.3	719	1433	36.51	46.93			Two LM5000PA
	S-250 (HD)	1983	88.500	7.370	26.0	716	1437	35.98	46.29			Two LM5000PA
	S-450 (HD)	1983	177.500	7.240	25.3	719	1433	36.51	47.12			Four LM5000PA
	S-450 (HD)	1983	177.700	7.340	26.0	716	1437	35.98	46.48			Four LM5000PA

		Year	Power (MW)	Heat Rate (BTU/MW hr)	ress. Ratio	EGT (K)	TET (K)	SC Efficiency (%)	CC Efficiency (%)	GT Power (MW)	ST Power (MW)	TURBINE
GE POWER GENERATION (cont)												
	LM2500 PE STIG (AE)	1986	24.790	9.200	18.4	801	1487	36.28	37.08			One LM2500PE
	LM2500 PE STIG (AE)	1986	23.740	9.480	18.6	802	1493	35.36	35.99			One LM2500PE
	LM2500 PH STIG (AE)	1986	26.560	8 880	20.0	804	1497	34.89	38.42			One LM2500PH
	LM2500 PH STIG (AE)	1986	25.040	9.150	20.0	805	1499	34.02	37.29			One LM2500PH
	LM5000PD STIG (AE)	1986	51.370	8.080	32.3	719	1433	36.51	42.23			One LM2500PD
	LM5000PD STIG (AE)	1986	47.510	8.370	32.0	716	1437	35.98	40.76			One LM2500PD
HITACHI												
	2025 (HD)	1988	69.130	7.148				32.31	47.73	44.860	24.270	Two H-25
	206B (HD)	1986	115.860	7.168	11.8	812	1377	31.42	47.60	76.120	39.740	Two MS6001B
	107EA (HD)	1989	122.970	7.072	12 4	803	1377	32.49	48.24	81.320	41.650	One MS7001E
	207EA (HD)	1989	247.560	7.028	12.4	803	1377	32.49	48.55	162.640	84.920	Two MS7001E
	307EA (HD)	1990	371.980	7.017	12.4	803	1377	32.49	48.62	243.960	128.020	Three MS7001E
	407EA (HD)	1992	498.250	6.985	12.4	803	1377	32.49	48.84	325.280	172.970	Four MS7001E
	109E (HD)	1986	172.200	7.246	12.1	802	1377	32.96	47.09	113.930	58.270	One MS9001E
	209E (HD)	1986	346.640	7.201	12.1	802	1377	32.96	47.38	227.860	118.780	Two MS9001E
	309E (HD)	1986	519.830	7.201	12.1	802	1377	32.96	47.38	341.790	178.040	Three MS9001E
INTERNATIONAL POWER TECHNOLOGY												
	CHENG S7 (HD)	1981	5.500	8.911					38.29			One
	CHENG S5 (HD)	1987	1.900	12.000					28.43			One
ISHIKAWAJIMA-HARIMA HEAVY INDUSTRIES												
	STIG LM1600 (AE)	1988	16.500	8.680	22.0	755	1459	36.00	39.31			One LM1600
	STIG LM2500 (AE)	1986	25.400	9.000	20.0	801	1487	36.28	37.91			One LM2500
	STIG IM5000 (AE)	1986	49.100	8.180	32.0	716	1437	35.98	41.71			One LM5000
	STIG IM5000 (AE)	1986	50.900	7.850	32.3	719	1433	36.51	43.46			One LM5000
JOHN BROWN ENGINEERING												
	Scotstag 103J (HD)	1979	14.500	9.180	7.2	799	1216	25.27	37.17	9.800	5.200	One PG3002J
	Scotstag 105P (HD)	1978	38.050	8.156	10.2	756	1230	28.86	41.83	25.248	12.802	One PG5001P
	Scotstag 205P (HD)	1980	77.000	8.061	10.2	756	1230	28.86	42.32	50.496	26.504	Two PG5001P
	Scotstag 106B (HD)	1980	55.900	7.447	11.8	812	1377	31.42	45.81	36.806	19.094	One PG6001B
	Scotstag 206B (HD)	1981	113.300	7.349	11.8	812	1377	31.42	46.43	73.613	39 687	Two PG6001B
	Scotstag 306B (HD)	1980	170.000	7.347	11.8	812	1377	31.42	46.44	110.419	59.581	Three PG6001B
	Scotstag 406B (HD)	1981	228.500	7.286	11.8	812	1377	31.42	46.83	147.226	81.274	Four PG6001B
	Scotstag 107E (HD)	1980	122.700	7.103	12.4	803	1377	32.49	48.03	80.006	42.694	One PG7001E
	Scotstag 207E (HD)	1981	247.350	7.048	12.4	803	1377	32.49	48.41	160.013	87.337	Two PG7001E
	Scotstag 307E (HD)	1980	373.000	7.010	12.4	803	1377	32.49	48.67	240.019	132.981	Three PG7001E
	Scotstag 109E (HD)	1980	172.500	6.973	12.1	802	1377	32.96	48.93	118 464	54.036	One PG9001E
	Scotstag 209E (HD)	1980	346.700	6.939	12.1	802	1377	32.96	49.17	236.928	109.772	Two PG9001E
KANIS ENERGINE												
	K COM 131 (HD)	1952	15.440	8.923	7.1	799	1216	25.61	38.24	9.970	5.760	One G3142(J)
	K COM 105PA (HD)	1976	38.200	8.140	10.2	756	1230	28.86	41.91	25.700	12.500	One PG5371PA
	K COM 205PA (HD)	1976	77.100	8.066	10.2	756	1230	28.86	42.30	50.600	26.500	Two PG5371PA
	K COM 106B (HD)	1978	56.500	7.370	11.8	812	1377	31.42	46.29	37.500	19.000	One PG6541B
	K COM 206B (HD)	1978	116.000	7.185	11.8	812	1377	31.42	47.49	75.000	41.000	Two PG6541B
	K COM 109E (HD)	1978	174.000	6.910	12.1	802	1377	33.09	49.37	114.900	59.100	One PG9161E
	K COM 209E (HD)	1978	352.400	6.825	12.1	802	1377	33.09	49.99	229.800	122.600	Two PG9161E
	K COM 109F (HD)	1987	319.500	6.640	13.5	856	1533	34.14	51.38	208.400	111.100	One PG9281F
	K COM 209F (HD)	1987	641.500	6.615	13.5	856	1533	34.14	51.58	418.800	224.700	Two PG9281F
KVAERNER EUREKA												
	S-106B (HD)	1987	57.420	7.250	11.5	810	1377	31.62	47.06			One MS6001B
	S-206B (HD)	1979	116.600	7.140	11.5	810	1377	31.62	47.78			Two MS6001B
	S-109B (HD)	1979	171.100	7.050	11.6	811	1377	33.32	48.39			One MS9001E
	S-209B (HD)	1979	34.464	7.000	11.6	811	1377	33.32	48.74			Two MS9001E
	S-107F (HD)	1987	218.910	6.690	13.5	856	1533	34.53	51.00			One MS7001F
	S-109F (HD)	1987	303.000	6.690	13.5	856	1533	34.14	51.00			One MS9001F
	S-225 (AE)	1979	57.000	7.280	18.7	789	1470	34.85	46.87			Two LM2500 PE
	S-250 (AE)	1983	84.600	7.560	30.0	722	1496	35.10	45.13			Two LM5000 PC
MAN GHH												
	THM 1304 (HD)	1990	25.970	8.086	10.0		1248	27.90	42.19			One THM 1304
	FT8 (AE)	1990	32.280	7.010	20.1	716	1359	38.12	48.67	24.700	7.580	One FT8
	FT8 Twin (AE)	1990	65.310	6.930	20.1	716	1359	38.12	49.23	49 660	15.650	Two FT8
MITSUBISHI HEAVY INDUSTRIES												
	MPCP1 (501D) (HD)	1981	144.000	7.260	14.0	794	1387	33.25	46.99	98.700	45.300	One MW-501D
	MPCP2 (501D) (HD)	1981	289.900	7.215	14.0	794	1387	33.25	47.29	197.400	92.500	Two MW-501D
	MPCP3 (501D) (HD)	1981	435.500	7.200	14.0	794	1387	33.25	47.39	296.100	139.400	Three MW-501D
	MPCP4 (501D) (HD)	1981	581.000	7.200	14.0	794	1387	33.25	47.39	394.800	186.200	Four MW-501D
	MPCP1 (701D) (HD)	1981	175.800	7.390	14.0	786	1372	33.88	46.17	119.600	56.200	One MW-701D
	MPCP2 (701D) (HD)	1981	353.400	7.360	14.0	786	1372	33.88	46.36	239.200	114.200	Two MW-701D
	MPCP3 (701D) (HD)	1981	530.900	7.350	14.0	786	1372	33.88	46.42	358.800	172.100	Three MW-701D
	MPCP4 (701D) (HD)	1981	708.200	7.340	14.0	786	1372	33.88	46.48	478.400	229.800	Four MW-701D
	MPCP1 (501F) (HD)	1989	222.000	6.645	14.0	851	1487	35.28	51.34			One 501F
	MPCP2 (501F) (HD)	1989	447.000	6.600	14.0	851	1487	35.28	51.69			Two 501F
	MPCP3 (501F) (HD)	1989	674.000	6.565	14.0	851	1487	35.28	51.97			Three 501F
	MPCP1 (701F) (HD)	1996	341.000	6.410	16.2	842	1497	37.04	53.23	232.500	108.500	One 701F
	MPCP2 (701F) (HD)	1996	685.000	6.380	16.2	842	1497	37.04	53.48	465.000	220.000	Two 701F
	MPCP3 (701F) (HD)	1996	1031.000	6.360	16.2	842	1497	37.04	53.64	697.500	333.500	Three 701F
	MPCP1 (501G) (HD)	1996	345.000	5.884	19.2	863	1593	39.04	57.98	230.000	115.000	One 501G
	MPCP2 (501G) (HD)	1996	690.000	5.884	19.2	863	1593	39.04	57.98	460.000	230.000	Two 501G

	Year	Power (MW)	Heat Rate (BTU/MW hr)	ress. Ratio	EGT (K)	TET (K)	SC Efficiency (%)	CC Efficiency (%)	GT Power (MW)	ST Power (MW)	TURBINE
MITSUI ENGINEERING & SHIPBUILDING											
SB30 (HD)	1985	7.700	8.968	6.7	786	1200	24.62	38.04	5.060	2.640	One SB30
SB60 (HD)	1985	17.650	8.230	12.1	729	1273	29.59	41.46	12.270	5.380	One SB60
SB90 (HD)	1985	24.200	8.706	6.2	783	1200	24.69	39.19	14.680	9.520	One SB90
SB120 (HD)	1985	32.810	8.048	11.7	748	1273	30.49	42.39	22.340	10.470	One SB120
NUOVO PIGNONE-TURBOTECNICA											
CC-210 (HD)	1988	27.500	7.765	14.0	735	1336	31.99	43.94	19.000	9.300	Two PGT10
CC-205 (HD)	1981	80.000	7.765	10.2	755	1230	29.16	43.94	51.400	29.600	Two MS5001
CC-106 (HD)	1989	56.500	7.348	11.5	810	1377	31.62	46.43	37.900	19.500	One MS6001
CC-206 (HD)	1981	116.000	7.193	11.5	810	1377	31.62	47.43	75.800	42.000	Two MS6001
CC-109 (HD)	1989	180.000	6.973	11.6	811	1377	33.32	48.93	121.000	62.000	One MS9001E
CC-209 (HD)	1981	360.000	6.833	11.6	811	1377	33.32	49.93	242.000	150.000	Two MS9001E
PRATT & WHITNEY CANADA											
FT8 (AE)	1990	32.280	7.010	20.3	716	1359	38.12	48.67	24.700	7.580	One FT8
FT8 Twin (AE)	1990	65.310	6.930	20.3	716	1359	38.12	49.23	49.660	15.650	Two FT8
V84.2 (HD)	1988	153.000	6.705	10.7	813	1337	33.38	50.88	99.000	56.000	One V84.2
V64.3 (HD)	1990	86.000	6.640	15.6	807	1444	35.16	51.38	58.500	29.000	One V64.3
ROLLS-ROYCE INDUSTRIAL POWER SYSTEM											
1xRB211 (AE)	1989	37.500	7.014	20.0	739	1397	35.63	48.64	26.500	11.000	One RB211
2xRB211 (AE)	1989	75.100	7.000	20.0	739	1397	35.63	48.74	52.900	22.200	Two RB211
1xTrent (AE)	1996	64.000	6.606	35.0	701	1504	41.56	51.65	49.600	14.400	One Trent
2xTrent (AE)	1996	129.200	6.600	35.0	701	1504	41.56	51.69	99.200	30.000	Two Trent
SIEMENS/KWU											
GUD 2.64.3 (HD)	1989	177.000	6.590	15.6	807	1444	35.16	51.77	117.000	63.000	Two V64.3
GUD 3.64.3 (HD)	1989	267.000	6.550	15.6	807	1444	35.16	52.09	175.500	96.000	Three V64.3
GUD 4.64.3 (HD)	1989	358.000	6 510	15.6	807	1444	35.16	52.41	234.000	130.000	Four V64.3
GUD 1.84.2 (HD)	1987	155.000	6.705	10.7	813	1337	33.38	50.88	99.000	59.000	One V84.2
GUD 2.84.2 (HD)	1987	313.000	6.665	10.7	813	1337	33.38	51.19	198.000	120.000	Two V84.2
GUD 3.84.2 (HD)	1987	472.000	6.625	10.7	813	1337	33.38	51.50	297.000	183.000	Three V84.2
GUD 1.94.2 (HD)	1977	227.000	6.680	15.6	818	1346	33.42	51.07	144.000	87.000	One V94.2
GUD 2.94.2 (HD)	1977	457.000	6.640	15 6	818	1346	33.42	51.38	288.000	177.000	Two V94.2
GUD 3.94.2 (HD)	1977	690.000	6 600	15 6	818	1346	33.42	51.69	432.000	269.000	Three V94.2
GUD 1S.64.3A (HD)	1994	101.000	6.355	16.6	838	1520	36.80	53.69	67.500	33.500	One V64.3A
GUD 2.64.3A (HD)	1994	205.000	6.260	16.6	838	1520	36.80	54.50	135.000	70.000	Two V64.3A
GUD 1S.84.3A (HD)	1995	250.000	5.985	16.5	835	1513	37.99	57.01	163.500	86.500	One V84.3A
GUD 2.84.3A (HD)	1995	499.000	5.995	16.5	835	1513	37.99	56.91	327.000	172.000	Two V84.3A
GUD 1S.94.3A (HD)	1996	354 000	5.965	16.6	835	1515	37.99	57.20	231.000	123.000	One V94.3A
GUD 2S.94.3A (HD)	1996	705.000	5.985	16.6	835	1515	37.99	57.01	462.000	243.000	Two V94.3A
SOLAR TURBINES											
Centaur CC (HD)	1981	4.160	9 640	9.4	722	1154	26.36	35.39	3.010	1.150	One Centaur
Centaur Type H (HD)	1985	5.265	8.325	9.3	789	1257	27.97	40.98	3.715	1.550	One Centaur H
Centaur Taurus (HD)	1989	5.930	9.145	11.0	772	1278	27.97	37.31	4.235	1.695	One Taurus
Mars CC (HD)	1981	11.330	8.420	15.7	739	1323	31.07	40.52	8.655	2.675	One Mars
IPS30 (HD)	1996	28.700	7.750	17.1	761	1390	32.45	44.02	21.390	7.310	Two Mars100
IPS40 (HD)	1996	43.100	7.730	17.1	761	1390	32.45	44.14	32.085	11.015	Three Mars100
IPS50 (HD)	1996	57.400	7.720	17.1	761	1390	32.45	44.19	42.780	14.620	Four Mars100
IPS60 (HD)	1996	70.950	7.715	17.1	761	1390	32.45	44.22	53.475	17.475	Five Mars100
SOVIET UNION											
GTG-35CC (HD)	1969	48.000		7.8	673	1043	24.80		32.000	16.000	One GTG-35
GTG-45CC (HD)	1989	81.000		7.8	738	1173	27.99		54.000	27.000	One GTG-45
GTG-115CC (HD)	1994	171.000		12.3	788	1413	33.00		114.000	57.000	One GTE-115
GTE-100CC (HD)	1969	157.500		13.0	673	1190	28.49		105.000	52.500	One GTE-100
GTE-150CC (HD)	1989	192.000		13.0	696	1223	30.49		128.000	64.000	One GTE-150
GTE-150CC (HD)	1990	235.500		13.0	803	1355	30.99		157.000	78.500	One GTE-150
GTE-200CC (HD)	1996	277.000		15.6	818	1523	32.59		185.000	92.500	One GTE-200
STEWART & STEVENSON											
CC-571 K (AE)	1986	7.700	7.730	12.7	806	1378	32.04	44.14	5.588	2.112	One 571-K
CC1-1600 (AE)	1987	17.900	7.127	22.0	755	1467	35.71	47.87	13.070	4.830	One LM1600
CC1-2500-33 (AE)	1973	30.120	6.859	18.7	801	1492	36.29	49.74	21.550	8.570	One LM2500
CC1-5000 (AE)	1984	43.620	7.144	28.8	719	1477	36.50	47.76	32.500	11.120	One LM5000
CC1-6000 (AE)	1990	54.100	6.400	29.5	723	1493	41.11	53.31	42.100	12.000	One LM6000
CC1-6000 (AE)	1990	108.800	6.350	29.5	723	1493	41.11	53.73	84.200	24.600	Two LM6000
SULZER BROTHERS											
Turbotur 206 (HD)	1974	9.500	8.160	10.0	740	1243	28.30	41.81	6.300	3.200	One Type 3
Turbotur 306 (HD)	1974	19.100	8.150	10.0	740	1243	28.30	41.86	12.600	6.500	TwoType 3
Turbotur 210 (HD)	1974	17.000	8.340	7.7	758	1198	24.99	40.91	10.580	6.420	One Type 7
Turbotur 310 (HD)	1974	34.000	8.330	7.7	758	1198	24.99	40.96	21.160	12.840	Two Type 7
Turbotur 221 (HD)	1981	31.400	7.170					47.58	20.800	10.600	One Type 10
Turbotur 321 (HD)	1981	63.100	7.120					47.92	41.600	21.500	Two Type 10
Turbotur 235 (HD)	1981	54.900	7.300	11.5	810	1377	31.62	46.74	37.900	17.000	One MS6001
Turbotur 335 (HD)	1981	110.100	7.270	11.5	810	1377	31.62	46.93	75.800	34.300	Two MS6001
Turbotur 2105 (HD)	1982	165.000	6.960	11.6	811	1377	33.32	49.02	115.600	49.400	One MS9001
Turbotur 3105 (HD)	1982	330.100	6.950	11.6	811	1377	33.32	49.09	231.200	98.900	One MS9001
THOMASSEN INTERNATIONAL											
STEG 106B (HD)	1980	59.000	7.080	11.5	816	1377	31.42	48.18	38.100	21.900	One PG6541(B)
STEG 109E (HD)	1986	185.200	6.730	12.1	811	1393	33.78	50.70	123.400	61.800	One PG9171(E)

	Year	Power (MW)	Heat Rate (BTU/MW hr)	ress. Ratio	EGT (K)	TET (K)	SC Efficiency (%)	CC Efficiency (%)	GT Power (MW)	ST Power (MW)	TURBINE
THOMASSEN STEWART & STEVENSON INT'L											
STEG 1600 (AE)	1988	18.900	6.965	22.5	760	1476	35.68	48.98	13.200	5.700	One LM1600
STEG 2500 (AE)	1984	29.860	6.960	18.8	801	1492	36.30	49.02	21.000	8.860	One LM2500
2 STEG 2500 (AE)	1984	60.000	6.800	18.8	801	1492	36.30	50.17	42.000	18.000	Two LM2500
STEG 5000 (AE)	1984	45.900	6.966	28.8	719	1476	36.50	48.98	33.000	12.900	One LM5000
STEG 6000 (AE)	1991	53.830	6.540	28.0	723	1475	40.93	52.17	40.500	13.330	One LM6000
TOSHIBA											
STAG109E (HD)	1982	151.500	7.880	11.6	811	1377	33.32	43.30			One MS9001E
STAG107E (HD)	1982	108.300	7.630	12.4	803	1377	32.49	44.72			One MS7001E
TURBO POWER											
FT8 (AE)	1990	32.280	7.010	20.3	716	1359	38.12	48.67	24.700	7.580	One FT8
FT8 Twin (AE)	1990	65.310	6.930	20.3	716	1359	38.12	49.23	49.660	15.650	Two FT8
V64.3 (HD)	1990	86.000	6.640	15.6	807	1444	35.16	51.38	58.500	29.000	One V64.3
V84.2 (HD)	1988	155.000	6.705	10.7	813	1337	33.38	50.88	99.000	59.000	One V84.2
WESTINGHOUSE											
PACE 60 (HD)	1982	68.430	7.600	15.3	783	1395	32.34	44.89	50.030	18.400	One CW251B12
PACE 150 (HD)	1981	152.400	7.050	14.2	794	1391	33.16	48.39	105.250	47.150	One W501D5
PACE 300 (HD)	1981	307.000	7.000	14.2	794	1391	33.16	48.74	210.500	96.500	Two W501D5
PACE 450 (HD)	1981	461.000	6.990	14.2	794	1391	33.16	48.81	315.750	145.250	Three W501D5
PACE 600 (HD)	1981	615.000	6.990	14.2	794	1391	33.16	48.81	421.000	194.000	Four W501D5
PACE 200 (F) (HD)	1989	240.000	6.700	14	851	1487	35.17	50.92	166.000	79.000	One 501F
1xRB211 (AE)	1989	37.500	7.014	20	739	1397	35.63	48.64	26.500	11.000	One RB211
2xRB211 (AE)	1989	75.100	7.000	20	739	1397	35.63	48.74	52.900	22.200	Two RB211
1xTrent (AE)	1996	64.000	6.606	35	701	1504	41.56	51.65	49.600	14.400	One Trent
2xTrent (AE)	1996	129.200	6 600	35	701	1504	41.56	51.69	99.200	30.000	Two Trent
1x1 501D (HD)	1981	144.000	7.260	14	794	1387	33.25	46.99	98.700	45.300	One MW-501D
2x1 501D (HD)	1981	289.900	7.215	14	794	1387	33.25	47.29	197.400	92.500	Two MW-501D
1x1 701D (HD)	1981	175.800	7.390	14	786	1372	33.88	46.17	119.600	56.200	One MW-701D
2x1 701D (HD)	1981	353.400	7.360	14	786	1372	33.88	46.36	239.200	114.200	Two MW-701D
1x1 501F (HD)	1989	222.000	6.645	14	851	1487	35.28	51.34	152.800	69.200	One 501F
2x1 501F (HD)	1989	447.000	6.600	14	851	1487	35.28	51.69	305.600	141.400	Two 501F
1x1 701F (HD)	1996	341.000	6.410	16 2	842	1497	37.04	53.23	232.500	108.500	One 701F
2x1 701F (HD)	1996	685.000	6.380	16.2	842	1497	37.04	53.48	465.000	220.000	Two 701F
1x1 501G (HD)	1996	345.000	5.884	19.2	863	1593	39.04	57.98	230.000	115.000	One 501G
2x1 501G (HD)	1996	690.000	5.884	19 2	863	1593	39.04	57.98	460.000	230.000	Two 501G

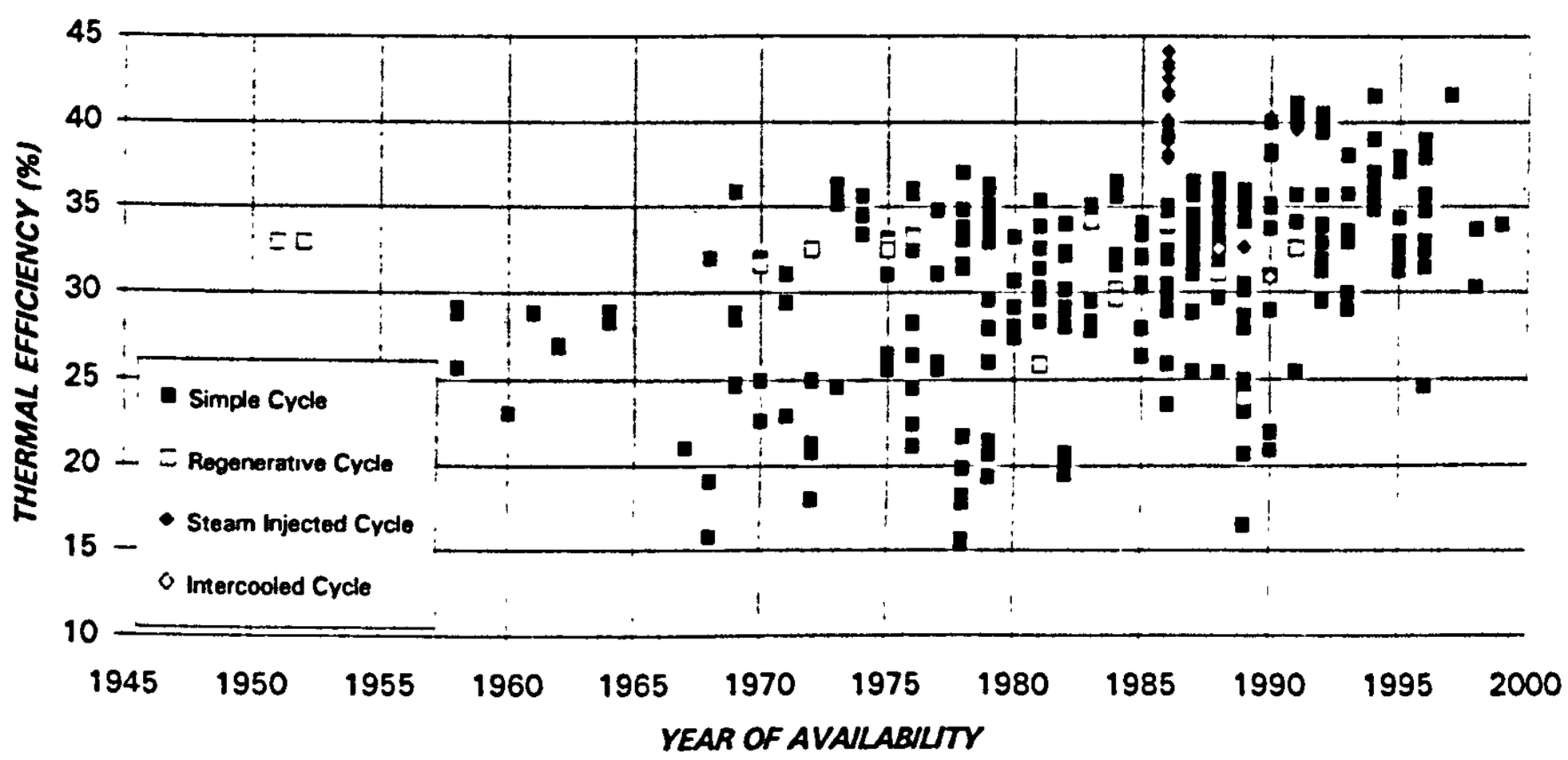

Figure 1.5. Thermal efficiency of simple cycle industrial gas turbines

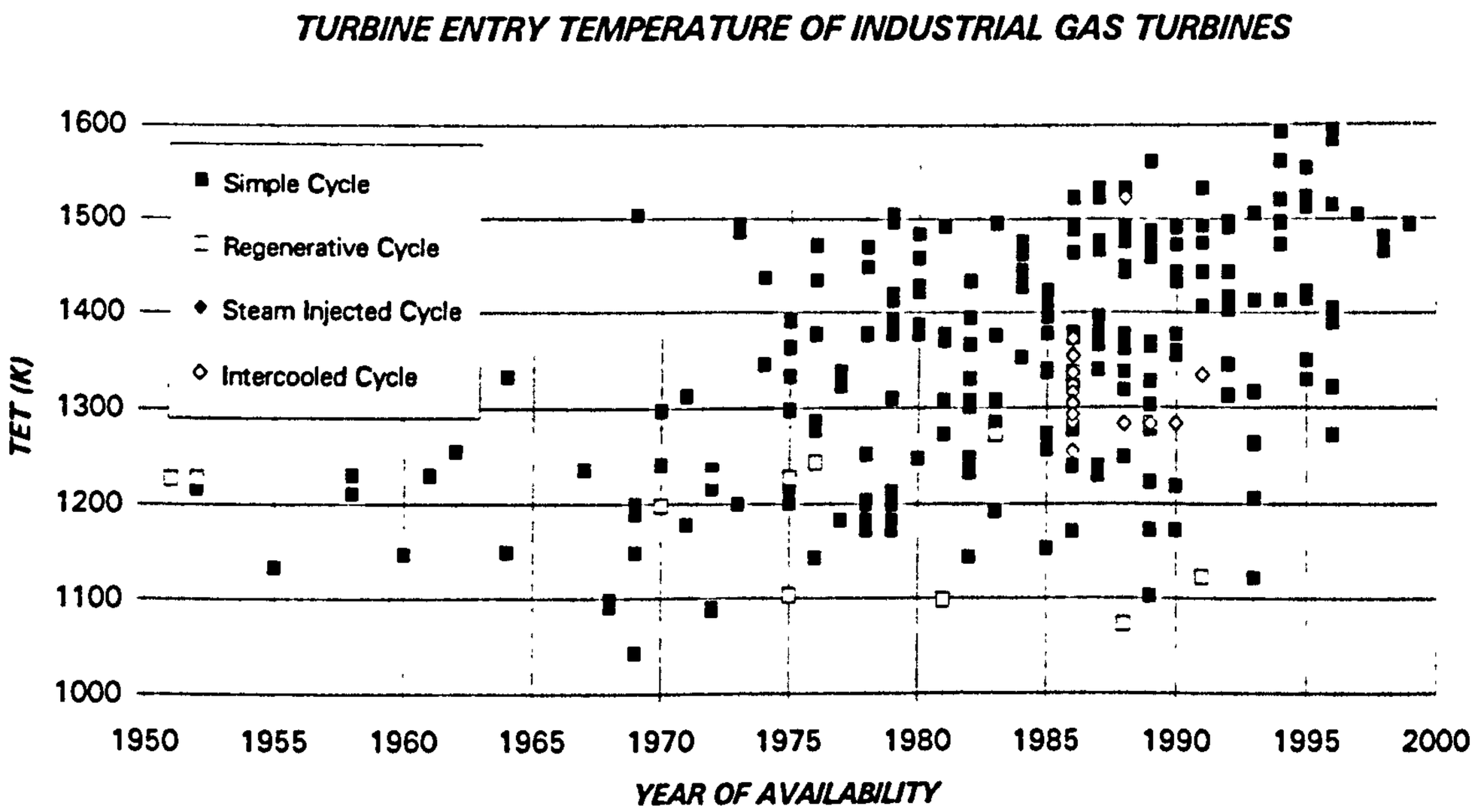

Figure 1.6. Turbine entry temperature of industrial gas turbines

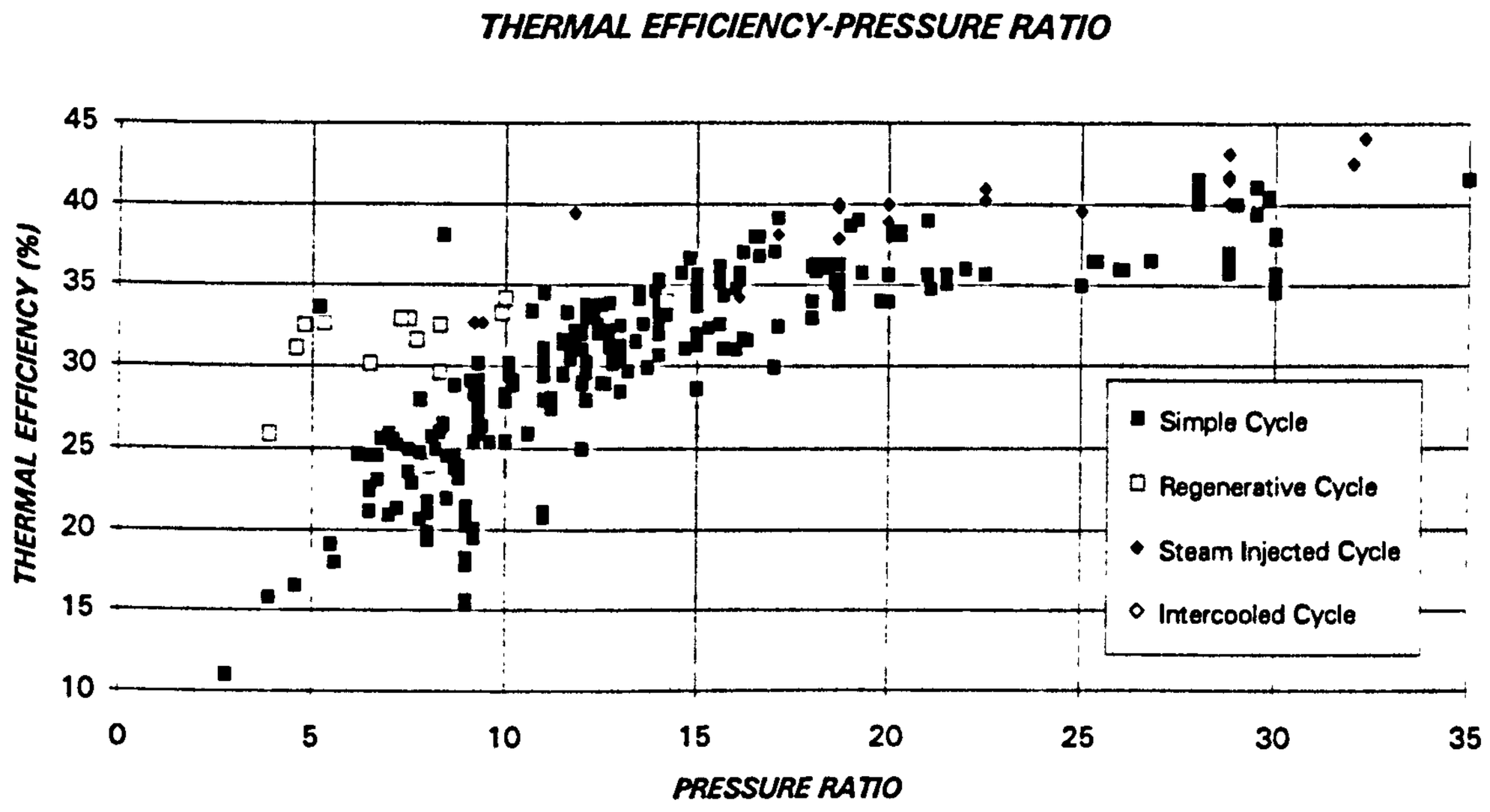

Figure 1.7. Pressure ratio of industrial gas turbines

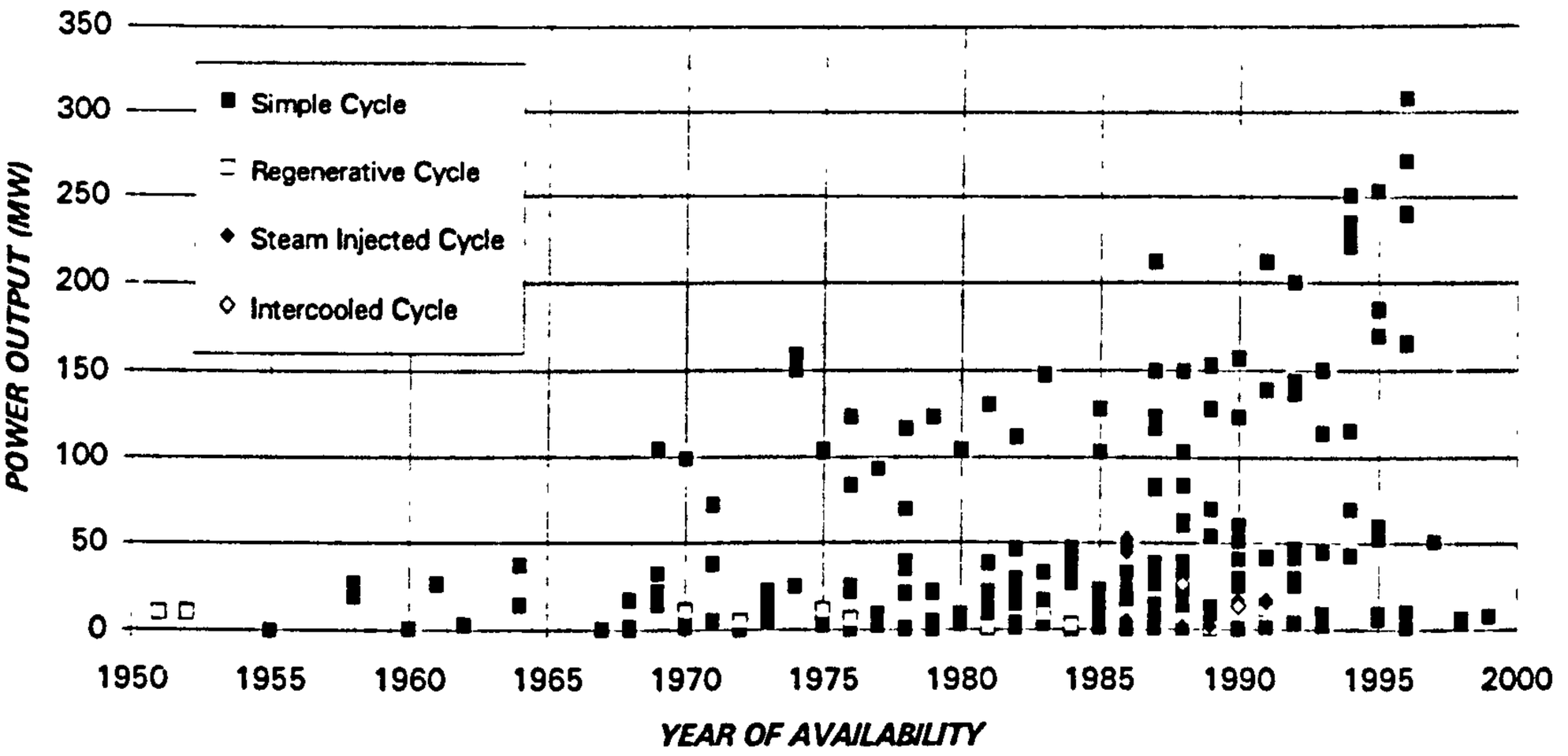

Figure 1.8. Power output of industrial gas turbines

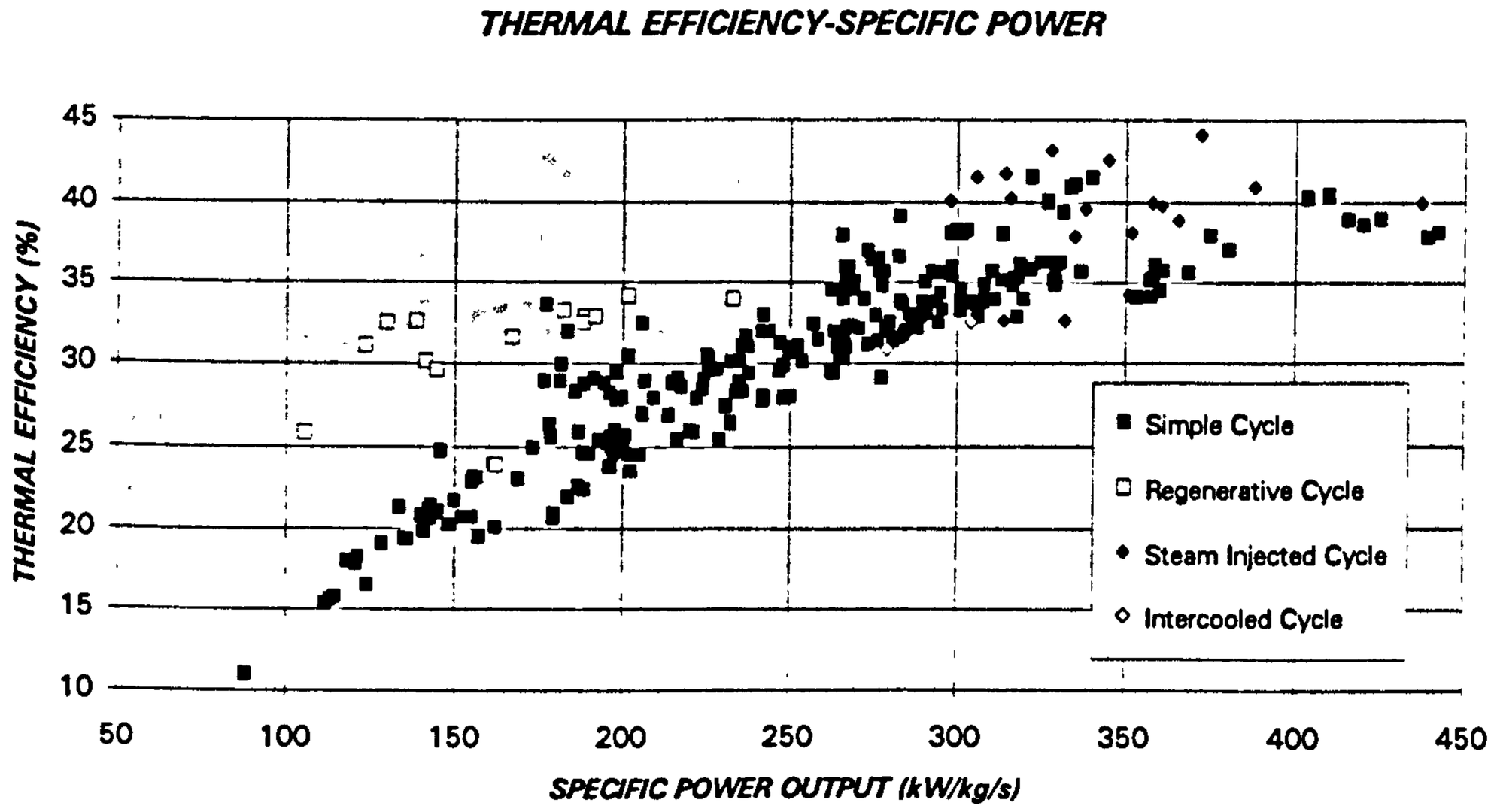

Figure 1.9. Correlation thermal efficiency - specific power output of industrial gas turbines

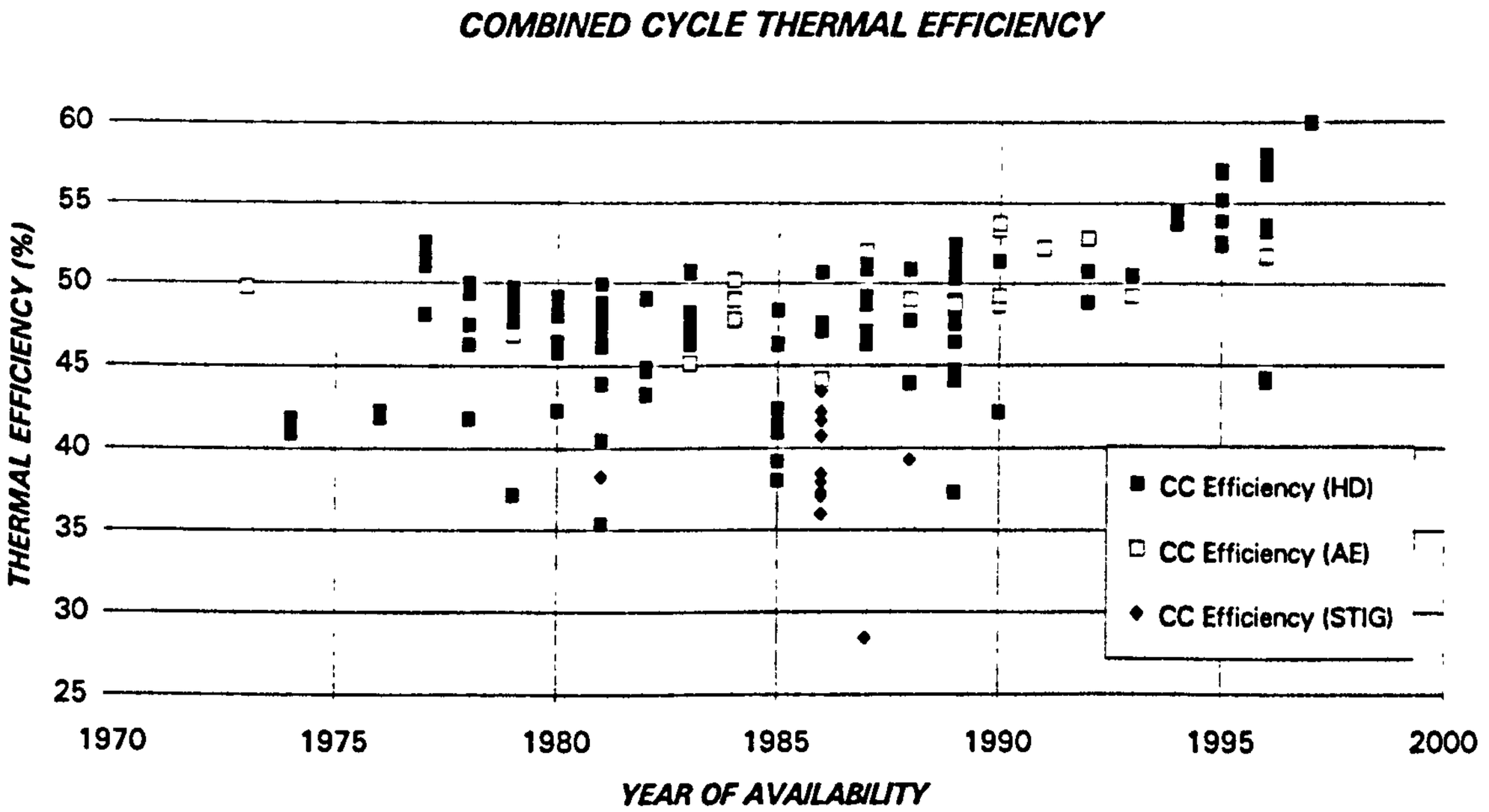

Figure 1.10a. Thermal efficiency of combined cycles vs. year of availability.

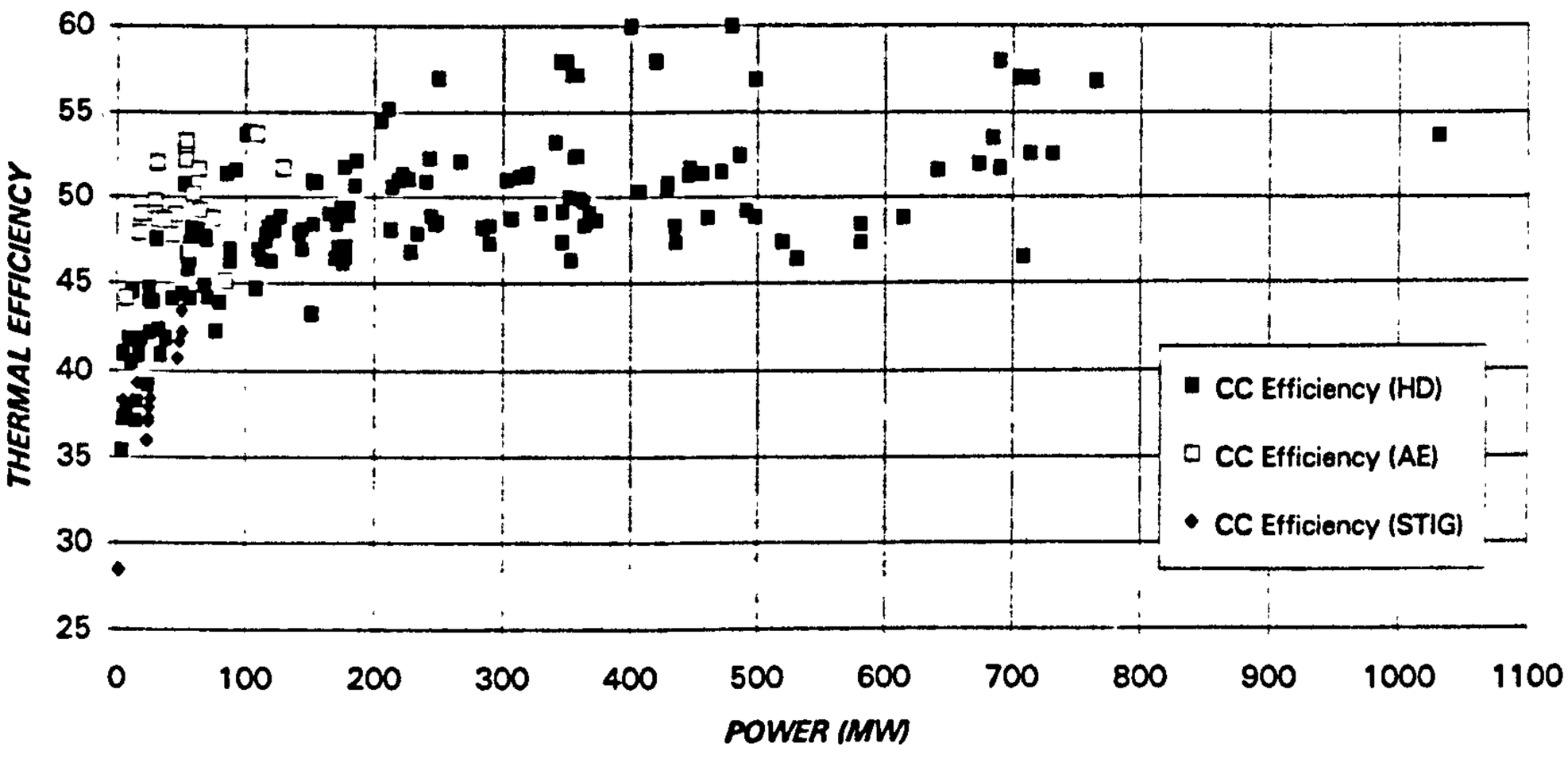

Figure 1.10b. Thermal efficiency of combined cycles vs. power output.

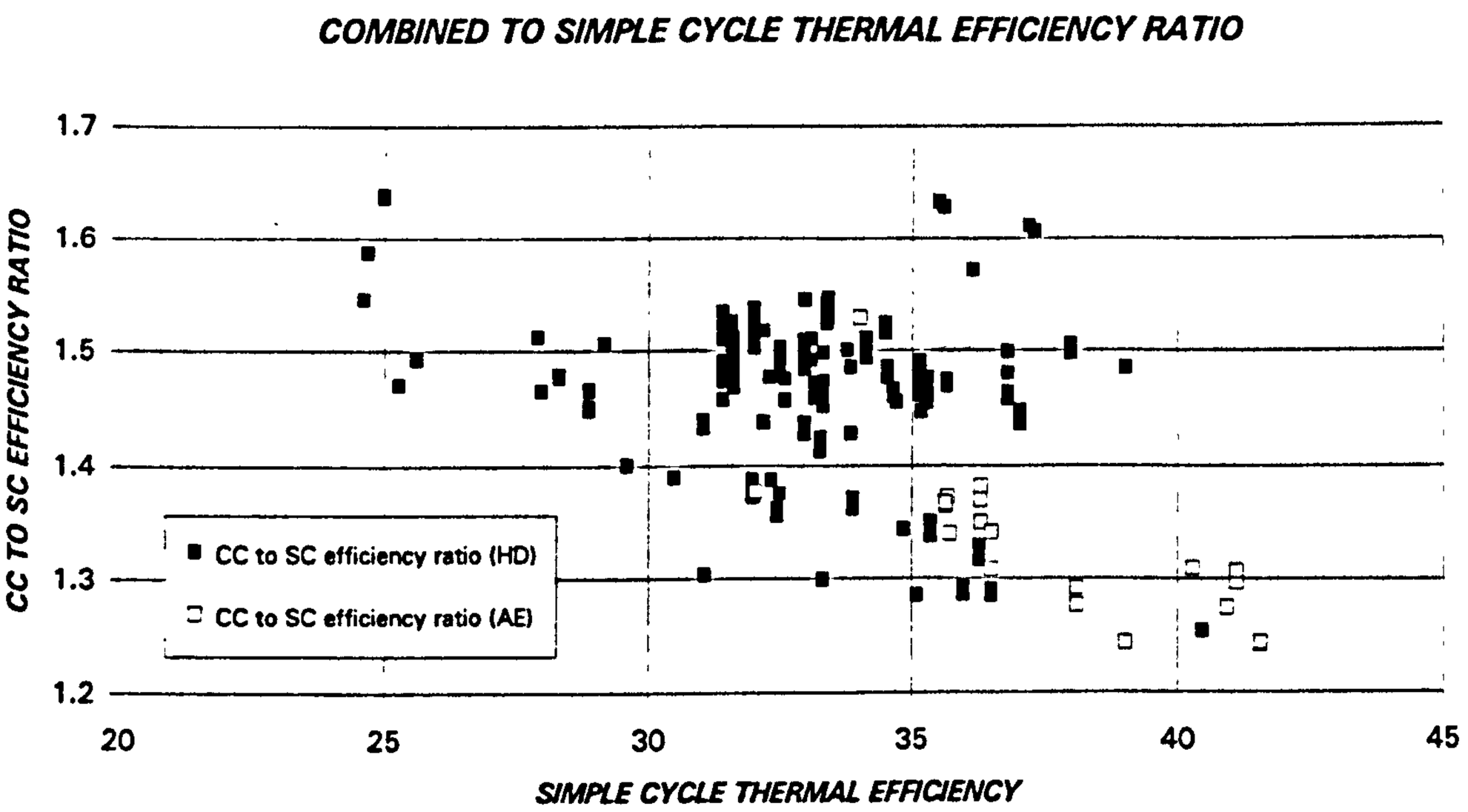

Figure 1.11. Relative increase in combined cycles power output

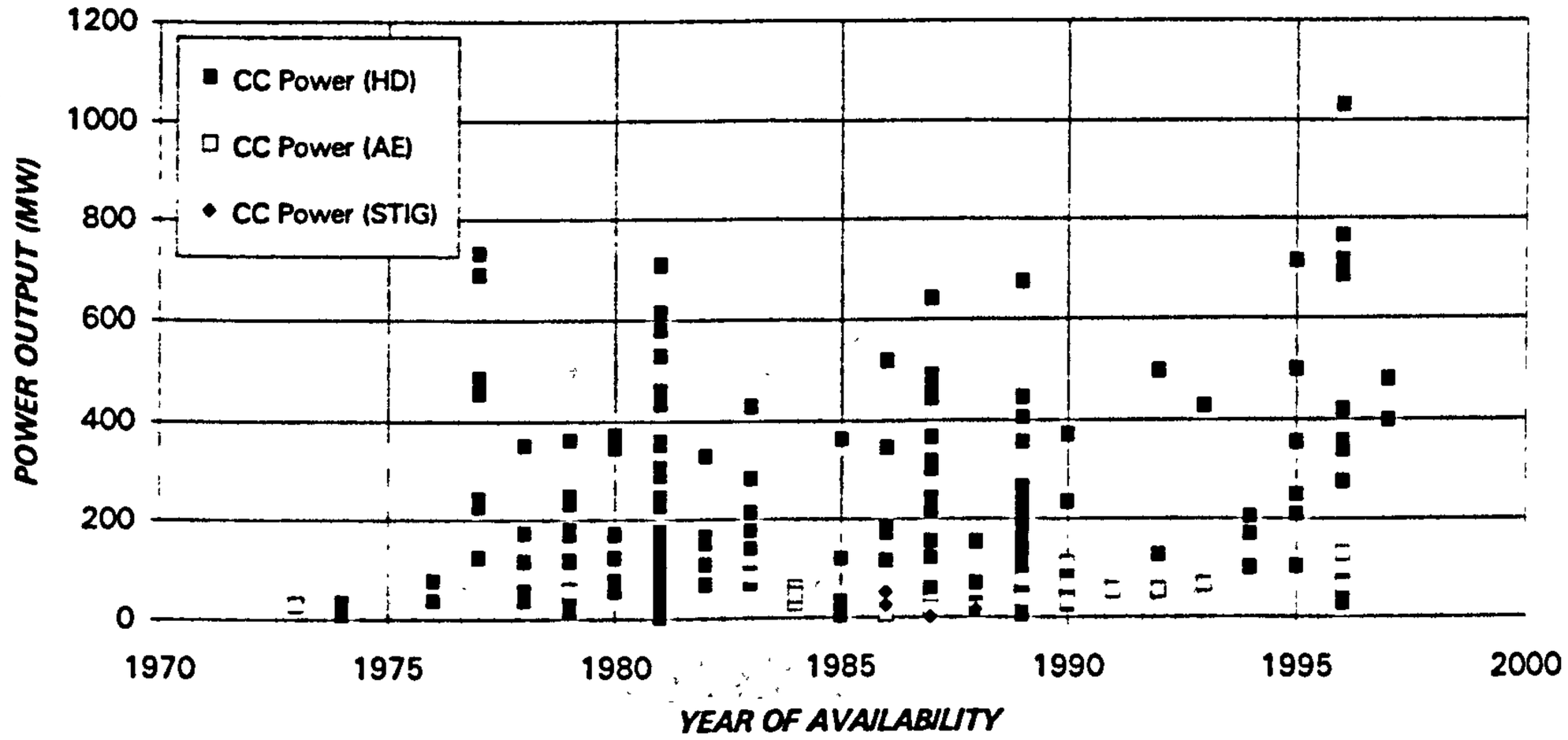

Figure 1.12. Power output of combined cycles vs. year of availability.

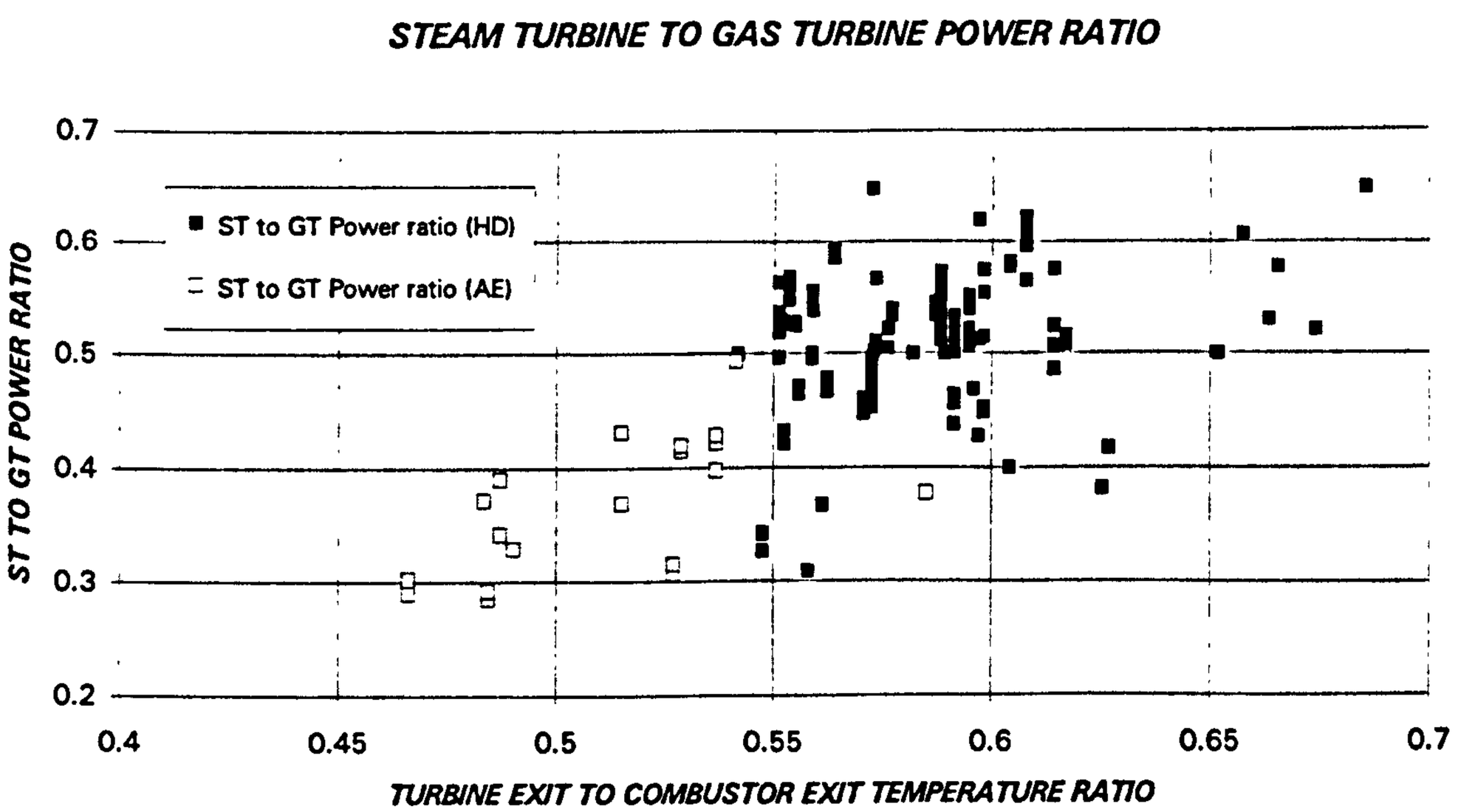

Figure 1.13. Steam turbine to gas turbine power ratio in combined cycles vs. turbine exit to combustor exit temperature ratio.

CHAPTER 2

THERMODYNAMIC ASPECTS OF GTSI PERFORMANCE CODE

2.1. INTRODUCTION TO PERFORMANCE SIMULATION CODES FOR INDUSTRIAL GAS TURBINES

For feasibility studies, conceptual, preliminary and detailed design, development, testing, growth and, in general, modifications of gas turbines, a basic tool is the performance simulation capability. The use of these computer programmes goes further, and constitutes the core of the prediction of performance degradation, no matter which method is employed.

At the very early stages of a design or development programme, when feasibility studies and conceptual design are carried out, the engineering tools employed are, mainly, the performance codes, to predict engine behaviour and evaluate various alternatives.

During preliminary design, the first phase of the development of a new machine, the performance is predicted using characteristics of similar components, before the aerodynamic group is able to provide new maps, with corrections derived from experience. Pressure ratios, efficiencies, different types of losses, cooling flows, auxiliary power extraction, etc. are estimated and introduced in the code to get the desired parameters.

During the detailed design, development & testing phase the component maps of the new engine are obtained and introduced in the code. These will be updated during the whole process. At this stage, more accurate prediction can be made, and the areas where improvement is required will be identified.

The models are corrected and validated during the testing phase. Here, deviations from theoretical predictions, introduced in the code as scaling factors, must be understood in order to gain not only experience, but knowledge, for future projects.

In some cases, the engine, or a major part of it, already exists, and the mission of the code is to evaluate possible modifications. The change from free power turbine to integral power turbine or vice versa, the addition of variable geometry, the introduction of steam/water injection, modifications in one or several components, etc., are examples of the kind of studies a performance code should be able to achieve.

The performance expectations of engine growth are predicted using the data of the baseline machine. In some cases growth is not purely a change that does not affect the turbomachinery, and existing components are modified or new ones are introduced. This is the case of single shaft machines where a booster is added to increase mass flow and power output.[1]

---

[1] When this modification of the compressor takes place it is very common to change the last turbine stages.

However, the use of performance programmes is not restricted to the design and development period. During the production and operation these are used to evaluate the most important performance parameters of every single machine.[2]

To be able to cope with these missions, a generic code should have the following capabilities, already outlined in the first chapter:

- Design and off-design performance calculations of most existing gas turbines, with projection for future power plants in a realistic way.
- Capability of introducing different control laws.
- Operation with different working fluids and fuels in a wide range of temperatures and pressures.
- Prediction of important component and/or engine parameters such as the thermal efficiency, power output, mass flow, turbine cooling flows, etc.
- Capability of introducing experimental component characteristics.
- Possibility of introducing new components and/or modifying the existing ones, operation with variable geometry in compressor and turbines, and changes in the working fluid composition as off-design studies.
- Capacity of changing the fuel with minor code modifications, with data from the most characteristic ones already introduced (natural gas, diesel No.2, kerosene,..).

The objectives of the development of GTSI was to produce a user friendly and robust programme, to support the TURBOMATCH code, already developed at Cranfield during the last three decades, enhancing the performance simulation capabilities. TURBOMATCH is a completely modular programme for design and off-design of open cycle gas turbines. The user can specify, with complete freedom, the turbomachinery arrangements, no matter how realistic, but it is not flexible in the control of the machine. The author decided to orientate GTSI in a slightly different direction.

2.2. THERMODYNAMIC ASPECTS OF GTSI

Being a performance simulation code for open, closed and semi-closed cycles, the main emphasis of the programme was to obtain the best calculation as possible of the thermodynamic properties of several gases, offering a large degree of flexibility to the user.

---

[2] The companies are contractually bind to satisfy a minimum performance on each machine in terms of power output, thermal efficiency, etc., at a certain condition (typically SL ISA day).

In most open cycles the air and combustion product properties are usually a function of the temperature and fuel to air ratio (*FAR*). The presence of water can also be evaluated [31], [32], [75] and [113], although in some cases its effect on performance is calculated using correlations. An example for a turbojet engine is given by Samuel and Gale [113], using weak quadratic functions of absolute humidity to correct the thrust, fuel flow, airflow, compressor speed and TET. In GTSI, the complete thermodynamic chart of water, as steam, mixture of steam and liquid, and liquid was generated. Therefore the water to air ratio (*WAR*) is introduced as an input, instead of using the correction factors mentioned above. The possibility of having hydrogen, kerosene, natural gas, diesel No.2 a standard mid calorific value fuel or a standard low calorific value fuel was added to the programme. However, if the user has the composition of a specific fuel, the code can be easily adapted to include it.[3]

For closed and semi-closed cycles, a generic mixture of air, argon, carbon dioxide, carbon monoxide, helium, hydrogen, nitrogen, oxygen and water vapour can be selected.

2.2.1. FUNCTIONS FOR ENTHALPY, ENTROPY AND CONSTANT PRESSURE SPECIFIC HEAT

The correct simulation of thermodynamic properties is one of the premises for the success of a performance code. As GTSI was written for open, closed and semi-closed cycles, employing different gases, the first idea was to obtain simple expressions for the constant pressure specific heat, enthalpy and entropy (or ϕ) of individual working fluids. Typically these thermodynamic properties are only a function of temperature. This is true at high temperatures. However, at high pressure and low temperatures, common conditions at the inlet of closed cycles, the pressure plays an important role. Hence, the GTSI thermodynamic properties (both static and total) will be a function of pressure and temperature:

$$c_p = c_p(t,p) \qquad C_p = C_p(T,P)$$
$$h = h(t,p) \qquad H = H(T,P)$$
$$\phi = \phi(t,p) \qquad \Phi = \Phi(T,P)$$

Using different sources with experimental data, such as [56] by Hilsenrath et al., [60] by Irvine and Liley or [68] by Keenan, Kaye and Chao, curve fitting was performed for the different gases. Resulting curves were checked against the NASA SP-273 [52].[4]

---

[3] The limitation in the fuel composition will be dictated by the products generated in the combustion. Only a combination of air (already a mixture of gases), argon, carbon dioxide, carbon monoxide, helium, hydrogen, nitrogen, oxygen and water vapour is possible in GTSI.

The general form of the constant pressure specific heat, enthalpy and Φ is:

$$C_P = \sum_{i=0}^{i=6} a_i T^i \qquad \text{for p = 1 bar}$$

$$C_P = \sum_{i=1}^{i=6} i a_i T^{(i-1)} \qquad \text{for p = 10 and 40 bars}$$

[2.1 and 2.2]

$$H = H_0 + \sum_{i=0}^{i=6} a_i \frac{T^{i+1}}{i+1} \qquad \text{for p = 1 bar}$$

$$H = \sum_{i=0}^{i=6} a_i T^i \qquad \text{for p = 10 and 40 bars}$$

[2.3 and 2.4]

$$\Phi = \Phi_0 + a_0 \ln T + \sum_{i=1}^{i=6} a_i \frac{T^i}{i} \qquad \text{for p = 1 bar}$$

$$\Phi = \Phi_0 + a_1 \ln T + \sum_{i=2}^{i=6} \frac{i}{i-1} a_i T^{(i-1)} \qquad \text{for p = 10 and 40 bars}$$

[2.5 and 2.6]

Although most of the gases have been simulated in this way, there are exceptions. Helium is one. Being a monoatomic gas, the value of C_P is almost constant for all pressures and temperatures. Argon is also a monoatomic gas, but it has a larger variation of properties than helium. At low pressure a simpler set of equations can been used. Hydrogen is also an exception, with the same type of equations for 1, 10 and 40 bars [2.1], [2.3] and [2.5]. The fourth one is water vapour. This fluid has been studied since the first boilers and steam turbines became operational. Hence, there are very good computational correlations for the properties, such as the ones developed by Hendricks and Peller [55] or by Irvine and Liley [60]. The last ones have been directly implemented in the GTSI thermodynamic subroutines.

The correlations for the thermodynamic properties of the different gases are given in the next sections.

2.2.2. OPEN CYCLE WITH KEROSENE

Kerosene is not very common for industrial gas turbines. but is the normal fuel for aero engines.

Its properties were taken from [121] by Sellers and Daniele, and are plotted in figure [2.1].

---

[4] This reference only offers data at low pressure, and for a temperature range starting at 300 K. Therefore, the low temperature and high pressure environment of a precooled closed cycle can not be covered with these results.

$$C_P^{Air} = 4185.767((((((((1.0116E-25\,T-1.4527E-21)T+7.6216E-18)T- \\ -1.5128E-14)T-6.7178E-12)T+6.5519E-8)T-5.1537E-05)T \\ +0.2502) \qquad [2.7]$$

$$H^{Air} = 2325.426((((((((((1.2644E-26\,T-2.0753E-22)T+1.2703E-18)T \\ -3.0257E-15)T-1.6795E-12)T+2.1840E-08)T-2.5768E-05)T \\ +2.5020E-01)T-1.7559) \qquad [2.8]$$

$$\Phi^{Air} = 4185.767(2.5020E-01\ln T+((((((1.4451E-26\,T-2.4211E-22)T \\ +1.5243E-18)T-3.7821E-15)T-2.2393E-12)T+3.2760E-08)T \\ -5.1577E-05)T+4.5432E-02) \qquad [2.9]$$

$$C_P^{Fuel} = 4185.767((((((((7.2679E-25\,T-1.3336E-20)T+1.0213E-16)T- \\ -4.2051E-13)T+9.9687E-10)T-1.3772E-06)T+1.2259E-03)T \\ +7.3817E-02) \qquad [2.10]$$

$$H^{Fuel} = 2325.426((((((((((9.0848E-26\,T-1.9051E-21)T+1.7021E-17)T \\ -8.4102E-14)T+2.4922E-10)T-4.5906E-07)T+6.1293E-04)T \\ +7.3817E-02)T+3.0582E01) \qquad [2.11]$$

$$\Phi^{Fuel} = 4185.767(7.3817E-02\ln T+((((((1.0383E-25\,T-2.2226E-21)T \\ +2.0426E-17)T-1.0513E-13)T+3.3229E-10)T-6.8860E-07)T \\ +1.2259E-03)T+6.4834E-01) \qquad [2.12]$$

$$C_P^{products} = \frac{C_P^{Air} + FAR\,C_P^{Fuel}}{1+FAR} \qquad [2.13]$$

$$H^{products} = \frac{H^{Air} + FAR\,H^{Fuel}}{1+FAR} \qquad [2.14]$$

$$\Phi^{products} = \frac{\Phi^{Air} + FAR\,\Phi^{Fuel}}{1+FAR} \qquad [2.15]$$

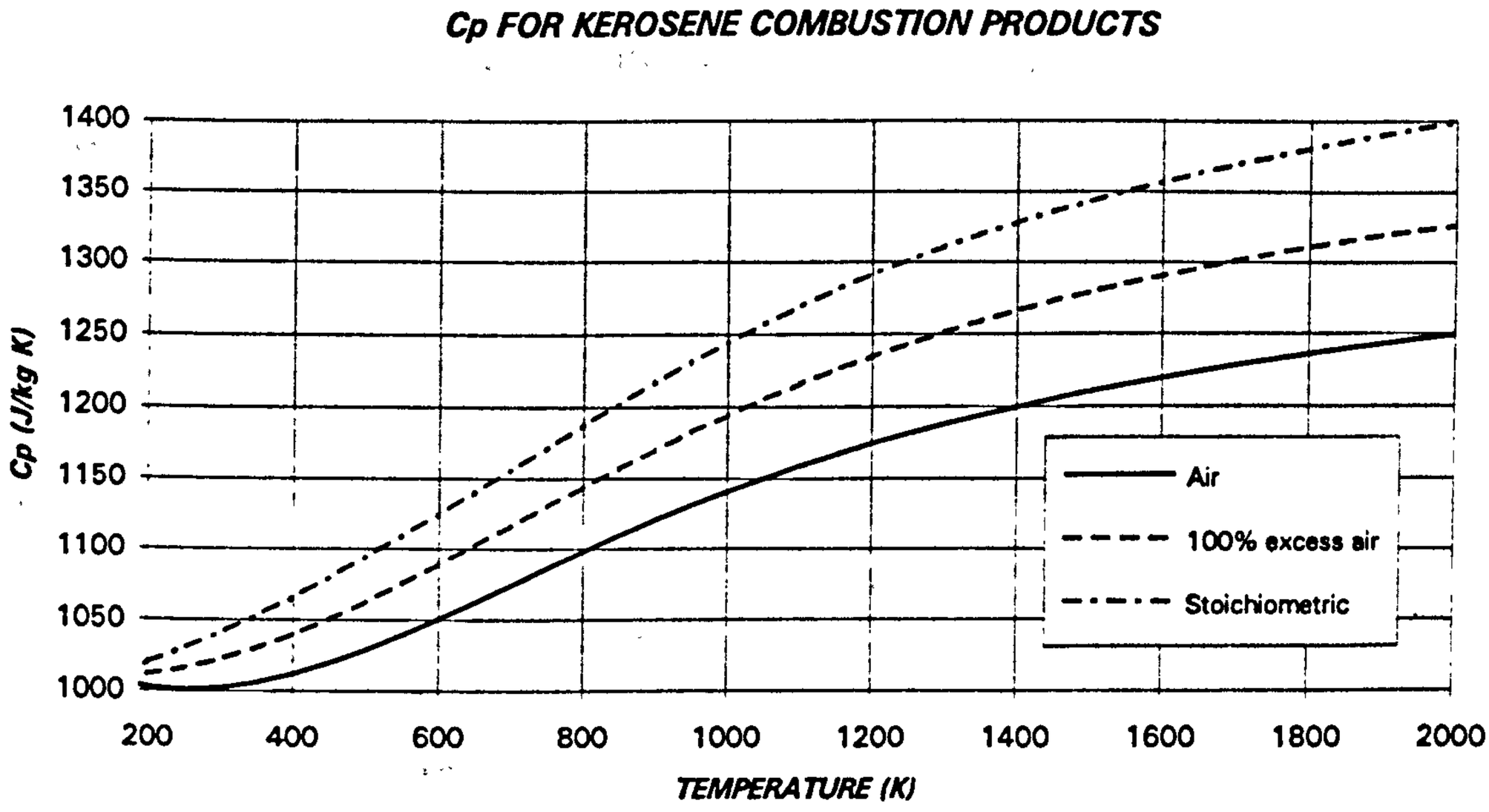

Figure 2.1. Constant pressure specific heat for kerosene combustion products at stoichiometric conditions and with 100% excess air

2.2.3. OPEN CYCLE WITH NATURAL GAS

Natural gas is, probably, the most common fuel for industrial gas turbines. But there is not a unique composition for this mixture of hydrocarbons. Hence, the thermodynamic properties will change according to the source. As the main element is methane, we have selected two possibilities: the first one considers natural gas as pure methane (CH_4), while the second one is $CH_{3.9}$. The differences between both cases are very small.

Although not very important for the composition, several requirements are usually established for the gaseous fuels contaminant content in terms of sulphur, vanadium, sodium, potassium, calcium, lead, zinc, cooper, iron, chlorine, magnesium, etc.

The thermodynamic properties are defined only as a function of temperature. After combustion the high pressure and low temperature environment is not realistic. The constant pressure specific heat, enthalpy and ϕ are, for stoichiometric conditions, as described by equations [2.1], [2.3] and [2.5], with the constants $H_0=a_7$ and $\Phi_0=a_8$. The coefficients a_i are given by Table 2.1 for methane and Table 2.2. for natural gas.

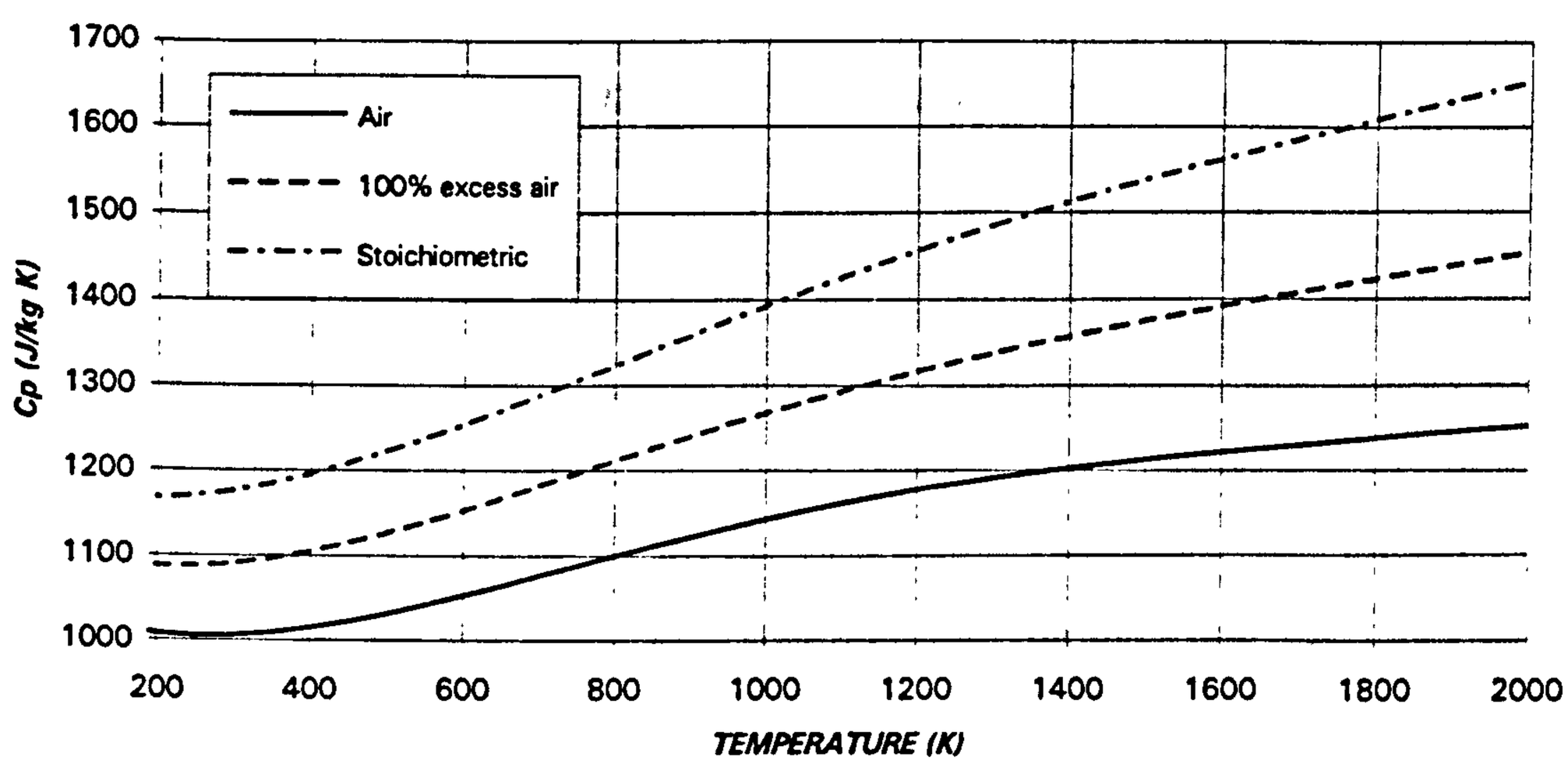

Figure 2.2. Constant pressure specific heat for methane (CH_4) combustion products at stoichiometric conditions and with 100% excess air

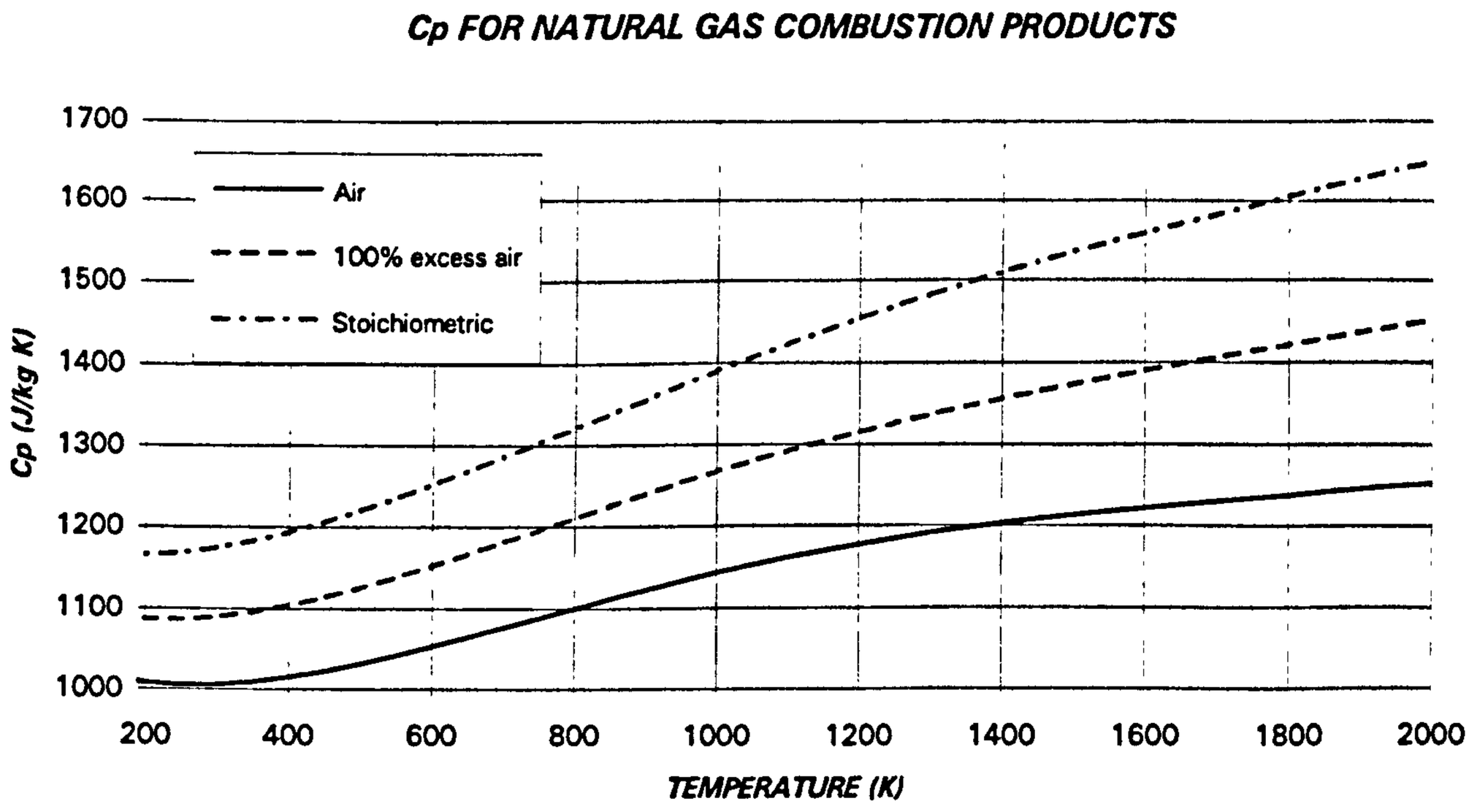

Figure 2.3. Constant pressure specific heat for Natural Gas ($CH_{3.9}$) combustion products at stoichiometric conditions and with 100% excess air

TABLE 2.1. CONSTANTS FOR METHANE COMBUSTION PRODUCTS

a_0=1.1955 E03	a_1=-3.5962 E-01	a_2=1.2098 E-03
a_3=-9.3580 E-07	a_4=3.2318 E-10	a_5=-4.2264 E-14
a_6=6.0526 E-20	a_7=-4.6467 E03	a_8=5.6577 E02

TABLE 2.2. CONSTANTS FOR NATURAL GAS COMBUSTION PRODUCTS

a_0=1.1955 E03	a_1=-3.5692 E-01	a_2=1.2055 E-03
a_3=-9.3350 E-07	a_4=3.2256 E-10	a_5=-4.2198 E-14
a_6=6.0237 E-20	a_7=-4.6281 E03	a_8=5.6902 E02

2.2.4. OPEN CYCLE WITH DIESEL No.2

Distillate Diesel No.2 is also a very common fuel for industrial gas turbines. A widely accepted composition is $CH_{1.56}$, equivalent to an 87% of carbon and a 13% of hydrogen (by mass), with limits in the aromatics (around 35% by volume) and olefins (around 5% by volume). The constant pressure specific heat, enthalpy and ϕ, at stoichiometric conditions, are given, as in the case of methane and Natural gas, by eq. [2.1], [2.3] and [2.5]. The coefficients are in table 2.3.

Cp FOR DISTILLATE DIESEL No.2 COMBUSTION PRODUCTS

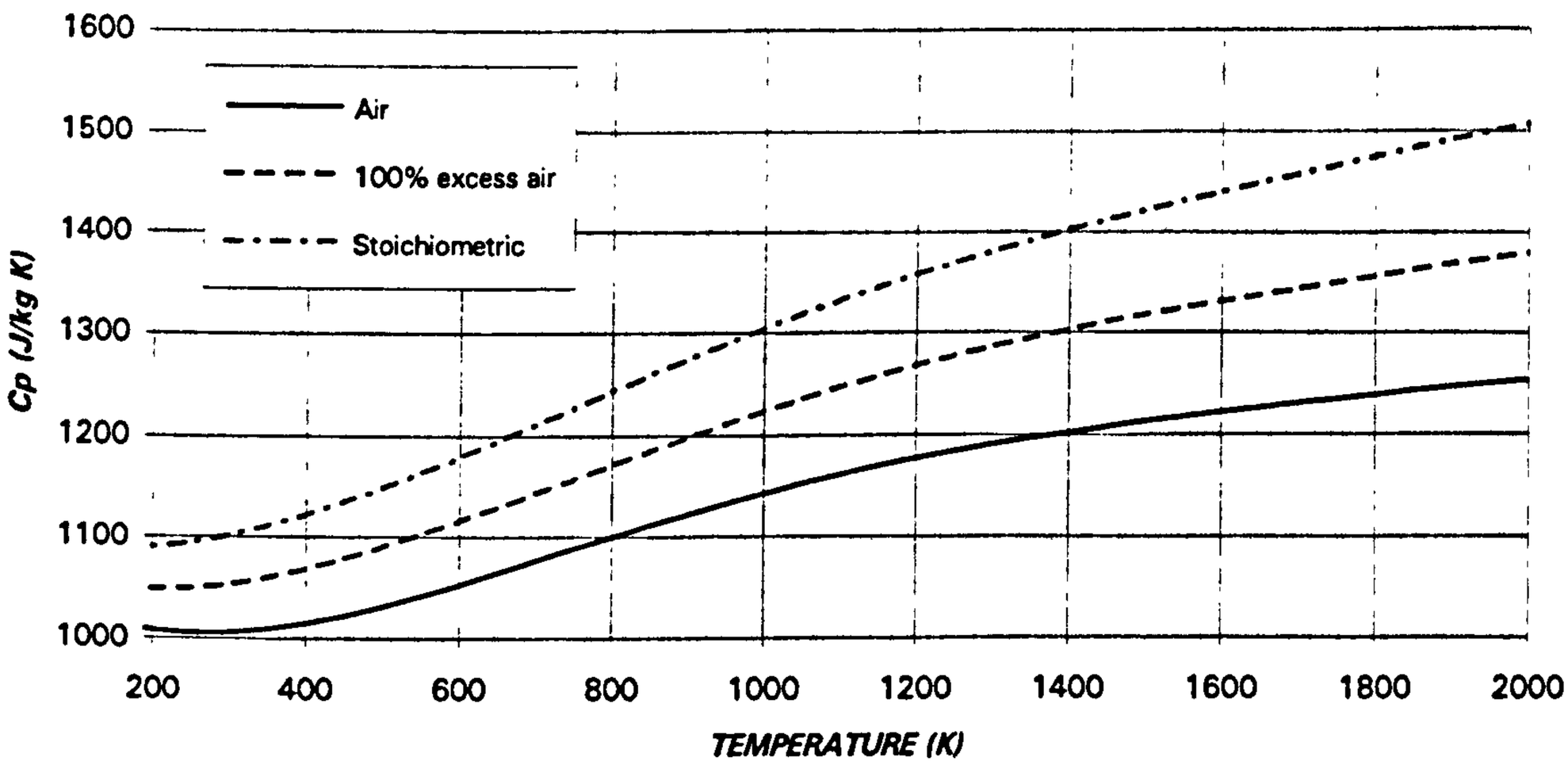

Figure 2.4. Constant pressure specific heat for Diesel No.2 ($CH_{1.56}$) combustion products at stoichiometric conditions and with 100% excess air

TABLE 2.3. CONSTANTS FOR DIESEL No.2 COMBUSTION PRODUCTS

a_0=1.1066 E03	a_1=-2.6224 E-01	a_2=1.0521 E-03
a_3=-8.5279 E-07	a_4=3.0078 E-10	a_5=-3.9880 E-14
a_6=5.0089 E-20	a_7=-3.9762 E03	a_8=6.8339 E02

As in the case of gaseous fuels, the fuel quality is an important requirement, with limits in the content of sulphur, vanadium, sodium, potassium, calcium, lead, zinc, cooper, etc. Maximum values of ash, carbon on 10% residuum, particulate, water and sediment are also established.

2.2.5. OPEN CYCLE WITH MID AND LOW CALORIFIC VALUE FUELS

While kerosene, methane, natural gas and diesel have high calorific values, located typically in the range of 40-50 MJ/kg, there are other fuels, coming from residuals, coal gasification, etc. that have a substantially lower calorific value.

It is not easy to make a clear division of what can be considered as low, mid or high calorific value. The following classification is made here: below 10 MJ/kg for low calorific value, between 10 and 30 MJ/kg for mid calorific value and above 30 MJ/kg for high calorific value.

There will be a very large number of fuel compositions. In Tables 2.4 and 2.5 two characteristic cases are shown. The thermodynamic properties are obtained, as in the previous sections, with equations [2.1], [2.3] and [2.5], where $H_0=a_7$ and $\Phi_0=a_8$.

TABLE 2.4. CONSTANTS FOR MID CV GAS COMBUSTION PRODUCTS

a_0=9.7261 E02	a_1=1.2611 E-01	a_2=5.2822 E-04
a_3=-5.1059 E-07	a_4=1.8826 E-10	a_5=-2.5101 E-14
a_6=1.2434 E-20	a_7=-1.0009 E02	a_8=9.2543 E02

TABLE 2.5. CONSTANTS FOR LOW CV GAS COMBUSTION PRODUCTS

a_0=1.0516 E03	a_1=-2.9073 E-02	a_2=7.4961 E-04
a_3=-6.4664 E-07	a_4=2.3089 E-10	a_5=-3.0459 E-14
a_6=2.7940 E-20	a_7=-1.5200 E03	a_8=8.0394 E02

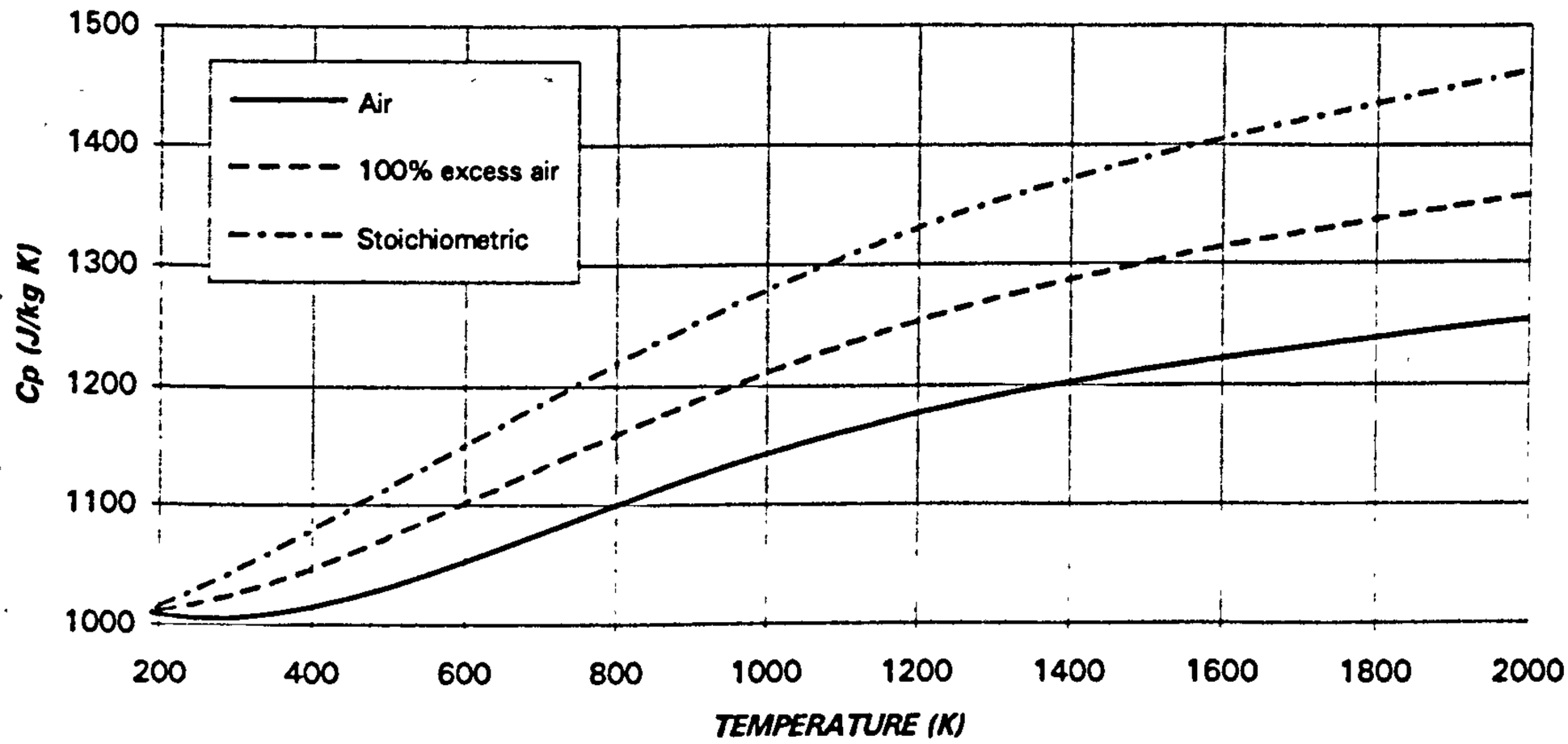

Figure 2.5. Constant pressure specific heat for mid calorific value gas combustion products at stoichiometric conditions and with 100% excess air

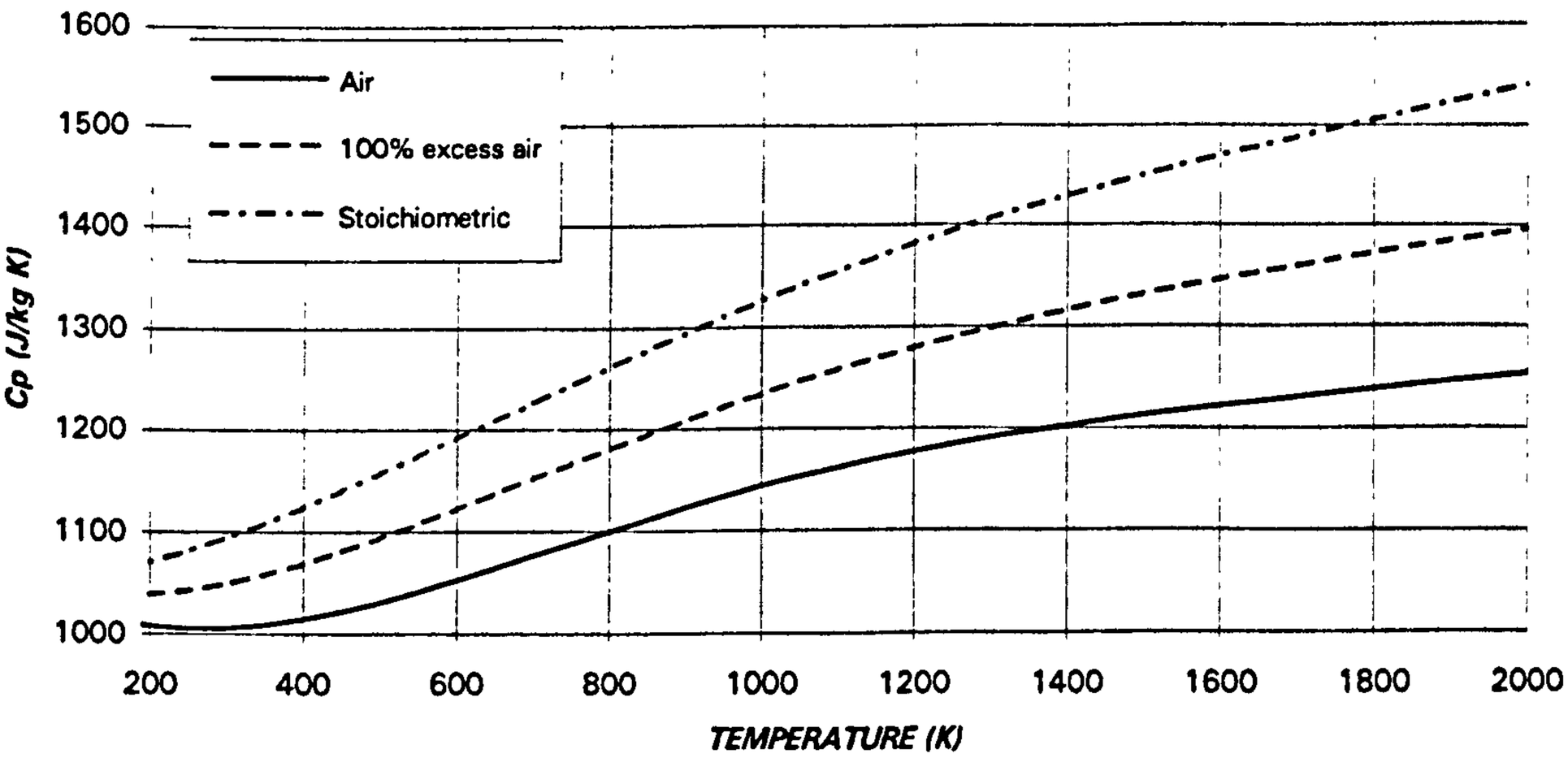

Figure 2.6. Constant pressure specific heat for low calorific value gas combustion products at stoichiometric conditions and with 100% excess air

2.2.6. OPEN CYCLE WITH HYDROGEN

Although still not in commercial use, hydrogen is, probably, the most promising fuel for gas turbines. It is clean (its combustion produces just water vapour, with no CO_x / NO_x emissions), with a very high calorific value (around 120 MW/kg) and the combustion product (water vapour) has a very high enthalpy. However, its manipulation, at ambient or high temperature, is very dangerous. Again, eq. [2.1], [2.3] and [2.5] describe the thermodynamic properties, and the coefficient for these equations are given in table 2.6.

TABLE 2.6. CONSTANTS FOR MID CV GAS COMBUSTION PRODUCTS

a_0=1.3050 E02	a_1=-5.7266 E-01	a_2=1.5100 E-03
a_3=-1.1200 E-06	a_4=3.7900 E-10	a_5=-4.9300 E-14
a_6=8.1700 E-20	a_7=-6.5748 E03	a_8=3.9581 E02

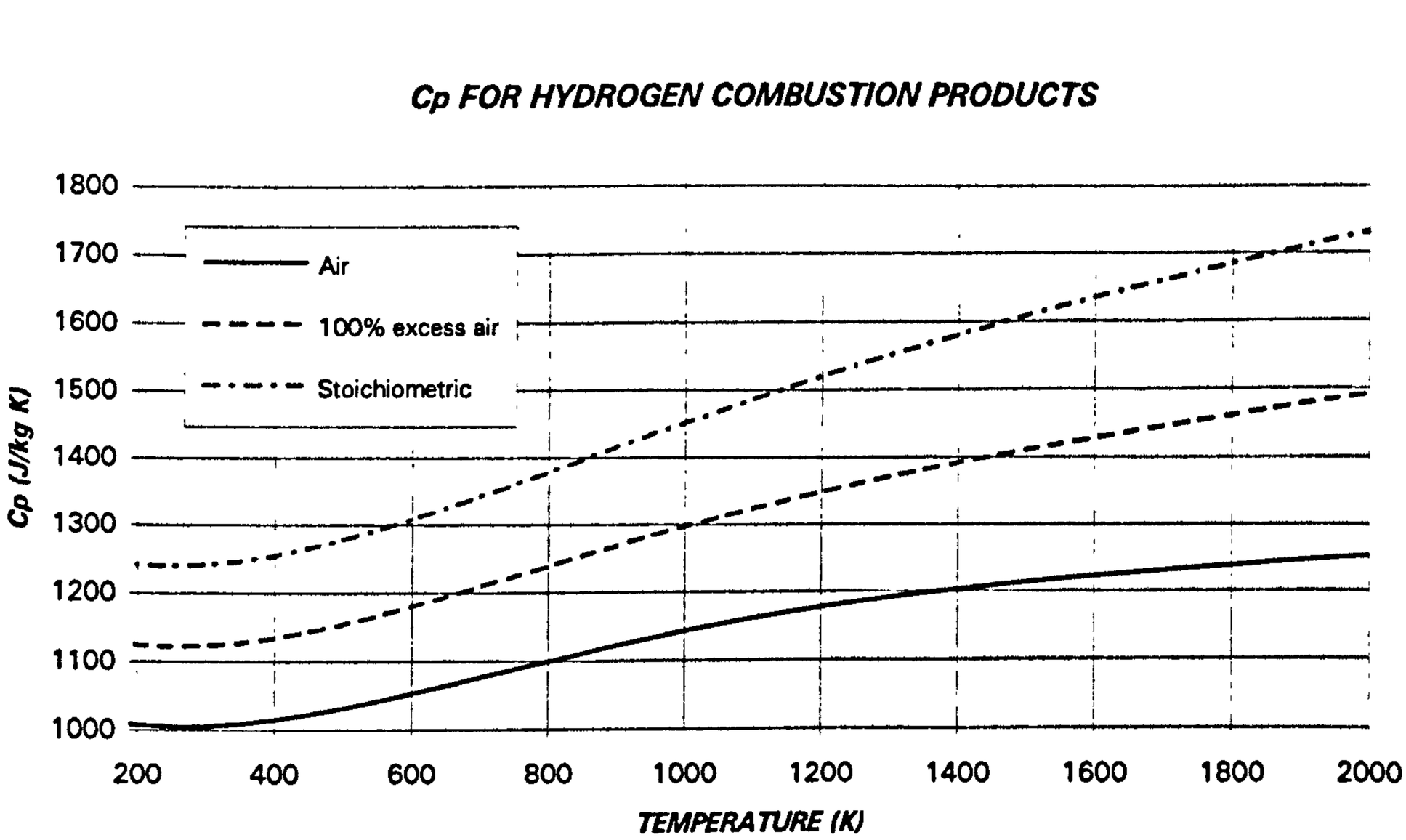

Figure 2.7. Constant pressure specific heat for hydrogen gas combustion products at stoichiometric conditions and with 100% excess air

2.2.7. CLOSED CYCLE GASES: AIR, ARGON, CARBON DIOXIDE, CARBON MONOXIDE, HELIUM, HYDROGEN, NITROGEN, OXYGEN AND WATER VAPOUR

In operational closed cycles the most common working fluids are air, helium, carbon dioxide, argon and xenon. The semi-closed cycle that will be extensively treated in this thesis will use carbon dioxide, argon and water vapour, burning a fuel that is a mixture of carbon monoxide, carbon dioxide and hydrogen, with the oxidizer being a mixture of oxygen and argon.

Therefore, the thermodynamic properties of the following gases will be simulated in detail: air, argon, carbon dioxide, carbon monoxide, helium, hydrogen, nitrogen, oxygen and water vapour. The author could not find the thermodynamic properties of xenon as a function of temperature and pressure. NASA SP-273 [52] gives the polynomial approximation of the properties for most of the gases as a function of temperature. Hence, this reference will be used for other gases.

Equations [2.1], [2.3] and [2.5] for 1 bar and [2.2], [2.4] and [2.6] for 10 and 40 bars, describe the thermodynamic properties of almost all the gases considered in this section with $H_0=a_7$ and $\Phi_0=a_8$ for the 1 bar case and $\Phi_0=a_7$. for the 10 and 40 bar cases. The exceptions are helium, that has constant C_P, hydrogen, that will be simulated with equations [2.1], [2.3] and [2.5] for 1, 10 and 40 bars and water vapour, that was taken from [60], Other exception could be the properties of argon at 1 bar, given by eq. [2.1], [2.3] and [2.5] and the coefficients of table 2.9A or by the following system:

$$C_P = a_0 + \frac{a_1}{T} \qquad [2.16]$$

$$H = H_0 + a_0 T + a_1 \ln T \qquad H_0 = a_2 \qquad [2.17]$$

$$\Phi = \Phi_0 + a_0 \ln T - \frac{a_1}{T} \qquad \Phi_0 = a_3 \qquad [2.18]$$

TABLE 2.7. CONSTANTS FOR ARGON AT 1 BAR

a_0=5.1997 E02	a_1=4.8161 E02	a_2=-2.8256 E03
a_3=9.1442 E03		

Tables A, B and C will give the constants for constant pressure specific heat, enthalpy and Φ (entropy) at 1, 10 and 40 bars respectively.

2.2.7.1. Thermodynamic Properties of Air

TABLE 2.8A. CONSTANTS FOR AIR AT 1 BAR

a_0=1.0590 E03	a_1=-4.9712 E-01	a_2=1.3360 E-03
a_3=-1.1073 E-06	a_4=4.0472 E-10	a_5=-5.5330 E-14
a_6=-9.8539 E-20	a_7=-5.2800 E03	a_8=-2.4304 E02

TABLE 2.8B. CONSTANTS FOR AIR AT 10 BAR

a_0=-1.1707 E04	a_1=1.0687 E03	a_2=-1.9415 E-01
a_3=3.0254 E-04	a_4=-1.4040 E-07	a_5=2.3730 E-11
a_6=-4.0032 E-16	a_7=2.9031 E01	

TABLE 2.8C. CONSTANTS FOR AIR AT 40 BAR

a_0=-3.5840 E04	a_1=1.1531 E03	a_2=-3.0047 E-01
a_3=3.6598 E-04	a_4=-1.5666 E-07	a_5=2.4357 E-11
a_6=-1.4208 E-16	a_7=-8.1485 E02	

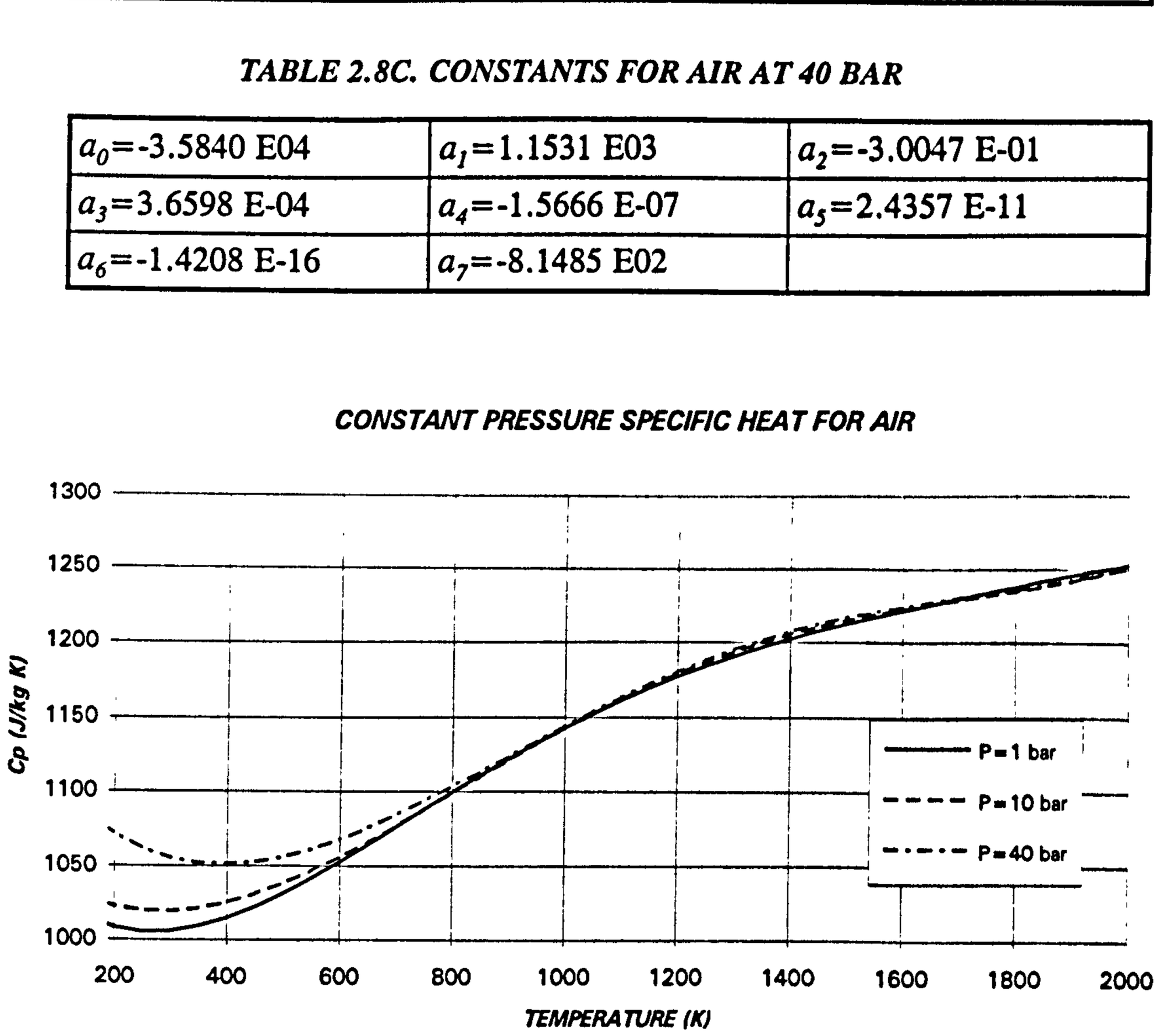

Figure 2.8. Constant pressure specific heat for air at 1, 10 and 40 bars

2.2.7.2. Thermodynamic Properties of Argon

TABLE 2.9A. CONSTANTS FOR ARGON AT 1 BAR

a_0=5.2510 E02	a_1=-1.8068 E-02	a_2=2.6017 E-05
a_3=-1.7662 E-08	a_4=5.6700 E-12	a_5=-6.9586 E-16
a_6=8.9744 E-22	a_7=-7.4812 E02	a_8=8.8624 E02

TABLE 2.9B. CONSTANTS FOR ARGON AT 10 BAR

a_0=-6.9068 E03	a_1=5.4539 E02	a_2=-3.5341 E-02
a_3=2.4701 E-05	a_4=-8.1883 E-09	a_5=9.2283 E-13
a_6=4.2449 E-17	a_7=3.0013 E02	

TABLE 2.9C. CONSTANTS FOR ARGON AT 40 BAR

a_0=-3.1762 E04	a_1=6.4684 E02	a_2=-1.9911 E-03
a_3=1.5547E-04	a_4=-5.8954 E-08	a_5=8.7622 E-12
a_6=-5.3610 E-17	a_7=-8.1485 E02	

CONSTANT PRESSURE SPECIFIC HEAT FOR ARGON

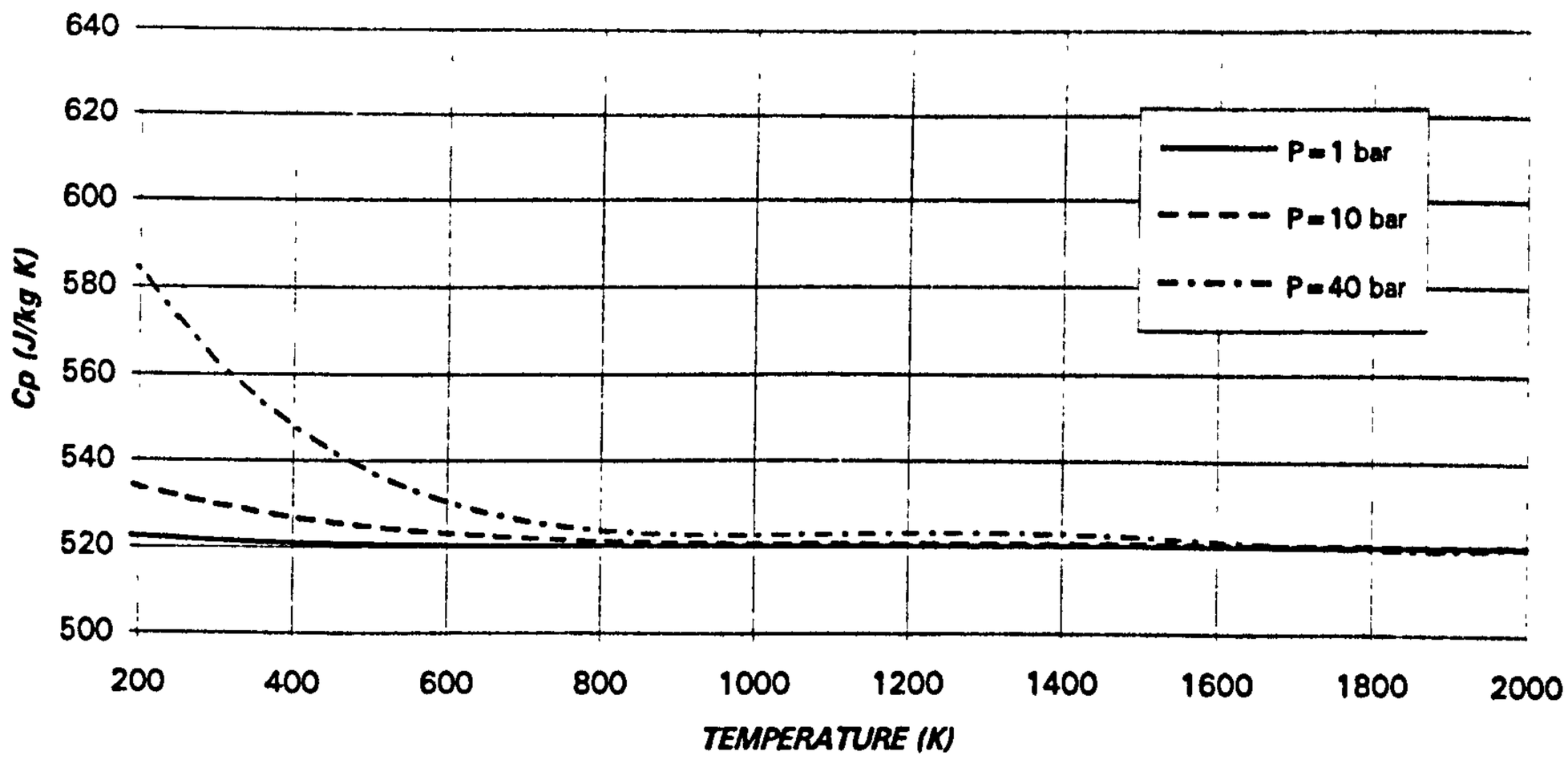

Figure 2.9. Constant pressure specific heat for argon at 1, 10 and 40 bars

2.2.7.3. Thermodynamic Properties of Carbon Dioxide

TABLE 2.10A. CONSTANTS FOR CARBON DIOXIDE AT 1 BAR

a_0=4.2422 E02	a_1=1.8618 E00	a_2=-1.8068 E-03
a_3=1.0375 E-06	a_4=-3.2606 E-10	a_5=4.3032 E-14
a_6=-1.5604 E-19	a_7=1.7637 E04	a_8=1.9550 E03

TABLE 2.10B. CONSTANTS FOR CARBON DIOXIDE AT 10 BAR

a_0=-2.6230 E04	a_1=6.1387 E02	a_2=5.8227 E-01
a_3=-2.5931 E-04	a_4=6.9978 E-08	a_5=-9.6851 E-12
a_6=3.8926 E-16	a_7=5.8465 E02	

TABLE 2.10C. CONSTANTS FOR CARBON DIOXIDE AT 40 BAR

a_0=-1.5540 E05	a_1=6.1387 E02	a_2=-2.8767 E-01
a_3=4.3619 E-04	a_4=-1.9901 E-07	a_5=3.1304 E-11
a_6=1.9894 E-17	a_7=-2.3545 E03	

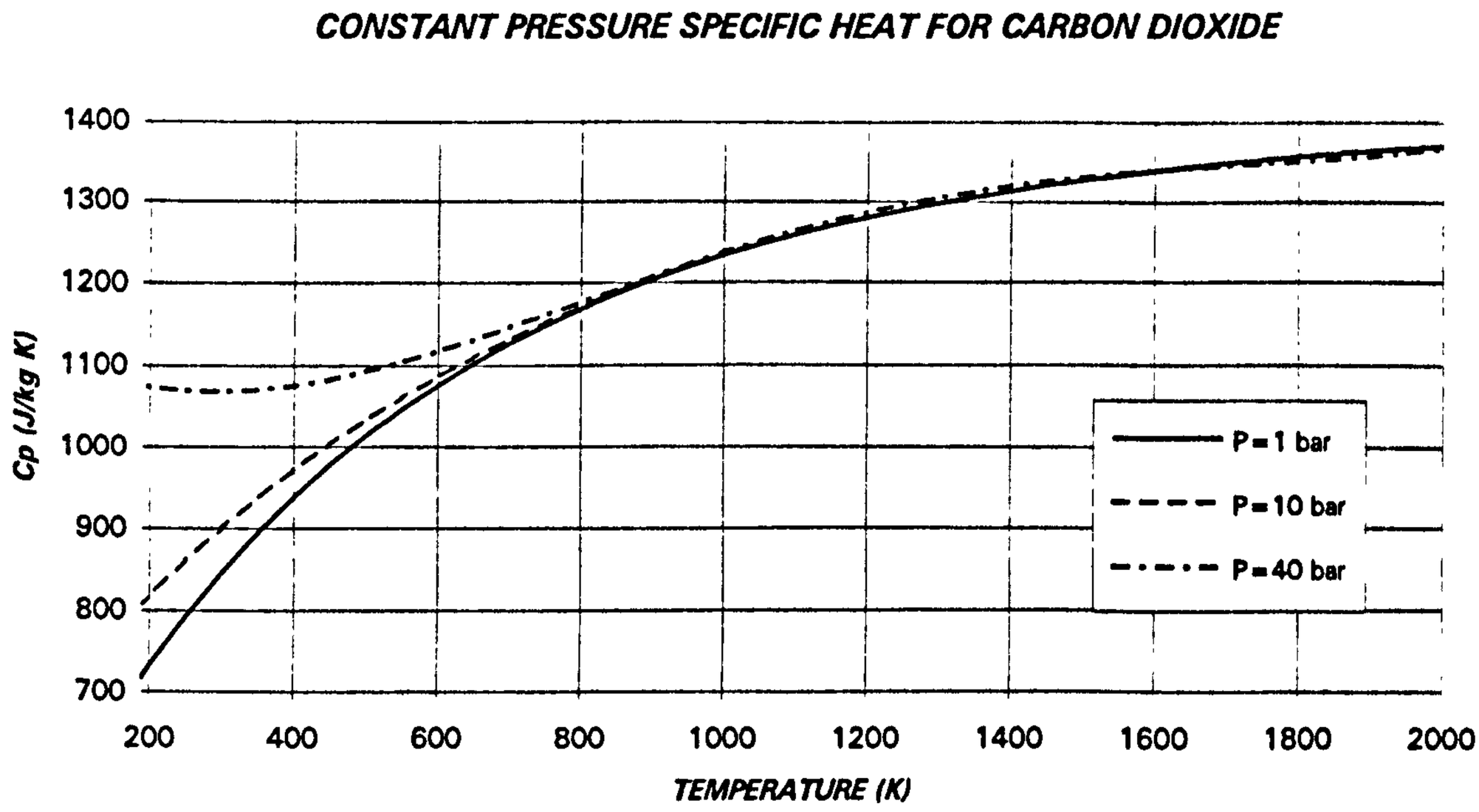

Figure 2.10. Constant pressure specific heat for CO_2 at 1, 10 and 40 bars

2.2.7.4. Thermodynamic Properties of Carbon Monoxide

TABLE 2.11A. CONSTANTS FOR CARBON MONOXIDE AT 1 BAR

a_0=1.1204 E03	a_1=-6.6026 E-01	a_2=1.6747 E-03
a_3=-1.3933 E-06	a_4=5.1439 E-10	a_5=-7.1479 E-14
a_6=-1.0008 E-20	a_7=-7.4171 E03	a_8=8.0186 E02

TABLE 2.11B. CONSTANTS FOR CARBON MONOXIDE AT 10 BAR

a_0=-4.5647 E04	a_1=1.2407 E03	a_2=-4.1559 E-01
a_3=4.8209 E-04	a_4=-2.0813 E-07	a_5=3.3073 E-11
a_6=-2.9641 E-16	a_7=-9.5210 E02	

TABLE 2.11C. CONSTANTS FOR CARBON MONOXIDE AT 40 BAR

a_0=-3.5840 E04	a_1=1.1531 E03	a_2=-3.0047 E-01
a_3=3.6598 E-04	a_4=-1.5666 E-07	a_5=2.4357 E-11
a_6=-1.4208 E-16	a_7=-8.1485 E02	

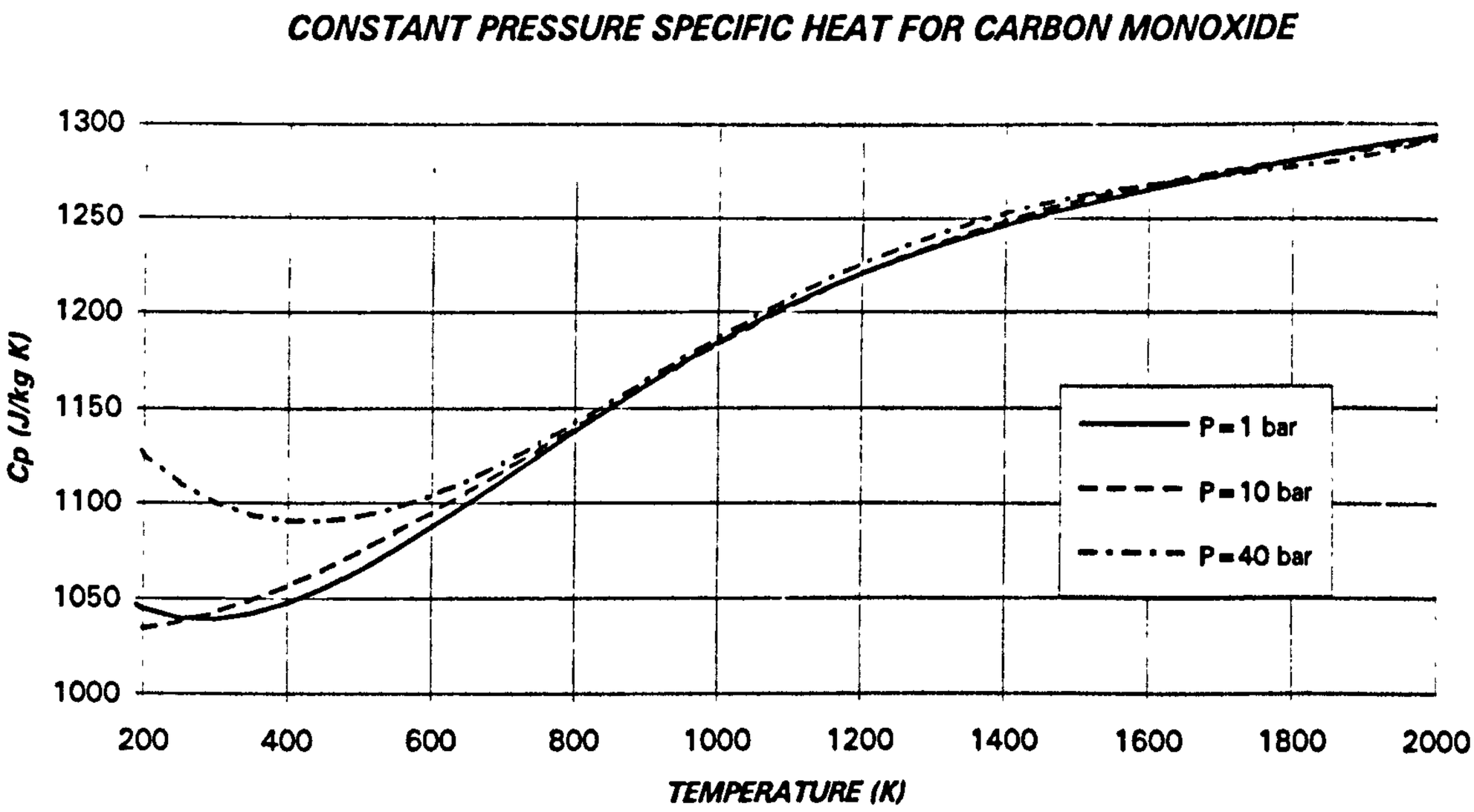

Figure 2.11. Constant pressure specific heat for CO at 1, 10 and 40 bars

2.2.7.5. Thermodynamic Properties of Helium

TABLE 2.12A. CONSTANTS FOR HELIUM AT 1, 10 AND 40 BAR

a_0=5.1931 E03	a_1=0.0000	a_2=0.0000
a_3=0.0000	a_4=0.0000	a_5=0.0000
a_6=0.0000	a_7=6.0547 E03	a_8=9.0705 E03

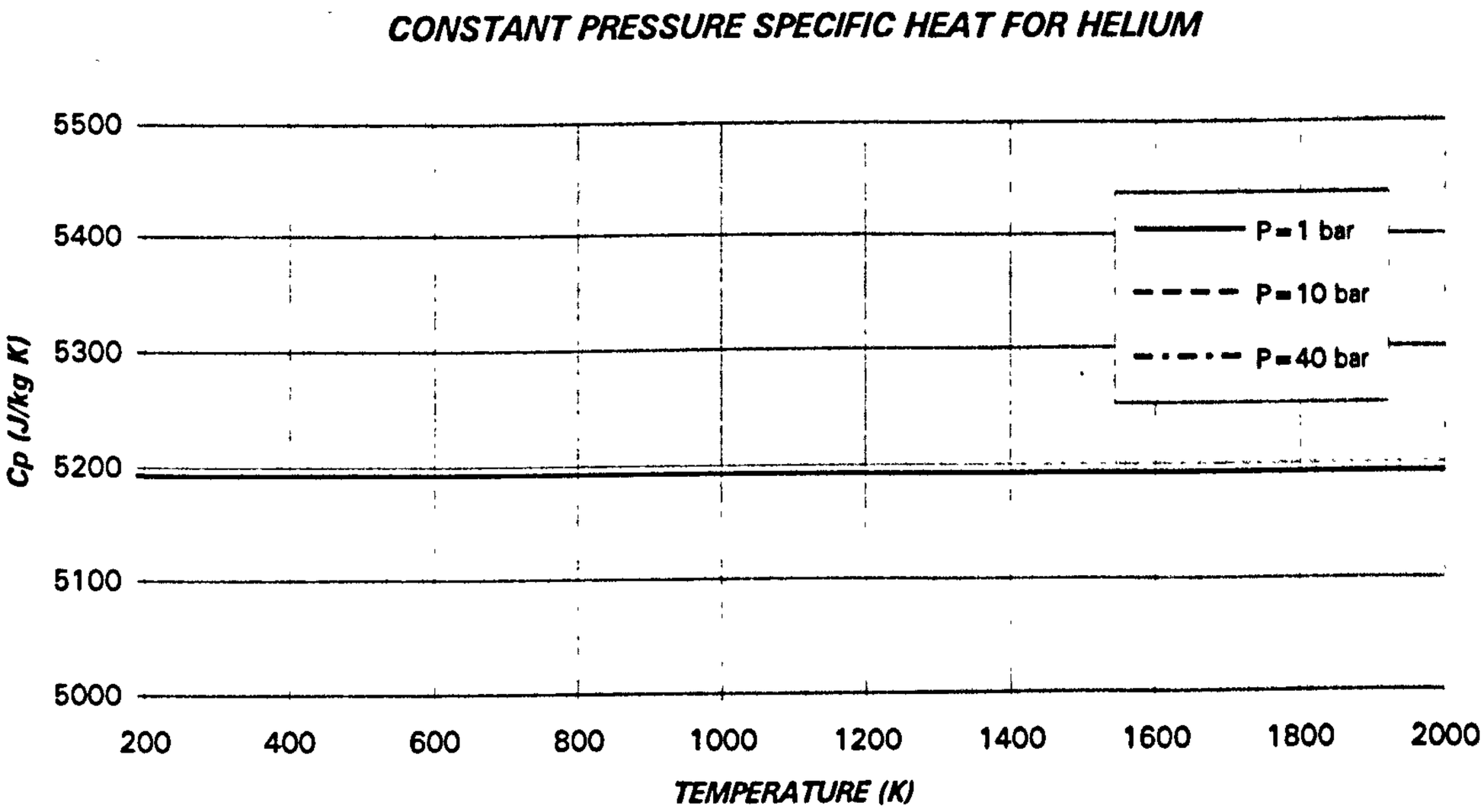

Figure 2.12. Constant pressure specific heat for helium at 1, 10 and 40 bars

2.2.7.6. Thermodynamic Properties of Hydrogen

TABLE 2.13A. CONSTANTS FOR HYDROGEN AT 1 BAR

a_0=1.2716 E04	a_1=9.4731 E00	a_2=-1.9290 E-02
a_3=1.8761 E-05	a_4=-7.9183 E-09	a_5=1.2276 E-12
a_6=-3.3185 E-18	a_7=1.2583 E05	a_8=-9.7873 E03

TABLE 2.13B. CONSTANTS FOR HYDROGEN AT 10 BAR

a_0=1.2533 E04	a_1=1.0948 E01	a_2=-2.2894 E-02
a_3=2.2514 E-05	a_4=-9.7064 E-09	a_5=1.5748 E-12
a_6=-1.7098 E-17	a_7=1.4305 E05	a_8=-1.8575 E05

TABLE 2.13C. CONSTANTS FOR HYDROGEN AT 40 BAR

a_0=1.2926 E04	a_1=9.1634 E00	a_2=-1.9765 E-02
a_3=1.9887 E-05	a_4=-8.6443 E-09	a_5=1.4026 E-12
a_6=-1.4050 E-17	a_7=9.6924 E04	a_8=-2.3589 E04

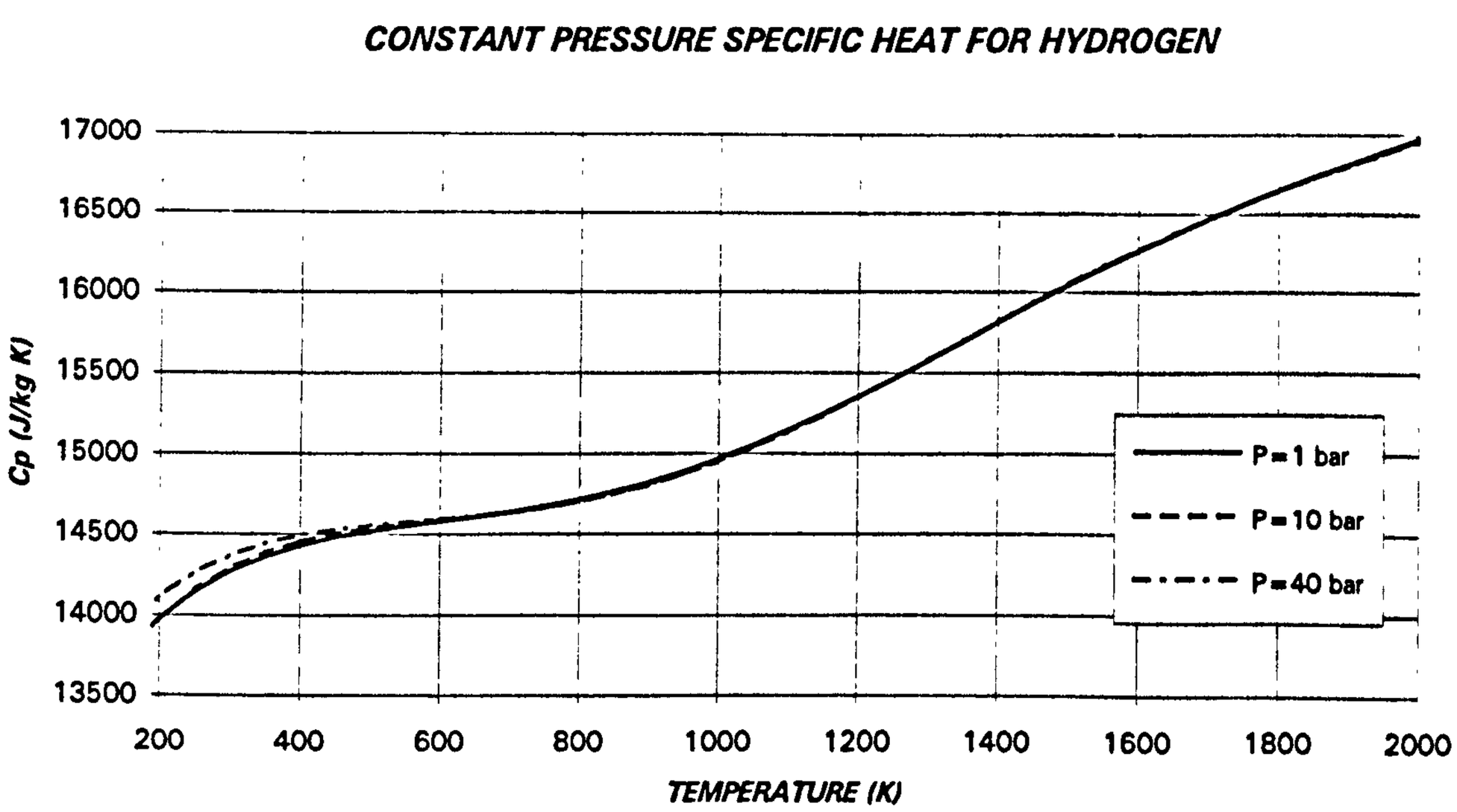

Figure 2.13. Constant pressure specific heat for hydrogen at 1, 10 and 40 bars

2.2.7.7. Thermodynamic Properties of Nitrogen

TABLE 2.14A. CONSTANTS FOR NITROGEN AT 1 BAR

a_0=1.1261E03	a_1=-6.5335 E-01	a_2=1.5330 E-03
a_3=-1.2095 E-06	a_4=4.2833 E-10	a_5=-5.7791 E-14
a_6=8.6364 E-20	a_7=-8.5332 E03	a_8=5.5542 E02

TABLE 2.14B. CONSTANTS FOR NITROGEN AT 10 BAR

a_0=-1.6844 E04	a_1=1.1438 E03	a_2=-2.9284 E-01
a_3=3.8508 E-04	a_4=-1.7118 E-07	a_5=2.8171 E-11
a_6=-4.5288 E-16	a_7=-2.4390 E02	

TABLE 2.14C. CONSTANTS FOR NITROGEN AT 40 BAR

a_0=-4.0259 E04	a_1=1.2253 E03	a_2=-3.9314 E-01
a_3=4.4285 E-04	a_4=-1.8492 E-07	a_5=2.8334 E-11
a_6=-1.7645 E-16	a_7=-1.0873 E03	

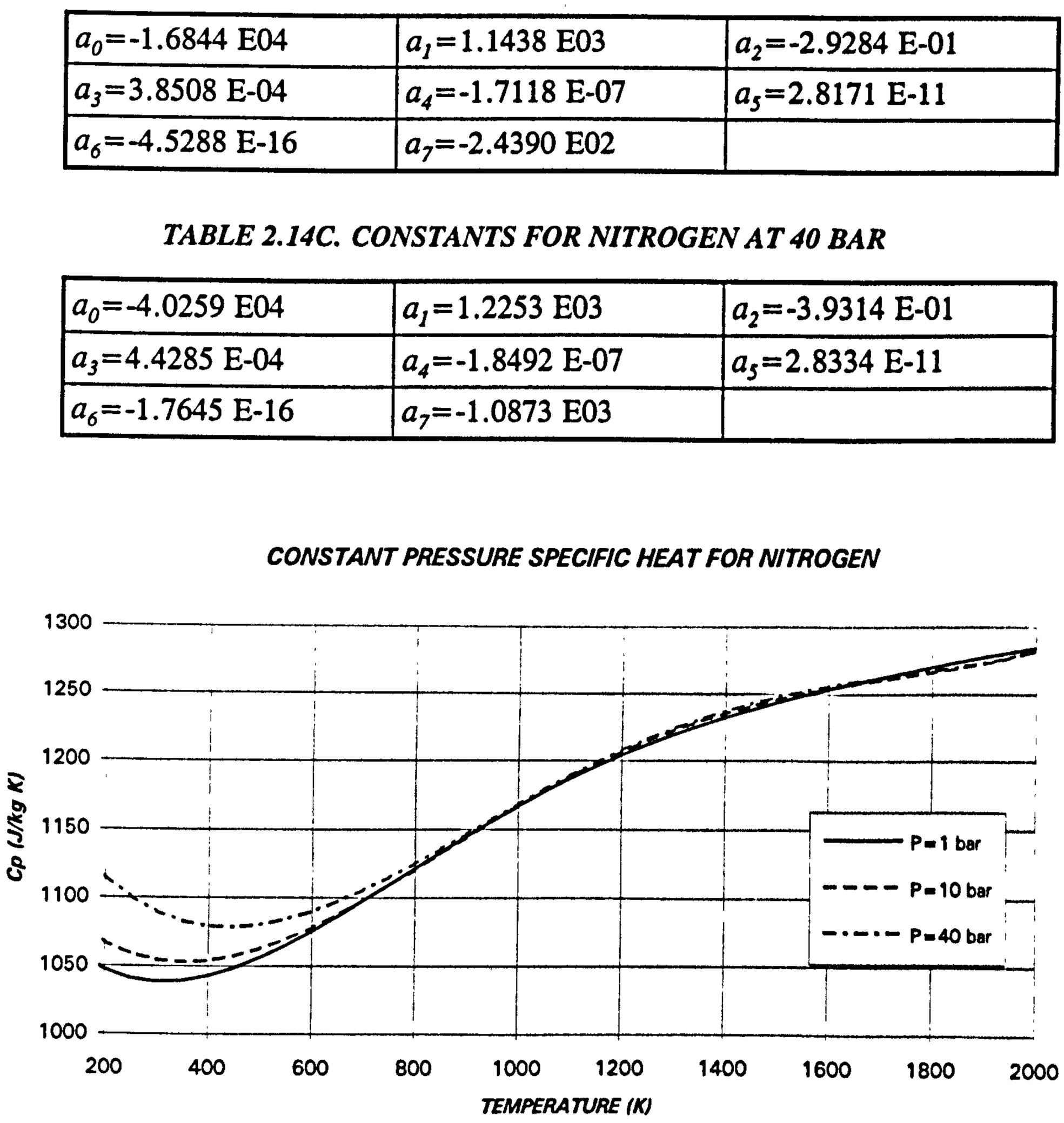

Figure 2.14. Constant pressure specific heat for nitrogen at 1, 10 and 40 bars

2.2.7.8. Thermodynamic Properties of Oxygen

TABLE 2.15A. CONSTANTS FOR OXYGEN AT 1 BAR

a_0=9.0012 E02	a_1=-1.8655 E-01	a_2=1.1492 E-03
a_3=-1.2147 E-06	a_4=5.2538 E-10	a_5=-8.2908 E-14
a_6=3.3399 E-19	a_7=3.1994 E03	a_8=1.2915 E03

TABLE 2.15B. CONSTANTS FOR OXYGEN AT 10 BAR

a_0=5.0559 E03	a_1=8.4345 E02	a_2=1.2505 E-01
a_3=4.1876 E-05	a_4=-4.4464 E-08	a_5=1.0047 E-11
a_6=-2.4590 E-16	a_7=9.1911 E02	

TABLE 2.15C. CONSTANTS FOR OXYGEN AT 40 BAR

a_0=-2.1415 E04	a_1=9.3653 E02	a_2=1.3420 E-03
a_3=1.2113 E-04	a_4=-6.7534 E-08	a_5=1.1894 E-11
a_6=-3.2348 E-17	a_7=7.1844 E01	

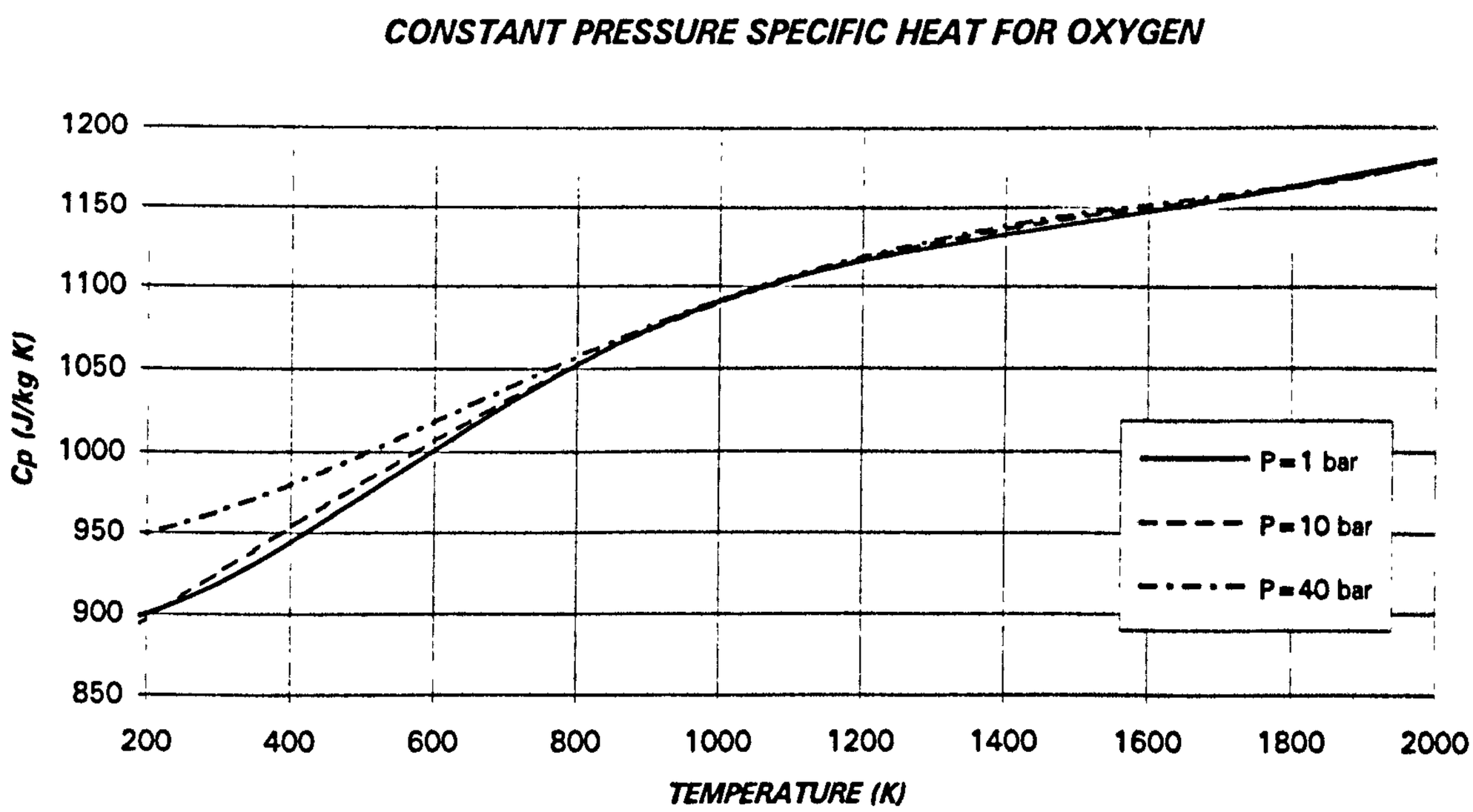

Figure 2.15. Constant pressure specific heat for oxygen at 1, 10 and 40 bars

2.2.7.9. Thermodynamic Properties of Water Vapour at Low Pressure

TABLE 2.16A. CONSTANTS FOR WATER VAPOUR AT 1 BAR

a_0=9.0012 E02	a_1=-1.8655 E-01	a_2=1.1492 E-03
a_3=-1.2147 E-06	a_4=5.2538 E-10	a_5=-8.2908 E-14
a_6=3.3399 E-19	a_7=3.1994 E03	a_8=1.2915 E03

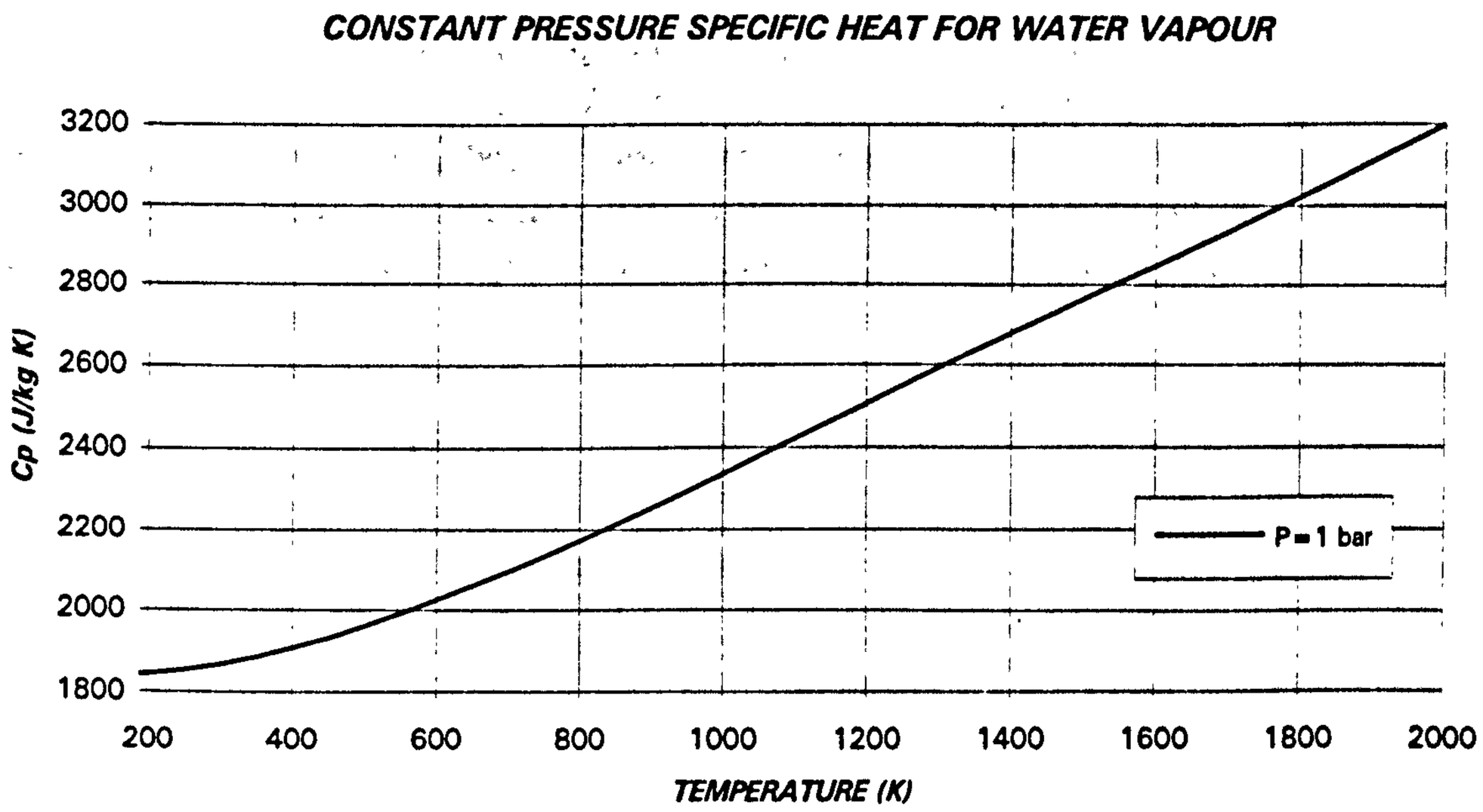

Figure 2.16. Constant pressure specific heat for water vapour at 1 bar

2.2.8. OPEN CYCLE WITH A GENERIC FUEL: MIXTURE OF GASES

When a generic fuel is used, the combustion products will be a combination of the gases considered in the previous section, mainly nitrogen, oxygen, carbon dioxide, argon and water vapour. Therefore, if the thermodynamic properties are calculated using a mixture of gases, almost any fuel could be easily simulated.

2.2.8.1. Thermodynamic Properties of Mixture of Gases

To evaluate the constant pressure specific heat, enthalpy and entropy of a mixture of gases the Dalton's Law is employed.

If the constant pressure specific heat is expressed, as a function of temperature, in the same way for all the gases of the mixture, as happen with air, argon, carbon monoxide, carbon dioxide, helium, nitrogen, oxygen and low pressure water vapour in the previous section, then it will be easy to write the enthalpy and phi with a unique expression. If the low pressure (1 bar) case is selected, C_P, H and Φ will be:

$$C_P = \sum_{j=0}^{j=6} a_j T^j \qquad [2.19]$$

$$C_P^{Mix} = \sum_{\forall i} x_i C_{P\,i} = \sum_{\forall i} x_i \left(\sum_{j=0}^{j=6} a_{ij} T^j \right) = \sum_{j=0}^{j=6} \left(\sum_{\forall i} x_i a_{ij} \right) T^j \qquad [2.20]$$

$$\begin{aligned} H^{Mix} &= H_0^{Mix} + \int_{T_0}^{T} \left(\sum_{\forall i} x_i C_{P\,i} \right) dT = H_0^{Mix} + \int_{T_0}^{T} \left(\sum_{\forall i} x_i \left(\sum_{j=0}^{j=6} a_{ij} T^j \right) \right) dT = \\ &= H_0^{Mix} + \sum_{j=0}^{j=6} \int_{T_0}^{T} \left(\sum_{\forall i} x_i a_{ij} \right) T^j dT = H_0^{Mix} + \sum_{j=0}^{j=6} \left(\sum_{\forall i} x_i a_{ij} \right) \frac{T^{j+1}}{j+1} \end{aligned} \qquad [2.21]$$

$$\begin{aligned} \Phi^{Mix} &= \Phi_0^{Mix} + \int_{T_0}^{T} \left(\sum_{\forall i} x_i C_{P\,i} \right) \frac{dT}{T} = \Phi_0^{Mix} + \int_{T_0}^{T} \left(\sum_{\forall i} x_i \left(\sum_{j=0}^{j=6} a_{ij} T^j \right) \right) \frac{dT}{T} = \\ &= \Phi_0^{Mix} + \sum_{j=0}^{j=6} \int_{T_0}^{T} \left(\sum_{\forall i} x_i a_{ij} \right) T^{j-1} dT = \Phi_0^{Mix} + \sum_{j=0}^{j=6} \left(\sum_{\forall i} x_i a_{ij} \right) \frac{T^j}{j} \end{aligned} \qquad [2.22]$$

Unfortunately, this situation will not be very frequent and, if the expressions are not the same, it will be necessary to unify them, using dummy coefficients for some terms:

$$C_P^{Mix} = \sum_{\forall i} x_i C_{P\,i} = \sum_{\forall i} x_i \left(\sum_{\forall j} a_{ij} f_j(T) \right) = \sum_{\forall j} \left(\sum_{\forall i} x_i a_{ij} \right) f_j(T) \qquad [2.23]$$

$$H^{Mix} = H_0^{Mix} + \int_{T_0}^{T} \sum_{\forall j} \left(\sum_{\forall i} x_i a_{ij} \right) f_j(T) dT \qquad [2.24]$$

$$\Phi^{Mix} = \Phi_0^{Mix} + \int_{T_0}^{T} \sum_{\forall j} \left(\sum_{\forall i} x_i a_{ij} \right) f_j(T) \frac{dT}{T} \qquad [2.25]$$

2.2.9. VALIDATION OF GAS MIXTURE METHOD

Dalton's law employed for gas mixtures is generally accepted for moderate pressures and temperatures. However, due to the great importance of the thermodynamic properties in the performance simulation codes, a validation exercise was made.

Three were the cases selected for this process: air at low pressure (figure 2.17) and stoichiometric mixture of air and kerosene (figure 2.18) and air at high pressure (figure 2.19). In all the cases the results were extremely good, giving small discrepancies between the initial constant pressure specific heat, from experimental results, and the one obtained as a mixture of individual gases.

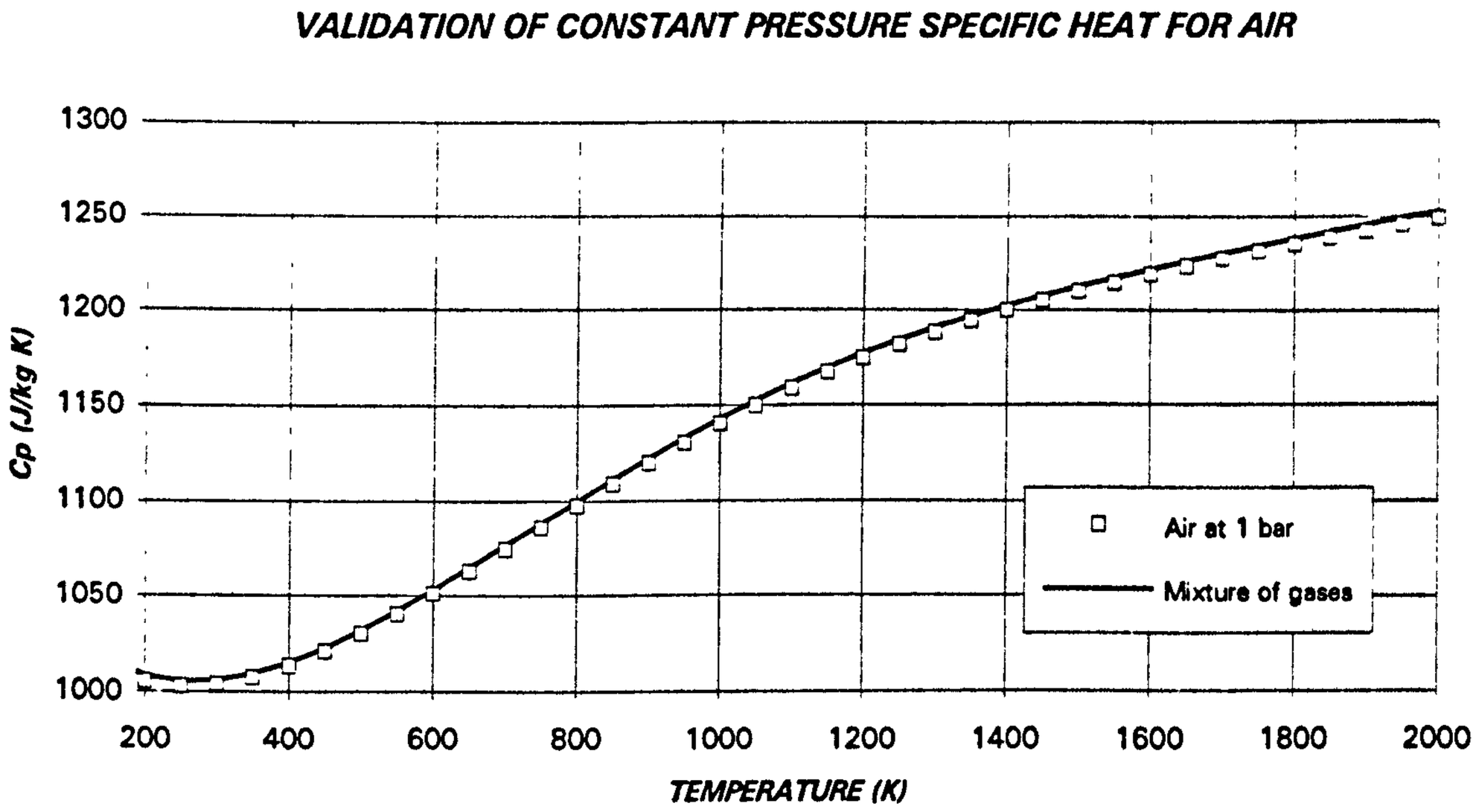

Figure 2.17. Constant pressure specific heat for air at low pressure. Validation of Dalton's Law

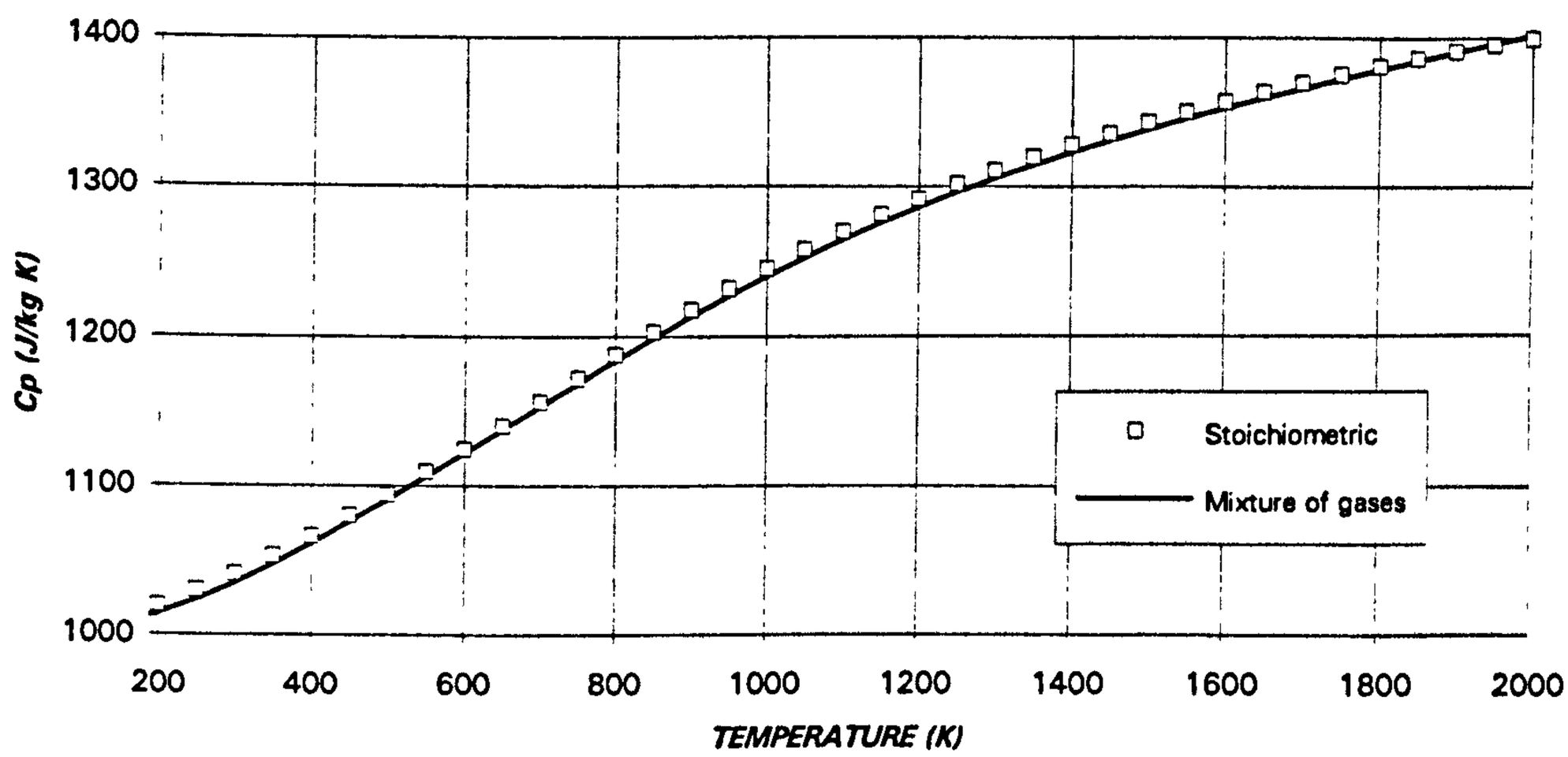

Figure 2.18. Constant pressure specific heat for kerosene combustion products.
Validation of Dalton's Law

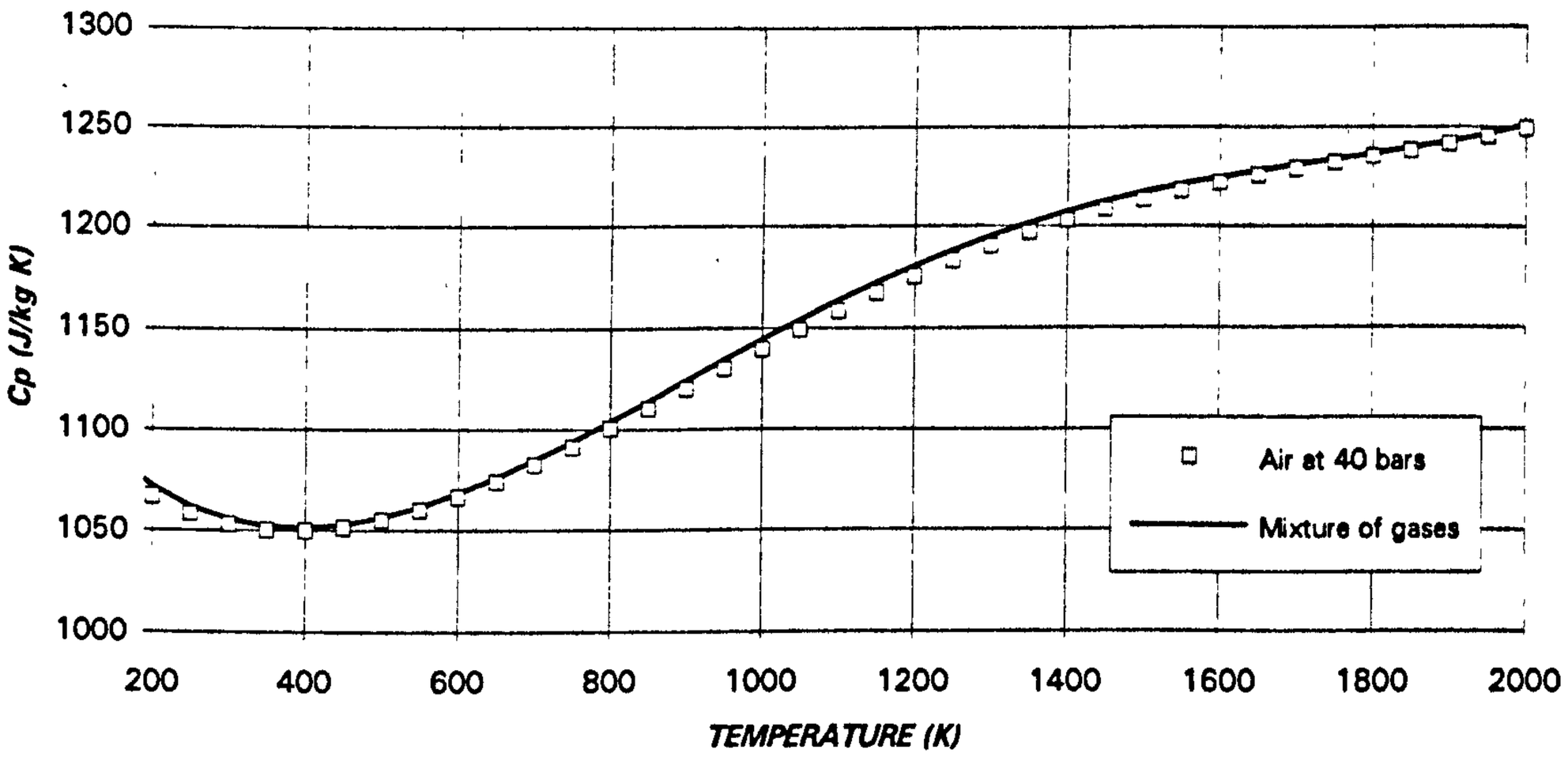

Figure 2.19. Constant pressure specific heat for air at high pressure.
Validation of Dalton's Law

2.3. TURBOMACHINERY CORRECTED PARAMETERS

Typically, turbomachinery maps are presented using non-dimensional mass flow, non-dimensional speed, pressure ratio or non-dimensional enthalpy and efficiency. However, in most cases, these terms cover just partially the Mach number similarity:

$$\text{Non dimensional mass flow} \quad \frac{W\sqrt{T}}{P}$$

$$\text{Non dimensional speed} \quad \frac{N}{\sqrt{T}}$$

$$\text{Non dimensional enthalpy} \quad \frac{\Delta H}{T}$$

Corrected mass flow, speed and enthalpy can also be employed:

$$\frac{W\sqrt{\theta}}{\delta}, \qquad \frac{N}{\sqrt{\theta}}, \qquad \frac{\Delta H}{\theta}$$

If the changes in the thermodynamic properties are relatively small, these approximations can be considered sufficient. In the case of closed cycles, comparison between cold flow tests and real engine behaviour or, in general, when the variation in thermodynamic properties are substantial, the full expression must be considered, as shown in refs. [32] and [75].

2.3.1. MASS FLOW CORRECTION FUNCTION

Non dimensional mass flow can be expressed as:

$$\frac{W\sqrt{T}}{AP} = \sqrt{\frac{\gamma}{R}} \frac{M_{AX}}{\left(1+\frac{\gamma-1}{2}M^2\right)^{\frac{\gamma+1}{2(\gamma-1)}}} \qquad [2.26]$$

Therefore, for two different conditions the flow correction factor, based on the Mach number similarity, will be

$$f_W = \sqrt{\frac{\gamma_2 R_1 T_1}{\gamma_1 R_2 T_2}} \frac{P_2}{P_1} \frac{\left(1+\frac{\gamma_1-1}{2}M^2\right)^{\frac{\gamma_1+1}{2(\gamma_1-1)}}}{\left(1+\frac{\gamma_2-1}{2}M^2\right)^{\frac{\gamma_2+1}{2(\gamma_2-1)}}} \qquad [2.27]$$

Typically, the Mach number term is neglected, as the error introduced is, most of the times, small enough. In figure 2.20, the ratio of both terms is shown for two cases:

- A change in the ratio of constant specific heats from 1.4 to 1.36, with the same gas constant, 287 J/kg K, entry temperatures of 300 and 475 K respectively and the same inlet pressure (CASE I)
- A change in the ratio of constant specific heats from 1.4 to 1.26, a variation in the gas constant from 287 to 189 J/kg K, the same entry temperature, 300 K, and the same inlet pressure (CASE II).

The Mach number will be changed between 0 and 1.

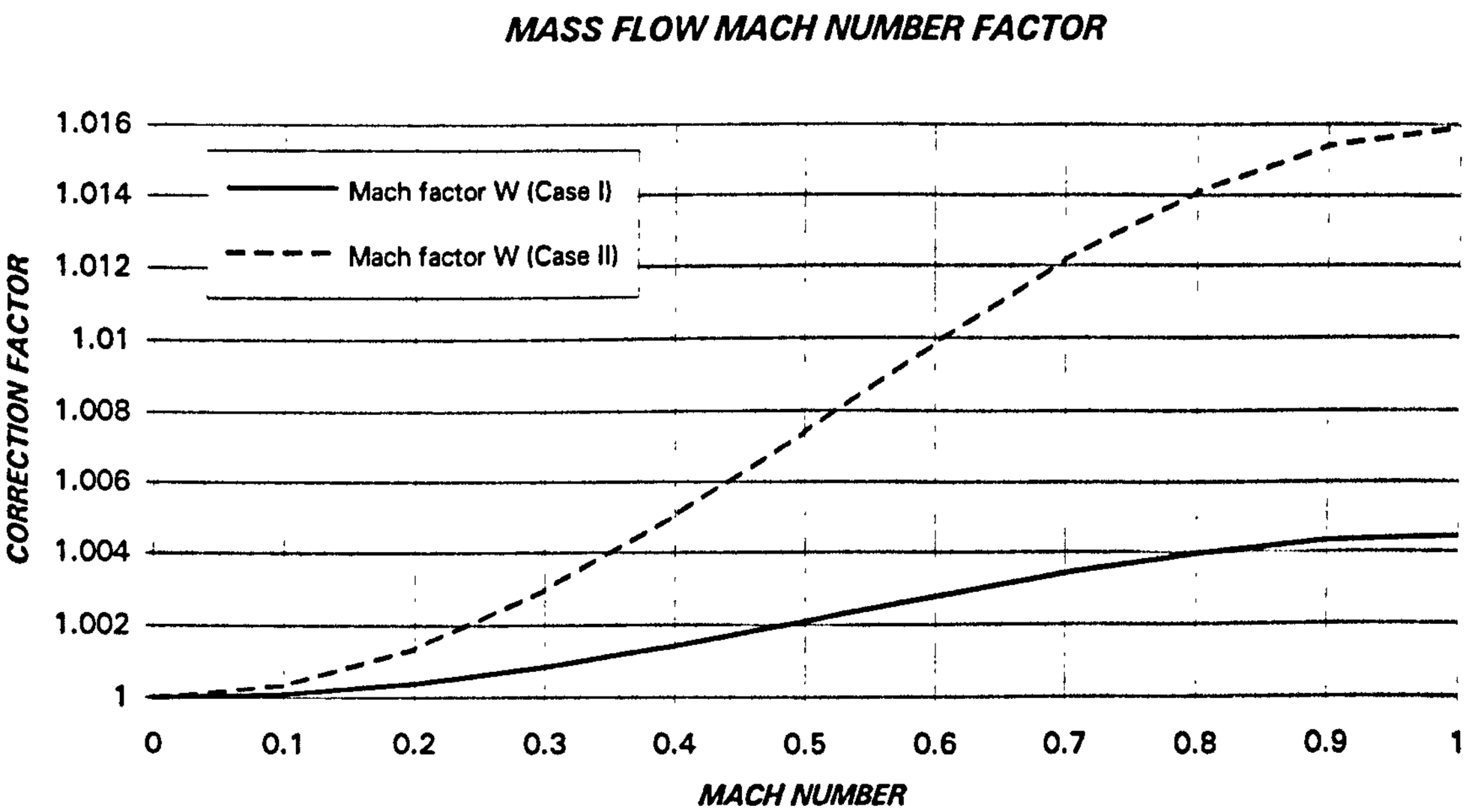

Figure 2.20. Mach number factor in the mass flow correction function

If the Mach number term is not considered or, in other words, its value is selected as zero, the flow correction factor will be:

$$f_W = \sqrt{\frac{\gamma_2 R_1 T_1}{\gamma_1 R_2 T_2}} \frac{P_2}{P_1} \qquad [2.28]$$

In many cases, to consider the Mach number terms, its value is assumed to be one. In turbomachinery simulation, specially in turbines, as the flow is close to sonic conditions, the error will be smaller than in the previous case, as demonstrated by Duponchel, Loisy and Carrillo [32]. The correction factor will then be:

$$f_W = \sqrt{\frac{\gamma_2 R_1 T_1}{\gamma_1 R_2 T_2}} \frac{P_2}{P_1} \frac{\left(\frac{\gamma_1 + 1}{2}\right)^{\frac{\gamma_1+1}{2(\gamma_1-1)}}}{\left(\frac{\gamma_2 + 1}{2}\right)^{\frac{\gamma_2+1}{2(\gamma_2-1)}}} \qquad [2.29]$$

The third option is to select a characteristic Mach number for each individual component, and employ the full expression:

$$f_W = \sqrt{\frac{\gamma_2 R_1 T_1}{\gamma_1 R_2 T_2}} \frac{P_2}{P_1} \frac{\left(1 + \frac{\gamma_1 - 1}{2} M_{DS}^{\ 2}\right)^{\frac{\gamma_1+1}{2(\gamma_1-1)}}}{\left(1 + \frac{\gamma_2 - 1}{2} M_{DS}^{\ 2}\right)^{\frac{\gamma_2+1}{2(\gamma_2-1)}}} \qquad [2.30]$$

The mass flow function will be, for the two cases described, as follows

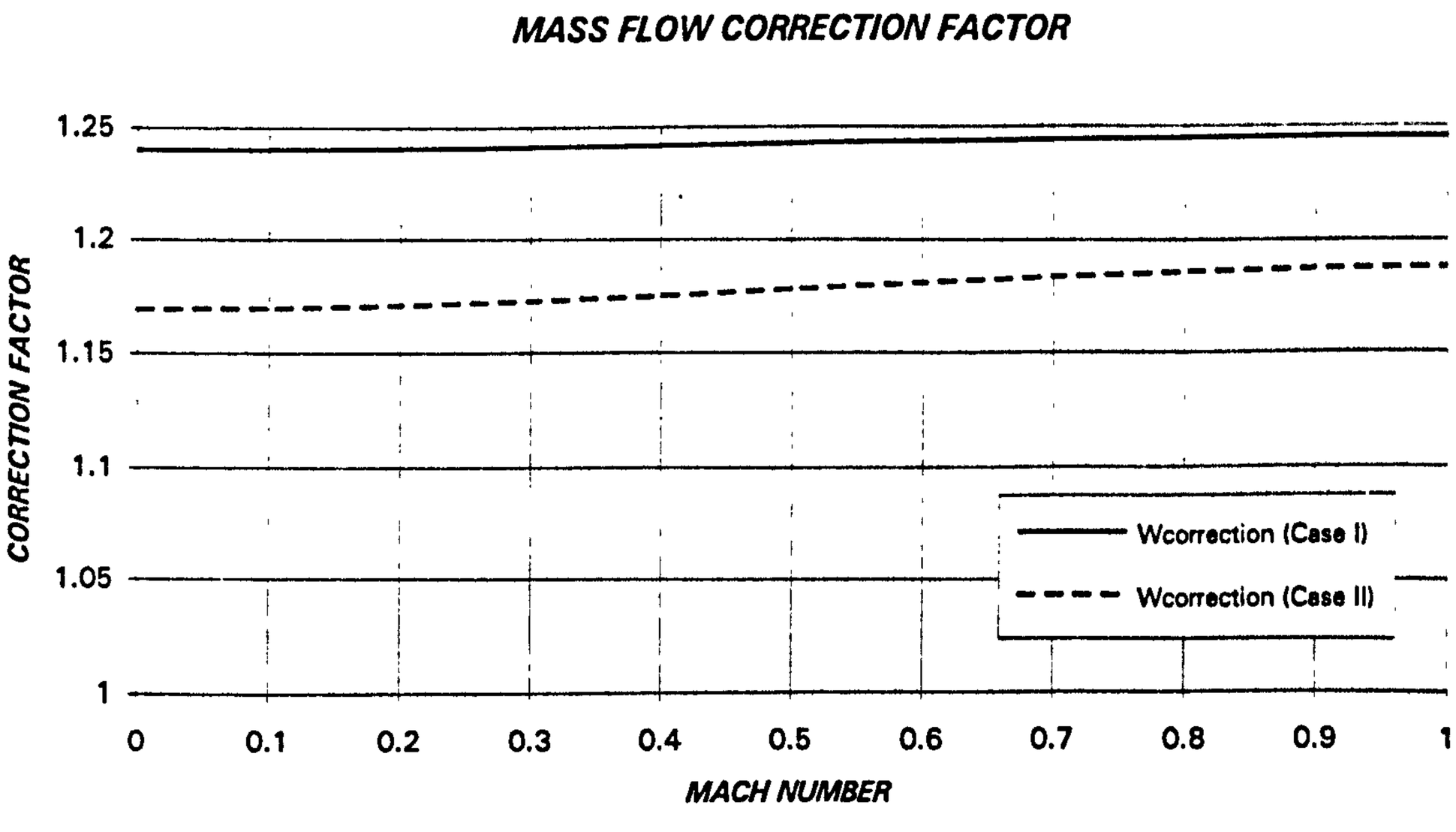

Figure 2.21. Mass flow correction function

2.3.2. SPEED CORRECTION FUNCTION

In a similar way as the corrected mass flow, the rotational speed, or circumferencial Mach number, can be written as:

$$M_\theta = 2\pi r \frac{N}{\sqrt{\gamma R t}} \qquad [2.31]$$

The speed correction factor can be expressed as:

$$f_N = \sqrt{\frac{\gamma_2 R_2 T_2}{\gamma_1 R_1 T_1} \frac{\left(1+\frac{\gamma_1 - 1}{2} M^2\right)}{\left(1+\frac{\gamma_2 - 1}{2} M^2\right)}} \qquad [2.32]$$

As in the previous case, the Mach number term is usually neglected, and the factor will be:

$$f_N = \sqrt{\frac{\gamma_2 R_2 T_2}{\gamma_1 R_1 T_1}} \qquad [2.33]$$

The error introduced by suppressing the Mach number term is plotted in the next figure for the cases specified in the previous section.

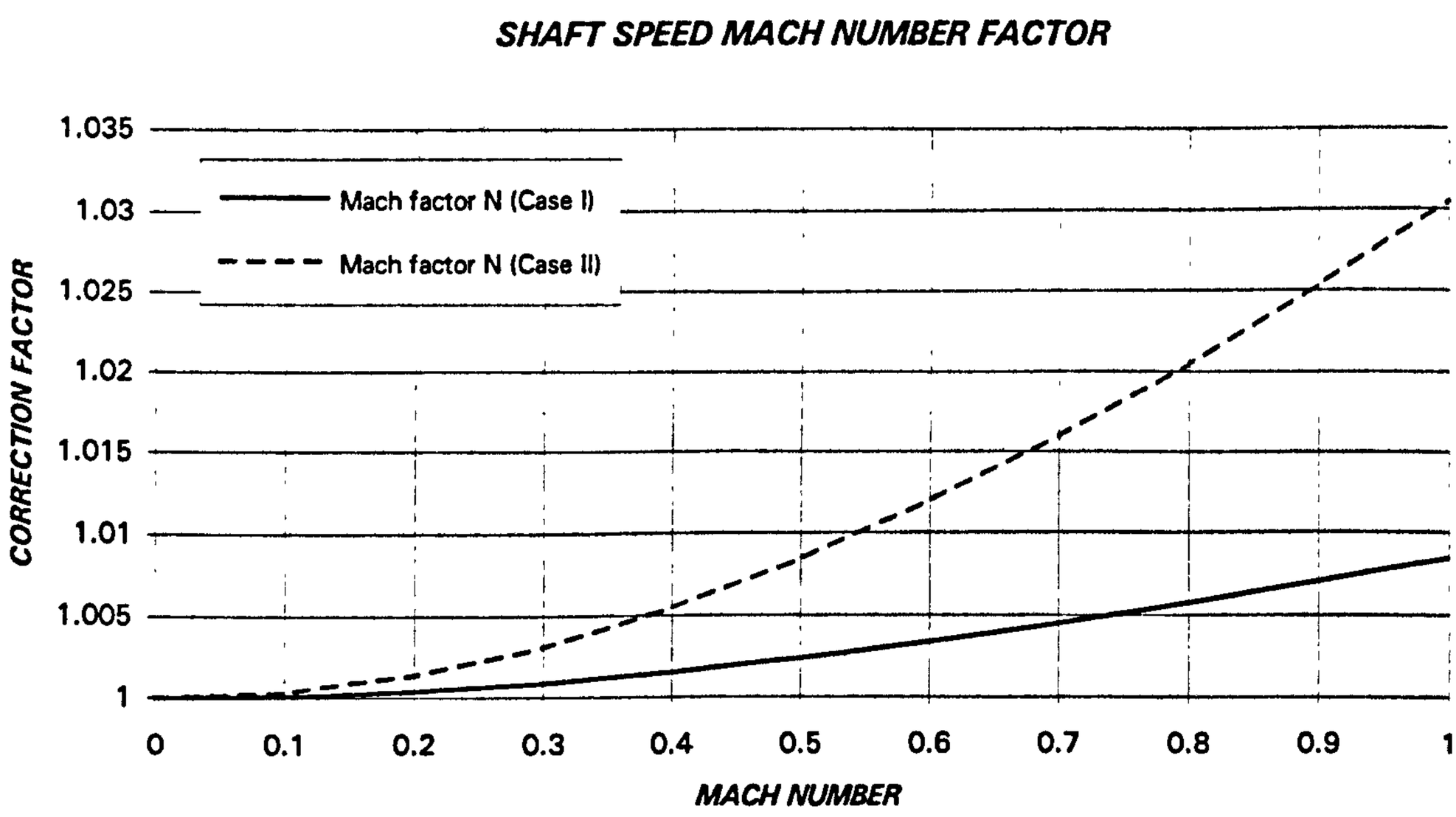

Figure 2.22. Mach number factor in the speed correction function

If the Mach number is taken as unity the speed factor will be:

$$f_N = \sqrt{\frac{\gamma_2 R_2 T_2}{\gamma_1 R_1 T_1} \frac{\gamma_1 + 1}{\gamma_2 + 1}} \qquad [2.34]$$

If the Mach number is selected for each component, the factor is:

$$f_N = \sqrt{\frac{\gamma_2 R_2 T_2}{\gamma_1 R_1 T_1} \frac{\left(1 + \frac{\gamma_1 - 1}{2} M_{DS}^2\right)}{\left(1 + \frac{\gamma_2 - 1}{2} M_{DS}^2\right)}} \qquad [2.35]$$

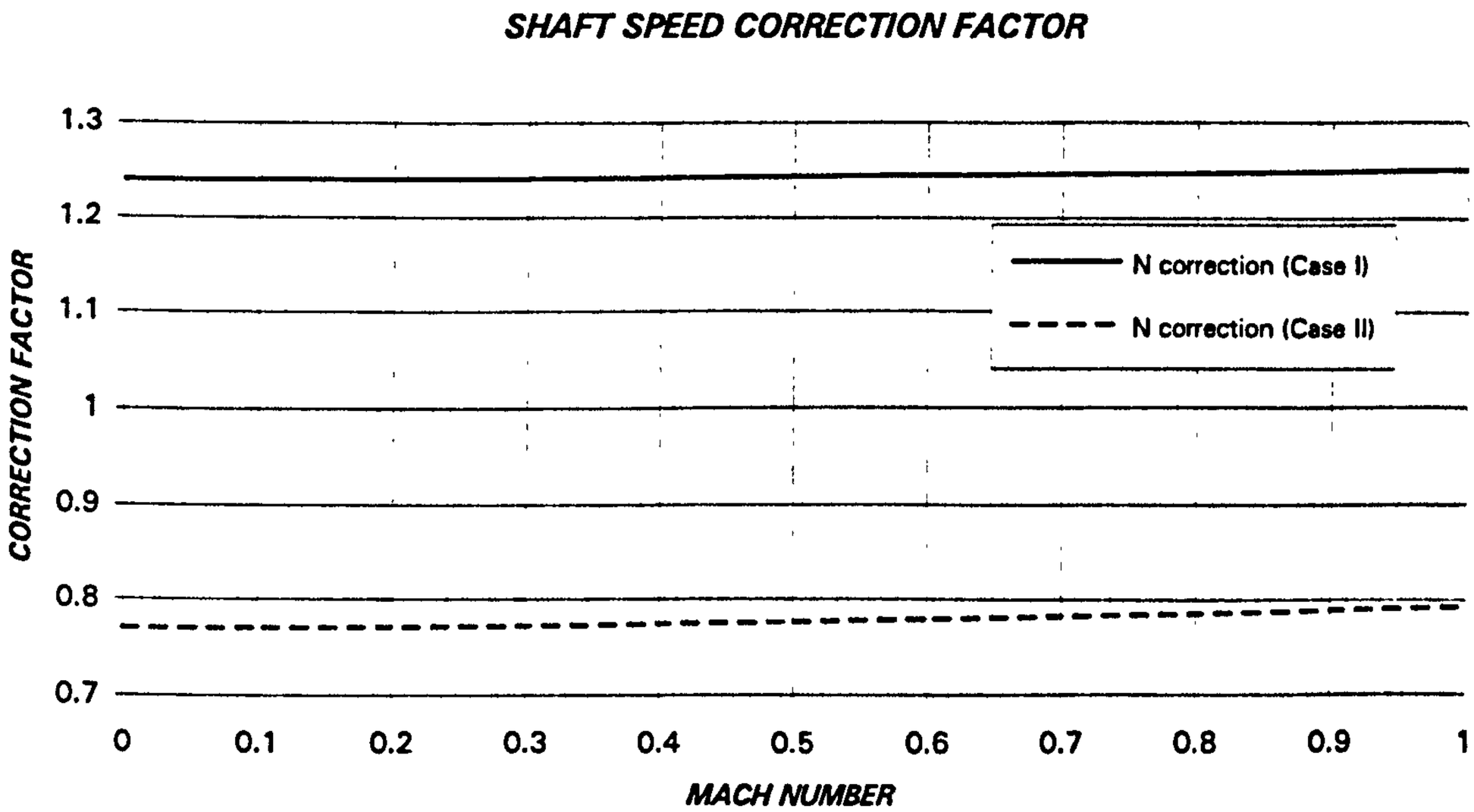

Figure 2.23. Speed correction function

2.3.3. SPECIFIC WORK CORRECTION FUNCTION

The specific work is proportional to rotational velocity squared. Hence, the terms will be, when neglecting the Mach number term, selecting the Mach number as unity or considering a design Mach number, as follows:

$$f_{\Delta H} = \frac{\gamma_2 R_2 T_2}{\gamma_1 R_1 T_1} \qquad [2.36]$$

$$f_{\Delta H} = \frac{\gamma_2 R_2 T_2}{\gamma_1 R_1 T_1} \frac{\gamma_1 + 1}{\gamma_2 + 1} \qquad [2.37]$$

$$f_{\Delta H} = \frac{\gamma_2 R_2 T_2}{\gamma_1 R_1 T_1} \frac{\left(1 + \frac{\gamma_1 - 1}{2} M_{DS}^{\ 2}\right)}{\left(1 + \frac{\gamma_2 - 1}{2} M_{DS}^{\ 2}\right)} \qquad [2.38]$$

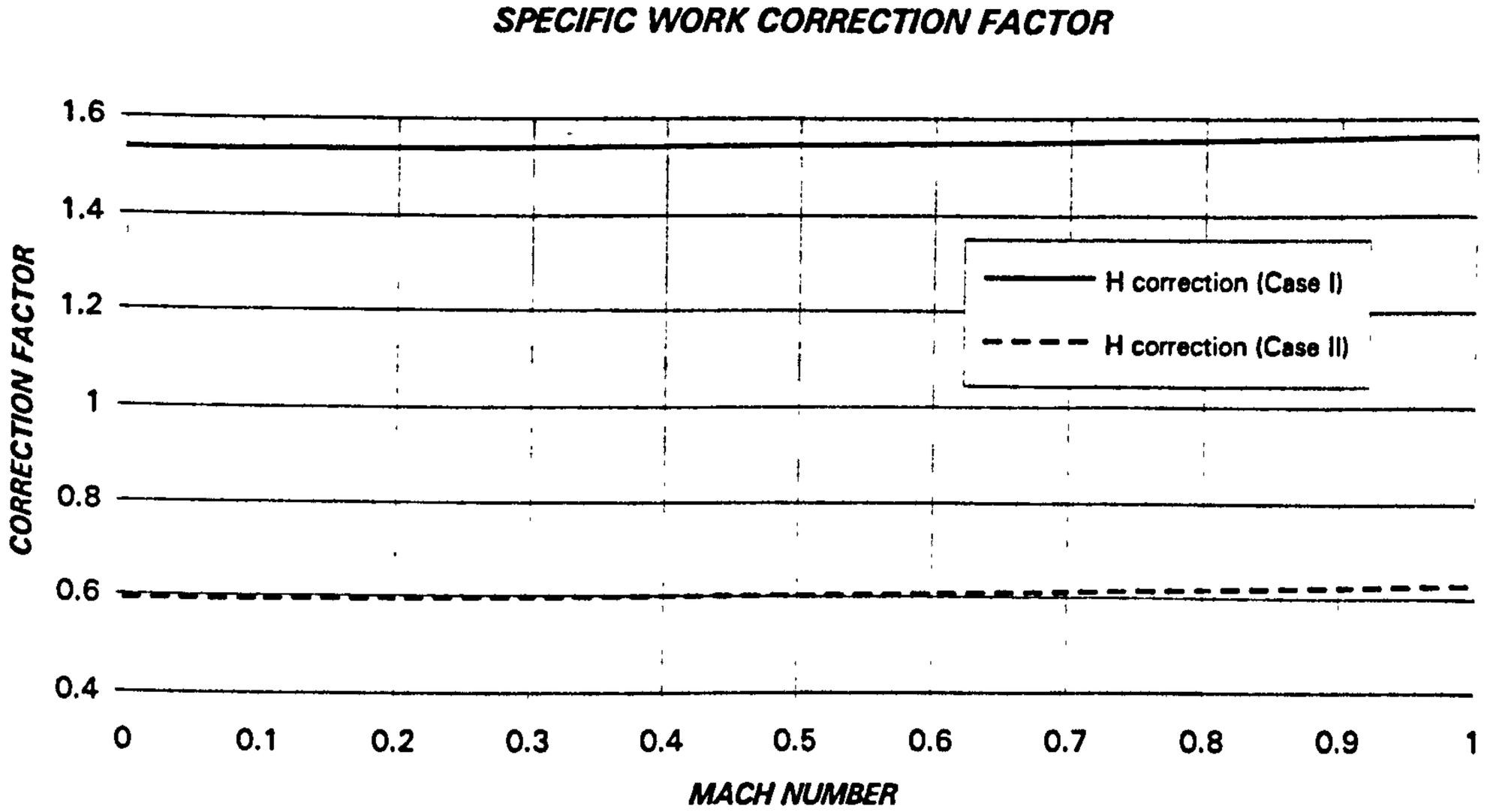

Figure 2.24. Specific work correction function

2.3.4. PRESSURE RATIO CORRECTION FUNCTION

The correction for the pressure ratio will be derived from the combination of specific work and efficiency, which has no correction function.

First, the isentropic enthalpy change, therefore the isentropic temperature, will be calculated. Then, using the isentropic process definition, the pressure ratio is found.

$$\eta = \frac{\Delta H}{\Delta H_{IS}} \qquad [2.39]$$

$$0 = \int_{T_1}^{T_{IS}} C_P \frac{dT}{T} - R \ln \frac{P_2}{P_1} \qquad [2.40]$$

CHAPTER 3

COMPONENT SIMULATION IN GTSI PERFORMANCE CODE

3.1. INTRODUCTION

The main objectives of the code are the realistic design and off-design performance calculations of most existing gas turbines, with projection for future power plants, together with implementing easily changes of different models in the modules.

One, two and three spool machines, with the option for a booster in the low pressure shaft (in the one and two spool cases), plus the possibility of adding an additional shaft for the free power turbine will constitute the skeleton of the programme.

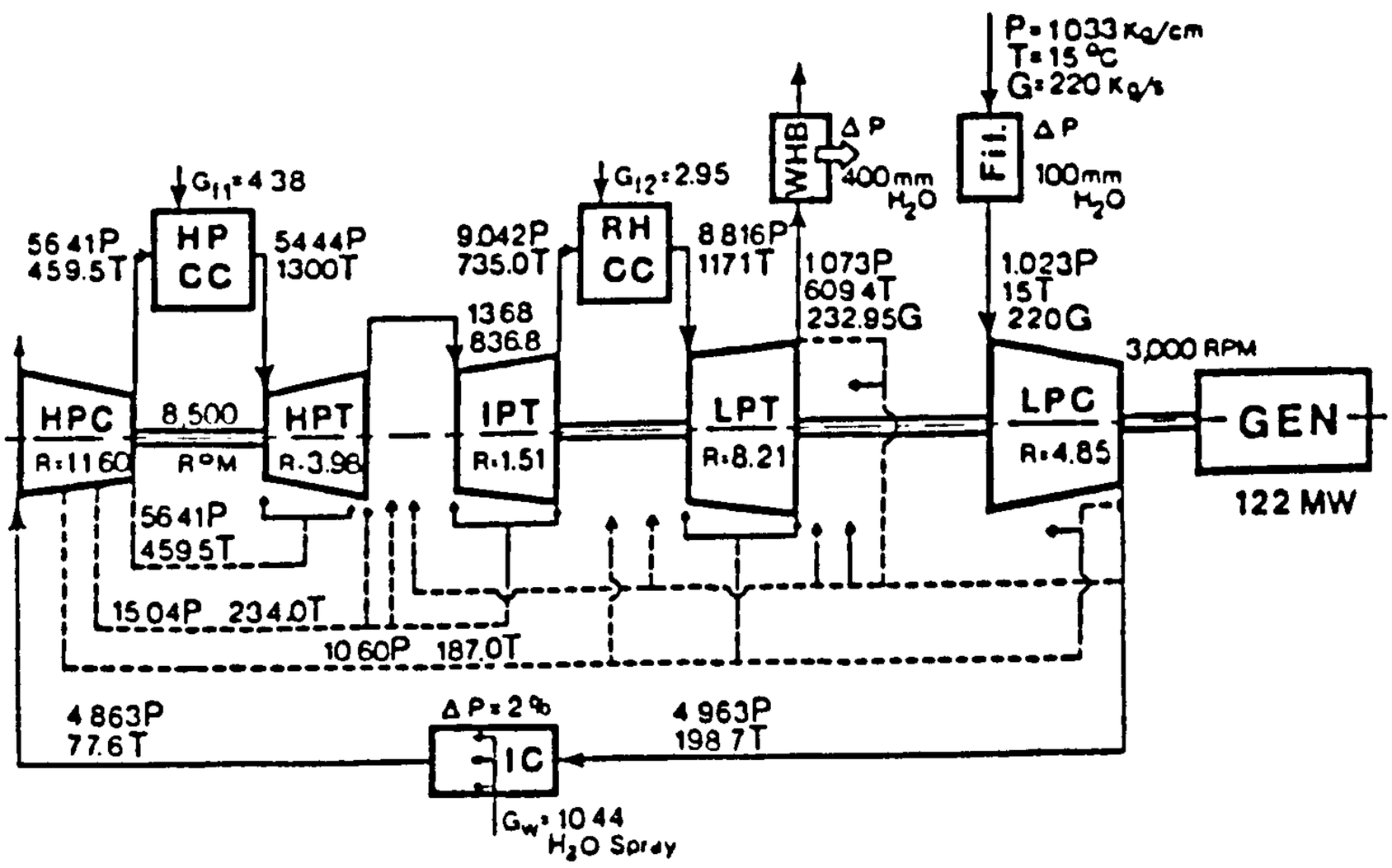

Figure 3.1. AGTJ-100A arrangement

Models for traditional components, such as the inlet, compressor and booster, turbine, combustion chamber, heat exchangers, regenerator and exhaust nozzle were developed. In addition, evaporative cooler[1], steam injection system[2], reheat[3], steam

---

1 One of the methods used as an intercooler is the evaporative cooler, where water is added to a hot stream. The cooling limit is reached when the relative humidity of the stream is 100%.

2 This system is becoming more and more popular, and several manufacturers have included this option in their standard machines. An increase in efficiency and power output, together with a very important reduction of NO_x emissions, make this system very competitive.

3 During the last decade at least two reheat gas turbines have been tested at full scale. The Japanese AGTJ-100A/B did not enter in production but the ABB GT24/GT26 are already in service. The complexity introduced by the reheat is impressive, but the advantages of very high specific power output, together with the suitability combined cycle application, make this system very attractive.

generator and bottoming cycle[4] models are necessary for industrial gas turbine simulation. An example that merges most of these features is the Japanese Moon Light Project [57], [90] and [127], where two advanced prototype gas turbines, the AGTJ-100A and AGTJ-100B, were built for on-site testing . The arrangement of this twin spool reheat gas turbine is shown in figure 3.1.

The transient capabilities, [32], [62], [69], [84], [114], [115], [120] and [121], have not been mentioned in detail. The main reason, outlined in the first chapter, is the lack of experimental data for validation. Also, some characteristics of the engines, such as shafts inertia, speeds, fuel and variable geometry schedules, acceleration / deceleration limits, etc., are not known. The transient simulation of heat exchangers has also been simplified. Accurate models for heat transfer must be developed, in order to obtain, in a realistic way, the behaviour of the gas turbine. In figure 3.2 the transient operation of a regenerative machine, with and without detailed simulation of the regenerator is presented. It can be appreciated that the presence of heat exchangers causes a very important modification in transient performance due to the different characteristic time response of the turbomachinery and the heat exchanger. If the acceleration/deceleration is slow enough to allow regenerator heat soakage, the transient and steady state simulations will be basically the same.

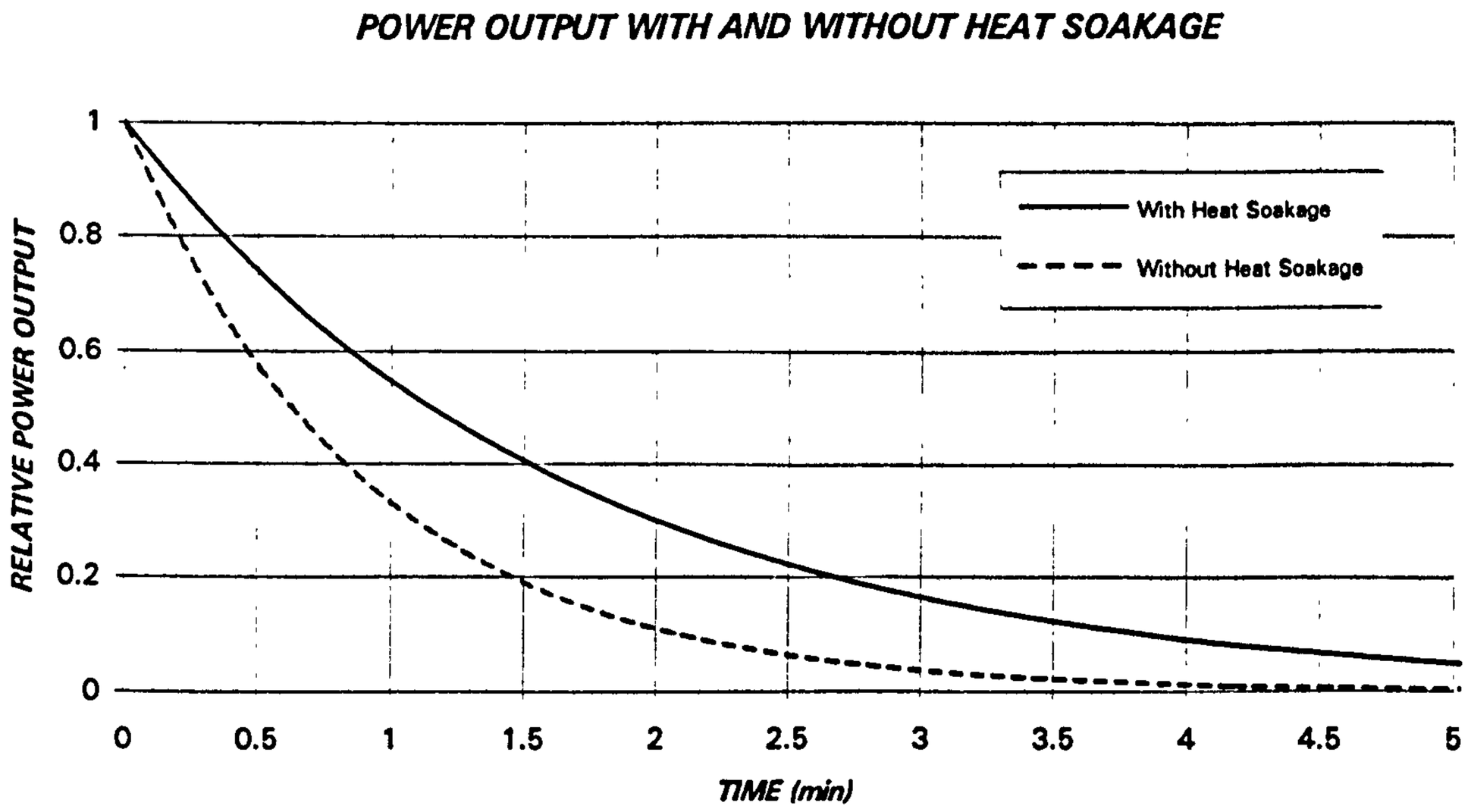

Figure 3.2. Transient operation of a regenerative gas turbine with and without detailed simulation of the heat exchanger.

[4] As shown in the first chapter, the efficiencies achieved by the combined cycles are in the range of 55%-60% and the target of 65% seems possible in the next few years. Hence, the simulation of the bottoming cycle, although not in detail, will be very useful.

3.2. INLET

Industrial gas turbine inlet generates pressure losses due to the bell-mouth inlet, acoustic silencers and other installation devices. These could be included as part of this system for analysis. Further details are given in [72], [75], [83] and [97].

Less frequent is the use of anti-icing valves. When this system is in operation the valves are open, and a bleed from the compressor is introduced, with the consequent increase in inlet temperature. The inlet pressure will not be substantially affected, as this flow is relatively small compared with the main flow.

The static/total pressure and temperature profile measurement in a section of given area is very important for the analysis of mass flow calculation.

3.2.1. INLET DESIGN POINT SIMULATION

The generic equations which model the inlet at design point (mass flow, species, momentum and energy conservation) are:

$$W_2 = W_1 + W_{anti-icing} = W_0 + W_{anti-icing} \qquad [3.1a]$$

$$x_2^i = \frac{x_1^i W_1 + x_{anti-icing}^i W_{anti-icing}}{W_1 + W_{anti-icing}} = \frac{x_0^i W_0 + x_{anti-icing}^i W_{anti-icing}}{W_0 + W_{anti-icing}} \qquad [3.2a]$$

$$P_2 = P_1\left(1 - \frac{\Delta P_{bell-mouth}^{DS}}{P_1}\right) = P_0\left(1 - \frac{\Delta P_{silencer}^{DS}}{P_0} - \frac{\Delta P_{other}^{DS}}{P_0}\right)\left(1 - \frac{\Delta P_{bell-mouth}^{DS}}{P_1}\right) = \qquad [3.3a]$$
$$= P_0\left(1 - \pi_{silencer}^{DS} - \pi_{other}^{DS}\right)\left(1 - \pi_{bell-mouth}^{DS}\right)$$

$$H_2 = \frac{(W_1 H_1 + W_{anti-icing} H_{anti-icing})}{W_1 + W_{anti-icing}} = \frac{(W_0 H_0 + W_{anti-icing} H_{anti-icing})}{W_0 + W_{anti-icing}} \qquad [3.4a]$$

The compressor inlet flow composition can be different from the upstream station if the anti-icing bleed employed has different species (i.e. flow extracted from the exit of the high pressure compressor with evaporative intercooler between LPC and HPC).

However, in most cases, there will be no mass flow addition across the inlet, and the installation losses (silencer,...) will not be considered, simplifying the equations above:

$$W_2 = W_1 = W_0 \qquad [3.1b]$$

$$x_2^i = x_1^i = x_0^i \qquad [3.2b]$$

$$P_2 = P_1\left(1-\frac{\Delta P^{DS}_{bell-mouth}}{P_1}\right) = P_0\left(1-\frac{\Delta P^{DS}_{bell-mouth}}{P_1}\right) = P_0\left(1-\pi^{DS}_{bell-mouth}\right) \qquad [3.3b]$$

$$H_2 = H_1 = H_0 \qquad [3.4b]$$

At design, the mass flow and inlet area (or desired Mach number) will be known, calculating the static temperature, static pressure and Mach number (or inlet area) from the following equations:

$$t_1 = \frac{T_1}{1+\frac{\gamma_1-1}{2}M_1^2} \qquad [3.5]$$

$$p_1 = \frac{P_1}{\left(1+\frac{\gamma_1-1}{2}M_1^2\right)^{\frac{\gamma_1}{\gamma_1-1}}} \qquad [3.6]$$

$$W_1 = \frac{A_1P_1}{\sqrt{T_1}}\sqrt{\frac{\gamma_1}{R_1}}\frac{M_1}{\left(1+\frac{\gamma_1-1}{2}M_1^2\right)^{\frac{\gamma_1+1}{2(\gamma_1-1)}}} \qquad [3.7]$$

The same equations can be employed to evaluate the variables at station 2 (compressor inlet face). However, as the Mach number at this station can be high, the exact thermodynamic relations were employed:

$$H_2 = h_2 + \frac{1}{2}V_2^2 = h_2 + \frac{1}{2}\gamma_2R_2t_2M_2^2 \qquad [3.8]$$

$$\Delta S_2 = 0 = (\Phi_{T_2} - \phi_{t_2}) - R_2 ln\frac{P_2}{p_2} \qquad [3.9]$$

$$W_2 = \rho_2V_2A_2 = \frac{p_2}{R_2t_2}\sqrt{\gamma_2R_2t_2}M_2A_2 \qquad [3.10]$$

For open cycles the water air ratio is given at station 0 (ambient). The calculation of the water air mixture properties at the static temperature of the flow can be performed in the following way (for station 2 analogous expressions will be obtained):

$$C_{P1} = \frac{C_{P1\,Dry\,Gas}(1+FAR_1)+C_{P1\,Vapor}WAR_1}{1+FAR_1+WAR_1} \qquad [3.11]$$

$$H_1 = \frac{H_{1\,Dry\,Gas}(1+FAR_1)+H_{1\,Vapor}WAR_1}{1+FAR_1+WAR_1} \qquad [3.12]$$

$$\Phi_1 = \frac{\Phi_{1\,Dry\,Gas}(1+FAR_1)+\Phi_{1Vapor}WAR_1}{1+FAR_1+WAR_1} \qquad [3.13]$$

$$R_1 = \frac{8314.5}{\frac{1+FAR_1+WAR_1}{\frac{1+FAR_1}{MW_{Dry\,Gas}}+\frac{WAR_1}{MW_{H_2O}}}} \qquad [3.14]$$

The fuel to air ratio at this section has been included to consider the possibility of hot gas recirculation, although in most cases the value will be zero.

If the areas at sections 1 and/or 2 are not known, reasonable values of the Mach numbers could be assumed to be able to determine the static temperature, lower than the total one, and, therefore, more prone to condensation. The presence of liquid water can be a problem, specially for the quality of the measurements.

3.2.2. OFF-DESIGN PERFORMANCE OF THE INLET

The mass flow, momentum and energy continuity equations are valid for both, design and off-design cases. The areas will be known, either because they have been given as design values or because they have been calculated from the Mach number. Therefore, the only unknown will be the total pressure drop.

The losses, accounting for turbulence and friction, will be known at design stage. At off-design the value will be calculated using the hypothesis that these losses are proportional to velocity square. For example, the bell-mouth inlet pressure drop could be expressed as follows:

$$\frac{\Delta P_{1-2}}{P_1} = \frac{\Delta P_{1-2}}{q_1}\frac{R_1}{2}\left(\frac{W_1\sqrt{T_1}}{A_1P_1}\right)^2 \qquad [3.15]$$

The dynamic head pressure losses are assumed to remain constant over a wide range of operating conditions. Equation [3.16] represents this:

$$\frac{\Delta P_{1-2}}{P_1} = K'_1\left(\frac{W_1\sqrt{T_1}}{A_1P_1}\right)^2 \qquad [3.16]$$

In this study the gas constant has not changed. This approximation is good enough for most cases. However, if during the off-design of a closed cycle there is a change in the working fluid, the value of R_I can be significantly different from the design point.[5] But in this situation, the assumption made in the previous paragraph can not be considered correct. Therefore, the suppression of the gas constant is just another simplification. Inlet distortion, which modifies inlet and compressor operation (mainly surge margin), as shown in [75] and [83], has not been introduced.

3.3. COMPRESSOR

Low, intermediate and high pressure compressors can be simulated using the same equations, with the only differences being the cooling bleeds, extracted typically from the high pressure compressor and, may be, the working fluid.

In this section the high pressure compressor, with two intermediate bleeds, will be considered.[6] The entry flow (engine section 25) can have large quantities of water, caused by the evaporative coolers. At engine section 253 there will be a flow extraction for power turbine cooling and at section 255 for the low pressure turbine. In addition to the blade, vane, disc and casing cooling, these flows are also employed for turbine interstage sealing. The amount and pressure of the bleed flows must be high enough to avoid hot gas ingestion into the internal air system through the turbine.[7] This subject will be considered in chapter 5, devoted to blade cooling.

At design stage there will be four possibilities of giving the input data:

- Pressure ratio and isentropic (adiabatic) efficiency data (CASE I):

$$\pi_{HPC} = \frac{P_3}{P_{25}} \qquad \eta_{is\,HPC} = \eta_{is\,25-3}$$

- Pressure ratio and polytropic efficiency data (CASE II):

$$\pi_{HPC} = \frac{P_3}{P_{25}} \qquad \eta_{poly\,HPC} = \eta_{poly\,25-3}$$

---

[5] This situation will occur in the semi-closed cycle exercise carried out in chapter 9, when the gas turbine working fluid changes from air (gas constant 287 J/kg K) to carbon dioxide-argon (gas constant 188 J/kg K).

[6] The use of inter-compressor anti surge valves has not been considered in this section, although GTSI has the possibility to switch on this mode of operation.

[7] If hot air ingestion takes place, the life of some turbine components could be drastically reduced, therefore it must be avoided. This is one of the key factors for the engine internal air system design and analysis.

- Increase in corrected enthalpy and isentropic efficiency data (CASE III):

$$\frac{\Delta H_{HPC}}{(\gamma R\theta)_{HPC}} = \frac{\Delta H_{25-3}}{\gamma_{25} R_{25} \theta_{25}} \qquad \eta_{is\,HPC} = \eta_{is\,25-3}$$

- Increase in corrected enthalpy and polytropic efficiency data (CASE IV):

$$\frac{\Delta H_{HPC}}{(\gamma R\theta)_{HPC}} = \frac{\Delta H_{25-3}}{\gamma_{25} R_{25} \theta_{25}} \qquad \eta_{poly\,HPC} = \eta_{poly\,25-3}$$

3.3.1. COMPRESSOR DELIVERY TEMPERATURE AND PRESSURE IF ISENTROPIC EFFICIENCY AND PRESSURE RATIO ARE GIVEN (CASE I)

If the isentropic efficiency and pressure ratio are given, the exit temperature can be calculated using the procedure described below.

The definition of isentropic efficiency is:

$$\eta_{25-3} = \frac{\Delta H^{IS}_{25-3}}{\Delta H_{25-3}} = \frac{\int_{T_{25}}^{T_3^{IS}} C_P dT}{\int_{T_{25}}^{T_3} C_P dT} \qquad [3.17]$$

therefore:

$$\int_{T_{25}}^{T_3} C_P dT = \frac{1}{\eta_{25-3}} \int_{T_{25}}^{T_3^{IS}} C_P dT \qquad [3.18]$$

If the isentropic exit temperature is determined, the real exit temperature will be found using an iterative procedure.

The Gibbs equation gives:

$$TdS = dH - \frac{1}{\rho} dP \qquad [3.19]$$

and for the complete compression process

$$\int_{T_{25}}^{T_3} dS = \int_{T_{25}}^{T_3} \frac{1}{T} dH - \int_{P_{25}}^{P_3} \frac{1}{T\rho} dP \qquad [3.20]$$

expressing dH as a function of T and ρ as a function of P, T and R

$$S_3 - S_{25} = \int_{T_{25}}^{T_3} C_P \frac{dT}{T} - \int_{P_{25}}^{P_3} \frac{R}{P} dP \qquad [3.21]$$

if R is constant the following expression is finally obtained:

$$S_3 - S_{25} = \int_{T_{25}}^{T_3} C_P \frac{dT}{T} - R_{25}\, Ln \frac{P_3}{P_{25}} = (\Phi_3 - \Phi_{25}) - R_{25}\, Ln \frac{P_3}{P_{25}} \qquad [3.22]$$

In the case of an isentropic process the equation above will be modified:

$$S_3^{IS} - S_{25} = 0 = \int_{T_{25}}^{T_3^{IS}} C_P \frac{dT}{T} - R_{25}\, Ln \frac{P_3^{IS}}{P_{25}} = (\Phi_3^{IS} - \Phi_{25}) - R_{25}\, Ln \frac{P_3^{IS}}{P_{25}} \qquad [3.23]$$

the final pressure will be the same in the real and in the isentropic processes, hence:

$$0 = \int_{T_{25}}^{T_3^{IS}} C_P \frac{dT}{T} - R_{25}\, Ln \frac{P_3}{P_{25}} = (\Phi_3^{IS} - \Phi_{25}) - R_{25}\, Ln \frac{P_3}{P_{25}} \qquad [3.24]$$

With this simple equation the compressor isentropic temperature can be easily calculated employing an iterative method. The first value of the isentropic temperature, to start the iterative process, is given by:

$$T_3^{IS} = T_{25} \left(\frac{P_3}{P_{25}} \right)^{\frac{\gamma_{25}-1}{\gamma_{25}}} \qquad [3.25]$$

3.3.2. COMPRESSOR DELIVERY TEMPERATURE AND PRESSURE IF POLYTROPIC EFFICIENCY AND PRESSURE RATIO ARE GIVEN (CASE II)

If the polytropic efficiency and pressure ratio are given, the exit temperature can be calculated using the following procedure.

The definition of polytropic efficiency is:

$$\eta_{25-3}^{POLY} = \frac{dH^{IS}}{dH} \qquad [3.26]$$

Employing the Gibbs equation in its differential form for an isentropic process:

$$dH^{IS} = \frac{1}{\rho} dP \qquad [3.27]$$

hence

$$\eta_{25-3}^{POLY} = \frac{\frac{1}{\rho}dP}{C_P dT} = \frac{R}{C_P}\frac{\frac{dP}{P}}{\frac{dT}{T}} \qquad [3.28]$$

The resultant equation will be:

$$\eta_{25-3}^{POLY}\int_{T_{25}}^{T_3} C_P \frac{dT}{T} = \int_{P_{25}}^{P_3} R\frac{dP}{P} \qquad [3.29]$$

if the gas constant does not change, the final expression relating the exit temperature with the polytropic efficiency and pressure ratio will be:

$$\eta_{25-3}^{POLY}\int_{T_{25}}^{T_3} C_P \frac{dT}{T} = \eta_{25-3}^{POLY}(\Phi_3 - \Phi_{25}) = R_{25}\, Ln\frac{P_3}{P_{25}} \qquad [3.30]$$

The only unknown in this equation is the exit temperature, that will be determined with an iterative procedure. A first estimation of its value can be done by assuming constant C_P during the compression process, resulting:

$$T_3 = T_{25}\left(\frac{P_3}{P_{25}}\right)^{\frac{\gamma_{25}-1}{\eta_{25}^{POLY}\gamma_{25}}} \qquad [3.31]$$

3.3.3. COMPRESSOR DELIVERY TEMPERATURE AND PRESSURE IF ISENTROPIC EFFICIENCY AND INCREASE IN CORRECTED ENTHALPY ARE GIVEN (CASE III)

If the isentropic efficiency and increase in corrected enthalpy are given, the exit temperature and pressure are determined as follows.

Equation [3.24], obtained in section 3.3.1., gives the relation between isentropic temperature and pressure ratio. Hence, if the isentropic temperature is found, the pressure ratio can be calculated.

From the isentropic efficiency definition the expression below can be determined:

$$\int_{T_{25}}^{T_3^{IS}} C_P dT = \eta_{25-3}\gamma_{25}R_{25}\theta_{25}\left(\frac{\Delta H_{25-3}}{\gamma_{25}R_{25}\theta_{25}}\right) \qquad [3.32]$$

the right hand side of the equation is known. Therefore, the isentropic temperature can be calculated as described in the previous cases. With this temperature the pressure ratio is found.

3.3.4. COMPRESSOR DELIVERY TEMPERATURE AND PRESSURE IF POLYTROPIC EFFICIENCY AND INCREASE IN CORRECTED ENTHALPY ARE GIVEN (CASE IV)

If the polytropic efficiency and increase in corrected enthalpy are given, the exit temperature and pressure are calculated as follows.

In CASE II, eq.[3.30] gives a relation between exit temperature, polytropic efficiency and pressure ratio. Hence, if the compressor discharge temperature is found, the pressure ratio will be easily obtained.

The corrected enthalpy is defined as:

$$\left(\frac{\Delta H_{25-3}}{\gamma_{25} R_{25} \theta_{25}}\right) = \frac{1}{\gamma_{25} R_{25} \theta_{25}} \int_{T_{25}}^{T_3} C_p dT \qquad [3.33]$$

where everything but the exit temperature is known. Once T_3 is found, the calculation of pressure ratio is straight forward, as described above.

At design stage the four cases can happen, while at off-design and transient, where the isentropic efficiency map is known, CASES I and III are the only possibilities. The situation of having polytropic efficiency maps is not considered, as the result of compressor testing is adiabatic efficiency. However, its use would be easy, changing from one efficiency map to the other with the functions already described.

3.3.5. COMPRESSOR WORK

Through the compressor there are several bleeds that are employed for turbine cooling, surge control, etc. At design stage, the relative position of these flow extraction points will be given in terms of enthalpy rise ratio, i.e. for the bleed *25i*:

$$\lambda_{25i} = \left(\frac{\Delta H_{25-25i}}{\Delta H_{25-3}}\right) \qquad [3.34]$$

The pressure will be calculated using the polytropic efficiency, assuming that all the compressor rows have the same one. The method described in 3.3.3 is used, and

the resulting pressure will be decreased for the total pressure drop close to the walls, where the flow is extracted from, additional pipe losses (if present), restrictors, etc.

Once the compressor bleed flows have been calculated the required work can be obtained from the following equation:

$$PW_{25} = W_3 \Delta H_{25-3} + \sum_{\forall i} W_{25i} \Delta H_{25-25i} = W_3 \Delta H_{25-3} + \sum_{\forall i} W_{25i} \lambda_{25i} \Delta H_{25-3} = \Delta H_{25-3} \left(W_3 + \sum_{\forall i} W_{25i} \lambda_{25i} \right) \quad [3.35]$$

3.3.6. OFF-DESIGN PERFORMANCE OF THE COMPRESSOR

In off-design performance very important figures are the running lines on the compressor map.

The requirement of variable geometry and/or valves to avoid surge, the possibility of changing the operating point to increase the efficiency, etc. are clearly shown in the pressure ratio vs. corrected mass flow and isentropic efficiency vs. corrected mass flow charts.

3.3.6.1. Compressor Maps

The compressor maps are functions that relate mass flow, rotational speed, pressure ratio or corrected enthalpy and adiabatic (isentropic) efficiency:

$$\left(\frac{\Delta H_{25-3}}{\gamma_{25} R_{25} \theta_{25}} \right) = f \left(\frac{W_{25} \sqrt{\theta_{25}}}{\delta_{25}} \sqrt{\frac{R_{25}}{\gamma_{25}}}, \frac{N_{HPS}}{\sqrt{\gamma_{25} R_{25} \theta_{25}}} \right) \quad [3.36]$$

$$\frac{P_3}{P_{25}} = f \left(\frac{W_{25} \sqrt{\theta_{25}}}{\delta_{25}} \sqrt{\frac{R_{25}}{\gamma_{25}}}, \frac{N_{HPS}}{\sqrt{\gamma_{25} R_{25} \theta_{25}}} \right) \quad [3.37]$$

$$\eta_{25-3} = f \left(\frac{W_{25} \sqrt{\theta_{25}}}{\delta_{25}} \sqrt{\frac{R_{25}}{\gamma_{25}}}, \frac{N_{HPS}}{\sqrt{\gamma_{25} R_{25} \theta_{25}}} \right) \quad [3.38]$$

Frequently, in open cycle gas turbines, the corrected speed, corrected mass flow and corrected enthalpy do not have the γ and R included. As the flow is always air there is almost no inaccuracy. However, when it is possible to use the same component with different working fluids or with the same fluid but different thermodynamic conditions, it is necessary to consider the gas properties. If the functions are carefully examined it is known that the term $\sqrt{\gamma_{25} R_{25} \theta_{25}}$ is closely related

with the sonic velocity at the compressor entry. Hence, the first term will be the axial Mach number, and the second one will be the rotational Mach number.

The problem of using these functions arises when the flow is choked, and for the same corrected mass flow there are several values of pressure, corrected enthalpy or efficiency. This effect is very common at high speeds, when the constant corrected speed lines become vertical. At intermediate speeds the opposite problem happens; near the surge line the constant corrected speed lines become horizontal, and for the same pressure ratio, efficiency or corrected enthalpy there are several mass flow values.

These two problems are solved introducing an additional parameter, called β. There is no physical meaning behind it, but allows the user to compute the compressor characteristics easily. There is not a unique definition of β. Here, the new functions are as follows:

$$\left(\frac{\Delta H_{25-3}}{\gamma_{25}R_{25}\theta_{25}}\right)=f_1\left(\beta_{HPC},\ \frac{N_{HPS}}{\sqrt{\gamma_{25}R_{25}\theta_{25}}}\right) \qquad [3.39]$$

$$\frac{P_3}{P_{25}}=f_2\left(\beta_{HPC},\ \frac{N_{HPS}}{\sqrt{\gamma_{25}R_{25}\theta_{25}}}\right) \qquad [3.40]$$

$$\eta_{25-3}=f_3\left(\beta_{HPC},\ \frac{N_{HPS}}{\sqrt{\gamma_{25}R_{25}\theta_{25}}}\right) \qquad [3.41]$$

$$\frac{W_{25}\sqrt{\theta_{25}}}{\delta_{25}}\sqrt{\frac{R_{25}}{\gamma_{25}}}=f_4\left(\beta_{HPC},\ \frac{N_{HPS}}{\sqrt{\gamma_{25}R_{25}\theta_{25}}}\right) \qquad [3.42]$$

Instead of using the approximated expressions, which neglect the Mach number term, it is also possible to employ the complete equations using the design compressor inlet Mach number:

$$\left(\frac{\Delta H_{25-3}\left(1+\frac{\gamma_{25}-1}{2}M^2_{25_{DS}}\right)}{\gamma_{25}R_{25}\theta_{25}}\right)=f_1\left(\beta_{HPC},\ \frac{N_{HPS}\sqrt{1+\frac{\gamma_{25}-1}{2}M^2_{25_{DS}}}}{\sqrt{\gamma_{25}R_{25}\theta_{25}}}\right) \qquad [3.43]$$

$$\frac{P_3}{P_{25}}=f_2\left(\beta_{HPC},\ \frac{N_{HPS}\sqrt{1+\frac{\gamma_{25}-1}{2}M^2_{25_{DS}}}}{\sqrt{\gamma_{25}R_{25}\theta_{25}}}\right) \qquad [3.44]$$

$$\eta_{25-3} = f_3\left(\beta_{HPC},\ \frac{N_{HPS}\sqrt{1+\frac{\gamma_{25}-1}{2}M^2_{25_{DS}}}}{\sqrt{\gamma_{25}R_{25}\theta_{25}}}\right) \qquad [3.45]$$

$$\frac{W_{25}\sqrt{\theta_{25}}}{\delta_{25}}\sqrt{\frac{R_{25}}{\gamma_{25}}}\left(1+\frac{\gamma_{25}-1}{2}M^2_{25_{DS}}\right)^{\frac{\gamma_{25}+1}{2(\gamma_{25}-1)}} = f_4\left(\beta_{HPC},\ \frac{N_{HPS}\sqrt{1+\frac{\gamma_{25}-1}{2}M^2_{25_{DS}}}}{\sqrt{\gamma_{25}R_{25}\theta_{25}}}\right) \qquad [3.46]$$

3.3.6.2. Scaling Factors

The programme will have several maps for a compressor, representing different technology levels. However, the pressure ratio, efficiency, etc., of a specific compressor will not be the same as the default ones, although its general behaviour can be very similar. To adapt the available map to the real compressor we want to study, the corrected parameters must be "scaled".

$$\left[\frac{\Delta H_{25-3}}{\gamma_{25}R_{25}\theta_{25}}\right]_{DESIGN} = sf_{H_{HPC}}\left[\frac{\Delta H_{25-3}}{\gamma_{25}R_{25}\theta_{25}}\right]_{MAP} \qquad [3.47]$$

$$\left[\frac{P_3}{P_{25}}-1\right]_{DESIGN} = sf_{\pi_{HPC}}\left[\frac{P_3}{P_{25}}-1\right]_{MAP} \qquad [3.48]$$

$$[\eta_{25-3}]_{DESIGN} = sf_{\eta_{HPC}}[\eta_{25-3}]_{MAP} \qquad [3.49]$$

$$\left[\frac{W'_{25}\sqrt{\theta_{25}}}{\delta_{25}}\sqrt{\frac{R_{25}}{\gamma_{25}}}\right]_{DESIGN} = sf_{W'_{HPC}}\left[\frac{W'_{25}\sqrt{\theta_{25}}}{\delta_{25}}\sqrt{\frac{R_{25}}{\gamma_{25}}}\right]_{MAP} \qquad [3.50]$$

The scaling factors are calculated at design, and it is assumed that the value will not change at off-design or transient conditions.[8]

If the full expressions are used, including the Mach number terms, the enthalpy and mass flow scaling factors will be:

---

[8] This is, clearly, the most simple approximation. When experimental data becomes available, via analysis by syntheis, the scaling factors will be modelled as function of other parameters, reflecting phisical phenomena not considered in the simplified approach.

$$sf_{H_{MPC}} = \frac{\left[\frac{\Delta H_{25-3}\left(1+\frac{\gamma_{25}-1}{2}M^2_{25_{DS}}\right)}{\gamma_{25}R_{25}\theta_{25}}\right]_{DESIGN}}{\left[\frac{\Delta H_{25-3}\left(1+\frac{\gamma_{25}-1}{2}M^2_{25_{DS}}\right)}{\gamma_{25}R_{25}\theta_{25}}\right]_{MAP}} \qquad [3.51]$$

$$sf_{W_{MPC}} = \frac{\left[\frac{W'_{25}\sqrt{\theta_{25}}}{\delta_{25}}\sqrt{\frac{R_{25}}{\gamma_{25}}}\left(1+\frac{\gamma_{25}-1}{2}M^2_{25_{DS}}\right)^{\frac{\gamma_{25}+1}{2(\gamma_{25}-1)}}\right]_{DESIGN}}{\left[\frac{W'_{25}\sqrt{\theta_{25}}}{\delta_{25}}\sqrt{\frac{R_{25}}{\gamma_{25}}}\left(1+\frac{\gamma_{25}-1}{2}M^2_{25_{DS}}\right)^{\frac{\gamma_{25}+1}{2(\gamma_{25}-1)}}\right]_{MAP}} \qquad [3.52]$$

3.3.6.3. Variable Geometry in the Compressor

There are two basic approaches to consider the variable stators in the performance simulation:

- Calculate the variables as a function of the stator angle, having performance maps for several angles.
- Consider a single parametric curve, which is function of the stator angle, for each performance variable.

The second approach has been employed in the code, while the first one can be easily implemented.

3.3.6.4. Compressor Work at Off-Design Conditions

The compressor inlet mass flow[9], discharge pressure, temperature, enthalpy, etc. will be calculated using the pressure ratio (or enthalpy rise) and efficiency from the component characteristics. To calculate the work it is also necessary to know the intercompressor bleed flows. The code has the capability of maintaining constant percentage relative to the inlet mass flow [3.53a] or a function (introduced by the user) of either the corrected inlet mass flow, pressure ratio or corrected shaft speed

---

[9] In some cases the maps are plotted against the discharge mass flow, although this situation is not very common.

[3.53b, 3.53c and 3.53d]. The value of λ_{25i} is assumed to remain constant. Once the value of the bleeds and enthalpy rise is obtained, the work is calculated using equation [3.35].

$$\frac{W'_{25i}}{W'_{25}} = K_{25i} \qquad [3.53a]$$

$$\frac{W'_{25i}}{W'_{25}} = f\left(\frac{W'_{25}\sqrt{\theta_{25}}}{\delta_{25}}\right) \qquad [3.53b]$$

$$\frac{W'_{25i}}{W'_{25}} = f\left(\frac{P_3}{P_{25}}\right) \qquad [3.53c]$$

$$\frac{W'_{25i}}{W'_{25}} = f\left(\frac{N_{25}}{\sqrt{\theta_{25}}}\right) \qquad [3.53d]$$

3.3.6.5. Different Off-Design Performance Simulation Methods if Schedules Vary

The way described here, where the compressor is simulated by single efficiency and pressure ratio (or enthalpy rise) maps, could not be the most accurate one, specially when the intercompressor bleeds are very large (or the order of 10-15%, or ever bigger, for the anti-surge valves). In that case, different maps should be obtained at several valve opening degrees. This situation is very common at low speeds, where large quantities of fluid are bled to avoid surge. Other simulation possibility will be to have different compressor maps for the stages that are before and after the bleed. The implementation of these capabilities, if required, could be done with minor code modifications.

3.3.6.6. Reynolds Number Correction

Compressor maps are given for a certain Reynolds number and changes in its value can widely modify the performance. Instead of using the absolute Reynolds number, a Reynolds number index is frequently employed, [32] and [75], which can be expressed, using the thermodynamic properties at compressor inlet face, as:

$$RNI = \frac{Re}{Re_{ref}} = \frac{\rho V L}{(\rho V L)_{ref}} \frac{\mu_{ref}}{\mu} \qquad [3.54]$$

For the same compressor the characteristic length can be canceled.[10] Therefore, the expression will be:

$$RNI = \frac{p M \sqrt{\frac{\gamma}{Rt}}}{p_{ref} M_{ref} \sqrt{\left(\frac{\gamma}{Rt}\right)_{ref}}} \frac{\mu_{ref}}{\mu} \qquad [3.55]$$

In some cases the static pressure and temperature are not available and the total magnitudes should be employed. A more simple approach can be done using the mass flow definition:

$$RNI = \frac{\rho V A}{(\rho V A)_{ref}} \frac{A_{ref}}{A} \frac{L}{L_{ref}} \frac{\mu_{ref}}{\mu} = \frac{W}{W_{ref}} \frac{A_{ref}}{A} \frac{L}{L_{ref}} \frac{\mu_{ref}}{\mu} \qquad [3.56]$$

where the only unknown will be the dynamic viscosity. Again, when the correction is applied to the same piece of hardware the geometric parameters disappear, giving:

$$RNI = \frac{W}{W_{ref}} \frac{\mu_{ref}}{\mu} \qquad [3.57]$$

These are the general expressions but, for air, a simpler one can be derived using an approximation of the dynamic viscosity for the typical range of compressor operating temperatures:

$$\mu = \mu_0 \left(\frac{t}{t_0}\right)^{0.75} \qquad [3.58]$$

hence, for a fixed Mach number and neglecting the variations in gas properties:

$$RNI = \frac{p \sqrt{\frac{1}{t}}}{p_{ref} \sqrt{\frac{1}{t_{ref}}}} \frac{\mu_{ref}}{\mu} = \frac{p \sqrt{\frac{1}{t}}}{p_{ref} \sqrt{\frac{1}{t_{ref}}}} \left(\frac{t_{ref}}{t}\right)^{0.75} = \frac{p}{p_{ref}} \left(\frac{t_{ref}}{t}\right)^{1.25} \qquad [3.59]$$

The whole maps, including the surge line, are modified with the Reynolds effect.

---

[10] If the maps have been obtained with a scale model the characteristic length must be maintained.

All the discussion above considers the properties at the compressor inlet face, with no rotating effect. For rotating turbomachinery, the Reynolds correction should include an additional term:

$$Re_{correction} = f\left(\left. \frac{pM\sqrt{\frac{\gamma}{Rt}}}{p_{ref} M_{ref} \sqrt{\left(\frac{\gamma}{Rt}\right)_{ref}}} \frac{L}{L_{ref}} \frac{\mu_{ref}}{\mu} \right|_{\substack{compressor \\ inlet}} , \frac{N\sqrt{(\gamma Rt)_{ref}}}{N_{ref}\sqrt{\gamma Rt}} \frac{D}{D_{ref}} \right) \quad [3.60]$$

For open cycle turbomachinery, neglecting the changes in thermodynamic properties and considering that the maps have been obtained for a compressor with the same dimensions, a simplified expression could be used:

$$Re_{correction} = f\left(\frac{p}{p_{ref}} \left(\frac{t_{ref}}{t} \right)^{1.25} , \frac{N\sqrt{T_{ref}}}{N_{ref}\sqrt{T}} \right) \quad [3.61]$$

3.3.7. COMPRESSOR TRANSIENT OPERATION

The transient of the compressor can include effects such as mass and heat storage, blade tip clearance changes, surge, distortion, internal air system variations, etc., refs. [22], [32], [69], [84] and [121]. Most of them are extremely difficult to evaluate and taken into account in a generic performance development code. However, from the point of view of a simplified transient simulation these effects can be introduced as time dependent scaling factors, and only the mass storage will be calculated, with the heat flow as an input from other disciplines.

3.4. DRY INTERCOOLER

The intercooler is a heat exchanger used to decrease the temperature between the compressors, increasing the specific power output substantially [50] and [122]. No mass or working fluid composition variation takes place, only the total pressure and temperature change.

3.4.1. DRY INTERCOOLER DESIGN PERFORMANCE CALCULATION

Assuming that the inlet conditions are known from the compressor discharge and the flow has no swirl component, the equations describing this system are equivalent

to [3.1b], [3.2b], [3.3b], [3.8], [3.9] and [3.10]. The only unknown is the exit enthalpy (or any other data that will enable us to calculate this variable).

$$H_{ex} \text{ given (or } T_{ex} \text{ given, or power extracted known)} \qquad [3.62]$$

If the area is not considered, only the total properties will be determined.

A simplified approach[11] can be done using equations analogous to [3.5], [3.6] and [3.7], for the mass flow, static pressure and static temperature.

If the heat exchanger characteristics, coolant mass flow and inlet temperature were known, the exit conditions given by eq.[3.62] would be directly obtained.

3.4.2. OFF-DESIGN PERFORMANCE OF THE DRY INTERCOOLER

As in the case of the inlet (section 3.2) the design equations are also valid for off-design, the only unknown being the total pressure losses. The exit temperature will be obtained from the energy equation and will constitute the control of the machine.[12]

The assumptions regarding the pressure losses will be same as in 3.2, obtaining the constant K' from the design point data (equations [3.15] and [3.16]).

3.5. EVAPORATIVE COOLER

The evaporative cooler or humid intercooler/aftercooler, refs. [12], [66], [85] and [86], decreases the main stream temperature, removing heat during the evaporation of small droplets of liquid water.[13] This system has two beneficial effects in addition to the increase in the gas turbine specific power output, as a conventional intercooler:

- A further increase in the specific power output, due to the larger mass flow through the turbines.
- An increase in the thermal efficiency. The value will lie between the simple and the steam injected cycle.

A good example of the use of this technology is the Humid Air Turbine (HAT®), [86], consisting in an evaporative aftercooler.

---

[11] The result of these equations will be acceptable if the Mach number is low enough.

[12] The real control will be the coolant mass flow & inlet temperature, with the exit emperature as feedback.

[13] Large quantities of energy are required to change the phase from liquid to vapour. Therefore with a modest amount of water a considerable decrease in temperature will take place.

The theoretical limit of the evaporative cooler will occur when the exit flow reaches 100% relative humidity. However, from the technological point of view, this condition is not fully achievable,[14] with the real limit being in the 95-98% region.

The water to be used in the evaporative cooler will have some requirements in terms of turbidity, pH, hardness ($CaCO_3$), sodium and potassium.

The use of this system in GTSI is limited to open cycles, although it would be possible to have the component in semi-closed cycles, where water is removed before starting the compression.

3.5.1. EVAPORATIVE COOLER DESIGN PERFORMANCE CALCULATION

The equations that solve the evaporative cooler are analogous to [3.1a], [3.2a], [3.3a], [3.4a], [3.8], [3.9] and [3.10]. The mass flow, spices and energy conservation [3.1a], [3.2a] and [3.4a] could be expressed as:

$$W_{out} = W_{in} + W_{injected}^{H_2O} \qquad [3.63]$$

$$W_{out}^{air} = W_{in}^{air} \qquad [3.64]$$

$$W_{out}^{fuel} = W_{in}^{fuel} \qquad [3.65]$$

$$W_{out}^{H_2O} = W_{in}^{H_2O} + W_{injected}^{H_2O} \qquad [3.66]$$

$$H_{out} = \frac{W_{in} H_{in} + W_{injected}^{H_2O} H_{liquid}^{H_2O}}{W_{out}} \qquad [3.67]$$

The relative humidity of the stream at the exit of the evaporative cooler will be:

$$RH_{out} = \frac{p_{out}^{vap}}{p_{out}^{sat}} = \frac{\dfrac{MW_{H_2O} WAR_{out}}{R_{out}}}{1 + \dfrac{MW_{H_2O} WAR_{out}}{R_{out}}} \frac{p_{out}}{p_{out}^{sat}} \qquad [3.68]$$

---

[14] The 100% relative humidity is the mathematical limit because the code is not able to handle with two-phase mixtures. Therefore it will not be possible to use this value without major subroutine modifications. Instead of 100%, 99.5% could be employed, giving almost the same result. It is also a technological limit, because if the real situation is considered, to obtain this condition it will be necessary to have not only a very long evaporator, but also a sophisticated injection system to ensure good homogeneous water-air mixture with no liquid phase at the exit. However, values extremely close to 100% are sometimes obtained.

The saturation pressure is obtained from the water-steam tables or equations.

In most cases the area is not known until the end of the preliminary design. Therefore, the Mach number, static pressure, static temperature, etc. will not be obtained, and the pressures used to calculate the relative humidity will be total instead of static.

Water mass flow, exhaust temperature, water to air ratio or relative humidity are some of the most common parameters that will be used to control the evaporative cooling at off-design, with the exhaust relative humidity being the typical control at design. For both, design and off-design, all the equations, except the one that gives the exit total pressure, are the same.

As in case of the dry intercooler, the simplified expressions for the mass flow, static pressure and static temperature can be used, provided that the Mach number is low enough.

3.5.2. OFF-DESIGN PERFORMANCE OF THE EVAPORATIVE INTERCOOLER

As in the case of the dry intercooler the only unknown will be the exit total pressure. This will be obtained using equations analogous to [3.15] and [3.16]. The exhaust humidity or temperature will be used as the control of the component, therefore specified by the user.

3.6. STEAM INJECTOR

The steam injector is one of the mechanisms most widely used in gas turbines to increase power and thermal efficiency [12], [13], [15], [76], [77], [85], [127], [130] and [145]. As for the evaporative cooler, the water must comply with some quality requirements. This system will only be considered in open cycles being, from the performance point of view, a constant area mixer. There are two possible situations:

- The static pressures of both streams are the same at the mixing plane
- The Mach number of the steam reaches sonic conditions.

3.6.1. MACH NUMBER/AREA, STATIC PRESSURE AND TEMPERATURE OF THE INLET CORE STREAM

The area (taking into account the blockage due to the injectors) or Mach number, mass flow total pressure and total temperature of the core stream at the mixing plane are known. Hence, the static properties are calculated, with equations analogous to [3.8], [3.9] and [3.10], assuming that no swirl is present in the flow:

$$H_3 = h_3 + \frac{1}{2}\gamma_3 R_3 t_3 M_3^2 \qquad [3.69]$$

$$\Delta S_3 = 0 = (\Phi_{T_3} - \phi_{t_3}) - R_3 \ln \frac{P_3}{p_3} \qquad [3.70]$$

$$W_3 = \frac{p_3}{R_3 t_3}\sqrt{\gamma_3 R_3 t_3}\, M_3 A_3 \qquad [3.71]$$

With these equations and the thermodynamics of the working fluid, the Mach number (or effective area), static pressure and static temperature are found. If the simplified expressions, equivalent to [3.5], [3.6] and [3.7], are considered accurate enough, the system will be:

$$t_3 = \frac{T_3}{1 + \frac{\gamma_3 - 1}{2} M_3^2} \qquad [3.72]$$

$$p_3 = \frac{P_3}{\left(1 + \frac{\gamma_3 - 1}{2} M_3^2\right)^{\frac{\gamma_3}{\gamma_3 - 1}}} \qquad [3.73]$$

$$W_3 = \frac{A_3 P_3}{\sqrt{T_3}}\sqrt{\frac{\gamma_3}{R_3}}\frac{M_3}{\left(1 + \frac{\gamma_3 - 1}{2} M_3^2\right)^{\frac{\gamma_3 + 1}{2(\gamma_3 - 1)}}} \qquad [3.74]$$

3.6.2. MACH NUMBER, STATIC PRESSURE AND TEMPERATURE OF THE INJECTED STREAM (SUPERHEATED STEAM)

As in the case of the core stream the total conditions of the steam (station 305) are known. In addition to these variables, either the mass flow or the area should be given. As mentioned at the beginning of this section, the static pressure at the injection plane or the Mach number in the direction of injection will be obtained from the Kutta-Jukowski condition eq.[3.75].

The exact equations could also be employed for a more accurate solution (eq. [3.69], [3.70] and [3.71]) specially at high Mach number operation.

The situation of having a convergent-divergent nozzle, with supersonic injection, has not been considered in this study.

$$M_{305} = \sqrt{\frac{2}{\gamma_3 - 1}\left(\left(\frac{P_{305}}{p_3}\right)^{\frac{\gamma_{305}-1}{\gamma_{305}}} - 1\right)} \Rightarrow$$

$$\Rightarrow \begin{cases} \text{if } M_{305} < 1 \rightarrow p_{305} = p_3 \\ \text{if } M_{305} \geq 1 \rightarrow M_{305} = 1 \;\&\; p_{305} = \dfrac{P_{305}}{\left(\dfrac{1+\gamma_{305}}{2}\right)^{\frac{\gamma_{305}}{\gamma_{305}-1}}} \end{cases} \qquad [3.75]$$

$$t_{305} = \frac{T_{305}}{1 + \dfrac{\gamma_{305}-1}{2} M_{305}^2} \qquad [3.76]$$

$$W_{305} = \frac{A_{305} P_{305}}{\sqrt{T_{305}}} \sqrt{\frac{\gamma_{305}}{R_{305}}} \frac{M_{305}}{\left(1 + \dfrac{\gamma_{305}-1}{2} M_{305}^2\right)^{\frac{\gamma_{305}+1}{2(\gamma_{305}-1)}}} \qquad [3.77]$$

3.6.3. THERMODYNAMIC VARIABLES AT THE EXIT OF THE MIXER

After steam injection, with the exit area known, the total and static pressure, temperature and Mach number will be obtained. There are two main injection systems: axial and perpendicular to the main stream. The following equations will be valid for both of them.[15]

The mass flow continuity gives:

$$W_{31} = W_3 + W_{305} \qquad [3.78]$$

The momentum equation, in axial direction, is:

$$A_3 p_3 \left(1 + \gamma_3 M_3^2\right) + A_{305} p_{305} \left(1 + \gamma_{305} M_{305ax}^2\right) = A_{31} p_{31} \left(1 + \gamma_{31} M_{31}^2\right) \qquad [3.79]$$

The energy balance, which gives the exit total enthalpy and, consequently, the total temperature, can be written in the following form:

$$H_{31} = \frac{W_3 H_3 + W_{305} H_{305}}{W_{31}} \qquad [3.80]$$

---

15 As a simplification, the exit is considered axial, without net perpendicular component.

The three additional equations that, together with [3.80], are required to calculate static and total pressure, static temperature and Mach number are:

$$H_{31} = h_{31} + \frac{1}{2}\gamma_{31} R_{31} t_{31} M_{31}^{\ 2} \qquad [3.81]$$

$$\Delta S_{31} = 0 = (\Phi_{T_{31}} - \phi_{t_{31}}) - R_{31}\, ln \frac{P_{31}}{p_{31}} \qquad [3.82]$$

$$W_{31} = \frac{p_{31}}{R_{31} t_{31}} \sqrt{\gamma_{31} R_{31} t_{31}}\, M_{31} A_{31} \qquad [3.83]$$

If the approximate expressions were employed, the calculation would be as follows:

$$\frac{P_{31}}{P_3} = \frac{W_{31}}{W_3} \sqrt{\frac{T_{31}}{T_3}} \frac{A_3}{A_{31}} \sqrt{\frac{\gamma_3}{R_3} \frac{R_{31}}{\gamma_{31}}} \frac{M_3 \left(1 + \frac{\gamma_{31} - 1}{2} M_{31}^2\right)^{\frac{\gamma_{31}+1}{2(\gamma_{31}-1)}}}{M_{31} \left(1 + \frac{\gamma_3 - 1}{2} M_3^2\right)^{\frac{\gamma_3+1}{2(\gamma_3-1)}}} \qquad [3.84]$$

The unknowns are the exhaust total pressure and Mach number, as the mass flow continuity gives directly the value of W_{31} and the exit area is also obtained from the assumption of constant area mixer.

Eq. [3.79] could be modified using the equation given below:

$$Ap = \frac{W \sqrt{T \frac{R}{\gamma}}}{M_{ax} \sqrt{1 + \frac{\gamma - 1}{2} M^2}} \qquad [3.85]$$

producing:

$$\frac{W_3 \sqrt{T_3 \frac{R_3}{\gamma_3}} \left(1 + \gamma_3 M_3^2\right)}{M_3 \sqrt{1 + \frac{\gamma_3 - 1}{2} M_3^2}} + \frac{W_{305} \sqrt{T_{305} \frac{R_{305}}{\gamma_{305}}} \left(1 + \gamma_{305} M_{305ax}^2\right)}{M_{305} \sqrt{1 + \frac{\gamma_{305} - 1}{2} M_{305}^2}} = \frac{W_{31} \sqrt{T_{31} \frac{R_{31}}{\gamma_{31}}} \left(1 + \gamma_{31} M_{31}^2\right)}{M_{31} \sqrt{1 + \frac{\gamma_{31} - 1}{2} M_{31}^2}} \qquad [3.86]$$

manipulating the expression above, a simplified form will be obtained[16]:

---

[16] The assumption of no inlet or exit swirl in the flow ($M_3 = M_{3ax}$ and $M_{31} = M_{31ax}$) will be used to generate a homogeneous expression

$$\Psi_{31}(\gamma_{31}, M_{31}, M_{31ax}) = \frac{M_{31}^2\left(1+\frac{\gamma_{31}-1}{2}M_{31}^2\right)}{\left(1+\gamma_{31}M_{31ax}^2\right)^2} =$$

$$= \left(\frac{W_{31}\sqrt{T_{31}\frac{R_{31}}{\gamma_{31}}}}{W_3\sqrt{T_3\frac{R_3}{\gamma_3}}\sqrt{\frac{1}{\Psi_3}}+W_{305}\sqrt{T_{305}\frac{R_{305}}{\gamma_{305}}}\sqrt{\frac{1}{\Psi_{305}}}}\right)^2 \qquad [3.87]$$

For the given inlet conditions, the value of Ψ_{31} is obtained and, therefore, the Mach number at that station (only the subsonic solution is considered here):

$$M_{31} = \sqrt{\frac{2\Psi_{31}}{(1-2\gamma_{31}\Psi_{31})+\sqrt{(1-2(\gamma_{31}+1)\Psi_{31})}}} \qquad [3.88]$$

An important advantage of axial steam injection is the increase in total pressure. In figure 3.3 the ratio of exit to inlet main stream total pressure is presented for typical injection rates of 5, 10, 15 and 20%.[17] The temperature, pressure, etc. are characteristic of a conventional industrial gas turbine.

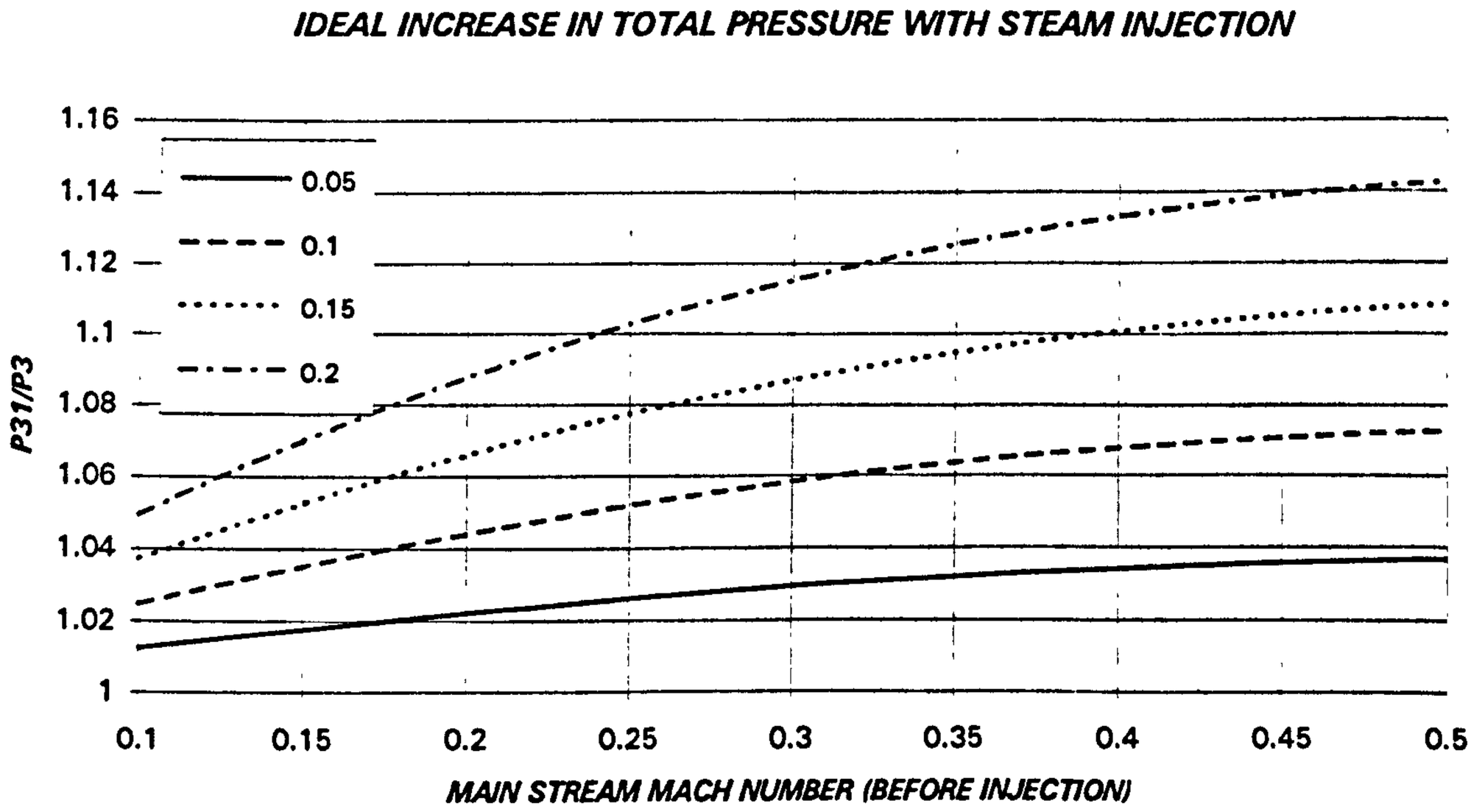

Figure 3.3. Increase in total pressure with axial steam injection (0.05 to 0.20 steam injection rates)

[17] The real increase in total pressure will be lower due to the losses inherent to a high turbulence mixing process. Nevertheless, experimental results have confirmed this beneficial effect.

When the injection is not axial, but with a certain angle, the incrase in total pressure is lower, as shown in figures 3.4 and 3.5 (5% and 15% injection rate respectively).

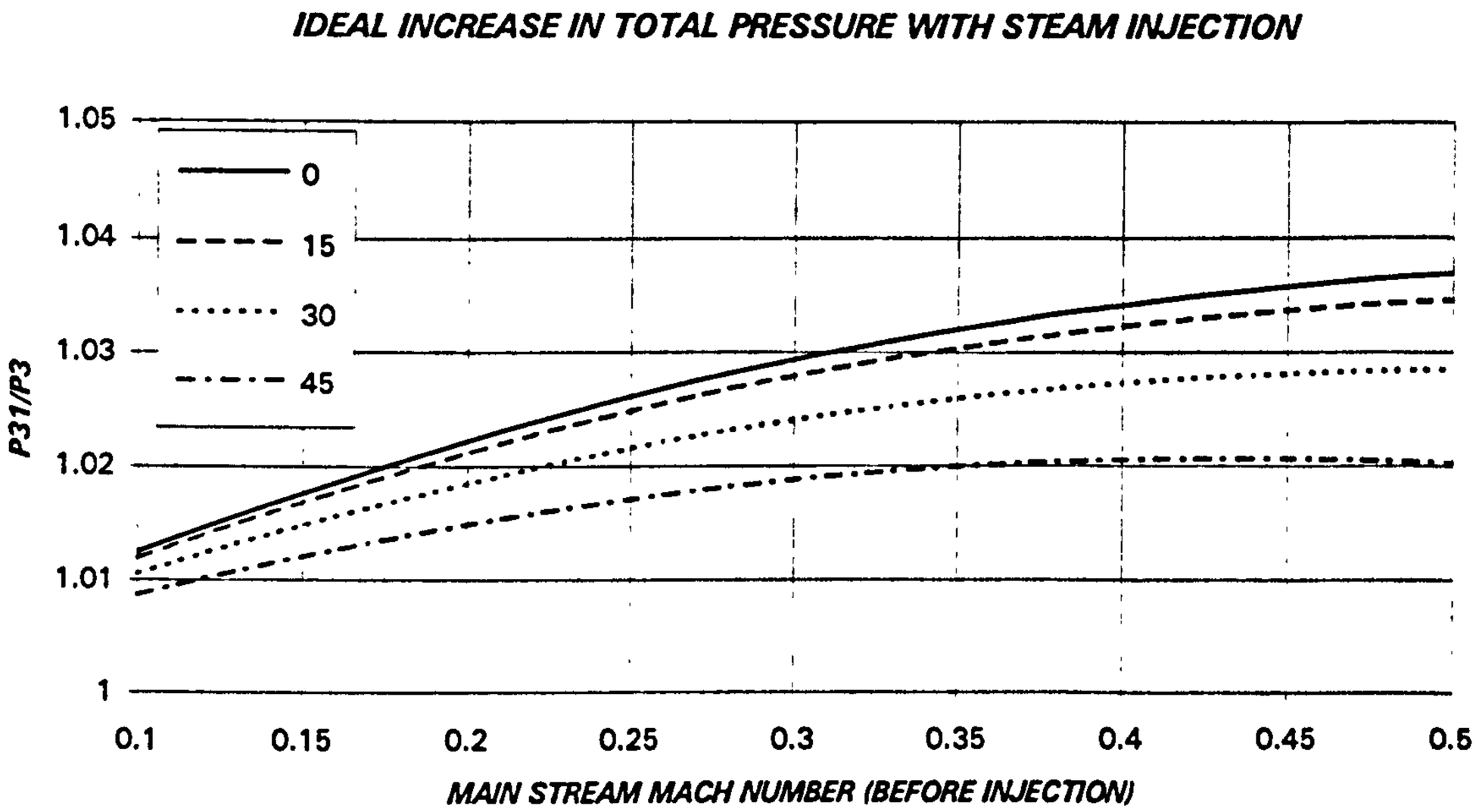

Figure 3.4. Increase in total pressure with 5% steam injection at different angles (0° to 45°)

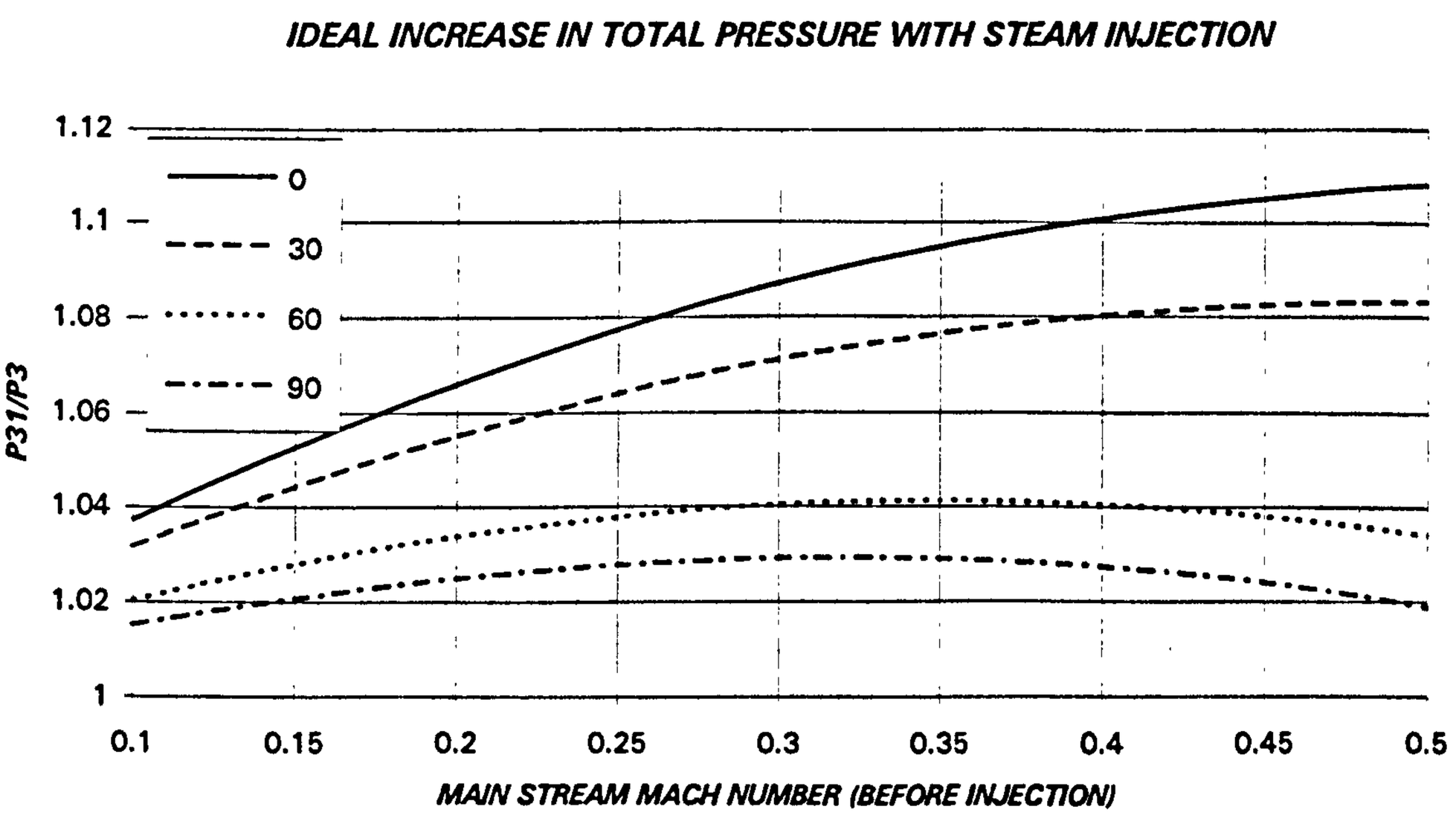

Figure 3.5. Increase in total pressure with 15% steam injection at different angles (0° to 90°)

3.7. REGENERATOR

The regenerator is a heat exchanger in which the turbine exhaust gases (hot flow) are used to increase the temperature of the working fluid prior to the combustion chamber inlet (cold flow), refs. [6], [12], [13], [41], [49], [117] and [122].

This method is employed when the simple cycle (gas turbine alone) thermal efficiency has to be optimised and, also, when the plant will operate, for long periods, at very different power conditions.

The closed cycle machines used in submarines or space applications are good examples of the use of the regenerator. Also, some open cycles have incorporated this system.[18] In general, the component is very expensive, with a relatively modest reliability, although the improvement in the efficiency can be substantial.

The parameter which describes the performance of the regenerator is the effectiveness:

$$\eta_{REG} = \frac{T_{Exit}^{Cold} - T_{Inlet}^{Cold}}{T_{Inlet}^{Hot} - T_{Inlet}^{Cold}} \qquad [3.89]$$

The equations of mass, momentum and energy conservation for this system are:

$$W_{out}^{Cold} = W_{in}^{Cold} + W_{Leakage}^{Cold} \qquad [3.90]$$

$$W_{out}^{Hot} = W_{in}^{Hot} + W_{Leakage}^{Hot} \qquad [3.91]$$

$$W_{out}^{Cold} H_{out}^{Cold} - W_{in}^{Cold} H_{in}^{Cold} + WQ_{Losses} = W_{in}^{Hot} H_{in}^{Hot} - W_{out}^{Hot} H_{out}^{Hot} \qquad [3.92]$$

$$P_{out}^{Cold} = P_{in}^{Cold}\left(1 - K_{in}^{'Cold}\left(\frac{W_{in}^{Cold}\sqrt{T_{in}^{Cold}}}{A_{in}^{Cold} P_{in}^{Cold}}\right)^2\right) \qquad [3.93]$$

$$P_{out}^{Hot} = P_{in}^{Hot}\left(1 - K_{in}^{'Hot}\left(\frac{W_{in}^{Hot}\sqrt{T_{in}^{Hot}}}{A_{in}^{Hot} P_{in}^{Hot}}\right)^2\right) \qquad [3.94]$$

$$H_{out}^{Cold} = h_{out}^{Cold} + \frac{1}{2}V_{out}^2 = h_{out}^{Cold} + \frac{1}{2}\gamma_{out}^{Cold} R_{out}^{Cold} t_{out}^{Cold} M_{out}^2 \qquad [3.95]$$

---

[18] Gas turbines for battle tanks, (i.e. the Lycoming (now Allied Signal) engine employed in the M1 Abrams [30]), marine propulsion (i.e. the Rolls Royce-Westinghouse ICR WR21 [122]), etc.

$$H_{out}^{Hot} = h_{out}^{Hot} + \frac{1}{2}V_{out}^2 = h_{out}^{Hot} + \frac{1}{2}\gamma_{out}^{Hot} R_{out}^{Hot} t_{out}^{Hot} M_{out}^2 \quad [3.96]$$

$$0 = (\Phi_{T_{out}}^{Cold} - \phi_{t_{out}}^{Cold}) - R_{out}^{Cold} \ln \frac{P_{out}^{Cold}}{p_{out}^{Cold}} \quad [3.97]$$

$$0 = (\Phi_{T_{out}}^{Hot} - \phi_{t_{out}}^{Hot}) - R_{out}^{Hot} \ln \frac{P_{out}^{Hot}}{p_{out}^{Hot}} \quad [3.98]$$

$$W_{out}^{Cold} = \rho_{out}^{Cold} V_{out}^{Cold} A_{out}^{Cold} = \frac{P_{out}^{Cold}}{R_{out}^{Cold} t_{out}^{Cold}} \sqrt{\gamma_{out}^{Cold} R_{out}^{Cold} t_{out}^{Cold}}\, M_{out}^{Cold} A_{out}^{Cold} \quad [3.99]$$

$$W_{out}^{Hot} = \rho_{out}^{Hot} V_{out}^{Hot} A_{out}^{Hot} = \frac{P_{out}^{Hot}}{R_{out}^{Hot} t_{out}^{Hot}} \sqrt{\gamma_{out}^{Hot} R_{out}^{Hot} t_{out}^{Hot}}\, M_{out}^{Hot} A_{out}^{Hot} \quad [3.100]$$

As in the case of the intercooler and evaporative cooler, provided that the Mach number is low enough, the simplified system could be employed. Also, if the area is not given, only the total magnitudes will be calculated.

3.8. COMBUSTION CHAMBER

The combustion chambers of industrial gas turbine have very different sizes, going from the small ones, characteristic of the aeroderivative machines, to the huge combustors of several manufacturers, where Siemens and ABB are good examples. Also the mechanisms to reduce the emissions can end up with exotic designs. However, from the performance point of view, the module will not change significantly between the different design approaches refs. [95] and [96].

3.8.1. COMBUSTOR EXIT MASS FLOW

The mass flow at the combustor exit is calculated using the continuity equation and accounting for the inefficiencies.[19]

---

[19] It will be assumed that the fuel flow that does not contribute to the temperature rise $(1-\eta_{cc})W_{FUEL}$ "disappears" after the combustor, although it will be considered for the cycle thermal efficiency calculation. This proposal is, of course, an approximation and considers, basically, that the "inefficient" fuel flow remains in liquid form through the turbines and HRSG. As the typical figure for combustor efficiency is around 99.9%, even for low calorific value fuels, where the typical fuel to air ratio is close to 0.1-0.15, the possible error introduced by this simplification would be 0.01%, considerably lower than the ones generated by other assumptions.

$$W_4 = W_{33} + \eta_{CC} W_{FUEL} \qquad [3.101]$$

3.8.2. COMBUSTOR EXIT PRESSURE

The pressure at the exit of the combustor will be:

$$P_4 = \pi_{33-4} P_{33} \qquad [3.102]$$

The pressure drop term has two contributors: the cold and hot pressure losses. The cold pressure losses are due to the wall friction and high turbulent flow (specially in the primary zone). The hot, or fundamental, pressure losses are caused by the heat addition in the combustor and will be estimated using two different approaches.

The pressure losses can be written as:

$$\frac{P_{33} - P_4}{P_{33}} = \left(\frac{P_{33} - P_4}{\frac{1}{2}\rho_{33} V_{33}^2} \right) \frac{\rho_{33} V_{33}^2}{2 P_{33}} \qquad [3.103]$$

The total pressure loss divided by inlet dynamic head term (rhs of the equation), known as pressure loss factor (PLF), is nearly constant for a given combustion chamber. The previous expression can be modified using the continuity equation:

$$\frac{P_{33} - P_4}{P_{33}} = \left(\frac{P_{33} - P_4}{\frac{1}{2}\rho_{33} V_{33}^2} \right) \left(\frac{R_{33}}{2} \right) \left(\frac{W_{33}\sqrt{T_{33}}}{A_{33} P_{33}} \right)^2 \qquad [3.104]$$

In general, the inlet corrected flow is also fairly uniform over the normal operating range. Hence, the fractional total pressure loss will be constant.

The PLF can be divided into cold and hot losses:

$$\frac{P_{33} - P_4}{\frac{1}{2}\rho_{33} V_{33}^2} = Cold\ Losses + Hot\ Losses = k_1 + Hot\ Losses \qquad [3.105]$$

The constant k_1 depends on the combustion chamber. As a first approach, all the combustor losses can be charged to the cold term (typically the hot losses are 10 to 20 times lower than the cold losses). Therefore, the PLF and k_1 will be nearly the same.

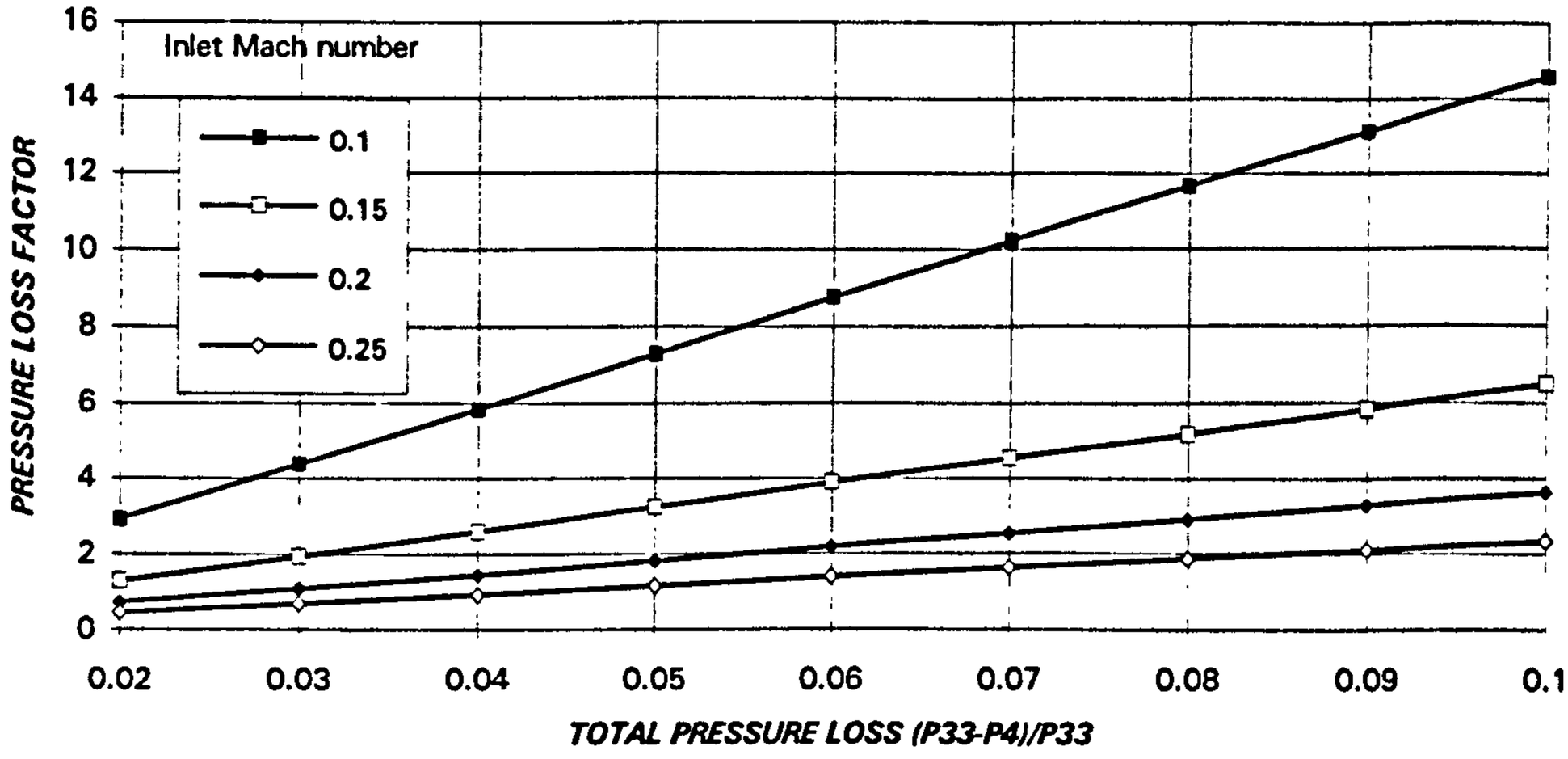

Figure 3.6. Pressure loss factor as a function of total pressure losses and inlet Mach number for a conventional open cycle (γ_{33}=1.360, γ_4=1.300)

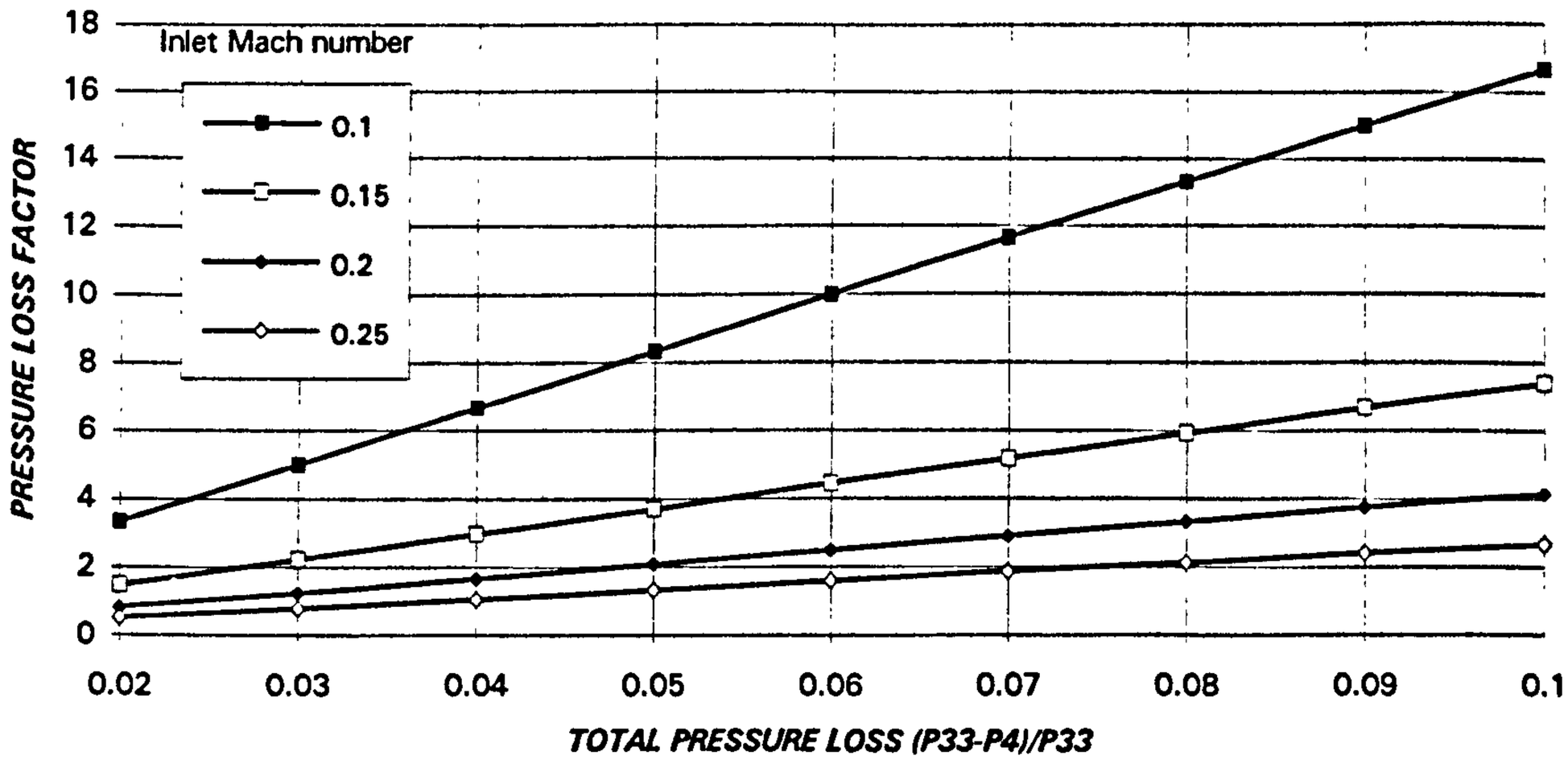

Figure 3.7. Pressure loss factor as a function of total pressure losses and inlet Mach number for a CO_2 semi-closed cycle (γ_{33}=1.200, γ_4=1.165)

In figures 3.6 and 3.7 the PLF is plotted for different total pressure losses and inlet Mach numbers for a conventional open cycle (γ_{33}=1.360, γ_4=1.300) and a CO_2 semi-closed cycle (γ_{33}=1.200, γ_4=1.165).

The hot losses have been neglected to obtain the first estimation of k_1, but now this term will be evaluated using two different methods.

3.8.2.1. Simple Estimation of Combustor Hot Pressure Losses (Incompressible & Constant Area Duct Approach)

As we have seen in the previous section, the pressure loss factor was divided in two terms: cold and hot pressure losses. If the flow is assumed to be incompressible, then

$$P_{33} - P_4 = (p_{33} - p_4) + \left(\frac{1}{2}\rho_{33}V_{33}^2 - \frac{1}{2}\rho_4 V_4^2\right) \qquad [3.106]$$

Using the momentum equation:

$$(A_{33}p_{33} - A_4 p_4) + (W_{33}V_{33} - W_4 V_4) = 0 \qquad [3.107]$$

If, for the purpose of this study, the combustor is simulated as a constant area duct[20] then, eq. [3.107] is simplified:

$$A_{33}(p_{33} - p_4) + W_{33}\left(V_{33} - \left(1 + \frac{W_F}{W_{33}}\right)V_4\right) = 0 \qquad [3.108]$$

Introducing this equation into [3.106]:

$$P_{33} - P_4 = \left(\frac{1}{2}\rho_{33}V_{33}^2 - \frac{1}{2}\rho_4 V_4^2\right) - \frac{W_{33}\left(V_{33} - \left(1 + \frac{W_F}{W_{33}}\right)V_4\right)}{A_{33}} \qquad [3.109]$$

Using the continuity equation:

$$W_{33} = \rho_{33}V_{33}A_{33} \qquad W_4 = \rho_4 V_4 A_{33} \qquad [3.110]$$

---

[20] In some cases the fuel flow is also neglected. However, this simplification is not valid if a low heating value gas is employed.

eq. [3.109] is simplified, giving:

$$P_{33} - P_4 = \left(\frac{1}{2}\rho_{33}V_{33}^2 - \frac{1}{2}\rho_4 V_4^2\right) - \left(\rho_{33}V_{33}^2 - \rho_4 V_4^2\right) = -\left(\frac{1}{2}\rho_{33}V_{33}^2 - \frac{1}{2}\rho_4 V_4^2\right) \qquad [3.111]$$

Expressing the pressure losses as a fraction of the dynamic head:

$$\frac{P_{33} - P_4}{\frac{1}{2}\rho_{33}V_{33}^2} = \frac{\rho_4 V_4^2}{\rho_{33}V_{33}^2} - 1 \qquad [3.112]$$

Using again the continuity equation, and bearing in mind that for the incompressible flows $\rho \propto 1/T$:

$$\frac{P_{33} - P_4}{\frac{1}{2}\rho_{33}V_{33}^2} = \frac{\rho_{33}}{\rho_4} - 1 \propto \frac{T_4}{T_{33}} - 1 \qquad [3.113]$$

This is the general expression of the hot losses when the incompressible assumption is used. Then, the loss term will be:

$$\frac{P_{33} - P_4}{\frac{1}{2}\rho_{33}V_{33}^2} = Cold\ Losses + Hot\ Losses = k_1 + k_2\left(\frac{T_4}{T_{33}} - 1\right) \qquad [3.114]$$

As k_1, the constant k_2 depends on the combustion chamber considered.

3.8.2.2. Detailed Estimation of Combustor Hot Pressure Losses (Compressible & Constant Area Duct Approach)

If the combustor is simplified as in 3.8.2.1., where it was considered as a constant area duct, employing the continuity and momentum equations over this component:

$$p_{33} + \frac{1}{2}\rho_{33}V_{33}^2 - C_D\rho_{33}V_{33}^2 = p_4 + \frac{1}{2}\rho_4 V_4^2 \qquad [3.115]$$

$$\left.\begin{aligned} W_{33} &= \rho_{33}V_{33}A \\ W_4 &= W_{33} + W_F = \rho_4 V_4 A \end{aligned}\right\} \Rightarrow \rho_{33}V_{33} = \frac{\rho_4 V_4}{1 + \frac{W_F}{W_{33}}} \qquad [3.116]$$

The ratio of static pressures is obtained from the momentum equation:

$$\frac{p_4}{p_{33}} = \frac{1+\gamma_{33}M_{33}^2\left(1-\frac{C_D}{2}\right)}{1+\gamma_4 M_4^2} \qquad [3.117]$$

Assuming low Mach numbers, the total pressure ratio will be:

$$\frac{P_4}{P_{33}} = \frac{p_4}{p_{33}} \frac{\left(1+\frac{\gamma_4-1}{2}M_4^2\right)^{\frac{\gamma_4}{\gamma_4-1}}}{\left(1+\frac{\gamma_{33}-1}{2}M_{33}^2\right)^{\frac{\gamma_{33}}{\gamma_{33}-1}}} \qquad [3.118]$$

Using equations [3.117] and [3.118] the following expression is obtained:

$$\frac{P_4}{P_{33}} = \left(\frac{1+\gamma_{33}M_{33}^2\left(1-\frac{C_D}{2}\right)}{1+\gamma_4 M_4^2}\right)\left(\frac{\left(1+\frac{\gamma_4-1}{2}M_4^2\right)^{\frac{\gamma_4}{\gamma_4-1}}}{\left(1+\frac{\gamma_{33}-1}{2}M_{33}^2\right)^{\frac{\gamma_{33}}{\gamma_{33}-1}}}\right) \qquad [3.119]$$

The cold losses term, C_D is, either an input or not considered in this calculation, adding those losses separately.

To be able to obtain the total pressure ratio, the exit Mach number must be calculated. Combining the continuity and gas state equations:

$$\frac{t_4}{t_{33}} = \frac{R_{33}}{R_4}\frac{p_4}{p_{33}}\frac{\rho_{33}}{\rho_4} \xrightarrow{continuity} \frac{t_4}{t_{33}} = \frac{R_{33}}{R_4}\frac{p_4}{p_{33}}\frac{V_4}{V_{33}}\frac{1}{\left(1+\frac{W_F}{W_{33}}\right)} \qquad [3.120]$$

Using now the Mach number, instead of the velocity:

$$\frac{t_4}{t_{33}} = \sqrt{\frac{R_{33}}{R_4}}\frac{p_4}{p_{33}}\frac{M_4\sqrt{\gamma_4 t_4}}{M_{33}\sqrt{\gamma_{33}t_{33}}}\frac{1}{\left(1+\frac{W_F}{W_{33}}\right)} \qquad [3.121]$$

The final expression for the static temperature ratio is:

$$\frac{t_4}{t_{33}} = \frac{R_{33}}{R_4}\left(\frac{p_4}{p_{33}}\right)^2 \frac{\gamma_4 M_4^2}{\gamma_{33} M_{33}^2} \frac{1}{\left(1+\frac{W_F}{W_{33}}\right)} =$$

$$= \frac{R_{33}}{R_4}\left(\frac{1+\gamma_{33} M_{33}^2\left(1-\frac{C_D}{2}\right)}{1+\gamma_4 M_4^2}\right)^2 \frac{\gamma_4 M_4^2}{\gamma_{33} M_{33}^2} \frac{1}{\left(1+\frac{W_F}{W_{33}}\right)} \qquad [3.122]$$

The total temperature ratio will be:

$$\frac{T_4}{T_{33}} = \frac{t_4}{t_{33}} \frac{\left(1+\frac{\gamma_4 - 1}{2} M_4^2\right)}{\left(1+\frac{\gamma_{33} - 1}{2} M_{33}^2\right)} \qquad [3.123]$$

Combining the last two equations, without the cold losses:

$$\frac{T_4}{T_{33}} = \left(\frac{R_{33}}{R_4}\right)\left(\frac{1+\gamma_{33} M_{33}^2}{1+\gamma_4 M_4^2}\right)^2 \left(\frac{1+\frac{\gamma_4 - 1}{2} M_4^2}{1+\frac{\gamma_{33} - 1}{2} M_{33}^2}\right)\left(\frac{\gamma_4 M_4^2}{\gamma_{33} M_{33}^2}\right) \frac{1}{\left(1+\frac{W_F}{W_{33}}\right)} \qquad [3.124]$$

In this expression the only unknown is the exit Mach number, that will be obtained using an iterative method. Figures 3.8 and 3.10 show the exit Mach number as a function of inlet Mach number and temperature ratio. The exit Mach number will be introduced in eq.[3.119] and the hot pressure loss will be then obtained.

In figures 3.9 and 3.11 the hot pressure losses for different inlet Mach numbers and temperature ratios are plotted for a conventional open cycle (γ_{33}=1.360, γ_4=1.300) and for a CO_2 semi-closed cycle (γ_{33}=1.200, γ_4=1.165). The conclusion extracted from these figures is that in the case of large cross-sectional area combustion chambers, where the Mach number is very low, the hot pressure losses are almost negligible. On the other hand, large temperature ratios lead to high hot pressure losses.

3.8.3. COMBUSTOR EFFICIENCY

In the industrial gas turbines industry it is very common to assume constant combustion efficiency (values from 99.5 to 99.9% are typical). The reasons are clear:

- The gas turbine is operating at high power settings most of the time, where the combustion efficiency is always close to 100%.

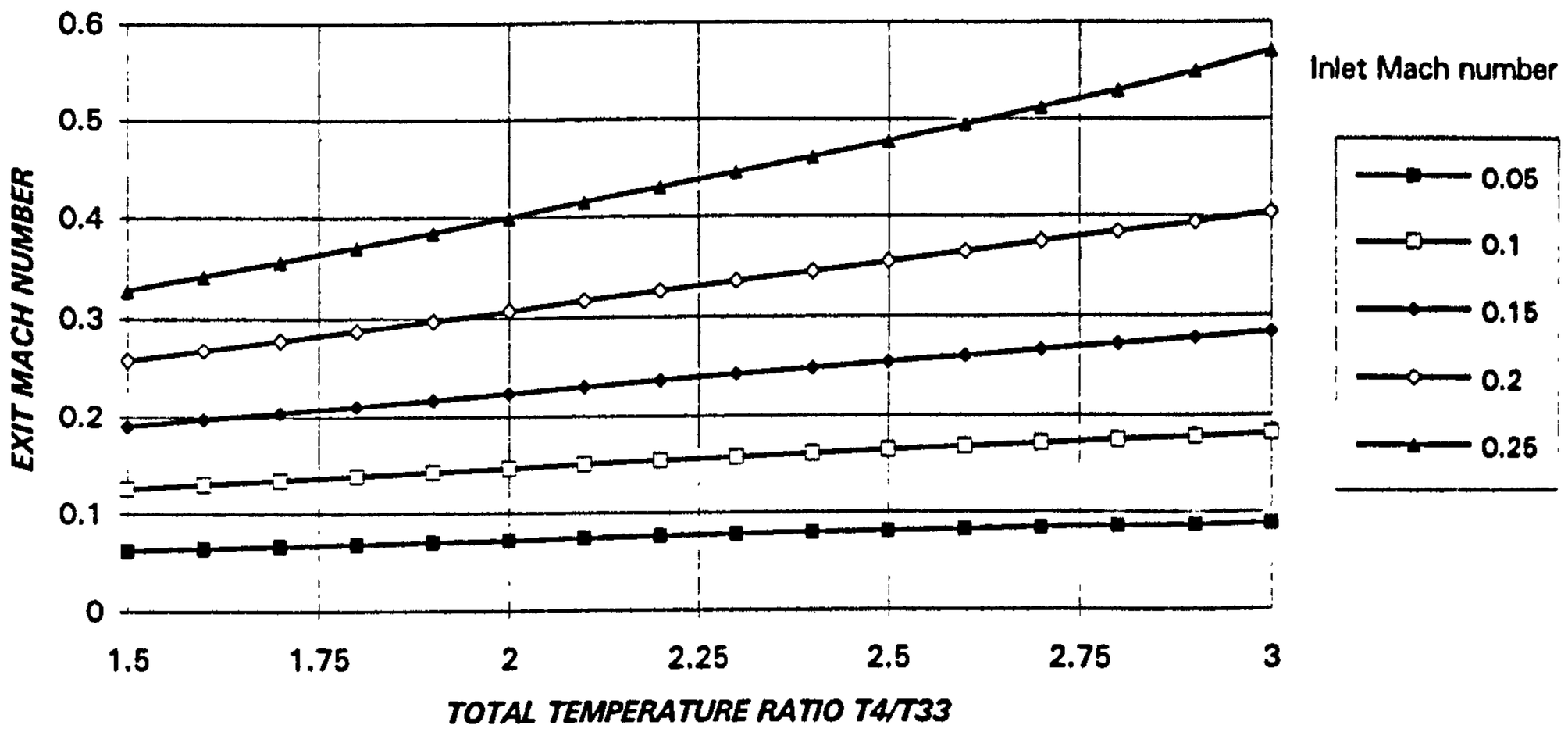

Figure 3.8. Exit Mach number as a function of inlet Mach number and total temperature ratio for a conventional open cycle (γ_{33}=1.360, γ_4=1.300)

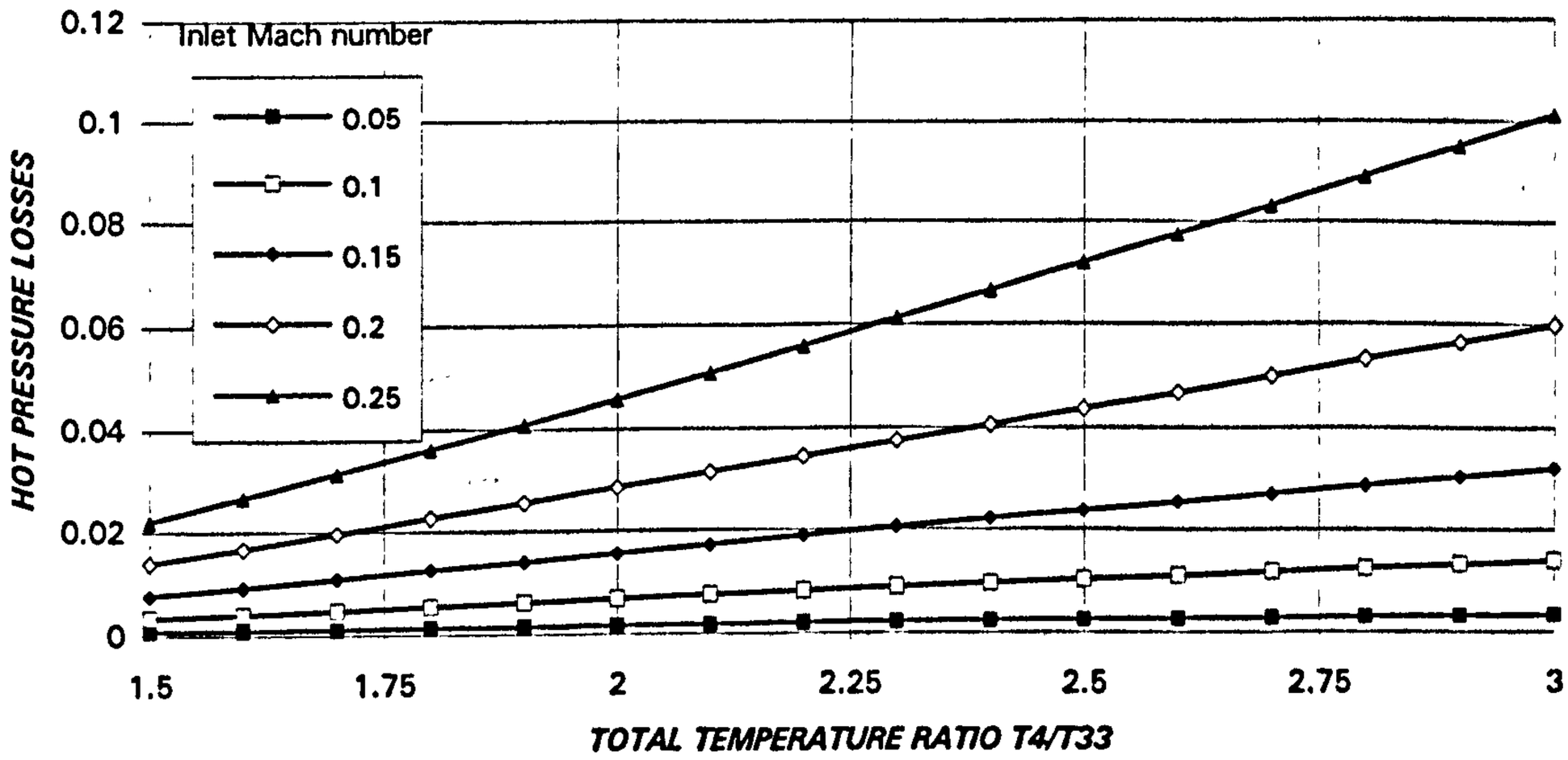

Figure 3.9. Hot losses as a function of total temperature ratio and inlet Mach number for a conventional open cycle (γ_{33}=1.360, γ_4=1.300)

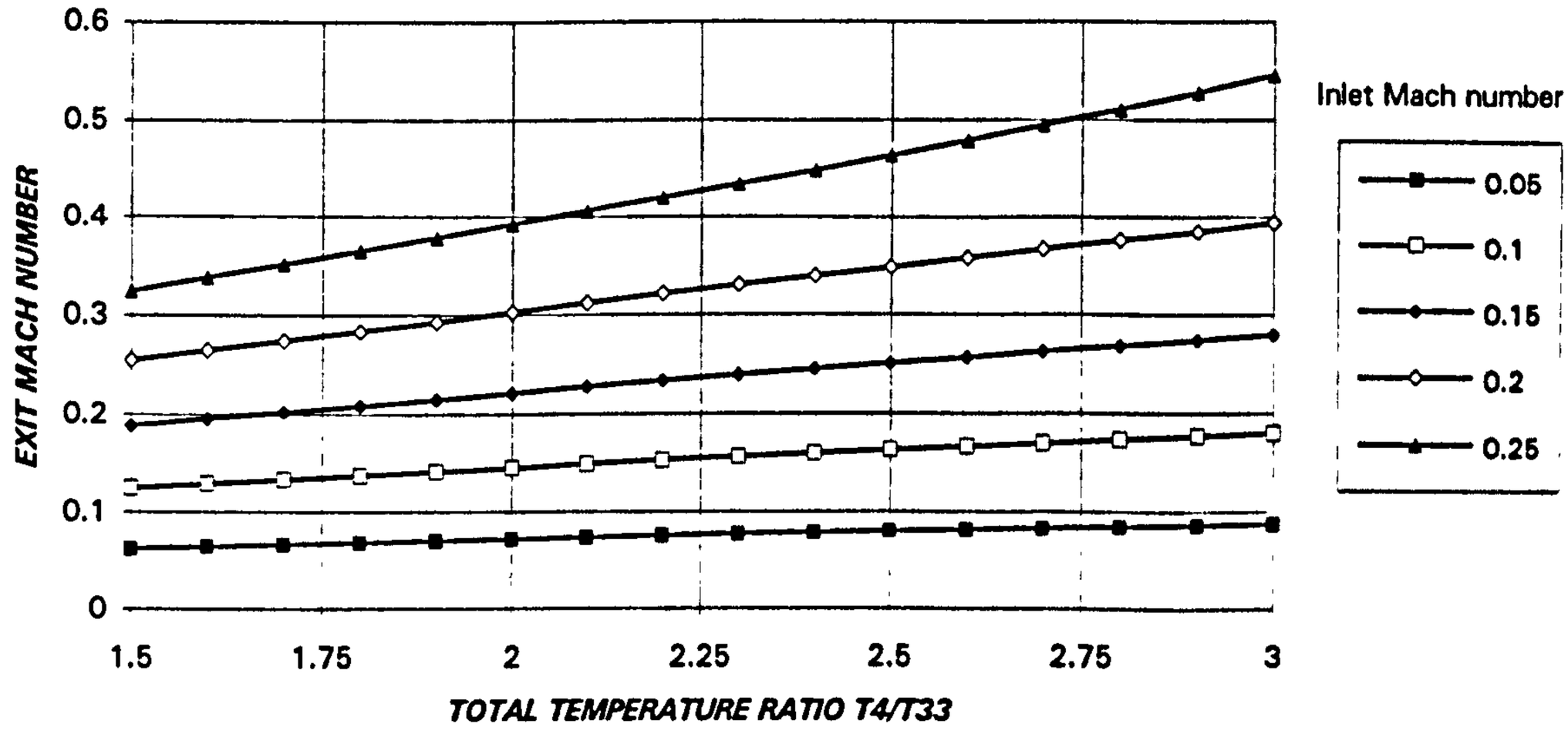

Figure 3.10. Exit Mach number as a function of inlet Mach number and total temperature ratio for a CO_2 semi-closed cycle (γ_{33}=1.200, γ_4=1.165)

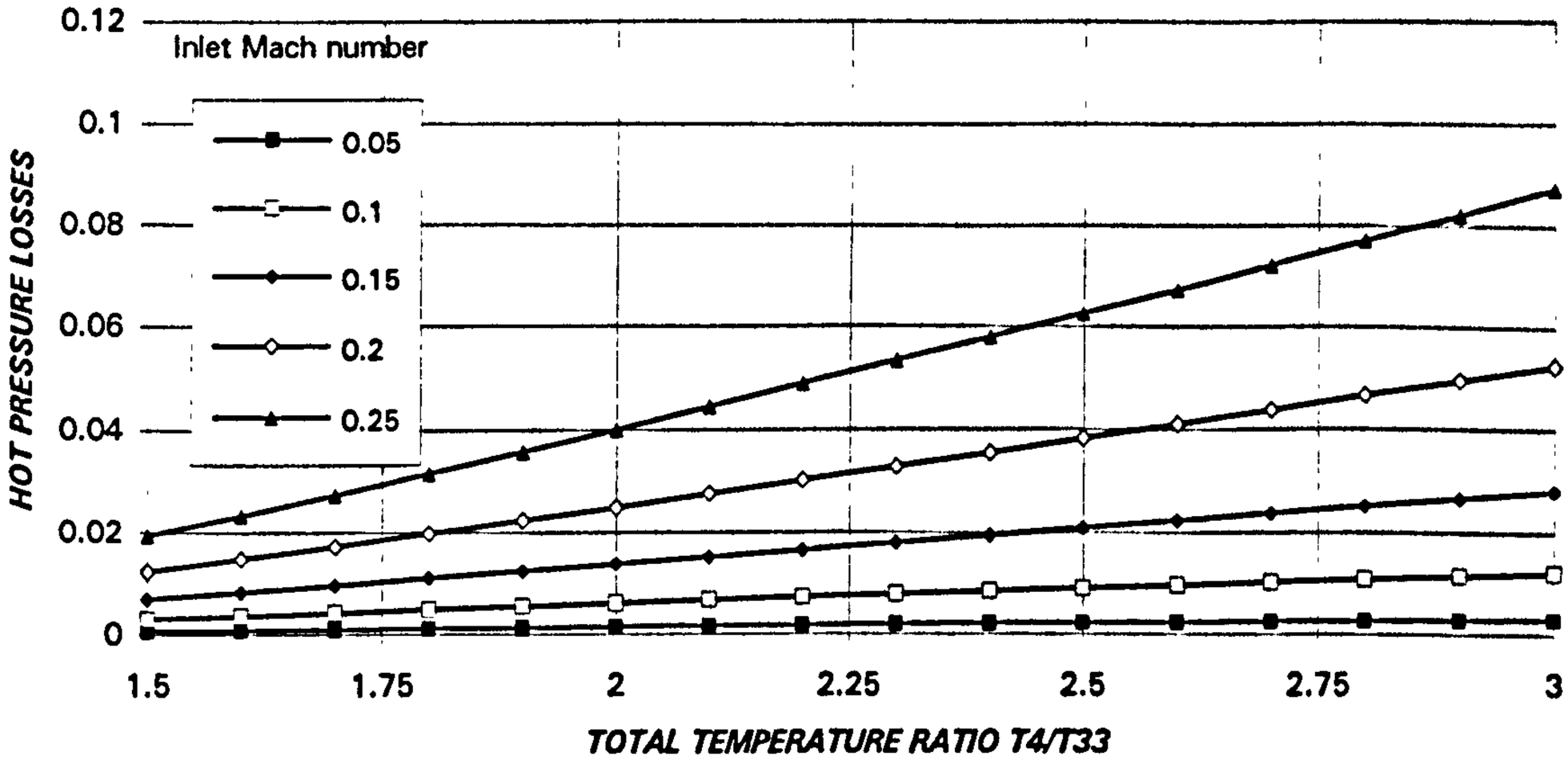

Figure 3.11. Hot losses as a function of total temperature ratio and inlet Mach number for a CO_2 semi-closed cycle (g_{33}=1.200, g_4=1.165)

- The ambient conditions suffer minor changes.
- The project timescales and resources are usually very limited, and the generation of a complete combustor efficiency map is very expensive and time consuming.

However, apart from the correlations developed by the manufacturers, there are some standard approaches that can be used as default [131].

The general expression of the correlations is:

$$\eta_{CC} = f\left(\phi_{PZ},\ \frac{P_{33}^{p} A_{CC} D_{CC}^{d} e^{\frac{T_{33}}{b}}}{W_{33}}\right) \quad \text{or} \quad \eta_{CC} = f\left(\phi_{PZ},\ \frac{P_{33}^{p} A_{CC} L_{CC}^{l} e^{\frac{T_{33}}{b}}}{W_{33}}\right) \qquad [3.125]$$

Where: ϕ_{PZ}: equivalence ratio of the primary zone
A_{CC}: Maximum casing cross sectional area
D_{CC}: Maximum casing diameter
L_{CC}: Combustor length (typically length of primary+seondary zones)
p: Pressure constant exponent to be determined experimentally
d: Diameter constant exponent to be determined experimentally
l: Length constant exponent to be determined experimentally
b: constant dependent on the primary zone equivalence ratio

Some of the most common correlations are:

$$\eta_{CC} = f\left(\frac{P_{33}^{1.75} A_{CC} D_{CC}^{0.75} e^{\frac{T_{33}}{300}}}{W_{33}}\right) \qquad [3.126]$$

$$\eta_{CC} = f\left(\frac{P_{33}^{1.8} A_{CC} D_{CC}^{0.75} e^{\frac{T_{33}}{300}}}{W_{33}}\right) \qquad [3.127]$$

$$\eta_{CC} = f\left(\frac{P_{33}^{1.75} A_{CC} L_{CC} e^{\frac{T_{33}}{300}}}{W_{33}}\right) = f\left(\frac{P_{33}^{1.75} Vol_{CC} e^{\frac{T_{33}}{300}}}{W_{33}}\right) \qquad [3.128a]$$

$$\eta_{CC} = f\left(\frac{P_{33}^{1.8} A_{CC} L_{CC} e^{\frac{T_{33}}{300}}}{W_{33}}\right) = f\left(\frac{P_{33}^{1.8} Vol_{CC} e^{\frac{T_{33}}{300}}}{W_{33}}\right) \qquad [3.128b]$$

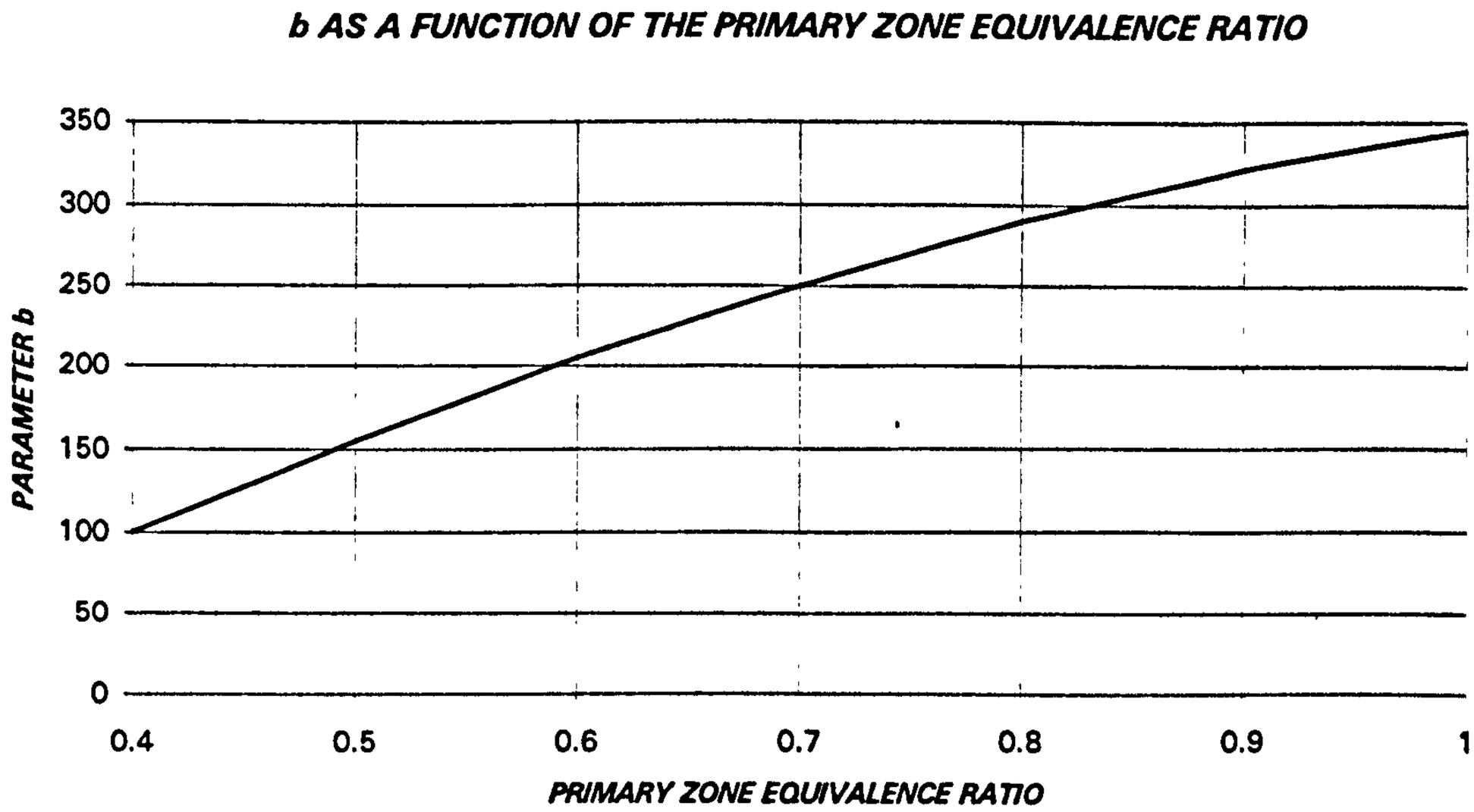

Figure 3.12. Parameter b as a function of the primary zone ratio

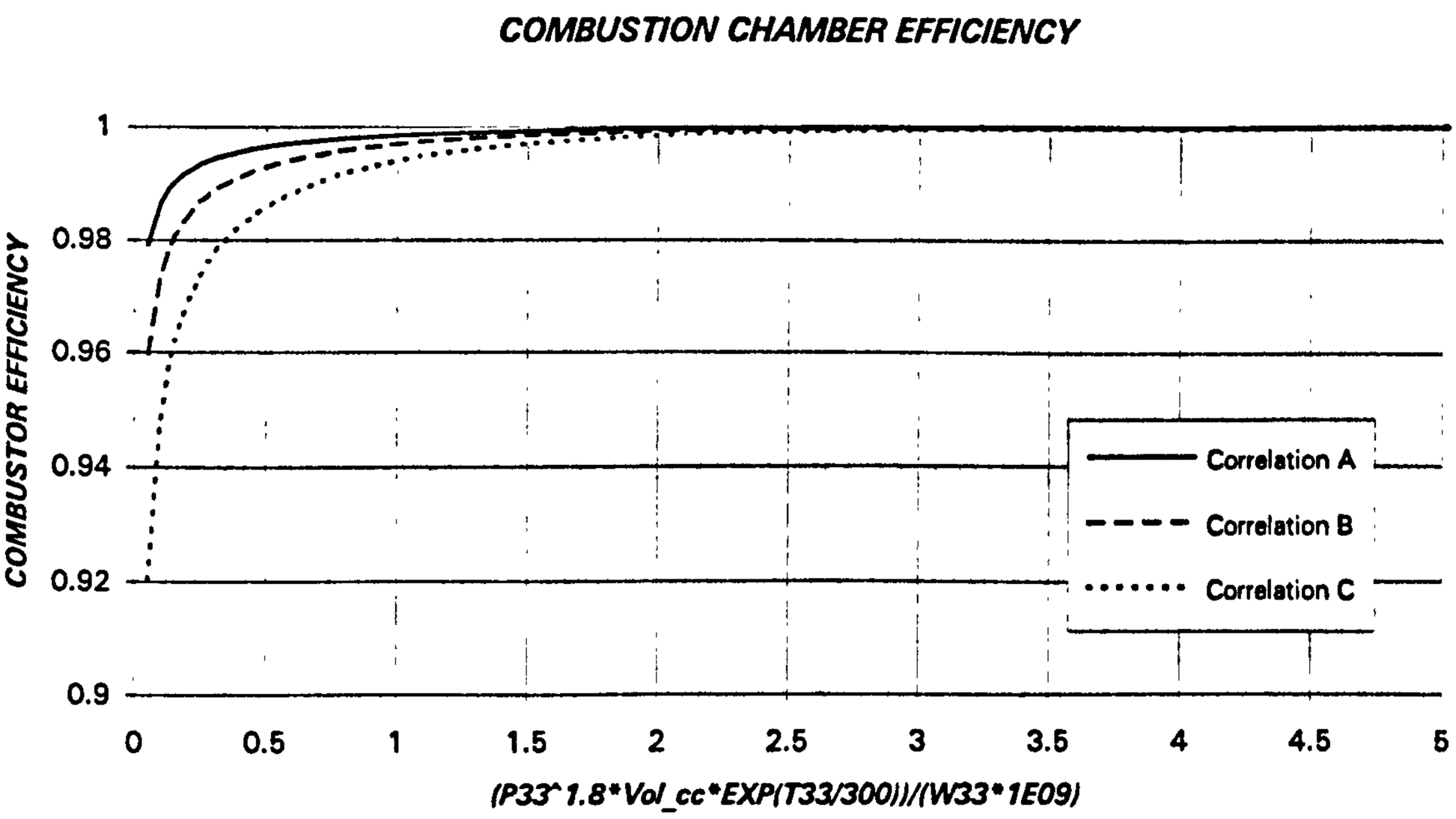

Figure 3.13. Combustion chamber efficiency using parameter of eq. [3.128b] for the correlation

The reason of eliminating the primary zone equivalence ratio is that, for conventional combustion chambers, it is always very close to one.[21] Eq.[3.128a] was developed by Longwell and Weiss [131] based on experiments using stirred reactors. They found that the parameter b is a function of the primary zone equivalence ratio, as shown in figure 3.12. In figure 3.13 some correlation efficiencies are plotted following the approach of equation [3.128b], similar to [3.128a].

In some cases the efficiency is calculated from correlations where the non-complete combustion is considered (generation of UHC, oxides of Nitrogen, carbon monoxide, ...).

3.8.4. COMBUSTOR EXIT TEMPERATURE

The exit temperature can be calculated in two ways:

- Employing the energy equation.
- Using experimental tables.

The first one will be described in this section.

3.8.4.1. Combustor Exit Temperature: Energy Equation

The general form of the energy equation, assuming that the exit water is gaseous, will be:

$$W_{33}H_{33}+\eta_{CC}W_{FUEL}LHV+\eta_{CC}W_{FUEL}\left(H^{T}_{FUEL}-H^{298}_{FUEL}\right)=\left(W_{33}+\eta_{CC}W_{FUEL}\right)H_{4} \qquad [3.129]$$

If the combustion products were known, the result given by this equation would be very accurate. However, if the products are not known, the errors could be important.

The first information should be the fuel composition (CH_x,CO, H_2, ...). From that input, the basic equations will be the following chemical reactions:

$$CH_x+\left(1+\frac{x}{4}\right)O_2\rightarrow CO_2+\frac{x}{2}H_2O \qquad [3.130]$$

$$H_2+\frac{1}{2}O_2\rightarrow H_2O \qquad [3.131]$$

---

[21] This method will not be valid for the modern lean pre-mixed low NO_x combustors.

$$CO + \frac{1}{2} O_2 \rightarrow CO_2 \qquad [3.132]$$

The carbon dioxide, nitrogen, inert gases (argon, helium,...), remaining oxygen, etc. will not react. The products will be carbon dioxide, water and the non-reactant gases. This approach will be good enough for moderate combustion temperatures, but not for high ones. In that case the products should be calculated using, at least, five equilibrium equations:

$$\frac{1}{2} O_2 + \frac{1}{2} N_2 \leftrightarrow NO \qquad [3.133]$$

$$H_2O \leftrightarrow H_2 + \frac{1}{2} O_2 \qquad [3.134]$$

$$H_2O \leftrightarrow OH + \frac{1}{2} H_2 \qquad [3.135]$$

$$CO_2 \leftrightarrow CO + \frac{1}{2} O_2 \qquad [3.136]$$

$$CO_2 + H_2 \leftrightarrow CO + H_2O \qquad [3.137]$$

This model will be adequate to simulate the combustor as a three parts component: primary zone, secondary zone and dilution zone. In the first one, due to the high temperatures, the complete set of equations is required. In the second region the combustion continues, although the oxides of nitrogen generated in the primary zone will not disappear. In the dilution part there is almost no chemical reaction, being just the mixture of two streams. The development of the complete component, as described above, was carried out as a separate module, because no validation data was available to the author. A remaining issue for future code development would be the introduction and validation of a more complex reaction system. The validity of this method should also be confirmed against the new technologies, such as the lean pre-mix combustor, to have confidence in the prediction of future systems.

3.9. TURBINE

High, intermediate and low pressure turbine as well as power turbine can be simulated using the same type of equations.

In this section a HPT will be considered. Between the entry flow (engine section 4) and the stator throat (engine station 405) there will be a cooling flow addition W_{B7}. Between the throat and the entry of the rotor (engine station 41) there is another

another cooling flow added to the main stream, W_2^{Bleed}. After the rotor (engine station 42), the last cooling flow is injected, W_3^{Bleed}.[22] The net value of the flows must take into account the internal air system contribution, (disks, firtrees, platforms and casings cooling). Due to the hot gas ingestion, these flows can, in some cases, be negative. A more detailed explanation will be found in chapter 5, dedicated to the treatment of cooling flows.

3.9.1. TURBINE THROAT

The equations of mass flow, energy and species conservation describe the flow evolution between the entry of the turbine and its throat, with no total pressure losses considered[23]:

$$W_{405} = W_4 + W_1^{Bleed} \qquad [3.138]$$

$$P_{405} = P_4 \qquad [3.139]$$

$$H_{405} = \frac{(W_4 H_4 + W_1^{Bleed} H_1^{Bleed})}{W_4 + W_1^{Bleed}} \qquad [3.140]$$

$$x_{i\,405} = \frac{(x_{i\,4} W_4 + x_{i\,1}^{Bleed} W_1^{Bleed})}{W_4 + W_1^{Bleed}} \qquad [3.141]$$

A particular case of the species conservation is the fuel to air ratio and water to air ratio calculation in the open cycles.

With this information it will be possible to evaluate the mass flow parameter at this station, crucial for the complete gas turbine behaviour.

$$\frac{W_{405}\sqrt{\theta_{405}}}{\delta_{405}} \sqrt{\frac{R_{405}}{\gamma_{405}}} \left(1 + \frac{\gamma_{405} - 1}{2} M_{405_{DS}}^2\right)^{\frac{\gamma_{405}+1}{2(\gamma_{405}-1)}} \qquad [3.142]$$

Typically, the Mach number will be unity, and the expression will be:

---

[22] The cooling flows W_1^{Bleed} and W_2^{Bleed} are used for the NGV and W_3^{Bleed} is used for the rotor.

[23] In single stage turbines it will not be difficult to derive a value of total pressure losses from the efficiency map, assuming a split between rotor and stator, with a further division inside the rows to account for the losses after and before the throat. In multi-stage turbines it would also be possible to make a guess and use a value of 0.02-0.05 of total pressure losses relative to the exit dynamic head. When the total pressure losses are not considered, a scaling factor for the mass flow parameter, comprising the errors in total pressure, temperature and area, will be employed.

$$\frac{W_{405}\sqrt{\theta_{405}}}{\delta_{405}}\sqrt{\frac{R_{405}}{\gamma_{405}}}\left(\frac{\gamma_{405}+1}{2}\right)^{\frac{\gamma_{405}+1}{2(\gamma_{405}-1)}} \qquad [3.143]$$

3.9.2. ROTOR ENTRY

As in 3.9.1., the equations of mass flow, energy and species conservation describe the flow evolution between the throat of the NGV and the rotor entry. Again, no total pressure losses are considered.

$$W_{41} = W_{405} + W_2^{Bleed} \qquad [3.144]$$

$$P_{41} = P_{405} \qquad [3.145]$$

$$H_{41} = \frac{(W_{405}H_{405} + W_2^{Bleed}H_2^{Bleed})}{W_{405} + W_2^{Bleed}} \qquad [3.146]$$

$$x_{i\,41} = \frac{(x_{i\,405}W_{405} + x_{i\,2}^{Bleed}W_2^{Bleed})}{W_{405} + W_2^{Bleed}} \qquad [3.147]$$

From the enthalpy, pressure and composition the stator outlet temperature, another essential gas turbine parameter, will be found.

3.9.3. TURBINE ROTOR

In the turbine rotor there will be no change in mass flow or species, and only a drop in temperature and pressure is considered. As in the case of the compressor design, there will be four possibilities:

- Pressure ratio and isentropic (adiabatic) efficiency data, CASE I. Occurs typically if the turbine is discharging to the exhaust nozzle:

$$\pi_{HPT} = \frac{P_{42}}{P_{41}} \qquad \eta_{is\,HPT} = \eta_{is\,41-42}$$

- Pressure ratio and polytropic efficiency data, CASE II. As in the previous case, takes place if the turbine is discharging to the exhaust nozzle:

$$\pi_{HPT} = \frac{P_{42}}{P_{41}} \qquad \eta_{poly\,HPT} = \eta_{poly\,41-42}$$

- Reduction in corrected enthalpy and isentropic (adiabatic) efficiency data, CASE III. Is the normal case of a turbine driving a compressor:

$$\frac{\Delta H_{HPT}}{(\gamma R\theta)_{HPT}} = \frac{\Delta H_{41-42}}{\gamma_{41} R_{41} \theta_{41}} \qquad \eta_{is\,HPT} = \eta_{is\,41-42}$$

- Reduction in corrected enthalpy and polytropic efficiency data, CASE IV. Again, is the common case of a turbine driving a compressor:

$$\frac{\Delta H_{HPT}}{(\gamma R\theta)_{HPT}} = \frac{\Delta H_{41-42}}{\gamma_{41} R_{41} \theta_{41}} \qquad \eta_{poly\,HPT} = \eta_{poly\,41-42}$$

3.9.4. TURBINE DELIVERY TEMPERATURE AND PRESSURE IF ISENTROPIC EFFICIENCY AND PRESSURE RATIO ARE GIVEN (CASE I)

When isentropic efficiency and pressure ratio are given, the exit temperature can be calculated using a procedure analogous to the one described in 3.3.1.

From the adiabatic efficiency definition the next equation is obtained:

$$\int_{T_{41}}^{T_{42}} C_P dT = \frac{1}{\eta_{41-42}} \int_{T_{41}}^{T_{42}^{IS}} C_P dT \qquad [3.148]$$

The isentropic exit temperature will be determined using the Gibbs equation (analogous to [3.24]):

$$0 = \int_{T_{41}}^{T_{42}^{IS}} C_P \frac{dT}{T} - R_{41}\, Ln \frac{P_{42}}{P_{41}} = \left(\Phi_{42}^{IS} - \Phi_{41}\right) - R_{41}\, Ln \frac{P_{42}}{P_{41}} \qquad [3.149]$$

With these equations the turbine isentropic and actual exit temperatures will be calculated employing an iterative method. The first value of the isentropic temperature will be obtained with the conventional relation between pressure and temperature as shown in eq.[3.25].

3.9.5 TURBINE DELIVERY TEMPERATURE AND PRESSURE IF POLYTROPIC EFFICIENCY AND PRESSURE RATIO ARE GIVEN (CASE II)

In the case of known polytropic efficiency and pressure ratio, the exit temperature can be calculated using a procedure similar to the one described in detail in 3.3.2.

The definition of polytropic efficiency for a turbine will be:

$$\eta_{41-42}^{POLY} = \frac{dH}{dH^{IS}} \qquad [3.150]$$

The expression that relates pressure ratio, exit temperature and polytropic efficiency, using the Gibbs equation and the definition of polytropic efficiency is:

$$\frac{1}{\eta_{41-42}^{POLY}} \int_{T_{41}}^{T_{42}} C_P \frac{dT}{T} = \frac{1}{\eta_{41-42}^{POLY}} (\Phi_{42} - \Phi_{41}) = R_{41} \, Ln \frac{P_{42}}{P_{41}} \qquad [3.151]$$

The exit temperature will be determined employing an iterative procedure. A first estimation of its value can be done by assuming constant C_p during the expansion process, obtaining an expression equivalent to [3.31]:

$$T_{42} = T_{41} \left(\frac{P_{42}}{P_{41}} \right)^{\frac{\eta_{41}^{POLY}(\gamma_{41}-1)}{\gamma_{41}}} \qquad [3.152]$$

3.9.6. TURBINE DELIVERY TEMPERATURE AND PRESSURE IF ISENTROPIC EFFICIENCY AND REDUCTION IN CORRECTED ENTHALPY ARE GIVEN (CASE III)

When the isentropic efficiency and drop in corrected enthalpy are given, the exit temperature and pressure are determined with the following procedure.

Equation [3.149] obtained in 3.9.4. gives the relation between isentropic temperature and pressure ratio. Hence, if the exhaust isentropic temperature is found, the pressure ratio will be immediately obtained.

Using the isentropic efficiency definition, the next equation is determined:

$$\int_{T_{41}}^{T_{42}^{IS}} C_P dT = \eta_{41-42} \gamma_{41} R_{41} \theta_{41} \left(\frac{\Delta H_{41-42}}{\gamma_{41} R_{41} \theta_{41}} \right) \qquad [3.153]$$

the rhs of the equation is known. Hence, the isentropic temperature can be easily calculated and, using eq.[3.149], the pressure ratio is easily obtained.

3.9.7 TURBINE DELIVERY TEMPERATURE AND PRESSURE IF POLYTROPIC EFFICIENCY AND REDUCTION IN CORRECTED ENTHALPY ARE GIVEN (CASE IV)

If the polytropic efficiency and decrease in corrected enthalpy are given, the exit temperature and pressure will be determined using the definition of corrected enthalpy:

$$\left(\frac{\Delta H_{41-42}}{\gamma_{41}R_{41}\theta_{41}}\right)=\frac{1}{\gamma_{41}R_{41}\theta_{41}}\int_{T_{41}}^{T_{42}}C_p dT \qquad [3.154]$$

The only unknown in this equation is the turbine discharge temperature T_{42}, that can be found using an iterative method.

With equation [3.151], derived in 3.9.5, relating pressure ratio, exit temperature and polytropic efficiency, the discharge pressure will be immediately obtained.

3.9.8. EXIT OF THE TURBINE

Once the rotor exit has been solved, the last cooling is introduced. This takes into account the rotor cooling flow and others that do not contribute to the turbine work.

As in 3.9.1. and 3.9.2. the equations of mass flow, energy and species conservation describe the flow evolution between the exit of the rotor and the exit of the turbine, with no total pressure losses being considered.

$$W_{43}=W_{42}+W_3^{Bleed} \qquad [3.155]$$

$$P_{43}=P_{42} \qquad [3.156]$$

$$H_{43}=\frac{(W_{42}H_{42}+W_3^{Bleed}H_3^{Bleed})}{W_{42}+W_3^{Bleed}} \qquad [3.157]$$

$$x_{i\,43}=\frac{(x_{i\,42}W_{42}+x_{i\,3}^{Bleed}W_3^{Bleed})}{W_{42}+W_3^{Bleed}} \qquad [3.158]$$

From the enthalpy, pressure and flow composition, the turbine outlet temperature, used for the control in most conventional gas turbines, will be obtained.

3.9.9. TURBINE OFF-DESIGN BEHAVIOUR

As in the case of the compressor, the turbine characteristics can be corrected using the mass flow, enthalpy drop or pressure ratio, shaft speed and efficiency:

$$\left(\frac{W_{405}\sqrt{\theta_{405}}}{A_{405}\delta_{405}}\sqrt{\frac{R_{405}}{\gamma_{405}}}\right)=f\left(\frac{\Delta H_{41-42}}{\gamma_{405}R_{405}\theta_{405}},\ \frac{N_{HPS}}{\sqrt{\gamma_{405}R_{405}\theta_{405}}}\right) \qquad [3.159]$$

$$\eta_{41}=f\left(\frac{\Delta H_{41-42}}{\gamma_{41}R_{41}\theta_{41}},\ \frac{N_{HPS}}{\sqrt{\gamma_{41}R_{41}\theta_{41}}}\right) \qquad [3.160]$$

$$\left(\frac{W_{405}\sqrt{\theta_{405}}}{A_{405}\delta_{405}}\sqrt{\frac{R_{405}}{\gamma_{405}}}\right)=f\left(\frac{P_{41}}{P_{42}},\ \frac{N_{HPS}}{\sqrt{\gamma_{405}R_{405}\theta_{405}}}\right) \quad [3.161]$$

$$\eta_{41}=f\left(\frac{P_{41}}{P_{42}},\ \frac{N_{HPS}}{\sqrt{\gamma_{405}R_{405}\theta_{405}}}\right) \quad [3.162]$$

When the Mach number is included, to improve the simulation capability, the next functions are obtained:

$$\frac{W_{405}\sqrt{\theta_{405}}}{A_{405}\delta_{405}}\sqrt{\frac{R_{405}}{\gamma_{405}}}\left(1+\frac{\gamma_{405}-1}{2}M^2_{405_{DS}}\right)^{\frac{\gamma_{405}+1}{2(\gamma_{405}-1)}}=$$

$$=f_1\left(\frac{\Delta H_{41-42}\left(1+\frac{\gamma_{405}-1}{2}M^2_{405_{DS}}\right)}{\gamma_{405}R_{405}\theta_{405}},\ \frac{N_{HPS}\sqrt{1+\frac{\gamma_{405}-1}{2}M^2_{405_{DS}}}}{\sqrt{\gamma_{405}R_{405}\theta_{405}}}\right) \quad [3.163]$$

$$\eta_{41-42}=f_2\left(\frac{\Delta H_{41-42}\left(1+\frac{\gamma_{405}-1}{2}M^2_{405_{DS}}\right)}{\gamma_{405}R_{405}\theta_{405}},\ \frac{N_{HPS}\sqrt{1+\frac{\gamma_{405}-1}{2}M^2_{405_{DS}}}}{\sqrt{\gamma_{405}R_{405}\theta_{405}}}\right) \quad [3.164]$$

Generic turbine maps can also be scaled to simulate our particular case:

$$\left[\frac{\Delta H_{41-42}}{\gamma_{405}R_{405}\theta_{405}}\right]_{DESIGN}=sf_{\Delta H_{HPT}}\left[\frac{\Delta H_{41-42}}{\gamma_{405}R_{405}\theta_{405}}\right]_{MAP} \quad [3.165]$$

$$\left[\frac{P_{41}}{P_{42}}-1\right]_{DESIGN}=sf_{\pi_{HPT}}\left[\frac{P_{41}}{P_{42}}-1\right]_{MAP} \quad [3.166]$$

$$[\eta_{41-42}]_{DESIGN}=sf_{\eta_{HPT}}[\eta_{41-42}]_{MAP} \quad [3.167]$$

$$\left[\frac{W_{405}\sqrt{\theta_{405}}}{\delta_{405}}\sqrt{\frac{R_{405}}{\gamma_{405}}}\right]_{DESIGN}=sf_{W_{HPT}}\left[\frac{W_{405}\sqrt{\theta_{405}}}{\delta_{405}}\sqrt{\frac{R_{405}}{\gamma_{405}}}\right]_{MAP} \quad [3.168]$$

If a more accurate definition of the non dimensional parameters where employed, the enthalpy and mass flow scaling factors would be:

$$sf_{\Delta H_{HPT}} = \frac{\left[\frac{\Delta H_{41-42}\left(1+\frac{\gamma_{405}-1}{2}M^2_{405_{DS}}\right)}{\gamma_{405}R_{405}\theta_{405}}\right]_{DESIGN}}{\left[\frac{\Delta H_{41-42}\left(1+\frac{\gamma_{405}-1}{2}M^2_{405_{DS}}\right)}{\gamma_{405}R_{405}\theta_{405}}\right]_{MAP}} \qquad [3.169]$$

$$sf_{W'_{HPT}} = \frac{\left[\frac{W_{405}\sqrt{\theta_{405}}}{\delta_{405}}\sqrt{\frac{R_{405}}{\gamma_{405}}}\left(1+\frac{\gamma_{405}-1}{2}M^2_{405_{DS}}\right)^{\frac{\gamma_{405}+1}{2(\gamma_{405}-1)}}\right]_{DESIGN}}{\left[\frac{W_{405}\sqrt{\theta_{405}}}{\delta_{405}}\sqrt{\frac{R_{405}}{\gamma_{405}}}\left(1+\frac{\gamma_{405}-1}{2}M^2_{405_{DS}}\right)^{\frac{\gamma_{405}+1}{2(\gamma_{405}-1)}}\right]_{MAP}} \qquad [3.170]$$

3.9.10. MULTI-STAGE TURBINE

For performance purposes the turbine is a black box characterised by two maps. When the turbine has more than one stage and the mass flow through the turbine changes, due to the cooling and sealing flows, the links between the power supplied, the efficiency and the exit temperature are not completely clear. The typical way to solve the problem is to have the following:

- An efficiency map which does not correspond with the aerodynamic efficiency, but produces the right exit temperature (enthalpy) for a given speed.
- A corrected mass flow map which produces the right work for the enthalpy drop and speed.

With this method it is possible to observe some paradoxes (i.e. improvements in the turbine efficiency as the cooling flow increases, with a clear drop in the efficiency of the machine). Therefore, the target is to find an inlet mass flow and enthalpy that give the right exit temperature and power with an efficiency that has some aerodynamic meaning, having information of the first NGV corrected mass flow. Chapter 5 will give a more detailed explanation on this subject.

3.9.11. REYNOLDS NUMBER CORRECTION

As in the case of the compressor, the turbine maps will also be corrected with the Reynolds number. The generic equations derived in 3.3.6.6 can be directly applied

for the turbine. For open cycles, using assumptions similar to the ones made for the compressor, the expression of the turbine Reynolds number correction will be:

$$Re_{correction} = f\left(\frac{p}{p_{ref}}\left(\frac{t_{ref}}{t}\right)^{1.15}, \quad \frac{N\sqrt{T_{ref}}}{N_{ref}\sqrt{T}}\right) \qquad [3.171]$$

However, it is very frequent to obtain the turbine maps running cold tests and using scale models.[24] Therefore, gas properties and scale corrections will be important, being necessary to employ the full expression given by equation [3.60].

3.10. REHEAT

The reheat gas turbine concept has been operating in the aeroengine field for over three decades as a mean of increasing the thrust (up to 50-60% relative to non-reheat operation) without any modification in the core of the machine [95]. The penalty is a large increase in specific fuel consumption. With no turbomachinery behind the afterburner the temperatures reach values close to stoichiometric (2000-2200 K).

In industrial gas turbines, the concept of reheat is not new, and in the early-mid 80s some papers showed the possible advantages of such system [37], [57], [58], [90], [104], [105], [106] and [107]. During the mid-late 80s the Japanese AGTJ-100A and 100B intercooled & reheat gas turbines were under full scale test for over three years [90] and [127]. However, it was in the early-mid 90s when this concept was implemented in production turbines (ABB-GT24 & GT26).

Unlike for the aero gas turbines, where the afterburner is mostly used for short periods of time, in the industrial field the reheat is employed during baseline continuous operation in combination with the combustor, and is located after one or more turbine stages, with additional expansion downstream. The reheat temperatures are far from stoichiometric, being the typical of a conventional combustor, or even lower [57], [90] and [127]. The arrangement of the system is also similar to a combustion chamber, not to an aeroengine afterburner.

In terms of efficiency, when used as a simple cycle, the result could not be the best, due to the large quantities of heat rejected to the atmosphere.[25] But when the reheat gas turbine is used in conjunction with a steam turbine bottoming cycle the thermal efficiency is excellent, achieving figures of the order of 55-60%.

---

[24] For situations where the engine Reynolds number is near the critical value it will be important to run the tests using this value, or a very close one.

[25] Only when very high overall pressure ratios are employed the exit temperature is adequate. As an example, the ABB GT-24 & GT-26 have a pressure ratio around 30.

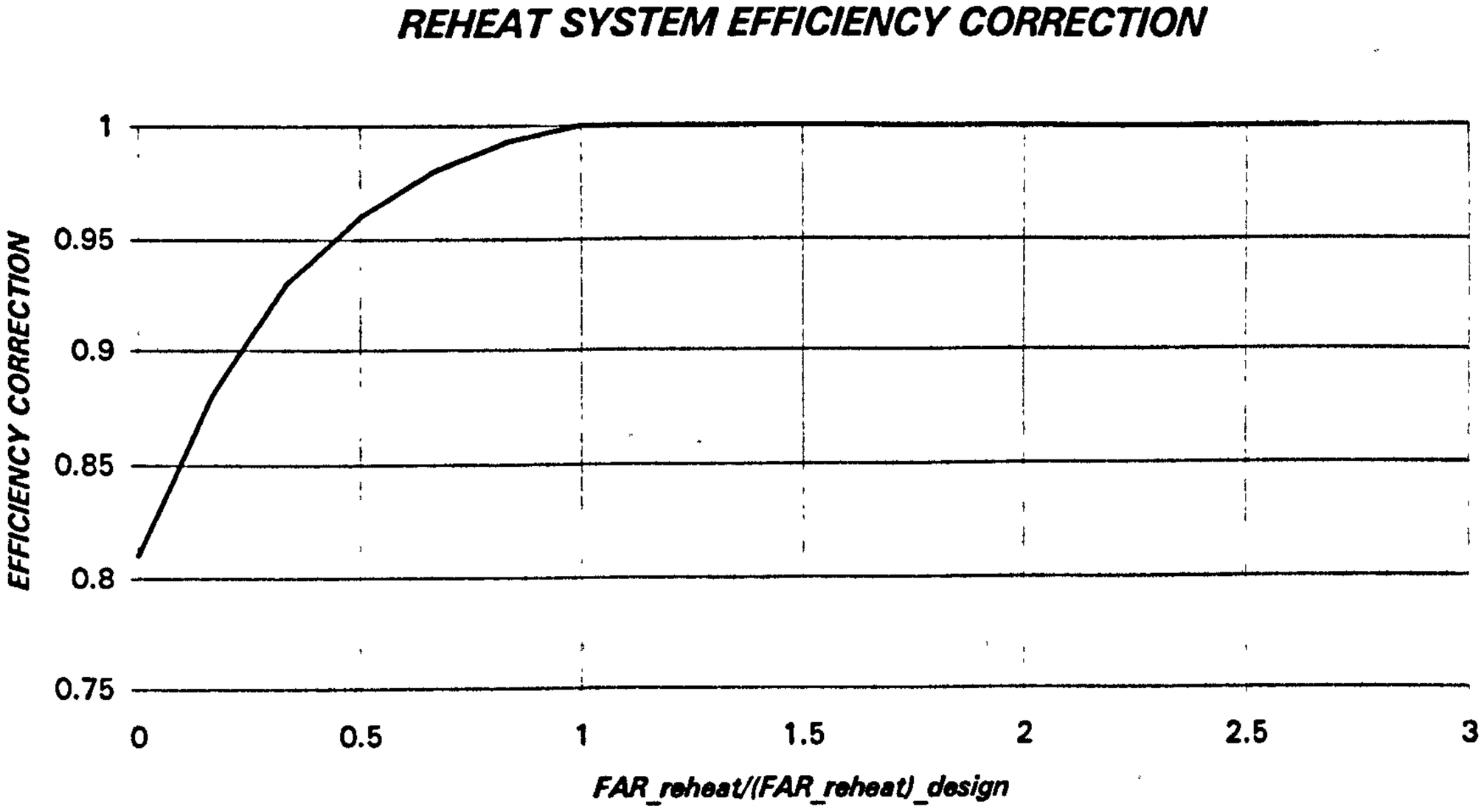

Figure 3.14. Reheat system efficiency correction for low fuel to air ratio operation

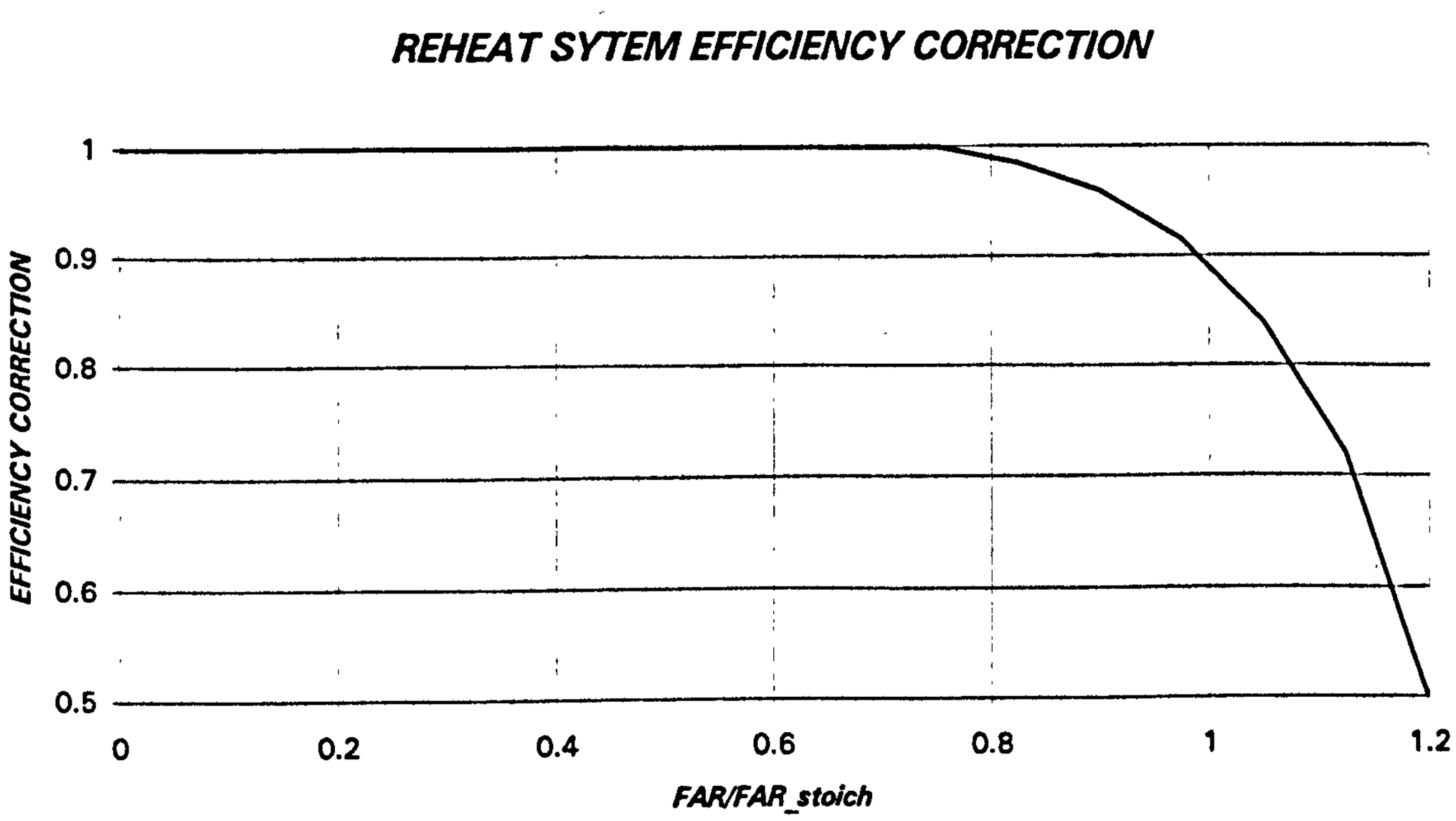

Figure 3.15. Reheat system efficiency correction for large fuel to air ratio operation

3.10.1. SIMULATION OF REHEAT

The reheat will be treated as another combustion chamber. The only difference will lie in the efficiency calculation. Figures 3.14 and 3.15 show factors that modify the conventional combustion efficiency.

3.11. EXHAUST DIFFUSER

While the aircraft propulsion engines try to accelerate the flow as much as possible, to produce thrust, the industrial gas turbines do not use the exit velocity. Therefore, the exhaust kinetic energy should be minimised to improve the performance, being a compromise between final area (or Mach number) and diffuser length, due to the limitation in the divergence angle (values around 5-7° are usually selected):

- Long diffuser=high wall friction losses & low exit Mach number[26]

- Short diffuser=low wall friction losses & high exit Mach number

If the exhaust is subsonic, which is the most common situation, the final static pressure will be ambient. If that is not the case, the exit Mach number will be one at section 8 and the static pressure will reach the critical value. The total pressure losses are, typically, a function of the inlet Mach number (or dynamic head) and swirl. The equations that solve the exhaust diffuser are the following:

$$W_8 = W_{-2} \qquad [3.172]$$

$$H_8 = H_{-2} \qquad (T_8 = T_{-2}) \qquad [3.173]$$

$$P_8 = P_{-2}\left(1 - \frac{\Delta P_{Friction}}{P_{-2}} - \frac{\Delta P_{Swirl}}{P_{-2}}\right) = P_{-2}\left(1 - K'_{-2}\left(\frac{W_{-2}\sqrt{T_{-2}}}{A_{-2}P_{-2}}\right)^2 - \frac{\Delta P_{Swirl}}{P_{-2}}\right) \qquad [3.174]$$

$$\left.\begin{aligned} &\frac{\Delta P_{Swirl}}{P_{-2}} = f(M_{-2}, \varphi_{-2}) \\ &\text{or} \\ &\frac{\Delta P_{Swirl}}{P_{-2}} = f(M_8, \varphi_8) \end{aligned}\right\} \qquad [3.175]$$

---

[26] The low energy boundary layer will be separated after a certain length, dictating the optimum diffuser length, as the region of the diffuser located after the separation is useless.

$$M_{8ax} = M_8 \cos\varphi_8 \qquad [3.176]$$

$$\left.\begin{array}{ccc} p_8 = p_{amb} & \& & M_{8ax} < 1 \\ \text{or} & & \\ M_{8ax} = 1 & \& & p_8 = p^* \end{array}\right\} \qquad [3.177]$$

$$H_8 = h_8 + \frac{1}{2} v_8^2 = h_8 + \frac{1}{2} \gamma_8 R_8 t_8 M_8^2 \qquad [3.178]$$

$$\Delta S_8 = 0 = (\Phi_{T_8} - \phi_{t_8}) - R_8 \ln \frac{P_8}{p_8} \qquad [3.179]$$

$$W_8 = \rho_8 V_{8ax} A_8 = \frac{p_8}{R_8 t_8} \sqrt{\gamma_8 R_8 t_8}\, M_{8ax} A_8 \qquad [3.180]$$

These expressions, together with the thermodynamic model, are enough to solve the exhaust system. For a first estimation, equations analogous to [3.75], [3.76] and [3.77] could be used. Also, if the exit Mach number if low, these will give an adequate solution.

3.12. EXHAUST HEAT EXCHANGER, HEAT RECOVERY STEAM GENERATOR, STEAM TURBINE AND STEAM GENERATOR

When the power plant is not a simple cycle but a combined cycle with a steam turbine bottoming cycle, [10], [11], [12], [19], [26], [39], [46], [47], [87], [104], [105], [129] and [139], a Cheng cycle (steam injected gas turbine), [12], [13], [15], [76], [77], [85], [127], [130] and [145], or a combined steam/heat and power, [2], [7], [24], [58], [77], [79], [91], [110], [111], [144] and [145], it is necessary to model three additional components: heat exchanger or heat recovery steam generator, steam turbine and steam generator.

The steam turbine is simulated here as a single pressure superheater steam cycle. Although it would be possible to increase the complexity of the bottoming cycle, the author has preferred to maintain its simplicity,[27] as this thesis is focused on the gas turbine side.

---

[27] The simple steam turbine module could be substitute either with a more complex one (double or triple pressure reheat turbine with deareator, intermediate bleeds, etc.) or linked with a commercial code.

3.12.1. HEAT EXCHANGER AND HEAT RECOVERY STEAM GENERATOR

The heat recovery steam generator and the heat exchanger are modeled as systems where heat is extracted from the high temperature gas turbine exhaust gases:

- The HRSG will be coupled with a steam turbine or a steam generator (to be used for steam injection or process), characterised by a difference between the HRSG inlet temperature from the gas turbine side and the maximum steam temperature (of the order of 50 K) and by a pinch point minimum temperature difference (of the order of 20 K) or a minimum exhaust temperature.
- The heat exchanger is coupled with other system characterised by a temperature drop. In this condition only the exhaust temperature and the pressure losses are given.

In the first situation, the most common and interesting one, the heat recovery steam generator is characterised by two of the three temperatures mentioned above and the total pressure drops in the economiser and superheater.

3.12.2. STEAM TURBINE AND STEAM GENERATOR

As it was mentioned at the beginning of this section the steam turbine and steam generator are very simple. Both are of the single pressure superheater type. The steam turbine main parameters are: isentropic efficiency, maximum pressure, exhaust back pressure, minimum exhaust moisture, pump isentropic efficiency and auxiliary losses. For the steam generator the parameters are the maximum pressure, pump isentropic efficiency, auxiliary losses and water inlet temperature and pressure.

3.13. PRECOOLER

A special case will be the precooler, a heat exchanger used to reduce the compressor inlet temperature increasing the T_4/T_2 ratio, as described in refs. [72] and [74]. The system will be specially effective if a cryogenic fluid is employed [74], causing a substantial drop in the main stream temperature. The equations to solve this component will be either the ones given in section 3.3 for the intercooler, if no data is available for the cold side, or the ones of section 3.5 for the regenerator, if the mass flow, temperature, etc. of the coolant are known.

CHAPTER 4

COMPONENT INTEGRATION AND CONTROL IN GTSI

4.1. INTRODUCTION

After the generation of models for each component of the gas turbine (inlet, compressor, combustor, turbine, ...) it is necessary to integrate them, to be able to build up the desired power plant & control, [32], [101], [121] and [131]. There will be two main simulation cases: design and off-design, that will be treated separately.

Different engine configurations will be examined, from the simple single shaft open cycle machine to a more complex system such as an intercooled & regenerated, steam injected & reheat gas turbine.

4.2. DESIGN POINT SIMULATION

The variables required to solve each component and a summary for the complete system will be given.

The first requirement is the power plant arrangement: open or closed cycle, number of spools and presence, or not, of intercoolers, steam injectors, regenerator, reheaters, free power turbine, steam turbine (for combined cycles), etc.

Some of the variables identified in this section will not be directly used for the design point calculations, but will be required to build the complete engine model (file MOTOR.DAT created each time a design point is run), an operation that is carried out at this stage. Some variables required for the off-design must be introduced by the user, while others are calculated internally by the code.

Four files will be necessary to run a design case:

- CONTROL.DAT: containing the control of the gas turbine and the name of the other files.
- DESIGN (the name of the file can be found in CONTROL.DAT): containing the design point values for the variables.
- ENGINE (the name of the file can be found in CONTROL.DAT): containing the component maps
- OUTDAT (the name of the file can be found in CONTROL.DAT): containing the output variables.

4.2.1. GENERAL CYCLE VARIABLES

Some parameters will affect not only a single component, but the complete gas turbine:

- Inlet mass flow
- Ambient pressure, temperature and relative humidity

- Working fluid composition (only for closed & semi-closed cycles)
- Fuel composition

4.2.2. INLET, DUCTS AND EXHAUST SYSTEM

These component will have similar treatment, requiring the same design point input variables:

- Total pressure losses, given as a fraction of the inlet total pressure.
- Area or Mach number
- Nozzle pressure ratio (only for the exhaust diffuser)
- Swirl angle (not necessary in the case of the intake).

4.2.3. COMPRESSOR

Two variables are required for a compressor: pressure ratio or enthalpy rise and isentropic or polytropic efficiency.

If the compressor has variable geometry, the stators angle at design stage will be taken as zero (reference). A flag will be activated to employ this capability at off-design.[1]

The turbine cooling, anti-surge and over board flows, will be treated in a separate section, but their values are required to complete the calculations.

Although not strictly required to solve the compressor at design point, it is necessary to have the design speed or, more rigorously, design relative speed, as well as the mathematical parameter beta, to be able to scale, if necessary, the component maps for off-design. Standard pressure, temperature, gamma and gas constant, used for maps generation, should also be supplied.

4.2.4. DRY INTERCOOLER

The exit total temperature, power extracted or decrease in enthalpy is the first parameter required. The second one will be the drop in total pressure.

---

1 The zero is just a reference for the code, and at off-design the stators can be opened (negative angle in CONTROL.DAT) or closed (positive angle in CONTROL.DAT, as this is the most common situation).

4.2.5. EVAPORATIVE COOLER

In addition to the pressure losses the other variable needed will be either the exit temperature, relative humidity, water to air ratio or water mass flow. For this component the selected value is not always adequate, (i.e. it is possible to select an exit total temperature lower than the value obtained with a 100% relative humidity, therefore impossible to achieve). In those cases an error message will be given by the code, indicating the problem.

4.2.6. STEAM INJECTOR

The pressure losses of core and steam injectors streams and the main stream Mach number are the only variables required at design stage. The steam pressure, temperature and total mass flow will be obtained from the steam generator and the gas turbine exit conditions.

4.2.7. REGENERATOR

Pressure losses of both, cold and hot streams, and regenerator effectiveness are the parameters needed.

4.2.8. COMBUSTOR OR MAIN HEAT EXCHANGER

The cold total pressure losses at design stage should be supplied by the user for either, combustor or main heat exchanger. For the conventional combustion chamber it is also possible to give the constants k_1 and k_2, together with the entry area, to calculate the cold and hot losses.

The second, and usually main engine control variable, would be either the combustor exit temperature, HPT stator outlet temperature, LPT stator outlet temperature, FPT stator outlet temperature, turbine exhaust temperature, fuel to air ratio, fuel flow or gas turbine power output. With any of these parameters it would be possible to obtain the combustor exit temperature. In the real machine the fuel flow is the control available, with turbine gas or metal temperature used as feedback.

In addition to the conventional variables, if a correlation similar to the ones presented in chapter 3 is used (equations [3.125] to [3.128b]), the volume of the primary+secondary zones is required to evaluate the combustion efficiency.

In the case of the main heat exchanger two parameters are required: the first one is the effectiveness and the second variable could be selected among the ones available for the combustor, except the fuel to air ratio or fuel flow, not present in this component.

4.2.9. TURBINE COOLING, ANTI-SURGE AND OVER-BOARD FLOWS

The design point turbine cooling flows will be either specified directly by the user or derived from a given technology and metal temperature limit for each row, using in the calculation some aerodynamic data from the turbine (blade speed, stage loading,...). To generate the engine model it is also necessary to have the variation of the flows with the pressure ratio, corrected speed, ...

Anti-surge, over-board and customer flows[2] should also be supplied, in order to have a proper design point definition.

4.2.10. TURBINE

As in the case of the compressor, it will be necessary to have two variables: pressure ratio or reduction in corrected enthalpy and isentropic or polytropic efficiency. The first ones are obtained directly from the power plant arrangement:

- For a turbine that does not discharge to ambient: turbine power demand (to obtain the corrected enthalpy drop)=compressor power+shaft output power+auxiliary system power extraction+shaft losses.
- For a turbine discharging to ambient: turbine exit total pressure (to obtain the pressure ratio), determined by ambient pressure, nozzle pressure ratio and pressure losses in the components present between turbine exit and gas turbine exhaust unit (regenerator, HRSG, precooling in the case of closed cycles, ...).

The losses and auxiliary power extraction should also be given at this stage.

Variable geometry will not be an option at design point, but at off-design, where the design throat areas are taken as reference.[3]

The design relative corrected speed and corrected enthalpy are required to scale the turbine maps for the off-design simulations. Standard pressure, temperature, gamma and gas constant should also be given.

---

[2] While it is very common to have over-board and customer bleed flows at design point, that is not the case for the anti surge flows, present at off-design points, when the compressor operating point is far from the initial position.

[3] As for the compressor, the design throat area will be the reference, with possibility of increasing or decreasing its value at off-design.

4.2.11. REHEATER

This system needs the same variables that a conventional burner: volume, to determine the efficiency, and either the component exit temperature, fuel flow, fuel to air ratio, power output or gas turbine exit temperature to derive the reheat exit temperature.

4.2.12. STEAM TURBINE AND STEAM GENERATOR

The variables will be:

- Difference between turbine exit and maximum steam temperature.
- Pinch point temperature difference.
- Maximum steam pressure.[4]
- Back-pressure (for steam turbine).
- Pressure losses in the economiser and superheater ducts.[5]
- Auxiliary systems losses (relative to steam turbine power).
- Split between steam injected at combustor, before the low pressure turbine and before the free power turbine.

A special characteristic of the steam turbine and steam generator is the way of solving these components. The gas turbine will be represented as a system of non-linear equations, and will be solved using the Newton-Raphson method. However, the heat recovery steam generator is treated separately. If the gas turbine has a steam bottoming cycle, the link between them will only be the heat exchanger. Therefore, the steam turbine will not have any effect on its topping cycle. But if the steam produced by the HRSG is injected into the gas turbine (Cheng cycle), the link is evident. In this case the steam mass flow, pressure and temperature are determined using a fixed point method. This linear technique is slower than a quadratic one, but more stable, a very important issue when solving steam injected cycles.

---

[4] Although the steam can be injected at three different locations: combustor entry, between high and low pressure turbine and between low and free power turbine, where the pressures will be very different, the steam pressure will be the same. This limitation will be avoid in a future code release, where some improvements will be done on the steam turbine/steam generator component.

[5] To simplify the evaporation process it is assumed that no pressure losses are present in the evaporator.

4.3. OFF-DESIGN CYCLE SIMULATION & CONTROL

Once the design point has been run, and the files containing all the gas turbine information (component maps, pressure losses, cooling flows, ...) are available, the off-design simulations can be carried out.

As mentioned in section 4.2, the file containing the variables that can be directly modified is called CONTROL.DAT. The engine model, component characteristics and output variables will be in different files.

An important capability, in some of the components, will be the possibility to modify the design value of certain parameters (efficiencies, pressure losses, flow capacity, etc.), running the new model as an off-design. With this special feature it will be possible to carry out the following studies:

- Assessment of the possibility of aero gas turbine industrialisation
- Feasibility of introducing a heat recovery steam generator, steam injection, intercooler, regenerator, etc. without modifications in other gas turbine elements
- Effect of replacing a component
- Deterioration of the gas turbine.

4.3.1. GENERAL CYCLE CONTROL VARIABLES

In addition to each component off-design control, that will be described below, the gas turbine has some variables affecting the complete cycle.

- Ambient pressure, temperature and relative humidity
- Working fluid composition (only for closed & semi-closed cycles). This modification will allow the user to study the changes in operating point matching when using the same turbomachinery with different working fluids.
- Fuel composition (widely used to evaluate the gas turbine performance burning Natural Gas, Diesel No.2, etc.)

4.3.2. INLET, DUCTS AND EXHAUST SYSTEM

In general there will be no variable required for these devices. For specific research topics, it would be possible to modify the design pressure losses or design areas in order to evaluate the impact on performance. These changes will be done in the engine model (DESIGN file) and not in the control file (CONTROL.DAT file). Using this capability it would be possible to determine, for example, the new gas turbine matching when a different exhaust unit is employed, when additional inlet losses are present due to installation problems, etc.

4.3.3. COMPRESSOR

Corrected speed and beta are the two parameters required to determine the compressor operating point.

The only independent control of the compressor will be the variable stators, if present, being one of the main gas turbine control systems. This parameter will be introduced as an angle value (relative to design).

The other possible exercise will be the modification of the compressor characteristics: efficiency, pressure ratio, flow capacity, ..., to simulate the engine deterioration, manufacturing errors, fouling, etc. As in the case of the inlet, ducts and exhaust unit, the changes will be carried out in the engine model file. The way to perform the task is altering the compressor scaling factors.

4.3.4. DRY INTERCOOLER

Exit total temperature, heat removed or, in general, any other variable that will give the flow energy conditions at the end of the intercooling process could be used as a control parameter.

As in a conventional duct, total pressure losses can be modified in the engine design file. This capability will be specially useful to simulate a very common and undesirable effect: the fouling of the heat exchanger.

4.3.5. EVAPORATIVE COOLER

The exit relative humidity, total temperature, etc. could be the independent control parameter. For convergence improvement relative humidity is strongly recommended.

As for the dry intercooler, it is also possible to change the pressure losses, altering the engine design file.

4.3.6. STEAM INJECTOR

The steam total pressure and injector discharge area will be the control parameters for this component.

Pressure losses in both, core and injected streams, as well as main stream area can be modified in the engine design file.

4.3.7. REGENERATOR

Once a regenerator effectiveness map has been introduced there is no control parameter over this device.

As in the intercooler and steam injector it would be possible to alter the design pressure losses to evaluate the impact of these changes. Also, the effectiveness could be modified to assess the performance modification with an improvement, or deterioration, in this key parameter.

4.3.8. COMBUSTOR, REHEAT SYSTEM OR MAIN HEAT EXCHANGER

Fuel flow (or fuel to air ratio) will be the combustion chamber and reheater control parameter. The analogous variable for the heat exchanger will be the heat addition.

Modifications in the turbine combustor volume, efficiency correlations, pressure losses, heat exchanger performance, etc. can be carried out by changing the values in the engine design file.

4.3.9. TURBINE COOLING, ANTI-SURGE AND OVER-BOARD FLOWS

Although there is not control over the turbine cooling flows, the value can be modified to simulate, for example, the effect of seal deterioration and the consequent changes in the engine internal air system. The new values will be supplied by the air system group. Anti-surge and over-board flows are, directly, control parameters.

4.3.10. TURBINE

Corrected speed and power are the parameters needed to set the turbine operating point.

The auxiliary power extraction is a control variable, although it is not very important for the engine cycle performance, except for the idle operating point definition.

The variable geometry will be the real independent control parameter of the turbine.[6] The ratio between actual and design throat area represents the degree of freedom.

---

[6] Although not very frequent in high pressure turbines, there are several low pressure and free power turbines with variable stators. The Rolls-Royce-Westinghouse ICR WR21 [122] is a good example.

4.3.11. STEAM TURBINE AND STEAM GENERATOR

Because of the simplified steam turbine model, steam pressure will be the main control variable. As for other components, it would be possible to modify, directly in the engine file, some design parameters, such as pressure losses, temperature difference at pinch point, etc., running the power plant in off-design mode.

4.4. EXAMPLE OF DESIGN & OFF-DESIGN CYCLE SIMULATION

Complete gas turbine and individual component variables have been described in the different sections of this chapter. However, when integrating the components to create a machine, not all the parameters necessary to determine the performance of a module can be used for control. Lets take a two spool, three shaft gas turbine with evaporative cooler, regenerator and reheat between high and low pressure turbine as an example (figure 4.1).

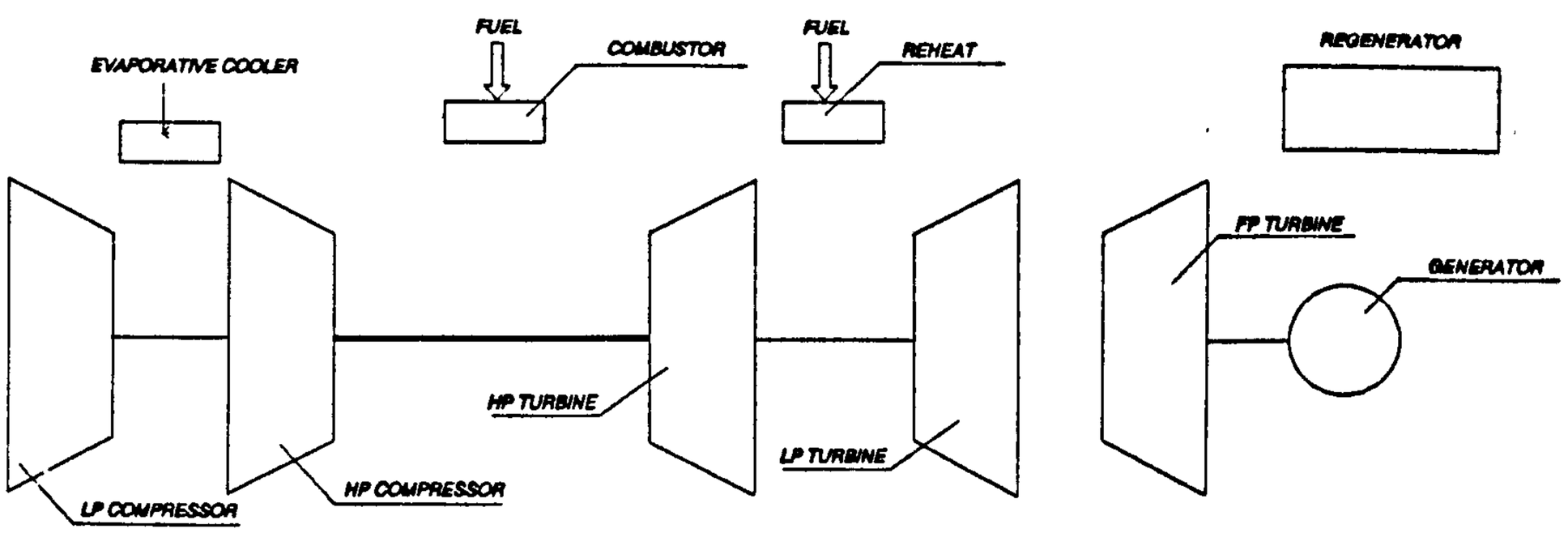

Figure 4.1. Scheme of the gas turbine selected for the simulation

After the selection of ambient conditions, fuel properties, turbomachinery variable geometry, design inlet mass flow and the mathematical control parameters, the gas turbine design variables could be:

- Inlet: total pressure losses and intake area
- Low pressure compressor (with variable geometry): pressure ratio and isentropic efficiency. Design corrected speed and beta for maps scaling.
- Evaporative cooler: total pressure losses and exit relative humidity
- High pressure compressor (with variable geometry): increase in corrected enthalpy and polytropic efficiency. Design corrected speed and beta for maps scaling.
- Regenerator: effectiveness and total pressure loses in cold and hot streams.
- Cooling and anti-surge bleeds: cooling bleed extraction position, anti-surge bleed mass flow, ..

- Combustor: k_1, k_2, inlet area, combustion chamber volume, efficiency correlation and HPT stator outlet temperature
- High pressure turbine: high pressure spool losses, isentropic efficiency and materials & aerodynamic characteristics to evaluate HPT cooling requirements (metal temperature, turbine stage loading factor, blade speed, ...). Design corrected speed and corrected enthalpy for maps scaling.
- Reheat: total pressure losses, reheat primary+secondary zone volume, efficiency correlation, free power turbine exit temperature
- Low pressure turbine: low pressure spool losses, polytropic efficiency and materials & aerodynamic characteristics to evaluate LPT cooling requirements (metal temperature, turbine stage loading factor, blade speed, ...). Design corrected speed and corrected enthalpy for maps scaling.
- Free power turbine (with variable geometry): free power turbine shaft losses, isentropic efficiency and materials & aerodynamic characteristics to evaluate LPT cooling requirements (metal temperature, turbine stage loading factor, blade speed, ...). Design corrected speed and corrected enthalpy for maps scaling.
- Exhaust diffuser: total pressure losses swirl angle and exit total to ambient static pressure ratio.

For a conventional off-design calculation, employing the design hardware without any deterioration, a possible set of gas turbine control variables would be:

- Low pressure compressor: variable stators angle position (eq. [4.1]).
- Evaporative cooler: exit relative humidity (eq. [4.2]).
- High pressure compressor: variable stators angle position (eq. [4.3]).
- Combustor: high pressure turbine stator outlet temperature (eq. [4.7]).
- Reheat: low pressure turbine stator outlet temperature (eq. [4.9]).
- Free power turbine: variable stators throat area ratio (eq. [4.11]) and power output shaft speed (eq. [4.12]).

In addition to these control variables the code will use others, to form a set of thirteen equations:

- High pressure compressor: flow capacity (eq. [4.4]).
- Regenerator: effectiveness (eq. [4.5]).
- High pressure turbine: flow capacity (eq. [4.6]).
- Low pressure turbine: flow capacity (eq. [4.8]).
- Free power turbine: flow capacity (eq. [4.10]).
- Exhaust diffuser: exit static pressure or exit area (eq. [4.13]).

No modification in the total pressure losses, position of cooling bleed, etc. is intended.

The equations of the system will be:

$$\frac{\alpha_2|_{Cycle}}{\alpha_2|_{Control}} - 1 = f_1 \qquad [4.1]$$

$$\frac{RH_{23}|_{Cycle}}{RH_{23}|_{Control}} - 1 = f_2 \qquad [4.2]$$

$$\frac{\alpha_{25}|_{Cycle}}{\alpha_{25}|_{Control}} - 1 = f_3 \qquad [4.3]$$

$$\frac{\left.\frac{W_{25}\sqrt{\theta_{25}}}{A_{25}\delta_{25}}\sqrt{\frac{R_{25}}{\gamma_{25}}}\right|_{Cycle}}{\left.\frac{W_{25}\sqrt{\theta_{25}}}{A_{25}\delta_{25}}\sqrt{\frac{R_{25}}{\gamma_{25}}}\right|_{Map}} - 1 = f_4 \qquad [4.4]$$

$$\frac{\eta_{regen}|_{Cycle}}{\eta_{regen}|_{Map}} - 1 = f_5 \qquad [4.5]$$

$$\frac{\left.\frac{W_{405}\sqrt{\theta_{405}}}{A_{405}\delta_{405}}\sqrt{\frac{R_{405}}{\gamma_{405}}}\right|_{Cycle}}{\left.\frac{W_{405}\sqrt{\theta_{405}}}{A_{405}\delta_{405}}\sqrt{\frac{R_{405}}{\gamma_{405}}}\right|_{Map}} - 1 = f_6 \qquad [4.6]$$

$$\frac{T_{41}|_{Cycle}}{T_{41}|_{Control}} - 1 = f_7 \qquad [4.7]$$

$$\frac{\left.\frac{W_{455}\sqrt{\theta_{455}}}{A_{455}\delta_{455}}\sqrt{\frac{R_{455}}{\gamma_{455}}}\right|_{Cycle}}{\left.\frac{W_{455}\sqrt{\theta_{455}}}{A_{455}\delta_{455}}\sqrt{\frac{R_{455}}{\gamma_{455}}}\right|_{Map}} - 1 = f_8 \qquad [4.8]$$

$$\frac{T_{46}\big|_{Cycle}}{T_{46}\big|_{Control}} - 1 = f_9 \qquad [4.9]$$

$$\frac{\left.\frac{W_{655}\sqrt{\theta_{655}}}{A_{655}\delta_{655}}\sqrt{\frac{R_{655}}{\gamma_{655}}}\right|_{Cycle}}{\left.\frac{W_{655}\sqrt{\theta_{655}}}{A_{655}\delta_{655}}\sqrt{\frac{R_{655}}{\gamma_{655}}}\right|_{Map}} - 1 = f_{10} \qquad [4.10]$$

$$\frac{\left.\frac{A_{655}}{A_{655}^{DS}}\right|_{Cycle}}{\left.\frac{A_{655}}{A_{655}^{DS}}\right|_{Control}} - 1 = f_{11} \qquad [4.11]$$

$$\frac{XN_{6^-\ Cycle}}{XN_{6^-\ Control}} - 1 = f_{12} \qquad [4.12]$$

$$\frac{A_{8\ Cycle}}{A_{8\ Control}} - 1 = f_{13} \qquad [4.13]$$

The well known Newton-Raphson method has been selected to solve the non-linear system of equations. The general form at iteration *n* could be:

$$\begin{pmatrix} \frac{\partial f_1(X_n)}{\partial x_1} & \cdots & \frac{\partial f_1(X_n)}{\partial x_i} & \cdots & \frac{\partial f_1(X_n)}{\partial x_N} \\ \cdots & & \cdots & & \cdots \\ \frac{\partial f_j(X_n)}{\partial x_1} & \cdots & \frac{\partial f_j(X_n)}{\partial x_i} & \cdots & \frac{\partial f_j(X_n)}{\partial x_N} \\ \cdots & & \cdots & & \cdots \\ \frac{\partial f_N(X_n)}{\partial x_1} & \cdots & \frac{\partial f_N(X_n)}{\partial x_i} & \cdots & \frac{\partial f_N(X_n)}{\partial x_N} \end{pmatrix} \begin{pmatrix} \Delta x_1 \\ \cdots \\ \Delta x_i \\ \cdots \\ \Delta x_N \end{pmatrix} = \begin{pmatrix} -f_1(X_n) \\ \cdots \\ -f_j(X_n) \\ \cdots \\ -f_N(X_n) \end{pmatrix} \qquad [4.14]$$

$$X_n = (x_1, x_2, \ldots, x_i, \ldots . x_N) \qquad [4.15]$$

Using the abbreviated notation:

$$\left[\frac{\partial f_j(X_n)}{\partial x_i}\right][\Delta x_i] = -[f_j(X_n)] \qquad [4.16]$$

The thirteen variables x_j, for the gas turbine considered, will be:

- Low pressure compressor: shaft speed, beta and variable stators angle ($x_8=XN_2$, $x_4=\beta_2$ and $x_1=\alpha_2$).
- Evaporative cooler: exit temperature ($x_2=T_{23}$).
- High pressure compressor: shaft speed, beta and variable stators angle ($x_6=XN_{25}$ $x_{13}=\beta_{25}$ and $x_3=\alpha_{25}$)
- Regenerator: exit temperature ($x_5=T_{33}$)
- Combustor: fuel to air ratio ($x_7=FAR_4$).
- Reheat: fuel to air ratio ($x_9=FAR_{45}$).
- Free power turbine: corrected enthalpy drop, shaft speed and variable throat area ($x_{12}=\Delta H_{67}/(\gamma_{67}R_{67}\theta_{67})$, $x_{10}=XN_{67}$ and $x_{11}=A_{655}$)

The variables have been selected to obtain a partial derivative matrix with the largest terms in the diagonal.

An equivalent procedure to the one described above will be followed for other gas turbine configurations.

For unconventional off-design studies, the efficiency, flow capacity, pressure ratio, etc. of the different components could be modified. Table 4.II gives a detailed list of the parameters.

4.5. OFF-DESIGN LIMITING VALUES

The gas turbine components have certain values that must not be exceeded during off-design operation. Compressor minimum surge margin, compressor and turbine maximum & minimum corrected speeds, maximum compressor discharge temperature and pressure, maximum turbine stator outlet temperature, maximum shaft speeds, maximum power output, etc. are examples of conventional limiting values.

From the simulation point of view there are two possible solutions when a limit is switch on and, during a run, its value is exceeded:

- The code runs normally, exceeding the limiting value, but a warning message will appear in an output file. If the control explicitly asks for a value in the parameter larger than the limit, and is not the result of controlling another variable, there will be no output message.
- The control of the gas turbine is changed, so the limiting parameter is not exceeded.

The first solution has been initially adopted in GTSI. The implementation of the second one should be done case by case, as there are several possibilities of controlling a single variable.[7]

4.6. CONTROL VARIABLES AND ERROR MESSAGES

An detailed description of the design and off-design variables has been carried out through the last sections of this chapter. A more extensive classification is presented in GTSI Computer User Guide, where all these variables, with the specific nomenclature, are explained. Nevertheless, when using the code, it is not difficult to make a mistake and select an inadequate control variable (i.e. try to control the surge margin with the variable stators and with the stator outlet temperature at the same time, leading to a mathematical error). In these cases the code does not run, producing error messages that will enable the user to fix the problem and generate the adequate DESIGN and CONTROL.DAT files. The list of specific messages is also given in GTSI User Guide.

[7] If the minimum compressor surge margin has been exceeded, the gas turbine can control its value using the combustor outlet temperature, compressor variable stators (if present), compressor bleed valves (if present), etc.

TABLE 4.I: DESIGN POINT VARIABLES

	DESIGN VARIABLES
Inlet	Pressure losses Area or Mach number
Compressor	Pressure ratio or increase in corrected enthalpy Isentropic or polytropic efficiency Relative corrected speed Beta parameter
Duct	Pressure losses Swirl angle Area or Mach number
Dry intercooler	Pressure losses Exit temperature, exit enthalpy, heat removed,...
Evaporative cooler	Pressure losses Exit temperature, exit relative humidity, ..
Steam injector	Inlet main stream area or Mach number Pressure losses in both streams
Regenerator	Regenerator effectiveness Pressure losses in both streams
Combustion chamber	Pressure losses Primary+secondary zone volume Efficiency correlation
Main heat exchanger	Pressure losses Efficiency
Turbine	Pressure ratio or decrease in enthalpy Isentropic or polytropic efficiency Relative corrected speed Relative corrected enthalpy drop Shaft losses Auxiliary power extraction

Reheater	Pressure losses Primary+secondary zone volume Efficiency correlation
Cooling & anti-surge bleeds	Cooling bleed mass flow relative to the HP compressor inlet mass flow Anti-surge mass flow relative to the compressor inlet mass flow (LP, IP or HP) Metal temperature of the vane/blade row, cooling technology and turbine main characteristics (loading factor & blade speed or number of stages) Pressure losses for the cooling system
Exhaust diffuser	Pressure losses Swirl angle Area, Mach number or nozzle pressure ratio
Steam turbine	Steam maximum pressure Steam turbine efficiency Economiser & superheater pressure losses Temperature drop between GT exit and steam Pinch point temperature difference Steam back pressure Liquid water pump efficiency Auxiliary system power losses relative to ST power
Steam generator	Steam maximum pressure Economiser & superheater pressure losses Temperature drop between GT exit and steam Pinch point temperature difference Liquid water pump efficiency Auxiliary system power losses relative to ST power

TABLE 4.II: CONVENTIONAL AND UNCONVENTIONAL OFF-DESIGN VARIABLES

	OFF-DESIGN VARIABLES
Inlet	Design pressure losses (Unconventional) Area (Unconventional)
Compressor	Variable stators angle Design flow capacity (Unconventional) Design efficiency (Unconventional) Design pressure ratio or corrected enthalpy rise (Unconventional)
Duct	Design pressure losses (Unconventional) Swirl angle (Unconventional) Area (Unconventional)
Dry intercooler	Exit temperature, exit enthalpy, heat removed,... Design pressure losses (Unconventional)
Evaporative cooler	Exit relative humidity, exit temperature, ... Pressure losses (Unconventional)
Steam injector	Main stream inlet area (Unconventional) Pressure losses in both streams (Unconventional)
Regenerator	Design effectiveness (Unconventional) Pressure losses in both streams (Unconventional)
Combustion chamber	Design efficiency correlation (Unconventional) Design pressure losses (Unconventional) Primary+secondary zone volume (Unconventional)
Main heat exchanger	Efficiency (Unconventional) Design pressure losses (Unconventional)

Turbine	Variable stators throat area ratio Auxiliary power extraction Design pressure ratio or corrected enthalpy drop (Unconventional) Design efficiency (Unconventional) Design shaft losses (Unconventional)
Reheater	Design efficiency (Unconventional) Design pressure losses (Unconventional) Primary+secondary zone volume (Unconventional)
Cooling & anti-surge bleeds	Anti-surge mass flow Design cooling mass flow (Unconventional) Design pressure losses (Unconventional)
Exhaust diffuser	Pressure losses (Unconventional) Swirl angle (Unconventional) Exit area (Unconventional)
Steam turbine	Steam maximum pressure Steam turbine design efficiency (Unconventional) Economiser & superheater design pressure losses (Unconventional) Temperature drop between GT exit and steam (Unconventional) Pinch point temperature difference (Unconventional) Steam back pressure (Unconventional) Auxiliary system power losses relative to ST power (Unconventional)
Steam generator	Steam maximum pressure Economiser & superheater design pressure losses (Unconventional) Temperature drop between GT exit and steam (Unconventional) Pinch point temperature difference (Unconventional) Auxiliary system power losses relative to ST power (Unconventional)

CHAPTER 5

BLADE COOLING MODELING IN GTSI PERFORMANCE CODE

5.1. BLADE COOLING CONSIDERATIONS

Blade cooling has been, probably, the technology that contributed most to the increase in turbine entry temperature in the past three decades. It is important to bear in mind that an increase of 50 K can provide corresponding increases of over 5% in power output and 0.5 to 2% in simple cycle efficiency. The cost benefit associated to these improvements will be significant, and more than $500,000/yr./100MW can be saved by the users of a combined cycle power plant. Hence, development of adequate turbine cooling continues to be one of the main challenges in advanced designs.

Until late 1960s and early 1970s, the rise in firing temperature paralleled the increase in alloy temperature capability. During the 1970s, however, firing temperature increases outstripped alloy advances. Two factors were responsible:

- Film cooling was introduced[1], which decoupled firing temperature from maximum metal temperature.
- As metal temperatures approached 870°C, hot corrosion became more life limiting than strength.

The concurrent increase in use of more contaminated fuels added another dimension to the corrosion problem. In figure 5.1 the evolution of blade metal temperature and base load stator outlet temperature (or turbine entry temperature in other cases) is plotted. It is evident that during the 1950s and 1960s there was an important increase in metal temperature, but in the late 1960s and specially in the early 1970s this tendency stopped. The most modern machines have peak load TET higher than 1700 K, although for base load the values can be substantially reduced to increase life of the hot parts.[2] For the stages subject to the highest temperatures blade coatings are frequently employed.

The turbine cooling airflow in the modern aeroderivative and heavy duty industrial gas turbines can be as high as 20% of the core flow, having a major effect on performance. This figure includes vane, blade, platform and disc cooling.

Film cooling has severe penalties in terms of aerodynamic efficiency, stress concentrations, larger manufacturing costs, increase in sensitivity to manufacturing tolerances, etc.

With this scenario it is easy to understand that an adequate simulation of the cooling flows, as well as a correct prediction of the amount of cooling needed for the turbines are essential.

---

[1] Blade cooling was introduced by the Germans in the Jumo engine in 1943 and the first cooled turbine blade entered airline service in 1960, in the Conway engine.

[2] The latest GE (Frame H) and Westinghouse (701F) machines have SOT over 1650 K, that represent an increase of 100 to 150 K relative to the previous designs.

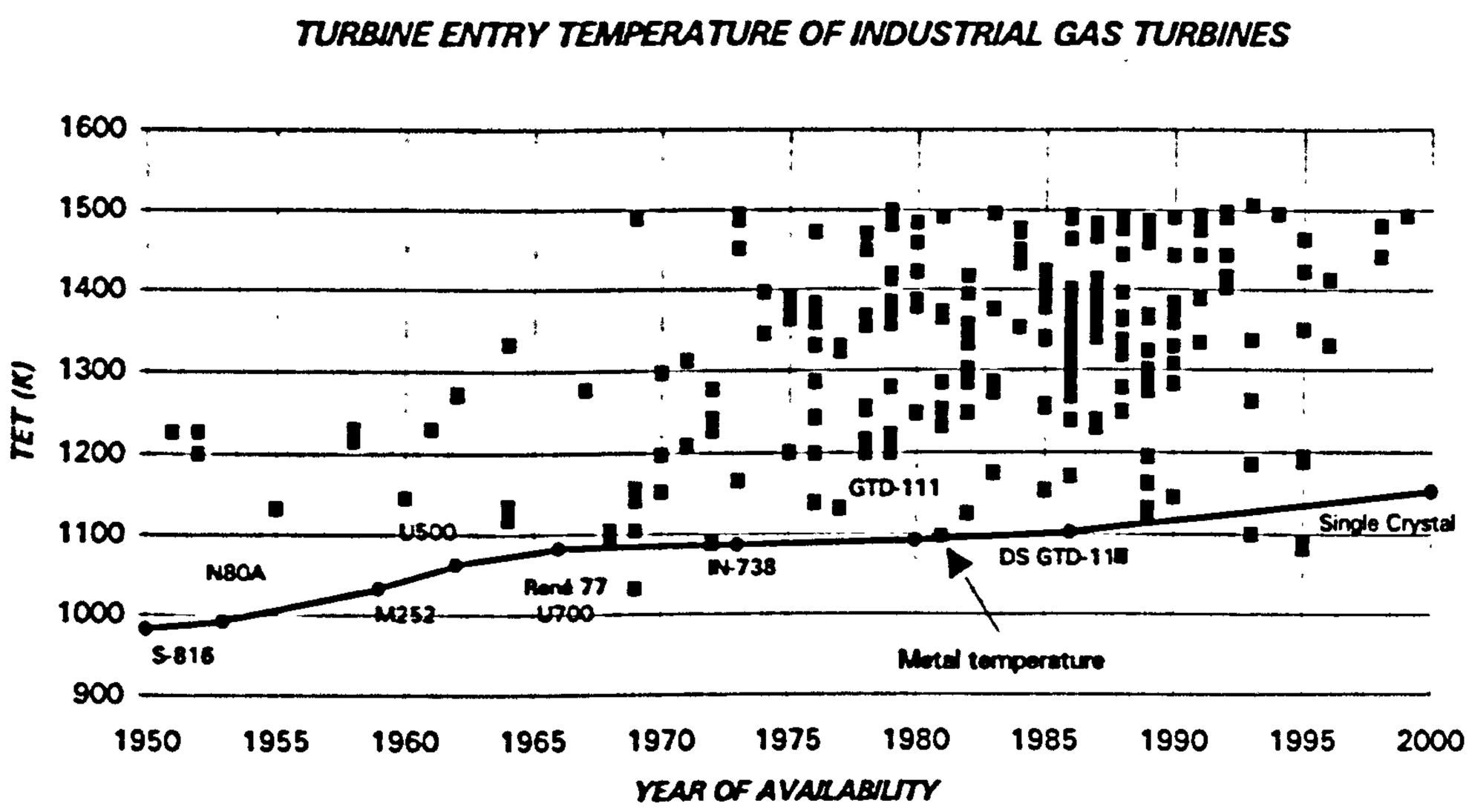

Figure 5.1. Turbine entry temperature and metal temperature of industrial gas turbines

5.2. BLADE COOLING MODELING

Most gas turbines, in operation or projected, employ film cooling, in addition to internal convection/impingement cooling.[3] Air is taken from different parts of the compressor: for the first stage the air is bled from the compressor discharge and, bypassing the combustor, cools the HPT NGVs and the HPT blades. For intermediate pressure stages the air is taken from the middle of the compressor. This method has a double benefit: reduces the compressor work, increasing the efficiency, and drops the cooling air temperature, decreasing the mass flow necessary to achieve a certain metal temperature.

In turbines where the cooling mass flow, number of stages, cooling technology and metal and firing temperatures are known, the simulation of blade cooling will be used to generate correlations to be employed in future gas turbines. This kind of work has been done by NASA during the past decades, and several reports have been written. Early experiments are covered by NASA TN D-5992 [43], NASA TM X-2580 [143] and NASA TP 1310 [89]. A summary is given in one of the chapters of NASA SP-290 [51], as well as in a chapter of *Aerothermodynamics of Aircraft Engine*

---

[3] Although even for moderately high operating temperatures film cooling has been employed in the last decades. Some novel technique have been proposed for internal blade cooling of small turbines, where film cooling represents also a manufacturing problem.

Components [95]. Furthermore, each year the number of papers on turbine cooling increases, achieving, progressively, a better understanding of the physical phenomena and, consequently, a better matching between predictions and experimental results.

For performance purposes four different types of blade cooling will be considered:

- Convection and impingement
- Convection, impingement and slots film cooling
- Conventional film cooling
- Full coverage film cooling

The first one corresponds to the earliest cooled gas turbines, while the last three are employed in gas turbine in operation and will be used in future ones. To improve the flexibility, the code allows the user to introduce his/her own cooling model.

Correlations for the first three types are taken from the references mentioned above, and are plotted in Figure 5.2. The last one was obtained from chapter 2 of *Steady and Transient Performance Prediction of Gas Turbine Engines* [99].

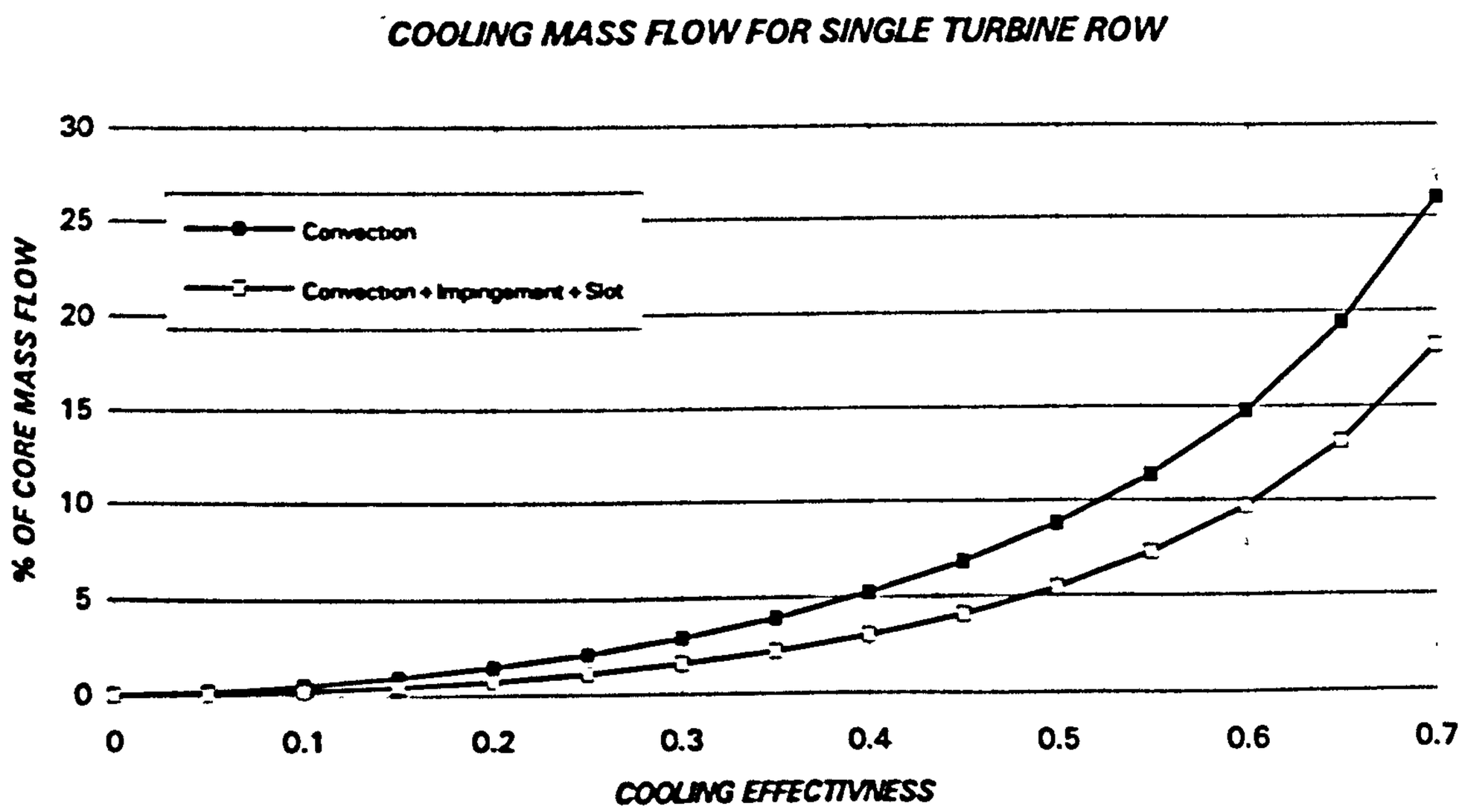

Figure 5.2. Cooling effectiveness-cooling mass flow for conventional cooling technology

5.2.1. FILM COOLING EFFECTIVENESS

Conventional and full coverage film cooling are the most widely employed methods in advanced turbines. The cooling achieved is expressed in terms of cooling effectiveness.

$$\varepsilon = \frac{T_{gas} - T_{metal}}{T_{gas} - T_{cooling}} \qquad [5.1]$$

From the performance point of view the metal temperature will be an average. However, it is important to consider that the real effectiveness will change considerably across the blade spanwise sections, according to the variations of local gas and metal temperature.

The value of mean cooling effectiveness is dependent on the complexity of the cooling design and also on the cooling flow rate through the blade. Turbine cooling engineers use a cooling flow coefficient which incorporates a heat transfer term, but for cycle analysis purposes it is necessary to convert this to simple cooling mass flow.

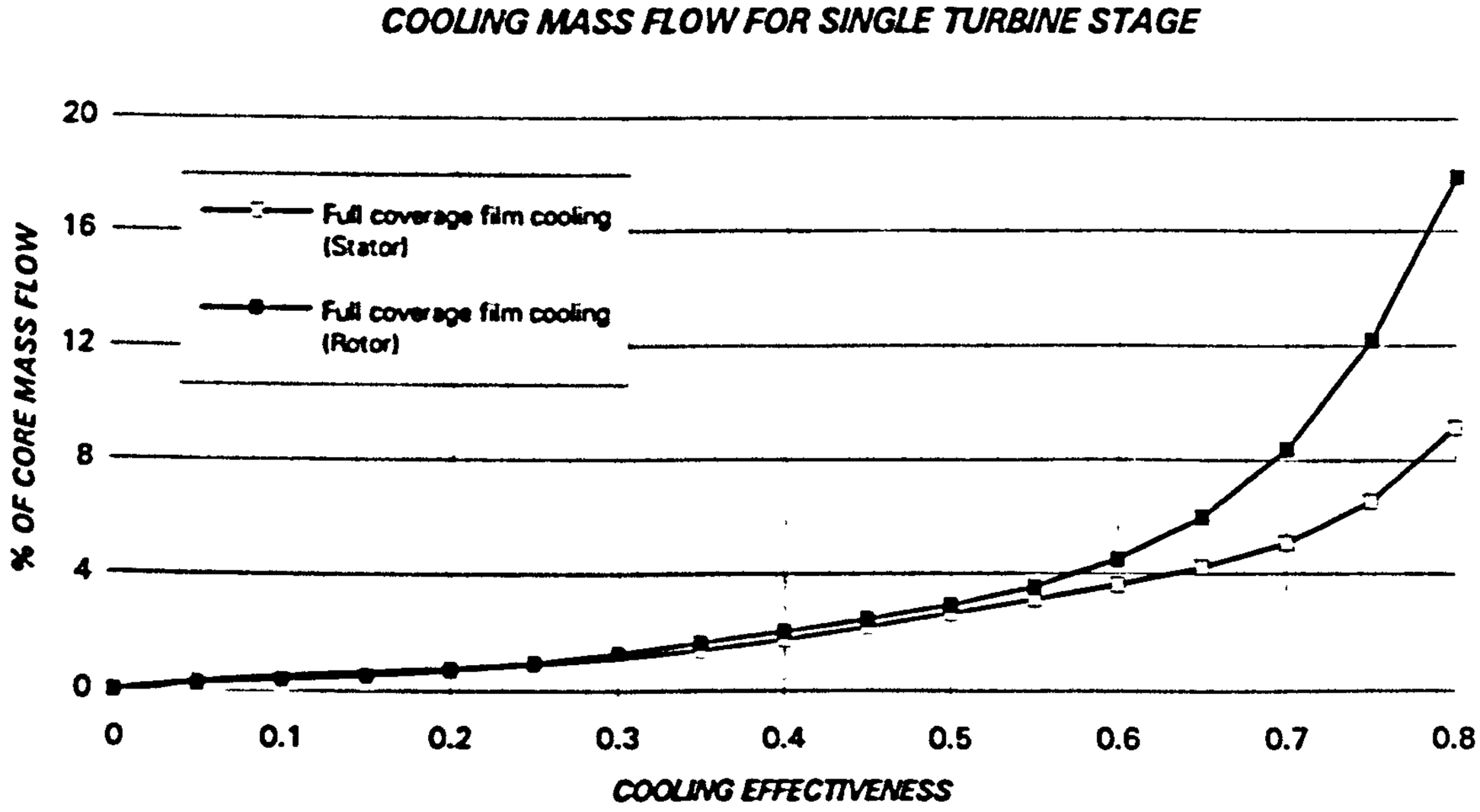

Figure 5.3. Cooling effectiveness-cooling mass flow for advanced film cooling technology

Figure 5.3 provides a correlation for full coverage film cooling that relates the cooling effectiveness with the percentage of cooling flow. The more complex internal cooling flow configurations allow to achieve a higher cooling effectiveness. Values of 0.75 to 0.8 can be found in the NGVs mean cooling effectiveness, with cooling mass

flow over 10%. For rotor blades, values of 0.55 to 0.60 are more typical, with cooling flow rates seldom exceeding 5%.

Since the NGVs are prone to the most severe temperature environment,[4] an additional cooling capability is frequently needed. However, as the stresses in the rotor are much higher, for the same material and life the NGVs could operate up to 100 K hotter than the rotor. For the rotor blade requirements, other important and beneficial effect must be taken into account: due to the rotation, the blade effectively "runs away" from the NGV exit flow, thereby reducing the relative total temperature. From the velocity triangles it can be shown that:

$$T_{rotor} = T_{41} - \frac{U^2}{2C_p}\left[\frac{\Delta H_{stg}}{U^2} - 2Rn + 1\right] \qquad [5.2]$$

Where:
- T_{rotor}: Relative total gas temperature at rotor inlet
- T_{41}: Absolute total gas temperature at rotor inlet
- U: Tangential blade speed
- ΔH_{stg}: Turbine stage work
- Rn: Degree of reaction

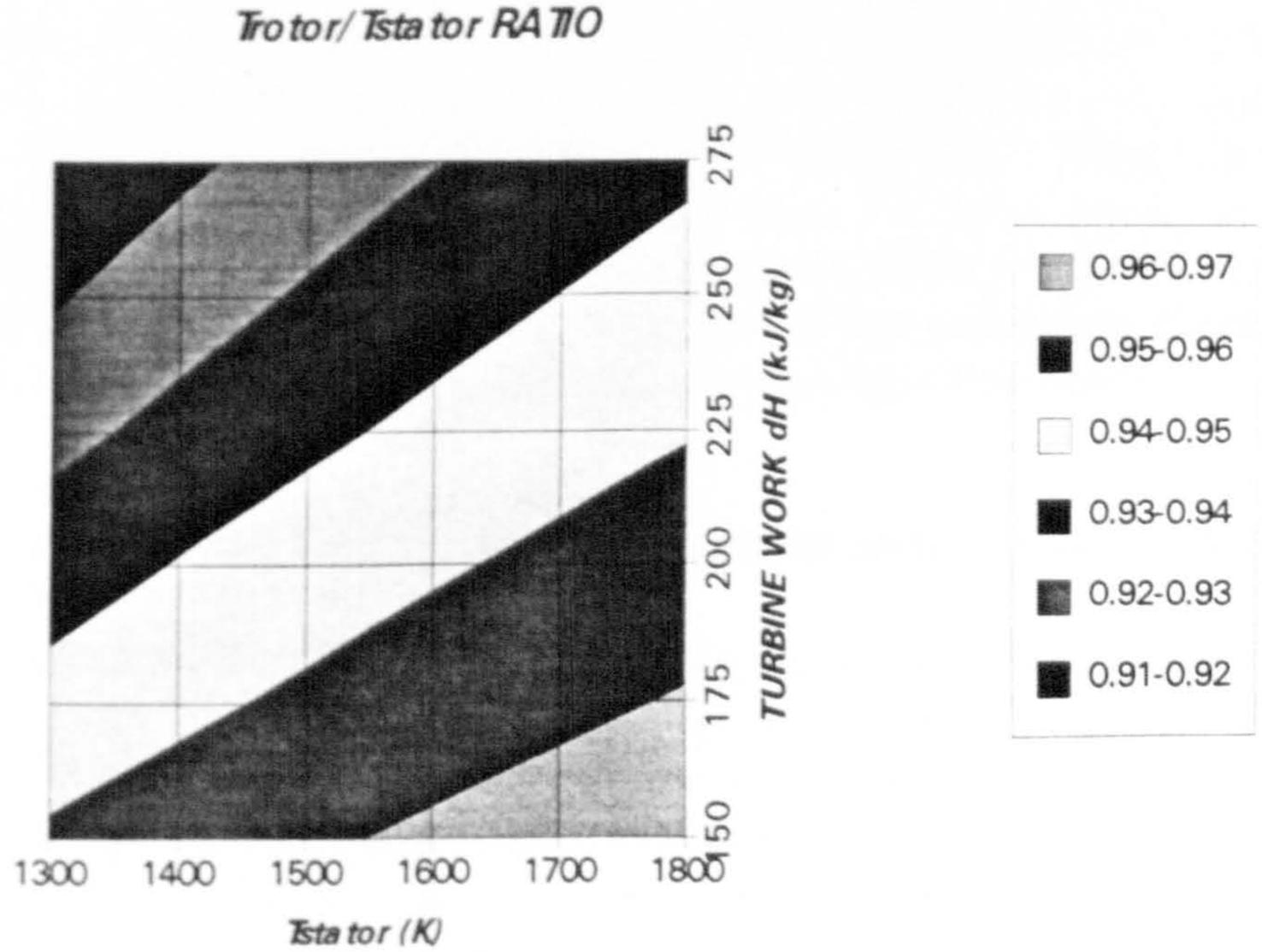

Figure 5.4. T_{rotor}/T_{41} ratio for different turbine work and stator outlet temperature

[4] Not only the temperature itself is higher, but, sometimes, also the temperature peaks (hot and cold spots) the high pressure turbine NGVs must withstand are more severe than in the rotor.

Despite that the determination of *Rn* requires aerodynamic blade details, most turbines for jet engine and industrial applications are designed close to 50% spanwise average Reaction (*Rn*=0.5), so the calculation can be easily done.[5] The equation is simplified now to:

$$T_{rotor} = T_{41} - \frac{\Delta H_{stg}}{2C_P} \qquad [5.3]$$

The value of C_P will also be evaluated as an average between the entry and exit of the turbine stage.

$$\Delta H_{stg} = \int_{T_{in}}^{T_{out}} C_P dT \approx \overline{C}_P \Delta T_{stg} \qquad [5.4]$$

Using current gas turbine values of enthalpy drop per stage, SOT and constant pressure specific heat, the ratio T_{rotor}/T_{41} is calculated (figure 5.4).

From this figure, a value of 0.93-0.94 can be taken as a reasonable empirical approximation for the first stage rotor temperature. In combination with the cooling effectiveness, the above procedure enables the stator outlet temperature to be related to rotor blade metal temperature. In spite of this effect, that decreases the relative total temperature, it is most often the first stage rotor temperature which sets the upper limit on combustion temperature in any given case. For that reason, in this thesis, the limiting temperature will be the stator outlet temperature (driven by the rotor metal temperature & cooling technology), instead of the combustor discharge temperature. Nevertheless, both can be related using the cooling of the stator.

5.2.2. EFFECTS OF COOLING FLOW ON CYCLE EFFICIENCY AND POWER.

The correct simulation of the cooling flows is essential for accurate prediction of efficiency and power. When designing a new machine, the number of turbine stages, loading coefficient, desired metal temperatures depending on the turbine materials and technology (conventional casting, directionally solidified, single crystal), fuel to be employed, time between overhauls, life, cost, etc., must be defined. Then, blade cooling technology will estimate the mass flow necessary to obtain these metal temperatures, depending on the available state-of-the-art and considering possible limitations, such as the feasibility in the manufacturing process, considerations in the

---

[5] To reduce the cooling flow requirements, improving the cycle efficiency, it is possible to reduce the degree of reaction, decreasing the total temperature relative to the rotor. However, to maintain an acceptable aerodynamic behaviour, the average value must be above 0.4-0.42.

holes size[6], etc. Just as an example of the effect of the cooling flows in the power output and thermal efficiency, the following different power plant arrangements, with a design point SOT of 1200°C, were studied at both, design and off-design:

- Simple open cycle gas turbine.
- Simple semi-closed cycle gas turbine.
- Combined plant with a simple gas turbine as topping cycle.
- Combined plant with a simple semi-closed gas turbine as topping cycle.

The systems are considered:

- With the adequate cooling flows
- With no cooling flow at all

In figures 5.5 to 5.12, the differences in thermal efficiency and power output are shown for an open and a semi-closed cycle running line in both simple and combined cycle arrangement.

---

[6] For example, if the fuel employed produces solid particles, very small cooling holes can be a problem. The solid deposits could block the cooling exits, with the consequent increase in metal temperature, that can destroy the turbine. On the other hand, adequate size of these holes can avoid erosion, due to the formation of a protective fluid layer.

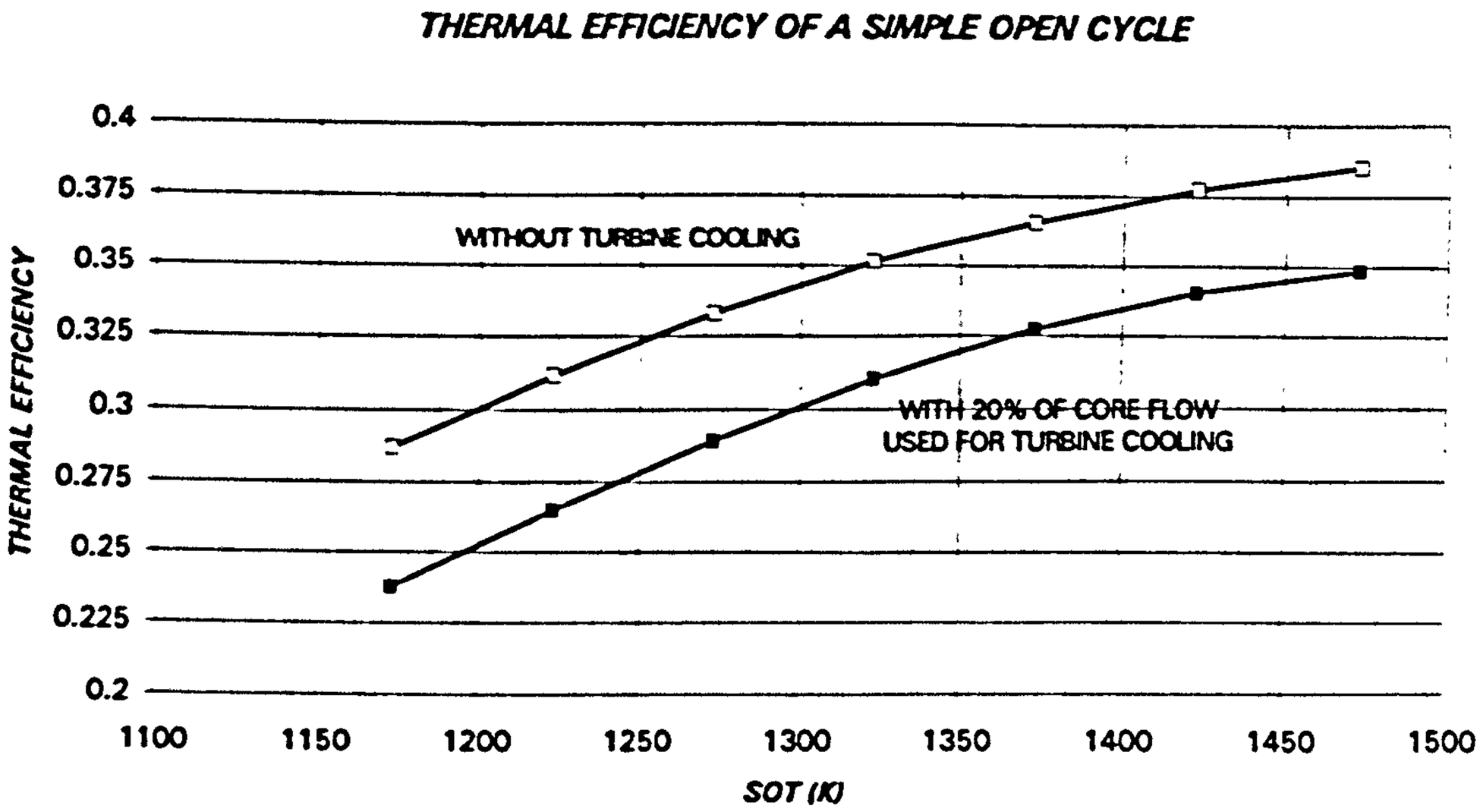

Figure 5.5. Simple open cycle thermal efficiency with and without cooling flows (running line from 1200°C down to 900°C)

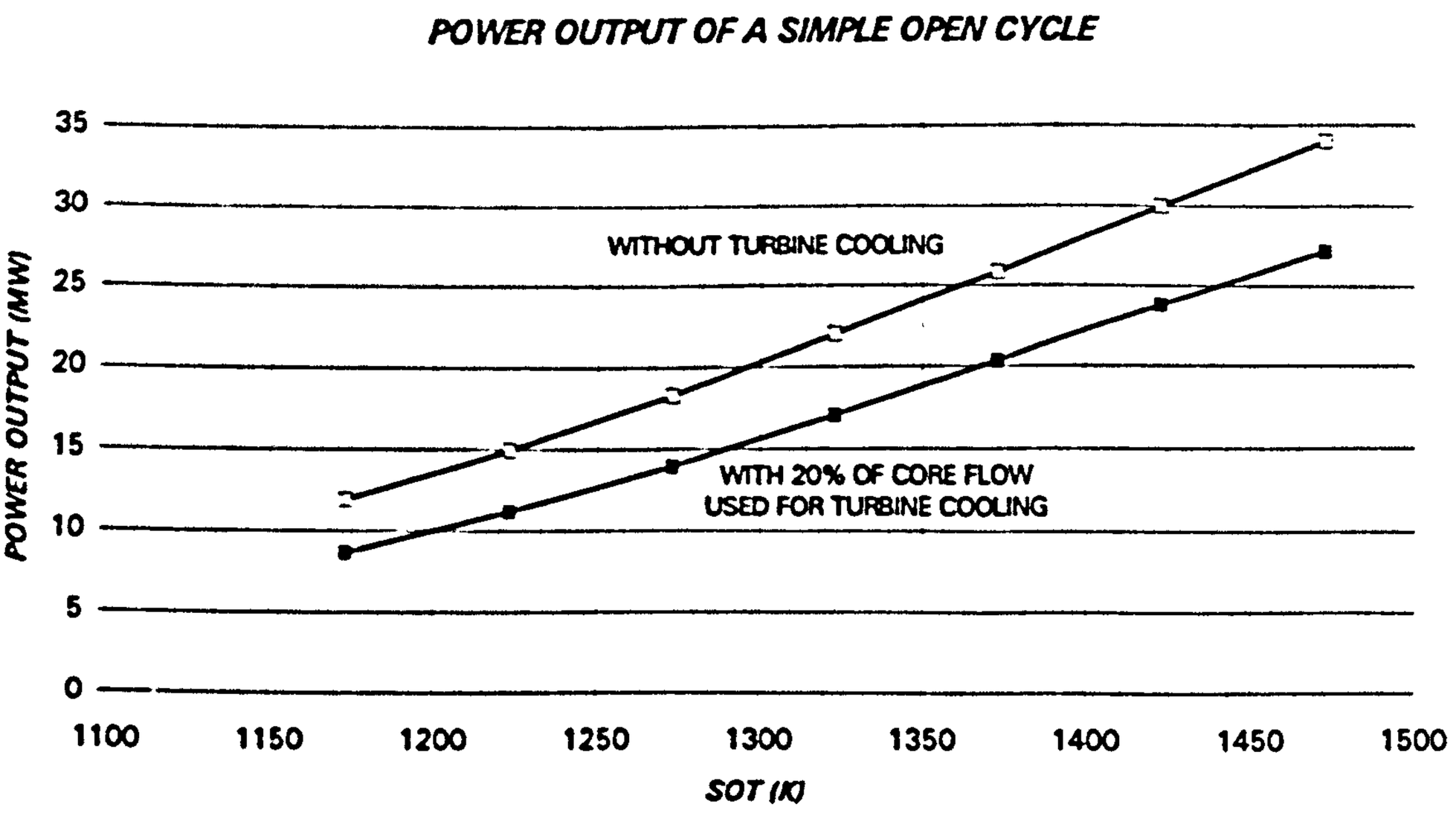

Figure 5.6. Simple open cycle power output with and without cooling flows (running line from 1200°C down to 900°C)

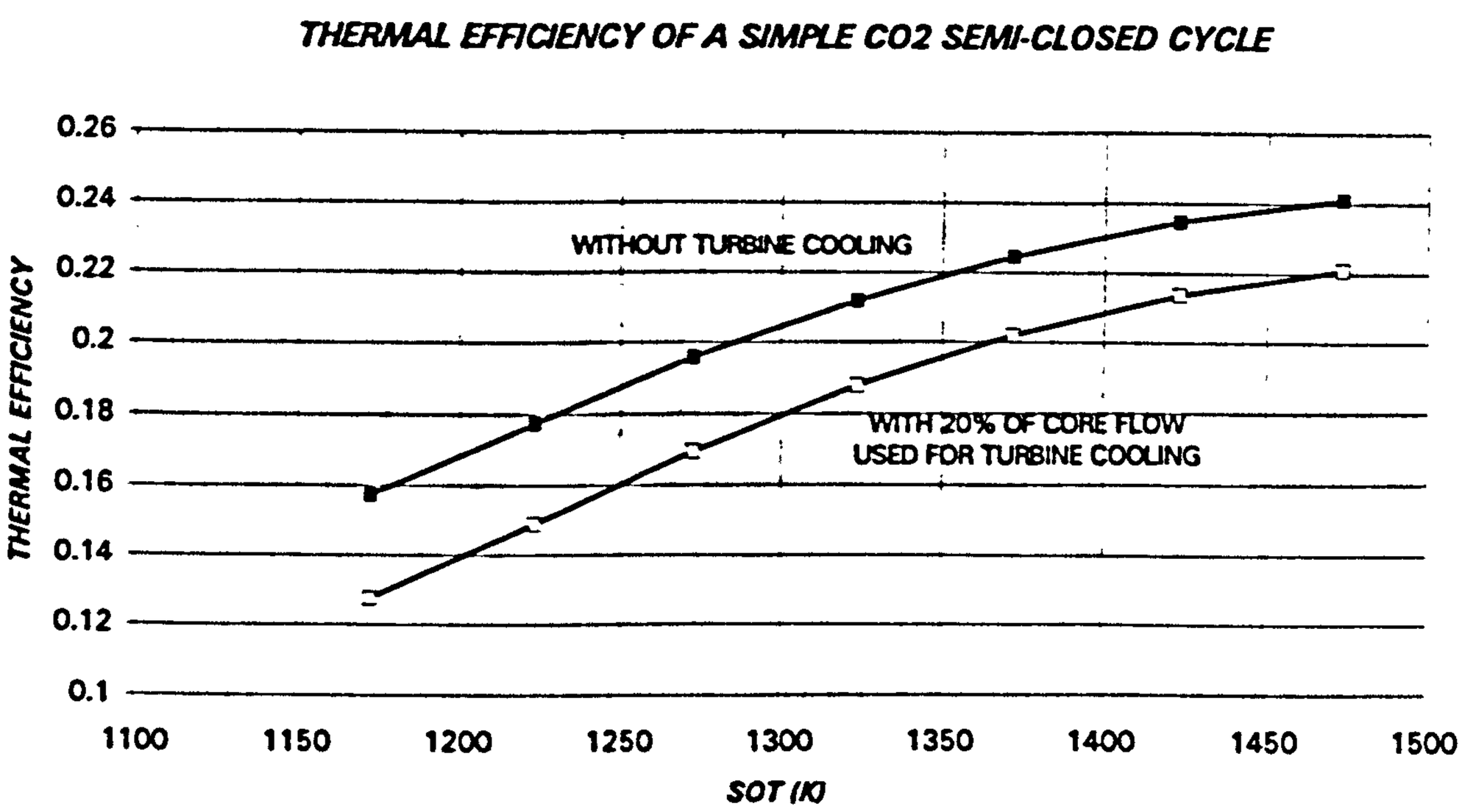

Figure 5.7. Simple semi-closed cycle thermal efficiency with and without cooling flows (running line from 1200°C down to 900°C)

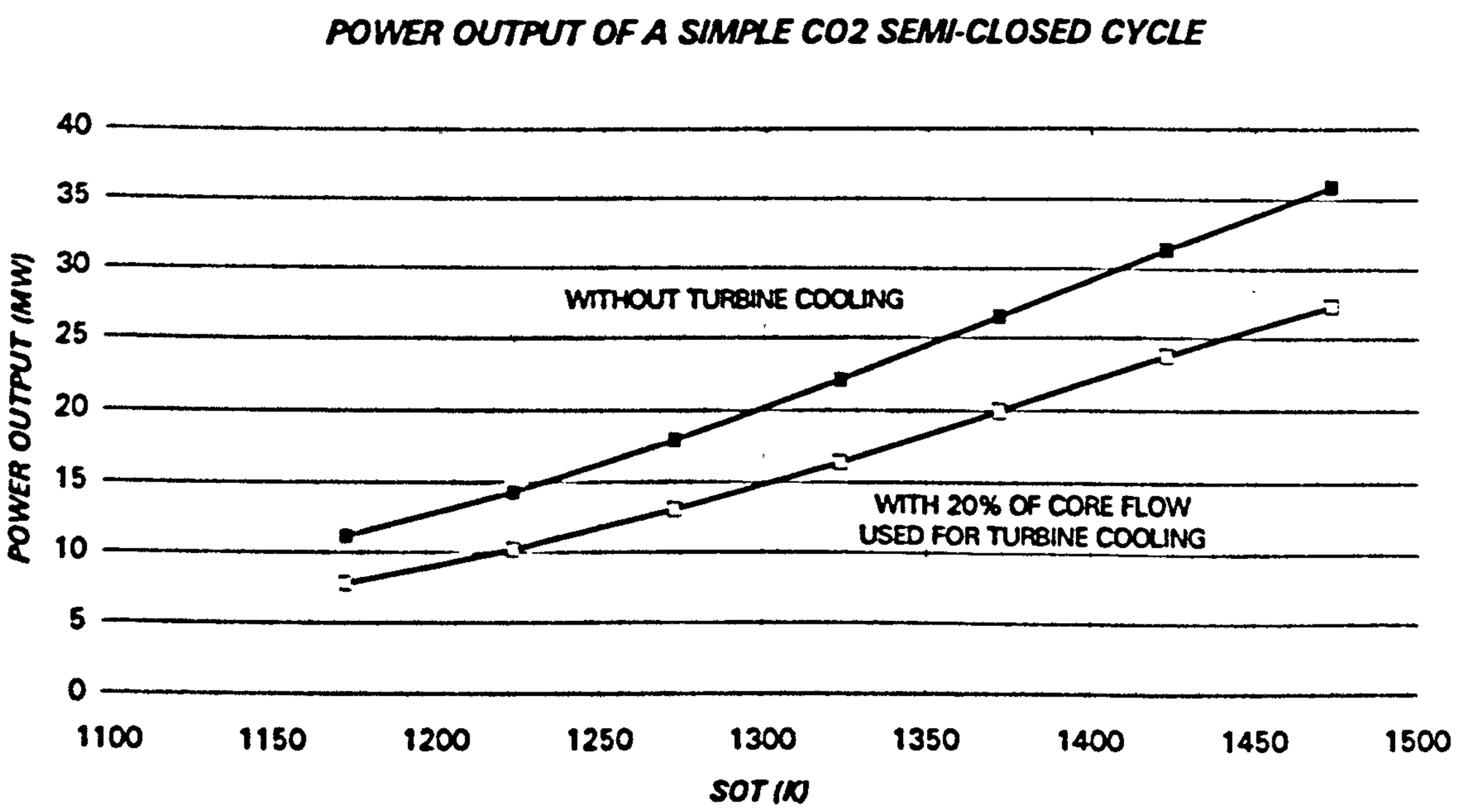

Figure 5.8. Simple semi-closed cycle power output with and without cooling flows (running line from 1200°C down to 900°C)

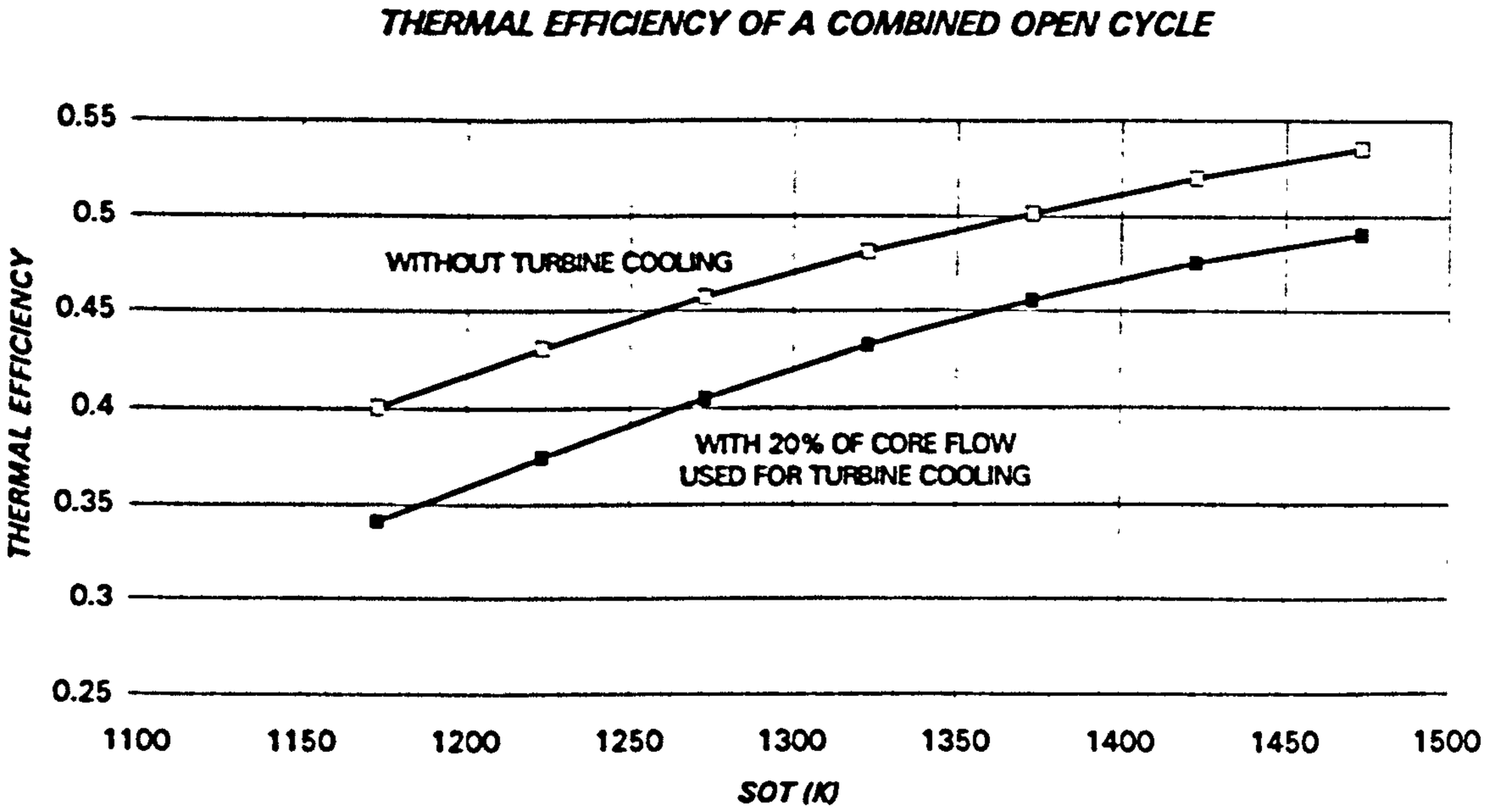

Figure 5.9. Combined open cycle thermal efficiency with and without cooling flows (running line from 1200°C down to 900°C)

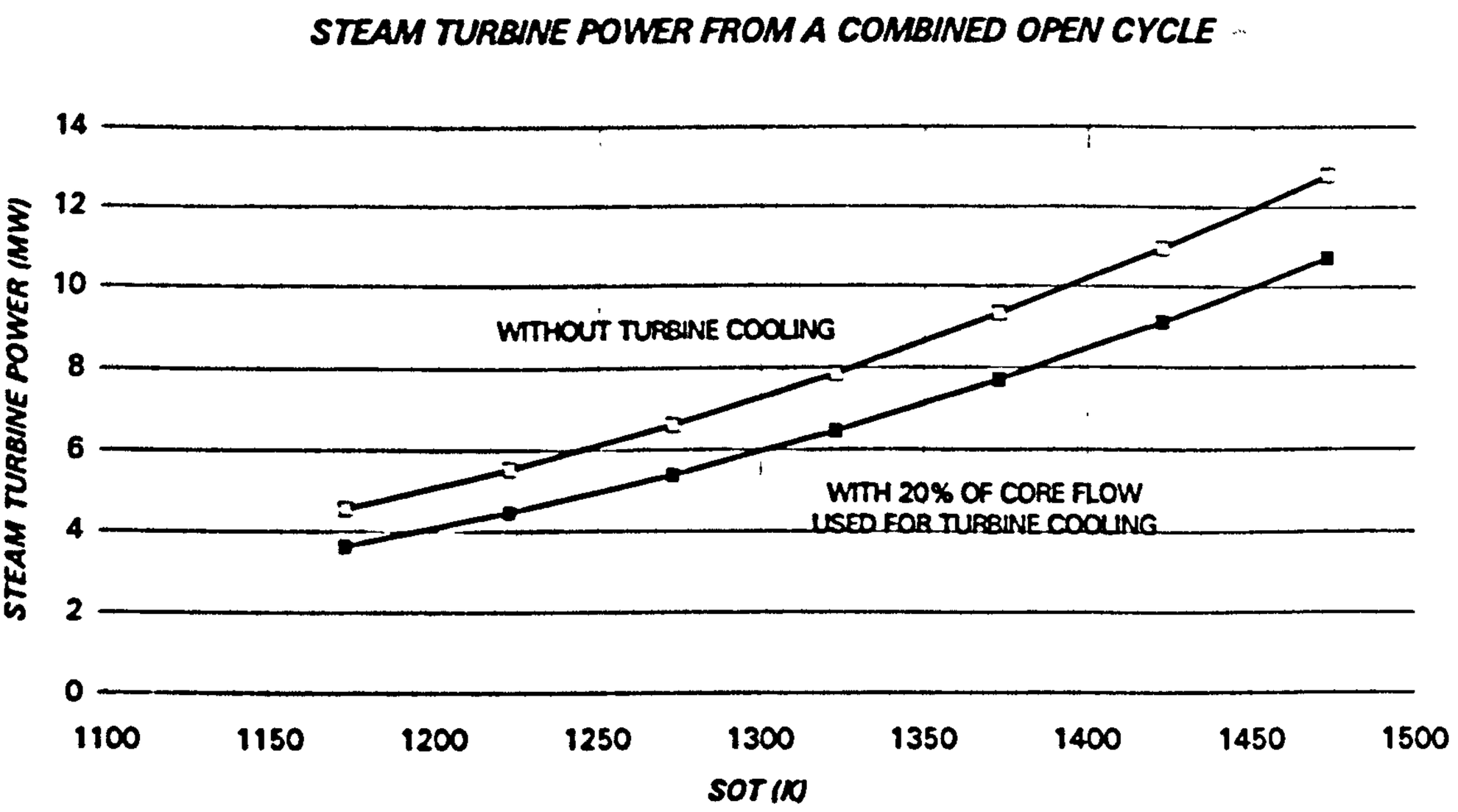

Figure 5.10. Combined open cycle steam turbine power with and without cooling flows (running line from 1200°C down to 900°C)

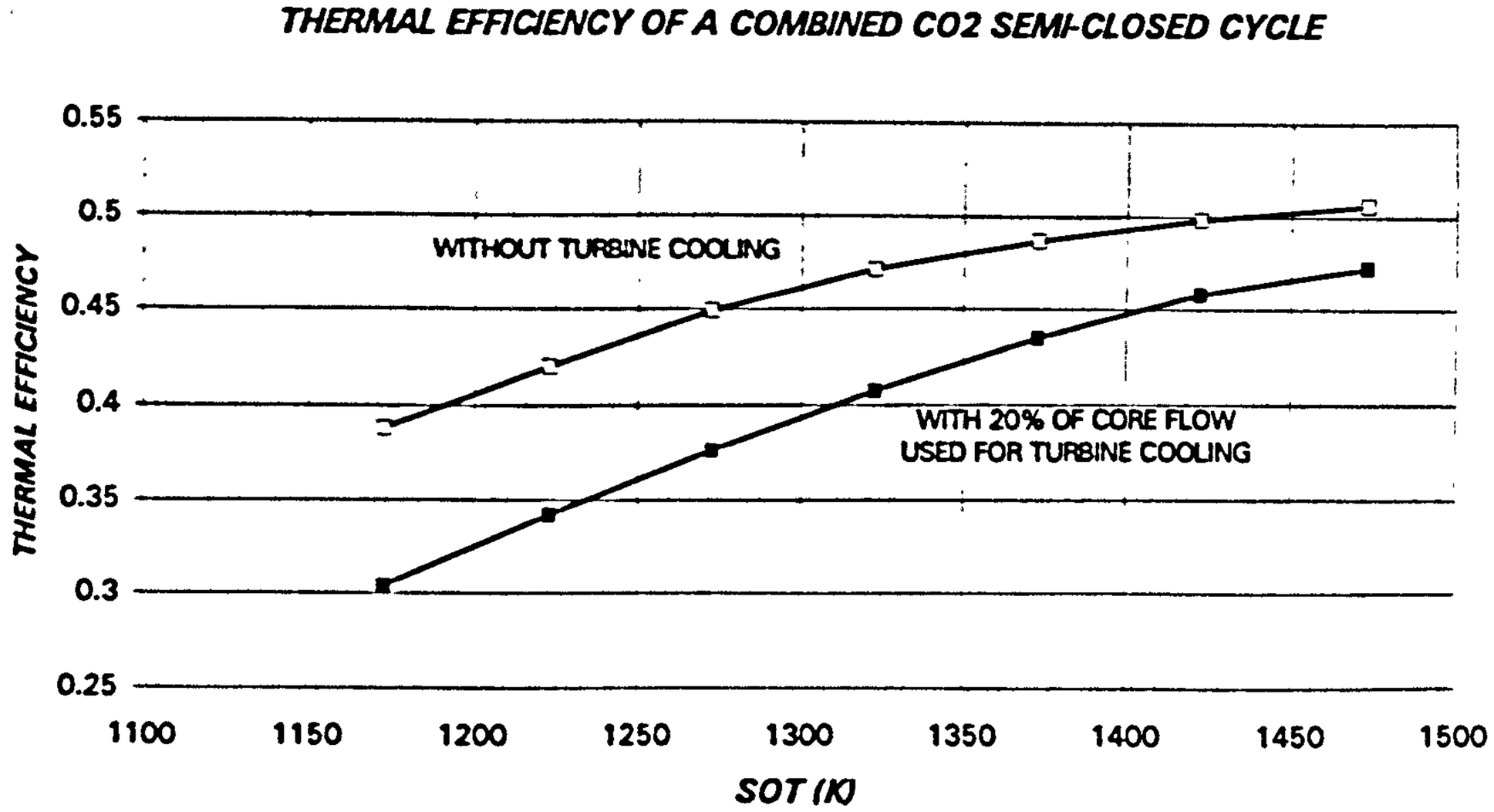

Figure 5.11. Combined semi-closed cycle thermal efficiency with and without cooling flows (running line from 1200°C down to 900°C)

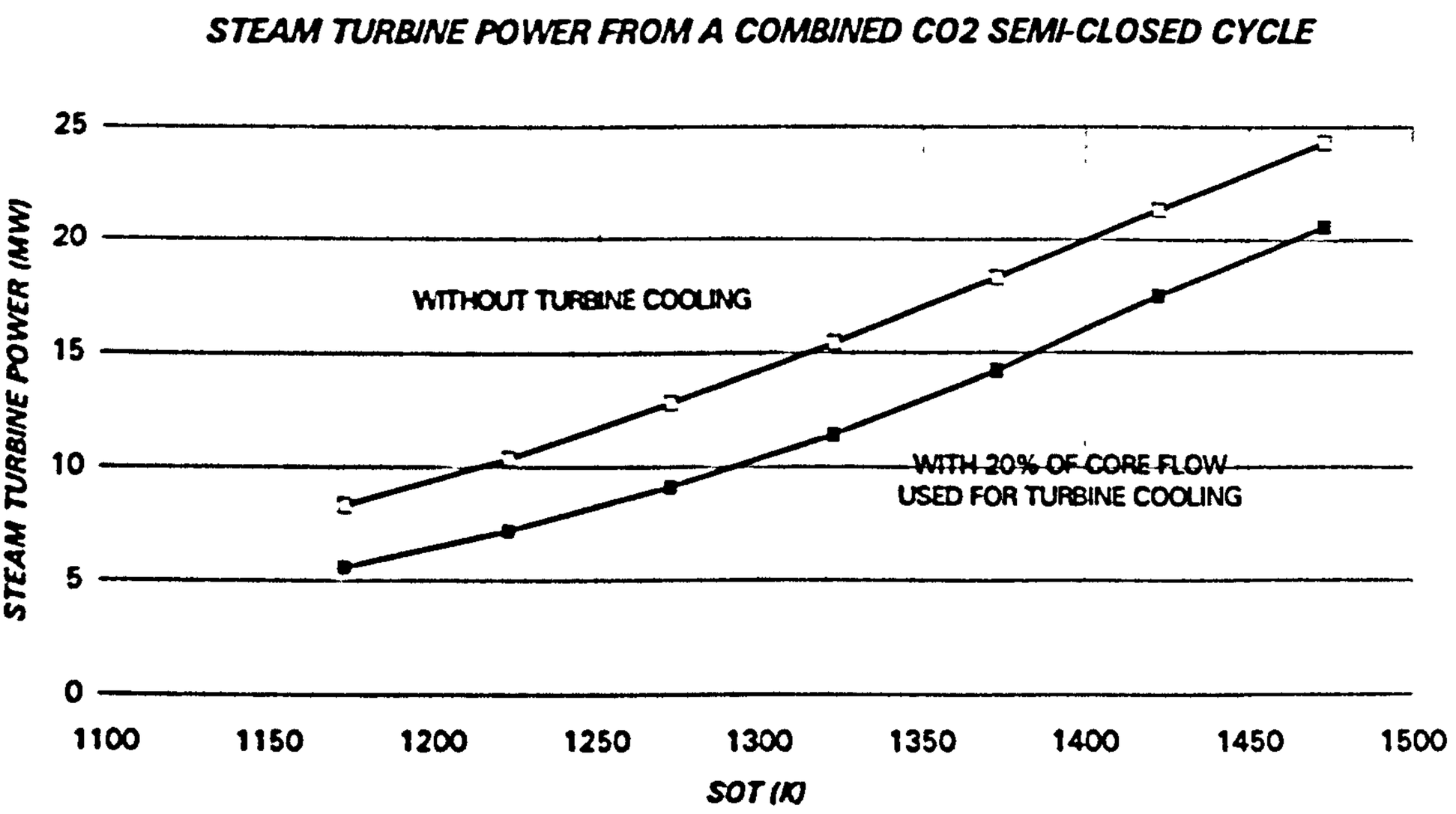

Figure 5.12. Combined semi-closed cycle steam turbine power with and without cooling flows (running line from 1200°C down to 900°C)

5.3. ESTIMATION OF THE COOLING FLOWS IN A TURBINE WITH PRESCRIBED NUMBER OF STAGES

If the number of stages is known, the basic assumptions for the estimation of the cooling flows will be the even distribution of enthalpy drop and the pressure ratio across the stages of the turbine. This is not necessarily true, specially if the turbine is the low pressure one. However, as this is not as hot as the high pressure turbine, the impact over the cooling flows will be small.

The pressure ratio per stage will be calculated using the following simplified expression.

$$\pi_{stg} = \left(\frac{P_4}{P_{43}} \right)^{\frac{1}{N_{stg}}} \qquad [5.5]$$

The total temperature of the stators will be:

$$T_i^{stator} = T_4 \left(\frac{1}{\pi_{stg}} \right)^{\frac{\eta_{poly}(\gamma-1)(i-1)}{\gamma}} \qquad i = 1 \rightarrow N_{stg} \qquad [5.6]$$

And for the rotors, with a 50% degree of reaction:

$$T_i^{rotor} = T_i^{stator} - \left(\frac{\Delta H}{\gamma RT} \right) \frac{\gamma RT}{2 C_P N_{stg}} = T_i^{stator} - \left(\frac{\Delta H_{stg}}{\gamma RT} \right) \frac{\gamma RT}{2 C_P} \qquad [5.7]$$

The value of C_P will be evaluated as an average between the entry and exit of the turbine and ΔH_{stg} will be:

$$\Delta H_{stg} = \int_{T_{out}}^{T_{in}} C_P dT \approx \overline{C}_P \Delta T_{stg} \qquad [5.8]$$

introducing this result in the rotor temperature equation:

$$T_i^{rotor} = T_i^{stator} - \frac{\Delta T_{stg}}{2} \qquad [5.9]$$

When the turbine has several stages the stator and rotor temperature at the entry of each one must be obtained. The temperature drop ΔT_{stg} will be very different for a turbine operating with air and another operating with helium. Hence, it will be more convenient to use ΔH_{stg}, which can be estimated using two main aerodynamic parameters: blade tangential speed U, and turbine stage loading coefficient Ψ.

$$\Delta H_{stg} = \Psi U^2 \qquad [5.10]$$

Depending on the technology and type of turbine different values of Ψ will be employed. Typical ranges are:

0.7-1.4: Low loading

1.4-2.1: Mid loading

2.1-2.8: High loading

2.8-3.5: Very high loading

The value of U is usually determined by a combination of aerodynamic (Mach number) and mechanical (stress) constraints and, in most cases, is limited by the compressor design group. However, in gases such as helium, with an extremely large speed of sound, only the mechanical limits will be considered. For conventional gases a value of 0.4-0.7 of the speed of sound can be employed.

With the stator and rotor temperatures it will be easy to find the cooling effectiveness that corresponds to the selected technology.

$$\varepsilon_i^{stator} = \frac{T_i^{stator} - T_i^{metal}}{T_i^{stator} - T_3} \qquad [5.11]$$

$$\varepsilon_i^{rotor} = \frac{T_i^{rotor} - T_i^{metal}}{T_i^{rotor} - T_3} \qquad [5.12]$$

In the early versions of the programme, the metal temperature of the stators for all the stages of the same turbine were the same. Identically for the rotors, where the user was able to specify a single temperature value. However, in real gas turbines, the rotor and stator metal temperature will not be necessary the same for all the stages, so the latest version has the possibility of selecting a different temperature for each blade or vane row.

The previous method has several simplifications that will be difficult to accept by a cooling specialist, although for performance calculations the results obtained are satisfactory. During the validation process, nine open cycle industrial gas turbine were simulated, and the values calculated by GTSI for the total cooling flows agreed within 10% with the real figures (differences of the order of 1% to 2% of core flow employed for cooling).

If, instead of the number of stages, the approximate pressure ratio per stage is given, the are calculated by and iterative method, and the process will be the same.

If the stage loading and blade speed are given, the number of stages can be easily calculated employing equation [5.10] to determine the enthalpy drop per stage.

5.4. SIMULATION OF TURBINE COOLING FLOWS IN A SINGLE STAGE TURBINE

Single stage turbines are becoming very frequent in advanced aero-engines, therefore in aeroderivative industrial machines, due to cost, weight and size reduction requirements. Furthermore, the stator of the LPT in a two shaft machine is sometimes eliminated with the introduction of counter-rotating turbines (the rotor of the HPT acts also as the stator of the LPT).

The most important turbine parameters for cycle definition and for the control of the machine, that will be strongly influenced by the cooling bleed modeling are:

$\left.\frac{W\sqrt{T}}{AP}\right\|_{NGV\ Throat}$	Non dimensional mass flow at NGV throat
$T\|_{Rotor\ Entry}$	Temperature at rotor entry / stator exit (SOT)
$T\|_{Rotor\ Exit}$	Temperature at rotor exit or turbine outlet temperature (TOT)
$\left.\frac{N}{\sqrt{T}}\right\|_{Rotor\ Entry}$	Non dimensional speed at rotor entry
$\Delta H\|_{Turbine}$	Specific power supplied by the turbine.

As mentioned in chapter 2, the non-dimensional mass flow at the NGV throat, non-dimensional speed at rotor entry and power supplied, shown above, are not rigorous. For cycles operating with a single gas or where the thermodynamic conditions do not change largely from the reference values, these are accurate enough. When the turbine is able to operate with different gases, or changing from cold to hot conditions, it is absolutely necessary to employ the following expressions:

$$\left.\frac{W\sqrt{T}}{AP}\sqrt{\frac{R}{\gamma}}\left(1+\frac{\gamma-1}{2}M^2\right)^{\frac{\gamma+1}{2(\gamma-1)}}\right|_{NGV\ Throat} \qquad [5.13]$$

$$\left.\frac{N\sqrt{1+\frac{\gamma-1}{2}M^2}}{\sqrt{\gamma RT}}\right|_{Rotor\ Entry} \qquad [5.14]$$

$$\left.\frac{\Delta H}{\gamma RT}\left(1+\frac{\gamma-1}{2}M^2\right)\right|_{Rotor\ Entry} \qquad [5.15]$$

However, the Mach number term in the non dimensional mass flow, speed and power, introduces only small corrections. These, in most cases, can be neglected, giving the final equations:

$$\left.\frac{W\sqrt{T}}{AP}\sqrt{\frac{R}{\gamma}}\right|_{NGV\ Throat} \qquad [5.16]$$

$$\left.\frac{N}{\sqrt{\gamma RT}}\right|_{Rotor\ Entry} \qquad [5.17]$$

$$\left.\frac{\Delta H}{\gamma RT}\right|_{Rotor\ Entry} \qquad [5.18]$$

The mass flow and total temperature at the NGV throat are influenced by the cooling flow introduced before this station, specially at the leading edge. The ratio of specific heats and the gas constant are also affected, although the effect is smaller. A similar analysis can be done for the corrected speed, SOT and corrected power supplied by the turbine, where the cooling flow introduced through the vanes, before and after the throat, modifies the mass flow, temperature, enthalpy, γ, R, etc., at the entry of the rotor. The rotor cooling flow will not contribute to the turbine work, although it will decrease the turbine outlet temperature.

5.4.1. COOLING ARRANGEMENT

There are three different cooling flows considered in the programme for a single stage turbine, as shown in figure 5.13:

- The first one, W_1^{Bleed}, cools the NGV, and enters before the throat of the stator.
- The second, W_2^{Bleed}, also cools the NGV, and enters after the throat of the stator.
- The third one, W_3^{Bleed}, cools the rotor, and enters after the rotor.

There will be other flows that are used to cool the platforms, discs, etc., and enter in different parts of the hot section. These flows can be considered at the design stage, and the method will be explained later.

The reason to have these three main cooling flows in each stage is clear. The NGV leading and trailing edges require a great amount of cooling, because the heat transfer coefficient is higher in those regions that in the rest of the blade. Also, in the high pressure turbine first NGV, an important amount of radiation heat comes from the combustion chamber, making even more difficult the cooling of the leading edge and pressure surface of the aerofoil.

As the mass flow through the turbine is, in most cases, controlled by the NGV throat, usually choked, the correct account of the cooling flow before this section is critical. The sum of the mass flows leaving the stator has also a substantial effect in the cycle calculation, because these flows contribute effectively to the work done over the rotor, while the rotor cooling flows do not make significant work over this stage, but they will do over the following ones.

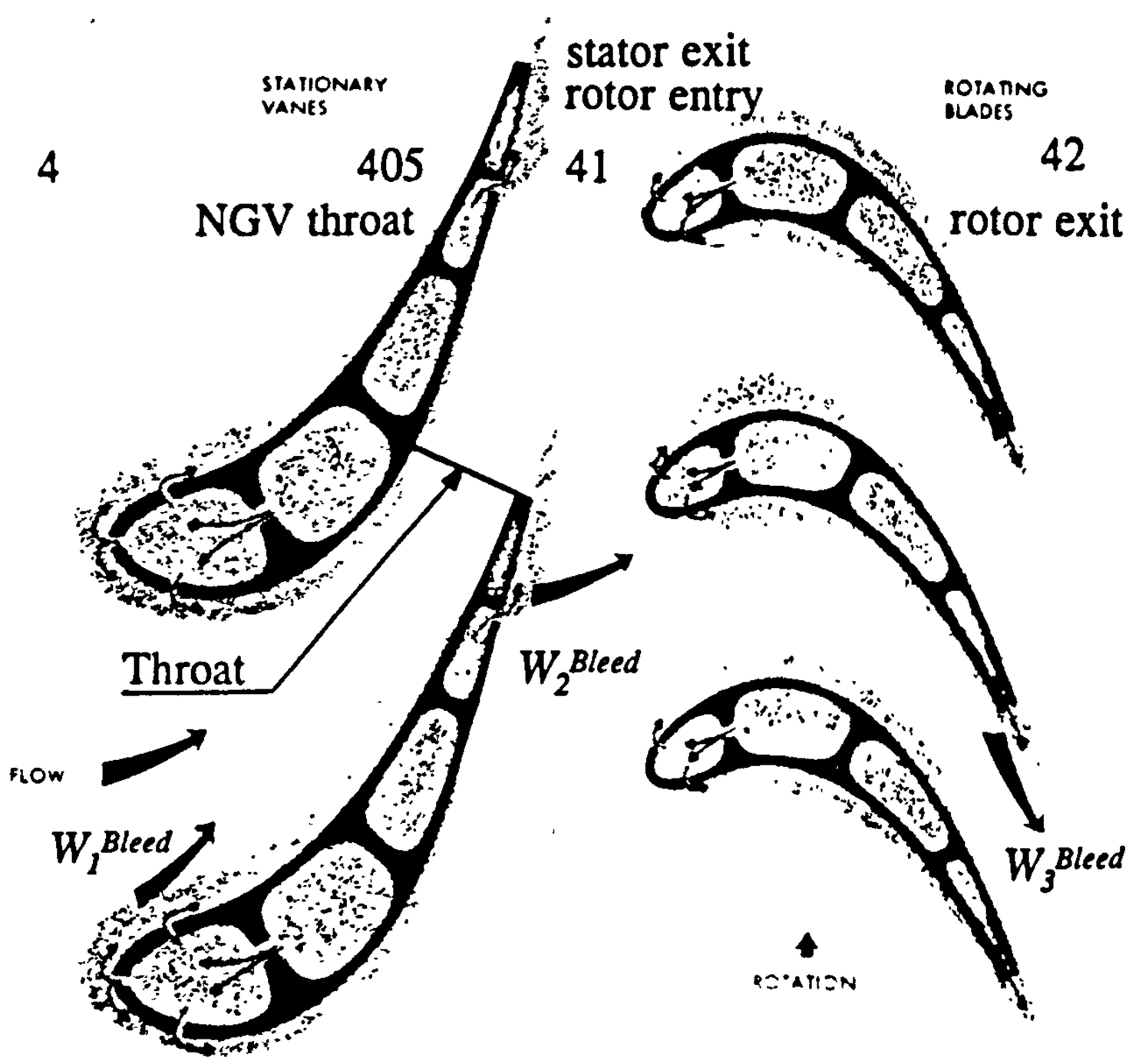

Figure 5.13. Single stage turbine cooling flows

From the performance point of view, a good approximation is to consider constant thermodynamic properties at the entry of each station. This will assume complete mixing between the cooling flows and the main stream before entering the next engine station downstream.

The actual physical process is very different. The radial and circumferential temperature profile at the combustor exit is not uniform, due to the presence of the burners, the dilution and cooling air injection at the combustion chamber walls and, in a less extend due to the heat transfer with the structure.[7] Figure 5.14 shows an example of temperature profile at the combustor exit. The conditions entering the rotor will also have strong gradients spanwise.

---

[7] The NGVs cooling flows will be tailored to those profiles, that can be predicted from previous experiments and analytical models. These cooling flows do not produce the same amount of work that an equivalent mass flow coming from the combustor or from a previous stage would produce.

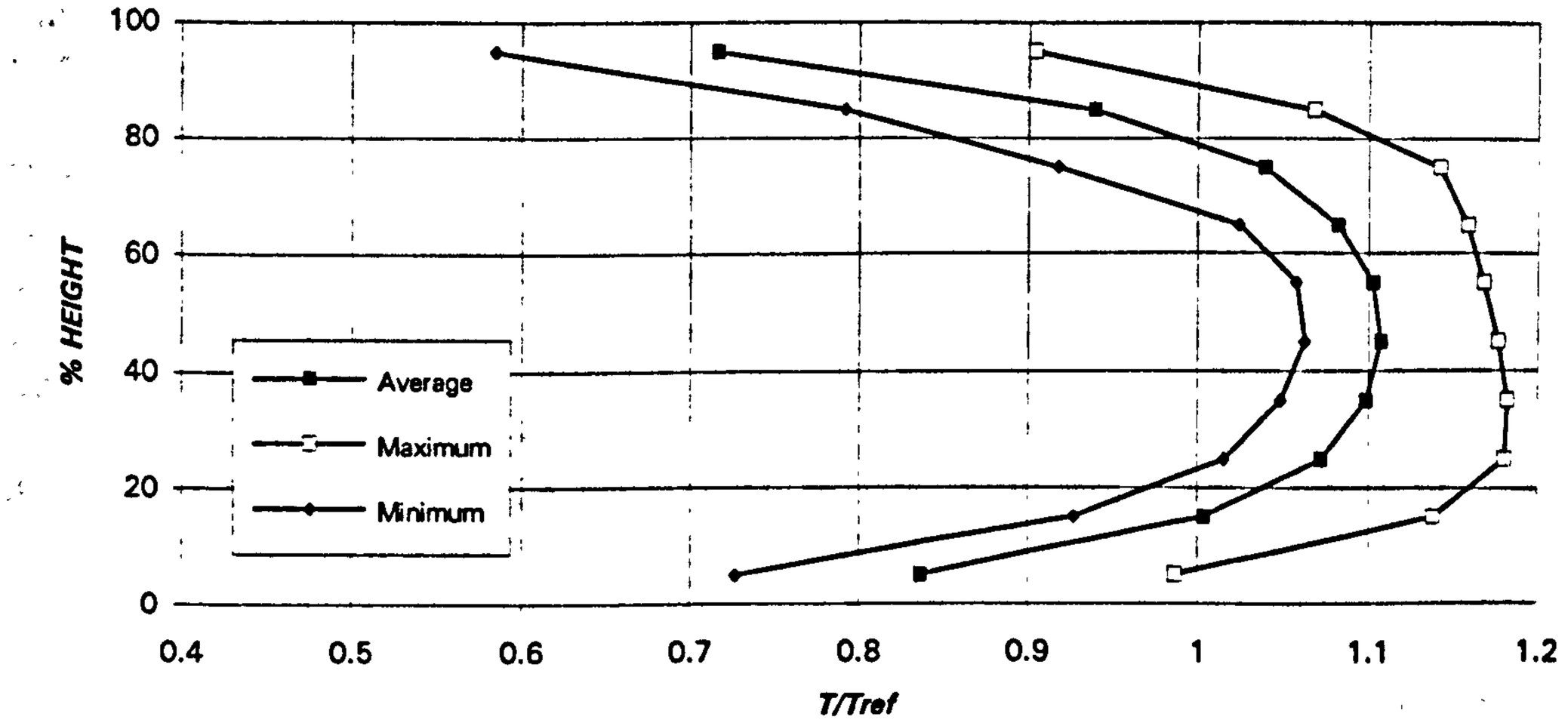

Figure 5.14. Radial temperature profile at the combustor exit, with minimum, average and maximum circumferential values

Employing the continuity, energy and gas model equations it is possible to find the mass flow, enthalpy, temperature, specific heats, etc. for each engine station. The influence of cooling bleeds on total pressure is not considered, assuming constant total pressure. For the case of a HPT the system will be:

$$W_{405} = W_4 + W_1^{Bleed} \qquad [5.19]$$

$$P_{405} = P_4 \qquad [5.20]$$

$$H_{405} = \frac{W_4 H_4 + W_1^{Bleed} H_1^{Bleed}}{W_4 + W_1^{Bleed}} \qquad [5.21]$$

The same procedure will be applied for the other stations where cooling flows, W_2^{Bleed} and W_3^{Bleed} are injected.

First HPT stage NGVs/Rotors with over 10% cooling flow are not uncommon. Therefore, errors of the order of 5% in turbine capacity and over 50 K in SOT could be introduced if a simplified method was employed.

5.4.2. COMPRESSOR BLEED POINTS

The cooling bleed location in the compressor depends on the pressure of the station where the flow will be injected and the pressure losses between the extraction and the injection points. For the high pressure turbine the flow is taken from the compressor exit, bypassing the combustion chamber, because the pressure at the first stage of the HPT is just slightly lower than the compressor discharge one. A simplification introduced in the programme assumes that for each turbine there is a unique extraction point. This is not necessarily true because, for example, the pressure in the second stage of a two stages HP turbine will be considerably lower than in the first one. Hence, the air could be bled from a compressor point with lower pressure. However, in order to simplify the design and, also, in some cases, due to manufacturing problems,[8] the assumption of one bleed point per turbine has been maintained. The errors introduced by this simplification will be small.

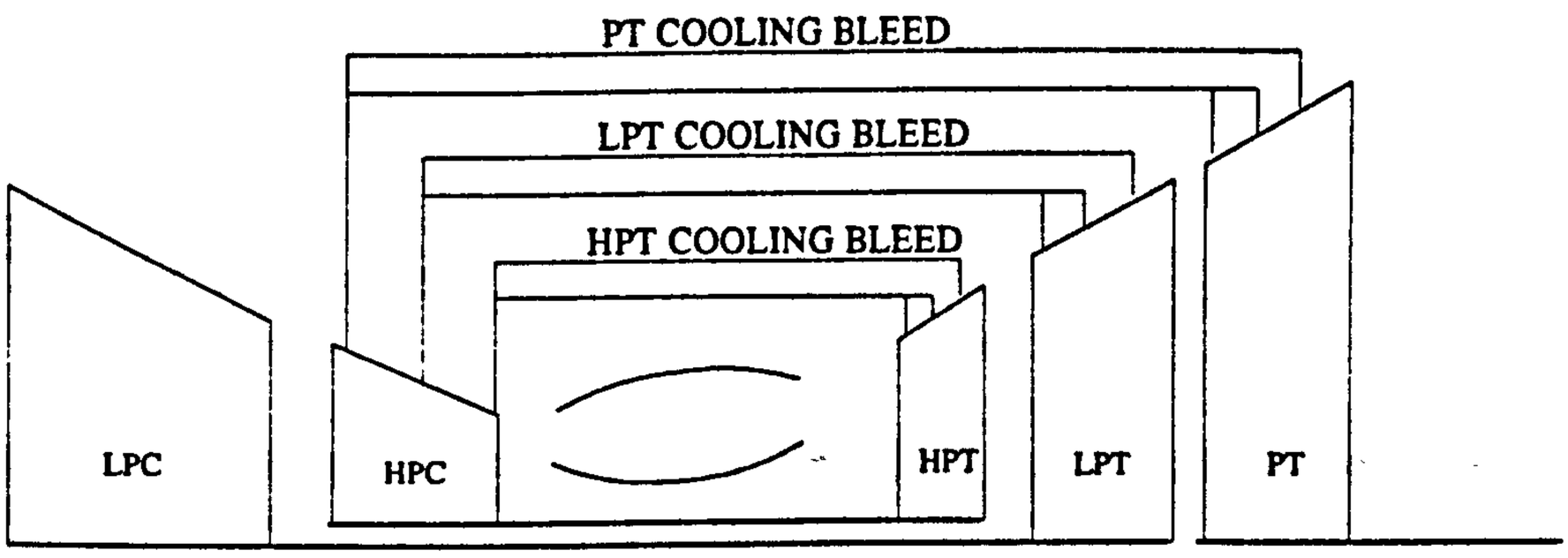

Figure 5.15. Cooling flow arrangement for a two spool - three shaft gas turbine

At the early stages of a project it is not usual to have details from each separate stage of the turbines. Therefore, it will not be possible to make a good estimation of the compressor bleed extraction point.

An easy method for estimating the position of the LPT cooling bleed in the compressor is based on the fact that the turbines are choked during normal operation. Hence, turbine pressure ratio will be constant, as well as non-dimensional mass flow.

---

[8] In the case of a two stage HPT, with a stage pressure ratio of 1.8, and with a compressor pressure ratio per stage of 1.4, it is easy to find that the cooling flow for the second turbine stage would be taken from the penultimate compressor stage. The difficulty to extract the flow from this stage, due to the small size of the last stages, together with the extra weight introduced by the additional ducts, seals, etc., can favor the solution of taking the complete turbine cooling flow from the compressor discharge.

$$\frac{W_{405}\sqrt{T_{405}}}{P_{405}} = K_1 \qquad [5.22]$$

$$\frac{W_{455}\sqrt{T_{455}}}{P_{455}} = K_2 \qquad [5.23]$$

The capacity of both turbines will be initially estimated using a simplified cycle.

The efficiency of the high pressure turbine can be found (if not given) with the following equation:

$$\eta_{41} = \frac{\Delta H}{\Delta H_{is}} \approx \frac{1-\left(\frac{T_{45}}{T_4}\right)}{1-\left(\frac{P_{45}}{P_4}\right)^{\frac{\gamma_4-1}{\gamma_4}}} \qquad [5.24]$$

Using the non dimensional mass flow at the HPT, and neglecting that the cooling flows are introduced at different stages (before and after the throat, etc.), the following expression can be derived:

$$\frac{W_{405}\sqrt{T_{405}}}{P_{405}} = \frac{W_{455}\sqrt{T_{455}}}{P_{455}}\frac{P_{455}}{P_{405}}\sqrt{\frac{T_{405}}{T_{455}}}\frac{W_{405}}{W_{455}} = \frac{W_{455}\sqrt{T_{455}}}{P_{455}}\frac{P_{455}}{P_{405}}\sqrt{\frac{T_{405}}{T_{455}}}\left(1-\frac{W_{BLEED}}{W_{455}}\right) \qquad [5.25]$$

Employing the adiabatic efficiency definition, the previous equation can be simplified, eliminating the temperature ratio:

$$\frac{W_{405}\sqrt{T_{405}}}{P_{405}} = \frac{W_{455}\sqrt{T_{455}}}{P_{455}}\frac{P_{455}}{P_{405}}\sqrt{\eta_{41}\left(\left(\frac{P_{405}}{P_{455}}\right)^{\frac{\gamma_4-1}{\gamma_4}}-1\right)+1}\left(1-\frac{W_{BLEED}}{W_{455}}\right) \qquad [5.26]$$

Introducing the constant turbine capacity, the combustion chamber pressure losses and safety factors for the bleed pressure (accounting for the injection pressure ratio, losses across the seals and metering holes, transient effects, lower pressure in the compressor boundary layer, etc.) the final equation will be:

$$K_1 = K_2\frac{(1-\zeta)P_{255}}{(1-\pi_{CC})P_3}\sqrt{\eta_{41}\left(\left(\frac{(1-\pi_{CC})P_3}{(1-\zeta)P_{255}}\right)^{\frac{\gamma_4-1}{\gamma_4}}-1\right)+1}\left(1-\frac{W_{BLEED}}{W_{455}}\right) \qquad [5.27]$$

If the amount of cooling bleed and the rest of the variables are known, the pressure P_{25} can be easily found.

This method will provide an acceptable estimation of the compressor bleed point, although it will be essential to cover the complete turbine operating range to ensure that the hot air ingestion risk has been minimised.

5.5 COOLING FLOW MODELING IN MULTI-STAGE TURBINE

In commercial aero-engines and industrial machines the most common situation is to have turbines with more than one stage (figure 5.16). In those cases the turbine is considered as the first NGV plus a black box representing the rest of the component. The cooling flow simulation method described in the previous section (one cooling flow injected before the first NGV throat, other after the NGV throat and a final one after the final rotor) does not reproduce the real engine behaviour, although the maps can be adequately modified to give the power, efficiency and mass flow.

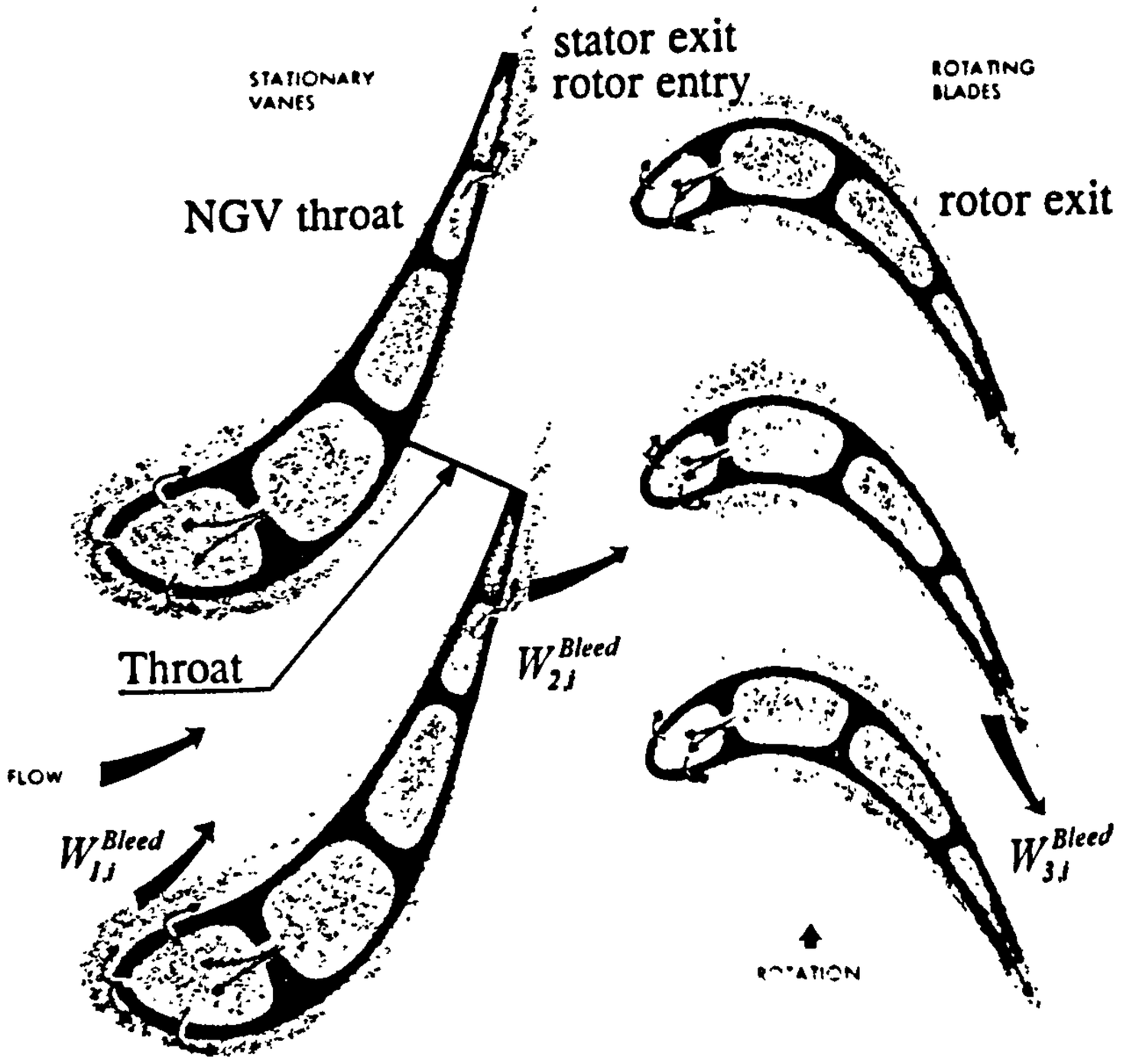

Figure 5.16. Scheme of the multi-stage turbine cooling bleeds (HPT)

The most intuitive approach will be to consider the multi-stage turbine as sequence of stages rotating at the same speed. In this situation the single-stage turbine method will be applicable. However, to follow this procedure it will be necessary to

have the performance data of each stage separately, which is not very common. For most cases only the performance of the whole turbine is available, and this will be the scenario considered in the study.

The main performance parameters in single and multi-stage turbines are the same: non-dimensional mass flow at the throat of the first NGV, total temperature at the entry of the first rotor, turbine outlet temperature, turbine power, corrected speed,...

The first target is the calculation of the number of turbine stages (if not specified by the user). As anticipated in the section devoted to the estimation of cooling requirements, with the stage loading and the tangential speed it is possible to find the enthalpy drop per stage. If the complete turbine enthalpy drop is known from the compressor and/or power output requirements, it will be simple to derive the number of stages.

Once the number of stages and the cooling flows necessary for each row are calculated, SOT, first NGV non-dimensional mass flow and corrected speed are found using the cooling results for the first stage.

To obtain the mass flow, temperature and enthalpy for the evaluation of the power of the turbine and, later, the exit temperature, an average considering all the cooling flows should be employed.

The average mass flow (W_{Av}) for turbine power calculations will then be:

$$W_{Av} = \frac{\left[\left(W_4 + W_{1,1}^{Bleed} + W_{2,1}^{Bleed}\right)N_{stg} + \sum_{i=2}^{N_{stg}}\left(W_{3,i-1}^{Bleed} + W_{1,i}^{Bleed} + W_{2,i}^{Bleed}\right)\left(N_{stg} - i + 1\right)\right]}{N_{stg}} \quad [5.28]$$

and the average enthalpy (H_{Av}) at the entry of the turbine will be:

$$H_{Av} = \frac{\left[\begin{array}{l}\left(W_4 H_4 + W_{1,1}^{Bleed} H_{1,1}^{Bleed} + W_{2,1}^{Bleed} H_{2,1}^{Bleed}\right)N_{stg} + \\ + \sum_{i=2}^{N_{stg}}\left(\begin{array}{l} W_{3,i-1}^{Bleed} H_{3,i-1}^{Bleed} + W_{1,i}^{Bleed} H_{1,i}^{Bleed} + \\ + W_{2,i}^{Bleed} H_{2,i}^{Bleed}\end{array}\right)\left(N_{stg} - i + 1\right)\end{array}\right]}{N_{stg} W_{Av}} \quad [5.29]$$

One of the main assumptions to derive these expressions is that all the stages of the turbine perform the same non-dimensional work. If the information of the work done by each stage is available it can be employed, giving equations [5.30] and [5.31]:

$$W_{Av} = \left(W_4 + W_{1,1}^{Bleed} + W_{2,1}^{Bleed}\right) + \sum_{i=2}^{N_{stg}}\left(W_{3,i-1}^{Bleed} + W_{1,i}^{Bleed} + W_{2,i}^{Bleed}\right)\xi_i \quad [5.30]$$

$$H_{Av} = \frac{\left[\begin{array}{l}\left(W_4 H_4 + W_{1,1}^{Bleed} H_{1,1}^{Bleed} + W_{2,1}^{Bleed} H_{2,1}^{Bleed}\right) + \\ + \sum_{i=2}^{N_{stg}} \left(W_{3,i-1}^{Bleed} H_{3,i-1}^{Bleed} + W_{1,i}^{Bleed} H_{1,i}^{Bleed} + W_{2,i}^{Bleed} H_{2,i}^{Bleed}\right) \xi_i\end{array}\right]}{W_{Av}} \quad [5.31]$$

where ξ_i is the work done by the stages from i to N_{stg} relative to the turbine work:

$$\xi_i = \frac{1}{\Delta H_{turbine}} \left[\sum_{j=i}^{N_{stg}} \Delta H_j\right] \quad [5.32]$$

Therefore, the cooling flow that contributes to the useful work will be:

$$W_{Av}^{Bleed} = \frac{\left(W_{1,1}^{Bleed} + W_{2,1}^{Bleed}\right) N_{stg} + \sum_{i=2}^{N_{stg}} \left(W_{3,i-1}^{Bleed} + W_{1,i}^{Bleed} + W_{2,i}^{Bleed}\right)\left(N_{stg} - i + 1\right)}{N_{stg}} \quad [5.33]$$

$$W_{Av}^{Bleed} = \left(W_{1,1}^{Bleed} + W_{2,1}^{Bleed}\right) + \sum_{i=2}^{N_{stg}} \left(W_{3,i-1}^{Bleed} + W_{1,i}^{Bleed} + W_{2,i}^{Bleed}\right) \xi_i \quad [5.34]$$

Once the enthalpy drop has been calculated employing the appropriate equation (work balance, exit pressure, component characteristics, ...) the remaining cooling flows, that do not make work, must be introduced.

The flow and enthalpy that enters the turbine are:

$$W_{in} = W_4 + \sum_{i=1}^{N_{stg}} \left(W_{1,i}^{Bleed} + W_{2,i}^{Bleed} + W_{3,i}^{Bleed}\right) \quad [5.35]$$

$$H_{in} = \frac{W_4 H_4 + \sum_{i=1}^{N_{stg}} \left(W_{1,i}^{Bleed} H_{1,i}^{Bleed} + W_{2,i}^{Bleed} H_{2,i}^{Bleed} + W_{3,i}^{Bleed} H_{3,i}^{Bleed}\right)}{W_{in}} \quad [5.36]$$

The flow and enthalpy already introduced are W_{Av}^{Bleed} and H_{Av}^{Bleed} . Hence, the difference between W_{in} and W_{Av}^{Bleed} for the mass flow and between H_{in} and H_{Av}^{Bleed} for the enthalpy are still to be injected into the main stream.

Special attention should be paid to the flows injected at the hub or tip region, characteristic of either internal vane/blade cooling, platform or casing cooling. Hot air ingestion between rows must also be contemplated in this study.

- The flows injected at hub or tip region will only produce useful work in the stages downstream.

- The hot air ingestion will be considered as a negative cooling flow.

With the method described in this section it is possible to perform the cooling bleed simulation in the turbine, with a high degree of accuracy, when only the complete turbine performance characteristics are known. Figure 5.17 shows the improvement in the performance calculations employing this technique. Of course, if detailed stage data are available the method for the single stage turbine would be applied.

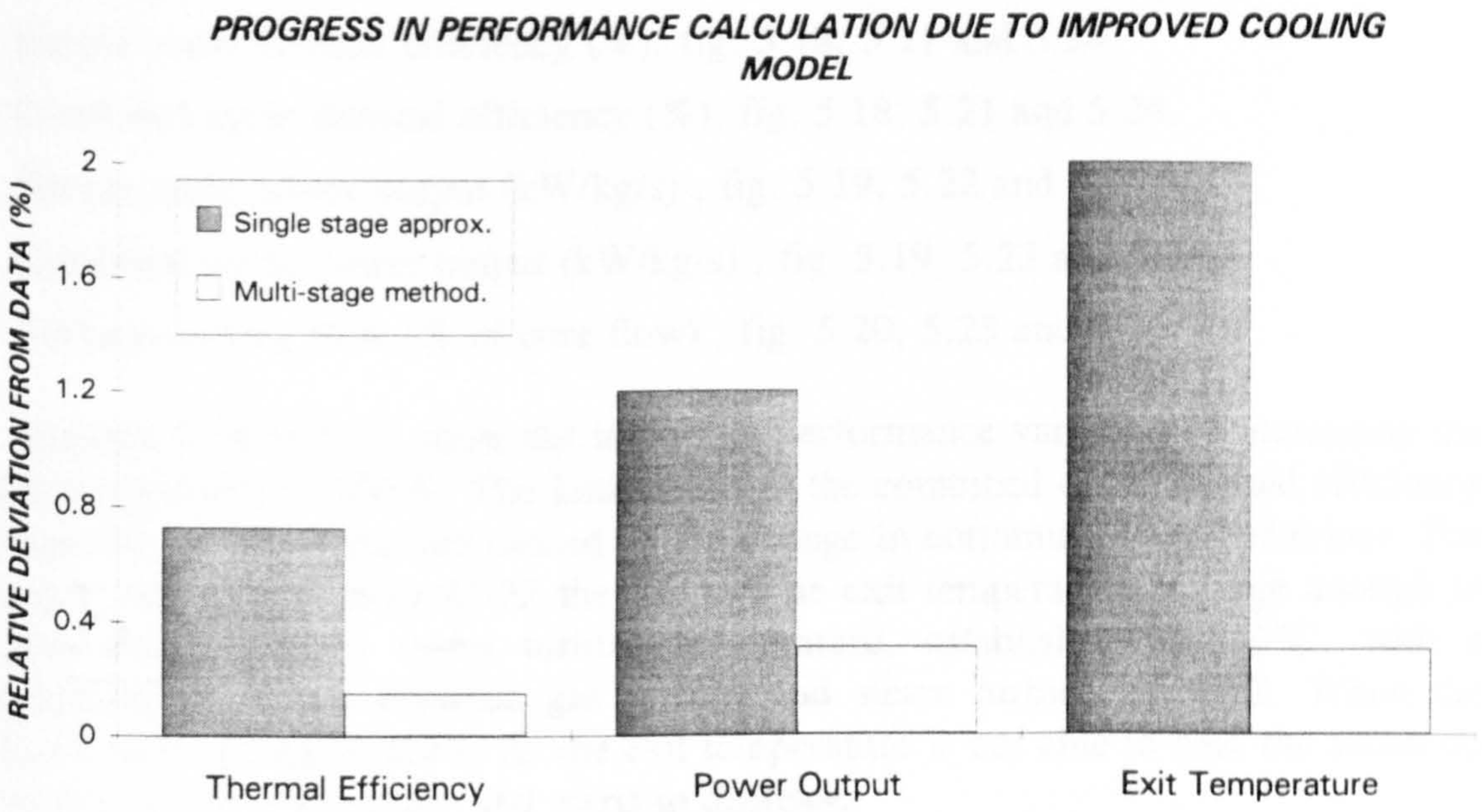

Figure 5.17. Performance deviation from engine data for a 4 stage turbine with single stage approximation and multi-stage method.

5.6. SENSITIVITY ANALYSIS

As previously stated, the effect of the cooling bleeds on the performance of the machine is not negligible. To evaluate this influence three cases have been studied, employing both, simple and combined cycles:

- Increase of 100 K in vanes and blades allowable metal temperature (full coverage film cooling employed), resulting in a reduction in cooling bleed flow, and consequently an improvement in performance.
- Change of cooling bleed method from convection, impingement & slot to full coverage film cooling, that again will cause an important decrease in turbine cooling flow, therefore a performance gain.

- Increase of 100 K in TET. The direct consequence is an improvement in performance, but the increase in cooling flow will reduce this effect.

For these simulations, a baseline gas turbine with a TET of 1300°C, vane and blade metal temperatures of 1100 K and 1075 K respectively, turbine tangential velocity of 375 m/s, stage loading coefficient of 1.9, and compressor and turbine polytropic efficiency of 0.89 and 0.87, has been employed. The steam turbine is of a single pressure type, with a polytropic efficiency of 0.85, and pressure optimised to give the highest combined cycle thermal efficiency.

The performance changes will be shown in terms of:

- Simple cycle thermal efficiency (%), fig. 5.18, 5.21 and 5.24.
- Combined cycle thermal efficiency (%), fig. 5.18, 5.21 and 5.24.
- Simple cycle power output (kW/kg/s) , fig. 5.19, 5.22 and 5.25.
- Combined cycle power output (kW/kg/s) , fig. 5.19, 5.22 and 5.25.
- Turbine cooling flow (% of core flow) , fig. 5.20, 5.23 and 5.26.

Figures 5.18 to 5.21 show the important performance variation of increasing the metal temperature in 100 K. The kink points in the combined cycle thermal efficiency and specific power output are caused by the change in bottoming cycle behaviour. For pressure ratios lower than 21-22 the gas turbine exit temperature is large enough to achieve the maximum steam turbine temperature, established at 540°C, with a temperature difference between gas turbine and steam turbine of 40°C. When the pressure ratio increases above 22 the exit temperature is not able to heat the steam up to the maximum temperature and starts to decrease.

Figures 5.21 to 5.23 show the changes of upgrading the cooling system from convection, impingement and slot to advanced full coverage film cooling. As in the previous case there is a kink point in the combined cycle thermal efficiency and specific power output, and the explanation is also the same. The performance improvements are of the same order that the ones achieved with the 100 K increase in metal temperature, with very significant gains in efficiency and power output for both, simple and combined cycles.

Figures 5.24 to 5.26 give the effect of increasing the TET in 100 K, with no variation in the allowable metal temperature of cooling method. The improvement in performance is now lower, especially for the simple cycle thermal efficiency, due to the increase in cooling flow, that offsets the gains caused by the 100 K rise in TET. The larger exit temperature has a considerable effect over the bottoming cycle. Hence, the combined cycle efficiency and, specially, the power output still have an important growth. The kink point in combined cycle thermal efficiency and specific power output is present as well in these figures.

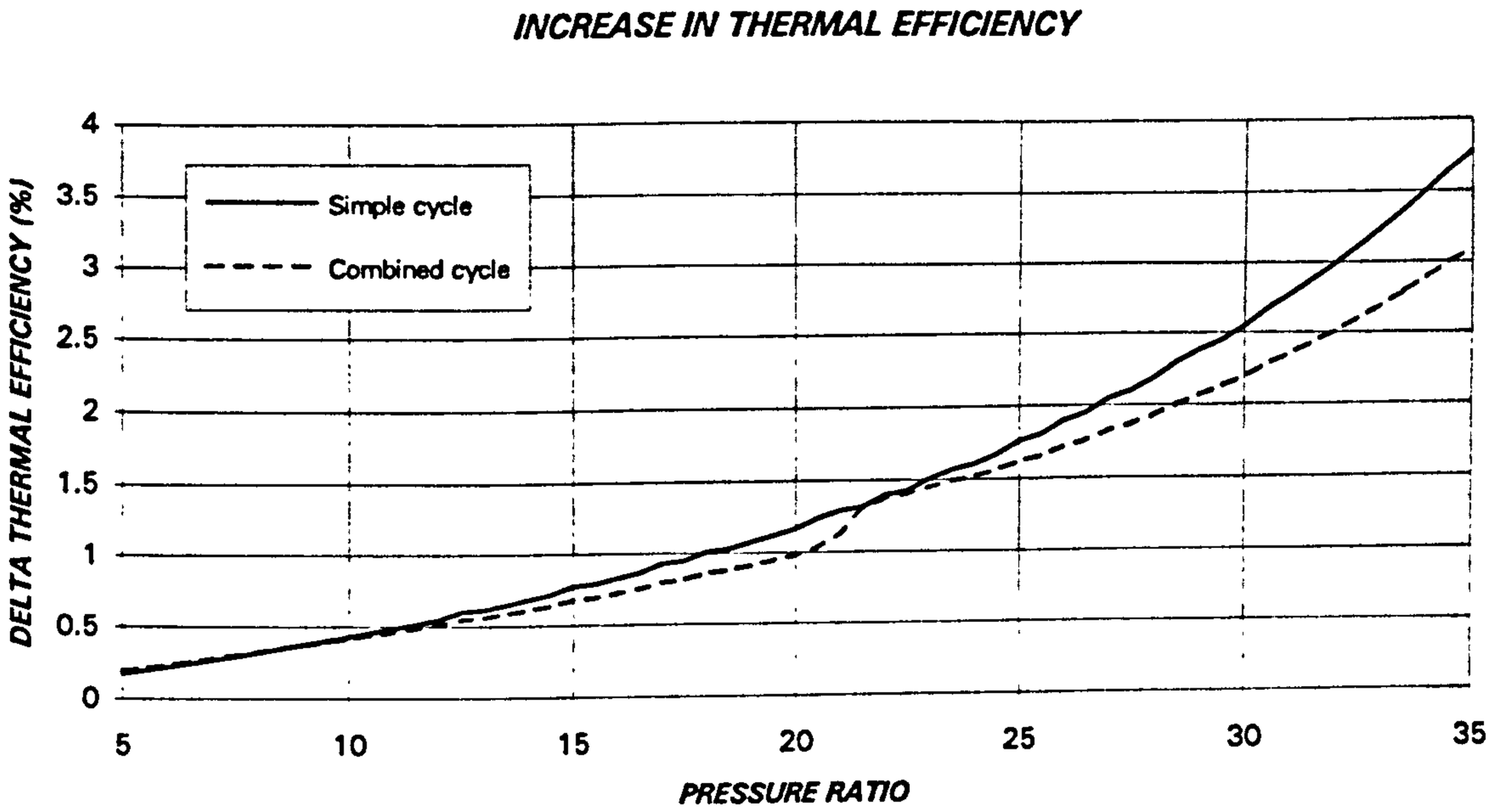

Figure 5.18. Increase in simple & combined cycle thermal efficiency for a 100 K increase in allowable metal temperature (%)

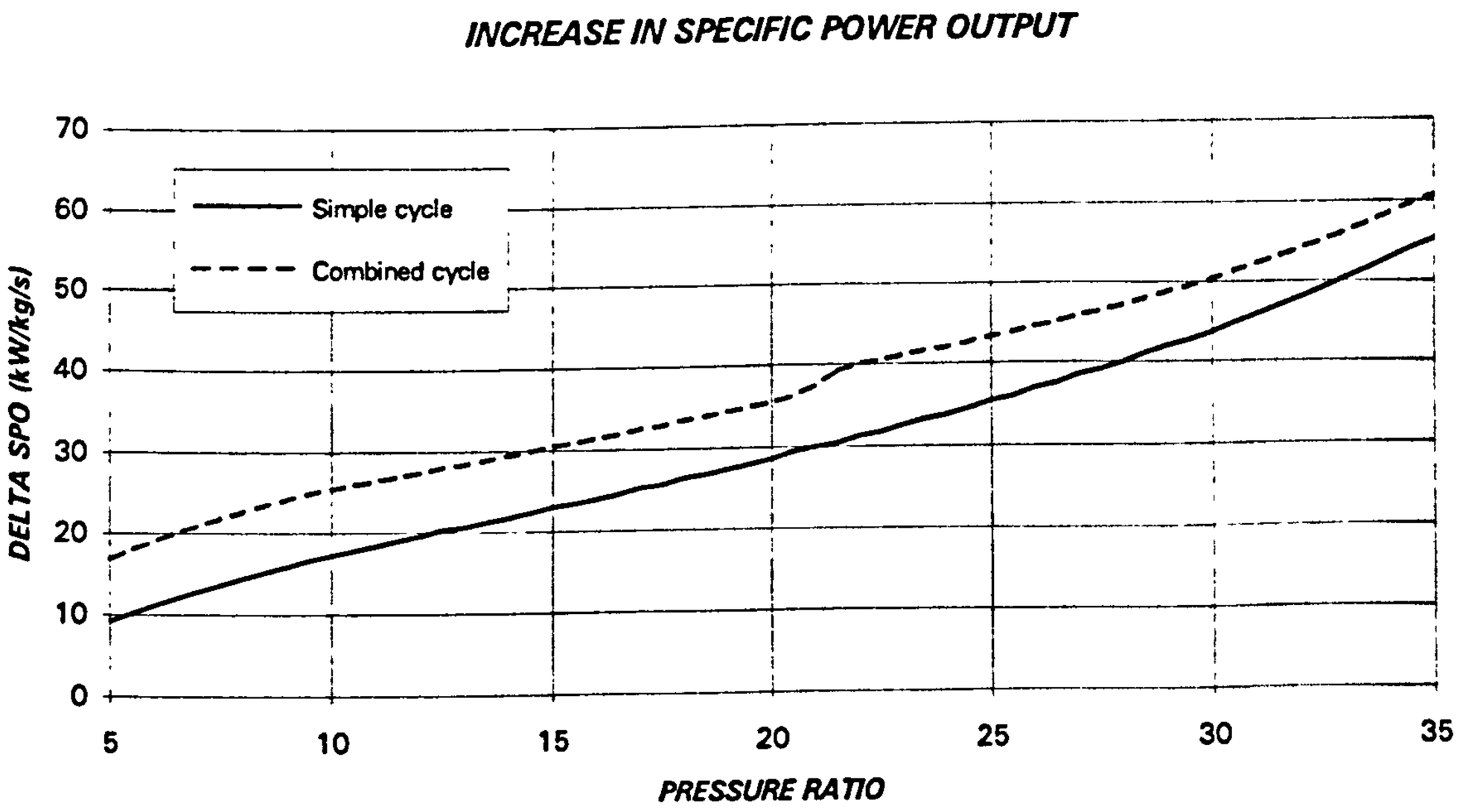

Figure 5.19. Increase in simple & combined cycle specific power output for a 100 K increase in allowable metal temperature (kW/kg/s)

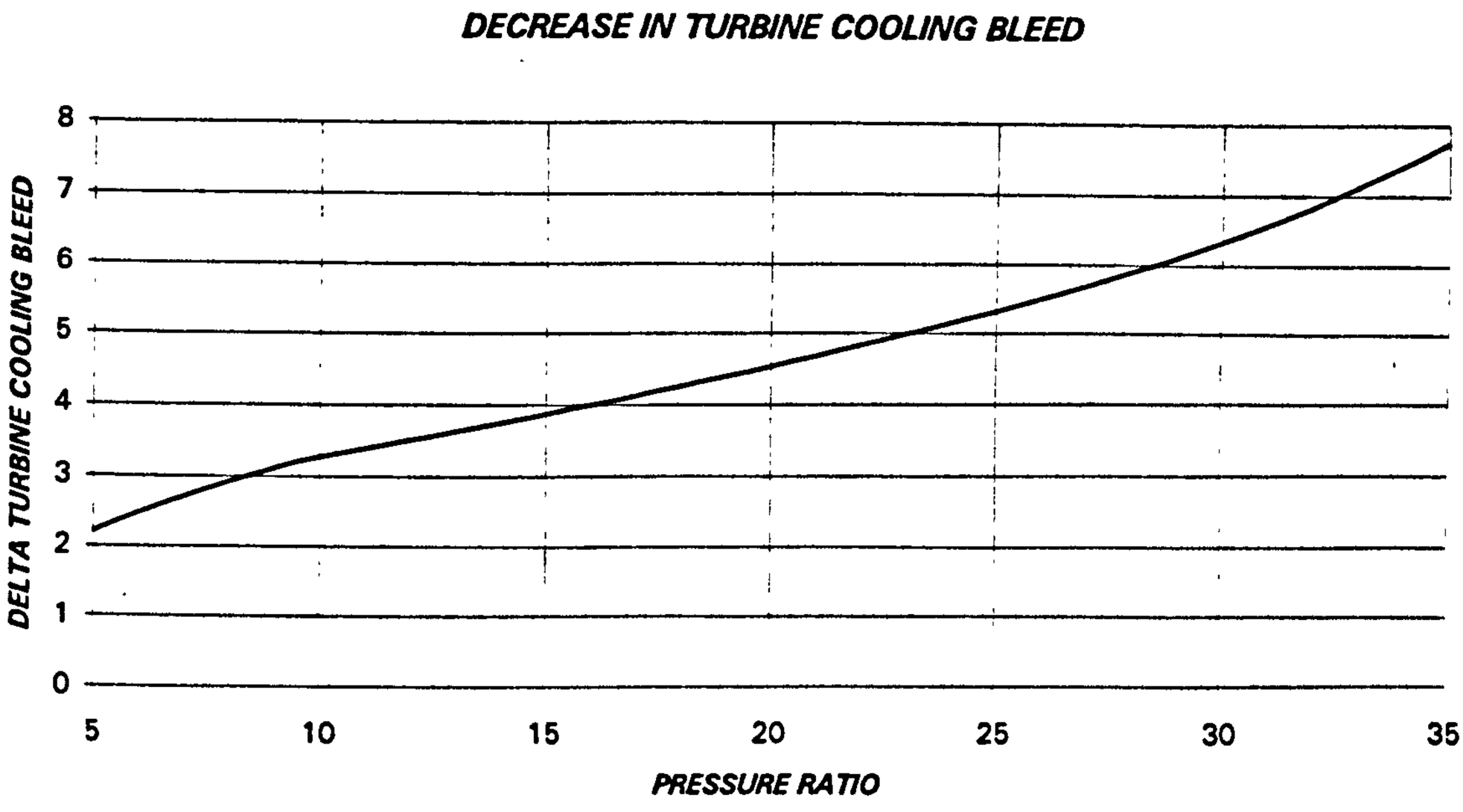

Figure 5.20. Decrease in gas turbine cooling flow for a 100 K increase in allowable metal temperature (% of core flow)

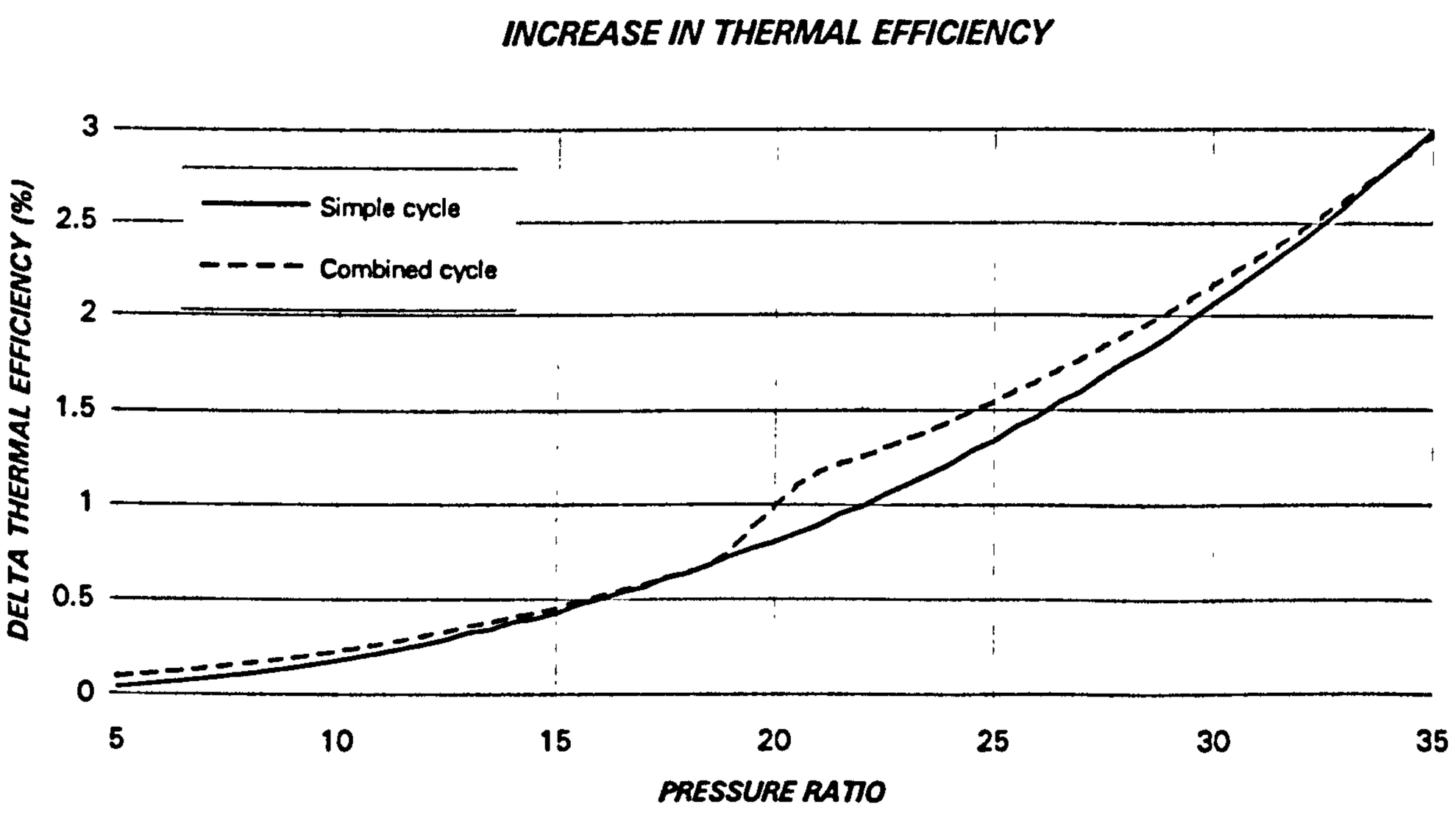

Figure 5.21. Increase in simple & combined cycle thermal efficiency for the upgrade in cooling flow method (%)

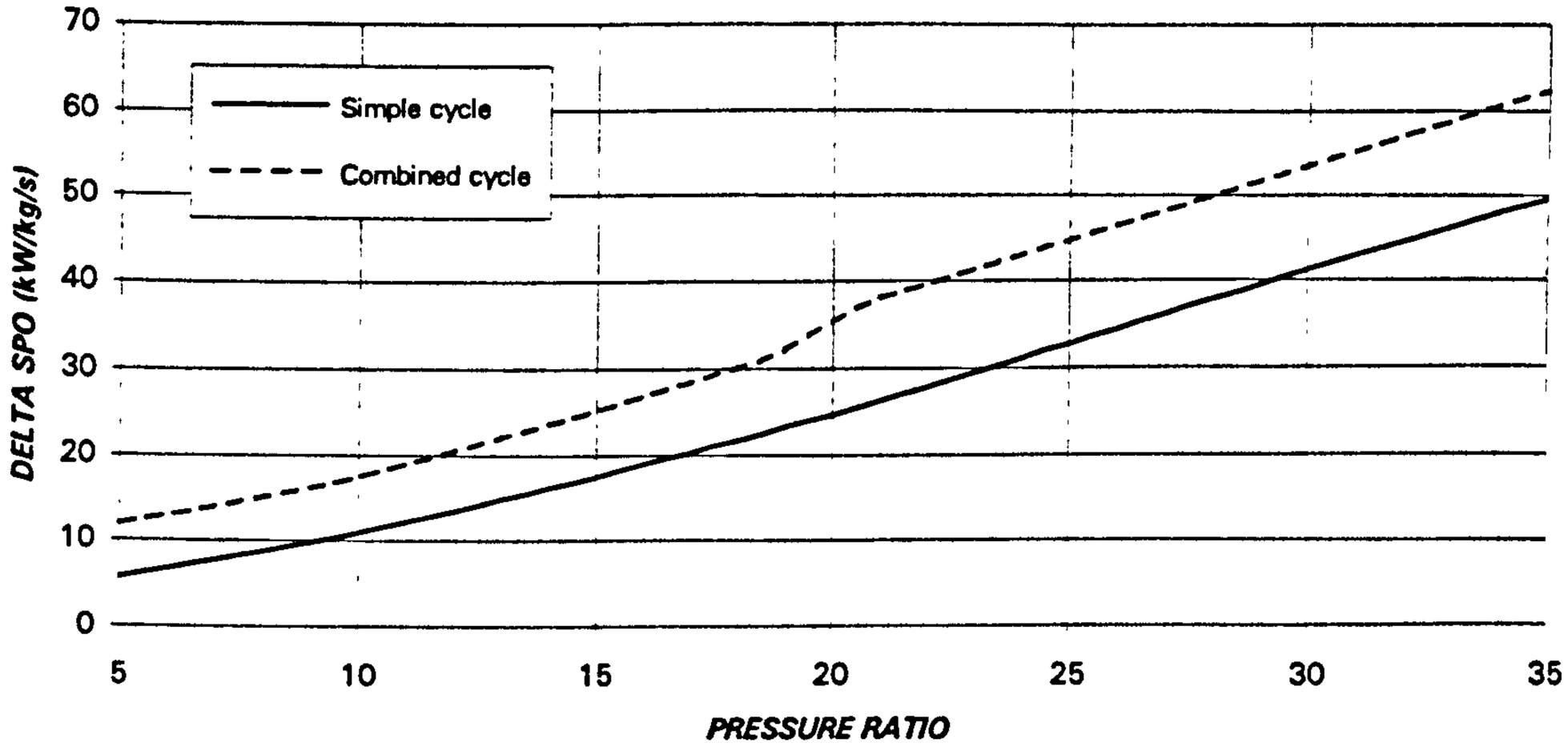

Figure 5.22. Increase in simple & combined cycle specific power output for the upgrade in cooling flow method (kW/kg/s)

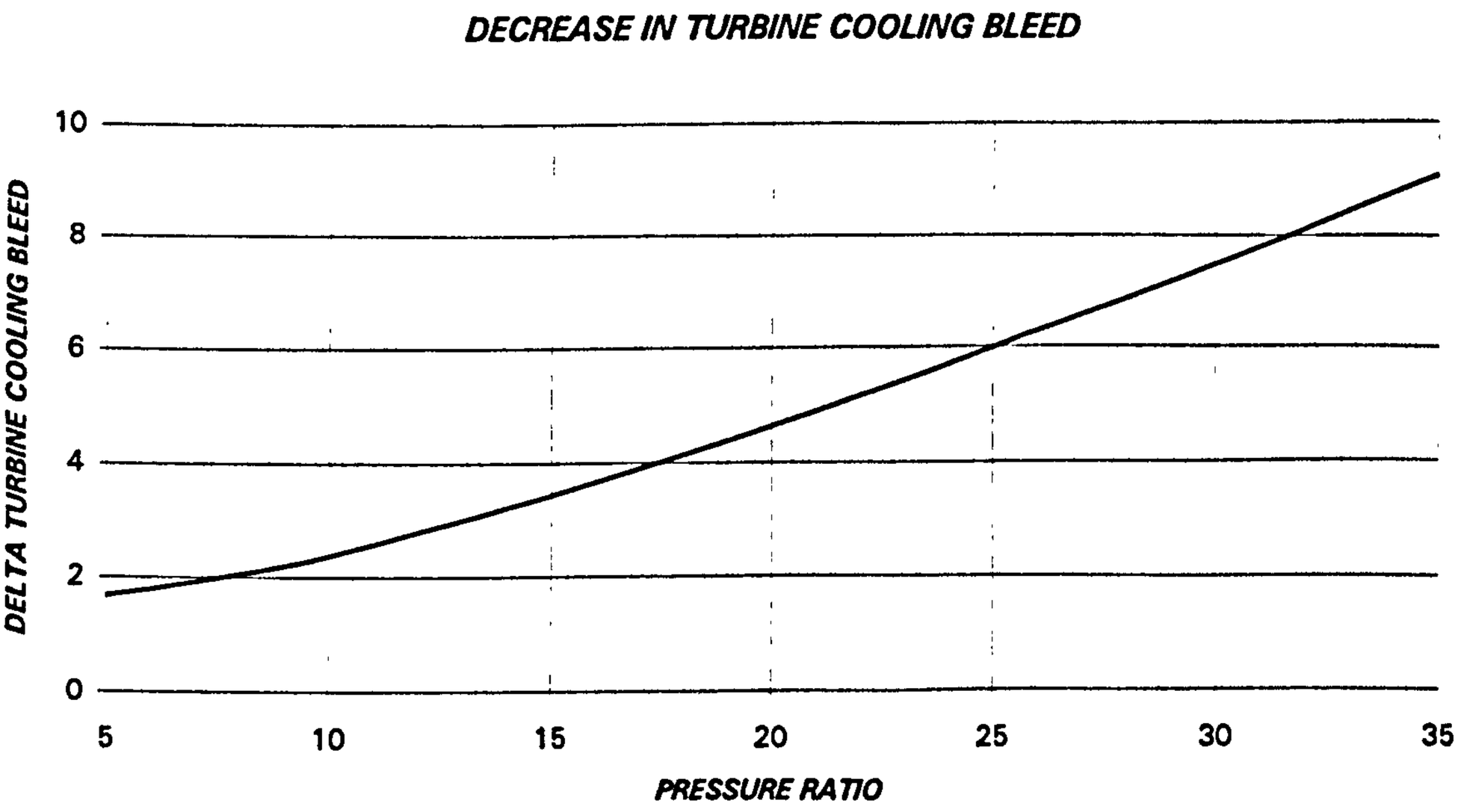

Figure 5.23. Decrease in gas turbine cooling flow for the upgrade in cooling flow method (% of core flow)

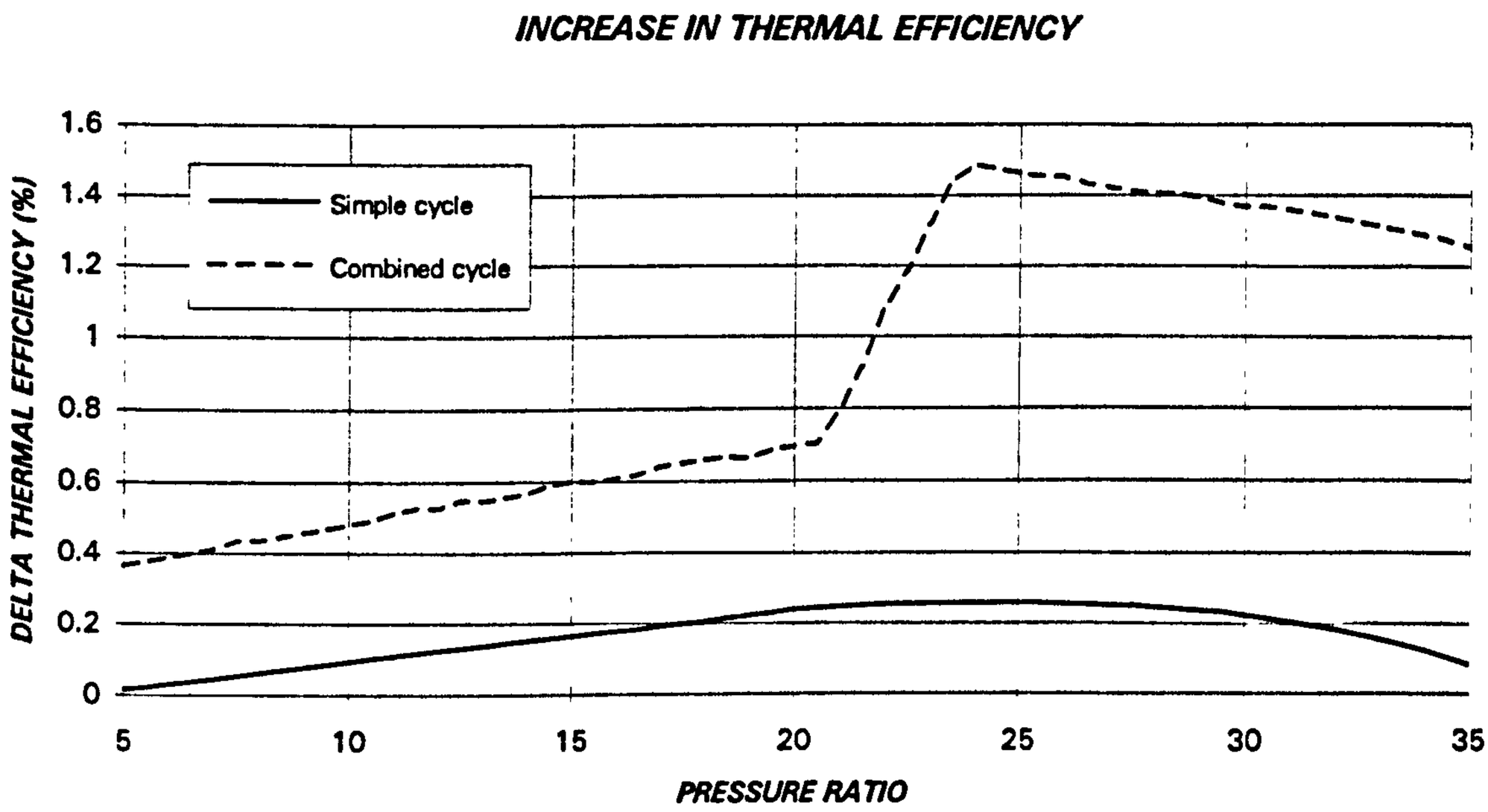

Figure 5.24. Increase in simple & combined cycle thermal efficiency for a 100 K increase in turbine entry temperature (%)

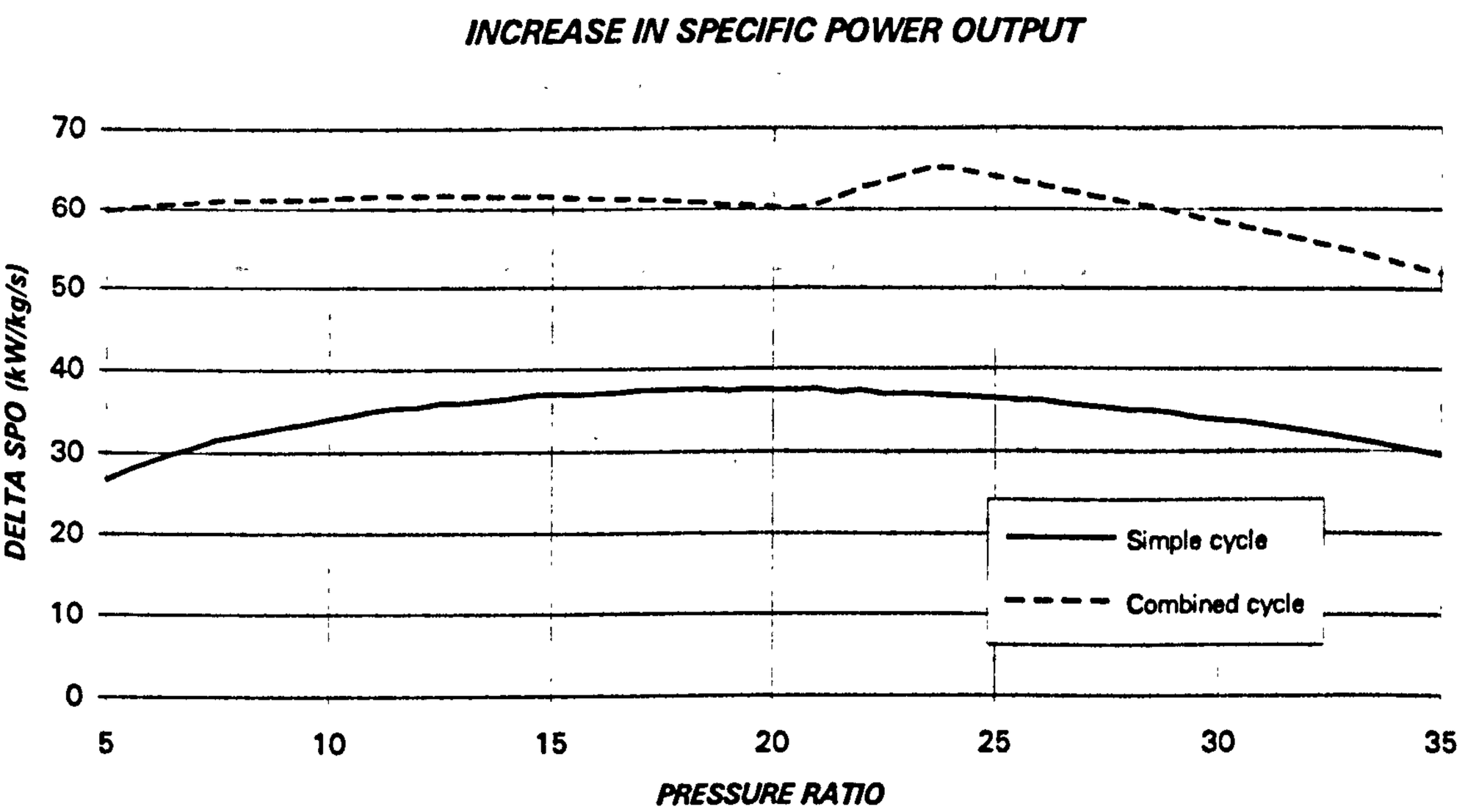

Figure 5.25. Increase in simple & combined cycle specific power output for a 100 K increase in turbine entry temperature (kW/kg/s)

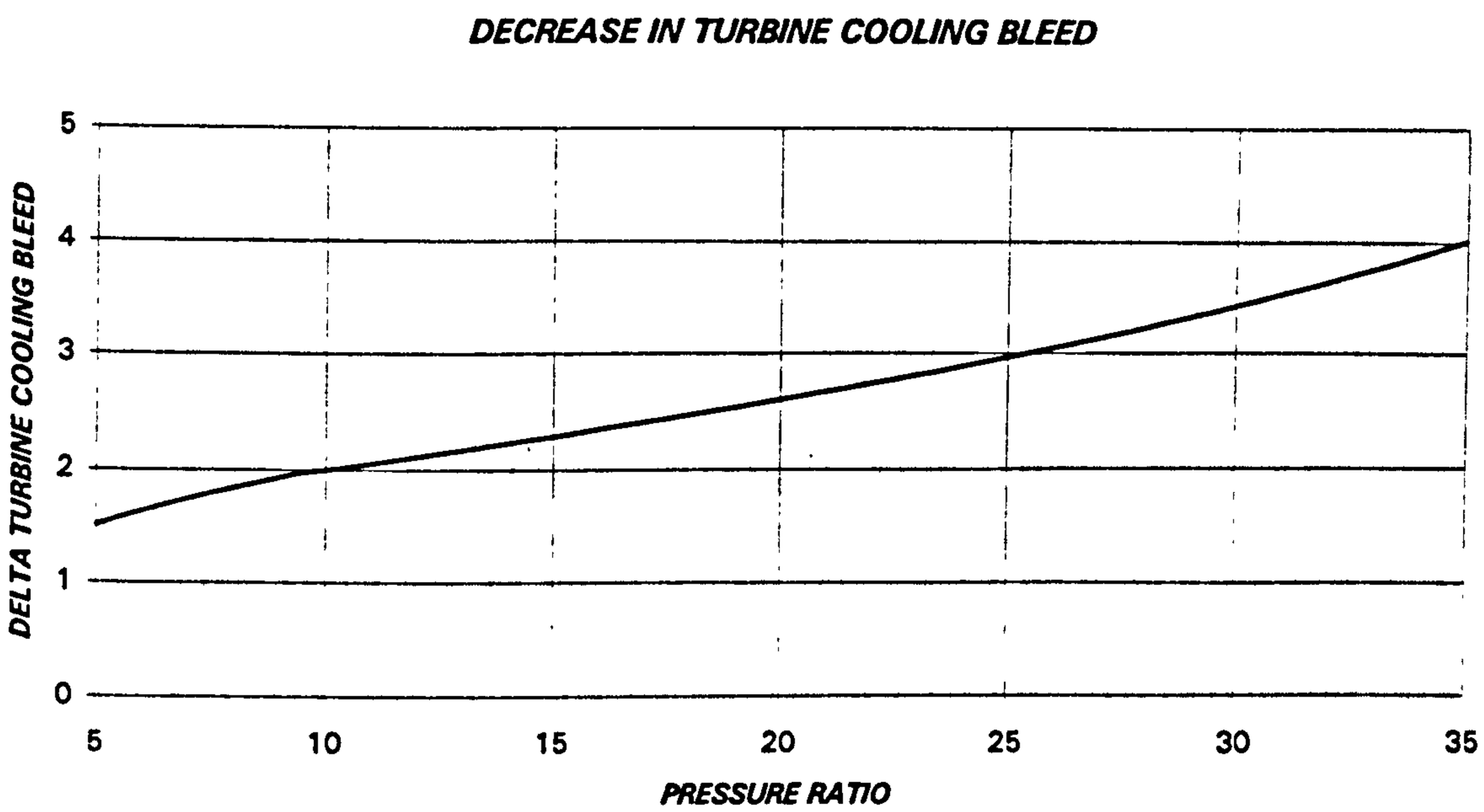

Figure 5.26. Increase in gas turbine cooling flow for a 100 K increase in Turbine entry temperature (% of core flow)

5.7. ADVANCED COOLING METHODS

The benefit of reducing the cooling mass flow has been demonstrated in this chapter. Hence, several methods should be considered in order to increase the performance of the gas turbine. Four solutions will be described here:

- Steam blade cooling, refs. [33], [107] and [109].
- Reduction in the cooling mass flow temperature using a heat exchanger with the steam turbine water as coolant.
- Reduction in the cooling mass flow temperature using a gas turbine precooling with the nitrogen coming from the oxygen separation (for semi-closed cycles).
- Use of the nitrogen coming from the oxygen separation for internal blade cooling (for semi-closed cycles).

5.7.1. STEAM BLADE COOLING

The possibility of using steam for blade cooling is not new. Thermal stress problems together with corrosion problems, have postponed its implementation in production units. However, the improved knowledge of blade cooling technology, temperature transients, thermal stresses, etc., have made this idea feasible. Some GE

production models already have steam vane/blade cooling and, in the near future, it is expected than many advanced gas turbines will have this system.

There are two very interesting arrangements of steam blade cooling: the first one consists on using it as multipassages internal cooling only, while in the second the steam is injected in the gas turbine after the internal cooling. In both cases the heat rejected by the blades is recovered by the complete cycle, either in the gas turbine or in the steam turbine.

For simulation purposes, internal blade cooling requires the integration of the performance of both machines, not just by the HRSG, but by the calculation of the steam mass flow required and heat rejected by the blades. The amount of steam will not be negligible. Although the steam specific heat is considerably larger than that for air, and only the NGVs will be steam cooled, two figures must be born in mind for advanced gas turbines: the typical ratio of steam to air inlet mass flow in a combined cycle is of the order of 0.15-0.20 and the ratio of total cooling (NGVs & rotors) to air inlet mass flow is also of the order of 0.15-0.20. The increase in steam temperature will act as a reheater for the bottoming cycle (if the steam is not mixed with the mainstream).

In the case of mixing the steam and the main stream, the gas turbine will behave as a steam injection machine, and the mass flows, pressures and temperatures must be determined at each station in order to accommodate the excess mass flow coming from the NGVs cooling.

Due to the inherent complexity of these methods and the potential reduction in reliability & availability of the power plant, implementation should be carefully assessed. Probably, its use in the HPT is well justified by the performance improvement, but in the LPT, where the temperatures can be considerably lower, a new cooling system is less beneficial.

5.7.2. REDUCTION IN COOLING MASS FLOW TEMPERATURE

The temperature of the mass flow used for blade cooling can decrease using several systems. For example, the Russian aeroengine Saturn Lyulka AL31-F employs a heat exchanger, where the hot side is the cooling air and the cold side is the bypass air. This system allows the engine to reduce the cooling mass flow by 40%.

In the case of the industrial gas turbines fitted with steam turbines, the cold water could be used to reduce drastically the temperature of the cooling air. Hence the mass flow requirement will decrease and the heat rejected will revert into the steam cycle, minimising the first law losses.

This system can be easily applied to part of the HPT and LPT cooling air, bled from the compressor and directed to the turbine shroud through external pipes, and not to the cooling flow that goes through the internal system and cools the discs and turbine hub.

5.7.3. ADDITIONAL COOLING SYSTEMS FOR SEMI-CLOSED CYCLES

The semi-closed cycle has several characteristics that can be employed to increase its low thermal efficiency. The low calorific value fuel is burnt with pure oxygen (or a mixture of 95% oxygen and 5% argon) coming from the air separation process, that requires around 0.86 MW/kg O_2. This takes place at a temperature below the critical temperature of the gas (154.4 K for the oxygen, 133 K for the air and 126.2 K for the nitrogen). The remaining mass flow of nitrogen, almost four times larger than the oxygen, can be employed to cool the compressor inlet flow. Also, due to the special characteristics of this plant, the total oxygen required is around 50% larger than the one employed in the gas turbine.[9] Nitrogen to engine inlet mass flow ratios of the order of 10 to 30%, depending on the pressure ratio and TET, may apply.

After the conventional precooler the carbon dioxide/argon is at 300 K approximately. However, a further reduction is possible using an additional cryogenic precooler. A preliminary study will show that a decrease of 50-110 K, depending on the nitrogen mass flow available, is feasible using the state-of-the-art technology.[10]

The nitrogen employed in the heat exchanger can be used afterwards to cool the turbine stators. The application of this system, together with the cryogenic precooler will improve efficiency and power output. In addition, the blade cooling detrimental effect on cycle thermal efficiency is larger in the semi-closed cycles, where the higher carbon dioxide temperatures in the LPT require considerable cooling flows. Hence, its use in both, HPT and LPT, will be justified by the performance benefit.

Appendices I and II show the variation in thermal efficiency, power output, etc. for two simple semi-closed cycle gas turbines, with SOT=1200°C and 1377°C respectively. Differences between the cryogenic precooling and the standard cycles (pp. I.i to I.iii and II.i to II.iii), between the cryogenic precooling with NGV internal cooling and the standard cycles (pp. I.iv to I.vi and II.iv to II.vi) and between the cryogenic precooling with NGV internal cooling and the cryogenic precooling cycles (pp. I.vii to I.ix and II.vii to II.ix) are presented.

---

[9] The generation of low calorific value gas fuel is the responsible for this additional requirement of oxygen.

[10] There is no phase change in the carbon dioxide, entering and leaving the heat exchanger in gas phase. If the cryogenic nitrogen is to be employed, a more sophisticated system should be used, as it will enter the precooler in liquid phase and leave in gaseous form.

CHAPTER 6

VALIDATION PROCESS OF GTSI PERFORMANCE CODE

6.1. INTRODUCTION

The importance of performance codes for project decisions has been outlined in different chapters of this thesis. These programmes must inspire a great degree of confidence. This is possible after a complete validation process, where discrepancies between different codes and between test results and code predictions are examined.

Very limited engine test results were available to the author at the present time. Therefore, despite the interest of carrying out such activity, this task has not been completely performed. Nevertheless the code has been checked against the results given by other performance codes and some engine results.

When compared with other codes the differences have been negligible, provided the engine model was the same.

When compared with engine performance data, it was very frequent to make assumptions, as only in a very few situations the complete engine model was available.[1] Control of the machine, real component maps, detailed interstage cooling data, thermodynamic modeling, fuel composition, exact component performance and corrections, etc. must be, sometimes, guessed.

To overcome one of the most common problems, the lack of turbomachinery maps, a suite of characteristics is available inside the code:[2]

- Compressor with a high pressure ratio per stage
- Compressor with a moderate pressure ratio per stage
- Single stage turbine with high pressure ratio per stage
- Multi stage turbine with moderate pressure ratio per stage

These ones will be scaled adequately to match the required design point.

6.2. CYCLES SELECTED

To carry out a representative validation several engines were considered:

- Single spool - single shaft (both heavy duty and aeroderivative)
- Single spool - single shaft closed cycle regenerated gas turbine, operating with helium (only design point available)

---

[1] Strictly, only one of the cases used for the validation process was completely defined. However the deficiencies in some models were very small: fuel exact composition, shaft losses, etc. Assuming default values and matching other data these parameters were obtained.

[2] If available, additional compressor and turbine maps can be easily introduced in GTSI.

- Single spool - double shaft
- Double spool - triple shaft (only design point available)
- Double spool - double shaft with evaporative cooler and reheat (only design point available)
- Single spool - double shaft with steam injection (only design point available)

A detailed description of each case is done in the next sections.

As can be inferred from the engine listed above, detailed information from closed and semi-closed cycle gas turbines is either not available or incomplete. Therefore, open cycle data will be used for most of the validation process.

6.2.1. SINGLE SPOOL-SINGLE SHAFT GAS TURBINE

For the aeroderivative case (a machine producing over 20 MW at max. continuous power) component maps, design point pressure temperatures and mass flow at entry and exit of each module as well as the basic performance data for a complete running line were available. The control of the machine (including anti-surge bleed at low pressure ratios) and detailed description of the cooling flows was not obtained.

For the heavy duty (a machine generating over 100 MW at max. continuous power) the design point thermodynamic parameters and component efficiencies, together with a complete off-design running line, were the data used for the code validation.

The design point performance of both engines has a great degree of confidence. Therefore, the generation of models which give a good matching at that condition were the initial target, successfully fulfill.

The results obtained for the running line of the heavy duty machine were excellent, with relative differences below 0.5%, while those for the aeroderivative gas turbine were not so good, with important discrepancies at part power conditions. These are presented in figures 6.1 to 6.3.[3] The larger mass flow obtained in the simulation for power conditions lower than 60-70%, together with the lower exit temperature are, probably, due to the opening of anti-surge compressor interstage valves.

---

[3] A non-dimensional presentation has been selected to preserve the confidentiality of the base-line data.

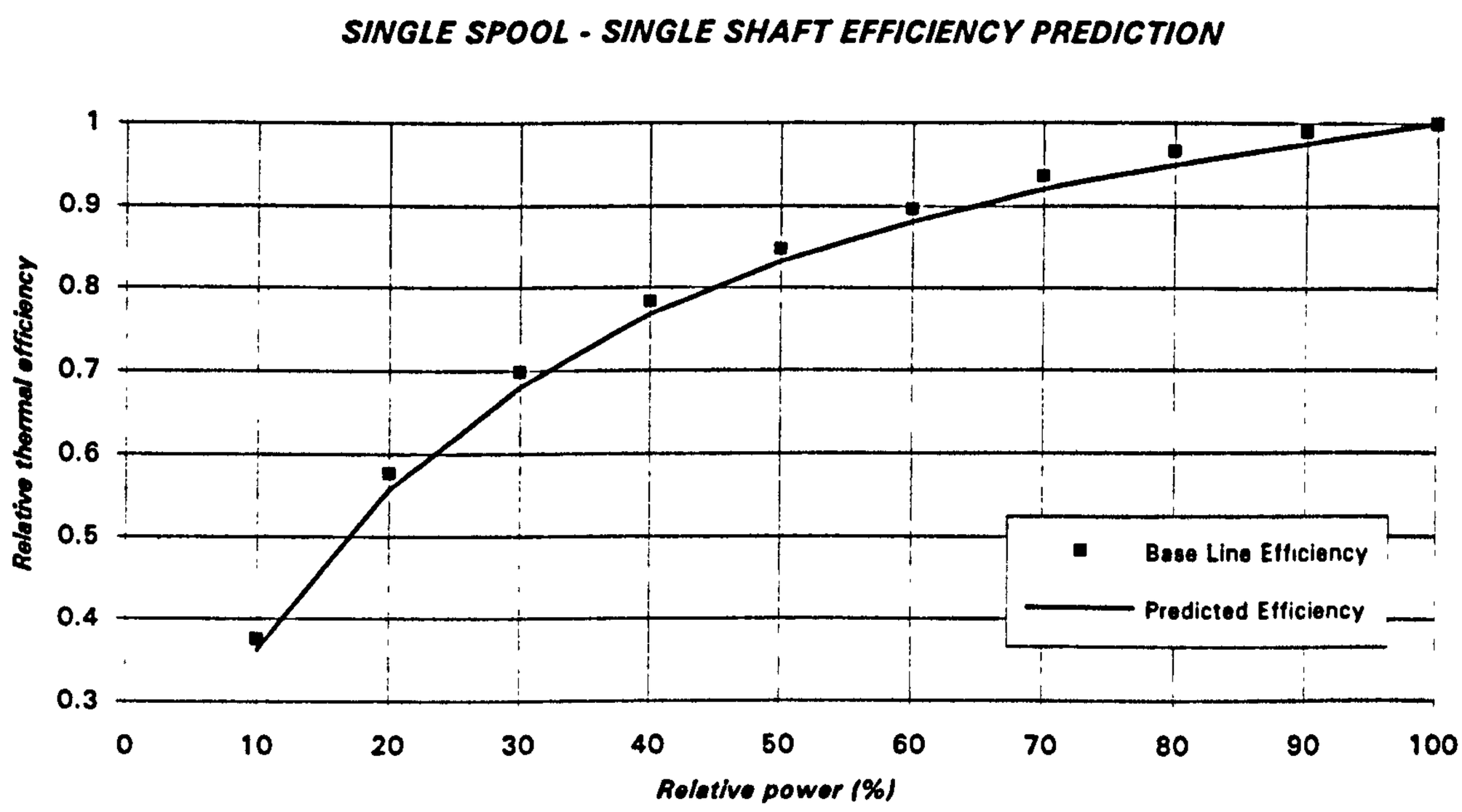

Figure 6.1. One spool - one shaft thermal efficiency prediction for a complete operating line

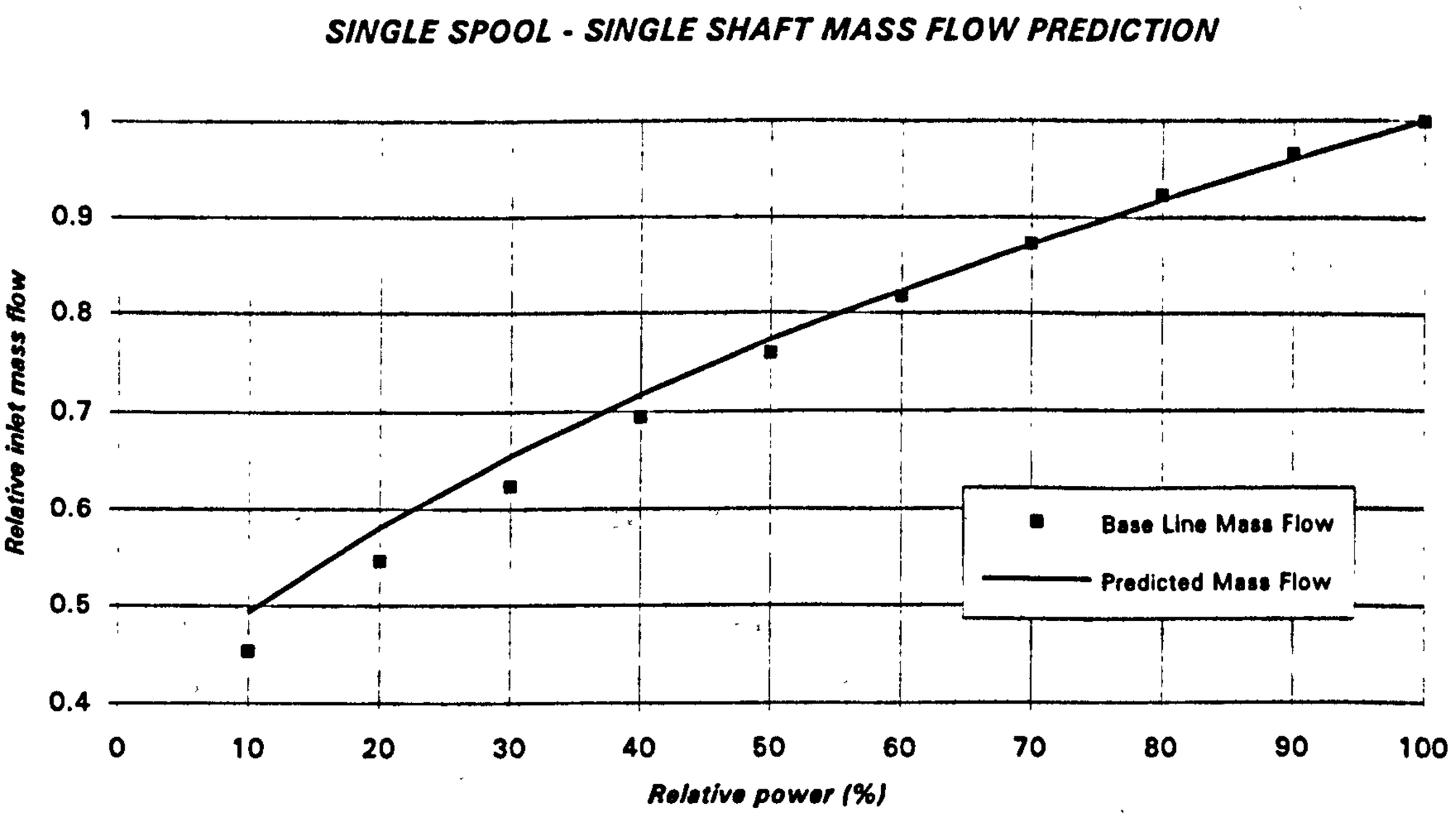

Figure 6.2. One spool - one shaft inlet mass flow prediction for a complete operating line

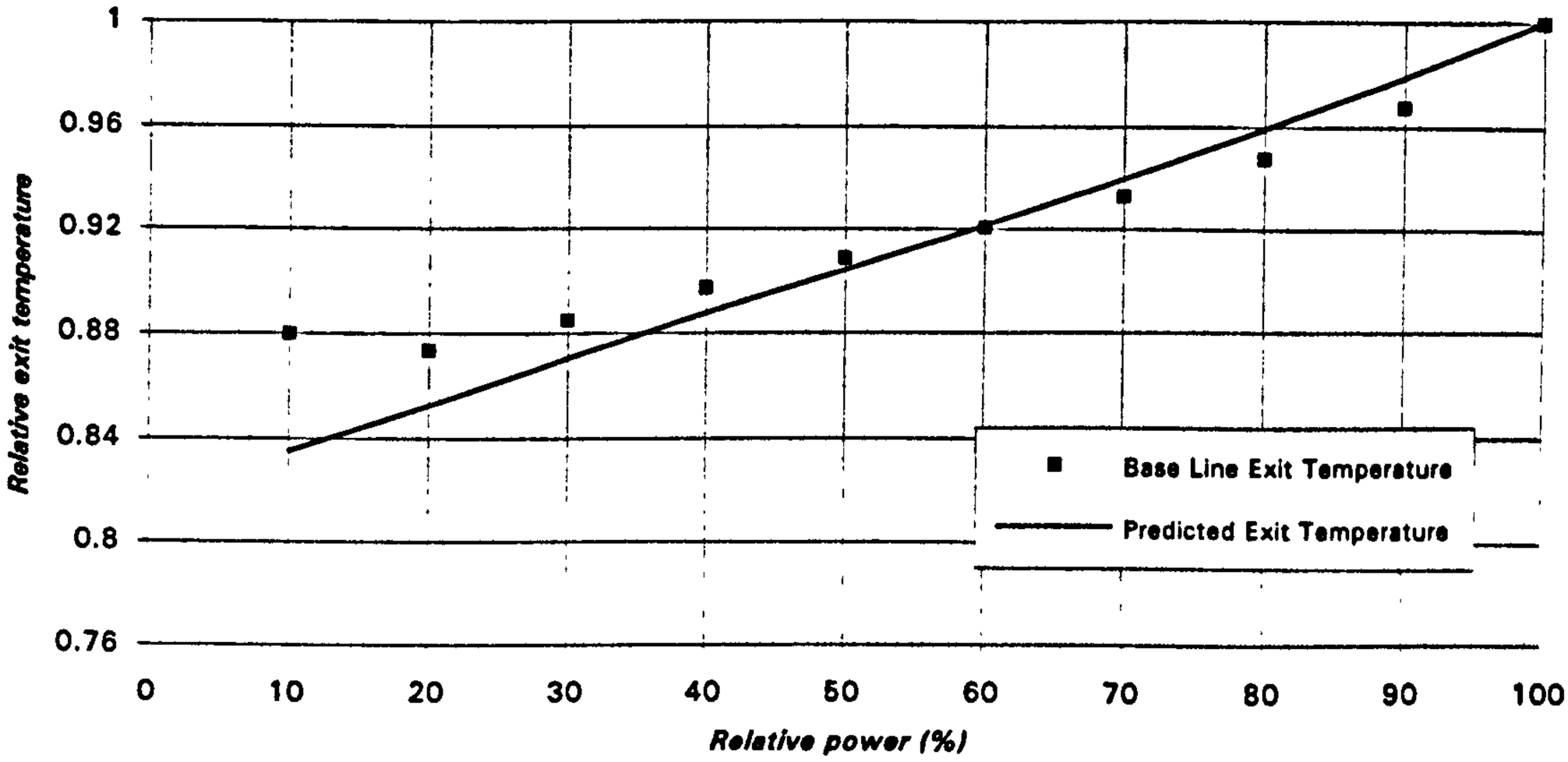

Figure 6.3. One spool - one shaft exit temperature prediction for a complete operating line

6.2.2. SINGLE SPOOL-SINGLE SHAFT CLOSED CYCLE REGENERATED GAS TURBINE

For the closed cycle regenerated gas turbine operating with helium only the design point performance data have been obtained: inlet mass flow, pressure losses, turbomachinery efficiencies and regenerator effectiveness, pressures and temperatures at main component inlet and exit planes were available. Despite the absence of proper validation results, this cycle will be used to check the handling of a non-conventional working fluid. In the simulation, the errors obtained in pressures, temperatures, mass flows, thermal efficiency and power were well below 0.01%. The reason for such a good matching lies in the absence of cooling flows, the constant C_p and γ of the gas and the simple modeling of the heat addition.

6.2.3. SINGLE SPOOL-DOUBLE SHAFT GAS TURBINE

As in the single spool-single shaft arrangement case, the data available is good enough for a proper performance check. For an aeroderivative turbine producing less than 10 MW, component characteristics, detailed controlled laws as well as thermodynamic conditions at each engine station were provided. Complete cooling flow details were not available.

The results are shown in the figures 6.4 to 6.6, showing an excellent agreement between the data and the code predictions.

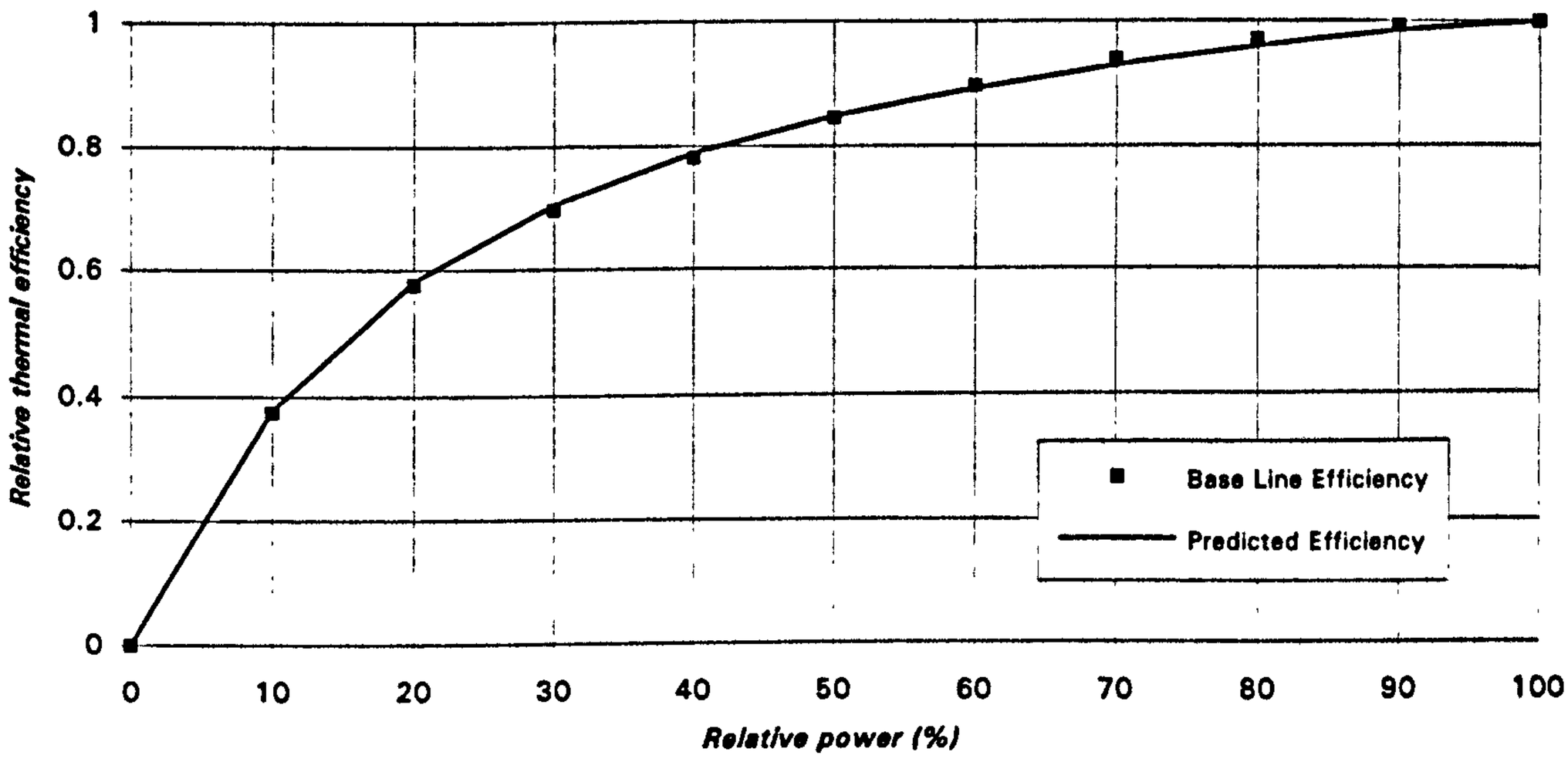

Figure 6.4. One spool - two shaft thermal efficiency prediction for a complete operating line

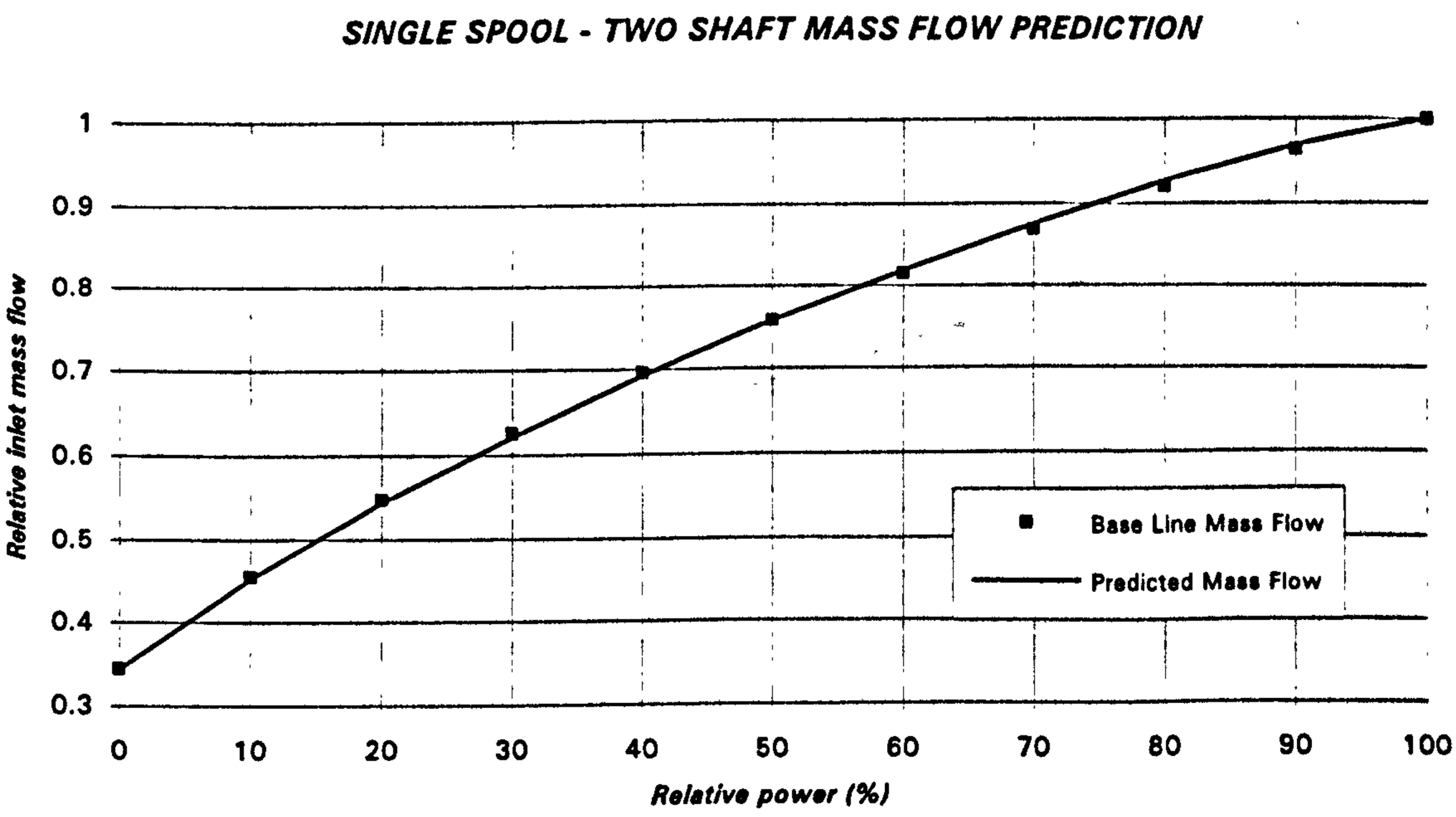

Figure 6.5. One spool - two shaft inlet mass flow prediction for a complete operating line

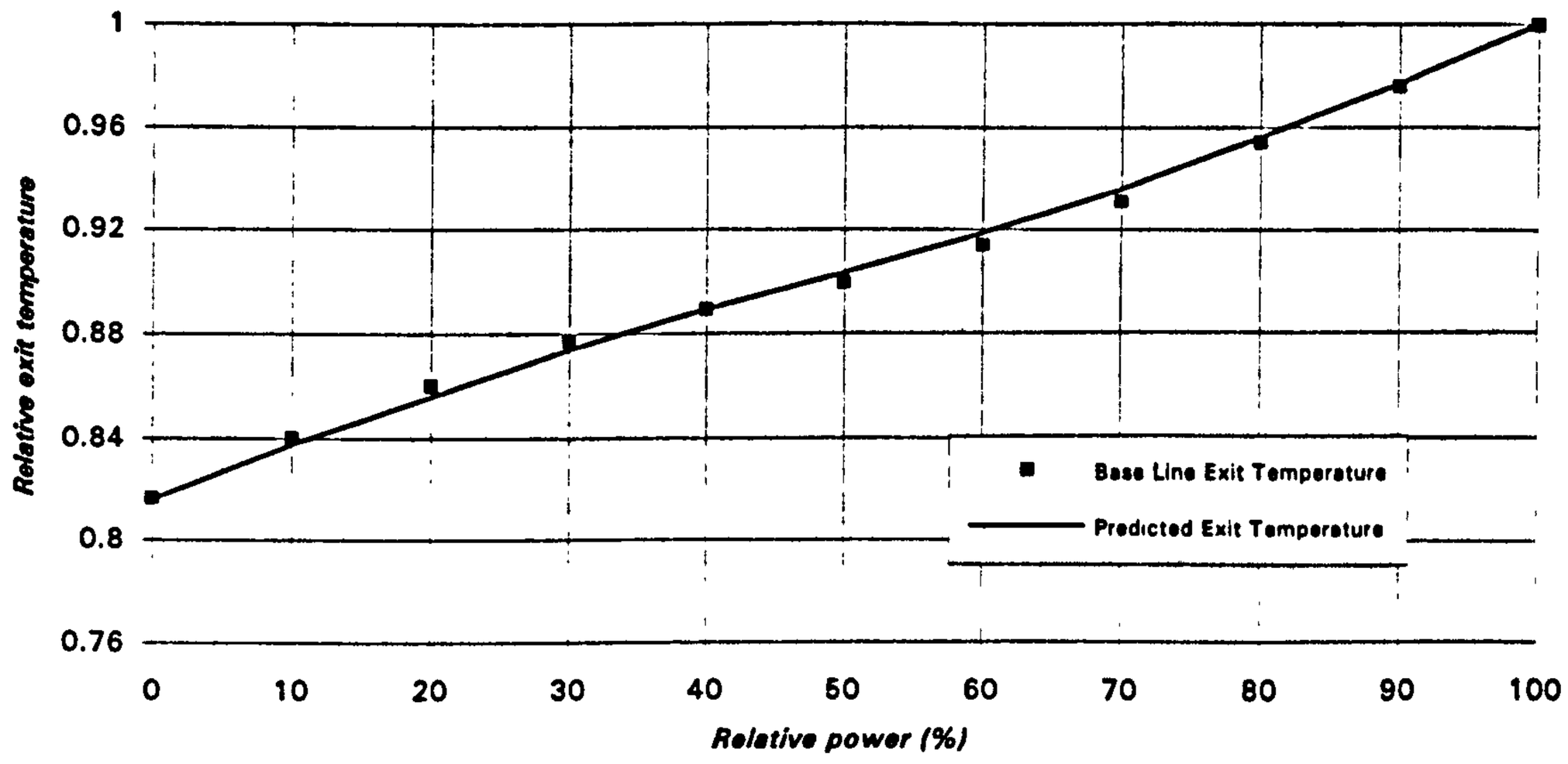

Figure 6.6. One spool - two shaft exit temperature prediction for a complete operating line

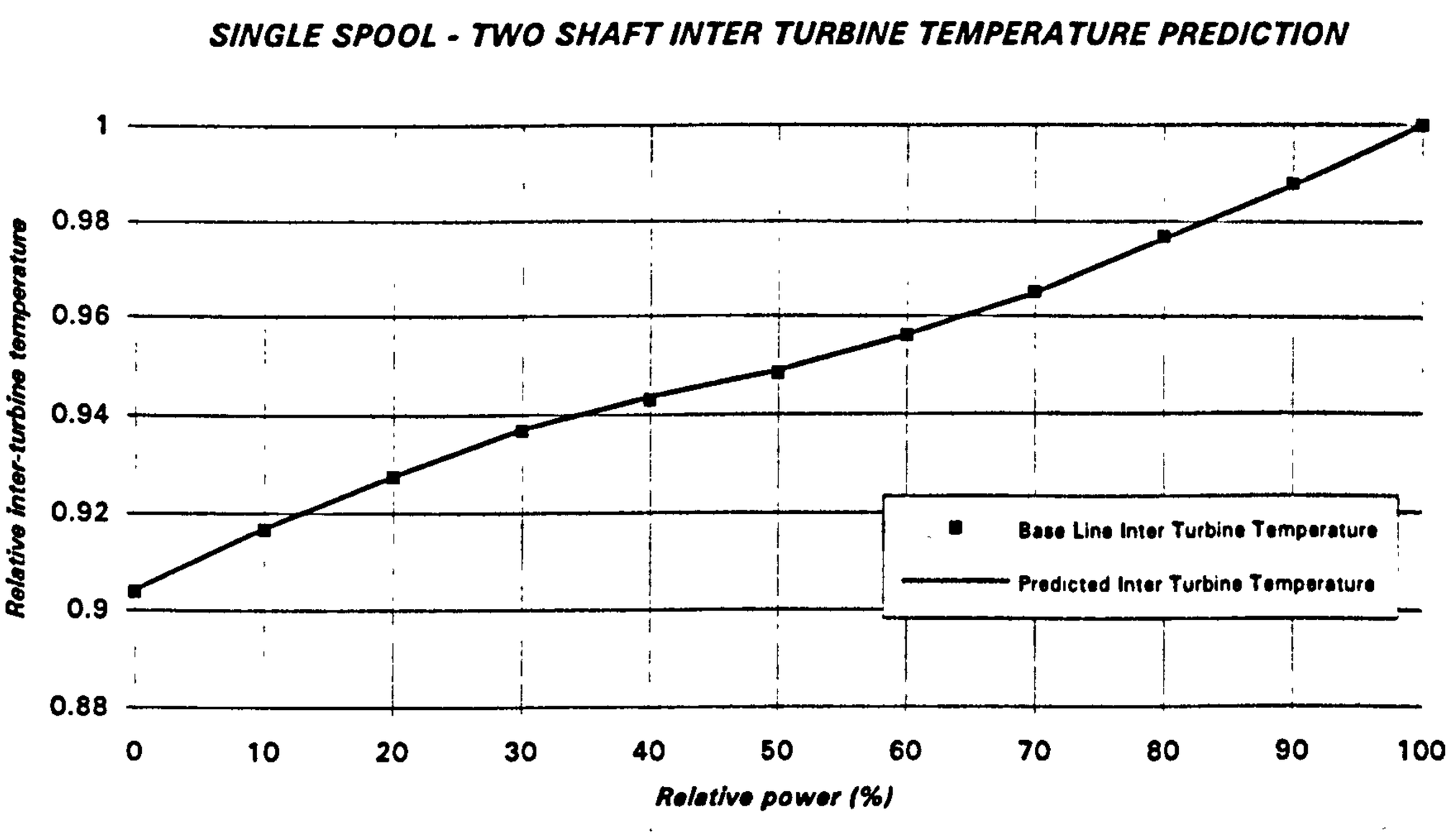

Figure 6.7. One spool - two shaft inter-turbine temperature prediction for a complete operating line

6.2.4. DOUBLE SPOOL-TRIPLE SHAFT GAS TURBINE

For this machine, an aeroderivative gas turbine producing over 20 MW at base load condition, only design point information was available (component efficiencies, fuel flow, power output and mass flow, pressure & temperature at different engine stations). The cooling scheme was given in great detail, with inter-turbine injection mass flows.

For the design point simulation, inlet mass flow, low and high compressor efficiency and pressure ratio, fuel flow, high and low pressure turbine efficiency and power output were used as data, while the free power turbine efficiency was modified to obtain the required power & exit pressure.

The results have been excellent, as shown in figure 6.8. The maximum discrepancy, lower than 0.1%, takes place in the high pressure turbine inlet temperature.

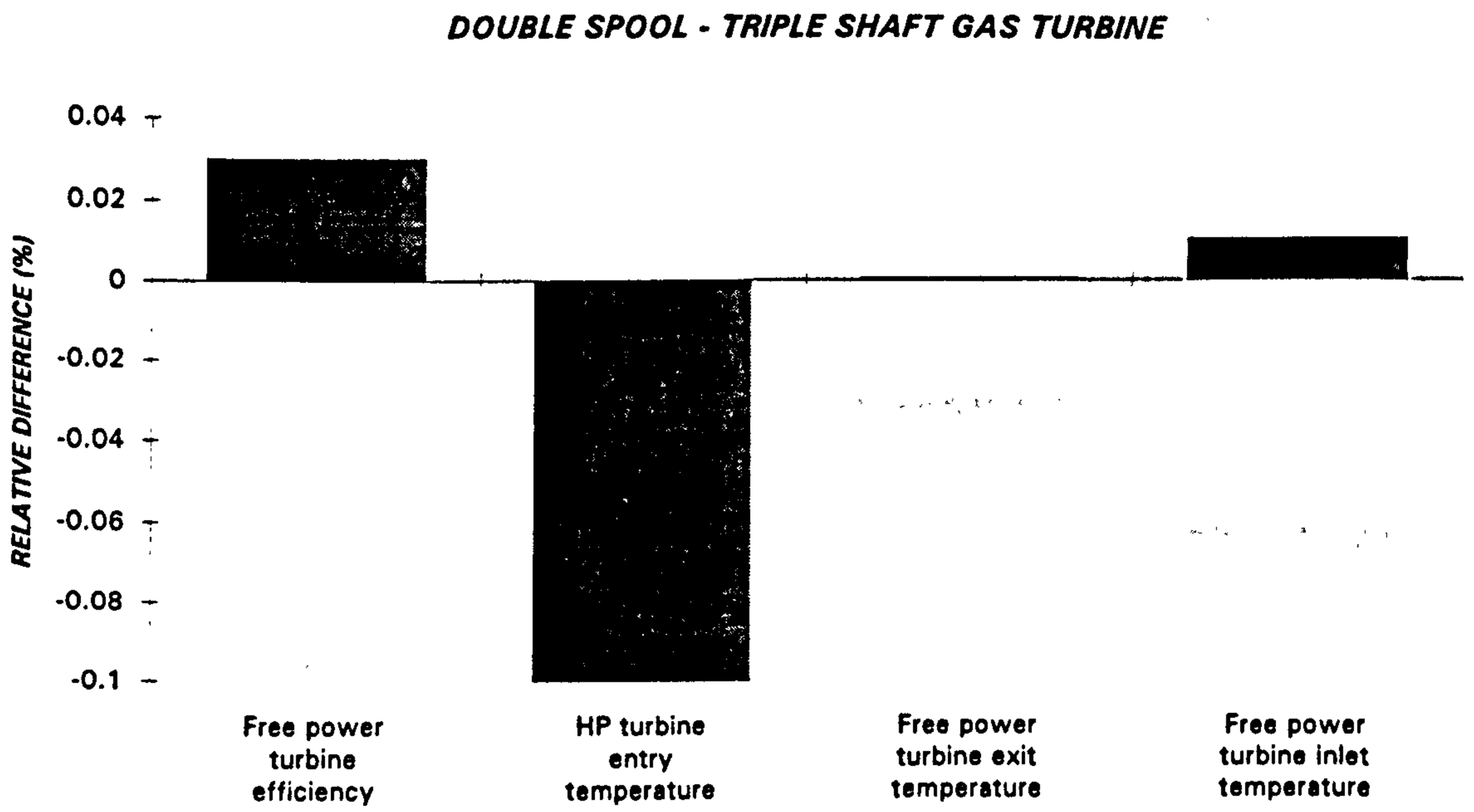

Figure 6.8. Two spool - three shaft gas turbine: design point discrepancies

6.2.5. DOUBLE SPOOL - DOUBLE SHAFT WITH EVAPORATIVE COOLER AND REHEAT

The data available for this engine was coming from different papers describing the design point of the Japanese AGTJ 100A & 100B [57], [90], [127]. The result of the simulation was excellent, with minor differences (of the order of 0.2%) in the hot

section of the gas turbine due, probably, to the different thermodynamic properties of the combustion products, because the fuel was not completely specified.

6.2.6. SINGLE SPOOL - DOUBLE SHAFT WITH STEAM INJECTION

For this steam injected gas turbine, rated at a baseline power under 20 MW, only design point performance data were available. Some of the cooling and steam injection details were unavailable. To overcome this problem, values from similar machines were used.

For the simulation, inlet mass flow, compressor efficiency and pressure ratio, fuel flow, high pressure turbine efficiency and power output were used as data, while the free power turbine efficiency was adjusted to obtain the required power & exit pressure.

The result shows important discrepancies in the turbine efficiency, free power turbine exit temperature and steam mass flow. The larger steam mass flow is consequence of the larger exit temperature & mass flow, resulting in a lower turbine efficiency to match the power output.

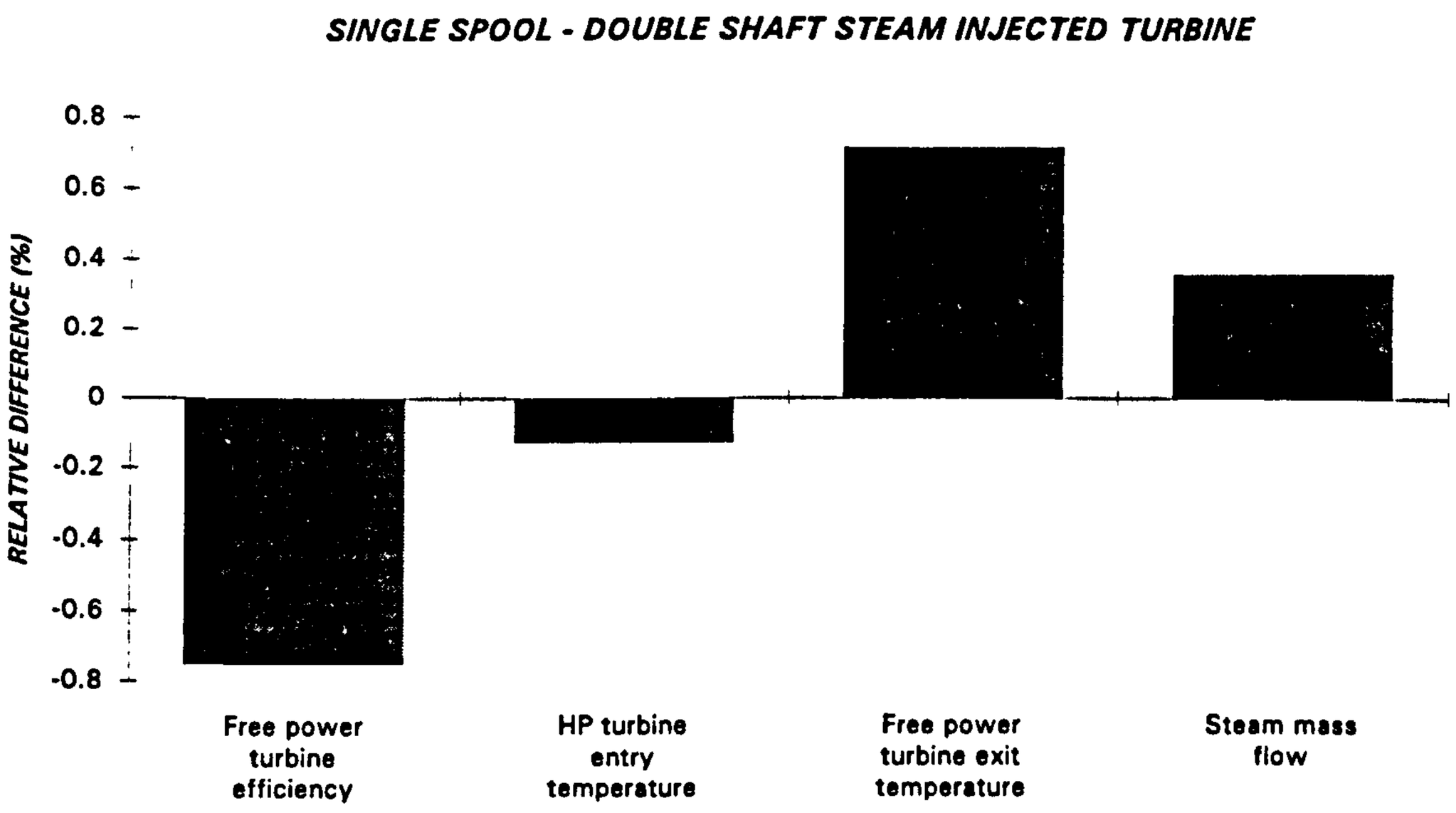

Figure 6.9. One spool - two shaft steam injected gas turbine: design point discrepancies

If the power was not the actual delivered by the free turbine (gross power), but the net power (without the auxiliaries), the matching is considerably better, with differences of the order of 0.1%.

CHAPTER 7

CARBON DIOXIDE/ARGON SEMI-CLOSED CYCLE SIMULATION

7.1. INTRODUCTION

The first stage of a new cycle design includes the following tasks:

- Identification of the preliminary power plant arrangement.
- Establish the working fluid (not necessary in the open cycles) and fuel, or heat source in general.
- Assumption of the efficiencies and losses of the components.
- Definition of the limits of different parameters such as temperatures, shaft speeds, surge margins, pressures, Mach numbers, etc.
- Identification of critical areas and situations (risk assessment).
- Conditions of the fluid at the entry and exit of each module.
- Definition of the operational envelope.

It is important to mention that these points are not in order of importance and, for example the use of a different working fluid can change the power plant arrangement completely, as well as the critical areas, etc. Also, some of the initial assumptions and/or calculations can change during the following phases of the design and development of the machine

When the cycle has been selected, after an optimisation process, and considering all the areas involved in the development of a new machine, not only the performance, an off-design analysis is carried out in order to prove that the final choice is reasonable for all operating conditions. This is very important in aero-engines, because they experience a wide range of inlet conditions and throttle settings. But also for industrial gas turbines, where large load variations are expected.

Transient analysis is also important in the industrial gas turbines, where starting and the time to achieve the full load condition of a peak/emergency machine can be crucial. The following situations are examples of the importance of the transients in the engine operation:

- When the surge margin of a compressor is controlled by the casing cooling air, a sudden change in temperature can increase tip clearance for a few seconds,[1] and surge can occur.
- If the engine acceleration from idle or part load up to full power creates an over shoot in the SOT of 15-20 K during a few seconds,[2] the life of the engine can be sensibly reduced.

---

[1] The different thermal behaviour of the casing, blades and discs is the responsible of the transient variation of the tip clearance. For this reason the cooling air is employed to control this mechanism.

- Overspeed protection during transients, as well as surge margin monitoring are critical.

During normal operation, when the transient from the starting and low speed idle to full power takes some minutes, to allow heat soakage,[3] gas and metal temperatures follow the same path and almost no transient thermal stresses are present. Under those circumstances, the transient simulation becomes less critical. Of course, shafts acceleration and deceleration limits should be specified, employing conservative schedules. Nevertheless, the transient response to sudden lad changes is interesting, in order to evaluate the stability in the frequency of the electricity generator. Also, as a limit case, the complete lost of load (when the shaft that carries the load breaks, or the electricity generator is suddenly disengaged) is of great interest to calculate the resulting overspeed, and study the possibilities to alleviate the burst condition. Hence, the transient study is not only interesting but, in some cases, essential.

Despite the discussions about the necessity of a detailed transient simulation, the off-design is always crucial. Some industrial machines will work at full power for over 8000 hours/year, while others will operate most of the time at part load. The operating conditions are also different depending on the period of the day, the season of the year or the geographic location.[4]

---

[2] Around 10-20 seconds is enough for the heat transfer mechanism to increase the metal temperature of a blade.

[3] In the case of a civil aeroengine, the typical minimum acceleration time from idle to 95% of the power at SL is of the order of 5 seconds, increasing to around 10 seconds at cruise altitude. For deceleration at SL the time will be around 3-4 seconds, increasing to 8 seconds at altitude. In a combat aircraft engine the typical periods of time will be 3-5 seconds for the SL acceleration from idle to the Max-Dry conditions, with 1-2 additional second to achieve Max-Reheat. The time at high altitude will be dependent on the Mach number (inlet total pressure) as well, and will be typically between 6-12 seconds to reach the Max-Dry condition, with 2-4 additional seconds to reach the Max-Reheat.

In a reheat industrial turbine, such as the AGTJ-100A/B or the Brown Boveri GT24/26, the time to achieve the Max-Reheat power will be slightly longer than in an aeroengine, where the reheat has no effect over the turbomachinery.

The moment of inertia of an aeroderivative gas turbine rotor (around 1-5 kg m^2 for a small machine and up to 50 kg m^2 for a large one) is of the order of 10 to 100 times smaller than the moment of inertia of a large heavy duty industrial machine. Hence, acceleration periods of the order of 10 to 100 times longer are expected.

[4] Taking, for example, the gas turbines employed in the gas pipelines in the desert, the change in temperature from day to night can be more than 40 K, with the consequent variation in off-design performance (28 K decrease in the inlet temperature of a modern aero-derivative gas turbine, such as the LM-6000, leads to an increase of 30% in power and 4.5% in thermal efficiency [72]).

The effect of changing the fuel, the possible introduction of steam injection for NO_x control, growth capability with minimum core changes, etc. should be determined before a new machine is launched, to be able to give the appropriate assessment for each specific case.

In the next sections some of these aspects, common for most of the projects, and others specific for the semi-closed cycle, will be discussed.

7.2. WORKING FLUID AND FUEL

The working fluid in the semi-closed cycle will be:

- Before combustion: Carbon dioxide or a mixture of carbon dioxide and argon. If an evaporator cooler or steam injection were used, water vapor would be also present.
- After combustion: Carbon dioxide and water vapor or a mixture of carbon dioxide, argon and water vapor, depending on the oxidizer employed.

The fuel composition has been given by other partners within the JOULE II project, and is given in the following table:

TABLE 7.1: COMPOSITION OF THE SEMI-CLOSED CYCLE FUEL

Gas	Mass fraction	Molar fraction
Carbon monoxide CO	71.40%	63.83%
Hydrogen H_2	1.62%	20.23%
Carbon dioxide CO_2	25.02%	14.23%
Methane CH_4	0.23%	0.36%
Sulphur S[5]	1.73%	1.34%
Chlorine	—	500 ppm

In closed cycles it is possible to select the working fluid considering different aspects. However, in a semi-closed cycle, the working fluid is imposed by the gas generated in the combustion process. If the oxidizer is pure oxygen, the products of a complete combustion will be carbon dioxide and water vapour, with a minimum content of sulphur dioxide. If argon is present in the oxidizer, being an inert gas, it will be also present in the combustion products.

This type of combustion constitutes a new area for the gas turbines, and will be treated in a deeper way in a following section dedicated to the critical areas.

---

[5] Some of the sulphur should be removed before injection in the combustor in order to avoid corrosion in the turbine caused by the sulfur compounds.

7.3. SEMI-CLOSED CYCLES SURVEY

Semi-closed cycles have not been seriously considered until this decade. The only reference the author has found (Harvey, Knoche and Richter, 1995, [54]) suggests a power plant where the fuel is pure methane, and the working fluid is a mixture of nitrogen, carbon dioxide and water. The cycle, shown in the next figure, proposes the reduction of combustion irreversibilities through off-gas recycling. Although the complexity involved in the design, development, control, normal operation and maintenance of a machine with three compressors, two intercoolers, one aftercooler, one combustion chamber, three turbines, two reheaters, one regenerator and two heat exchangers (one for the intercooler water and other one working as a precooler for the recycling gases) is scaring, the cycle itself is interesting to be considered for further research, with some simplifications that will not have a large detrimental effect on the efficiency.

The cycle consists on the following processes:

1-2: Combustion of part of the fuel with enough air to raise the temperature from 1186 K up to 1533 K.

2-3: Expansion from 20.6 bar down to 7.5 bar.

3-4: Reheat injecting additional air, rising the temperature up to 1533 K.

4-5: Expansion from 7.5 down to 2.7 bar.

5-6: Reheat injecting additional air, rising the temperature up to 1533 K.

6-7: Expansion from 2.7 down to 1 bar.

7-8: Recuperator: the cold gas temperature increased to 1186 K, and the hot stream temperature reduced from 1267 down to 539 K.

8-9: Gas-water heat exchanger.

9-10: Precooler, with 300 K as the final inlet temperature.

10-11: Compression from 1 up to 2.7 bar.

11-12: Evaporative intercooler.

12-13: Compression from 2.7 up to 7.5 bar.

13-14: Evaporative intercooler.

14-15: Compression from 7.5 up to 20.6 bar.

15-16: Evaporative aftercooler.

16-1: Cold side of the recuperator.

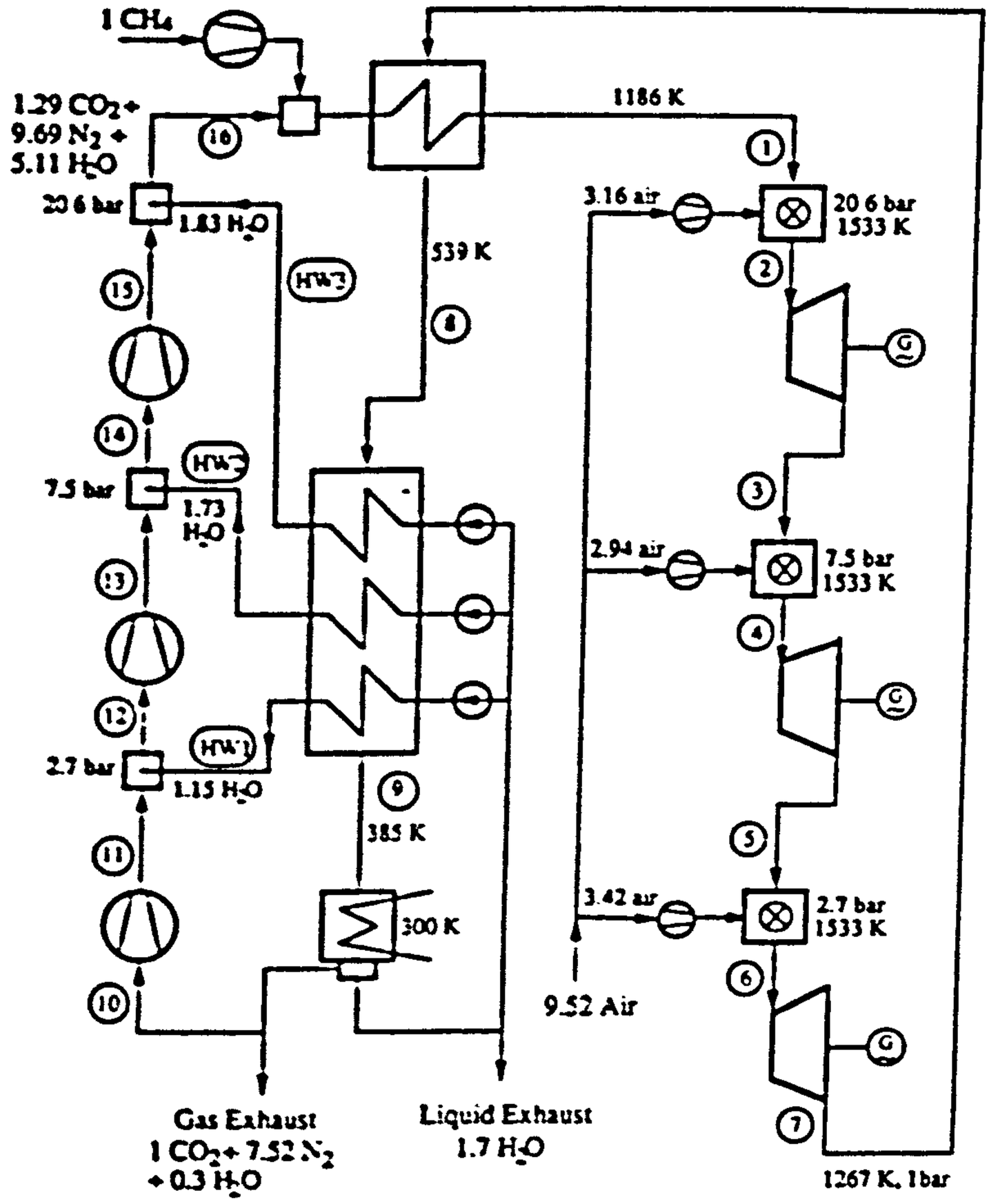

Figure 7.1. Semi closed cycle gas turbine with recycled exhaust gases

7.3.1. ASPECTS TO BE CONSIDERED IN THE HARVEY et al. CYCLE

The results obtained by Harvey et al. can not be accepted as representative of a real cycle, because the following losses have not been taken into account:

- Pressure losses in the intercooler-aftercooler (of the order of 1-2% each).
- Pressure losses in the recuperator (of the order of 2-4% at each side).
- Pressure losses in the combustor and reheaters (of the order of 3-5% each).
- Pressure losses in the gas-water heat exchanger (of the order of 2-4%).
- Pressure losses in the precooler (of the order of 1-2%).
- Exhaust NPR to drive the flow (of the order of 1-2%)
- Blade cooling problems. With all the turbines subjected to a very high temperature this will become a key issue. The solution of using ceramic technology, with potential temperatures up to 1675 K, is still unrealistic, specially for a land based continuous operation system, where the reliability is, in most cases, more

important than a small change in thermal efficiency. A fairly large amount of cooling should then be employed for the three turbines.

- Vitiation problems in the reheat system, specially at low pressure levels. The typical combustion efficiency value, 99.5-100%, is adequate for the conventional high pressure combustors. Reheat systems operating at high pressure after a lean combustor and burning far away from the stoichiometric mixtures will have efficiency figures of the same order.[6] In this case, where all the combustors are burning stoichiometrically from the oxygen point of view (all the fuel is injected before the first combustor and air is injected progressively), the problems will occur in both, combustion chamber and reheat systems. An efficiency drop between 1-5% is expected in each combustor, with the largest figures corresponding to the lowest pressure burners.

7.3.2. MAJOR TECHNOLOGICAL CHALLENGES

From the technology point of view, combustion, recuperator and control will be the major challenges.

- In all the current combustors the fuel is injected in an oxygen rich environment, and the liner walls are cooled with the excess gas. In this semi-closed cycle the gas that enters into the combustor and reheaters contains the fuel, and air is injected to burn it. In an area where a lot of research, both experimental and theoretical, has been carried out during the last decades to achieve optimum efficiency with the lowest emissions as possible, such a big change, that can modify most of the design concepts drastically, seems unreachable in a reasonable period of time. The large amount of radiation in the combustor could also be a problem, due to the important amount of triatomic molecules (water and carbon dioxide) present in the working fluid. The use of methane as fuel, with a large hydrogen to carbon weight, will attenuate this effect.

- The problem with the recuperator is the high temperature in both sides, with the additional difficulty of the high pressure in the cold side. In table 7.2, of the section 7.4.1., the maximum temperatures of closed cycle heat exchangers are given. The values for base load operating plants are below 1050 K, with prospect to reach 1150 K. In this semi-closed cycle, even the temperature of the cold side is higher than 1150 K, with the consequent technological requirements. It is important to bear in mind that the heat exchanger is one of the systems with lower

---

[6] This is the case of the ABB GT 24 and GT 26, where two annular combustor operate in serie, but far from stoichiometric and at high pressure, specially the first one (TET=1500 K, PR=30). The second combustor is located after a HPT stage expansion. At that engine station the pressure will be high enough, and there will be free oxygen for a further combustion process. The increase in temperature will no be very large. Therefore, the fuel to air ratio will not reach the stoichiometric value at the exit of the second combustor.

reliability/availability, which decreases when the gas temperature increases. Also, the large temperature variation in the recuperator, over 700 K in the hot side and even larger in the cold side, lead to a very complex device.

- The control of the plant is the third area of serious troubles. It is not clear to deduce from the scheme given if figure 7.1 the shaft arrangement of the plant. The one shaft configuration seems a little bit difficult, due to the high pressure of the machine.[7] In any case, the starting sequence should be carefully simulated, with the required synchronism between the main system fuel injection, the air pumping compressors, the water injection valves, etc.[8] The part load operation, the response to sudden changes in load, failures of one of the sub-systems, etc., will demand a complete study. Even if control laws are obtained for all the systems, reversionary models should be derived from experimental and/or theoretical calculations, to be able to answer quickly to a failure in the determination of one or more parameters involved in the engine control[9] or to a real failure in a component.[10]

An additional difficulty of every innovative gas turbine is the uncertainty in the failure rates of the new systems. For this configuration, where almost everything is new, the uncertainty will be larger. An extensive test programme should be carried out in order to find out, experimentally, the behaviour of the plant. In addition, a relatively long period of normal operation of a pilot plant would be essential.[11]

---

7 Although it is not the most suitable configuration for off-design, pressure ratios around 30 can be found in a single shaft configuration (ABB GT24 & GT26)

8 The incorrect pressure of the air injected in the different burners can modify the exit pressure, hence the LP compressor inlet pressure, generating instabilities. Also, a failure in the air and/or fuel flow can represent the presence of oxygen in the recycled gases; a hazardous situation when the temperature of the gas is increased in the recuperator, with the methane already injected.

9 Typically a few measurements are needed for the different engine control laws. When one of these measurements fails, an approximate value can be derived from other engine parameters, avoiding a possible critical failure. In some cases it will be necessary to stop the machine to replace the probe or rake, but in others it will continue its normal operation. In this machine, where different types of measurements are required, the accuracy and reliability of the devices used for this purpouse are extremely important.

10 If, for example, one of the water injection systems fails, the rest of the engine must have a quick response to this problem, changing the rest of the control laws. As in the case of a measurement, some failures will require the immediate stop of the machine, in most of the cases the machine will be able to operate partially, with a later stop, while other ones will be just warnings of the control system.

11 The AGTJ-100A, a very good example of an innovative machine, was in operation, for performance and endurance cycles at the Sodegaura Power Station of the Tokyo Electric Power Co, Inc. (TEPCO) for over 3 years.

In most of the actual open cycle gas turbines, fuel flow is the parameter driving the off-design behaviour and control of the machine, having the most common limiting parameters as feedback, with bleed valves, variable IGVs, etc. as minor contributors. In other cases steam injection is present as well, and, in a few cases, variable low pressure/power turbines NGVs are employed. In the case of the proposed semi-closed cycle the number of sub-systems seems unreasonable for safe continuous operation.

7.4. CRITICAL AREAS

The cycle we are interested in has two main critical areas:

- The use of carbon dioxide or a mixture of carbon dioxide, argon and water vapour as a working fluid.
- The combustion of a low calorific value gas, obtained from coal gasification, with pure oxygen or a mixture of oxygen and argon (95%/5%) in a carbon dioxide environment.

7.4.1. PROBLEMS ASSOCIATED WITH THE USE OF CARBON DIOXIDE AS WORKING FLUID

In general, the use of a gas different than air for the cycle will be a critical point. The experience with gases such as helium, argon, mixtures of helium and xenon, carbon dioxide, etc., is restricted to a very few closed cycles, all of them with low turbine entry temperature (of the order of 1100 K). The closed cycles with helium have been used for base load electricity generation, hence designed for optimum efficiency. However, in other cases, the closed cycles gas turbines have been used for submarine and space applications, where several important factors other than thermal efficiency, should be considered. Table 7.2 gives the characteristics of several closed cycles using different working fluids.

The optimisation of the turbomachinery will be a very important subject for the carbon dioxide cycle. Most of the CFD codes available, either commercially or developed in house by the gas turbine companies, use air as a working fluid. Some code improvements will be necessary to be able to switch from air to carbon dioxide, a mixture of carbon dioxide and argon or a mixture of carbon dioxide, argon and water vapor. The most difficult and expensive activity will be the validation of the codes with experimental data. For the moment the author has not found any CFD validation data set using the gases we are interested in. Hence, some experiments should be run in order to obtain the necessary information.

TABLE 7.2: CLOSED CYCLE PERFORMANCE

	Oberhausen I	Oberhausen II	NASA BRU	Terrestrial AC
Fuel	Coal Coke oven gas	Coke oven gas	Radioisotope	Radioisotope
Working Fluid	Air	Helium	XeHe84	Argon
Power Output (MW)	13.75	50	0.006	0.015
Heat Output (MW)	18.5-28	53.5		
Efficiency %	29.5	31.3	36.0	
Fuel utilisation %	65.6	65.0		
SOT (K)	983	1023	1144	960
CDP (bar)	32	28	1.9	2.9
Commissioning	1960	1975		
Availability (%)	79			

Other critical aspect is turbine cooling. Vanes, blades and platforms, as well as discs, must be cooled in order to maintain the surface at an acceptable temperature. With 1200°C selected as the target SOT, a fairly large amount of cooling must be employed to keep the metal temperature at a reasonable level. The appropriate internal air system configuration will be critical to extend the life of the hot section of the gas turbine. As we have seen previously, the optimisation of the cooling bleeds is necessary to increase the cycle efficiency. These ideas must be borne in mind in this cycle, where the optimum pressure ratios are very high, leading to a high cooling temperature, and where the lower temperature drop in the turbine will increase the operating temperature of second and subsequent stages.[12]

As the working fluid is, mainly, carbon dioxide, the radiation problems will increase. In the case of having an open cycle gas turbine, the main components in the combustor will be nitrogen and unburnt oxygen, with some carbon dioxide, water vapor and argon present as well. The symmetric diatomic molecules, N_2 and O_2, are almost transparent to radiation. However, the presence of triatomic molecules, such as CO_2 and H_2O, leads to luminous radiation. A lot of research has been conducted to investigate radiation in open cycles gas turbines, using natural gas, kerosene and diesel as fuels. An increase in the combustor liner metal temperature occurs when the combustion gas radiation is stronger. Hence, it will be absolutely necessary to investigate the radiation phenomena in a carbon dioxide atmosphere and burning a low heating value gas, where the fuel to air ratio will be of the order of 5 times

---

[12] Just as an example the temperature drop in the turbine of a machine operating with carbon dioxide and with a pressure ratio 20 can be 50% lower than in other one using air as working fluid and with a pressure ratio 10. The higher exit temperature will lead to a larger amount of turbine cooling flows.

greater than with natural gas. The increase in radiation will also have an important effect on the mass flow necessary for the HPT NGVs leading edge and pressure surface cooling. Figure 7.2 shows the maximum combustor wall temperature in an open cycle gas turbine using different fuels, indicating the need for improvements in wall cooling technology to maintain acceptable durability of combustor liners when burning conventional low hydrogen content fuels. The situation will be critical if this content decreases to values close to 1-2%, as happens with fuel derived from coal gasification.

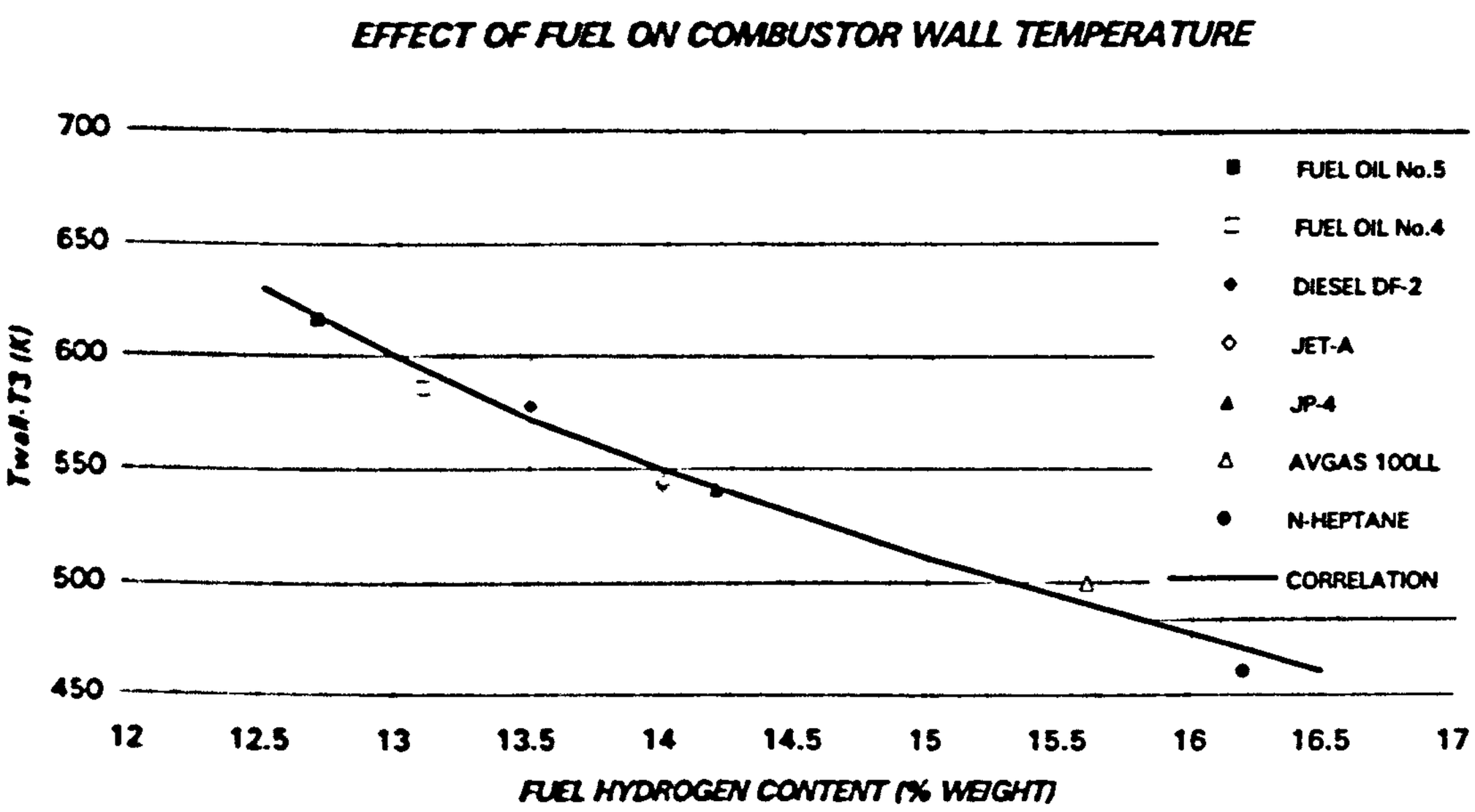

Figure 7.2. Effect of the fuel hydrogen content on combustor wall temperatures

7.4.2. PROBLEMS ASSOCIATED WITH THE USE OF A LOW HEATING VALUE FUEL DERIVED FROM COAL GASIFICATION

The low heating value gases will be burnt with oxygen in an inert atmosphere. In the gas turbine combustion discipline there is no previous experience with this kind of processes. The efficient mixing between the fuel and the oxidizer, to achieve complete combustion, will be a challenge. Also the necessity to avoid hot spots, that would cause damage in the turbines, is an area that requires an important research effort.

The most common fuel properties investigated in relation with the gas turbine operation and performance are:

- Aromatic content: related with carbon and smoke formation
- Hydrogen content: related with combustor liner temperatures

- Lower heating value: related with fuel consumption and auxiliary power
- Olefin content: related with gum formation
- Carbon residue: related with combustor and fuel nozzle coke deposition and turbine blades deposition and erosion, as well as pollutants formation.
- Water and sediment: related with fuel system fouling and erosion, as well as pollutants formation.
- Ash content: related with hot end corrosion, erosion and fouling as well as pollutants formation.
- Sulphur content: related with SO_2 generation and hot end corrosion
- Trace metals (vanadium, sodium, potassium, calcium, lead, iron, copper, magnesium, etc.): related with hot end corrosion and pollutant formation.
- Flash point: related with handling safety.

Other properties such as viscosity, pour point, cloud point, freeze point, vapor pressure and distillation will not apply to gaseous fuels.

The hydrogen content, carbon residue, water and sediment, ash content and sulphur content seem to be the most serious problems for the semi-closed cycle gas turbine.

As the fuel used is coming from coal gasification, although cyclons will be undoubtedly employed, a relatively large content of sulphur will be present in the final gas injected in the combustor. Therefore, additional cooling is required to decrease the turbine metal temperature and avoid sulphidation.

Even if full coverage film cooling or transpiration cooling are employed, the contaminated gas stream could damage the turbine. Hot particles coming from the combustor can reach the blades and be retained at the surface. The mechanisms for the deposition phenomenon can be: direct impingement[13], vapor diffusion[14], turbulent diffusion[15], electrophoresis[16], thermophoresis[17], magnetophoresis[18], photophoresis[19],

---

[13] Impingement is controlled by particle size.

[14] Vapor diffusion is controlled by the vapor pressure of the different individual elements of the hot gas mixture.

[15] Turbulent diffusion is controlled by the boundary layer characteristics.

[16] Electrophoresis is controlled by the electric charge of the particles.

[17] Thermophoresis is controlled by temperature gradients.

[18] Magnetophoresis is controlled by the magnetic charge of the particles.

[19] Photophoresis is controlled by light.

molecular diffusion[20], brownian diffusion, diffusiophoresis, etc. The effectiveness of each of the mechanisms depends upon many factors, such as particle size and density, concentration, intensity of electrostatic charge, magnetic intensity, temperature, pressure, viscosity, velocity and density of the hot gas stream, blade surface temperature and roughness, local turbulence, etc. Phenomena, generally overlooked in the gas turbine world, such as the electrophoresis and magnetophoresis can play an adverse role in a contaminated environment. The effect using a coal derived fuel in a carbon dioxide environment must be investigated experimentally.

Some difficulties could also be present in the bottoming cycle heat exchanger, where the combination of high temperatures, due to the lower temperature drop in the turbine, with the fuel contaminants should be studied.

In the final cooler the problem will be the combination of low temperatures with the sulphur content in the gas, with the possibility of sulphuric acid formation. This module will be one of the most critical, despite being a relatively cold one.

All of these items will lead to a sequence of tests to prove the feasibility of the system that, in order to be completely representative, should be done at almost full scale, and under the same operating conditions as the real gas turbine.[21]

However, some individual aspects can be proved at scale models, or using different systems.[22]

Deposition will be a problem, not only in the HP turbine NGVs and blades, but also in the combustor, where the high wall temperatures, due to radiation problems, will be more difficult to overcome.

Even when a very high purity fuel is employed, the deposition rate increases dramatically with the temperature of the liner walls. In figures 7.3 and 7.4, from Chin, Hermanson and Spadaccini, [20], the deposition data for commercial methane and ultra high purity (UHP) methane / natural gas are plotted against combustor wall temperature. Considering that in the case of the carbon dioxide semi-closed cycle these temperatures will be of the order of 1100 K or higher, the deposition rate when using commercial methane can be of the order of 50 mg/cm²h. After one year of operation, the deposition will be of the order of 0.5 g/cm². The critical effects

---

20 The brownian diffusion and molecular diffusion affects to the smaller particles. In the first case the size range is 0.5 to 1 microns, while in the case of the diffusion is 0.01 to 0.5 microns.

21 It is not just Murphy's Law, but the experience of the gas turbine companies, what dictates that the most serious failures will take place in the parts not taken into account during the various risk analysis exercises carried out during the design & development phases, and also not considered in the preliminary tests. For this reason, the experiments must be carried out as close as possible to the real engine conditions, and using, if possible, the same hardware, measurement devices, etc. This philosophy can save a lot of money and time during the development period of a new engine.

22 For example the flow pattern in the combustion chamber can be initially visualised using the water analogy.

associated with the deposition are the blockage of the liner cooling holes, with the consequent increase in temperatures and the possibility of burning the liner, and the periodic detachment of the carbon layer, that can seriously damage the turbines.

It is very difficult to extrapolate this tendency to a new fuel coming from coal gasification. The necessity of carrying out the appropriate experiments using a representative full scale combustor sector is, again, clear.

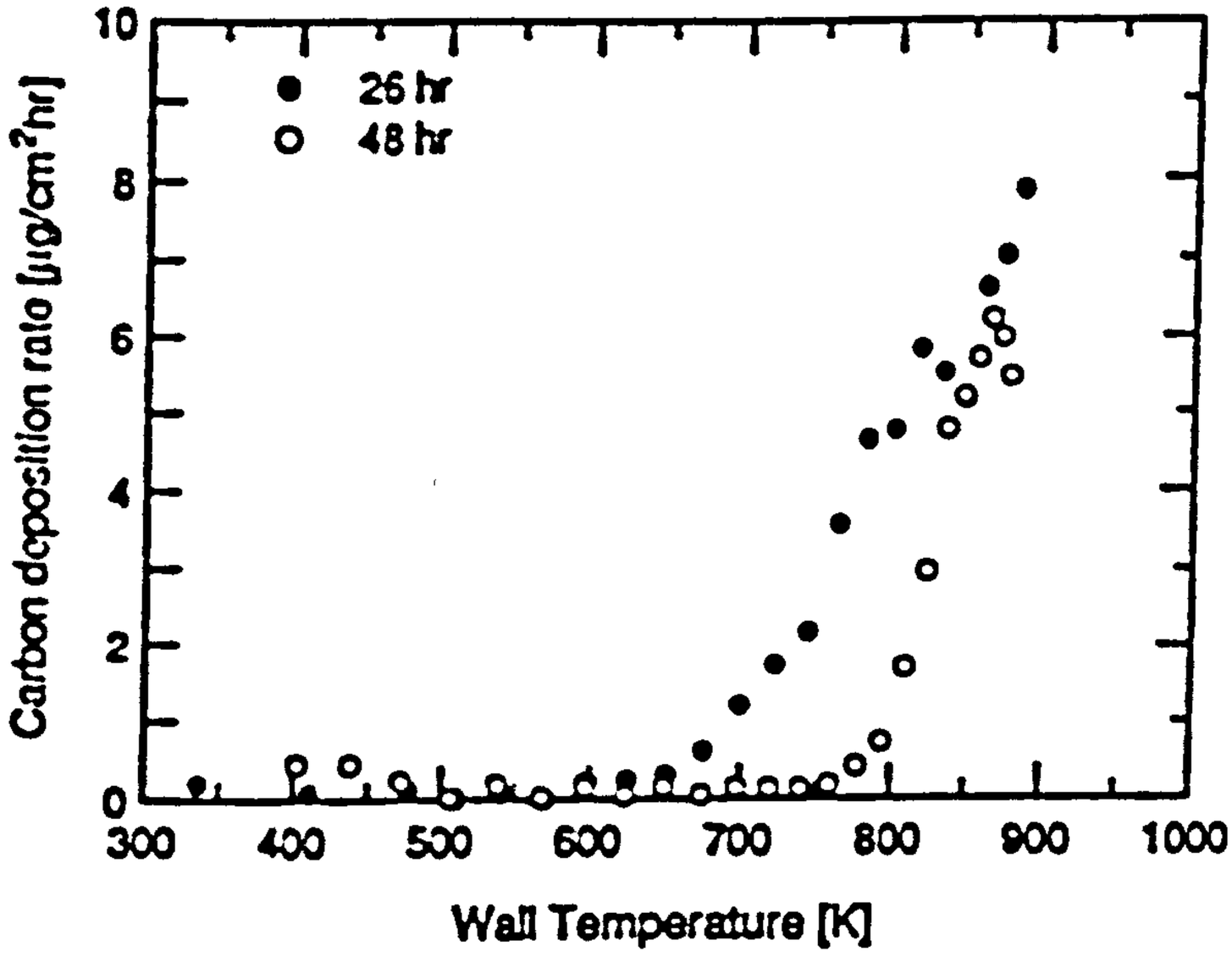

Figure 7.3. Deposition rates for commercial methane as a function of combustor wall temperatures

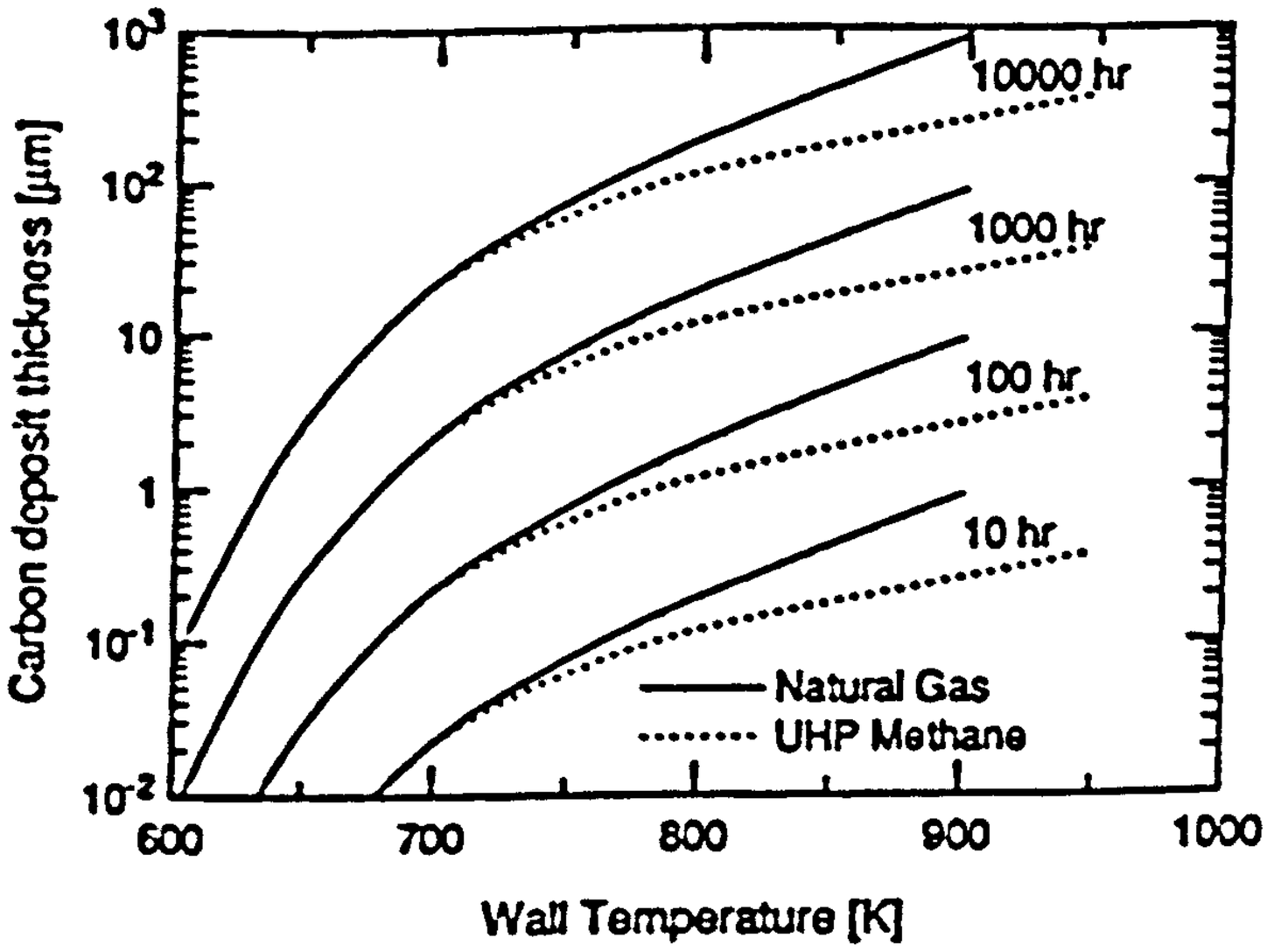

Figure 7.4. Estimated deposition rates for ultra high purity methane and natural gas as a function of combustor wall temperatures

7.5. LIMITING VALUES OF THE CYCLE

It is very important to clearly identity the limiting parameters of the cycle before starting the project. An error at this stage could cause very serious problems during the design and development of the machine.

7.5.1. GAS TURBINE LIMITING PARAMETERS

The values suggested, according to experience in conventional open cycle machines are, in the case of a two spools machine:

- Maximum continuous low pressure shaft speed[23]: 103% of the design value
- Maximum instantaneous low pressure shaft speed[23]: 125-130% of the design value
- Minimum continuous low pressure shaft speed: 35% of the design value
- Maximum corrected speed of the low pressure compressor: 110% of the design value
- Minimum low pressure compressor surge margin $(PR_{SM}-1)/(PR-1)$: 8%
- Maximum continuous high pressure shaft speed[24]: 102.5% of the design value
- Maximum instantaneous high pressure shaft speed[24]: 120% of the design value
- Minimum continuous high pressure shaft speed: 50% of the design value
- Maximum corrected speed of the high pressure compressor: 106% of the design value
- Minimum high pressure compressor surge margin $(PR_{SM}-1)/(PR-1)$: 12%
- Maximum compressor delivery temperature (CDT): 900 K
- Maximum compressor delivery pressure (CDP): 80 bar
- Combustor wall temperatures: 1150 K (1075 K if sulphur becomes finally a problem)
- Temperature profile quality at the exit of the combustor $(T_{\_}-T_{\_})/T_{\_}$ better than 10%.
- Maximum stator outlet temperature (SOT): 1500 K
- Maximum deviation in SOT (SOT_u-SOT_{ss}) during normal transients: 10 K

---

[23] It is assumed that the power turbine is not in the low pressure shaft.

[24] It is assumed that the power turbine is not in the high pressure shaft.

- Maximum HPT nozzle guide vanes metal temperature: 1125 K (1075 K if sulphur becomes finally a problem)
- Maximum HPT blade metal temperature: 1100 K (1050 K if sulphur becomes finally a problem)
- Maximum LPT and PT nozzle guide vanes metal temperature: 1100 K (1050 K if sulphur becomes finally a problem)
- Maximum LPT and PT blade metal temperature: 1075 K (1050 K if sulphur becomes finally a problem)
- Maximum continuous free power turbine shaft speed: 110% of the design value
- Maximum instantaneous free power turbine shaft speed: 140% of the design value
- Maximum turbine exit temperature: 1150 K (1050 K if sulphur becomes finally a problem)
- Minimum steam cycle heat exchanger exit temperature: 415 K (to avoid water liquefaction and the possibility of sulphuric acid formation)

The maximum continuous shaft speed limit will be an important mechanical design criteria, due to the increase in creep, fatigue, etc., relative to the baseline shaft speed. The instantaneous overspeed will be a major issue for mechanical integrity, specially discs and shafts. For the power turbine shaft, the continuous overspeed limit is less restrictive, and typically between 105 and 110% of the design value is allowed, with values around 125-130% for the instantaneous overspeed in the case of the two spool-two shaft configuration, and around 140-150% for the two spool-three shaft arrangement (free power turbine).[25] The variation of speed at base load is very dependent on the configuration, type of control, etc., and is, sometimes, fixed by government regulations regarding the stability of the electricity frequency.[26] The lower limit of the shaft speed is due to aeroelasticity problems for stable operation.

The minimum value of surge margin in industrial gas turbines can be lower than in aeroengines, where values of 15 to 25% are usually employed, as there is no need to have an additional reserve for manoeuvres, large inlet flow distortion, etc. The margin is higher in the HPC, because the surge problem in this component is more serious than in the LPC, as it is possible to have combustor air through the compressor, with catastrophic results in this component, and to produce a flame-out.

---

[25] For the instantaneous overspeed, coming from a shaft, clutch, etc. failure, resulting in an immediate lost of load, the presence of a compressor in the same shaft acts as a brake, due to the efficiency drop at high corrected speeds, increase in mass flow and pressure ratio (therefore in compressor power demand) is very beneficial, with the free power turbine configuration having a maximum transient value considerably larger.

[26] Typical frequency stability limits are: ±2% from idle to 50% power, and ±1% above 50% power.

The maximum compressor delivery temperature is limited by the materials of the last stages, and the maximum pressure by the combustor liner loads. Pressure of the order of 80 bars have been achieved in the Japanese AGTJ 100A and 100B.

The maximum metal temperatures of the combustor walls, NGVs and blades of the high pressure turbine are determined by the limitations imposed by the materials. For the combustor and NGVs the loads are just the aerodynamic ones, while in the turbine blades the centrifugal stresses are also present.[27] For the semi-closed cycle we are considering the blades running 25°C cooler than the vanes. This is the most common tendency, although in some cases the opposite selection is made.[28]

In addition to the difficulties associated with high temperature, such as creep and thermal stresses, the presence of sulphur in the fuel becomes a problem if the temperature is raised above 815°C (1088 K), as may happen in the case of the high pressure turbine blades and vanes. The sulphidation phenomenon is less dramatic in single crystal blades, as metal sulphides are formed in the grain boundaries. Sulphur has a particular affinity for nickel. Hence, alloys with high nickel content will be specially prone to sulphidation.[29] The combination of sulphur and vanadium with sodium and potassium, to form sulphates and vanadates, have proved particularly troublesome, because they have sufficiently high vapor pressure to emerge from flames in vapor form and then condense on metal surfaces that operate at temperatures below 815°C. The low pressure turbine will suffer from these problems. These sulfates and vanadates are liquid at temperatures above 650°C, and in this form react with the oxide films that would normally protect the alloy surface. A fairly rapid attack occurs under these films, that can be accelerated if chlorides or lead are also present.

For the case of the coal derived fuel sulphur will be the main problem, as vanadium is usually not present in sufficient quantities, although a very detailed investigation is required. Therefore, an important effort should be carried out in order to remove the sulphur during the gasification process.

The corrosion caused by the combustion products will be stronger in the case of semi-closed cycles than in open cycle gas turbines, even if clean fuel was employed. In that situation, if the metal temperature is kept above the dew point of the water vapor present in the combustion products, there is little difference between the corrosion rates in air and in combustion products, as long as the fuel-air ratio (fuel-oxidizer ratio for our particular case) remains either above or below the

---

[27] It is important to note that most of the materials employed in turbines have a sharp drop in the properties above a certain temperature. Therefore, an accurate estimation of the metal temperature is essential

[28] For example in the Westinghouse 501D the HPT stator was hotter than the rotor, and in the 501F the rotor was hotter than the stator.

[29] Most of the actual turbine alloys are nickel based

stoichiometric value. However, if the atmosphere fluctuates between oxidizing and reducing conditions, the scale formed during oxidizing conditions tends to flake off during a shift to reducing conditions, and a very rapid attack can occur. In a semi-closed cycle the fuel to oxidizer ratio has to be kept extremely close to the stoichiometric value, and this problem will, probably, arise.

The SOT over shoot during transients can reduce the life of the turbine dramatically. This will not be a problem if a smooth starting/acceleration is employed, but it should be considered in the control schedules.

The temperature profile quality at the exit of the combustor affects turbine life. HP turbine vane/blade cooling is designed according to the turbine gas inlet temperature pattern to maintain the metal temperature. If this profile oscillates, the metal temperatures will have an important gradient, with the consequent loss in life.

The power turbine maximum exit temperature is limited by the heat recovery for the bottoming cycle. The heat exchanger will not be cooled, as turbine aerofoils are, and any increase in its temperature will have a large impact on the cost of the power plant. The minimum temperature at the exit of this component is limited by the sulphur content of the fuel. However, the problem will be transferred to the precooler, where the water is removed from the carbon dioxide/argon mixture at temperatures lower than exit temperature of the HRSG, making the precooler a critical component. Its life must be carefully estimated. Again, sulphur appears as a key issue for the feasibility of this power plant.

7.5.2. STEAM TURBINE LIMITING PARAMETERS

The parameters considered in this section will be the ones that have a direct effect on combined cycle efficiency and gas turbine/steam turbine interface.

- Maximum temperature: 813 K (540°C)
- Maximum pressure: 120 bar
- Minimum steam quality: 87%

The typical temperature range of the bottoming cycle steam turbine is 400°C to 540°C, with pressure going from 15 to 120 bar. The maximum temperature of 540°C is a very common value in steam turbines, requiring no further material research. The maximum pressure has also been maintained at 120 bar. Although in supercritical steam cycles considerably higher values are found, the intention of a combined cycle is to recover as much heat as possible, with a minimum decrease in the reliability and availability of the system. Higher temperatures and pressures could have the undesirable effect of making the steam cycle a risky area.

The minimum steam quality is limited by corrosion in the last stages of the turbine. Experience shows that values higher than 85-87% are acceptable. However,

it is very common to design for no liquid fraction at the exit, tolerating small figures at off-design.

7.6. PERFORMANCE PARAMETERS OF THE COMPONENTS

The design efficiencies, pressure losses, power output, etc. are specified in this section for both, the gas turbine and the steam turbine.

7.6.1. GAS TURBINE DESIGN PERFORMANCE PARAMETERS

- Low pressure compressor inlet temperature: 300 K
- Inlet pressure losses: 0.5%
- Low pressure compressor polytropic efficiency: 90%
- Low pressure compressor relative shaft speed: defined by the base load operating point.
- Low pressure compressor surge margin: 40% (55% if steam injection is considered as a possible future option with no major re-design).
- Intercompressor casing pressure losses: 0.2%
- Intercooler exit temperature: 310 K
- Intercooler pressure losses: 2%
- High pressure compressor polytropic efficiency: 89%
- High pressure compressor relative shaft speed: defined by the base load operating point.
- High pressure compressor surge margin: 30% (45% if steam injection is considered as a possible future option with no major re-design).
- LPT blade cooling extraction point: $(H_{255}-H_{25})/(H_3-H_{25})=0.45$
- Polytropic efficiency loss in the LPT cooling bleed due to walls: 5%
- Excess mass flow compressor polytropic efficiency: 85%
- Regenerator effectiveness: 80%
- Regenerator pressure losses: 3% in the cold side
  3% in the hot side
- External consumption maximum bleed: 1%
- Combustor efficiency: 99.9%
- Combustor & diffuser pressure losses: 5%

- Stator outlet temperature (SOT): 1473 K and 1650 K
- High pressure turbine polytropic efficiency: 87%
- High pressure shaft friction losses: 0.1%
- High pressure shaft power off-take: 0.4%
- HPT nozzle guide vanes metal temperature: 1100 K (1050 K if sulphur becomes finally a problem)
- HPT blade metal temperature: 1075 K (1025 K if sulphur becomes finally a problem)
- HPT stage loading: $\Psi=\Delta H/U^2=1.7$
- HPT blade speed (Mach number): $M=0.5$
- Low pressure turbine polytropic efficiency: 87%
- Low pressure shaft friction losses: 0.3%
- LPT and PT nozzle guide vanes metal temperature: 1075 K (1025 K if sulphur becomes finally a problem)
- LPT and PT blade metal temperature: 1050 K (1000 K if sulphur becomes finally a problem)
- LPT stage loading: $\Psi=\Delta H/U^2=1.7$
- LPT blade speed (Mach number): $M=0.4$
- Turbine casing pressure losses: 0.5%
- Power turbine polytropic efficiency: 87%
- Power turbine losses, including generator losses: 2%
- Bottoming cycle heat exchanger pressure losses: 5%
- Temperature at the exit of the bottoming cycle heat exchanger: 420 K
- Precooler pressure losses: 2%
- Nozzle pressure ratio: 1.02

The compressor inlet temperature is determined by the water temperature used to precool the gas (around 10-15°C can be assumed). With 15°C as cooling temperature, a recuperator effectiveness of 91% and a hot side inlet gas temperature of 150°C, the precooler exit/compressor inlet temperature will be 27°C (300 K).

The efficiencies of both, LP and HP compressors are characteristic of those employed in industrial gas turbines, where a larger number of stages with a lower work done per stage and a slightly higher efficiency, is preferred over the weight and cost reduction derived from the reduction in number of stages. In figure 7.5 a scheme of the range of efficiencies for axial compressors using air as working fluid is shown.

The pressure ratio per stage has a direct relation with blade speed and work coefficient as shown in figure 7.6, where different aero and industrial compressor technologies are classified according to their pressure ratio, mean corrected speed and work coefficient. If the relative velocity of the blade is transonic or supersonic the pressure ratio will grow, but then the losses will come not only from boundary layer friction or secondary flows, but also from shock waves.

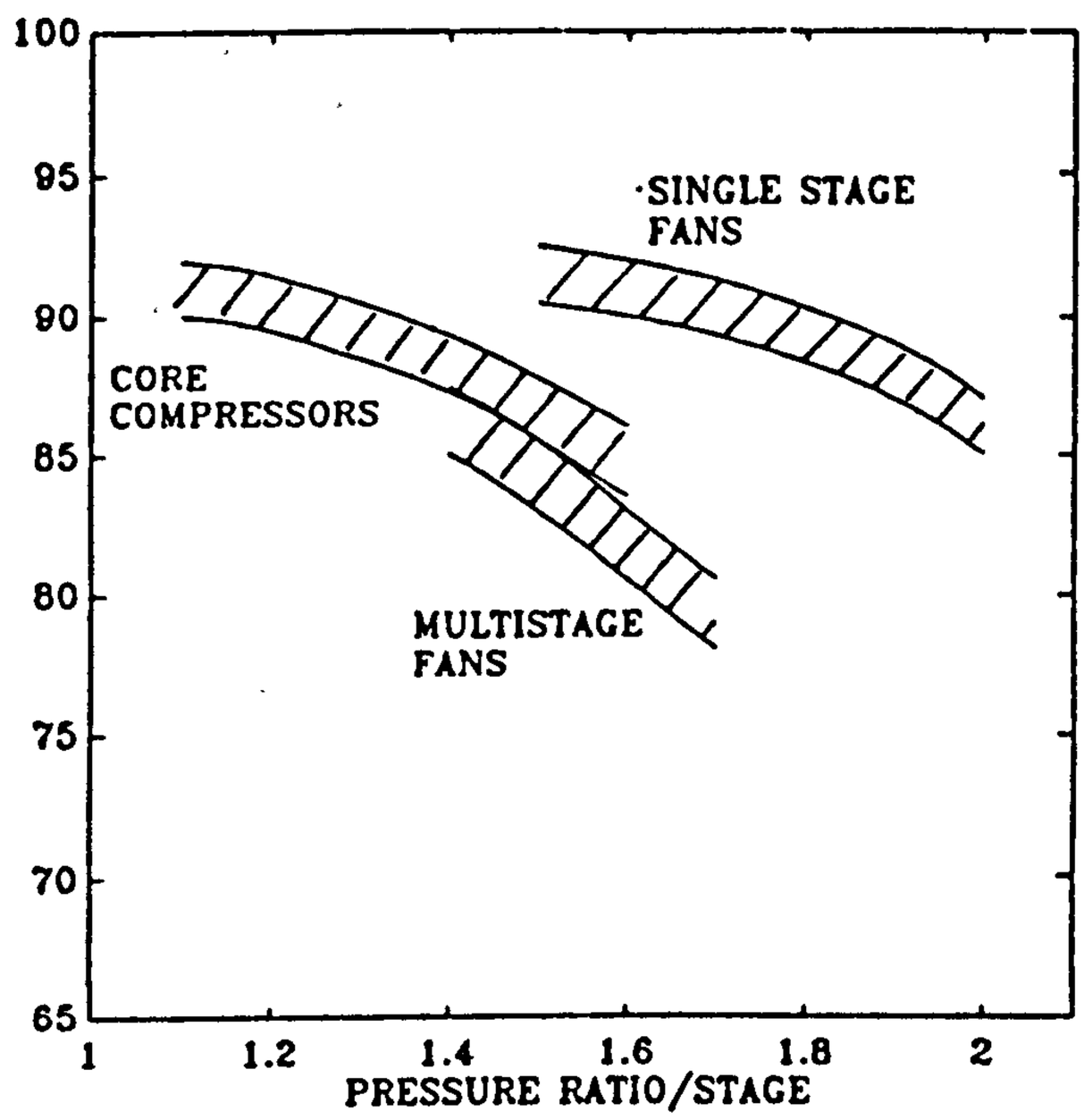

Figure 7.5. Compressor polytropic efficiency vs. stage pressure ratio

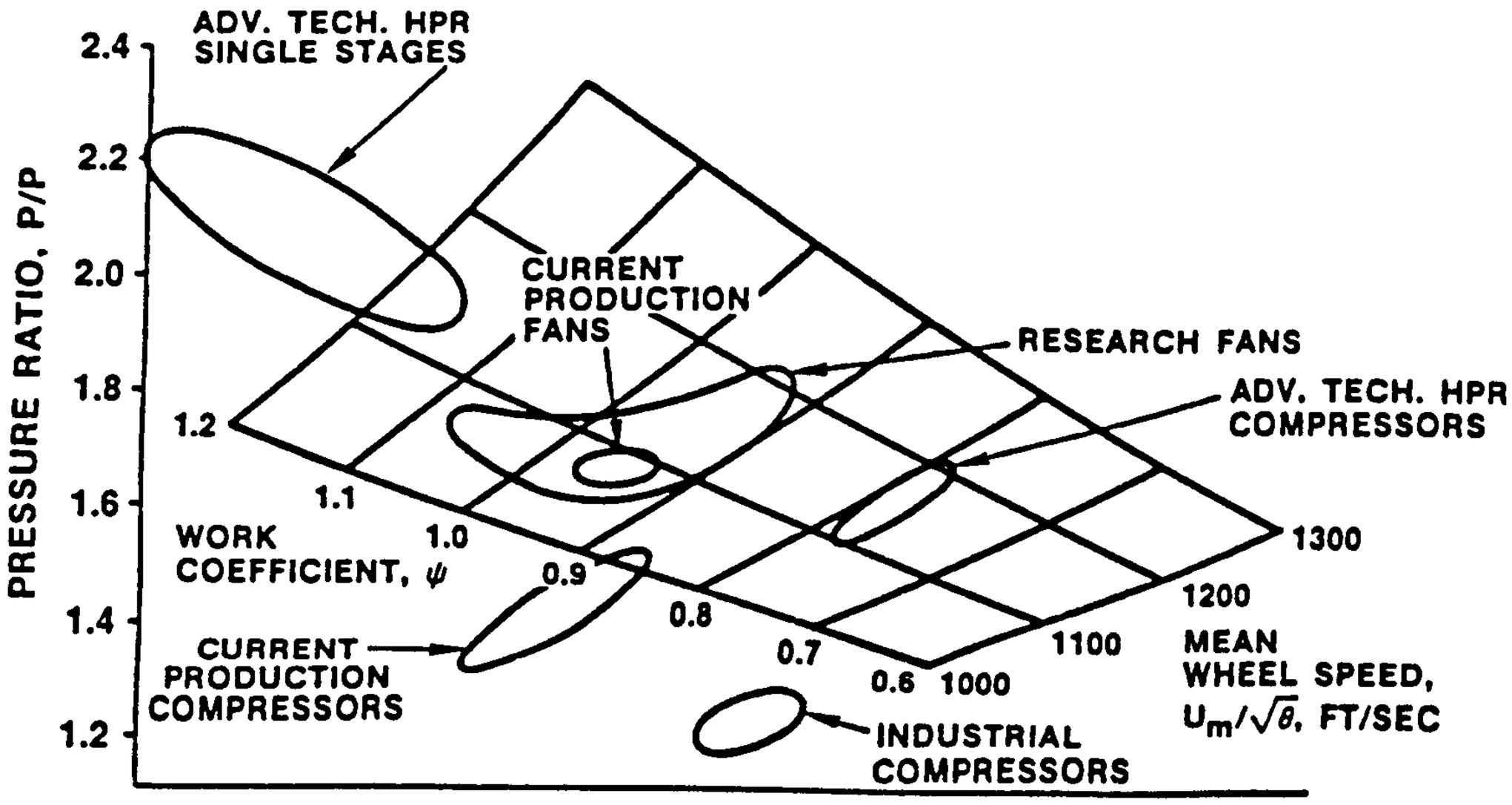

Figure 7.6. Pressure ratio per stage as a function of work coefficient and corrected speed

The optimisation of the blade design should be done for the base load operating point, where this power plant will operate for at least 80% of its life. In other machines a complete study of the possible duty cycles should be carried out, in order to determine clearly the operating point where the turbomachinery efficiency must be maximise.

The compressor surge margin is a very important subject. If the same turbomachinery has to suit both, steam injection and simple cycle gas turbines, the surge margin must be larger than for a conventional cycle.[30] As it was explained in previous chapters, the most common reasons for steam injection are the reduction in NO_x levels together with a very high efficiency in a compact pack, and the possibility of having an integrated cogeneration / combined cycle system. In these cycles the reasons will be the second and third ones, because no NO_x emissions will take place. In addition to the reduction in surge margin if steam injection is used, it was observed during the first off-design runs of this cycle that the LP compressor running line approached the surge line quicker than in an open cycle gas turbine.[31] This unexpected effect changed the initial design surge margins, fixed in 20% for the LPC and 25% for the HPC, to 40% and 30% respectively. In the case of compatibility between simple cycle and steam injection the values would be 55% and 45%. The increase could be lower, however the steam to inlet flow ratio is expected to be higher than in a conventional open cycle gas turbine, due to its higher power turbine exit temperature, leading to a larger steam mass flow generation.

The recuperator effectiveness is representative of that of a large device employing mature technology. Values around 85% could be achieved using advanced materials and methods. The pressure losses have been estimated from existing machines, and a more accurate prediction should be made as soon as the final arrangement is decided.

The efficiency of the compressor used to increase the pressure of the excess of carbon dioxide bled before the entry of the combustor is characteristic of a centrifugal one. If the excess mass flow was large enough, an axial compressor, with a higher efficiency, could be employed.

Combustion efficiency must be nearly 100%. The 5% pressure loss in the diffuser and combustor is a very common value. Slightly lower losses could be obtained employing larger combustors, with the consequent reduction in velocity. However, figures between 3 and 6% are expected.

As it has been stated, the peak load SOT is high, specially if the fuel contains large proportions of impurities. However, after a reduction of around 100°C for the

---

[30] An example of compatibility between simple and steam injection cycles is given by the Allison 501-KH. Being an aeroderivative of the T56-501K turboprop engine, the 501-KB had a surge margin in excess of 45 percent. Hence, it was feasible to modify the industrial turbine, adding the possibility of steam injection, without major re-designs.

[31] It is important to notice that this effect, not expected initially, does not modify the optimisation calculations done before.

base load, the resultant value would be acceptable. It is important to bear in mind that the cooling flows will be designed for the peak value, giving an important increase in life when the turbine works at part load.

The HP, LP and power turbine efficiencies are conservative values obtained from experience with open cycles. Usually, the HP turbine has a lower efficiency, due to its higher load per stage and interaction between main flow and cooling flows. In the semi-closed cycle, as the drop in temperature per stage is lower, even the last stages would need some cooling. For that reason a constant polytropic efficiency has been taken.[32]

The shaft losses, HP shaft power off-take, power turbine and generator losses values are typical for industrial gas turbines in operation.

The pressure losses of the bottoming cycle heat recovery are quite important. However, the flow will experience a very large temperature drop, and the heat exchanger must be large enough to allow this heat transfer. The precooler losses and the nozzle pressure ratio have also been obtained from different experimental and production machines.

7.6.2. STEAM TURBINE DESIGN PERFORMANCE PARAMETERS

A simple steam turbine is assumed for the optimisation process, to avoid iterative loops in the bottoming cycle calculations. A detailed treatment of the steam turbine should be done when the final cycle arrangement has been decided. The steam turbine main parameters are:

- Temperature drop between gas turbine exit and steam turbine entry: 40 K
- Temperature difference in the pinch point: 20 K
- Steam turbine isentropic efficiency: 85%
- Condenser pressure: 6 mbar
- Pump efficiency: 70%
- Economiser pressure losses: 8%
- Superheater pressure losses: 7%
- Auxiliary power for steam turbine ancillaries and generator pressure losses: 2%

---

[32] Perhaps a 1-2% increase in efficiency between the first and last turbine would be more accurate. However, if different efficiencies were employed for low pressure and power turbine, the design performance for the free power configuration will not give the same results as in the case of power turbine in the HP or LP shaft. Metal temperatures for both, stator and rotor, cooling technology, etc. should also be the same, to minimise the possible performance differences generated by the vane/blade cooling calculations.

The temperature drop between the exit of the power turbine and the inlet of the steam turbine and temperature difference in the pinch point have been taken from references [11], [48] and [87].

The efficiency of the power turbine, as well as the pump efficiency and pressure losses in the economiser and superheater have been obtained from the TVA Bull Run power plant [48], as well as from other references on steam power plants [11], [19], [25], [47] and [98].

Several steam turbines used in combined cycles have been examined to obtain a reasonable value of the condenser back pressure. A range from 1.2'' up to 15'' Hg was identified, and 1.8'' Hg was finally selected.

Auxiliary power and generator losses between 1.5 and 4% are very common. The highest values usually include the pump power, that has been calculated separately. Therefore, a value of 2% was chosen.

7.7. POWER PLANT ARRANGEMENT

The possible arrangements of the power plant depend on the final cycle selection. Four possible gas turbine cycles will be investigated:

- Simple cycle
- Intercooled cycle
- Recuperated cycle
- Intercooled and recuperated cycle

The one spool/single shaft arrangement is usually preferred for electricity generation, due to its better stability and power change response. However, this configuration is not feasible for very high pressure ratio gas turbines. Off-design problems caused by very high pressure ratio compressors limit the use of single shaft power plants. One of the drivers in the allowable pressure ratio is the change in density from inlet to outlet of the compressor. Due to the different thermodynamic properties of carbon dioxide, or carbon dioxide/argon, compared with air, larger density changes will happen for the same pressure ratio. Initial studies have confirmed that the optimum pressure ratios will be higher than with air. From the open cycle data, where the maximum pressure ratio for a conventional compressor is limited to values around 20,[33] and bearing in mind that carbon dioxide is an unconventional

---

[33] A higher value can be found, for example, in the high pressure compressor of the aero gas turbine GE-90, with a pressure ratio of 20 or in the heavy duty ABB GT24 and GT26 models with a pressure ratio of 30. However, the control of this kind of compressor is far more difficult, and slightly lower values are desirable.

working fluid, the limiting value chosen for each compressor of the semi-closed cycle has been 12.

With these considerations, the two spool arrangement seems to be the most adequate. The power turbine can be either a free power turbine[34] (two spools/three shafts) or located in the low pressure spool[35] (two spools/two shafts). Schemes of the possible configurations are shown in figures 7.7 to 7.10.

7.8. CONDITIONS AT THE ENTRY AND EXIT OF EACH MODULE AND OPERATIONAL ENVELOPE

Typically, pressure and temperature distributions at the entry of the compressors, turbines, combustor, etc. are not uniform. For our purposes these non-uniformities will be neglected, and only the high pressure turbine peak temperatures will be considered for cooling flow calculations of the NGVs.

No temperature change is assumed between the extraction and injection points for any of the cooling flows.

The operational envelope does not suffer from inlet pressure and/or temperature variations, as in the case of open cycles, where hot climate and operation at altitude decrease the efficiency and power output.[36] Only the changes in the temperature of the water, used to pre-cooled the gas leaving the bottoming cycle heat exchanger and the condenser, affect the compressor inlet temperature. These will result in minor performance changes. However, the necessity of a constant water supply for the precooler is an important logistic factor to be considered. The variations in inlet pressure will be dictated by the limitations imposed in the condenser. It would be desirable to change the power output of the plant by changing the inlet pressure, as in the case of closed cycles gas turbines, but the limited range of pressure-temperature combination for water liquefaction make this option very difficult, although some modifications in this pressure are allowed.

---

[34] The aeroderivative GE LM5000, RR RB211, ... are examples of two shaft + free power turbine machines.

[35] The Japanese project AGJ100A/B and the GE LM6000 are examples of a two shaft with the power turbine incorporated in the low pressure shaft

[36] The change in altitude has also an effect over the Reynolds number, that affects the compressor efficiency as well as the combustion efficiency in the aeroengines. However, in the case of the industrial gas turbines these changes are relatively small (maximum variations of the order of 20-30% in Reynolds number).

For closed cycles, where the power is controlled mainly with the inlet pressure, the Reynolds number will experience important deviations from the design value, and the effect on compressor efficiency could be substantial.

CARBON DIOXIDE/ARGON SEMI-CLOSED CYCLE SIMULATION

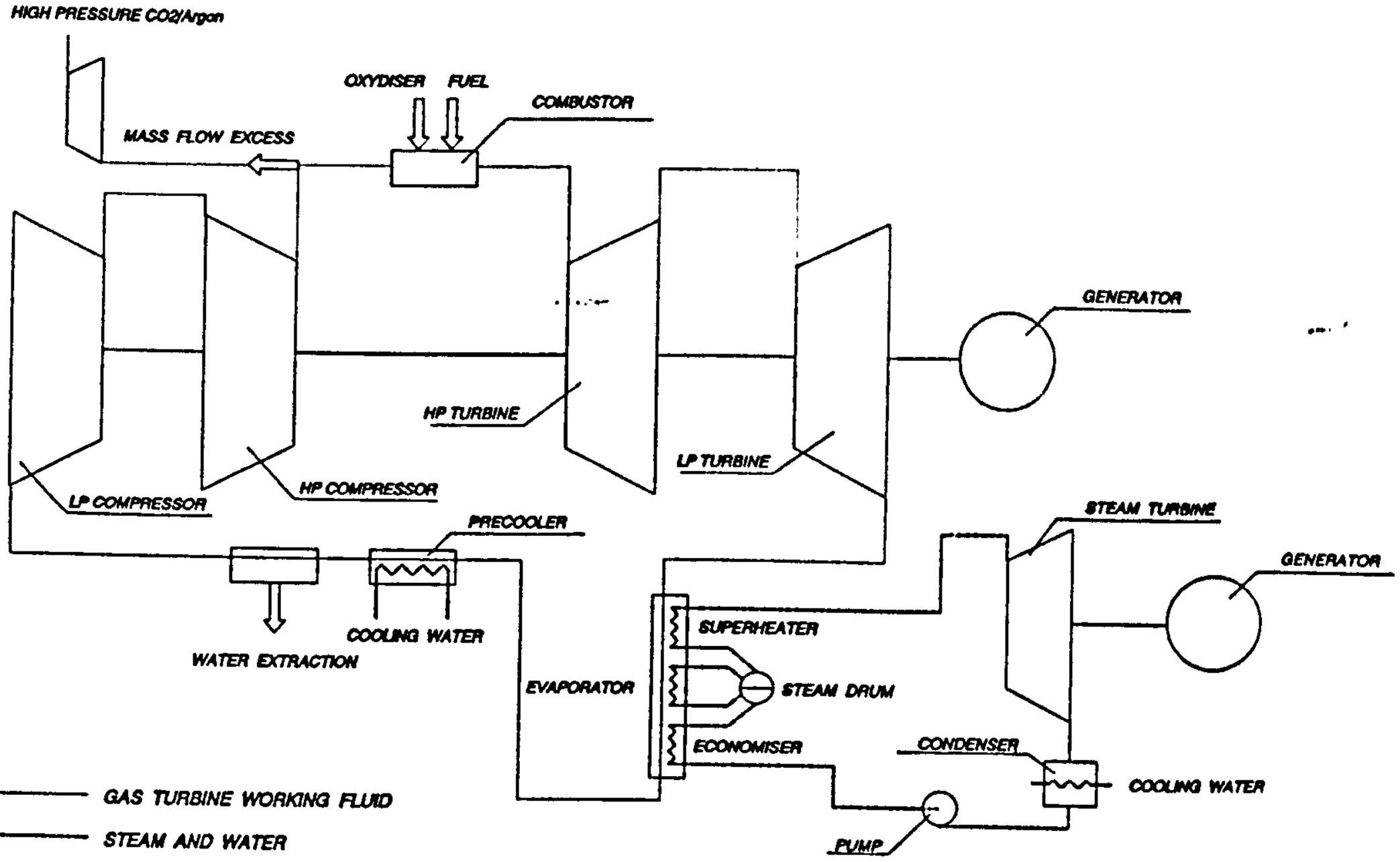

Figure 7.7. Semi-closed simple cycle with steam bottoming cycle.

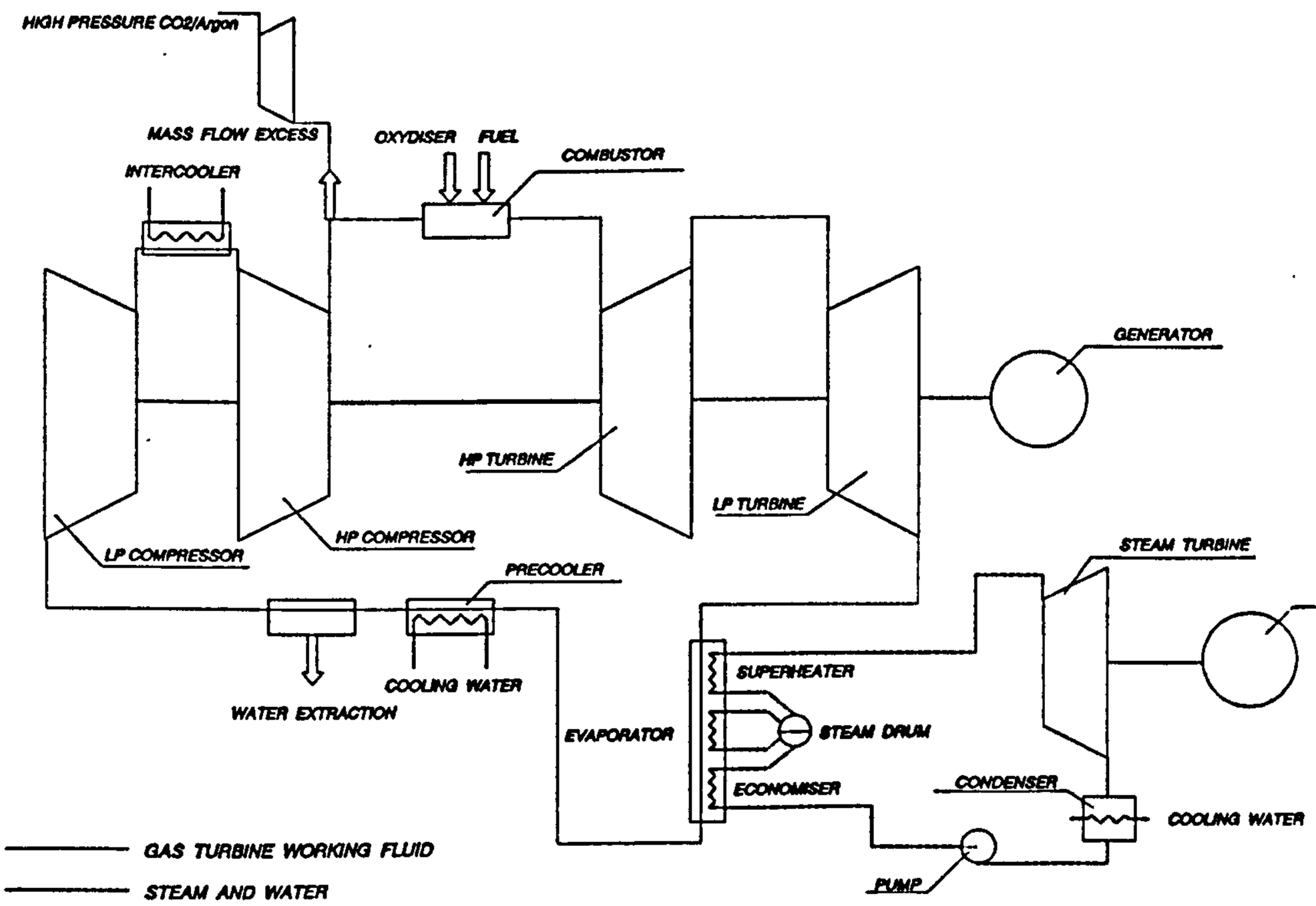

Figure 7.8. Semi-closed regenerated cycle with steam bottoming cycle.

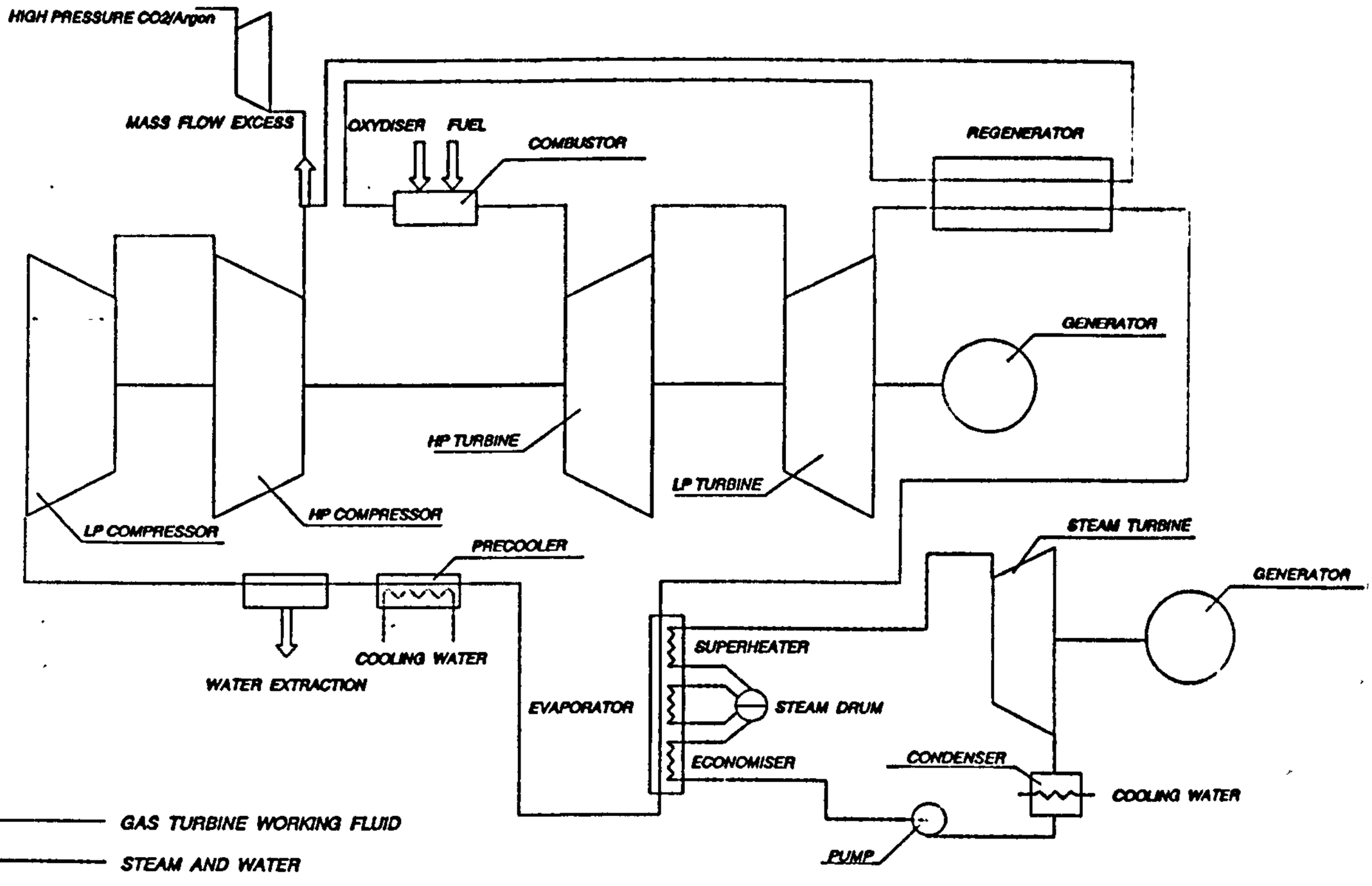

Figure 7.9. Semi-closed intercooled cycle with steam bottoming cycle.

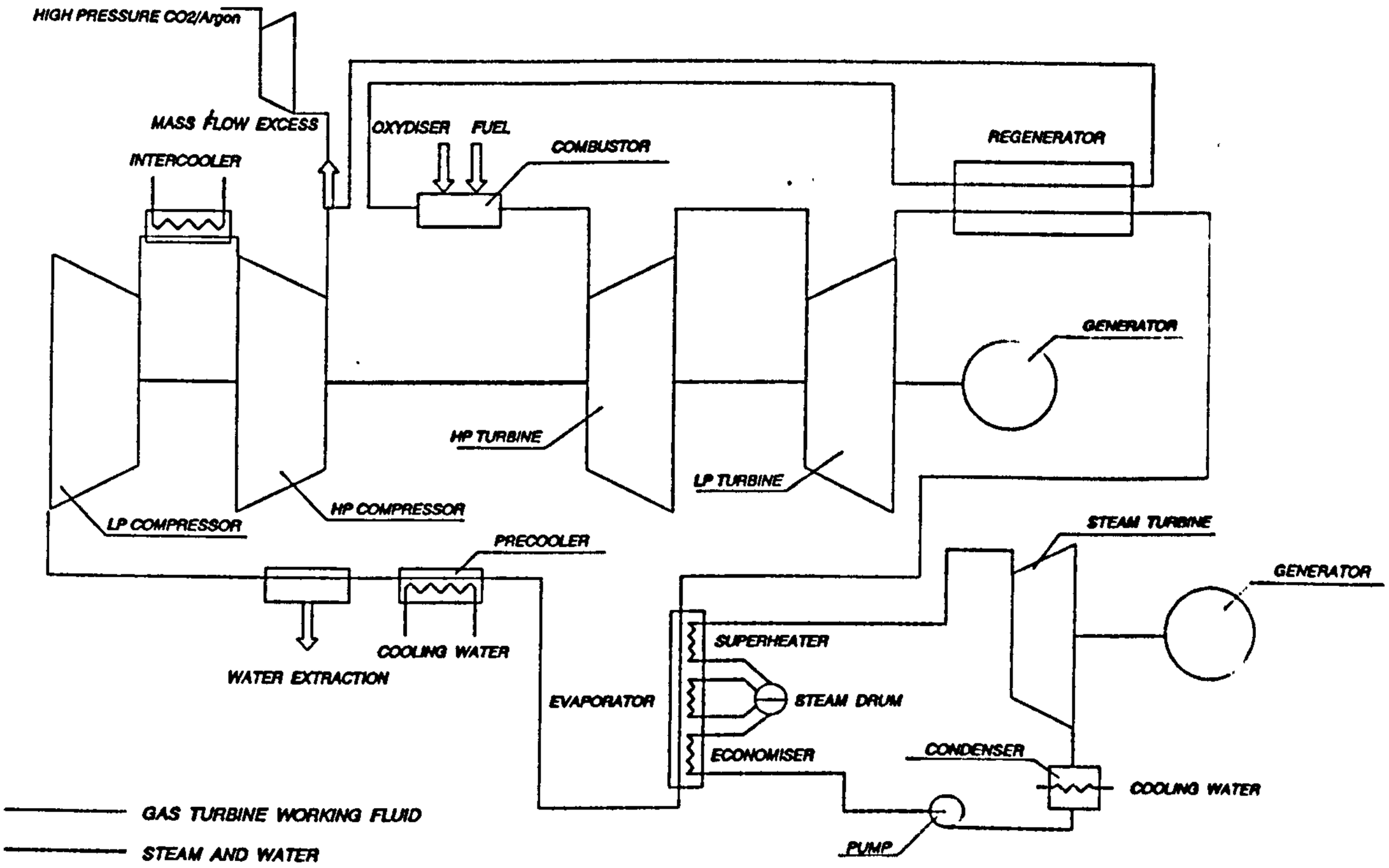

Figure 7.10. Semi-closed intercooled & recuperated cycle with steam bottoming cycle

7.9. PERFORMANCE COMPARISON OF THE POWER PLANT WITH CO_2 AND CO_2/ARGON AS WORKING FLUIDS

Initially both, pure carbon dioxide and a mixture of carbon dioxide and argon can be employed as working fluids. As it has been already mentioned, carbon dioxide will be the operating gas when the oxidizer is pure oxygen, and carbon dioxide/ argon if the oxidizer is a mixture of oxygen and argon (95%/5%). In both cases the oxygen comes from air separation, but in the second one the argon is left with the oxygen. The result is a more economical and simpler air separation process.

All the calculations, for the simple, intercooled, regenerated and intercooled & regenerated cycles, were done with both working fluids and a SOT of 1473 K. The results are presented in Appendix III for the case of pure oxygen oxidizer (CO_2 working fluid) and in App.IV for the oxygen/argon oxidizer (CO_2/Argon working fluid).

Figures 1, 25, 49 and 73 show the combined cycle thermal efficiency of the four cycles studied, considering the losses originated by the air separation process, carbon dioxide compression process, fuel compression process, etc., not only for the gas turbine but for the complete power plant, including also the energy required for the fuel gasification process. In all cases, the CO_2/Argon cycle has a slightly larger efficiency than the pure CO_2 one, as can be clearly seen when figures 25 of App.III and IV are compared.

Figures 2, 26, 50 and 74 are the combined cycle ideal thermal efficiency, where none of the losses inherent to the semi-closed cycle are considered. In this case there is almost no difference between the CO_2 and CO_2/Argon cycles. The conclusion is clear: the differences found when comparing figures 1, 25, 49 and 73 of App.III and IV are caused mainly by the excess energy required to separate the argon, and not by the different thermodynamic behaviour of the working fluid (additional 0.107 MJ/kg O_2 are required for the pure oxygen generation).

Figures 3, 27, 51 and 75 show the simple cycle thermal efficiency considering all the power plant losses. As for the combined cycle thermal efficiency, the CO_2/Argon cycle offers slightly larger values.

Figures 4, 28, 52 and 76 are the simple cycle ideal thermal efficiency. Again, when the air separation losses, etc. are not taken into account, CO_2 and CO_2/Argon cycles have the same performance.

Figures 5, 29, 53 and 77 are the complete power plant combined cycle specific power output (kW/kg/s). In parallel with the combined cycle efficiency the power output is slightly larger for the CO_2/Argon cycle.

Figures 6, 30, 54 and 78 present the combined cycle ideal specific power output (kW/kg/s), where the power required to compress the fuel and the excess CO_2 and to separate the oxygen or oxygen/argon is not considered. The difference between the CO_2 and CO_2/Argon cycles is negligible.

Figures 7, 31, 55 and 79 show the gas turbine specific power (kW/kg/s) and do not change significantly between App.III and IV.

A similar conclusion can be obtained when figures 8, 32, 56 and 80, that represent the steam turbine specific power output (kW/kg/s) and figures 9, 33, 57 and 81, that represent the gas turbine to steam turbine power ratio, of Appendices III and IV are compared.

Figures 10, 34, 58 and 82 give the auxiliary (fuel compression, air separation and excess carbon dioxide compression specific power) to useful power ratio. There is a clear difference between the CO_2 and CO_2/Argon cycles, with smaller values for the second case.

Figures 11, 35, 59 and 83 present the excess carbon dioxide or carbon dioxide/argon compression specific power (kW/kg/s), almost the same for both cases.

The main difference appears when figures 12, 36, 60 and 84, representing the oxygen or oxygen/argon separation specific power (kW/kg/s), are considered. When argon is present in the working fluid, the power required by the air separation process is lower, as can be clearly appreciated comparing Appendices III and IV.

Figures 13, 37, 61 and 85 are for the fuel compression specific power (kW/kg/s), and no major difference can be appreciated between the values calculated with CO_2 and with CO_2/Argon.

The same conclusion is obtained for the fuel to compressor inlet mass flow ratio (equivalent to the fuel to air ratio in open cycles) shown in figures 14, 38, 62 and 86 and for the gas turbine exit temperature (K), shown in figures 15, 39, 63 and 87.

The high pressure turbine design parameters are the same for both working fluids. Number of HPT stages (figures 16, 40, 64 and 88), HPT cooling bleed (% relative to compressor inlet mass flow, figures 17, 41, 65 and 89), HPT stators cooling bleed (% relative to compressor inlet mass flow, figures 18, 42, 66 and 90) and HPT rotor cooling bleed (% relative to compressor inlet mass flow, figures 19, 43, 67 and 91) are almost identical for Appendices III and IV.

The low pressure turbine behaviour is the same with CO_2 and with CO_2/Argon. Number of LPT stages (figures 20, 44, 68 and 92), turbine cooling bleed (figures 21, 45, 69 and 93), stator cooling bleed (figures 22, 46, 70 and 94) and rotor cooling bleed (figures 23, 47, 71 and 95) do not suffer variations with the change in working fluid.

The optimum steam turbine pressures, that maximise the combined cycle thermal efficiency, are also the same for the CO_2 and CO_2/Argon cycles, as shown in figures 24, 48, 72 and 96 of Appendices III and IV.

After the comparison, the main conclusion is that almost no differences in the performance results exist between the simulations carried out with CO_2 (Appendix III) and with CO_2/Argon (Appendix IV) for the four cycles considered: simple, intercooled, regenerated and intercooled & regenerated. Slightly higher simple and

combined cycle efficiency and specific power output were obtained using the mixture of carbon dioxide and argon, due to the lower energy required by the air separation process. In other areas, such as combustion, cooling, etc., the author has not identified any detrimental effect caused by the presence of argon. Therefore, the mixture of oxygen/argon as oxidizer, that ends up with the CO_2/Argon working fluid, is selected for further studies.

7.10. PERFORMANCE COMPARISON BETWEEN THE SIMPLE, INTERCOOLED, REGENERATED AND INTERCOOLED & REGENERATED CYCLES WITH CO_2/ARGON AS WORKING FLUID

Once the CO_2/Argon has been selected as the most adequate working fluid, in terms of performance and power plant complexity, it is necessary to decide the power plant arrangement. As mentioned earlier, simple, intercooled, regenerated and intercooled & regenerated cycles have been initially considered, always in the two spool-two shaft arrangement,[37] and fitted with a steam turbine bottoming cycle to evaluate the combined cycle performance.

Appendix IV shows the performance results of the complete power plant simulation, including the energy required for the coal gasification process as well as for the fuel compression, oxygen/argon separation and excess CO_2/Argon compression, when the SOT is 1473 K (conservative cycle concept). Appendix V considers the 1650 K SOT case (advance cycle concept).

7.10.1. PERFORMANCE STUDY FOR THE 1473 K SOT CYCLE (APPENDIX IV)

Figures 1, 25, 49 and 73 show the combined cycle thermal efficiency for the complete power plant. For the simple cycle arrangement the peak efficiency (η_{th}~ 0.35^{+}) is obtained at pressure ratios around 50. The intercooled cycle highest values (η_{th}~0.35^{-}) take place at a pressure ratio lower than 40 (LPC PR~3-3.5, HPC PR~ 12). For the regenerated cycle the peak values (η_{th} ~0.36) happen at pressure ratios around 30. Finally, the peak efficiencies for the intercooled & regenerated cycle (η_{th}~ 0.37^{-}) take place at pressure ratios slightly lower than 30 (LPC PR~2.5, HPC PR~ 11). The differences between the four configurations are not very large, and only the

---

[37] For the lowest pressures ratios, i.e. between 4 and 20, the one spool-single shaft configuration would be the right choice. But, as the preliminary studies demonstrated that the peak efficiencies take place at pressure ratios above 40, the complete study is carried out with the two spool - two shaft arrangement. It would have been possible to employ a two spool - three shaft configuration, with free power turbine, but, as this cycle will be mainly dedicated to the electricity generation, the two shaft arrangement seems to be more appropriate.

intercooled cycle offers a relatively poorer efficiency, while the intercooled & regenerated cycle has a better performance.

The combined cycle ideal thermal efficiency, shown in figures 2, 26, 50 and 74, has a maximum around 0.48-0.5 for the four power plant arrangements.

Figures 3, 27, 51 and 75 present the complete power plant simple cycle (gas turbine alone) thermal efficiency. The maximum efficiencies for the simple cycle configuration (η_{th}~0.16^{+}) are obtained at pressure ratios around 60-70. For the intercooled cycle, the peak values (η_{th} ~0.20^{-}) take place at pressure ratios larger than 80 (LPC PR~8, HPC PR~12). In the regenerated case, the maximum values (η_{th} ~ 0.23) are for pressure ratios around 20-25. For the intercooled & regenerated cycle the maximum efficiencies (η_{th} ~0.27) are for pressure ratios around 50, although there is a large region of relatively high thermal efficiency.

The simple cycle (gas turbine alone) ideal thermal efficiency, shown in figures 4, 28, 52 and 76, does not follow the same behaviour as the combined cycle, where the maximum values were the same for all the cycles. In this case the simple cycle is the lowest, with a value of η_{th} ~0.33^{-}. The intercooled has a peak ideal efficiency of η_{th} ~ 0.34^{+}. The regenerated cycle maximum values are around η_{th} ~0.35^{+}, and the intercooled & regenerated shows the best efficiency, with η_{th} ~0.40.

The complete plant combined cycle specific power output (kW/kg/s) is presented in figures 5, 29, 53 and 77. In the simple cycle arrangement the maximum values take place at low pressure ratios, while for the peak combined cycle efficiency pressure ratios the specific power output is around 325-350 kW/kg/s. The intercooled cycle has a larger specific power output, with values close to 400 kW/kg/s, and slightly lower (390 kW/kg/s) for the peak combined cycle efficiency points. The regenerated cycle has a very poor specific power output, with maximum figures around 285 kW/kg/s. The intercooled & regenerated arrangement offers slightly better values, that for the maximum combined cycle efficiency are around 300 kW/kg/s.

The combined cycle ideal specific power output (kW/kg/s) of figures 6, 30, 54 and 78, follows a parallel behaviour to the previous parameter, this one being, of course, larger, due to the no consideration of the auxiliary power requirements (coal gasification, fuel compression, oxygen/argon separation and excess CO_2/Argon compression).

Figures 7, 31, 55 and 79 show the gas turbine specific power output (kW/kg/s). The simple cycle configuration has the maximum, around 285 kW/kg/s, for the same pressure ratios where the combined cycle efficiency has the peak values. The intercooled cycle has the largest specific power output, with values over 370 kW/kg/s for pressure ratios larger than 100. For the region where the thermal efficiency was maximum, the specific power output is approximately 330 kW/kg/s. The regenerated cycle offers top specific power output of 285 kW/kg/s located in the pressure ratios where the maximum combined cycle thermal efficiencies take place. Finally, the intercooled & regenerated cycle largest specific power outputs, with values over 350

kW/kg/s, take place for very large pressure ratios. The specific power output for optimum thermal efficiency region is around 310 kW/kg/s. The main conclusion is that the differences in gas turbine specific power output, for the pressure ratios where the thermal efficiency is maximum, are not very large for the four cycles considered (285, 330, 285 and 310 kW/kg/s respectively)

The steam turbine specific power output (kW/kg/s) is presented in figures 8, 32, 56 and 80. For the simple cycle arrangement the maximum values (320 kW/kg/s) can be found at low pressure ratios, where the exit temperatures are larger. But for the pressure ratios where the combined cycle thermal efficiency is optimum, the specific power output is around 200 kW/kg/s. The behaviour for the intercooled cycle is almost the same as for the simple cycle, with very small differences and, although the pressure ratios where the optimum thermal efficiency is located are very different the value of the steam turbine specific power output is also around 200-210 kW/kg/s. The regenerated cycle shows a completely different panorama, with a very uniform specific power output. The maximum values, around 126 kW/kg/s, can be found at pressure ratios above 90, while for the maximum thermal efficiency region the figures would be 105-110 kW/kg/s. The scenario in the intercooled and regenerated cycle is similar to the regenerated case, with very small variations for the whole range of pressure ratios. The location of the peak values, around 85 kW/kg/s for LPC pressure ratios of 2-2.5, coincides in this cycle with the region of the maximum thermal efficiency.

Figures 9, 33, 57 and 81 show the gas to steam turbine power ratio. For the simple cycle configuration, a figure around 1.5 is obtained for the peak thermal efficiency region. A similar value is found for the intercooled cycle arrangement. For the regenerated cycle the ratio for the maximum thermal efficiency region is 2.5, increasing up to 3.5 for the intercooled & regenerated case.

The details of the auxiliary losses are presented in figures 10 to 13 for the simple cycle power plant arrangement, 34 to 37 for the intercooled cycle, 58 to 61 for the regenerated cycle and 82 to 85 for the intercooled & regenerated configuration. It is important to stress the large losses caused by the oxygen separation and fuel compression, as well as for the excess carbon dioxide compression at low pressure ratios, responsible all of them for the low performance exhibited by the different power plant configurations.

The fuel to compressor inlet mass flow is shown in figures 14, 38, 62 and 86 for the four cycles considered. The main characteristic is the large amount of fuel required, due to the low heating value, specially for the simple and the intercooled cycles.

The gas turbine exit temperature (K) is presented in figures 15, 39, 63 and 87. It is important to observe the large temperatures (up to 1200 K) found for the simple and intercooled cycles, with variations of 500 K for the pressure ratios considered. In the regenerated and intercooled & regenerated cycles case the exhaust temperatures are much lower and uniform (around 700-800 K for the regenerated and 600-700 K

for the intercooled & regenerated plant). The difficulty for the last two cycles will be located in the regenerator, with very high operating temperatures.

The HPT stage number and cooling bleed requirements are shown in figures 16 to 19, 40 to 43, 64 to 67 and 88 to 91. The relatively large cooling bleed flow requirements used in the simple and regenerative cycle arrangements is drastically reduced in the intercooled and intercooled & regenerated configurations, due to the decrease in the cooling flow temperature. In these two cycles the constant mass flow cooling lines are horizontal, due to the constant temperature for each HPC pressure ratio, independent on the LPC pressure ratio.

The LPT details are shown in figures 20 to 23, 44 to 47, 68 to 71 and 92 to 95. The most important characteristic is the large number of turbine stages required to drive the LPC and generate the power output. Although the number of stages is larger, due to the lower temperature, the cooling flow requirements are less than for the HPT. However this figure will be larger than for a similar turbine operating with air, became the temperature drop is lower in a turbine using CO_2 as working fluid. The iso-cooling lines are not completely horizontal for the intercooled and intercooled & regenerated cycles, due to the different LPT inlet temperatures.

The steam turbine optimum pressure is presented in figures 24, 48, 72 and 96 of appendix IV. The large exit temperatures of the first two cycles, simple and intercooled, make the optimum steam turbine pressure considered to be over 50 bars for most of the pressure ratios, with a much lower value for the regenerated and intercooled & regenerated cycles, where the values are around 10 bars.

7.10.2. PERFORMANCE STUDY FOR THE 1650 K SOT CYCLE (APPENDIX V)

The combined cycle thermal efficiency for the complete power plant running at 1650 K SOT is shown in figures 1, 25, 49 and 73 of App.V. The peak efficiency of the simple cycle arrangement peak efficiency (η_{th} ~0.36^{+}) is obtained at pressure ratios around 55. For the intercooled cycle the highest values (η_{th} ~0.36^{-}) are found at a pressure ratios slightly larger than 40 (LPC PR~3.5, HPC PR~12). In the case of the regenerated cycle the peak values (η_{th} ~0.38^{+}) happen at pressure ratios around 25-30. For the intercooled & regenerated cycle, the peak efficiencies (η_{th} ~0.39^{-}) take place at pressure ratios around 30 (LPC PR~2.5, HPC PR~12). The differences between the four cycles are larger than for the 1473 K SOT case. The intercooled & regenerated cycle has the best performance, slightly larger than the regenerated cycle, these two offering a combined cycle efficiency 2-2.5 points better than the simple cycle or intercooled cycle arrangements.

The combined cycle ideal thermal efficiency of figures 2, 26, 50 and 74, has a maximum around 0.50-0.52 for the four power plant arrangements, 2 points higher than the 1473 K case.

In figures 3, 27, 51 and 75 the complete power plant simple cycle (gas turbine alone) thermal efficiency can be observed. For the simple cycle configuration the maximum efficiencies (η_{th} ~0.17) are obtained at pressure ratios around 70-80. For the intercooled cycle, the peak values (η_{th} ~0.20^{+}) are located at pressure ratios larger than 90 (LPC PR~9, HPC PR~12). In the regenerated case the largest values (η_{th} ~ 0.23) are for pressure ratios around 25-30. The maximum efficiencies of the intercooled & regenerated cycle (η_{th} ~0.27) are for pressure ratios around 50, although there is an extensive region of high simple cycle thermal efficiency. When comparing these figures with the 1473 K SOT case the differences obtained are very small. The excess energy required to produce the additional fuel & oxygen, to increase the temperature from 1473 up to 1650 K, and the larger cooling flows cancel the benefits of having a higher SOT. Nevertheless, the rise in turbine exit temperature make the steam turbine bottoming cycle more effective, increasing the combined cycle thermal efficiency, as shown in the first paragraph of this section.

The simple cycle (gas turbine alone) ideal thermal efficiency is shown in figures 4, 28, 52 and 76. The simple cycle arrangement has the lowest value of the four power plant configurations, with a value of η_{th} ~0.33. The intercooled has a maximum ideal efficiency of η_{th} ~0.35^{+}. The regenerated cycle peak values are around η_{th} ~0.35^{+}, and the intercooled & regenerated offers the best efficiency, with η_{th} ~0.40^{+}.

The complete power plant combined cycle specific power output (kW/kg/s) is presented in figures 5, 29, 53 and 77 of App.V. In the simple cycle configuration the maximum values (over 430 kW/kg/s) take place at pressure ratios around 12, while for the pressure ratios where the peak combined cycle efficiencies are located, the specific power output is around 380-400 kW/kg/s. The intercooled cycle has a slightly larger maximum specific power output, with values close to 460 kW/kg/s, and above 450 kW/kg/s for the peak combined cycle efficiency cases. The regenerated cycle does not offer a good specific power output, with maximum figures around 340 kW/kg/s. The location of the maximum specific power output coincides with the maximum combined cycle thermal efficiency pressure ratios. The intercooled & regenerated arrangement has slightly better values than the regenerated cycle, with maximum values around 360 kW/kg/s, and figures around 350 kW/kg/s for the maximum combined cycle efficiency cases. The values found here are around 50 kW/kg/s larger than the ones obtained with the 1473 K SOT cycles.

The combined cycle ideal specific power output (kW/kg/s) of figures 6, 30, 54 and 78, follows a similar trend than the combined cycle specific power output, with values between 100 and 170 kW/kg/s larger than the previous case (1473 K SOT).

Figures 7, 31, 55 and 79 present the gas turbine specific power output (kW/kg/s). The simple cycle configuration has its maximum, around 315 kW/kg/s, for the same pressure ratios where the combined cycle efficiency has the peak values. The intercooled cycle has the highest specific power output, with values in excess of 420 kW/kg/s for very large pressure ratios. For the pressure ratios where the highest

combined cycle thermal efficiency occurs, the gas turbine specific power output is around 375 kW/kg/s. The regenerated cycle has its best gas turbine specific power outputs, 310-315 kW/kg/s, located close to the pressure ratios where the highest combined cycle thermal efficiencies take place. The intercooled & regenerated cycle largest specific power outputs, with values higher than 400 kW/kg/s, are located at pressure ratios over 100. The specific power output for the optimum combined cycle thermal efficiency region is around 360 kW/kg/s. In general, a better gas turbine specific power output has been found when the stator outlet temperature has been increased from 1473 K up to 1650 K.

The steam turbine specific power output (kW/kg/s) is shown in figures 8, 32, 56 and 80 of appendix V. The simple cycle arrangement presents peak values around 360 kW/kg/s for the lowest pressure ratios, where the exit temperatures are larger. However, for the pressure ratios where the combined cycle thermal efficiency is highest, the specific power output is around 240-250 kW/kg/s. As in the 1473 K SOT case, the steam turbine specific power output of the intercooled cycle is almost the same as in the simple cycle arrangement. For the pressure ratios where the combined cycle thermal efficiency is optimum, the steam turbine specific power output is also around 250 kW/kg/s. The regenerated cycle has a considerably lower and constant steam turbine specific power output, and the highest values, around 151 kW/kg/s, are located at pressure ratios above 100. For the peak thermal efficiency region the specific power outputs are between 137 and 141 kW/kg/s. For the intercooled & regenerated cycle the specific power output is also fairly low, with small variations for the whole range of pressure ratios. The largest values are located at LPC pressure ratios of 2-2.5, where the maximum combined cycle thermal efficiency is obtained.

Analogous to appendix IV, figures 9, 33, 57 and 81 of appendix V present the gas turbine to steam turbine power ratio. The simple cycle will have a ratio of 1.5 for the maximum combined cycle thermal efficiency pressure ratios. A slightly larger value, around 1.6, is obtained for the intercooled cycle configuration. For the regenerated cycle this ratio is 2.2, increasing up to 3 for the intercooled & regenerated one.

The calculations of the auxiliary losses are shown in figures 10 to 13 for the simple cycle power plant arrangement, 34 to 37 for the intercooled cycle, 58 to 61 for the regenerated cycle and 82 to 85 for the intercooled & regenerated configuration. The considerations are similar than the ones made for the 1473 K SOT case, with the figures having a very similar shape, but lower values relative to the useful power output.

The fuel to compressor inlet mass flow ratio can be found in figures 14, 38, 62 and 86. The quantities of fuel required are even larger than for the 1473 K SOT cycles, with relative values up to 15%.

The gas turbine exhaust temperature (K), prior to the bottoming cycle heat recovery steam generator, is shown in figures 15, 39, 63 and 87 of App.V. The values are, due to the increase in SOT, higher than the ones found in the previous

section. The simple and intercooled cycles have temperatures larger than 1300 K, with variations over 500 K for the range of pressure ratios considered. In the other two cycles the low pressure turbine discharge temperatures are considerably lower and more uniform for the complete range of pressure ratios (around 775-825 K for the regenerated and 650-750 K for the intercooled & regenerated plant).

The HPT number of stages and cooling bleeds for the 1650 K SOT cycles can be found in figures 16 to 19, 40 to 43, 64 to 67 and 88 to 91. The number of stages if very similar to the 1473 K SOT case, with a small reduction, due to the increase in the constant pressure specific heat and in the velocity of sound, although the flow through the turbine is lower, because the cooling flows are now considerably larger. For low cooling flow cycles, as the intercooled or intercooled & regenerated, the reduction in the number of stages with the increase in SOT is more evident.

The LPT characteristics are given in figures 20 to 23, 44 to 47, 68 to 71 and 92 to 95. As for the HPT, the number of stages is also very similar to the 1473 K case, and the cooling flows required are considerably larger, due to the higher temperature.

The values of the optimum pressure for the steam turbine are presented in figures 24, 48, 72 and 96 of appendix V. The highest value, found in the simple and intercooled cycles, is the same as for the 1473 K SOT case, due to the limitation in the maximum steam turbine operating temperature. For the regenerated and intercooled & regenerated cycle the steam cycle pressures are higher in the 1650 K SOT case, as the gas turbine exhaust temperature is now higher, but still lower than the maximum allowed by the steam turbine.

7.11. POWER PLANT PERFORMANCE IMPROVEMENTS

The efficiencies obtained with the configurations shown in figures 7.9 to 7.12 are considerably lower than those of a conventional open cycle gas turbine fitted with a steam turbine bottoming cycle.

Nevertheless, carbon dioxide is a fairly good working fluid, with low constant pressure specific heat at low temperatures and lower compressor discharge temperature than the correspondent open cycle. Therefore, compressor work will be lower. At high temperatures the large change in the ratio of specific heats increases considerably the C_P and, although the turbine exit temperature is much higher than with air, the turbine work is just slightly lower. Hence, the reason for such a low value in the combined cycle thermal efficiency must be found in the large amount of energy employed for the oxygen separation plant (0.935 MJ/kg O_2 for the case of pure oxygen and 0.828 MJ/kg O_2 for the case of Oxygen/Argon) and to compress the large quantities of fuel required, due to the low heating value. The energy required to compress the excess CO_2 up to 60 bar contributes as well to the reduction in the efficiency.

A way to recover part of this energy is to employ the nitrogen resultant from the liquefaction process. Large quantities of cryogenic N_2 are produced, which can be used to cool the entry of the gas turbine. Furthermore, after precooling the working fluid the nitrogen is still at very low temperature (of the order of 265-270 K), and can be passed through internal NGVs and blade passages, serving as turbine cooling, as shown in figure 7.13.

The implementation of the precooling system would require a considerable amount of development effort, due to the extremely low temperatures. However it seems feasible.

An additional benefit, if cryogenic nitrogen is employed just for precooling, is the reduction in the turbine cooling mass flow, due to the lower compressor temperatures.

The concept of blade cooling using an external flow is not new. Water, steam, etc. have been suggested as potential candidates.[38] In this case, the application of the cold nitrogen could be possible if there was no leakage. This will be difficult to achieve in a real machine, although it would yield an important benefit in terms of thermal efficiency and specific power output.

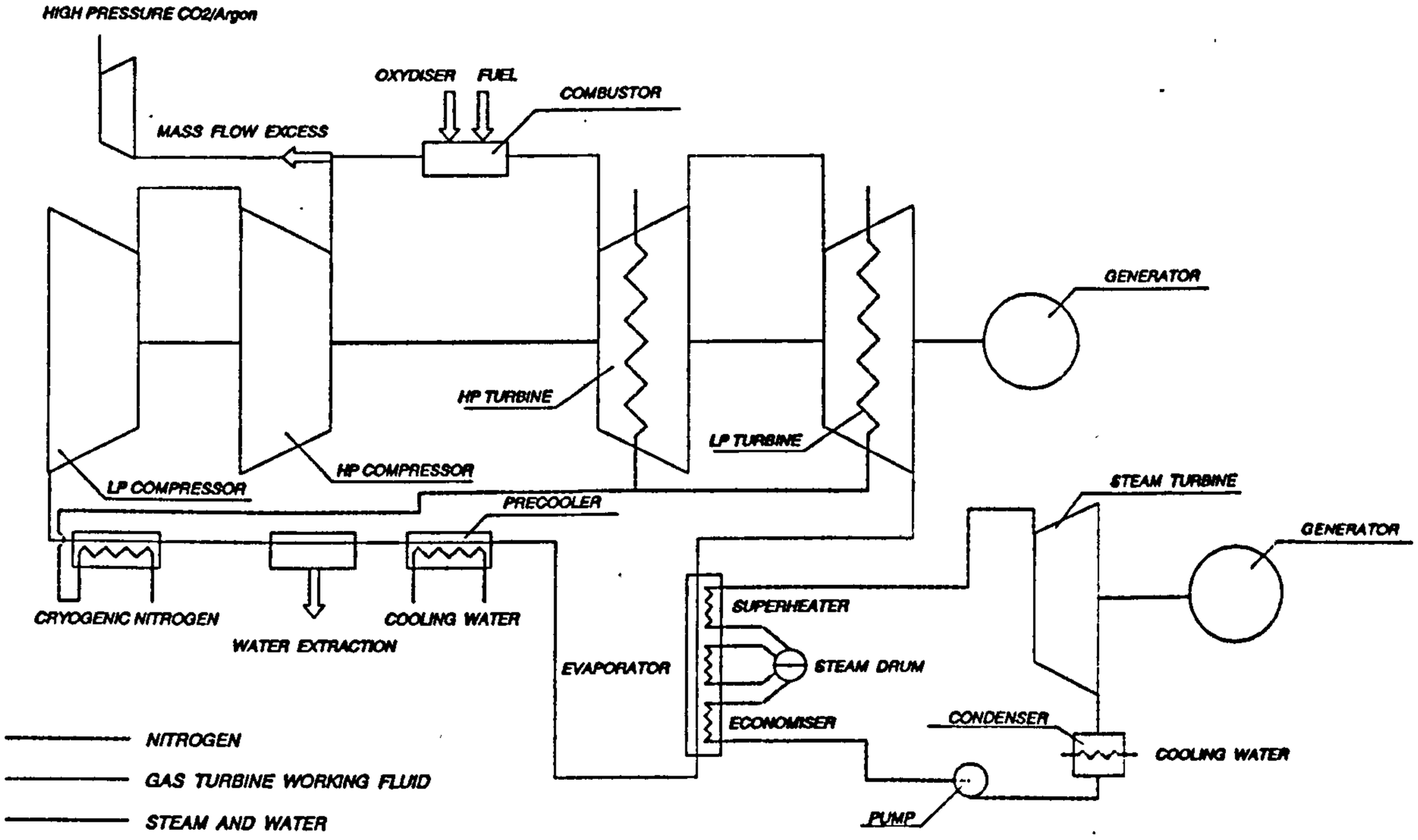

Figure 7.13. Semi-closed combined cycle with additional N_2 precooling and NGV internal cooling

[38] The General Electric 9001H, already in production, uses steam for the NGVs cooling.

An additional way of rising the efficiency and specific power output will be the modification of the fuel. An increase in the heating value, modifying, for example, the hydrogen and/or methane content, will have the benefit of decreasing the fuel compressor work. The excess carbon dioxide compression power will also change. But, due to the fact that we are trying to design close to the 60 bar compressor discharge pressure region, this effect will be negligible or none.

7.11.1. PERFORMANCE STUDY FOR THE 1650 K SOT CYCLES WITH CRYOGENIC NITROGEN PRECOOLING (APPENDIX VI)

The complete plant combined cycle thermal efficiency for the 1650 K SOT cycle with cryogenic nitrogen precooling is given in figures 1, 25, 49 and 73 of Appendix VI. The simple cycle arrangement optimum values (η_{th} ~0.38^{+}) are obtained at pressure ratios around 70. For the intercooled cycle the peak efficiencies (η_{th} ~0.38^{-}) are found at a pressure ratios over 55 (LPC PR~5.5, HPC PR~10-11). The regenerated cycle peak values (η_{th} ~0.40^{+}) are obtained at pressure ratios around 35-40 and, finally, the intercooled & regenerated cycle maximum combined cycle thermal efficiencies (η_{th} ~0.41^{-}) take place at pressure ratios above 40 (LPC PR~5, HPC PR~8-9). The use of cryogenic nitrogen precooling increases the combined cycle thermal efficiency in 2 points. This efficiency improvement is very important for these semi-closed cycles, which have an important deficit compared with the conventional open cycles burning high calorific value fuels.

The combined cycle ideal thermal efficiency of figures 2, 26, 50 and 74 achieves its peak value around 0.52-0.54 for the four cases, with an increase of 2 points relative to the 1650 K SOT conventional cycles.

Figures 3, 27, 51 and 75 give the complete power plant simple cycle (gas turbine alone) thermal efficiency. The simple cycle configuration maximum efficiencies (η_{th} ~ 0.22^{+}) are obtained at pressure ratios above 100. For the intercooled cycle, the peak values (η_{th} ~0.22^{-}) are also obtained at pressure ratios larger than 100 (LPC PR~12, HPC PR~12). The regenerated cycle has its maximum values (η_{th} ~0.28^{+}) for pressure ratios around 40 (LPC PR~5, HPC PR~8). The intercooled & regenerated cycle maximum efficiencies (η_{th} ~0.31^{+}) are found at pressure ratios above 60 (LPC PR~8, HPC PR~8). The difference between these and the conventional 1650 K SOT cases is large, with an improvement of 2 to 5 points in efficiency. The reason is the large increase in the T_4/T_2 ratio, that is a key parameter for the cycle performance. In an open cycle the rise in efficiency would be more important, because the larger fuel flow required in the precooling cycles does not have the penalty present in the semi-closed cycle gas turbine (air separation and low calorific value fuel compression).

The simple cycle ideal thermal efficiency is presented in figures 4, 28, 52 and 76 of App.VI. The simple cycle arrangement has the lowest value of the four power plant configurations, with a value of η_{th} ~0.37. The intercooled one has a maximum

ideal efficiency of η_{th} ~0.39. The regenerated cycle peak values are around η_{th} ~0.41, and the intercooled & regenerated offers the best efficiency, with η_{th} ~0.45-.

The complete power plant combined cycle specific power output (kW/kg/s) is given in figures 5, 29, 53 and 77. The simple cycle arrangement has the maximum values (over 480 kW/kg/s) at pressure ratios around 20-25, while for the pressure ratios where the peak combined cycle efficiencies are found, the specific power output is around 460-470 kW/kg/s. The intercooled cycle has larger maximum values, around 500 kW/kg/s, and 480-490 kW/kg/s for the pressure ratios where the combined cycle efficiency is optimum. The explanation for the unconventional shape of the surface is easy: for the lowest LPC pressure ratios the temperature at the exit of this component is not high enough to have a standard intercooler, therefore the arrangement is of the simple cycle type. The regenerated cycle offers a poor specific power output, having the maximum values around 360-380 kW/kg/s for a very wide range of pressure ratios. Finally, the specific power output obtained with the intercooled & regenerated cycle arrangement has its peak values, around 400 kW/kg/s, for high pressure ratios, while for the pressure ratios where the maximum efficiencies are located the specific power output is around 380-390 kW/kg/s. The increase, relative to the 1650 K SOT conventional cycle, is approximately 30-40 kW/kg/s.

The combined cycle ideal specific power output (kW/kg/s) of figures 6, 30, 54 and 78, follows a similar trend than the combined cycle specific power output, offering peak values around 150-175 kW/kg/s larger than the maximum found in that case.

The specific power output (kW/kg/s) of the gas turbine alone is shown in figures 7, 31, 55 and 79. The simple cycle configuration has a maximum value around 420 kW/kg/s, coinciding with the pressure ratios of maximum combined cycle thermal efficiency. The intercooled cycle has the highest gas turbine specific power outputs, with values close to 500 kW/kg/s for pressure ratios over 100. For the pressure ratios where the peak combined cycle thermal efficiency occurs the gas turbine specific power output is around 430 kW/kg/s. The highest values for the regenerated cycle, 400 kW/kg/s, are located at pressure ratios slightly larger than the ones where the maximum combined cycle thermal efficiencies take place. The specific power output of the intercooled & regenerated cycle has its peak value, around 470 kW/kg/s, for pressure ratios in excess of 100, with figures close to 400 kW/kg/s for the region of optimum combined cycle thermal efficiency. An average improvement of 40 kW/kg/s has been obtained relative to the conventional cycles operating at 1650 K SOT.

The specific power output (kW/kg/s) of the steam turbine bottoming cycle is presented in figures 8, 32, 56 and 80 of Appendix VI. In the simple, intercooling and intercooling & regenerated cycle arrangements the values are basically the same as the ones obtained with the non-precooling 1650 K SOT cycles. For the regenerated cycle a similar behaviour is also obtained, although the values are now slightly lower, with a decrease in the steam turbine specific power output of 20 kW/kg/s.

Figures 9, 33, 57 and 81 show the gas turbine to steam turbine power ratio. The simple cycle configuration will have a ratio of 2 for the pressure ratios of maximum combined cycle thermal efficiency, growing up to 2.2 for the intercooled cycle. In the regenerated cycle the ratio for the optimum combined cycle efficiency is 3.25, with values around 4-4.5 for the intercooled & regenerated arrangement.

The auxiliary losses (kW/kg/s), including the excess CO_2/Argon compression, oxygen separation and fuel compression, are shown in figures 10 to 13 for the simple cycle power plant arrangement, 34 to 37 for the intercooled cycle, 58 to 61 for the regenerated cycle and 82 to 85 for the intercooled & regenerated configuration. The general behaviour is very similar to the one obtained in the conventional 1650 K SOT cycles of App.V, although the losses are now lower.

The fuel to compressor inlet mass flow is given in figures 14, 38, 62 and 86. In the non-intercooled cycles the fuel required is now larger than in the conventional 1650 K SOT cycles, as the compressor discharge temperature is lower. In the intercooled cycles there will be no change, because the temperature at the entry of the combustor has not decreased due to the presence of the cryogenic nitrogen precooler. In the case of the intercooled cycle there is a clear discontinuity, caused, as explained before, by the impossibility of having an intercooler when the temperature at the exit of the LPC is not high enough.

The gas turbine exit temperature (K), prior to the HRSG can be observed in figures 15, 39, 63 and 87. The values are very similar to the ones obtained for the non-precooled 1650 K SOT cycles, with minor differences caused by the differences in compressor work, cooling mass flows and temperatures.

The number of stages and cooling bleeds of the high pressure turbine are given in figures 16 to 19, 40 to 43, 64 to 67 and 88 to 91. The number of stages for the simple and regenerated cycle arrangements is lower than for the non cryogenic precooling case, due, basically, to the reduction in the cooling flows. The intercooler and intercooler & regenerated cycles have similar figures in the 1650 K SOT conventional cycles of App.V and in the 1650 K SOT N_2 cryogenic precooling cycles because the behaviour and cooling requirements of the high pressure spool are the same.

The low pressure turbine number of stages and cooling flows are presented in figures 20 to 23, 44 to 47, 68 to 71 and 92 to 95. The conclusions are the same as the ones obtained for the HPT: in the simple and regenerated configurations the number of stages and cooling flows are lower than in the 1650 K SOT conventional cycles, while for the intercooler and intercooler & regenerated cycles the values are the almost the same with and without cryogenic precooler.

The optimum steam turbine pressure is presented in figures 24, 48, 72 and 96. The values are, again, similar to the ones got in App.V, as the exhaust temperatures are roughly the same.

7.11.2. PERFORMANCE STUDY FOR THE 1650 K SOT CYCLES WITH CRYOGENIC NITROGEN PRECOOLING AND NGVs NITROGEN INTERNAL COOLING (APPENDIX VII)

In these cycles, along with N_2 cryogenic precooling, the stators of the turbine will not require compressor cooling flow, because the nitrogen used for the precooling will be employed afterwards in the NGVs. This technique will have an improvement in the performance of the machine.

The results of the simple, intercooler, regenerated and intercooled & regenerated power plant arrangements are given in appendix VII. In general the differences between having the cryogenic precooling with and without NGV nitrogen internal cooling are relatively small. In terms of efficiency the gain is smaller than one point. The improvement in combined cycle specific power output is around 30-40 kW/kg/s, with larger values in both, gas and steam turbine. The most clear gain is, of course, in the cooling flow requirements, with an over 50% reduction relative to the cycle without internal cooling. The reason for the relatively low improvement is clear: the decrease in cooling flow requires an additional fuel and oxygen injection, because the mass flow through the core will be larger. Therefore, although the power output increases, the auxiliary power required by the low heating value fuel compressor and by the air separation plant will also be larger. The ratio of auxiliaries to useful power ratio decreases, but not enough to have a noticeable effect on the combined cycle thermal efficiency. In a conventional open cycle gas turbine, where the high heating value fuel requires very small power for compression, the improvement caused by a reduction larger than 50% in the total amount of cooling flow will be very significant.

7.12. POWER PLANT SELECTION

Once all the power plant arrangements have been examined, the final design point selection should be carried out. Two cycles will be chosen: one representing the conservative approach and other for the advance cycle technology.

Only the combined cycle arrangement, with the simple cycle gas turbine fitted with a steam turbine bottoming cycle, will be considered. The main reason is the extremely low thermal efficiency of the CO_2/Ar semi-closed cycle gas turbine, except for the intercooled & regenerated configuration, that has a peak value of 0.27, also considerably lower than the homologous advanced open cycle machines.

7.12.1. CONSERVATIVE CYCLE SELECTION

The cycles running at a design SOT of 1473 K, described in section 7.10.1 and Appendix IV, had a very similar complete plant combined cycle thermal efficiency and specific power output. The intercooled & regenerated cycle has a slightly better

efficiency, with the intercooled cycle showing the worst performance. However, the specific power output is larger for the intercooled and simple cycles, with lower values for the other two. The already complex cycle, due to the new technologies involved in its design and development, together with the substantial deterioration of the intercooler and regenerator during normal operation, that can modify the performance results shown in section 7.9., will favour the selection of the simple cycle machine. The overall pressure ratio would be close to 60, to simplify, or eliminate, the excess CO_2/Argon compression system.

7.12.2. ADVANCED CYCLE SELECTION

These cycles, operating at a design SOT of 1650 K and with the possibility of using a cryogenic nitrogen precooler and a nitrogen turbine stator cooling, are described in sections 7.10.2 (standard cycle), 7.11.1 (with cryogenic precooler) and 7.11.2 (with cryogenic precooler & NGVs internal cooling).

Bearing in mind that these cycles would be developed in several years, the possibility of using the precooler and the turbine stator internal cooling seems feasible.

The efficiency and specific power output combination of the simple cycle tend to favour this arrangement, although the intercooled & regenerated configuration is also very attractive. Due to the new and advanced technologies involved in the design and development of such power plants, and considering these as cycles for the future, it will be interesting to evaluate both possibilities, unless the off-design analysis favour, clearly, one of them.

CHAPTER 8

OFF-DESIGN PERFORMANCE OF CO_2/ARGON SEMI-CLOSED CYCLES

8.1. INTRODUCTION

As it was outlined in chapter 7, after a preliminary selection of a cycle design point, the off-design study should be carried out in order to verify that the performance requirements for all the representative operating points of the machine is fulfilled. The necessity of variable geometry (variable compressor and/or turbine stators, variable bleed valves, ...) will be also determined during this exercise.

In an open cycle the changes in compressor inlet conditions (pressure and temperature) are significant. However, in the semi-closed cycles the inlet conditions are fairly stable, depending only on the water used in the precooler. For that reason, while for open cycles variations in ambient temperature between -20°C and 50°C and pressure between 110 kPa and 75 kPa can take place, for semi-closed cycles the inlet temperature will be fairly constant, with oscillations of ±10 K as an average. For the same reason, if an intercooler is employed, the gas exit temperature will also be very stable, with a variation of ±10 K. The pressure will also be constant and, although the closed cycles can change the power output just by increasing the pressure level (hence the mass flow) across the cycle, that is not the case for the semi-closed cycle considered here. The reason is the necessity of water condensation before entering the LPC. Small pressure changes could be made but, initially, this situation will not be considered.

In the case of the semi-closed cycle employing cryogenic nitrogen for additional precooling, the inlet temperature will change according to the amount of fuel burnt.

8.2. CYCLES CONSIDERED FOR THE OFF-DESIGN STUDY

Two cycles have been considered for the **preliminary off-design** study:

- Two spool - three shaft gas turbine with a design SOT of 1473 K (**CYCLE I:** LP compressor - HP compressor - combustor - HP turbine - LP turbine - Power turbine).
- Two spool - two shaft gas turbine with a design SOT of 1473 K (**CYCLE II:** LP compressor - HP compressor - combustor - HP turbine - LP turbine)

For the **detailed off-design** three cycles have been selected:

- Two spool - two shaft gas turbine with a design SOT of 1650 K (**CYCLE III:** LP compressor - HP compressor - combustor - HP turbine - LP turbine)
- Two spool - two shaft gas turbine with cryogenic N_2 precooler, N_2 turbine stator internal cooling and design SOT of 1650 K (**CYCLE IV:** Nitrogen precooler - LP compressor - HP compressor - combustor - HP turbine - LP turbine)
- Two spool - two shaft intercooled & regenerated gas turbine with cryogenic N_2 precooler, N_2 turbine stator internal cooling and design SOT of 1650 K (**CYCLE**

V: Nitrogen precooler - LP compressor - intercooler - HP compressor - cold side of regenerator - combustor - HP turbine - LP turbine - hot side of regenerator)

During the design point selection, carried out in the previous chapter, the component efficiencies were the same for the conservative and advanced technology cycles. However, for the final study, some minor modifications will be introduced in order to consider the possible improvement in the turbomachinery associated with the advanced technology.

The performance parameters, at design point, employed in these five cycles have been:

TABLE 8.I: DESIGN POINT PERFORMANCE PARAMETERS

	I	II	III	IV	V
Low pressure compressor total inlet temperature (K)	300	300	300	216	237
Inlet pressure losses (%)	0.50	0.50	0.50	0.50	0.50
Low pressure compressor adiabatic efficiency[1] (%)	85.8	85.8	87.9	88.1	88.2
Low pressure compressor pressure ratio	6.00	6.00	7.00	5.00	5.00
Low pressure compressor surge margin (%)	30.0	30.0	42.0	37.0	37.0
Intercompressor casing pressure losses (%)	0.20	0.20	0.20	0.20	0.20
High pressure compressor adiabatic efficiency[2] (%)	85.8	85.8	86.9	86.2	86.2
High pressure compressor pressure ratio	8.00	8.00	8.00	12.0	12.0
High pressure compressor surge margin (%)	33.0	33.0	45.0	50.0	50.0
LPT blade cooling extraction point, as per $(H_{255}-H_{25})/(H_3-H_{25})*100$	45.0	45.0	45.0	45.0	45.0
Polytropic efficiency loss in the LPT cooling bleed due to walls (%)	5.00	5.00	5.00	5.00	5.00
Excess mass flow compressor polytropic efficiency (%)	85.0	85.0	85.0	85.0	85.0

[1] As the development would take place in not less than 10 years, a 2% improvement in LPC polytropic efficiency has been considered in the cycles selected for the final off-design study.

[2] As the development would take place in not less than 10 years, a 2% improvement in HPC polytropic efficiency has been considered in the cycles selected for the final off-design study.

External consumption maximum bleed (%)	1.00	1.00	1.00	1.00	1.00
Combustor efficiency (%)	99.9	99.9	99.9	99.9	99.9
Combustor & diffuser pressure losses (%)	5.00	5.00	4.50	4.50	4.50
Burner outlet temperature (K)	1510	1510	1720	1650	1650
Stator outlet temperature (K)	1473	1473	1650	1650	1650
High pressure turbine polytropic efficiency (%)	87.9	87.9	87.9	87.7	87.7
High pressure shaft friction losses (%)	0.10	0.10	0.10	0.10	0.10
High pressure shaft power off-take & additional losses (%)	0.40	0.40	0.40	0.40	0.40
HPT nozzle guide vanes metal temperature[3] (K)	1100	1100	1100	1100	1100
HPT blade metal temperature[4] (K)	1075	1075	1075	1075	1075
HPT stage loading ($\Psi = \Delta H/U^2$)	1.70	1.70	1.70	1.70	1.70
HPT blade speed (M_U)	0.50	0.50	0.50	0.50	0.50
HPT nozzle guide vanes cooling technology	FCFC	FCFC	FCFC	FCFC	FCFC
HPT blades cooling technology	FCFC	FCFC	FCFC	NIC	NIC
Low pressure turbine polytropic efficiency (%)	87.6	89.1	89.2	89.3	89.3
Low pressure shaft friction losses (%)	0.10	0.10	0.10	0.10	0.10
Low pressure shaft power off-take & additional losses (%)	0.10	0.30	0.30	0.30	0.30
LPT nozzle guide vanes metal temperature[5] (K)	1075	1075	1075	1075	1075
LPT blade metal temperature[6] (K)	1050	1050	1050	1050	1050

[3] The HPT NGVs metal temperature will be reduced from 1100 K down to 1050 K if sulphur becomes a problem.

[4] The HPT blade metal temperature will be reduced from 1075 K down to 1025 K if sulphur becomes a problem.

[5] The LPT NGVs metal temperature will be reduced from 1075 K down to 1025 K if sulphur becomes a problem.

[6] The LPT blade metal temperature will be reduced from 1050 K down to 1000 K if sulphur becomes a problem.

LPT stage loading ($\Psi=\Delta H/U^2$)	1.70	1.70	1.70	1.70	1.70
LPT blade speed (M_U)	0.45	0.45	0.45	0.45	0.45
LPT nozzle guide vanes cooling technology	FCFC	FCFC	FCFC	FCFC	FCFC
LPT blades cooling technology	FCFC	FCFC	FCFC	NIC	NIC
LPT exhaust guide vanes & diffuser pressure losses (%)	N/A	0.5	0.5	0.5	0.5
Power turbine polytropic efficiency	88.4	N/A	N/A	N/A	N/A
Power turbine shaft friction losses (%)	0.10	N/A	N/A	N/A	N/A
Power turbine shaft power off-take & additional losses (%)	0.20	N/A	N/A	N/A	N/A
PT nozzle guide vanes metal temperature[7] (K)	1075	N/A	N/A	N/A	N/A
PT blade metal temperature[8] (K)	1050	N/A	N/A	N/A	N/A
PT stage loading ($\Psi=\Delta H/U^2$)	1.70	N/A	N/A	N/A	N/A
PT blade speed (M_U)	0.40	N/A	N/A	N/A	N/A
PT nozzle guide vanes cooling technology	FCFC	N/A	N/A	N/A	N/A
PT blades cooling technology	FCFC	N/A	N/A	N/A	N/A
PT exhaust guide vanes & diffuser pressure losses (%)	0.50	N/A	N/A	N/A	N/A
Generator losses (%)	2.00	2.00	2.00	2.00	2.00
Bottoming cycle heat exchanger pressure losses (%)	5.00	5.00	5.00	5.00	5.00
Minimum temperature at the exit of the bottoming cycle heat exchanger (K)	420	420	420	420	420
Precooler pressure losses (%)	2.00	2.00	2.00	2.00	2.00
Nozzle pressure ratio	1.02	1.02	1.02	1.02	1.02

[7] The PT NGVs metal temperature will be reduced from 1075 K down to 1025 K if sulphur becomes a problem.

[8] The PT blade metal temperature will be reduced from 1050 K down to 1000 K if sulphur becomes a problem.

8.3. PRELIMINARY OFF-DESIGN STUDIES

Initially, a simple simulation was run for the first two configurations, operating at a SOT of 1200°C. The exercise was performed **without any variable geometry** in the turbomachinery, to evaluate the necessity of this feature, as well as the general behaviour of the machine in simple (gas turbine) and combined cycle (gas+steam turbine) arrangement.

The running lines of the compressors are shown in figures 8.1 to 8.4, with the resultant surge margin plotted in figures 8.11 and 8.12. Looking at these results it is clear that the LPC will need variable geometry to comply with the restriction of a minimum surge margin of 10%. Initially, the HPC will not require variable stators, although a more detailed study would be needed prior to a final decision of having a high pressure compressor with variable geometry, anti-surge valves, or other solution to prevent surge.

Simple and combined cycle thermal efficiency[9] and specific power output are plotted in figures 8.5 to 8.8. The value of the simple cycle thermal efficiency is too low for an industrial machine. The combined cycle offers a better performance, although still far from the 60% obtained with a modern power plant.

The relative power for both, simple and combined cycles, is shown in figures 8.9 and 8.10 respectively, taking as a baseline the design power of CYCLE I.

The exhaust temperature is plotted in figure 8.13.

---

[9] In both, preliminary and final off-design assessments, the power required to compress the excess CO_2 up to 60 bars, the one needed for the air liquefaction, the additional power required to liquefy the air used by the coal gasifier burner (50% relative to the air employed by the gas turbine), as well as the energy necessary to compress the low calorific value synthetic gas fuel, have been considered for the thermal efficiency calculations. In some studies and papers related with low calorific value gases, the supplementary energy required to generate and compress them is not considered, making the efficiency figure larger than it is in reality.

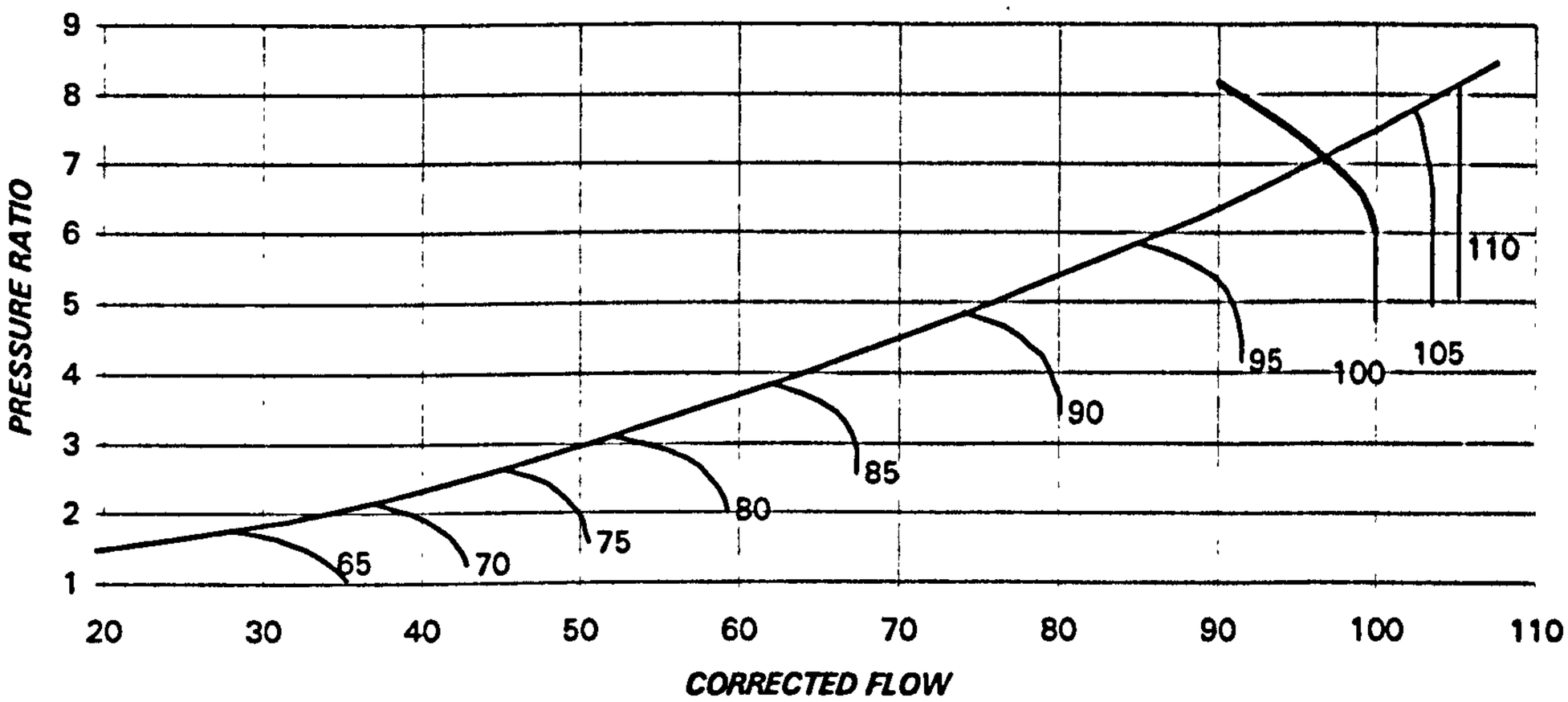

Figure 8.1. Low pressure compressor operating line (CYCLE I)

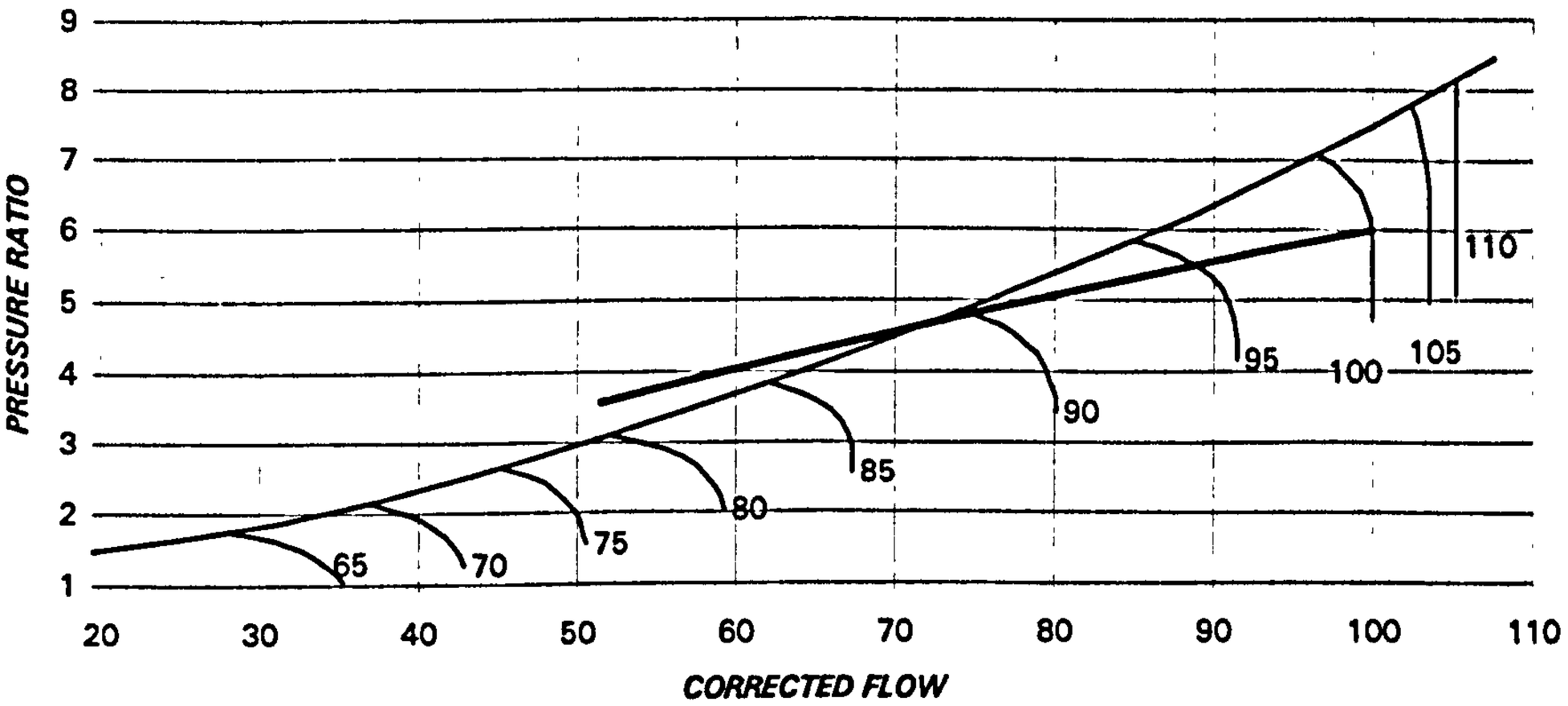

Figure 8.2. Low pressure compressor operating line (CYCLE II)

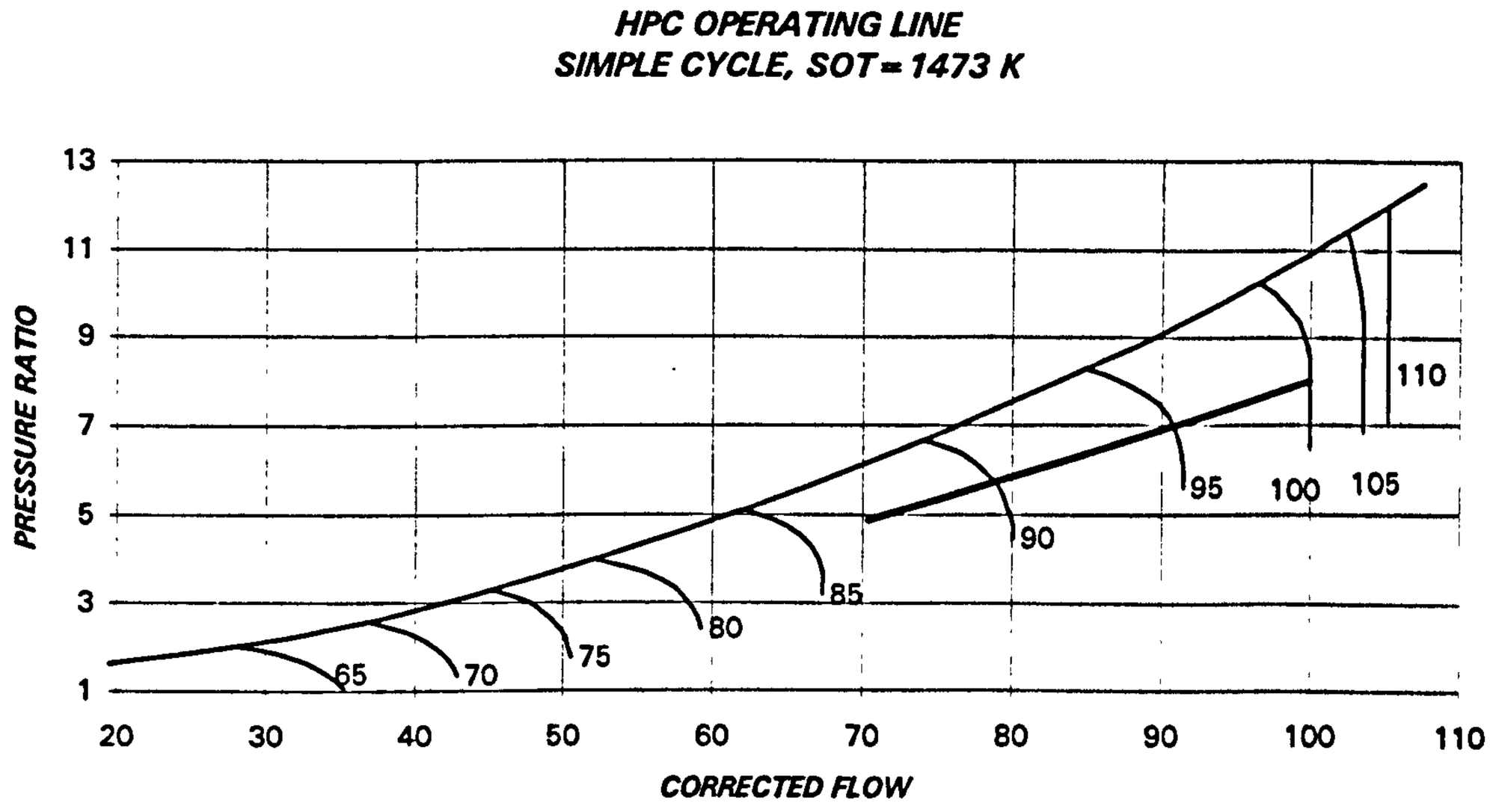

Figure 8.3. High pressure compressor operating line (CYCLE I)

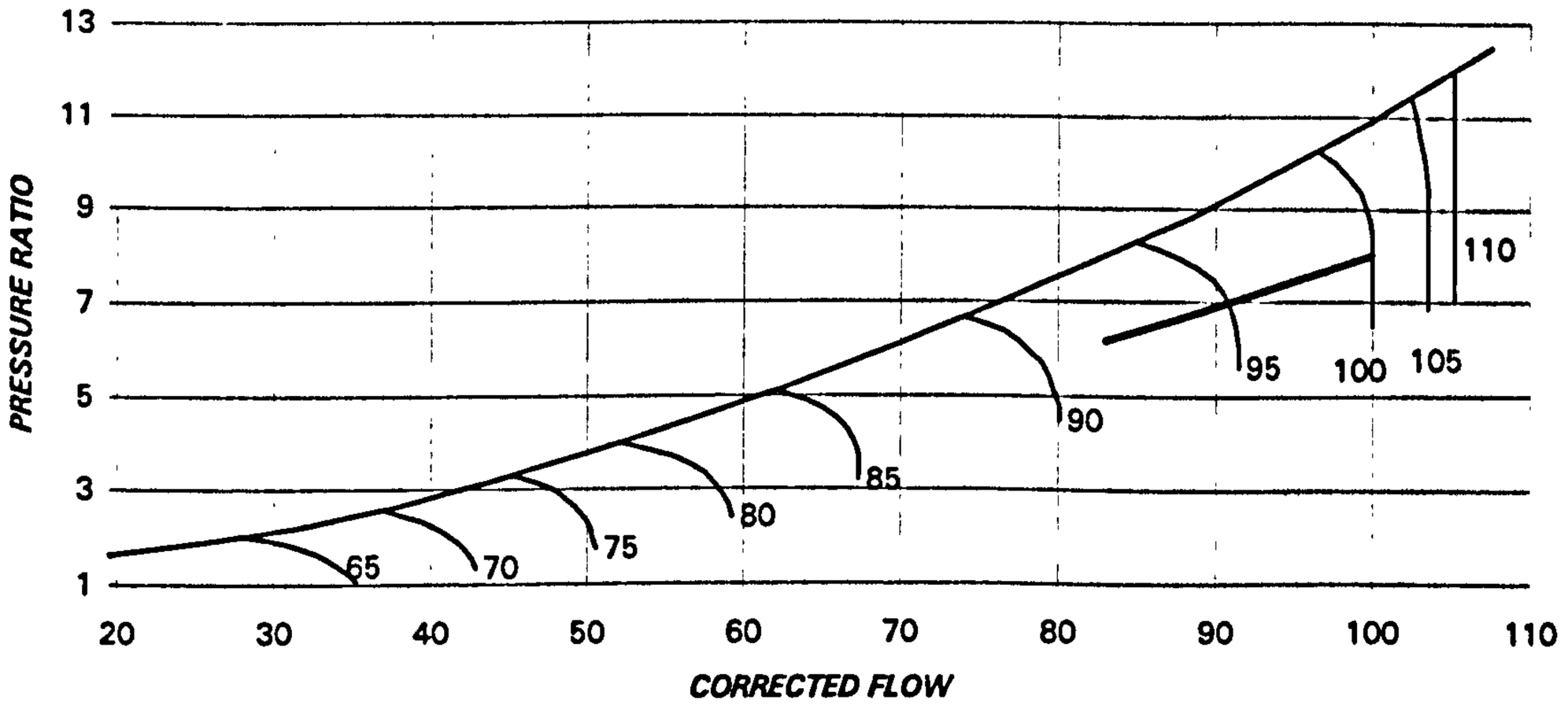

Figure 8.4. High pressure compressor operating line (CYCLE II)

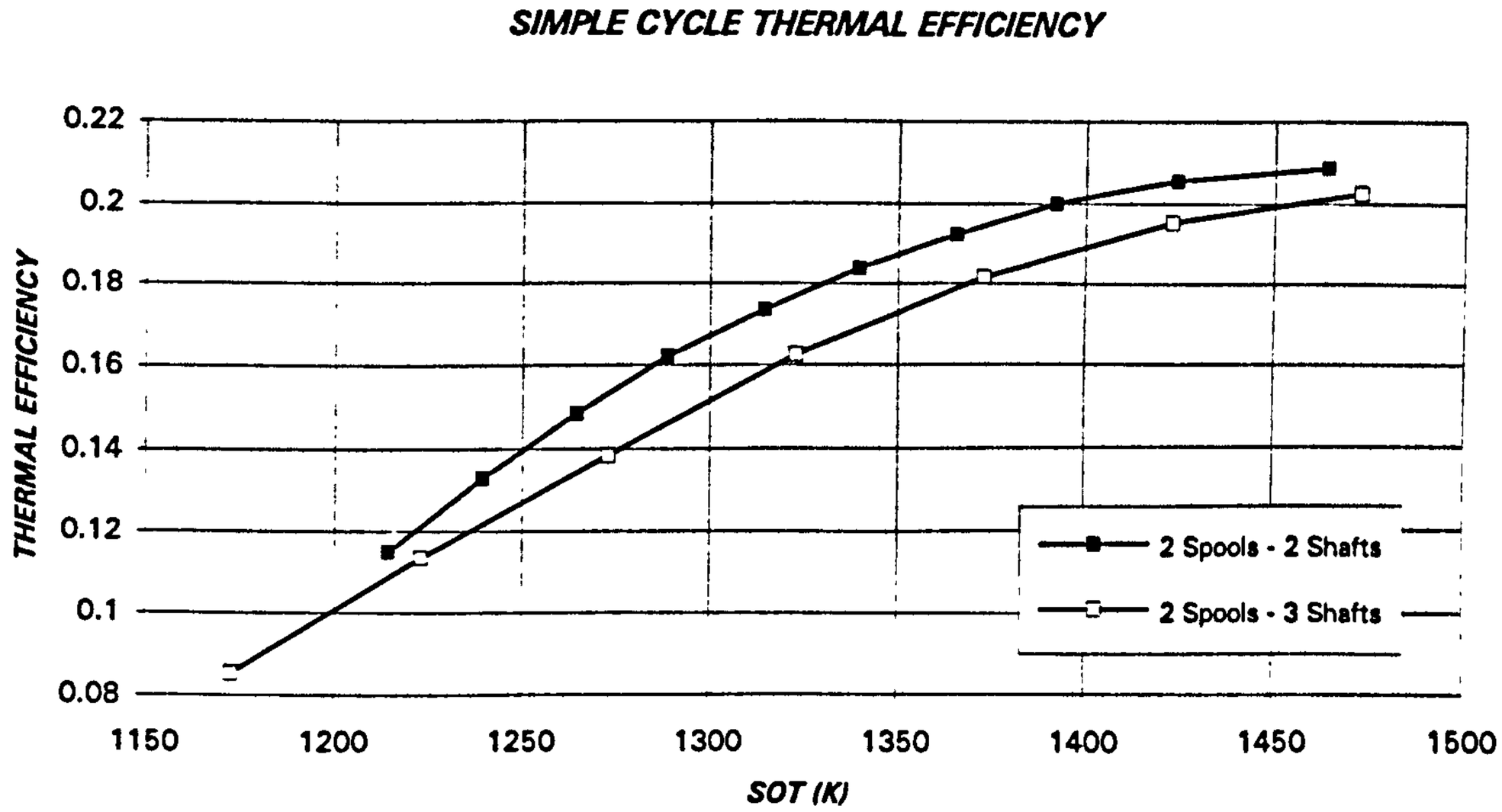

Figure 8.5. Simple cycle thermal efficiency (CYCLES I and II)

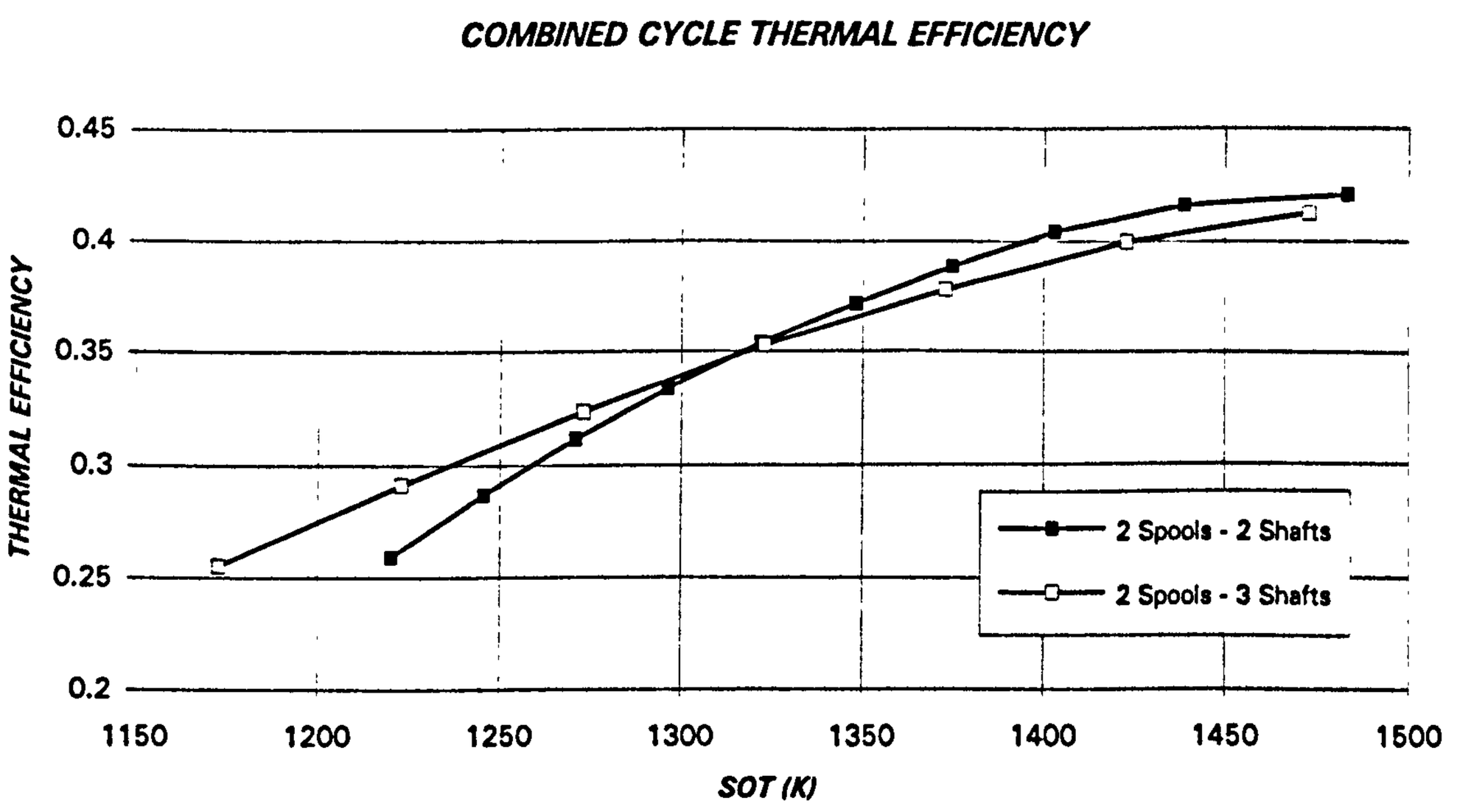

Figure 8.6. Combined cycle thermal efficiency (CYCLES I and II)

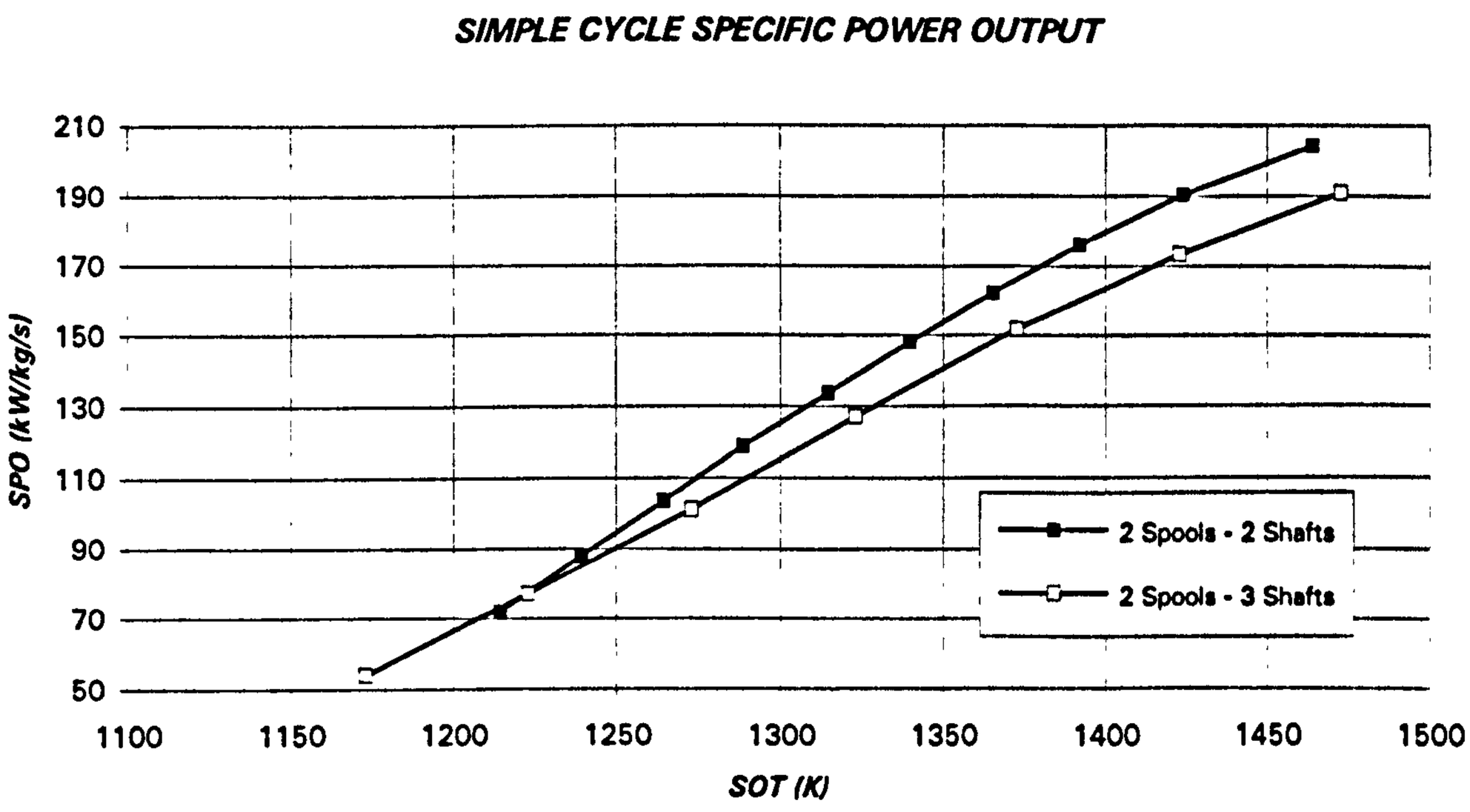

Figure 8.7. Simple cycle specific power output (kW/kg/s) (CYCLES I and II)

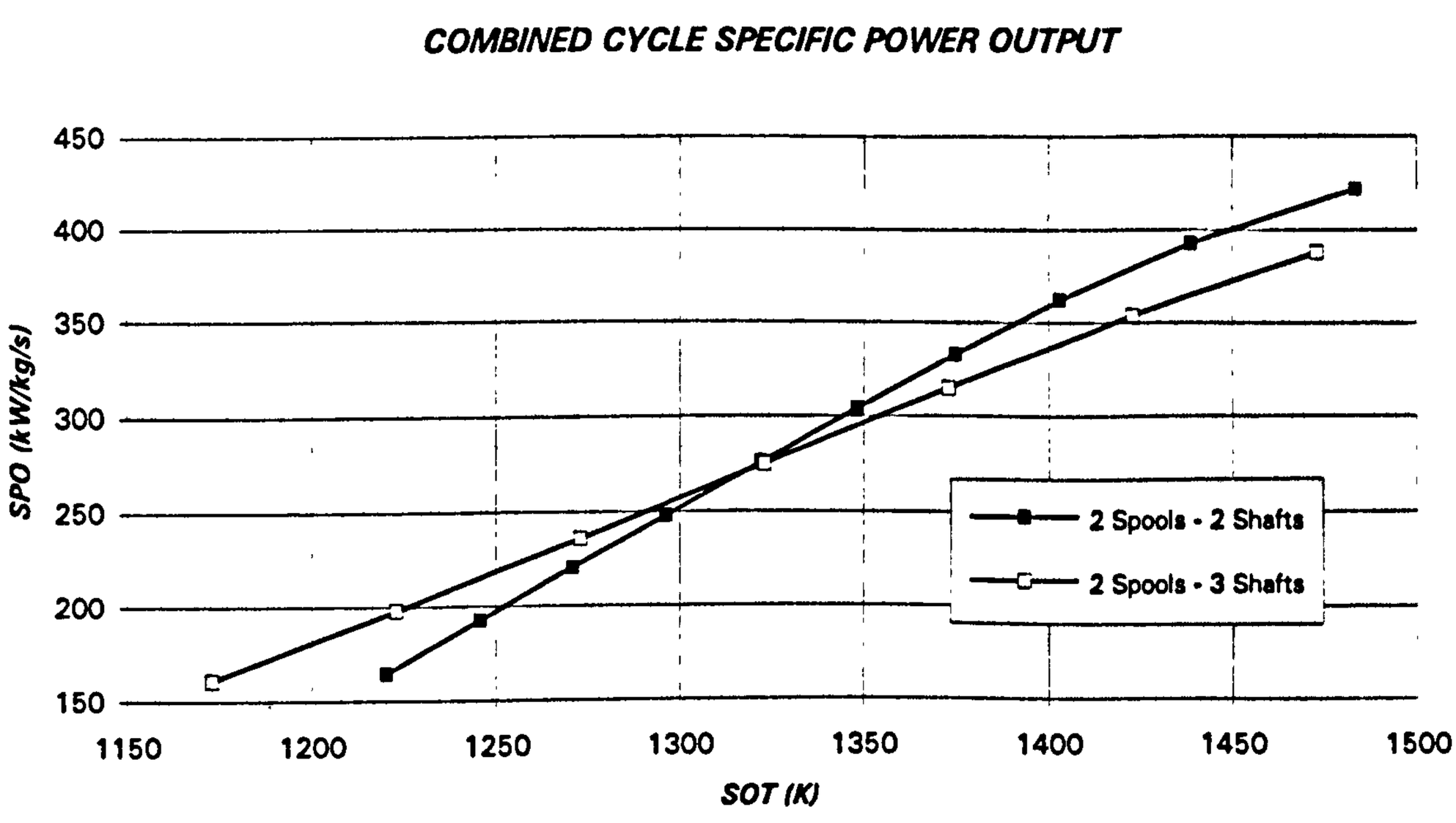

Figure 8.8. Combined cycle specific power output (kW/kg/s) (CYCLES I and II)

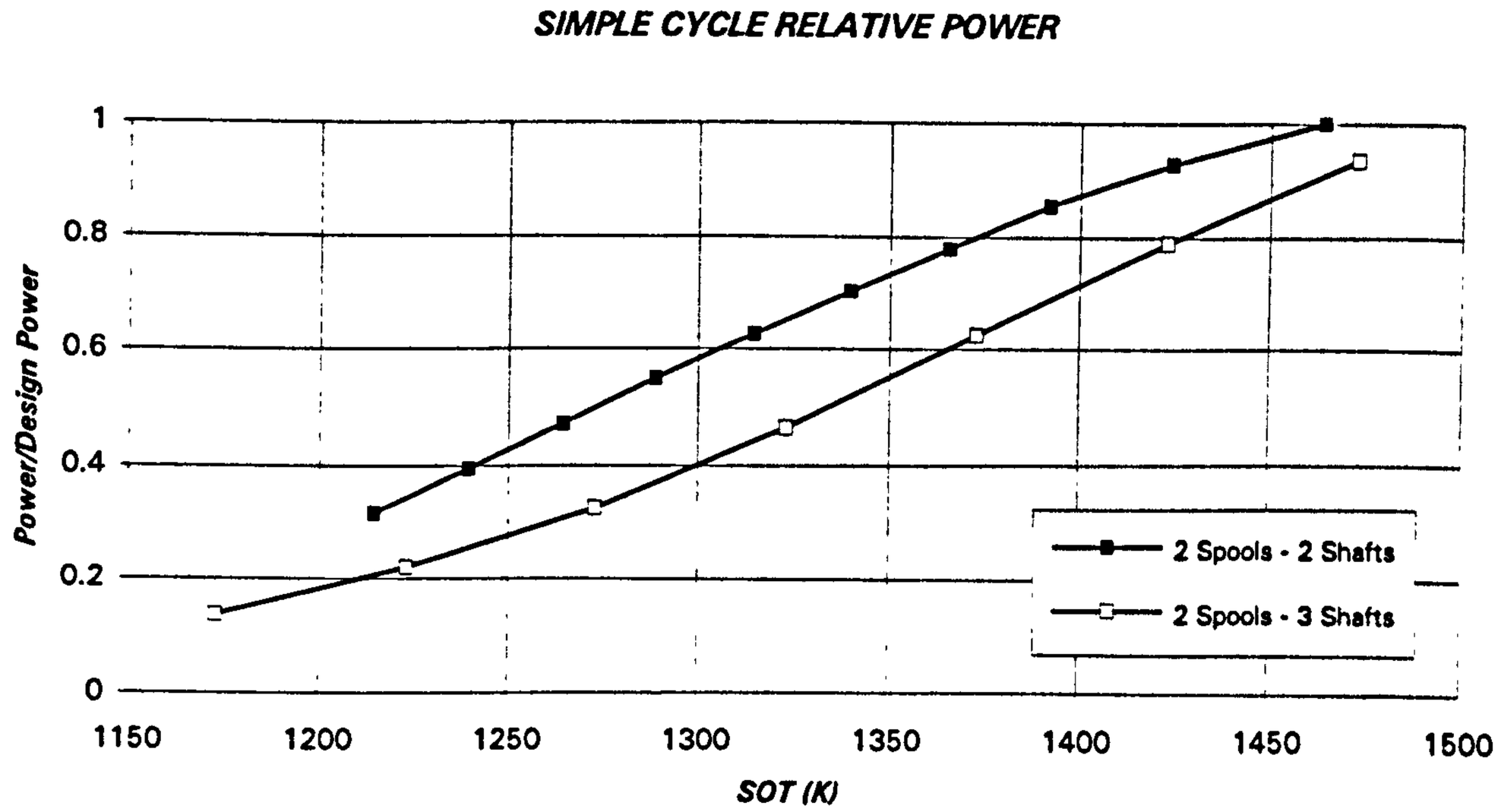

Figure 8.9. Simple cycle relative power (baseline: design power of CYCLE I) (CYCLES I and II)

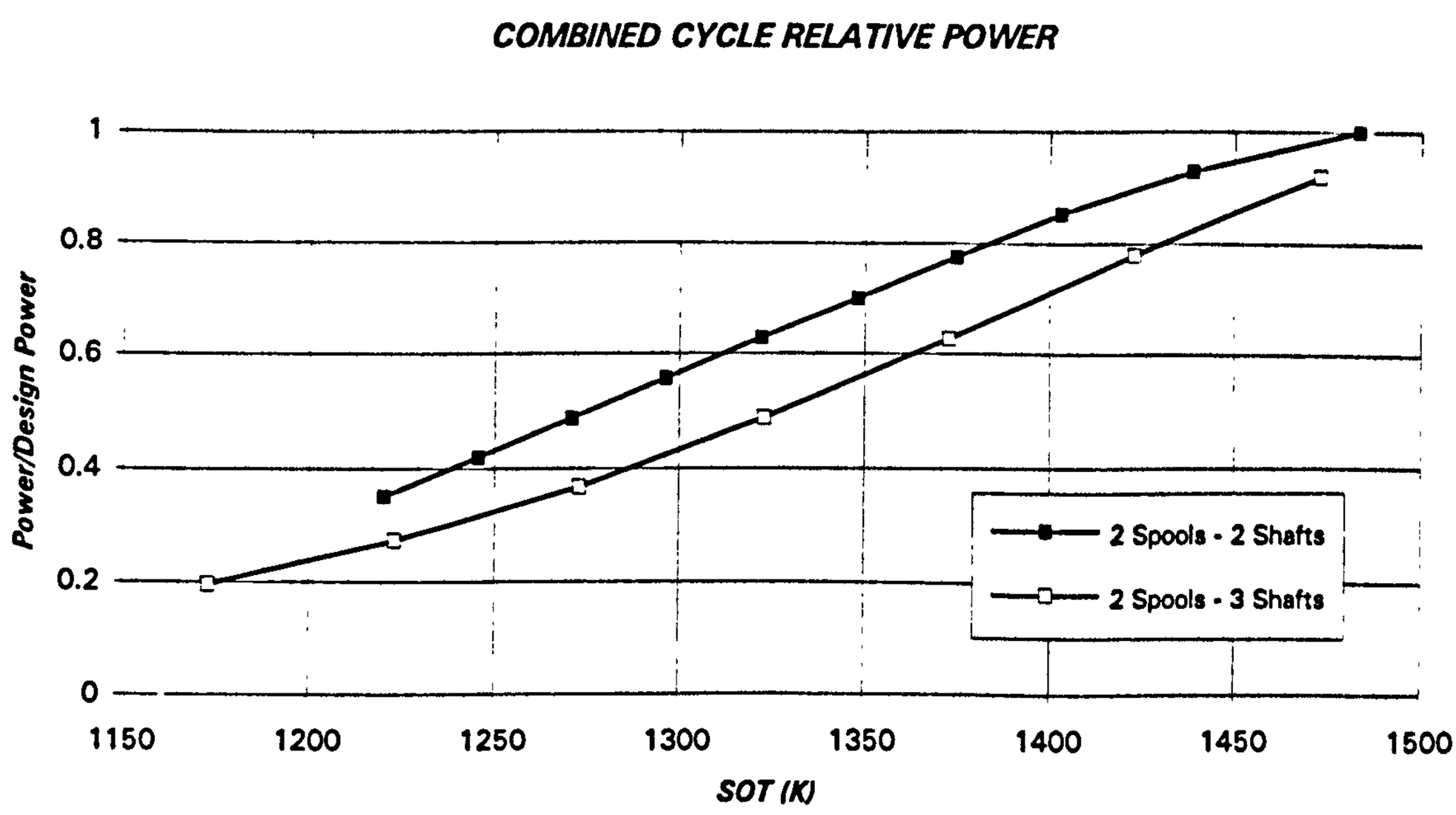

Figure 8.10. Combined cycle relative power (baseline: design power of CYCLE I) (CYCLES I and II)

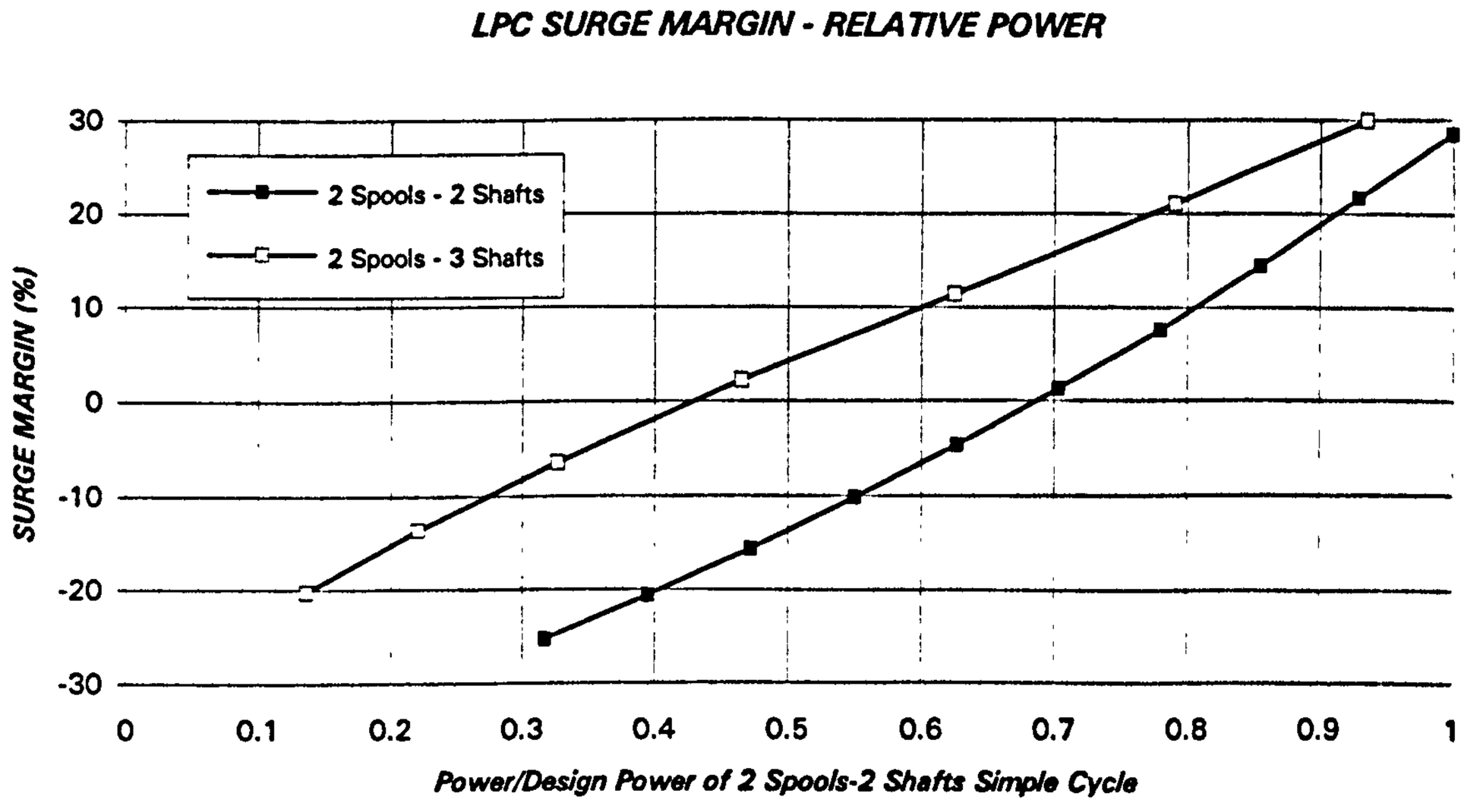

Figure 8.11. Low pressure compressor surge margin (CYCLES I and II)

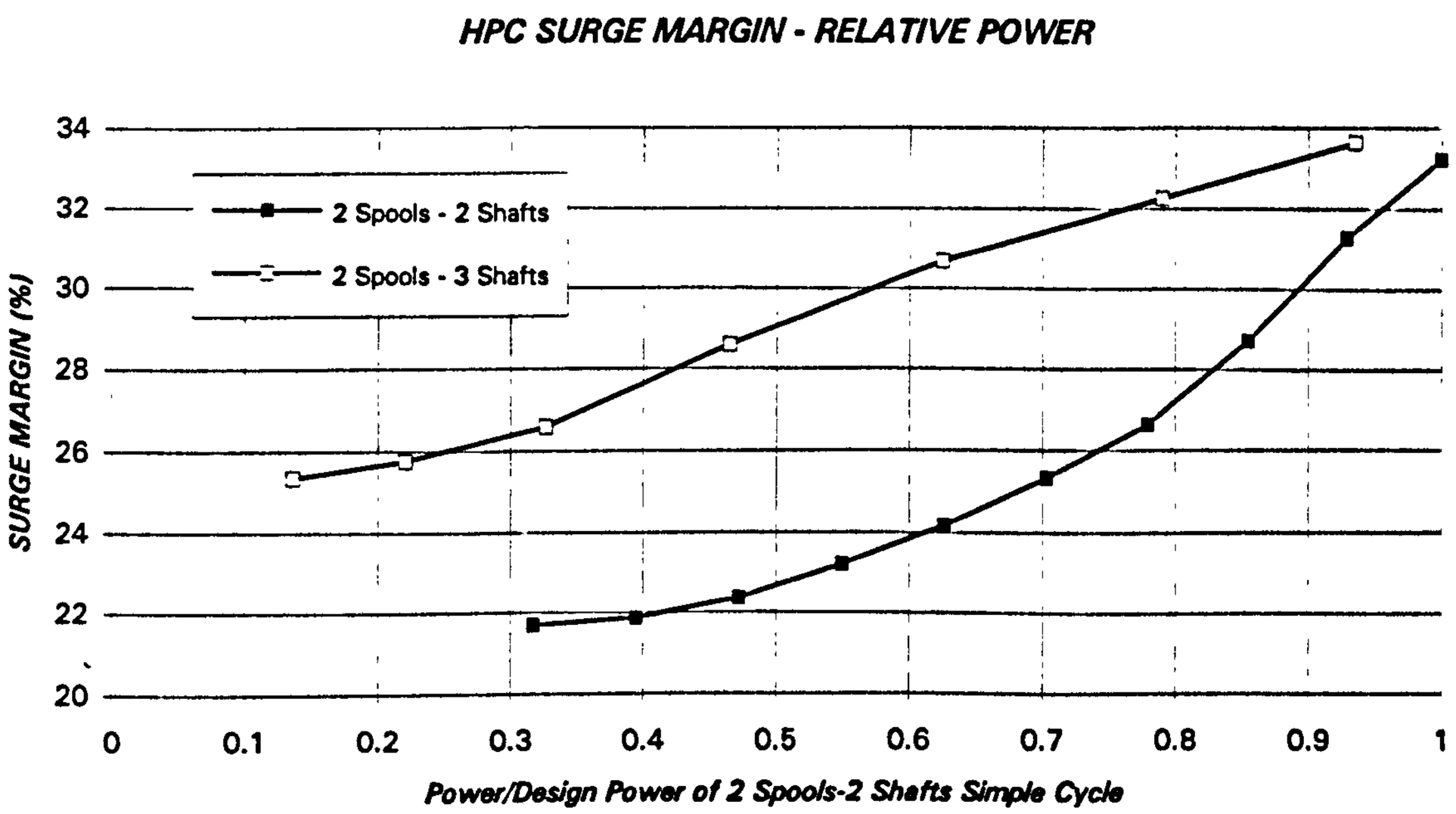

Figure 8.12. High pressure compressor surge margin (CYCLES I and II)

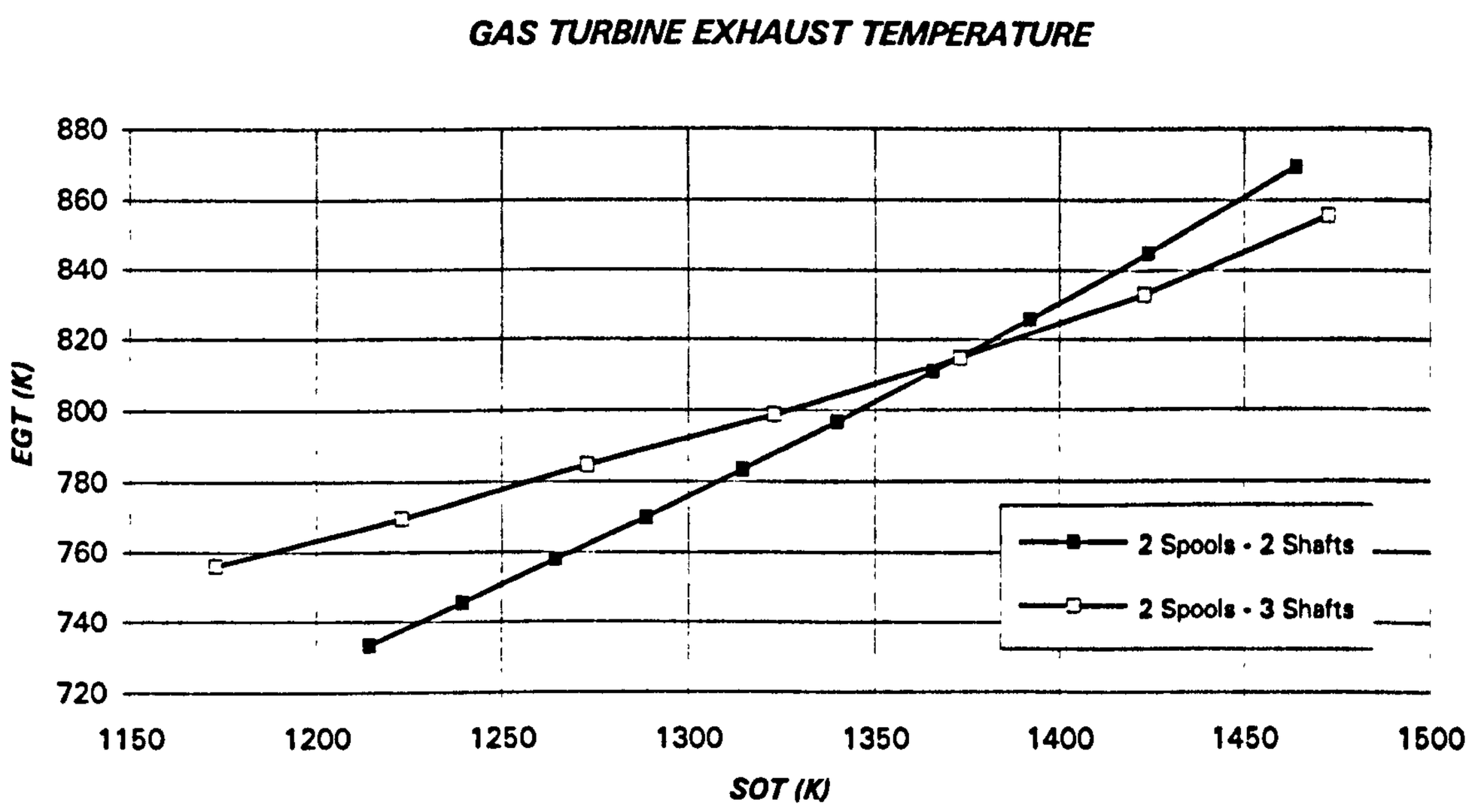

Figure 8.13. Exhaust gas temperature (K) (CYCLES I and II)

8.4. OFF-DESIGN OF THE TWO SPOOL-TWO SHAFT GAS TURBINE AT SOT=1650 K

Temperatures, pressures, etc. of CYCLE III, IV and V, described in section 8.2, would be the real target for the semi-closed cycle technology. Due to the relatively low thermal efficiency, high technology required and fuel availability, it is unlikely that such cycle will be built in the near future. However, in the mid-long term future, if natural gas sources decrease, this kind of technology could be attractive. Therefore, the high temperature and advance technologies considered will not be, probably, a major problem.

8.4.1. OFF-DESIGN PERFORMANCE STUDY AT BASELINE PRE & INTER-COOLER TEMPERATURE: COMPARISON BETWEEN CYCLES III, IV AND V

As it was outlined in the first section of this chapter, inlet temperature (prior to the cryogenic precooler) and intercooler temperature, will not suffer large changes. Therefore, the baseline off-design simulation, which runs at 300 K inlet temperature, for the conventional precooler, and 310 K intercooler exit temperature, will be very representative of the behaviour of the cycles.

In all cases, when the LPC surge margin decreases below 10%, variable stators were employed to ensure safe compressor operation. In the case of the HPC the minimum surge margin control with variable geometry was not initially considered, because this problem appeared only at very low power settings, hence the complexity of the turbomachinery design could be avoided using variable bleed valves at those extreme conditions. However, a more detailed study is required.

Low and high pressure compressor operating lines for the three cycles are plotted in figures 8.14 to 8.19. The LPC behaviour is shown with and without variable stators (solid and dotted lines respectively), with the component characteristics plotted for the fully open and fully close positions. From these figures, the variable geometry requirement for the low pressure compressor can be understood. Also, for CYCLE IV and V, the high pressure compressor will require a system to increase the surge margin.

Figures 8.20 and 8.21 show the combined cycle thermal efficiency and relative power output. At design point the intercooled & regenerated cycle with precooling offers the best efficiency, but at off-design the simple cycle with precooling is better. This cycle is also the best one in terms of power output, although for SOTs lower than 1400 K the three configurations have a similar behaviour.

The simple cycle thermal efficiency and relative power output, figures 8.22 and 23 respectively, do not follow the same tendency, with the intercooled & regenerated arrangement offering the best performance in both parameters. For the efficiency, the differences at design point are significant, with over 10 points relative to the simple

cycle with cryogenic precooling and over 15 points when compared with the conventional simple cycle.

The combined cycle specific power output (kW/kg/s), presented in figure 8.24, is around 20% larger for the simple cycle with precooling compared with the intercooled & regenerated cycle and the simple cycle. The last two configurations have similar values, although slightly lower for the simple cycle.

If the specific power output (kW/kg/s) of the turbine alone, figure 8.25, is now considered, the intercooled and regenerated cycle exhibits the best performance, although the difference with the cryogenic precooling simple cycle is not very large, specially close to design point operating conditions. For this region the simple cycle offers a poor behaviour, when compared with the other two.

The relative inlet mass flow at off-design, shown in figure 8.26, is very different for the three cycles. The simple cycle has, for the same SOT, substantially larger inlet mass flow than the intercooled and regenerated one, with this having also considerably higher values than the cryogenic precooling simple cycle.

The low pressure compressor surge margin, presented in figure 8.26, decreases very quickly when the turbine entry temperature is reduced, requiring variable geometry for most of the operating range. The problem is even worst for the N_2 precooling cycle, which demands variable stators for SOTs just below 1500 K. The other two cycles need this system for SOTs lower than 1400 K.

The variable stator angle capable of maintaining a 10% surge margin in the low pressure compressor is shown in figure 8.28. As can be easily appreciated, the values for low power settings are extremely large, and it can be questioned feasibility of the solution for these operating points. If the angles were limited to a maximum of 30-35°, and no other surge margin control mechanism was employed, the simple and the intercooled & regenerated cycles could not operate below 10-15% power. With the same restriction, the simple cycle with N_2 precooling could not work below 20% power. Bearing in mind that the machine will be dedicated to electricity generation, operating between 70% and full power most of the time, the situations that are not covered by the variable geometry could be solved by the introduction of bleed valves. This solution will alleviate the variable stators turbomachinery design problem.

The high pressure compressor surge margin, presented in figure 8.29, is adequate in the case of the simple cycle. However, for the simple cycle with cryogenic precooling and the intercooled & regenerated cycle, the surge margin shows a substantial decrease at low power setting conditions. For SOTs below 1050-1100 K the value is lower than 10%. As mentioned at the beginning of this section, no additional control was initially introduced to overcome this problem. Bleed valves and variable stators should be evaluated.

The fuel to compressor inlet mass flow ratio is shown in figure 8.30. Due to the very low Fuel Heating Value associated to synthetic gas, ratios of 10 to 13% are found. The largest values correspond to the simple cycle with cryogenic precooling.

The other two cycles have very similar figures. Typically, the intercooled & regenerated cycle would have lower fuel to compressor mass flow ratio than the simple cycle. But, it must be considered that intercooled & regenerated cycle has also cryogenic nitrogen precooling, that increases the fuel demand due to the reduction in compressor discharge temperature.

The control parameters are presented in figure 8.31, turbine exhaust temperature vs. SOT, figure 8.32, turbine exhaust temperature vs. relative power, figure 8.33, high pressure spool speed vs. SOT and figure 8.34, high pressure spool speed vs. relative power. The simple cycle with cryogenic precooling will be, initially, more difficult to control. The sensibility of power output to variations in high pressure spool speed at high power settings, and turbine exhaust temperature at lower power settings, is poorer than for the other two cycles.

The low pressure compressor inlet temperature is presented in figure 8.35, showing the cryogenic precooling effect in CYCLE IV and V. The reduction in SOT, hence in fuel demand, leads to an increase in inlet temperature.

8.4.2. OFF-DESIGN OF THE CRYOGENIC PRECOOLING SIMPLE CYCLE WITH NGVs NITROGEN INTERNAL COOLING AT DIFFERENT INLET TEMPERATURES

Although the conventional precooler exit temperatures will not suffer large changes, oscillations of ±10 K can be found[10]. Therefore, it is necessary to study the performance variations of the power plant at different inlet temperatures.

For the base temperature operation, when the LPC surge margin decreased below 10%, variable stators were employed to maintain this minimum surge margin. For the ±10 K cases the stator law previously found has not been modified, to be able to evaluate if a single schedule can be used for different operating temperatures.

The figure with the operating lines for the three cases has not been included, because there was almost no difference between them.

Figure 8.36 gives the combined cycle thermal efficiency for the three temperatures, the main characteristic being the small variation at full power. On the other hand, the combined cycle relative power output, shown in figure 8.37, changes substantially with the inlet temperature, specially at high power settings.

---

[10] The change in precooler temperature will be caused by the variation in the temperature of the cooling water and/or the deterioration of the heat exchangers. The temperature at the exit of the cryogenic precooler will be modified as a consequence of the change in its inlet (exit of the conventional precooler) conditions, fuel flow demand (change in nitrogen available for cryogenic precooling), etc.

The simple cycle (gas turbine alone) thermal efficiency of figure 8.38 follows a behaviour similar to the combined cycle efficiency, having a relatively small difference for the largest SOTs, increasing this difference when reducing the power. The relative power output for this configuration, given in figure 8.39, is almost identical to the combined cycle relative power output.

The combined cycle specific power output, shown in figure 8.40, is almost the same for the three conditions, with the low inlet temperature cycle performing slightly better. For the simple cycle specific power output, figure 8.41, the differences between the three cases are larger, specially at low SOTs, with the T_{ref}-10 K case having always the best performance.

The relative mass flow has also a significant variation with inlet temperature. The largest differences take place for the highest SOTs, as can be seen in figure 8.42.

The LPC surge margin, figure 8.43, is extremely close to zero for the T_{ref}+10 K case. Therefore it would be necessary to modify the stator law with the inlet temperature. A simple shift of 3-4° seems to be enough. A similar behaviour can be observed for the HPC surge margin, shown in figure 8.45, decreasing the value as the inlet temperature increases.

The fuel to compressor inlet mass flow ratio, given in figure 8.46, is very similar for the three temperatures considered, being slightly larger for the lowest inlet temperature.

The high pressure spool speed vs. SOT, shown in figure 8.49, is not affected by inlet temperature variations. That is not the case if the speed is plotted against the relative power output (figure 8.50). The other main control parameter, the exhaust gas temperature, is shown in figures 8.47 and 8.48, changing considerably with the inlet temperature.

The low pressure compressor inlet temperature is plotted in figure 8.51 for the three cases. As a result of the ±10 K change in the conventional precooler exit temperature, the actual inlet temperature to the machine is modified in almost the same value.

8.4.3. OFF-DESIGN OF THE INTERCOOLED & REGENERATED CYCLE WITH CRYOGENIC PRECOOLER AND NGVs NITROGEN INTERNAL COOLING AT DIFFERENT INLET AND INTERCOOLER TEMPERATURES

The off-design behaviour of this cycle will be examined for changes of ±10 K in the conventional precooler and intercooler exit temperatures.

As in previous sections, the stator schedule has not been modified, to evaluate the possibility of using a single law for different operating temperatures.

The combined cycle thermal efficiency is given in figure 8.52. For SOTs above 1400 K the variation is very small. Then kink point at 1150-1200 K is caused by the

change from combined cycle to simple cycle, as the gas turbine exhaust temperature is not high enough to produce steam for the bottoming cycle.

For power settings close to 100%, the simple cycle thermal efficiency of figure 8.54 does not alter its value due to variations in inlet and intercooler temperatures, having large differences when decreasing the SOT.

As in the previous cycle, combined cycle relative power (figure 8.53) and simple cycle relative power (figure 8.55) are very sensitive to changes in inlet and intercooler temperatures, specially at high SOTs.

The combined cycle specific power output, given in figure 8.56, is almost the same for the three conditions at high power settings. At low SOTs, when the turbine exit temperature is not enough to generate steam, becoming a simple cycle, the difference is larger. This conclusion matches with figure 8.57, where specific power output of the gas turbine alone is plotted. For both configurations, simple and combined cycle, the lowest temperature case, T_{ref} -10 K, offers the best performance.

The inlet relative mass flow has a significant variation with the changes in temperature. The differences are of the same order for the complete range of SOTs considered, as can be observed in figure 8.58.

The LPC surge margin is given in figure 8.59. For the largest temperature cycle, the compressor will approach, dangerously, the surge line. The HPC surge margin, shown in figure 8.61, is also lower for the T_{ref} +10 K case, with the operating line close to surge at low power settings.

The fuel to compressor inlet mass flow ratio, given in figure 8.62, is basically the same for the three temperatures considered and the complete range of SOTs.

The exhaust gas temperature, shown in figures 8.63 and 8.64, changes considerably for the three cases. Therefore, this parameter is very adequate for the control of the machine.

The high pressure spool speed vs. SOT, shown in figure 8.65, is almost independent of the conventional precooler and intercooler temperatures. However, if the speed is plotted against the relative power output, figure 8.66, three curves can be easily distinguished.

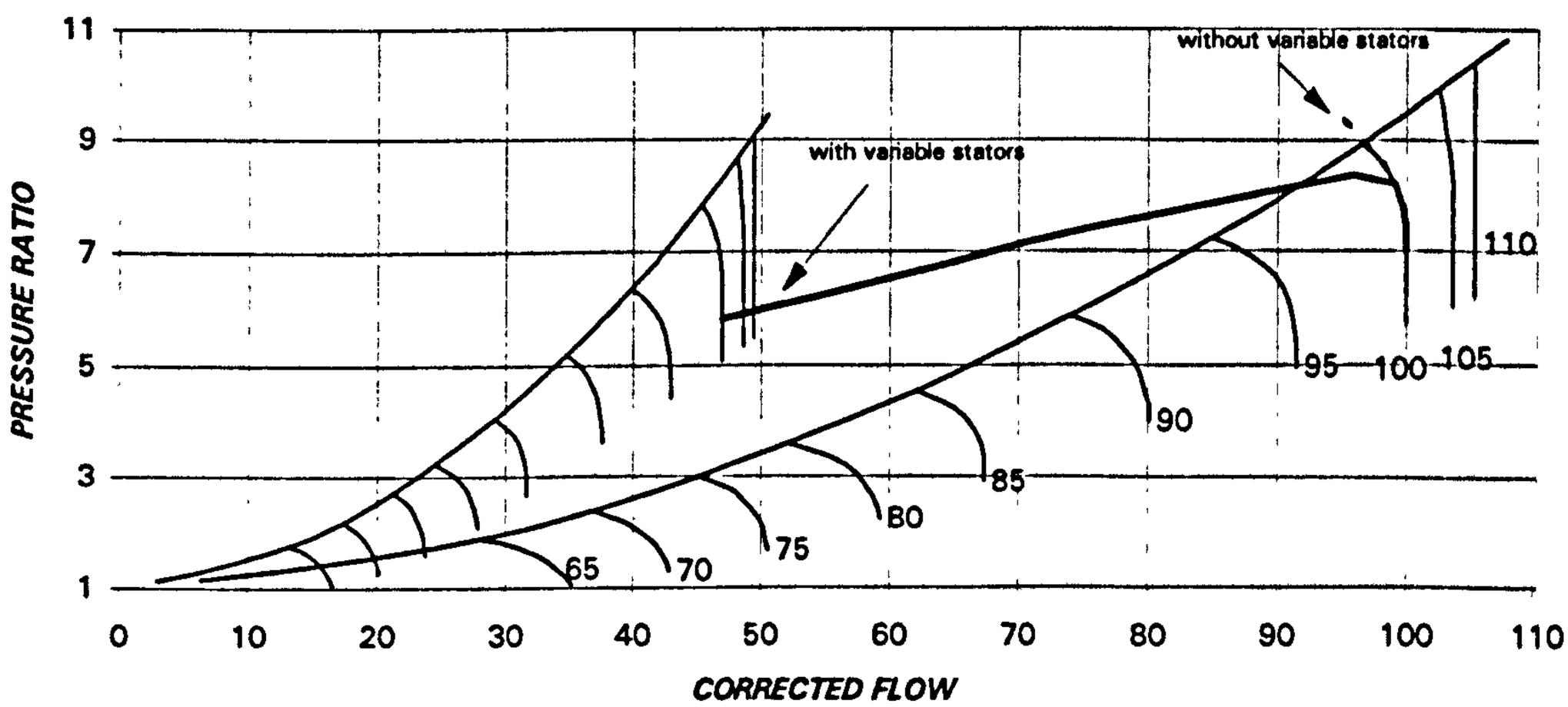

Figure 8.14. Low pressure compressor operating line (with variable stators effect on map) (CYCLE III)

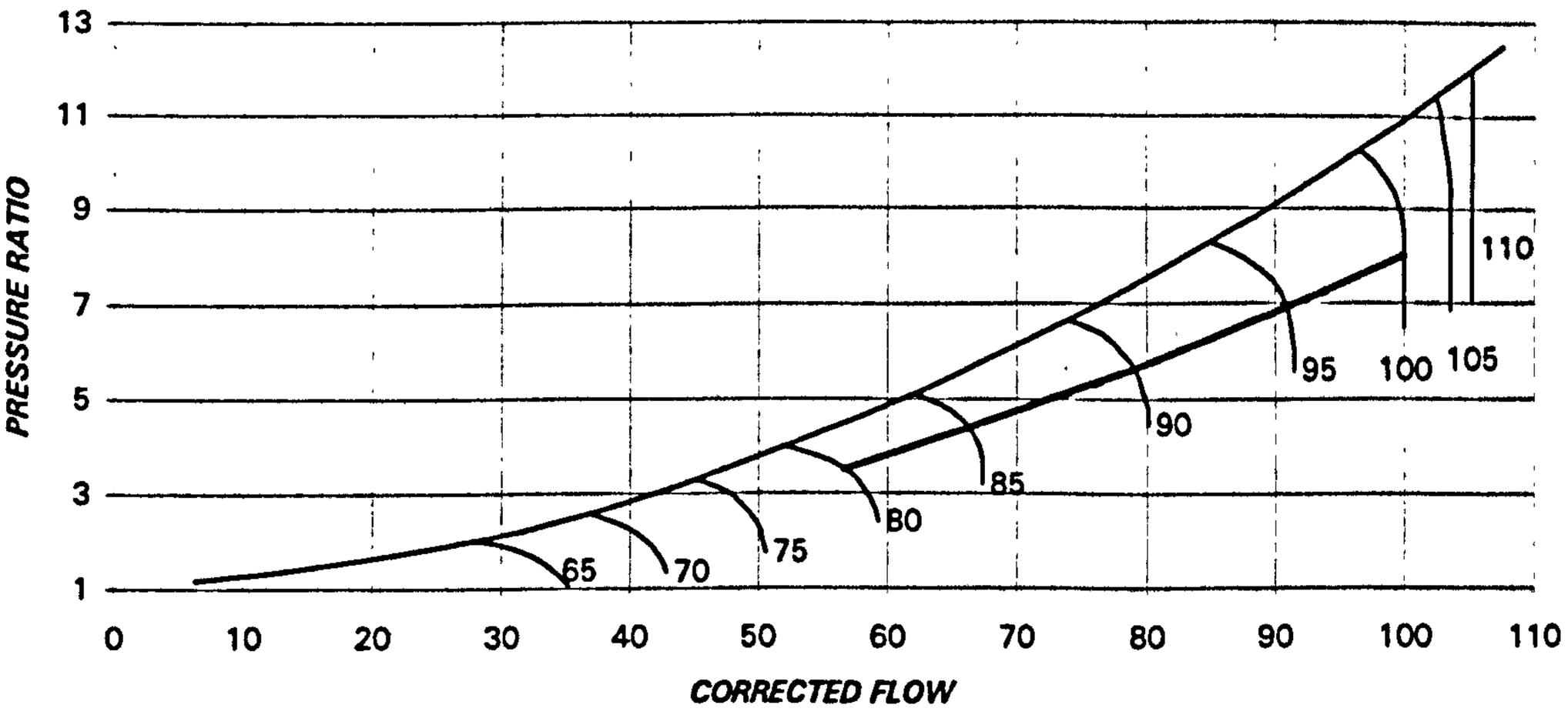

Figure 8.15. High pressure compressor operating line (CYCLE III)

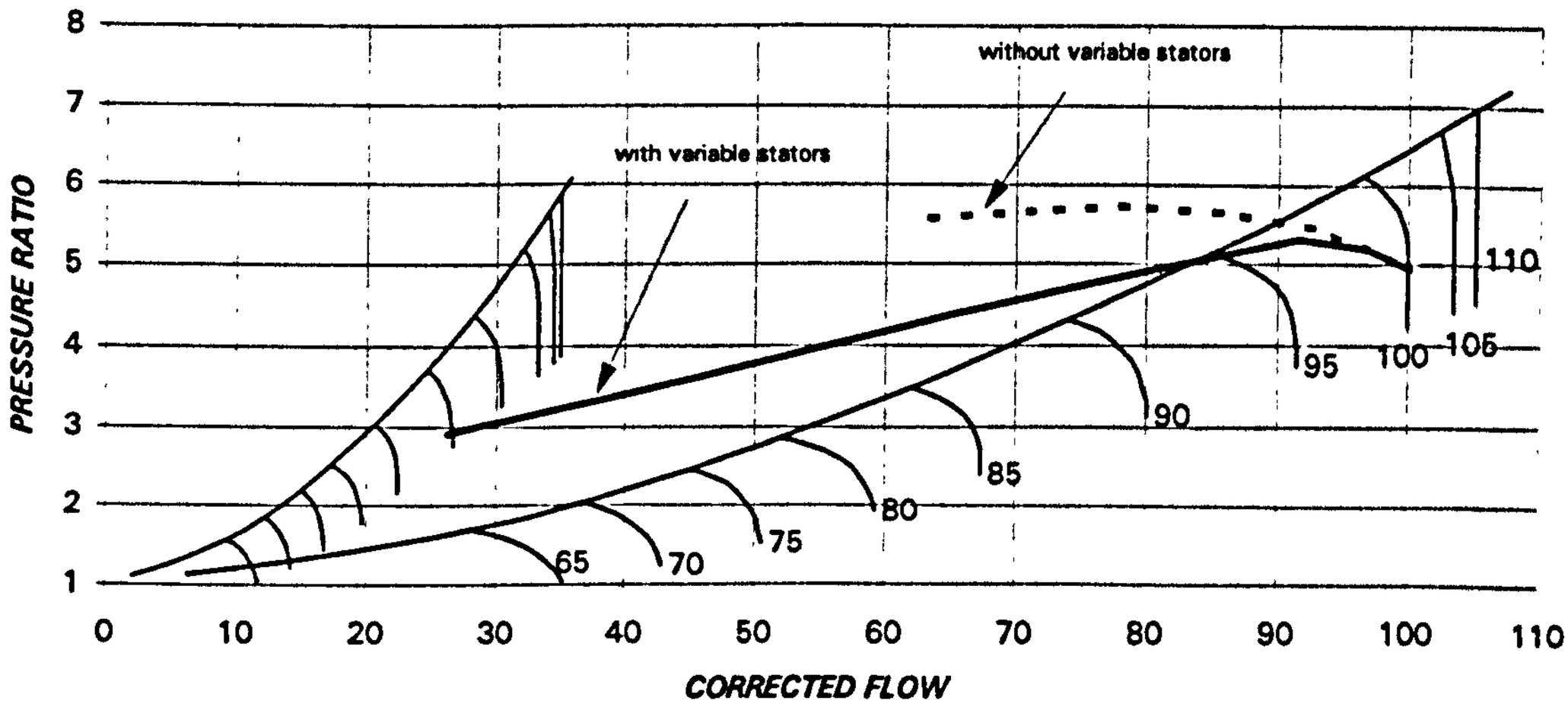

Figure 8.16. Low pressure compressor operating line (with variable stators effect on map) (CYCLE IV)

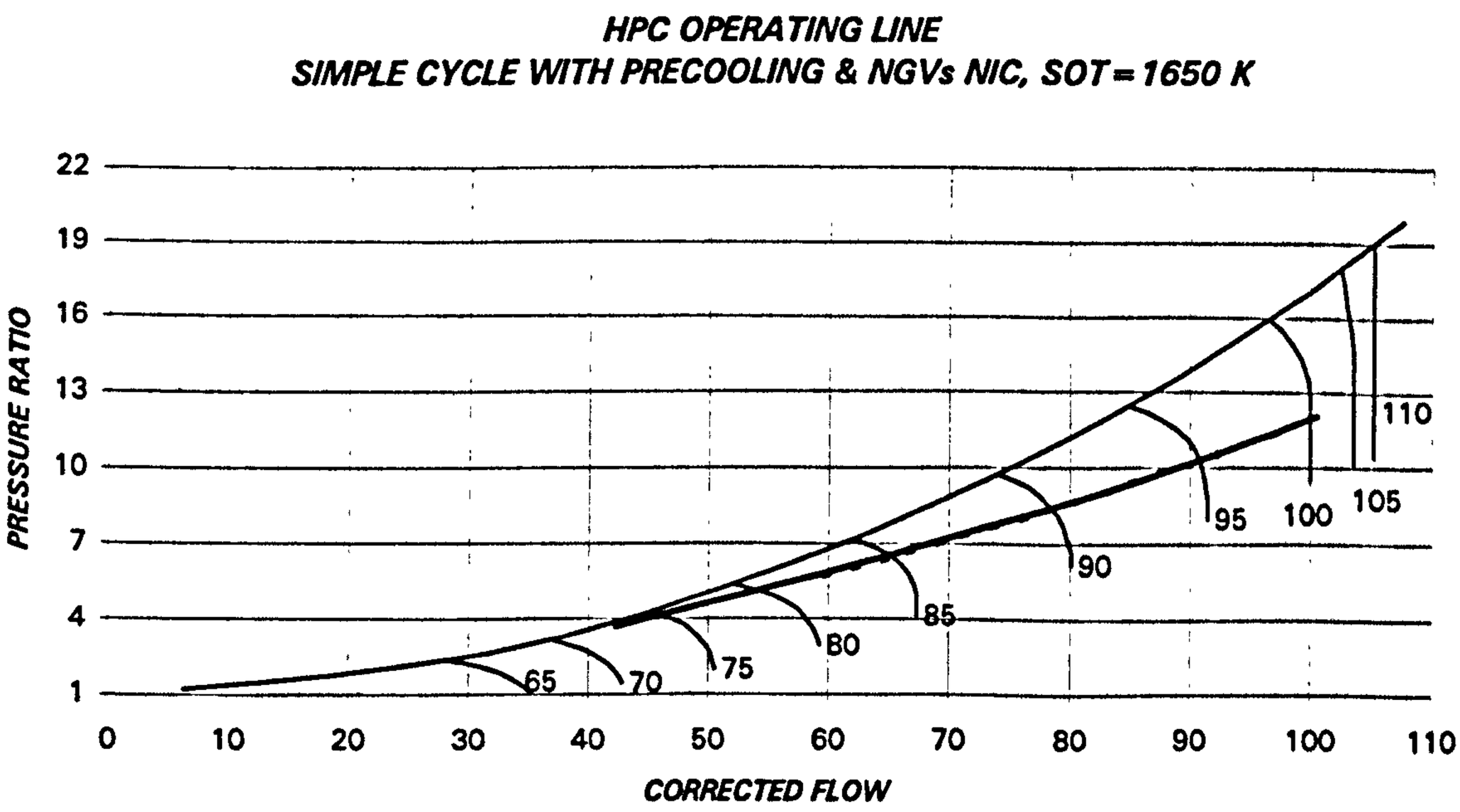

Figure 8.17. High pressure compressor operating line (CYCLE IV)

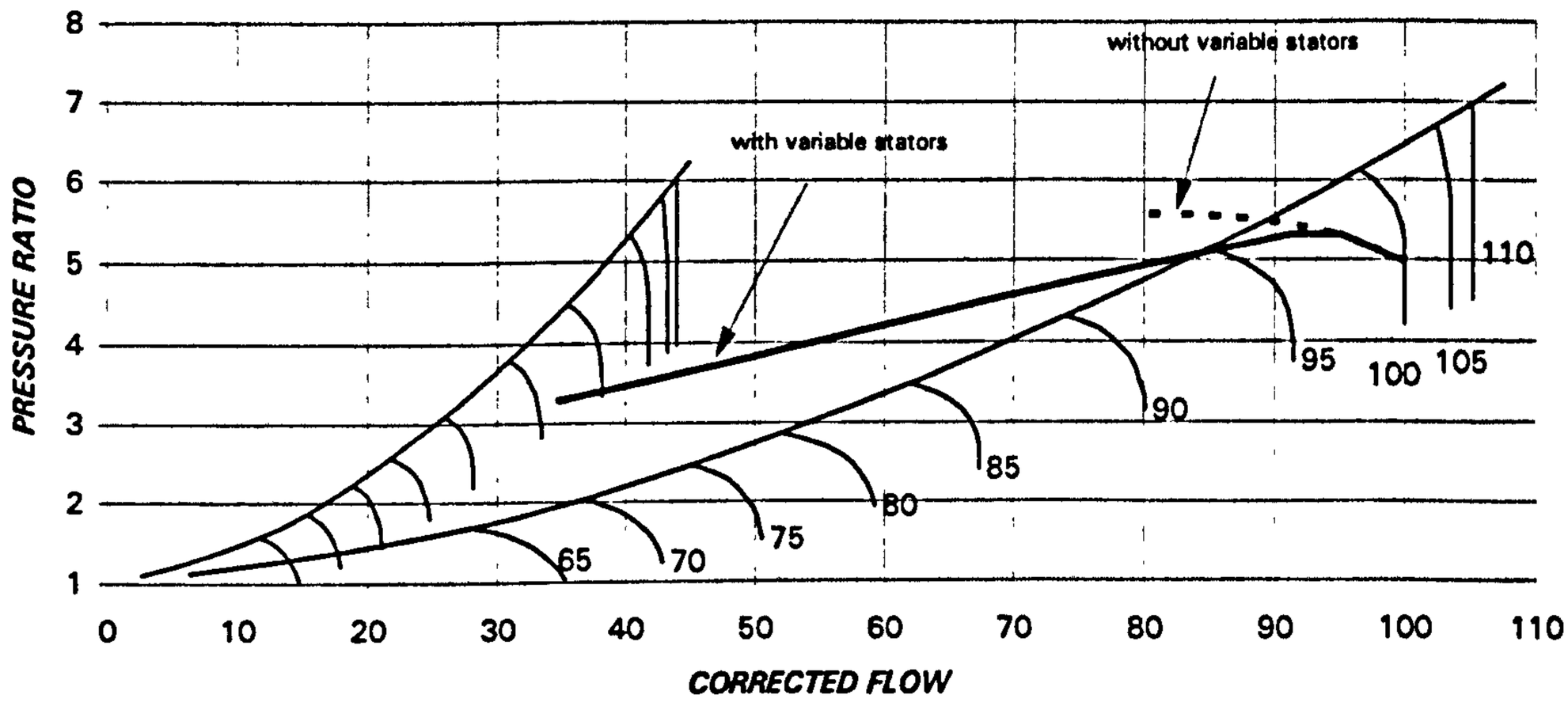

Figure 8.18. Low pressure compressor operating line (with variable stators effect on map) (CYCLE V)

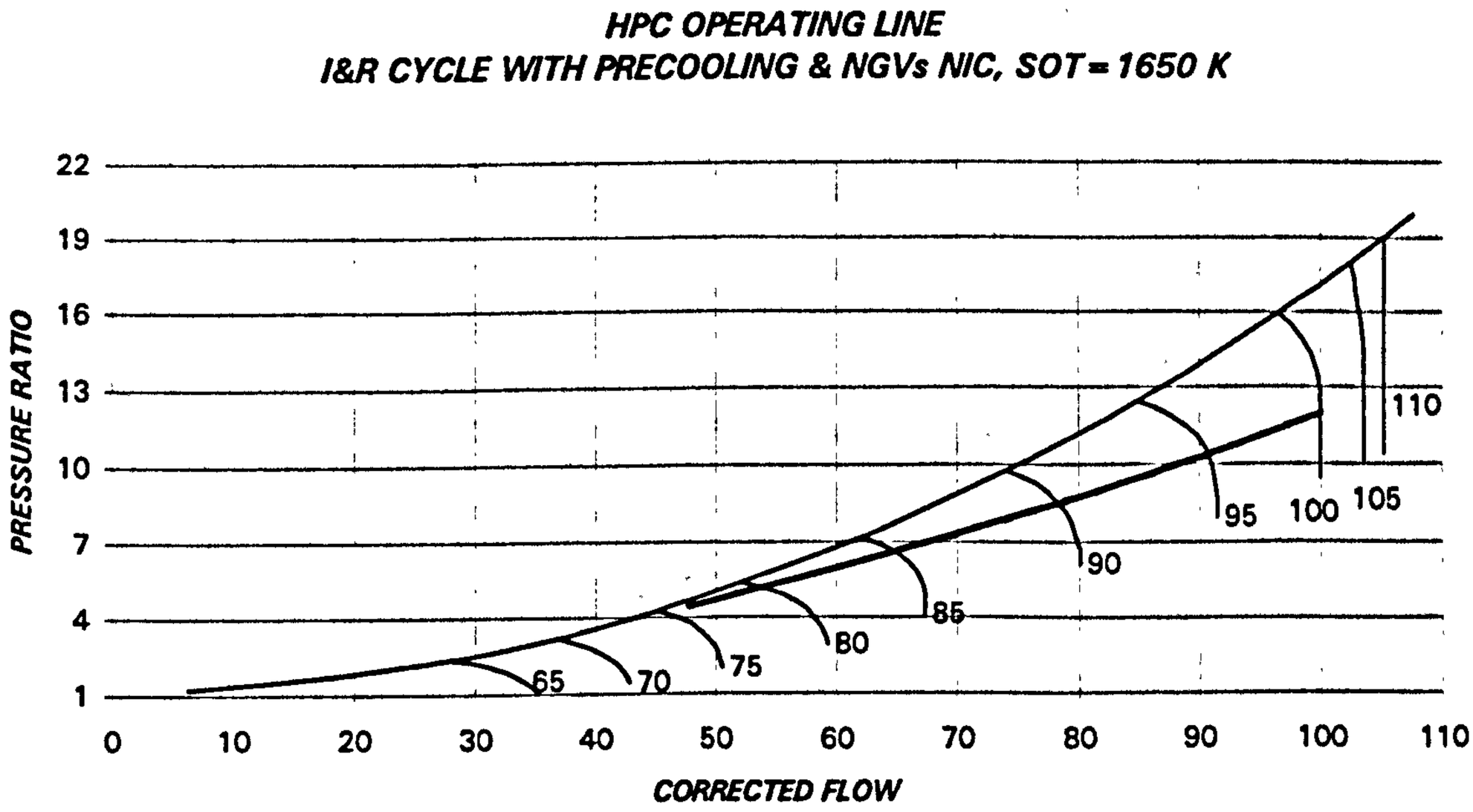

Figure 8.19. High pressure compressor operating line (CYCLE V)

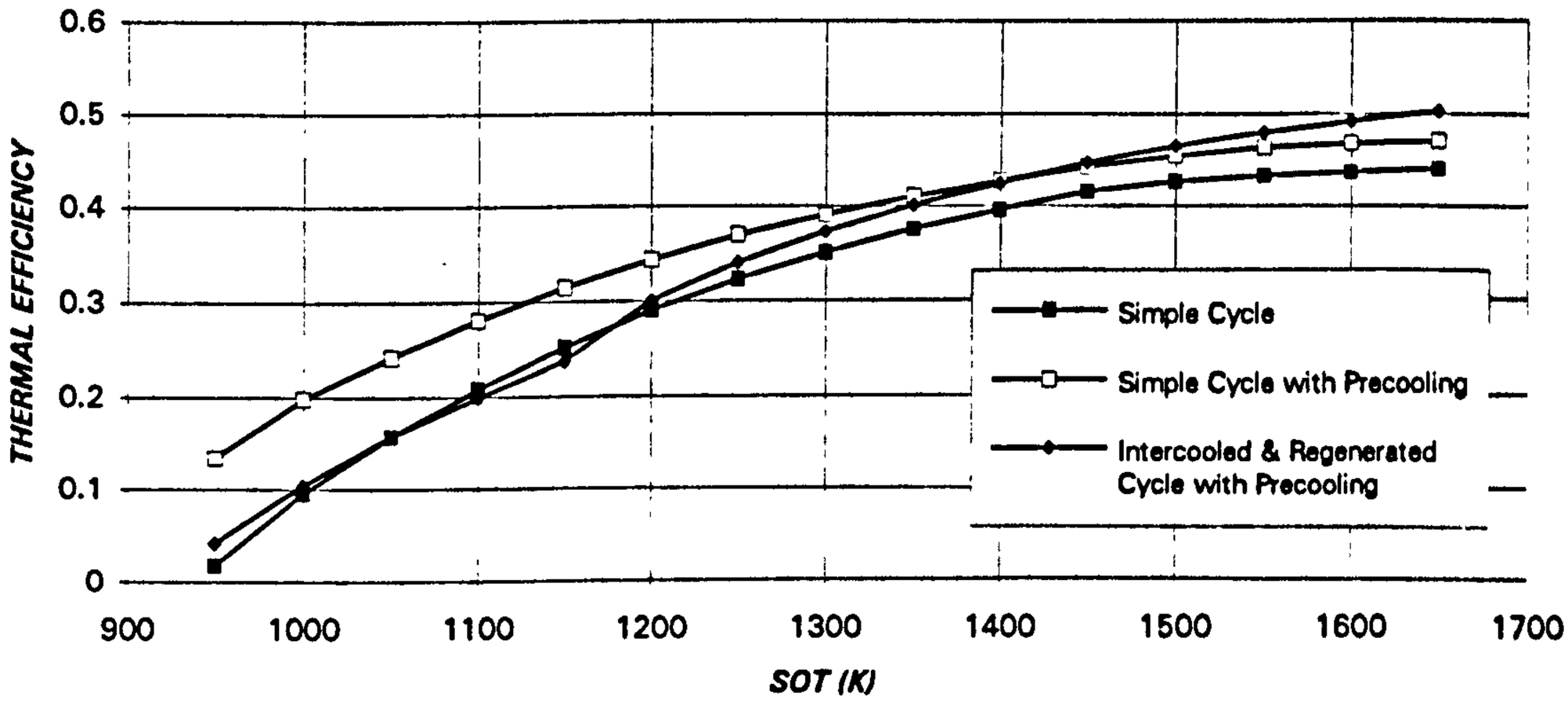

Figure 8.20. Combined cycle thermal efficiency (CYCLES III, IV and V)

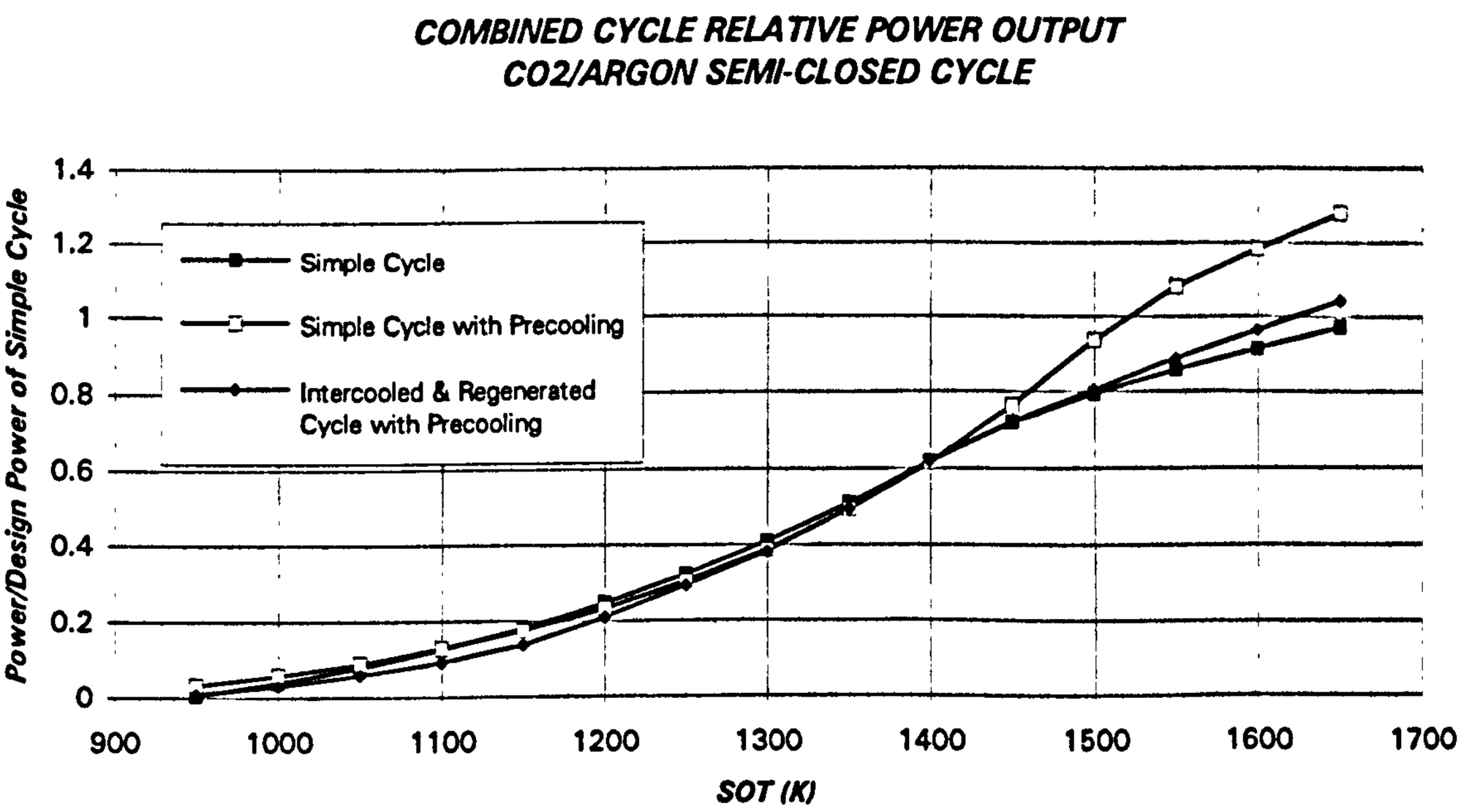

Figure 8.21. Combined cycle relative power (baseline: design power of CYCLE I) (CYCLES III, IV and V)

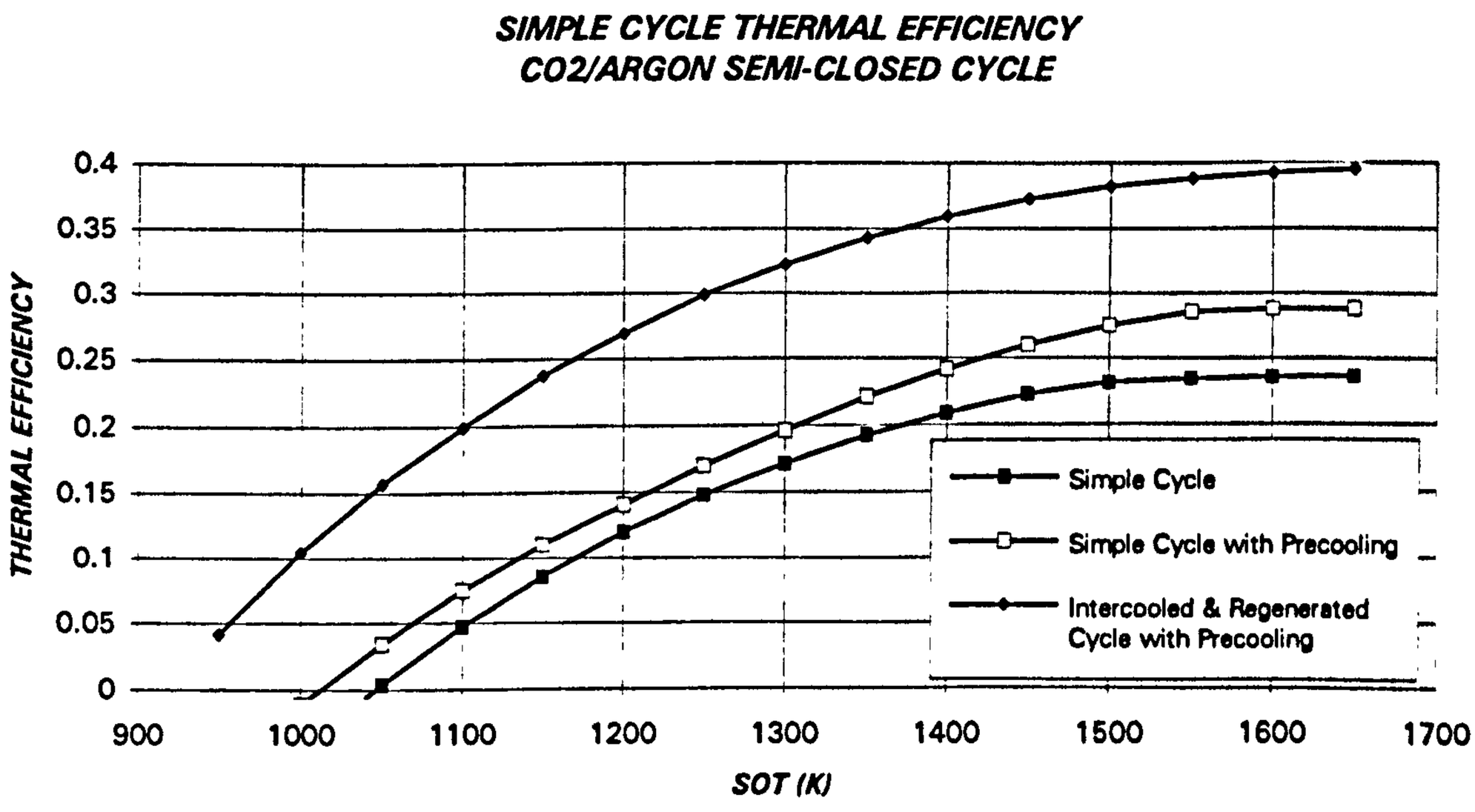

Figure 8.22. Simple cycle thermal efficiency (CYCLES III, IV and V)

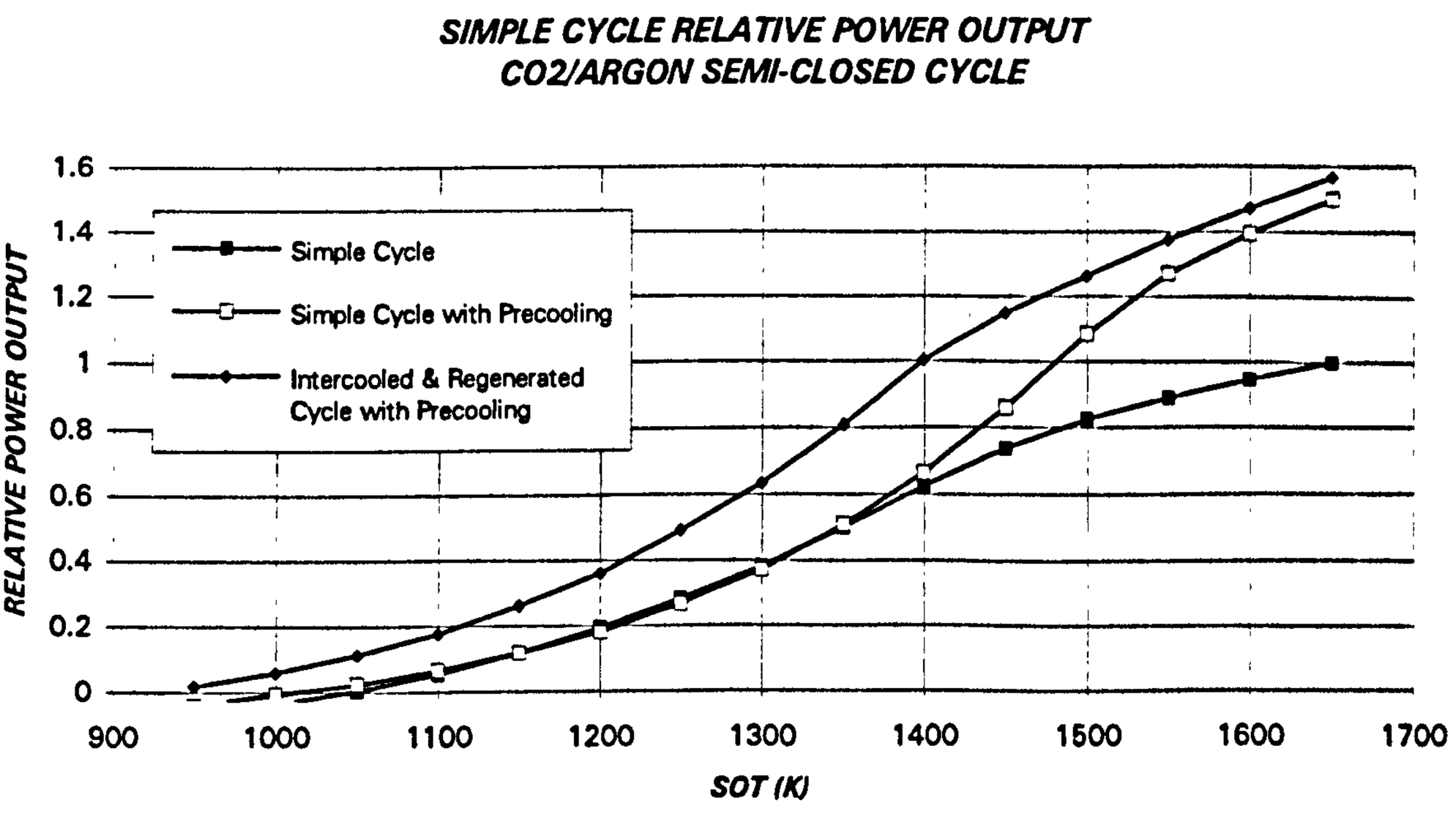

Figure 8.23. Simple cycle relative power (baseline: design power of CYCLE I) (CYCLES III, IV and V)

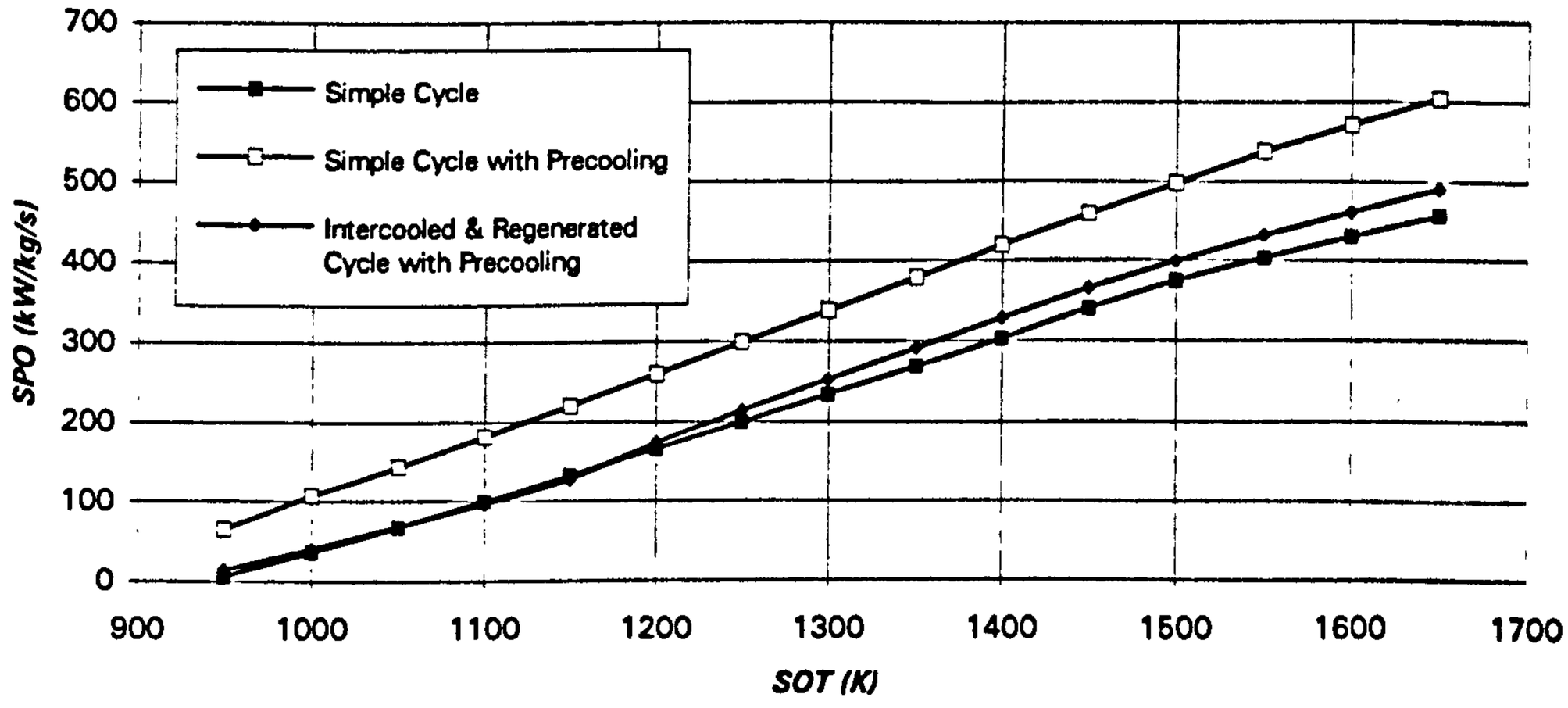

Figure 8.24. Combined cycle specific power output (kW/kg/s) (CYCLES III, IV and V)

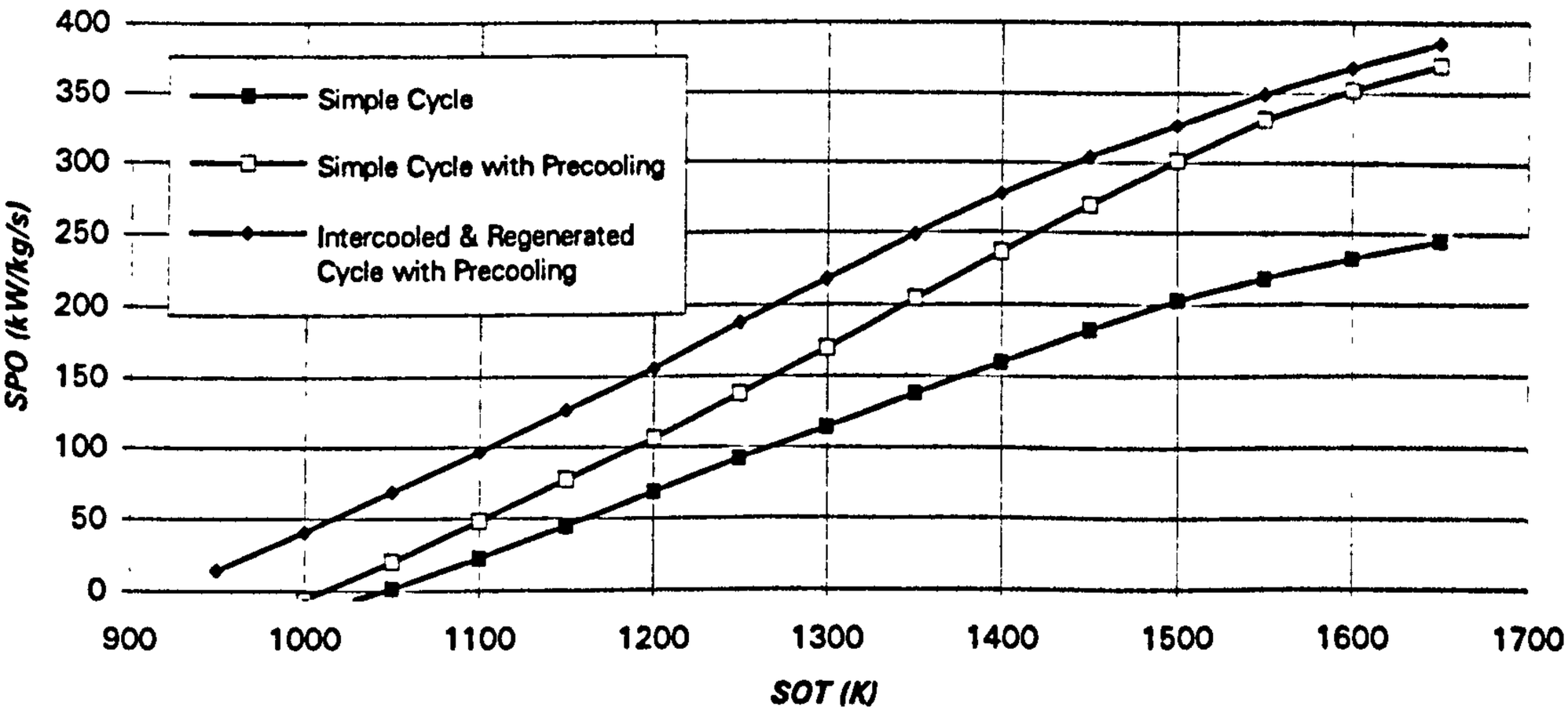

Figure 8.25. Simple cycle specific power output (kW/kg/s) (CYCLES III, IV and V; kW/kg/s)

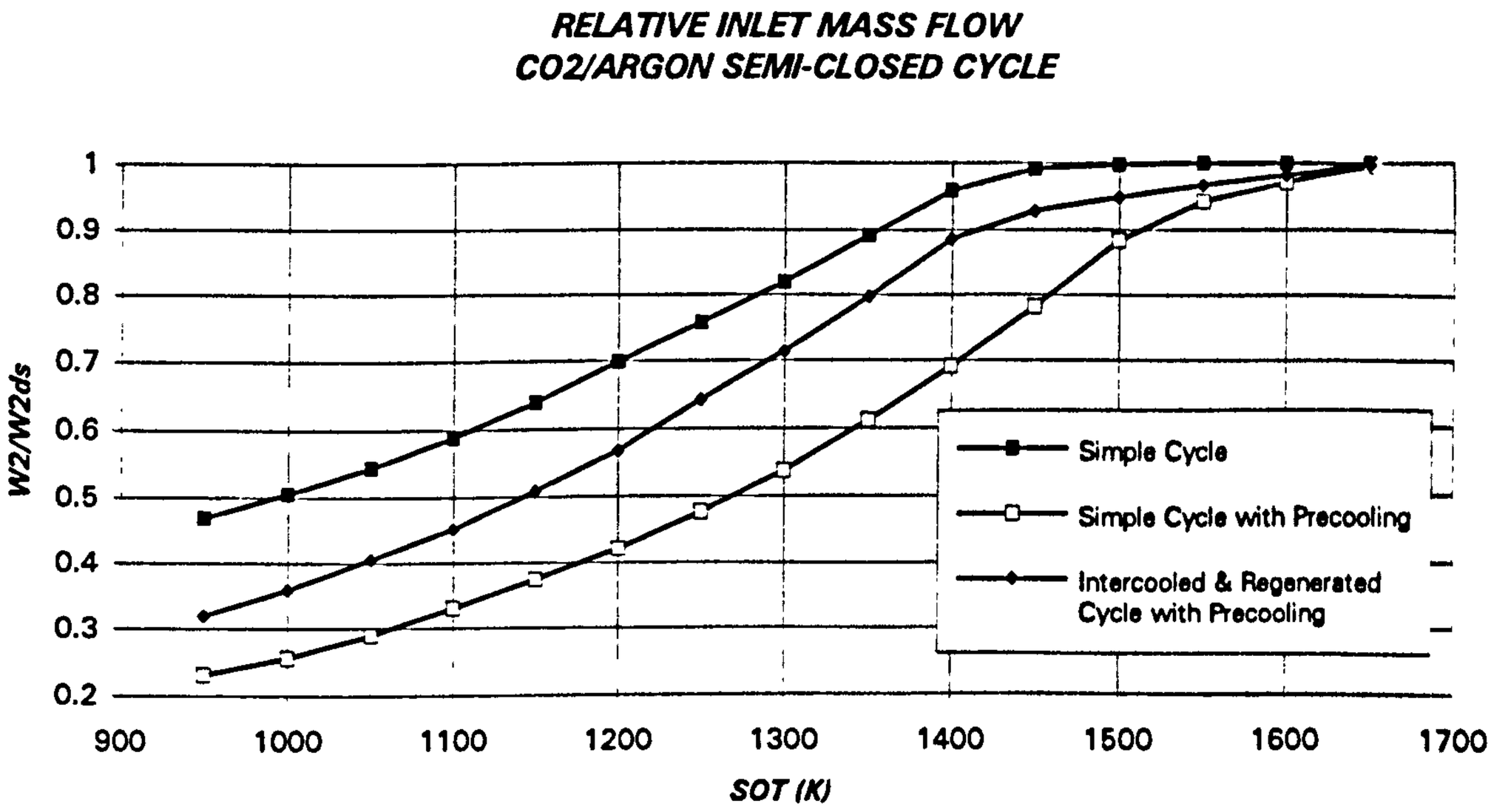

Figure 8.26. Relative compressor inlet mass flow (CYCLES III, IV and V)

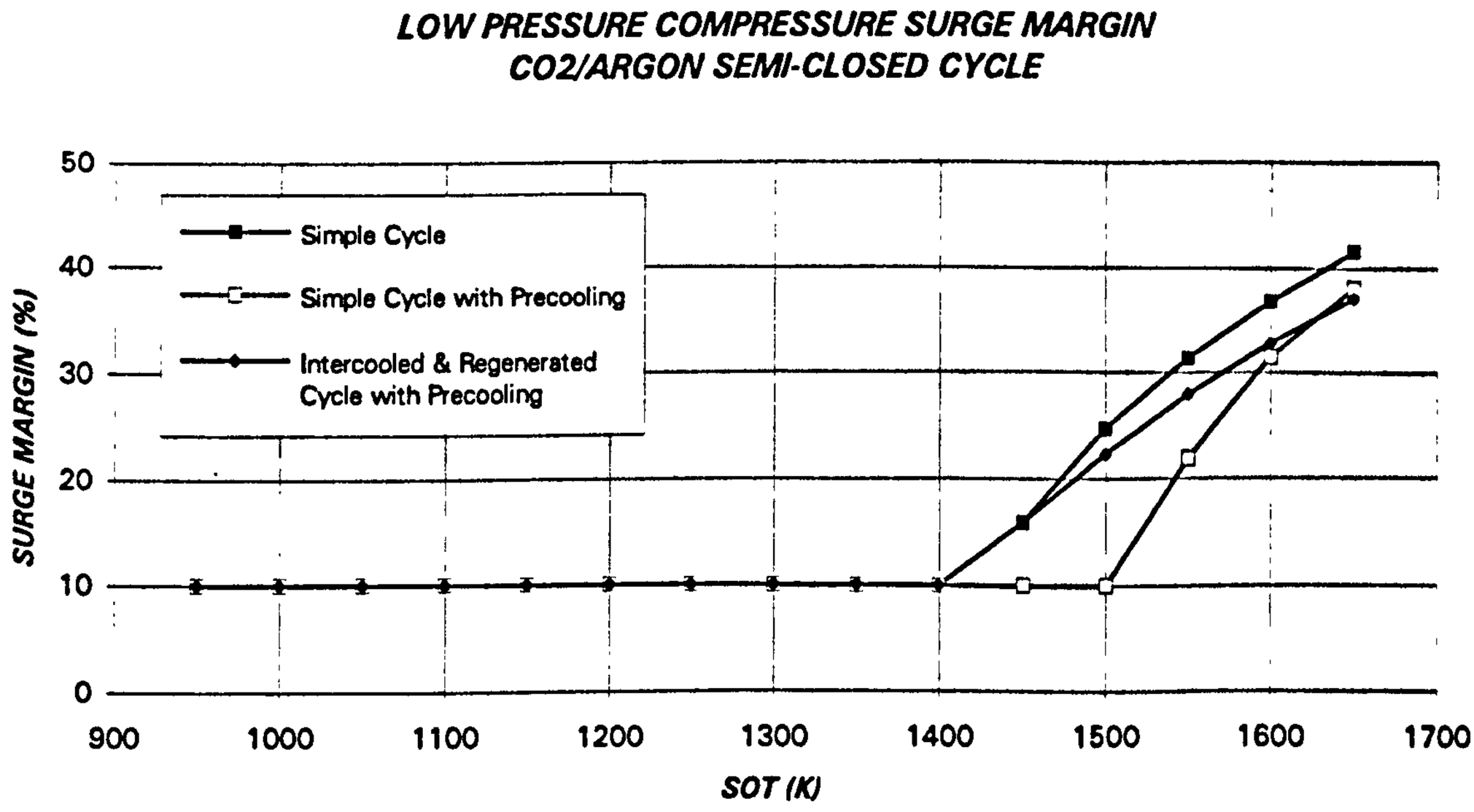

Figure 8.27. Low pressure compressor surge margin (CYCLES III, IV and V)

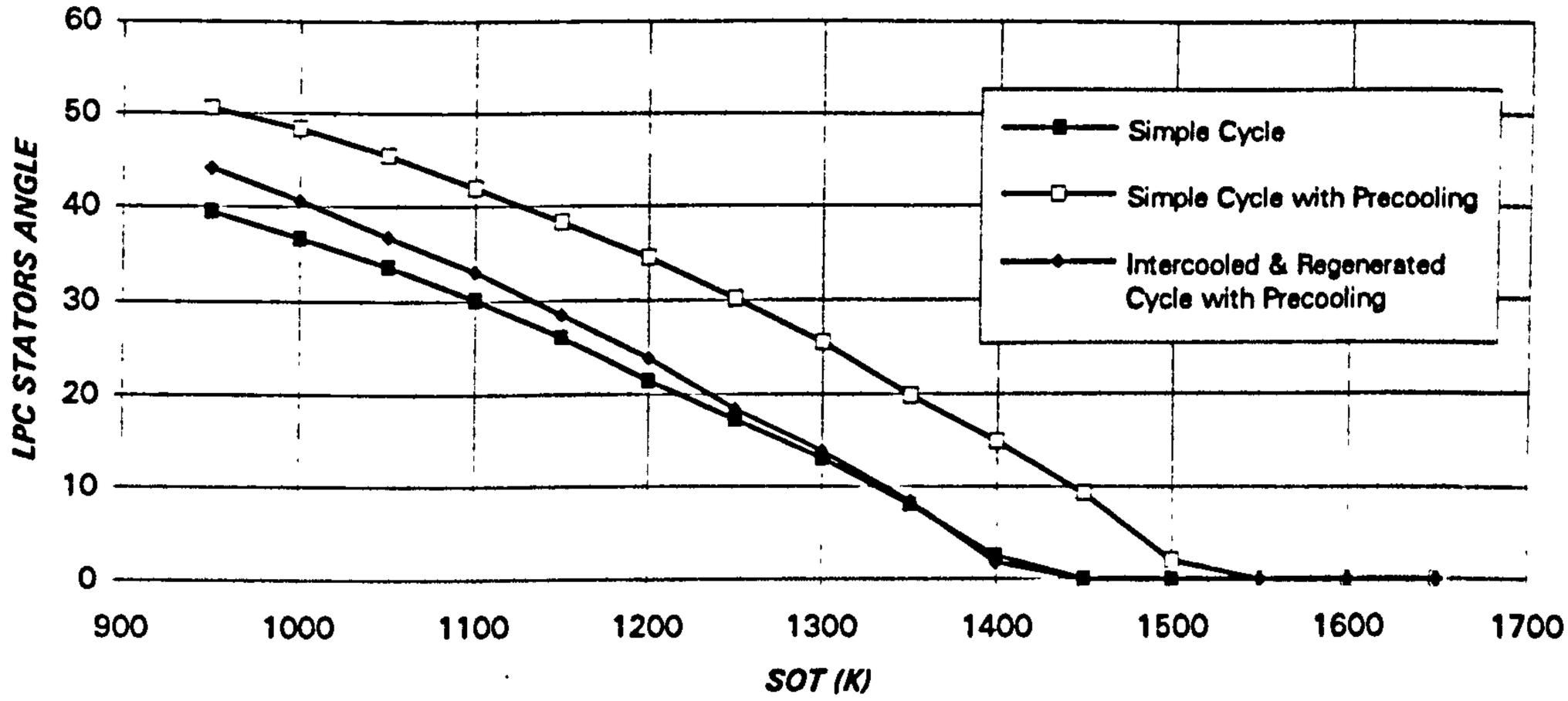

Figure 8.28. Low pressure compressor variable stators angle (CYCLES III, IV and V)

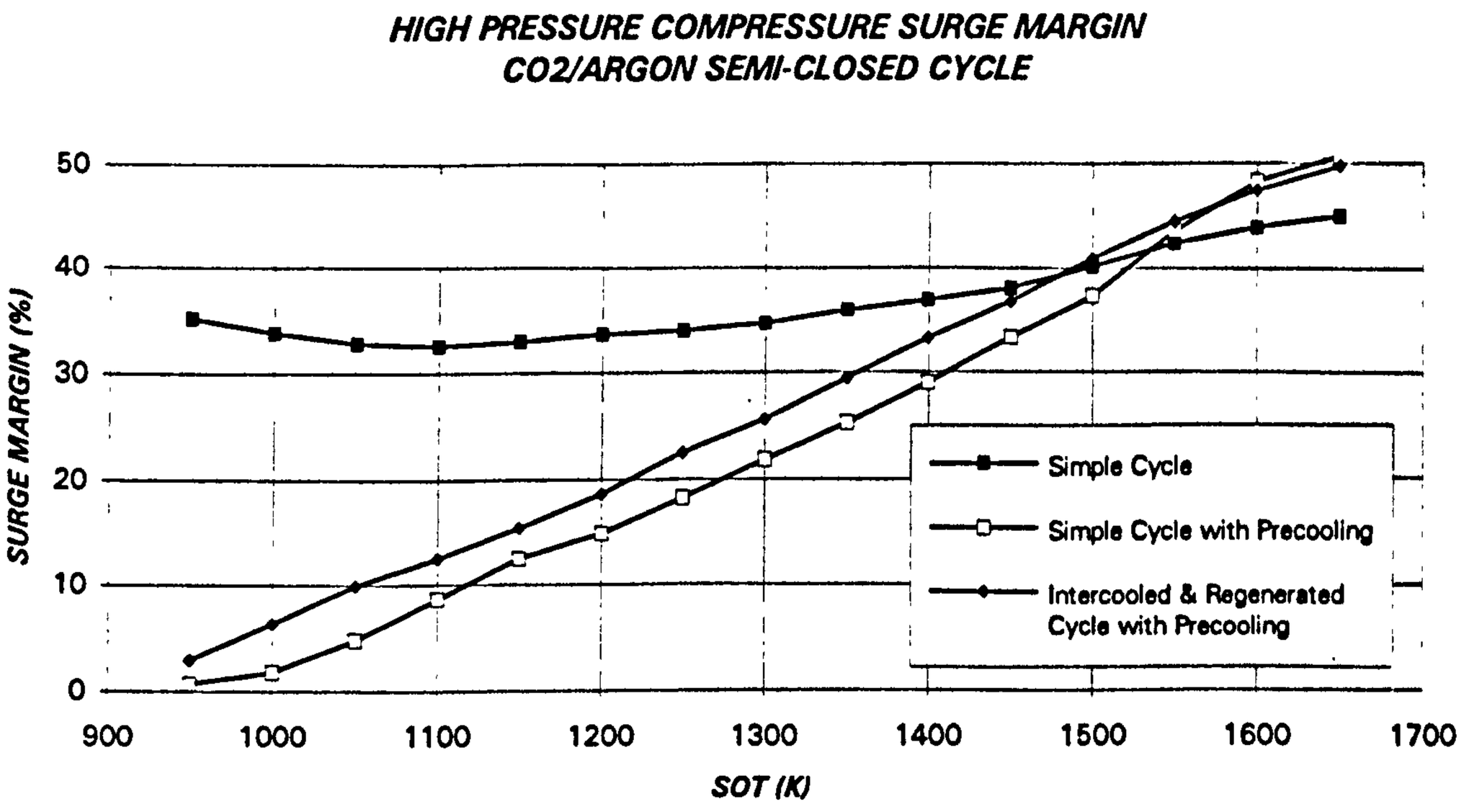

Figure 8.29. High pressure compressor surge margin (CYCLES III, IV and V)

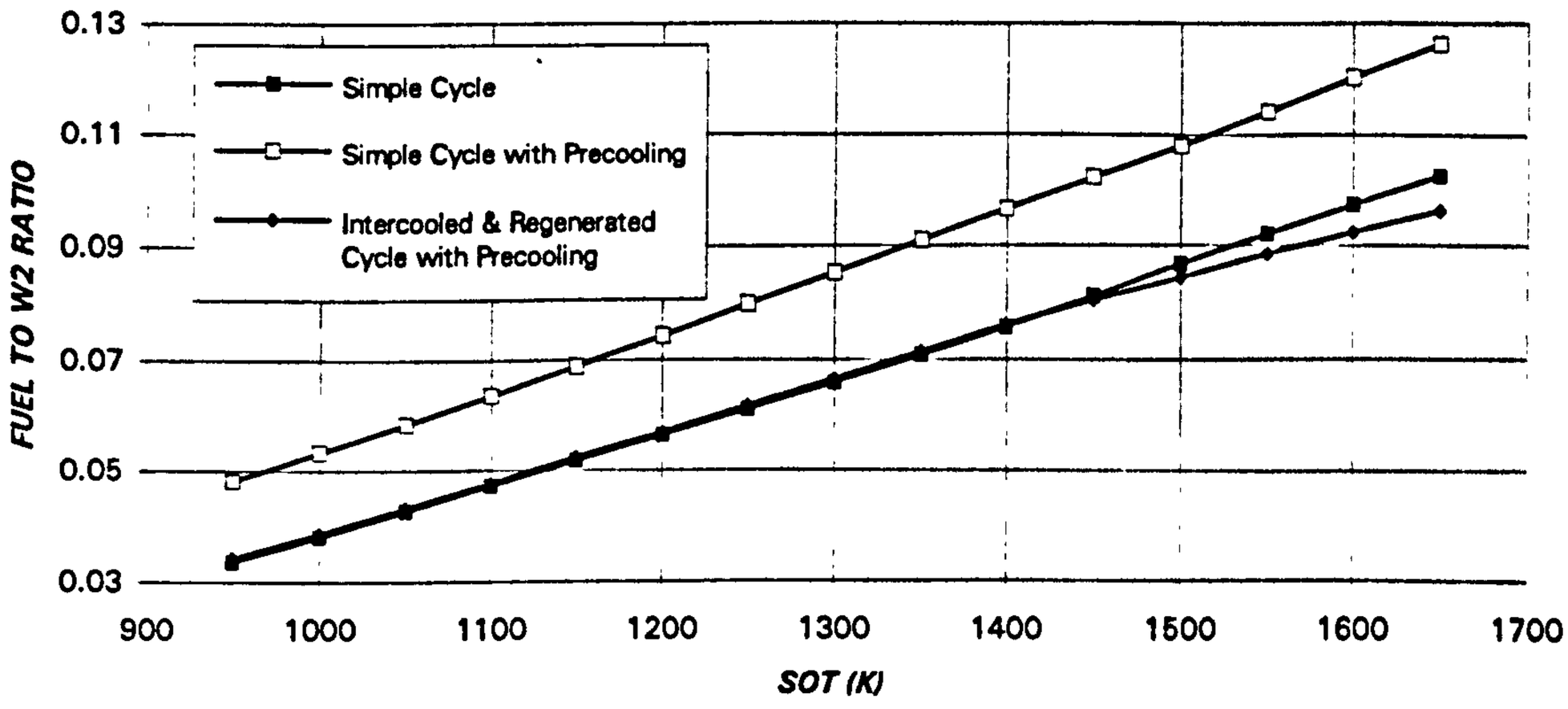

Figure 8.30. Fuel to compressor inlet mass flow ratio (CYCLES III, IV and V)

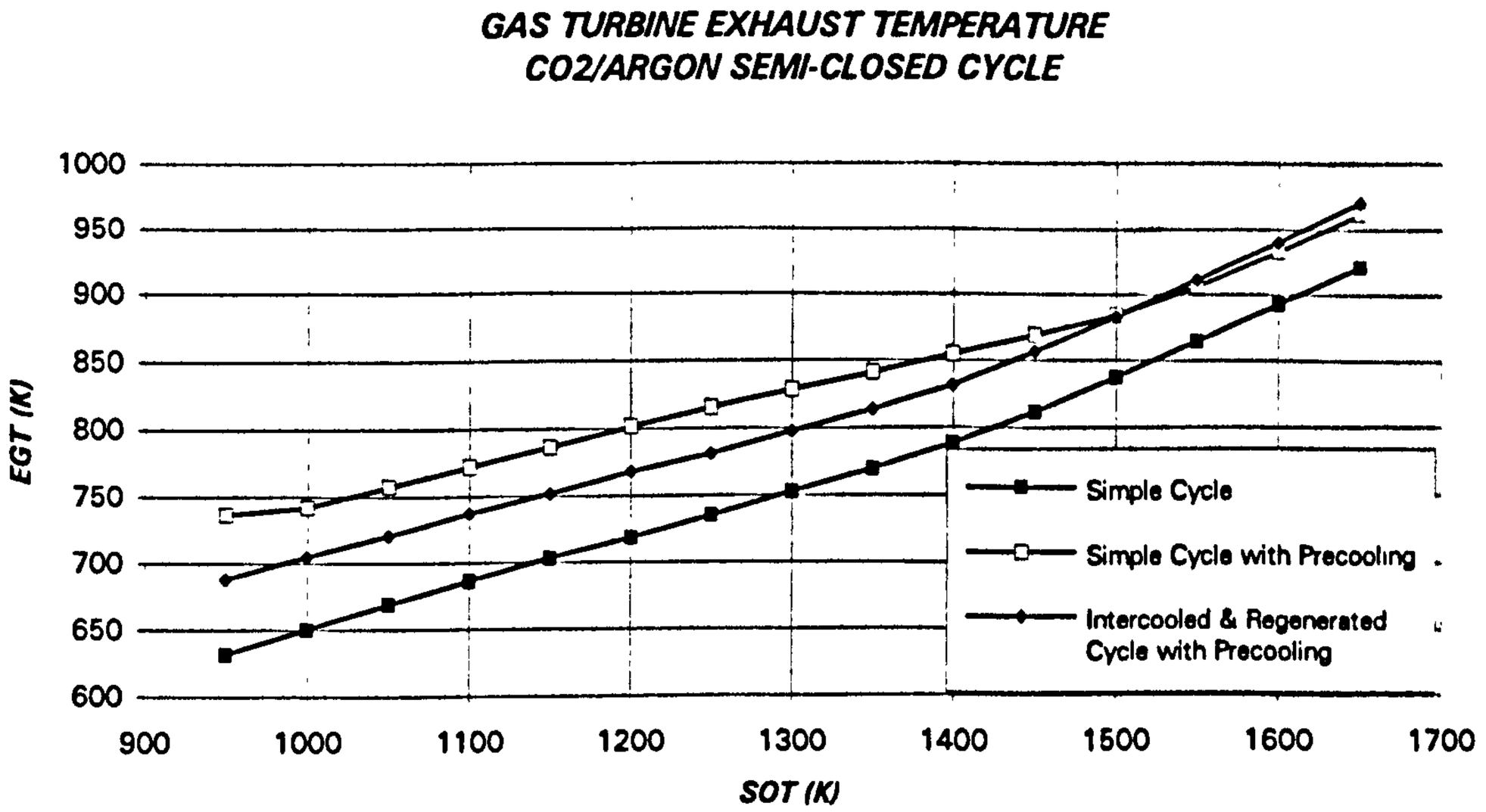

Figure 8.31. Turbine exhaust temperature vs. SOT (CYCLES III, IV and V)

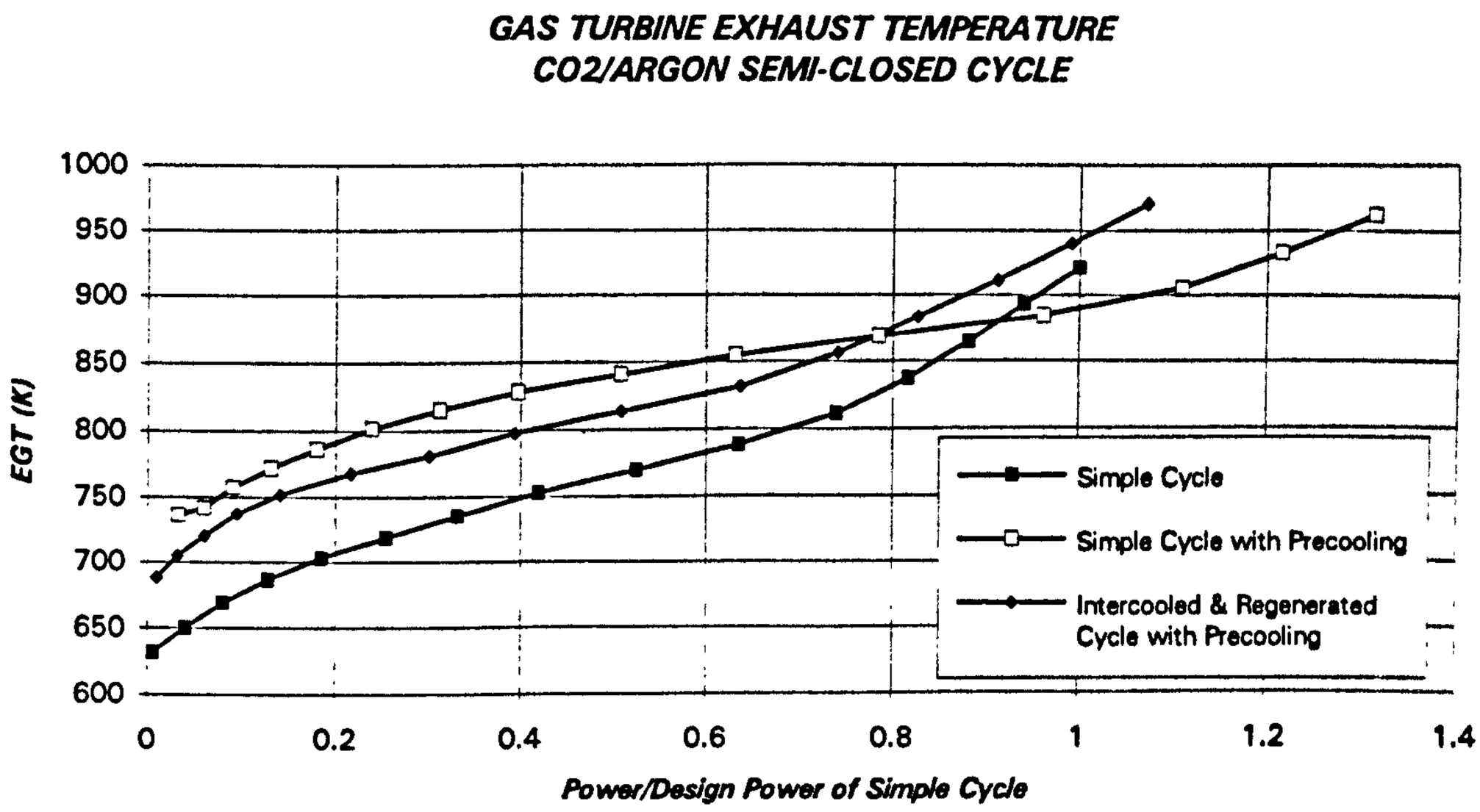

Figure 8.32. Turbine exhaust temperature vs. relative power (CYCLES III, IV and V)

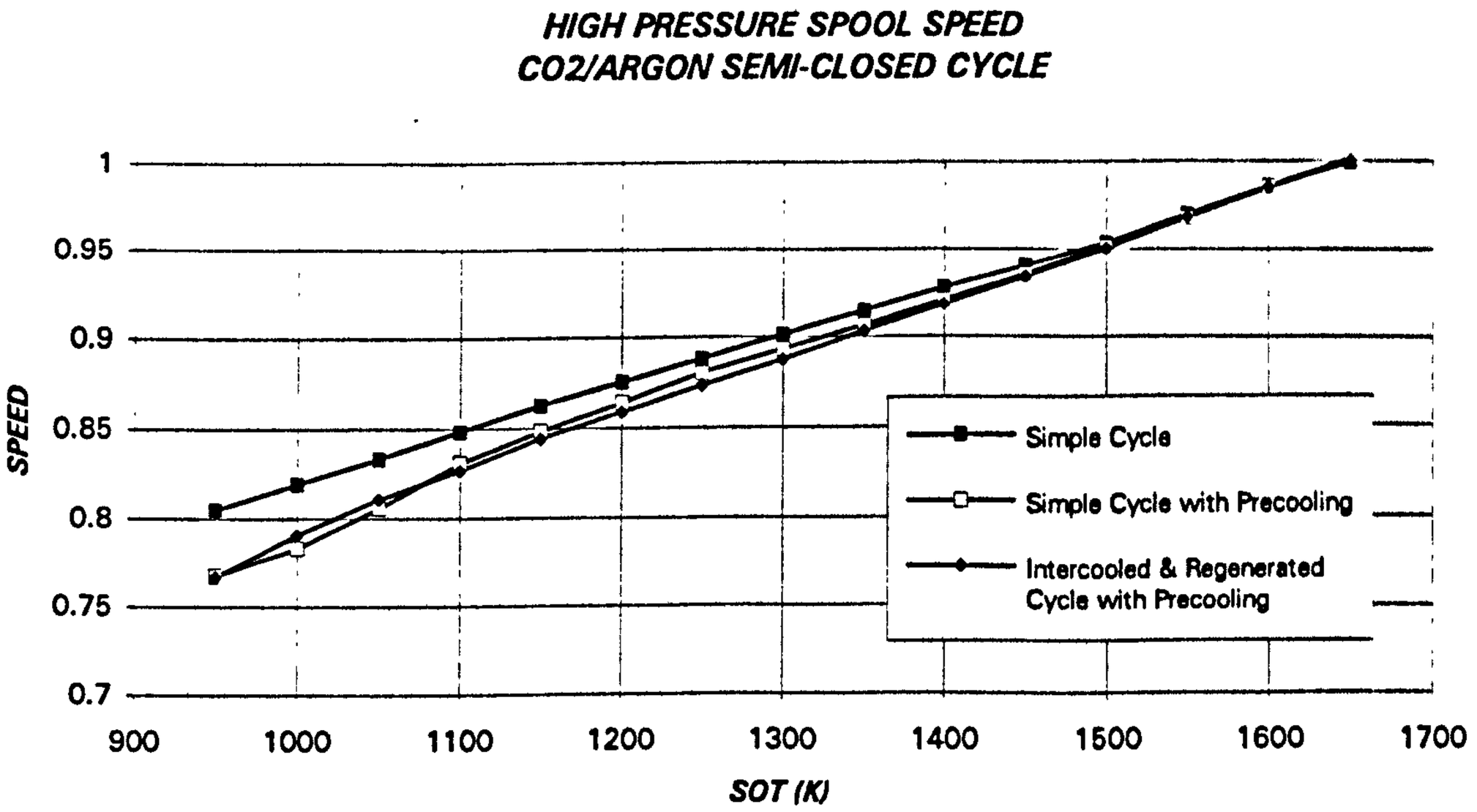

Figure 8.33. High pressure spool speed vs. SOT (CYCLES III, IV and V)

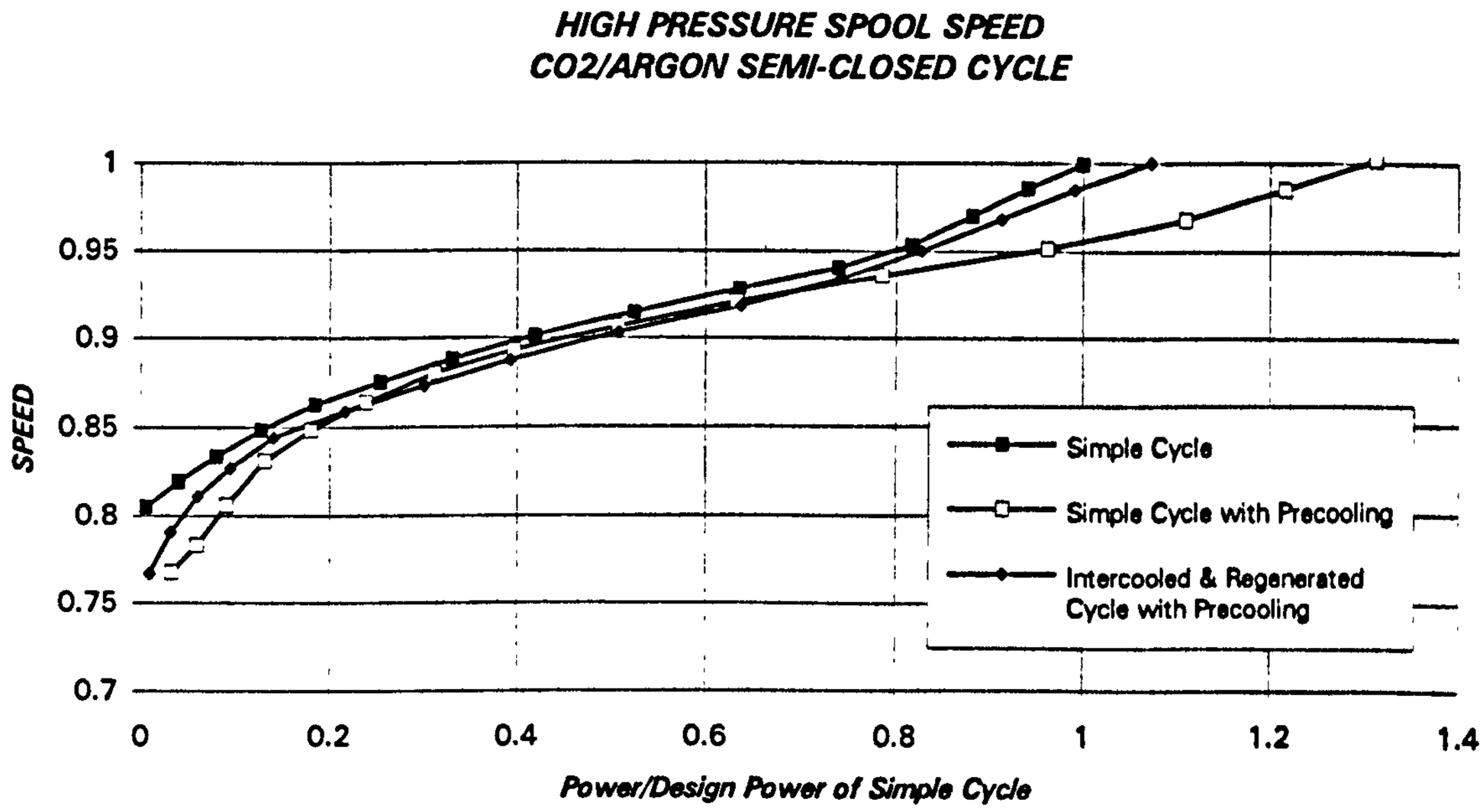

Figure 8.34. High pressure spool speed vs. relative power (CYCLES III, IV and V)

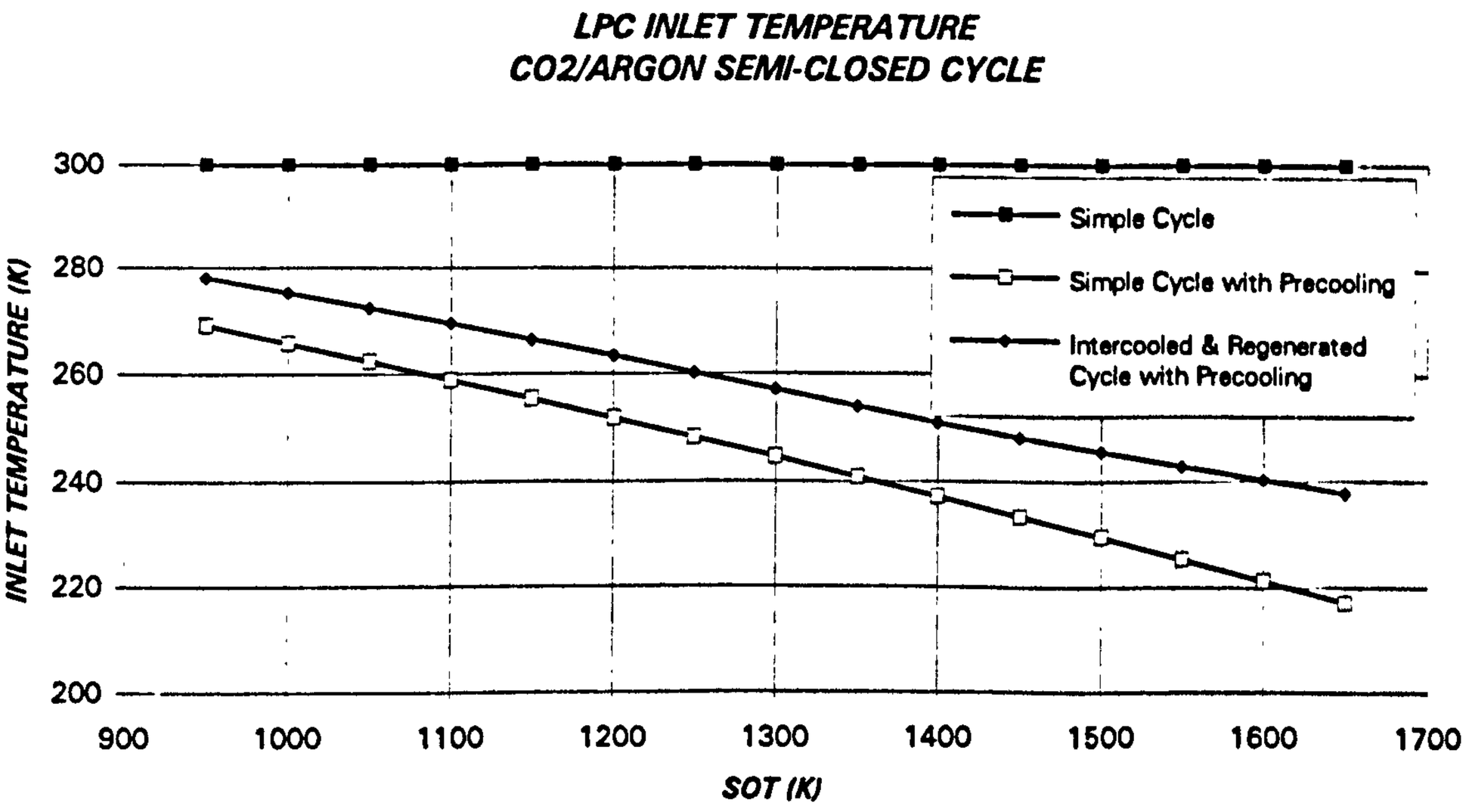

Figure 8.35. Low pressure compressor inlet temperature (after the precoolers) (CYCLES III, IV and V)

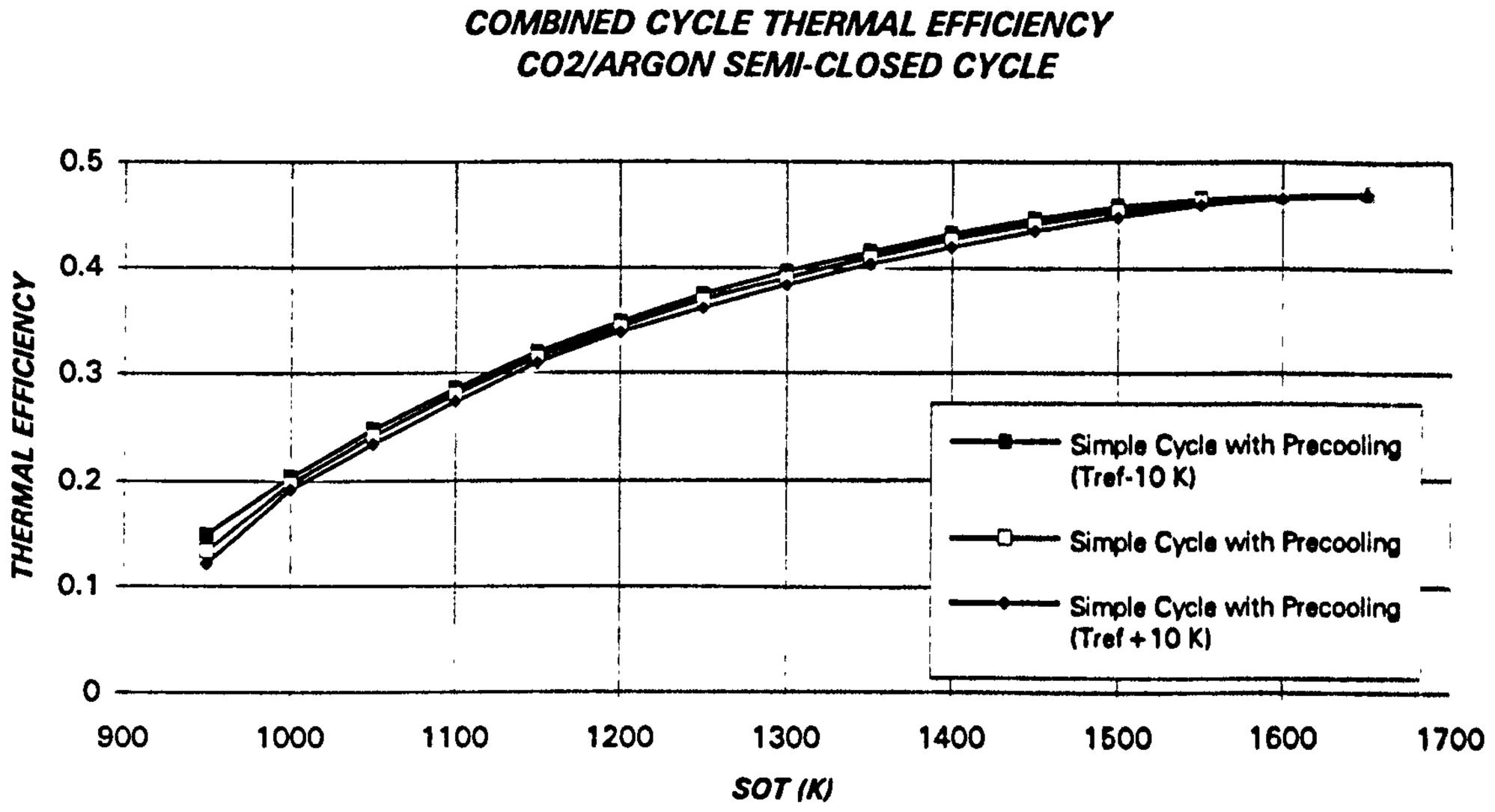

Figure 8.36. Combined cycle thermal efficiency (CYCLE IV at T_{ref} and T_{ref}±10 K)

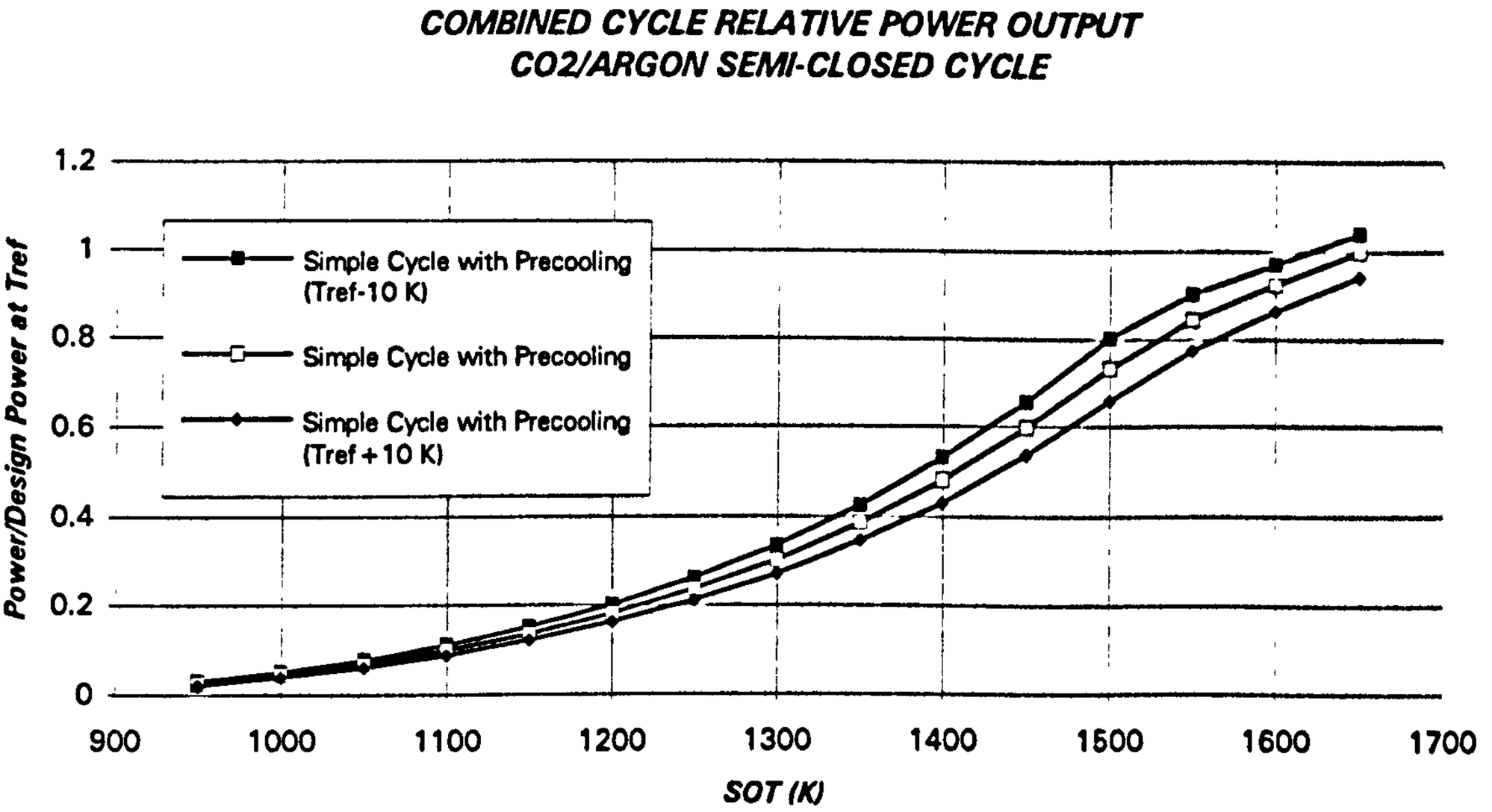

Figure 8.37. Combined cycle relative power (baseline: design power of CYCLE V at T_{ref}) (CYCLE IV at T_{ref} and T_{ref}±10 K)

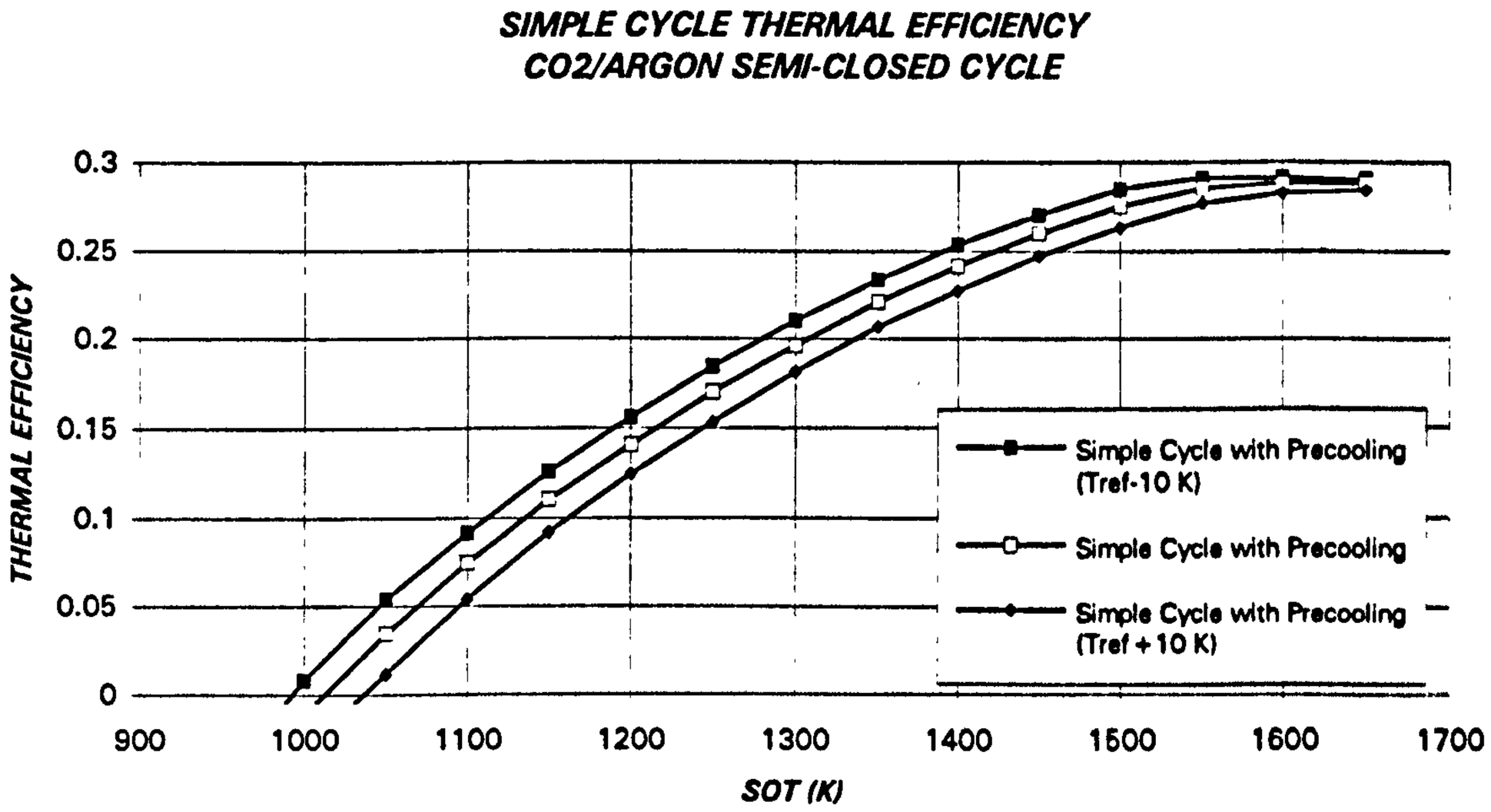

Figure 8.38. Simple cycle thermal efficiency (CYCLE IV at T_{ref} and T_{ref}±10 K)

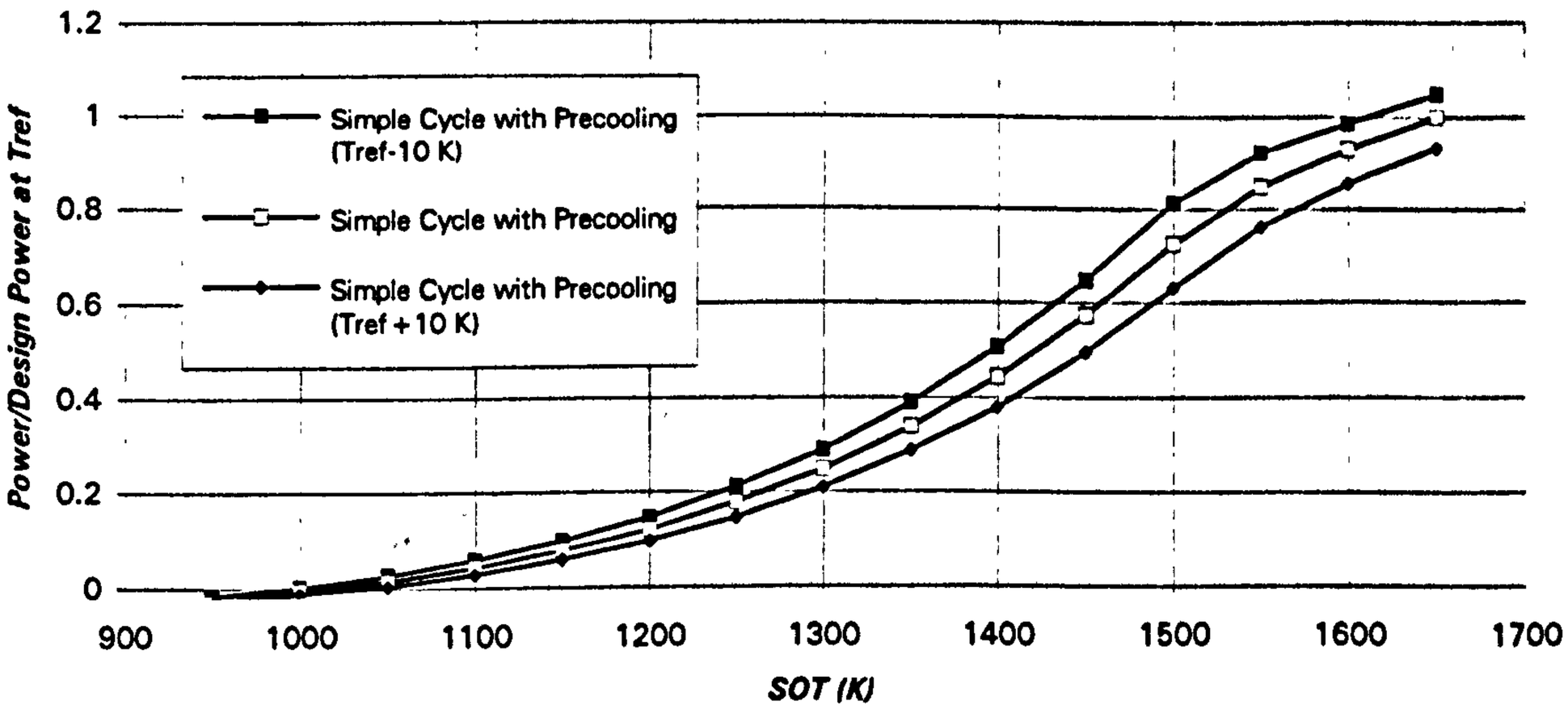

Figure 8.39. Simple cycle relative power (baseline: design power of CYCLE IV at T_{ref}) (CYCLES IV at T_{ref} and T_{ref}±10 K)

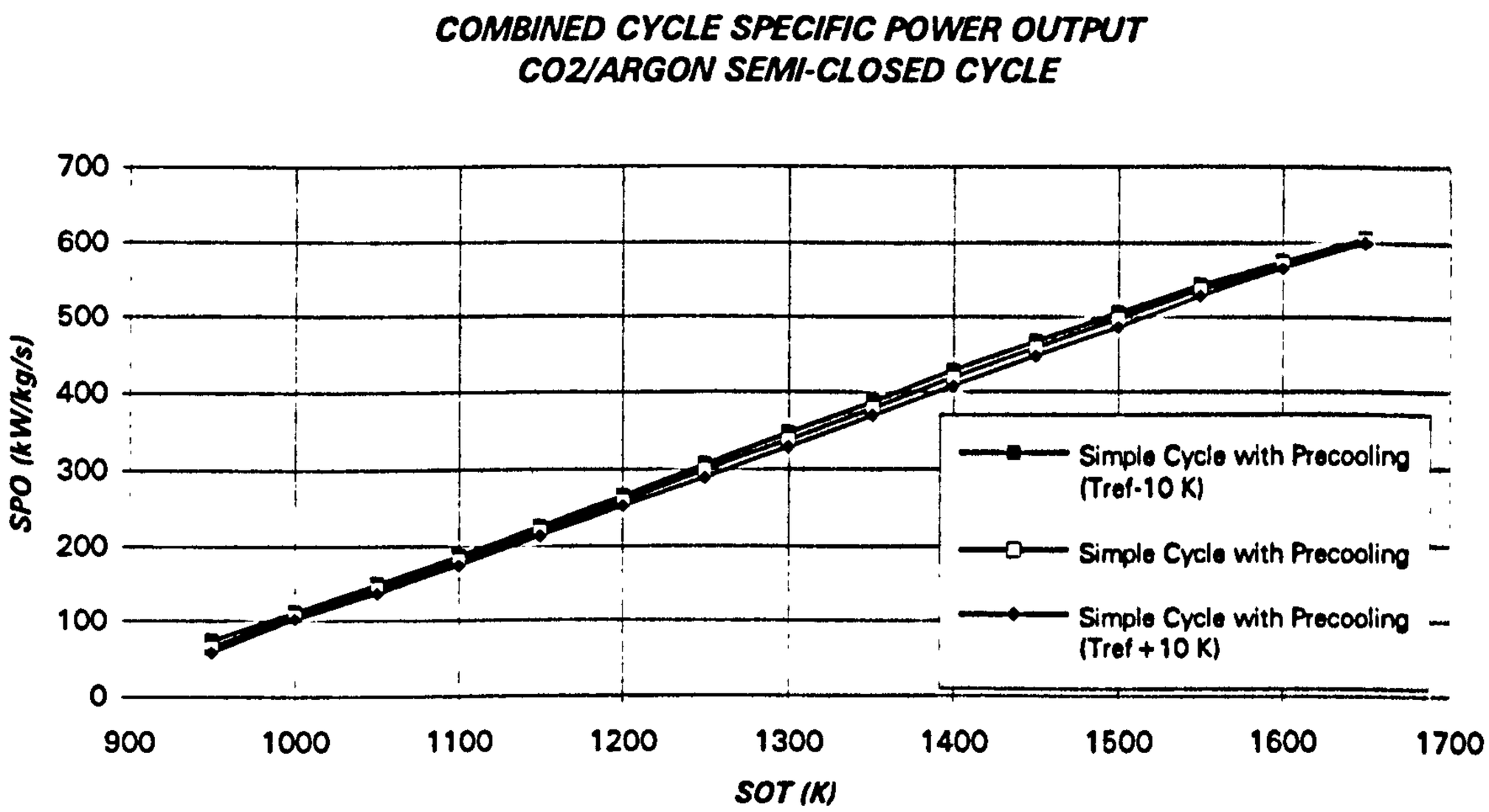

Figure 8.40. Combined cycle specific power output (kW/kg/s) (CYCLE IV at T_{ref} and T_{ref}±10 K)

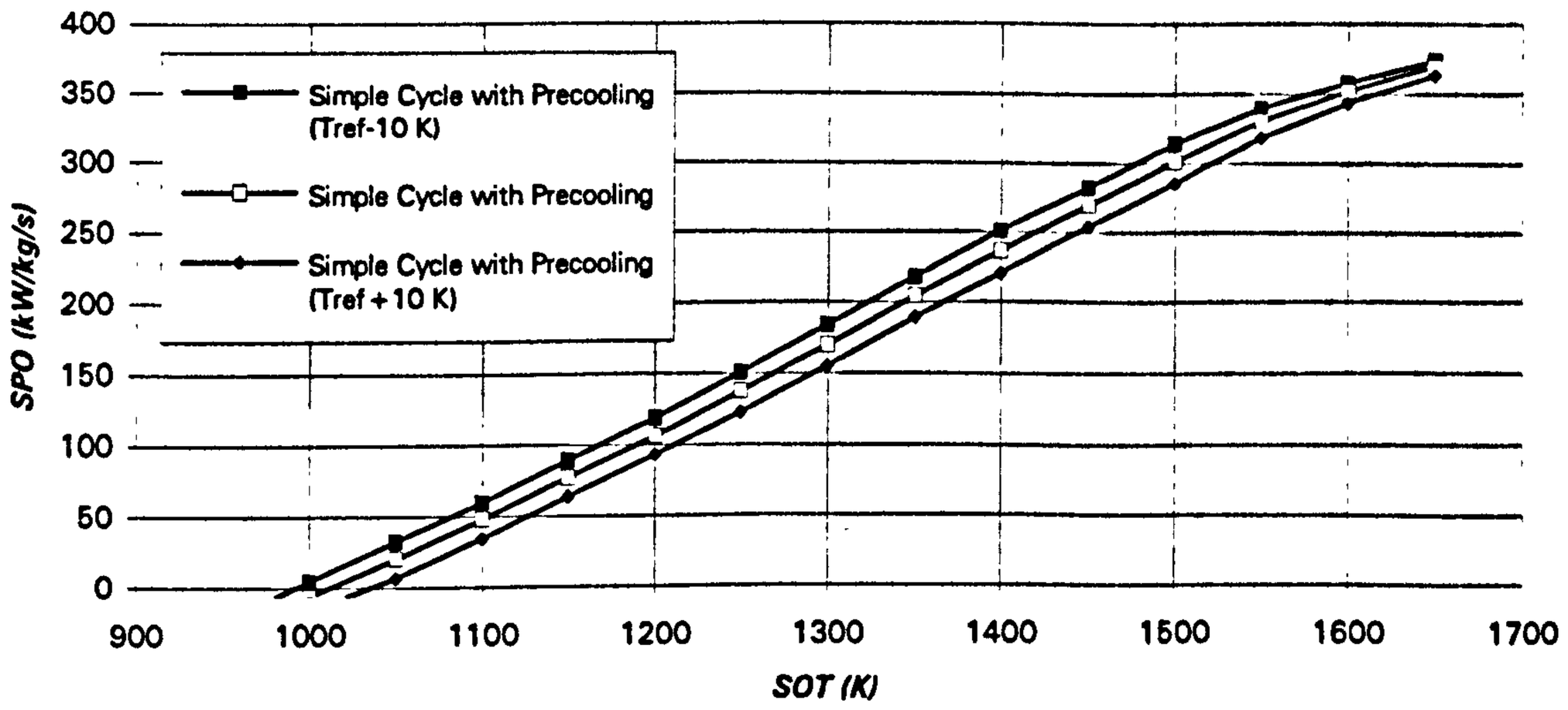

Figure 8.41. Simple cycle specific power output (kW/kg/s) (CYCLE IV at T_{ref} and T_{ref}±10 K)

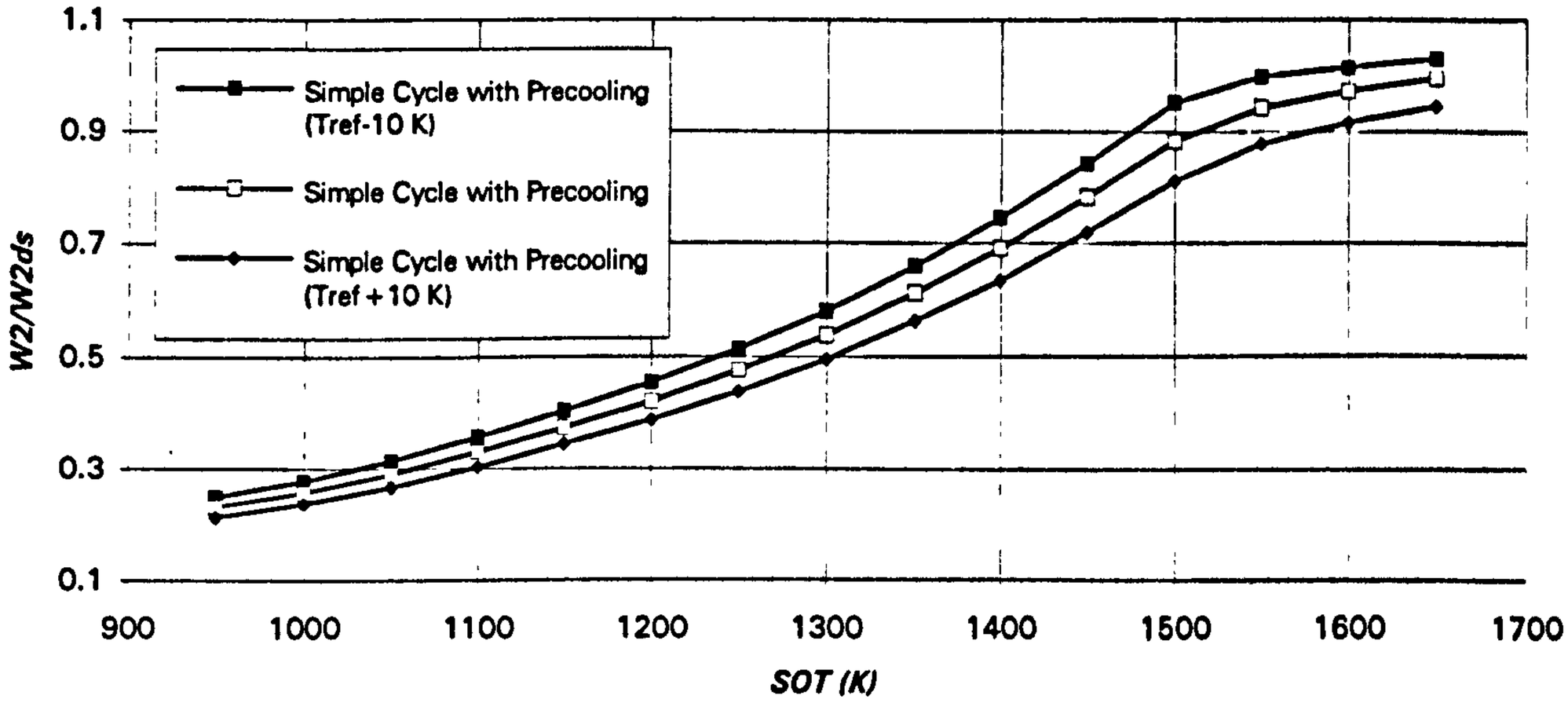

Figure 8.42. Relative mass flow (baseline: mass flow of CYCLE IV at T_{ref}) (CYCLE IV at T_{ref} and T_{ref}±10 K)

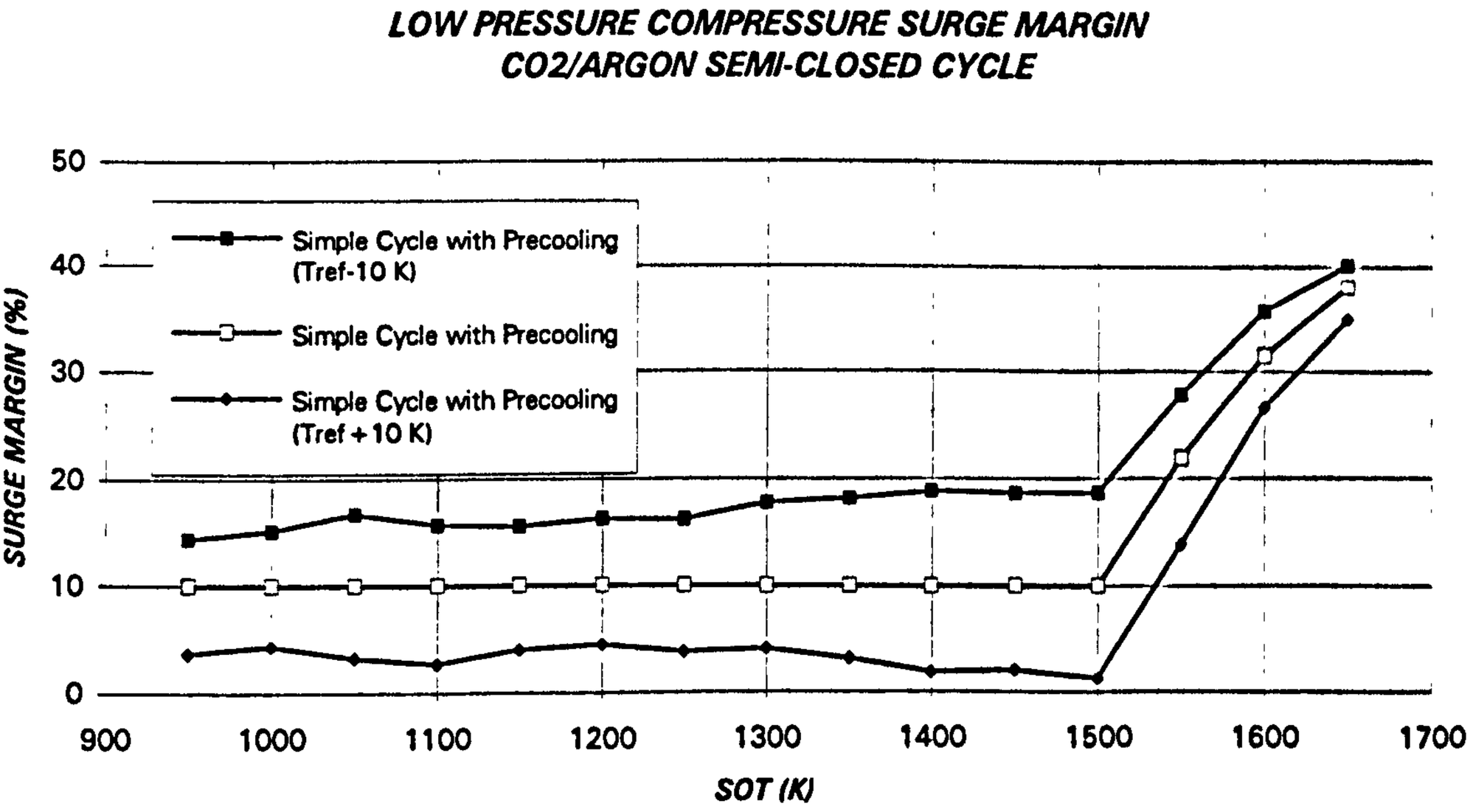

Figure 8.43. Low pressure compressor surge margin (CYCLE IV at T_{ref} and T_{ref}±10 K)

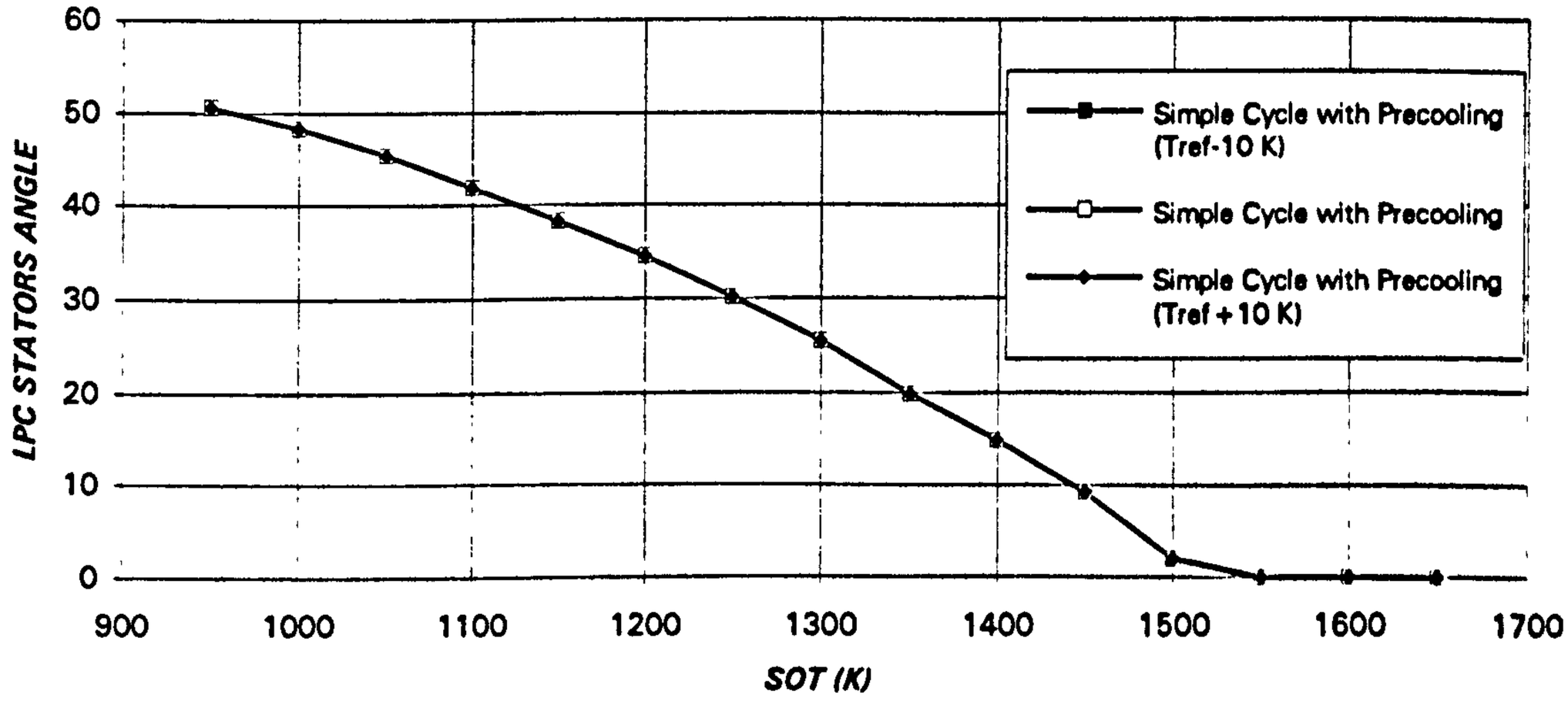

Figure 8.44. Low pressure compressor variable stators angle (CYCLE IV at T_{ref} and T_{ref}±10 K)

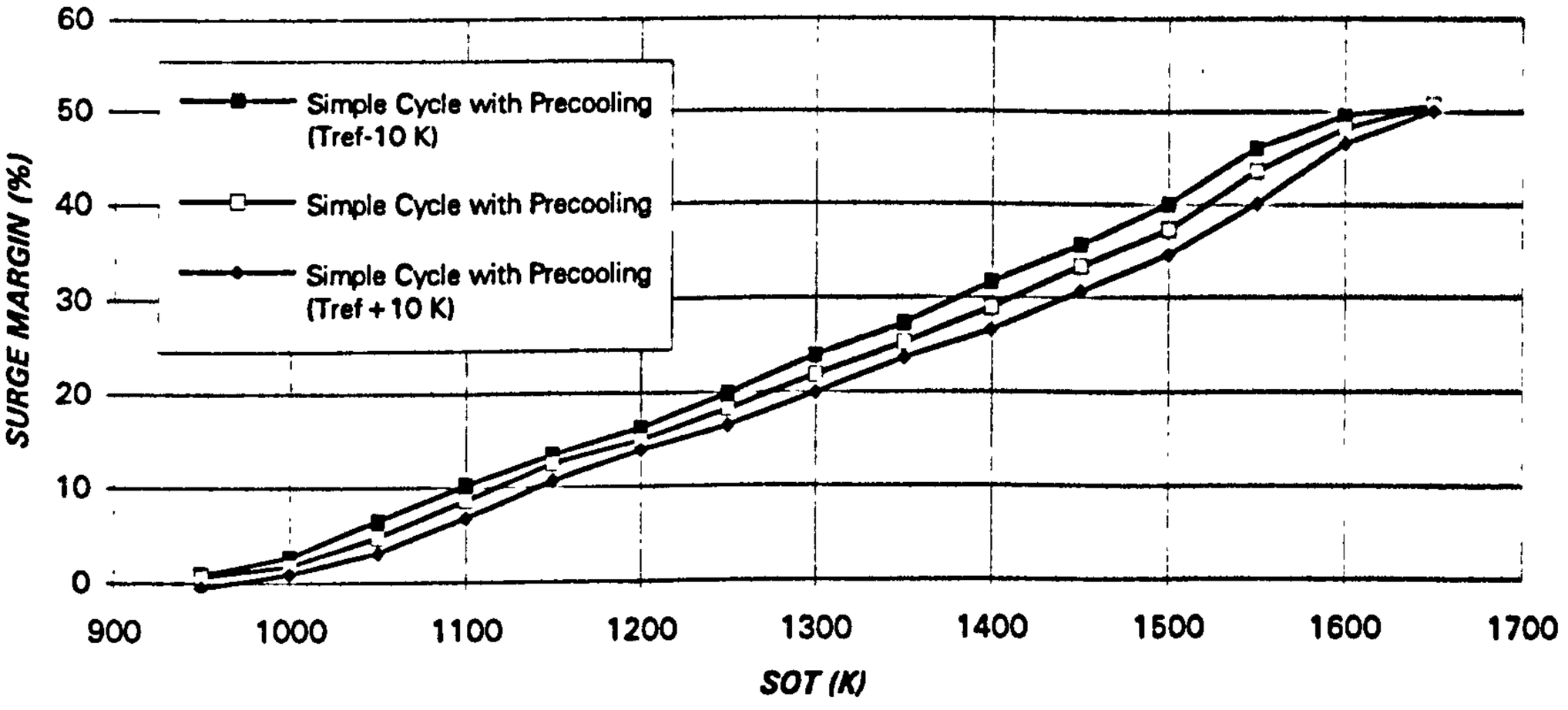

Figure 8.45. High pressure compressor surge margin (CYCLE IV at T_{ref} and T_{ref}±10 K)

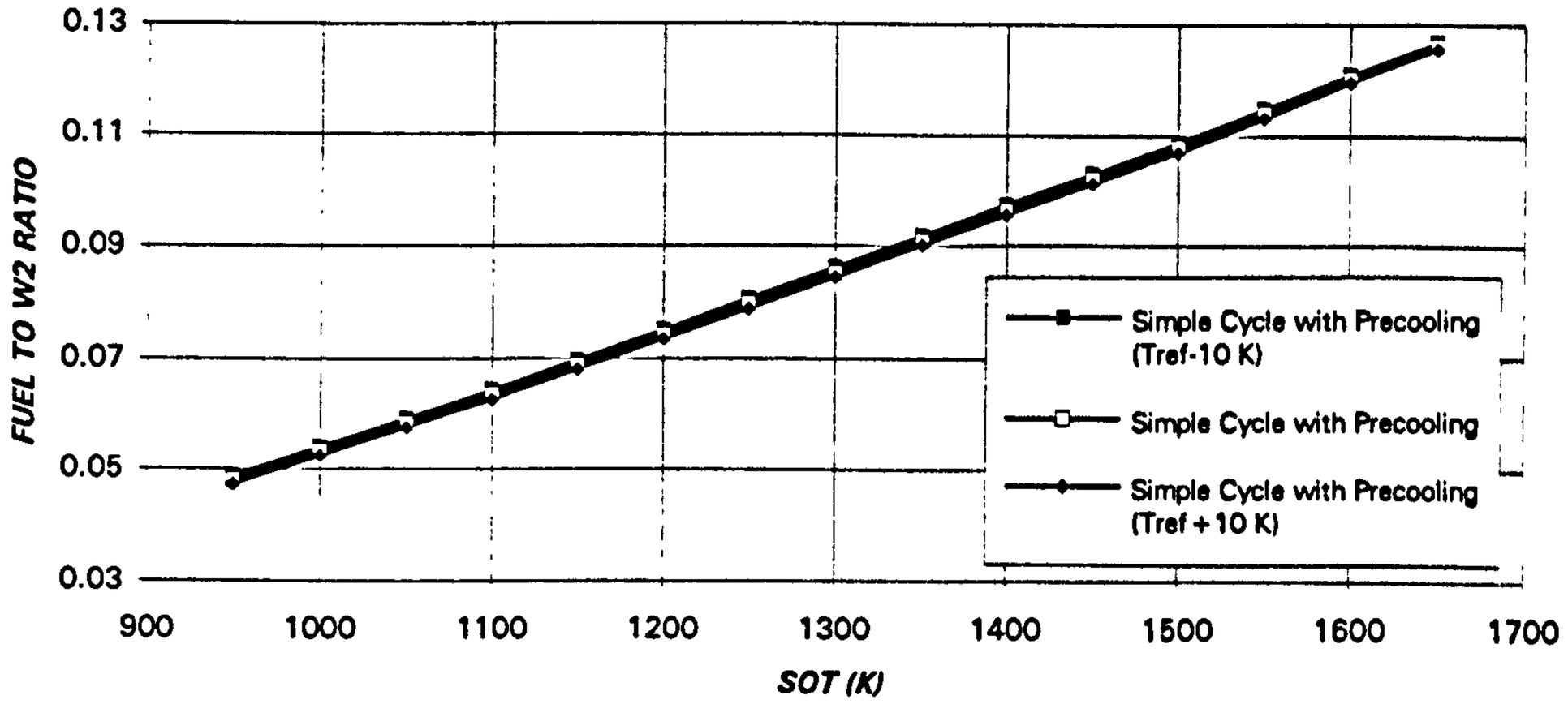

Figure 8.46. Fuel to compressor inlet mass flow ratio (CYCLE IV at T_{ref} and T_{ref}±10 K)

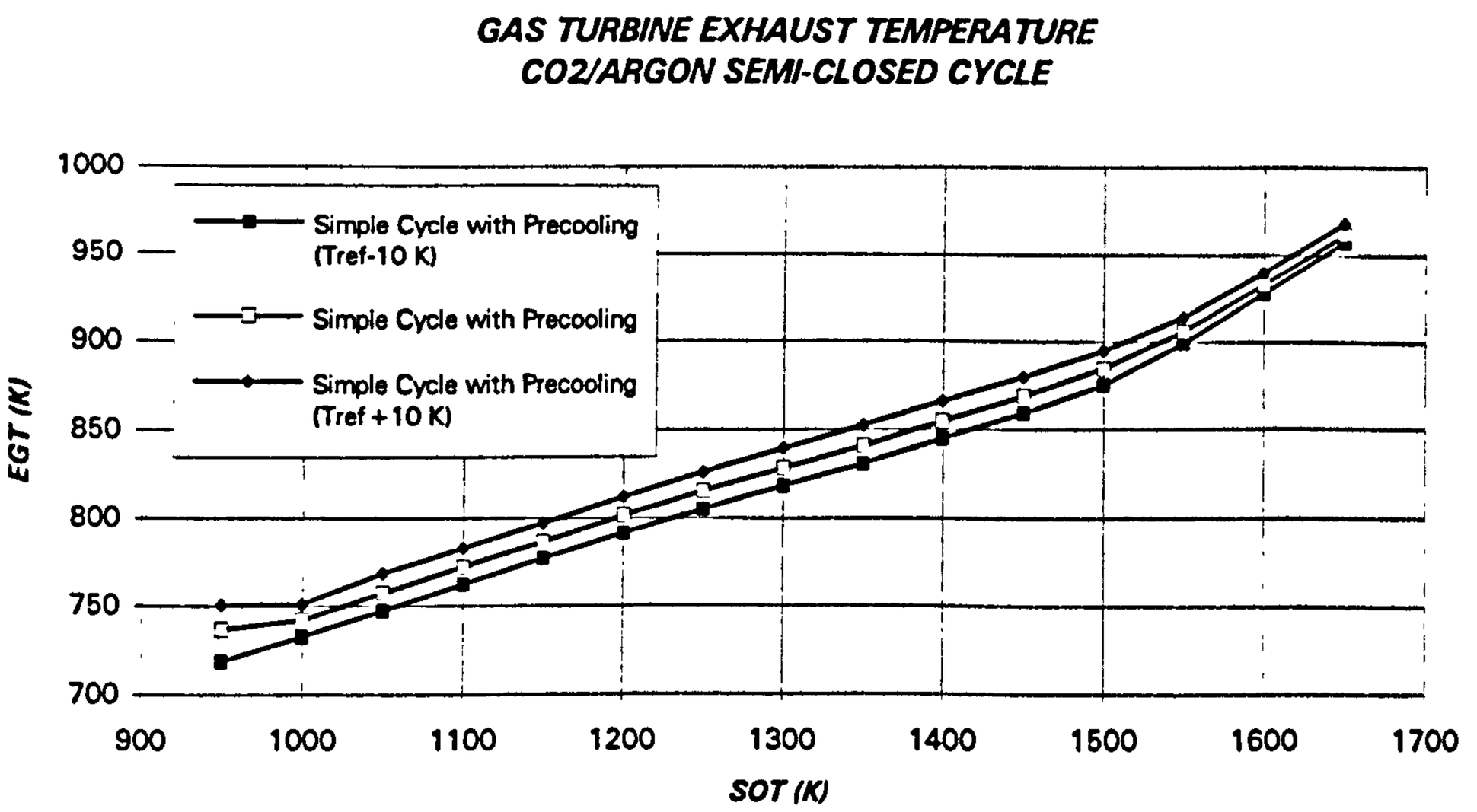

Figure 8.47. Turbine exhaust temperature vs. SOT (CYCLE IV at T_{ref} and T_{ref}±10 K)

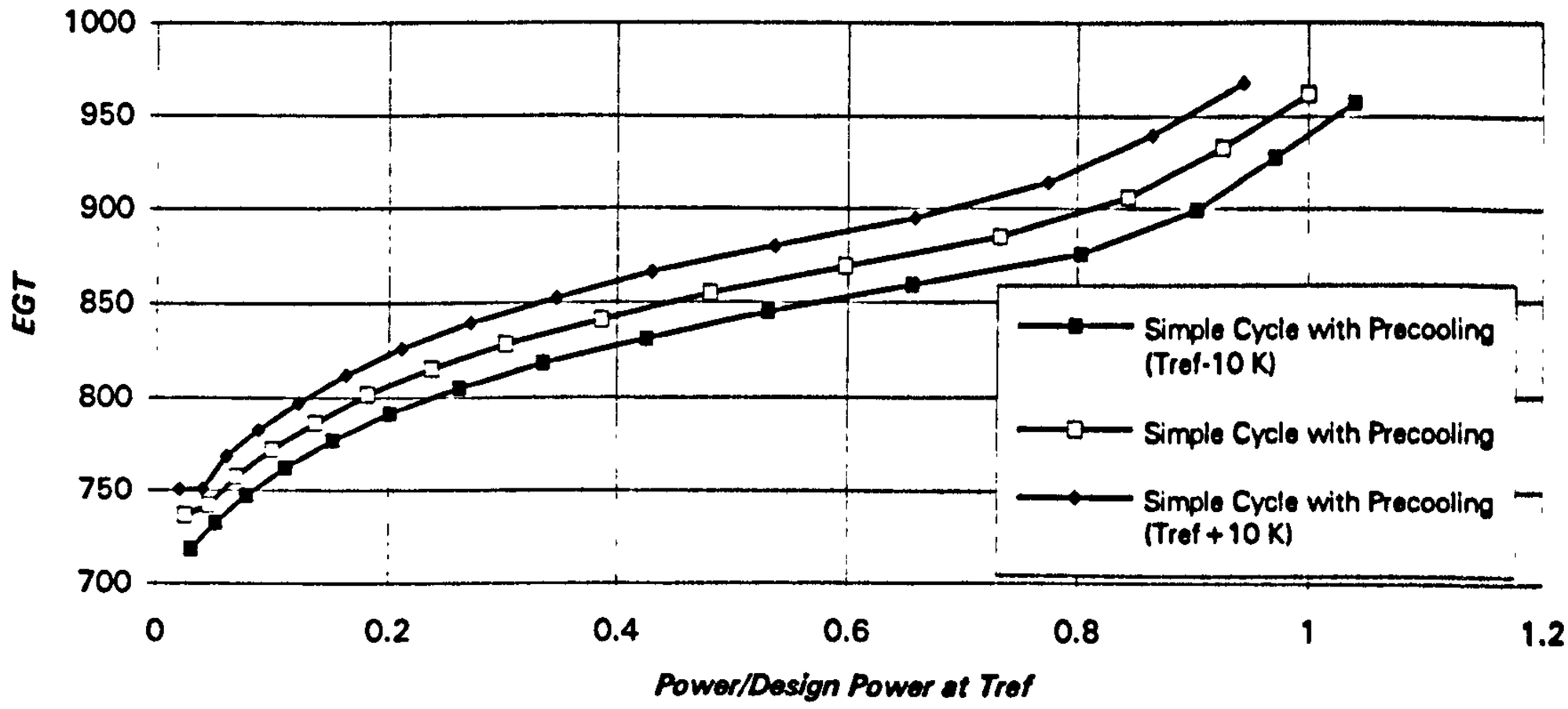

Figure 8.48. Turbine exhaust temperature vs. relative power (CYCLE IV at T_{ref} and T_{ref}±10 K)

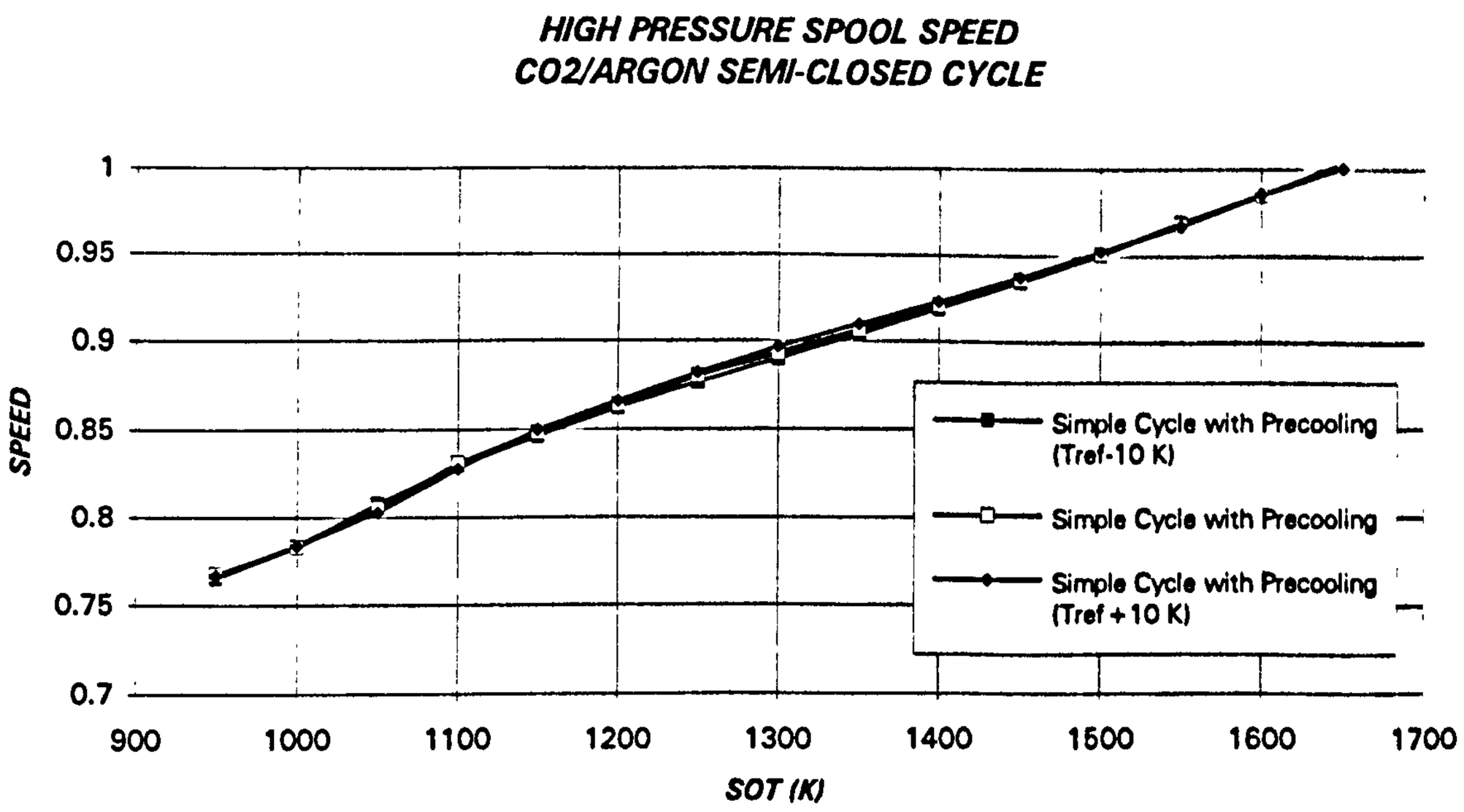

Figure 8.49. High pressure spool speed vs. SOT (CYCLE IV at T_{ref} and T_{ref}±10 K)

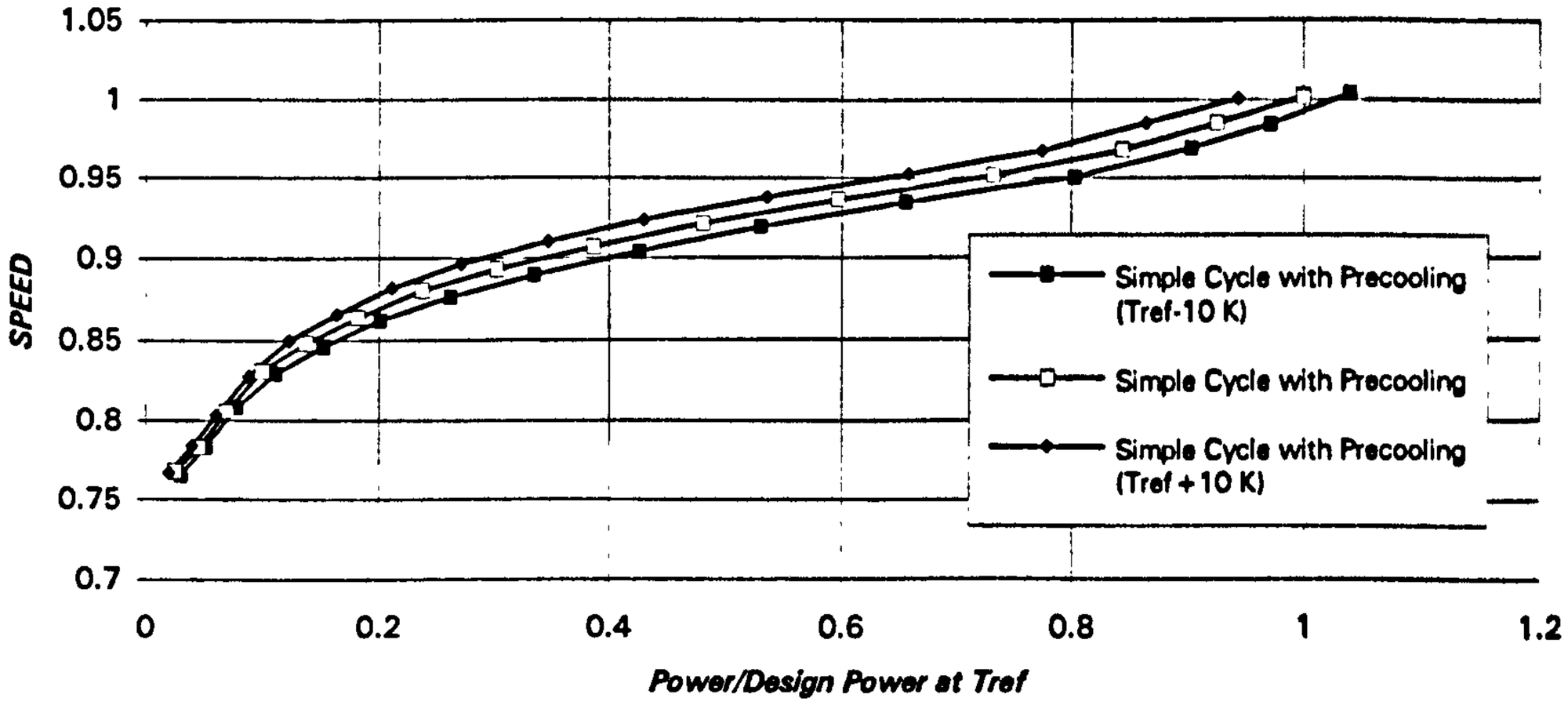

Figure 8.50. High pressure spool speed vs. relative power (CYCLE IV at T_{ref} and T_{ref}±10 K)

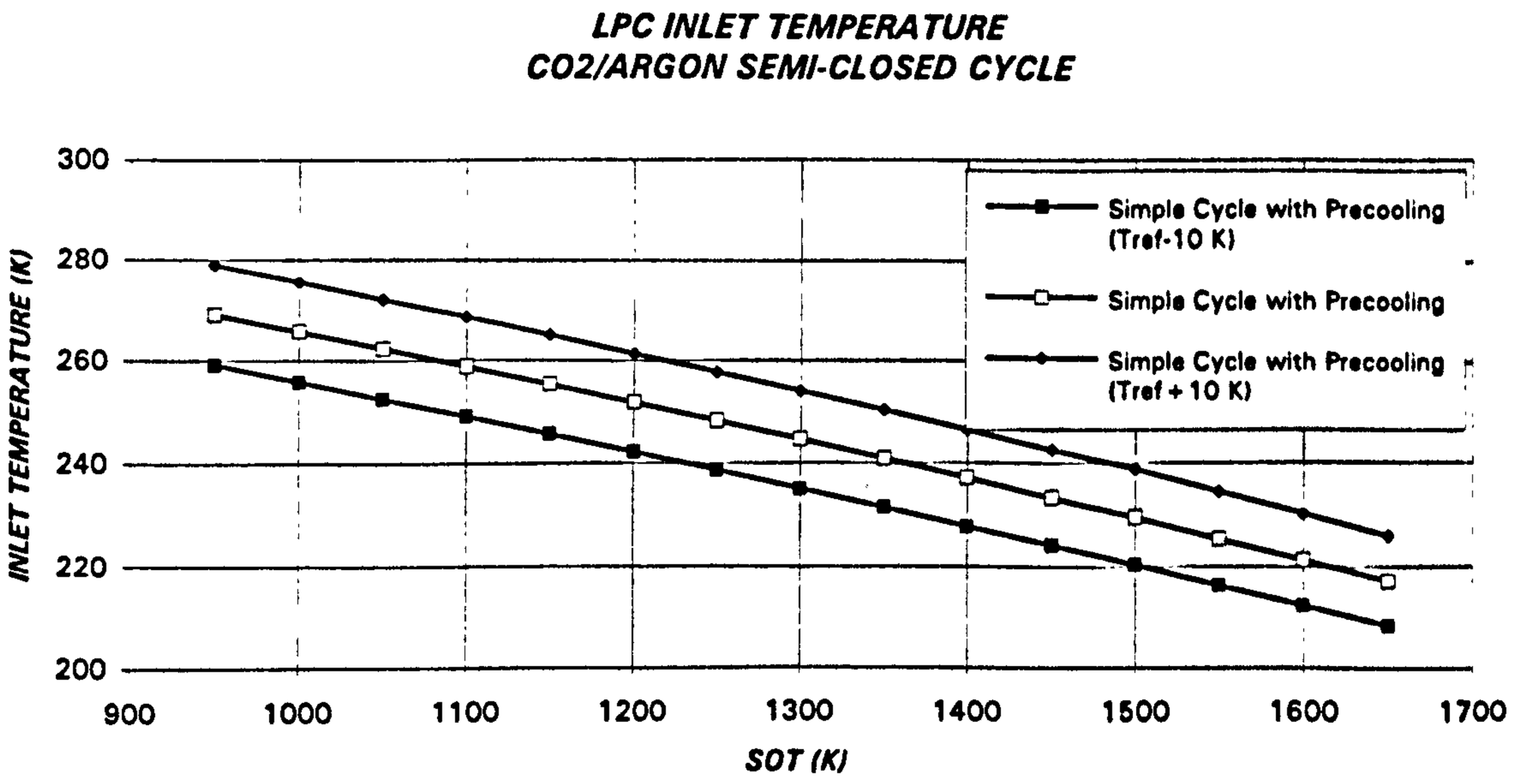

Figure 8.51. Low pressure compressor inlet temperature (after the precoolers) (CYCLE IV at T_{ref} and T_{ref}±10 K)

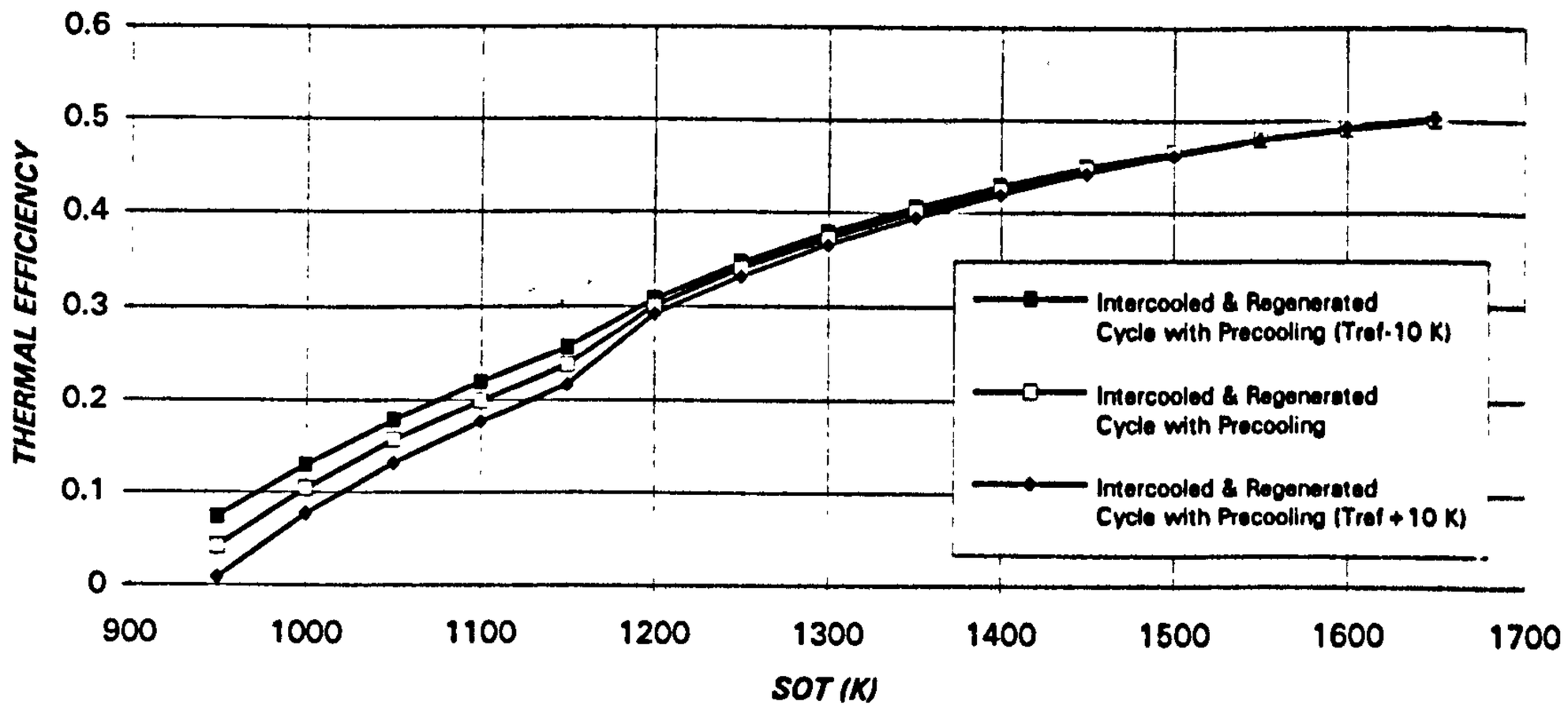

Figure 8.52. Combined cycle thermal efficiency (CYCLE V at T_{ref} and T_{ref}±10 K)

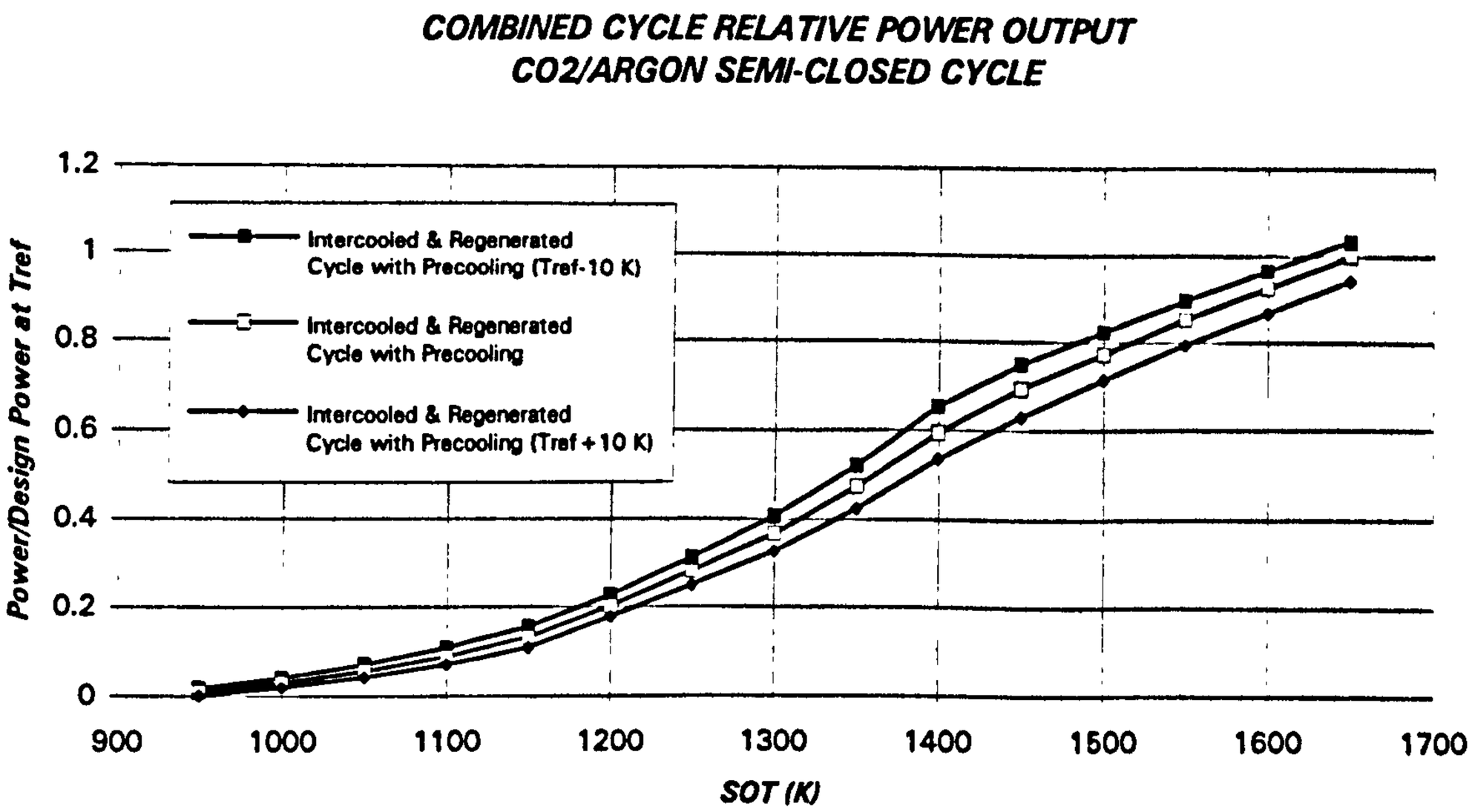

Figure 8.53. Combined cycle relative power (baseline: design power of CYCLE V at T_{ref}) (CYCLE V at T_{ref} and T_{ref}±10 K)

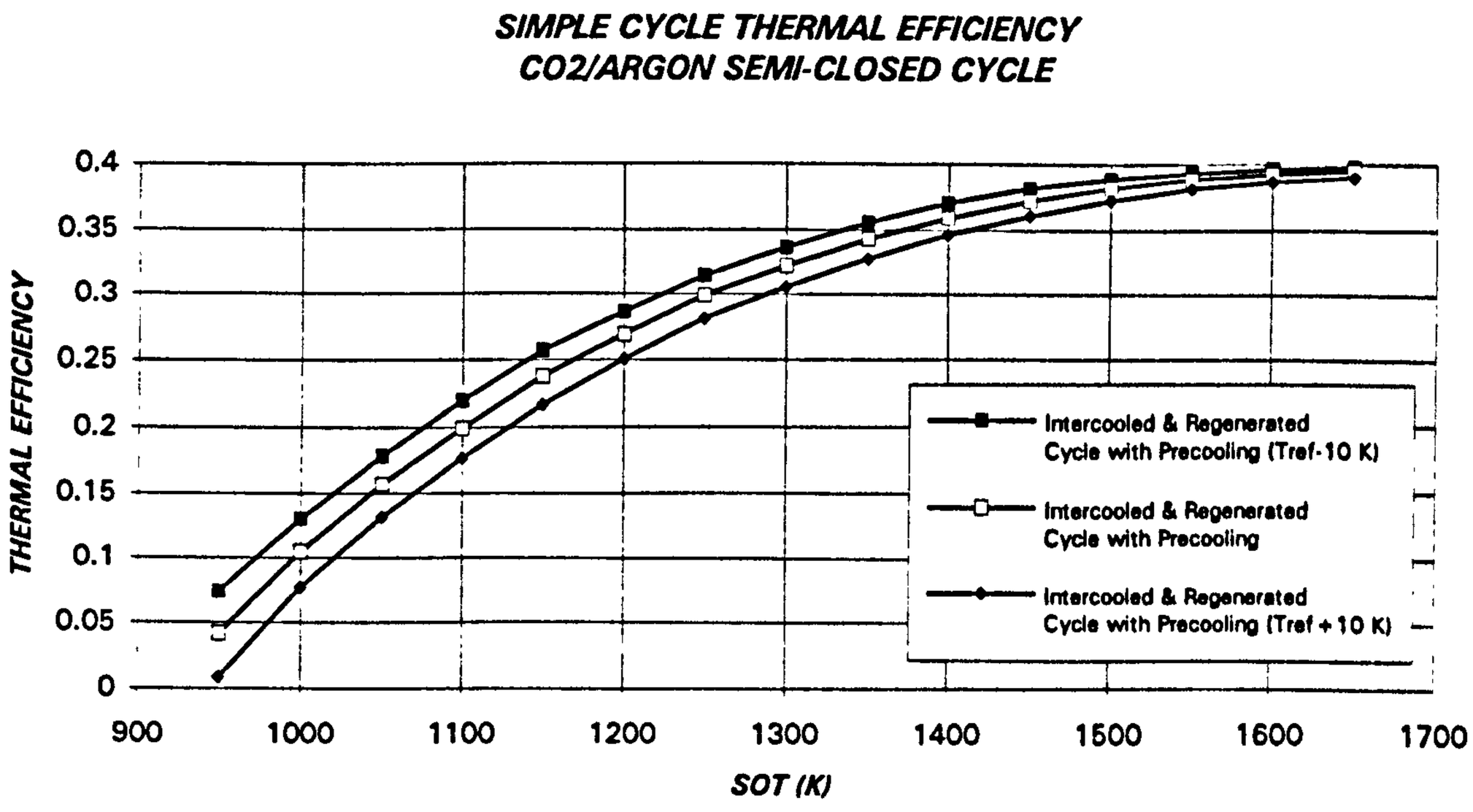

Figure 8.54. Simple cycle thermal efficiency (CYCLE V at T_{ref} and T_{ref}±10 K)

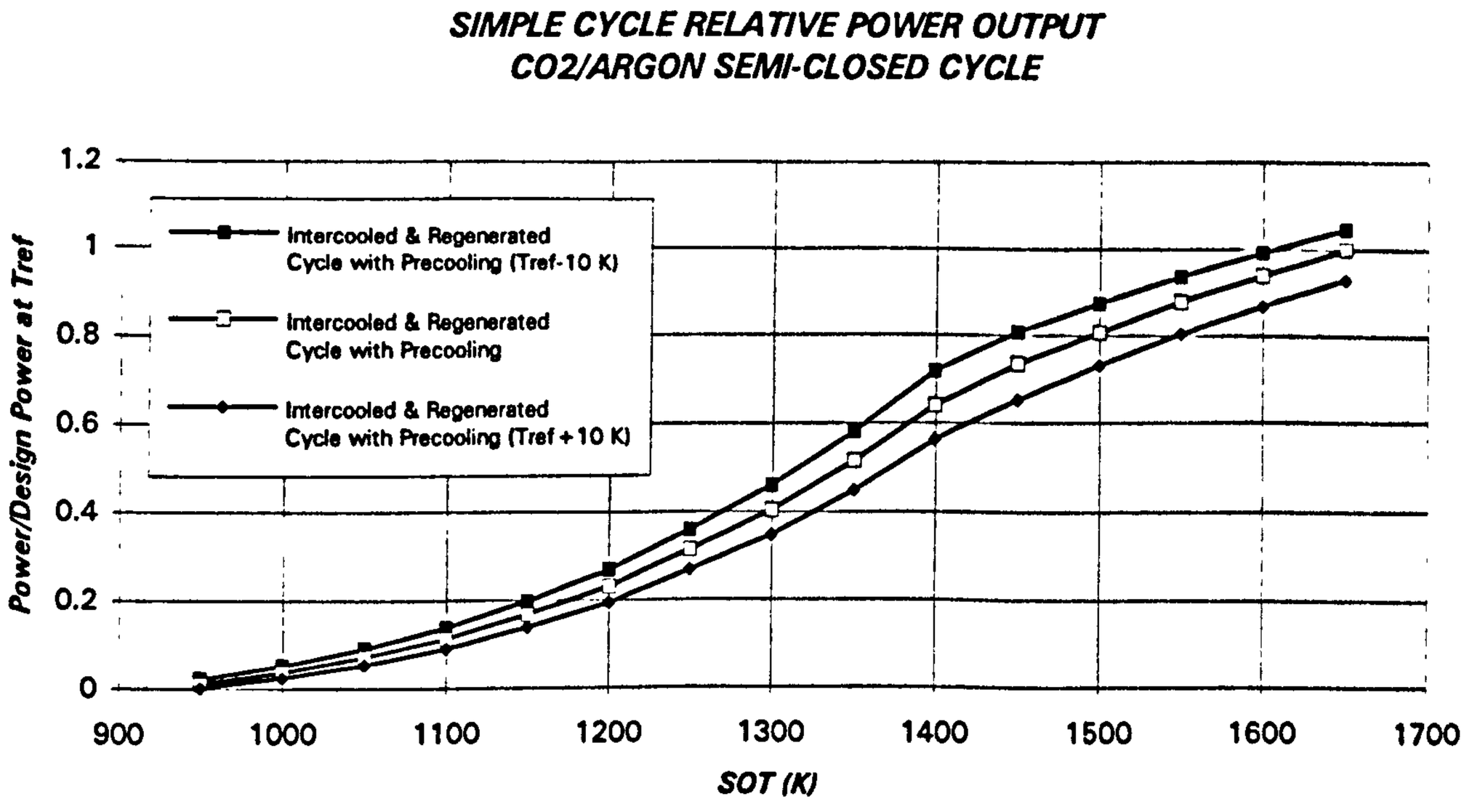

Figure 8.55. Simple cycle relative power (baseline: design power of CYCLE V at T_{ref}) (CYCLES V at T_{ref} and T_{ref}±10 K)

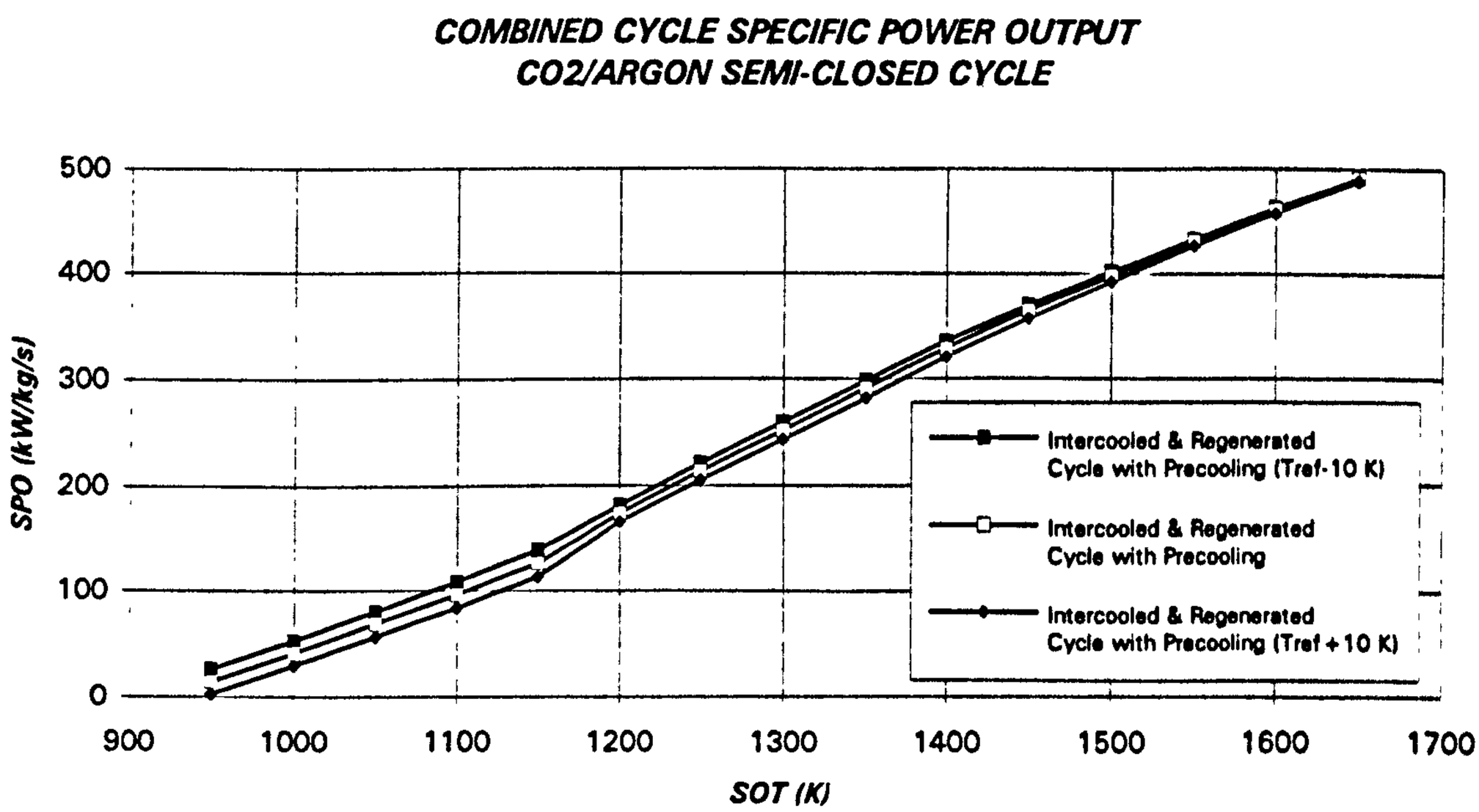

Figure 8.56. Combined cycle specific power output (kW/kg/s) (CYCLE V at T_{ref} and T_{ref}±10 K)

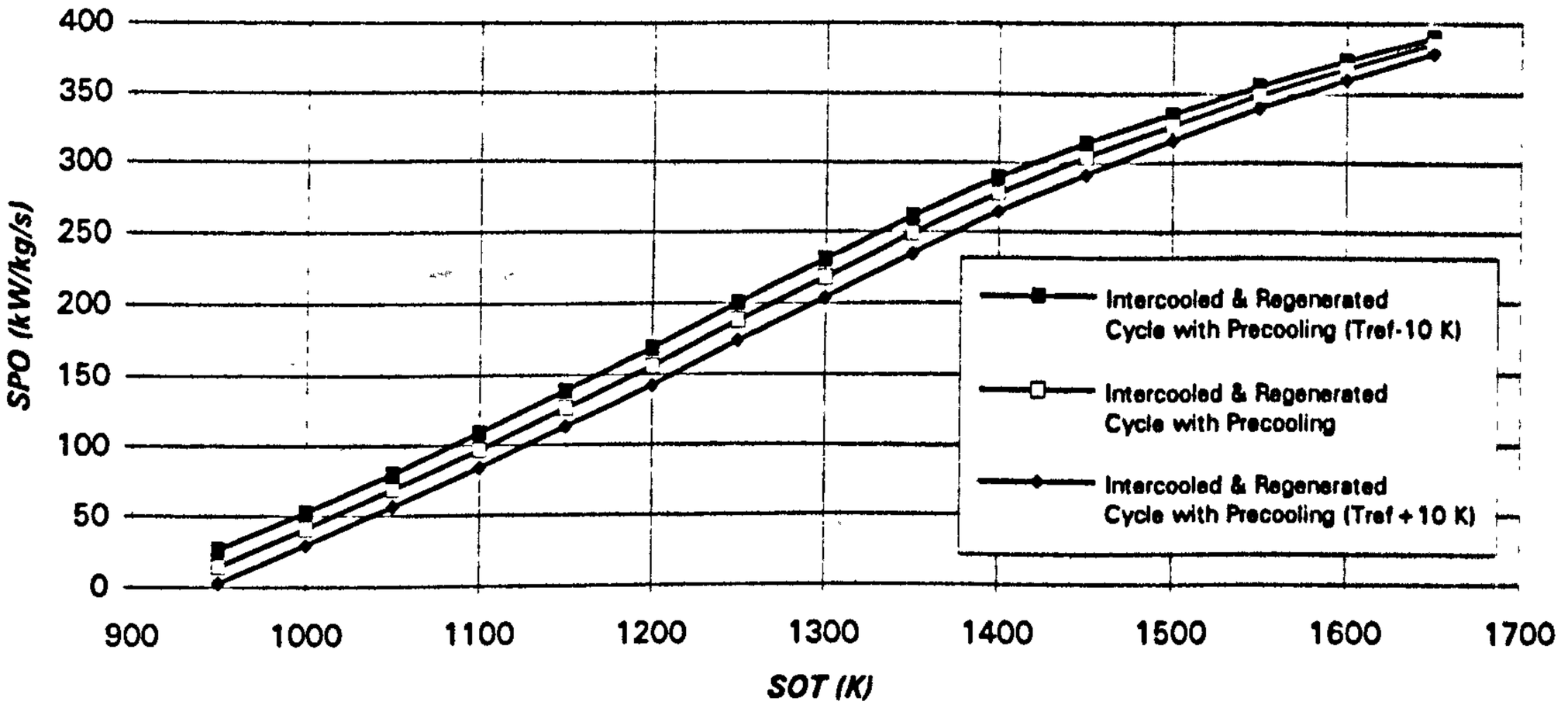

Figure 8.57. Simple cycle specific power output (kW/kg/s) (CYCLE V at T_{ref} and T_{ref}±10 K)

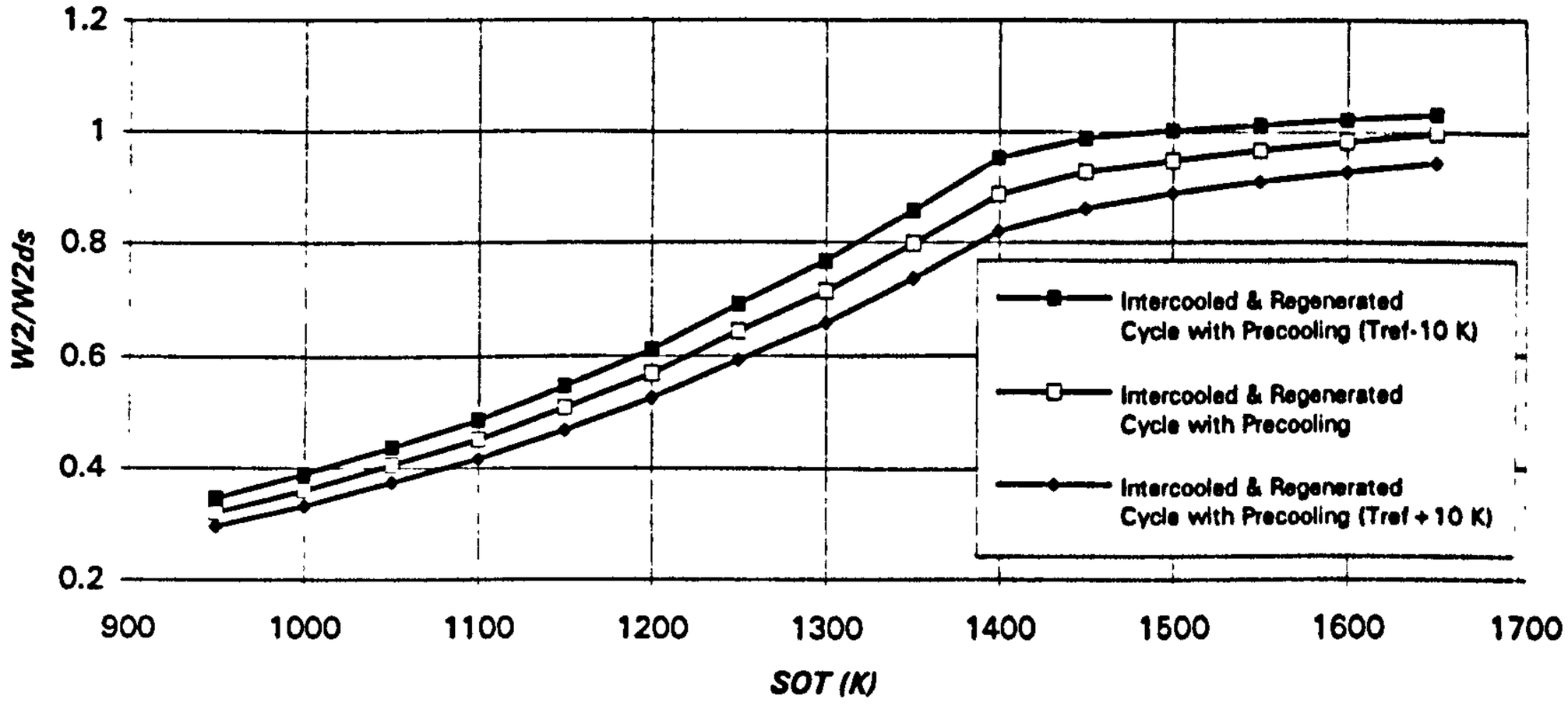

Figure 8.58. Relative mass flow (baseline: mass flow of CYCLE V at T_{ref}) (CYCLE V at T_{ref} and T_{ref}±10 K)

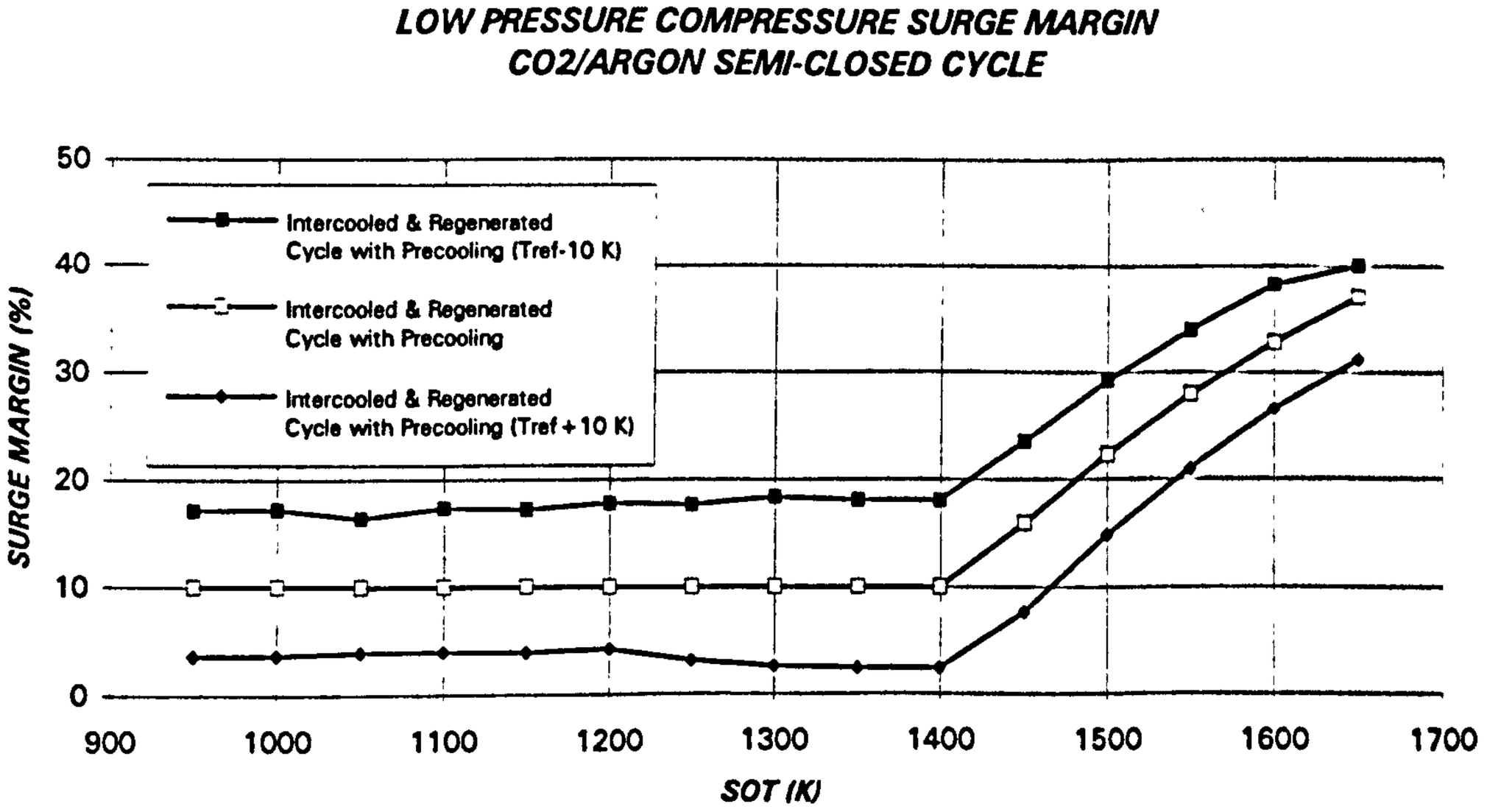

Figure 8.59. Low pressure compressor surge margin (CYCLE V at T_{ref} and T_{ref}±10 K)

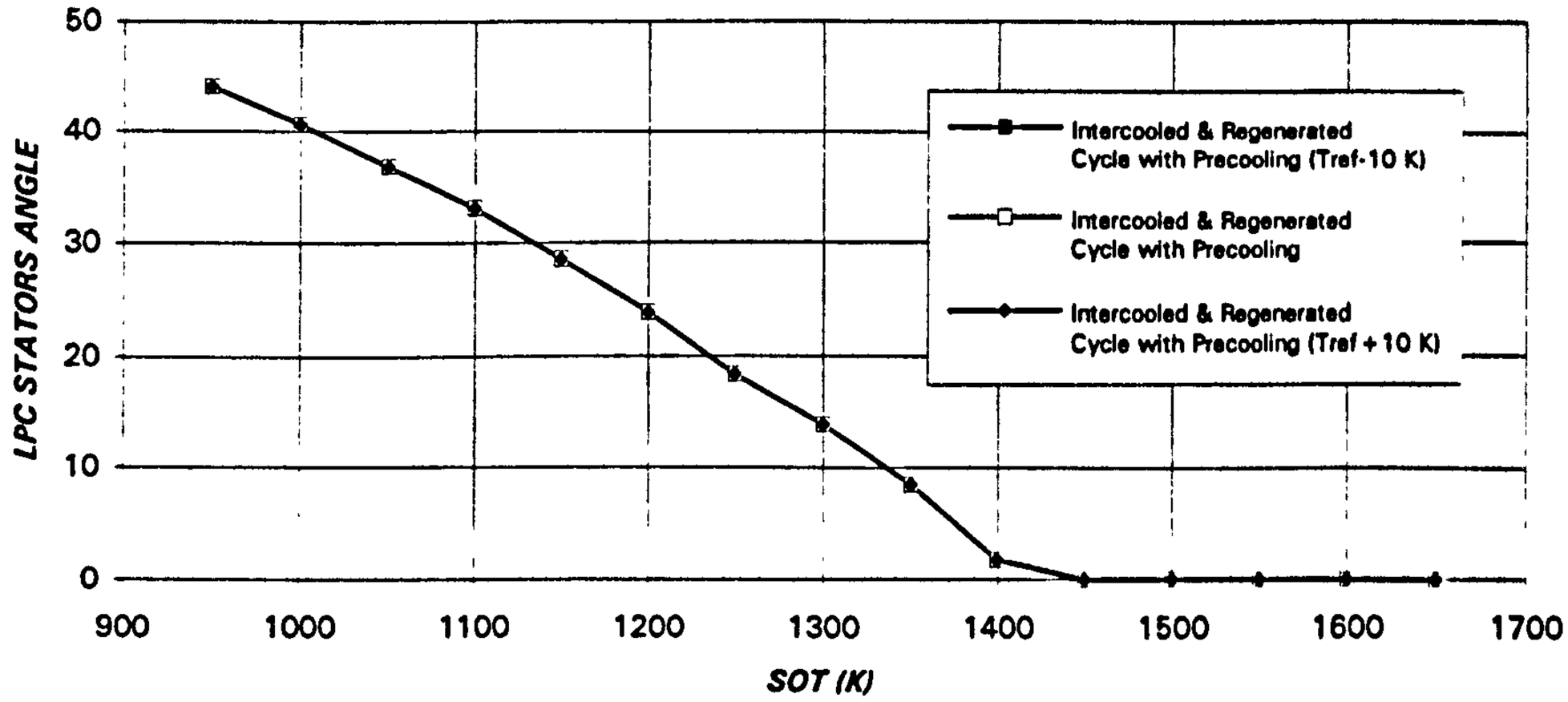

Figure 8.60. Low pressure compressor variable stators angle (CYCLE V at T_{ref} and T_{ref}±10 K)

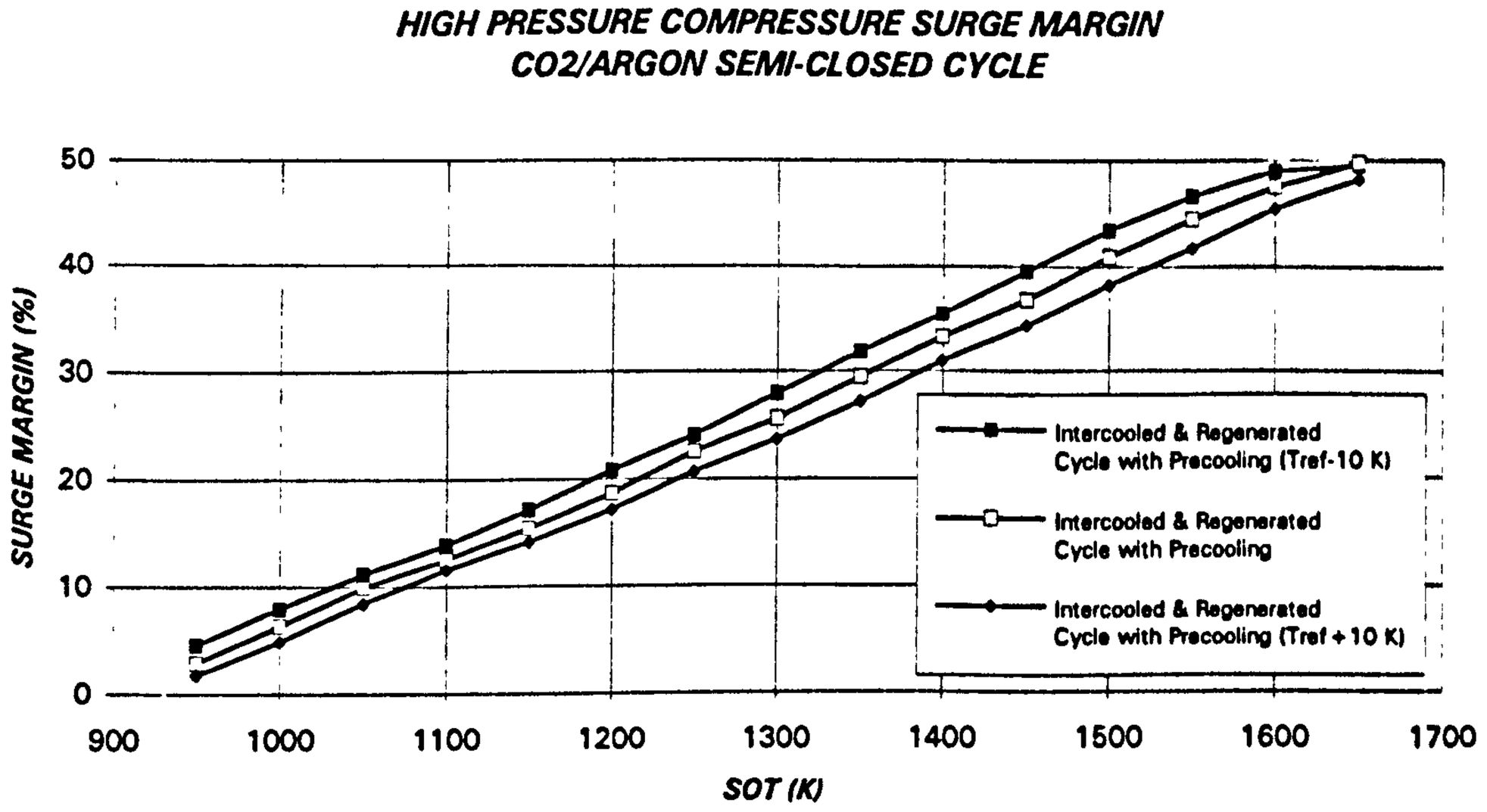

Figure 8.61. High pressure compressor surge margin (CYCLE V at T_{ref} and T_{ref}±10 K)

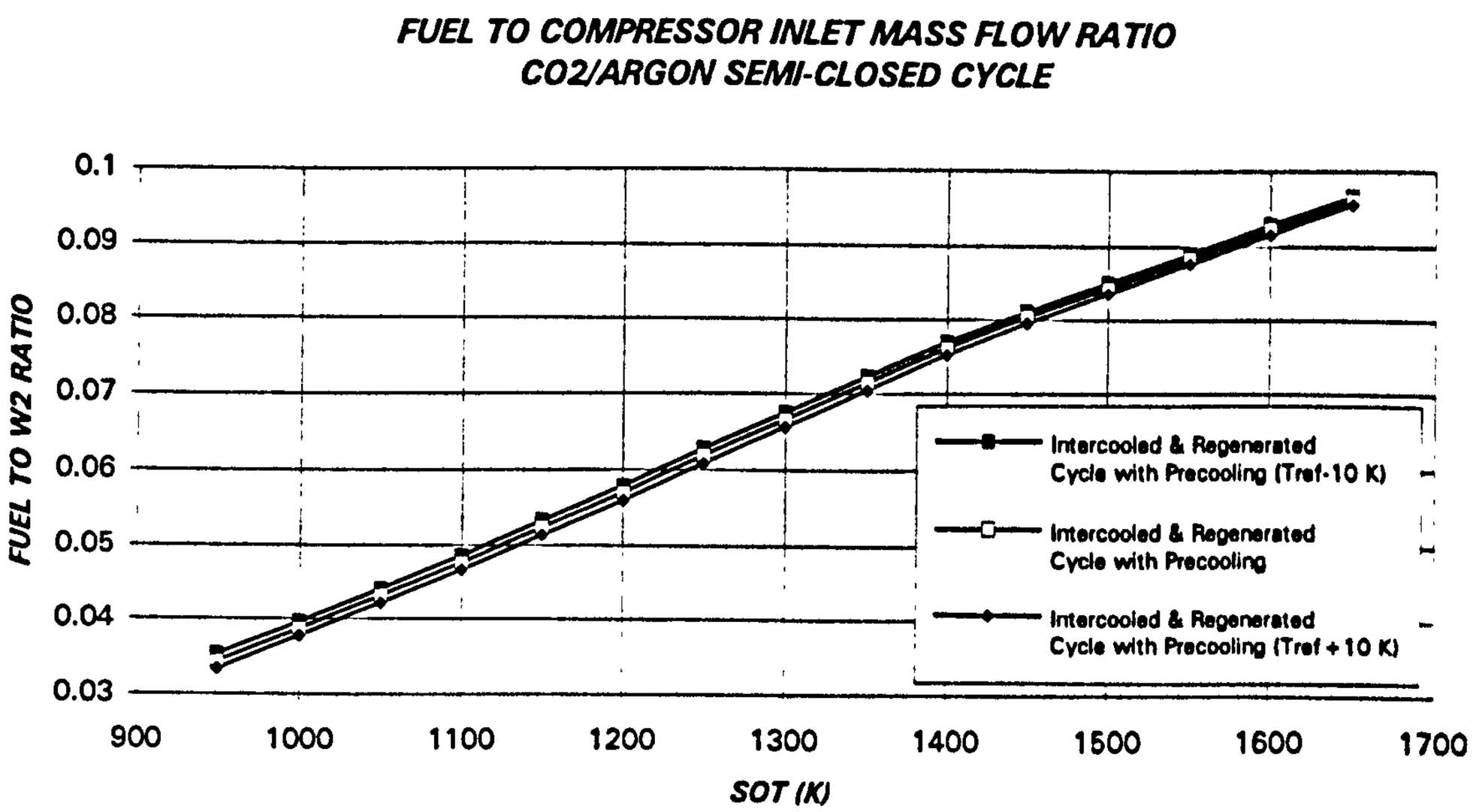

Figure 8.62. Fuel to compressor inlet mass flow ratio (CYCLE V at T_{ref} and T_{ref}±10 K)

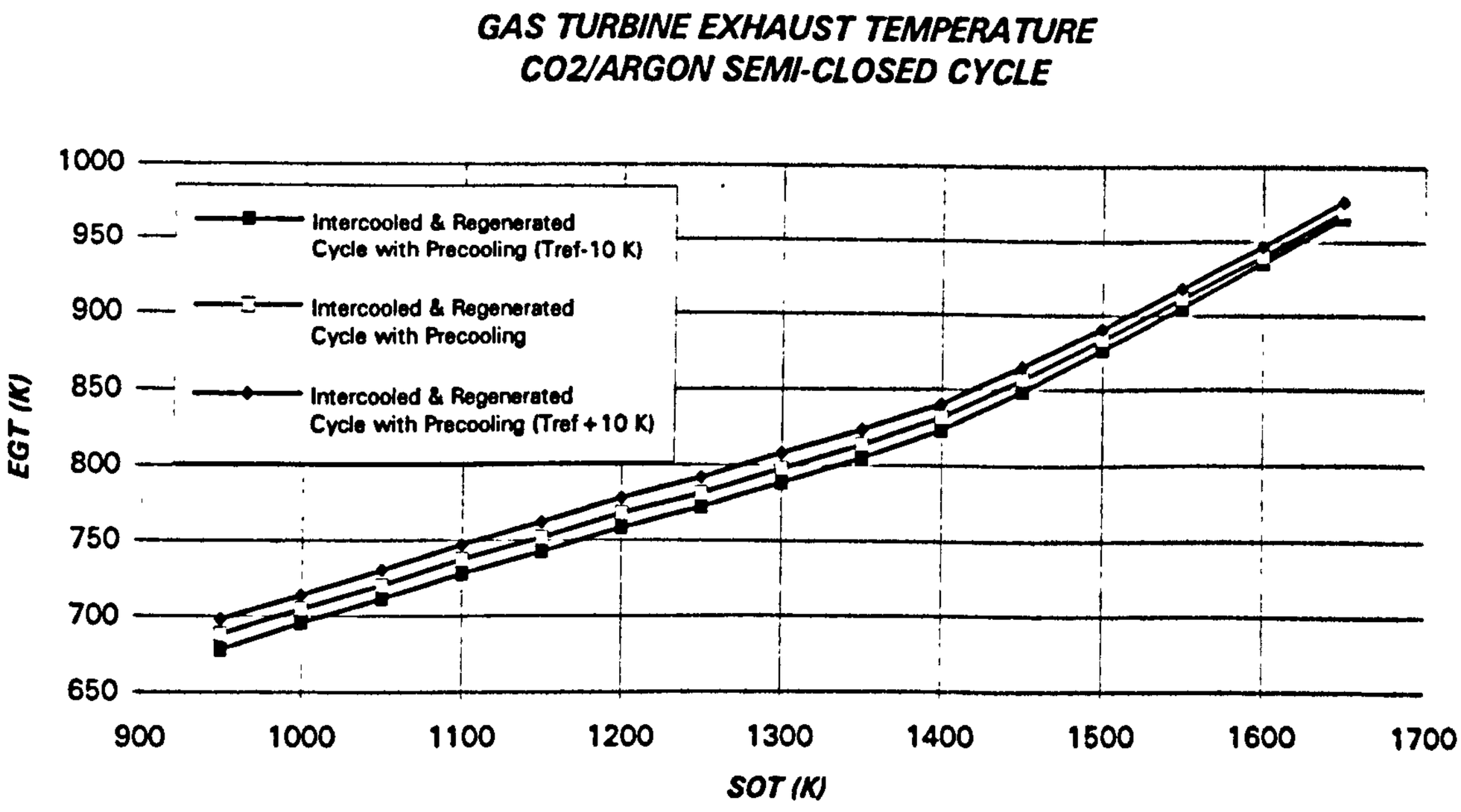

Figure 8.63. Turbine exhaust temperature vs. SOT (CYCLE V at T_{ref} and T_{ref}±10 K)

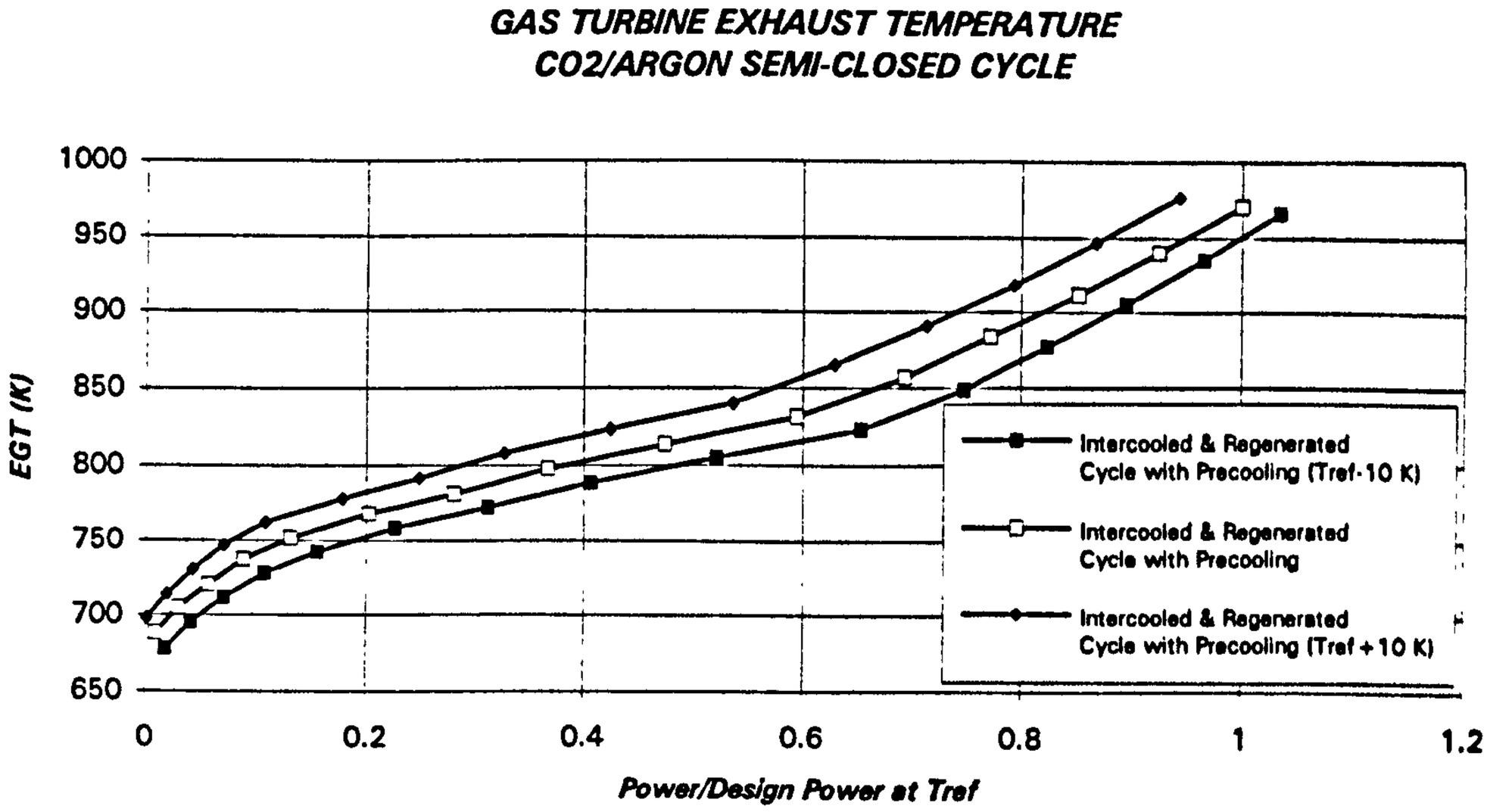

Figure 8.64. Turbine exhaust temperature vs. relative power (CYCLE V at T_{ref} and T_{ref}±10 K)

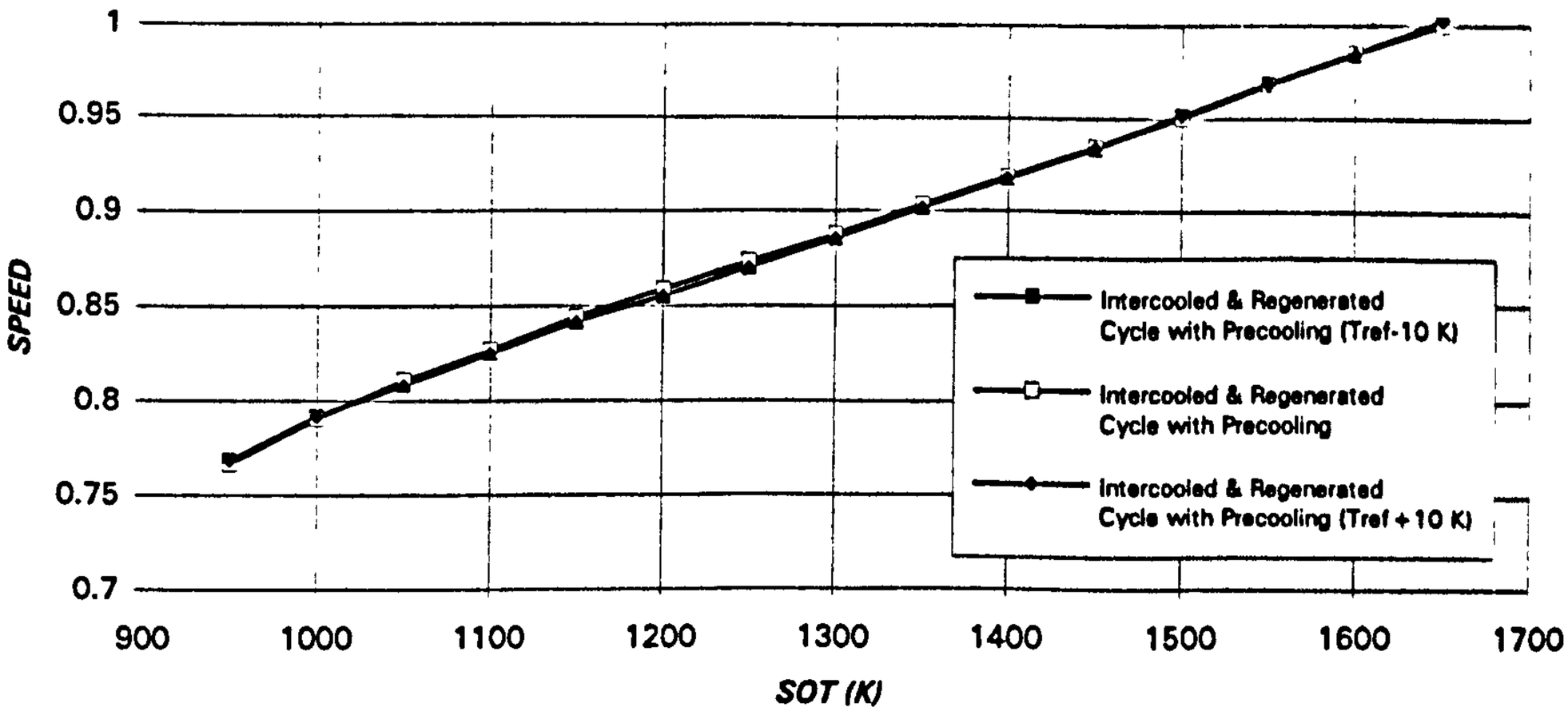

Figure 8.65. High pressure spool speed vs. SOT (CYCLE V at T_{ref} and T_{ref}±10 K)

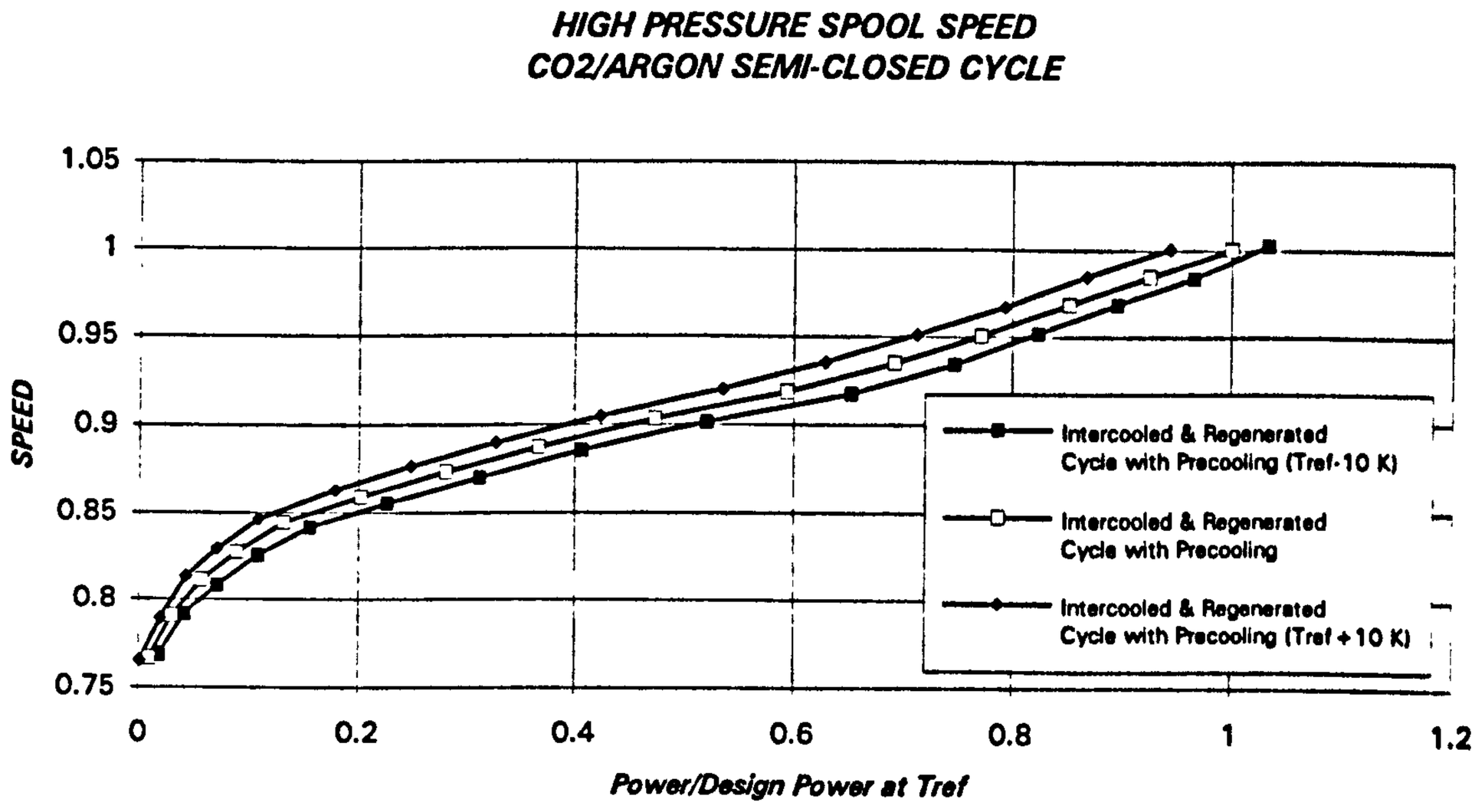

Figure 8.66. High pressure spool speed vs. relative power (CYCLE V at T_{ref} and T_{ref}±10 K)

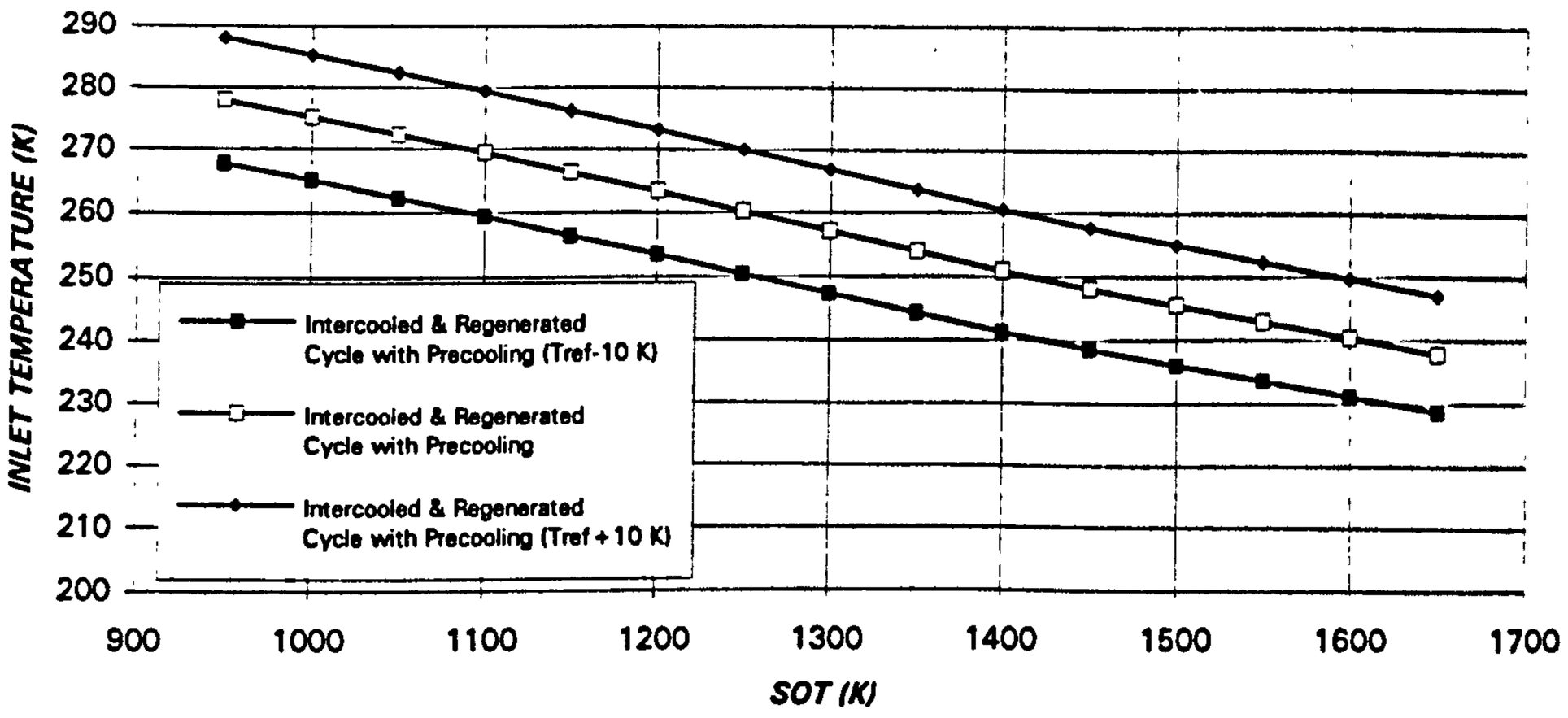

Figure 8.67. Low pressure compressor inlet temperature (after the precoolers) (CYCLE V at T_{ref} and T_{ref}±10 K)

8.5. STARTING AND IDLE HANDLING OF THE SEMI-CLOSED CYCLE GAS TURBINE

This section outlines the starting and idle handling of the semi-closed cycle gas turbine.

Starting is considered to be the phase beginning with the engine stationary and ending with the engine at synchronous speed and no load, with air as working fluid and natural gas fuel. The engine is started from rest by external power coupled to the HP shaft, and brought to synchronous speed.

The idle handling involves the change of working fluid, from air to carbon dioxide/argon, and the switch of fuel, from natural gas to coal synthetic gas.

Operating lines of the starting, change in working fluid and loading up to full power of CYCLE III are shown in figures 8.68 and 8.69 for the LPC and HPC respectively. Variable stator schedule, shaft speeds, temperatures, etc. will be shown for the different parts of the process.

8.5.1. STARTING

This phase starts with the rotor at rest. Power is provided from an external source, bringing the gas turbine to a self sustaining condition. Then, the engine is accelerated to the LP shaft design speed.

The performance at these conditions is, as with all gas turbines, very difficult to predict, because the behaviour of the individual components is not well understood.

The power of the auxiliary starting device required to bring the LP shaft to a speed of about 70 percent is estimated to be around 1% of the power supplied by the gas turbine at its design point, or 0.6% of the combined cycle power at the same operating point. This speed and power were chosen after examining figure 8.70, where the high pressure spool power is given. It appears to be at this condition where an acceptable performance level of all the components is got. High pressure shaft speed is shown in figure 8.71. Variable stator setting for LP and HP compressors is plotted in figures 8.72 and 8.73. Turbine inlet (stator outlet) and exit temperatures are given in figures 8.74 and 8.75. For very low speeds, below 67.5%, the turbine exit temperature achieves a limiting value of 590°C. This behaviour is consistent with the low pressure ratio at this operating conditions. The fuel to compressor inlet mass flow ratio is shown in figure 8.76.

8.5.2. CHANGE OF WORKING FLUID AND FUEL AT IDLE

Once the engine has stabilised at synchronous idle, the working fluid is changed from air to carbon dioxide/argon and, afterwards, the fuel is switched to synthetic

gas. The main reasons for doing this now is the oxygen requirement using natural gas as fuel and the stability of the gas turbine.

If the change of working fluid was done at lower speeds it would be possible to have a deceleration that could lead to an unexpected shut down of the plant.

Also, if the change of fuel was done at full power, the oxygen requirement as the turbine is loaded increases, leading to a value higher than the demand when synthetic fuel is employed.

The transition process of changing the working fluid has been investigated as a sequence of steady state points. Initially, due to the large time scale involved, the transient study is not considered, necessary.

During the operation, the LP shaft speed is kept constant, changing the rest of the parameters. Figures 8.77 to 8.81 show the HP shaft speed, the LPC variable stator (the HPC stators remain at the fully open position), the turbine entry and exit temperatures and the fuel to compressor inlet mass flow ratio, with the content of carbon dioxide/argon as a parameter.

The differences in thermodynamic properties between air and the mixture of carbon dioxide and argon lead to a moderate change in corrected mass flow and a significant variation in the corrected speed.

At the end of this phase the fuel will be switched from natural gas to coal synthetic gas. Under these circumstances it may be necessary to have a rich oxygen mixture to ensure combustion of the fuel while the change is taking place. The difference in performance is relatively small, with variations of the order of 1% in mass flows and pressures and 1.5% in temperatures.

Once the engine is operating at synchronous idle with the correct working fluid and fuel the normal loading takes place, increasing the useful power that will be absorbed by the electricity generators. The process will take place slowly, as in all large heavy duty gas turbines, due to the considerable heat soakage period required by the engine thermal mass. The performance variables of CYCLE III at part load are shown in section 8.4.

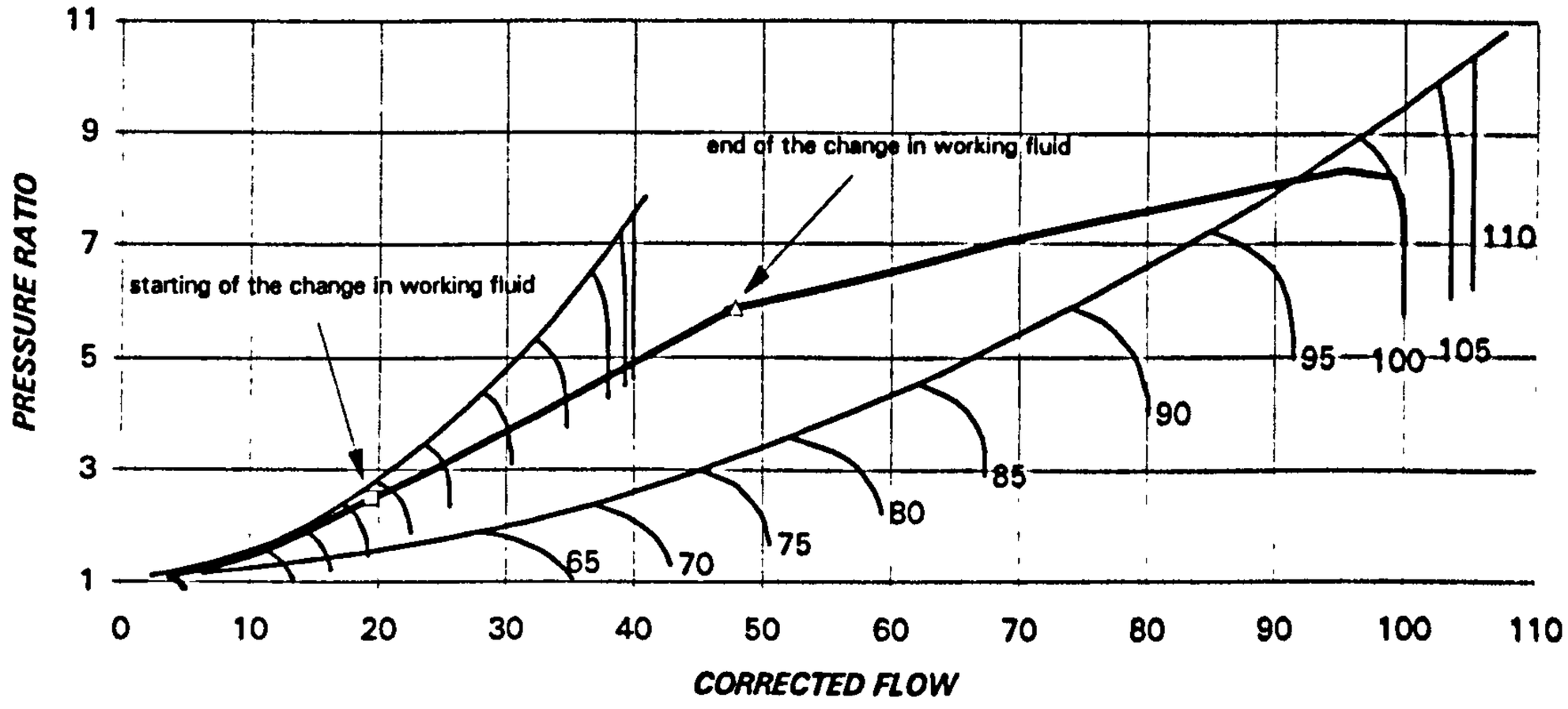

Figure 8.68. Low pressure compressor operating line during starting, change in working fluid, change in fuel and loading up to full power

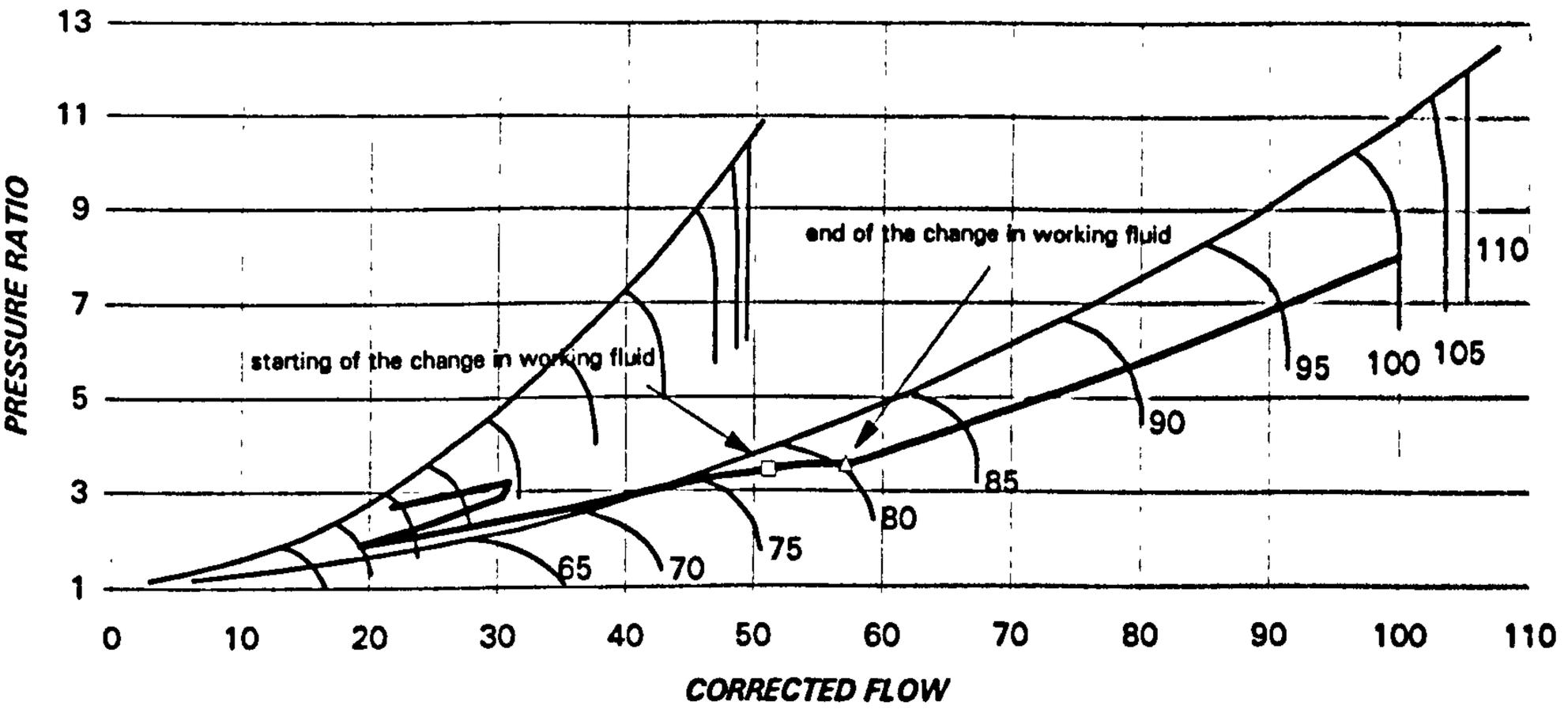

Figure 8.69. High pressure compressor operating line during starting, change in working fluid, change in fuel and loading up to full power

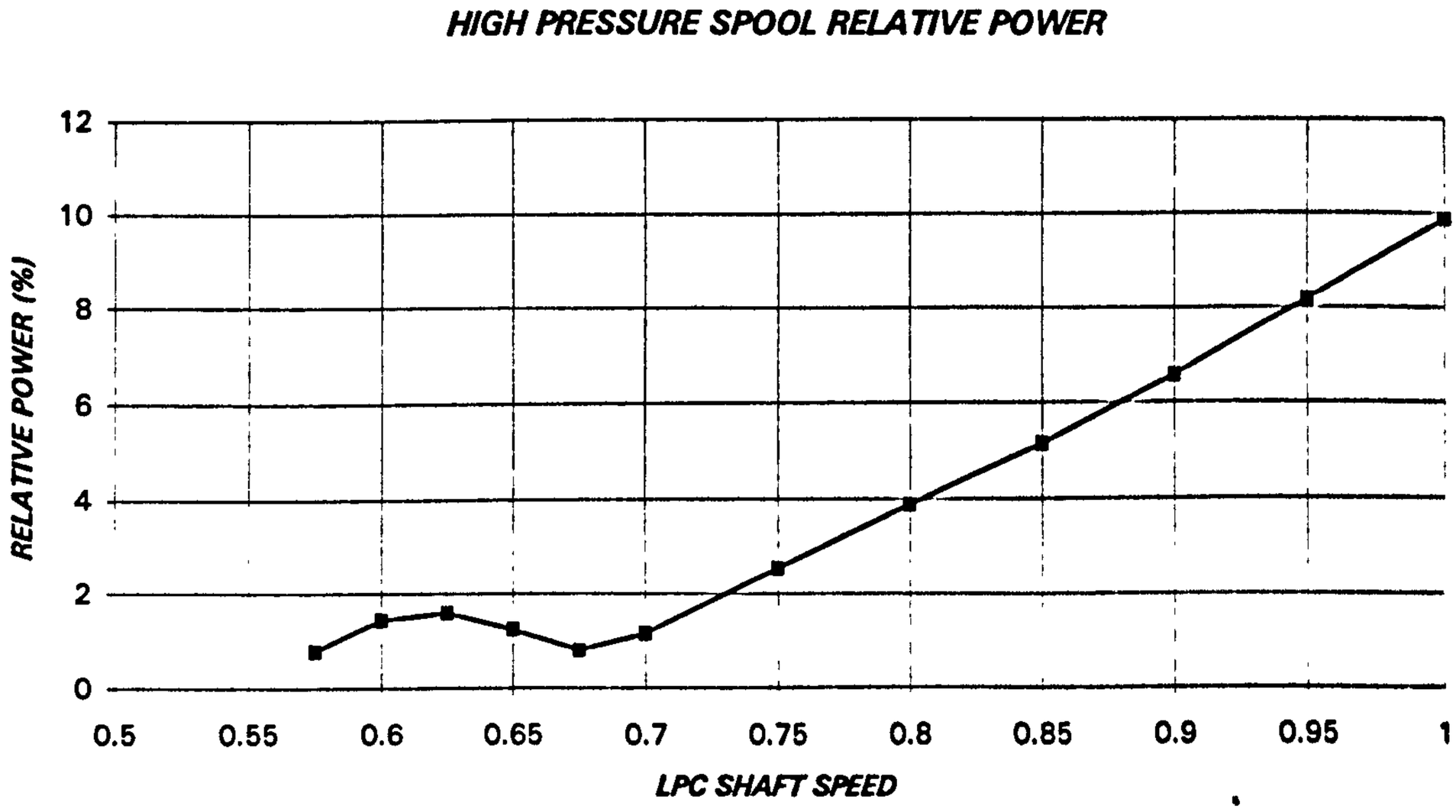

Figure 8.70. High pressure spool power (% relative to gas turbine design power)

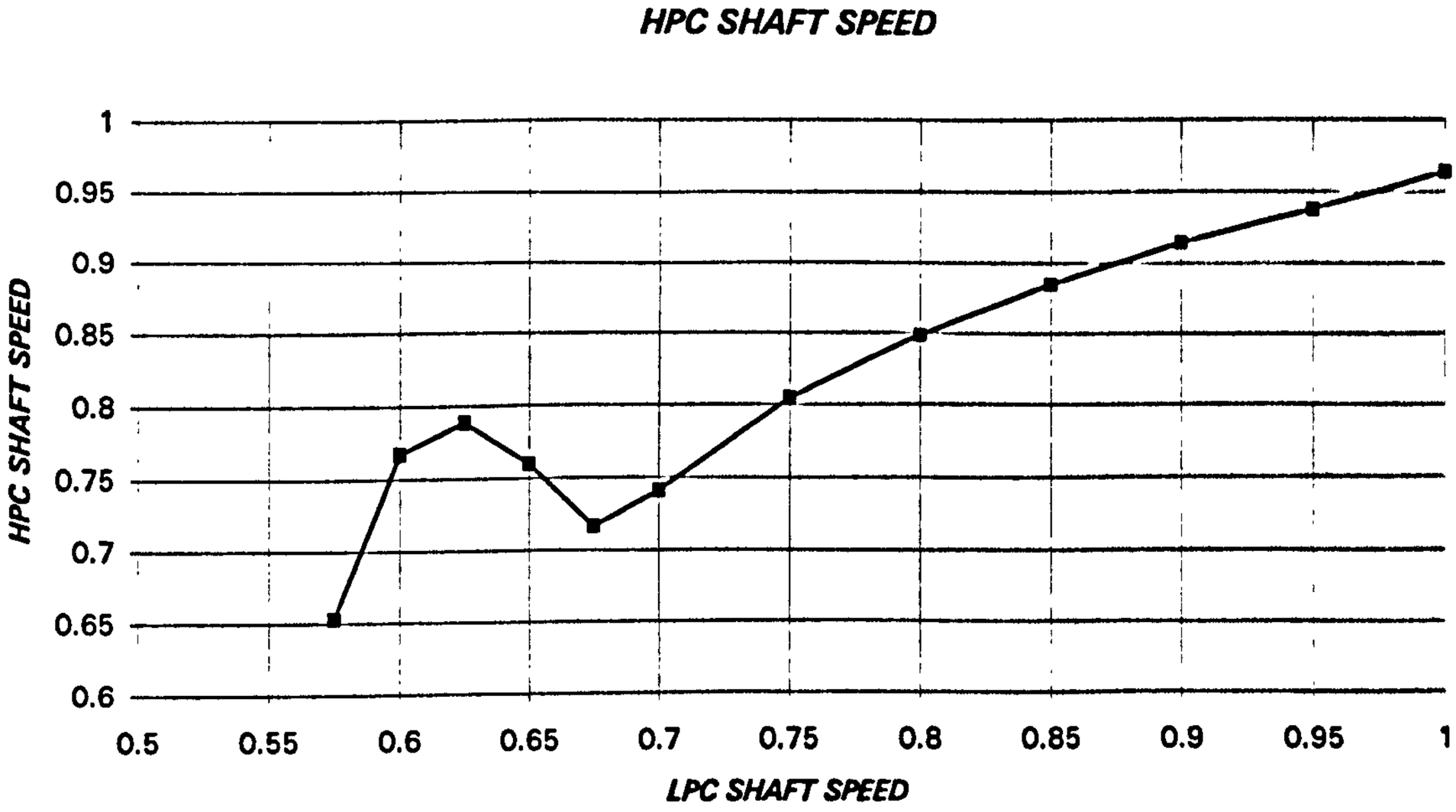

Figure 8.71. High pressure spool speed during starting

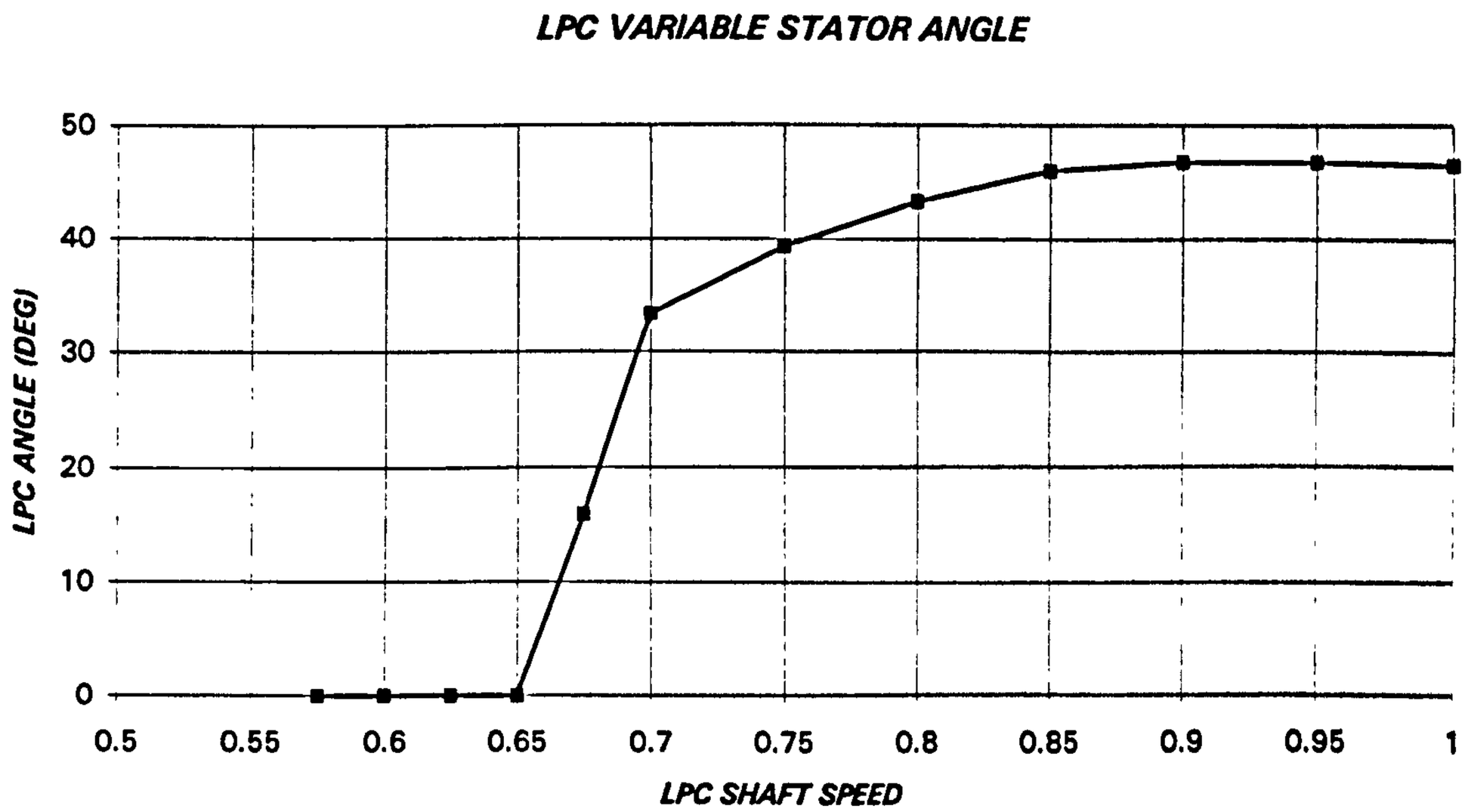

Figure 8.72. Low pressure compressor variable stator angle during starting

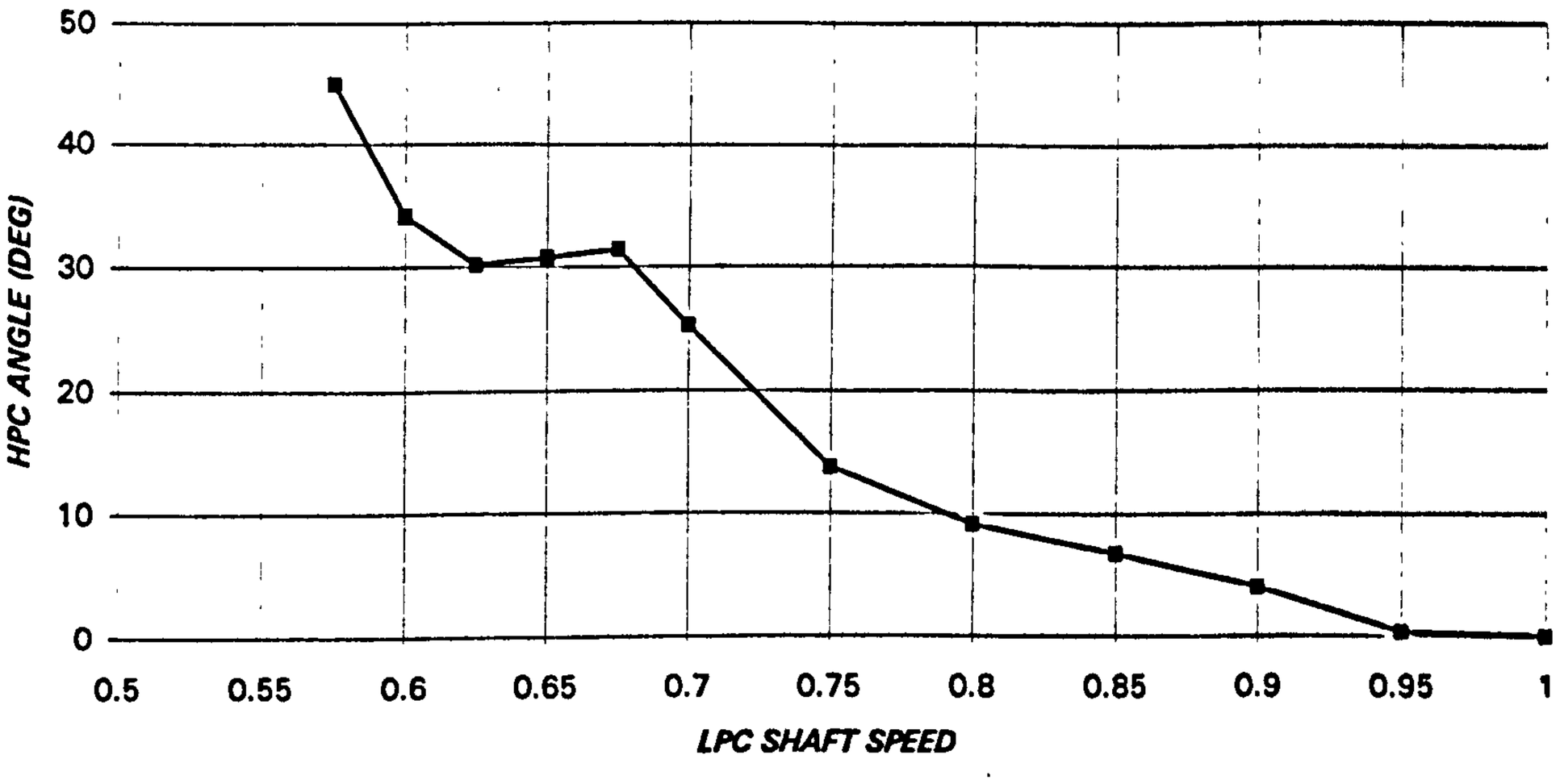

Figure 8.73. High pressure compressor variable stator angle during starting

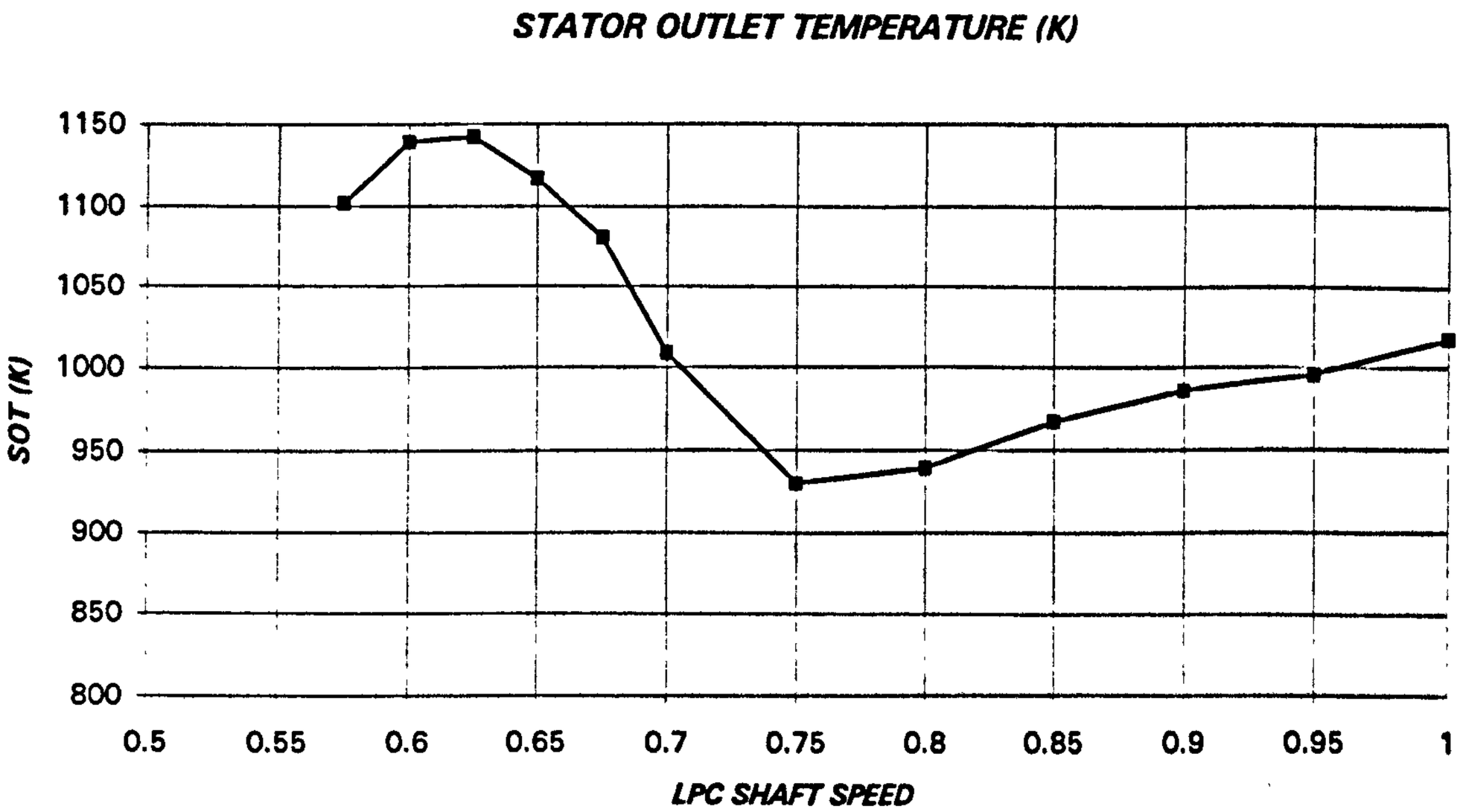

Figure 8.74. Stator outlet temperature during starting

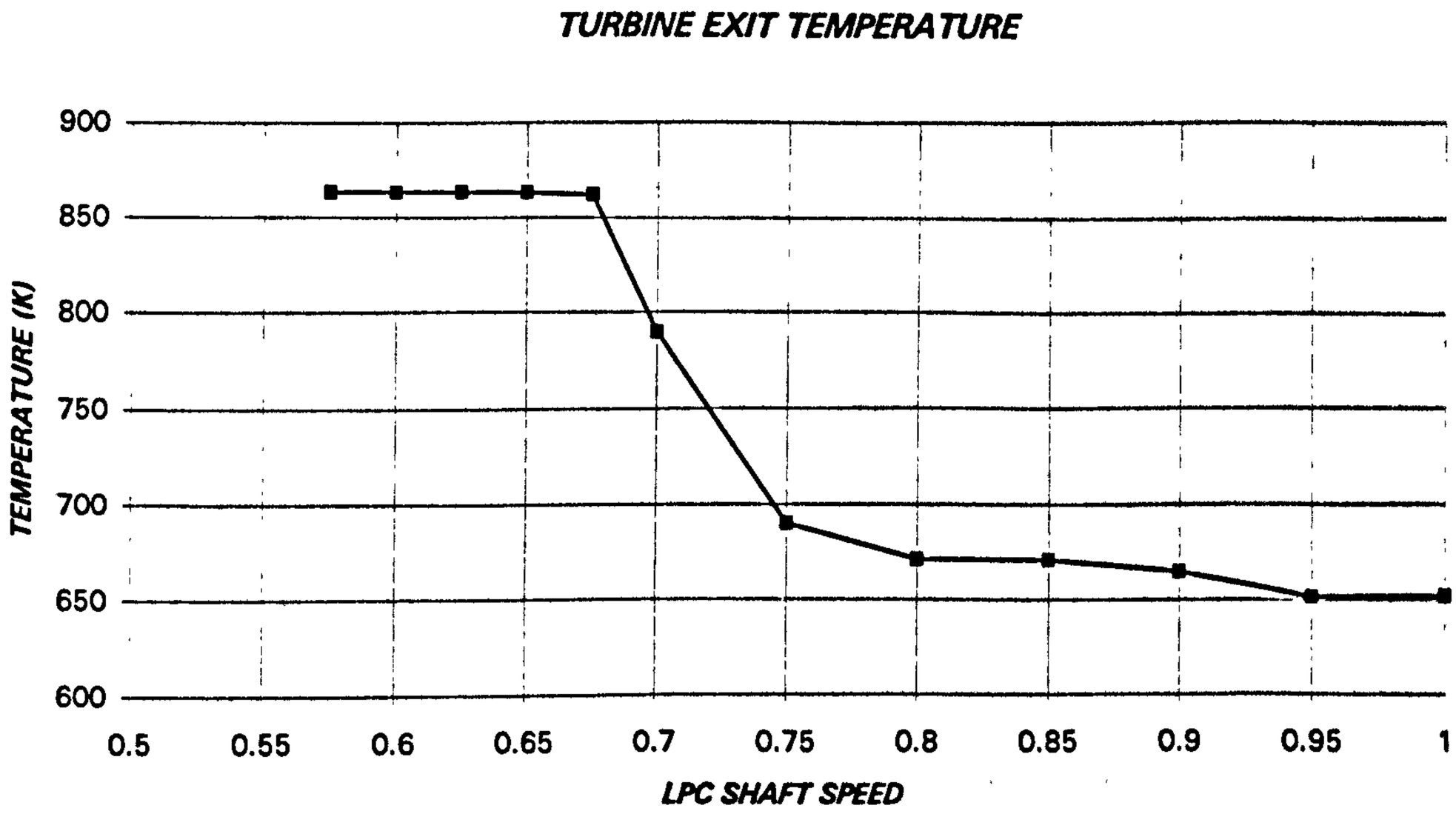

Figure 8.75. Turbine exit temperature during starting

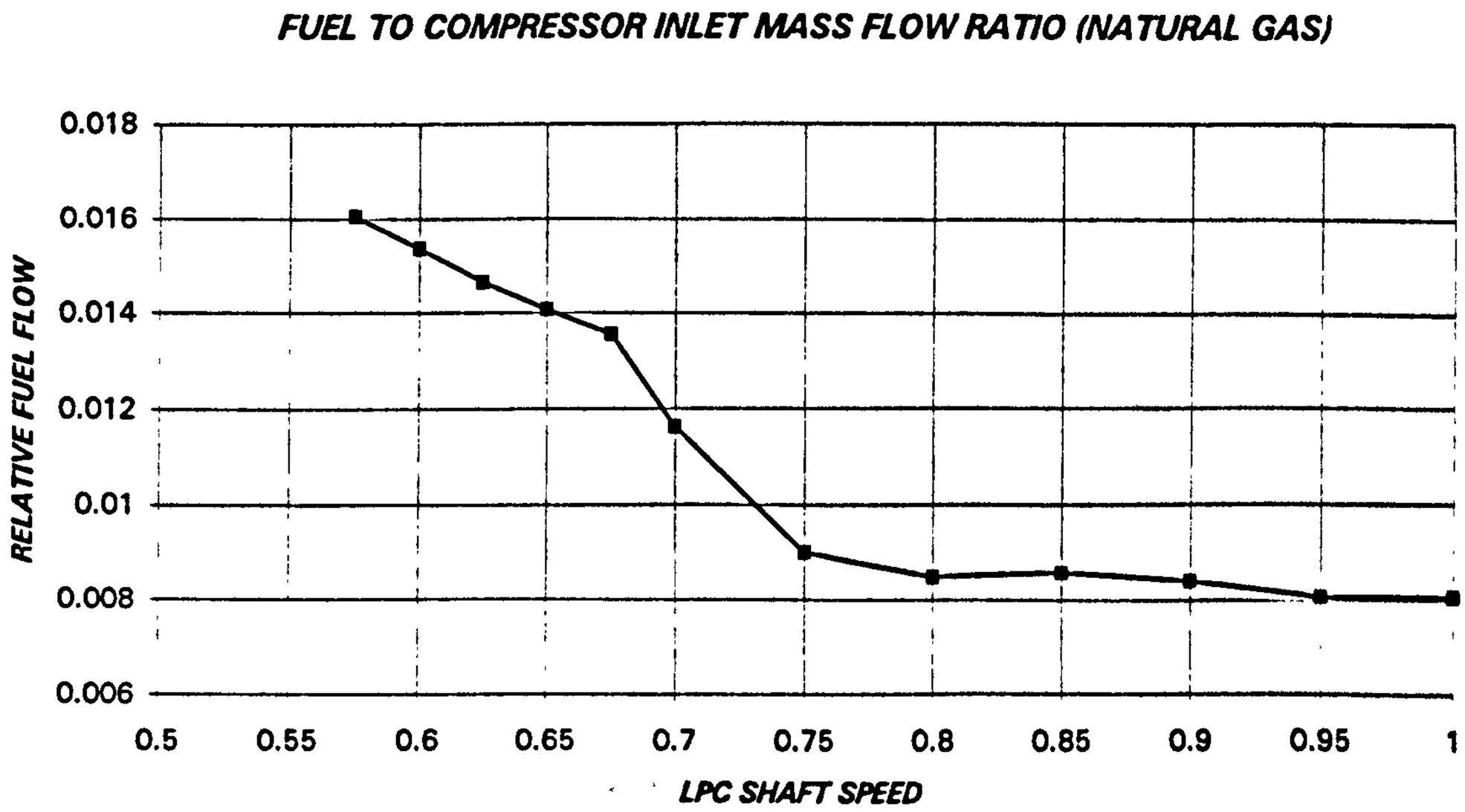

Figure 8.76. Fuel to compressor inlet flow ratio during starting (Natural Gas)

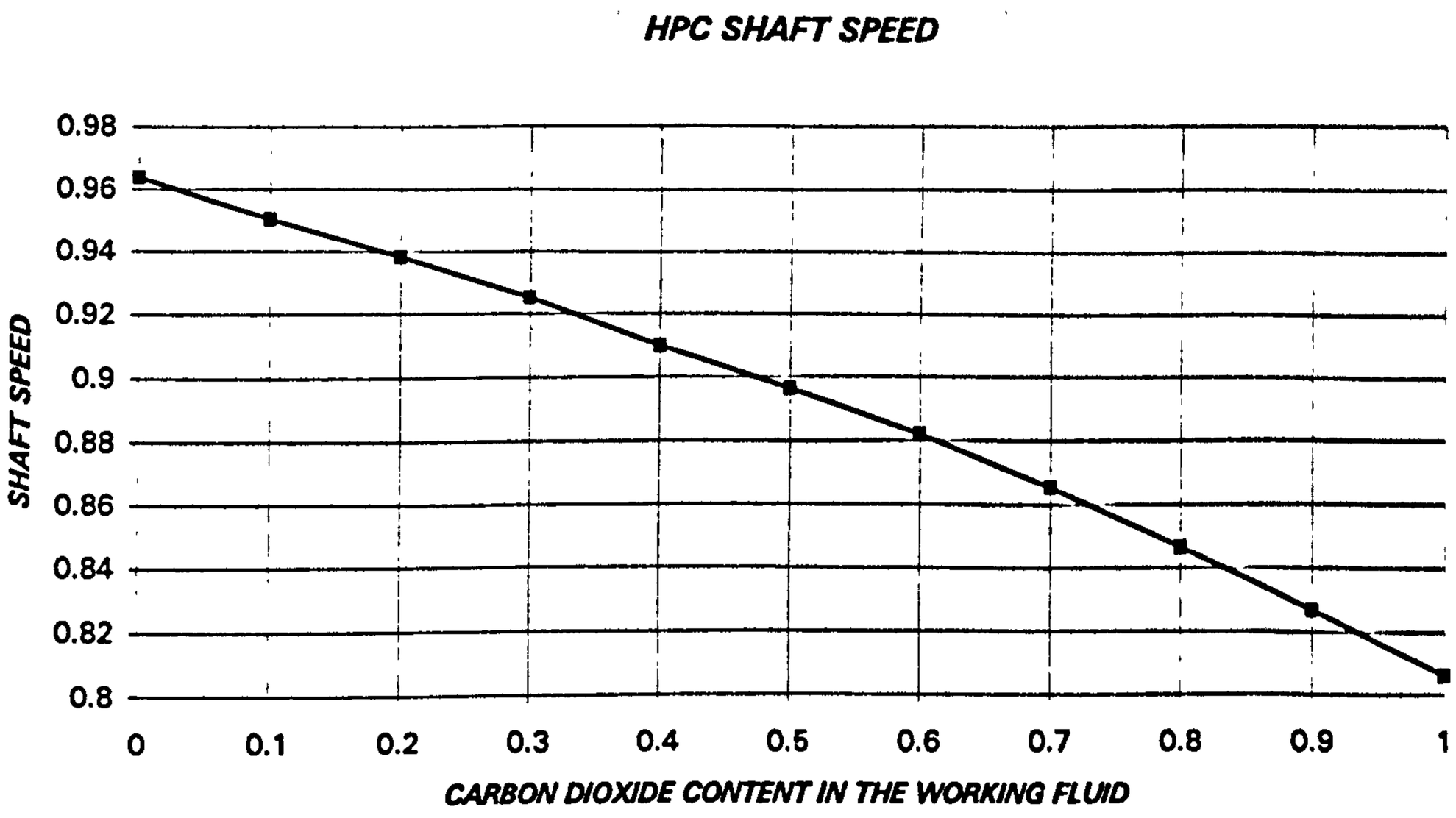

Figure 8.77. High pressure shaft speed during the change from air to carbon dioxide/argon

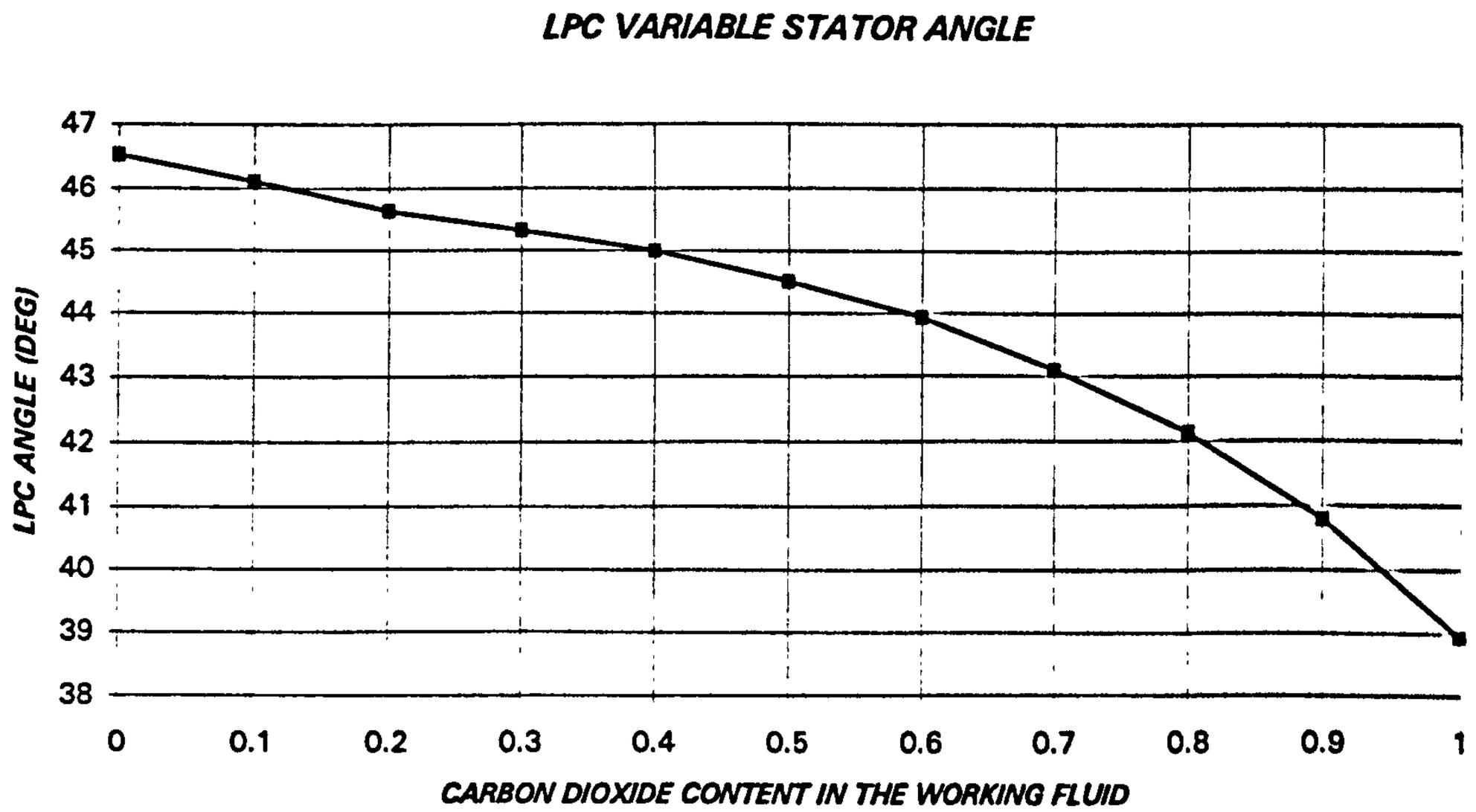

Figure 8.78. Low pressure compressor variable stator angle during the change from air to carbon dioxide/argon

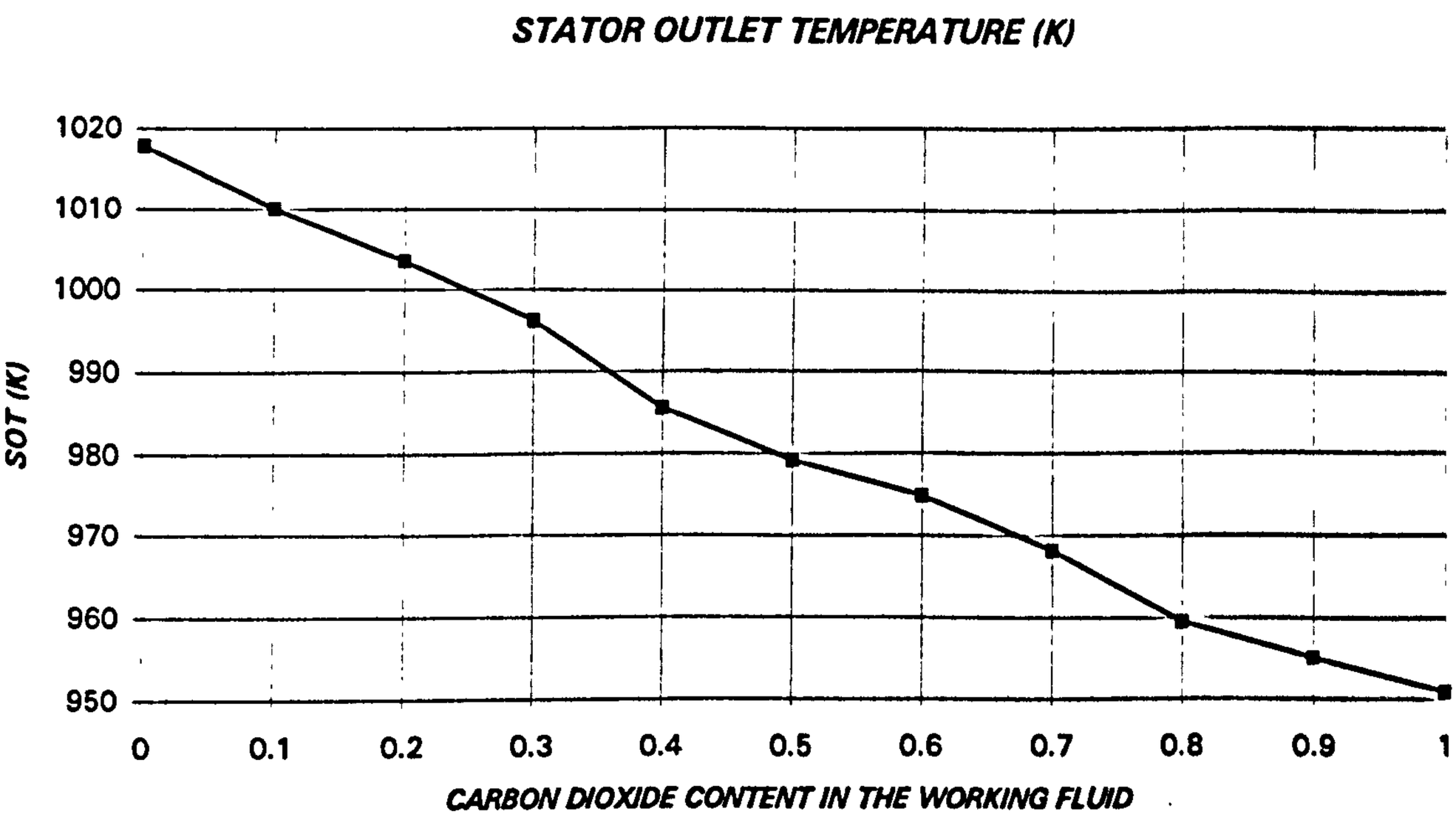

Figure 8.79. Stator outlet temperature during the change from air to carbon dioxide/argon

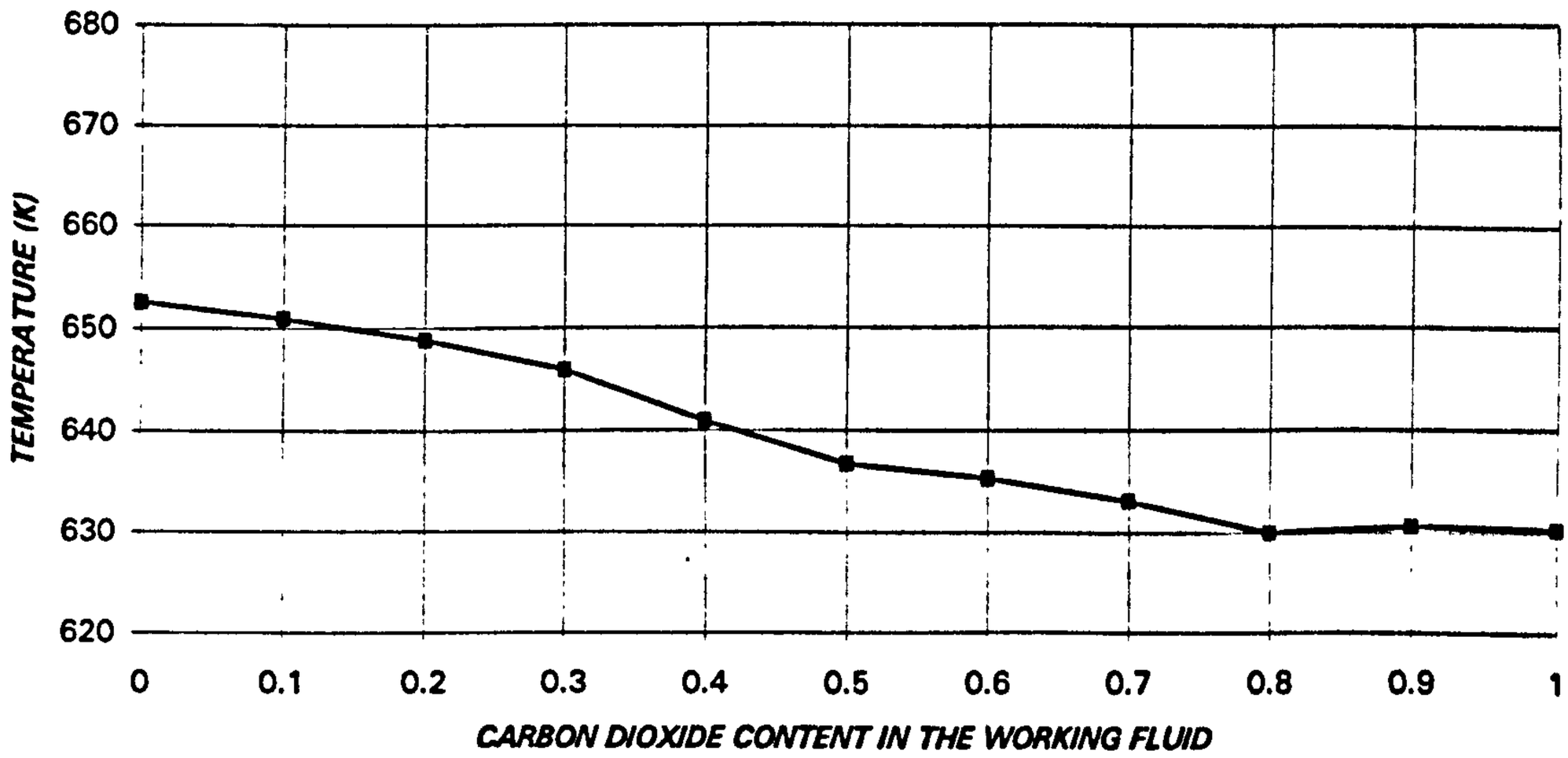

Figure 8.80. Turbine exit temperature during the change from air to carbon dioxide/argon

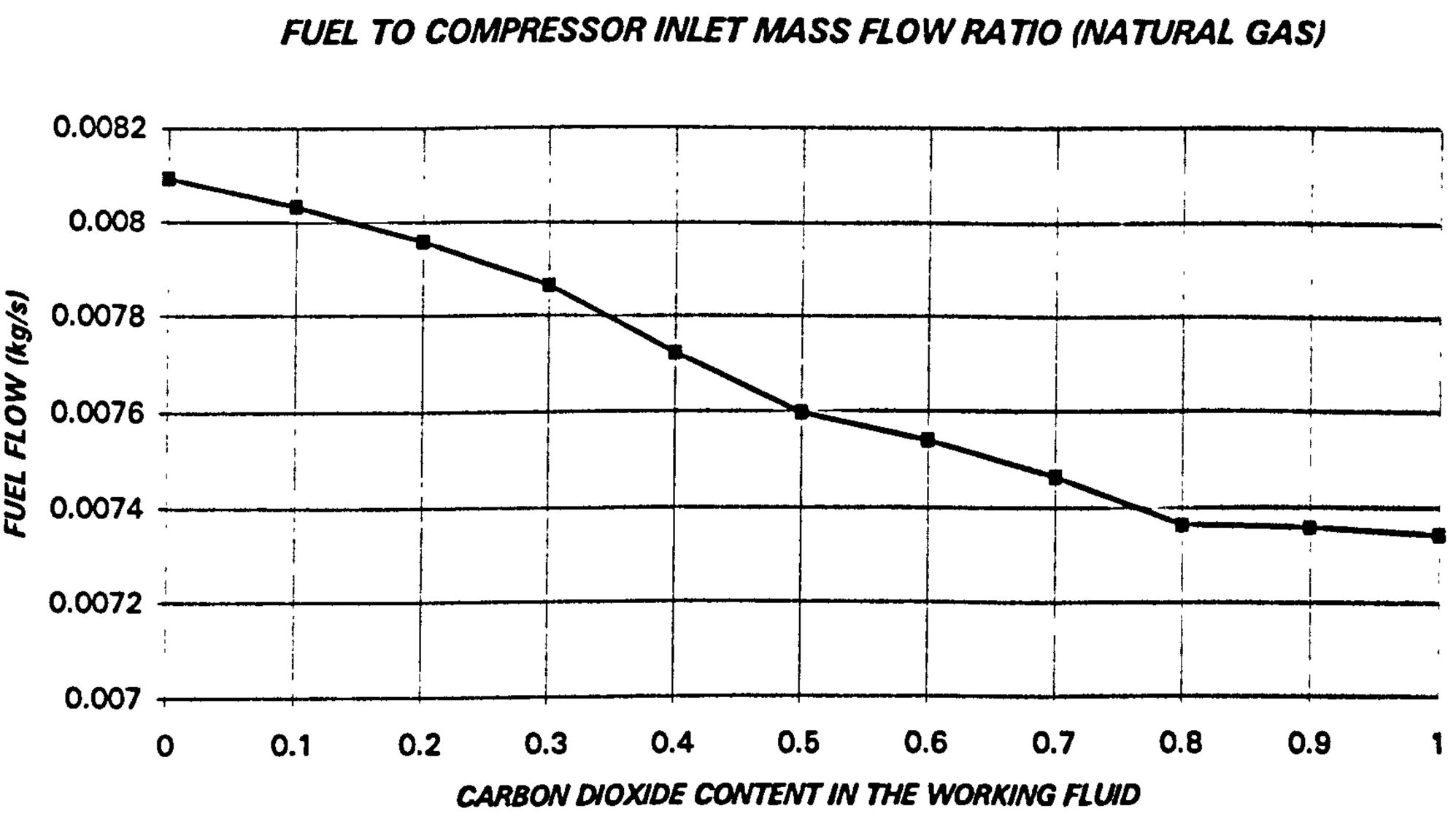

Figure 8.81. Fuel to compressor inlet flow ratio during the change from air to carbon dioxide/argon

CHAPTER 9

CHANGE IN SEMI-CLOSED CYCLES WORKING FLUID

9.1. INTRODUCTION

When designing a semi-closed cycle operating with a mixture of carbon dioxide and argon as working fluid, one major problem is the impossibility of verifying the aerodynamic behaviour of a gas turbine employing that fluid before a prototype or a development machine is built. But, the large investment required to manufacture and test a technology demonstrator can stop its development. However, if it was possible to use existing hardware, the cost would be drastically reduced.

That is the idea explored here with the following performance exercise:

- Convert a conventional existing open cycle gas turbine turbomachinery, designed for air, into a closed cycle machine.
- Change, progressively, the working fluid from air to carbon dioxide/argon (operating as a closed cycle).

The main aim of this exercise is the evaluation of the changes in compressor and turbine aerodynamic behaviour. Therefore, the possibility of running the gas turbine with working fluids considerably different from its original design.

The assessment of cycle performance employing inadequate turbomachinery is of second interest. Hence, after the complete change of working fluid, as a closed cycle, it would be possible to go further, and perform simulations with the gas turbine in semi-closed cycle configuration, burning low heating value gas.

Initial combustion studies, probably at small scale, should be carried out independently, to be able to discern whether the problems are coming from one or other discipline. But if the exercise concludes that it will be feasible to run the existing air design turbomachinery with CO_2/Ar, it would be possible to perform full scale combustion experiments at a relatively low cost.

9.2. CASES SELECTED AND METHOD EMPLOYED

To cover some representative gas turbine arrangements, four cases have been selected:

- One spool - one shaft (compressor - combustor - turbine)
- One spool - two shaft (compressor - combustor - turbine - free power turbine)
- Two spool - two shaft (LP compressor - HP compressor - combustor - HP turbine - LP turbine)
- Two spool - three shaft (LP compressor - HP compressor - combustor - HP turbine - LP turbine - Power turbine)

The method to carry out the performance simulation will be:

- Generate a design case for each configuration with characteristics (pressure ratio, component efficiencies, cooling bleeds, etc.) similar to actual open cycle gas turbines. For example, in the case of the single spool - single shaft, a machine equivalent to a heavy duty GE Frame 7 was employed and in the two spool - three shaft, a gas turbine similar to the aeroderivative GE LM5000 model has been selected.
- Go from open cycle to closed cycle, employing air as working fluid, as an off-design, preserving the turbomachinery, i.e. with the same characteristics.
- Modify, progressively, the working fluid, from 100% air/0% carbon dioxide-argon to 0% air/100% carbon dioxide-argon. The reason to do this part of the study in several steps is a code convergence problem (initial conditions)

9.3. ONE SPOOL - ONE SHAFT CASE

As already mentioned, the model selected is similar to the GE Frame-7 gas turbine.

- Inlet mass flow: 361 kg/s
- Pressure ratio: 15.0
- HPC adiabatic efficiency: 88.2%
- Base load SOT: 1450 K
- HPT/PT adiabatic efficiency: 92.3%
- Exhaust gas temperature 823 K.
- Thermal efficiency: 34.7%
- Power output: 119.5 MW

The results of running the turbomachinery as a closed cycle changing the working fluid composition from 100% air to 100% CO_2/Ar are presented in Appendix VIII, showing the evolution of mass flow, pressure ratio, compressor & turbine efficiency, compressor & turbine corrected speed, power output, etc. The initial change from open cycle to closed cycle using air is not presented here.

9.3.1. COMPRESSOR BEHAVIOUR (Appendix VIII, fig. 1 to 6)

The shaft speed is kept constant (single shaft gas turbine for electricity generation). Therefore, with the substantial drop in both, gas constant and ratio of specific heat, although the inlet temperature is slightly larger than the design case (300 K vs. 288.15 K), the corrected speed increases significantly (26% larger with CO_2/Ar) going beyond the safe limits of the compressor map (corrected speed at

continuous operation is limited to values 10-15% higher than design). With these conditions, the aerodynamic behaviour of the compressor is far from optimum, and the adiabatic efficiency drops from 0.88 to 0.58.

9.3.2. TURBINE BEHAVIOUR (Appendix VIII, fig. 7 to 12)

Following a similar trend as the compressor, the limitation of constant shaft speed ends up with an important increase in the turbine corrected speed (larger than 30%). The corrected enthalpy increases also in 24% when using CO_2/Ar. Two other important parameters for turbine performance are the loading coefficient ($\Delta H/U^2$) and the flow coefficient V_{ax}/U. Both experience a decrease in 25% relative to the open cycle. The Mach number increases in over 15% relative to the design case, with larger figures at part load, where the sonic velocity is lower. This detrimental effect, together with the decrease in flow coefficient, will have an important penalty in the turbine efficiency that could not be completely reflected in the performance simulation. It would also be possible to find that the increase in the Mach number causes a situation of limit loading and, due to the decrease in incidence angle, a vibration/flutter problem could emerge, due to the possible presence of a pressure surface recirculation bubble.

9.3.3. GENERAL PERFORMANCE (Appendix VIII, fig. 13 to 17)

The inlet mass flow increases, when changing the working fluid to CO_2/Ar, from 339 kg/s up to 458 kg/s, with a rise in the corrected flow from 350 kg/s up to 458 kg/s. The exit temperature has also a substantial rise when running at constant SOT. Therefore, it would be probably required to run at lower temperature. Specific power output and thermal efficiency are also presented, showing a considerable drop in both performance parameters.

9.4. ONE SPOOL - TWO SHAFT CASE

The model selected has been a modified GE Frame-7 gas turbine type that, instead of having a single shaft, it is fitted with a free power turbine.

- Inlet mass flow: 361 kg/s
- Pressure ratio: 15.0
- HPC adiabatic efficiency: 88.2%
- Base load SOT: 1450 K
- HPT adiabatic efficiency: 91.0%
- LPT/PT adiabatic efficiency: 89.0%

- Exhaust gas temperature 820 K.
- Thermal efficiency: 35.1%
- Power output: 120.7 MW

Appendix IX contains the results of the simulation.

9.4.1. COMPRESSOR BEHAVIOUR (Appendix IX, fig. 1 to 6)

In this cycle the gas generator speed is not necessarily constant (free power turbine for electricity generation). As a consequence, there is a reduction in the core shaft speed that, together with the drop in the gas constant and ratio of specific heat and the increase in inlet temperature, increase the corrected speed in less than 3% relative to the open cycle design. Therefore, the aerodynamic behaviour of the compressor is close to the optimum, and the adiabatic efficiency drops from 88% to 84%.

9.4.2. TURBINE BEHAVIOUR (Appendix IX, fig. 7 to 18)

In parallel with the compressor, the HP turbine corrected speed increases just 6% relative to the design case, and the corrected enthalpy increases in 10%. The loading factor, flow coefficient and Mach number change less than 6%. All these figures suggest that the change in working fluid has a minor impact on HPT performance

However, the FPT modifies its operating point in a similar way as the HPT did in the single shaft case. The corrected speed, driven by the constant speed limitation, is increased by 25%, and the corrected enthalpy by 29%. The loading factor and flow function are decreased by 18% and 20% respectively, with an increase in Mach number of 12%. The conclusions for this turbine are analogous to the ones obtained for the HPT in the single spool - single shaft configuration (section 9.3.2.)

9.4.3. GENERAL PERFORMANCE (Appendix IX, fig. 19 to 23)

The inlet mass flow increases, when changing the working fluid to CO_2/Ar, from 328 kg/s up to 422 kg/s, with a rise in the corrected flow from 338 kg/s up to 368 kg/s. The exit temperature increases in over 150 K for the design SOT. Hence, as in the single spool - single shaft case, the turbine entry temperature should be reduced. The simple cycle thermal efficiency suffer an important decrease, but considerably smaller than in the single spool - single shaft. The specific power output does not change its value between the air and CO_2/Ar cycles.

9.5. TWO SPOOL - TWO SHAFT CASE

In the following case, a gas turbine similar to the GE LM6000[1] has been selected. The main performance parameters are:

- Inlet mass flow: 126.5 kg/s
- LPC pressure ratio: 3.5
- LPC adiabatic efficiency: 84.6%
- HPC pressure ratio: 7.46
- HPC adiabatic efficiency: 82.6%
- Base load SOT: 1450 K
- HPT adiabatic efficiency: 89.2%
- LPT/PT adiabatic efficiency: 91.1%
- Exhaust gas temperature 725 K.
- Thermal efficiency: 35.5%
- Power output: 33.7 MW

The results of the simulation are shown in the figures of Appendix X.

9.5.1. COMPRESSOR BEHAVIOUR (Appendix X, fig. 1 to 12)

As the carbon dioxide/argon content increases, the mass flow and corrected mass flow increase as well. The low pressure shaft speed is kept constant (coupled to the electricity generator). Therefore, the LPC corrected speed grows up significantly, due to the drop in the gas constant and specific heat ratio between air and CO_2/Ar. The high pressure shaft speed decreases, but the HPC corrected speed grows, as the reduction in speed can not compensate the drop in R and γ. The LPC and HPC pressure ratios rise and surge margins improve. An important detrimental effect is experience in the LPC adiabatic efficiency, due to the large corrected speeds found: around 117% for the CO_2/Ar cycle compared with 92.5% for the air cycle at base load design point. The HPC does not suffer this effect, as the final values of corrected speed are around 98% with CO_2/Ar and 95% with air.

---

[1] The LM6000 will have a lower LPC pressure ratio and a higher HPC pressure ratio, with a simple cycle thermal efficiency around 40%.

9.5.2. TURBINE BEHAVIOUR (Appendix X, fig. 13 to 24)

For the design SOT, the HPT corrected enthalpy ($\Delta H/\gamma RT$) grows to a value of 112% relative to the original open cycle design. The corrected speed is 106% of the initial value. The loading factor does not change between air and CO_2/Ar cycles, and the flow coefficient decreases to 95% of the design value, with a minor effect on HPT aerofoil incidence. The turbine rotor characteristic Mach number will not change significantly.

Again, for the highest SOT, the LPT corrected enthalpy ($\Delta H/\gamma RT$) grows to a value of 142% and the corrected speed increases to 124% compared with the initial design values!!. The loading factor is 91.4% and the flow coefficient is 80.4% relative to the open cycle design values. Hence, the decrease in LPT aerofoil incidence angle will be considerable, with a serious increase in losses. The turbine rotor characteristic Mach number will rise by approximately 10-12% compared with the design value, with the detrimental effect in efficiency, and the possibility of limit loading phenomenon.

9.5.3. GENERAL PERFORMANCE (Appendix X, fig. 25 to 29)

The inlet mass flow experience a huge increase (around 50%). The gas turbine exit temperature increases, as for the one spool - one shaft and one spool - two shaft, in 150 K at design SOT. Specific power output do not have a significant change, but thermal efficiency drops considerably.

9.6. TWO SPOOL - THREE SHAFT CASE

A gas turbine similar to the GE LM5000[2] has been selected. The main performance characteristics are:

- Inlet mass flow: 126.5 kg/s
- LPC pressure ratio: 3.5
- LPC adiabatic efficiency: 84.6%
- HPC pressure ratio: 7.46
- HPC adiabatic efficiency: 82.6%
- Base load SOT: 1450 K
- HPT adiabatic efficiency: 89.2%
- LPT adiabatic efficiency: 89.7%

---

[2] The LM5000 will have a lower LPC pressure ratio and a higher HPC pressure ratio

- FPT adiabatic efficiency: 90.5%
- Exhaust gas temperature 724 K.
- Thermal efficiency: 36.15%
- Power output: 33.3 MW

The figures showing the results of the simulation are in Appendix XI..

9.6.1. COMPRESSOR BEHAVIOUR (Appendix XI, fig. 1 to 12)

The performance of the compressors is similar to the one spool-two shaft arrangement. The presence of the FPT removes the restriction in the speed of the gas generator shafts. The consequence is a reduction of around 22% in HP and LP shaft speed when the working fluid has been completely changed. With these reductions, the corrected speeds are less than 4% away from the initial design point, and the LPC and HPC adiabatic efficiencies drop around 5%.

9.6.2. TURBINE BEHAVIOUR (Appendix XI, fig. 13 to 30)

As in the case of the compressors, the HPT and FPT behave in the same way as in the one spool-two shaft arrangement. The LPT follows a trend similar to the HPT.

The HPT corrected enthalpy grows to a value of 112% and the corrected speed to a 107% compared with the initial open cycle design. The loading factor suffers minor changes between the air and CO_2/Ar cycles, with the flow coefficient decreasing to 93% of the design value, resulting in incidence angles away from the design, with a reduction in the component efficiency. The turbine rotor characteristic Mach number will not change significantly.

The LPT corrected enthalpy grows to a value of 110% and the corrected speed increases to 106% relative to the open cycle design point. These figures are considerably lower than the ones found in the two spool-two shaft configuration. The loading factor is, practically, constant, as well as the Mach number, with the flow coefficient decreasing by 5%. This variation should not have a great impact on turbine aerodynamic behaviour.

The largest changes appear in the FPT, with increases of 40% and 22% in corrected enthalpy and corrected speed respectively. The loading factor was dropped by 5%, the flow coefficient by 18% and the Mach number was risen by 10%. The conclusions for this turbine are equivalent to the ones obtained for the LPT in the two spool - two shaft arrangement: large changes in aerofoil incidence and higher Mach numbers. These resulting in a considerably poorer turbine performance, that is not fully reflected in the simulation, mainly because the operating points were out of the available turbine map, and the values were extrapolated.

9.6.3. GENERAL PERFORMANCE (Appendix XI, fig. 31 to 35)

The inlet mass flow increases, when changing the working fluid to CO_2/Ar, from 113 kg/s up to 170 kg/s, with a rise in the corrected flow from 114 kg/s and 124 kg/s up to 147 kg/s and 143 kg/s for the LPC and HPC respectively. Turbine exit temperature increases in more than 150 K for the design SOT. Thermal efficiency and specific power output do change significantly between air and CO_2/Ar cycles.

9.7. CONCLUSIONS

The main conclusion from the four representative cycles run is that in all the cases one or more components finished in a medium-high risk area (vibrations, flutter, stall, ...). One possible solution could be to select the single spool - two shaft case, where the core components do not change significantly their performance, and take the free power turbine from another machine. Apparently this would be the only feasible solution if an existing gas turbine is intended to be used for the carbon dioxide/argon cycle. A further detailed study is required, investigating this possibility.

The two spool gas turbines present the same problems that the single spool ones, with the additional complexity of having an extra spool. Hence, their use is not recommended.

CHAPTER 10

CONCLUSIONS AND RECOMMENDATIONS FOR FURTHER WORK

10.1. CONCLUSIONS

The main aims of this thesis, explained in the first two chapters, were:

- **Generation and validation of a general robust and accurate gas turbine performance code oriented not just to open cycles with conventional components and fuels, but able to simulate open, closed and semi-closed cycles with exotic working fluids, new components and unorthodox fuels.**
- **Selection of the power plant arrangement and performance study of an innovative semi-closed cycle operating with a mixture of carbon dioxide and argon as working fluid and burning low calorific value gas obtained from coal gasification.**

These goals have been successfully achieved with the conception and development of GTSI code and the design & off-design study of various semi-closed cycle configurations.

Thermodynamic properties for different fluids (nitrogen, oxygen, carbon dioxide, carbon monoxide, ...) as a function of temperature and pressure have been employed in the model, considering also the effect of water as a real gas. The combustion products for different hydrocarbon fuels have been already implemented as default options, but the user has the possibility to specify, easily, the properties of other combustion gases.

The components developed for the code (inlet, compressor, intercooler, evaporator cooling, steam injector, combustor, reheat system, turbine, cooling system, etc.) were created with the maximum generality. Variable geometry was introduced in the turbomachinery, steam injectors, etc.

A simple steam turbine model was generated to be able to simulate the combined cycles. A steam generator module was created as well for the steam injected cycles.

The component subroutines were integrated in such a way that open, closed and semi-closed cycles can be studied at design point, and also at off-design, using different control laws. The possibility of introducing component deterioration was also considered. The complete system is solved using a conventional Newton-Raphson method for non-linear systems.

As special off-design cases, the change from open to closed or semi-closed cycle can be done with a minimum effort, as well as the substitution of a single component, leaving the rest of the modules unchanged.

When the code was ready, a comprehensive validation was carried out with several gas turbines configurations. Also, some analytical results from different sources using gases other than air (i.e. helium), were examined. The results of the validation have been extremely good, giving confidence in the predictions of the code.

After the validation of GTSI, the semi-closed cycle was designed. Initially, the selection of working fluid, between pure carbon dioxide and carbon dioxide / argon, and the choice of power plant arrangements were carried out. Characteristic values of the state-of-the-art technology were used for component efficiencies, cooling requirements, etc. The two spool-two shaft gas turbine was selected due to the very high pressure ratio needed to obtain high thermal efficiencies. Simple, intercooled, regenerated and intercooled & regenerated cycles were initially considered (fitted, in every case, with an optimum steam turbine bottoming cycle). With small differences in thermal efficiency, the main parameter for a base load machine, between the four cycles, and in order to simplify the already difficult machine, the two spool-two shaft simple cycle machine was chosen.

However, not only a conventional turbine, with a moderate firing temperature, has been considered in this thesis. Advanced high temperature cycles employing cryogenic nitrogen precooling, used also for turbine stator cooling, were studied. These have shown important increases in thermal efficiency and specific power output, although the technological challenges are considerably larger than for the conventional, low temperature, cycle. In the analysis, not only the components of the gas turbine, but also the inefficiencies due to air separation, coal gasification and carbon dioxide liquefaction have been taken into account in order to have realistic performance values. In general, the simple cycle efficiencies obtained are very low. The combined cycle values, where the exhaust heat is used for the steam cycle, are also quite low compared with open cycle machines. A better performance if offered by the advanced high temperature cycles, but still not as good as by a modern combined open cycle. The differences can be explained by the significant installation inefficiencies associated to the semi-closed cycle.

Once the cycles have been selected, the off-design study was carried out. The inlet temperature will not change significantly (affected only by the precooling water temperature that should be fairly stable). The inlet pressure will be controlled to give ambient pressure at compressor inlet. Designed for electricity generation, the low pressure spool will operate at constant speed. Preliminary off-design studies shown the necessity of having variable geometry in the low pressure compressor for part power operation. Further off-design simulations indicated the need of high pressure compressor variable geometry. The use of bleed valves at part load, common in open cycles, will be very restricted in this case, where the operating fluid is mainly carbon dioxide.

The starting process was studied as a sequence of steady-state points. At low shaft speed the working fluid was air, firing natural gas. When the gas generator reached the synchronous idle condition, the air was changed to carbon dioxide/argon, employing natural gas as fuel and oxygen as oxidizer. Finally, the fuel was switch to a low calorific value synthetic gas, also with oxygen as oxidizer.

With the uncertainties associated to the turbomachinery design, operating mainly with carbon dioxide, and to the new combustion technology, a demonstrator seems to be a reasonable way of validating some of the innovative aspects of the semi-closed

cycles. Using the capabilities of GTSI, the application of an existing open cycle gas turbine hardware was considered, showing possible problems, risk areas and difficulties associated with this proposal.

10.2. RECOMMENDATIONS FOR FURTHER WORK

As stated in the first section of this chapter, all the initial objectives have been successfully accomplished. However, a performance code must be always open to modifications, improvements, introduction of new methodologies, etc. Therefore, a continuous improvement should always be carried out, adding more capabilities. It is also important to bear in mind that the new versions must be compatible with the previous ones, in order to be able to run old cases with the new programme.

Although the code has been extensively validated against published and private performance data of various gas turbine arrangements, with different technology levels, a continuous effort should be made, when new data becomes available, to follow with this activity. Experimental data of gas turbines with variable geometry[1], burning fuels other than Natural Gas, Diesel No.2 or kerosene and using different working fluids, would be desirable.

GTSI has been written for synthesis, and has a limited analysis (diagnostics) capability. The introduction of this feature appears as a major task for the improvement of the code. This modification will take a large amount of time, as it will be necessary to observe different configurations for the instrumentation, etc.

The capability of simulating component deterioration has already been implemented in the code. But, if the analysis capability was fully introduced, it would be possible to create an extremely powerful tool for engine monitoring.

Finally, the input files of the code, for design and control of the machine, are quite easy to produce with the help of the Programme User Guide. However, it would be desirable to have an interactive Graphical User Interface to generate the input, and some effort should be devoted in this direction.

---

[1] Not only the component characteristics as a function of the variable geometry should be available, but also the control laws of the machine, to reproduce the operating conditions as accurate as possible.

BIBLIOGRAPHY AND REFERENCES

BIBLIOGRAPHY AND REFERENCES

1. Adelman, S.T., Hoffman, M.A. and Baughn, J.W., *A Methane-Steam Reformer for a Basic Chemically Recuperated Gas Turbine*, Transactions of the ASME, Journal for Gas Turbines and Power, Vol. 117, January 1995, pp. 16-23.

2. Allen, R.P. and Kovacik J.M., *Gas Turbine Cogeneration-Principles and Practice*, Transactions of the ASME, Journal for Gas Turbines and Power, Vol. 106, July 1984, pp. 725-730.

3. Amagasa, S., Shimomura, K., Kadowaki, M., Takeishi, K., Kawai, H., Aoki, S and Aoyama, K., *Study on the Turbine Vane and Blade for a 1500°C Class Industrial Gas Turbine*, Transactions of the ASME, Journal for Gas Turbines and Power, Vol. 116, July 1994, pp. 597-604.

4. Ammari, H.D., Hay, N. and Lampard, D., *Simulation of Cooling Film Density Ratios in a Mass Transfer Technique*, ASME paper 89-GT-200, Toronto, Canada, 1989.

5. Baggenstoss, W.G. and Ashe, T.L. *Mission Design Drivers for Closed Brayton Cycle Space Power Conversion Configuration*, Transactions of the ASME, Journal for Gas Turbines and Power, Vol. 114, October 1992, pp. 721-726.

6. Bammert, K. and Groschup, G., *Status Report on Closed-Cycle Power Plants in the Federal Republic of Germany*. Transactions of ASME, Journal of Engineering for Power, Vols. 98-99, 1976-77.

7. Baughn, J.W. and Kerwin, R.A., *A Comparison of the Predicted and Measured Thermodynamic Performance of a Gas Turbine Cogeneration System*, Transactions of the ASME, Journal for Gas Turbines and Power, Vol. 109, January 1987, pp. 32-38.

8. Baughn, J.W. and Bagheri, N., *The Effect of Thermal Matching on the Thermodynamic Performance of Gas Turbine and IC Engine Cogeneration Systems*, Transactions of the ASME, Journal for Gas Turbines and Power, Vol. 109, January 1987, pp. 39-45.

9. Becker, B. and Schetter, B., *Gas Turbines Above 150 MW for Integrated Coal Gasification Combined Cycles (IGCC)*, Transactions of the ASME, Journal of Engineering for Gas Turbines and Power, Vol. 114, October 1992, pp. 660-664.

10. Boissenin, Y. and Castanier, A., *Choosing the Right Combined Cycle Power Plant*, Alsthom AGTR 8807, 1988.

11. Bolland, O., *A Comparative Evaluation of Advanced Combined Cycles Alternatives*, Transactions of the ASME, Journal of Engineering for Gas Turbines and Power, Vol. 113, April 1991, pp. 190-197.

12. Bolland, O. and Stadaas, J.F., *Comparative Evaluation of Combined Cycles and Gas Turbine Systems With Water Injection, Steam Injection and Recuperation*, Transactions of the ASME, Journal for Gas Turbines and Power, Vol. 117, January 1995, pp. 138-145.

13. Boyle, R.J., *Effect of Steam Addition on Cycle Performance of Simple and Recuperated Gas Turbines*, NASA TP 1440, Lewis Research Center, Cleveland Ohio, 1979.

14. Brander, J.A. and Chase, D.L., *Repowering Applications Considerations*, Transactions of the ASME, Journal of Engineer for Gas Turbines and Power, Vol. 114, October 1992, pp. 643-652.

15. Burnham, J.B., Giuliani, M.H. and Moeller, D.J., *Development, Installation, and Operating Results of a Steam Injection System (STIG^{TM}) in a General Electric LM5000 Gas Generator, Transactions of the ASME*, Journal of Engineering for Gas Turbines and Power, Vol. 109, July 1987, pp. 257-262.

16. Cambel, A.B. and Koomanoff, F.A., *High Temperature Superconductors and CO_2 Emissions*, Energy Vol. 14, No. 6, pp. 309-322, 1989.

17. Carlson, R.J., West, P.M. and Azouz, D.E., *Digital Control System Development for an Intercooled Recuperated Gas Turbine*, Transactions of the ASME, Journal for Gas Turbines and Power, Vol. 117, January 1995, pp. 172-175.

18. Carnevale E. and De Lucia, M., *The Use of Oxygen in Combustion Process: Experimental Results in Some Industrial Plants*, Proceedings of the 23rd Intersociety Energy Conversion Engineering Conference, July-August 1988, Denver, Colorado.

19. Cerri, G., *Parametric Analysis of Combined Gas-Steam Cycles*, Transactions of the ASME, Journal of Engineering for Gas Turbines and Power, Vol. 109, January 1987, pp. 46-54.

20. Chin, D., Hermanson, J.C. and Spadaccini, L.J., *Thermal Stability and Heat Transfer Characteristics of Methane and Natural Gas Fuels*, Transactions of the ASME, Journal for Gas Turbines and Power, Vol. 117, July 1995, pp. 462-467.

21. Choo, Y.K., *Analysis of Potential Benefits of Integrated-Gasifier Combined Cycles for a Utility System*, NASA TP 2172, Lewis Research Center, Cleveland Ohio, 1983.

22. Crawford, R.A., *Quantitative Evaluation of Transient Heat Transfer on Axial Flow Compressor Stability*, AIAA paper 85-1352, July 1985, Monterey, California.

23. Davis, N.T., McDonell, V.G. and Samuelsen, G.S., *Effects of Cycle Operating Conditions on Combustor Performance*, Transactions of the ASME, Journal for Gas Turbines and Power, Vol. 119, January 1997, pp. 45-49.

24. De Lucia, M. and Tucci, M., *Increasing the Power-to-Heat Ratio Through Application of a Combined Cycle to a Cogeneration Plant.*

25. Deschamps, P.J., Mathieu, Ph. and Singh, R., *Off-Design Performance of Repowered Steam Cycle Power Plants*, 19th International Congress on Combustion Engines, Florence 1991.

26. Dechamps, P.J., Pirard, N. and Mathieu, Ph., *Part-Load Operation of Combined Cycle Plants With and Without Supplementary Firing*, Transactions of the ASME, Journal for Gas Turbines and Power, Vol. 117, July 1995, pp. 475-483.

27. Dharmadhikari, S., *Gas Turbine for the Process Industries*, The Chemical Engineer, February 1989, pp. 16-20.

28. Dhole, V.R. and Zheng, J.P., *Applying Combined Pinch and Exergy Analysis to Closed-Cycle Gas Turbine System Design*, Transactions of the ASME, Journal for Gas Turbines and Power, Vol. 117, January 1995, pp. 47-52.

29. Diesel and Gas Turbine World Wide, *Rolls-Royce Releases Details of Dry Low Emissions Program*, October 1992, pp. 44-46.

30. Diesel and Gas Turbine World Wide, *Testing Battle Tank Gas Turbines*, January-February 1993, pp. 36-38.

31. Duponchel, J.P. and Leturcq, R., *Humidity Effects on Gas Turbine Performance - SNECMA methodology*, AGARD Committee 72-5, Madrid, May 1990.

32. Duponchel, J.P., Loisy, J. and Carrillo, R., *Steady and Transient Performance Calculation Method for Prediction,* AGARD Lecture Series 183, *Steady and Transient Performance Prediction of Gas Turbine Engines*, May 1992.

33. Edwards, J.P., *Liquid and Vapour Cooling Systems for Gas Turbines*, ARC/CP-1127, London, 1970.

34. El-Masri, M.A. and Magnusson, J.H., *Thermodynamics of an Isothermal Gas Turbine Combined Cycle*, Transactions of the ASME, Journal of Engineering for Gas Turbines and Power, Vol. 106, October 1984, pp. 743-749.

35. El-Masri, M.A., *On Thermodynamics of Gas Turbine Cycles: Part 1-Second Law Analysis of Combined Cycles*, Transactions of the ASME, Journal of Engineering for Gas Turbines and Power, Vol. 107, October 1985, pp. 880-889.

36. El-Masri, M.A., *On Thermodynamics of Gas Turbine Cycles: Part 2-A Model for Expansion in Cooled Turbines*, Transactions of the ASME, Journal of Engineering for Gas Turbines and Power, Vol. 108, January 1986, pp. 151-159.

37. El-Masri, M.A., *On Thermodynamics of Gas Turbine Cycles: Part 3-Thermodynamic Potential and Limitations of Cooled Reheat-Gas-Turbine Combined Cycles*, Transactions of the ASME, Journal of Engineering for Gas Turbines and Power, Vol. 108, January 1986, pp. 160-170.

38. El-Masri, M.A., *Exergy Analysis of Combined Cycles: Part 1-Air Cooled Brayton-Cycle Gas Turbines*, Transactions of the ASME, Journal of Engineering for Gas Turbines and Power, Vol. 109, April 1987, pp. 228-236.

39. El-Masri, M.A., *Exergy Analysis of Combined Cycles: Part 2-Analysis and Optimization of Two-Pressure Steam Bottoming Cycles*, Transactions of the ASME, Journal of Engineering for Gas Turbines and Power, Vol. 109, April 1987, pp. 237-243.

40. El-Masri, M.A., *GASCAN-an Interactive Code for Thermal Analysis of Gas Turbine Systems*, Transactions of the ASME, Journal of Engineering for Gas Turbines and Power, Vol. 110, April 1988, pp. 201-207.

41. El-Masri, M.A., *A Modified, High-Efficiency, Recuperator Gas Turbine Cycle*, Transactions of the ASME, Journal of Engineering for Gas Turbines and Power, Vol. 110, April 1988, pp. 233-240.

42. Emanuel, G., *Advanced Classical Thermodynamics*, AIAA Educational Series, Washington D.C., 1987.

43. Esgar, J.B., Colladay, R.S. and Kaufman, A., *An Analysis of the Capabilities and Limitations of Turbine Air Cooling Methods*, NASA TN D-5992, Lewis Research Center, Cleveland, Ohio, 1970.

44. Farmer, R., *GT-60 Turbine Repowered by an LM1600 Gas Generator is Rated at 18000 hp*, Gas Turbine World, December 1988, pp. 10-23.

45. Fatemi, H., *Influence of Operating Environment on the Performance and Selection of Industrial Gas Turbines*, MSc Thesis, Cranfield Institute of Technology, Cranfield, Bedford, 1985.

46. Finckh, H.H. and Pfost, H., *Development Potential of Combined Cycle (GUD) Power Plant With and Without Supplementary Firing*, Transactions of the ASME, Journal of Engineering for Gas Turbines and Power, Vol. 114, October 1992, pp. 653-659.

47. Foster-Pegg, R.W., *Steam Bottoming Plants for Combined Cycles*, Transactions of ASME, Journal of Engineering for Power, Vol. 100, pp. 203-211, April 1978.

48. Fraas, A.P., *Engineering Evaluation of Energy Systems*, McGraw-Hill Book Company, New York, 1982.

49. Frutschi, H.U., *The Relationship of Power and Heat Production with Closed Cycle Gas Turbines*, Transactions of the ASME, Journal of Engineering for Power, Vol. 102, April 1980, pp. 288-291.

50. Gill, A.B., *Power Plant Performance*, Butterworths, 1984.

51. Glassmann, A.J. (ed.), *Turbine Design and Application*, Vols. 1-3, NASA SP-290, 1972.

52. Gordon, S. and McBride, B.J., *Computer Program for Calculation of Complex Chemical Equilibrium Composition, Rocket Performance, Incident and Reflected Shocks, and Chapman-Jouget Detonations*, NASA SP-273, Lewis Research Center, Cleveland, Ohio, 1971.

53. Harman, R.T.C., *Gas Turbine Engineering*, The MacMillan Press, 1981.

54. Harvey, S.P., Knoche, K.F. and Richter, H.J., *Reduction of Combustion Irreversibility in a Gas Turbine Power Plant Through Off-Gas Recycling*, Transactions of the ASME, Journal for Gas Turbines and Power, Vol. 117, January 1995, pp. 24-30.

55. Hendricks, R.C. and Peller, I.C., *WASP-A Flexible Fortran IV Computer Code for Calculating Water and Steam Properties*, NASA TN-D-7391, Lewis Research Center, Cleveland, Ohio, 1973.

56. Hilsenrath, J. et al., *Tables of Thermodynamic and Transport Properties of Air, Argon, Carbon Dioxide, Carbon Monoxide, Hydrogen, Nitrogen, Oxygen and Steam*, Pergamon Press, Oxford, 1960.

57. Hori, A. and Takeya, K., *Outline of Plan for Advanced Reheat Gas Turbine*, Transactions of the ASME, Journal of Engineering for Power, Vol. 103, October 1981, pp. 772-850.

58. Huang, F.F. and Wang, L., *Thermodynamic Study of an Indirect Fired Air Turbine Cogeneration System with Reheat*, Transactions of the ASME, Journal of Engineering for Gas Turbines and Power, Vol. 109, January 1987, pp. 16-21.

59. Hunter, I., *Design of Turbomachinery for Closed and Semi Closed Gas Turbine Cycles*, MSc Thesis, 1993-94, Cranfield University.

60. Irvine, T.F. and Liley, P.E., *Steam and Gas Tables with Computer Equations, Appendices I, II, V and VII*. Academic Press, Orlando, 1984.

61. Issa, M., *Modification of an Aero-Engine (Rolls-Royce Spey RB 168-66) to an Industrial/Marine/Unit By-Pass Heat Exchanger Version*, MSc Thesis, Cranfield Institute of Technology, Cranfield, Bedford, 1985.

62. Itoh, M., Ishigaki, T. and Sagiya, Y., *Simulation Study of Transient Performance Matching of Turbofan Engine Using an Analogue Computer to Evaluate Its Usefulness as Design Tool*, Transactions of ASME, Journal of Engineering for Power, Vol. 97, pp. 369-374, July 1975.

63. Jericha, H. and Hoeller, F., *Combined Cycle Enhancement*, Transactions of the ASME, Journal of Engineering for Gas Turbines and Power, Vol. 113, April 1991, pp. 198-202.

64. Johnson, M.S., *Prediction of Gas Turbine On-and Off-Design Performance When Firing Coal-Derived Syngas*, Transactions of the ASME, Journal for Gas Turbines and Power, Vol. 114, April 1992, pp. 380-385.

65. Johnson, R.C., *Tables of Critical-Flow Functions and Thermodynamic Properties for Methane and Computational Procedures for Both Methane and Natural Gas*, NASA SP-3074, Lewis Research Center, Cleveland Ohio, 1972.

66. Johnson, R.S., *The Theory and Operation of Evaporative Coolers for Industrial Gas Turbine Installations*, Transactions of the ASME, Journal of Engineering for Gas Turbines and Power, Vol. 111, April 1989, pp. 327-334.

67. Kalina, A.I., *Combined-Cycle System With Novel Bottoming Cycle*, Transactions of the ASME, Journal of Engineering for Gas Turbines and Power, Vol. 106, October 1984, pp. 737-742.

68. Keenan, J.H., Kaye, J. and Chao, J., *Gas Tables: International Version 2nd Edition (SI Units)*, 1983.

69. Khalid, S.J. and Hearne, R.E., *Enhancing Dynamic Model Fidelity for Improved Prediction of Turbofan Engine Transient Performance*, AIAA paper 80-1083, Hartford, Connecticut, 1980.

70. Kimura, S.G., Spiro, C.L. and Chen, C.C., *Combustion and Deposition in Coal-Fired Turbines*, Transactions of the ASME, Journal for Gas Turbines and Power, Vol. 109, July 1987, pp. 319-324.

71. Kolp, D.A. and Moeller, D.J., *World's First Full STIG™ LM5000 Installed at Simpson Paper Company*, Transactions of the ASME, Journal of Engineering for Gas Turbines and Power, Vol. 111, April 1989, pp. 200-210.

72. Kolp, D.A., Flye, W.M. and Guidotti, H.A., *Advantages of Air Conditioning and Supercharging an LM6000 Gas Turbine Inlet*, Transactions of the ASME, Journal for Gas Turbines and Power, Vol. 117, Jul. 1995, pp. 513-527.

73. Kotas, T.J., *The Exergy Method of Thermal Plant Analysis*, Butterworths, 1985.

74. Krey, G., *Utilisation of the Cold by LNG Vaporisation with Closed Cycle Gas Turbine*, Transactions of the ASME, Journal of Engineering for Power, Vol. 102, April 1980, pp. 225-230.

75. Kurzke, J., *Calculation of Installation Effects within Performance Computer Programs*, AGARD Lecture Series 183, *Steady and Transient Performance Prediction of Gas Turbine Engines*, May 1992.

76. Larson, E.D. and Williams, R.H., *Steam Injected Gas Turbines*, Transactions of the ASME, Journal of Engineering for Gas Turbines and Power, Vol. 109, January 1987, pp. 55-63.

77. Larson, E.D. and Williams, R.H., *Biomass-Gasifier Steam-Injected Gas Turbine Cogeneration*, Transactions of the ASME, Journal of Engineering for Gas Turbines and Power, Vol. 112, April 1990, pp. 157-163.

78. Lee, J.C., Campbell, J.Jr. and Wright, D.E., *Closed Cycle Gas Turbine Working Fluids*, Transactions of ASME, Journal of Engineering for Power, Vol. 103, 1981.

79. Leibowitz, H. and Tabb, E., *The Integrated Approach to a Gas Turbine Topping Cycle Cogeneration System*, Transactions of the ASME, Journal of Engineering for Gas Turbines and Power, Vol. 106, October 1984, pp. 731-736.

80. Leonard, G. and Stegmaier, J., *Development of an Aeroderivative Gas Turbine Dry Low Emissions Combustion System*, Transactions of the ASME, Journal for Gas Turbines and Power, Vol. 116, July 1994, pp. 542-546.

81. Little, W.J., *Tables of Thermodynamic Properties of Argon from 100 to 3000 K*, AEDC-TDR-64-68, 1964.

82. Livingood, J.N.B., *1971 NASA Turbine Cooling Research Status Report*, NASA TM-X-2384, Lewis Research Center, Cleveland, Ohio, 1971.

83. Longley, J.P. and Greitzer, E.M. *Inlet Distortion Effects in Aircraft Propulsion System Integration*, AGARD Lecture Series 183, *Steady and Transient Performance Prediction of Gas Turbine Engines*, May 1992.

84. Maccallum, N.R.L. and Qi, Q.F., *The Transient Behaviour of Aircraft Gas Turbines*, University of Glasgow, September 1989.

85. Macchi, E., Consonni, S., Lozza, G. and Chiesa, P., *An Assessment of the Thermodynamic Performance of Mixed Gas-Steam Cycles: Part A-Intercooled and Steam Injected Cycles*, Transactions of the ASME, Journal for Gas Turbines and Power, Vol. 117, July 1995, pp. 489-498.

86. Macchi, E., Consonni, S., Lozza, G. and Chiesa, P., *An Assessment of the Thermodynamic Performance of Mixed Gas-Steam Cycles: Part B-Water Injected and HAT Cycles*, Transactions of the ASME, Journal for Gas Turbines and Power, Vol. 117, July 1995, pp. 489-498.

87. Marston, C.H. and Hyre, M., *Gas Turbine Bottoming Cycles: Triple Pressure Steam Versus Kalina*, Transactions of the ASME, Journal for Gas Turbines and Power, Vol. 117, January 1995, pp. 10-15.

88. Maughan, J.R., Elward, K.M., De Pietro, S.M. and Bautista, P.J., *Field Test Results of a Dry Low NO_x Combustion System for the MS3002J Regenerative Cycle Gas Turbine*, Transactions of the ASME, Journal for Gas Turbines and Power, Vol. 119, January 1997, pp. 50-57.

89. Meitner, P.L., *Analysis of Metal Temperature and Coolant Flow with a Thermal-Barrier Coating on a Full-Coverage Film-Cooled Turbine Vane*, NASA TP 1310, AVRADCOM Technical Report 78-20, Lewis Research Center, Cleveland, Ohio, 1978.

90. Mori, K., Kitajima, J., Kimura, T. and Miki, S., *Preliminary Study on Reheat Combustors for Advanced Gas Turbines*, Transactions of the ASME, Journal of Engineering for Power, Vol. 104, January 1982, pp. 1-8.

91. Nainiger, J.J., Burns, R.K. and Easley, A.J., *Performance and Operational Economics Estimates for Coal Gasification Combined-Cycle Cogeneration Power Plant*, NASA TM 82729, Lewis Research Center, Cleveland Ohio, 1982.

92 Nakata, T., Sato, M., Ninomiya, T., Yoshine, T. and Yamada, M., *Effect of Pressure on Combustion Characteristics in LBG-Fueled 1300°C-Class Gas Turbine*, Transactions of the ASME, Journal for Gas Turbines and Power, Vol. 116, July 1994, pp. 554-558.

93. Navaratnam, M., *The Investigation of an Aero Derivative Gas Turbine Using Alternative Working Fluids in Closed/Semi Closed Cycles*, MSc Thesis, 1993-94, Cranfield University.

94. Novack, M., Roffe, G. and Miller, G., *Combustion of Coal/Water Mixtures With Thermal Preconditioning*, Transactions of the ASME, Journal for Gas Turbines and Power, Vol. 109, July 1987, pp. 313-318.

95. Oates, G.C., *Aerothermodynamics of Aircraft Engine Components*, AIAA Education Series, Washington DC, 1985.

96. Oates, G.C., *Aerothermodynamics of Gas Turbine and Rocket Propulsion*, AIAA Education Series, revised and enlarged edition, Washington DC, 1988.

97. Oates, G.C., *Aircraft Propulsion Systems Technology and Design*, AIAA Education Series, Washington DC, 1989.

98. Oliker, I., *Steam Turbines for Cogeneration Power Plants*, Transactions of the ASME, Journal of Engineering for Power, Vol. 102, April 1980, pp. 482-485.

99. Philpot, M.G., *Practical Considerations in Designing the Engine Cycle*, AGARD Lecture Series 183, *Steady and Transient Performance Prediction of Gas Turbine Engines*, May 1992.

100. Pai, B.R., *Utilisation of Sludge Gas for Power Generation Through Aero Gas Turbines*, Sandhana Vol. 7, Part 3, November 1984, pp. 223-236.

101. Perz, E., *A Computer Method for Thermal Power Cycle Calculation*, Transactions of the ASME, Journal for Gas Turbines and Power, Vol. 113, April 1991, pp. 184-189.

102. Rahnke, C.J., *The Variable Geometry Power Turbine*, International Automotive Engineering Congress, Jan. 1969, Detroit, Michigan.

103. Raj, R., *Deposition Results of a Transpiration Air-Cooled Turbine Vane Cascade in a Contaminated Gas Stream*, Transactions of the ASME, Journal of Engineering for Power, Vol. 105, October 1983, pp. 826-833.

104. Rice, I., *The Combined Reheat Gas Turbine/Steam Turbine Cycle, Part I-A Critical Analysis of the Combined Reheat Gas Turbine/Steam Turbine Cycle*, Transactions of the ASME, Journal of Engineer for Power, Vol. 102, January 1980, pp. 35-41.

105. Rice, I., *The Combined Reheat Gas Turbine/Steam Turbine Cycle, Part II-The LM 5000 Gas Generator Applied to the Combined Reheat Gas Turbine/Steam Turbine Cycle*, Transactions of the ASME, Journal of Engineer for Power, Vol. 102, January 1980, pp. 42-49.

106. Rice, I. and Jenkins, P.E., *Comparison of the HTTT Reheat-Gas Turbine Combined Cycle with the HTTT Nonreheat Gas-Turbine Combined Cycle, Transactions of the ASME*, Journal of Engineering for Power, January 1982, Vol. 1982, pp. 129-142.

107. Rice, I.G., *The Reheat Gas Turbine with Steam-Blade Cooling-A Means of Increasing Reheat Pressure, Output, and Combined Cycle Efficiency*, Transactions of the ASME, Journal of Engineering for Power, Vol. 104, January 1982, pp. 9-22.

108. Rice, I.G., *Steam-Cooled Gas Turbine Casings, Struts, and Disks in a Reheat Gas Turbine Combined Cycle: Part I-Compressor and Combustor*, Transactions of the ASME, Journal of Engineering for Power, Vol. 105, October 1983, pp. 844-850.

109. Rice, I.G., *Steam-Cooled Gas Turbine Casings, Struts, and Disks in a Reheat Gas Turbine Combined Cycle: Part II-Gas Generator Turbine and Power Turbine*, Transactions of the ASME, Journal of Engineering for Power, Vol. 105, October 1983, pp. 851-858.

110. Rice, I.G., *Thermodynamic Evaluation of Gas Turbine Cogeneration Cycles: Part I-Heat Balance Method Analysis*, Transactions of the ASME, Journal of Engineering for Gas Turbines and Power, Vol. 109, January 1987, pp. 1-7.

111. Rice, I.G., *Thermodynamic Evaluation of Gas Turbine Cogeneration Cycles: Part II-Complex Cycle Analysis*, Transactions of the ASME, Journal of Engineering for Gas Turbines and Power, Vol. 109, January 1987, pp. 8-15.

112. Rieke, K.L., Lew, H.G. and Rovesti, W.C., *ITSL Coal Liquid as a Combustion Turbine Fuel*, Transactions of the ASME, Journal for Gas Turbines and Power, Vol. 109, July 1987, pp. 305-312.

113. Samuels, J.C. and Gale, B.M., *Effect of Humidity on Performance of Turbojet Engines*, NACA TN 2119, June 1950.

114. Saravanamuttoo, H.I.H. and Fawke, A.J., *Simulation of Gas Turbine Dynamic Performance*, ASME paper 70-GT-23, Brussels, Belgium, 1970.

115. Saravanamuttoo, H.I.H. and Fawke, A.J., *Digital Computer Methods for Prediction of Gas Turbine Dynamic Response*, SAE paper 710550, Montreal, Canada, 1971.

116. Sawyer, J.W., *Sawyer's Gas Turbine Engineering Handbook, Volume I Theory and Design*. 3rd Edition, 1985.

117. Sawyer, J.W., *Sawyer's Gas Turbine Engineering Handbook, Volume II Selection and Application*, Chapters 1, 7, 8 and 9. 3rd Edition, 1985.

118. Scalzo, A.J., McLaurin, L.D., Howard, G.S., Mori, Y., Hiura, H. and Sato, T., *A New 150 MW High-Efficiency Heavy-Duty Combustion Turbine*, Journal of Engineer for Gas Turbines and Power, Vol. 111, April 1989, pp. 211-217.

119. Schilke, P.W., Foster, A.D., Pepe, J.J. and Beltran, A.M., *Land-Based Gas Turbines*, Advanced Materials and Processes 4/92, pp. 22-30.

120. Schobeiri, M.T., Attia, M. and Lippke, C., *GETRAN: A Generic, Modularly Structured Computer Code for Simulation of Dynamic Behaviour of Aero- and Power Generation Gas Turbine Engines*, Transactions of the ASME, Journal of Engineer for Gas Turbines and Power, Vol. 116, July 1994, pp. 483-494.

121. Sellers, J.F. and Daniele, C.J., *DYNGEN - a Program for Calculating Steady-State and Transient Performance of Turbojet and Turbofan Engines*, NASA TN D-7901, Lewis Research Center, Cleveland Ohio, 1975.

122. Shepard, S.B., Bowen, T.L. and Chiprich, J.M., *Design and Development of the WR-21 Intercooled Recuperated (ICR) Marine Gas Turbine*, Transactions of the ASME, Journal for Gas Turbines and Power, Vol. 117, Jul. 1995, pp. 557-562.

123. Spiro, C.L., Kimura, S.G. and Chen, C.C., *Ash Behavior During Combustion and Deposition in Coal-Fueled Gas Turbines*, Transactions of the ASME, Journal for Gas Turbines and Power, Vol. 109, July 1987, pp. 325-330.

124. Stamatis, A., Mathioudakis, K. and Papailiou, K.D., *Adaptive Simulation of Gas Turbine Performance,* Transactions of the ASME, Journal of Engineering for Gas Turbines and Power, Vol. 112, April 1990, pp. 168-175.

125. Takano, H., Kitauchi, Y. and Hiura, H., *Design for the 145 MW Blast Furnace Gas Firing Gas Turbine Combined Cycle Plant*, Transactions of the ASME, Journal of Engineering for Gas Turbines and Power, Vol. 111, April 1989, pp. 218-224.

126. Takeishi, K., Aoki, S. and Sato, T., *Film Cooling on a Gas Turbine Rotor Blade*, Transactions of the ASME, Journal of Turbomachinery, Vol. 114, October 1992.

127. Takeya, K. and Yasui, H., *Performance of the Integrated Gas and Steam Cycle (IGSC) for Reheat Gas Turbines*, Transactions of the ASME, Journal for Gas Turbines and Power, Vol. 110, April 1988, pp. 220-232.

128. Touchton, G.L., *Influence of Gas Turbine Combustor Design and Operating Parameters on Effectiveness of NO_x Suppression by Steam or Water*, Transactions of the ASME, Journal for Gas Turbines and Power, Vol. 107, July 1985.

129. Tuccillo, R., Fontana, G. and Jannelli, E., *Coal-Derived Gas Utilization in Combined Gas-Steam Cycle Power Plants*, ASME paper 90-GT-366, June 1990, Brussels, Belgium.

130. Tuzson, J., *Status of Steam Injected Gas Turbines*, Transactions of the ASME, Journal of Engineering for Gas Turbines and Power, Vol. 114, October 1992, pp. 682-686.

131. Ulizar, I., *Design and Off-Design Performance Study of a Variable Cycle Engine with Convergent-Divergent Nozzle*, MSc Thesis, Cranfield Institute of Technology, Cranfield, Bedford, 1992.

132. Ulizar, I., *A Semi-Closed Cycle Gas Turbine with Carbon Dioxide-Argon as Working Fluid*, Journal of Engineering for Gas Turbines and Power, Vol. 119, July 1997, pp. 612-616.

133. Ulizar, I., *GTSI-Simulation of Gas Turbines with Unorthodox Working Fluids and Fuels*, Proceedings of Turbmacchine 96, Genova, Italy, July 1996.

134. Ulizar, I., *Design of a Semiclosed Cycle Gas Turbine with Carbon Dioxide-Argon as Working Fluid*, presented in the ASME Turbo Expo 1997, Orlando, Florida (accepted for publication in the Transactions of the ASME).

135. Ulizar, I., *Handling of the Semiclosed Cycle Gas Turbine with Carbon Dioxide-Argon as Working Fluid*, to be presented in the ASME Turbo Expo 1998, Stockholm, Sweden.

136. Urban, L.A., *Gas Turbine Engine Parameter Interrelationships*, United Technologies Hamilton Standard, 2nd Edition.

137. Wachsmuth, M., *Technical and Economical Considerations of Combined Cycles*, MSc Thesis, Cranfield Institute of Technology, Cranfield, Bedford, 1989.

138. Weisman, J. and Eckart, L.E., *Modern Power Plant Engineering*.

139. Wright, M.R., *Combined Gas/Steam Cycle Power Generation from a User's Viewpoint*, MPhil Thesis, Cranfield Institute of Technology, Cranfield, Bedford, 1990.

140. Wolf, J. and Moskowitz, S., *Development of the Transpiration Air-Cooled Turbine for High-Temperature Dirty Gas Streams*, Transactions of the ASME, Journal of Engineering for Power, Vol. 105, October 1983, pp. 821-825.

141. Wu, C.S. and Louis, J.F., *A Comparative Study of the Influence of Different Means of Cooling on the Performance of a Combined (Gas and Steam Turbines) Cycle*, Transactions of the ASME, Journal of Engineering for Power, Vol. 106, October 1984, pp. 750-755.

142. Yamada, H., Shimodaira, K. and Hayashi, S., *On-Engine Evaluation of Emissions Characteristics of a Variable Geometry Lean-Premixed Combustor*, Transactions of the ASME, Journal for Gas Turbines and Power, Vol. 119, January 1997, pp. 66-69.

143. Yeh, F.C., Gladden, H.J. and Gauntner, J.W., *Comparison of Heat Transfer Characteristics of Three Cooling Configurations for Air Cooled Turbine Vanes Tested in a Turbojet Engine*, NASA TM-X-2580, Lewis Research Center, Cleveland, Ohio, 1972.

144 Yokoyama, R. and Ito, K., *Multi-objective Optimisation in Unit Sizing of a Gas Turbine Cogeneration Plant*, Transactions of the ASME, Journal for Gas Turbines and Power, Vol. 117, January 1995, pp. 53-59.

145. Yokoyama, R., Ito, K. and Matsumoto, Y., *Optimal Operation of Cogeneration Plants with Steam-Injected Gas Turbines*, Transactions of the ASME, Journal for Gas Turbines and Power, Vol. 117, January 1995, pp. 60-66.

146. Zelina, J. and Ballal, D.R., *Combustor Stability and Emissions Research Using a Well-Stirred Reactor*, Transactions of the ASME, Journal for Gas Turbines and Power, Vol. 119, January 1997, pp. 70-75.

147. Zhu, P. and Saravanamuttoo, H.I.H., *Simulation of an Advanced Twin-Spool Industrial Gas Turbine*, Transactions of the ASME, Journal for Gas Turbines and Power, Vol. 114, April 1992, pp. 180-186.

APPENDIX I

EFFECT OF THE CRYOGENIC PRECOOLING AND NGVs NITROGEN INTERNAL COOLING (TET=1473 K)

EFFECT OF THE CRYOGENIC PRECOOLING & NGVs N_2 COOLING (TET=1473 K)

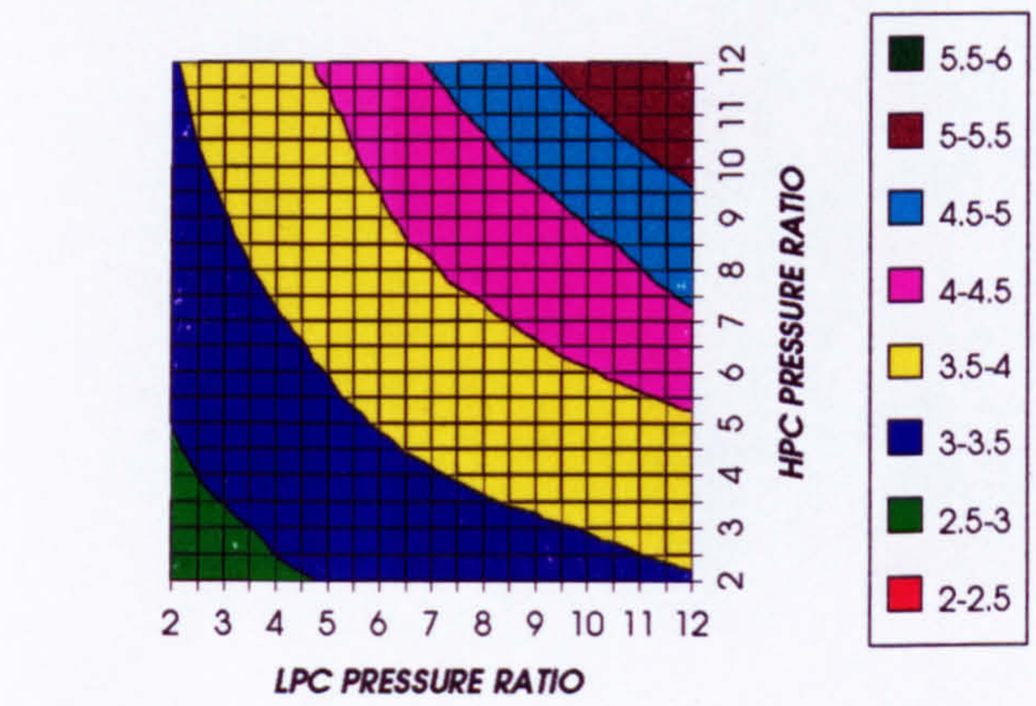

Figure 1. Increase in simple cycle thermal efficiency
Difference between precooling and standard

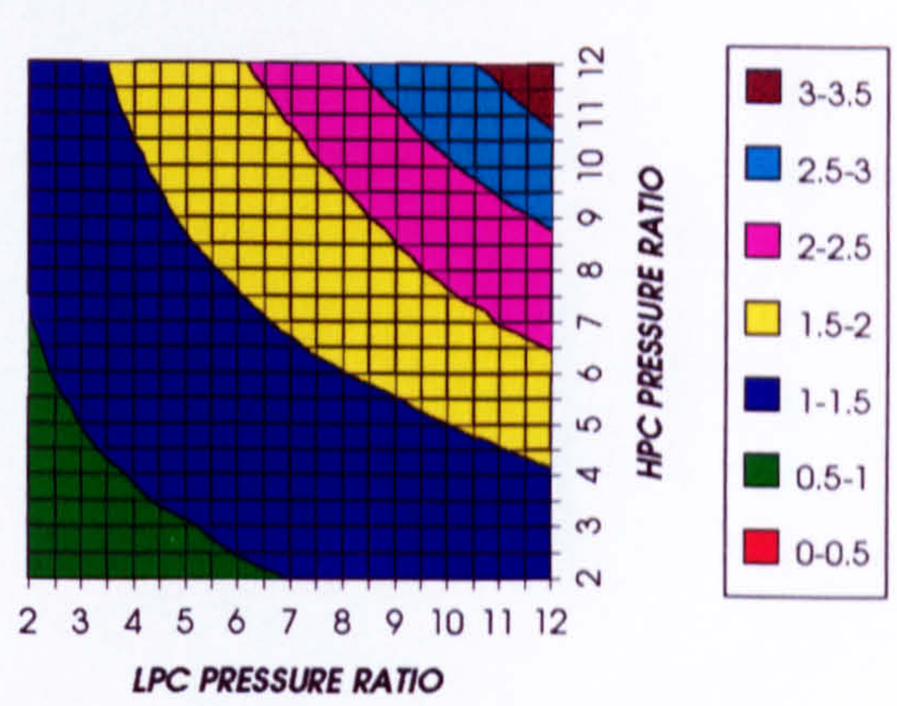

Figure 2. Increase in combined cycle thermal efficiency
Difference between precooling and standard

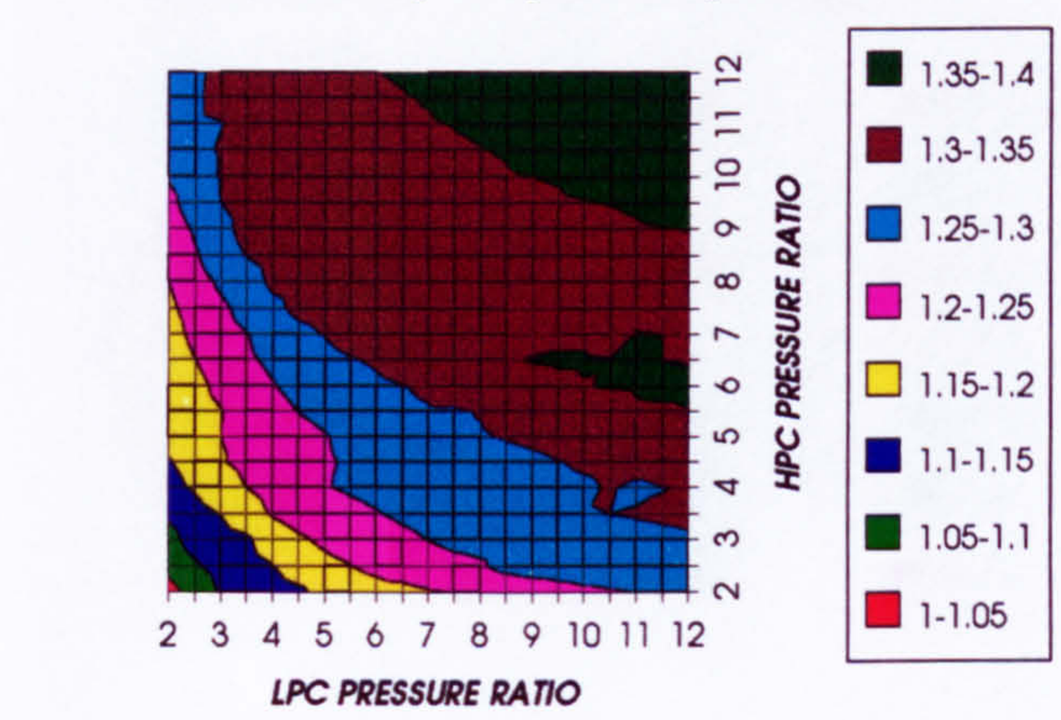

Figure 3. Increase in fuel to inlet mass flow ratio
Difference between precooling and standard

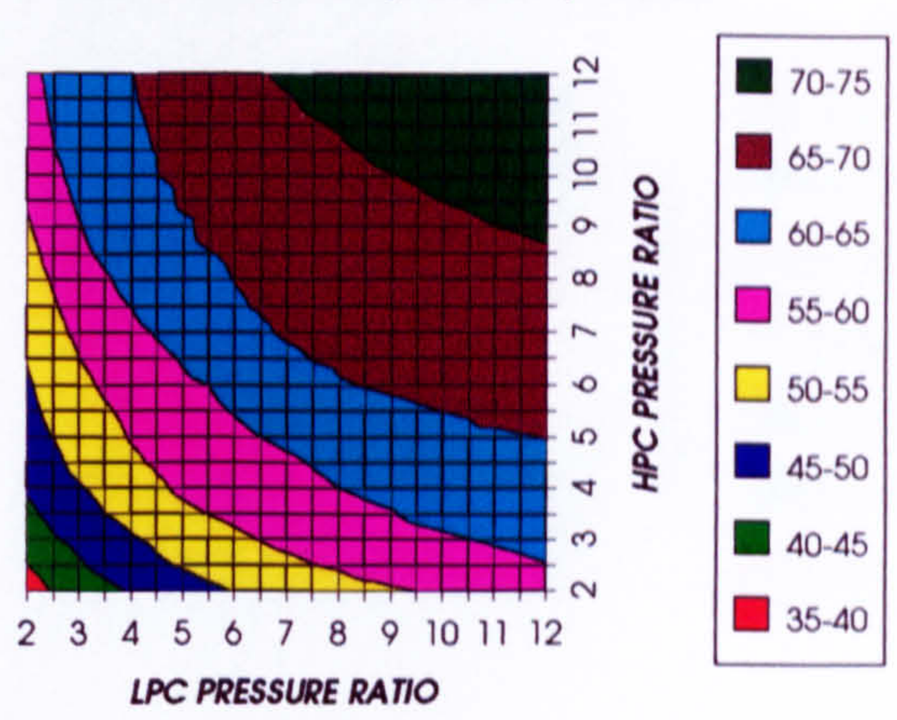

Figure 4. Increase in combined cycle specific power output
Difference between precooling and standard

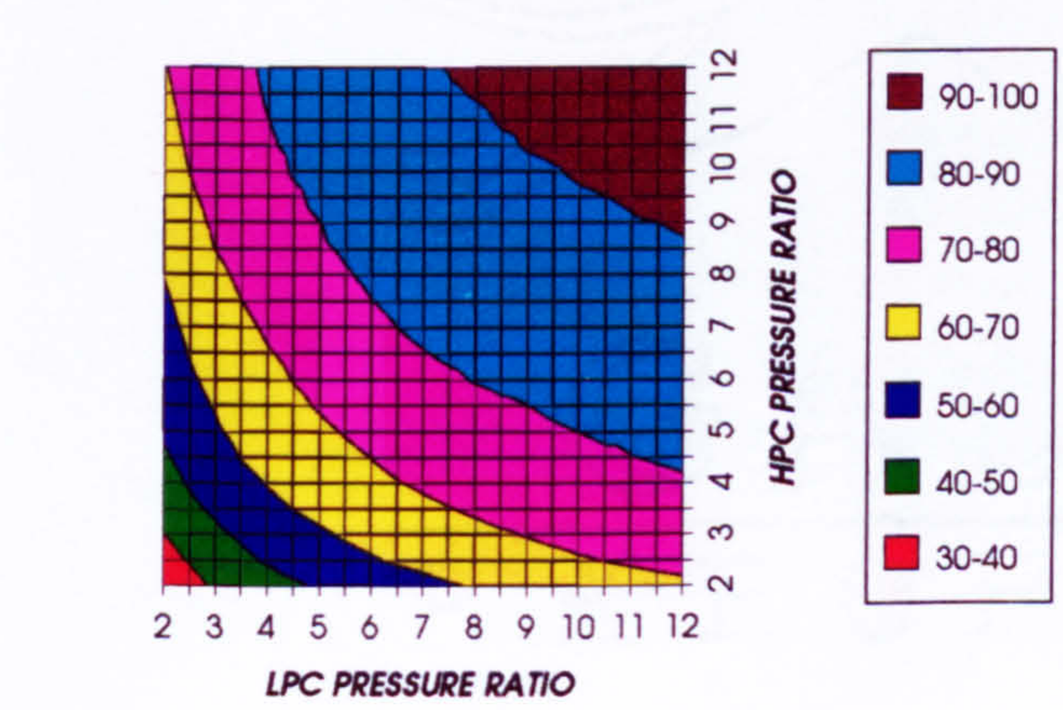

Figure 5. Increase in gas turbine specific power output
Difference between precooling and standard

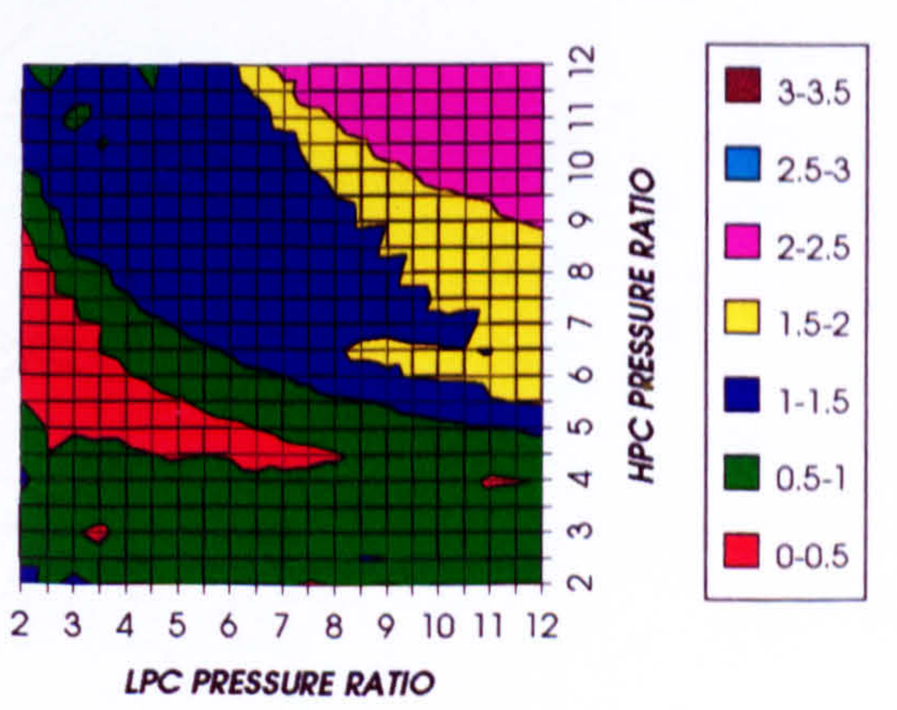

Figure 6. Increase in steam turbine specific power output
Difference between precooling and standard

EFFECT OF THE CRYOGENIC PRECOOLING & NGVs N_2 COOLING (TET=1473 K)

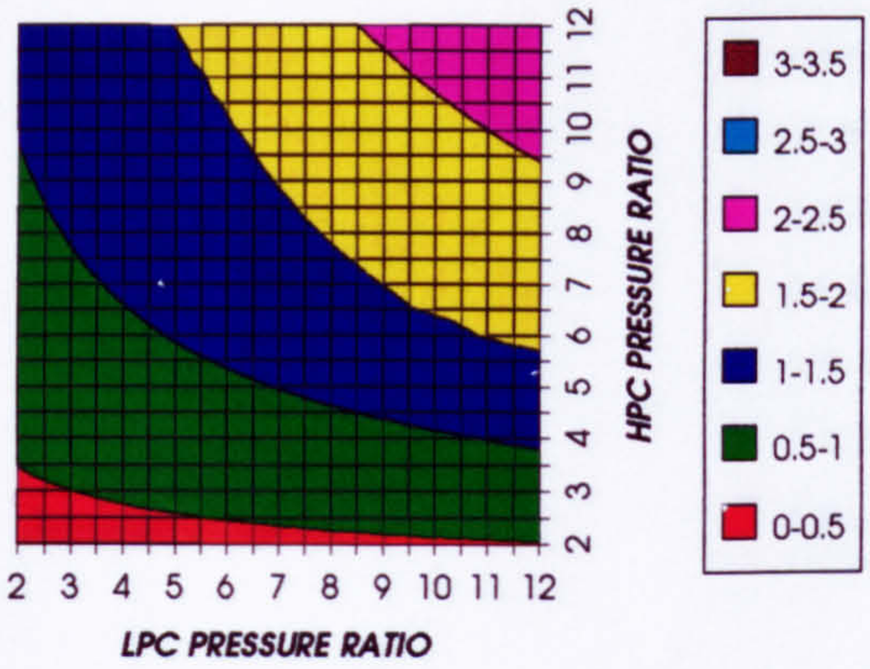

Figure 7. Decrease in HPT stator relative cooling flow
Difference between precooling and standard

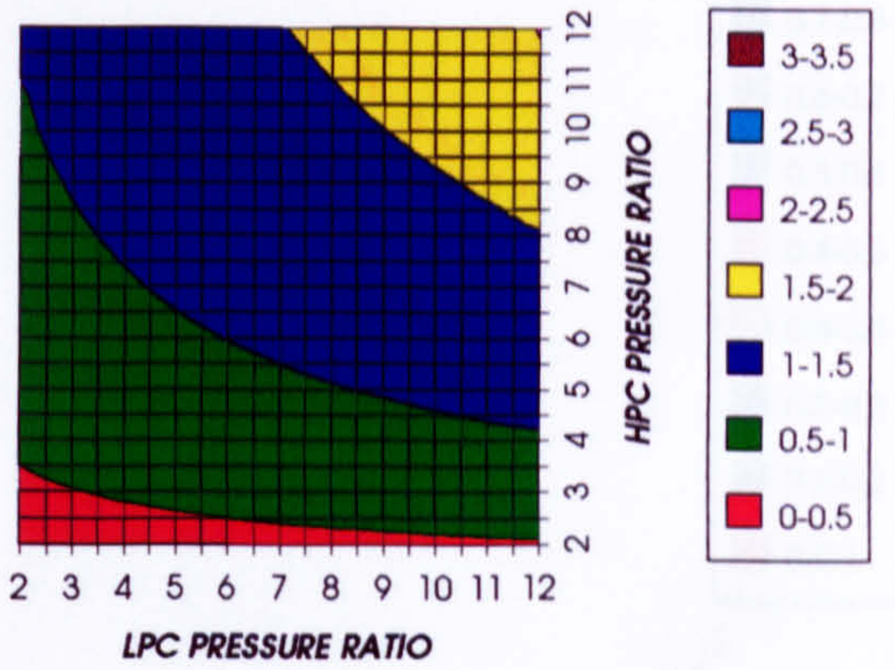

Figure 8. Decrease in HPT rotor relative cooling flow
Difference between precooling and standard

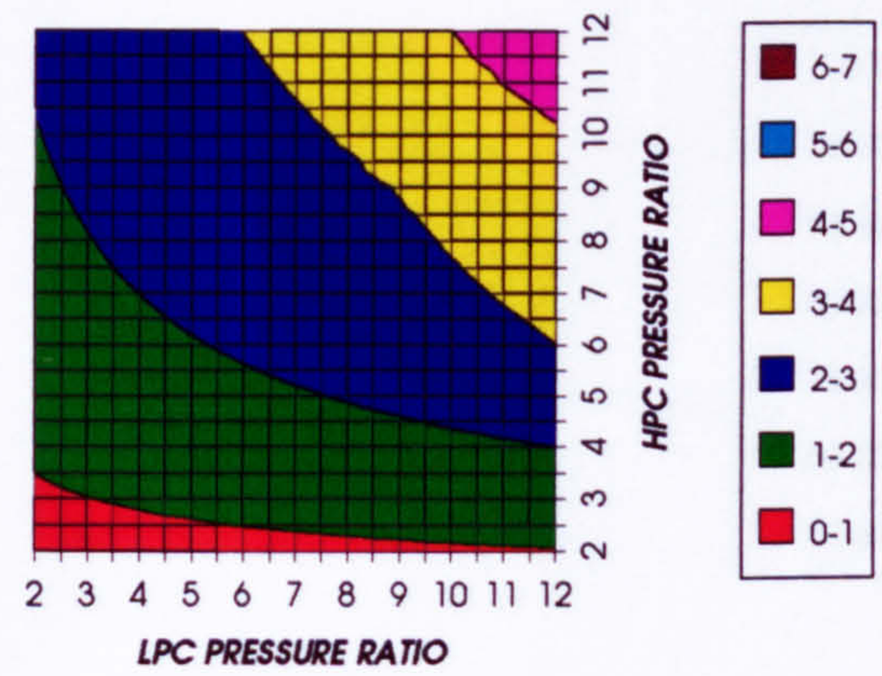

Figure 9. Decrease in HPT relative cooling flow
Difference between precooling and standard

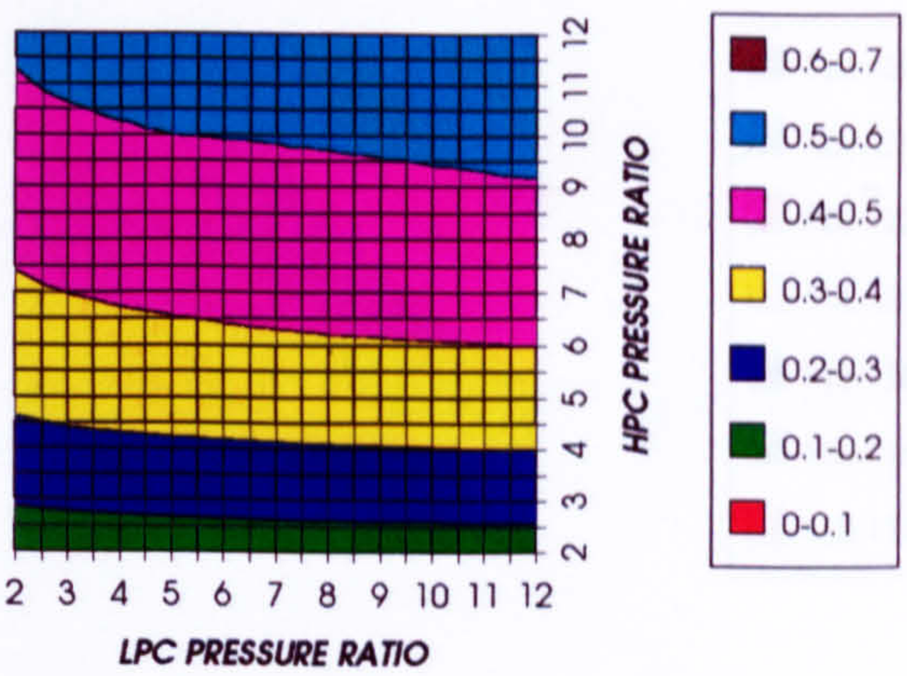

Figure 10. Decrease in HPT number of stages
Difference between precooling and standard

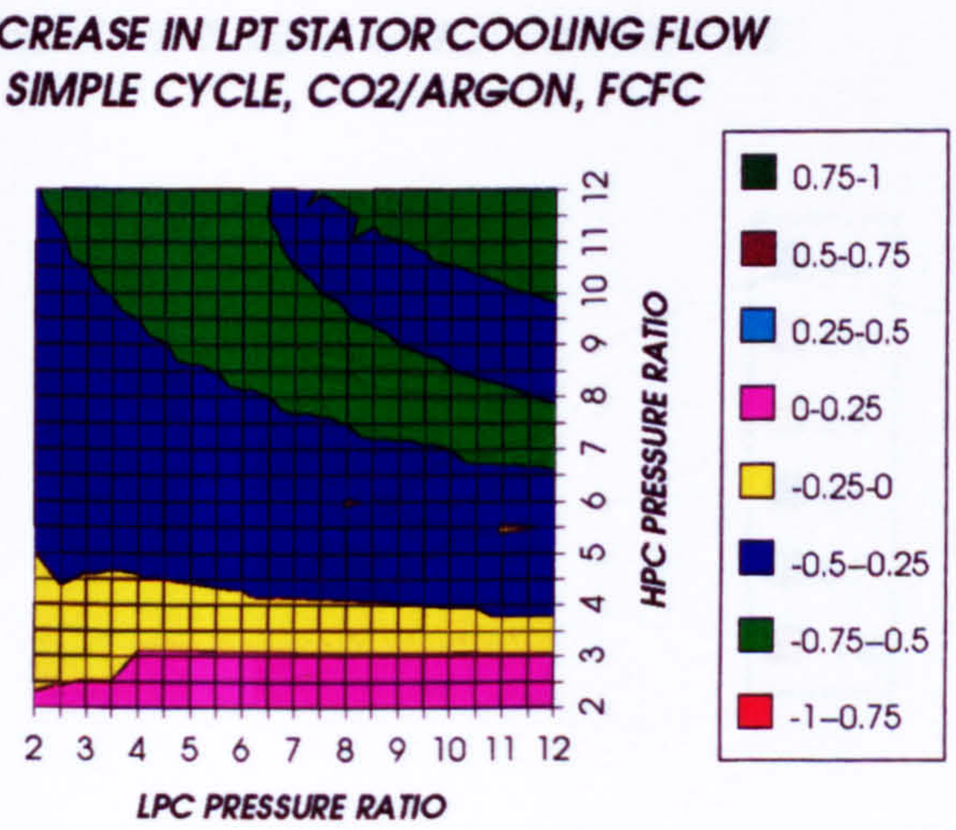

Figure 11. Decrease in LPT stator relative cooling flow
Difference between precooling and standard

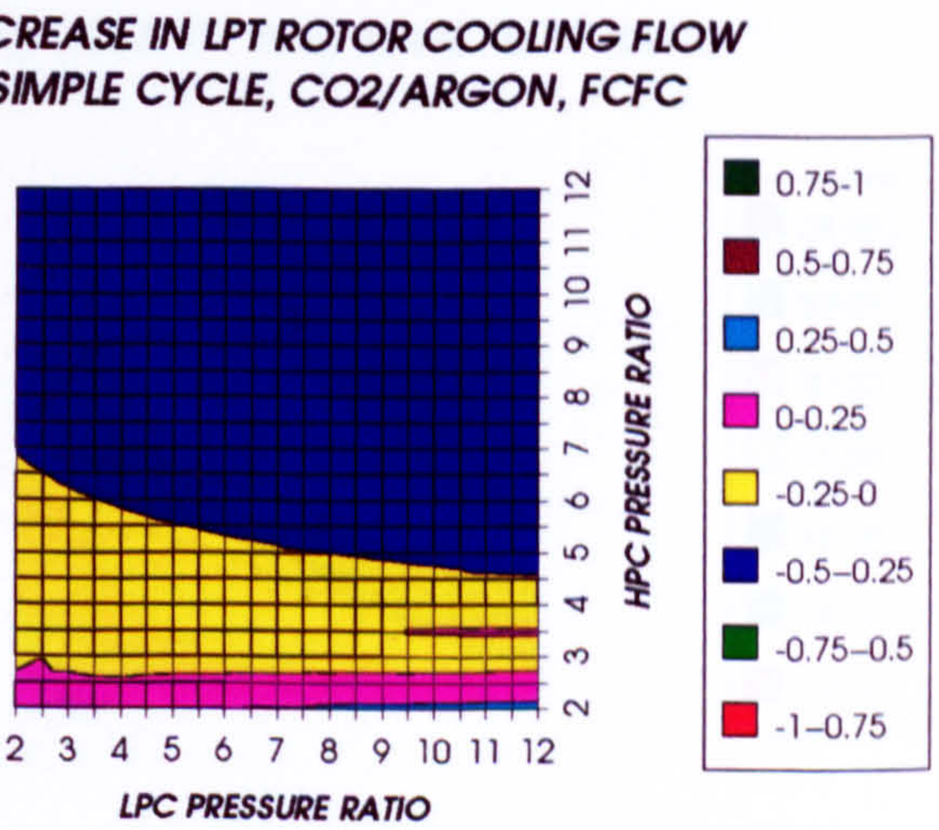

Figure 12. Decrease in LPT rotor relative cooling flow
Difference between precooling and standard

EFFECT OF THE CRYOGENIC PRECOOLING & NGVs N_2 COOLING (TET=1473 K)

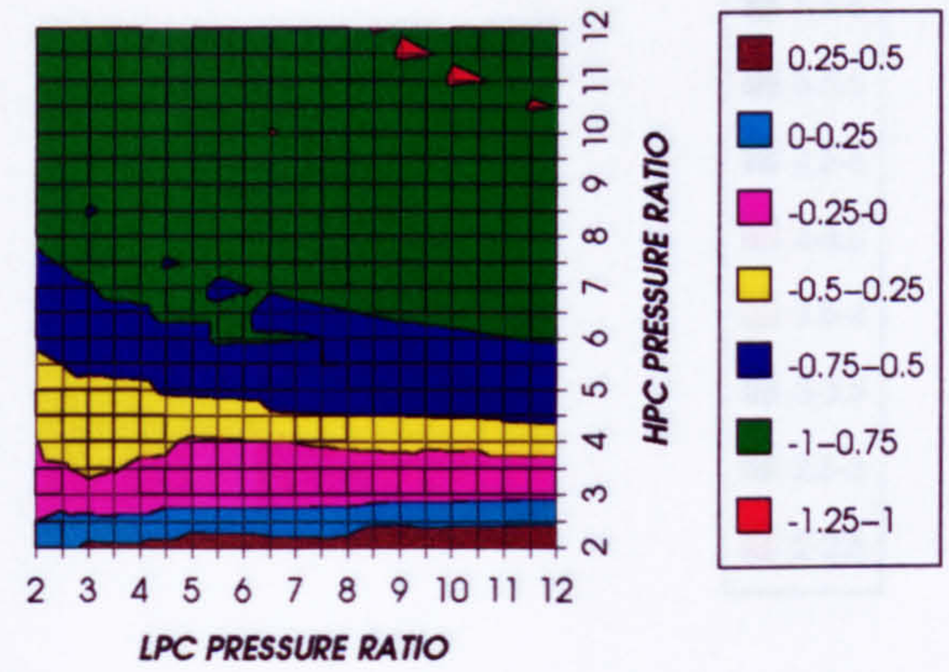

Figure 13. Decrease in LPT relative cooling flow
Difference between precooling and standard

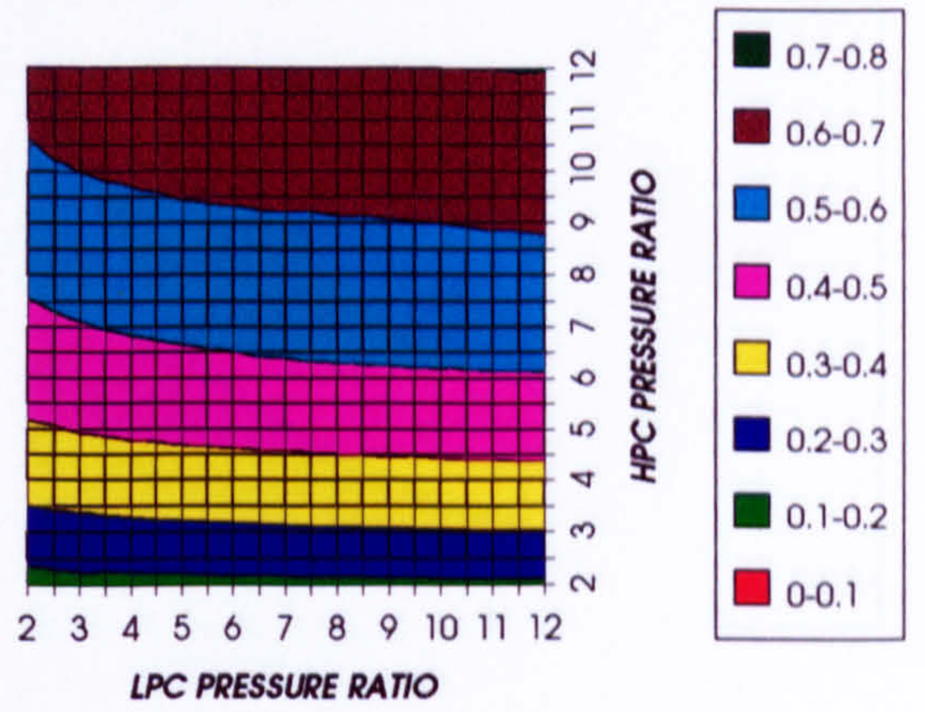

Figure 14. Increase in LPT number of stages
Difference between precooling and standard

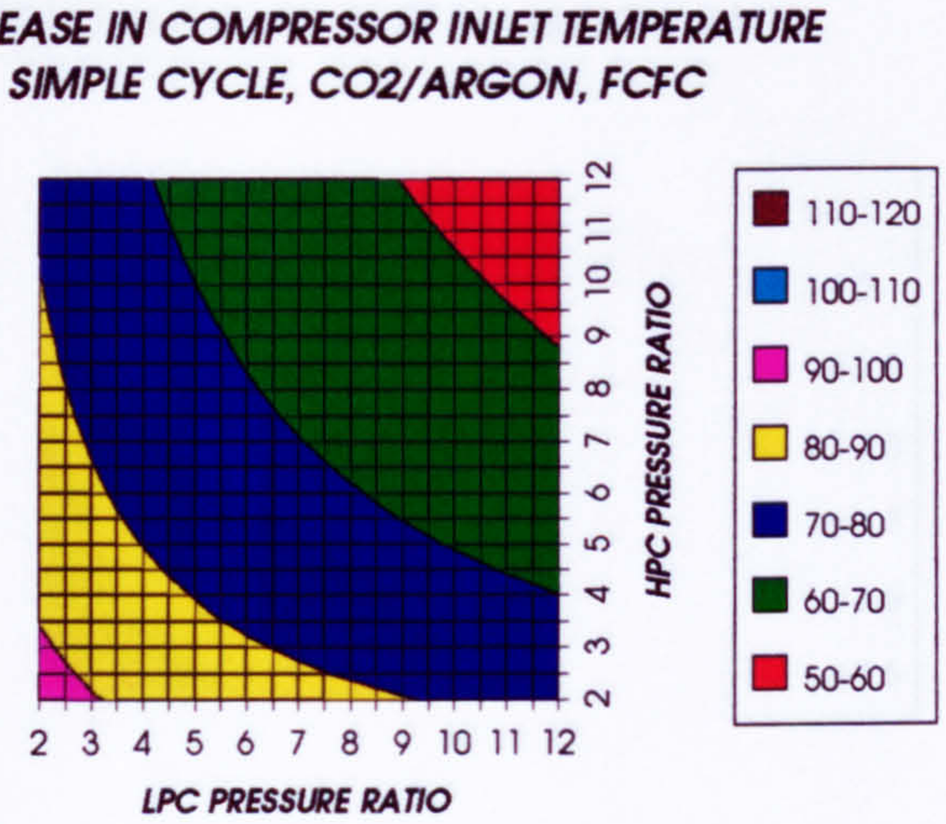

Figure 15. Decrease in compressor inlet temperature
Difference between precooling and standard

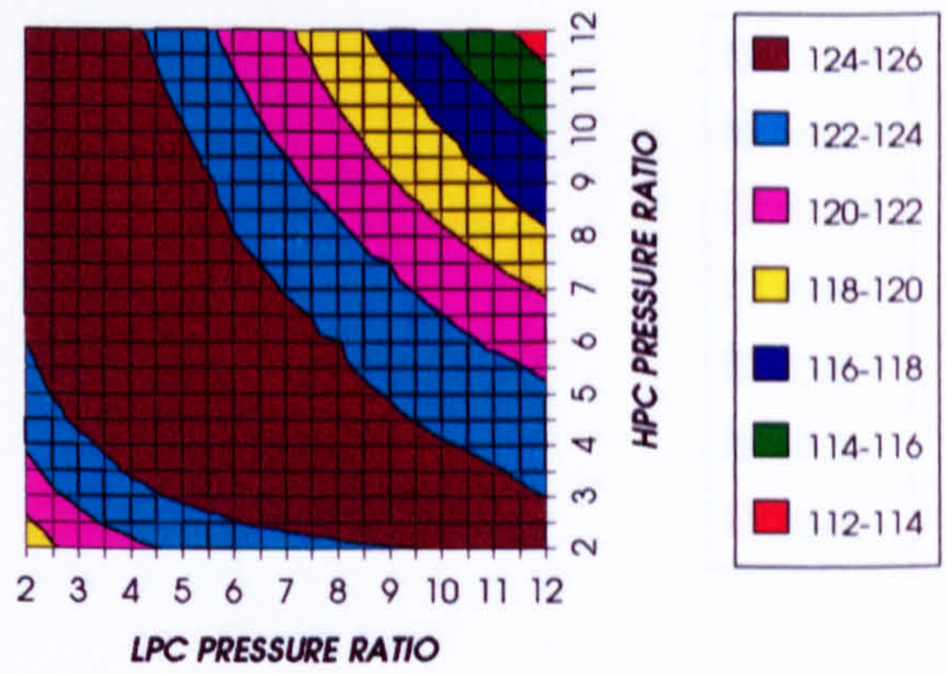

Figure 16. Decrease in compressor outlet temperature
Difference between precooling and standard

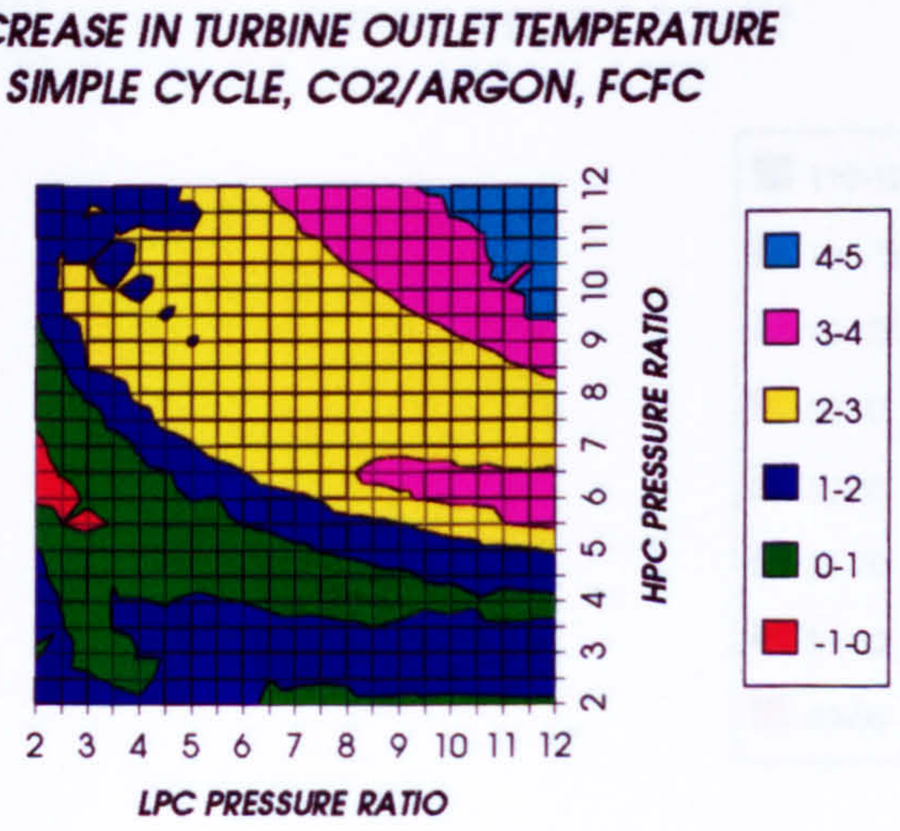

Figure 17. Increase in turbine exit temperature
Difference between precooling and standard

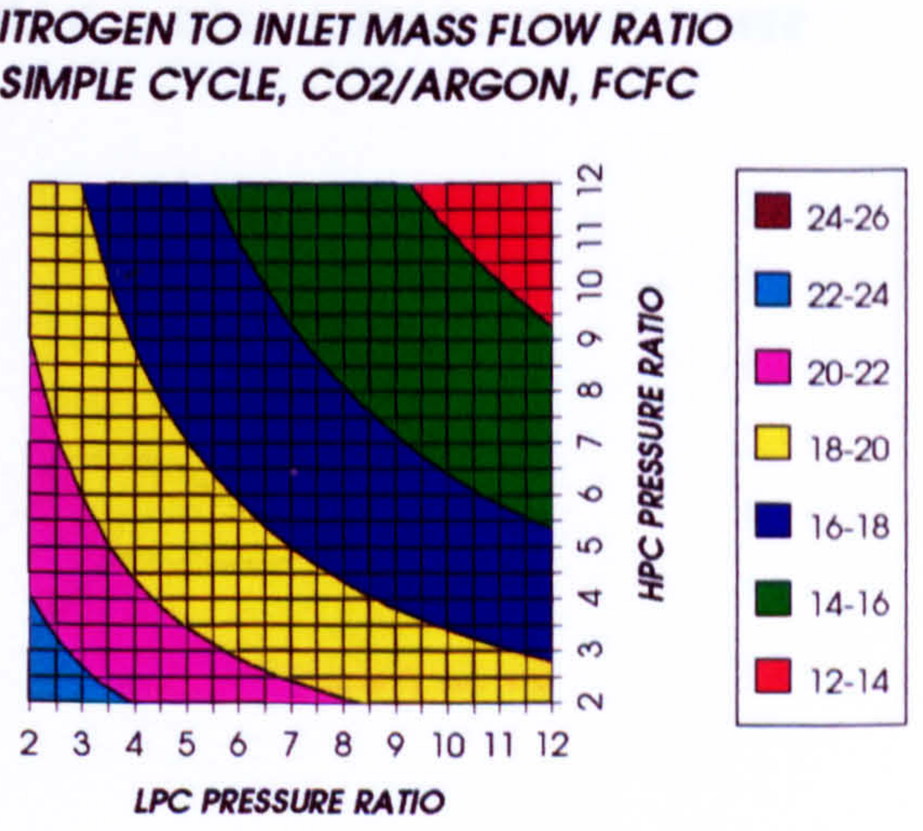

Figure 18. Nitrogen to inlet mass flow ratio for the standard case

EFFECT OF THE CRYOGENIC PRECOOLING & NGVs N_2 COOLING (TET=1473 K)

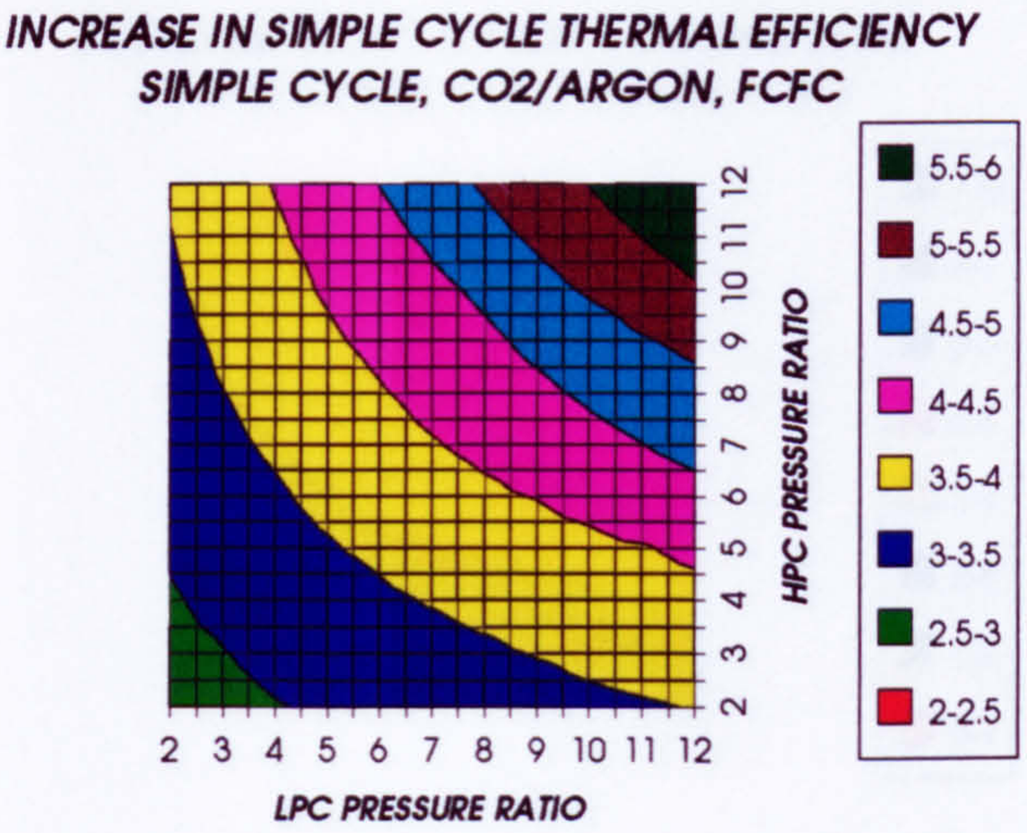

Figure 19. Increase in simple cycle thermal efficiency
Difference between precooling + NGV cool and standard

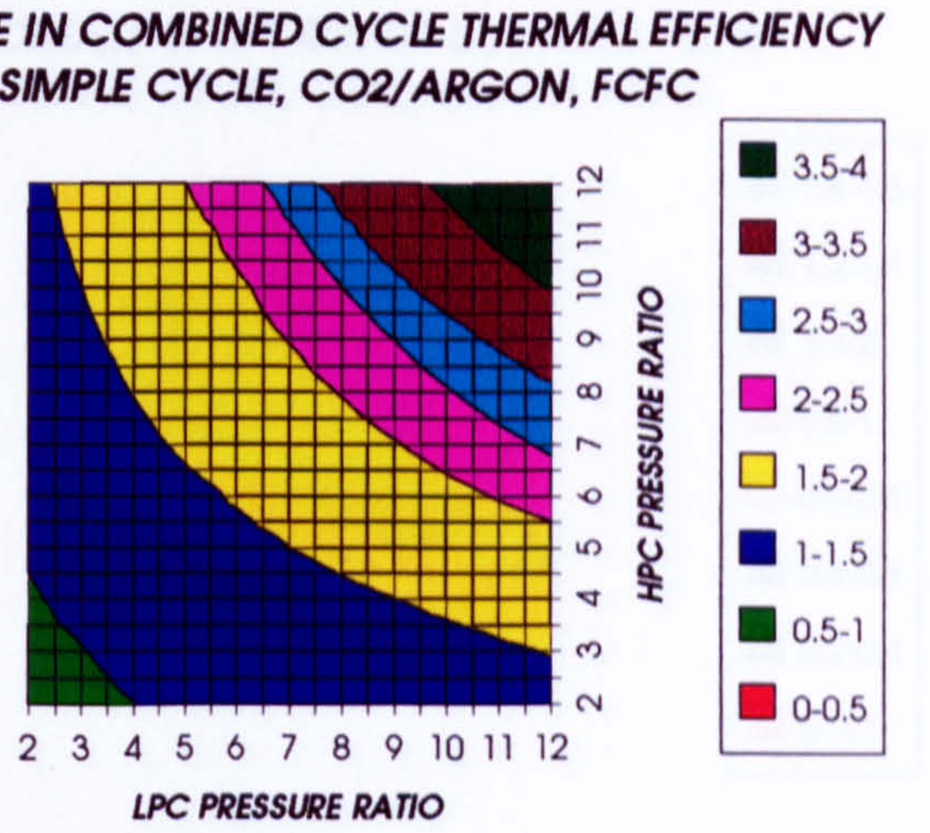

Figure 20. Increase in combined cycle thermal efficiency
Difference between precooling+ NGV cool and standard

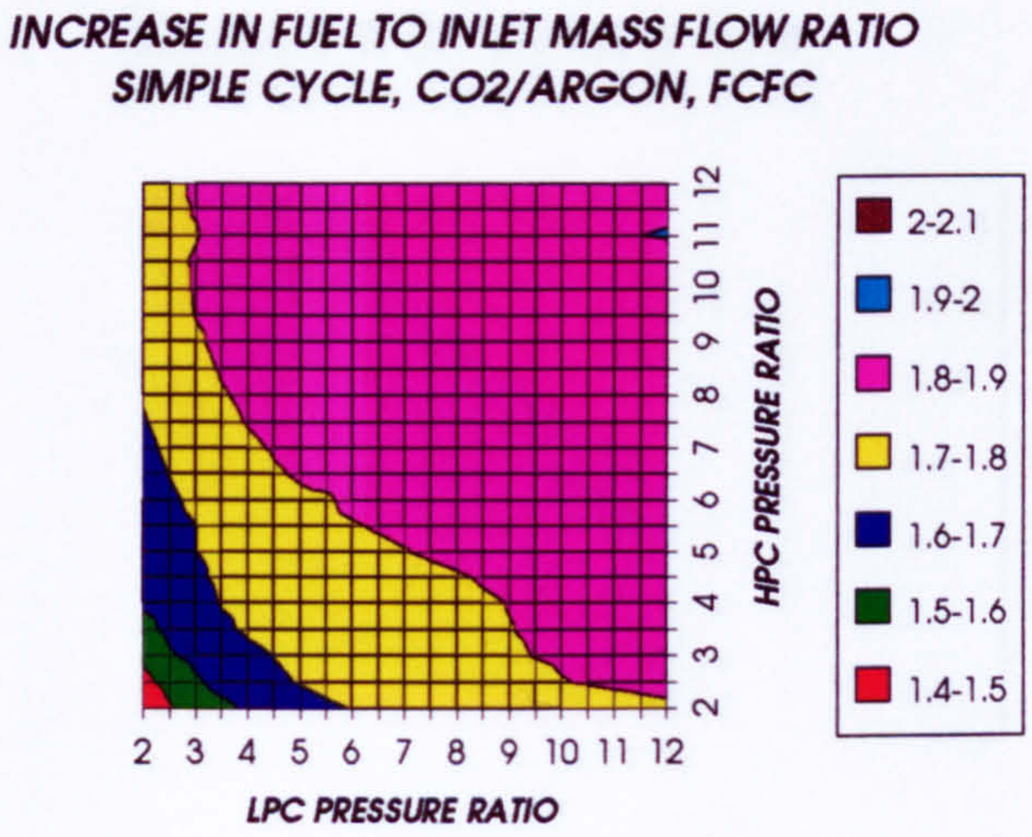

Figure 21. Increase in fuel to inlet mass flow ratio
Difference between precooling+ NGV cool and standard

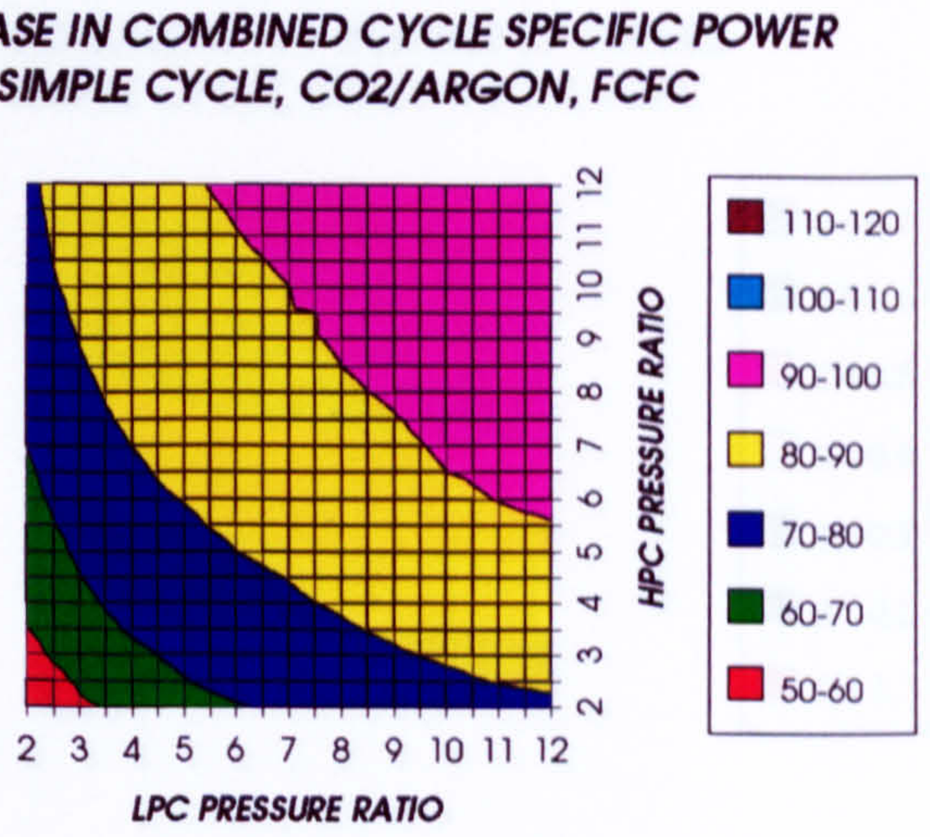

Figure 22. Increase in combined cycle specific power output
Difference between precooling+ NGV cool and standard

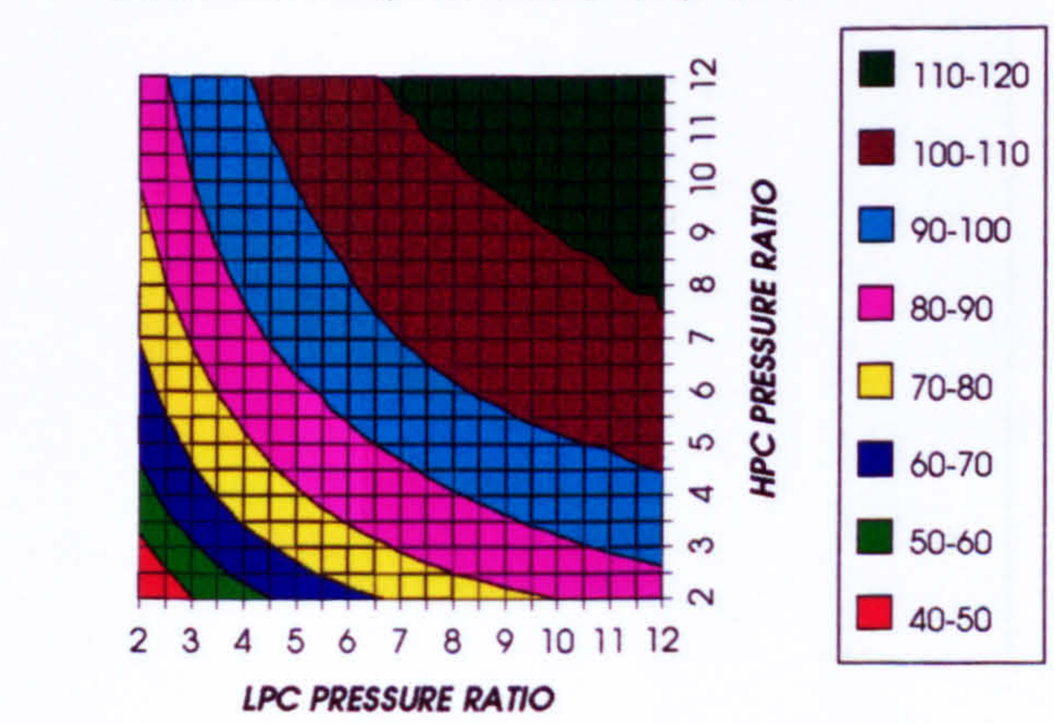

Figure 23. Increase in gas turbine specific power output
Difference between precooling+ NGV cool and standard

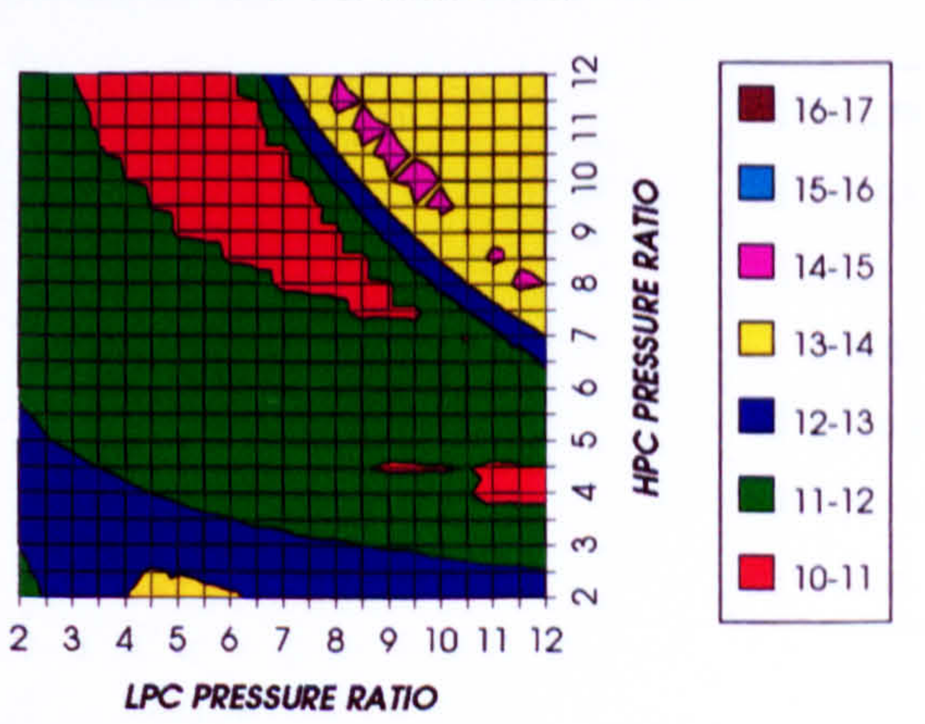

Figure 24. Increase in steam turbine specific power output
Difference between precooling+ NGV cool and standard

EFFECT OF THE CRYOGENIC PRECOOLING & NGVs N_2 COOLING (TET=1473 K)

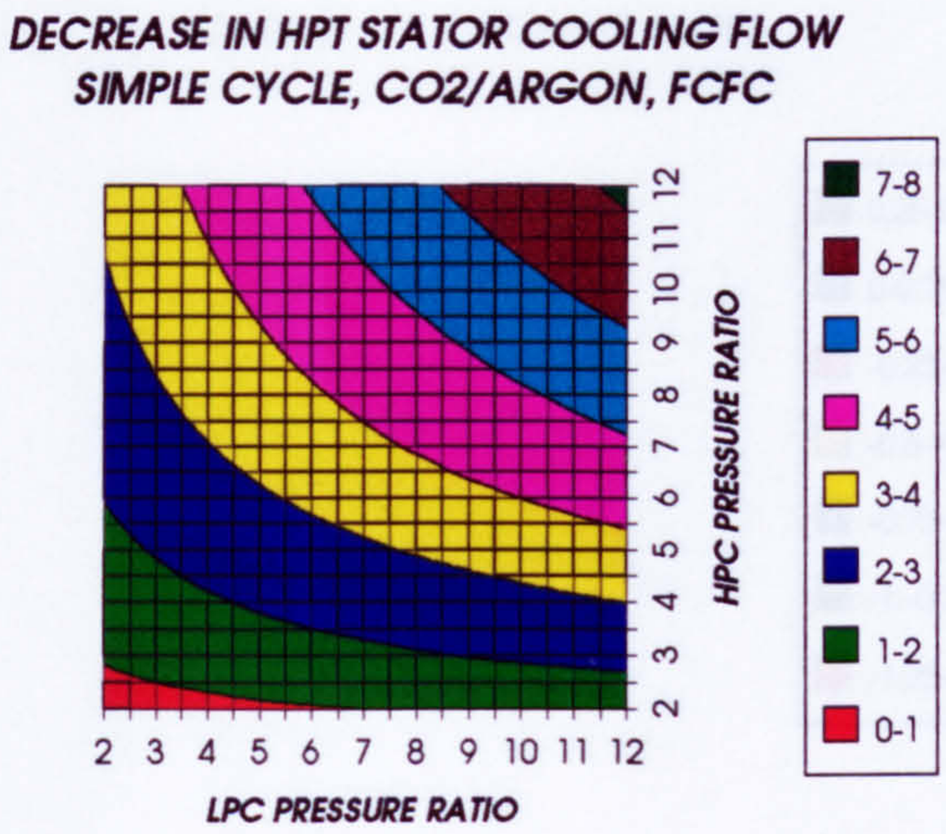

Figure 25. Decrease in HPT stator relative cooling flow.
Difference between precooling + NGV cool and standard

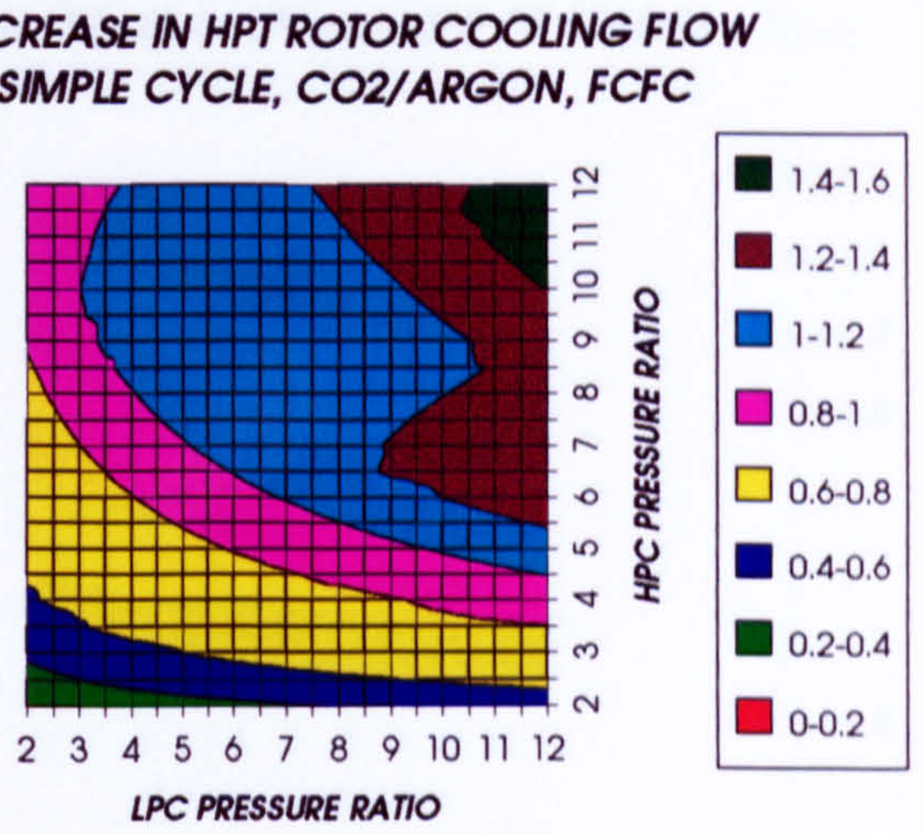

Figure 26. Decrease in HPT rotor relative cooling flow.
Difference between precooling + NGV cool and standard

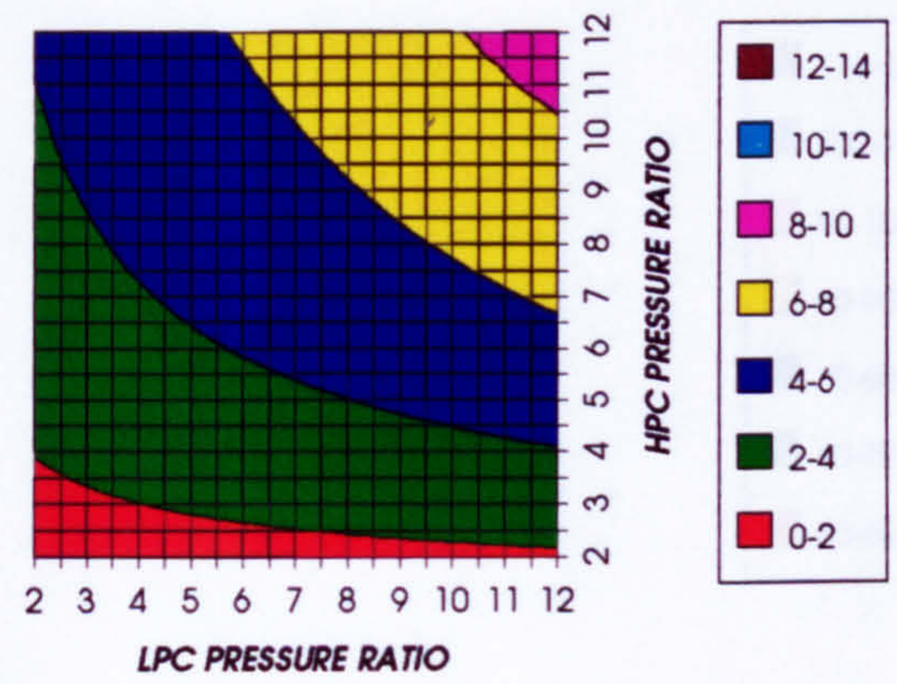

Figure 27. Decrease in HPT relative cooling flow.
Difference between precooling + NGV cool and standard

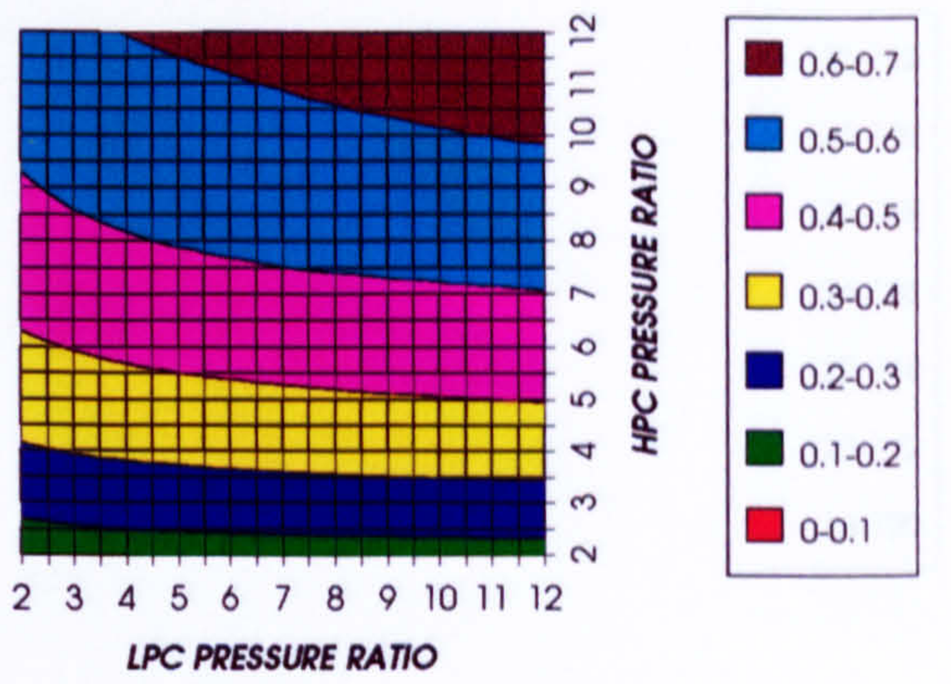

Figure 28. Decrease in HPT number of stages
Difference between precooling + NGV cool and standard

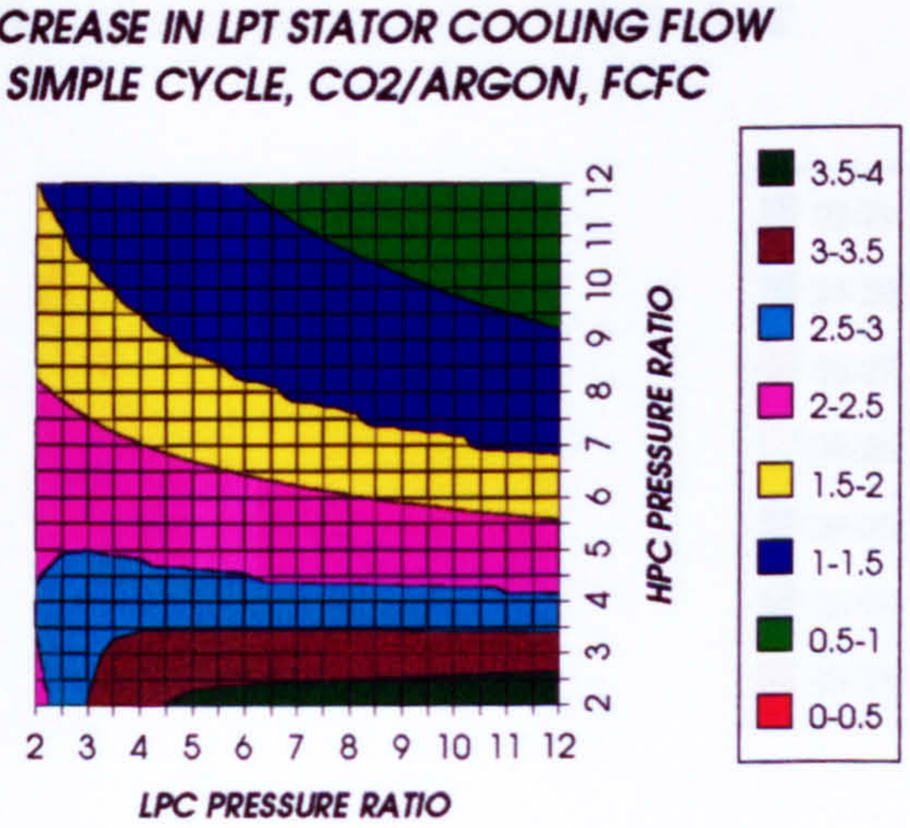

Figure 29. Decrease in LPT stator relative cooling flow.
Difference between precooling + NGV cool and standard

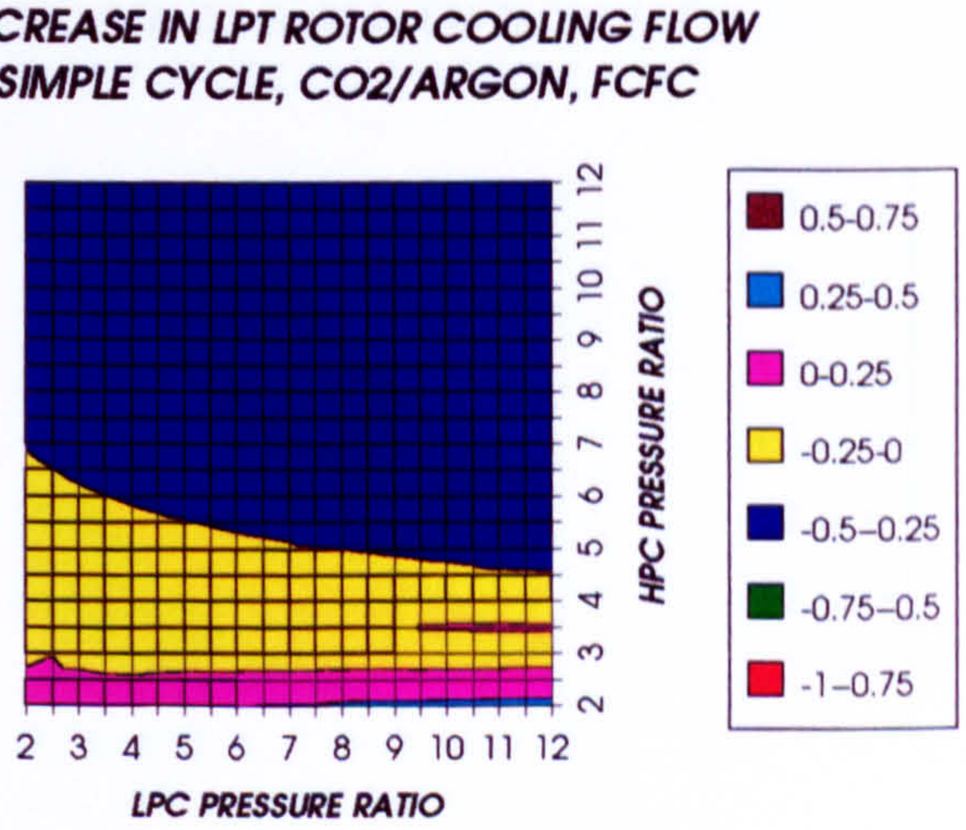

Figure 30. Decrease in LPT rotor relative cooling flow.
Difference between precooling + NGV cool and standard

EFFECT OF THE CRYOGENIC PRECOOLING & NGVs N_2 COOLING (TET=1473 K)

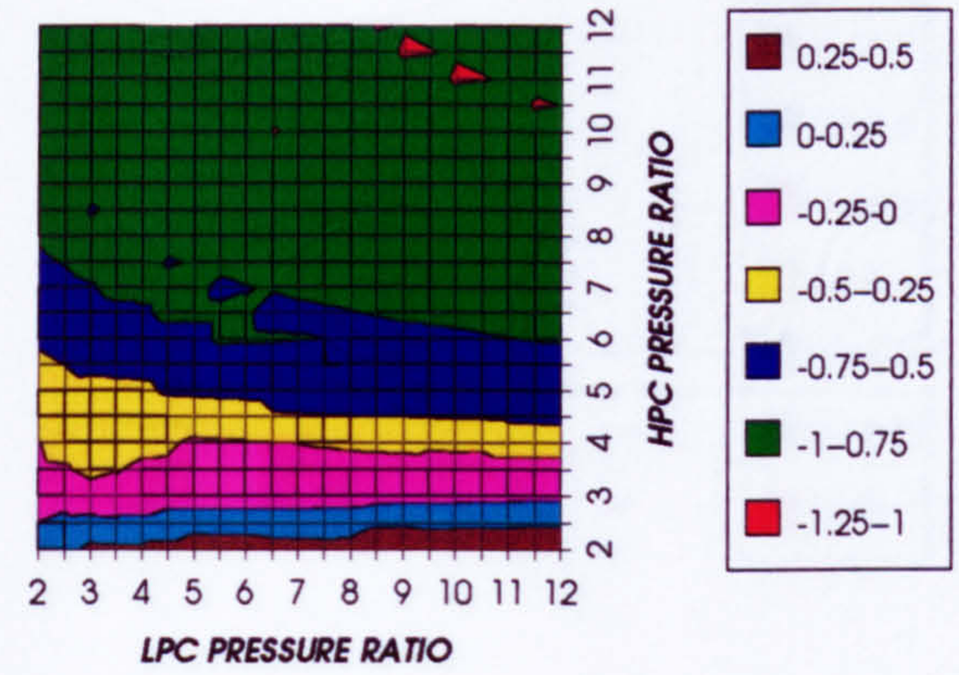

Figure 31. Decrease in LPT relative cooling flow
Difference between precooling +NGV cool and standard

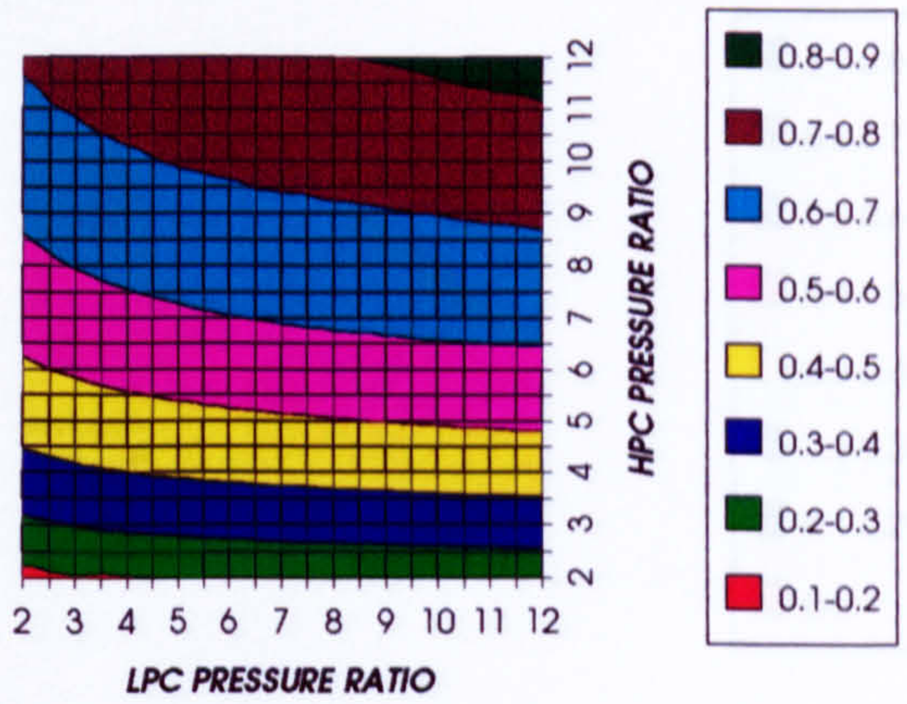

Figure 32. Increase in LPT number of stages
Difference between precooling+NGV cool and standard

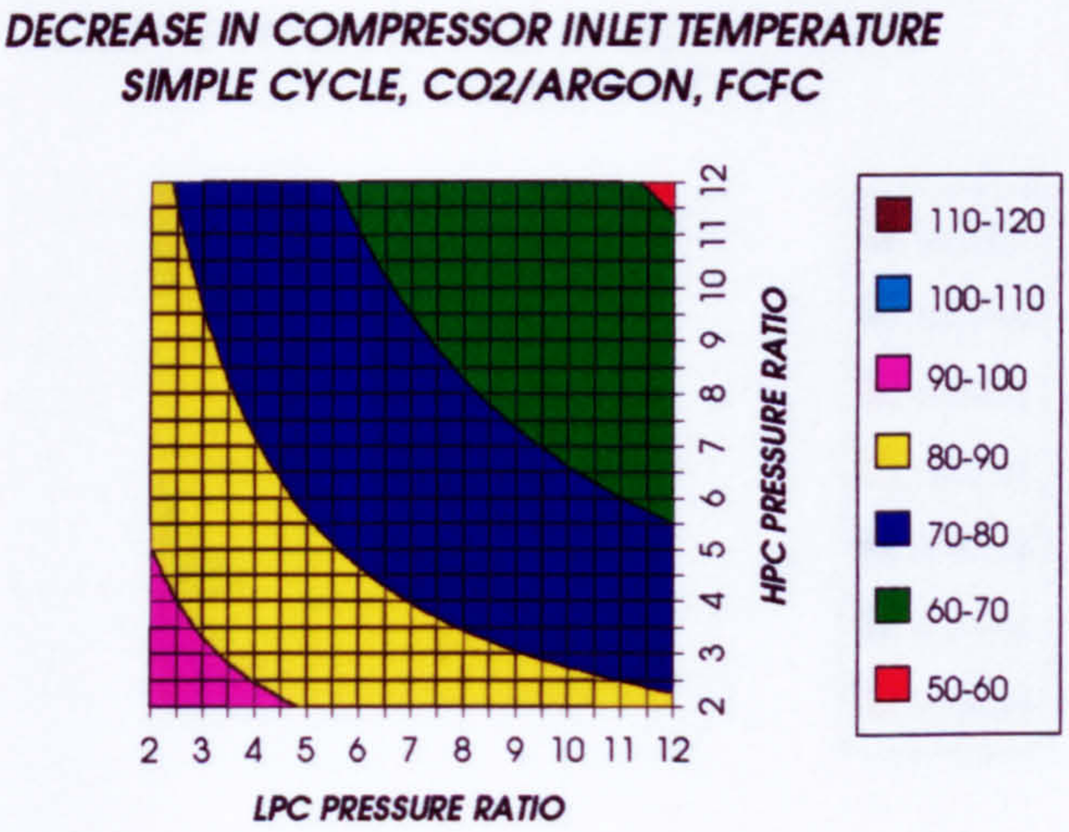

Figure 33. Decrease in compressor inlet temperature
Difference between precooling +NGV cool and standard

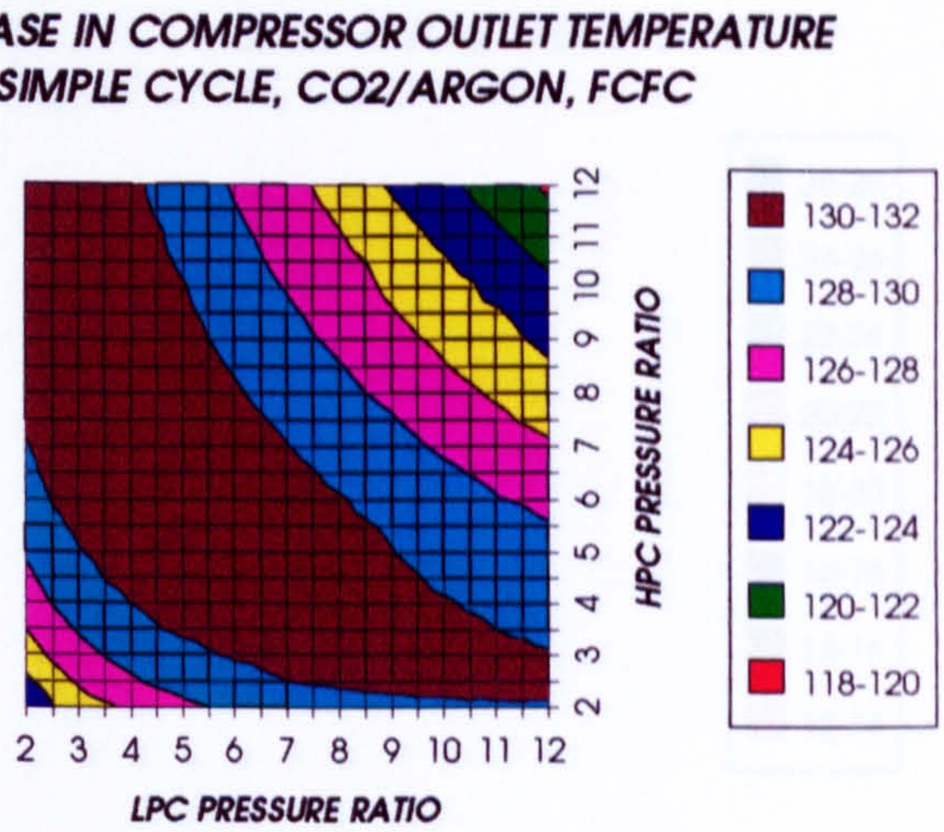

Figure 34. Decrease in compressor outlet temperature
Difference between precooling +NGV cool and standard

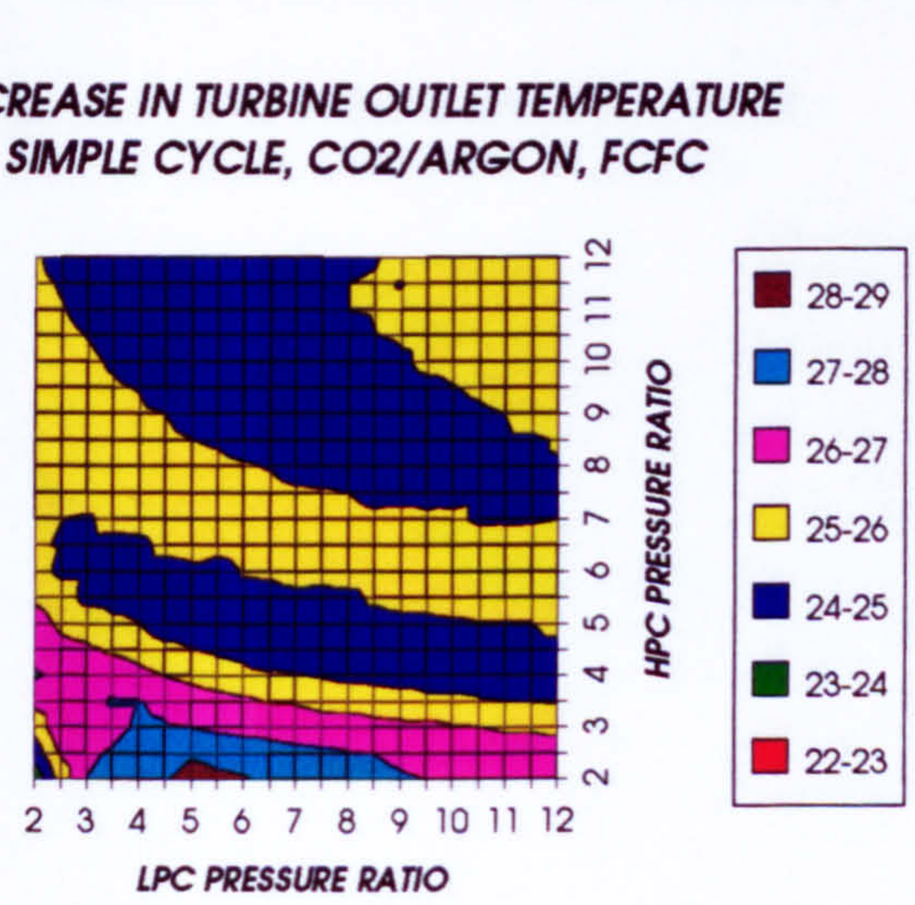

Figure 35. Increase in turbine exit temperature
Difference between precooling +NGV cool and standard

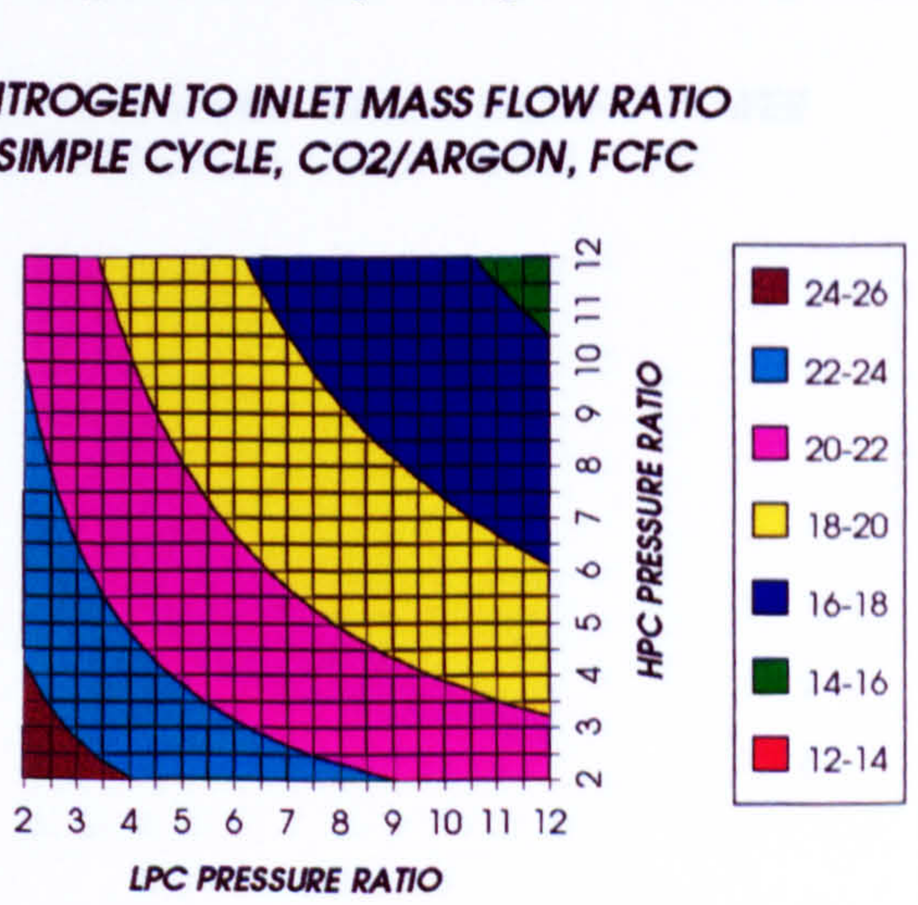

Figure 36. Nitrogen to inlet mass flow ratio for the N_2 cryogenic precooling case

EFFECT OF THE CRYOGENIC PRECOOLING & NGVs N_2 COOLING (TET=1473 K)

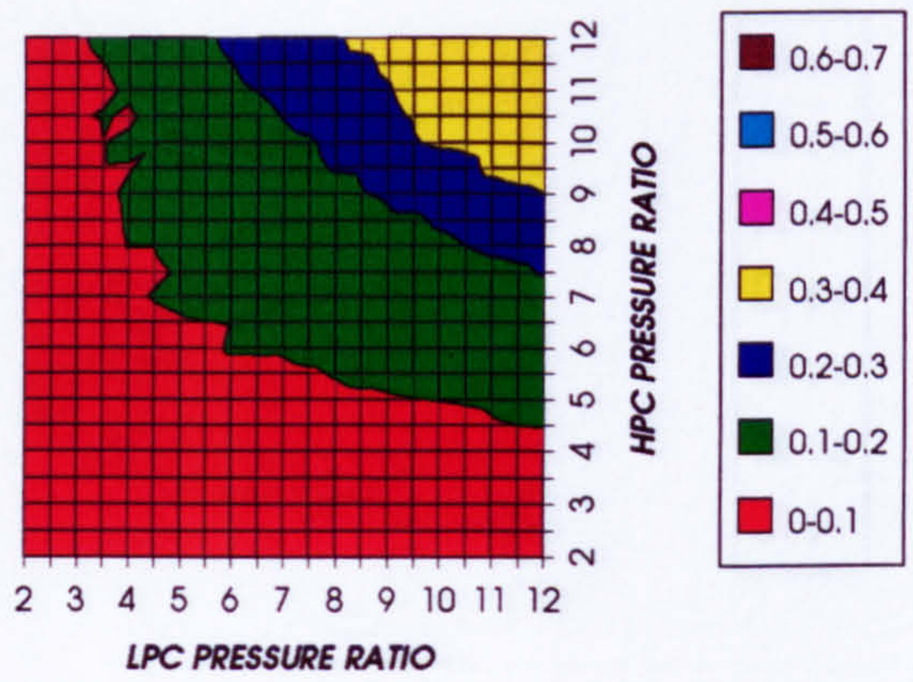

Figure 37. Increase in simple cycle thermal efficiency
Difference between precooling + NGV cool and precool

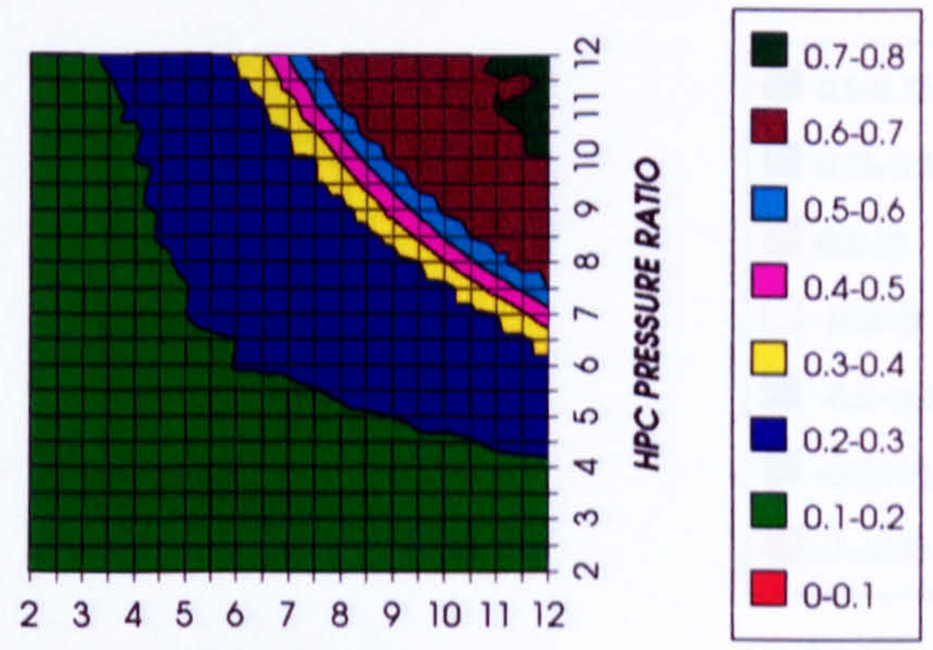

Figure 38. Increase in combined cycle thermal efficiency
Difference between precooling+ NGV cool and precool

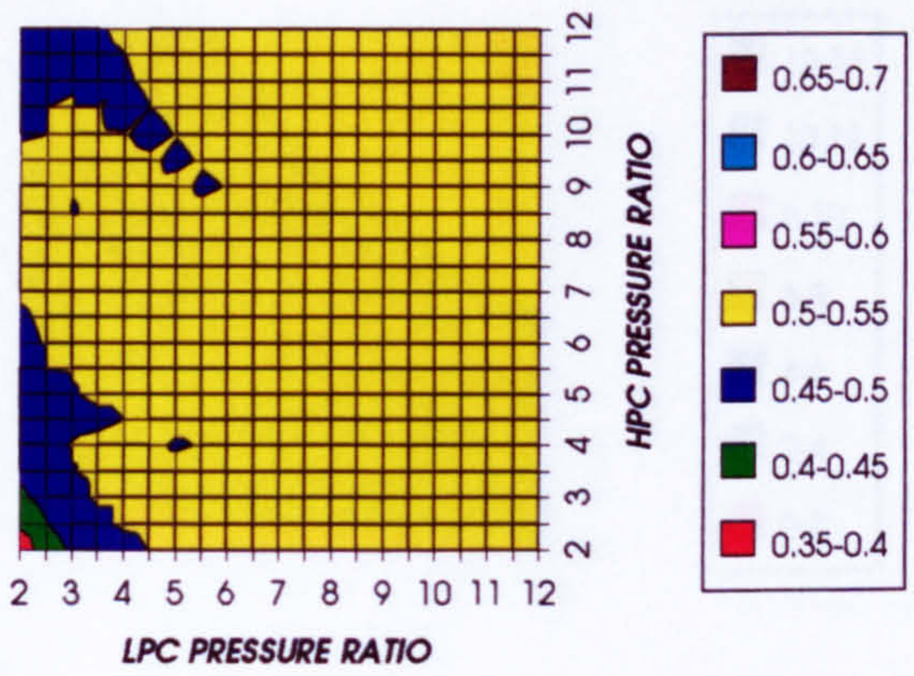

Figure 39. Increase in fuel to inlet mass flow ratio
Difference between precooling+ NGV cool and precool

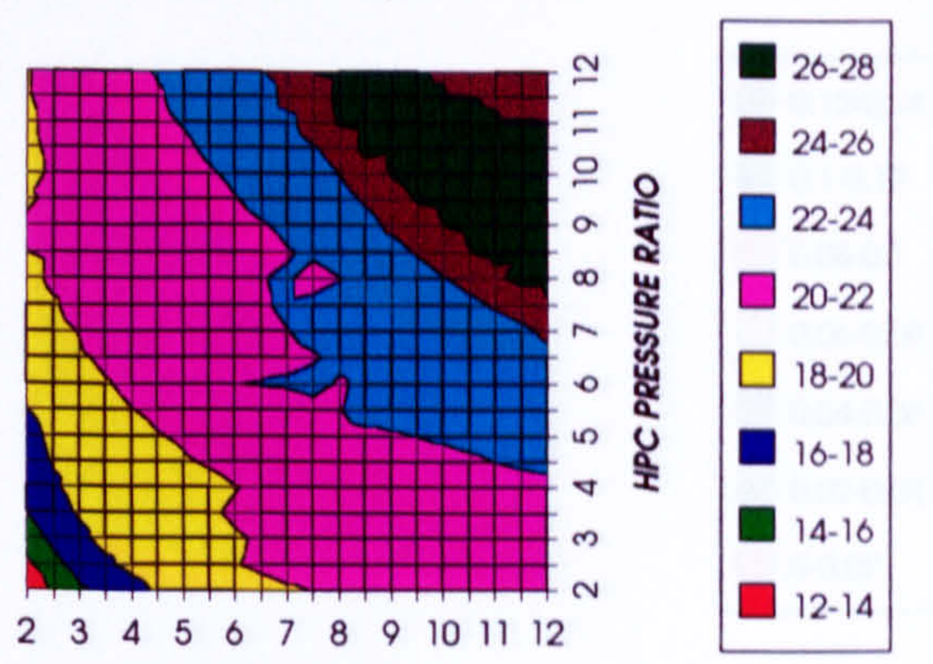

Figure 40. Increase in combined cycle specific power output
Difference between precooling+ NGV cool and precool

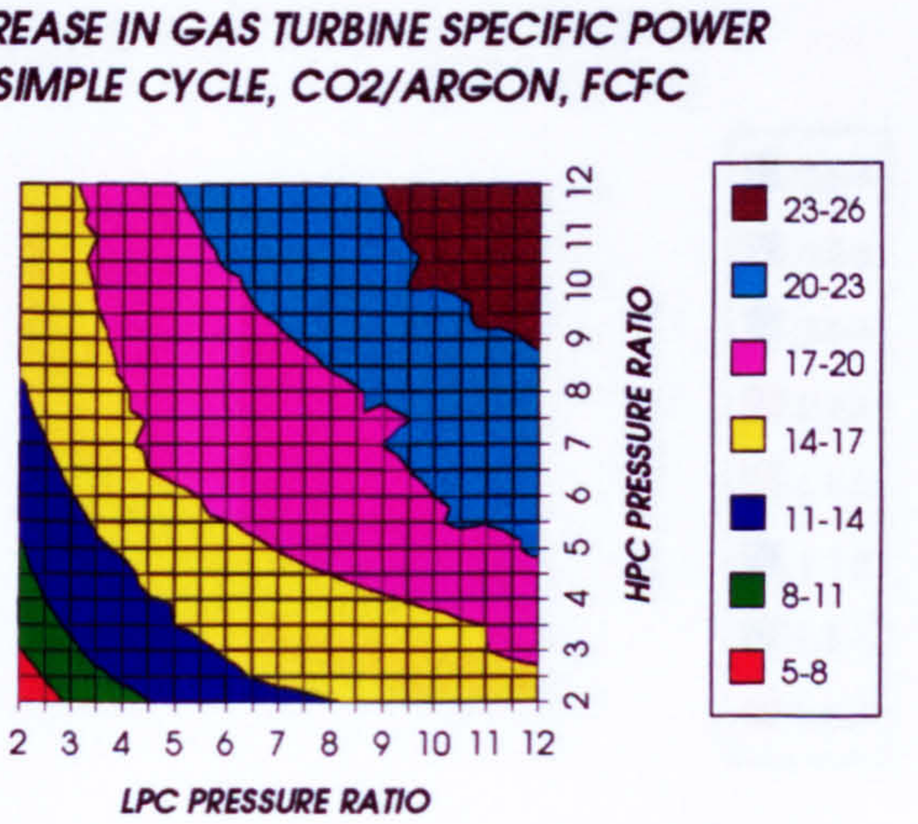

Figure 41. Increase in gas turbine specific power output
Difference between precooling+ NGV cool and precool

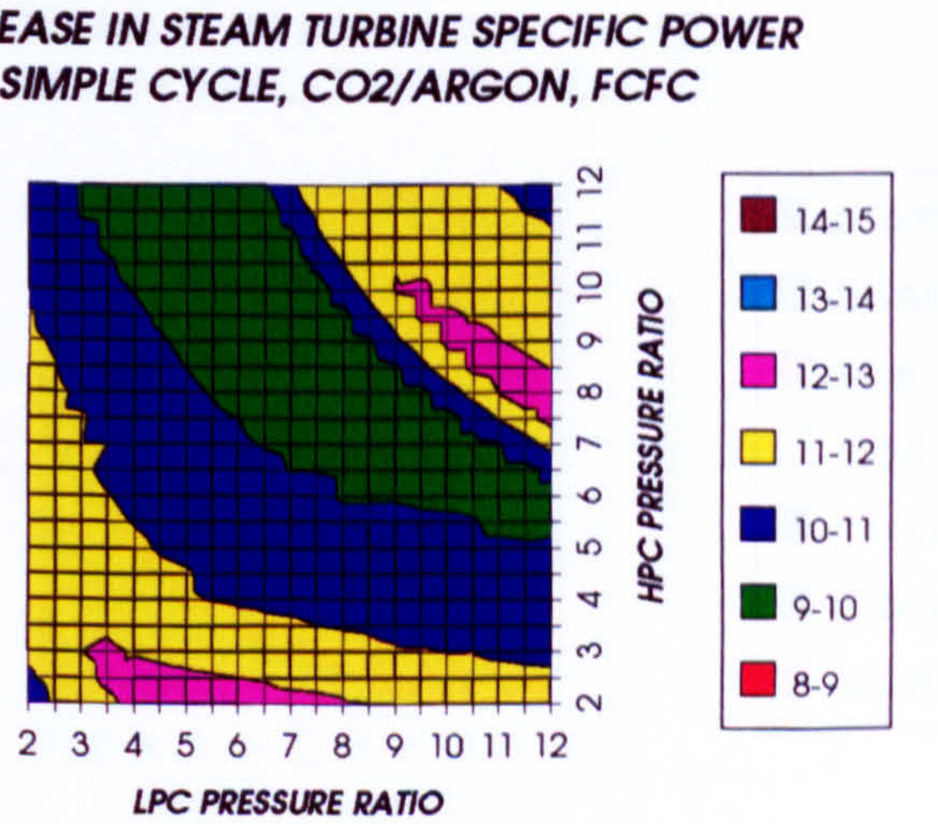

Figure 42. Increase in steam turbine specific power output
Difference between precooling+ NGV cool and precool

EFFECT OF THE CRYOGENIC PRECOOLING & NGVs N_2 COOLING (TET=1473 K)

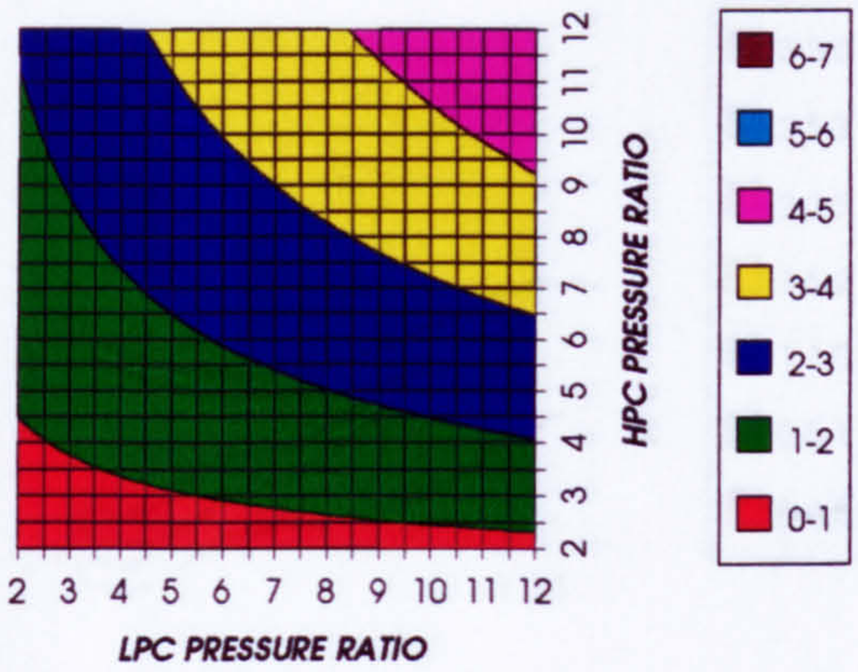

Figure 43. Decrease in HPT stator relative cooling flow
Difference between preecoling + NGV cool and precool

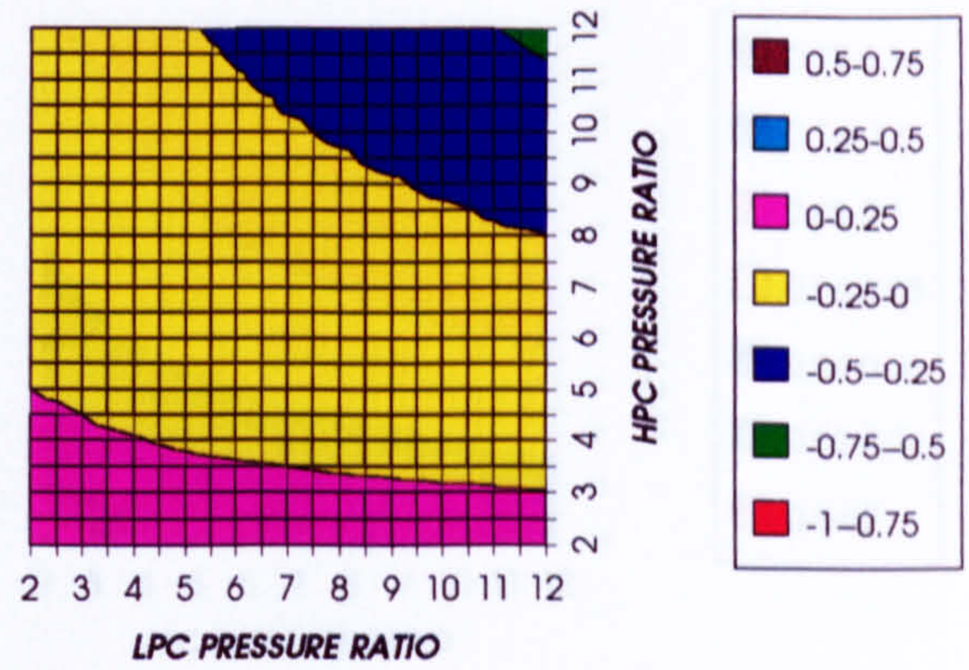

Figure 44. Decrease in HPT rotor relative cooling flow
Difference between preecoling + NGV cool and precool

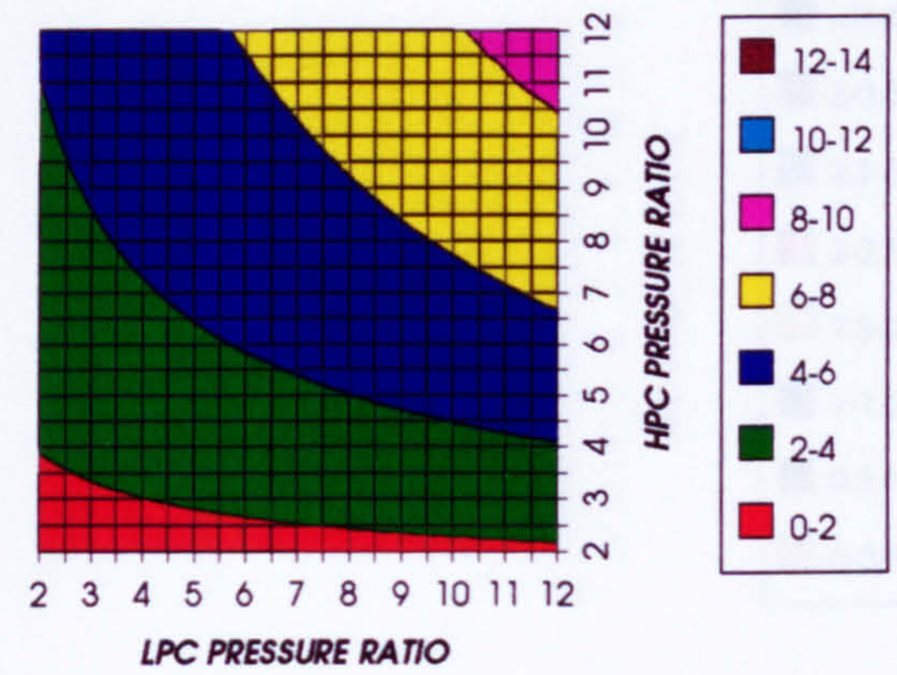

Figure 45. Decrease in HPT relative cooling flow
Difference between preecoling + NGV cool precool

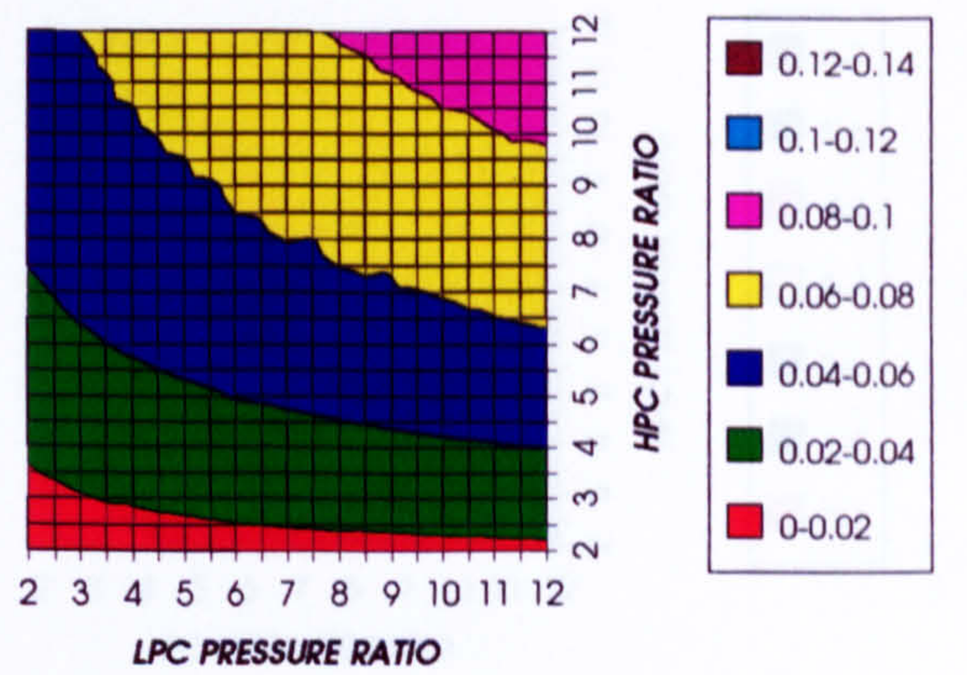

Figure 46. Decrease in HPT number of stages
Difference between preecoling + NGV cool and precool

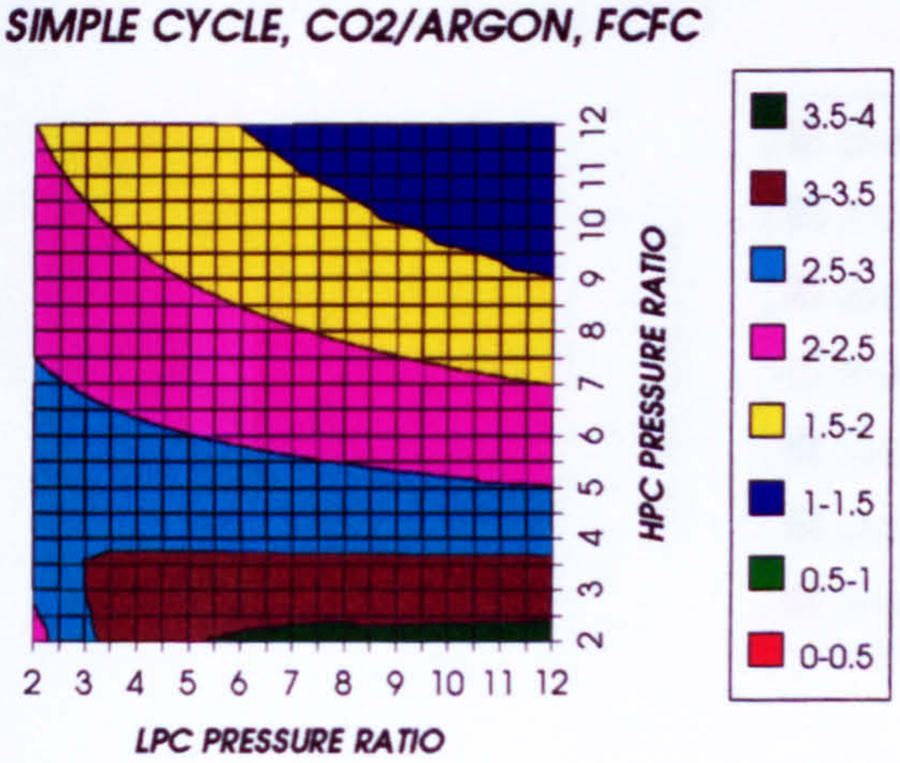

Figure 47. Decrease in LPT stator relative cooling flow.
Difference between preecoling + NGV cool and precool

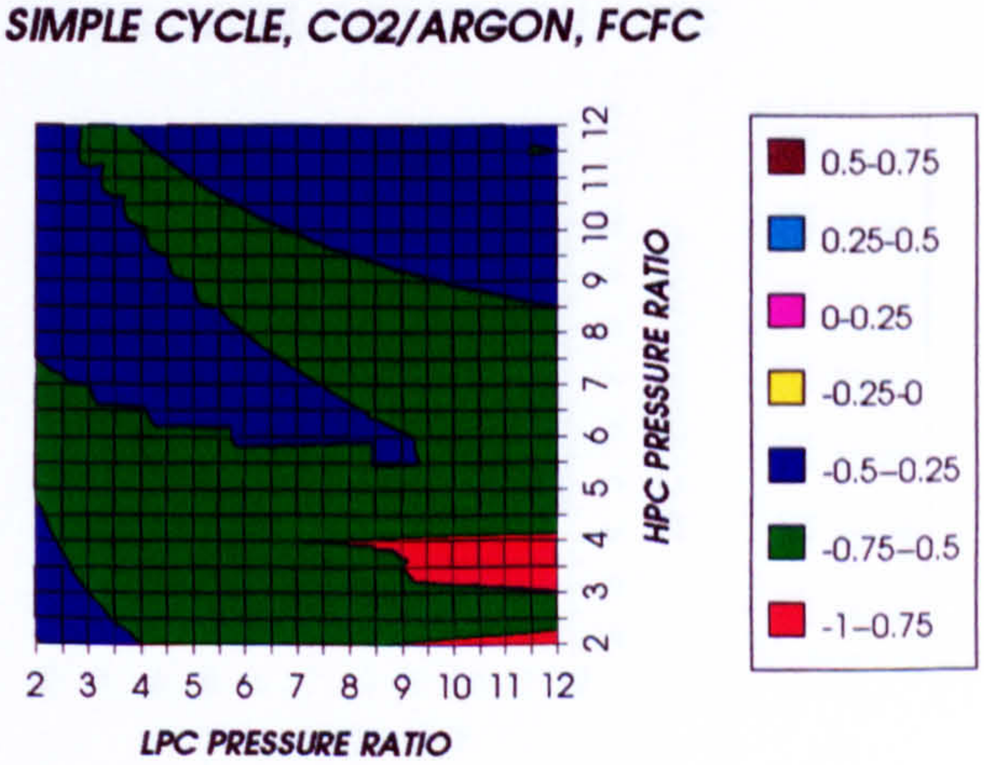

Figure 48. Decrease in LPT rotor relative cooling flow.
Difference between preecoling + NGV cool and precool

EFFECT OF THE CRYOGENIC PRECOOLING & NGVs N_2 COOLING (TET=1473 K)

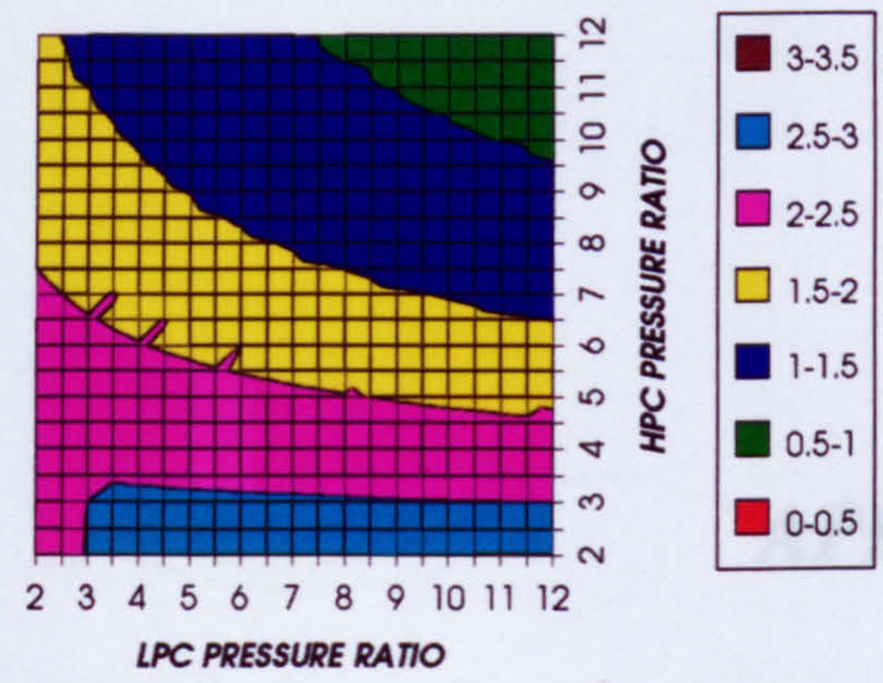

Figure 49. Decrease in LPT relative cooling flow
Difference between precooling + NGV cool and precool

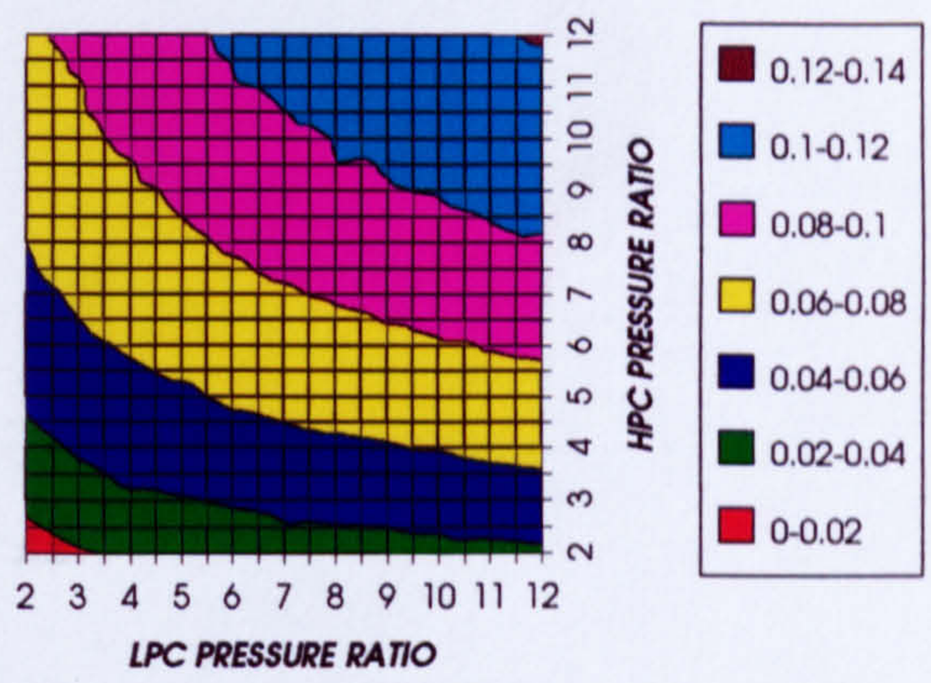

Figure 50. Increase in LPT number of stages
Difference between precooling + NGV cool and precool

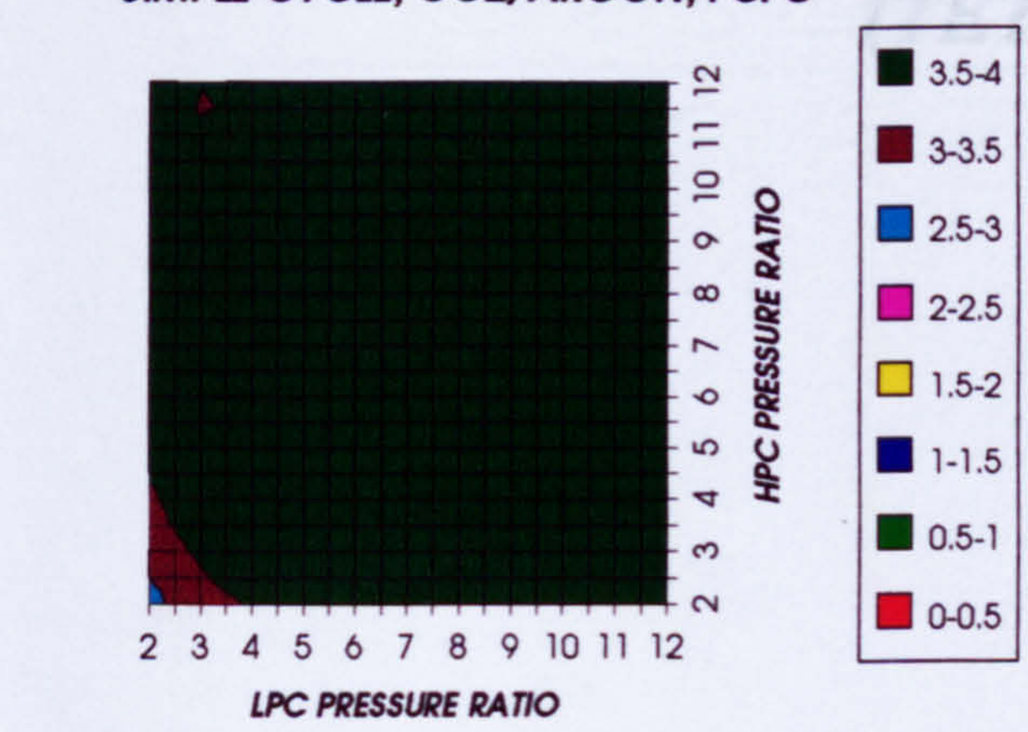

Figure 51. Decrease in compressor inlet temperature
Difference between + NGV cool precooling and precool

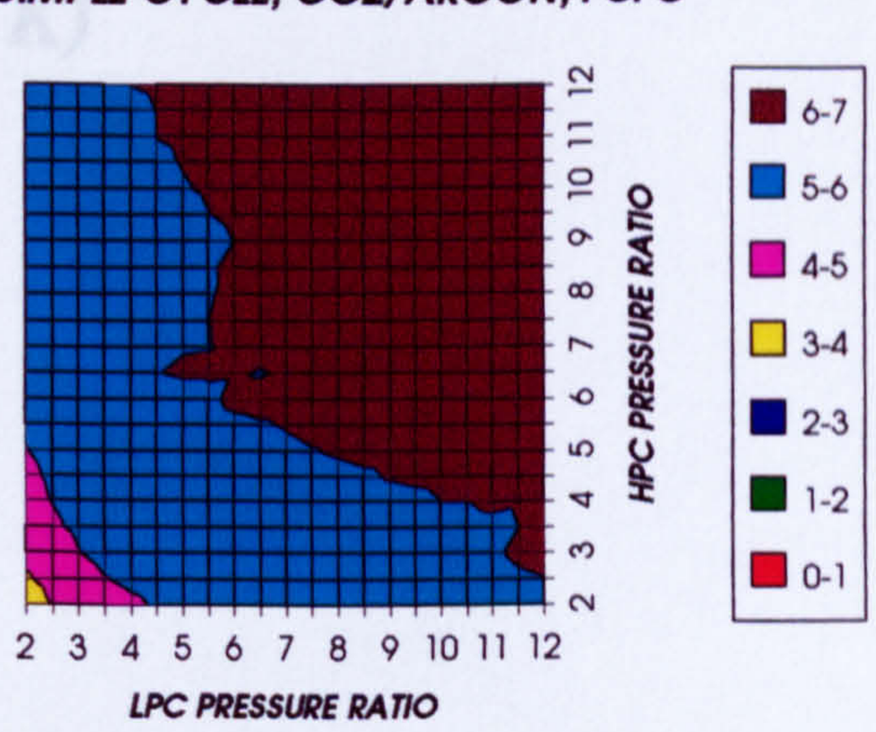

Figure 52. Decrease in compressor outlet temperature
Difference between precooling + NGV cool and precool

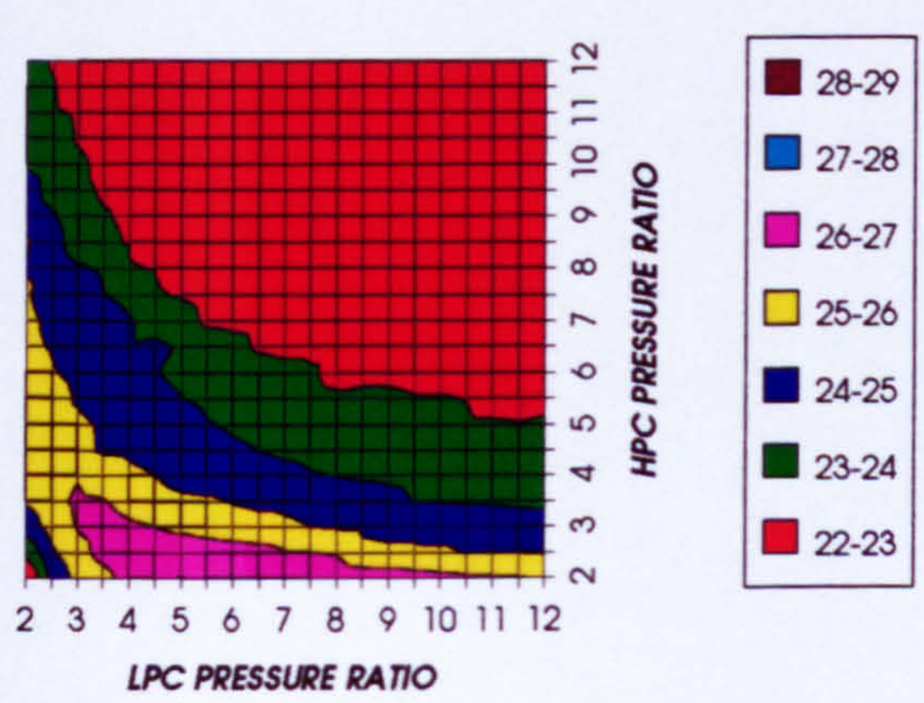

Figure 53. Increase in turbine exit temperature
Difference between precooling + NGV cool and precool

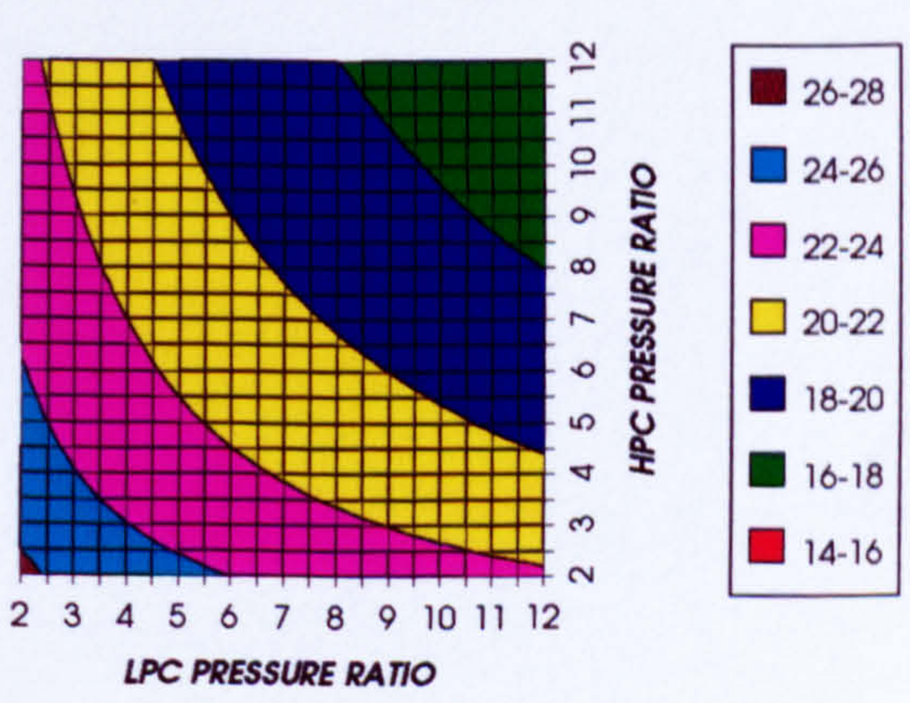

Figure 54. Nitrogen to inlet mass flow ratio for the N_2 cryogenic precooling + N_2 NGV cooling

APPENDIX II

EFFECT OF THE CRYOGENIC PRECOOLING AND NGVs NITROGEN INTERNAL COOLING (TET=1650 K)

EFFECT OF THE CRYOGENIC PRECOOLING & NGVs N_2 COOLING (TET=1650 K)

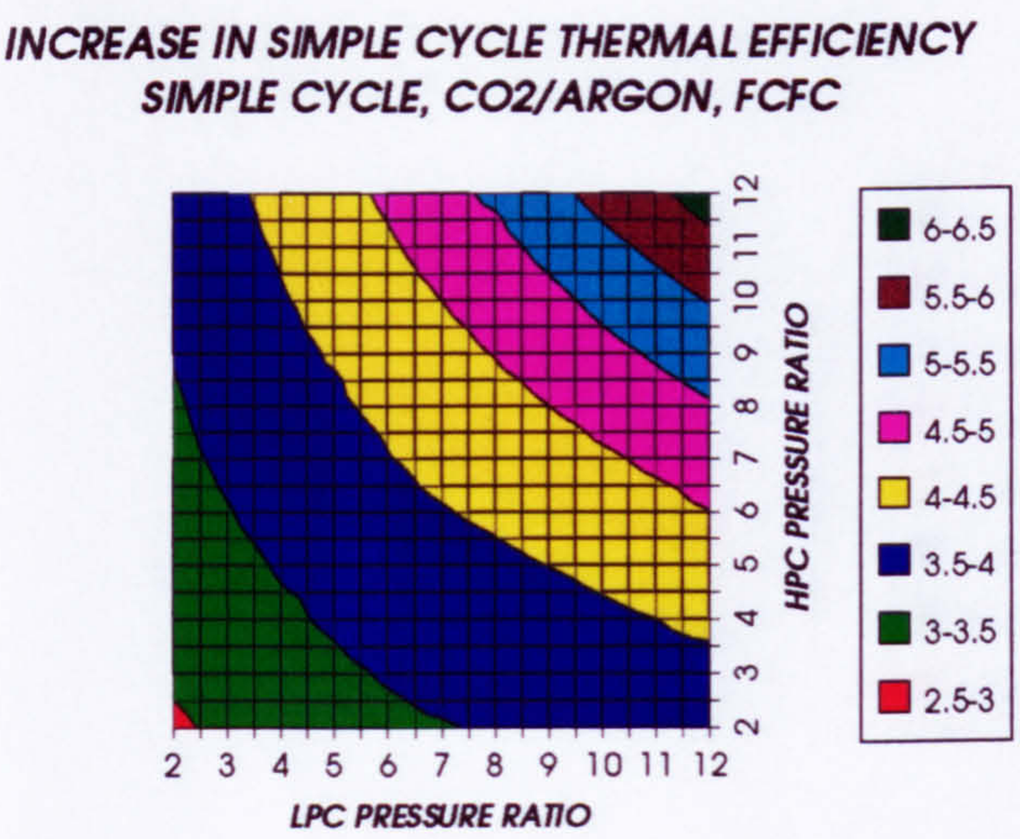

Figure 1. Increase in simple cycle thermal efficiency
Difference between precooling and standard

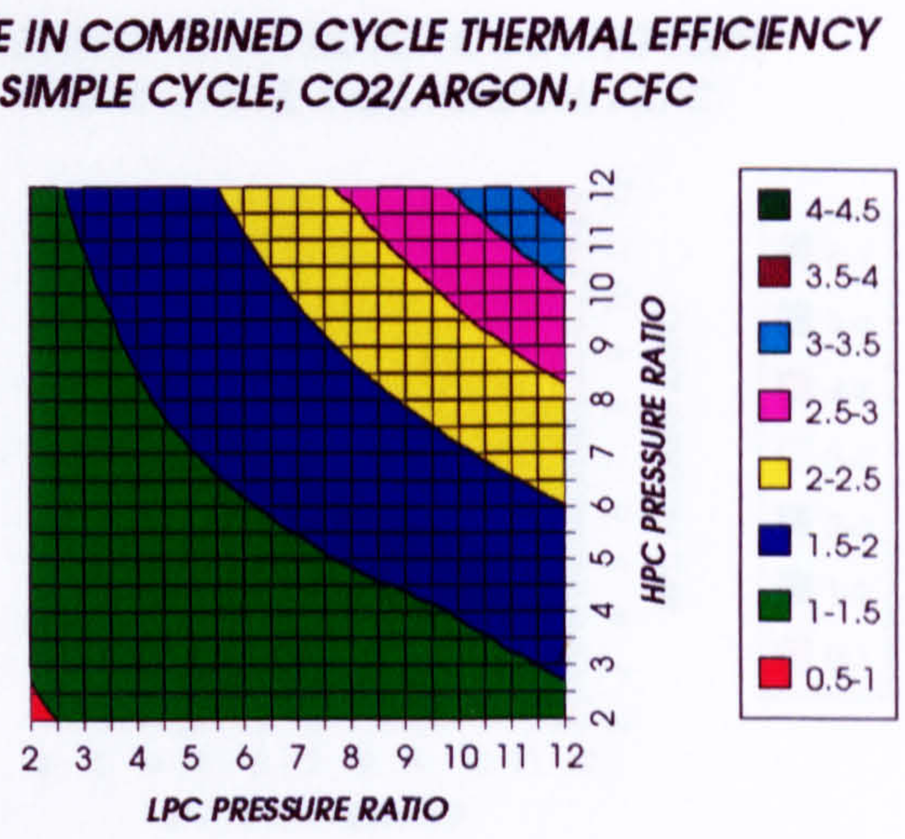

Figure 2. Increase in combined cycle thermal efficiency
Difference between precooling and standard

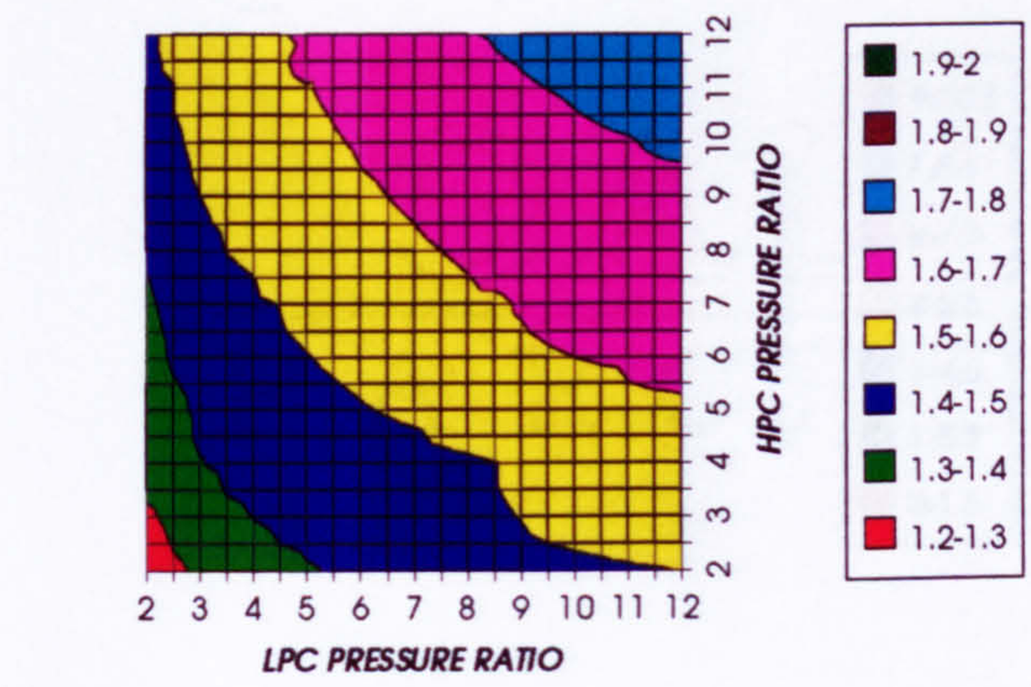

Figure 3. Increase in fuel to inlet mass flow ratio
Difference between precooling and standard

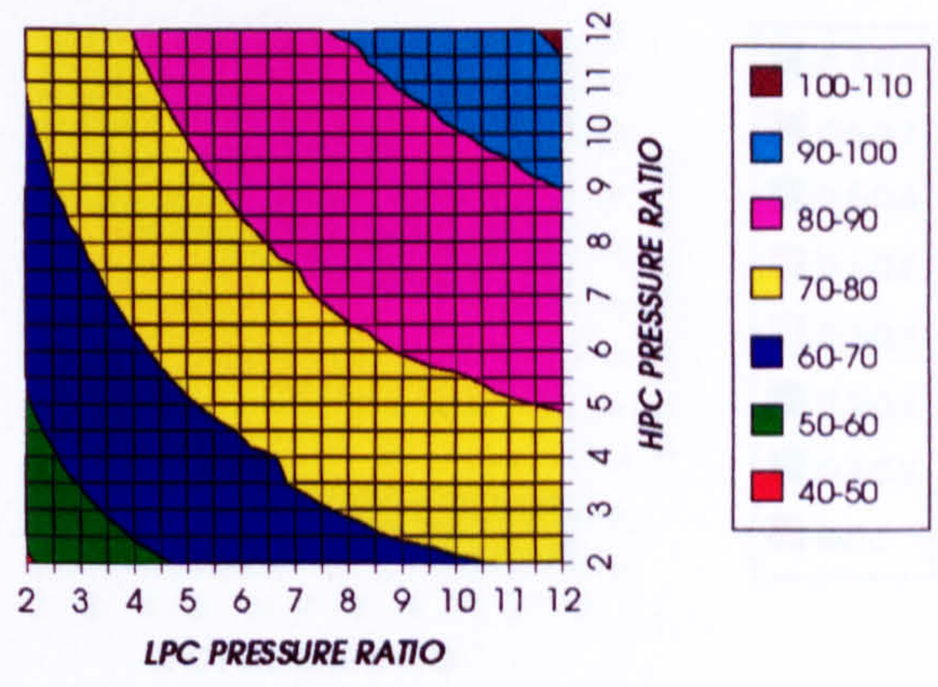

Figure 4. Increase in combined cycle specific power output
Difference between precooling and standard

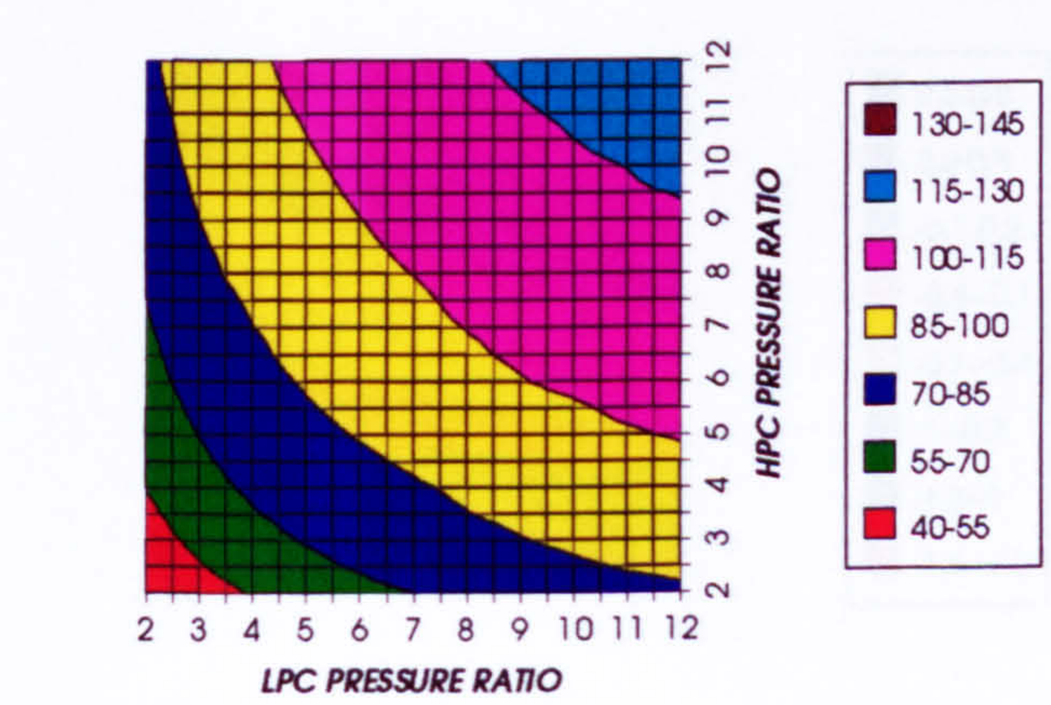

Figure 5. Increase in gas turbine specific power output
Difference between precooling and standard

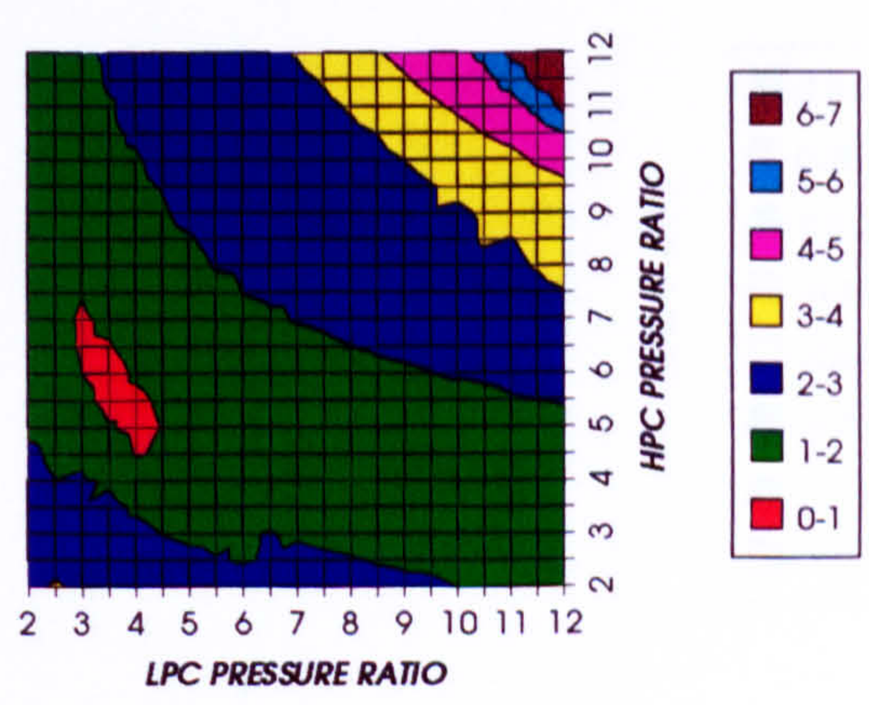

Figure 6. Increase in steam turbine specific power output
Difference between precooling and standard

EFFECT OF THE CRYOGENIC PRECOOLING & NGVs N_2 COOLING (TET=1650 K)

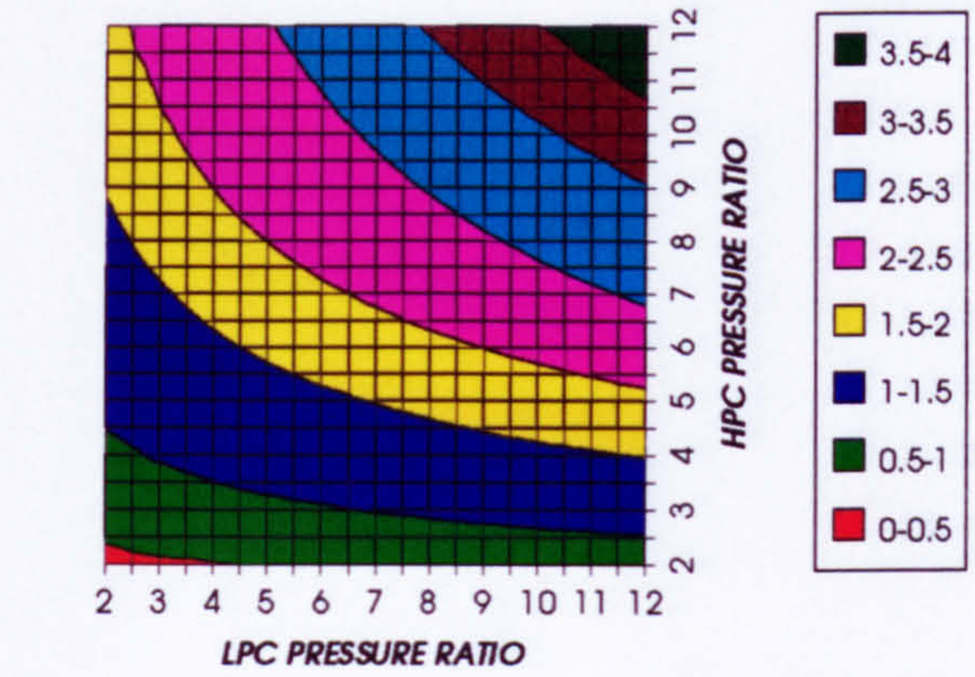

Figure 7. Decrease in HPT stator relative cooling flow
Difference between precooling and standard

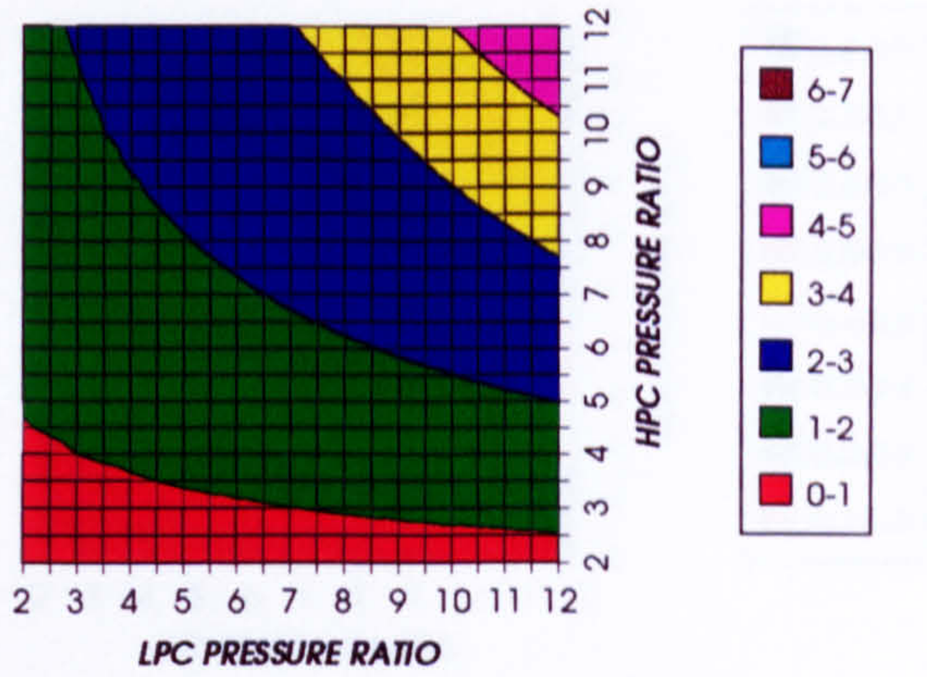

Figure 8. Decrease in HPT rotor relative cooling flow
Difference between precooling and standard

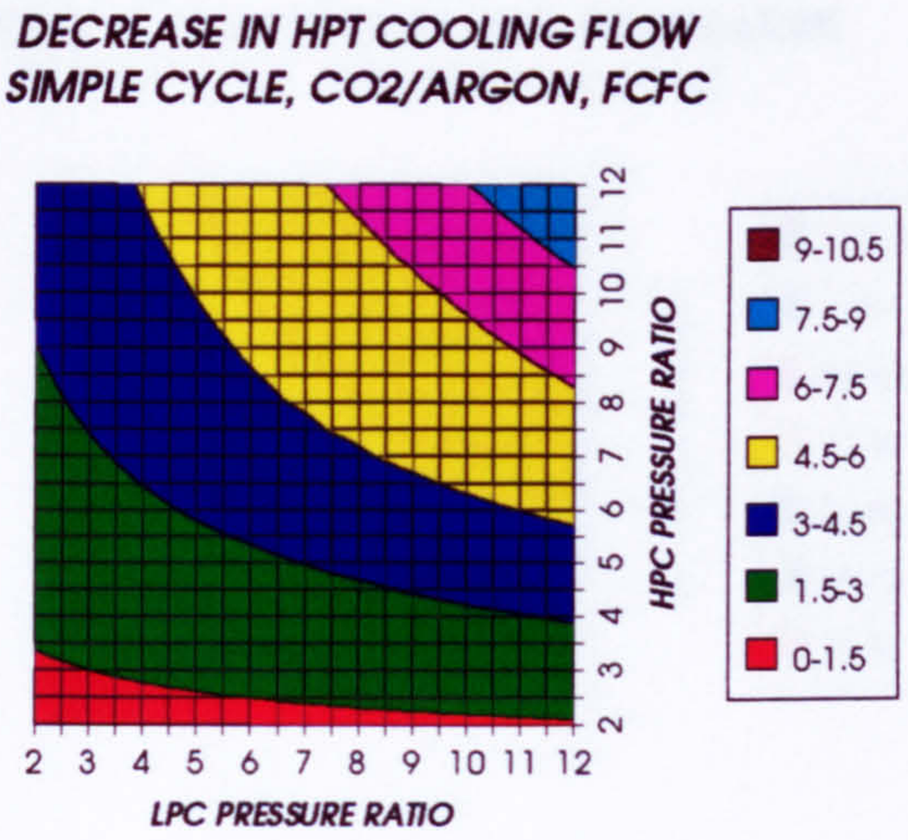

Figure 9. Decrease in HPT relative cooling flow
Difference between precooling and standard

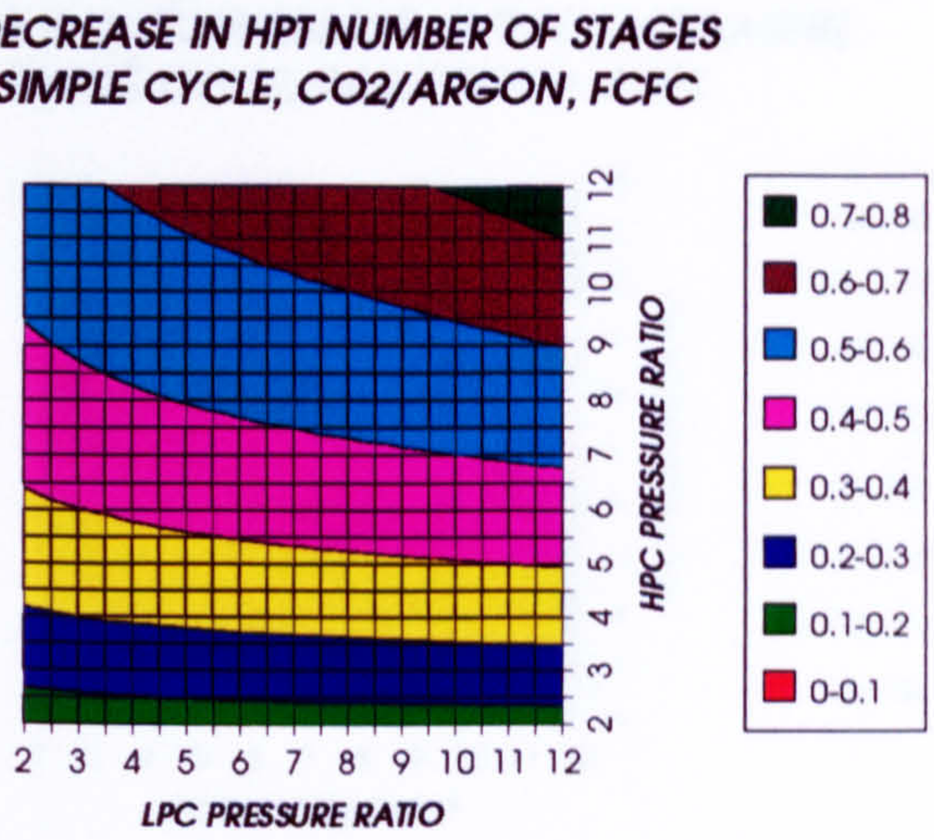

Figure 10. Decrease in HPT number of stages
Difference between precooling and standard

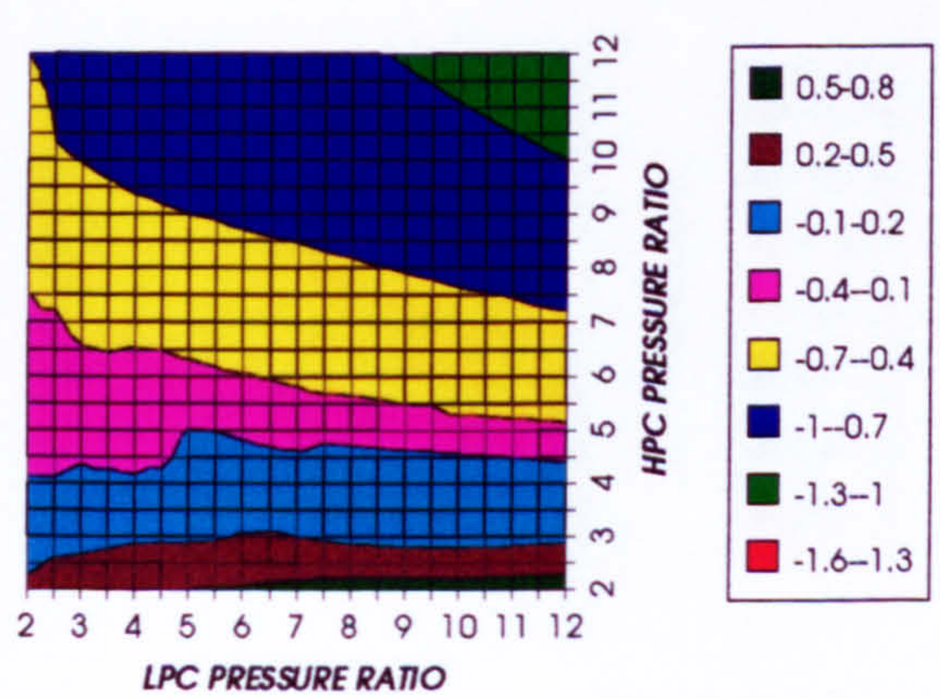

Figure 11. Decrease in LPT stator relative cooling flow
Difference between precooling and standard

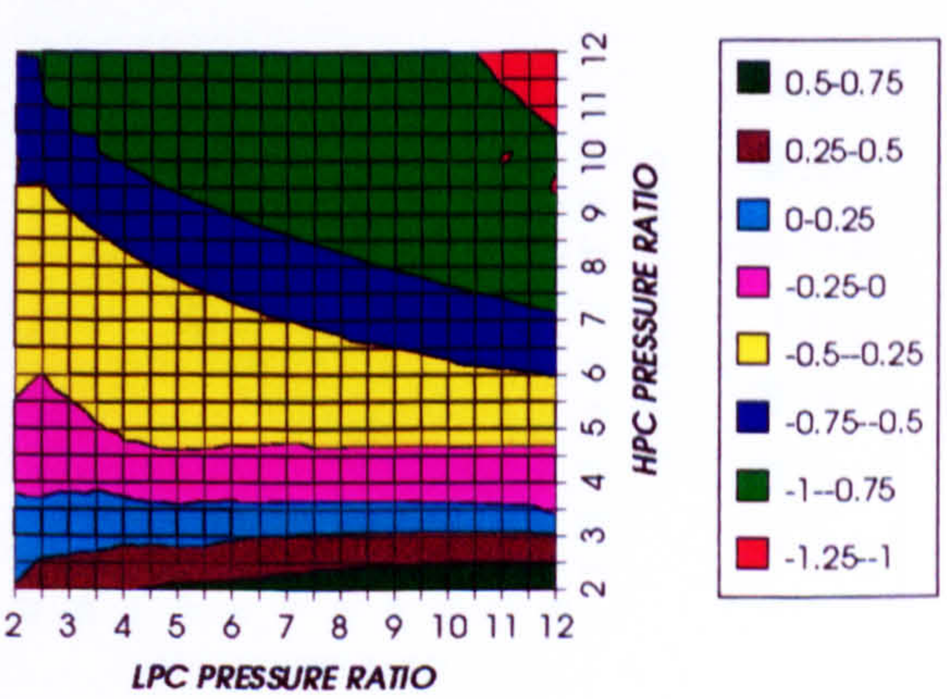

Figure 12. Decrease in LPT rotor relative cooling flow
Difference between precooling and standard

EFFECT OF THE CRYOGENIC PRECOOLING & NGVs N_2 COOLING (TET=1650 K)

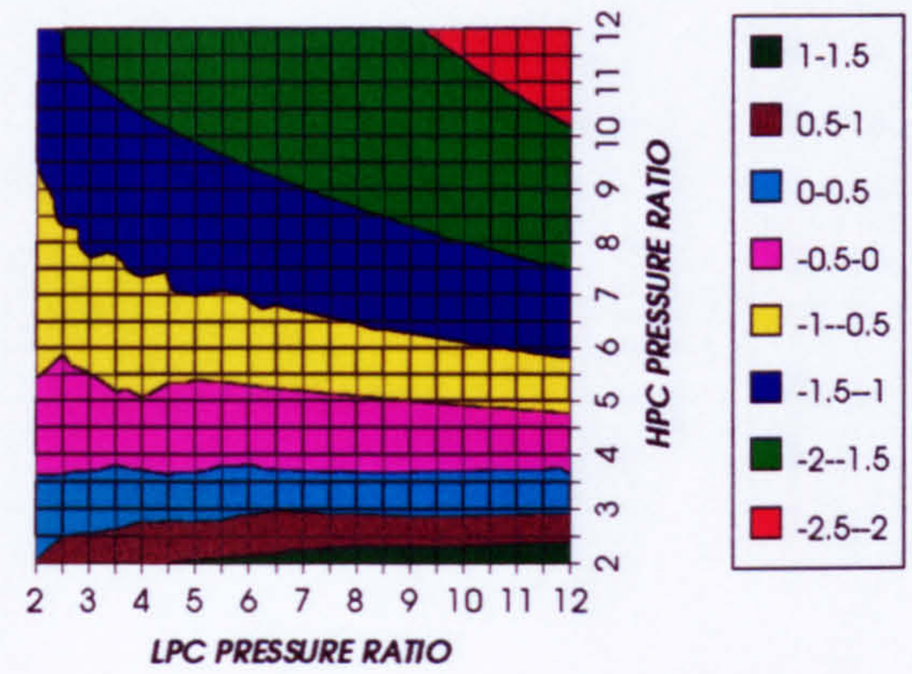

Figure 13. Decrease in LPT relative cooling flow
Difference between precooling and standard

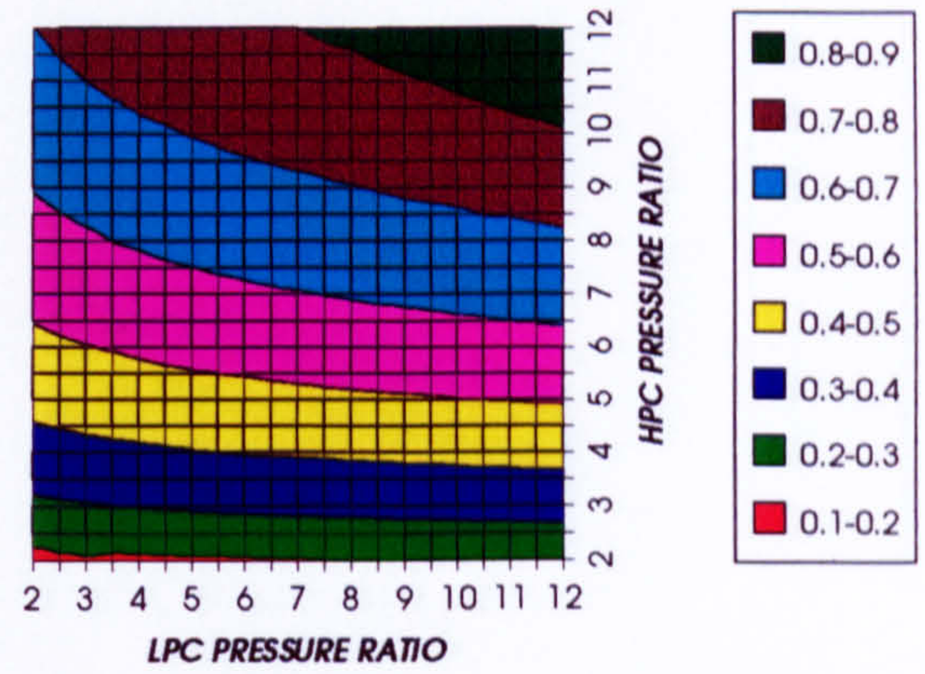

Figure 14. Increase in LPT number of stages
Difference between precooling and standard

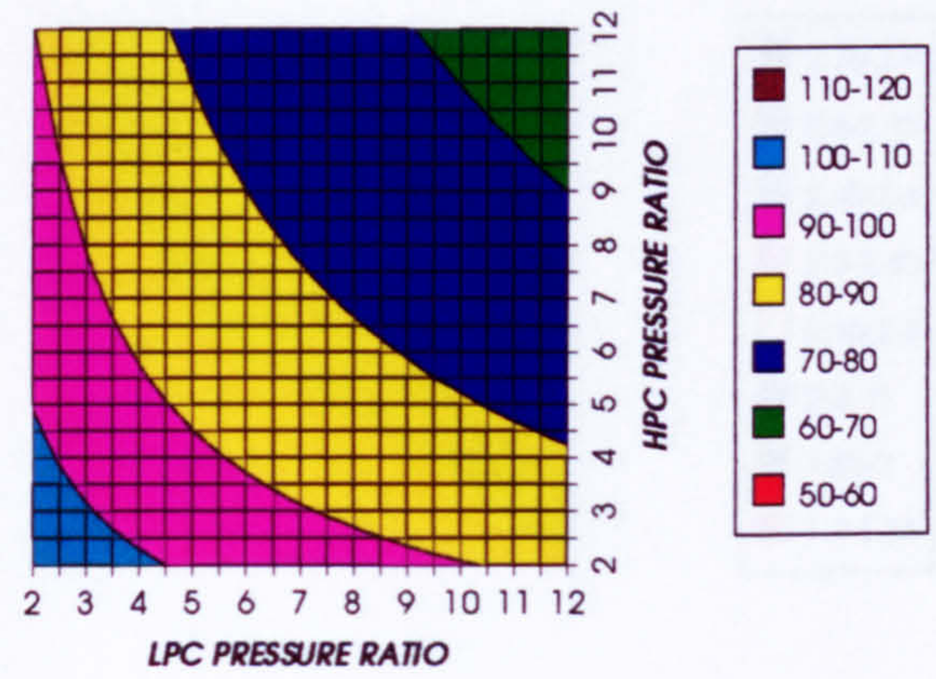

Figure 15. Decrease in compressor inlet temperature
Difference between precooling and standard

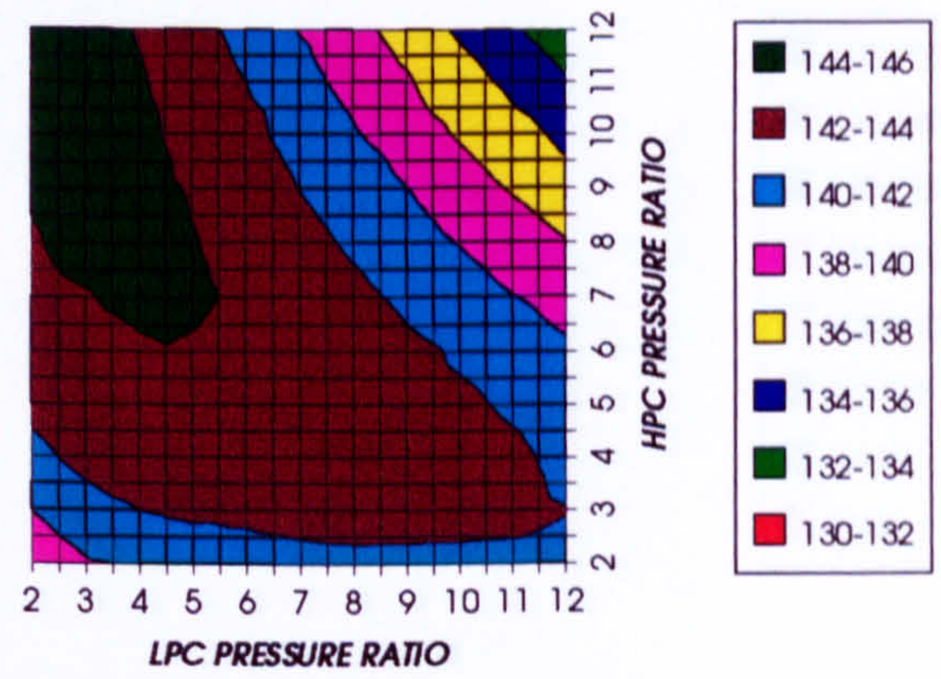

Figure 16. Decrease in compressor outlet temperature
Difference between precooling and standard

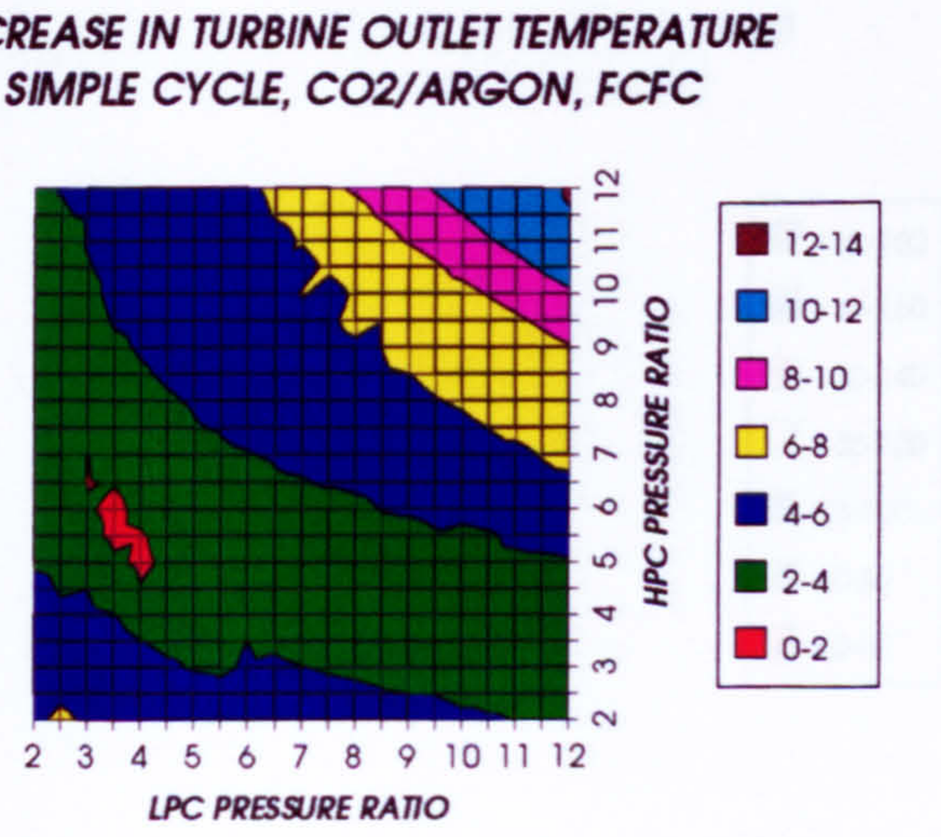

Figure 17. Increase in turbine exit temperature
Difference between precooling and standard

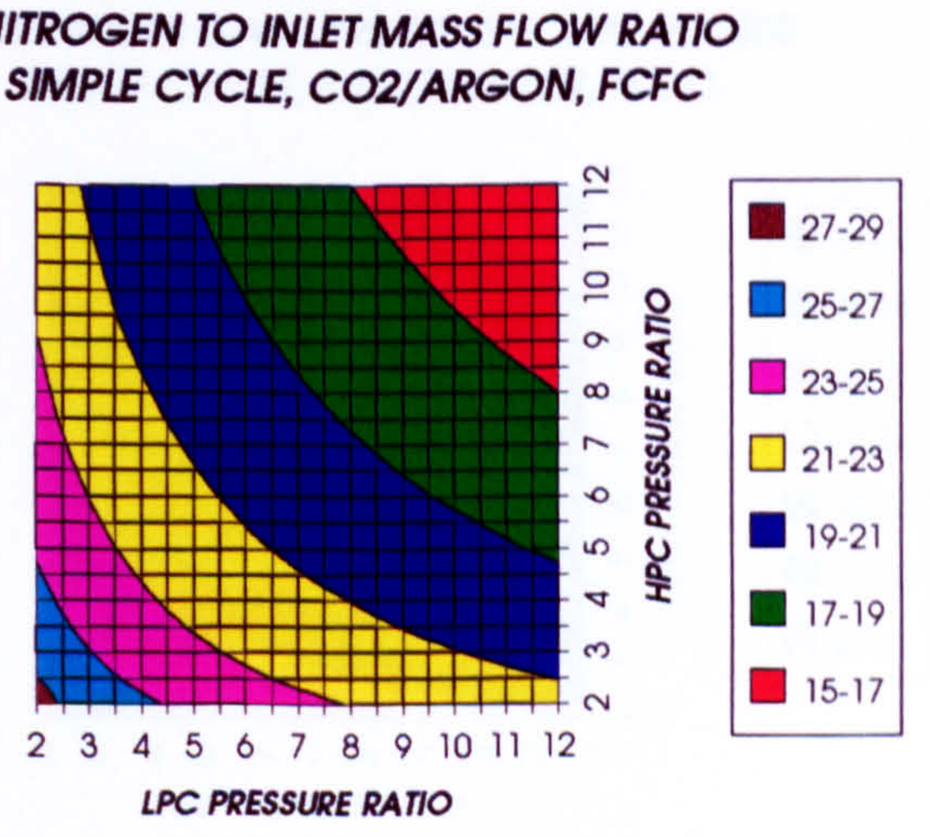

Figure 18. Nitrogen to inlet mass flow ratio for the standard case

EFFECT OF THE CRYOGENIC PRECOOLING & NGVs N_2 COOLING (TET=1650 K)

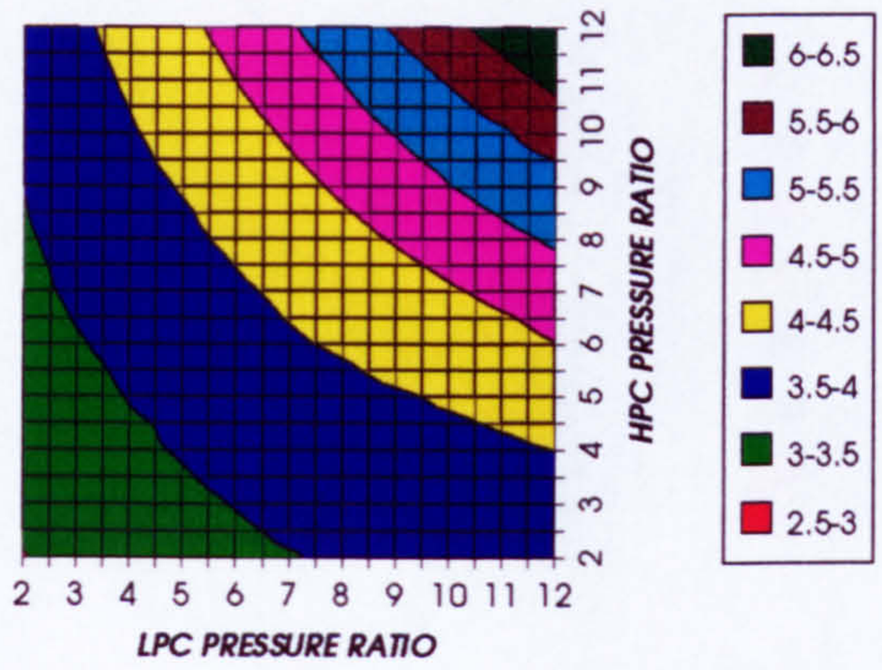

Figure 19. Increase in simple cycle thermal efficiency
Difference between precooling + NGV cool and standard

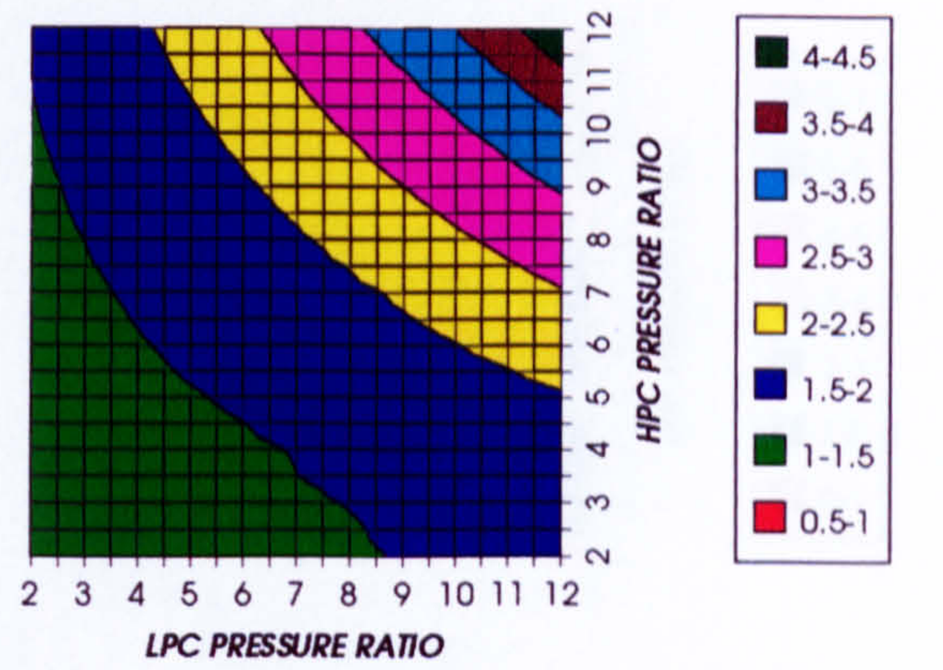

Figure 20. Increase in combined cycle thermal efficiency
Difference between precooling + NGV cool and standard

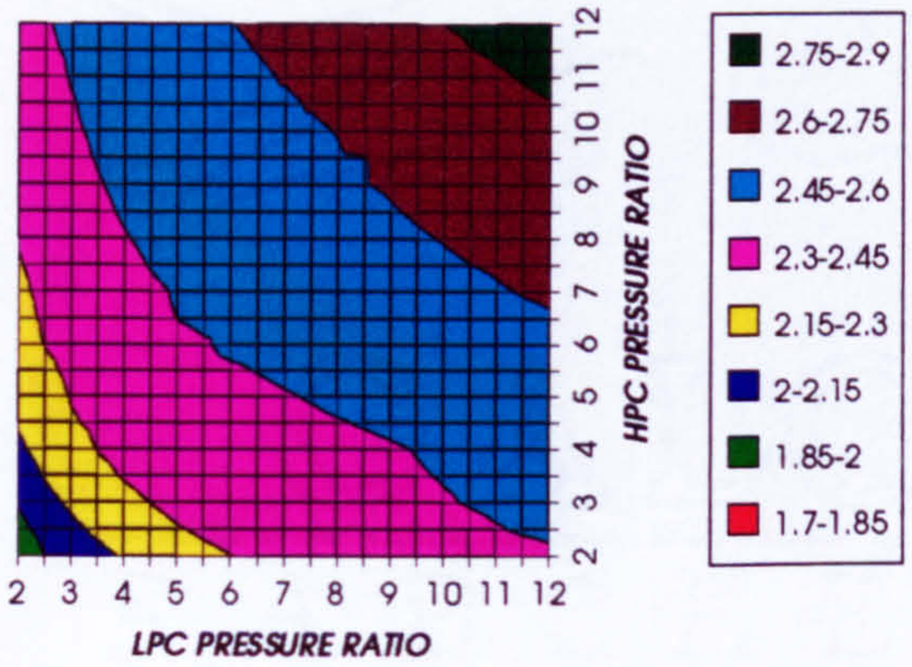

Figure 21. Increase in fuel to inlet mass flow ratio.
Difference between precooling + NGV cool and standard

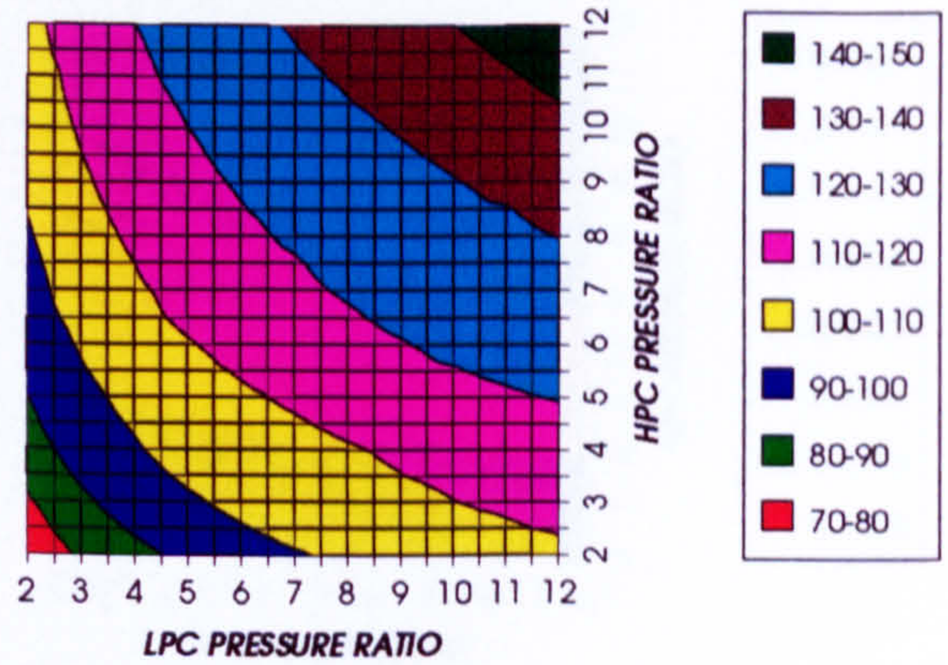

Figure 22. Increase in combined cycle specific power output
Difference between precooling + NGV cool and standard

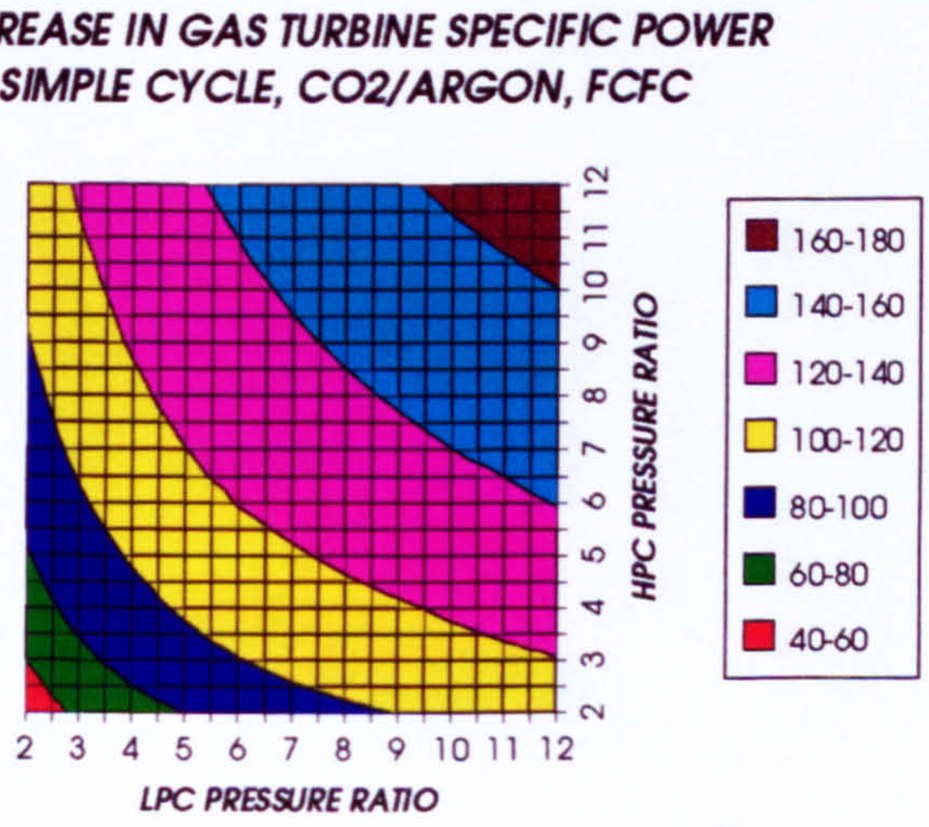

Figure 23. Increase in gas turbine specific power output
Difference between precooling + NGV cool and standard

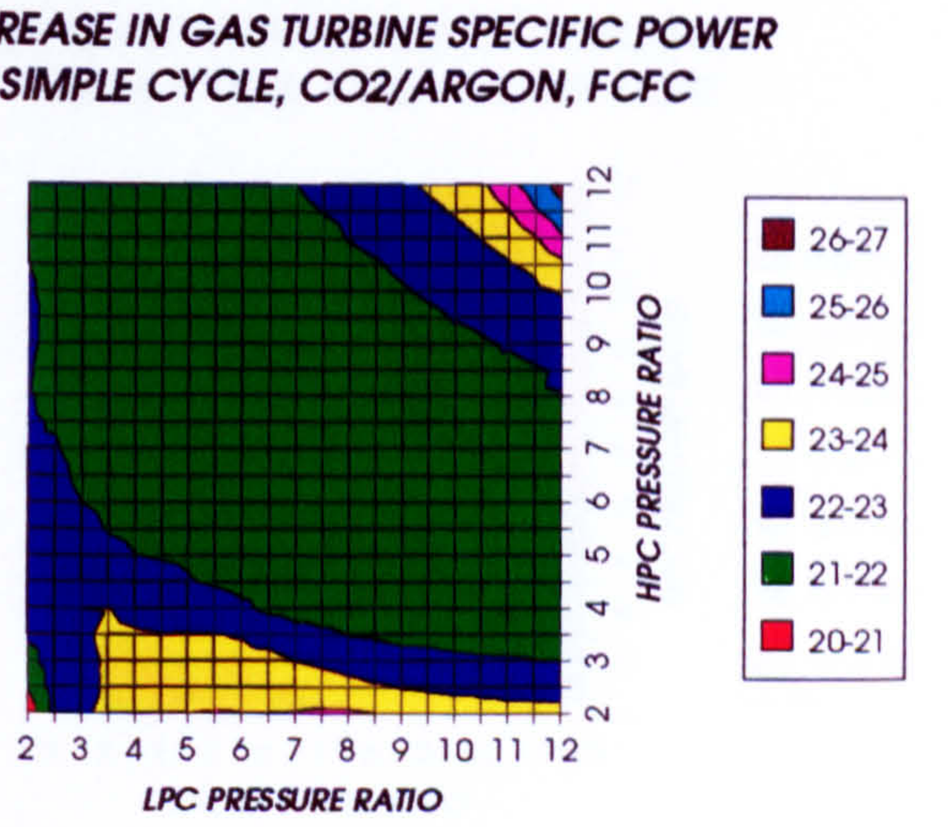

Figure 24. Increase in steam turbine specific power output
Difference between precooling + NGV cool and standard

EFFECT OF THE CRYOGENIC PRECOOLING & NGVs N_2 COOLING (TET=1650 K)

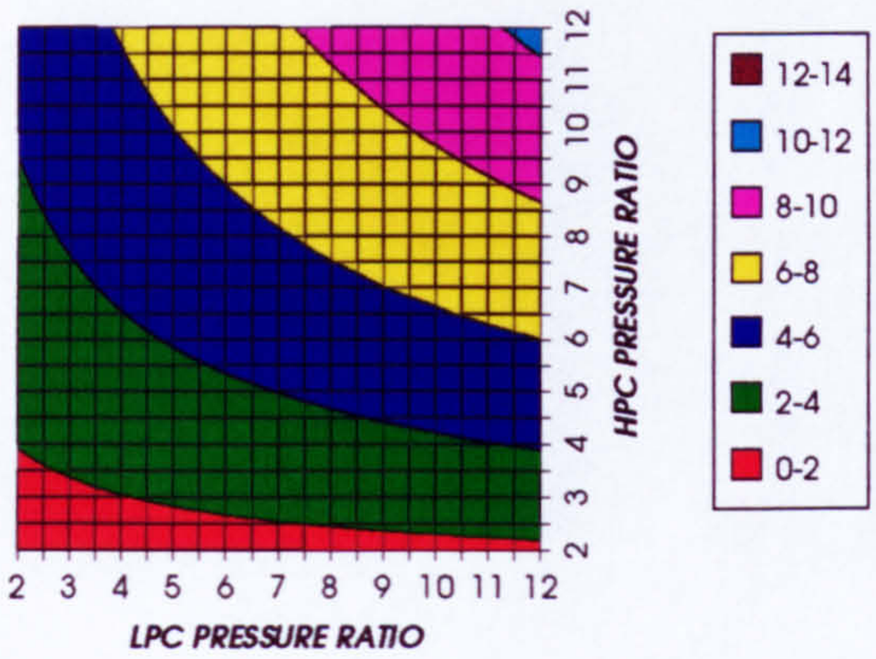

Figure 25. Decrease in HPT stator relative cooling flow
Difference between precooling + NGV cool and standard

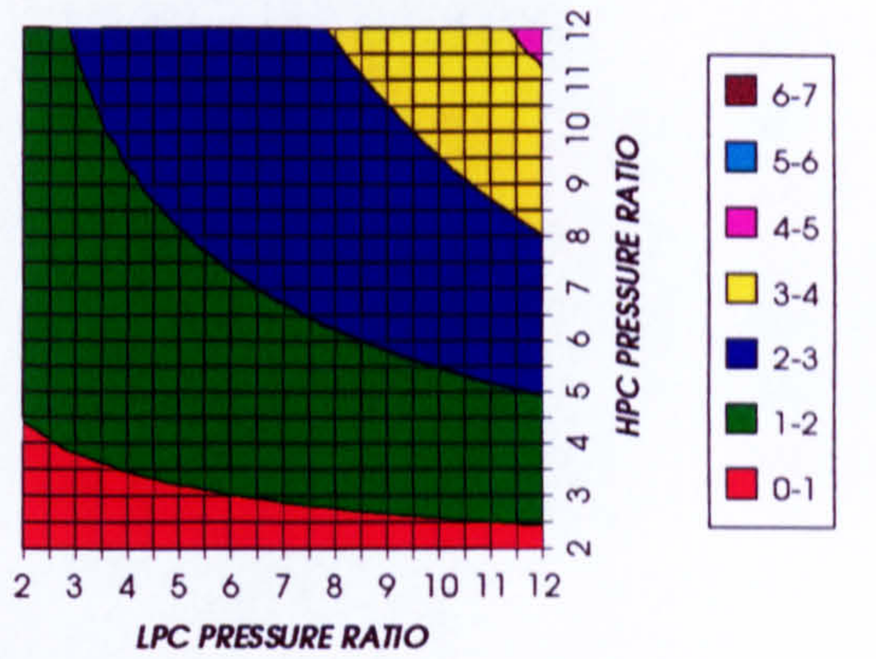

Figure 26. Decrease in HPT rotor relative cooling flow
Difference between precooling + NGV cool and standard

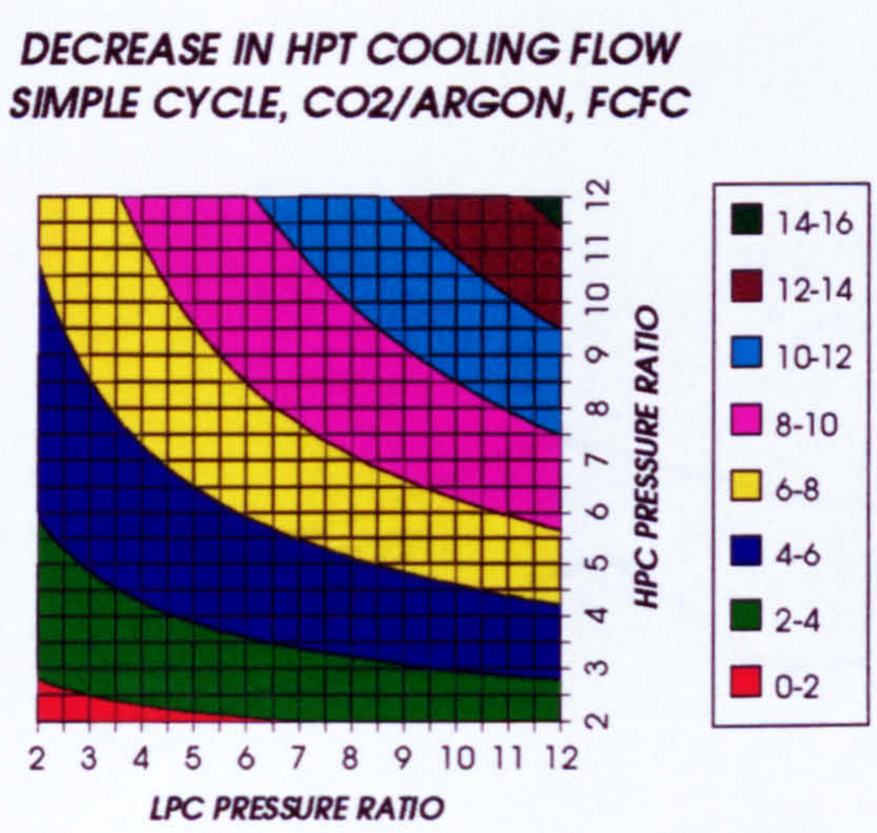

Figure 27. Decrease in HPT relative cooling flow
Difference between precooling + NGV cool and standard

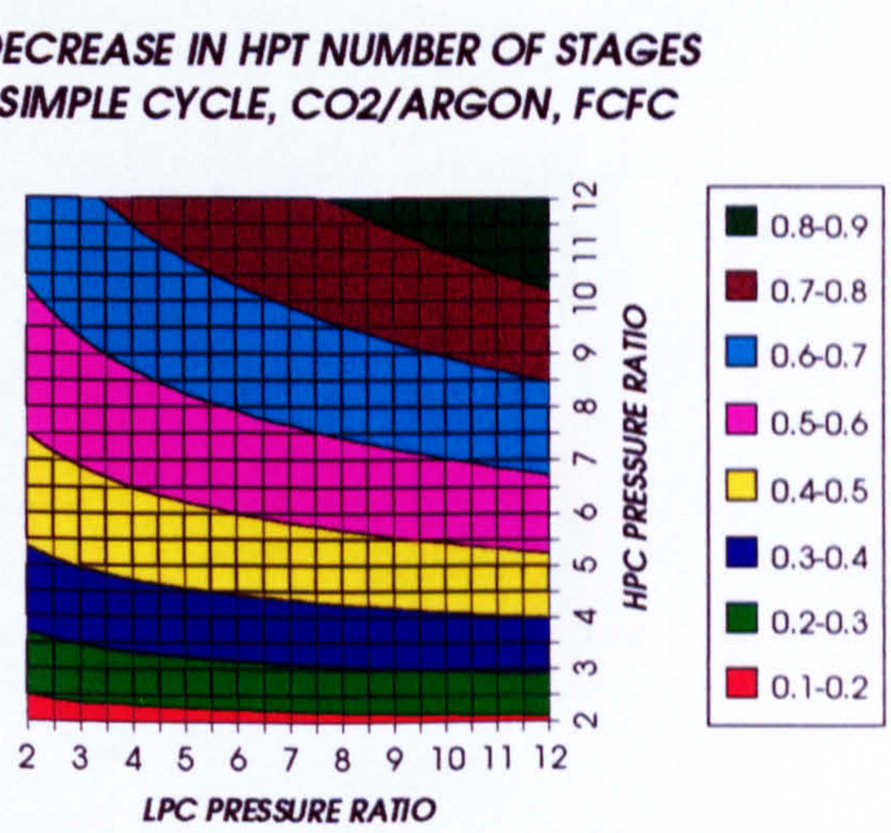

Figure 28. Decrease in HPT number of stages
Difference between precooling + NGV cool and standard

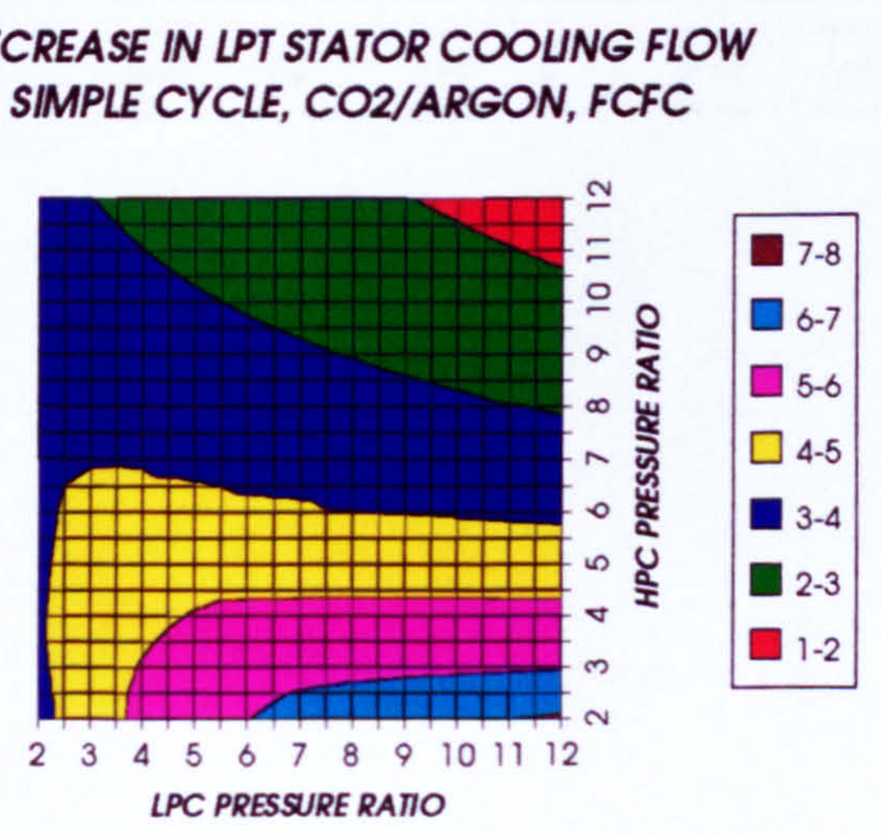

Figure 29. Decrease in LPT stator relative cooling flow.
Difference between precooling + NGV cool and standard

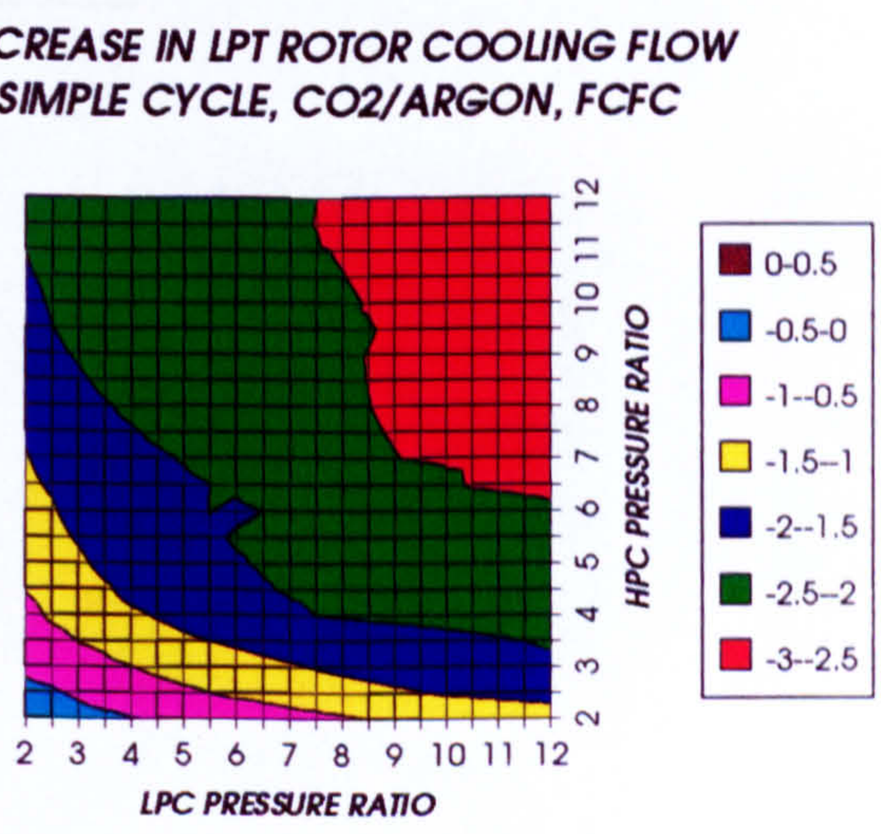

Figure 30. Decrease in LPT rotor relative cooling flow.
Difference between precooling + NGV cool and standard

EFFECT OF THE CRYOGENIC PRECOOLING & NGVs N_2 COOLING (TET=1650 K)

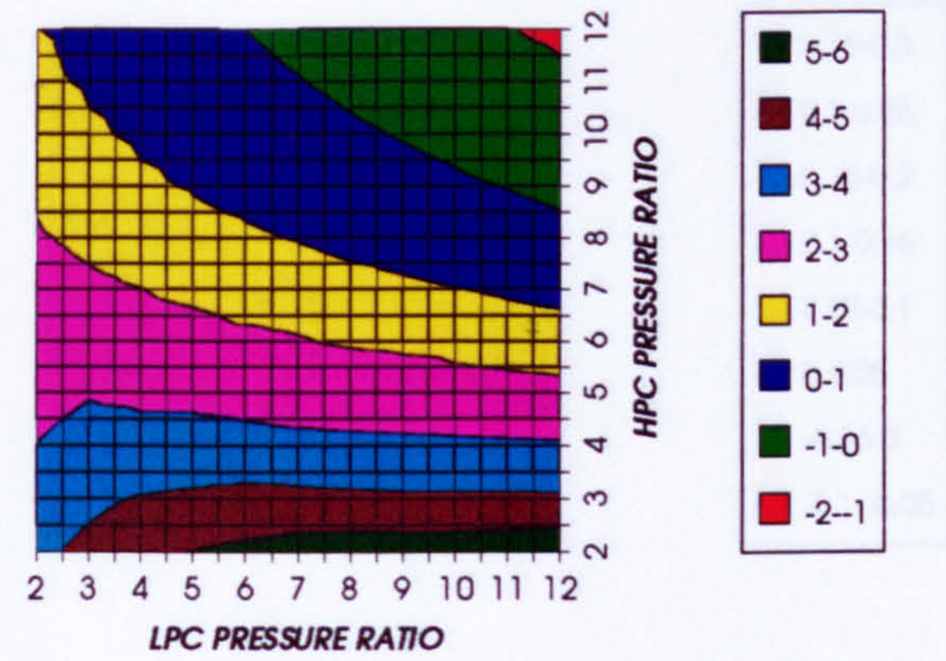

Figure 31. Decrease in LPT relative cooling flow
Difference between precooling + NGV cool and standard

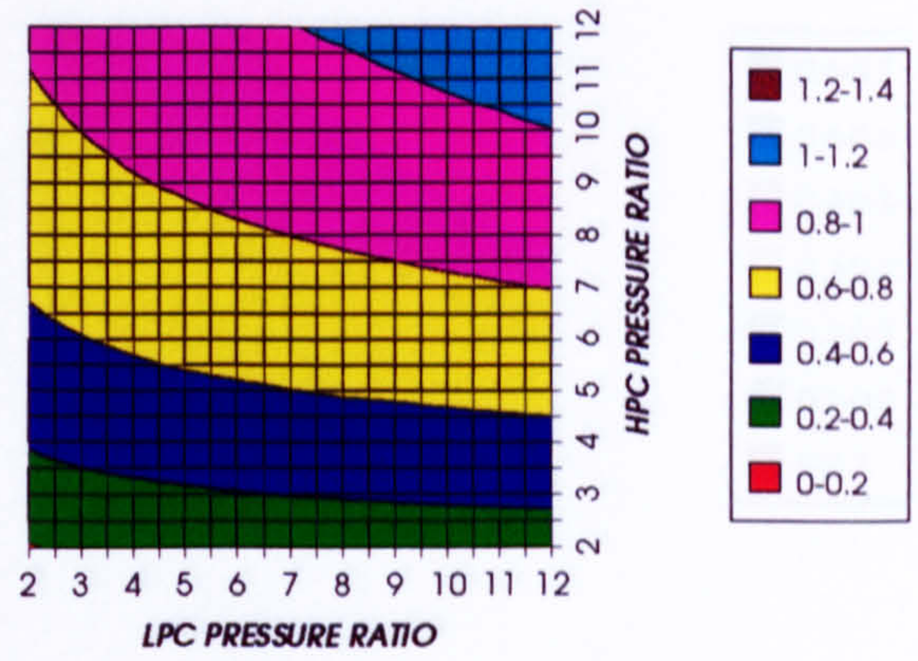

Figure 32. Increase in LPT number of stages
Difference between precooling + NGV cool and standard

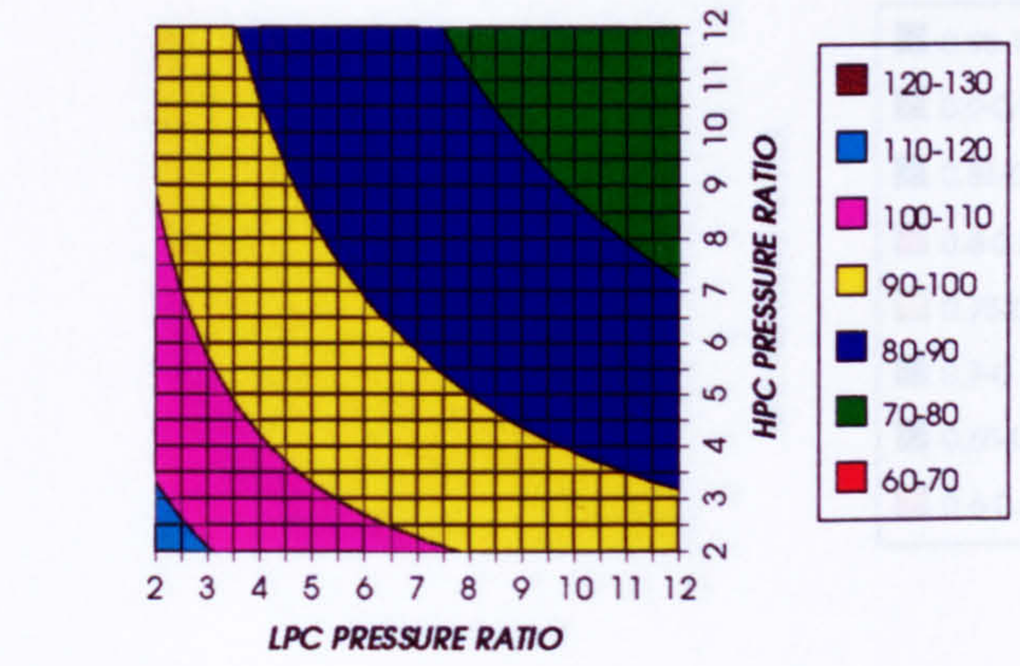

Figure 33. Decrease in compressor inlet temperature
Difference between precooling + NGV cool and standard

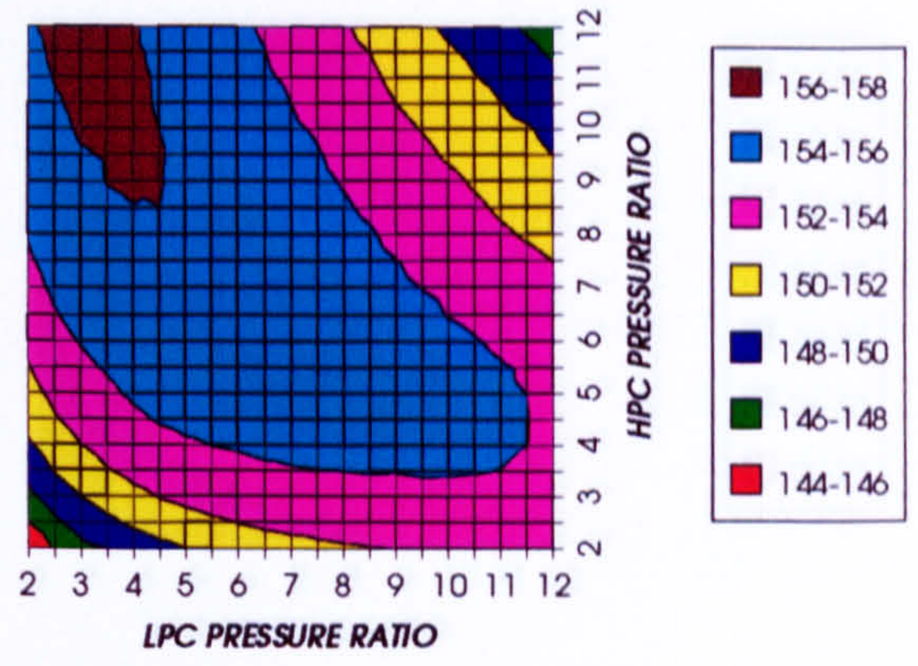

Figure 34. Decrease in compressor outlet temperature
Difference between precooling + NGV cool and standard

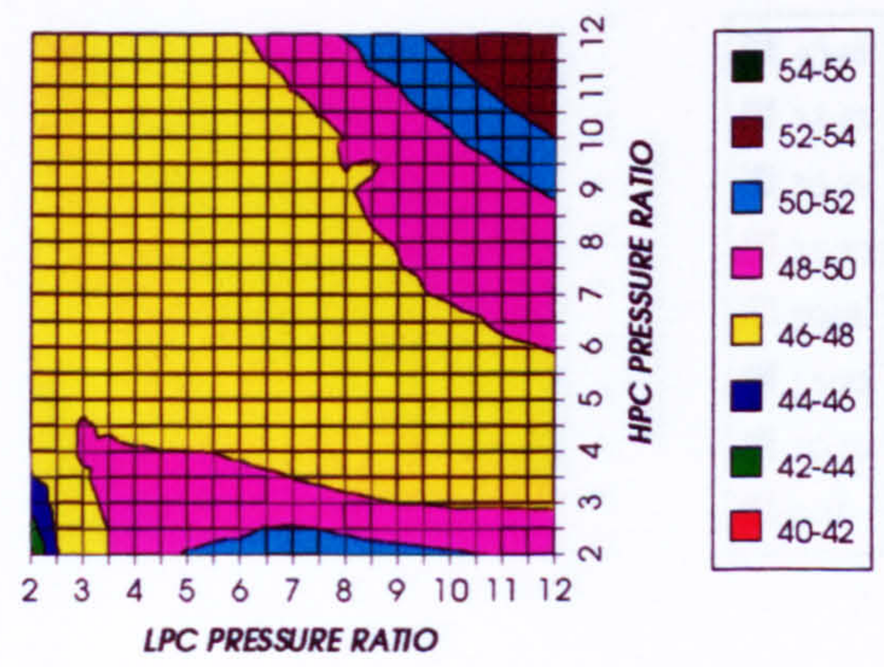

Figure 35. Increase in turbine exit temperature
Difference between precooling + NGV cool and standard

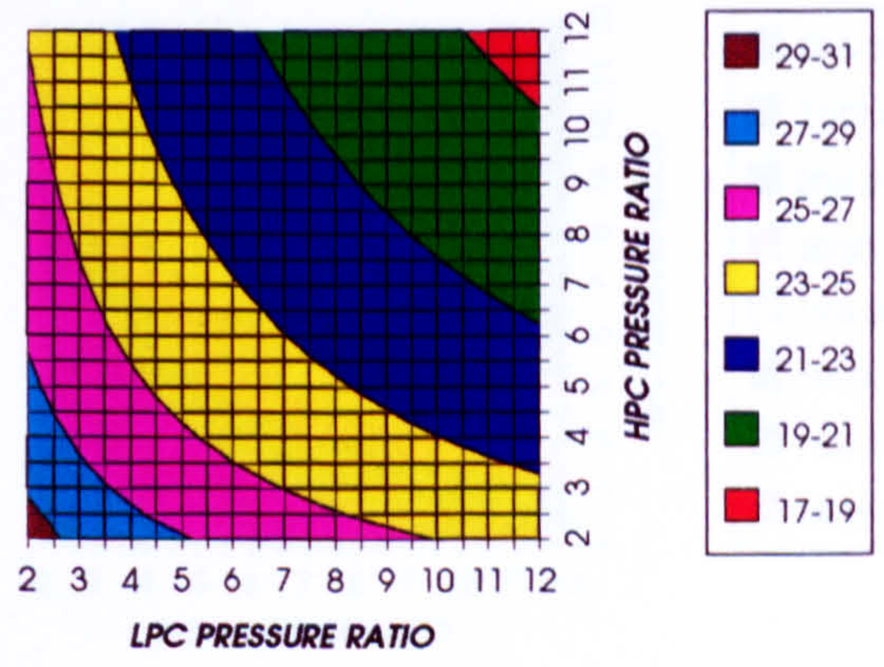

Figure 36. Nitrogen to inlet mass flow ratio for the N_2 cryogenic precooling case

EFFECT OF THE CRYOGENIC PRECOOLING & NGVs N_2 COOLING (TET=1650 K)

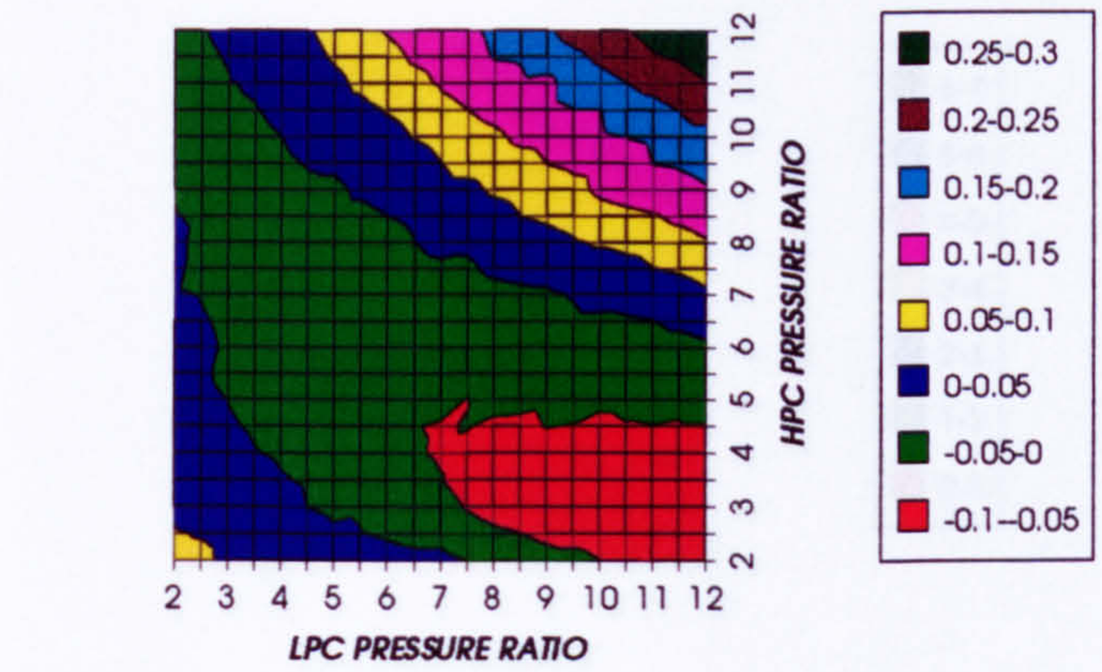

Figure 37. Increase in simple cycle thermal efficiency
Difference between precooling + NGV cool and precool

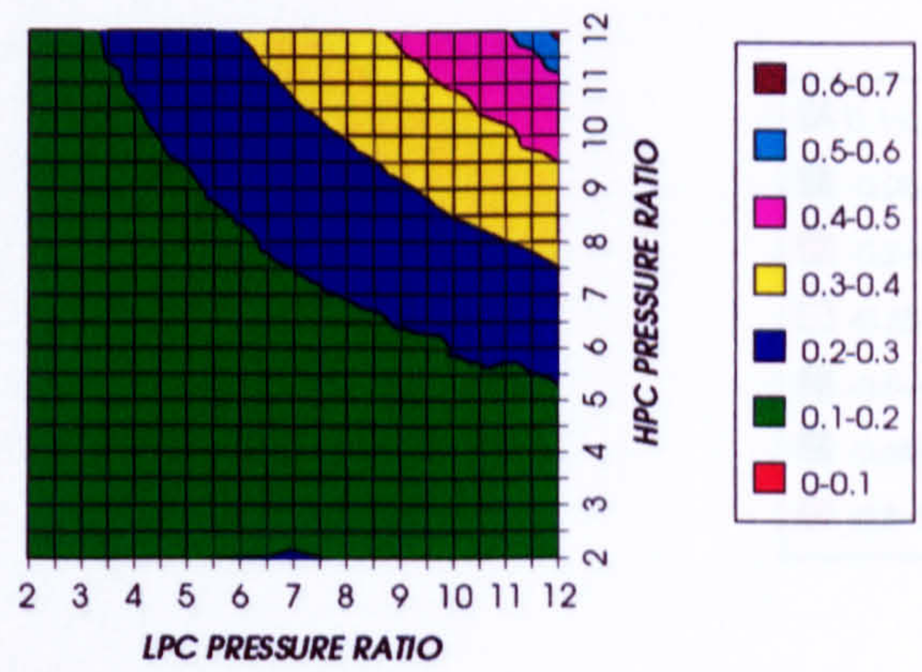

Figure 38. Increase in combined cycle thermal efficiency
Difference between precooling + NGV cool and precool

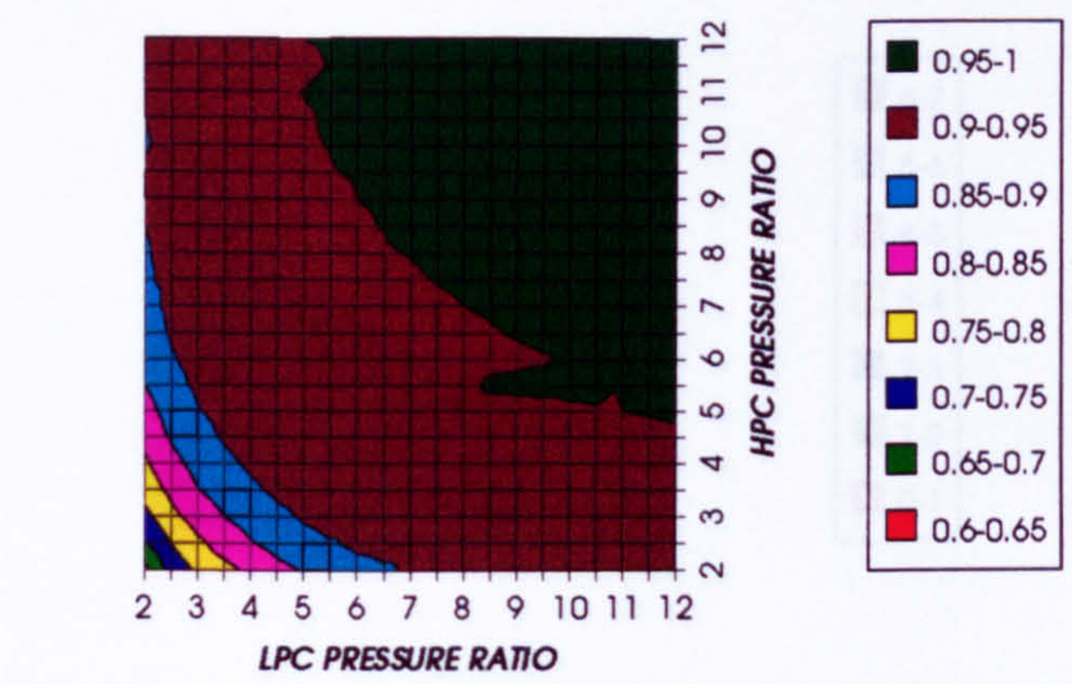

Figure 39. Increase in fuel to inlet mass flow ratio
Difference between precooling + NGV cool and precool

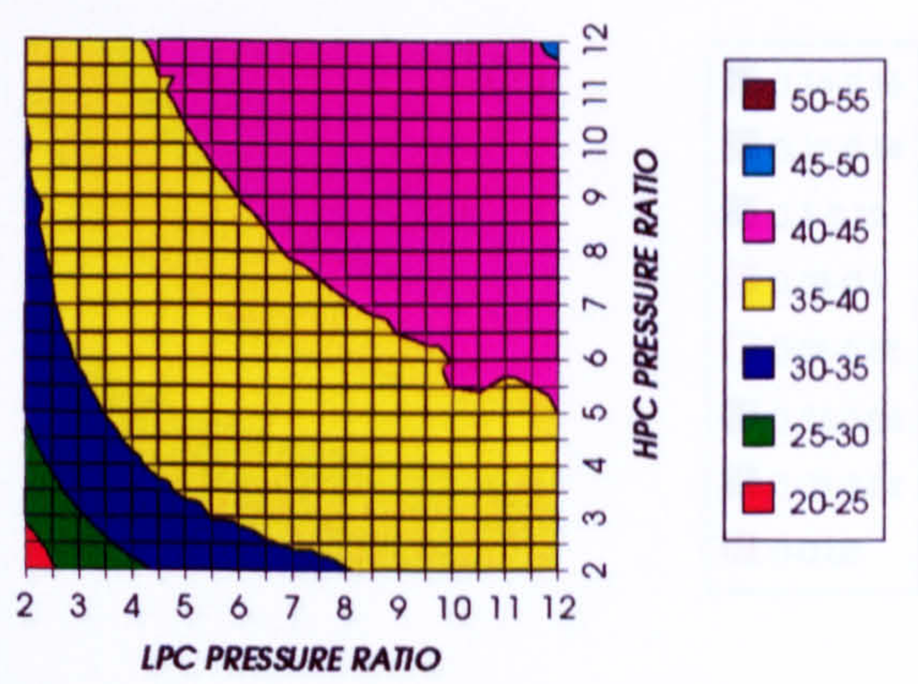

Figure 40. Increase in combined cycle specific power output
Difference between precooling + NGV cool and precool

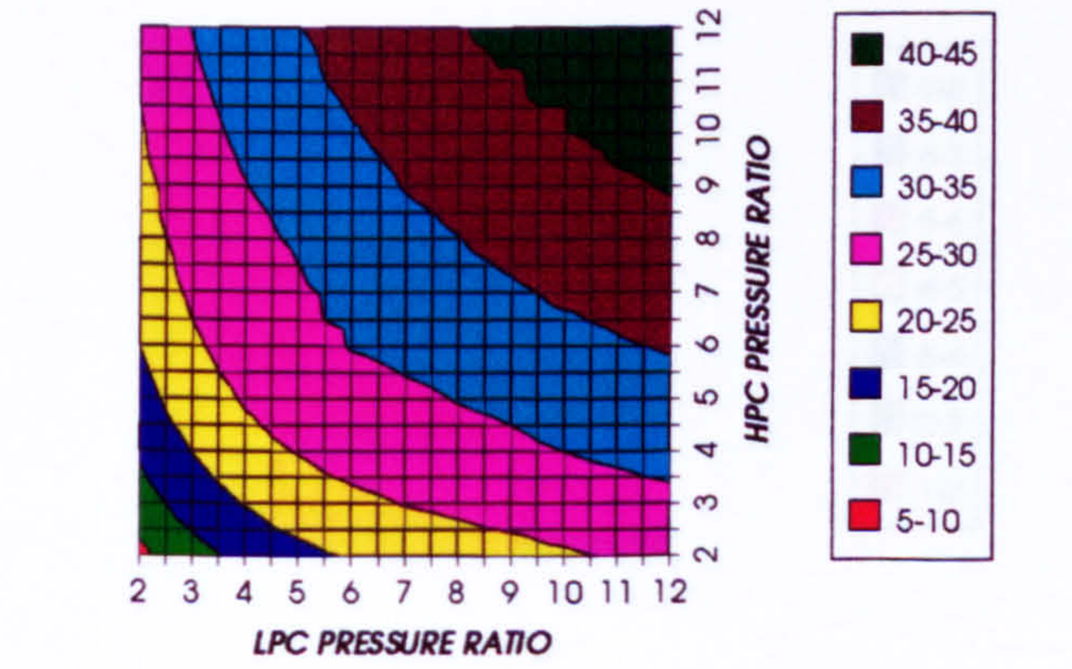

Figure 41. Increase in gas turbine specific power output
Difference between precooling + NGV cool and precool

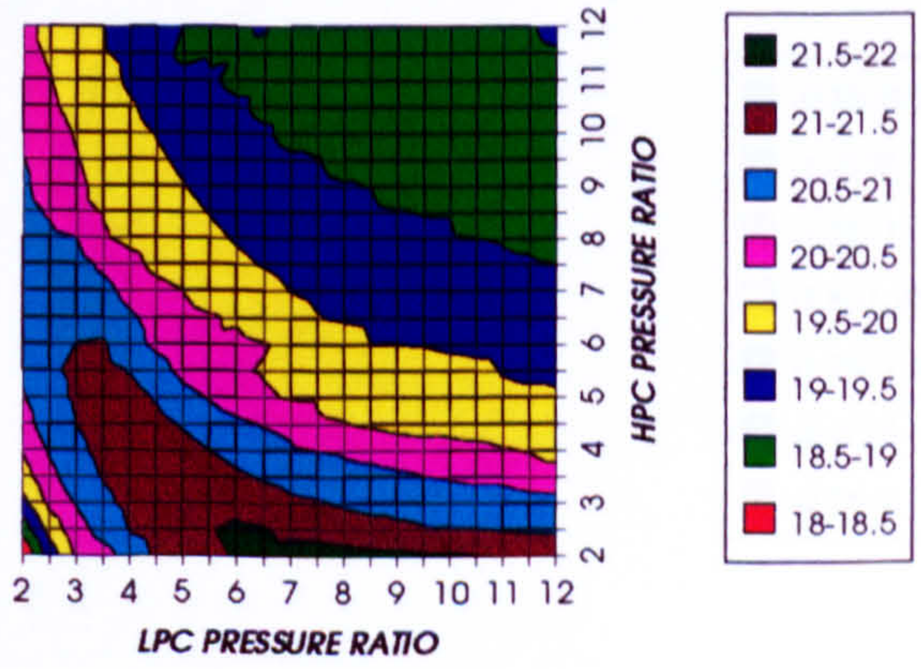

Figure 42. Increase in steam turbine specific power output
Difference between precooling + NGV cool and precool

EFFECT OF THE CRYOGENIC PRECOOLING & NGVs N_2 COOLING (TET=1650 K)

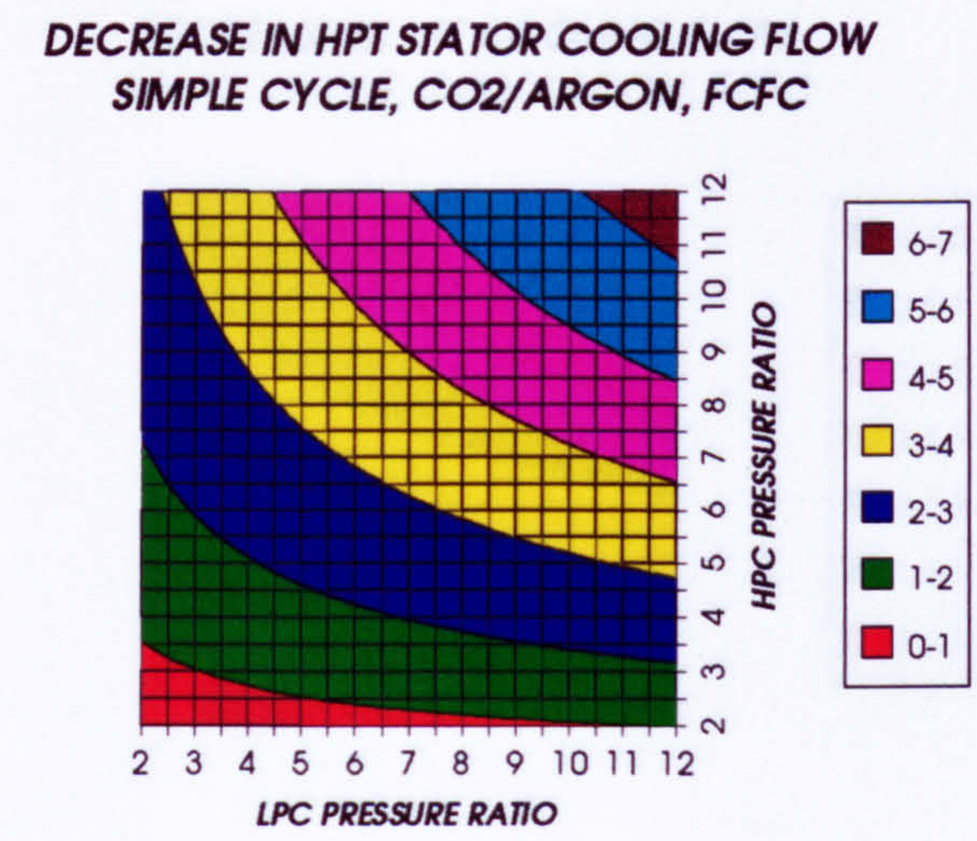

Figure 43. Decrease in HPT stator relative cooling flow
Difference between precooling + NGV cool and precool

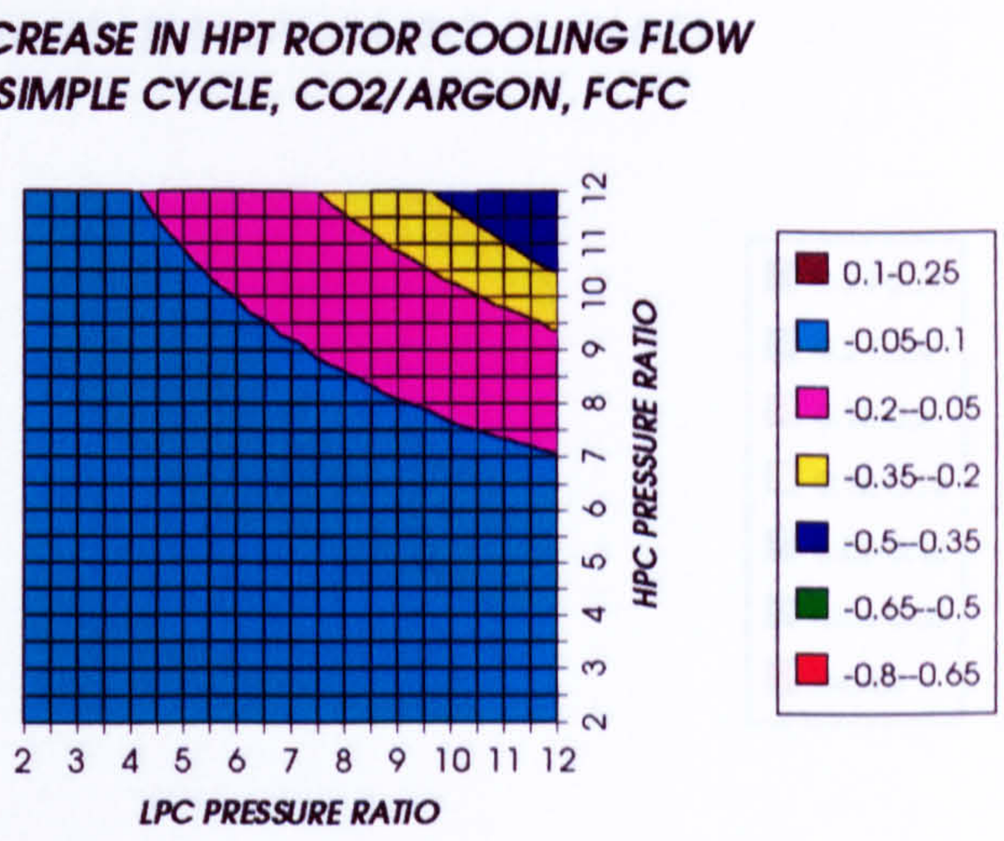

Figure 44. Decrease in HPT rotor relative cooling flow
Difference between precooling + NGV cool and precool

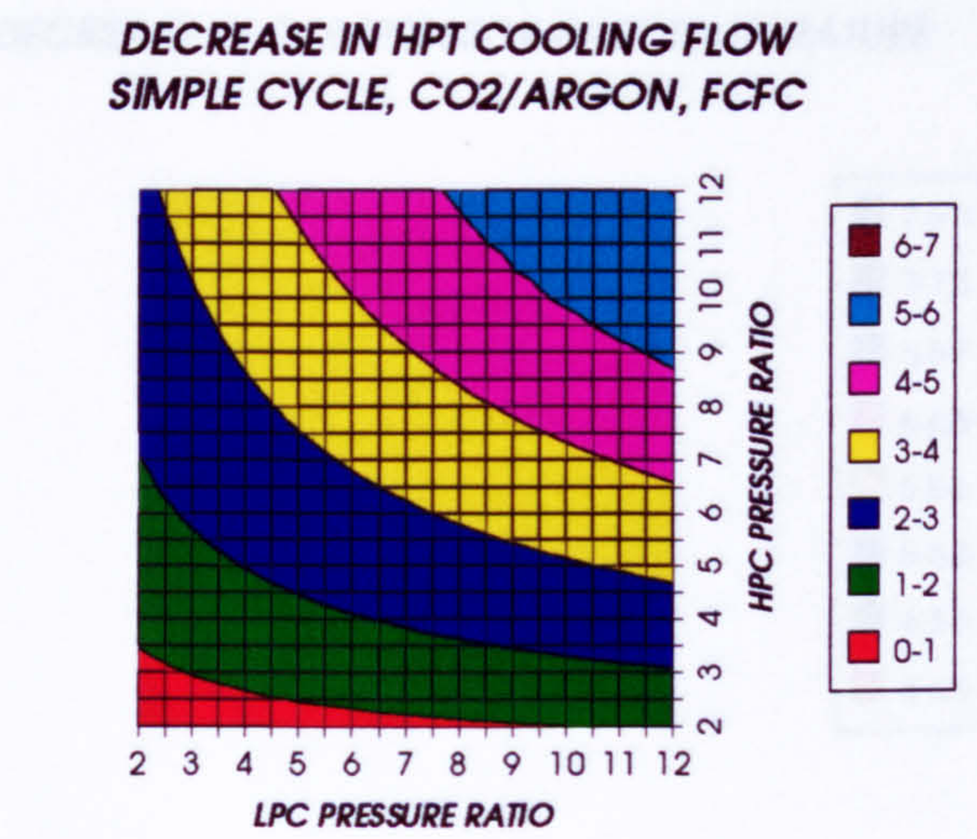

Figure 45. Decrease in HPT relative cooling flow
Difference between precooling + NGV cool and precool

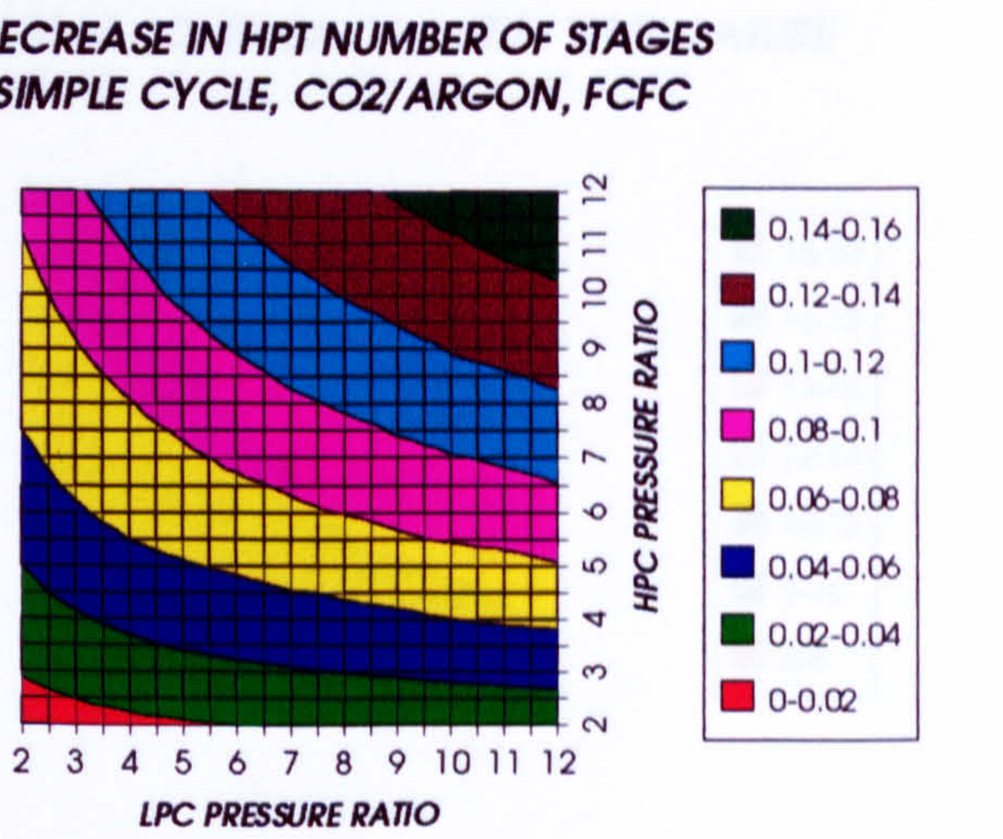

Figure 46. Decrease in HPT number of stages
Difference between precooling + NGV cool and precool

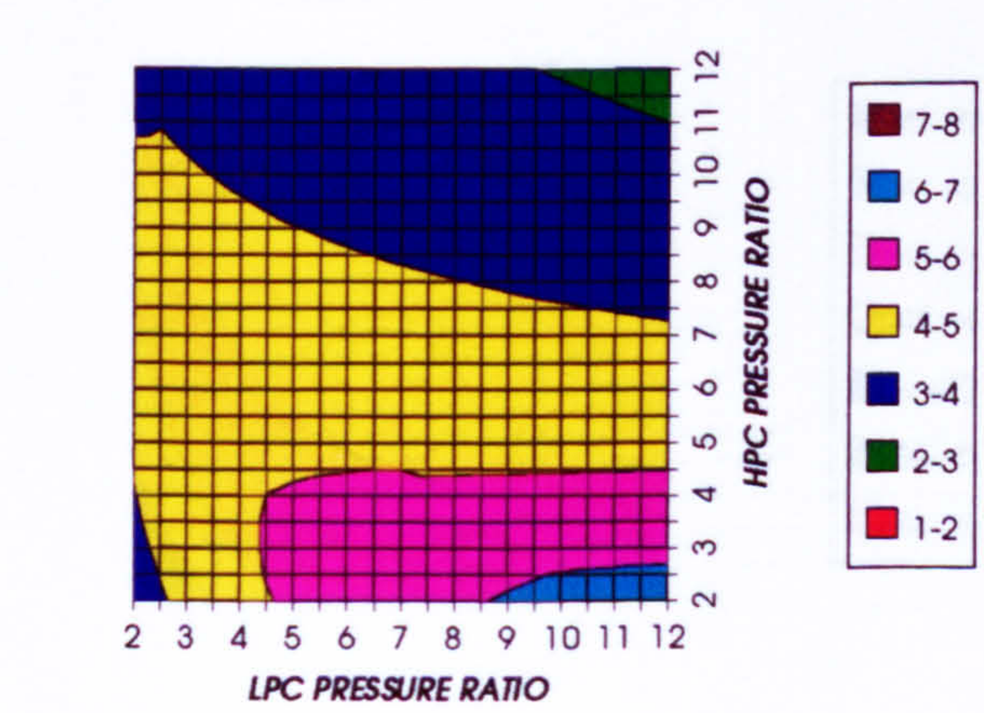

Figure 47. Decrease in LPT stator relative cooling flow
Difference between precooling + NGV cool and precool

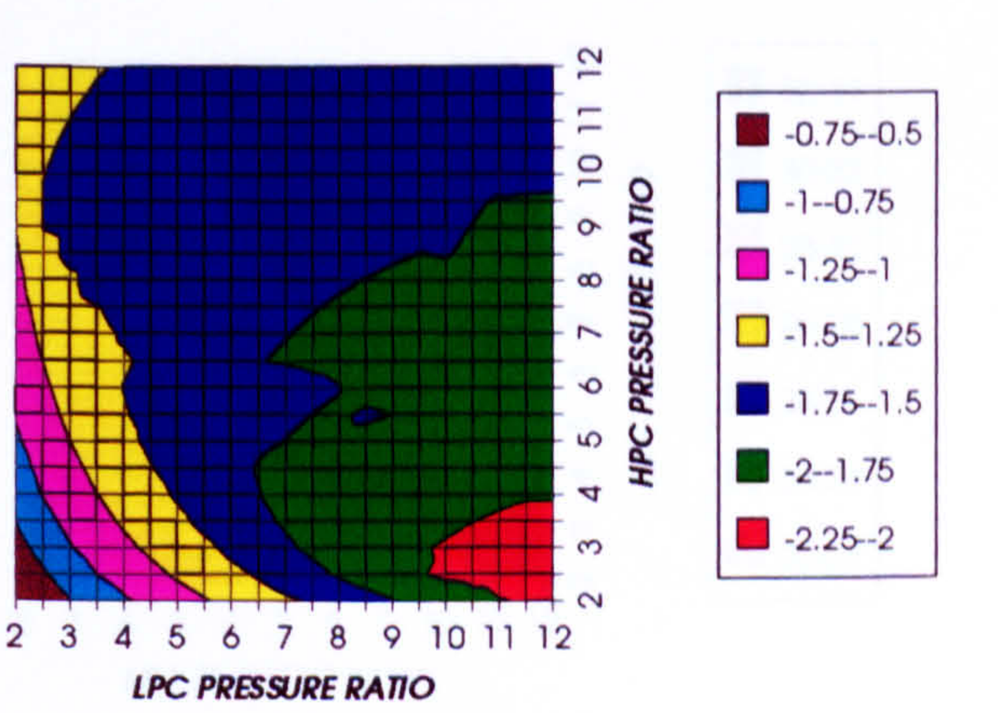

Figure 48. Decrease in LPT rotor relative cooling flow
Difference between precooling + NGV cool and precool

EFFECT OF THE CRYOGENIC PRECOOLING & NGVs N_2 COOLING (TET=1473 K)

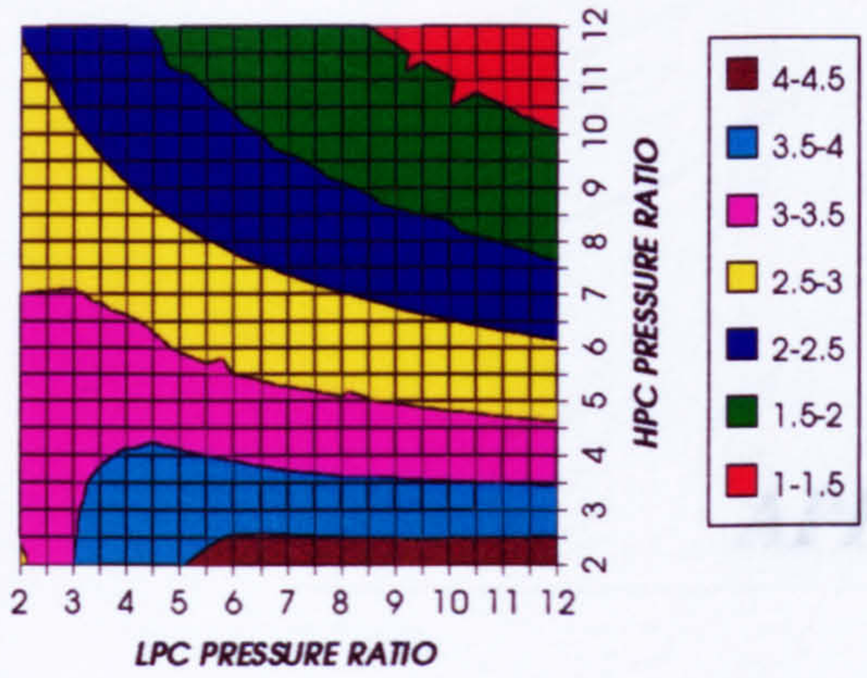

Figure 49. Decrease in LPT relative cooling flow
Difference between precooling + NGV cool and precool

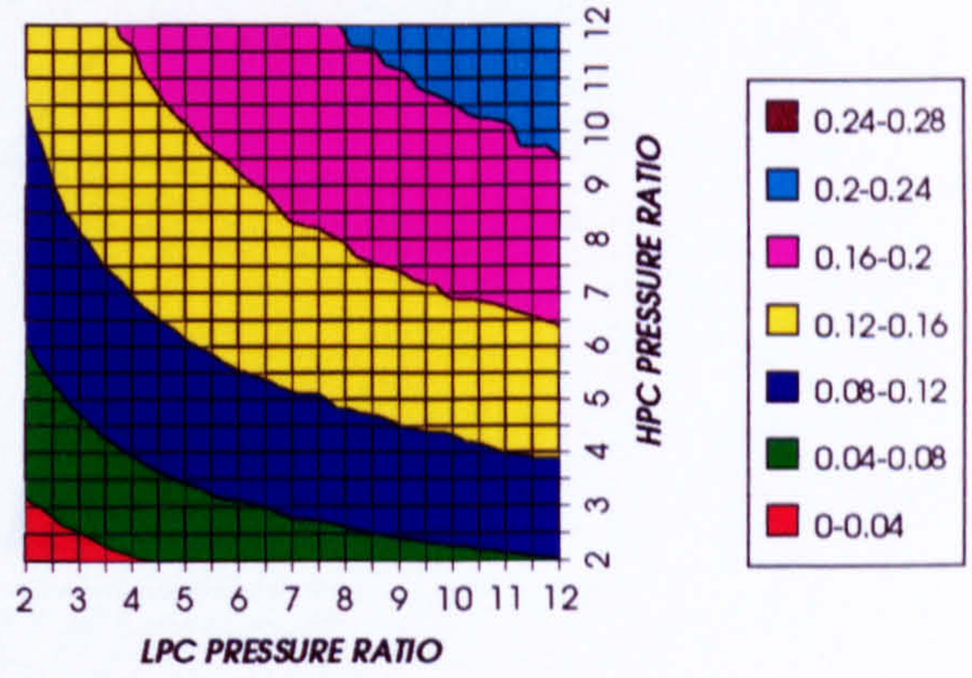

Figure 50. Increase in LPT number of stages
Difference between precooling + NGV cool and precool

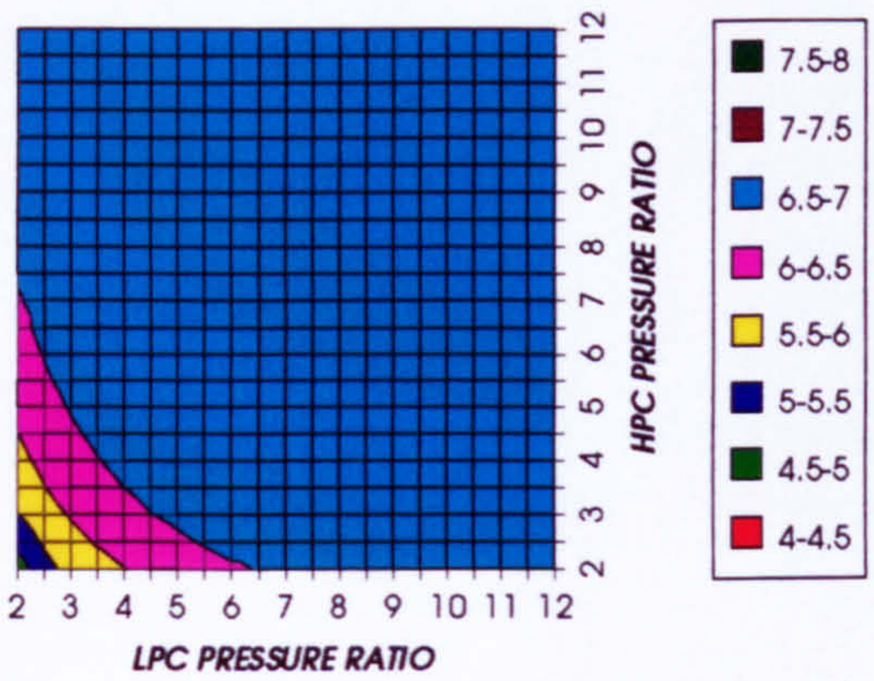

Figure 51. Decrease in compressor inlet temperature
Difference between precooling + NGV cool and precool

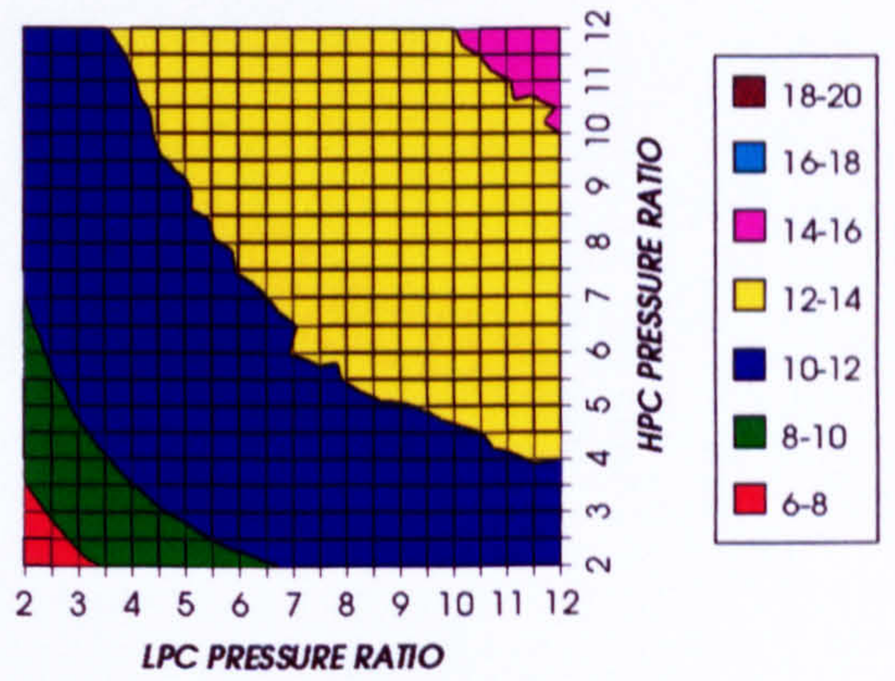

Figure 52. Decrease in compressor outlet temperature
Difference between precooling + NGV cool and precool

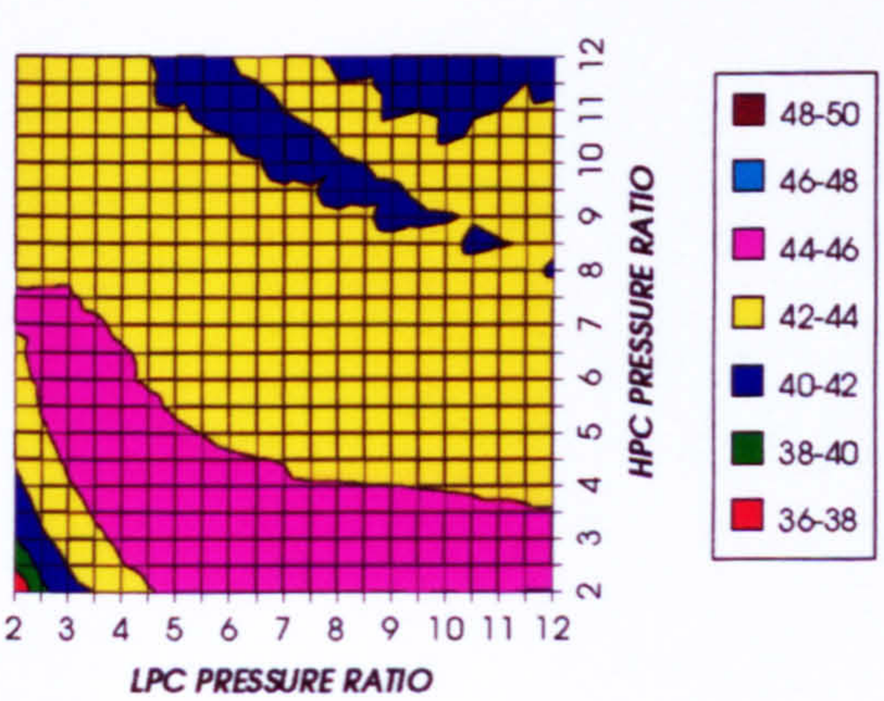

Figure 53. Increase in turbine exit temperature
Difference between precooling + NGV cool and precool

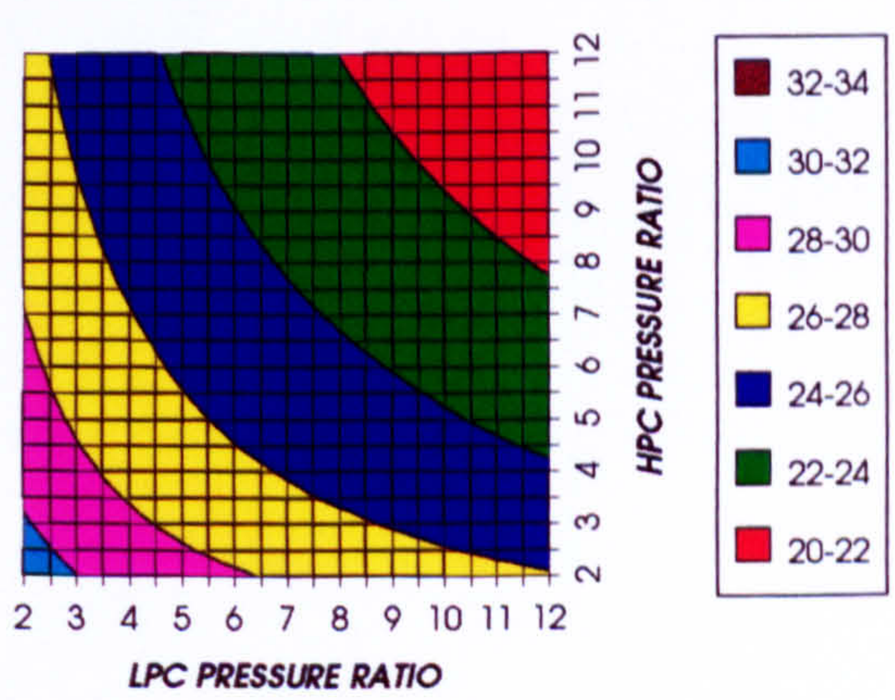

Figure 54. Nitrogen to inlet mass flow ratio for the N_2 cryogenic precooling + N_2 NGV cooling

APPENDIX III

COMPLETE PLANT PERFORMANCE (WORKING FLUID CO_2, TET=1473 K)

COMPLETE PLANT (TET=1473K)

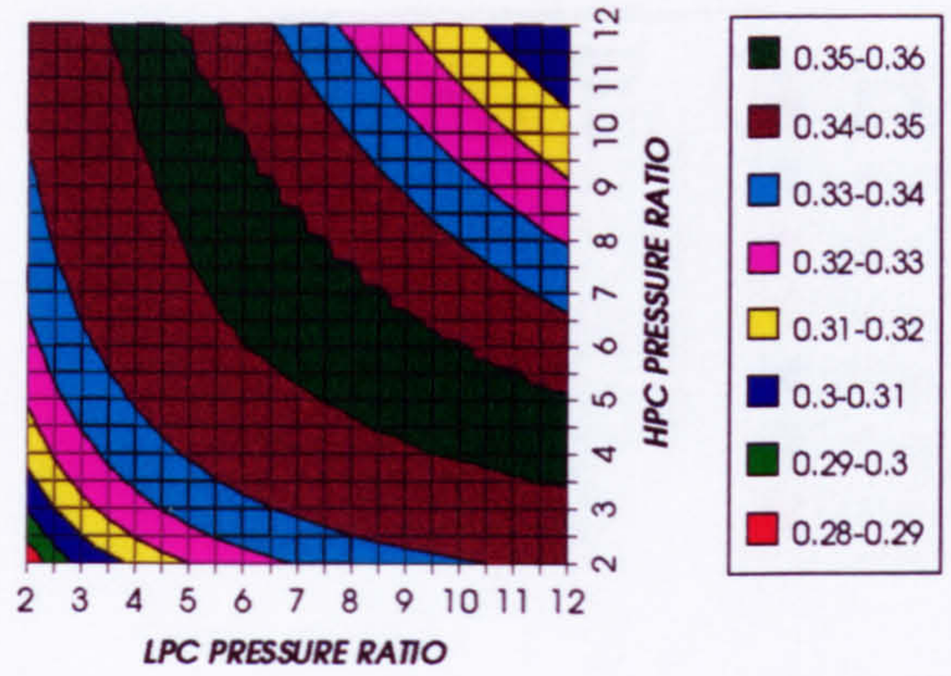

Figure 1. Combined cycle thermal efficiency

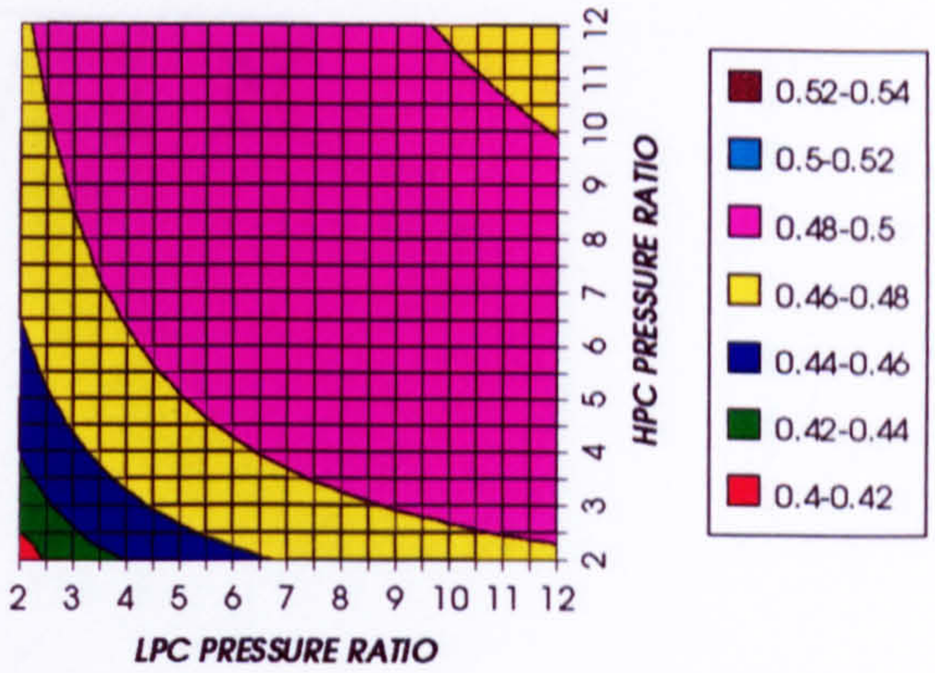

Figure 2. Combined cycle ideal thermal efficiency

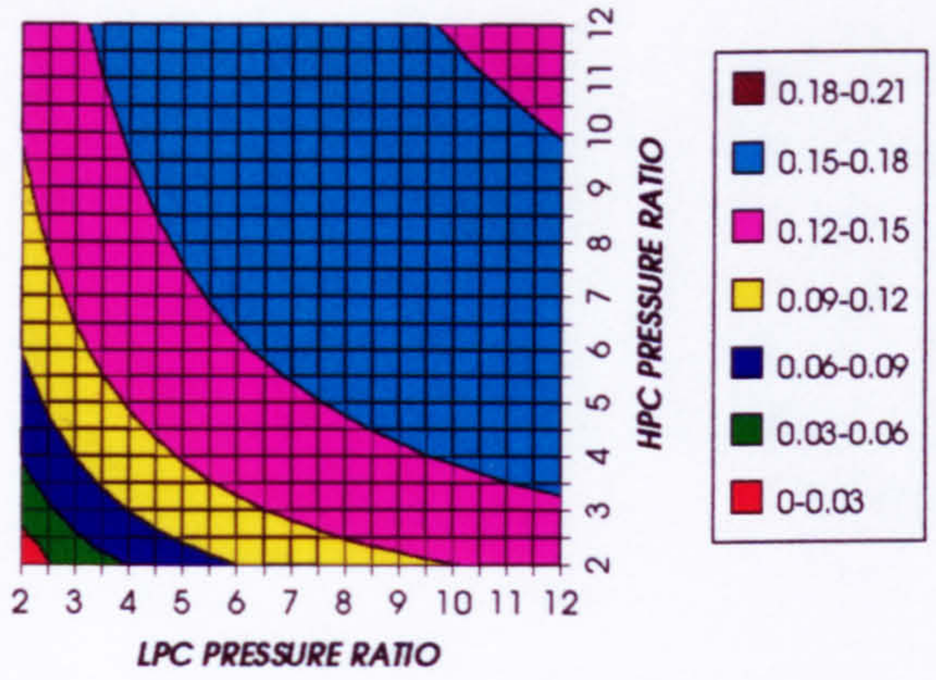

Figure 3. Simple cycle thermal efficiency

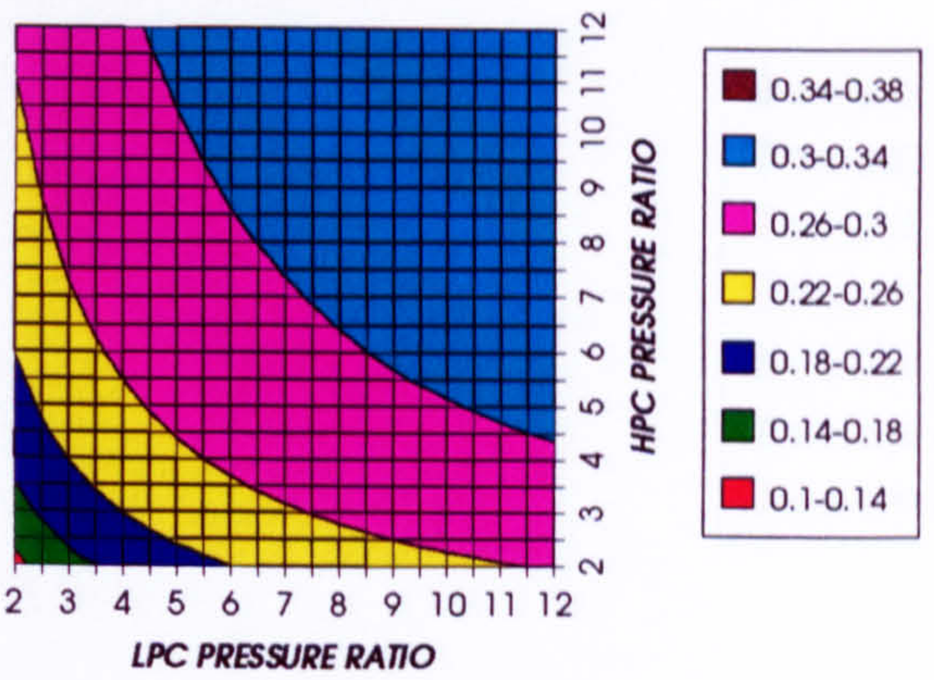

Figure 4. Simple cycle ideal thermal efficiency

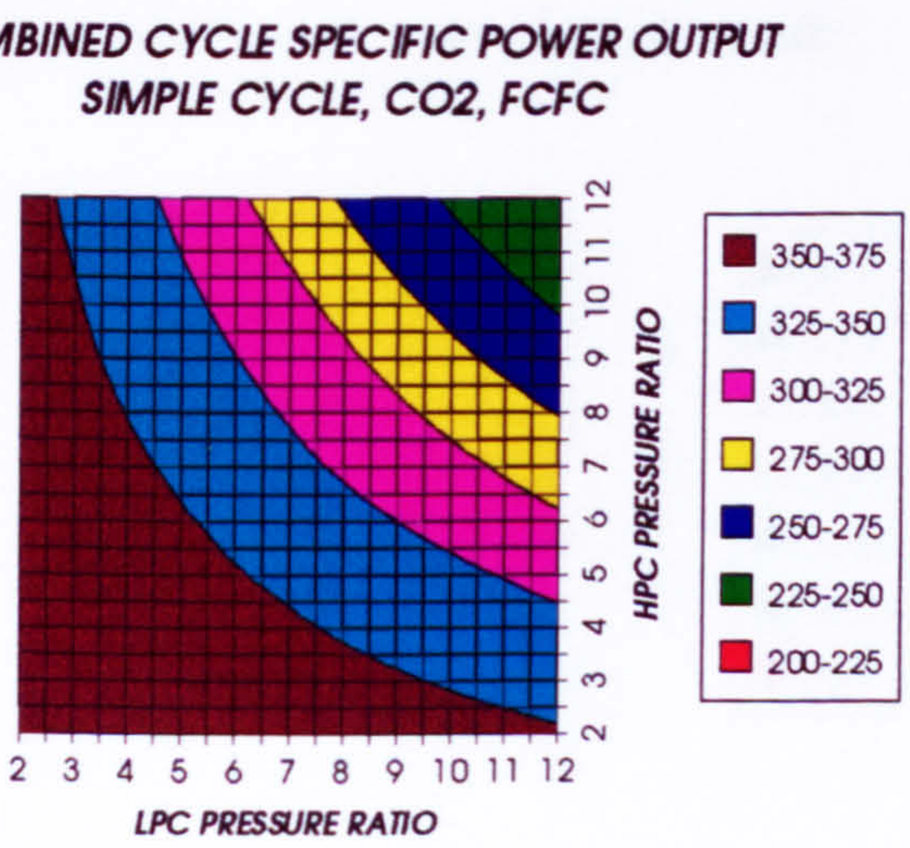

Figure 5. Combined cycle specific power output

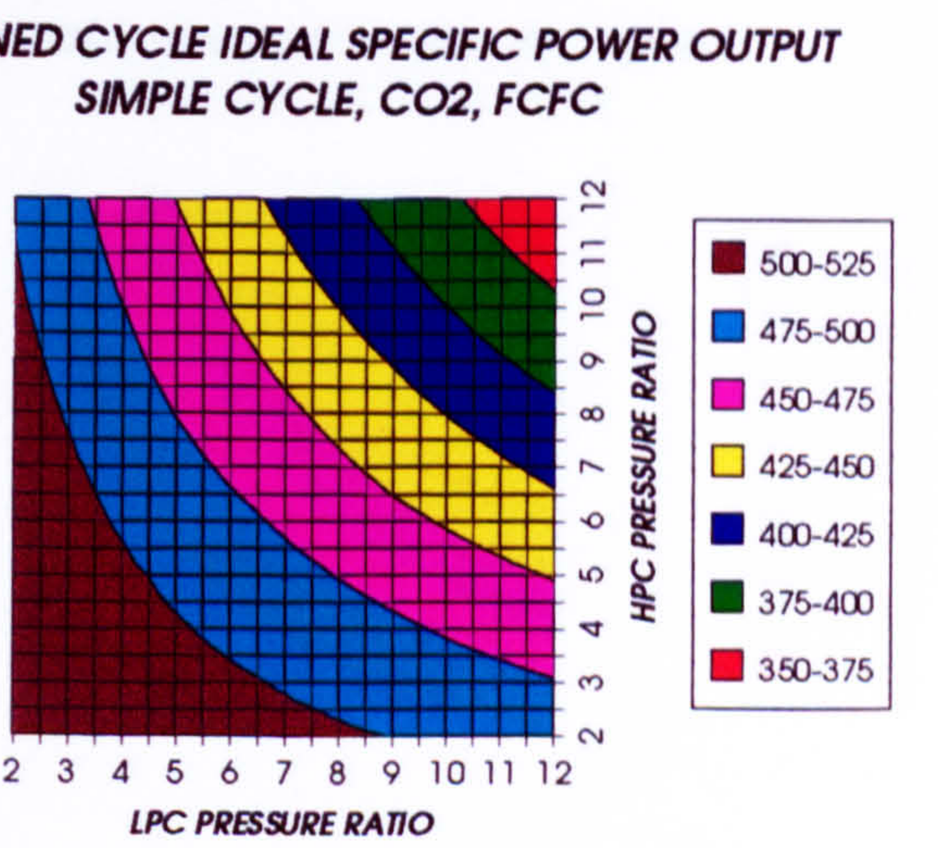

Figure 6. Combined cycle ideal specific power output

COMPLETE PLANT (TET=1473 K)

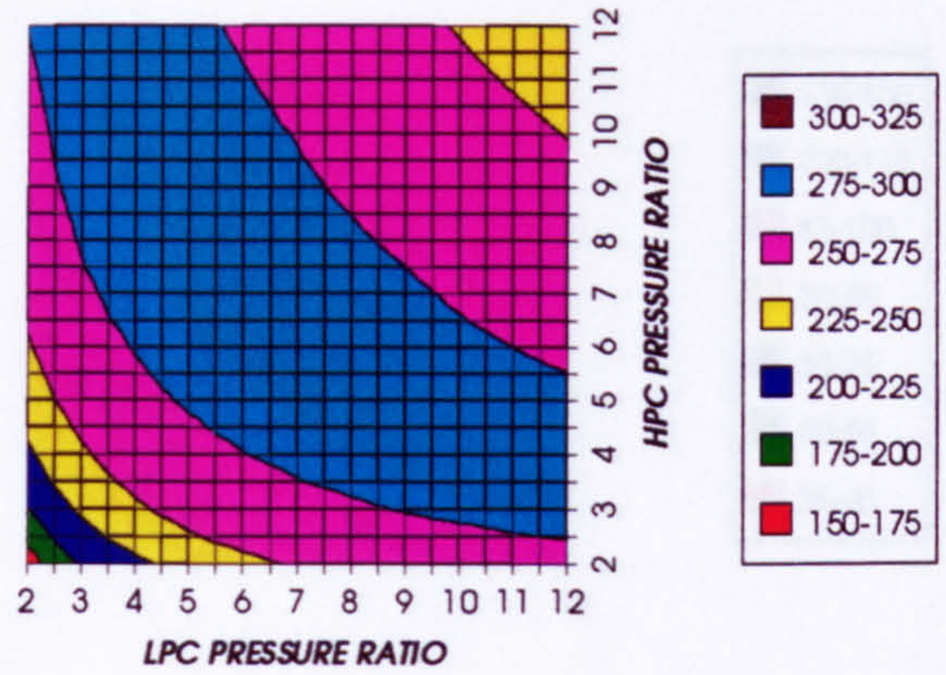

Figure 7. Gas turbine specific power output

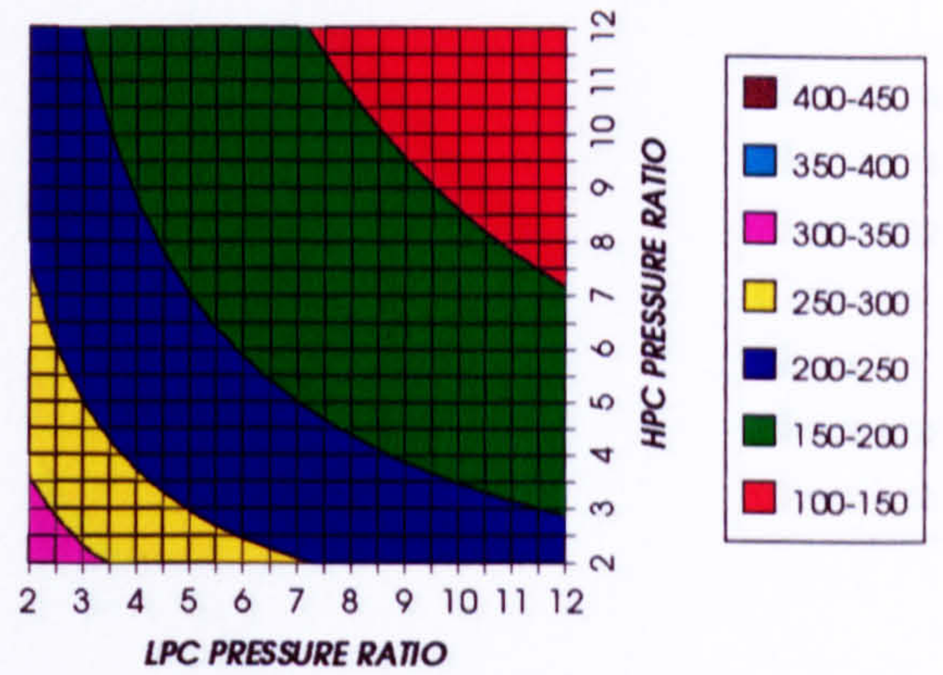

Figure 8 Steam turbine specific power output

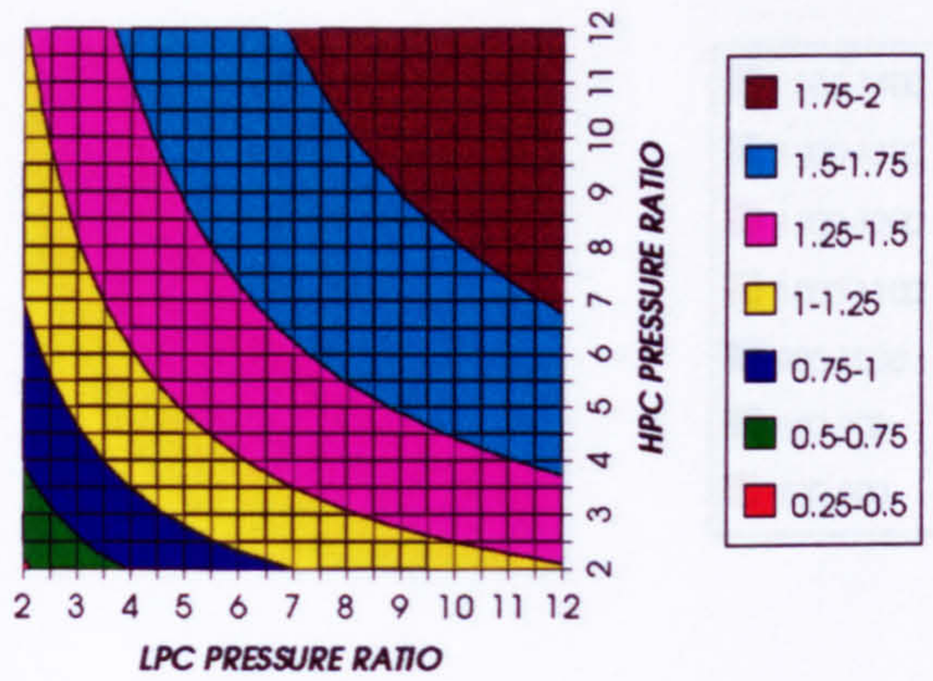

Figure 9. Gas turbine to steam turbine power ratio

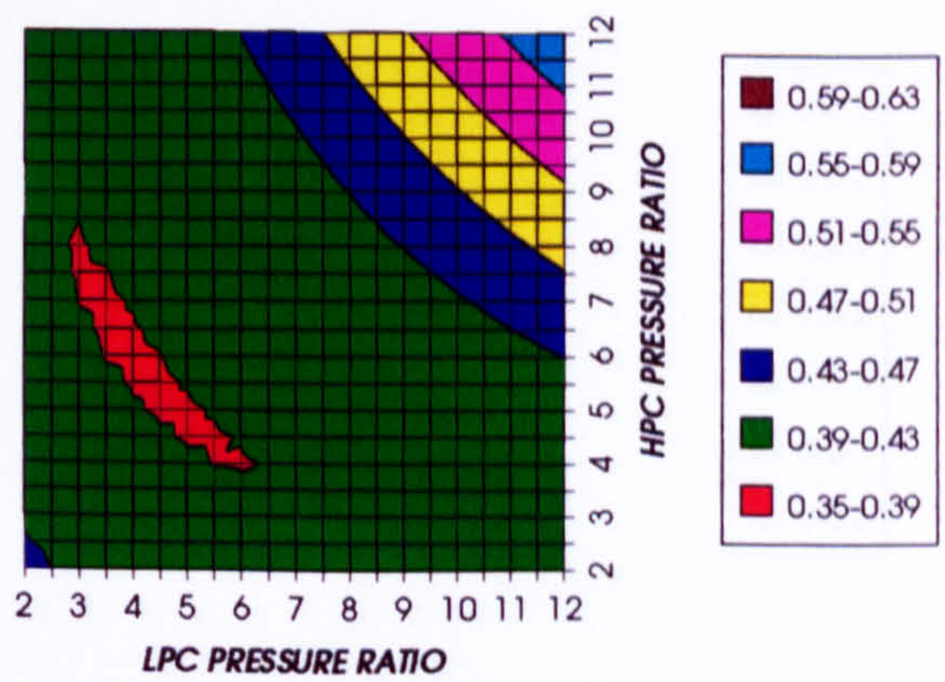

Figure 10. Auxiliary (CO2, O2 & Fuel) to usefuel power ratio

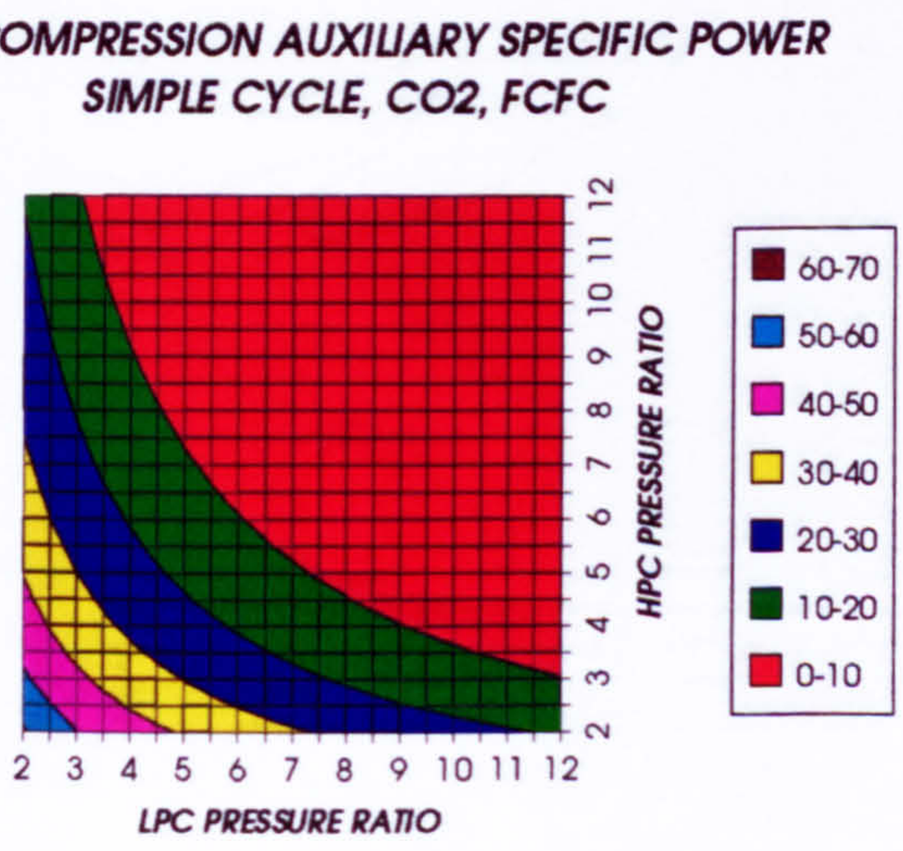

Figure 11. CO2 compression specific power

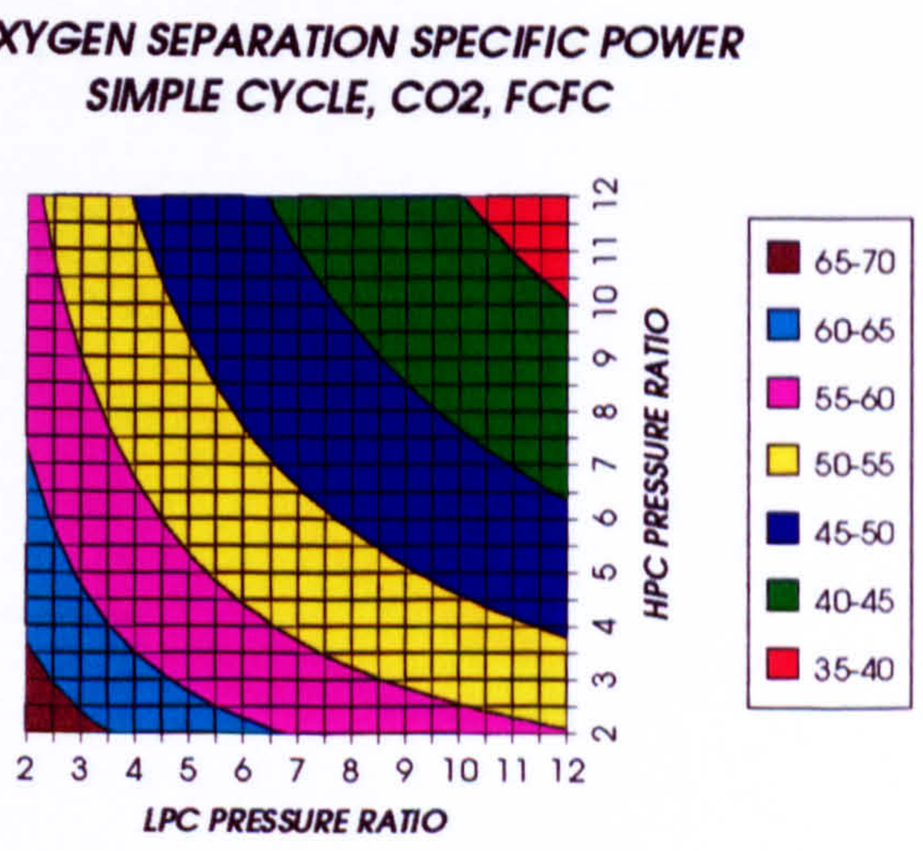

Figure 12. Oxygen separation specific power

COMPLETE PLANT (TET=1473 K)

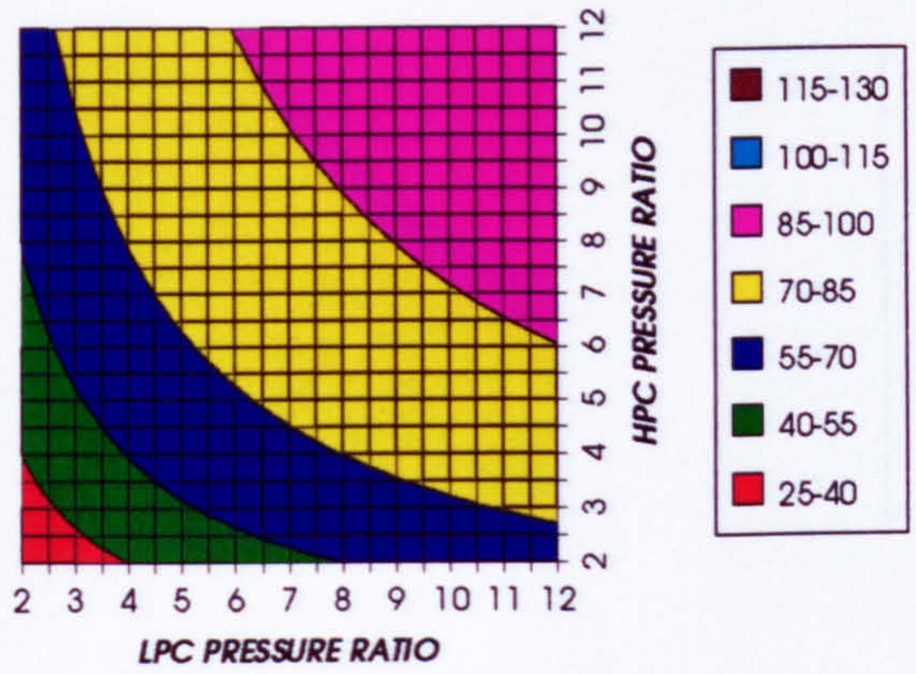

Figure 13. Fuel compression specific power

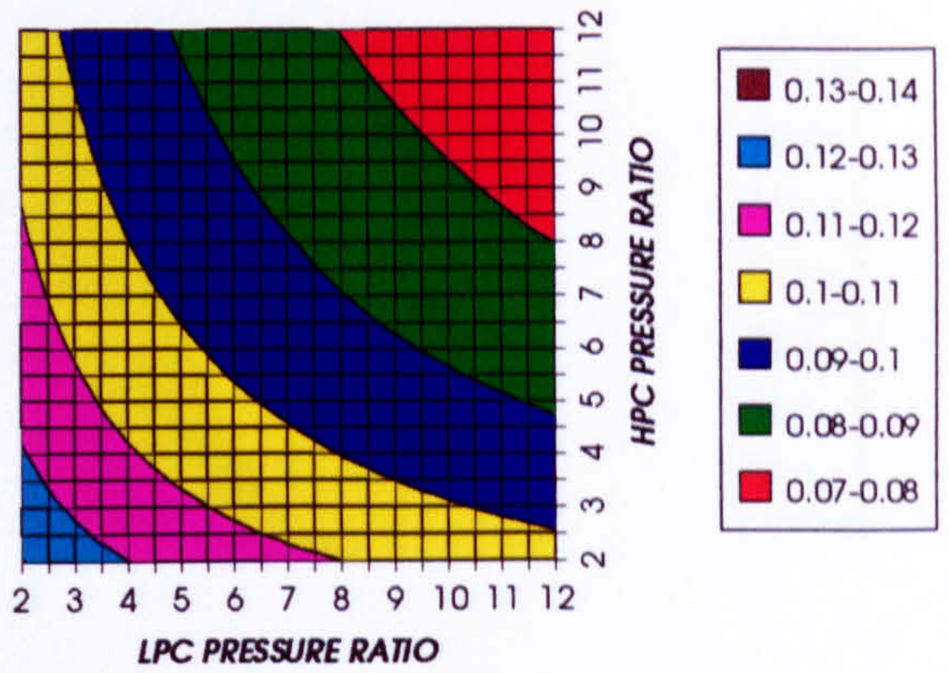

Figure 14 Fuel to compressor inlet mass flow ratio

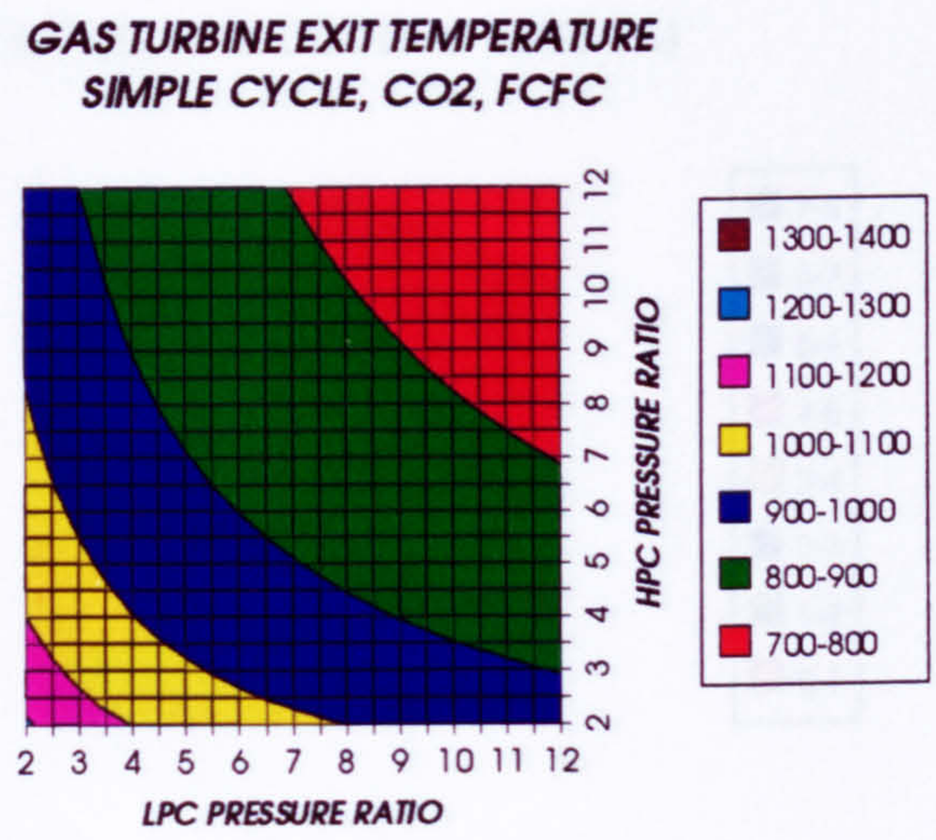

Figure 15. Gas turbine exit temperature

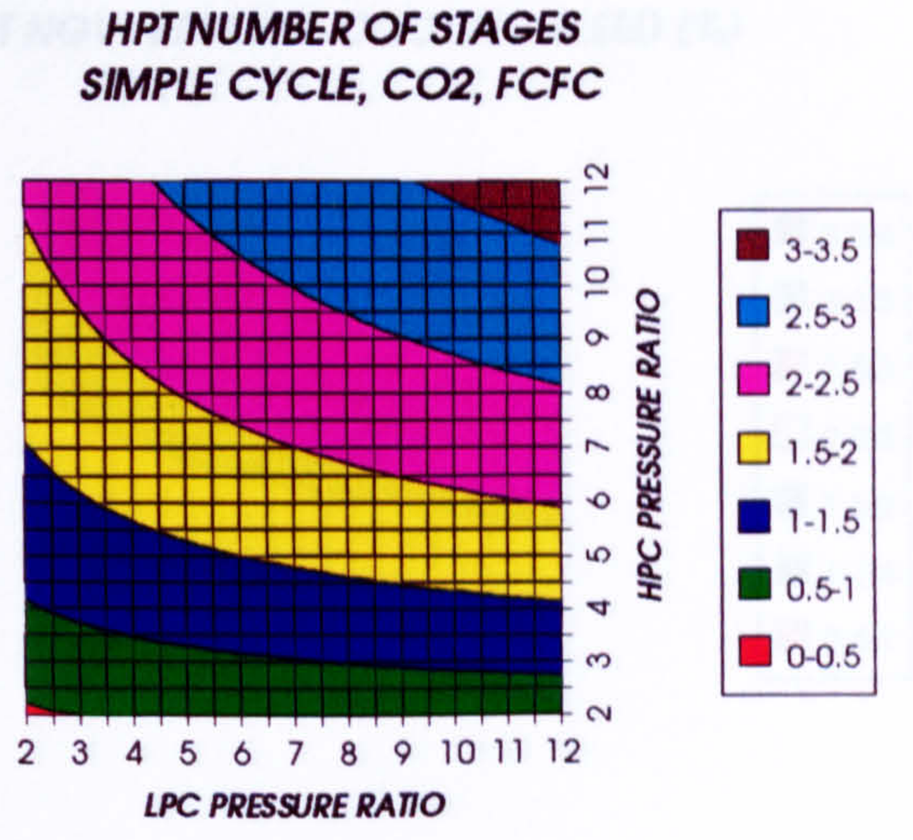

Figure 16. Number of HPT stages

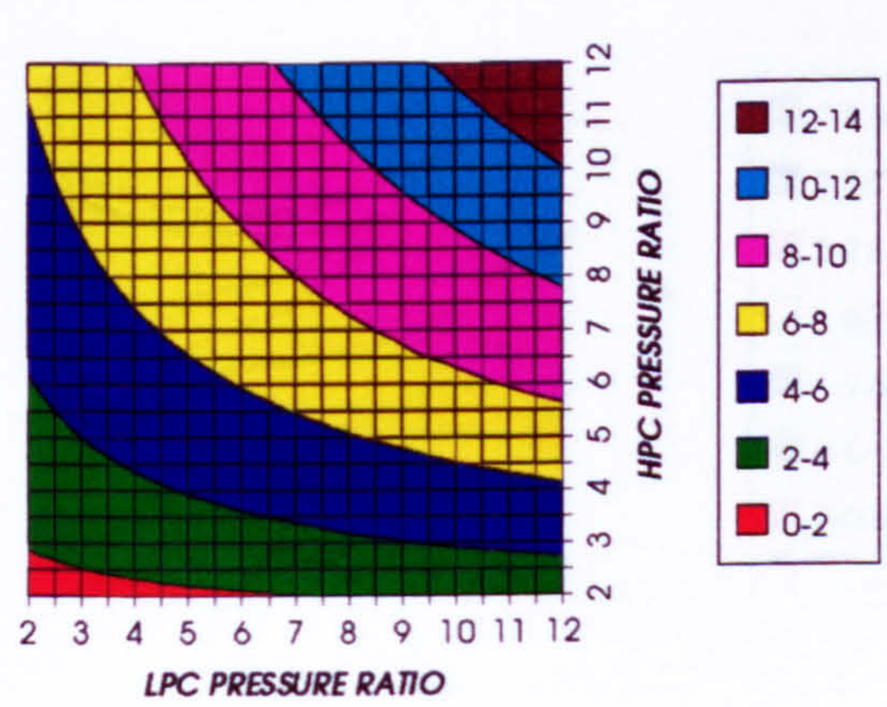

Figure 17. HPT cooling to compressor inlet mass flow ratio

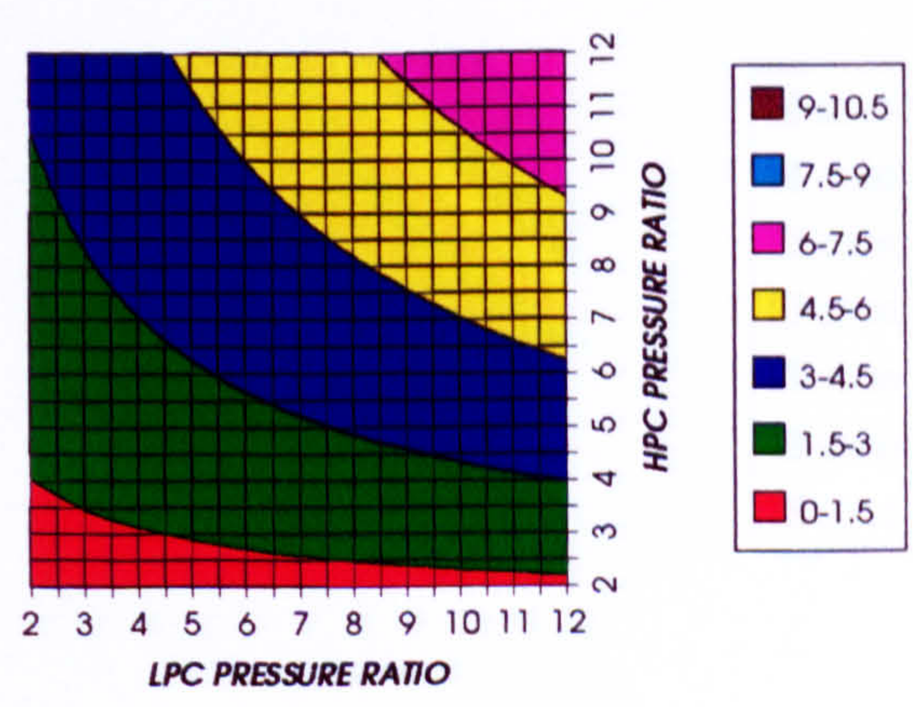

Figure 18. HPT NGVs cooling to compressor inlet mass flow ratio

COMPLETE PLANT (TET=1473 K)

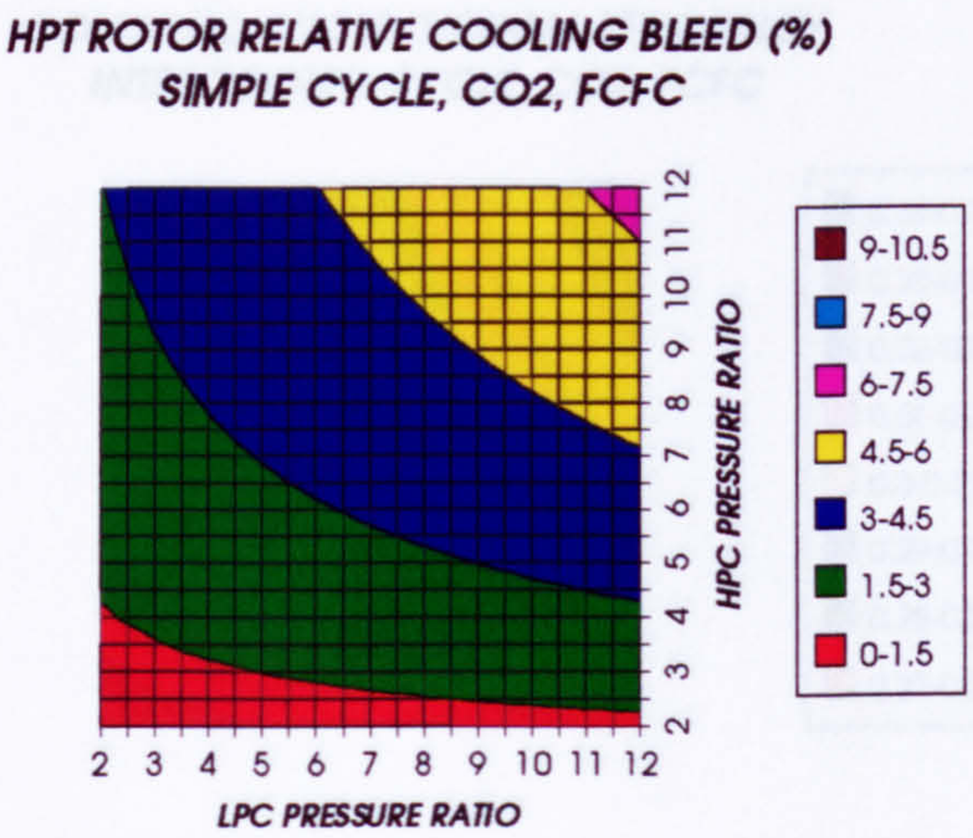

Figure 19. HPT rotor cooling to compressor inlet mass flow ratio

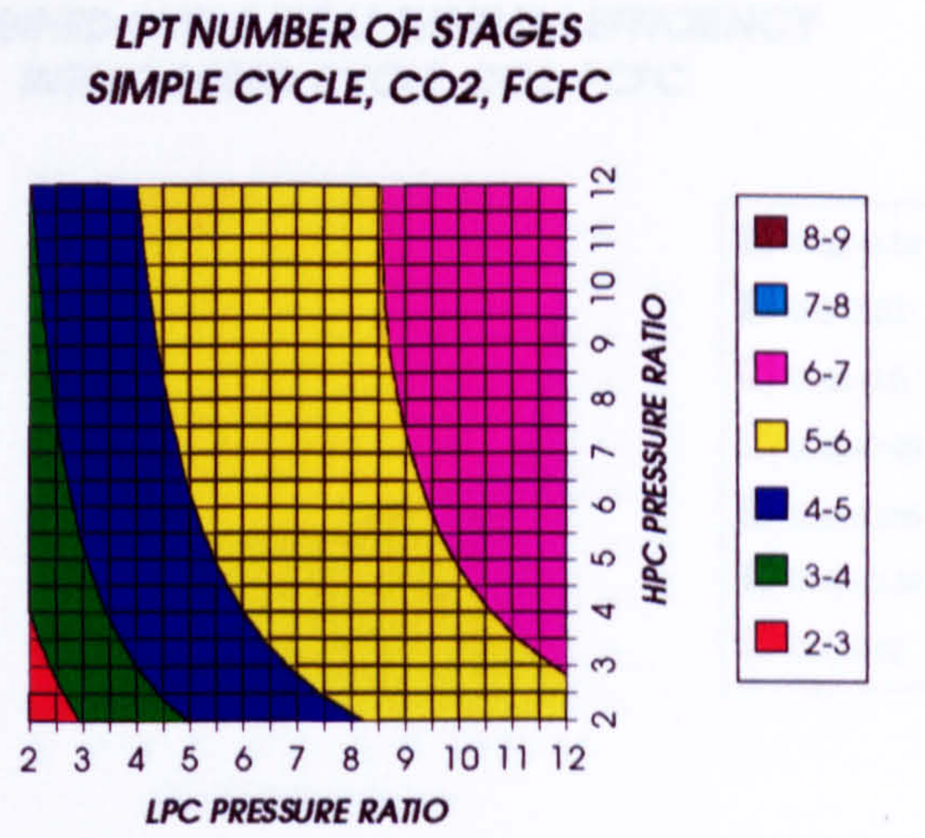

Figure 20. Number of LPT stages

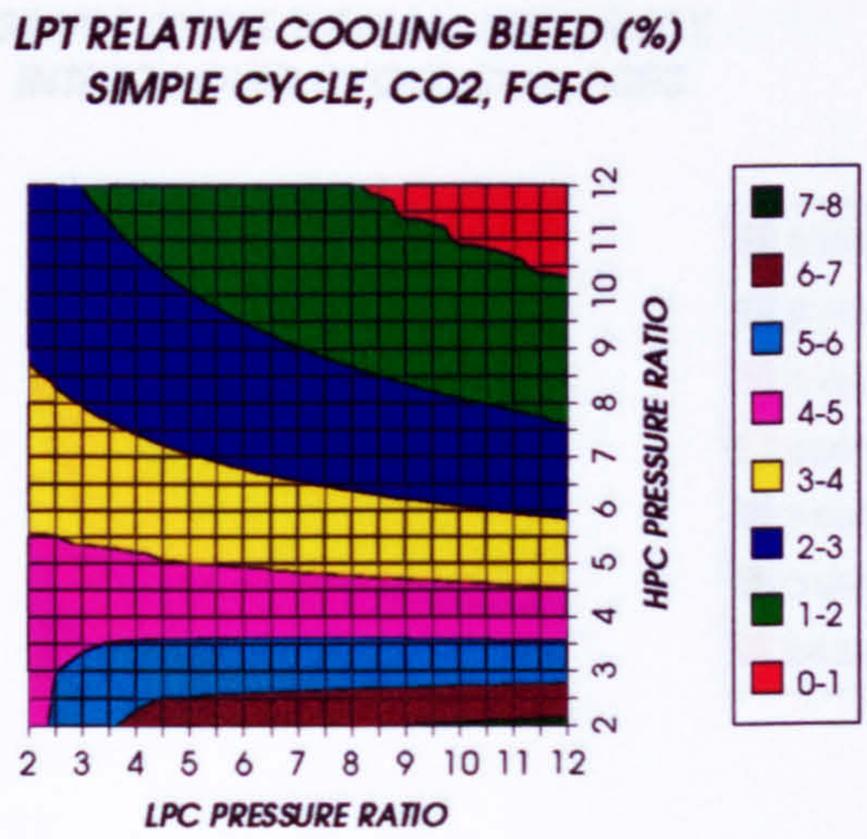

Figure 21.LPT cooling to compressor inlet mass flow ratio

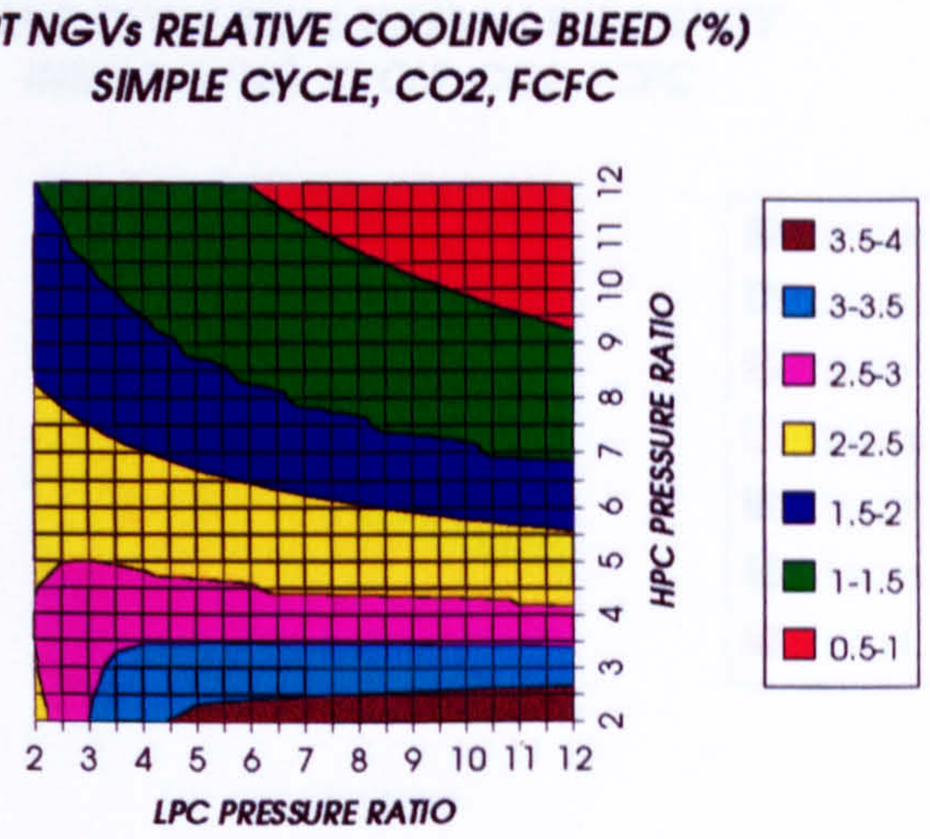

Figure 22. LPT NGVs cooling to compressor inlet mass flow ratio

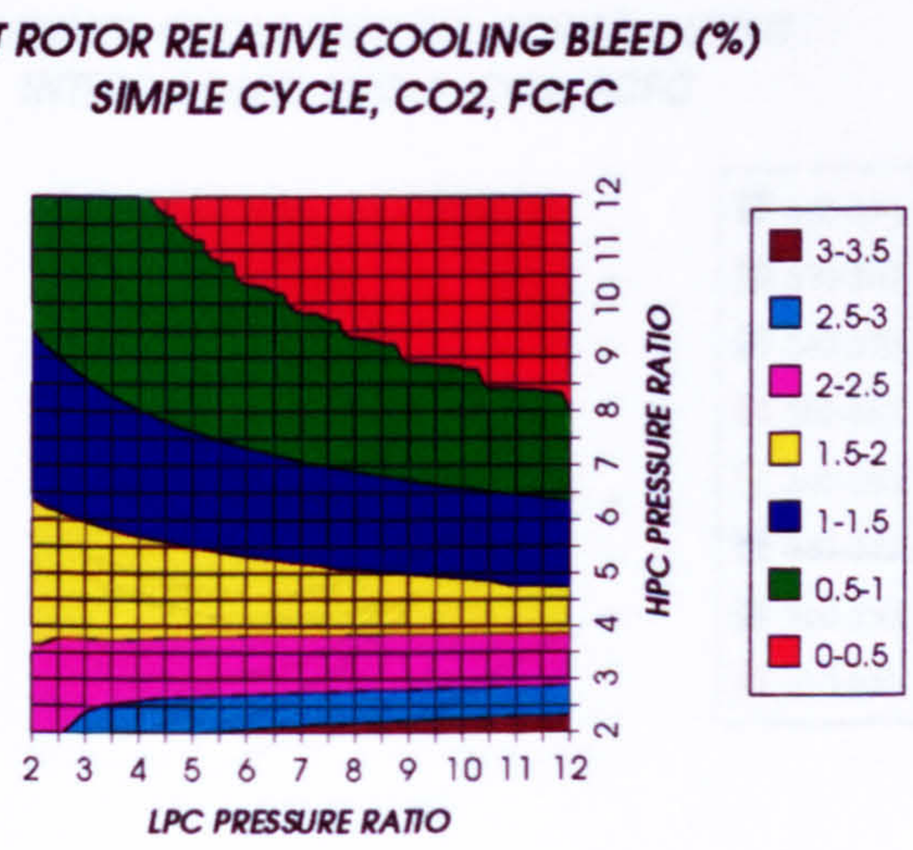

Figure 23. LPT rotor cooling to compressor inlet mass flow ratio

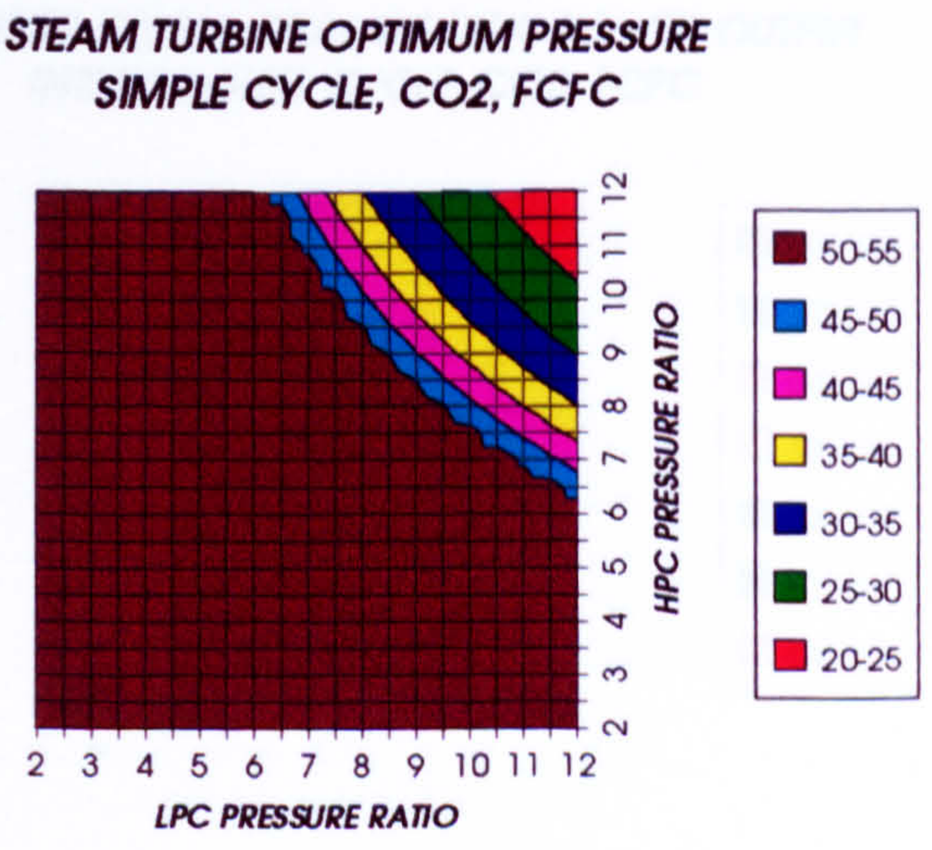

Figure 24. Steam turbine optimum pressures (maximum)

COMPLETE PLANT (TET=1473K)

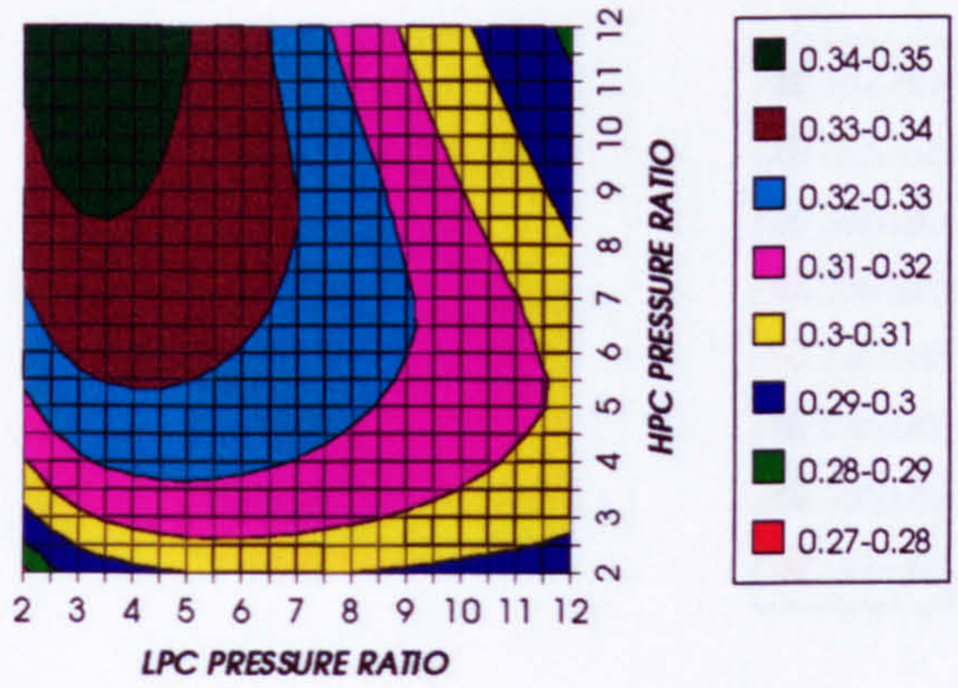

Figure 25. Combined cycle thermal efficiency

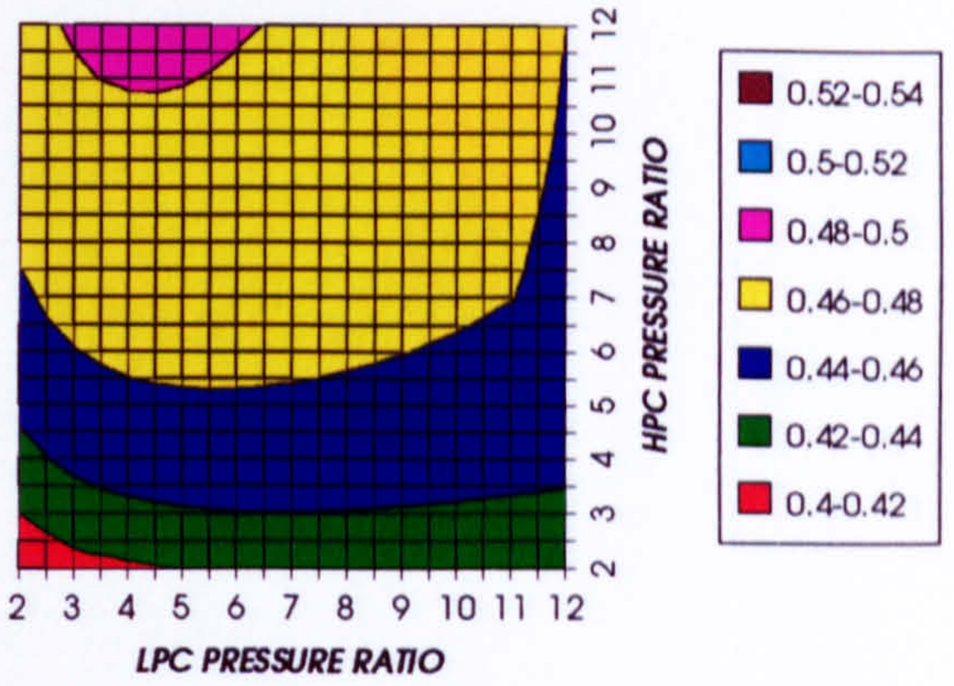

Figure 26. Combined cycle ideal thermal efficiency

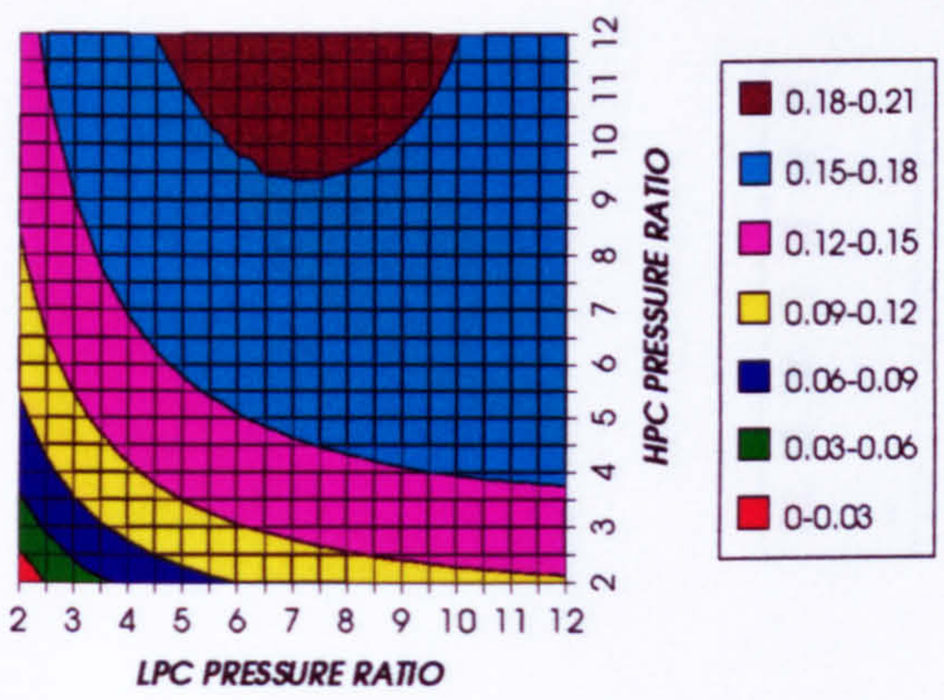

Figure 27. Simple cycle thermal efficiency

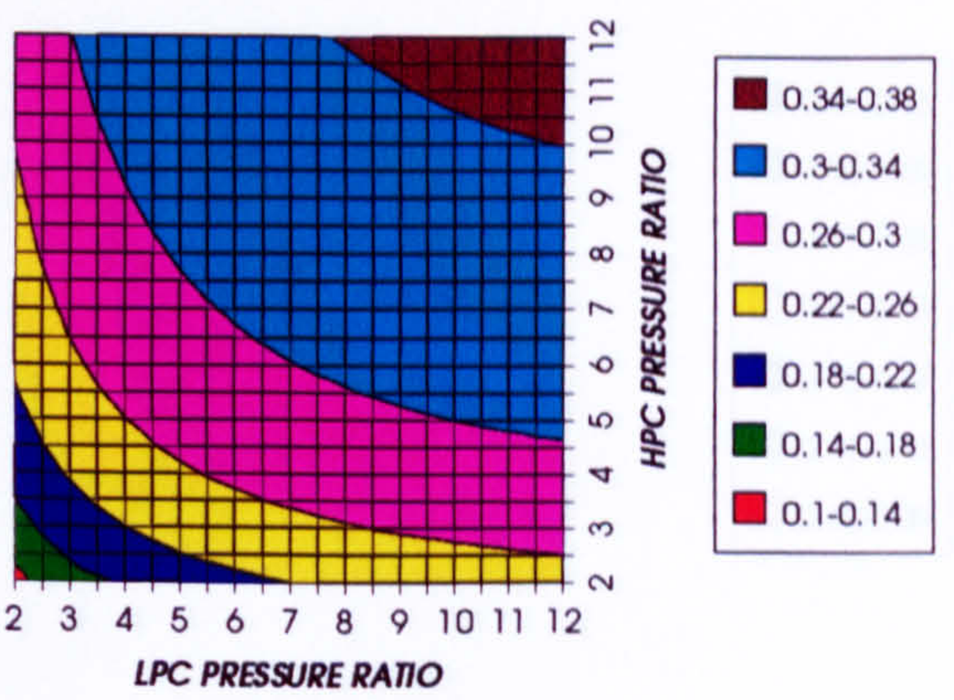

Figure 28. Simple cycle ideal thermal efficiency

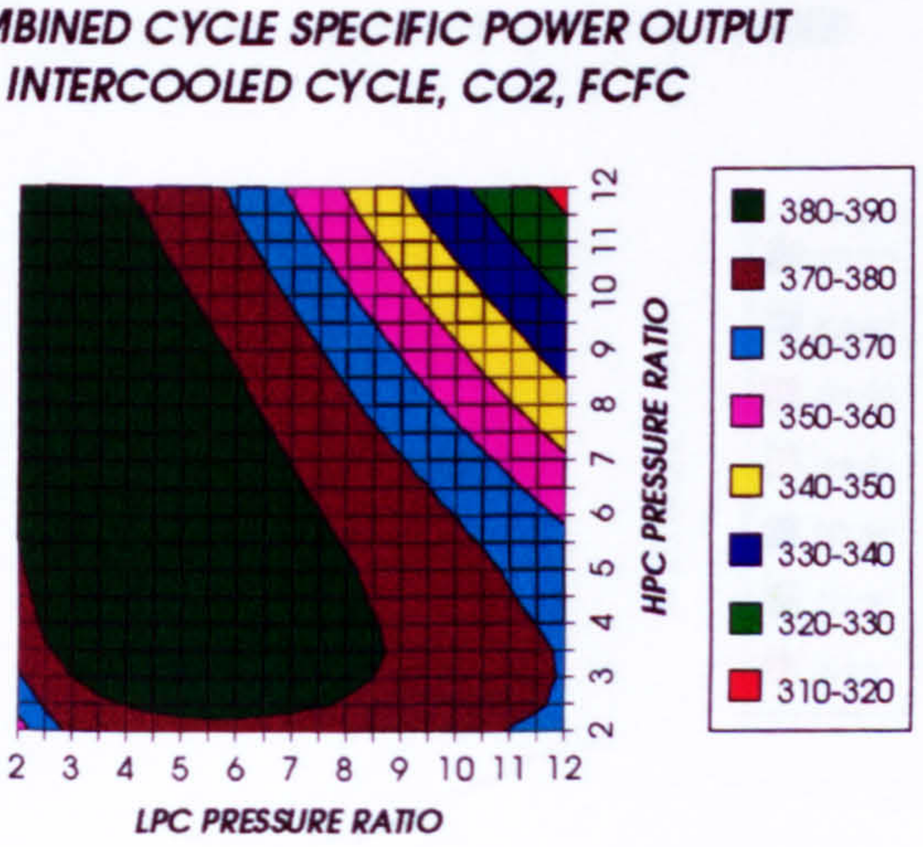

Figure 29. Combined cycle specific power output

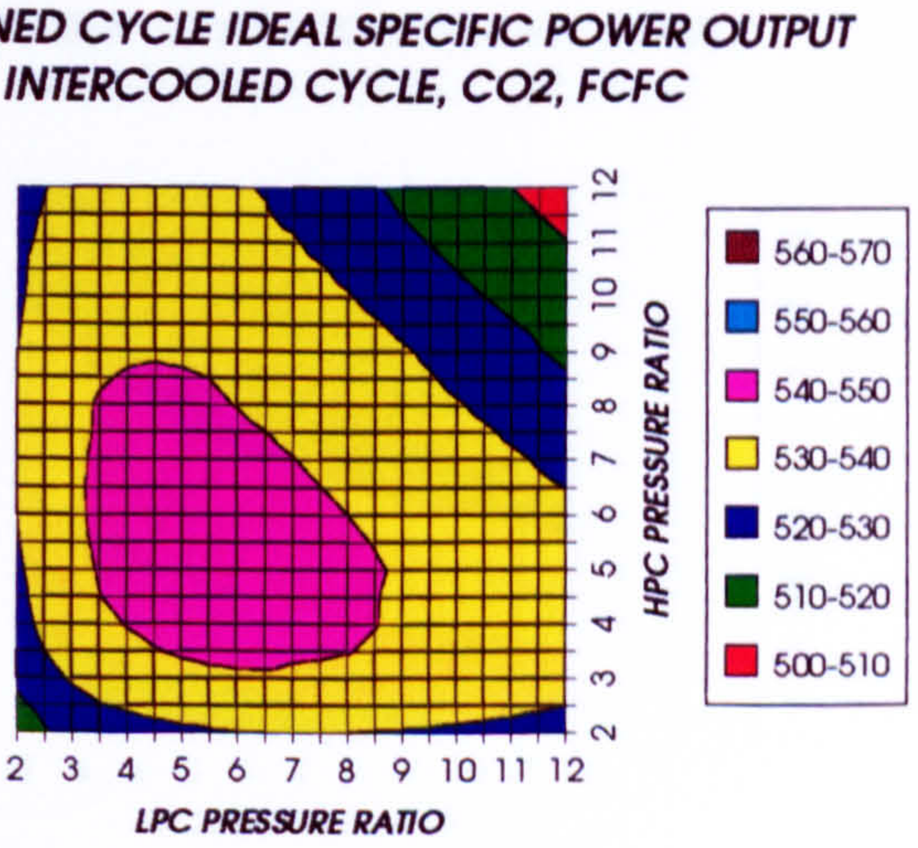

Figure 30. Combined cycle ideal specific power output

COMPLETE PLANT (TET=1473 K)

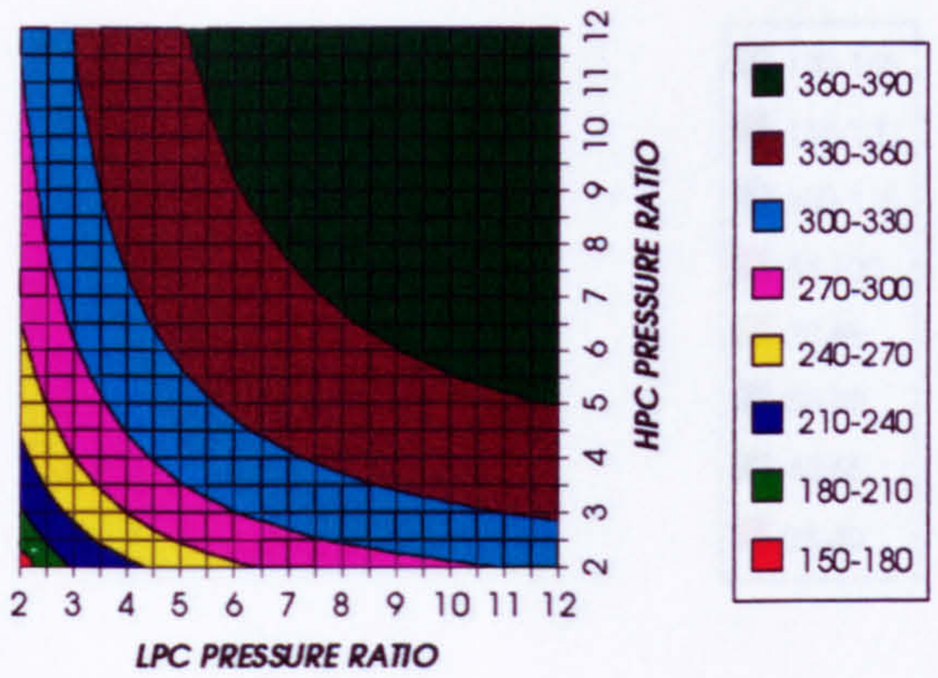

Figure 31. Gas turbine specific power output

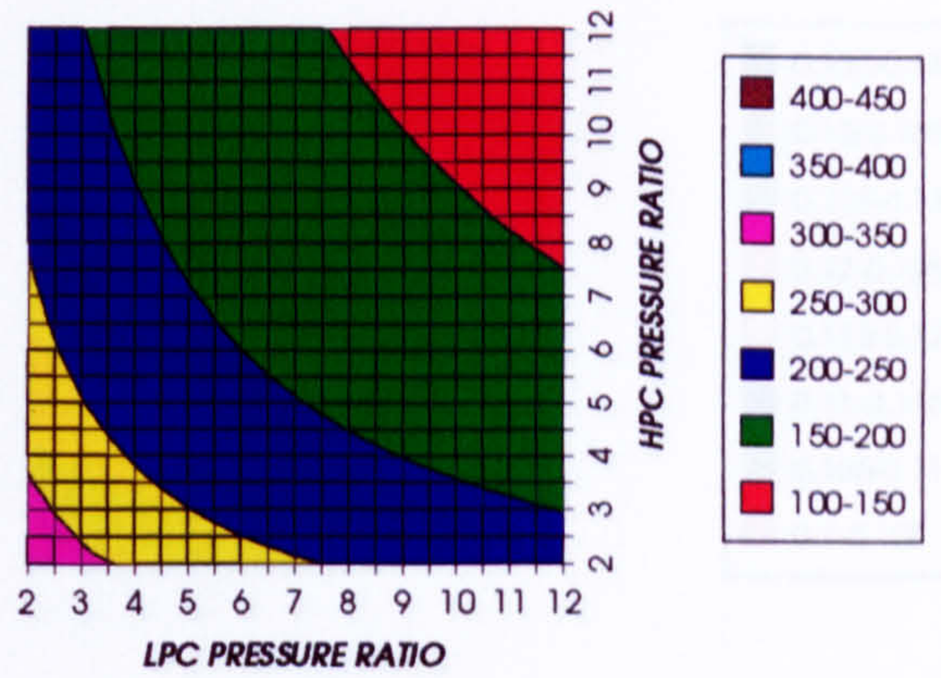

Figure 32 Steam turbine specific power output

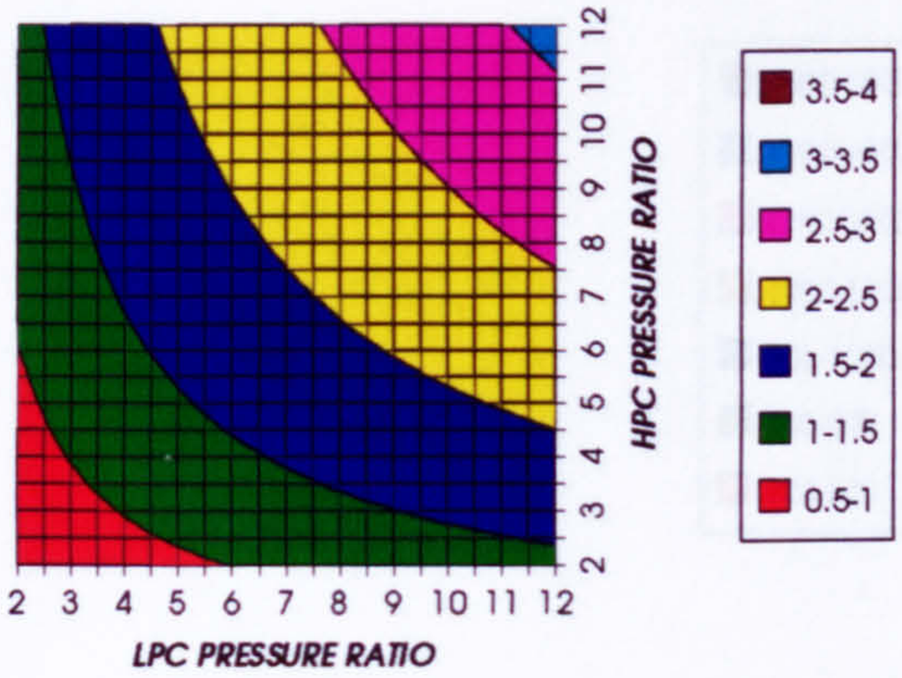

Figure 33. Gas turbine to steam turbine power ratio

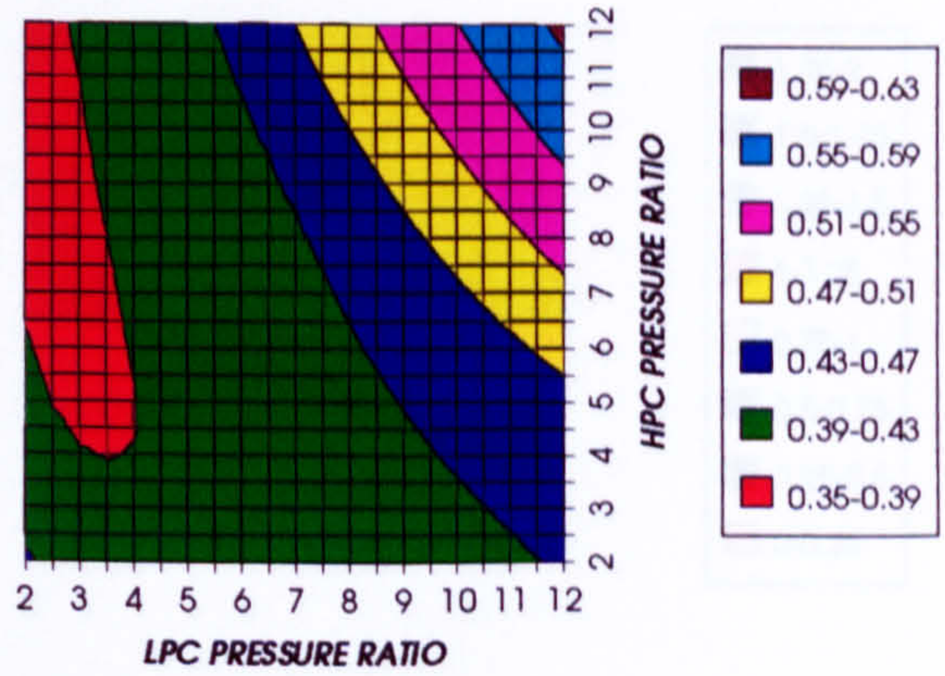

Figure 34. Auxiliary (CO2, O2 & Fuel) to usefuel power ratio

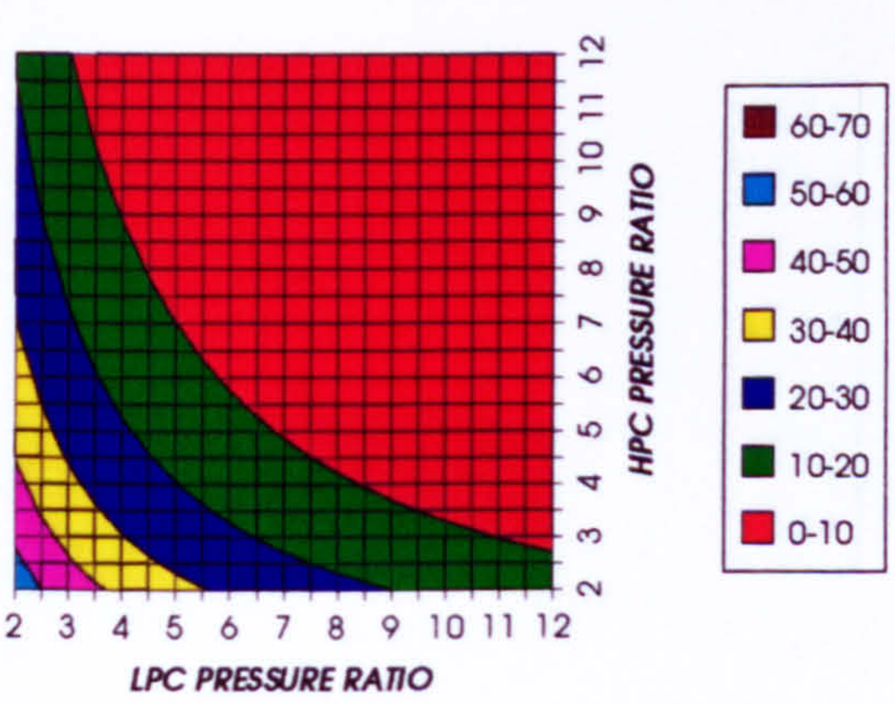

Figure 35. CO2 compression specific power

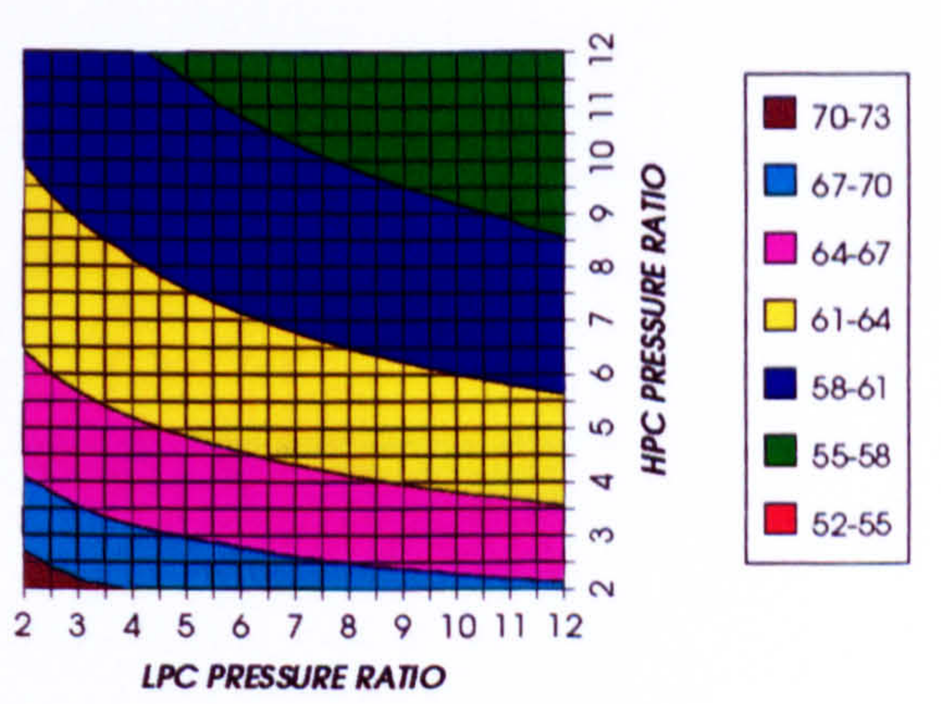

Figure 36. Oxygen separation specific power

COMPLETE PLANT (TET=1473 K)

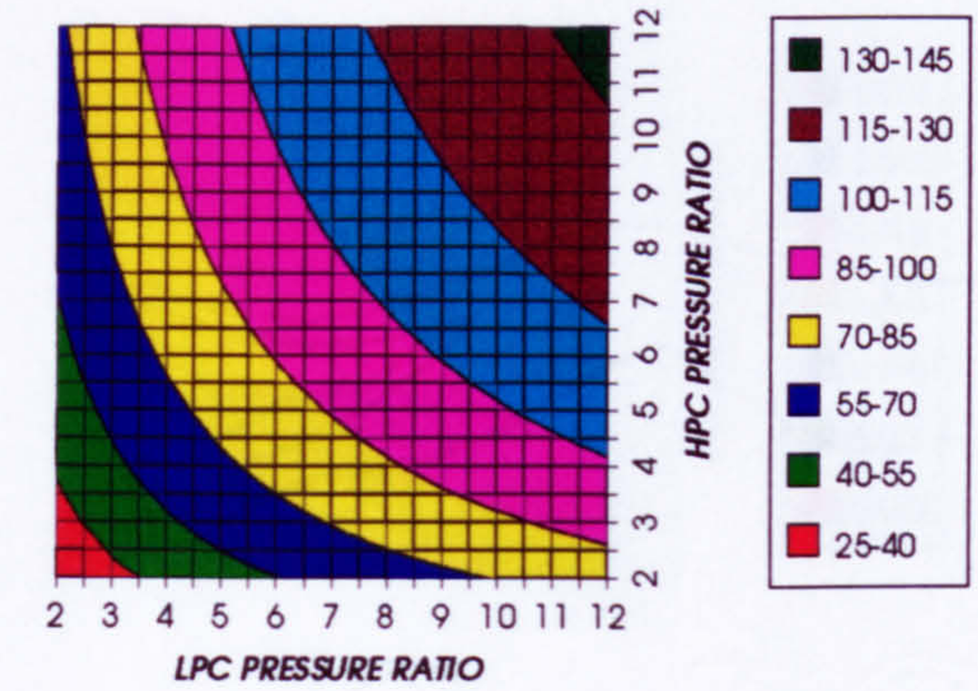

Figure 37. Fuel compression specific power

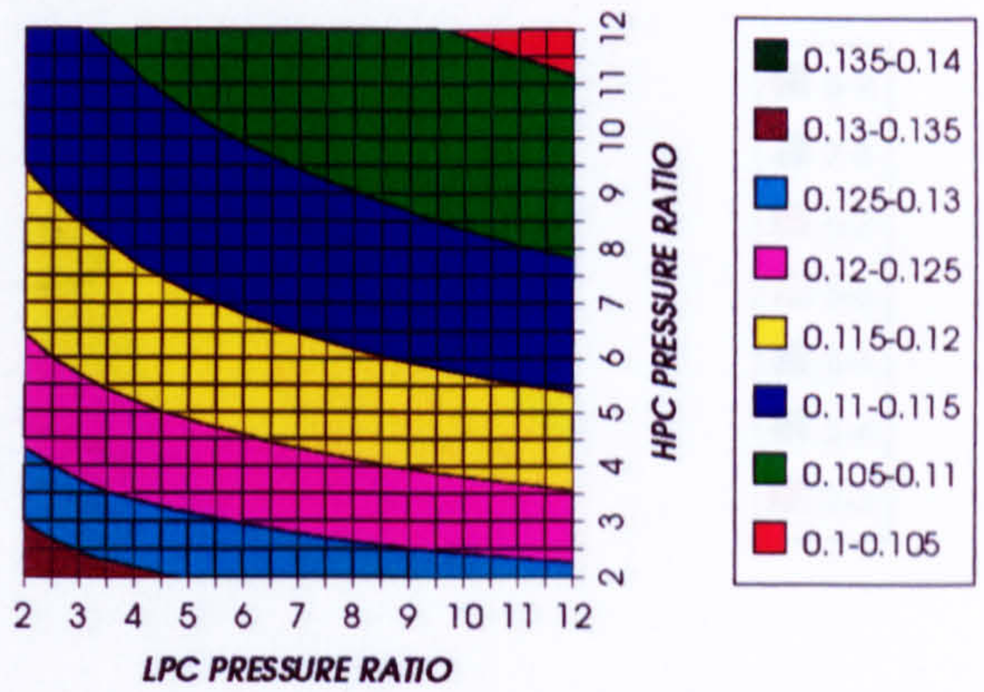

Figure 38 Fuel to compressor inlet mass flow ratio

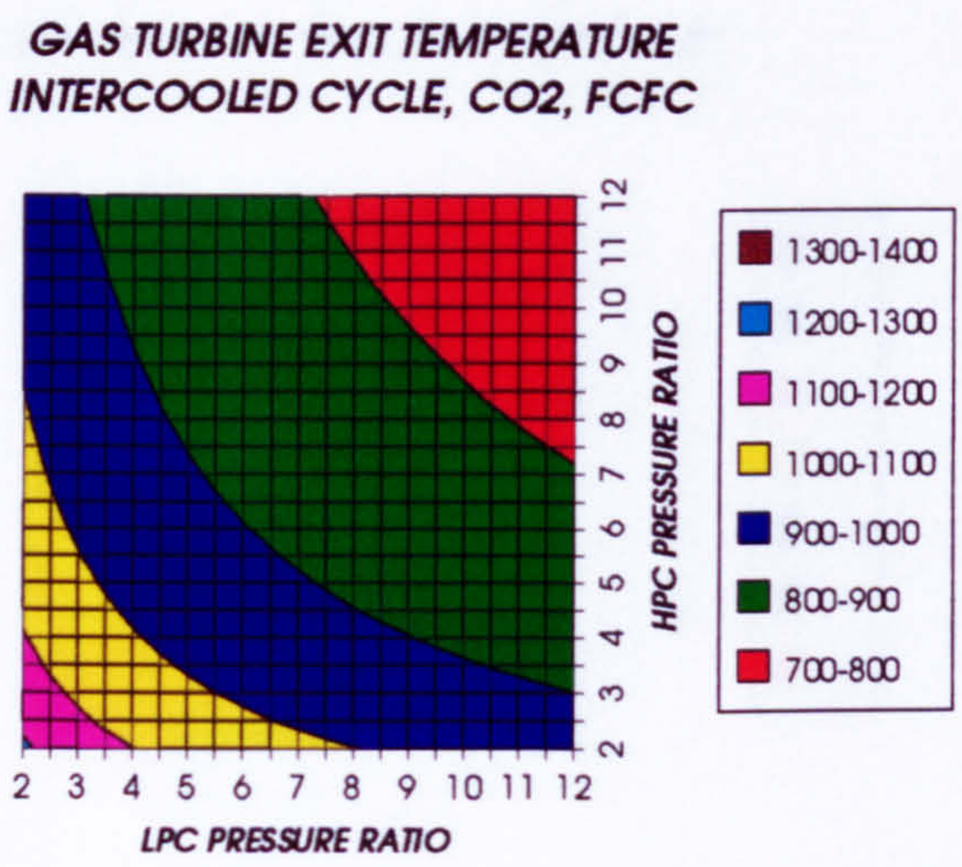

Figure 39. Gas turbine exit temperature

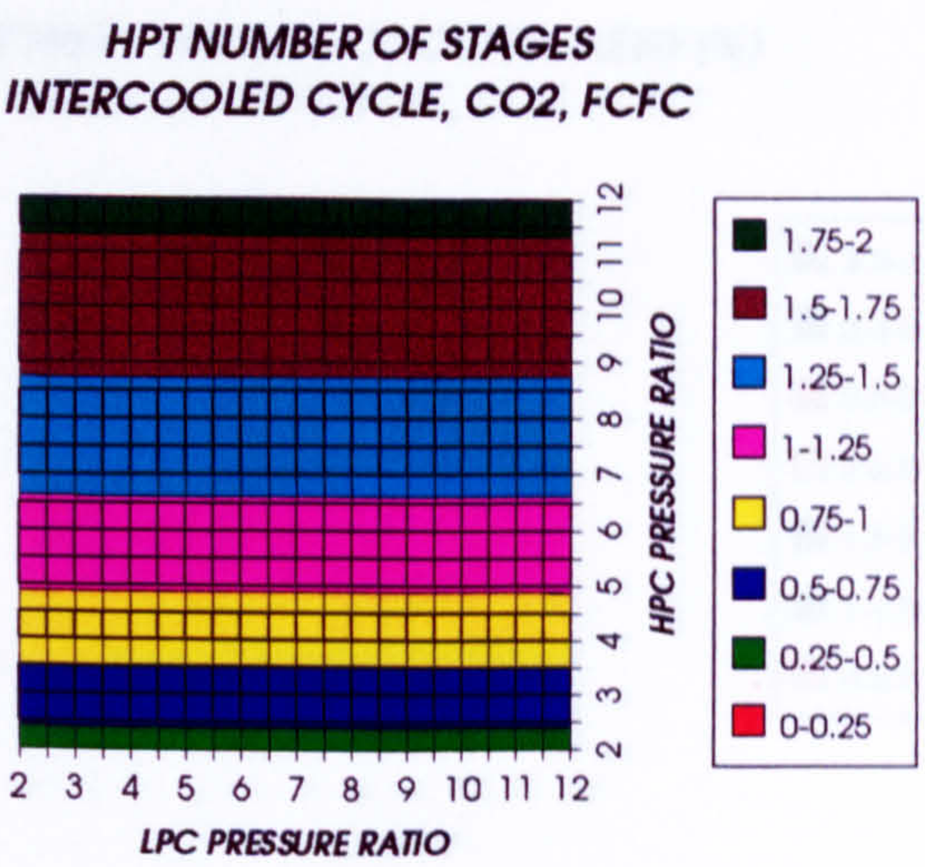

Figure 40. Number of HPT stages

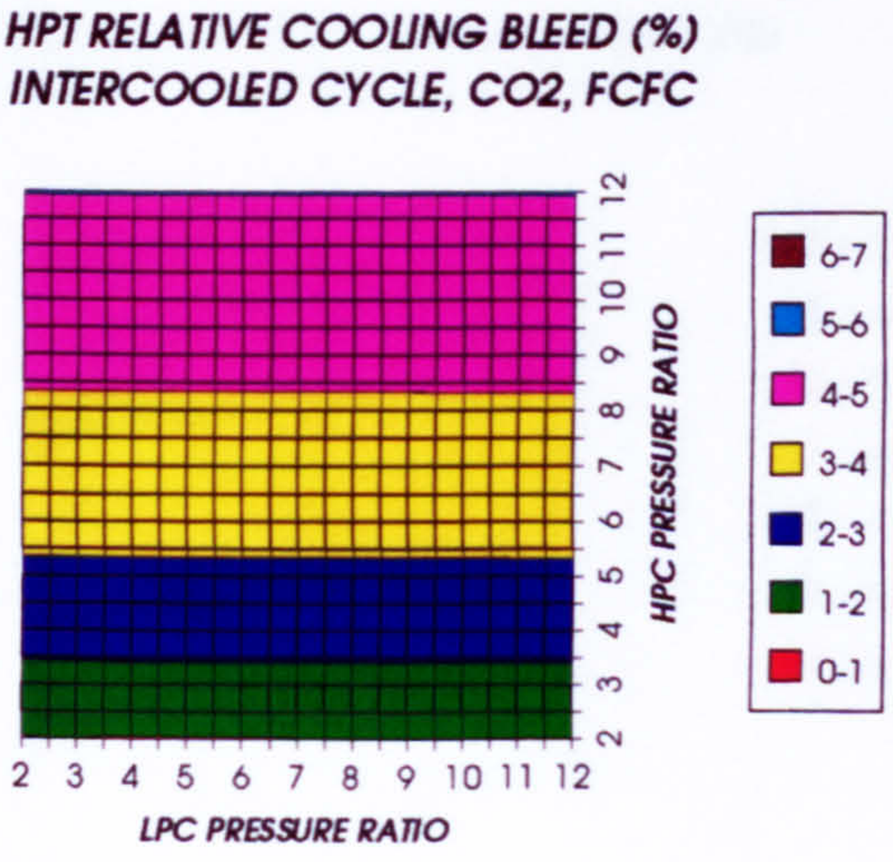

Figure 41. HPT cooling to compressor inlet mass flow ratio

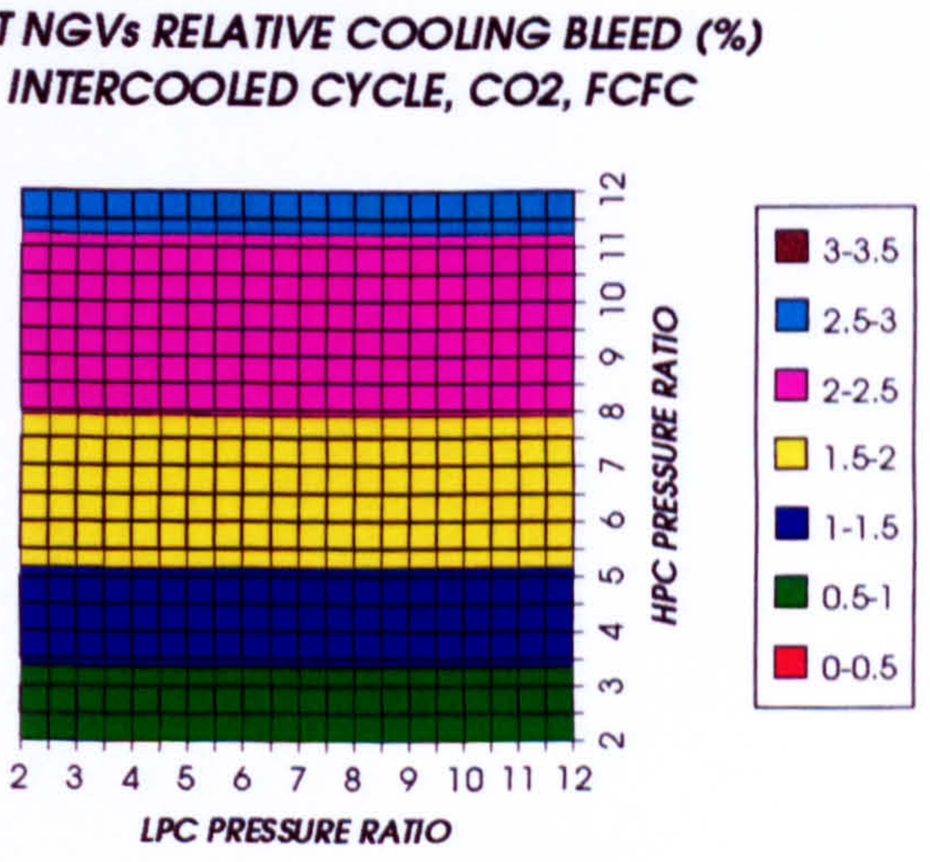

Figure 42. HPT NGVs cooling to compressor inlet mass flow ratio

COMPLETE PLANT (TET=1473 K)

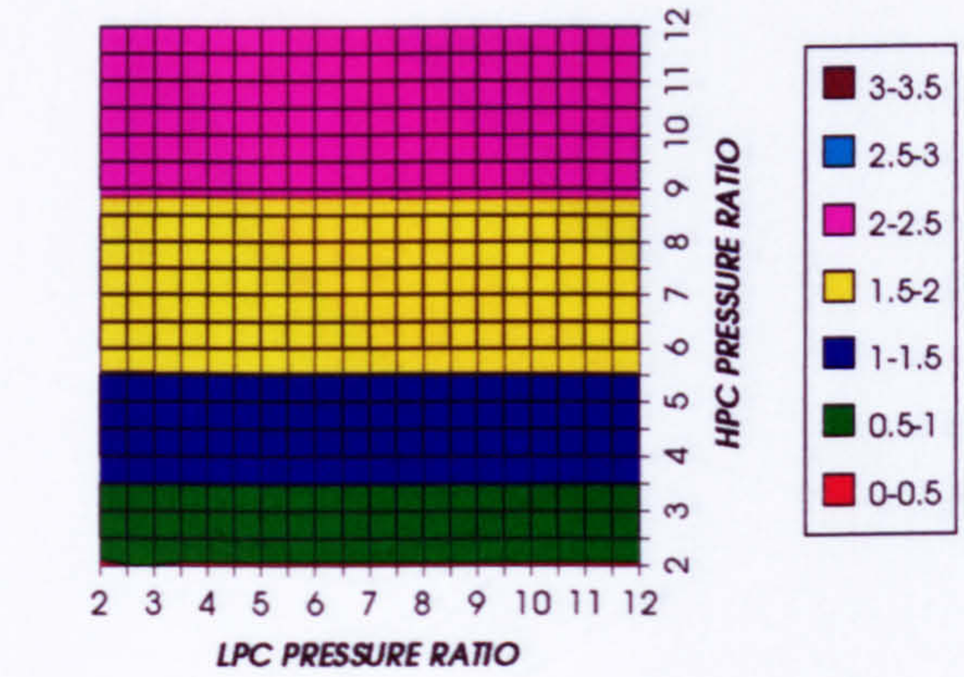

Figure 43. HPT rotor cooling to compressor inlet mass flow ratio

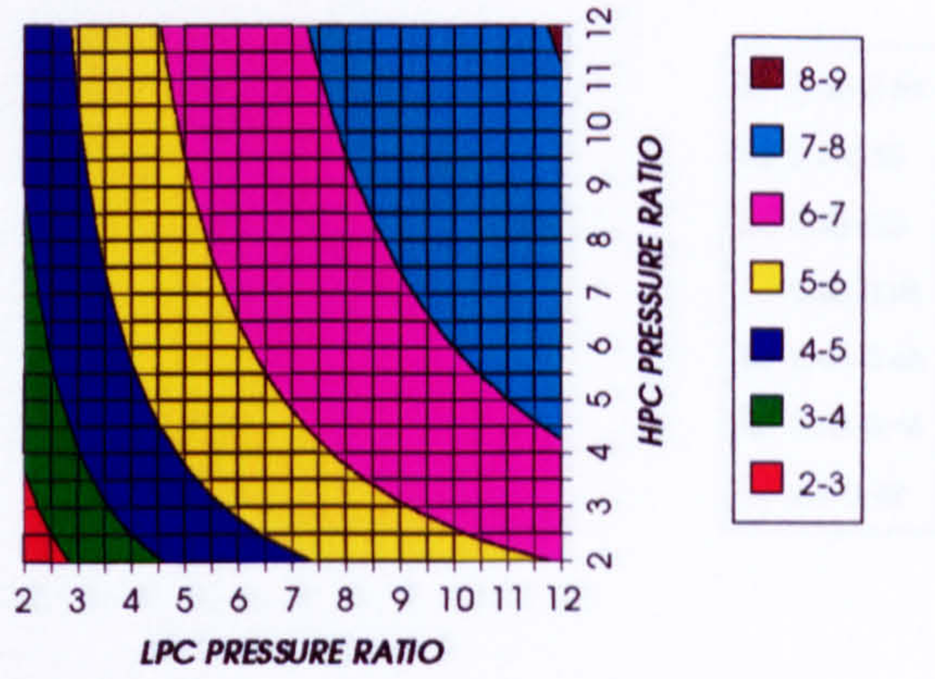

Figure 44. Number of LPT stages

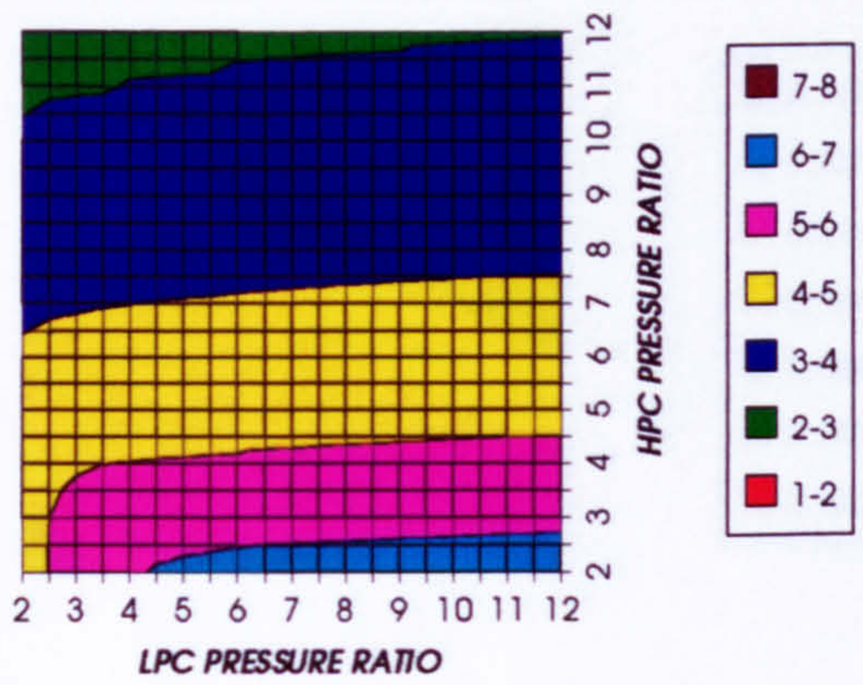

Figure 45.LPT cooling to compressor inlet mass flow ratio

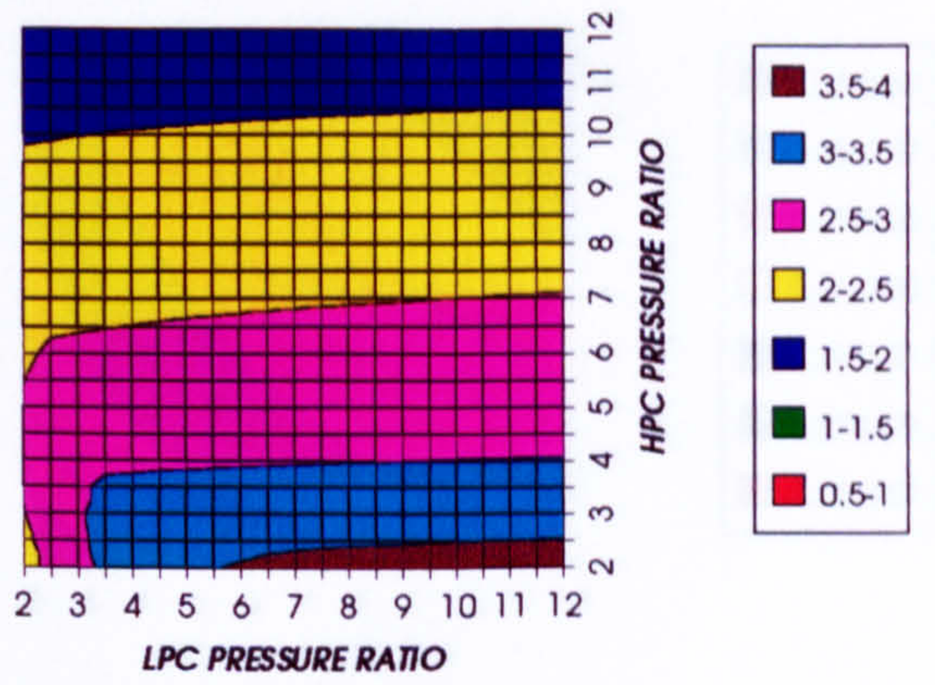

Figure 46. LPT NGVs cooling to compressor inlet mass flow ratio

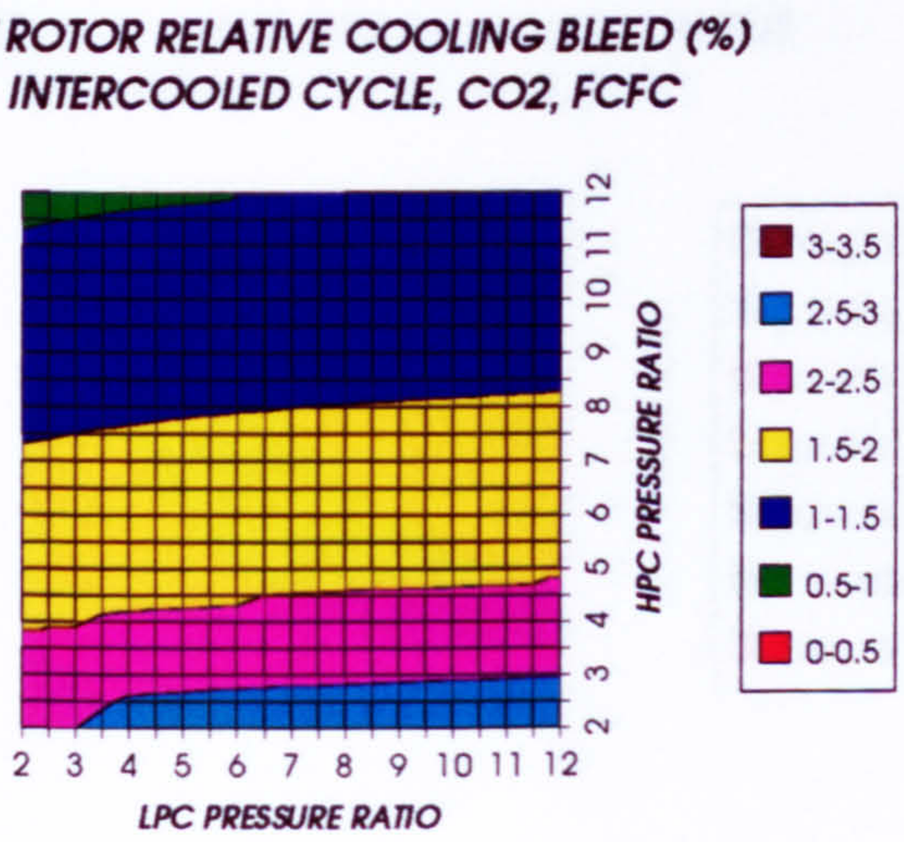

Figure 47. LPT rotor cooling to compressor inlet mass flow ratio

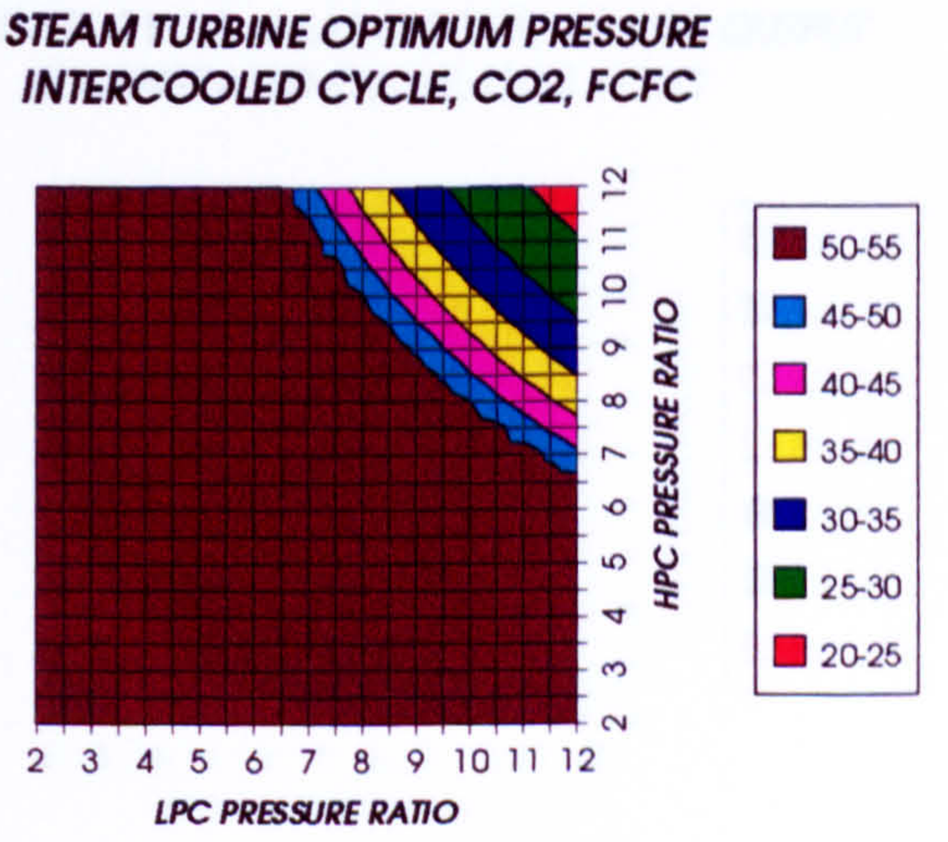

Figure 48. Steam turbine optimum pressures (maximum)

COMPLETE PLANT (TET=1473K)

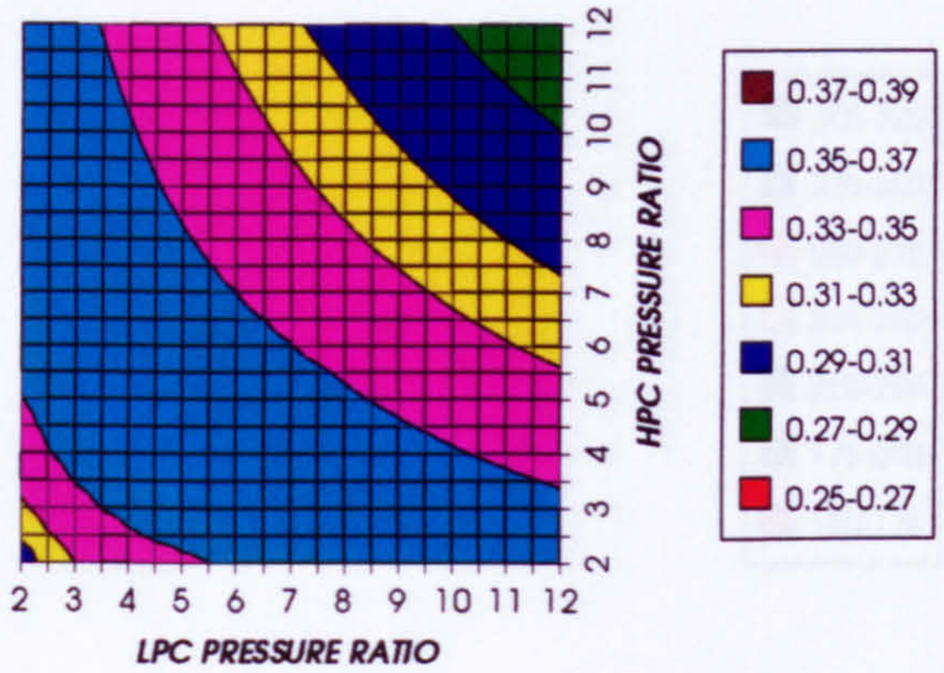

Figure 49. Combined cycle thermal efficiency

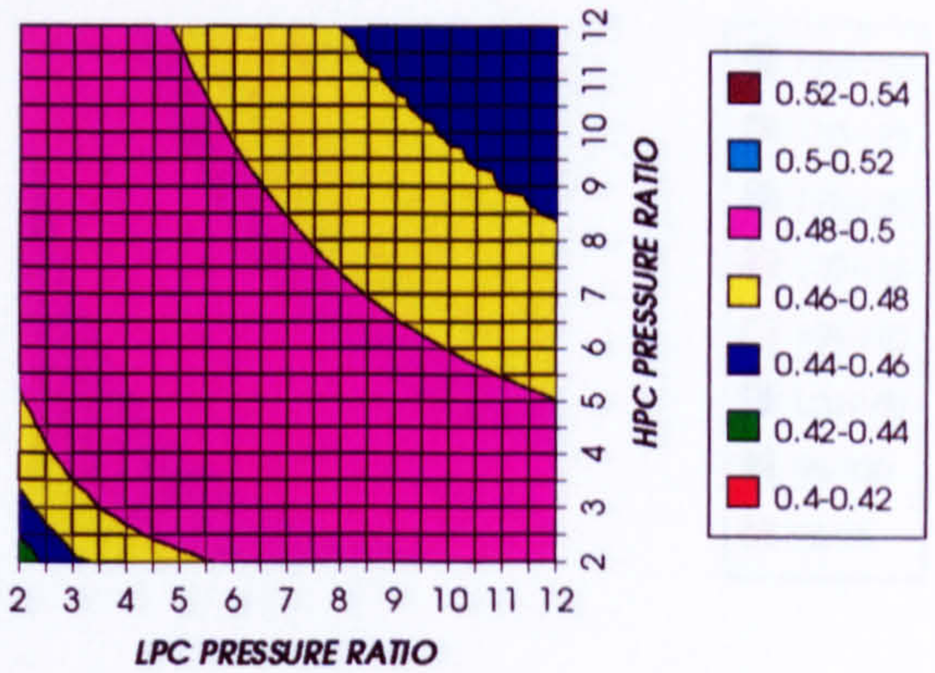

Figure 50. Combined cycle ideal thermal efficiency

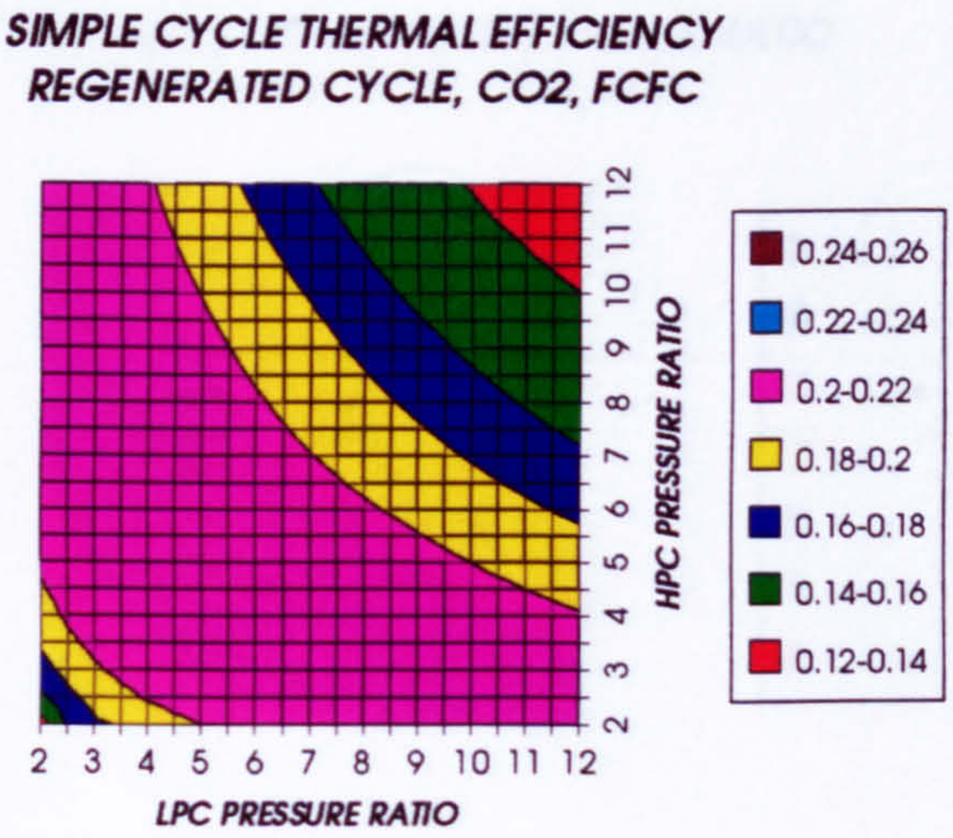

Figure 51. Simple cycle thermal efficiency

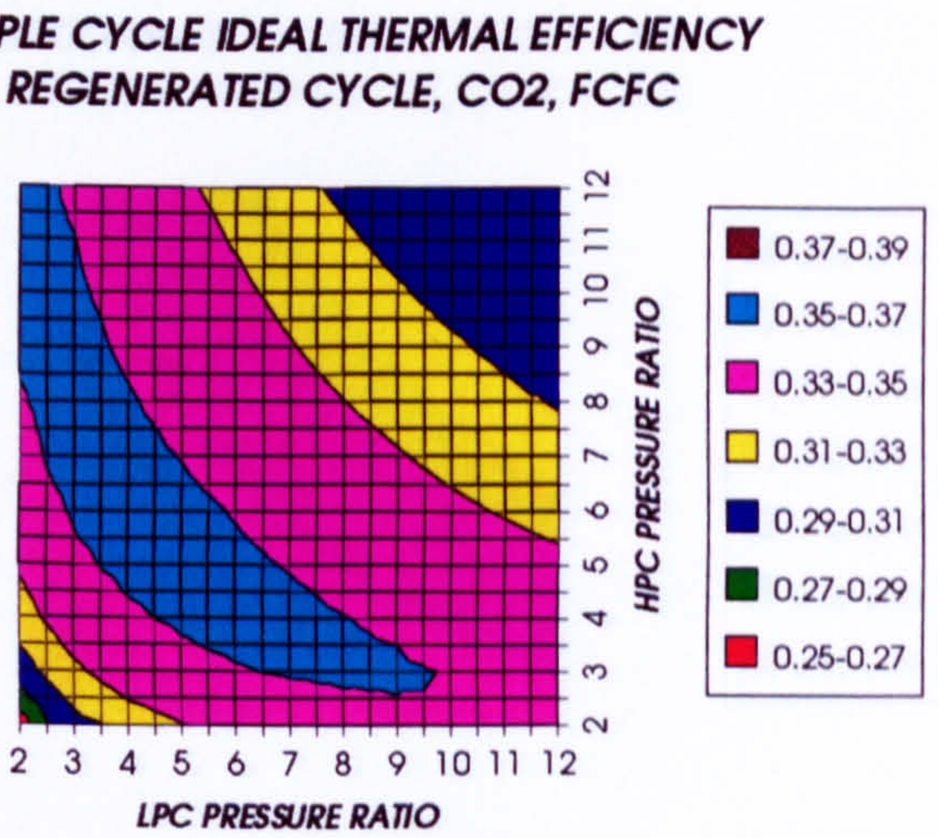

Figure 52. Simple cycle ideal thermal efficiency

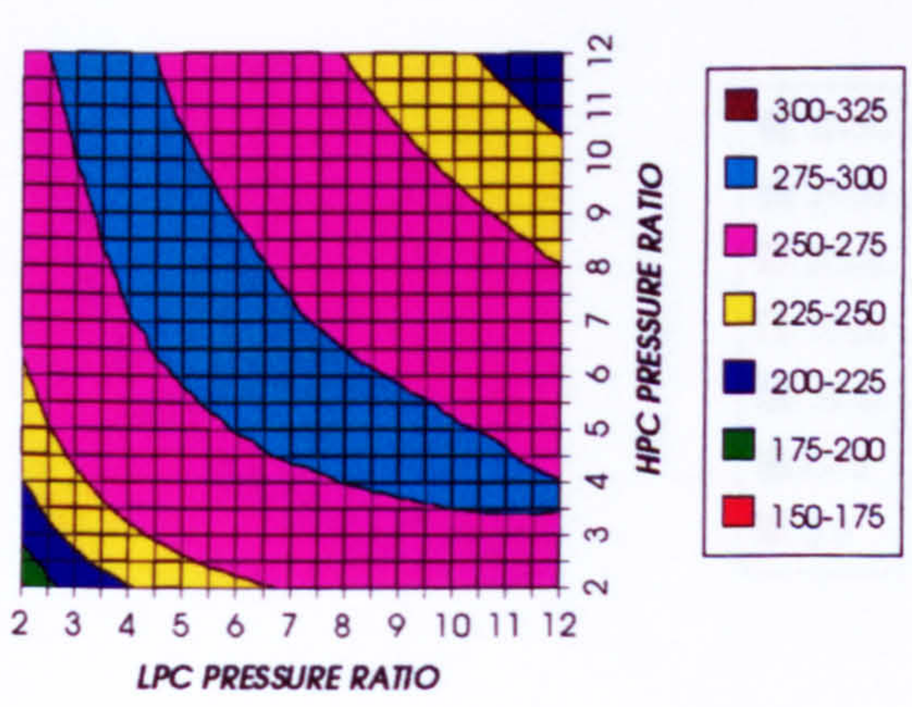

Figure 53. Combined cycle specific power output

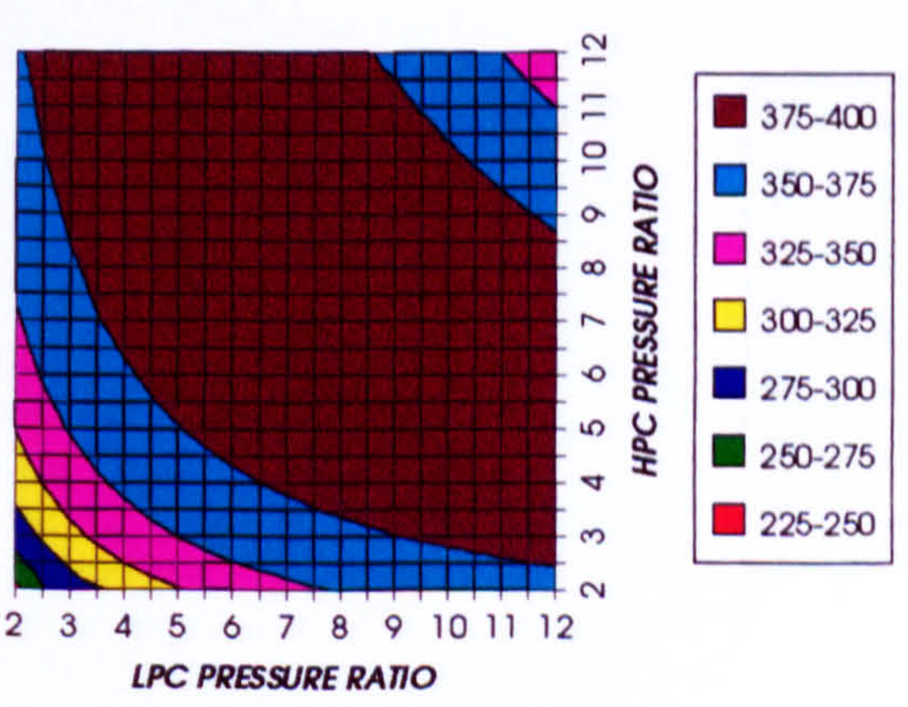

Figure54. Combined cycle ideal specific power output

COMPLETE PLANT (TET=1473 K)

GAS TURBINE SPECIFIC POWER OUTPUT
REGENERATED CYCLE, CO2, FCFC

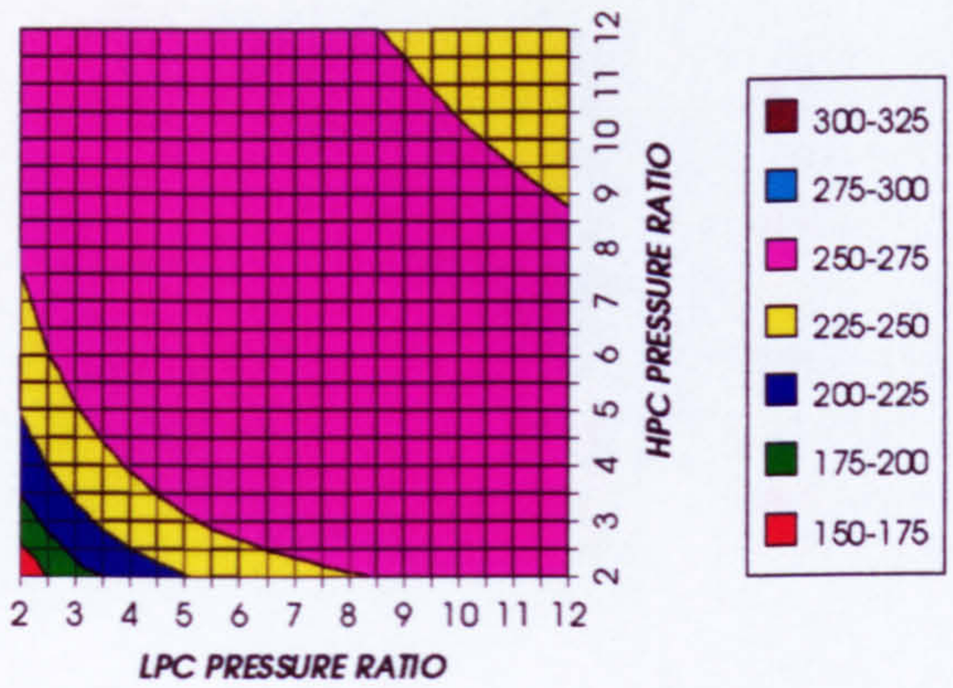

Figure 55. Gas turbine specific power output

STEAM TURBINE SPECIFIC POWER OUTPUT
REGENERATED CYCLE, CO2, FCFC

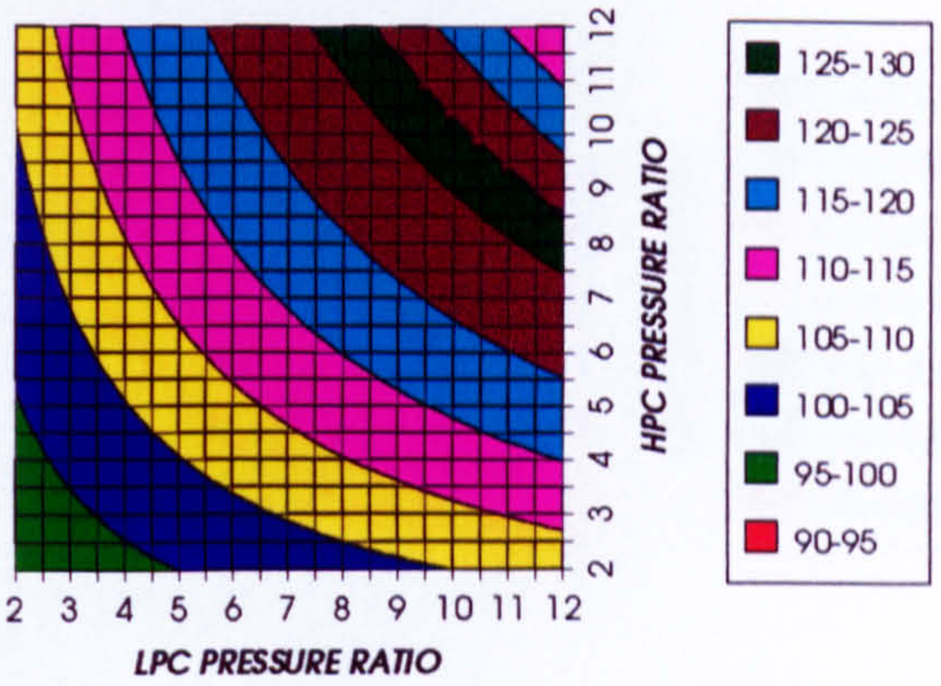

Figure 56. Steam turbine specific power output

GAS TURBINE TO STEAM TURBINE POWER RATIO
REGENERATED CYCLE, CO2, FCFC

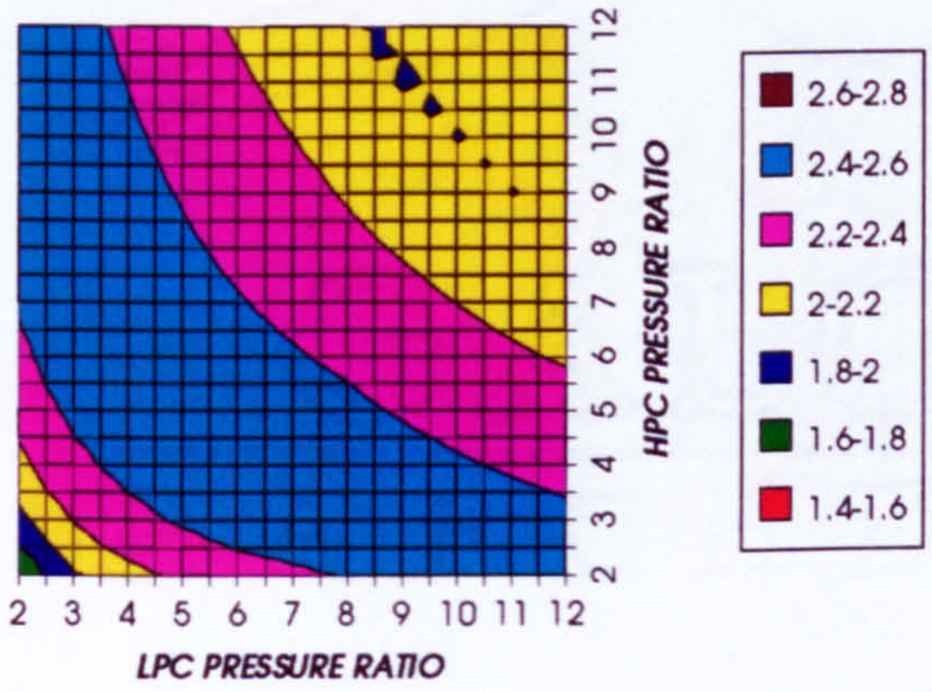

Figure 57. Gas turbine to steam turbine power ratio

AUXILIARIES TO USEFUL POWER RATIO
REGENERATED CYCLE, CO2, FCFC

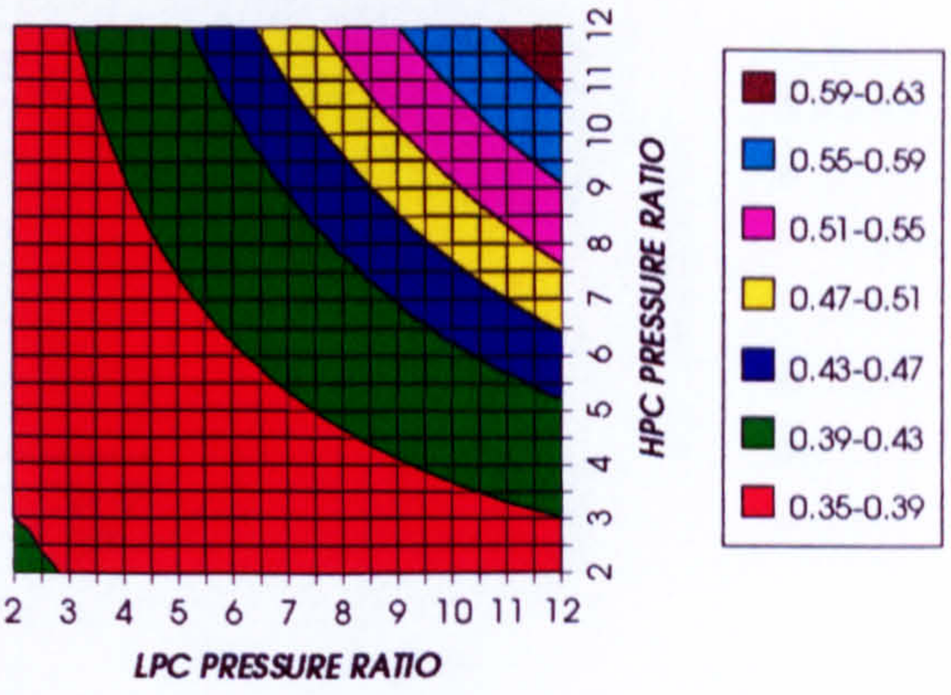

Figure 58. Auxiliary (CO2, O2 & Fuel) to usefuel power ratio

CO2 COMPRESSION AUXILIARY SPECIFIC POWER
REGENERATED CYCLE, CO2, FCFC

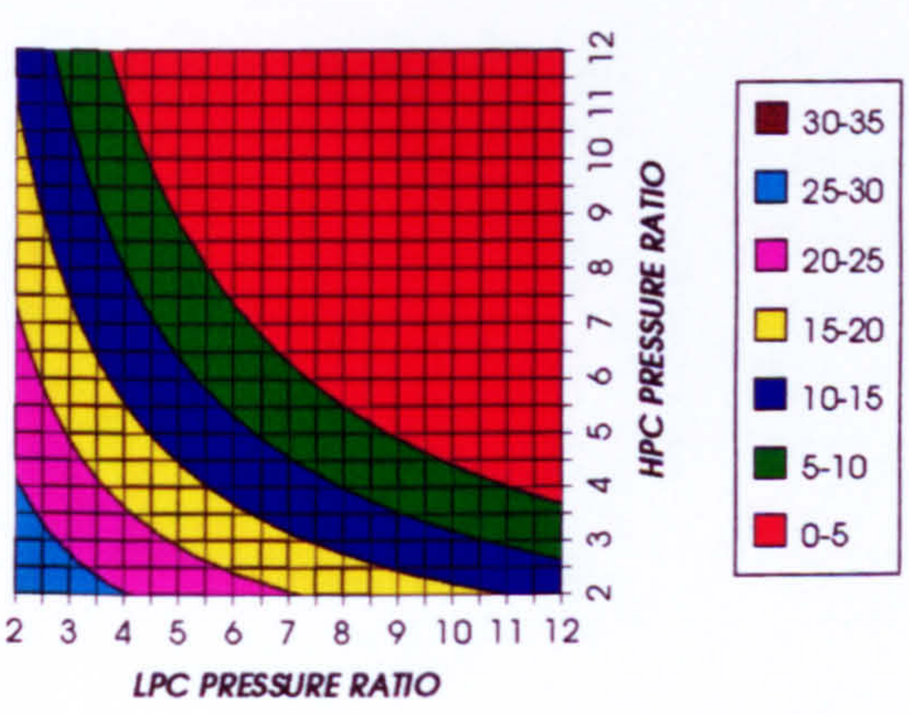

Figure 59. CO2 compression specific power

OXYGEN SEPARATION SPECIFIC POWER
REGENERATED CYCLE, CO2, FCFC

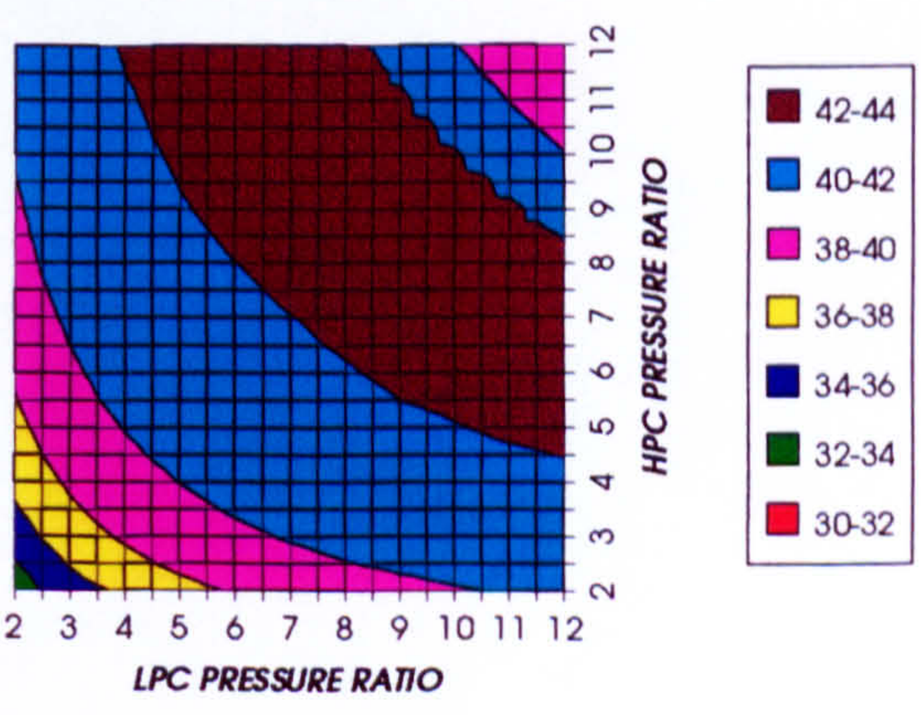

Figure 60. Oxygen separation specific power

COMPLETE PLANT (TET=1473 K)

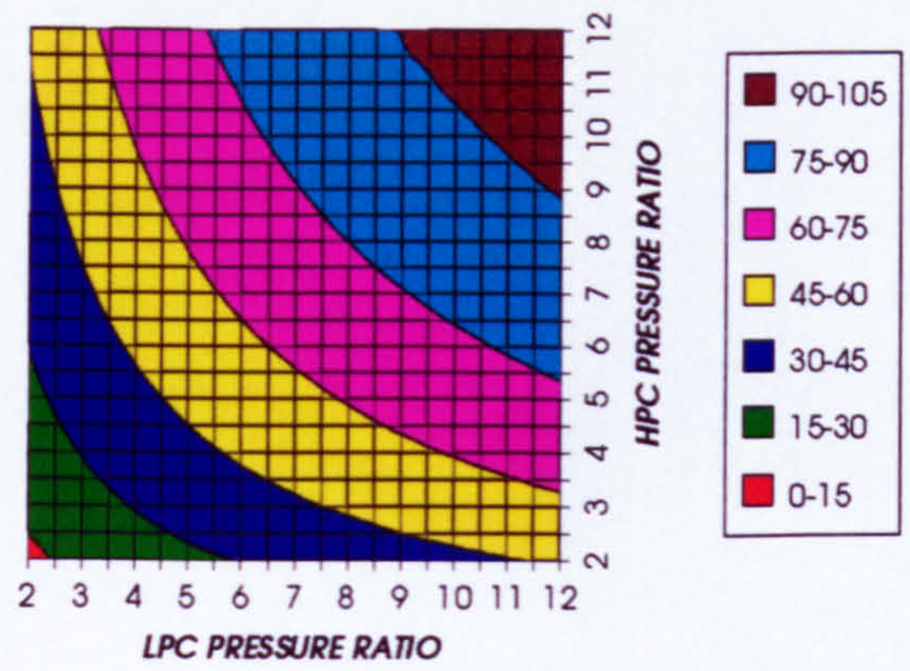

Figure 61. Fuel compression specific power

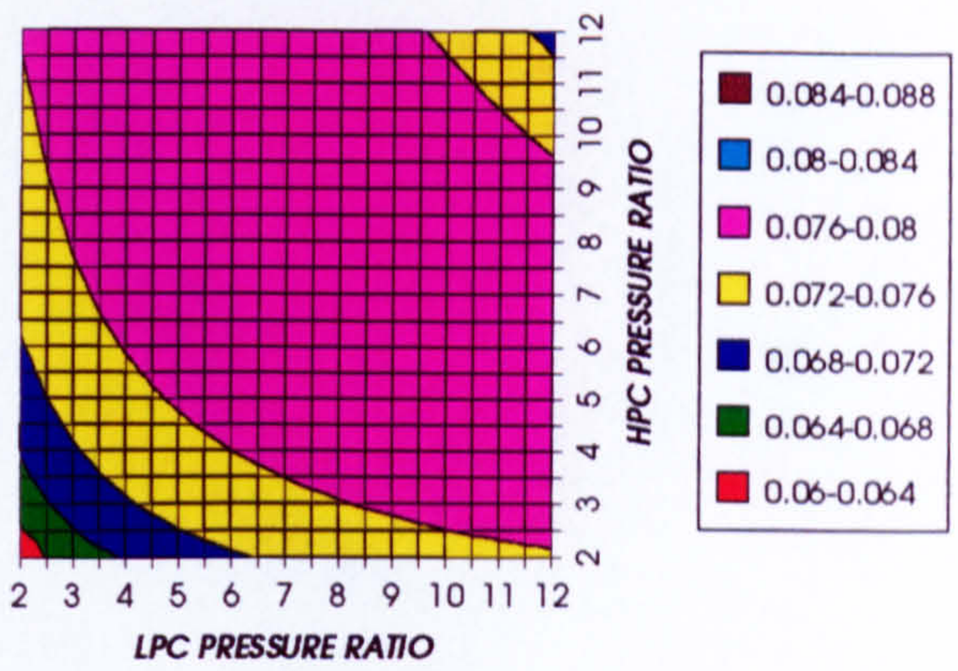

Figure 62. Fuel to compressor inlet mass flow ratio

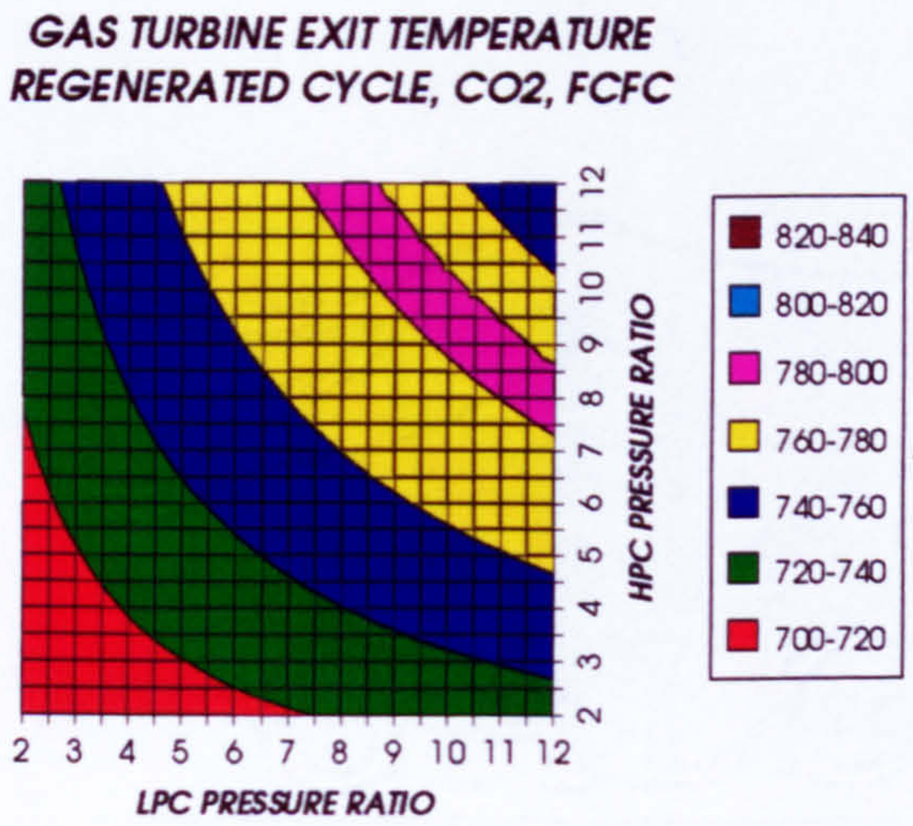

Figure 63. Gas turbine exit temperature

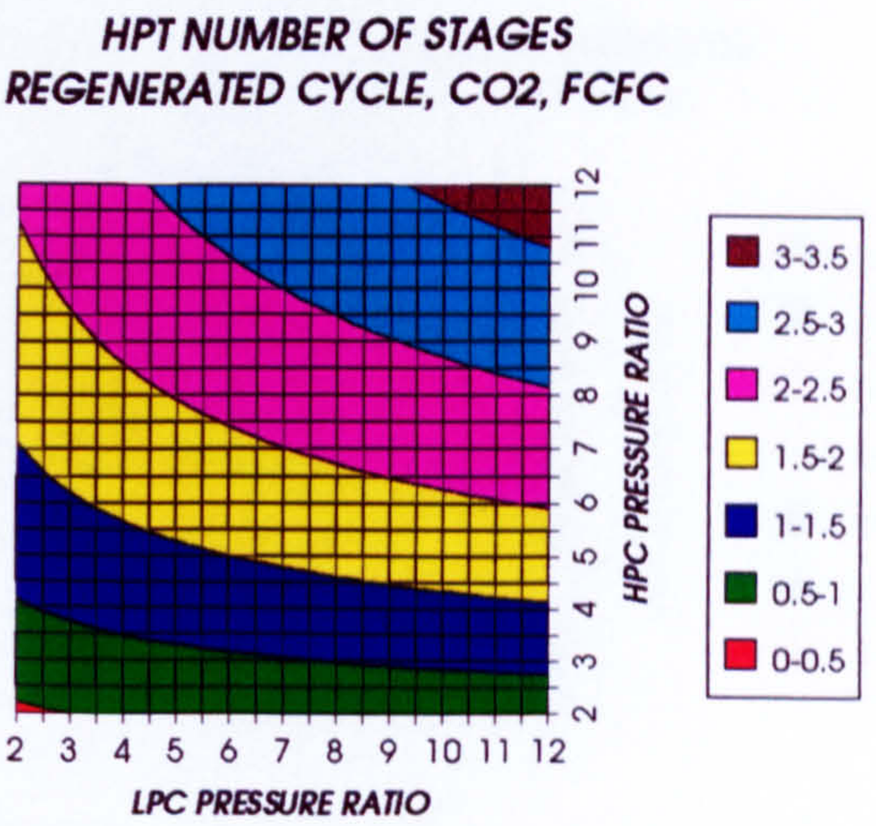

Figure 64. Number of HPT stages

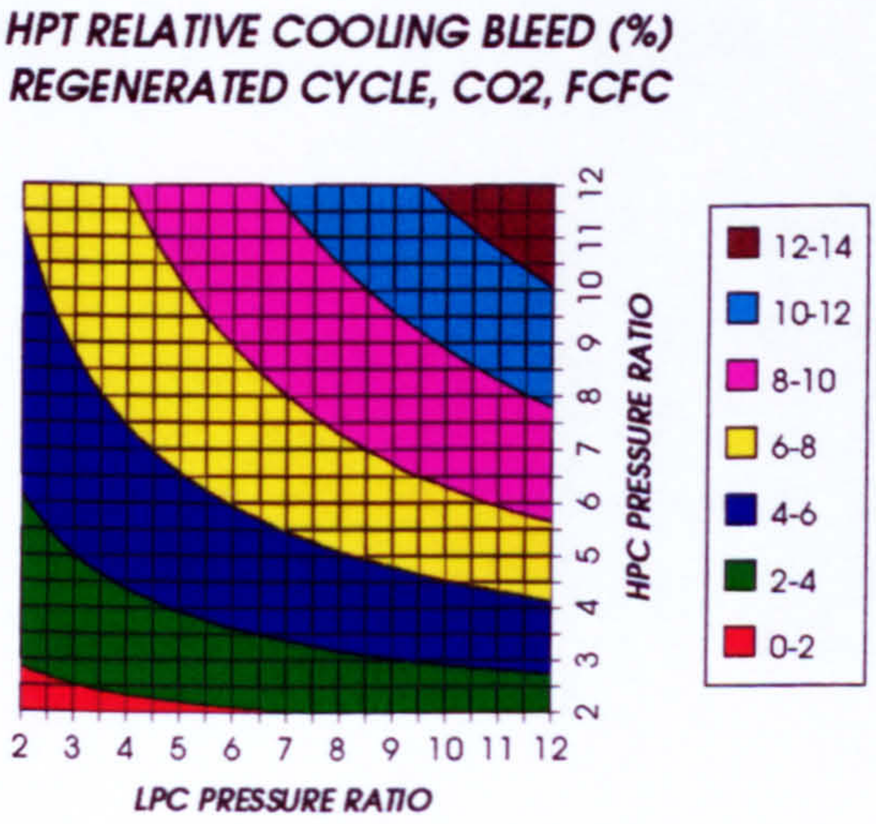

Figure 65. HPT cooling to compressor inlet mass flow ratio

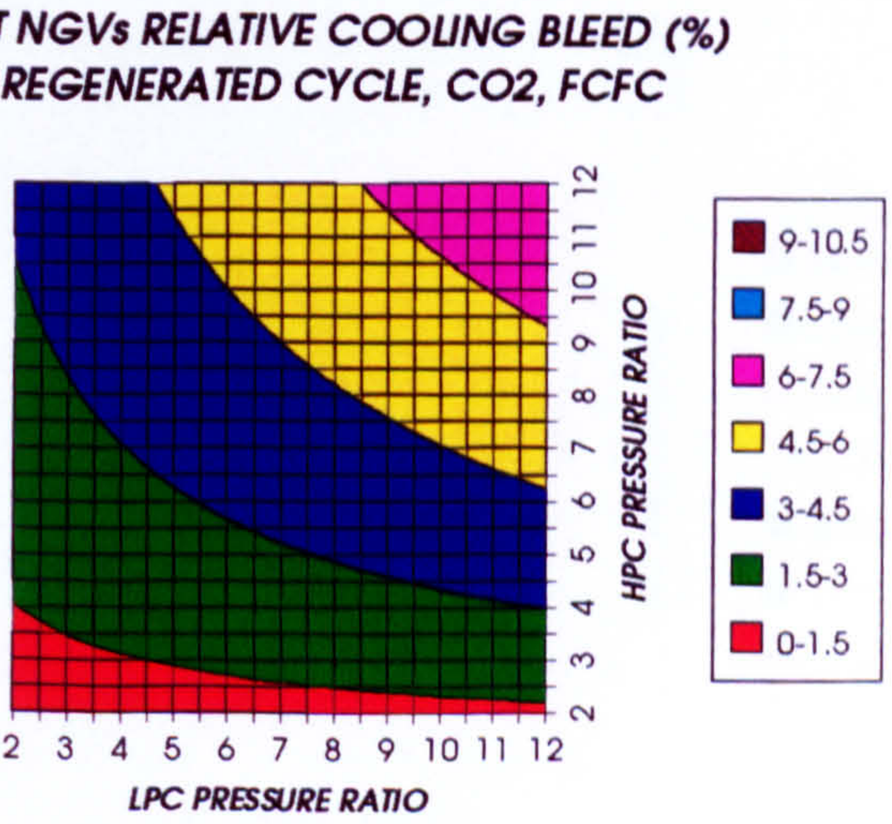

Figure 66. HPT NGVs cooling to compressor inlet mass flow ratio

COMPLETE PLANT (TET=1473 K)

HPT ROTOR RELATIVE COOLING BLEED (%)
REGENERATED CYCLE, CO2, FCFC

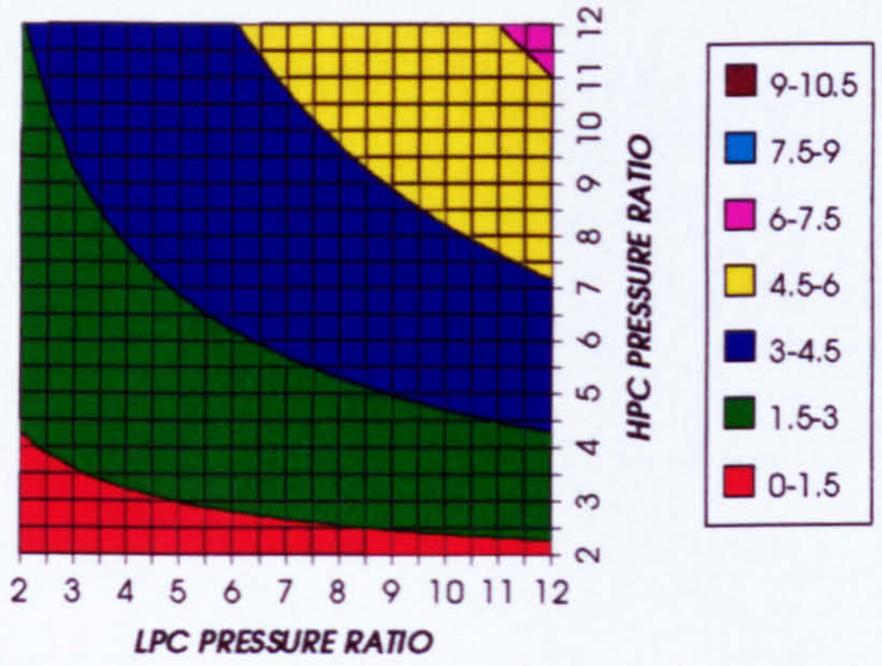

Figure 67. HPT rotor cooling to compressor inlet mass flow ratio

LPT NUMBER OF STAGES
REGENERATED CYCLE, CO2, FCFC

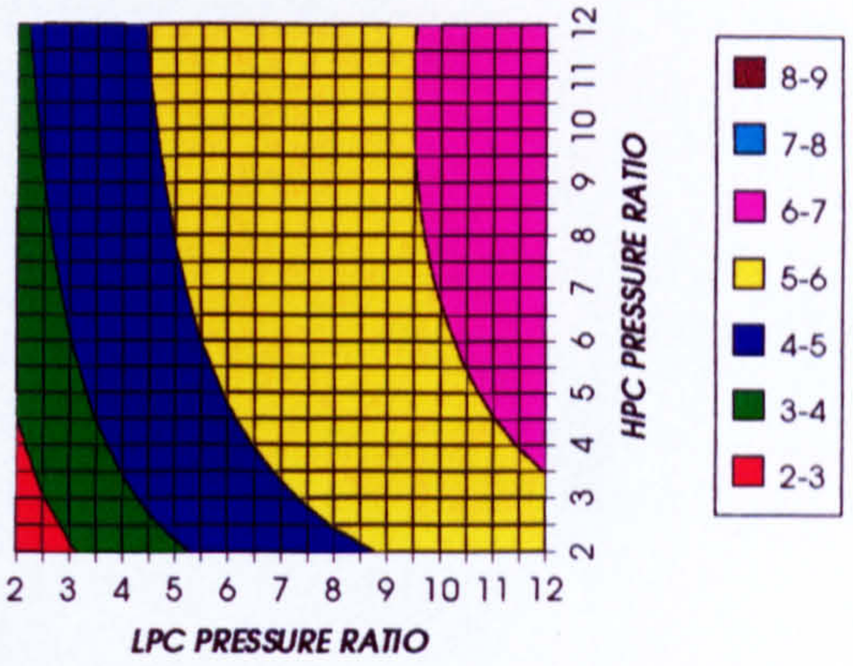

Figure 68. Number of LPT stages

LPT RELATIVE COOLING BLEED (%)
REGENERATED CYCLE, CO2, FCFC

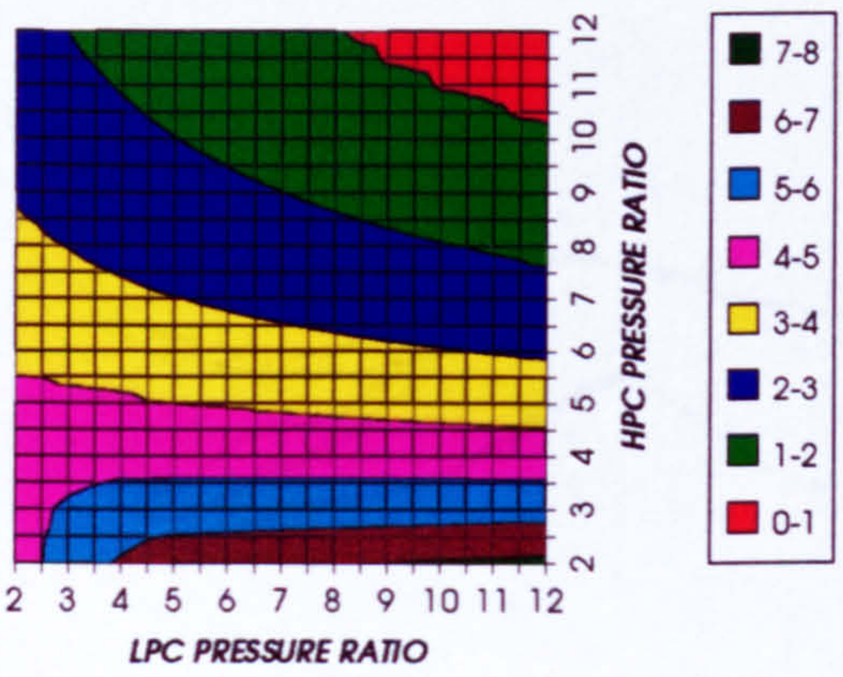

Figure 69.LPT cooling to compressor inlet mass flow ratio

LPT NGVs RELATIVE COOLING BLEED (%)
REGENERATED CYCLE, CO2, FCFC

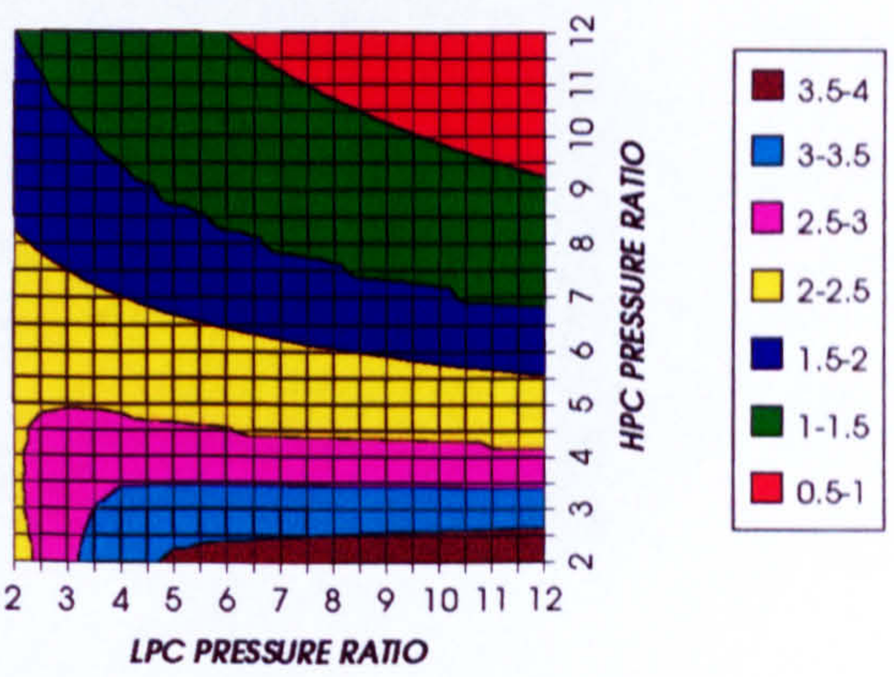

Figure 70. LPT NGVs cooling to compressor inlet mass flow ratio

LPT ROTOR RELATIVE COOLING BLEED (%)
REGENERATED CYCLE, CO2, FCFC

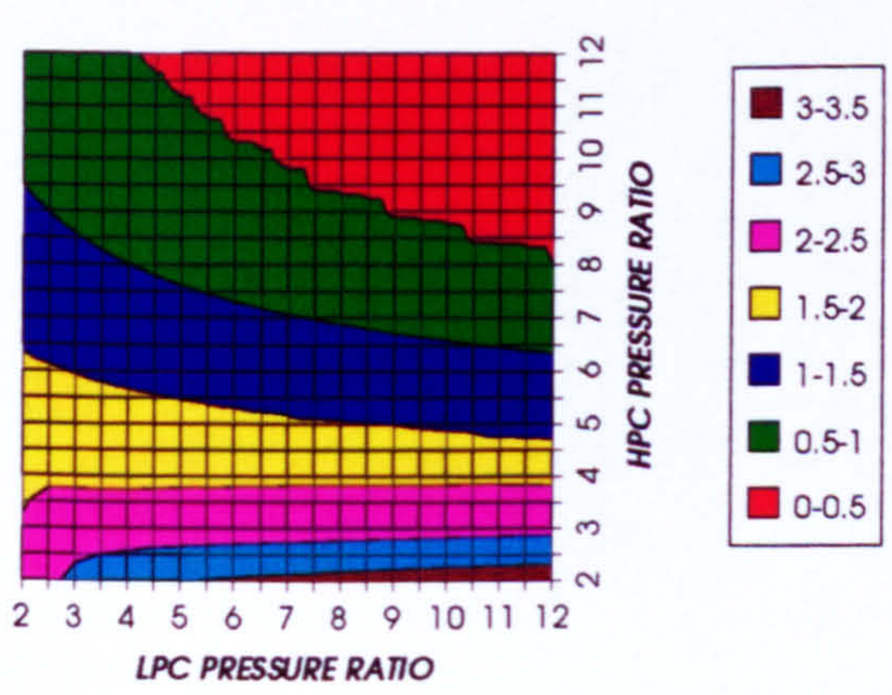

Figure 71. LPT rotor cooling to compressor inlet mass flow ratio

STEAM TURBINE OPTIMUM PRESSURE
REGENERATED CYCLE, CO2, FCFC

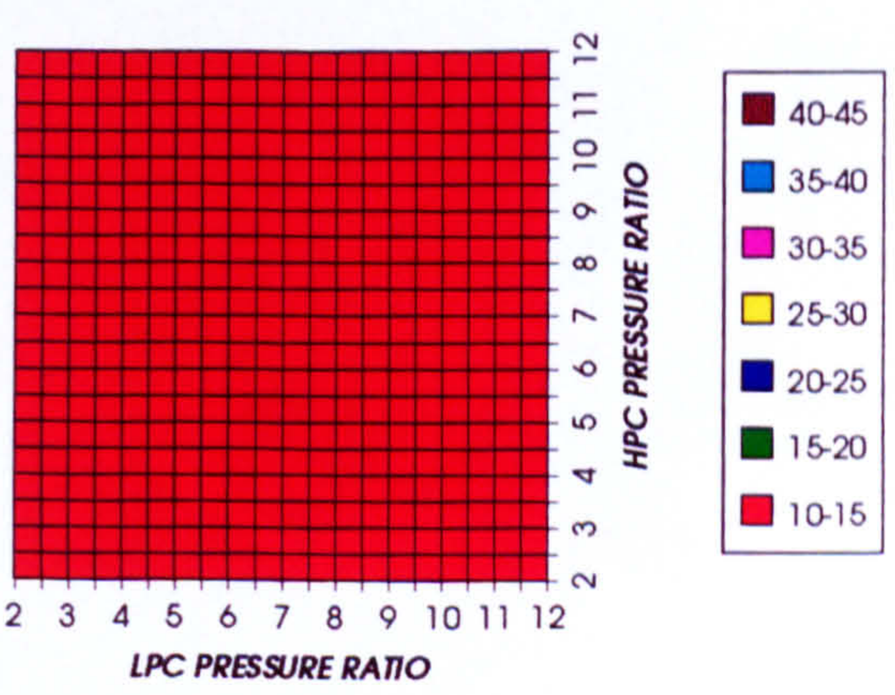

Figure 72. Steam turbine optimum pressures (maximum)

COMPLETE PLANT (TET=1473K)

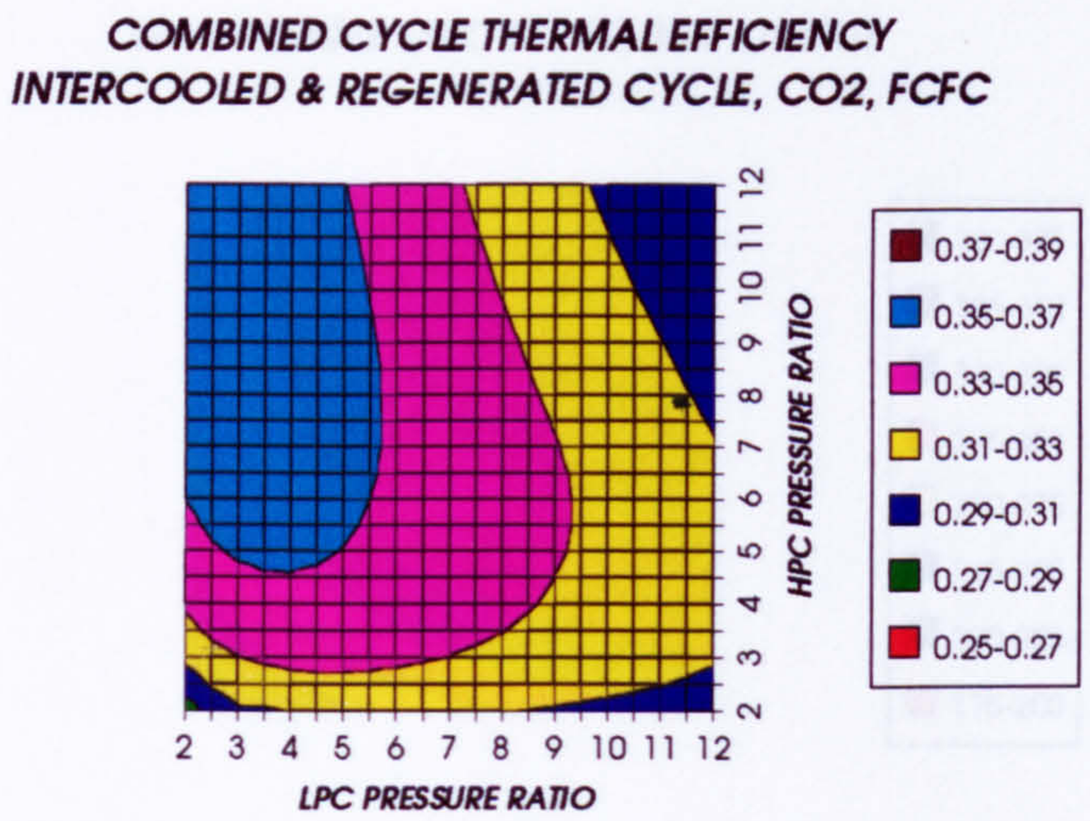

Figure 73. Combined cycle thermal efficiency

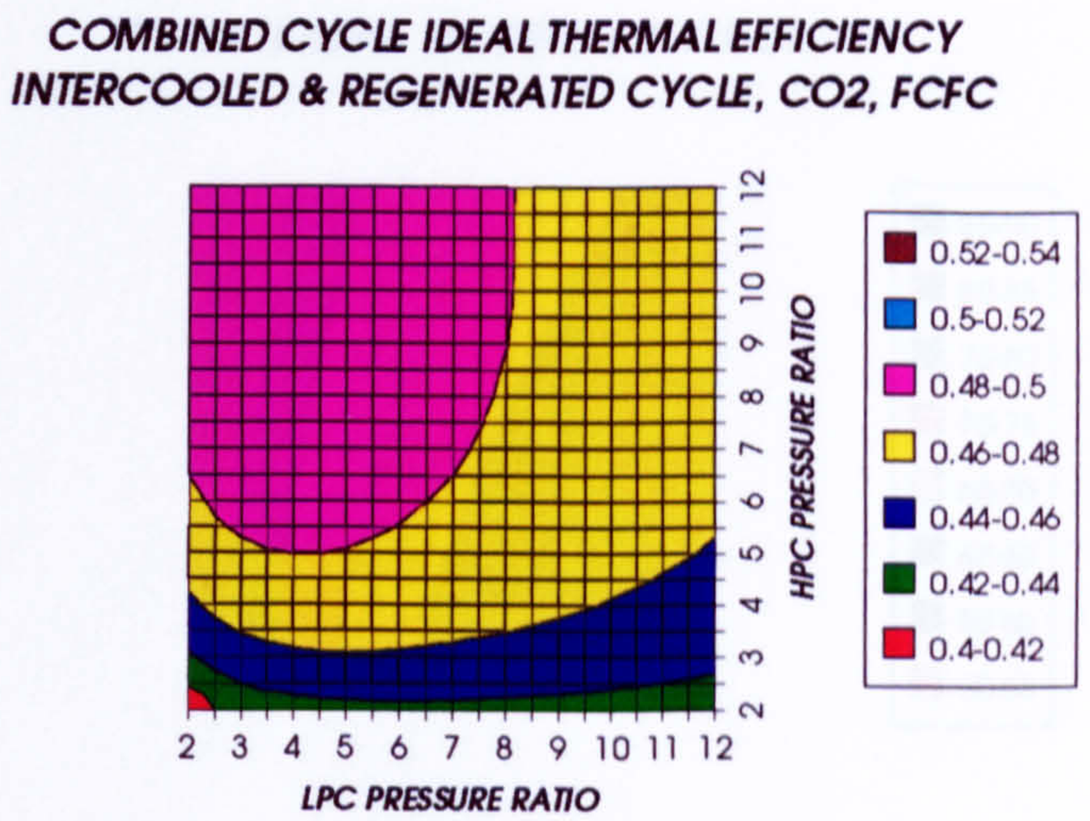

Figure 74. Combined cycle ideal thermal efficiency

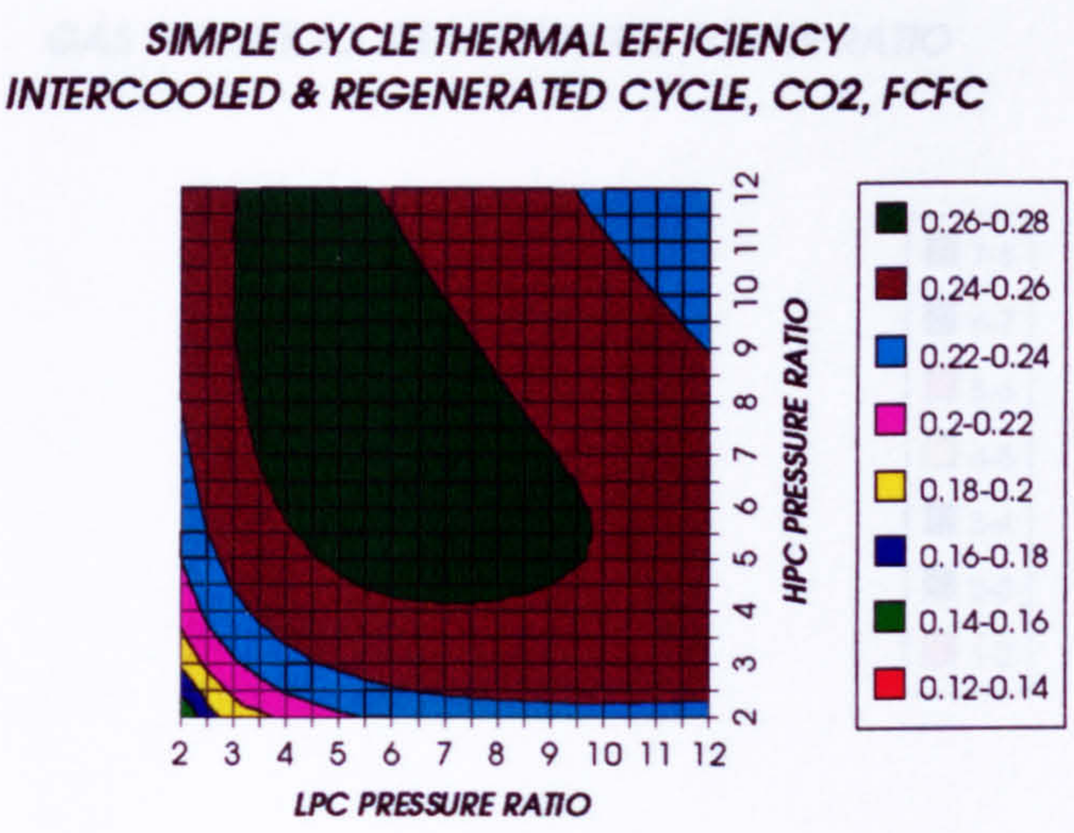

Figure 75. Simple cycle thermal efficiency

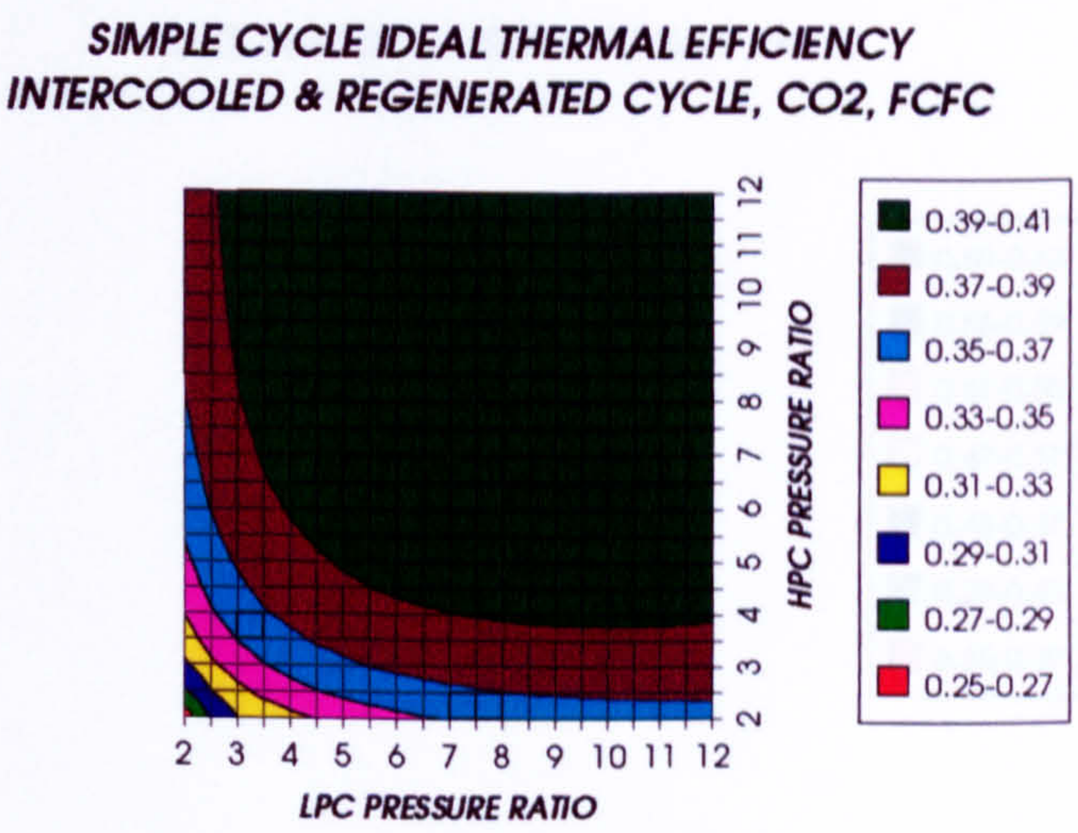

Figure 76. Simple cycle ideal thermal efficiency

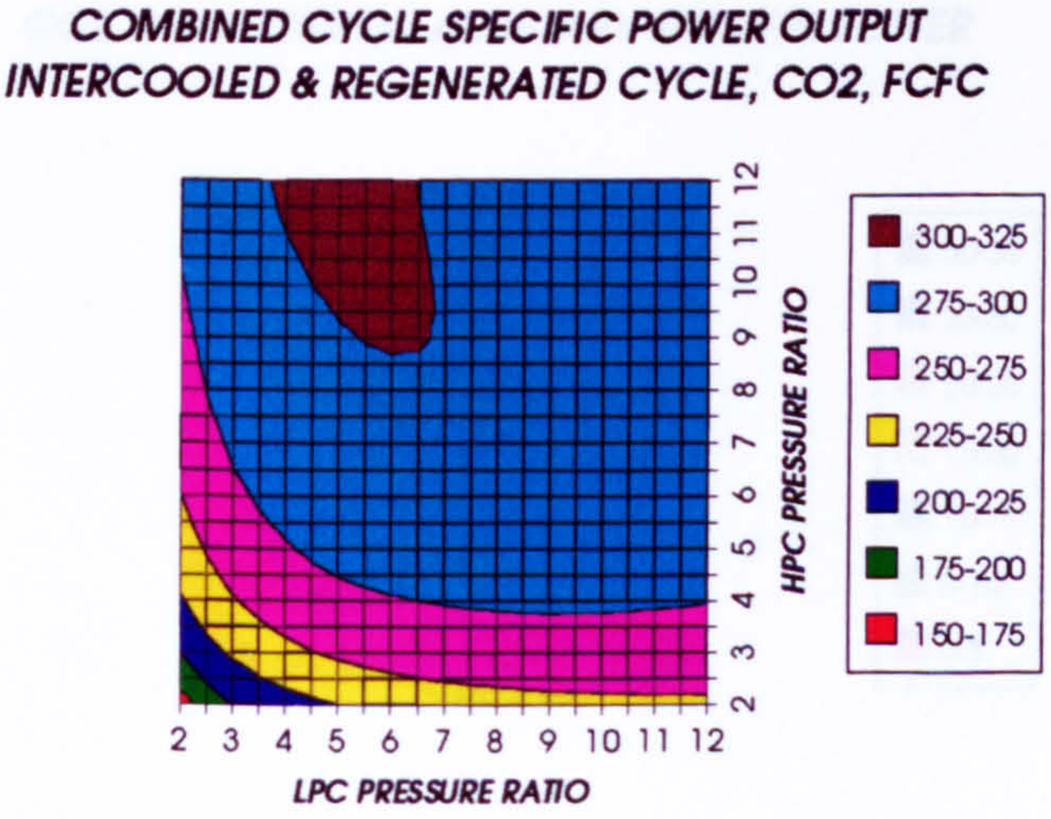

Figure 77. Combined cycle specific power output

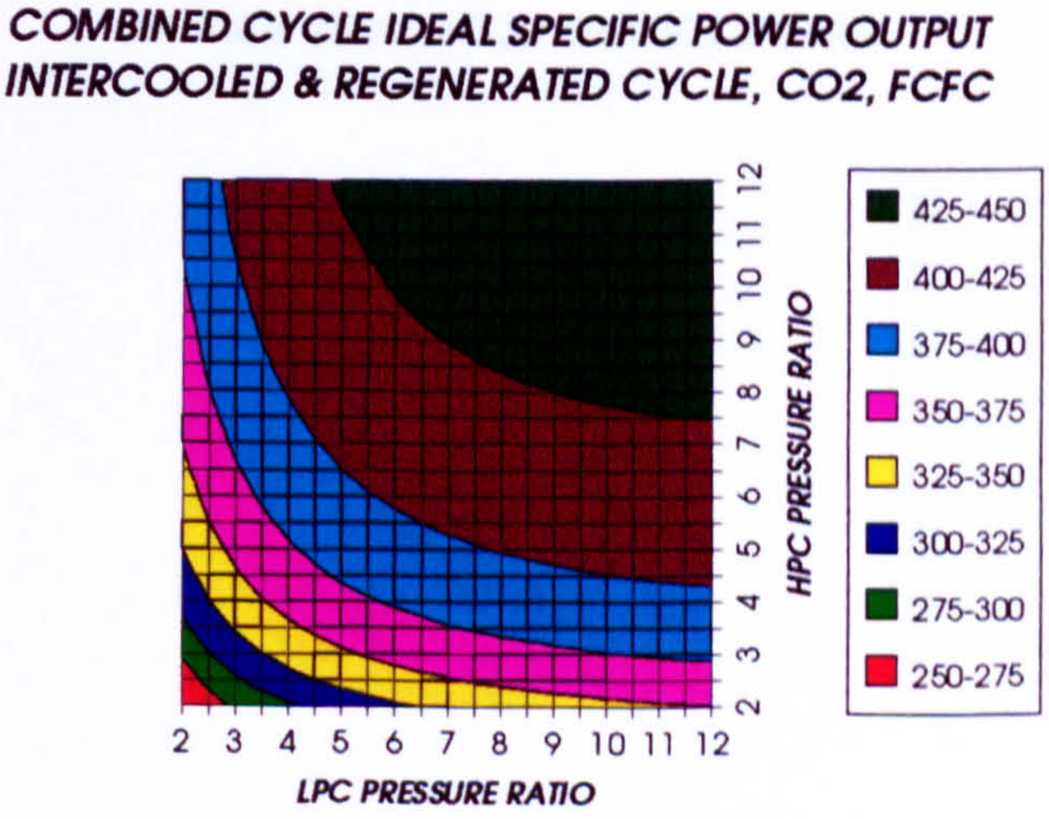

Figure78. Combined cycle ideal specific power output

COMPLETE PLANT (TET=1473 K)

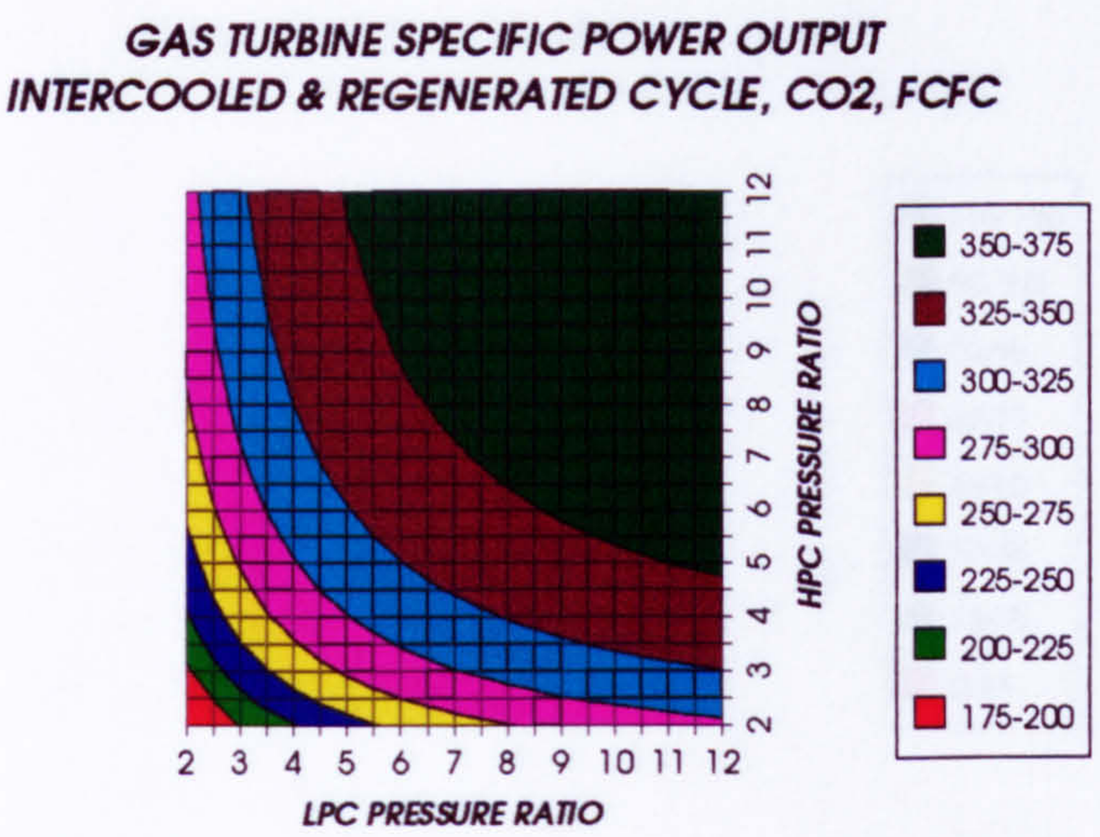

Figure 79. Gas turbine specific power output

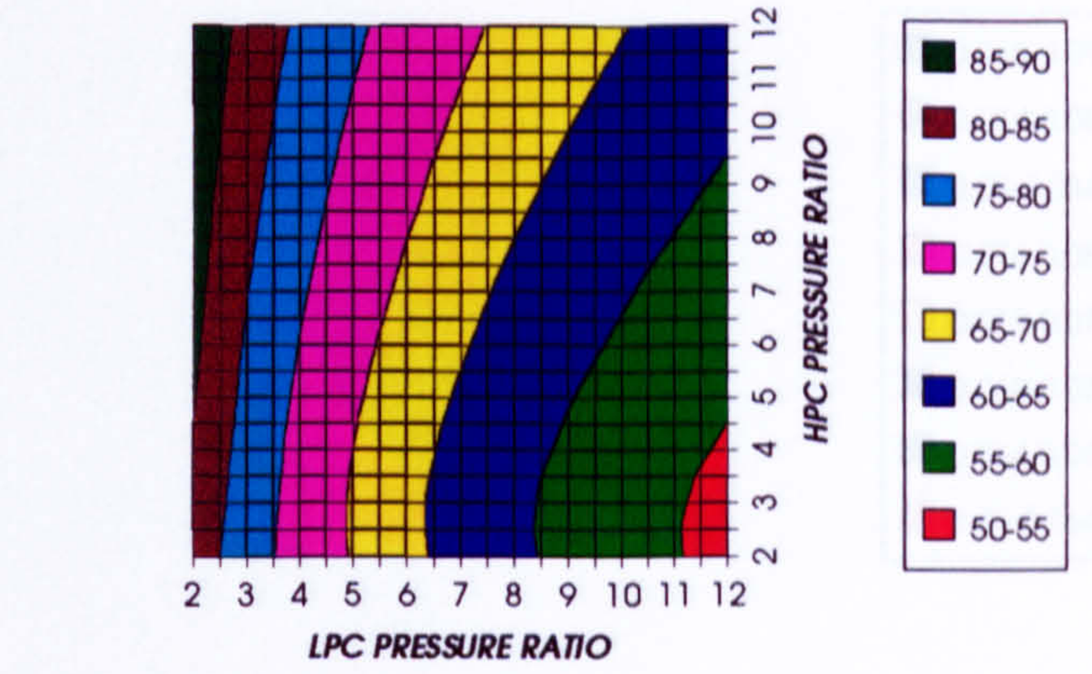

Figure 80. Steam turbine specific power output

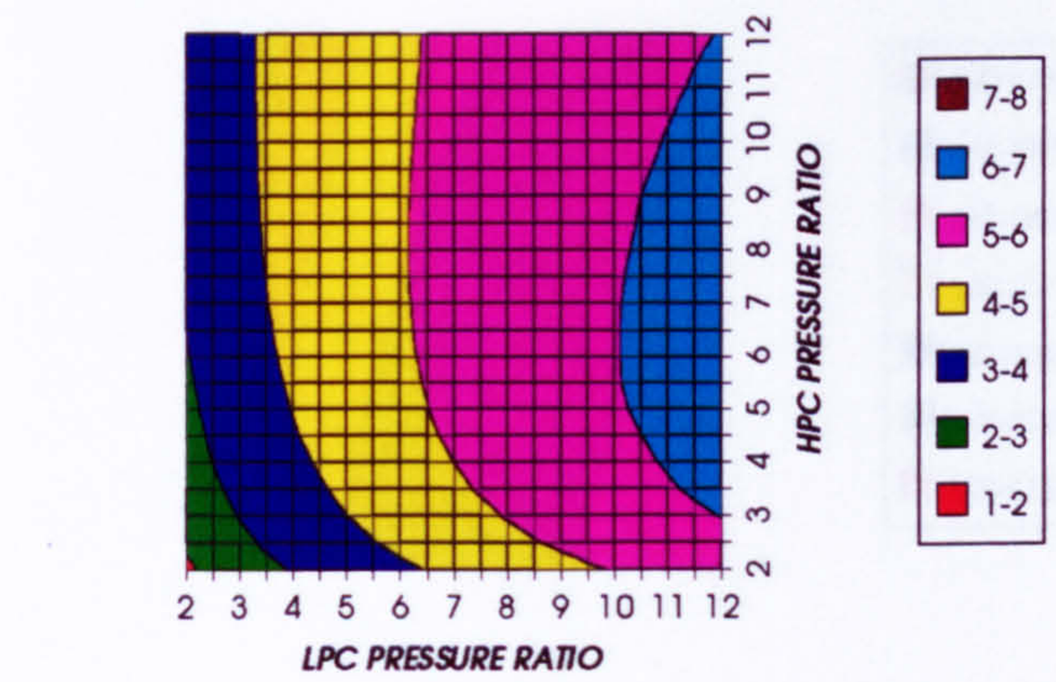

Figure 81. Gas turbine to steam turbine power ratio

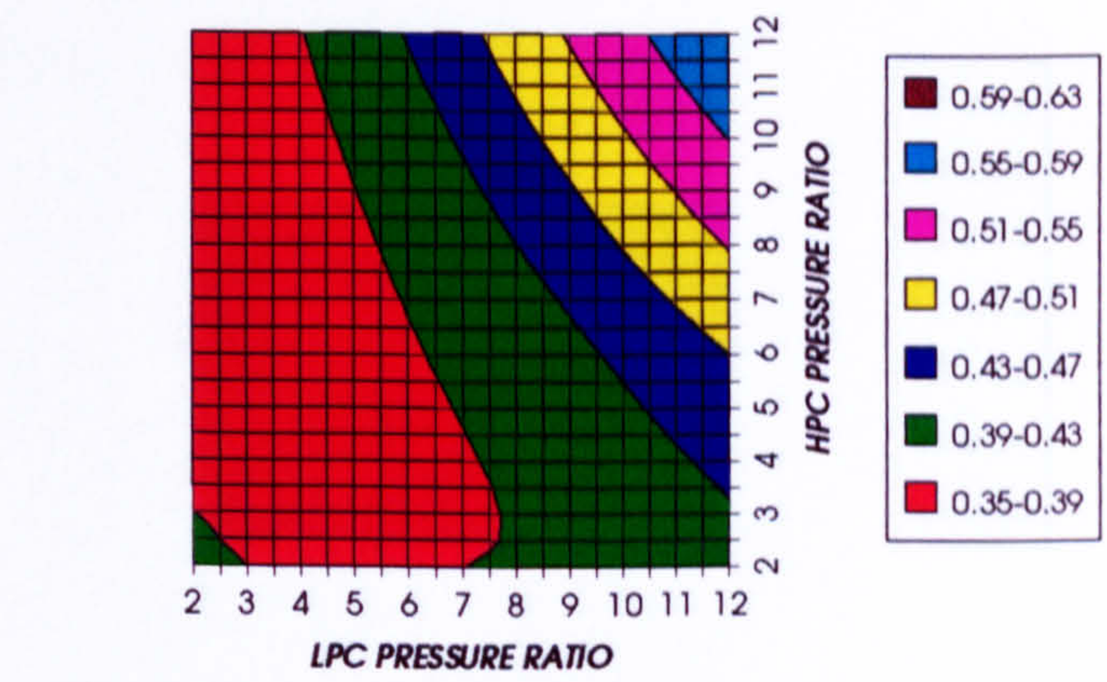

Figure 82. Auxiliary (CO2, O2 & Fuel) to usefuel power ratio

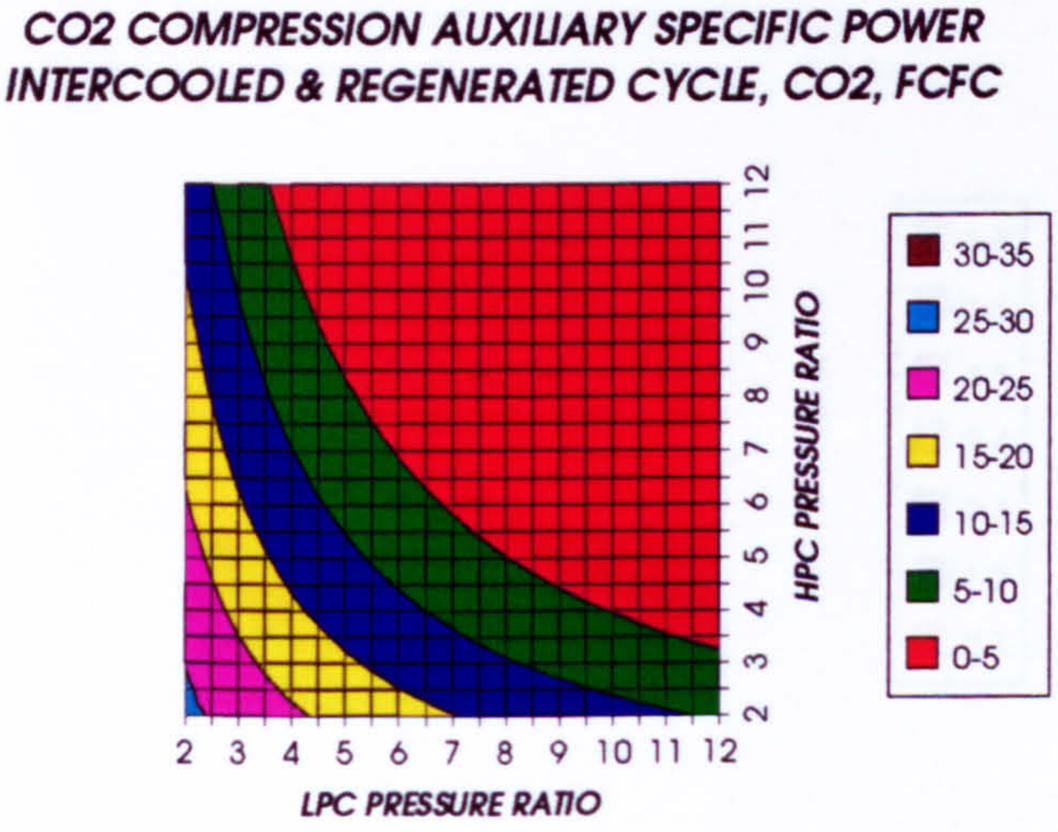

Figure 83. CO2 compression specific power

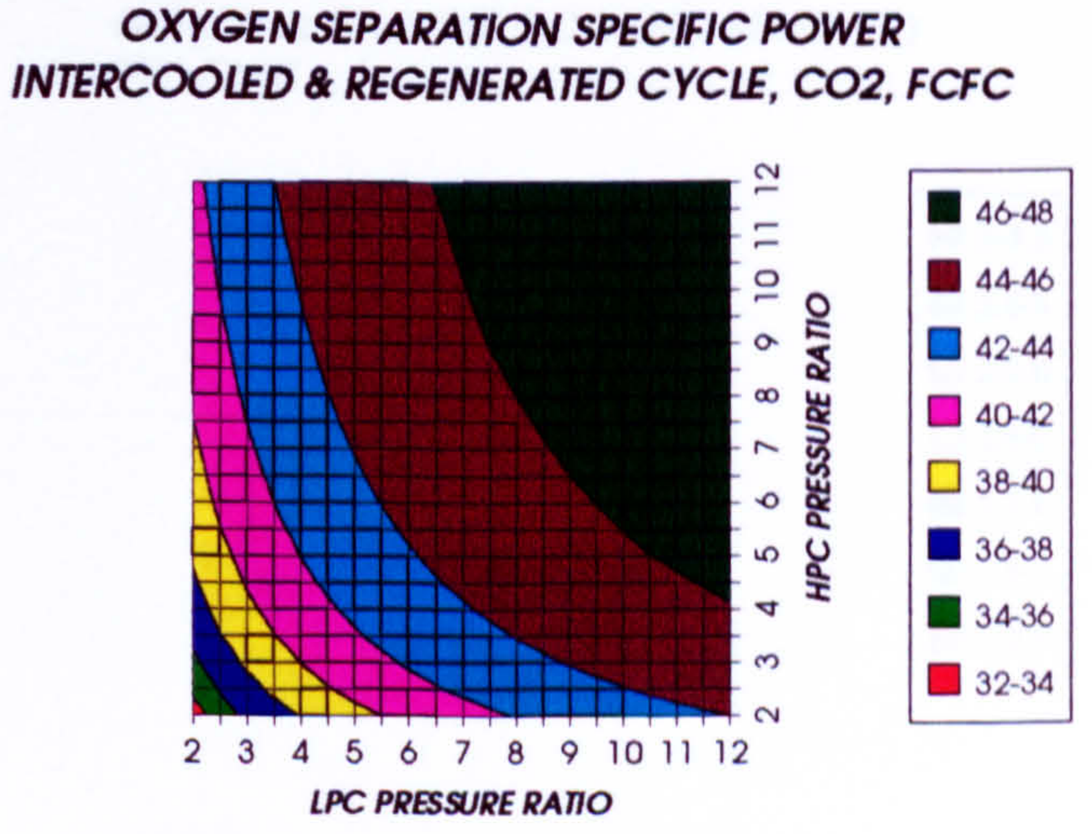

Figure 84. Oxygen separation specific power

COMPLETE PLANT (TET=1473 K)

FUEL COMPRESSION SPECIFIC POWER
INTERCOOLED & REGENERATED CYCLE, CO2, FCFC

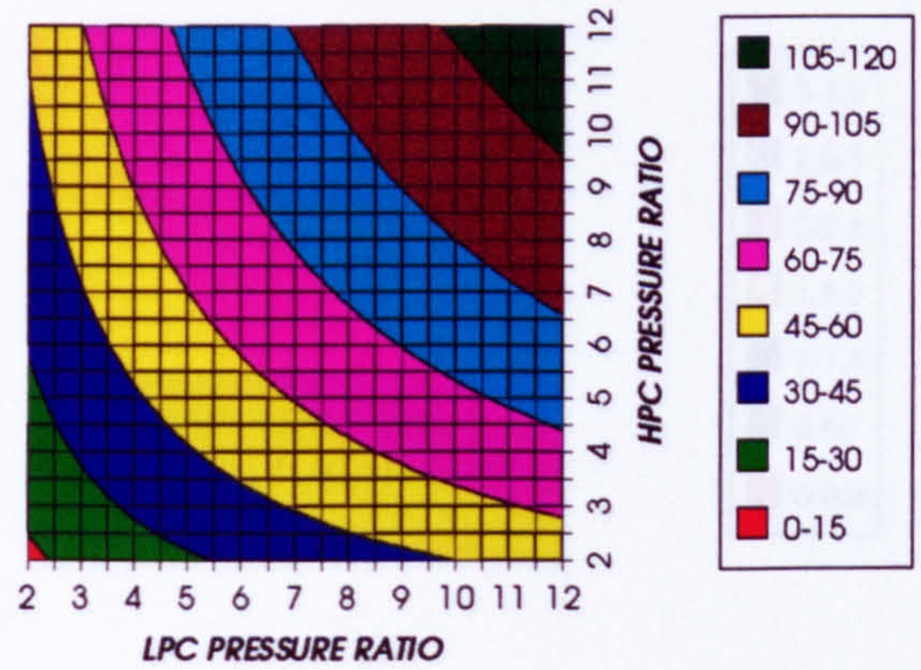

Figure 85. Fuel compression specific power

FUEL TO COMPRESSOR INLET MASS FLOW RATIO
INTERCOOLED & REGENERATED CYCLE, CO2, FCFC

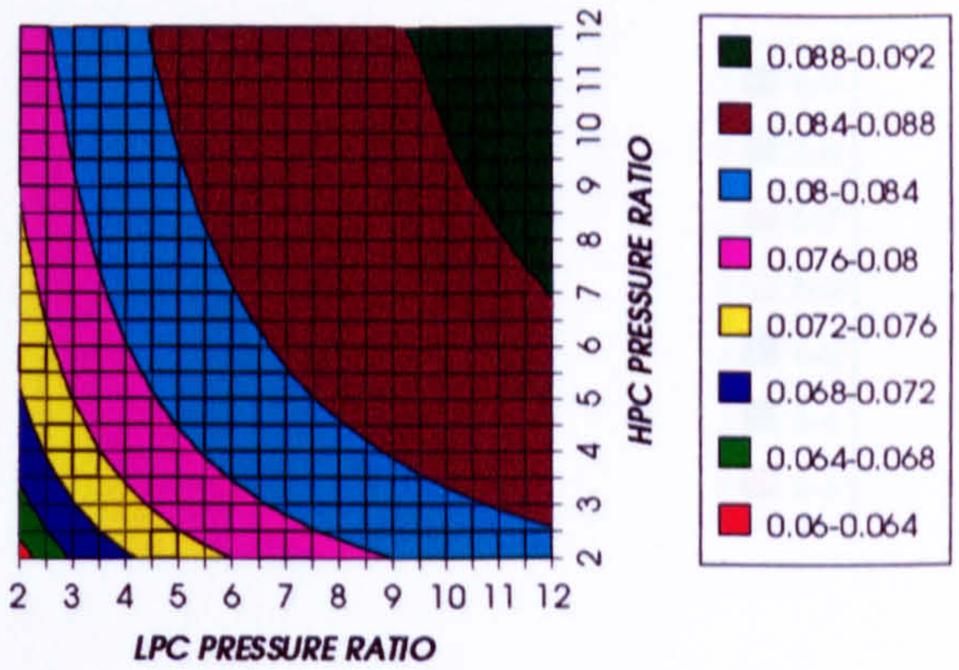

Figure 86. Fuel to compressor inlet mass flow ratio

GAS TURBINE EXIT TEMPERATURE
INTERCOOLED & REGENERATED CYCLE, CO2, FCFC

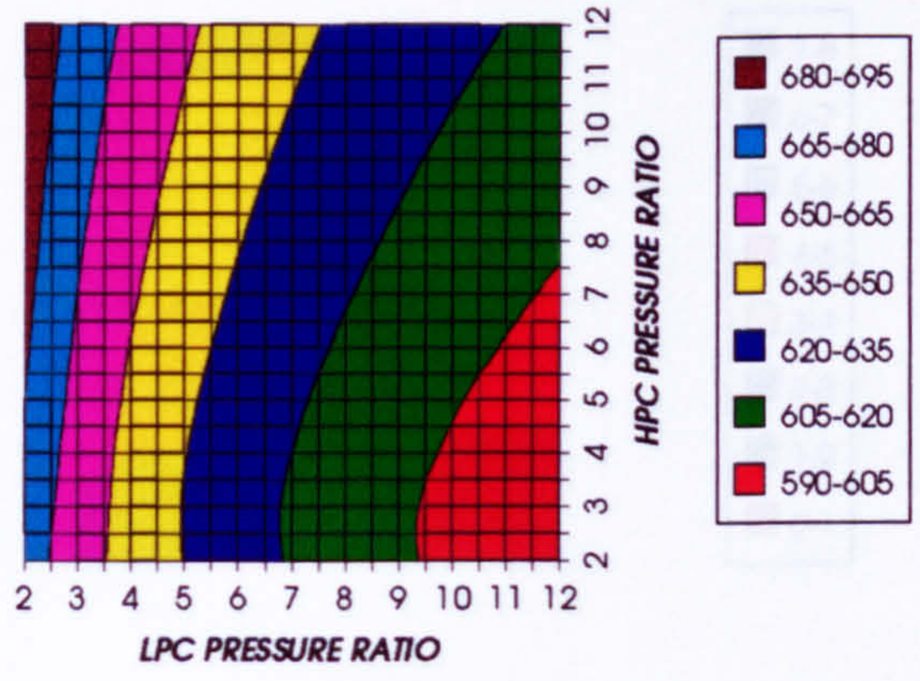

Figure 87. Gas turbine exit temperature

HPT NUMBER OF STAGES
INTERCOOLED & REGENERATED CYCLE, CO2, FCFC

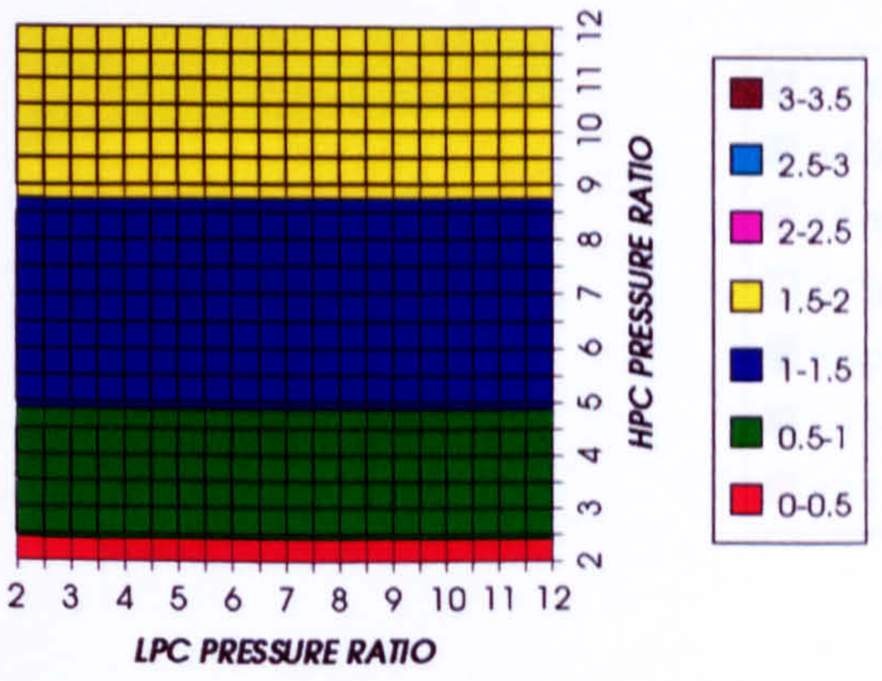

Figure 88. Number of HPT stages

HPT RELATIVE COOLING BLEED (%)
INTERCOOLED & REGENERATED CYCLE, CO2, FCFC

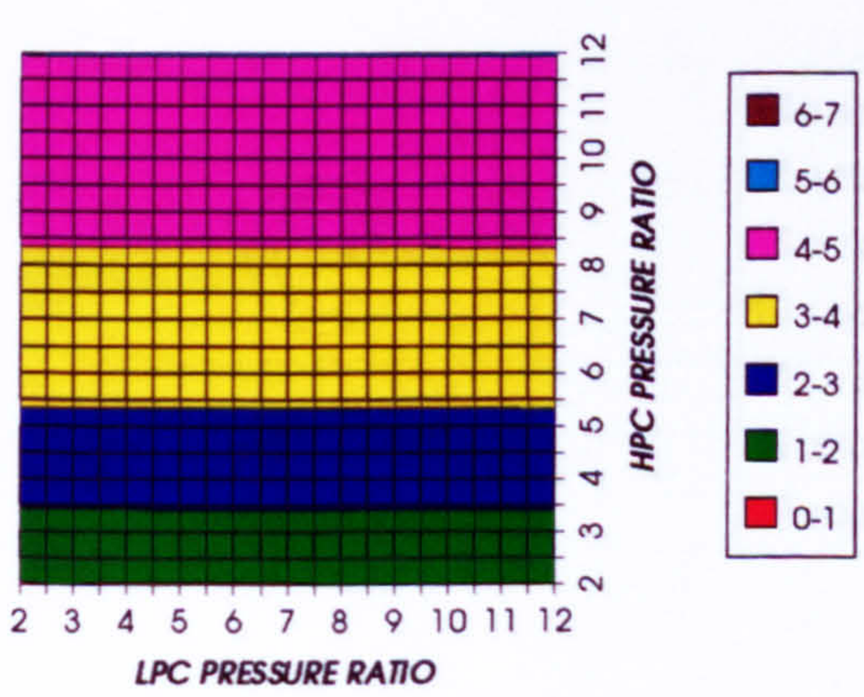

Figure 89. HPT cooling to compressor inlet mass flow ratio

HPT NGVs RELATIVE COOLING BLEED (%)
INTERCOOLED & REGENERATED CYCLE, CO2, FCFC

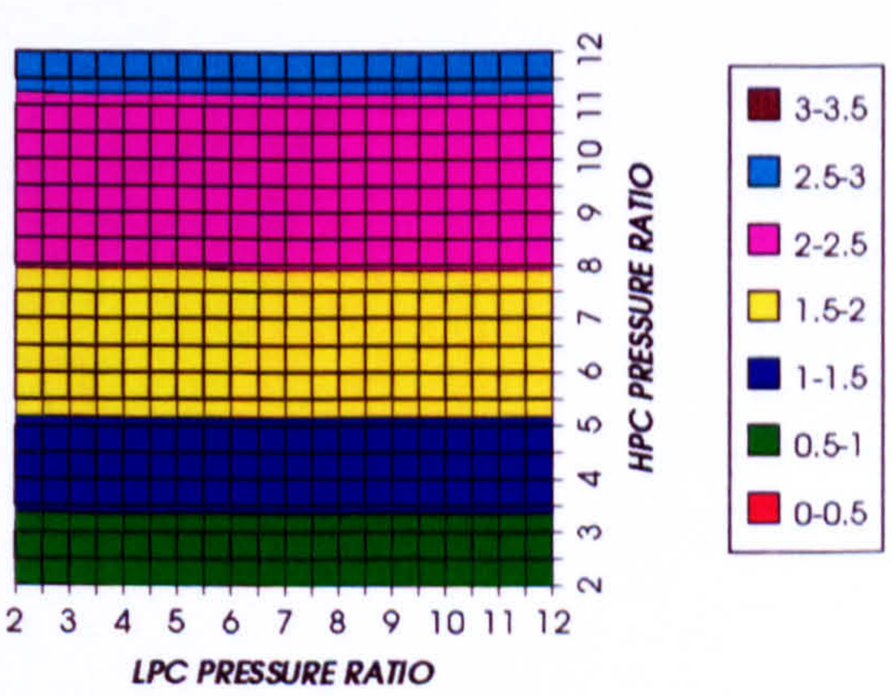

Figure 90. HPT NGVs cooling to compressor inlet mass flow ratio

HPT ROTOR RELATIVE COOLING BLEED (%)
INTERCOOLED & REGENERATED CYCLE, CO2, FCFC

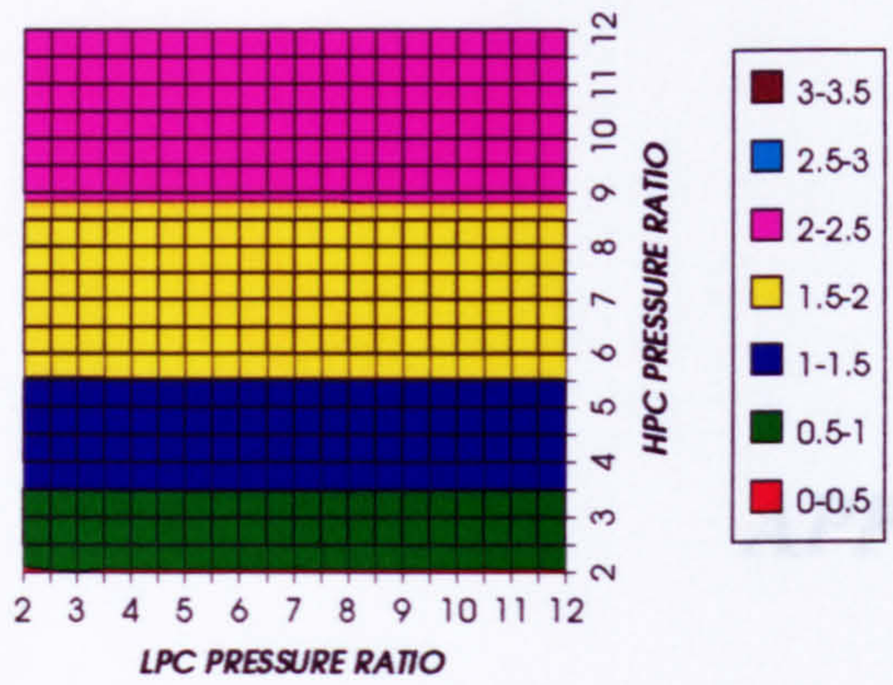

Figure 91. HPT rotor cooling to compressor inlet mass flow ratio

LPT NUMBER OF STAGES
INTERCOOLED & REGENERATED CYCLE, CO2, FCFC

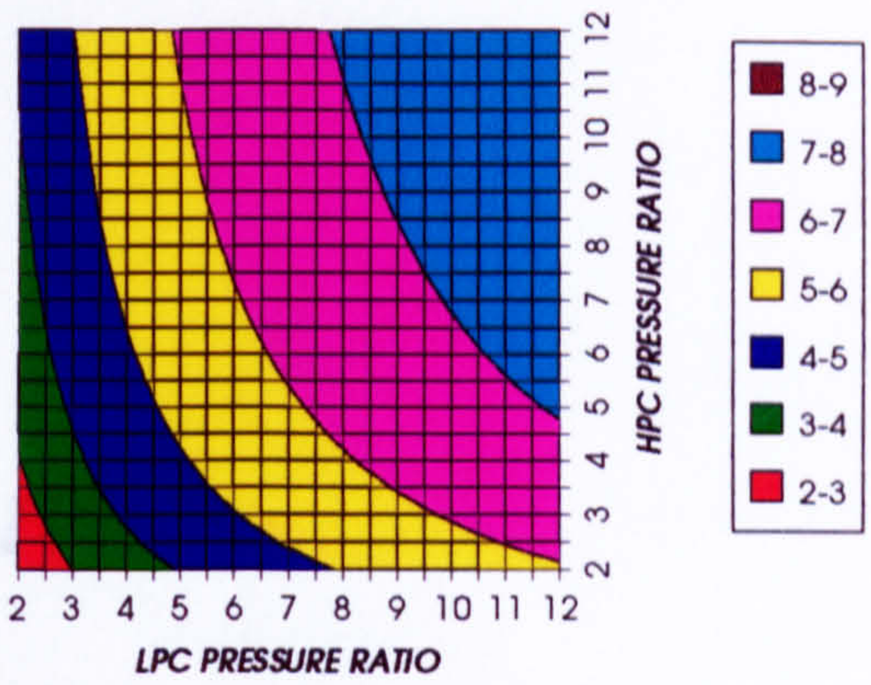

Figure 92. Number of LPT stages

LPT RELATIVE COOLING BLEED (%)
INTERCOOLED & REGENERATED CYCLE, CO2, FCFC

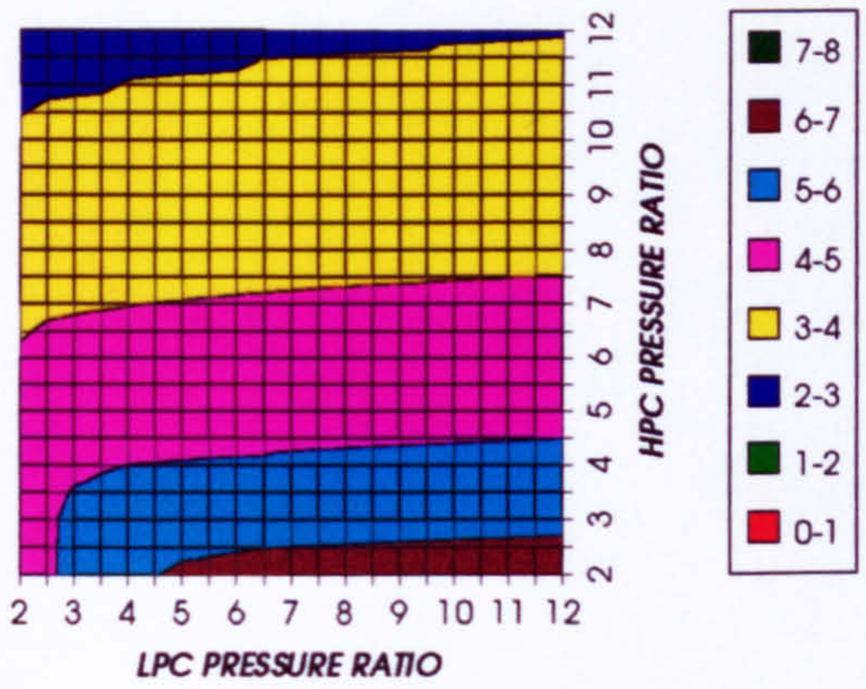

Figure 93.LPT cooling to compressor inlet mass flow ratio

LPT NGVs RELATIVE COOLING BLEED (%)
INTERCOOLED & REGENERATED CYCLE, CO2, FCFC

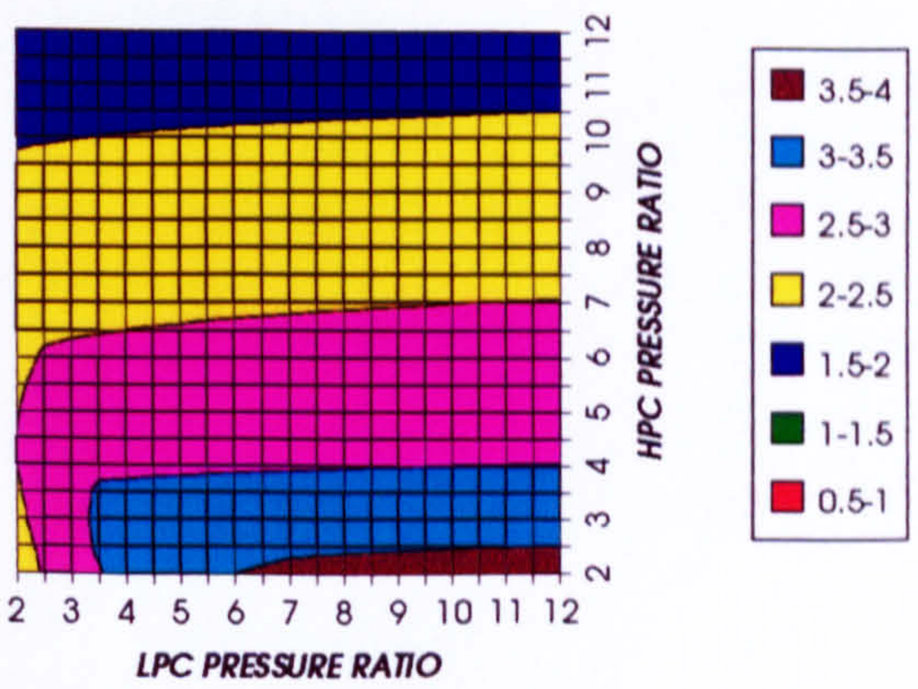

Figure 94. LPT NGVs cooling to compressor inlet mass flow ratio

LPT ROTOR RELATIVE COOLING BLEED (%)
INTERCOOLED & REGENERATED CYCLE, CO2, FCFC

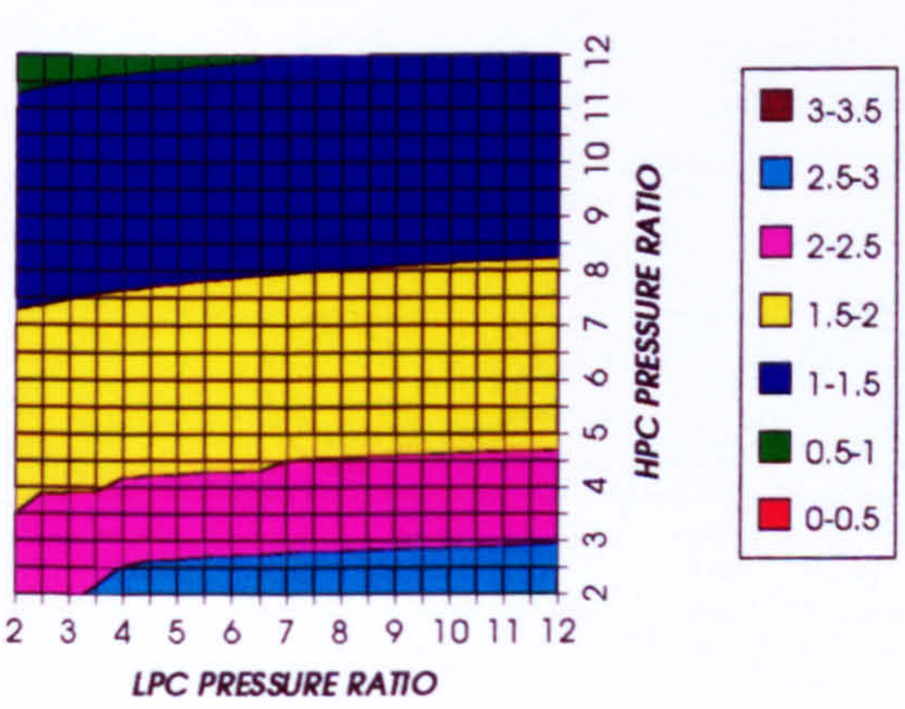

Figure 95. LPT rotor cooling to compressor inlet mass flow ratio

STEAM TURBINE OPTIMUM PRESSURE
INTERCOOLED & REGENERATED CYCLE, CO2, FCFC

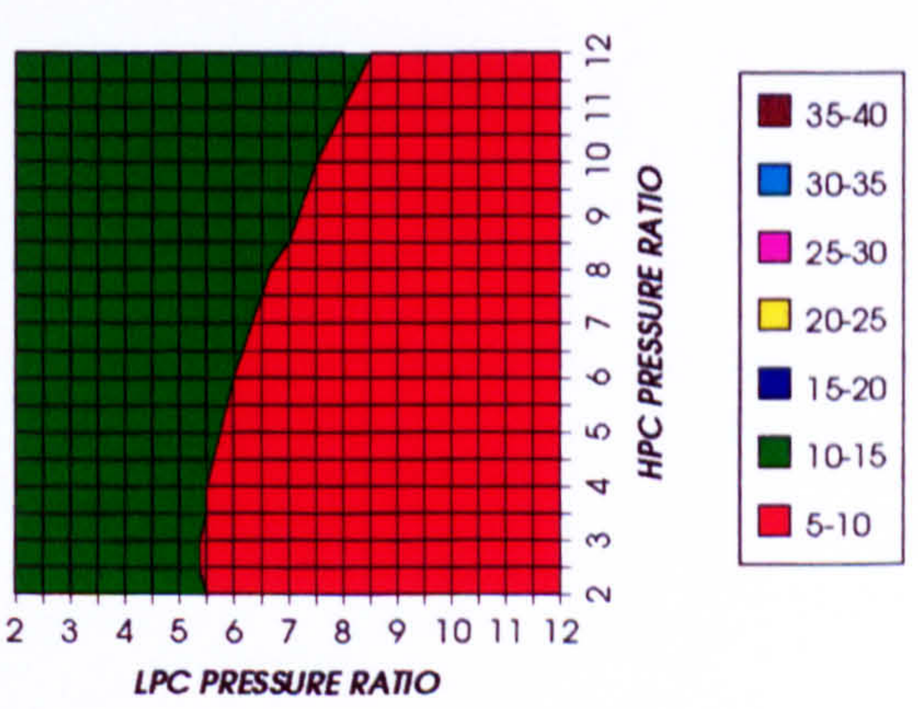

Figure 96. Steam turbine optimum pressures (maximum)

APPENDIX IV

COMPLETE PLANT PERFORMANCE (WORKING FLUID CO_2/ARGON, TET=1473 K)

COMPLETE PLANT (TET=1473K)

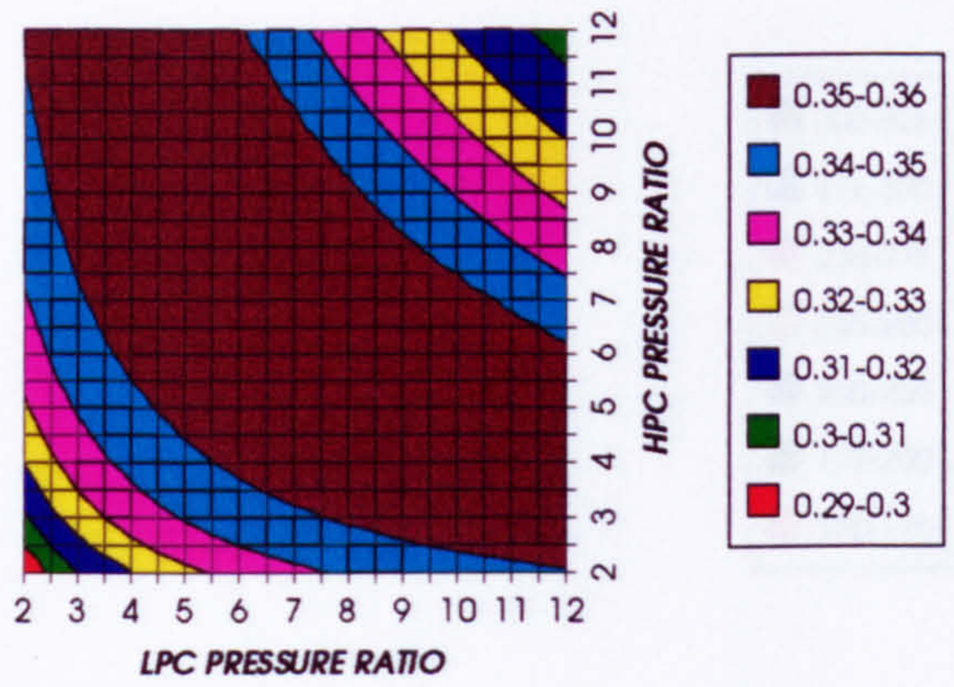

Figure 1. Combined cycle thermal efficiency

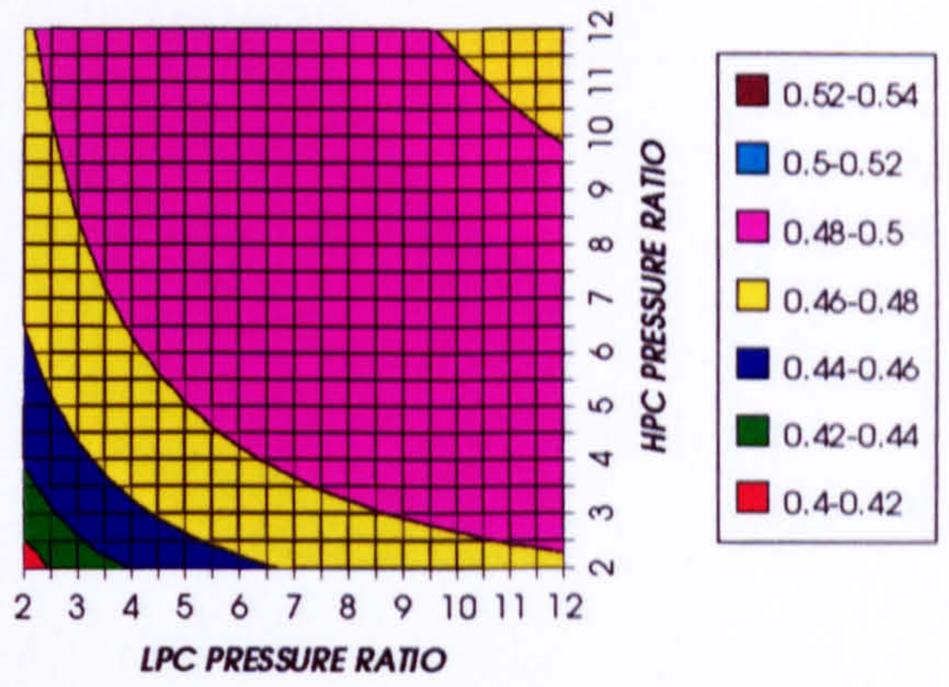

Figure 2. Combined cycle ideal thermal efficiency

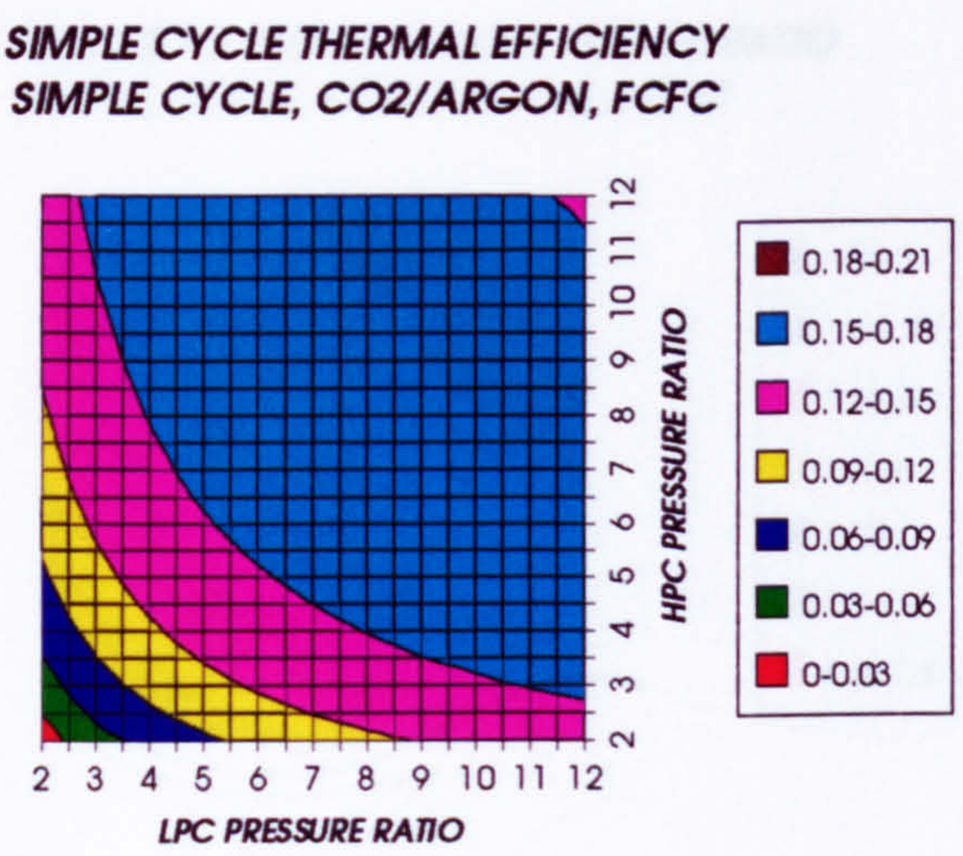

Figure 3. Simple cycle thermal efficiency

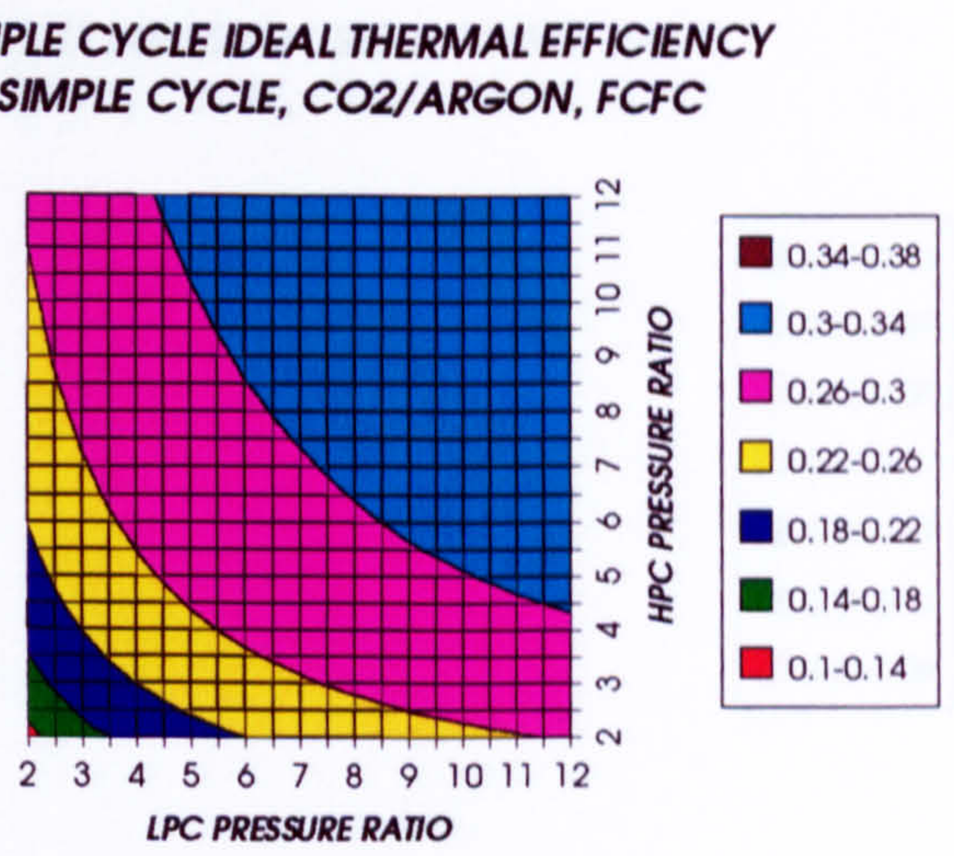

Figure 4. Simple cycle ideal thermal efficiency

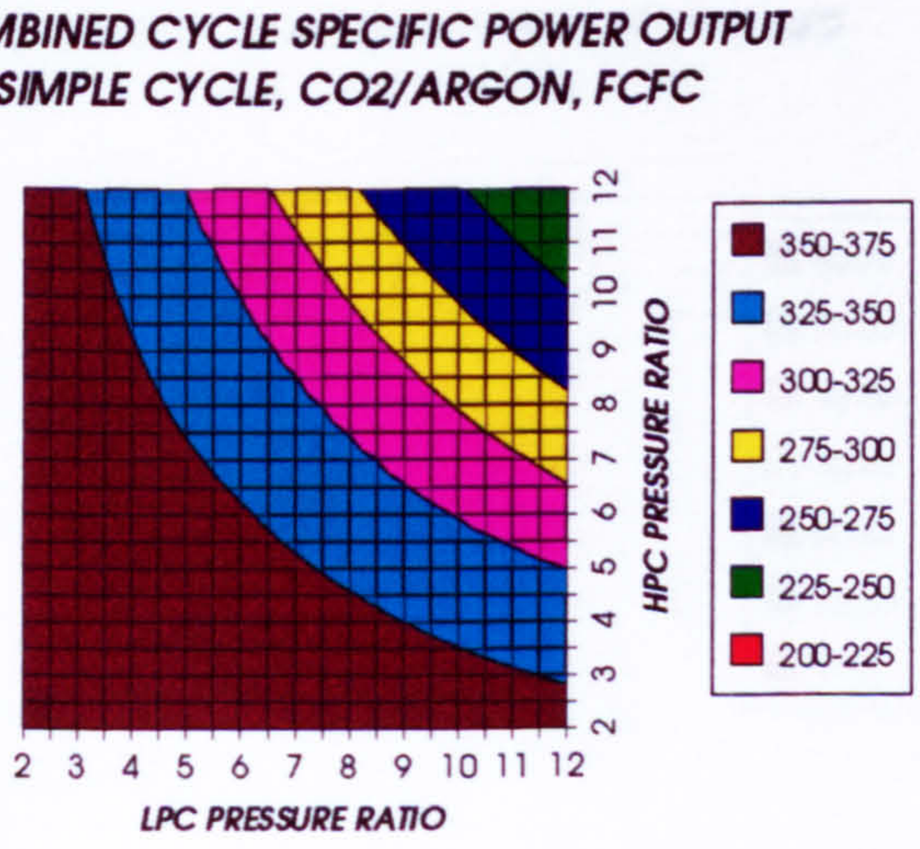

Figure 5. Combined cycle specific power output

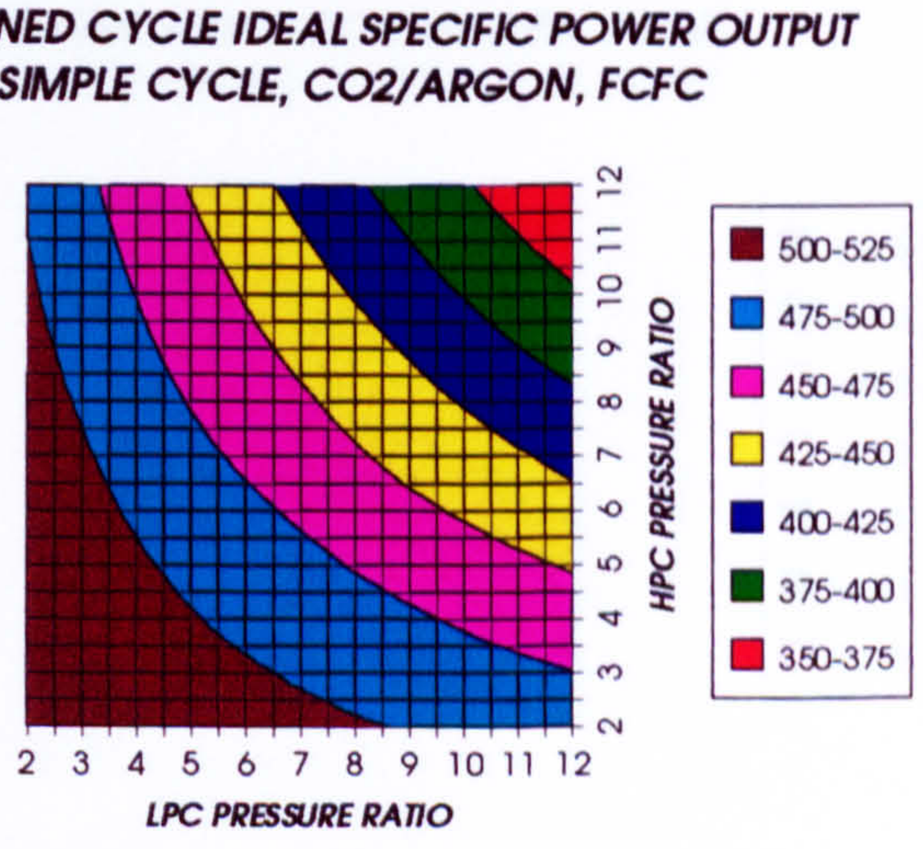

Figure 6. Combined cycle ideal specific power output

COMPLETE PLANT (TET=1473 K)

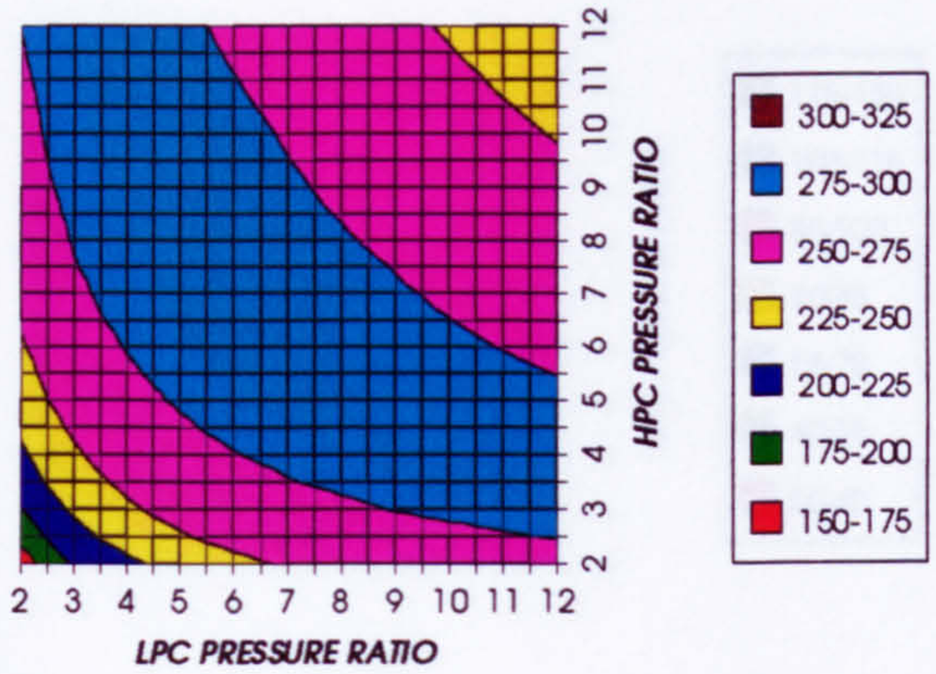

Figure 7. Gas turbine specific power output

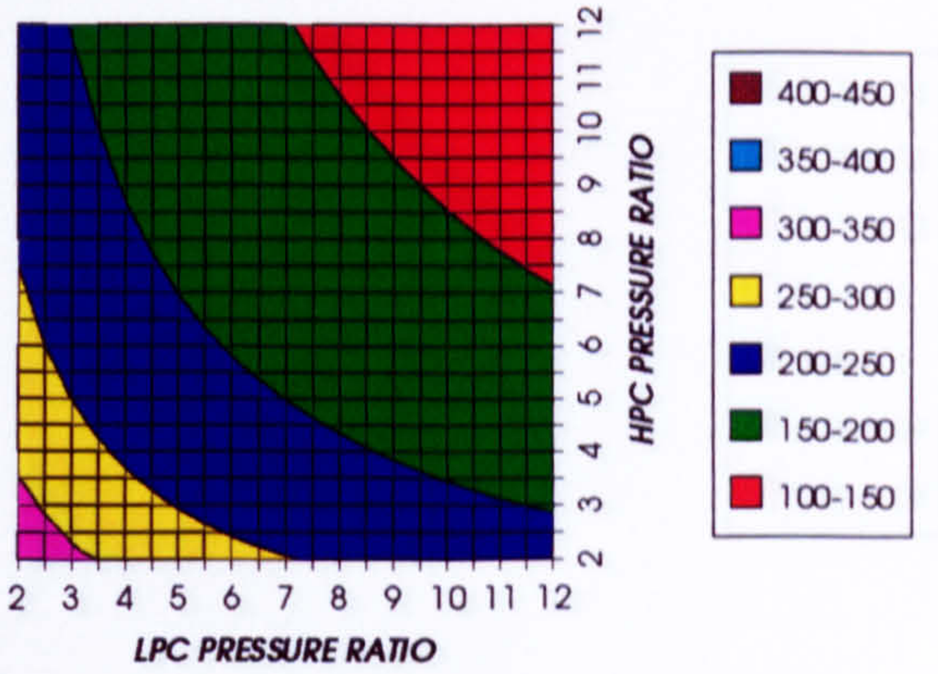

Figure 8. Steam turbine specific power output

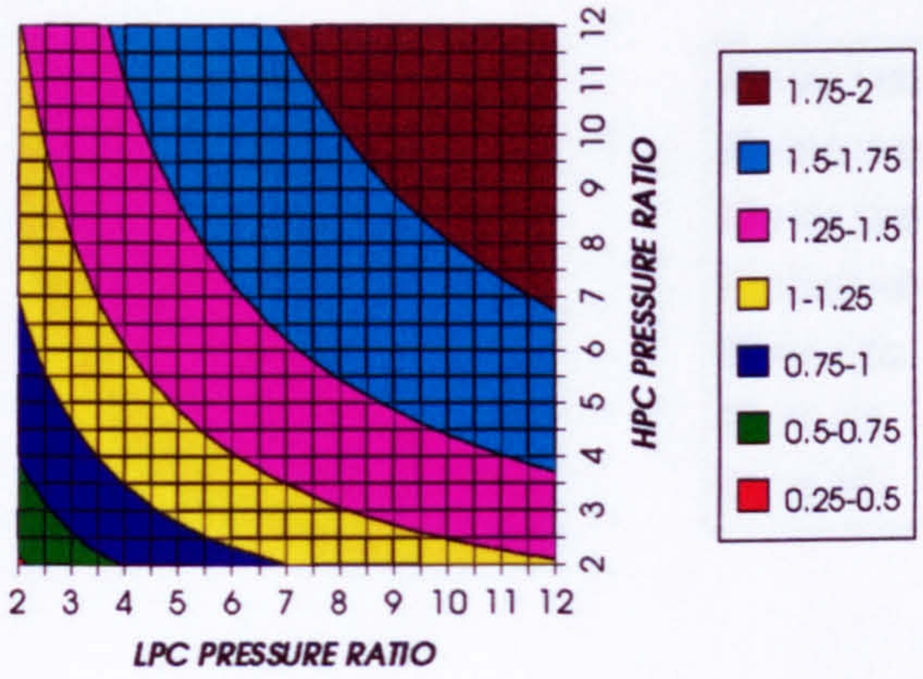

Figure 9. Gas turbine to steam turbine power ratio

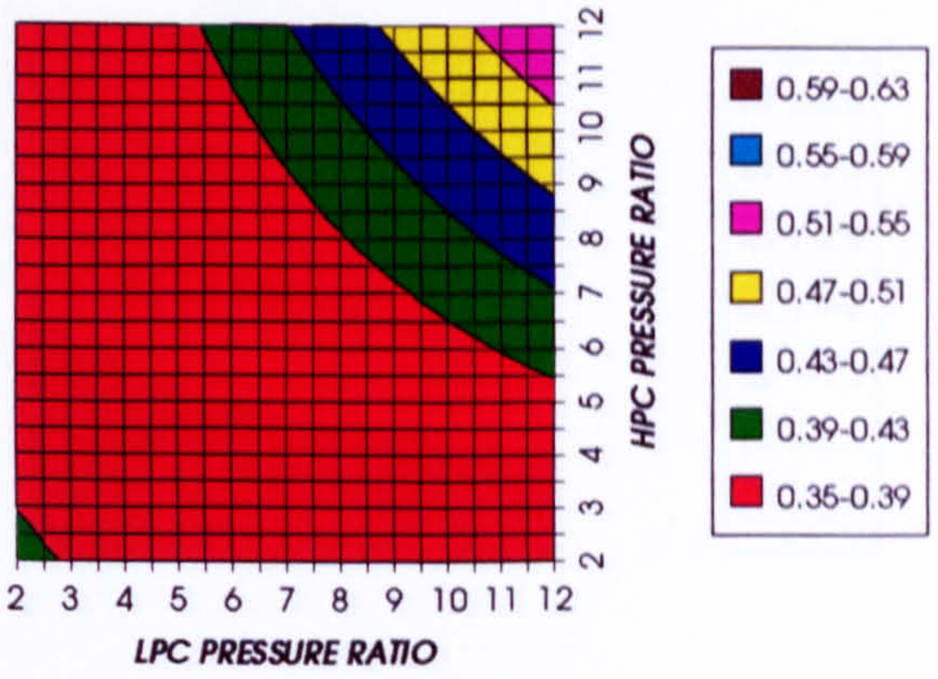

Figure 10. Auxiliary (CO2/Argon, O2 & Fuel) to usefuel power ratio

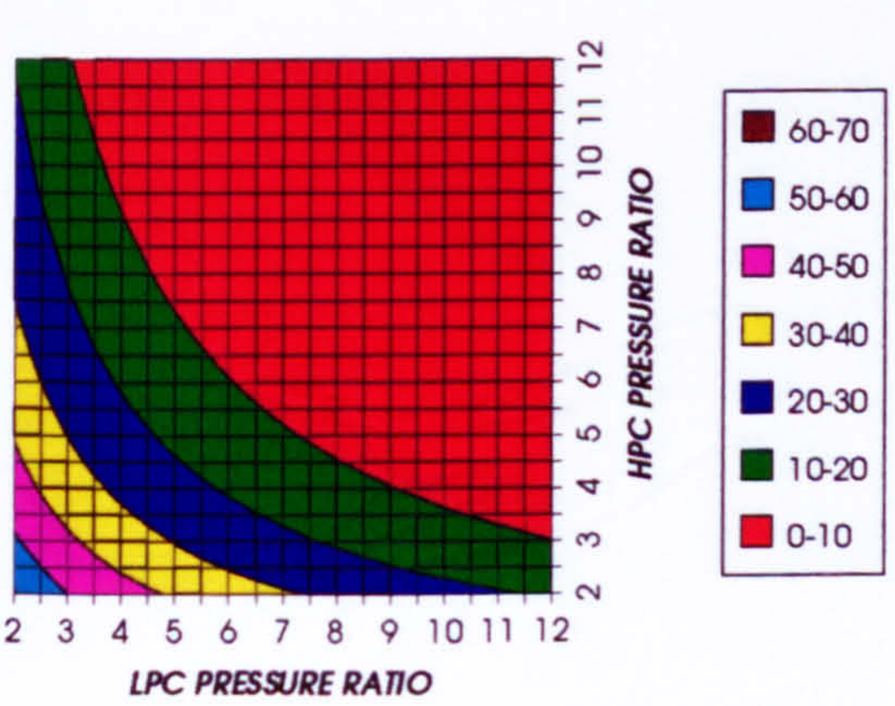

Figure 11. CO2/ Argon compression specific power

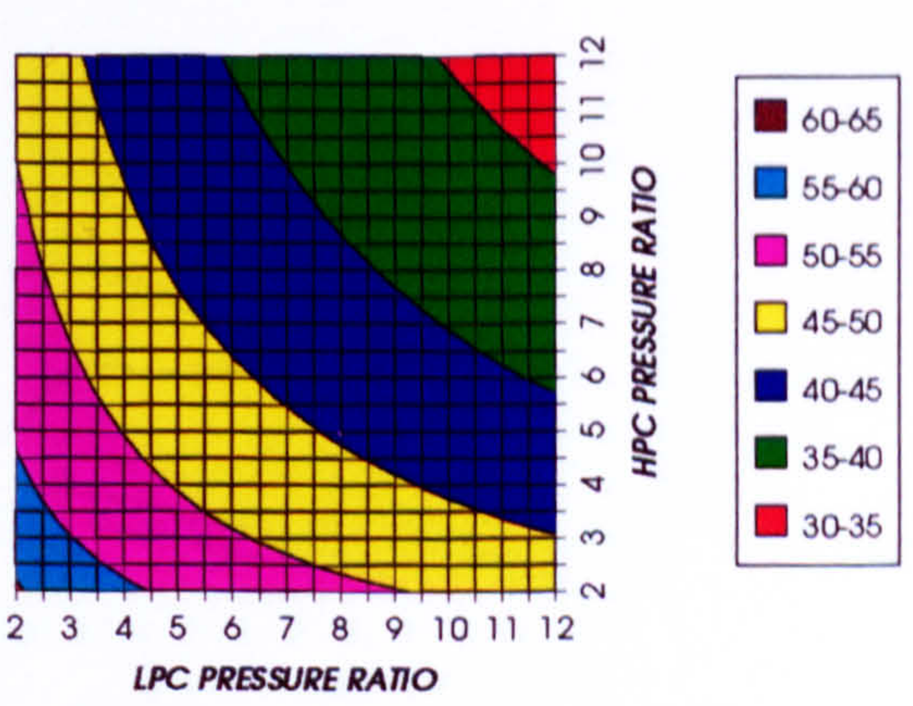

Figure 12. Oxygen separation specific power

COMPLETE PLANT (TET=1473 K)

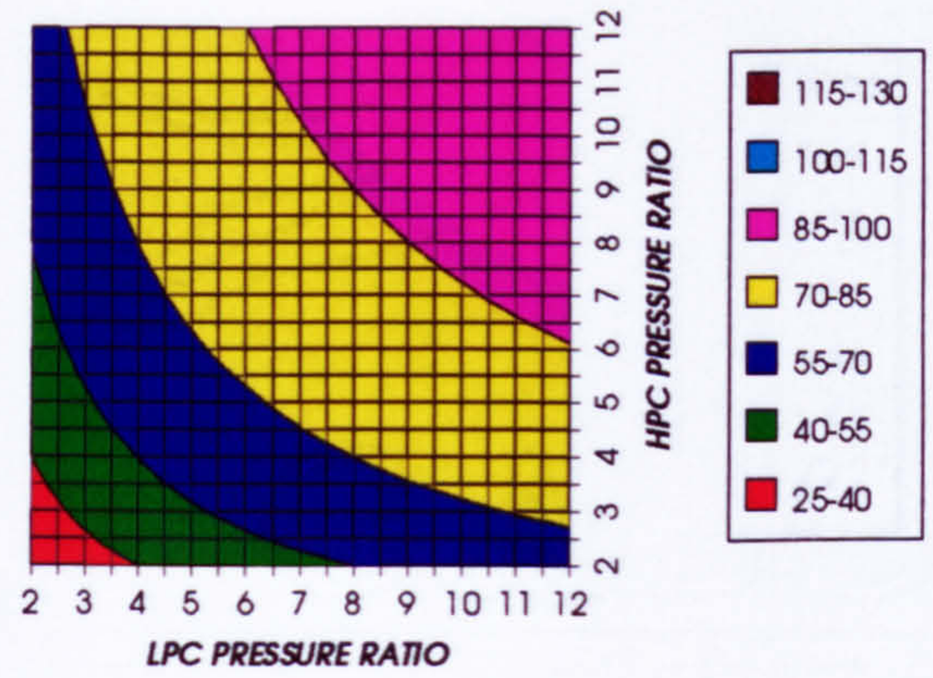

Figure 13. Fuel compression specific power

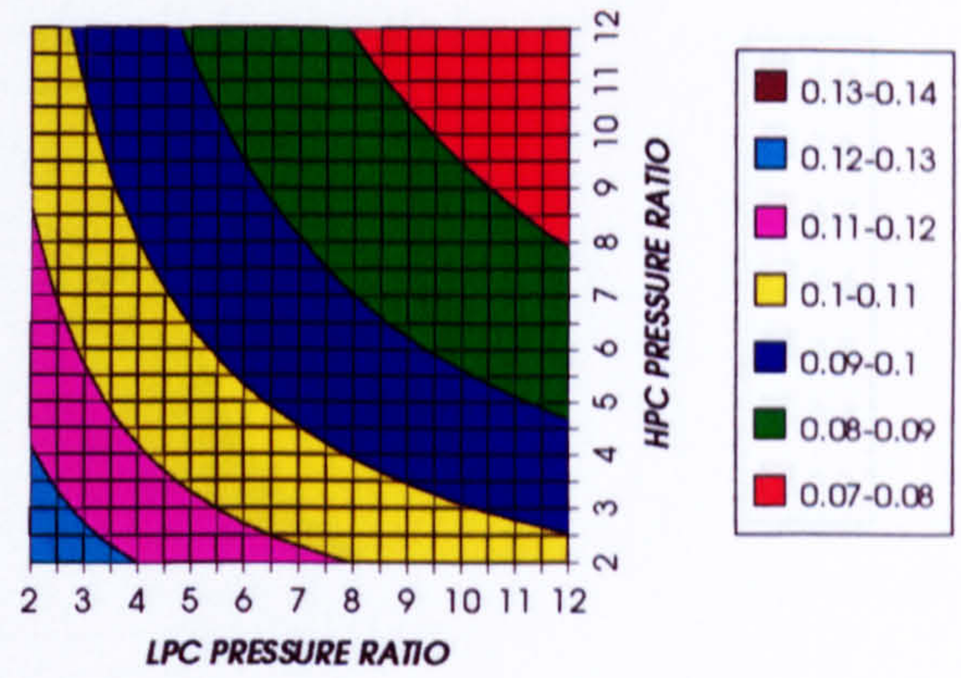

Figure 14. Fuel to compressor inlet mass flow ratio

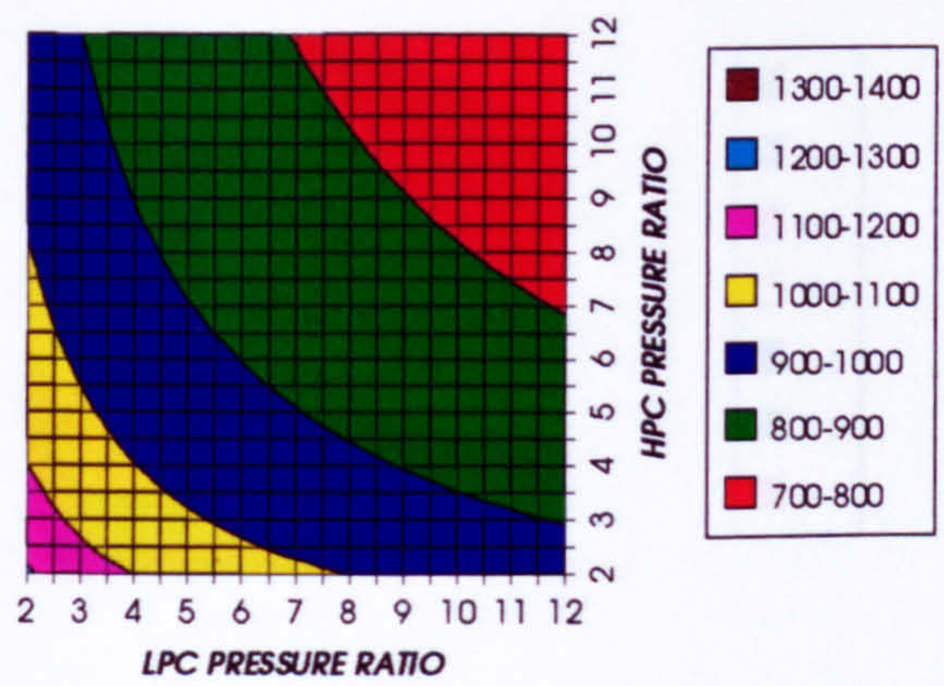

Figure 15. Gas turbine exit temperature

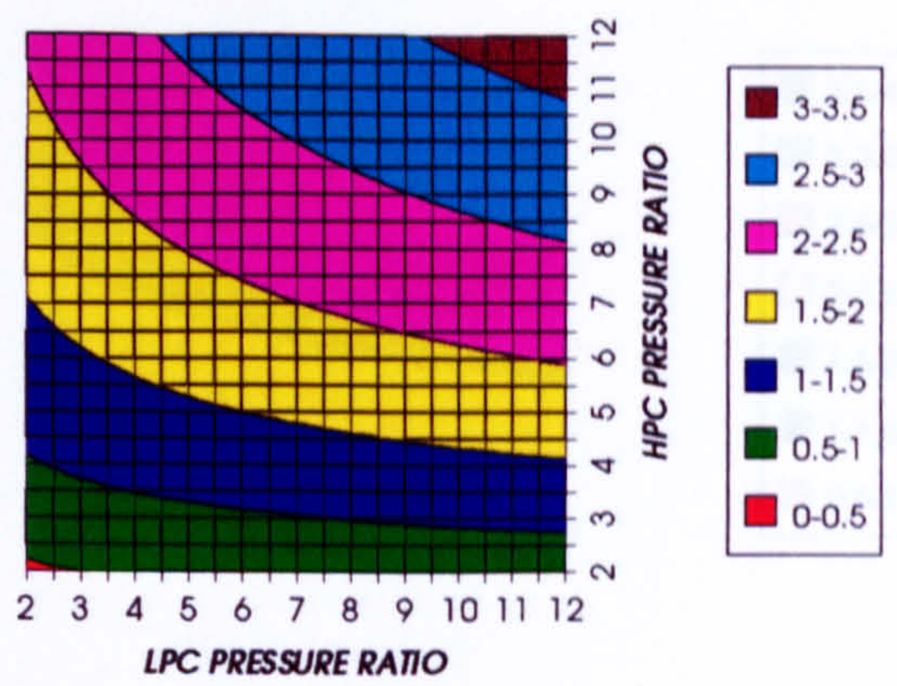

Figure 16. Number of HPT stages

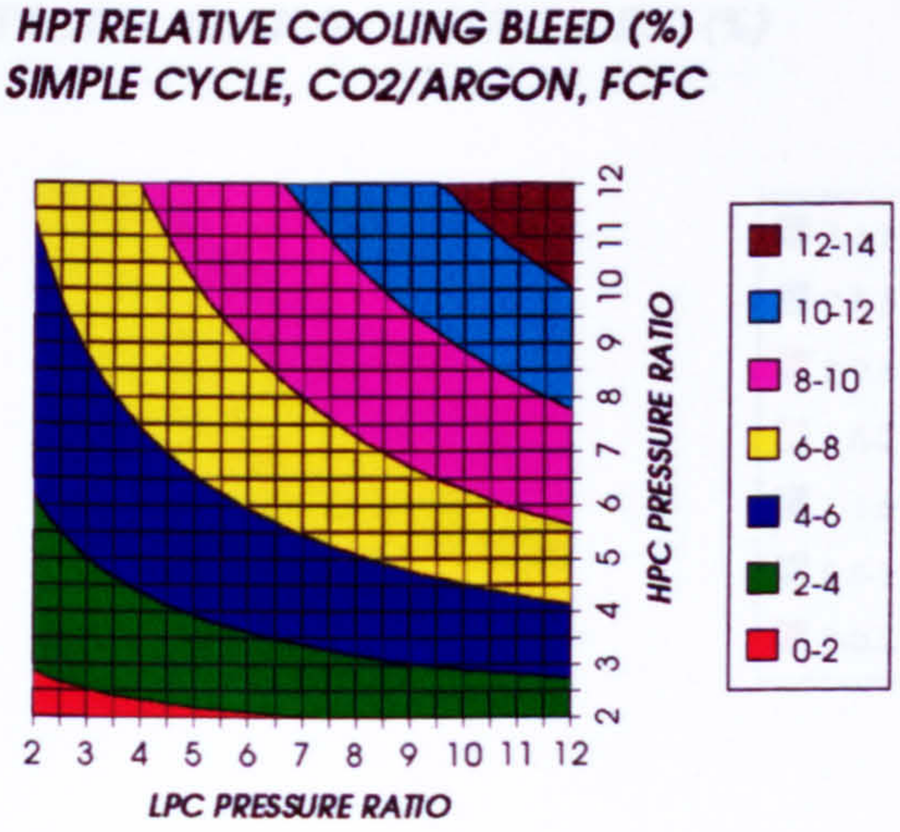

Figure 17. HPT cooling to compressor inlet mass flow ratio

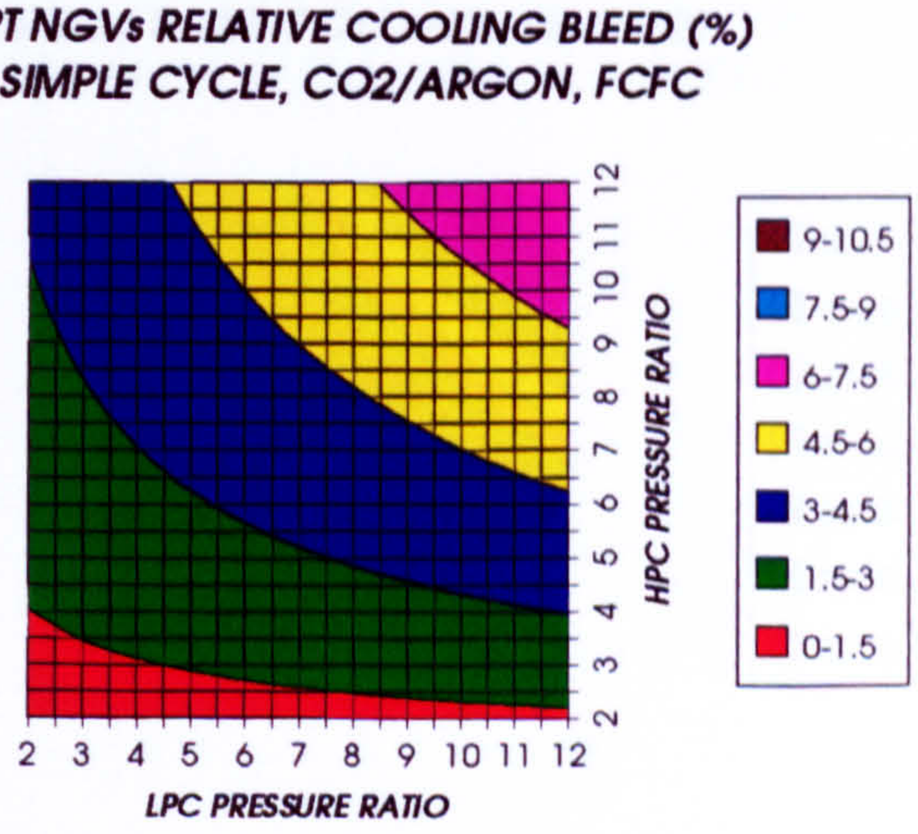

Figure 18. HPT NGVs cooling to compressor inlet mass flow ratio

COMPLETE PLANT (TET=1473 K)

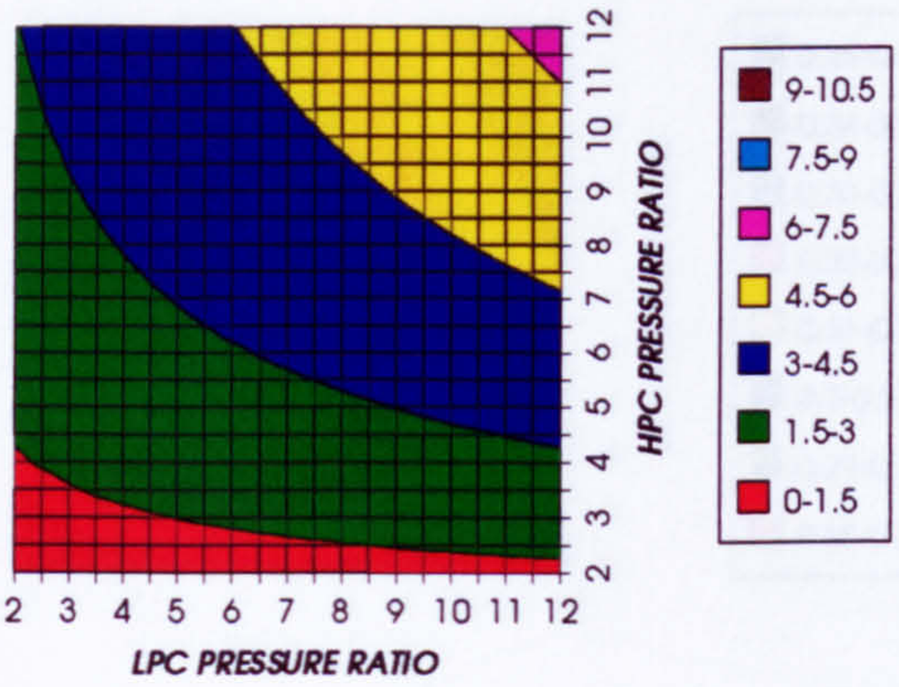

Figure 19. HPT rotor cooling to compressor inlet mass flow ratio

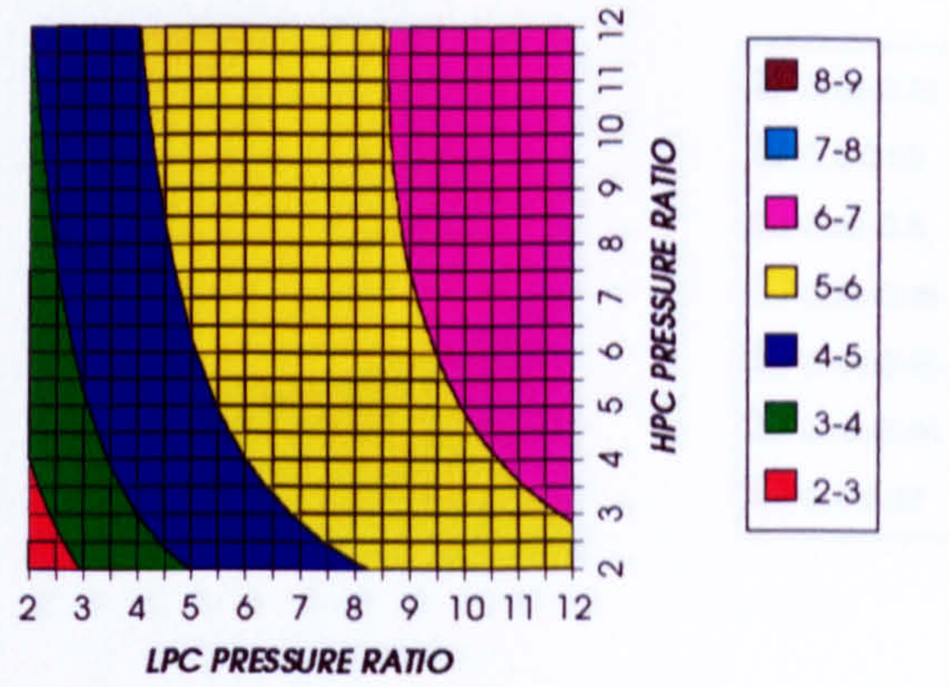

Figure 20. Number of LPT stages

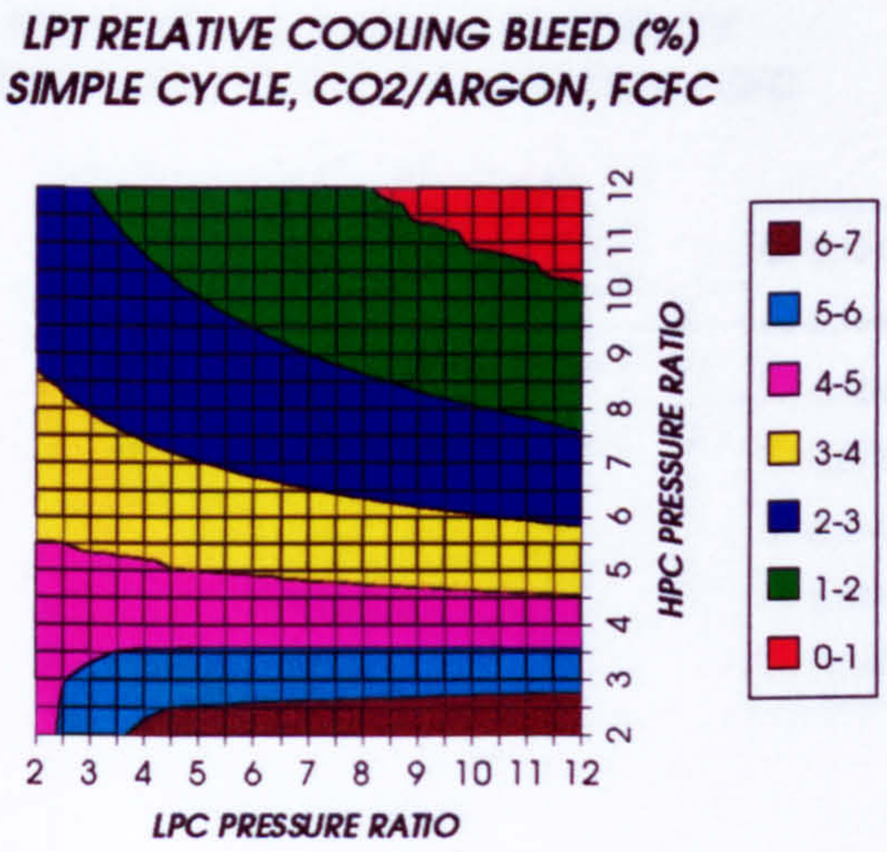

Figure 21.LPT cooling to compressor inlet mass flow ratio

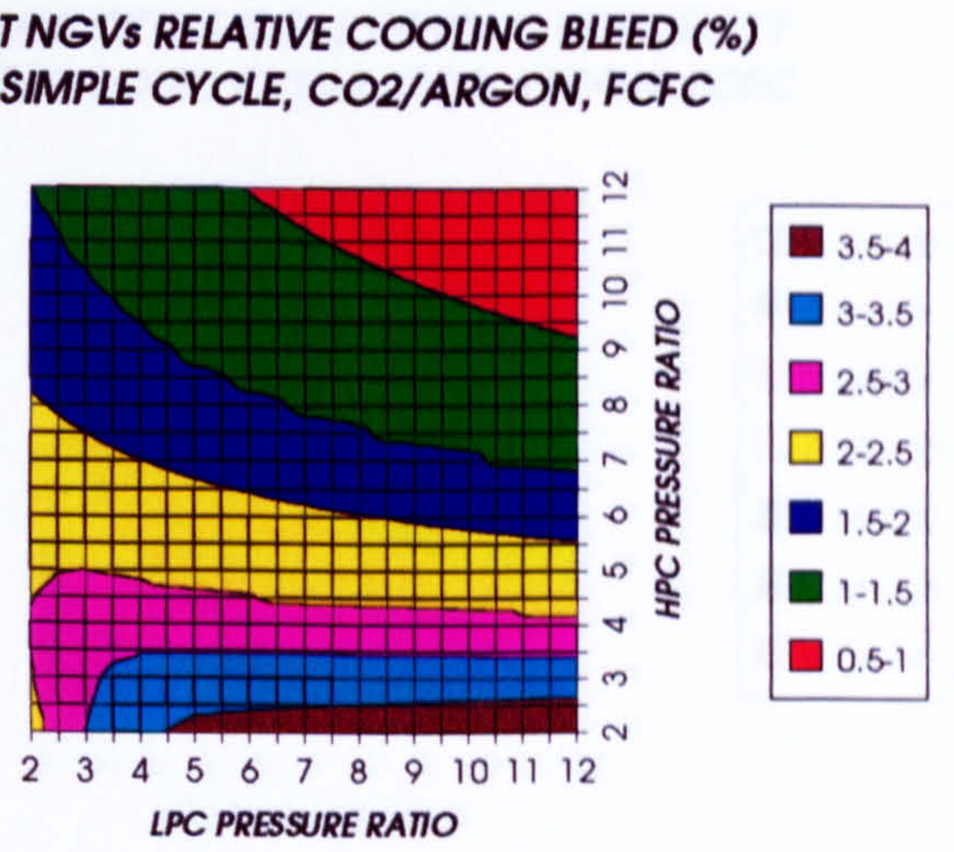

Figure 22. LPT NGVs cooling to compressor inlet mass flow ratio

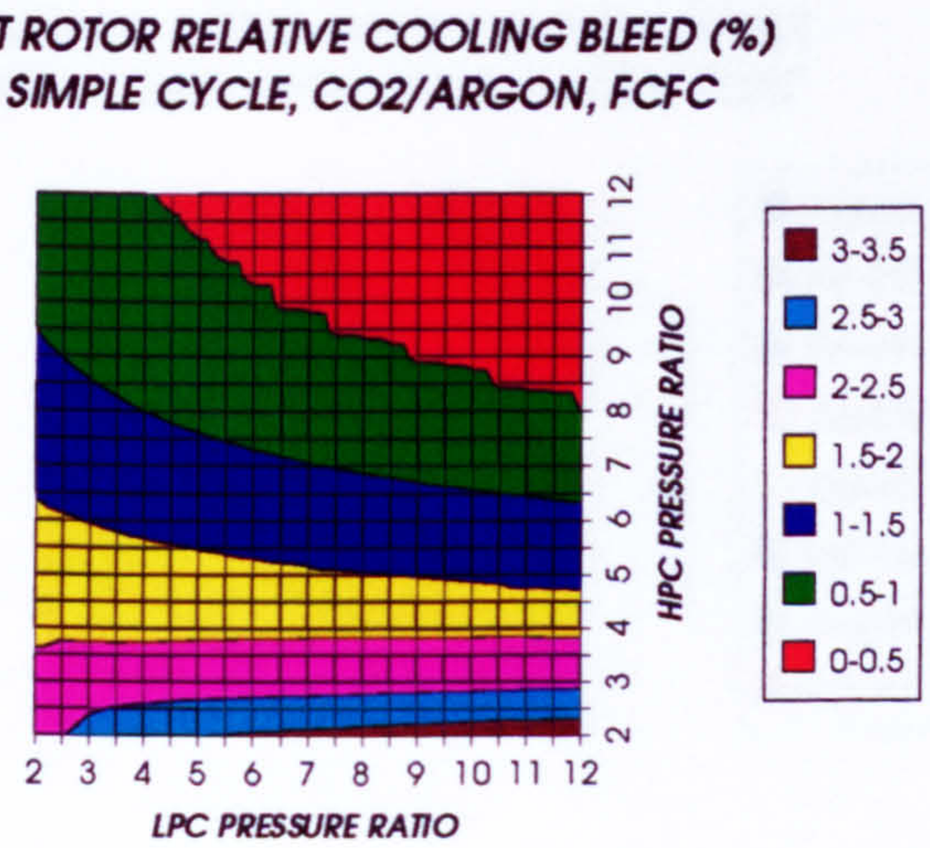

Figure 23. LPT rotor cooling to compressor inlet mass flow ratio

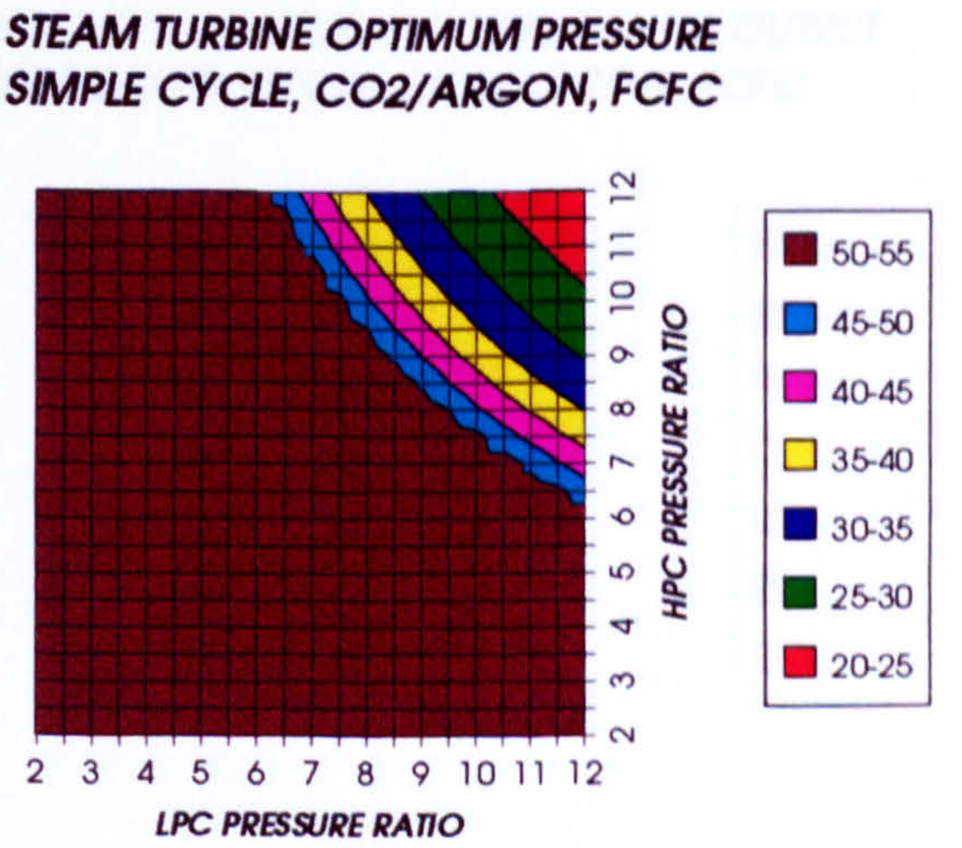

Figure 24. Steam turbine optimum pressures (maximum)

COMPLETE PLANT (TET=1473K)

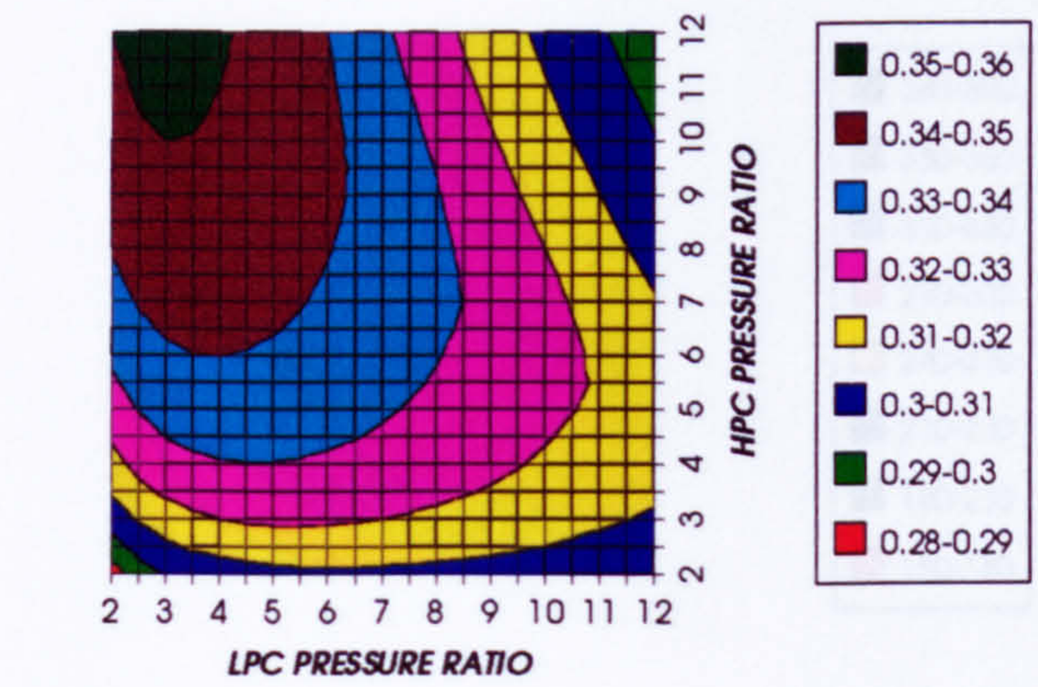

Figure 25. Combined cycle thermal efficiency

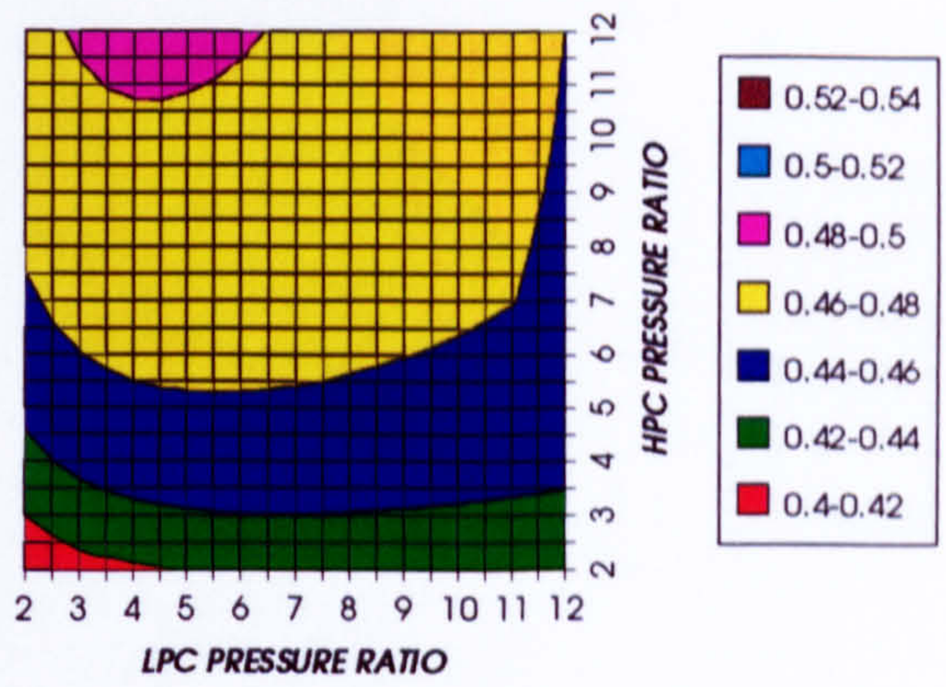

Figure 26. Combined cycle ideal thermal efficiency

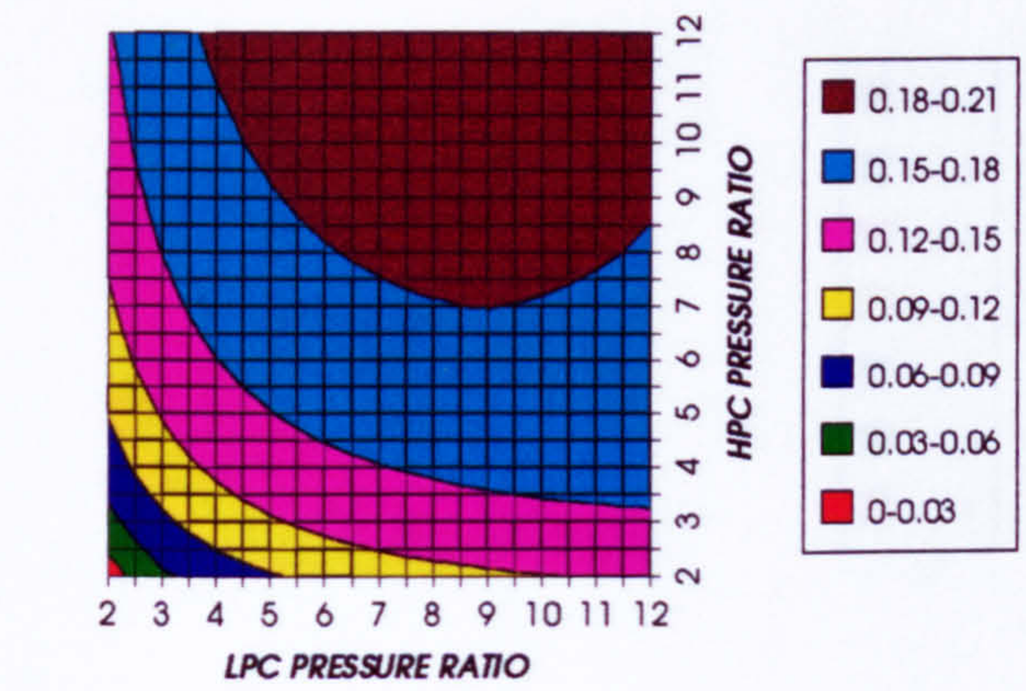

Figure 27. Simple cycle thermal efficiency

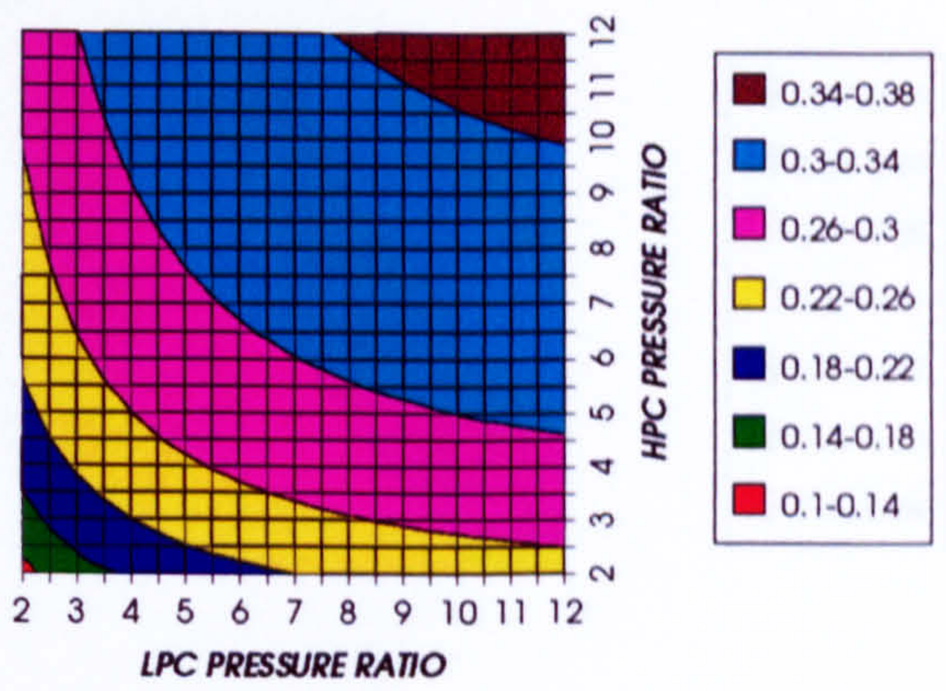

Figure 28. Simple cycle ideal thermal efficiency

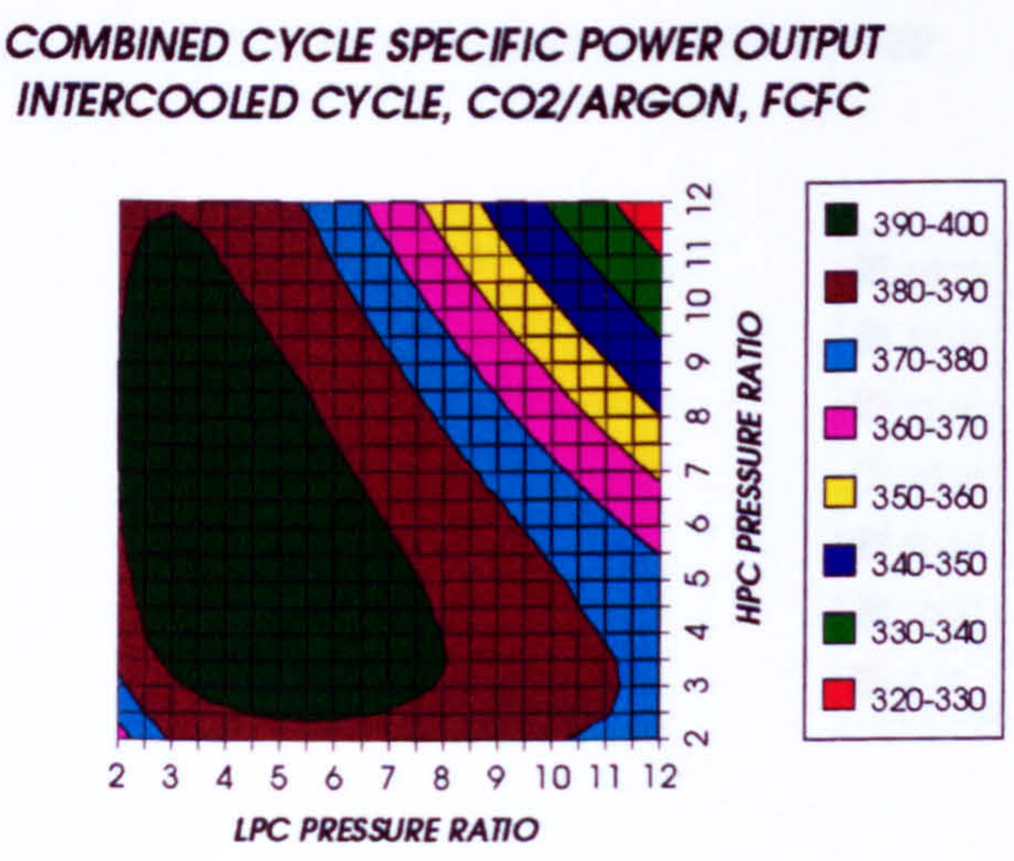

Figure 29. Combined cycle specific power output

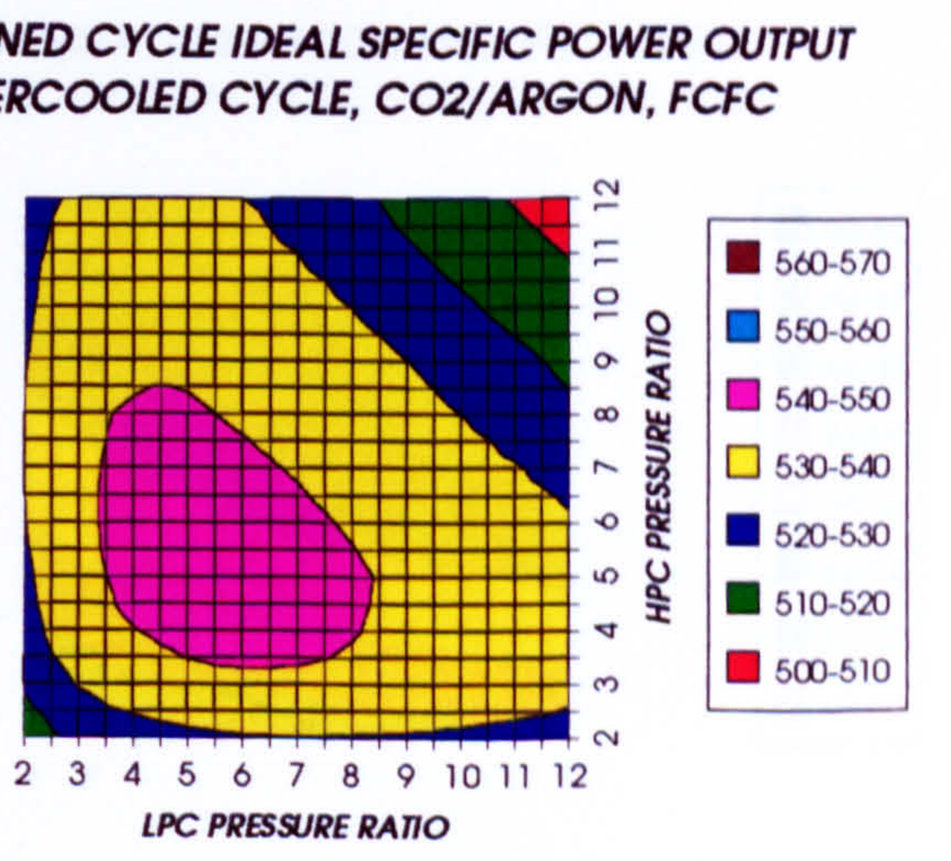

Figure 30. Combined cycle ideal specific power output

COMPLETE PLANT (TET=1473 K)

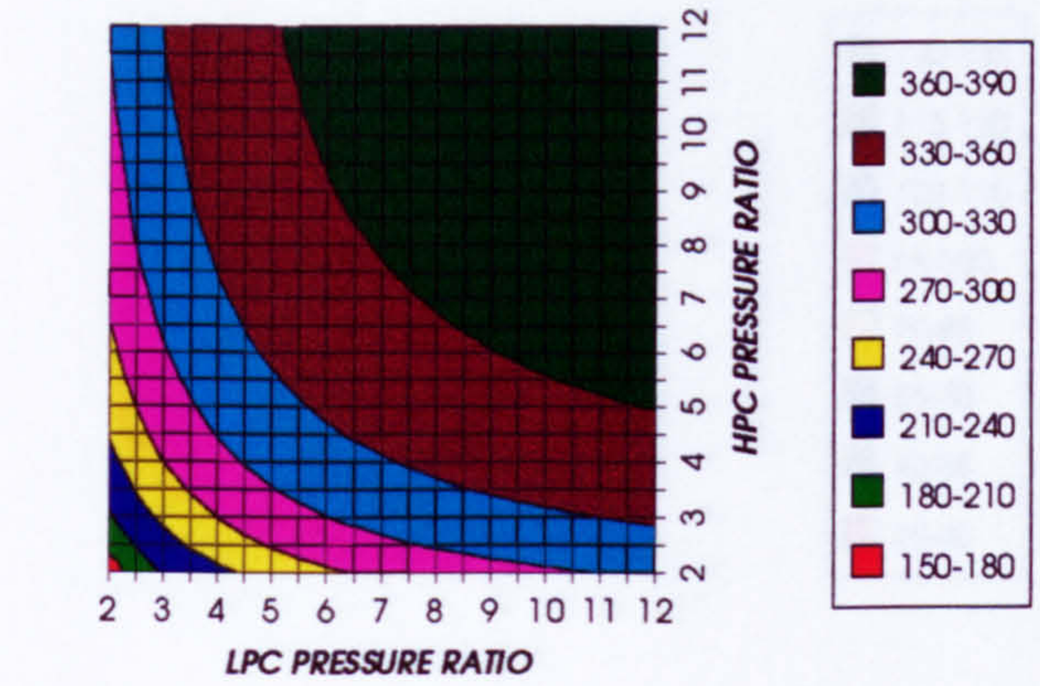

Figure 31. Gas turbine specific power output

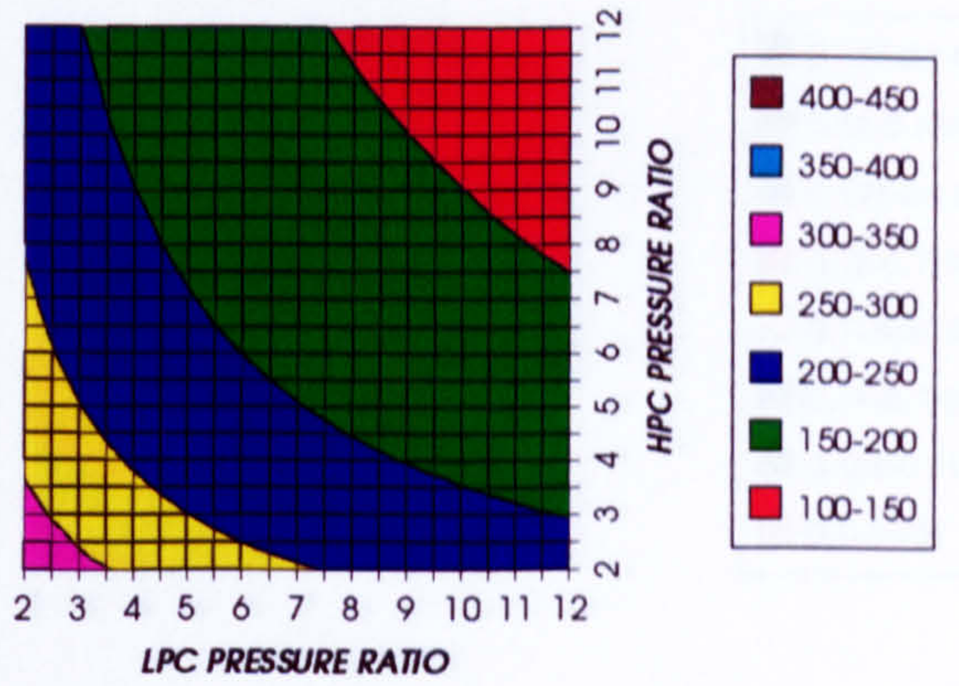

Figure 32. Steam turbine specific power output

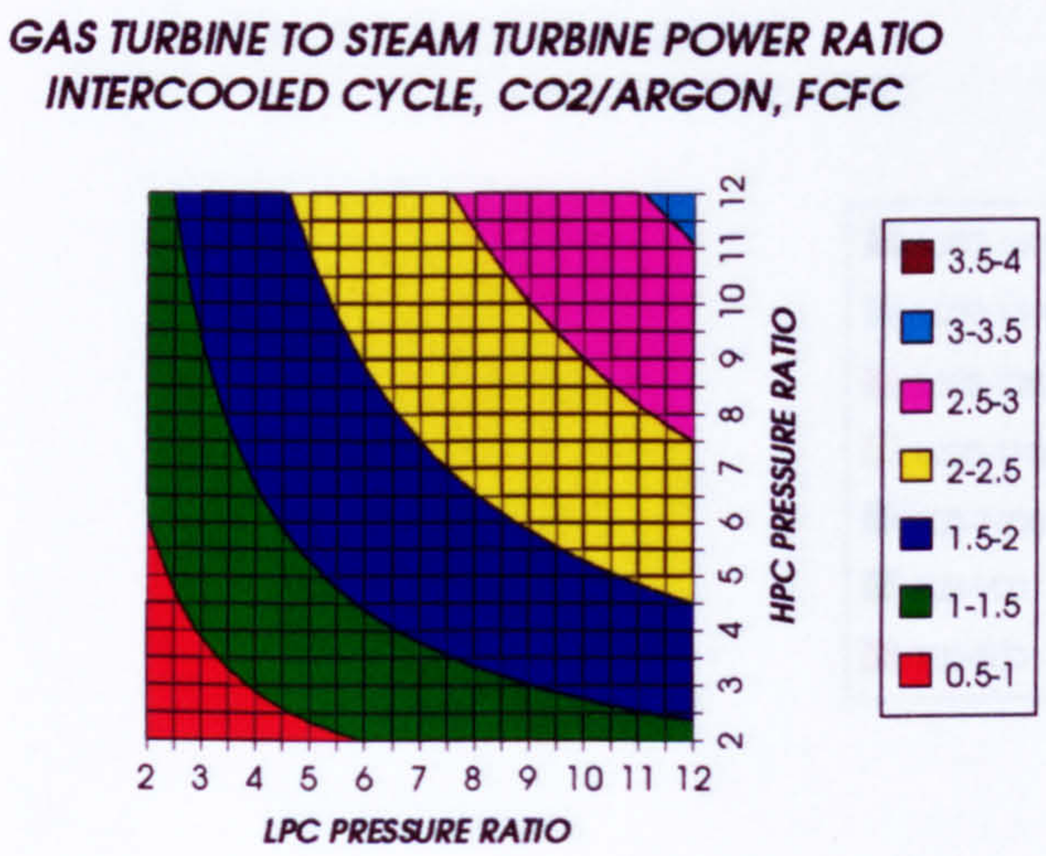

Figure 33. Gas turbine to steam turbine power ratio

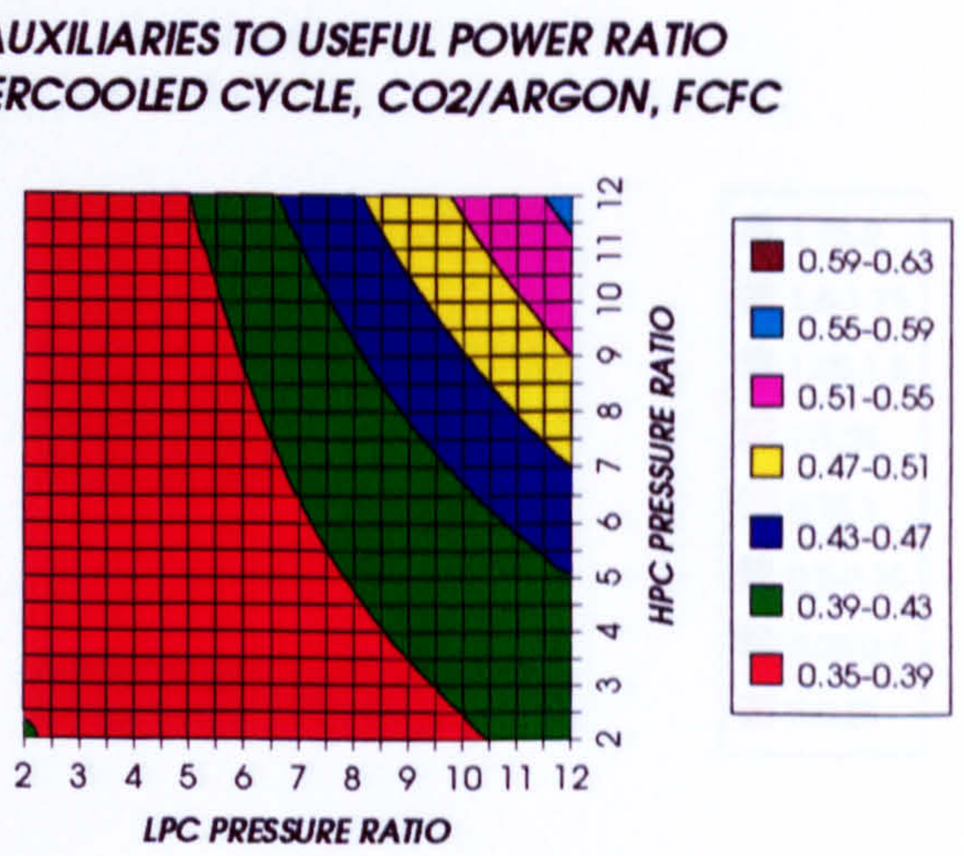

Figure 34. Auxiliary (CO2/Argon, O2 & Fuel) to usefuel power ratio

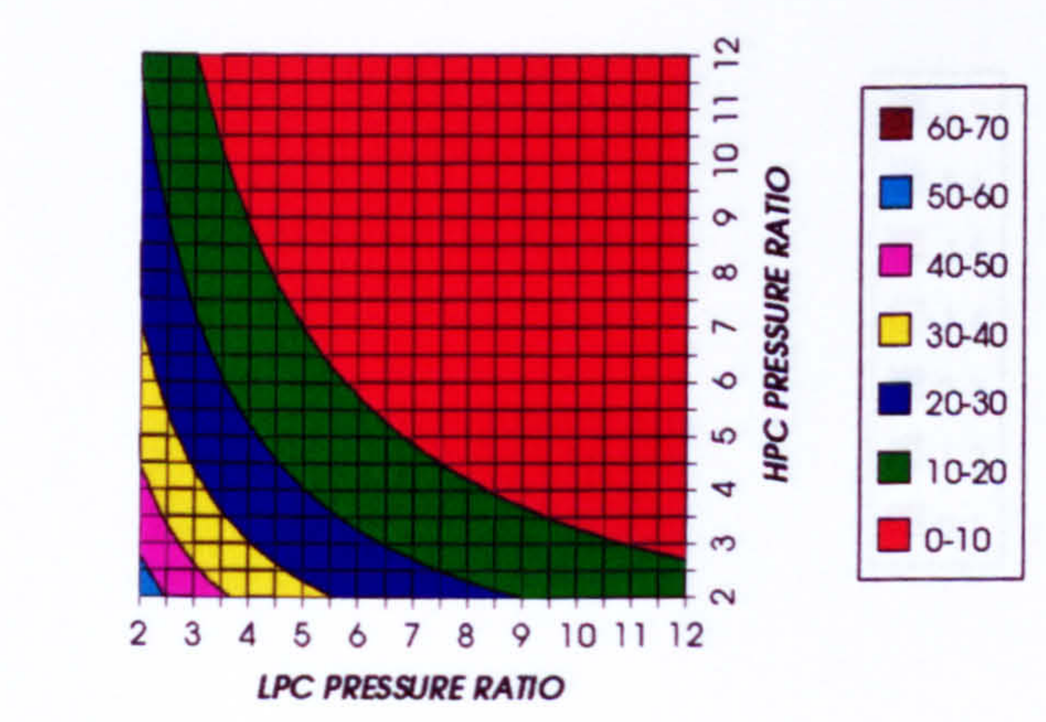

Figure 35. CO2/Argon compression specific power

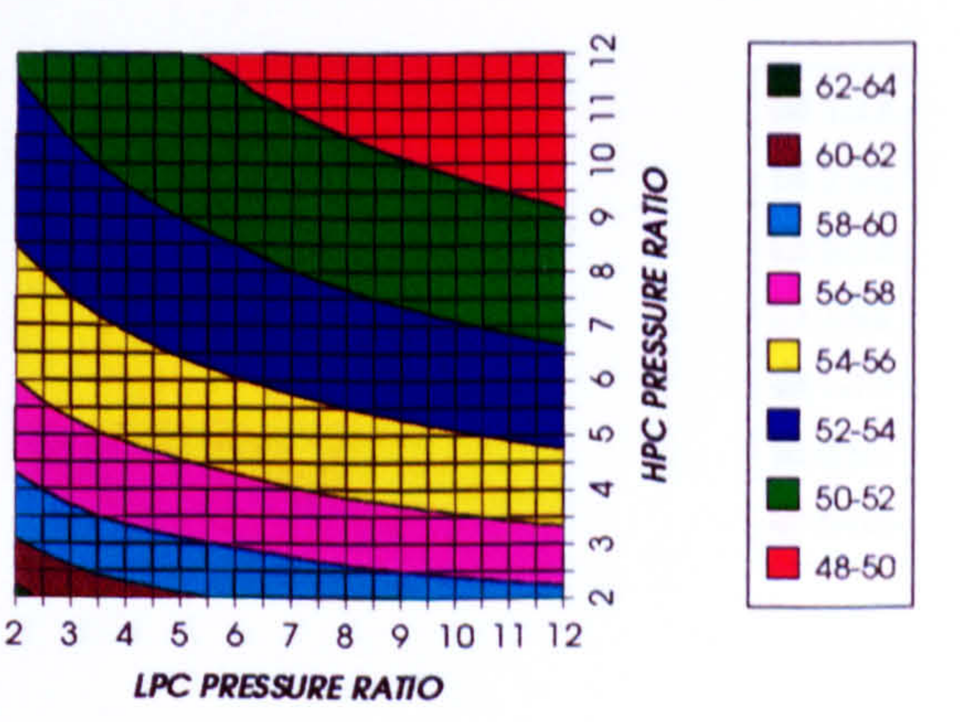

Figure 36. Oxygen separation specific power

COMPLETE PLANT (TET=1473 K)

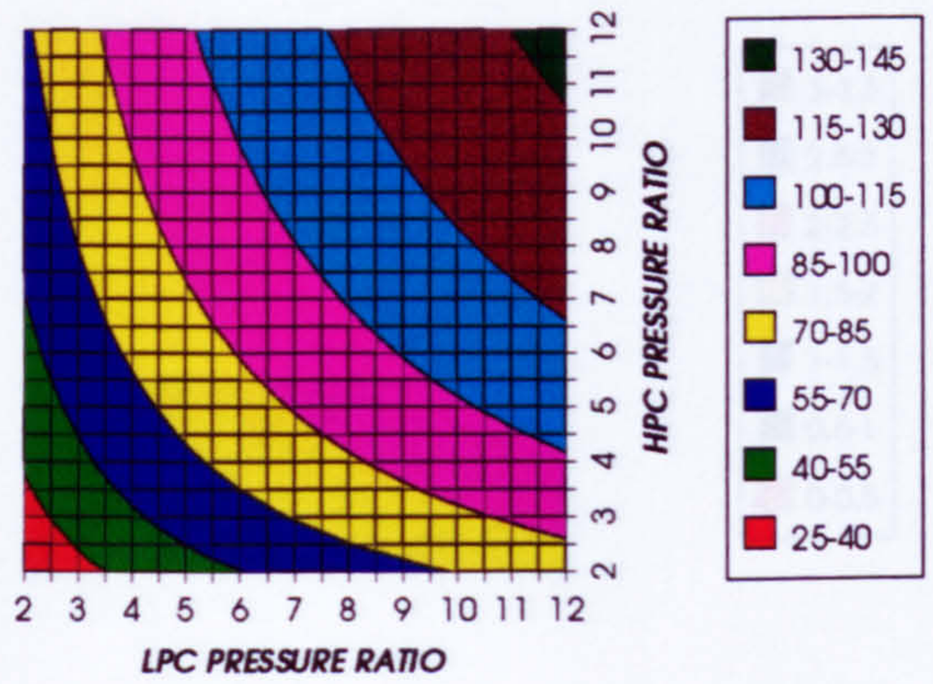

Figure 37. Fuel compression specific power

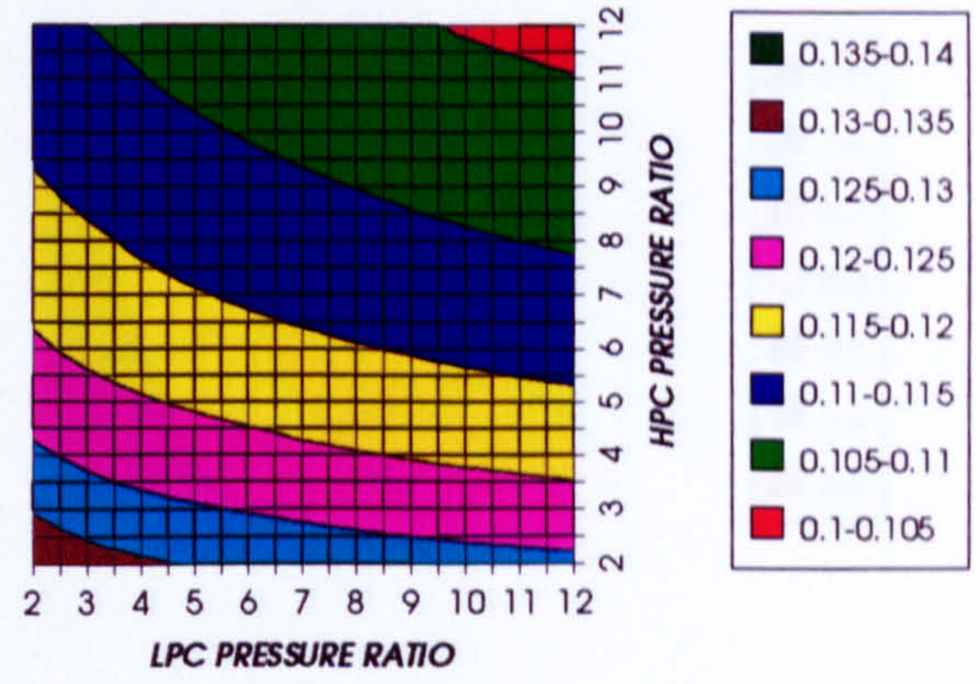

Figure 38. Fuel to compressor inlet mass flow ratio

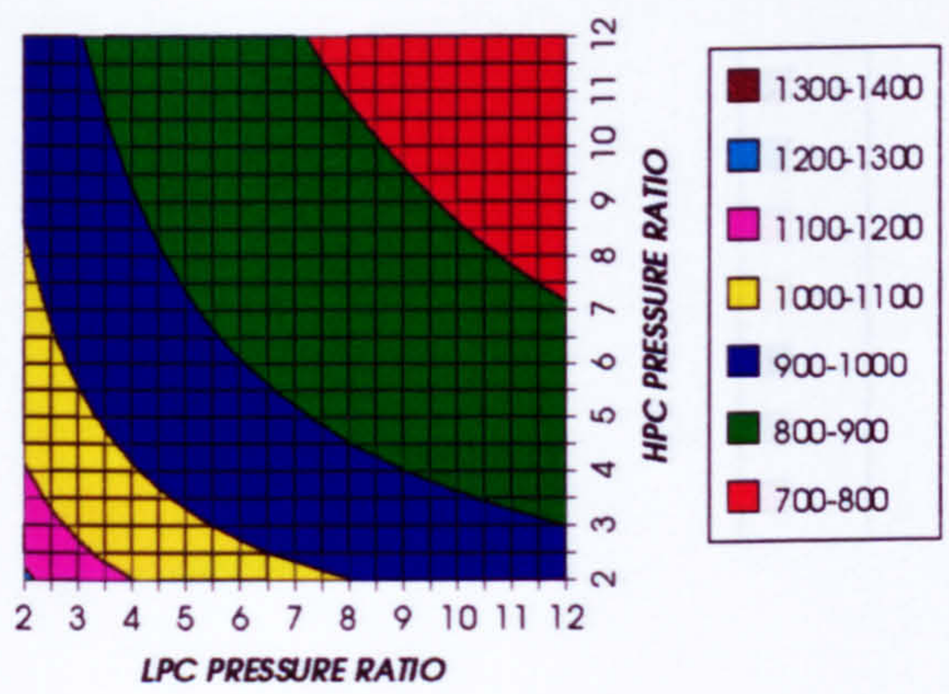

Figure 39. Gas turbine exit temperature

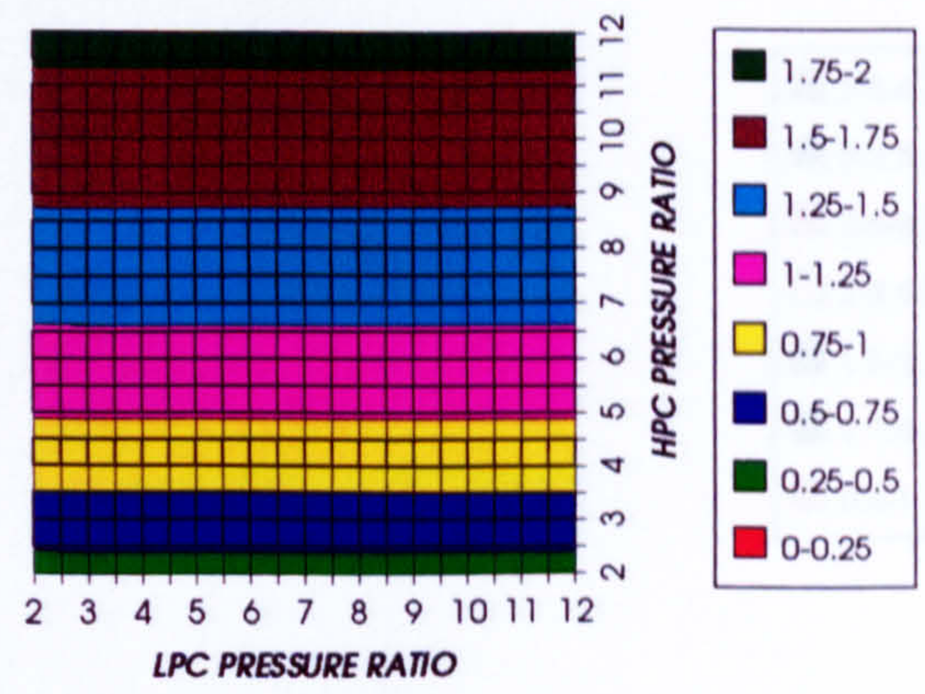

Figure 40. Number of HPT stages

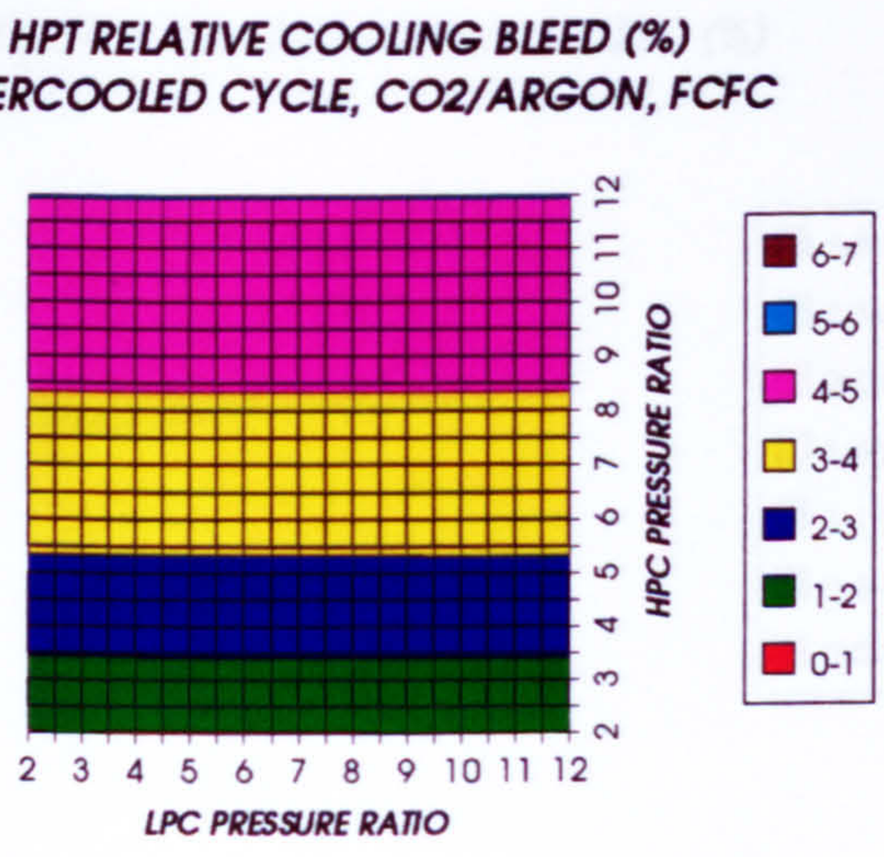

Figure 41. HPT cooling to compressor inlet mass flow ratio

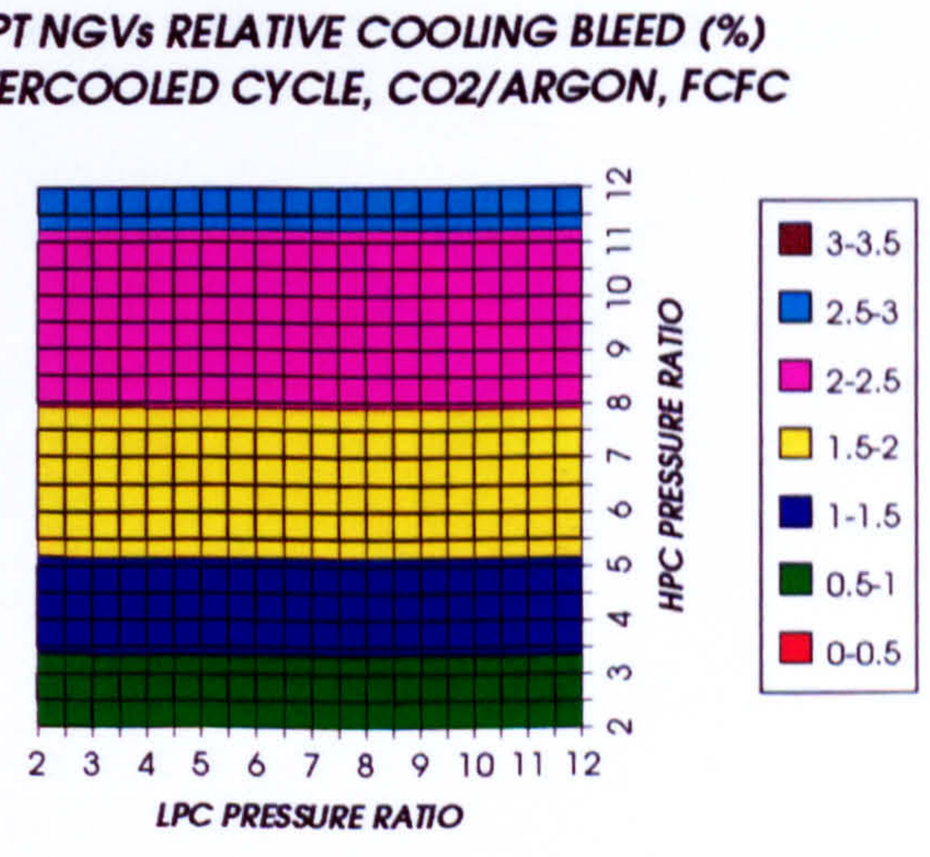

Figure 42. HPT NGVs cooling to compressor inlet mass flow ratio

COMPLETE PLANT (TET=1473 K)

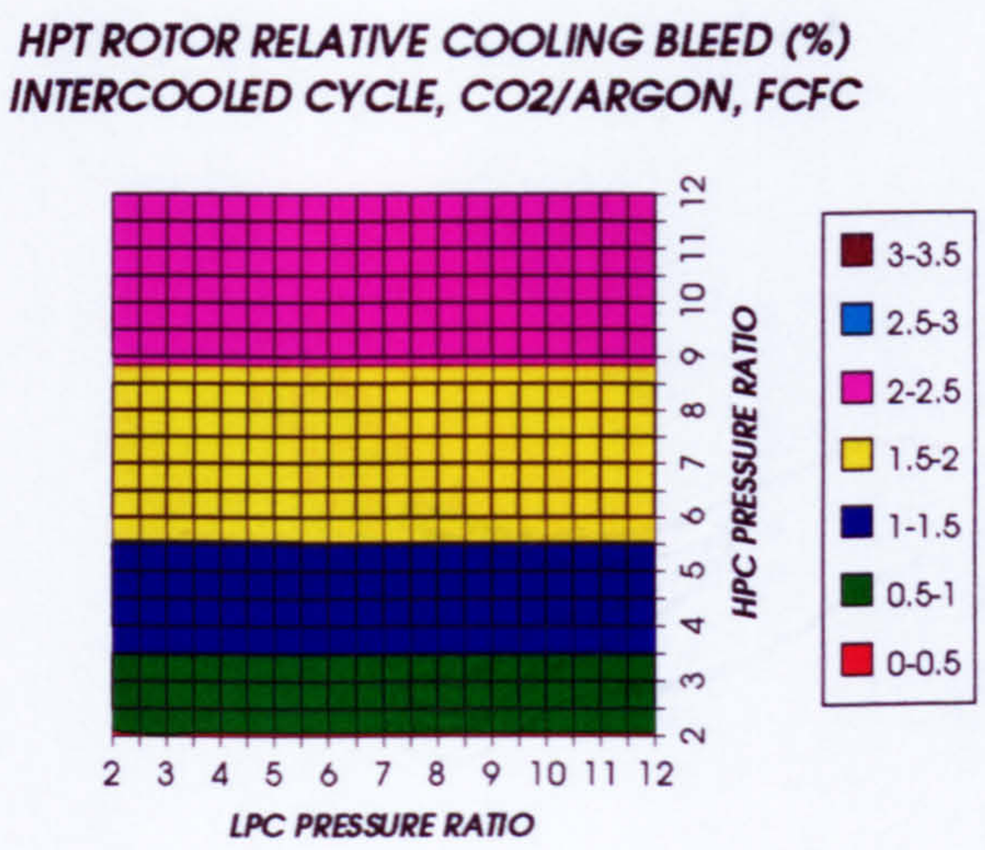

Figure 43. HPT rotor cooling to compressor inlet mass flow ratio

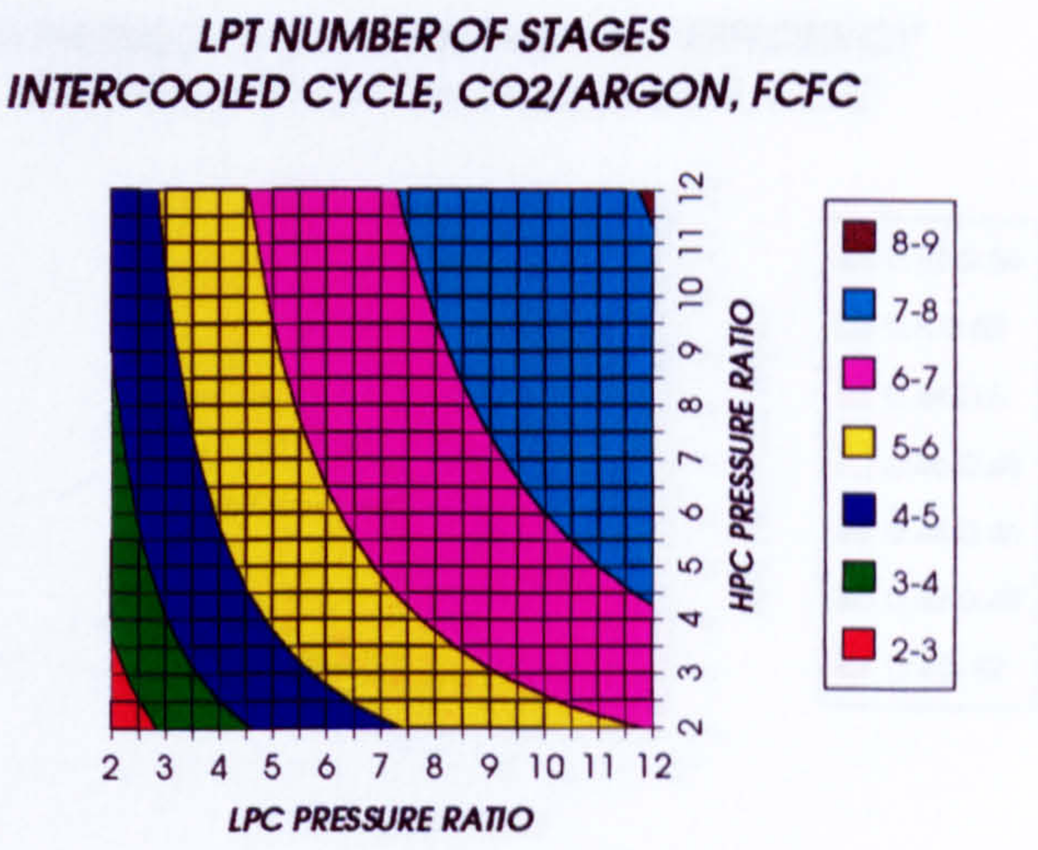

Figure 44. Number of LPT stages

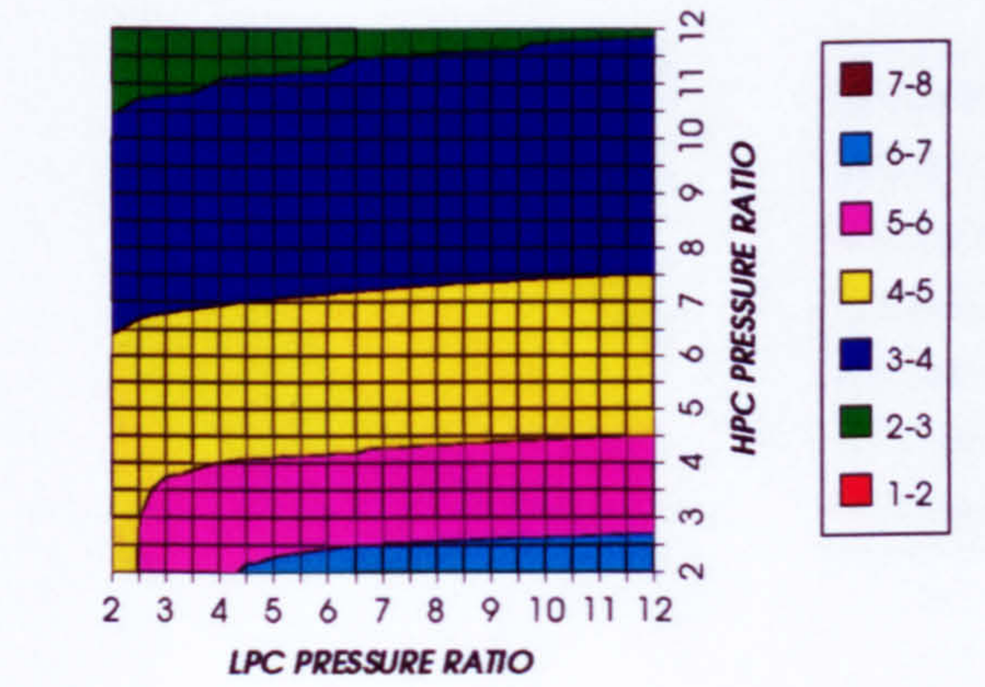

Figure 45.LPT cooling to compressor inlet mass flow ratio

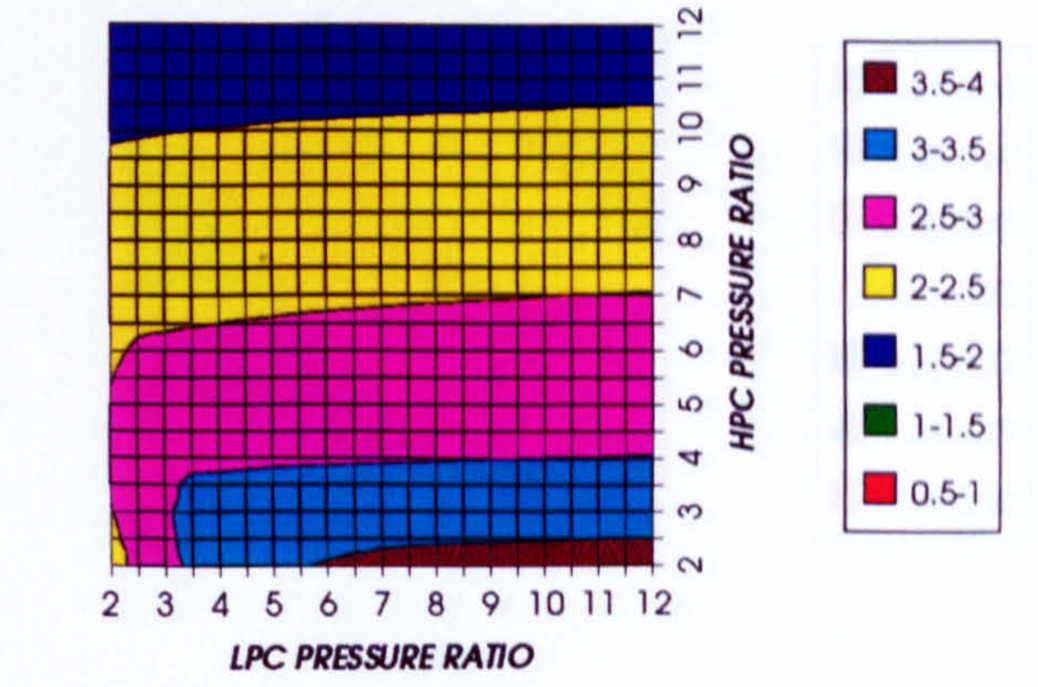

Figure 46. LPT NGVs cooling to compressor inlet mass flow ratio

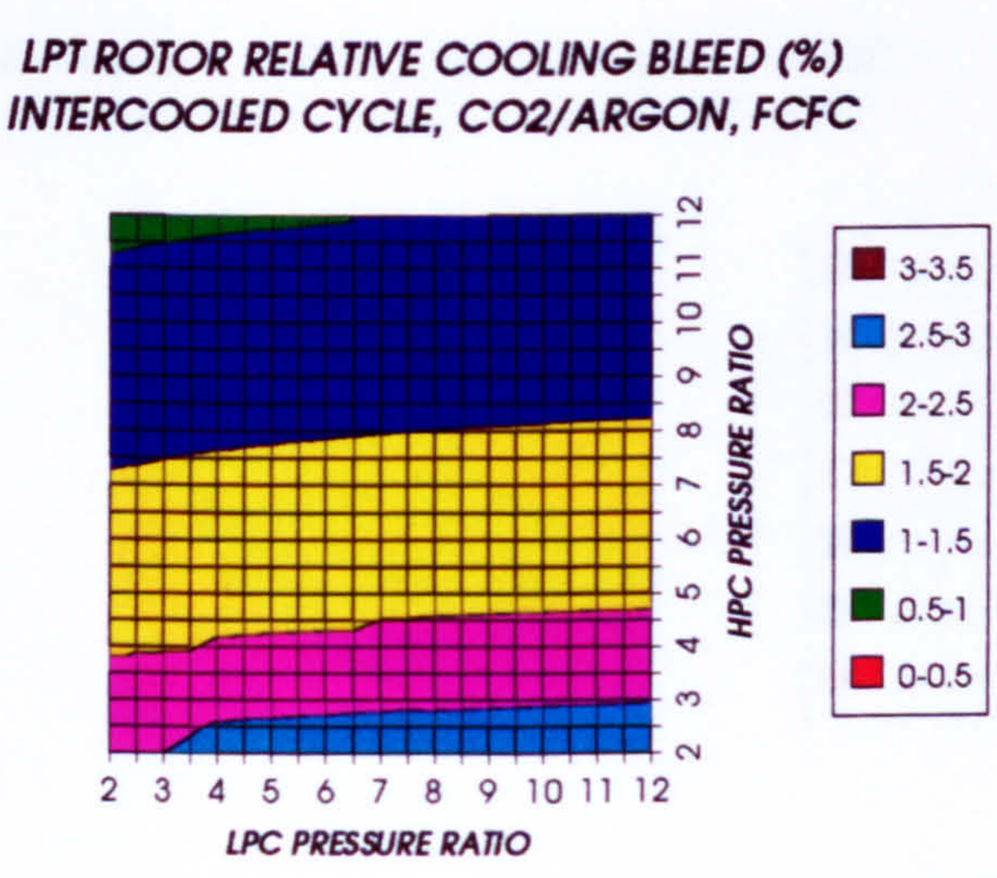

Figure 47. LPT rotor cooling to compressor inlet mass flow ratio

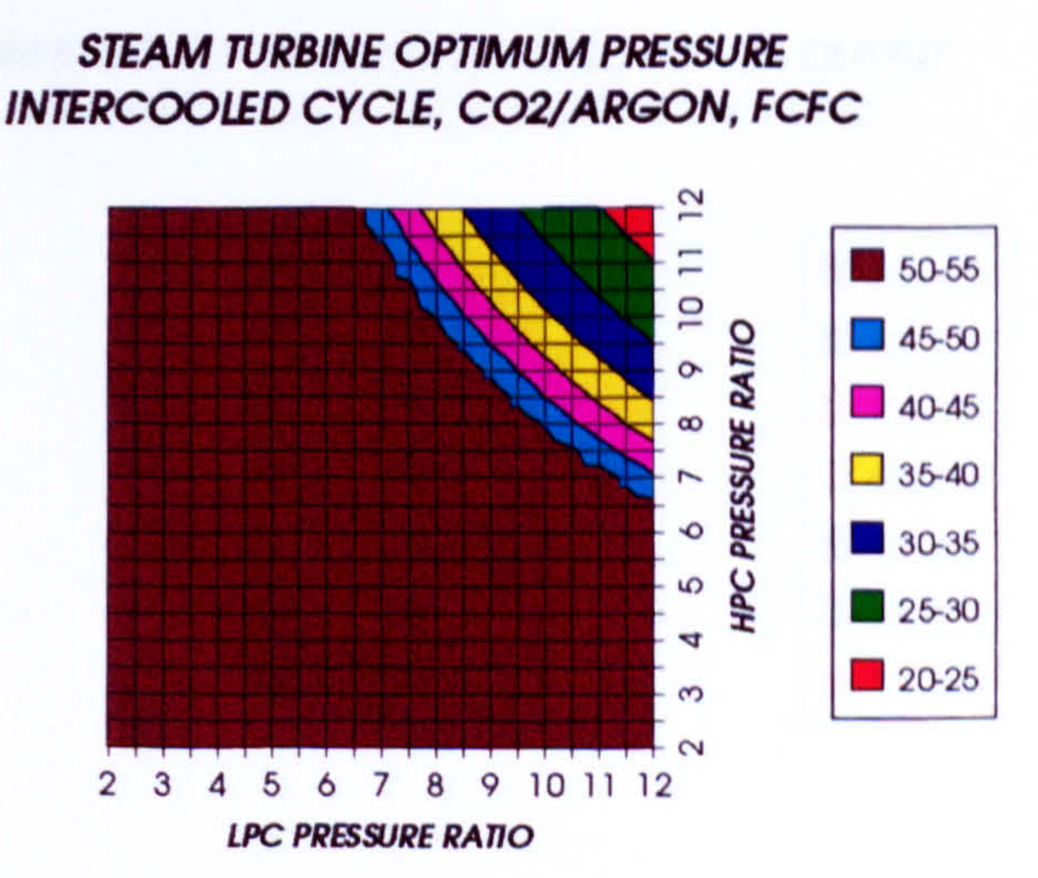

Figure 48. Steam turbine optimum pressures (maximum)

COMPLETE PLANT (TET=1473K)

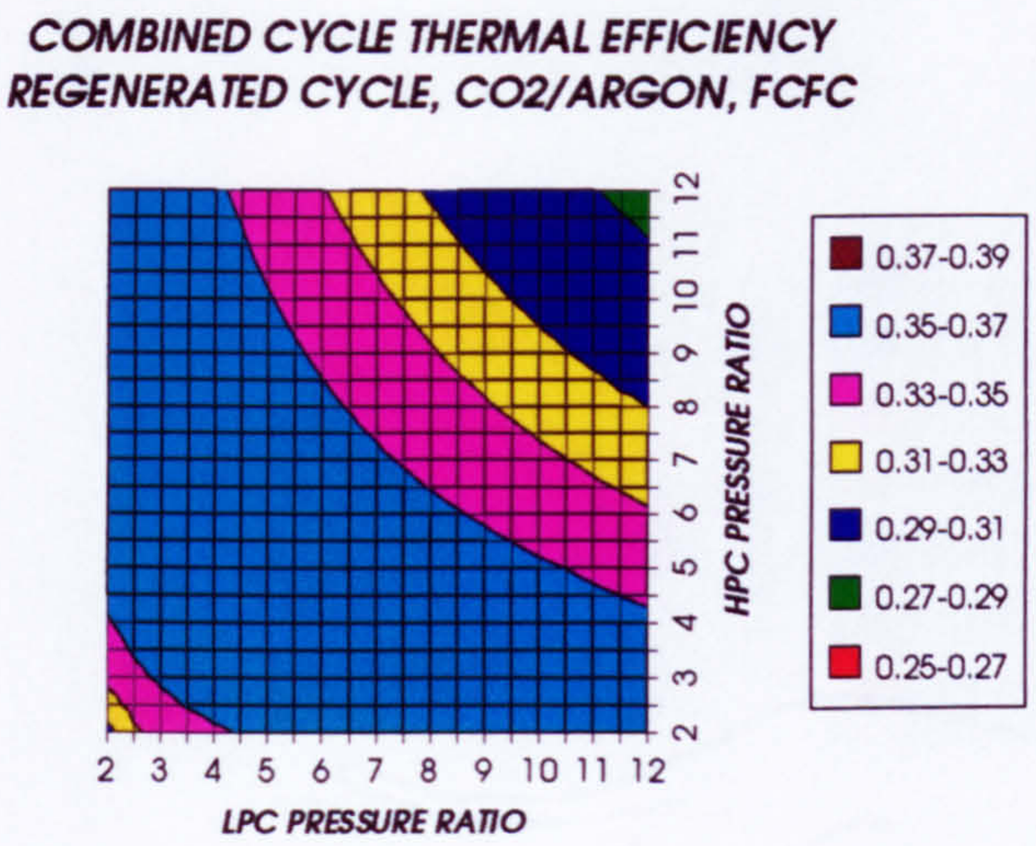

Figure 49. Combined cycle thermal efficiency

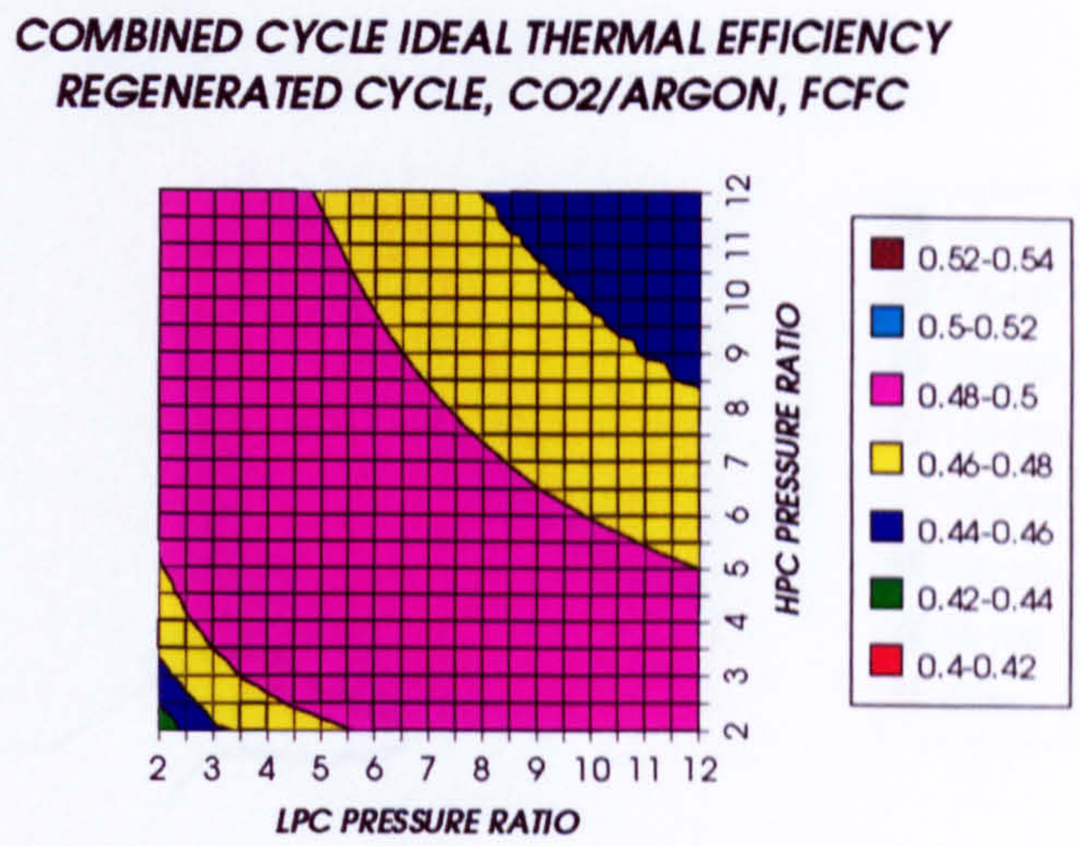

Figure 50. Combined cycle ideal thermal efficiency

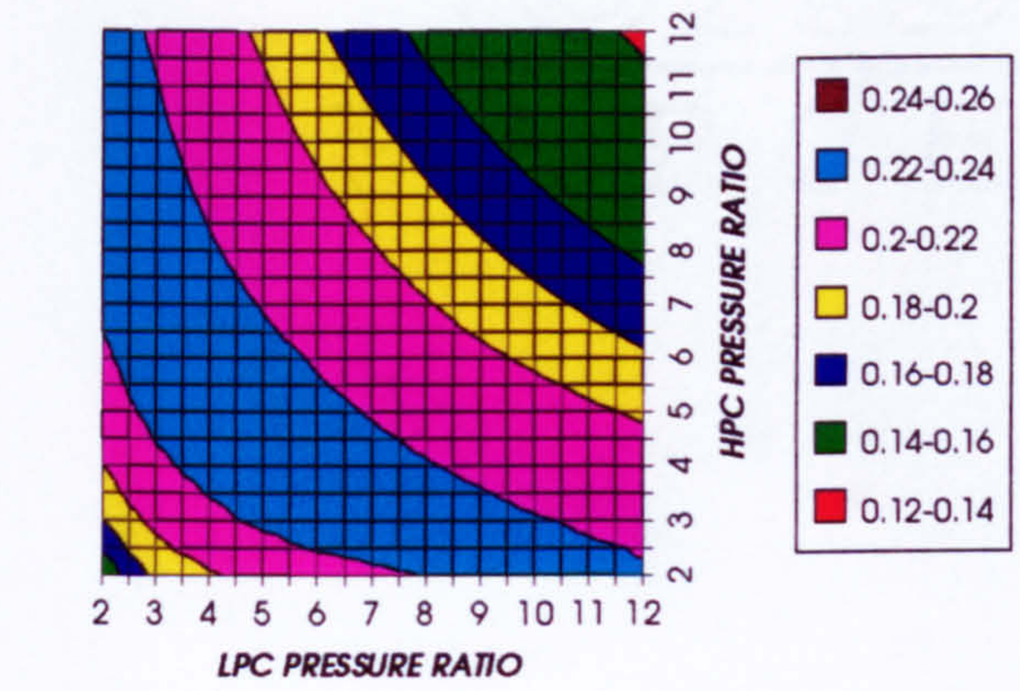

Figure 51. Simple cycle thermal efficiency

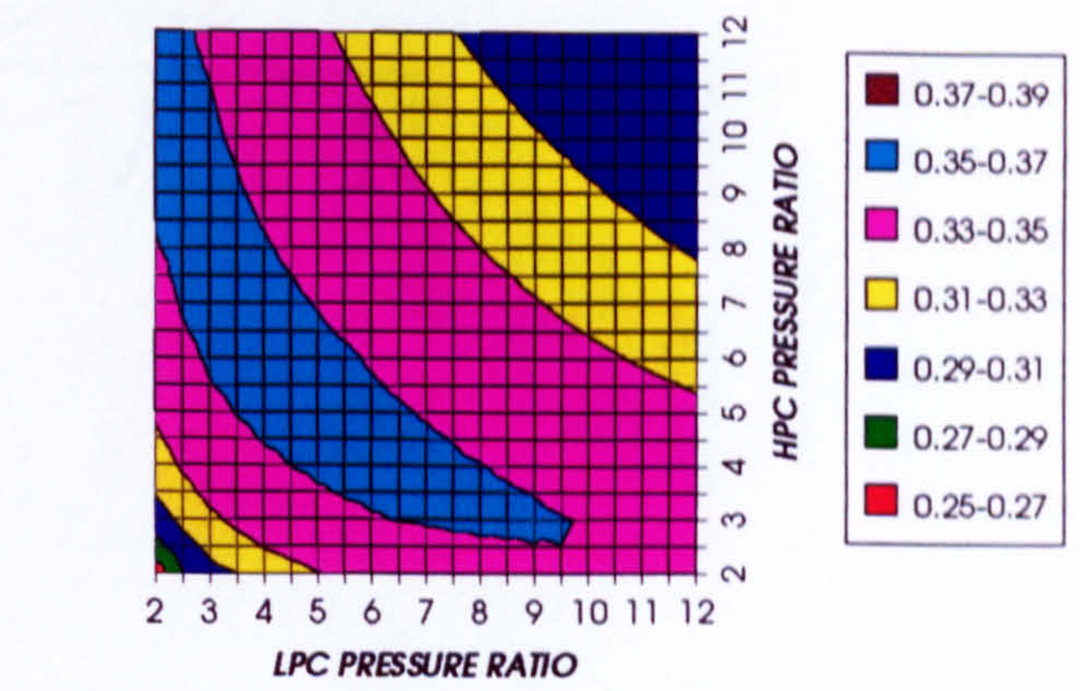

Figure 52. Simple cycle ideal thermal efficiency

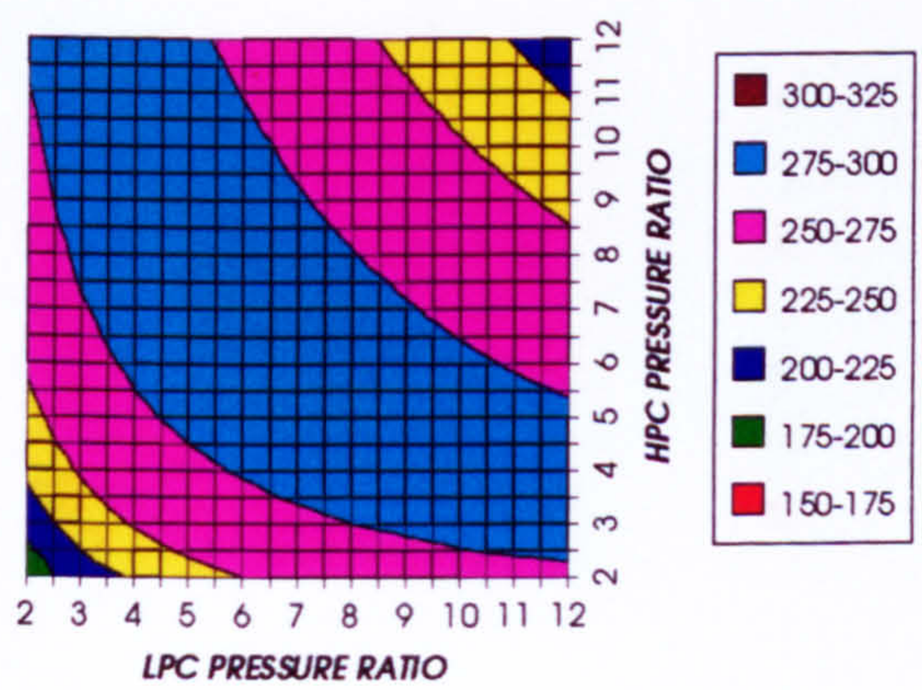

Figure 53. Combined cycle specific power output

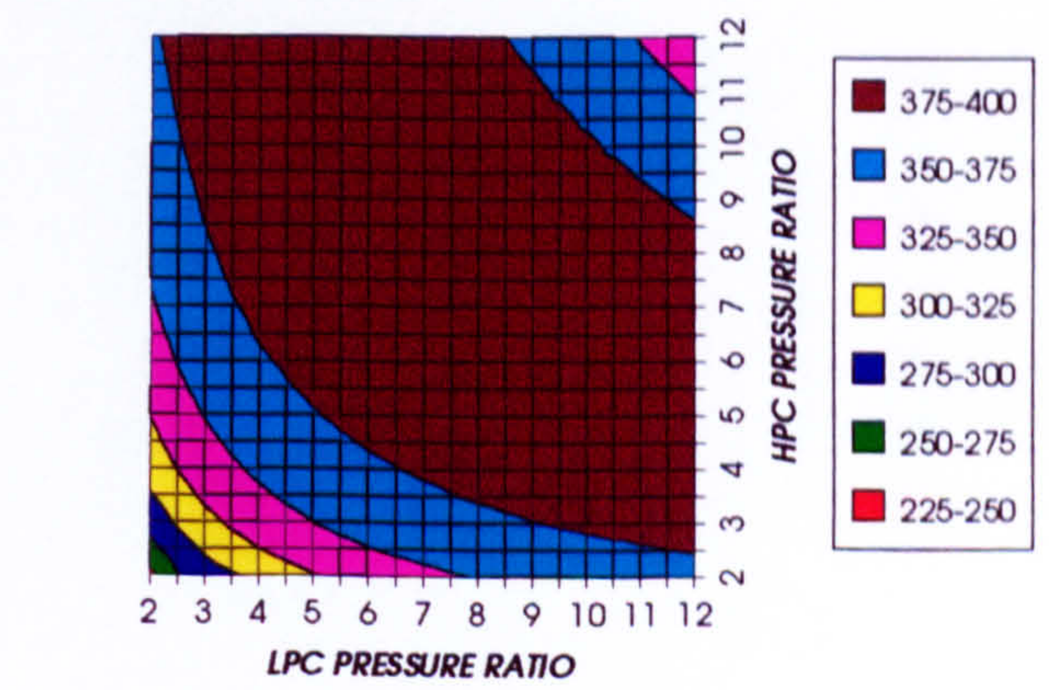

Figure54. Combined cycle ideal specific power output

COMPLETE PLANT (TET=1473 K)

GAS TURBINE SPECIFIC POWER OUTPUT REGENERATED CYCLE, CO2/ARGON, FCFC

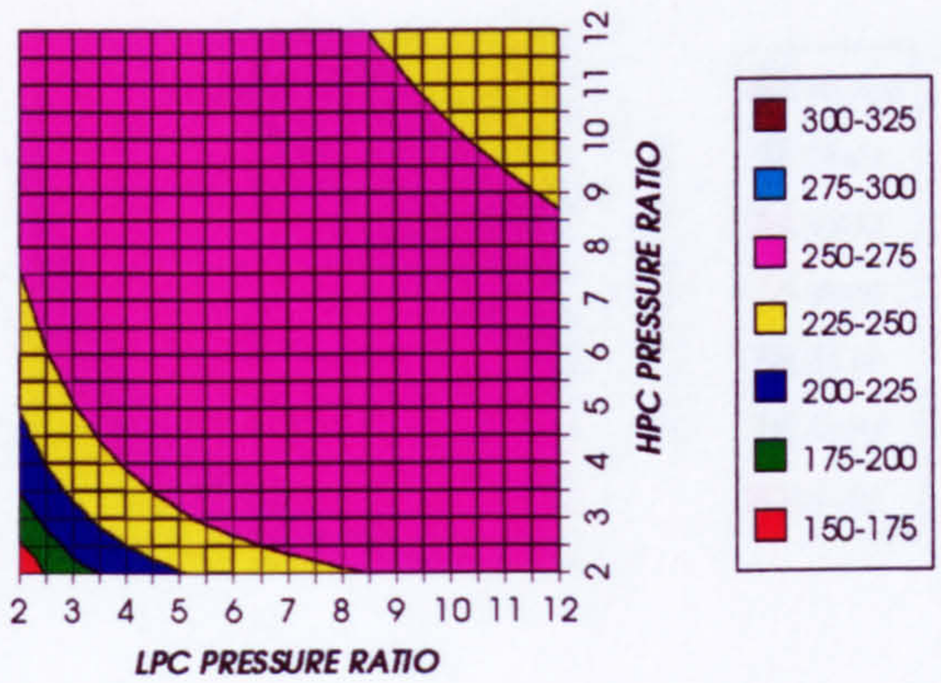

Figure 55. Gas turbine specific power output

STEAM TURBINE SPECIFIC POWER OUTPUT REGENERATED CYCLE, CO2/ARGON, FCFC

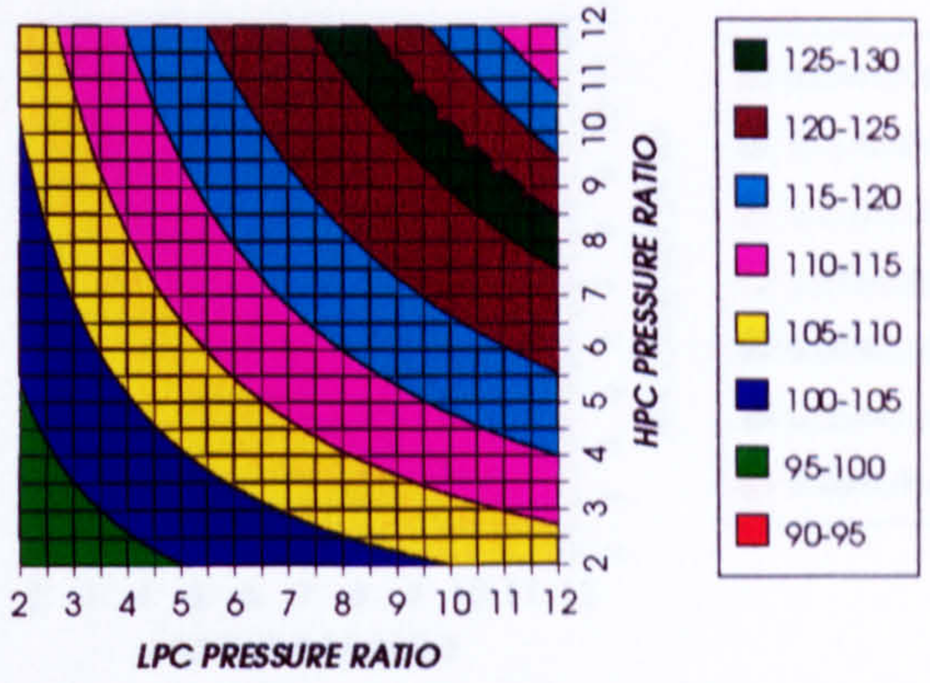

Figure 56. Steam turbine specific power output

GAS TURBINE TO STEAM TURBINE POWER RATIO REGENERATED CYCLE, CO2/ARGON, FCFC

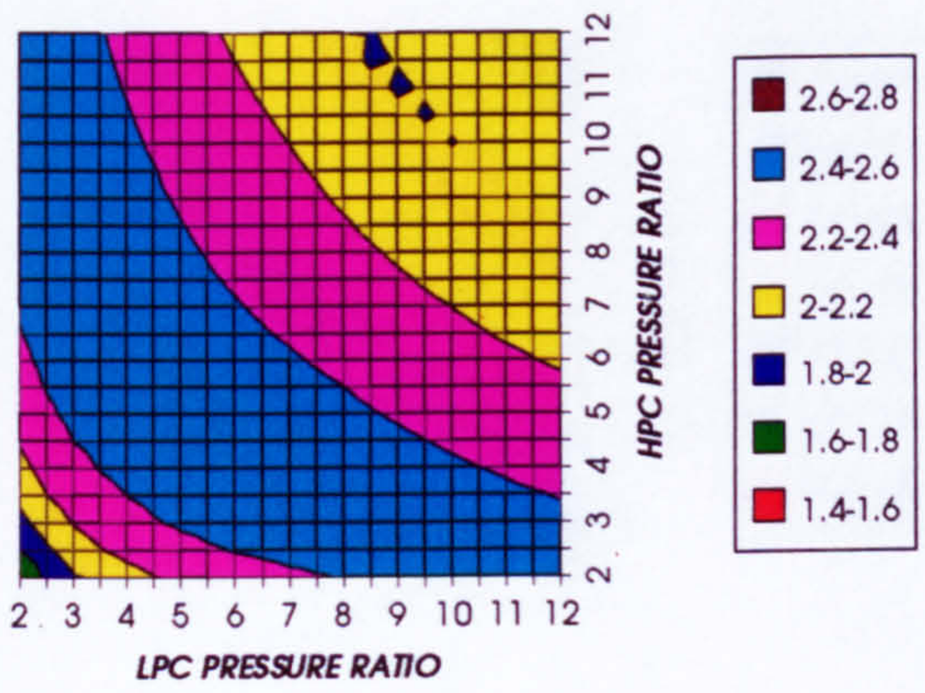

Figure 57. Gas turbine to steam turbine power ratio

AUXILIARIES TO USEFUL POWER RATIO REGENERATED CYCLE, CO2/ARGON, FCFC

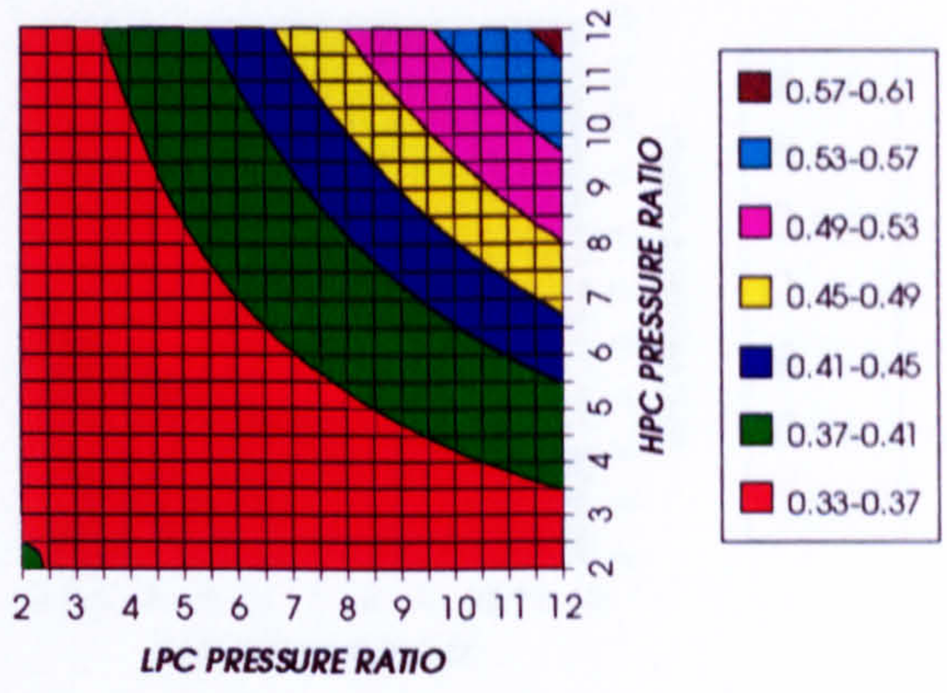

Figure 58. Auxiliary (CO2/Argon, O2 & Fuel) to usefuel power ratio

CO2 COMPRESSION AUXILIARY SPECIFIC POWER REGENERATED CYCLE, CO2/ARGON, FCFC

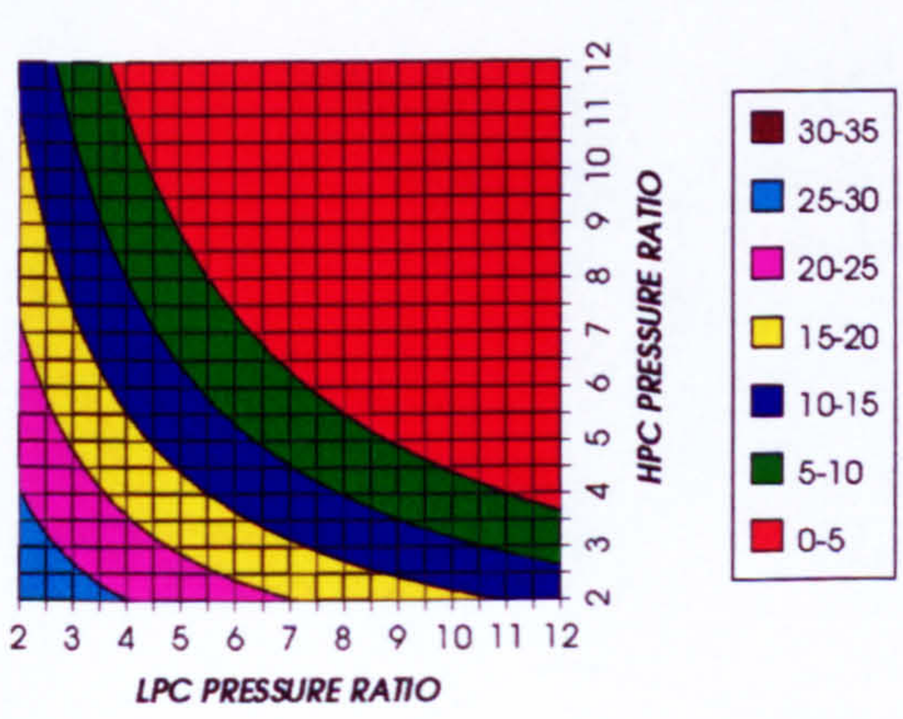

Figure 59. CO2/Argon compression specific power

OXYGEN SEPARATION SPECIFIC POWER REGENERATED CYCLE, CO2/ARGON, FCFC

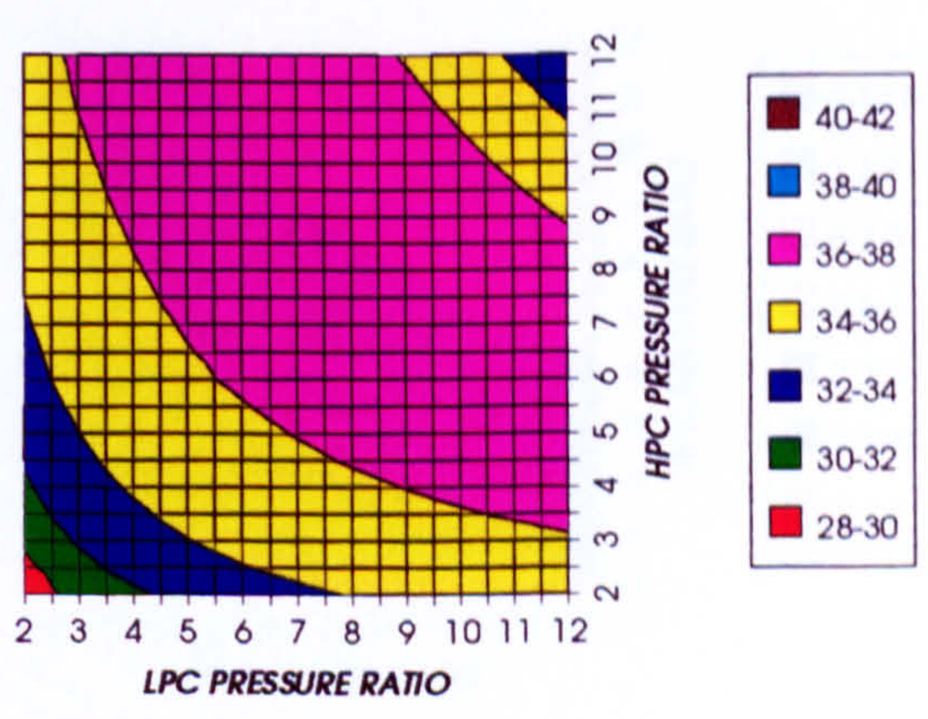

Figure 60. Oxygen separation specific power

COMPLETE PLANT (TET=1473 K)

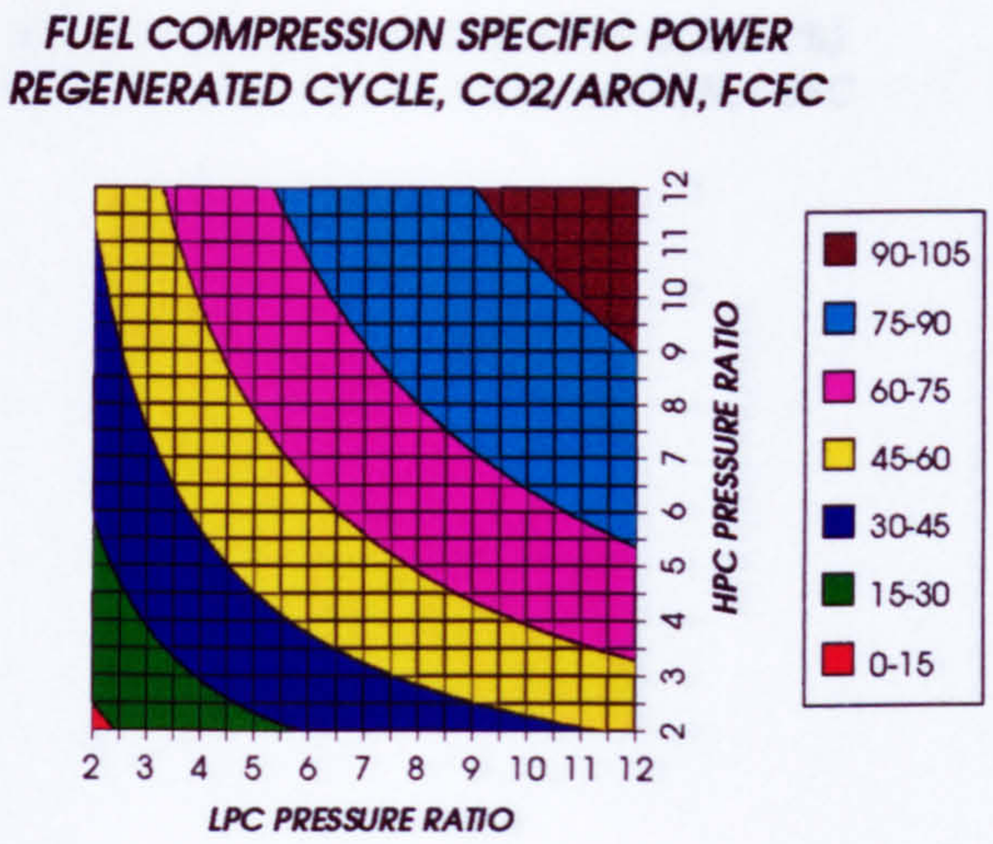

Figure 61. Fuel compression specific power

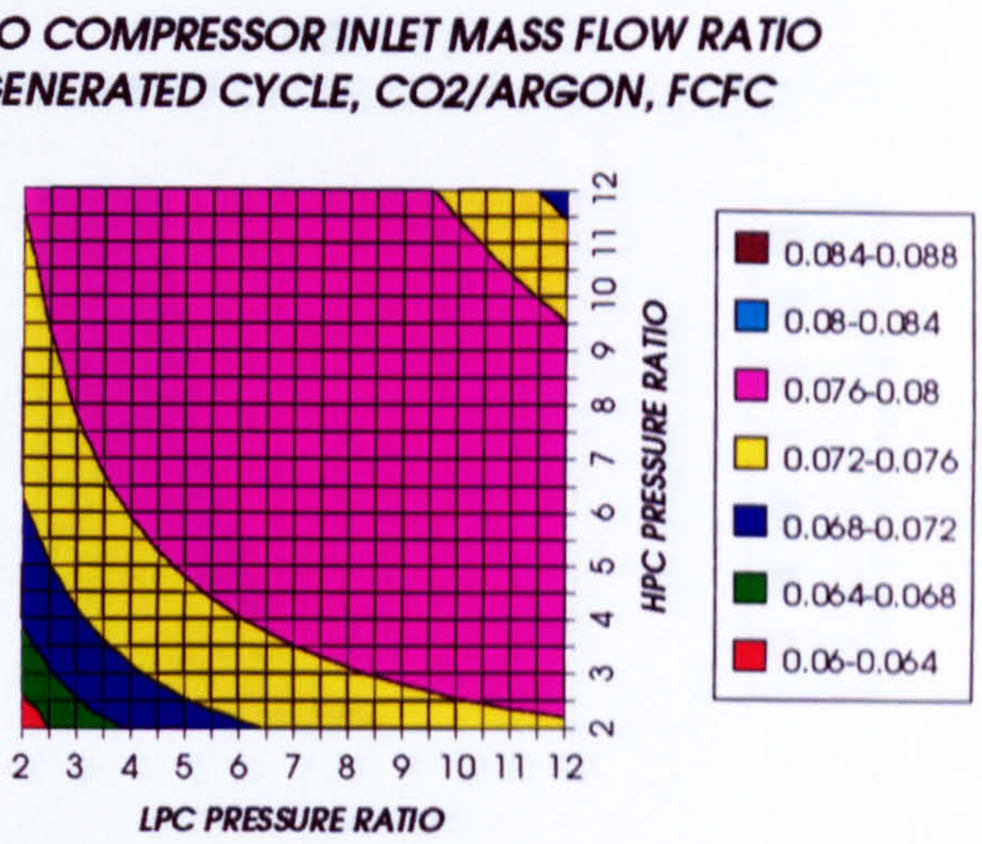

Figure 62. Fuel to compressor inlet mass flow ratio

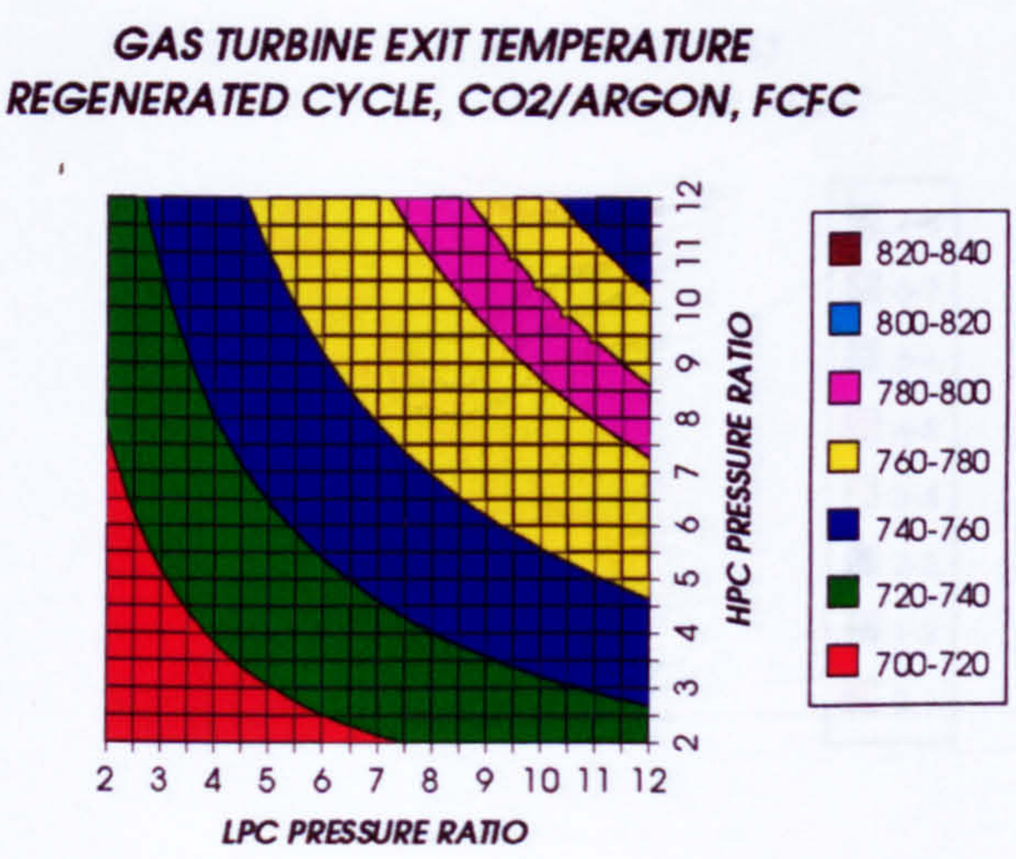

Figure 63. Gas turbine exit temperature

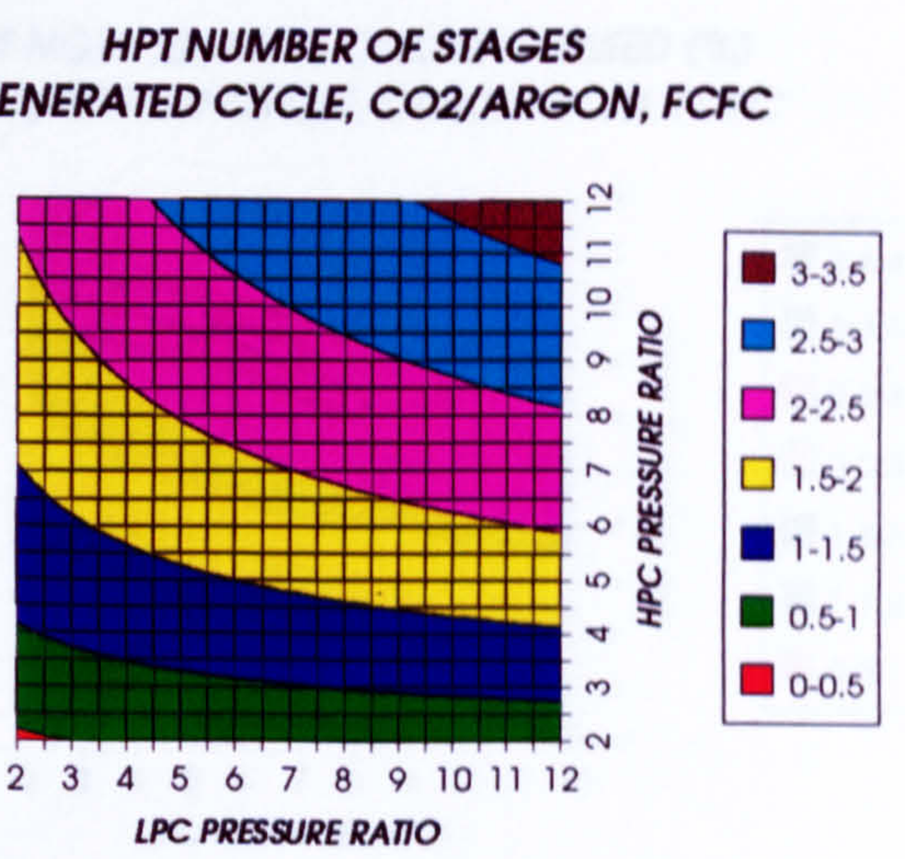

Figure 64. Number of HPT stages

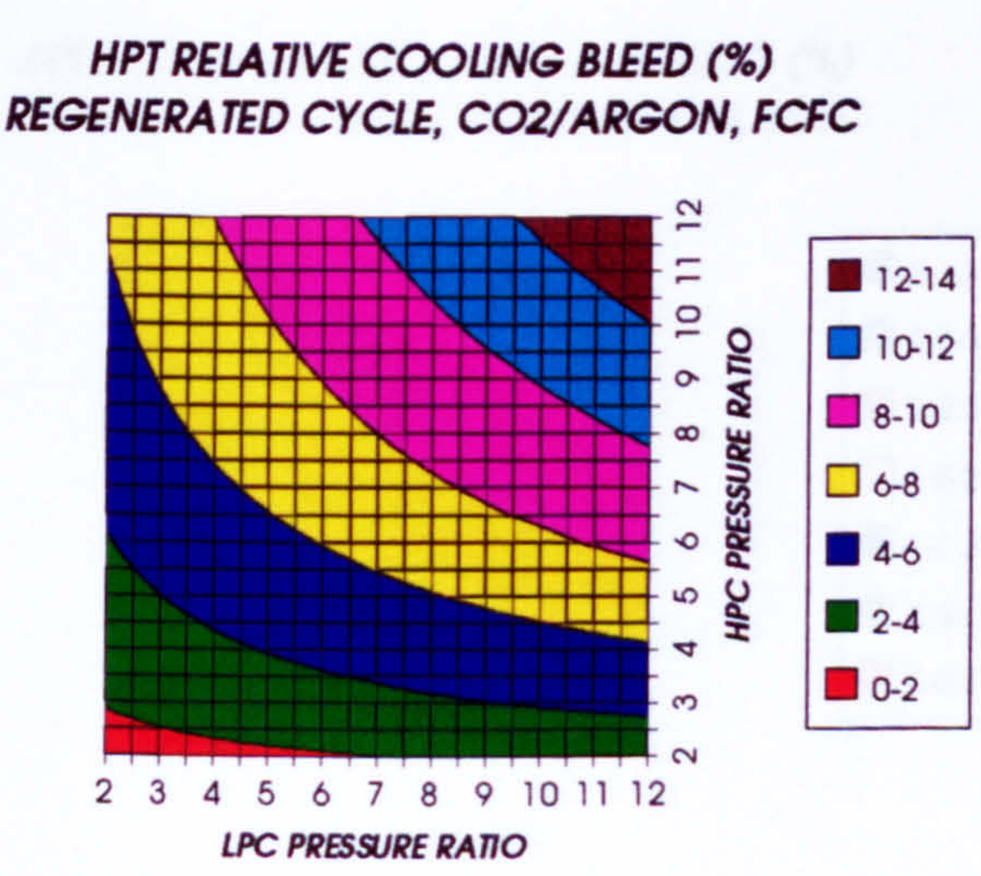

Figure 65. HPT cooling to compressor inlet mass flow ratio

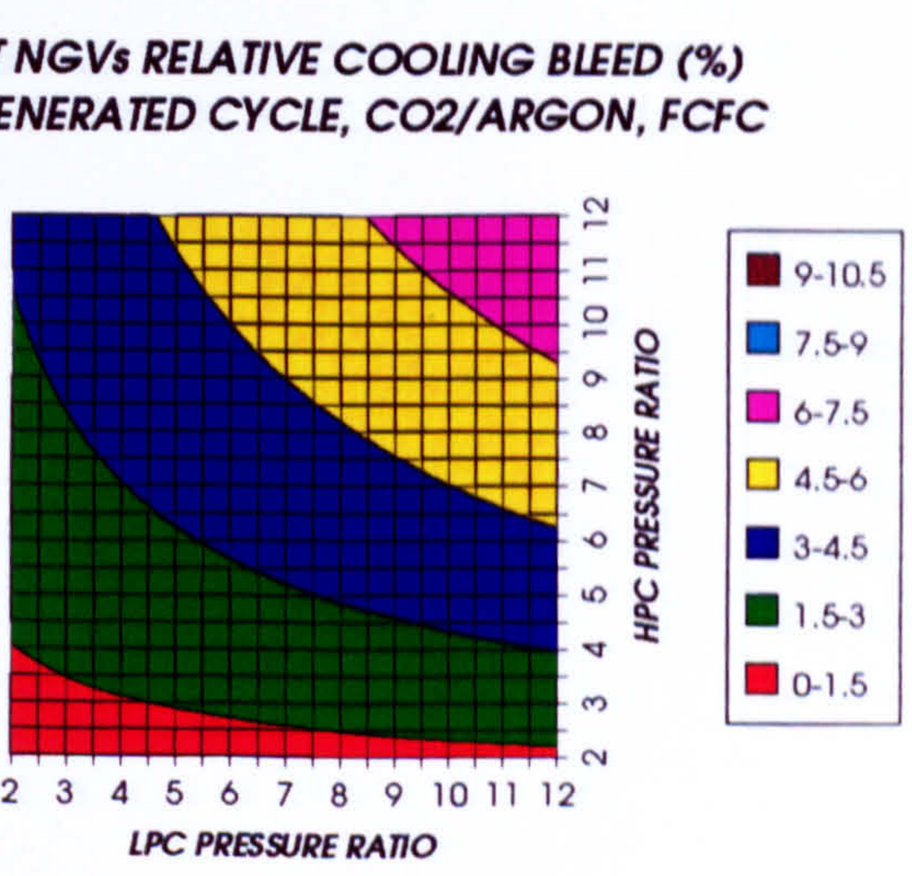

Figure 66. HPT NGVs cooling to compressor inlet mass flow ratio

HPT ROTOR RELATIVE COOLING BLEED (%)
REGENERATED CYCLE, CO2/ARGON, FCFC

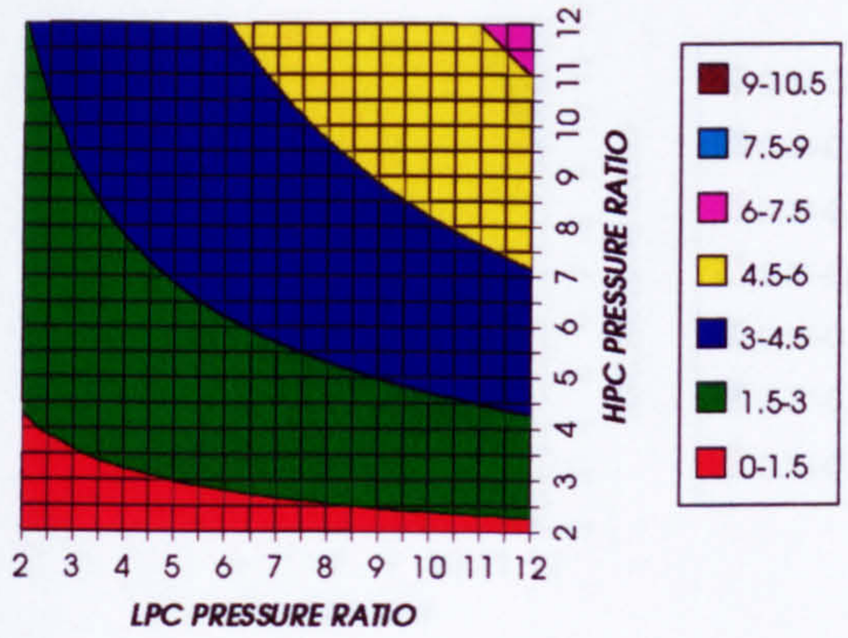

Figure 67. HPT rotor cooling to compressor inlet mass flow ratio

LPT NUMBER OF STAGES
REGENERATED CYCLE, CO2/ARGON, FCFC

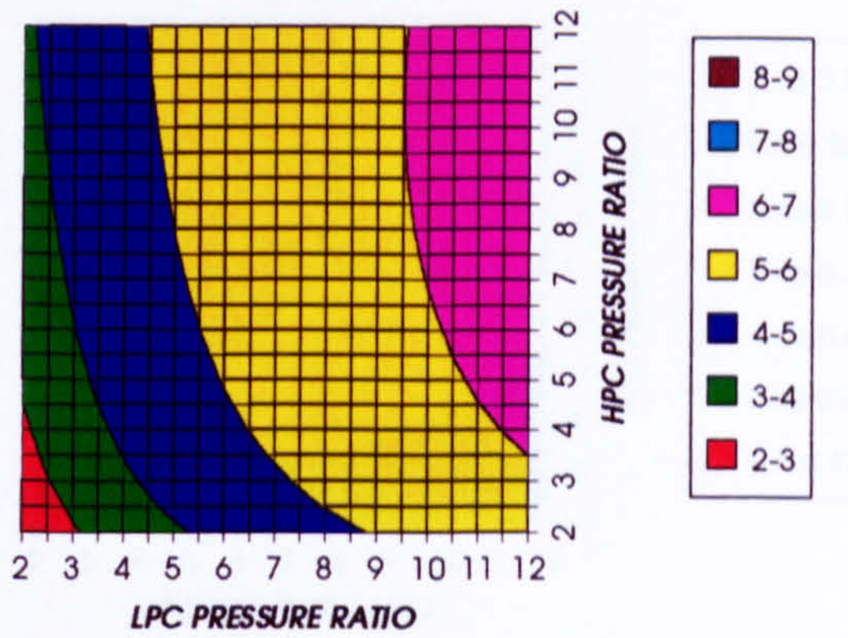

Figure 68. Number of LPT stages

LPT RELATIVE COOLING BLEED (%)
REGENERATED CYCLE, CO2/ARGON, FCFC

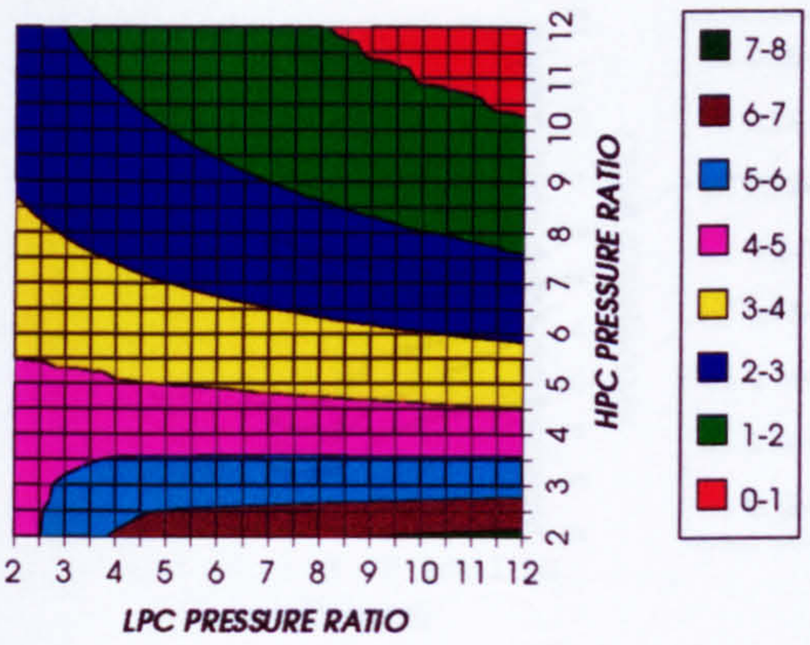

Figure 69.LPT cooling to compressor inlet mass flow ratio

LPT NGVs RELATIVE COOLING BLEED (%)
REGENERATED CYCLE, CO2/ARGON, FCFC

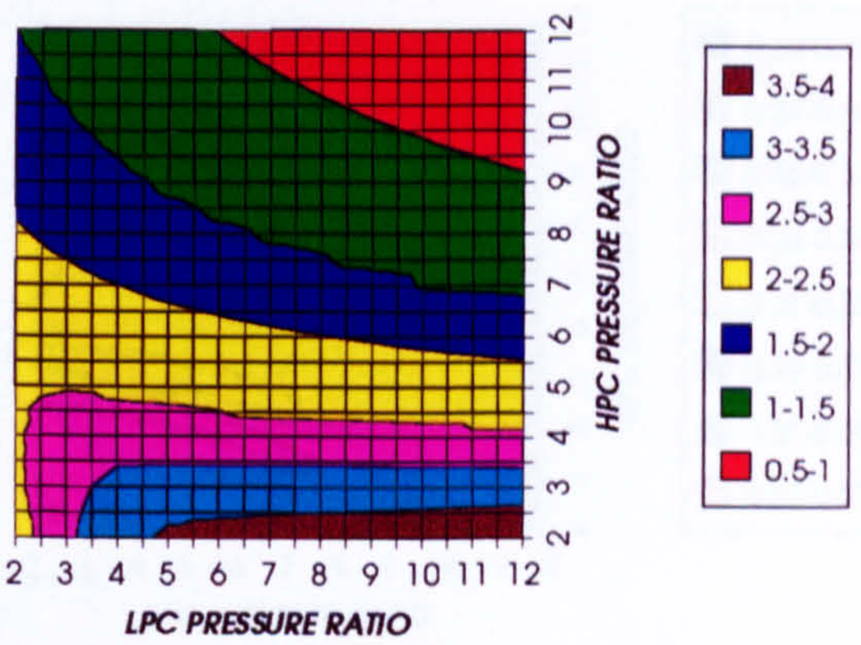

Figure 70. LPT NGVs cooling to compressor inlet mass flow ratio

LPT ROTOR RELATIVE COOLING BLEED (%)
REGENERATED CYCLE, CO2/ARGON, FCFC

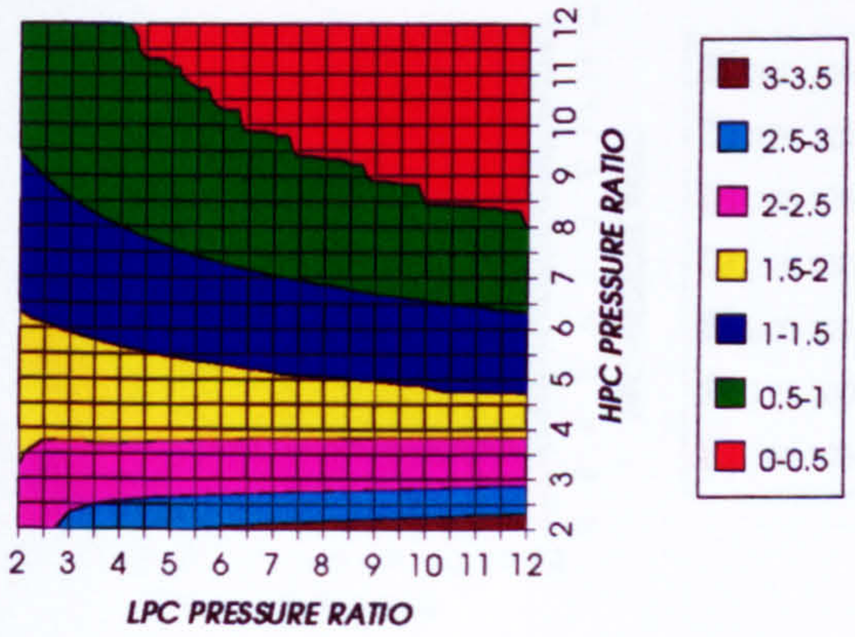

Figure 71. LPT rotor cooling to compressor inlet mass flow ratio

STEAM TURBINE OPTIMUM PRESSURE
REGENERATED CYCLE, CO2/ARGON, FCFC

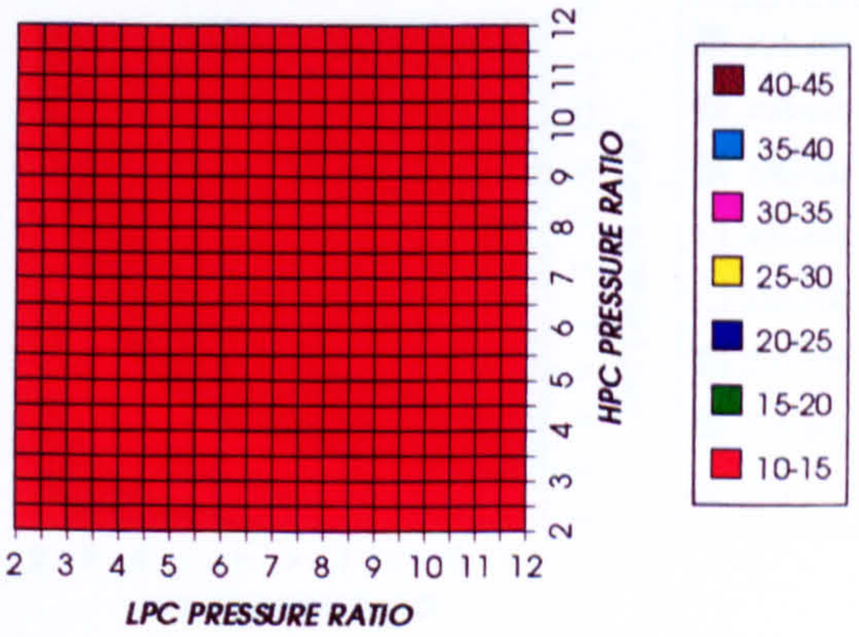

Figure 72. Steam turbine optimum pressures (maximum)

COMPLETE PLANT (TET=1473K)

COMBINED CYCLE THERMAL EFFICIENCY INTERCOOLED & REGENERATED, CO2/ARGON, FCFC

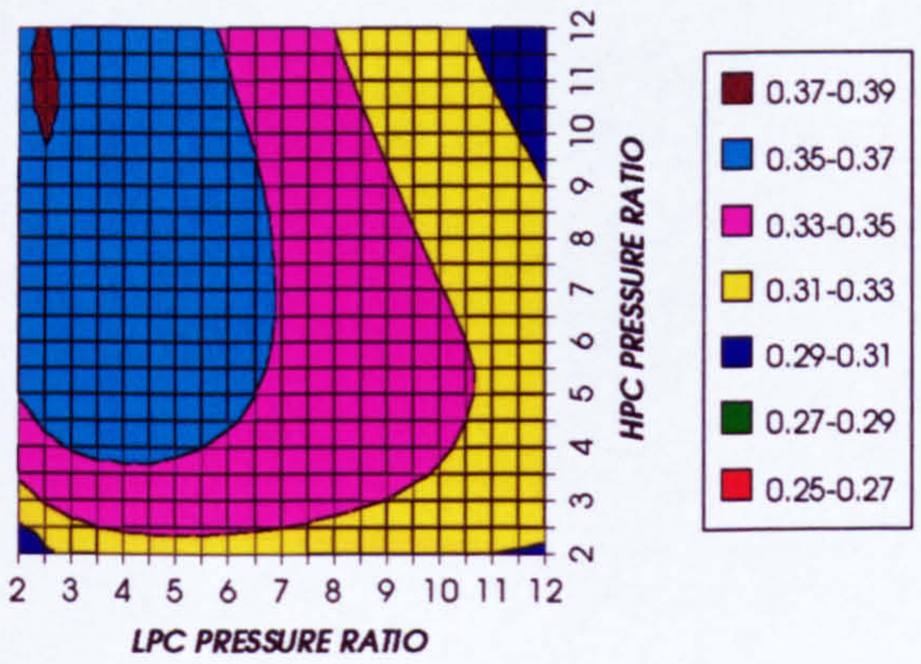

Figure 73. Combined cycle thermal efficiency

COMBINED CYCLE IDEAL THERMAL EFFICIENCY INTERCOOLED & REGENERATED, CO2/ARGON, FCFC

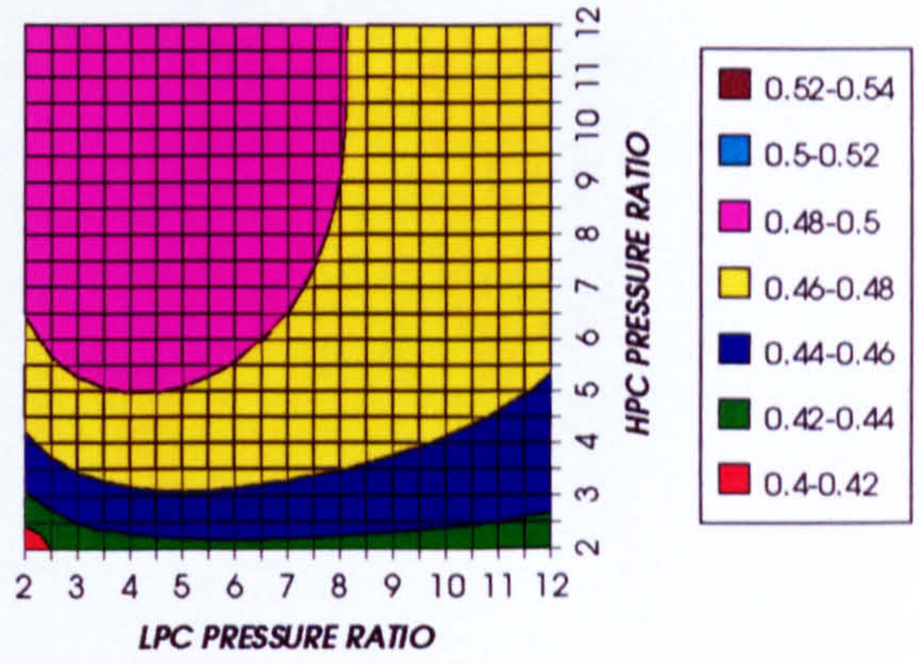

Figure 74. Combined cycle ideal thermal efficiency

SIMPLE CYCLE THERMAL EFFICIENCY INTERCOOLED & REGENERATED, CO2/ARGON, FCFC

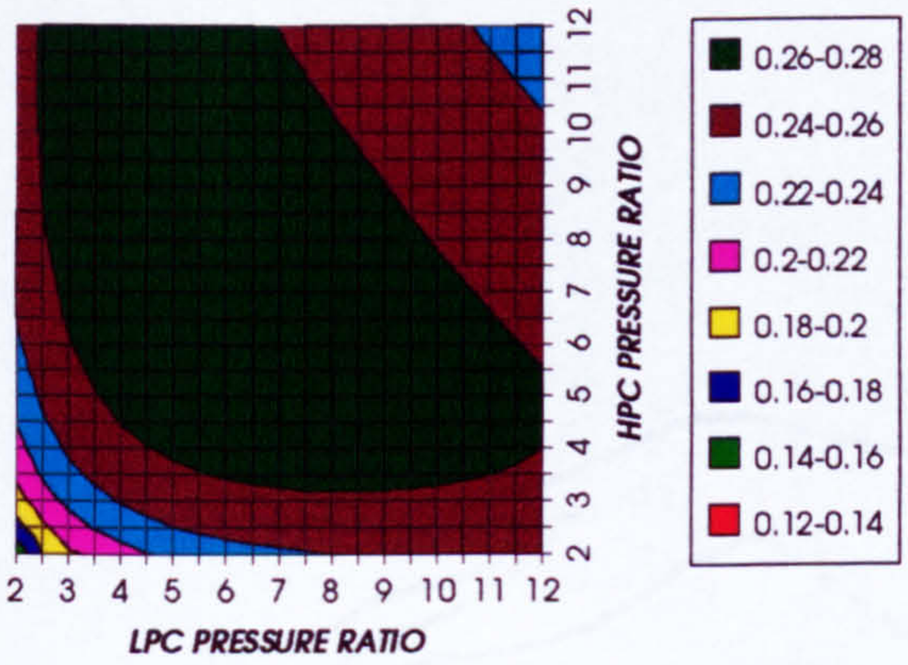

Figure 75. Simple cycle thermal efficiency

SIMPLE CYCLE IDEAL THERMAL EFFICIENCY INTERCOOLED & REGENERATED, CO2/ARGON, FCFC

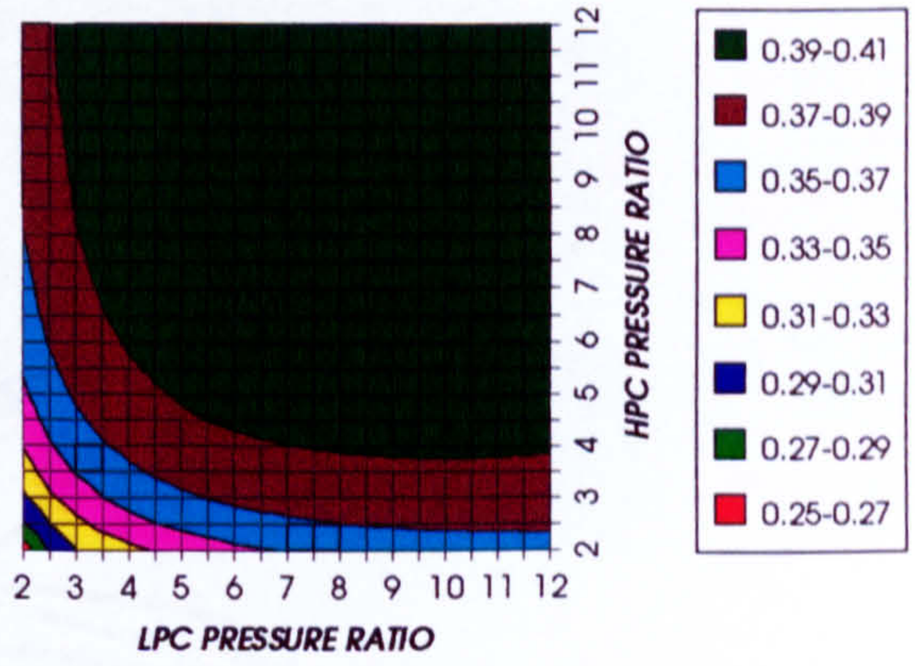

Figure 76. Simple cycle ideal thermal efficiency

COMBINED CYCLE SPECIFIC POWER OUTPUT INTERCOOLED & REGENERATED, CO2/ARGON, FCFC

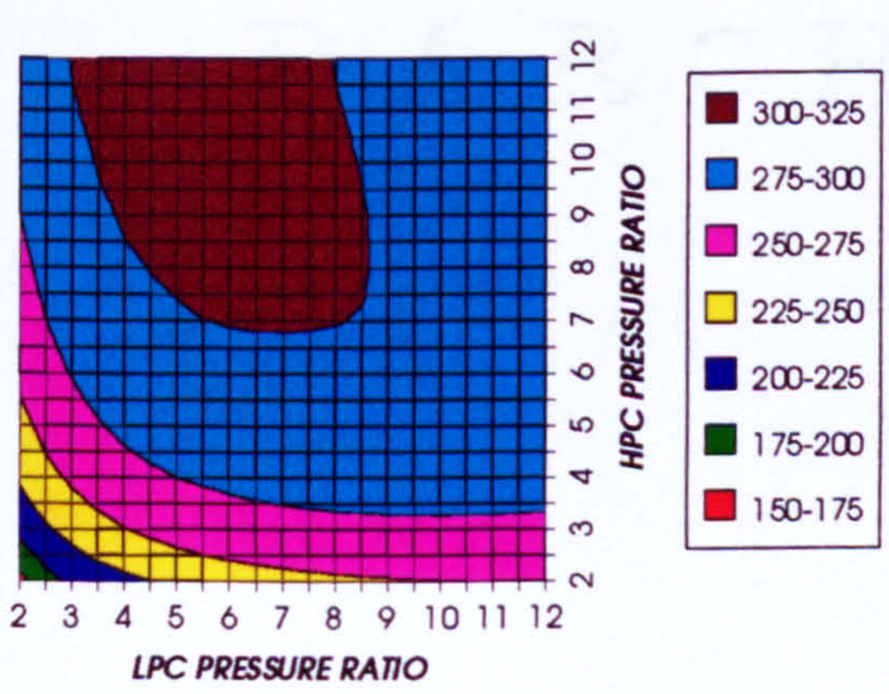

Figure 77. Combined cycle specific power output

COMBINED CYCLE IDEAL SPECIFIC POWER OUTPUT INTERCOOLED & REGENERATED, CO2/ARGON, FCFC

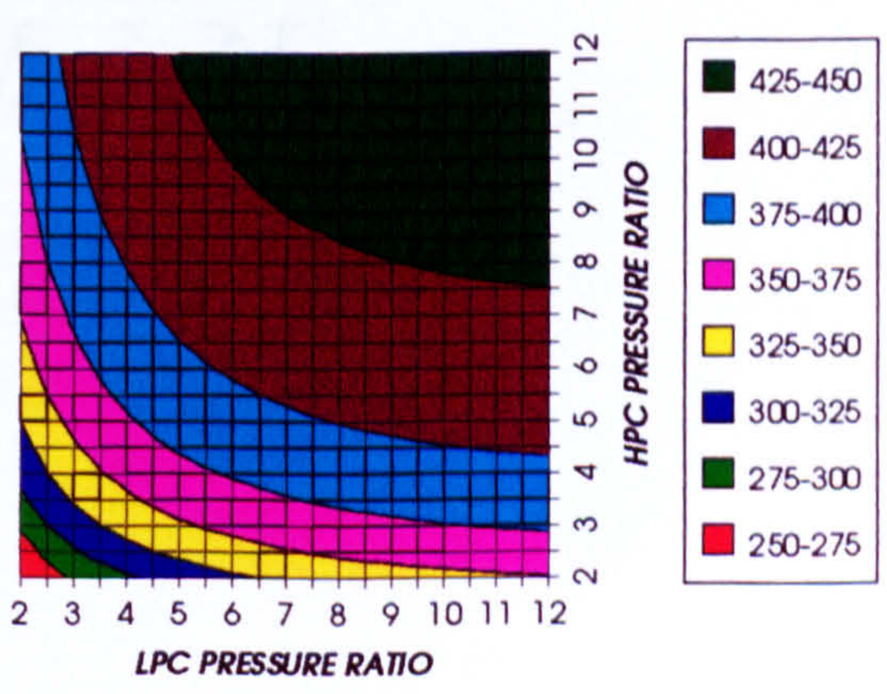

Figure78. Combined cycle ideal specific power output

COMPLETE PLANT (TET=1473 K)

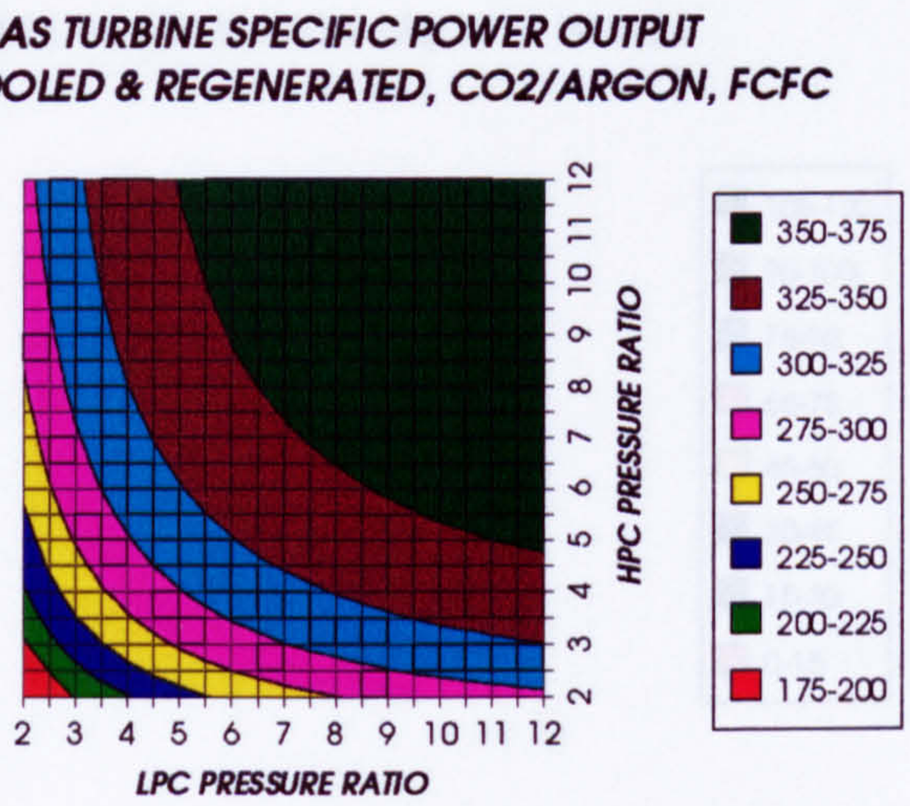

Figure 79. Gas turbine specific power output

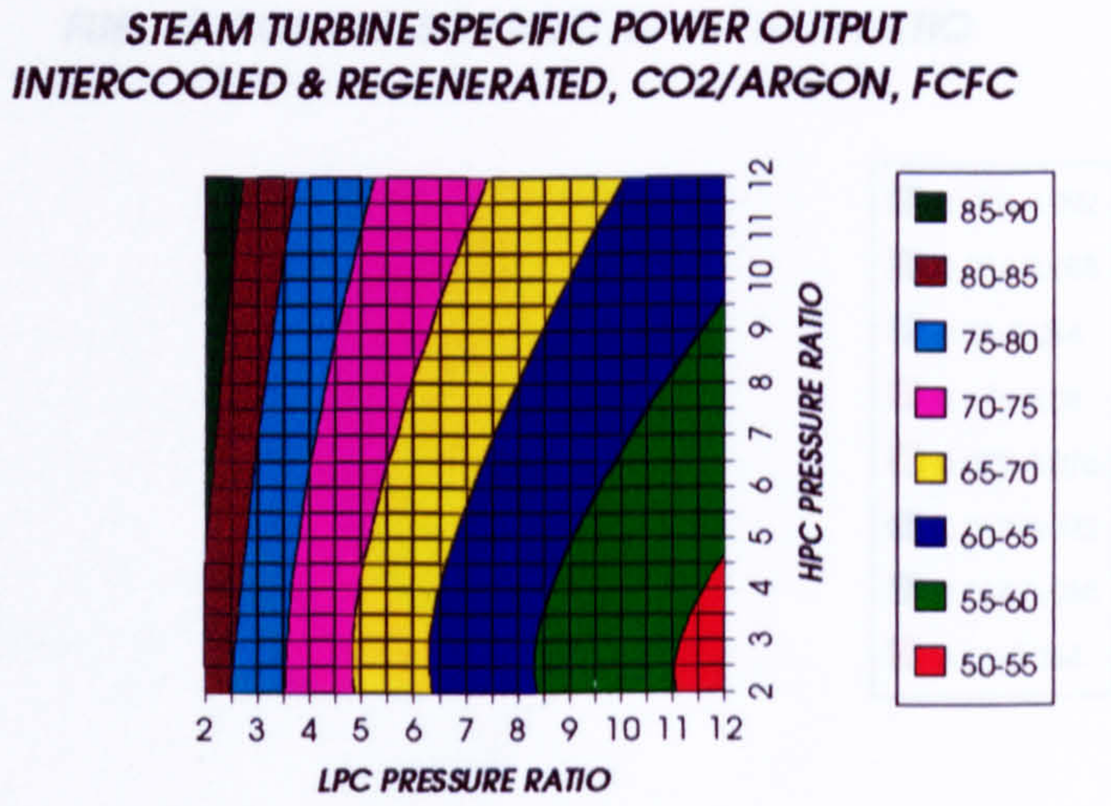

Figure 80. Steam turbine specific power output

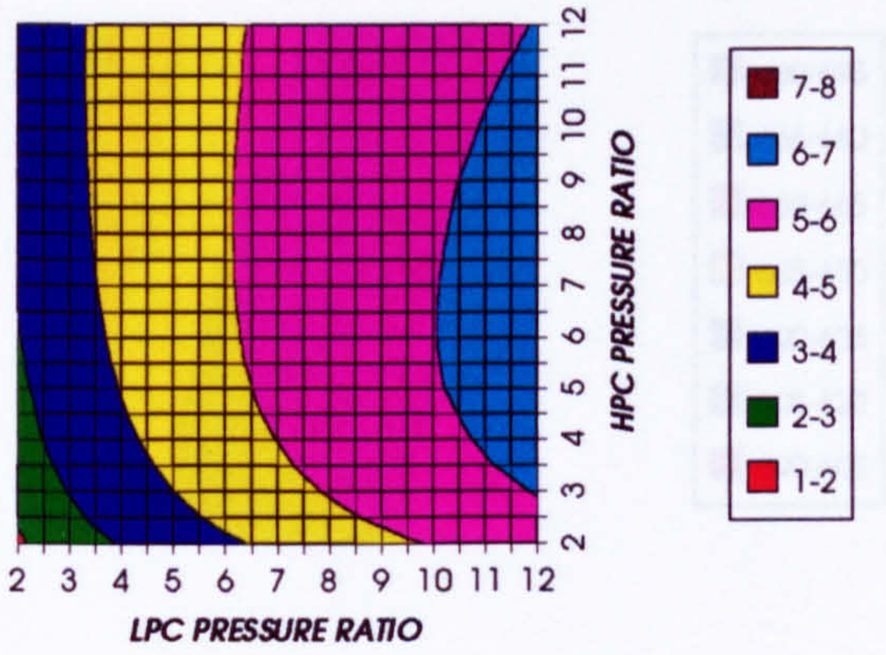

Figure 81. Gas turbine to steam turbine power ratio

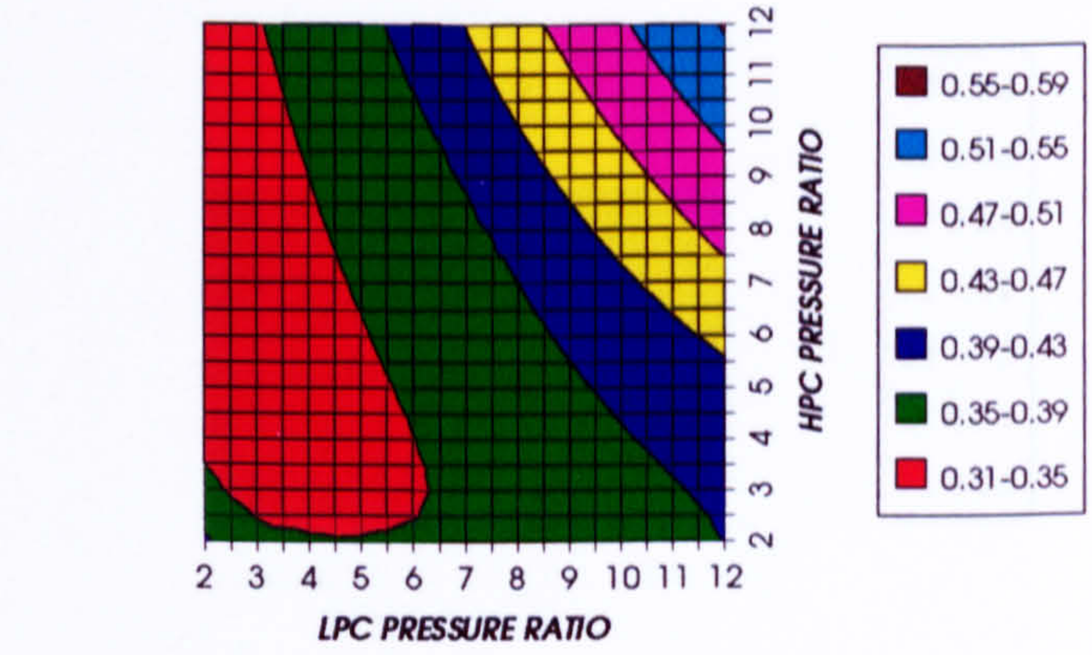

Figure 82. Auxiliary (CO2/Argon, O2 & Fuel) to usefuel power ratio

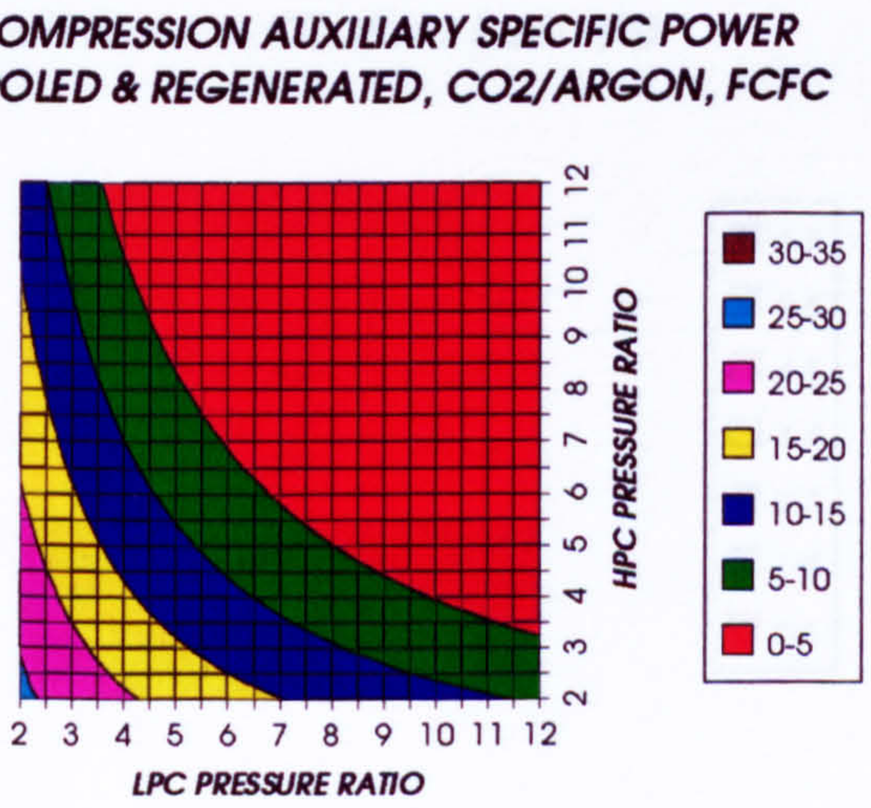

Figure 83. CO2/Argon compression specific power

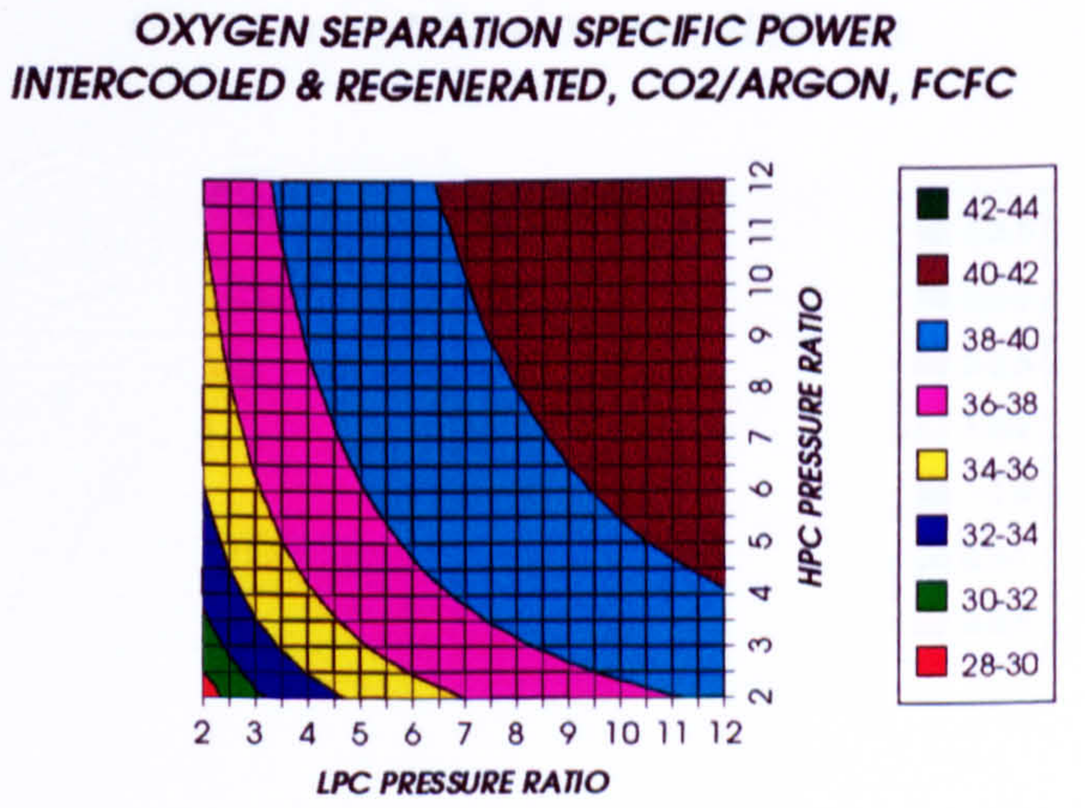

Figure 84. Oxygen separation specific power

COMPLETE PLANT (TET=1473 K)

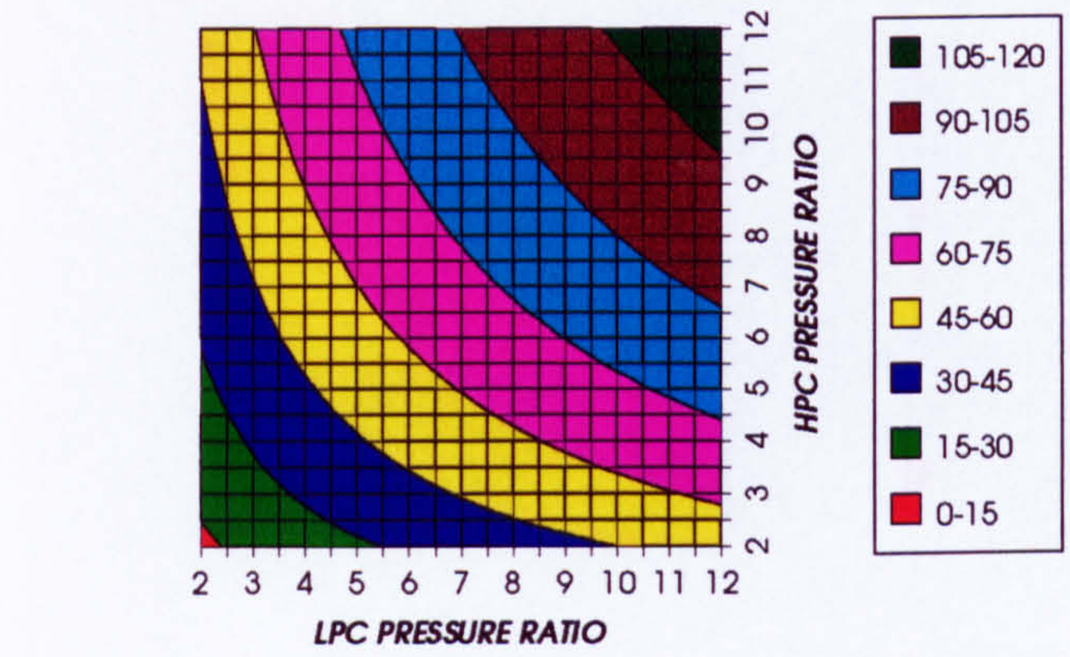

Figure 85. Fuel compression specific power

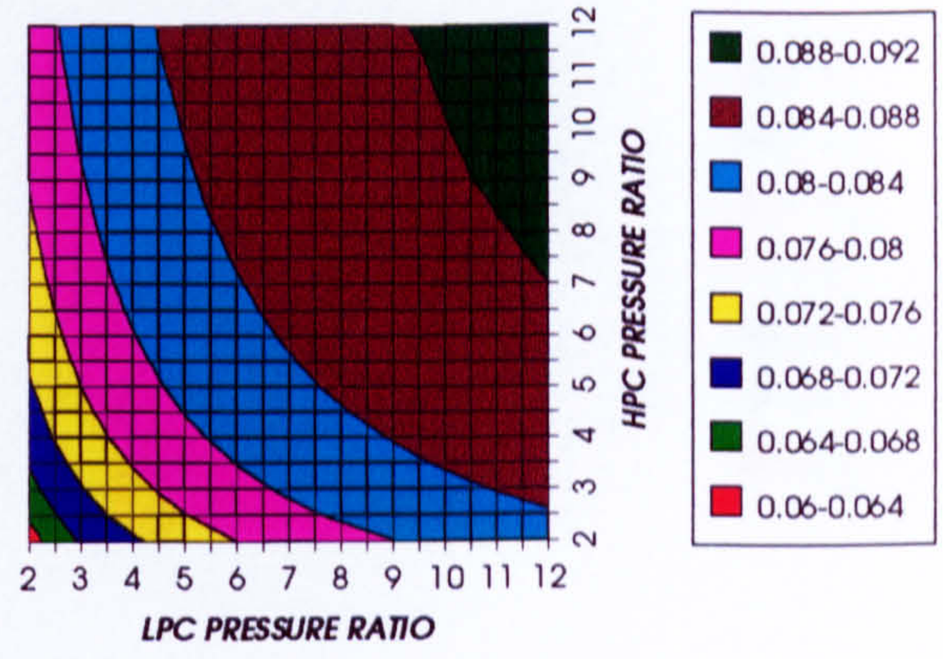

Figure 86. Fuel to compressor inlet mass flow ratio

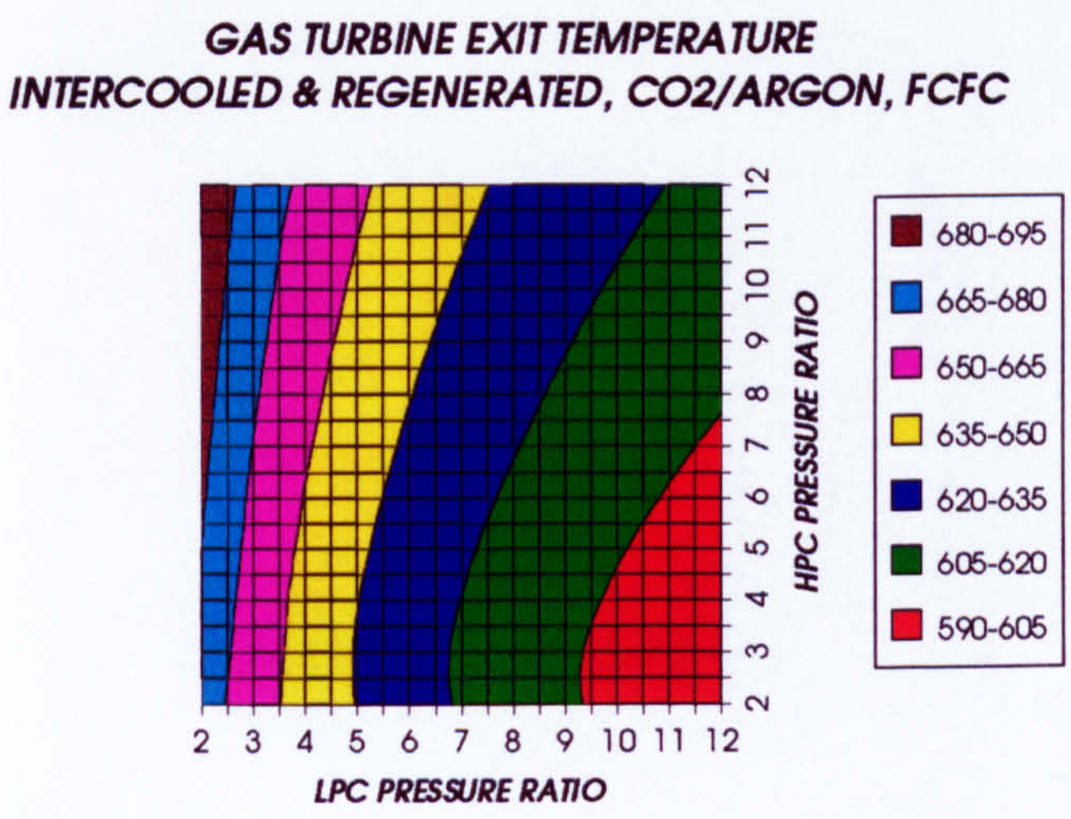

Figure 87. Gas turbine exit temperature

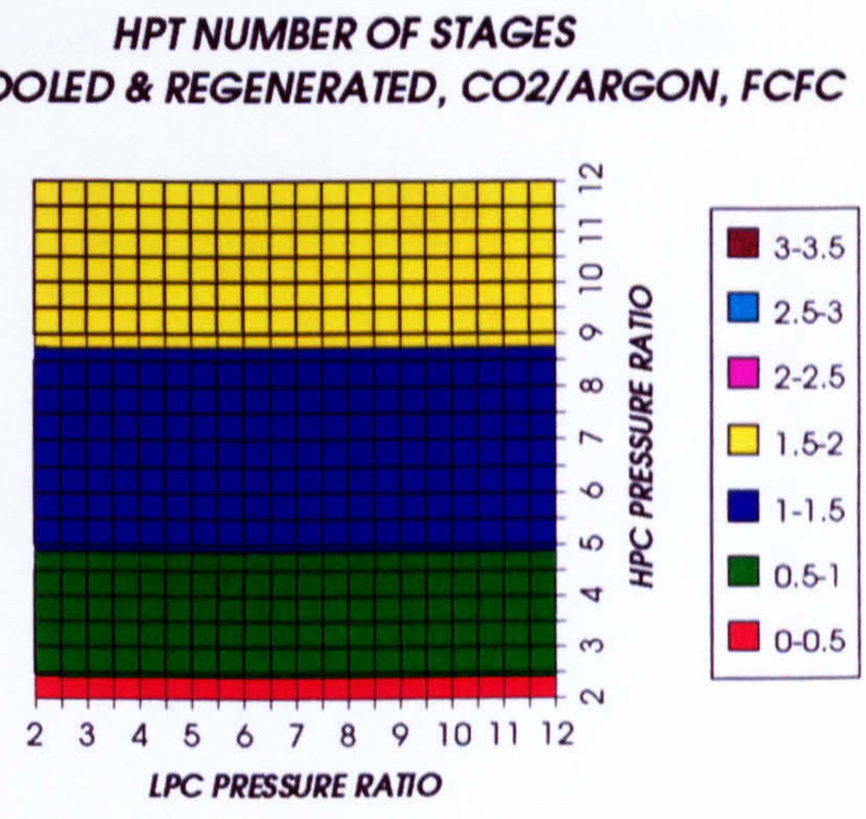

Figure 88. Number of HPT stages

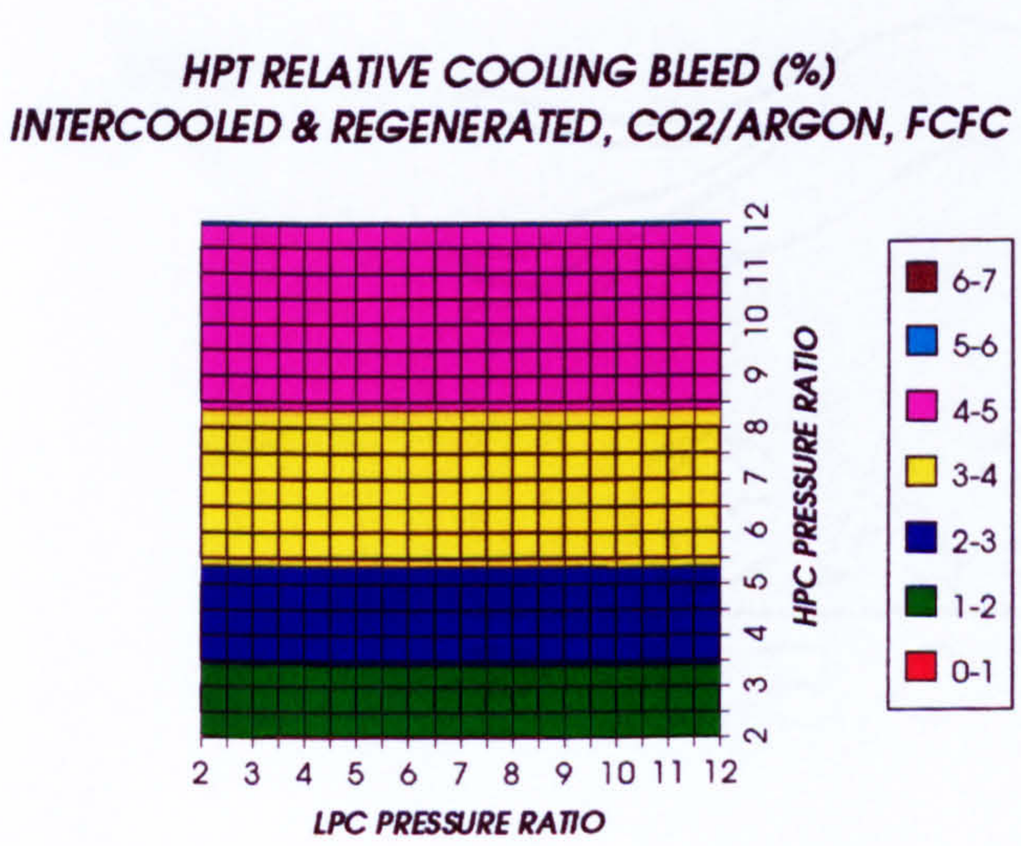

Figure 89. HPT cooling to compressor inlet mass flow ratio

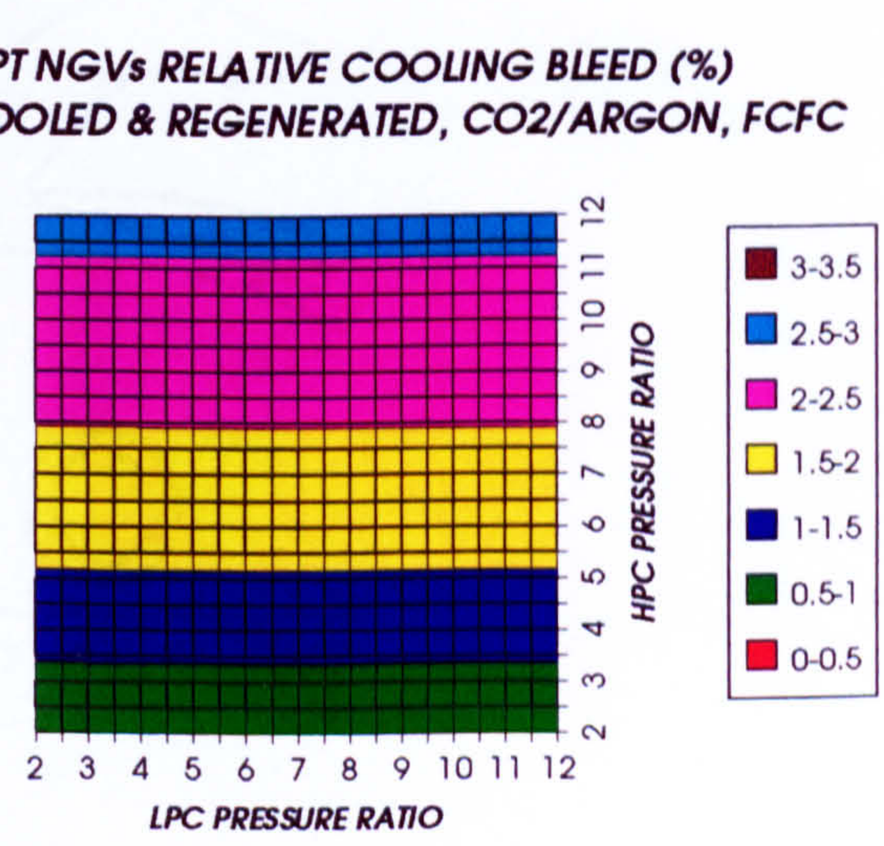

Figure 90. HPT NGVs cooling to compressor inlet mass flow ratio

HPT ROTOR RELATIVE COOLING BLEED (%)
INTERCOOLED & REGENERATED, CO2/ARGON, FCFC

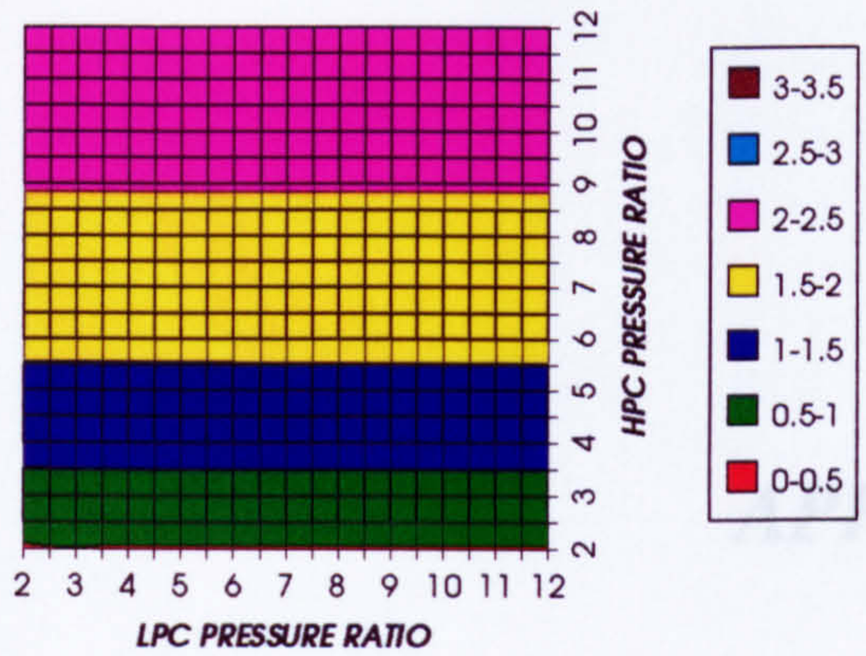

Figure 91. HPT rotor cooling to compressor inlet mass flow ratio

LPT NUMBER OF STAGES
INTERCOOLED & REGENERATED, CO2/ARGON, FCFC

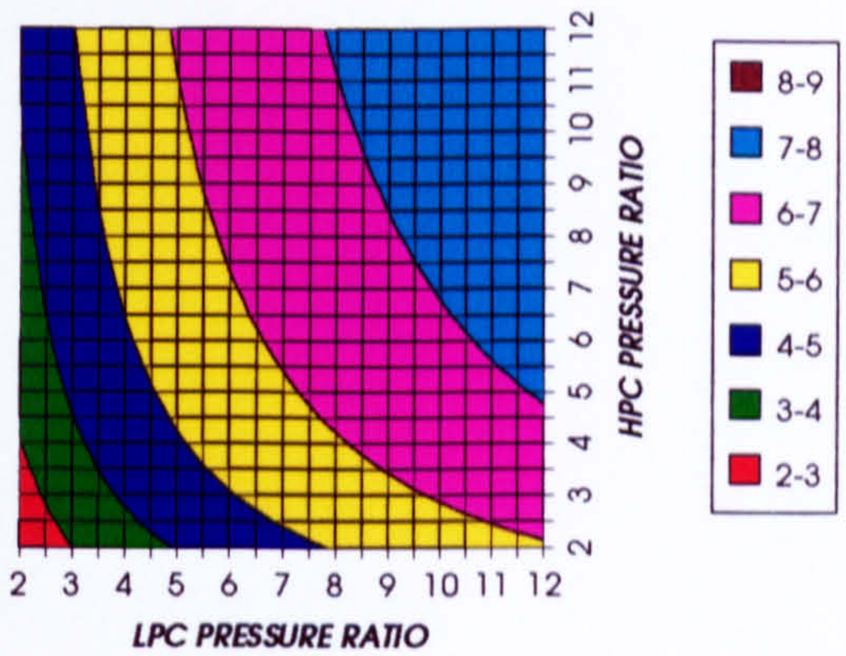

Figure 92. Number of LPT stages

LPT RELATIVE COOLING BLEED (%)
INTERCOOLED & REGENERATED, CO2/ARGON, FCFC

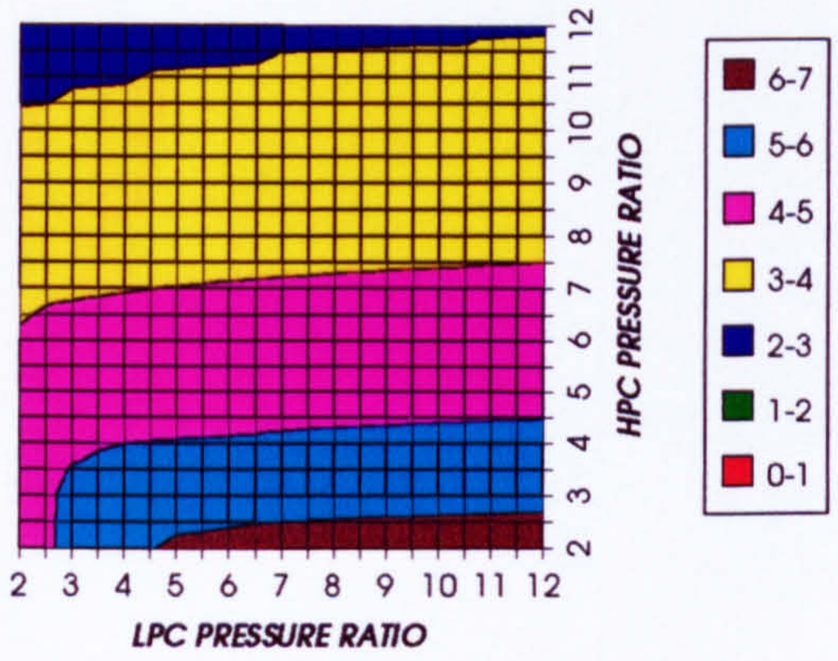

Figure 93. LPT cooling to compressor inlet mass flow ratio

LPT NGVs RELATIVE COOLING BLEED (%)
INTERCOOLED & REGENERATED, CO2/ARGON, FCFC

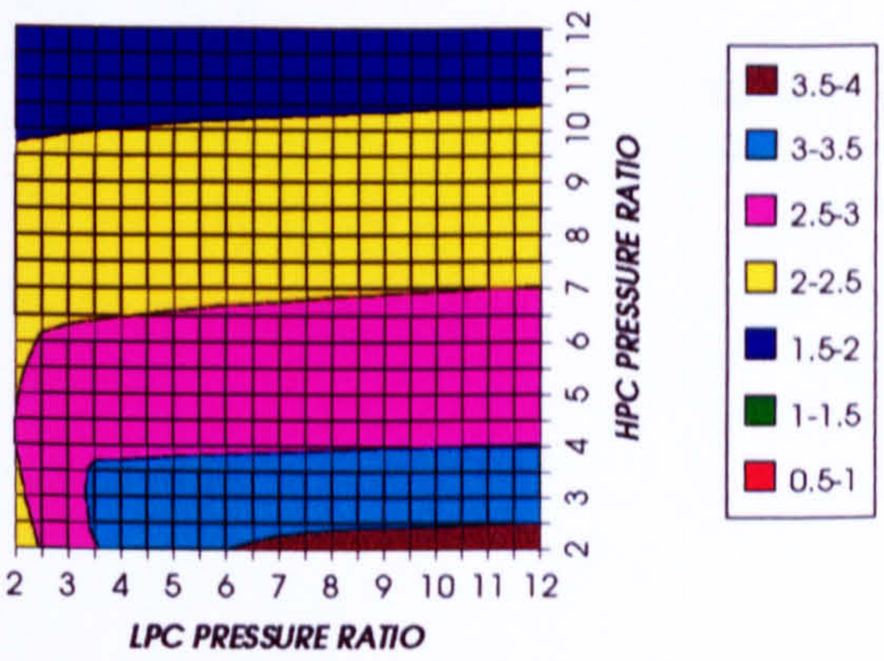

Figure 94. LPT NGVs cooling to compressor inlet mass flow ratio

LPT ROTOR RELATIVE COOLING BLEED (%)
INTERCOOLED & REGENERATED, CO2/ARGON, FCFC

Figure 95. LPT rotor cooling to compressor inlet mass flow ratio

STEAM TURBINE OPTIMUM PRESSURE
INTERCOOLED & REGENERATED, CO2/ARGON, FCFC

Figure 96. Steam turbine optimum pressures (maximum)

APPENDIX V

COMPLETE PLANT PERFORMANCE (WORKING FLUID CO_2/ARGON, TET=1650 K)

COMPLETE PLANT (TET=1650 K)

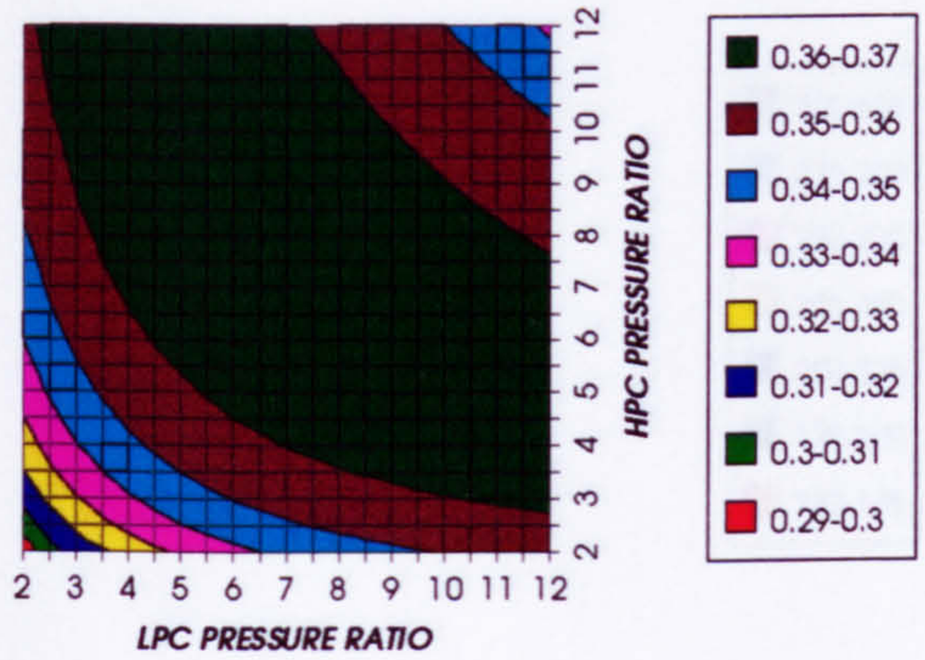

Figure 1. Combined cycle thermal efficiency

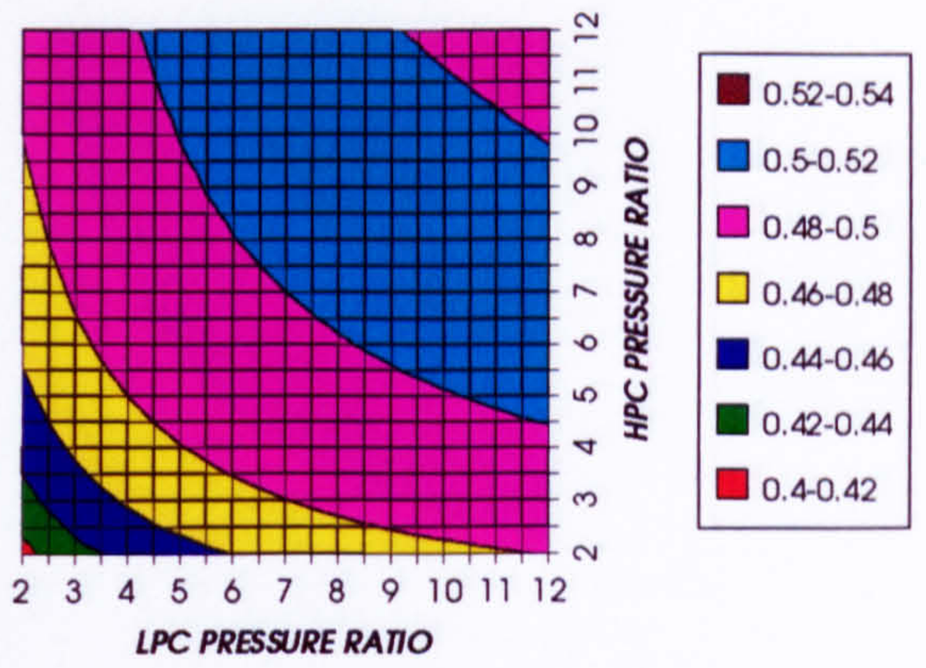

Figure 2. Combined cycle ideal thermal efficiency

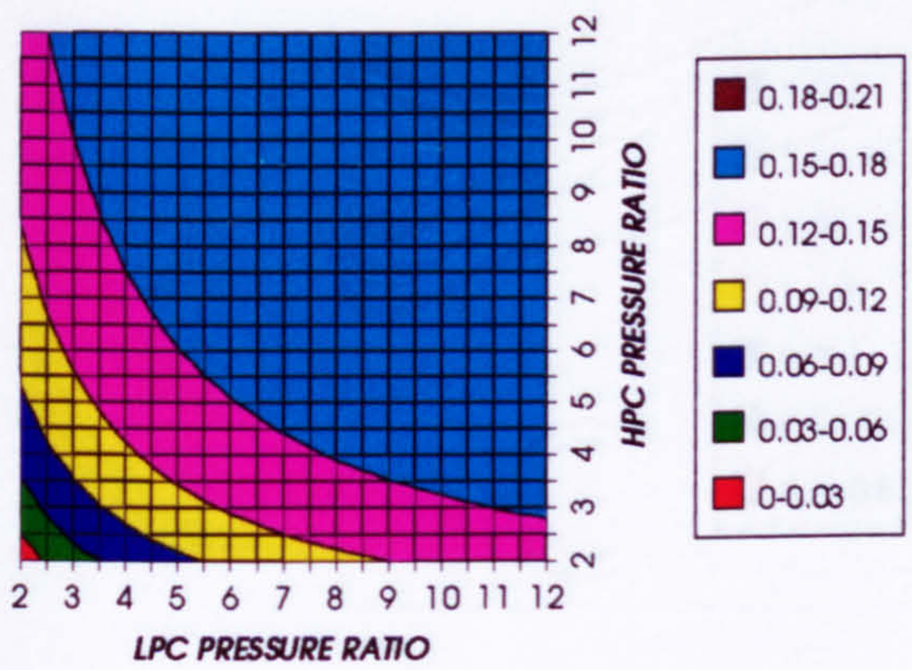

Figure 3. Simple cycle thermal efficiency

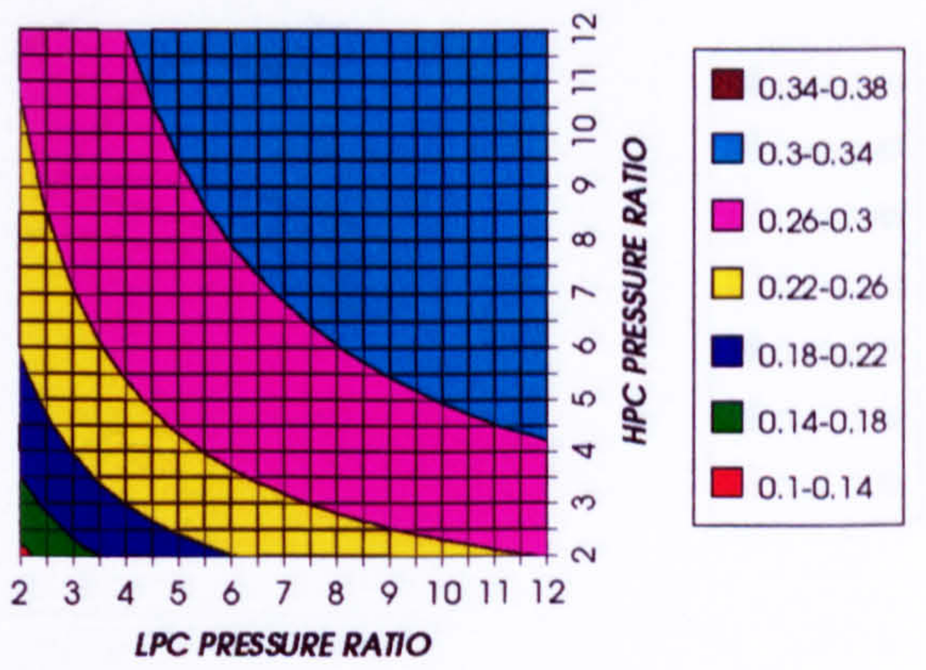

Figure 4. Simple cycle ideal thermal efficiency

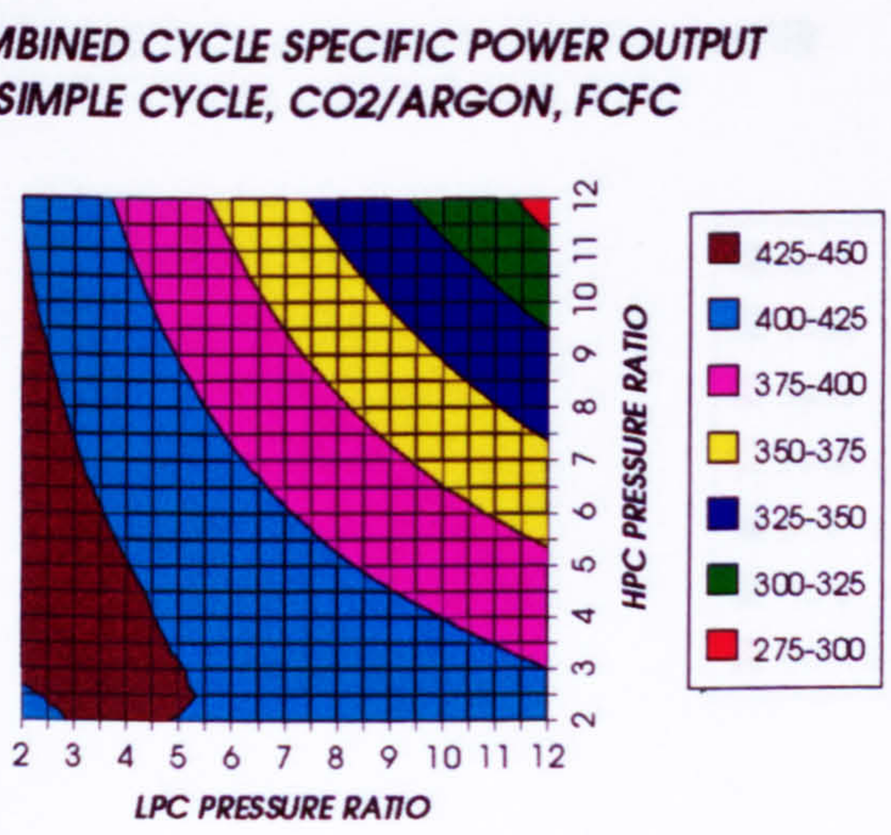

Figure 5. Combined cycle specific power output

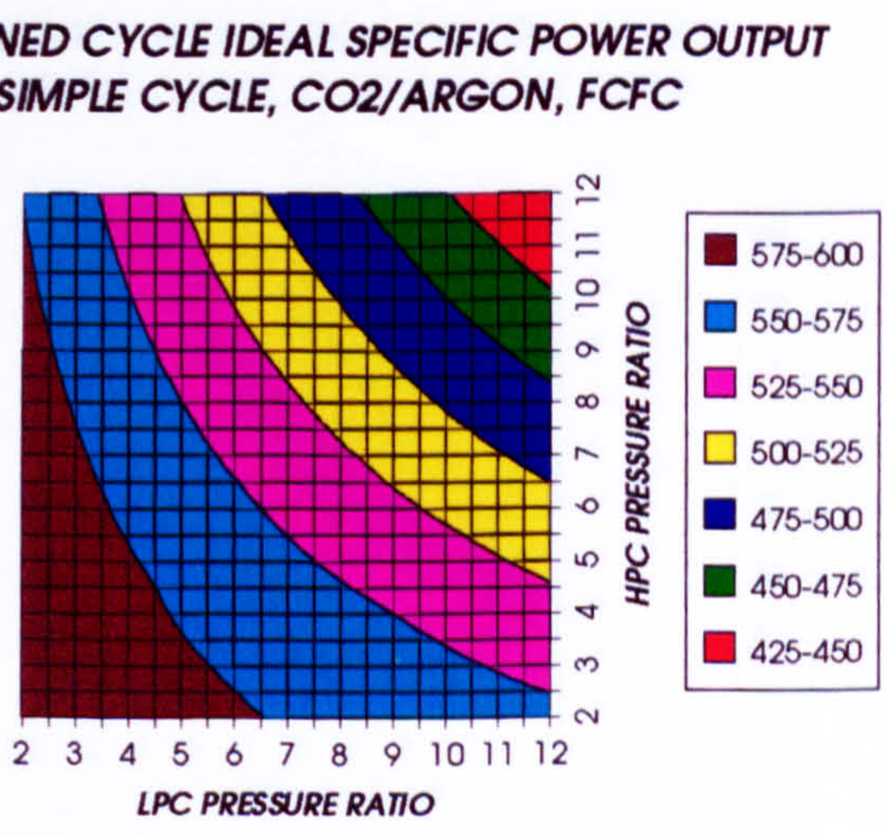

Figure 6. Combined cycle ideal specific power output

COMPLETE PLANT (TET=1650 K)

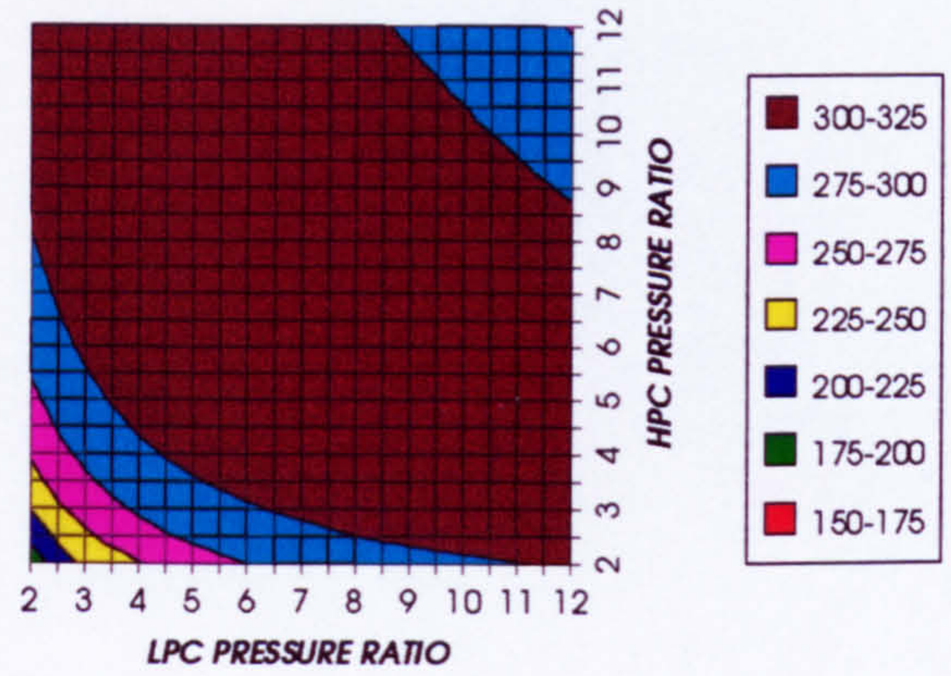

Figure 7. Gas turbine specific power output

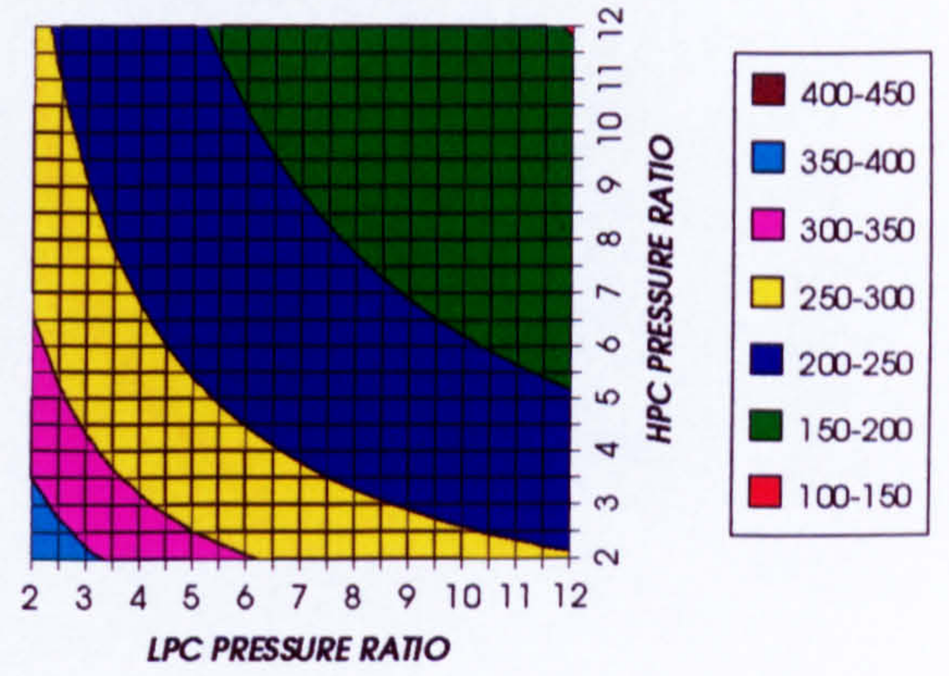

Figure 8. Steam turbine specific power output

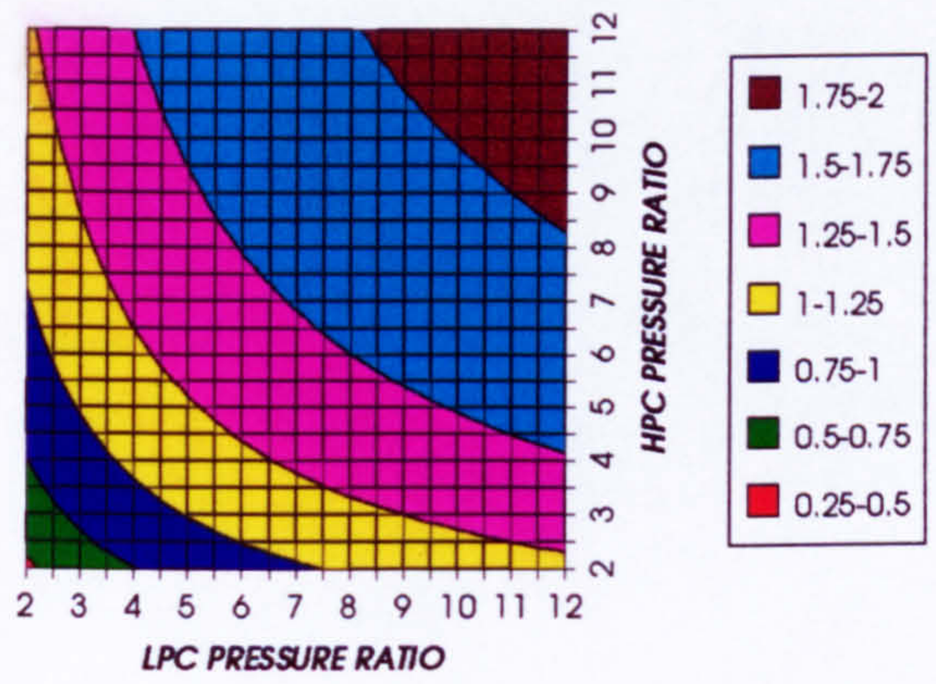

Figure 9. Gas turbine to steam turbine power ratio

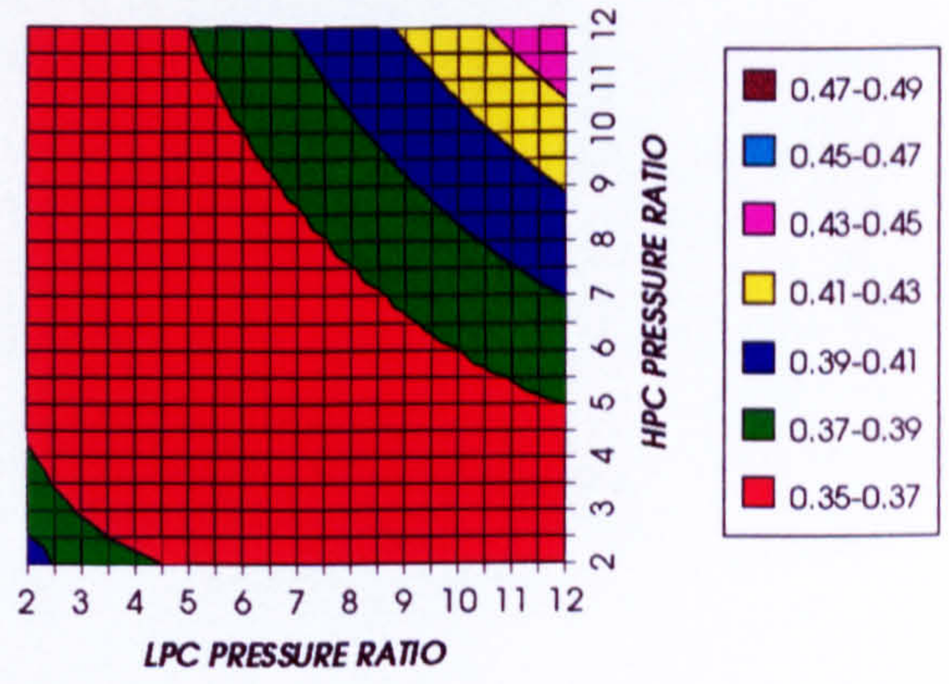

Figure 10. Auxiliary (CO2/Argon, O2 & Fuel) to usefuel power ratio

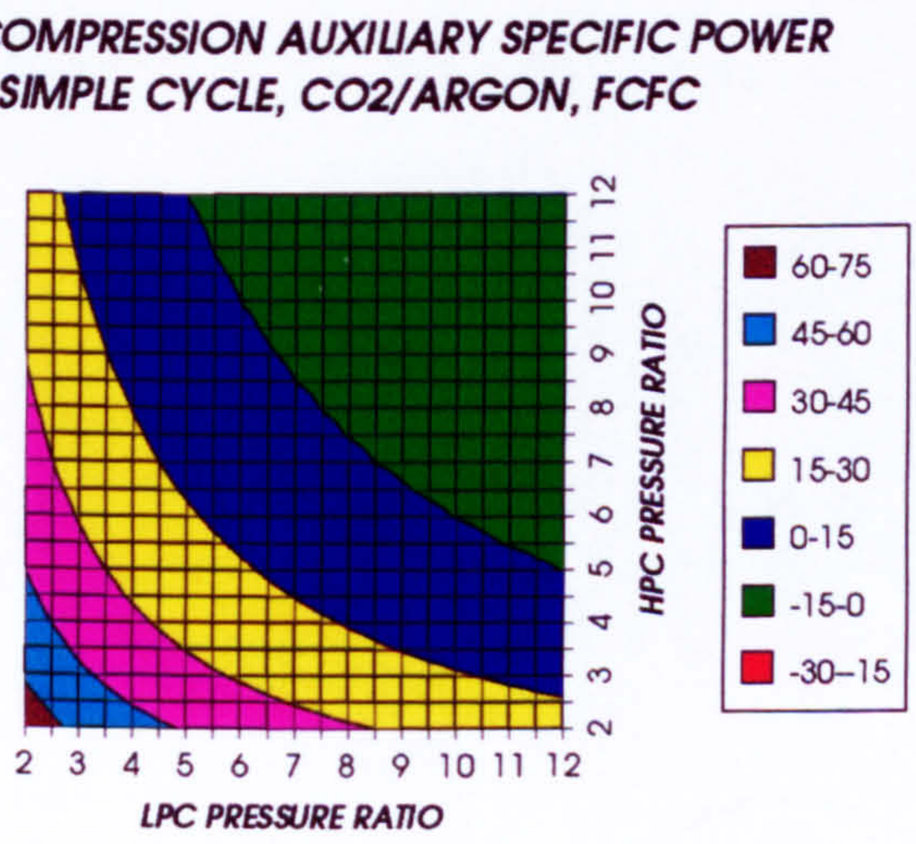

Figure 11. CO2/Argon compression specific power

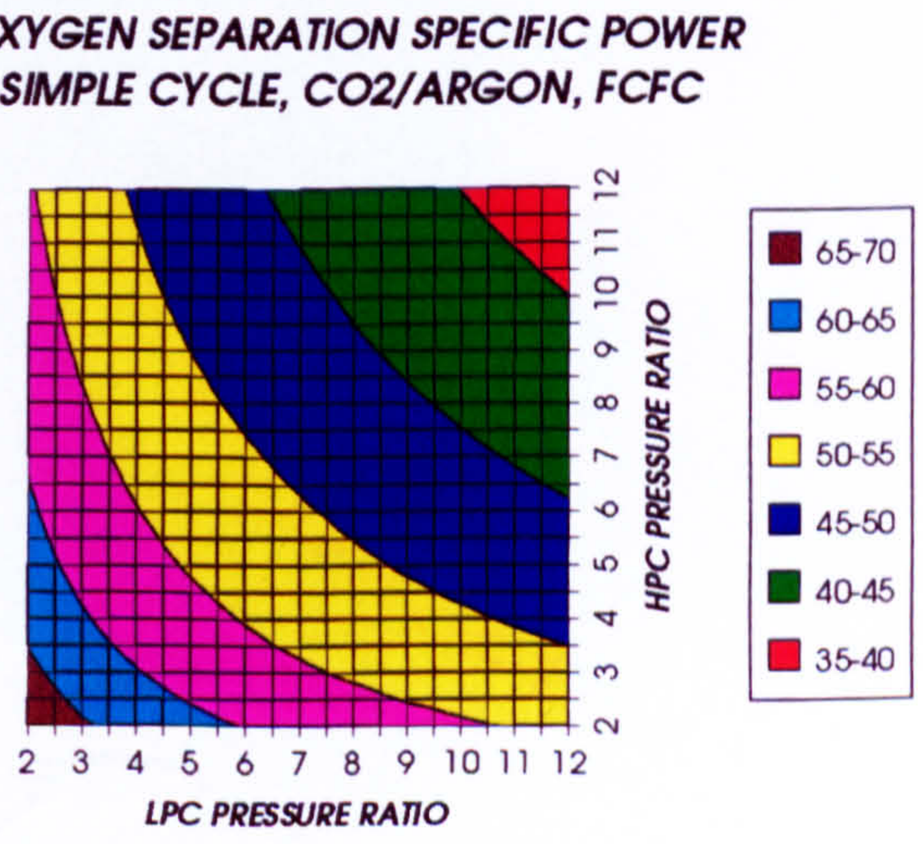

Figure 12. Oxygen separation specific power

COMPLETE PLANT (TET=1650 K)

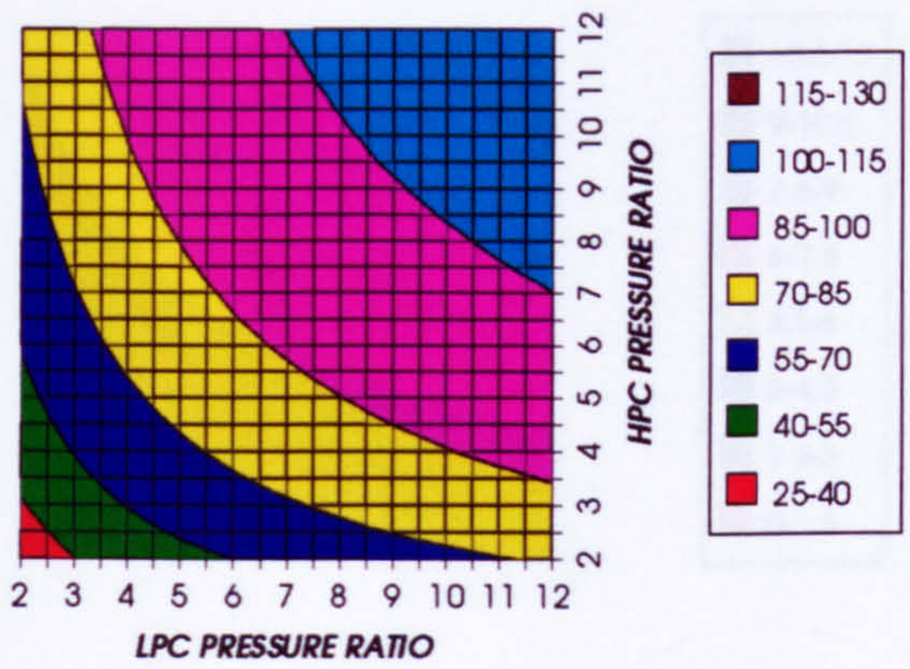

Figure 13. Fuel compressio specific power

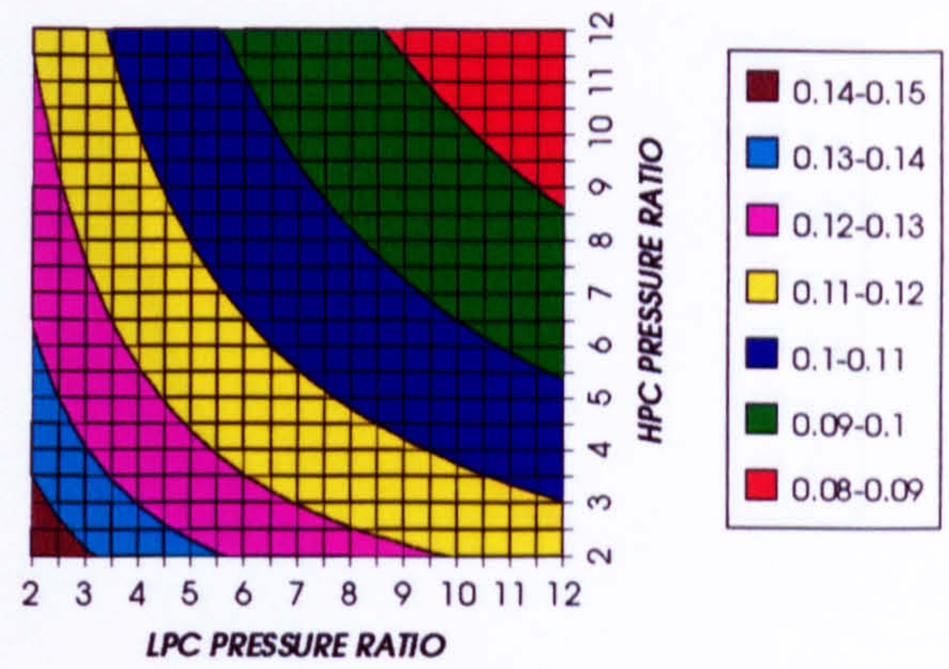

Figure 14. Fuel to compressor inlet mass flow ratio

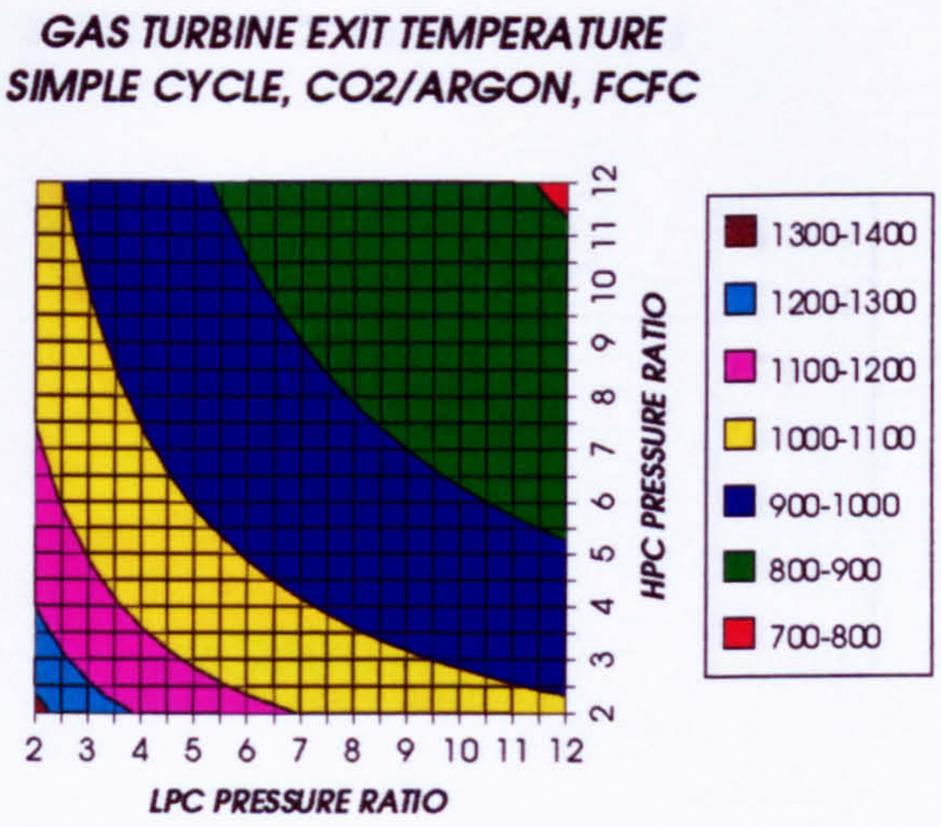

Figure 15. Gas turbine exit temperature

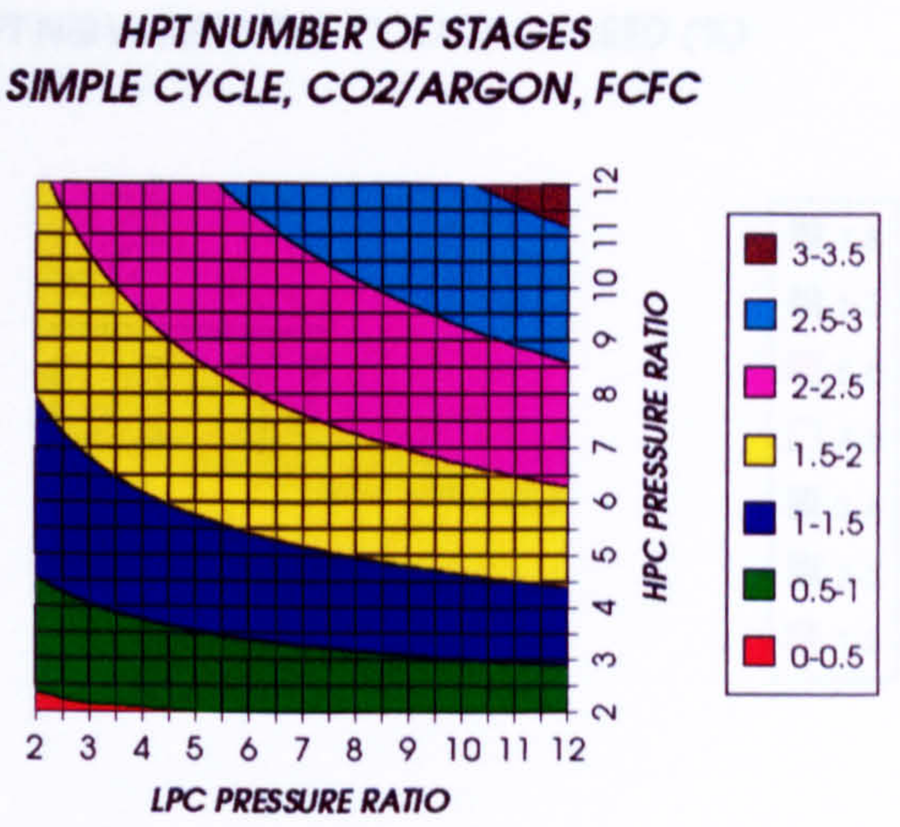

Figure 16. Number of HPT stages

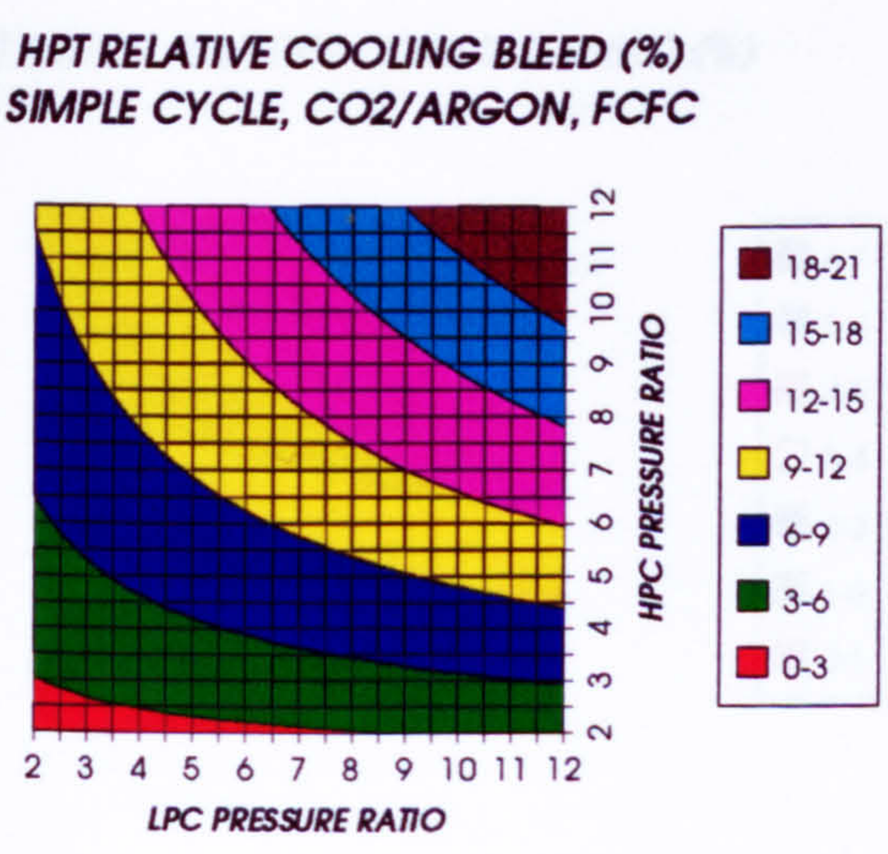

Figure 17. HPT cooling to compressor inlet mass flow ratio

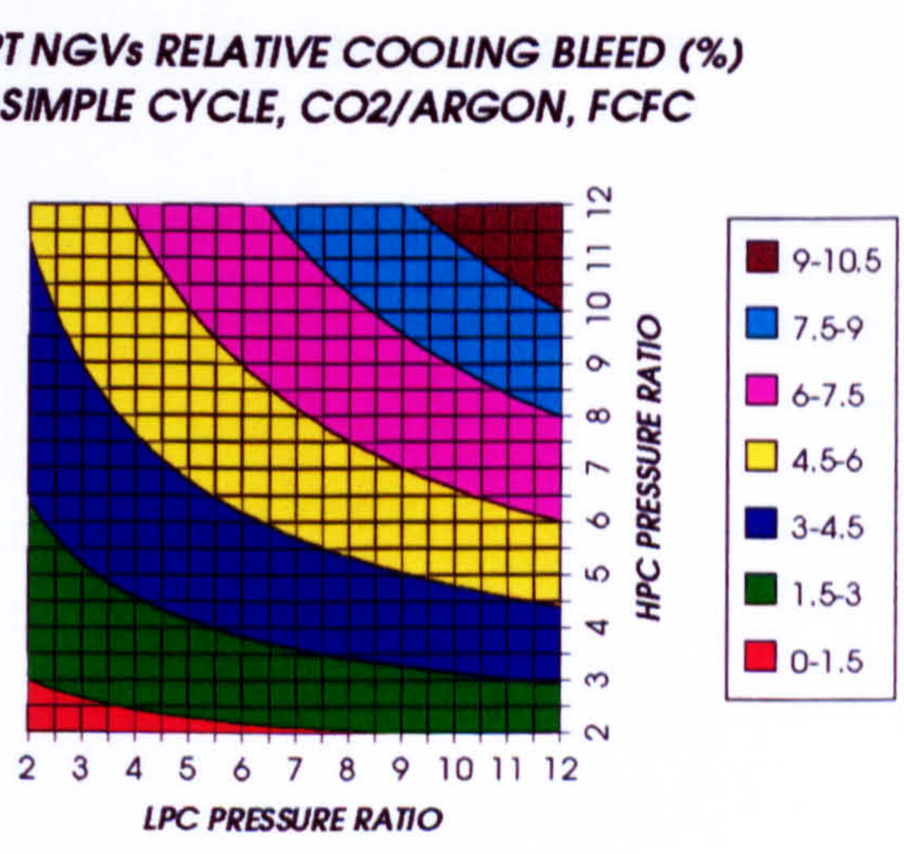

Figure 18. HPT NGVs cooling to compressor inlet mass flow ratio

COMPLETE PLANT (TET=1650 K)

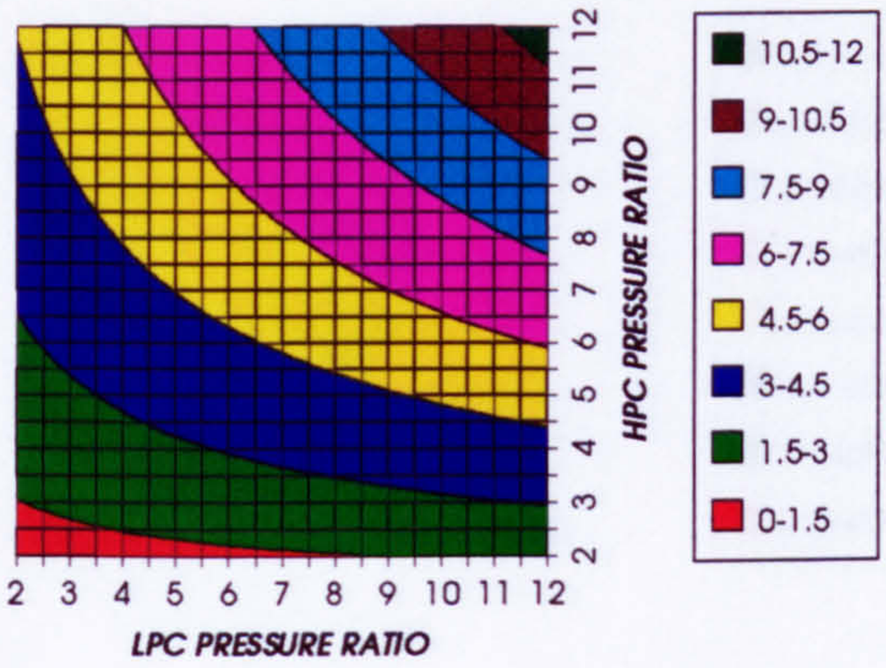

Figure 19. HPT rotor cooling to compressor inlet mass flow ratio

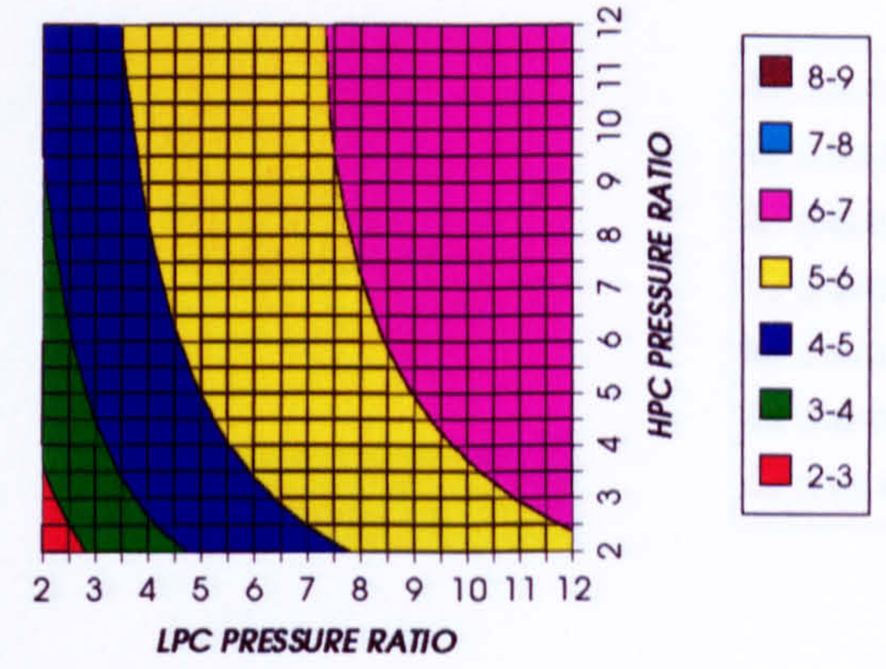

Figure 20. Number of LPT stages

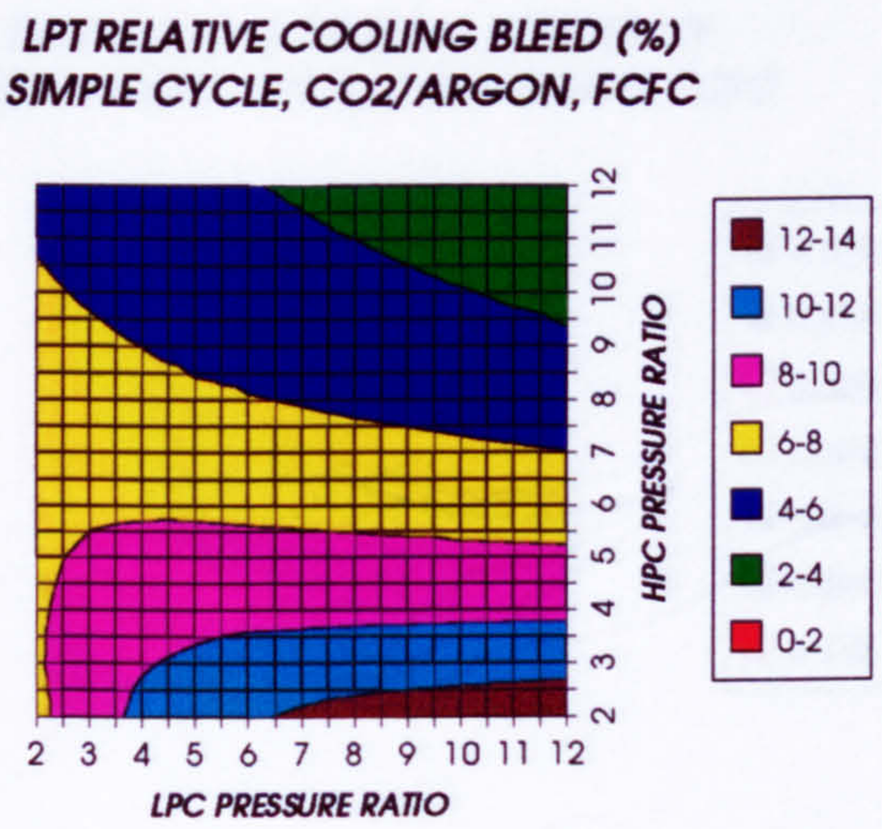

Figure 21. LPT cooling to compressor inlet mass flow ratio

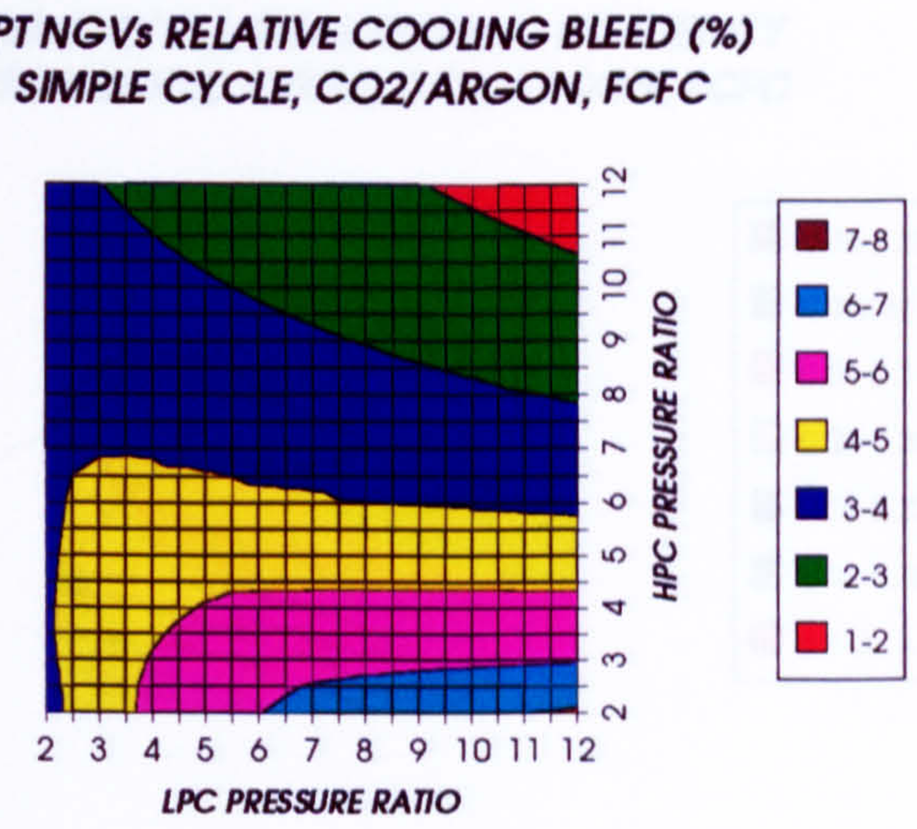

Figure 22. LPT NGVs cooling to compressor inlet mass flow ratio

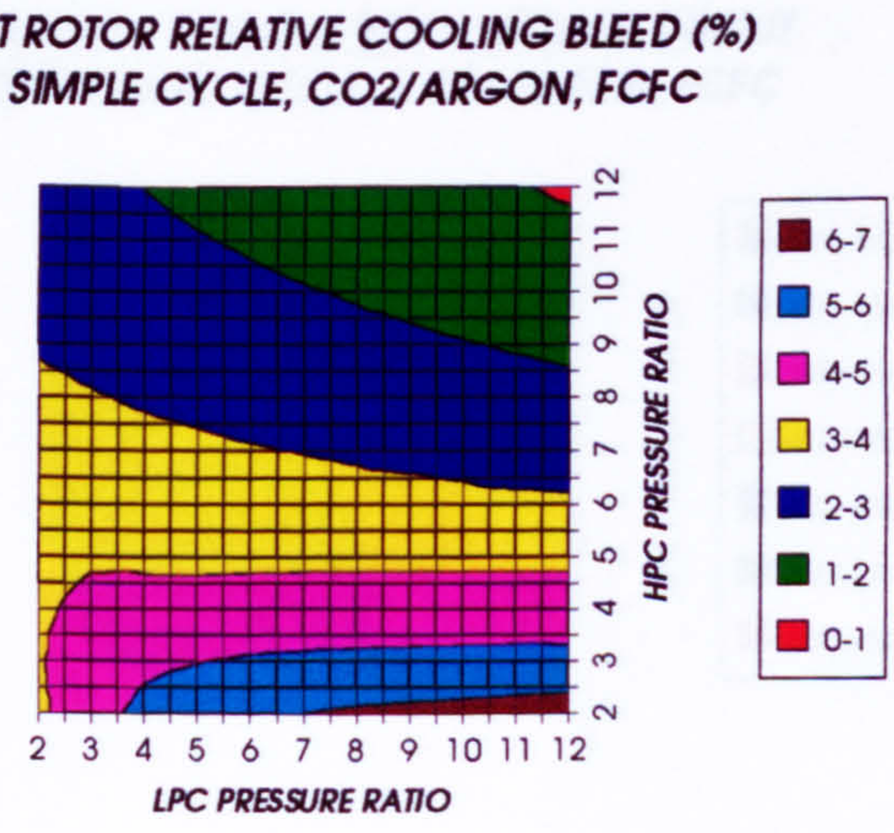

Figure 23. LPT rotor cooling to compressor inlet mass flow ratio

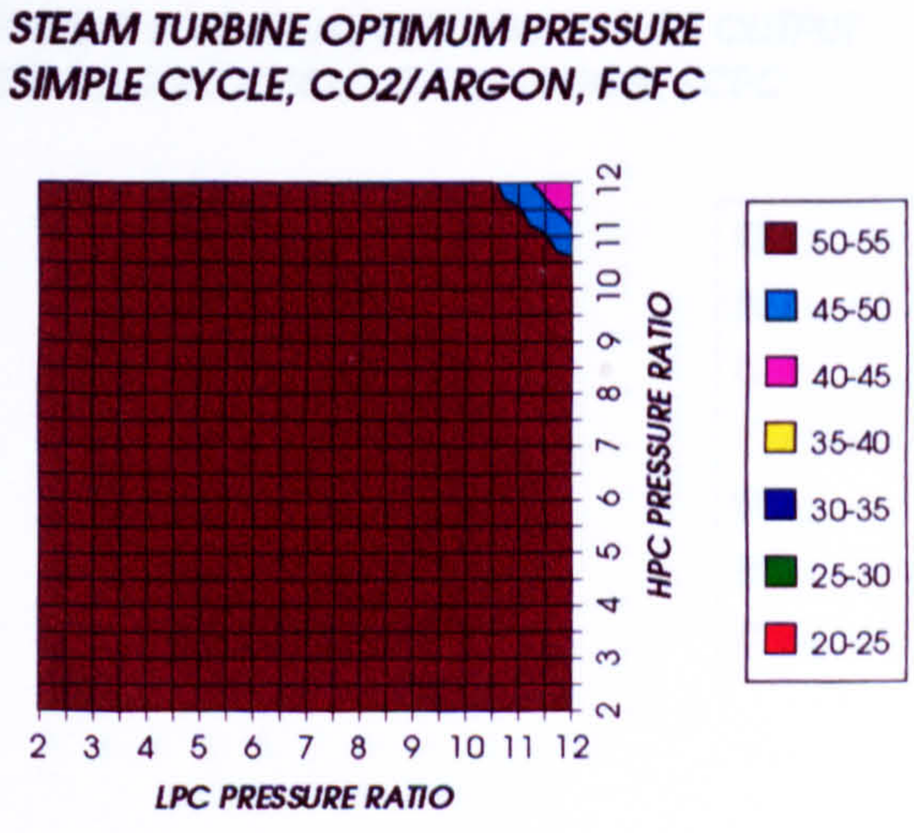

Figure 24. Steam turbine optimum pressures (maximum)

COMPLETE PLANT (TET=1650 K)

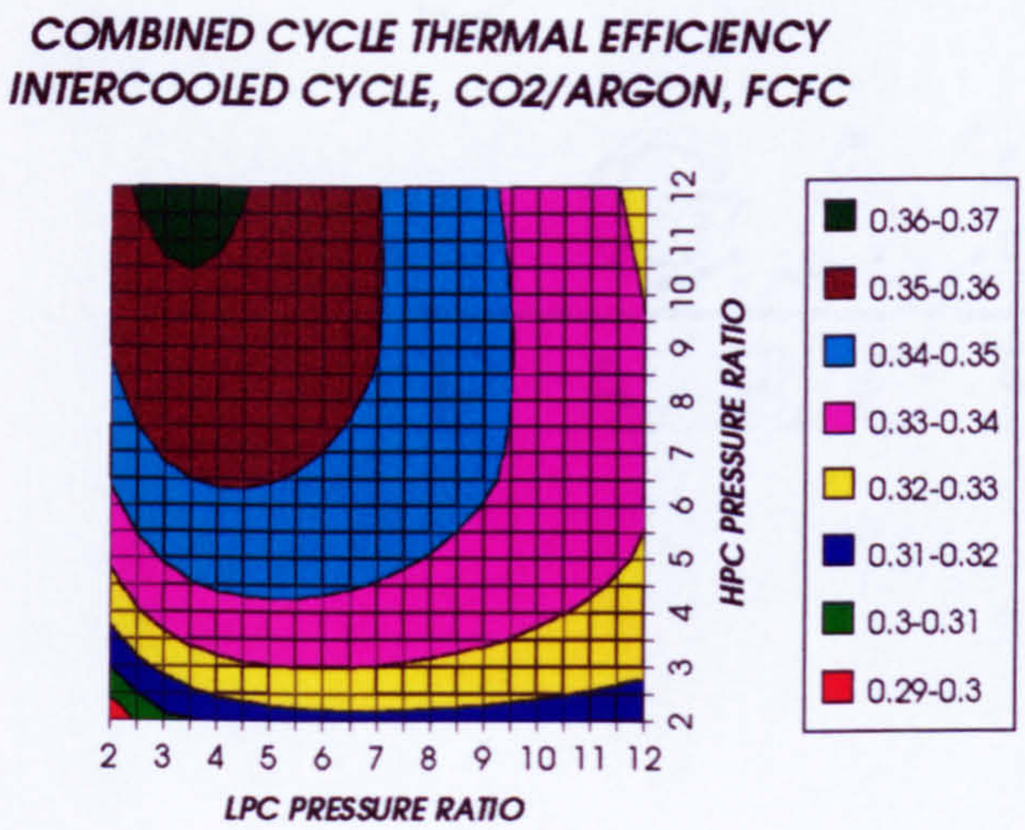

Figure 25. Combined cycle thermal efficiency

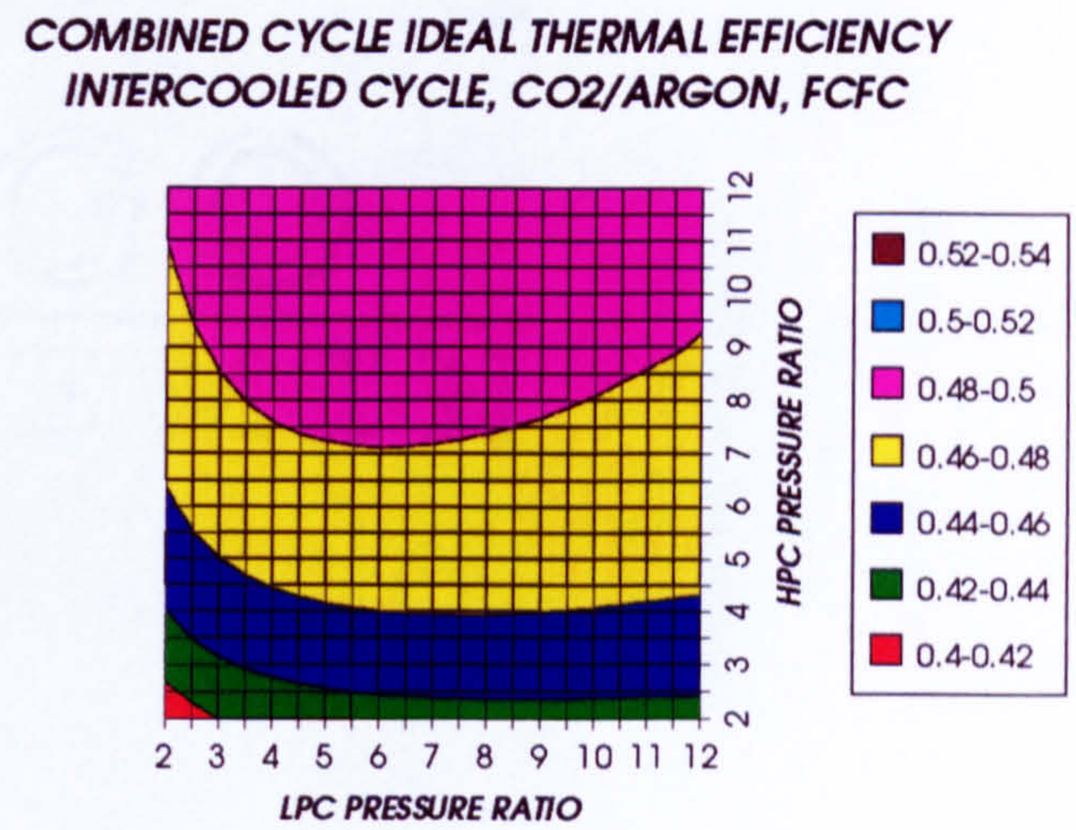

Figure 26. Combined cycle ideal thermal efficiency

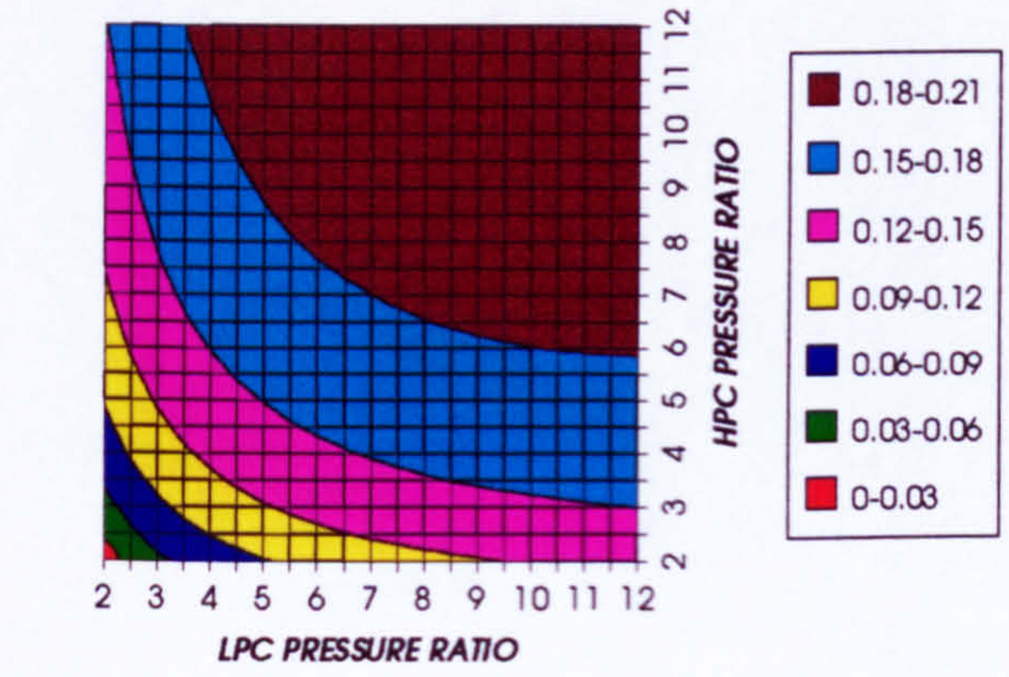

Figure 27. Simple cycle thermal efficiency

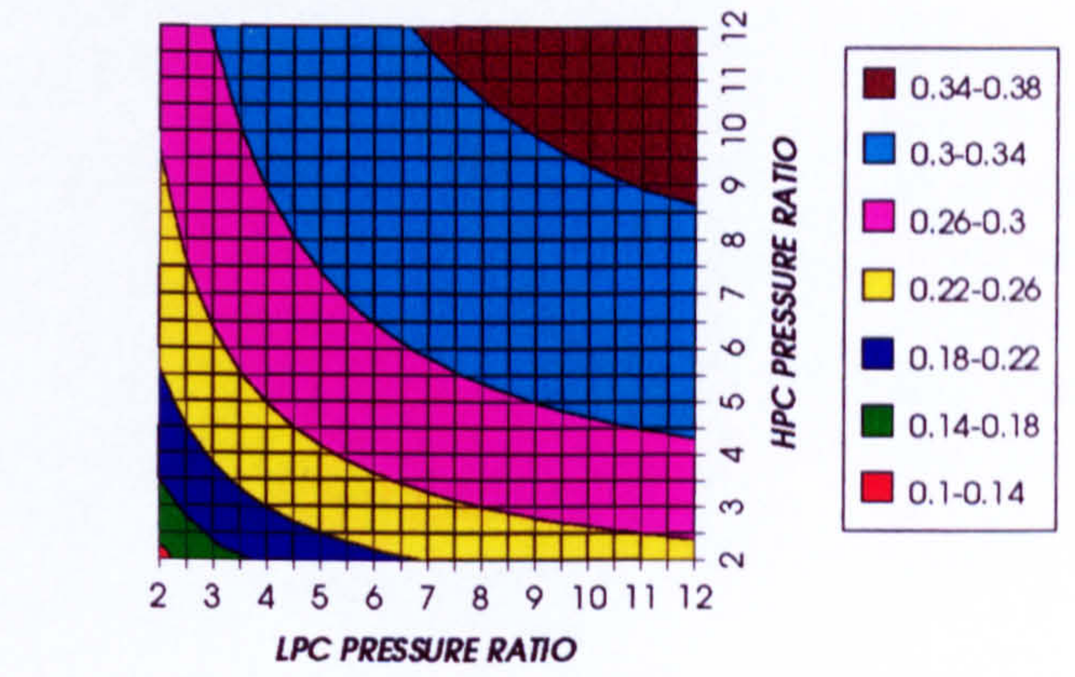

Figure 28. Simple cycle ideal thermal efficiency

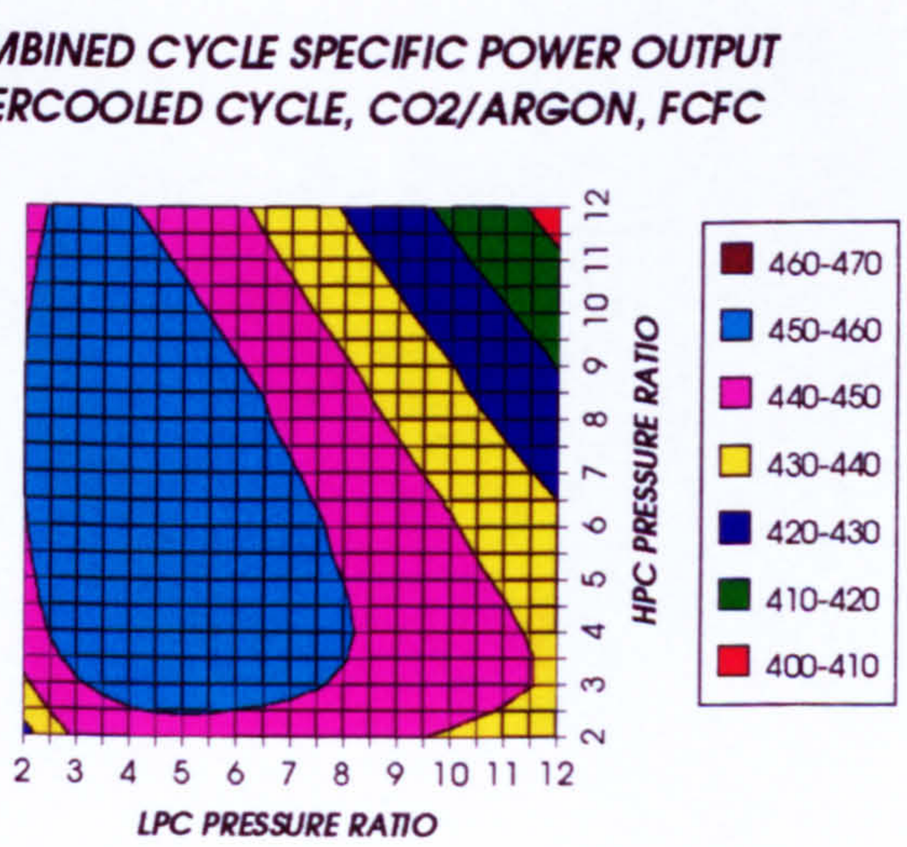

Figure 29. Combined cycle specific power output

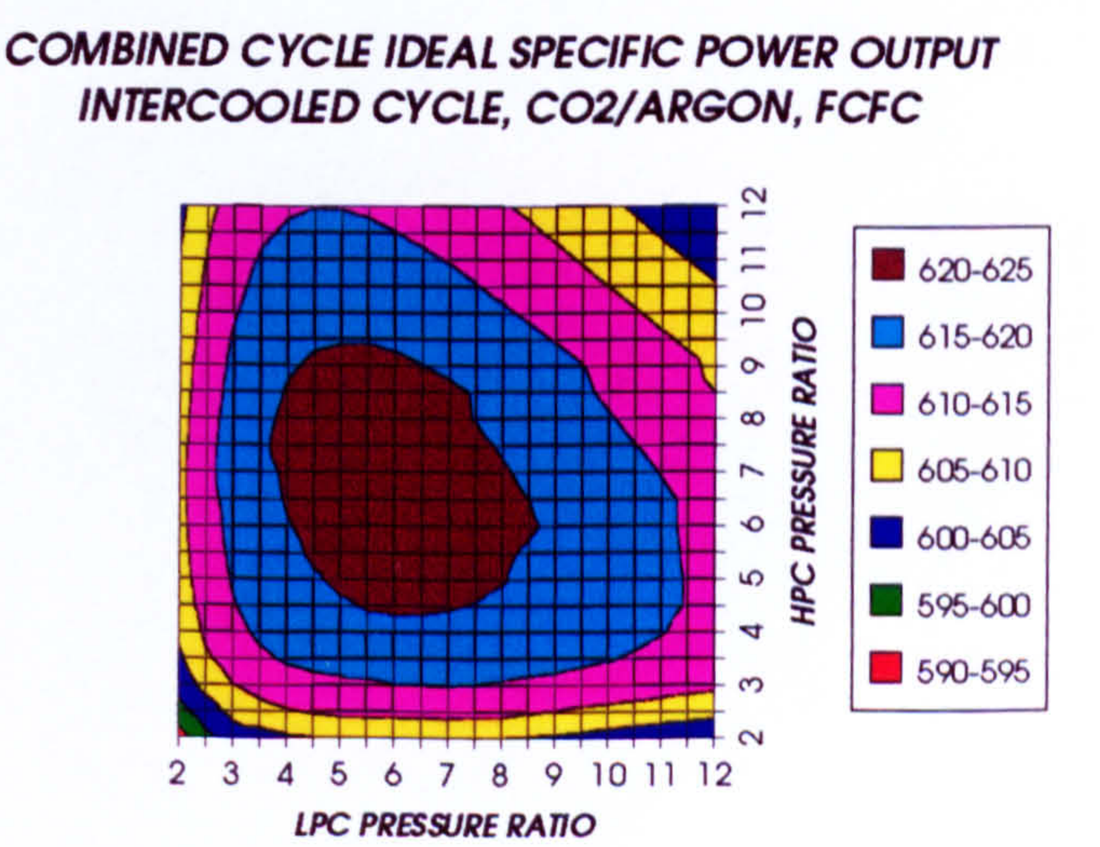

Figure 30. Combined cycle ideal specific power output

COMPLETE PLANT (TET=1650 K)

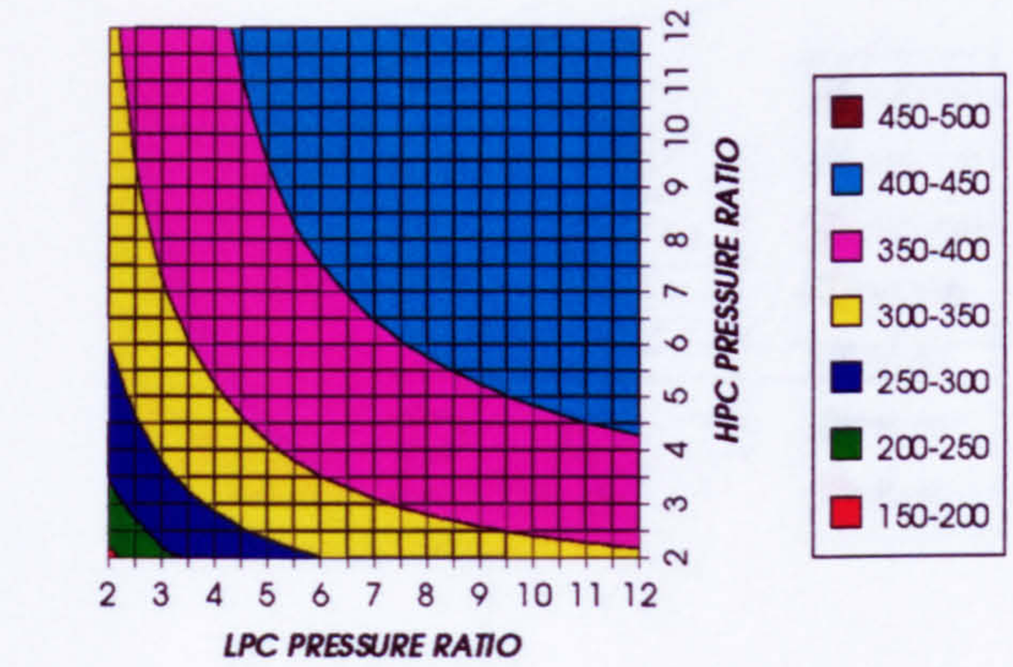

Figure 31. Gas turbine specific power output

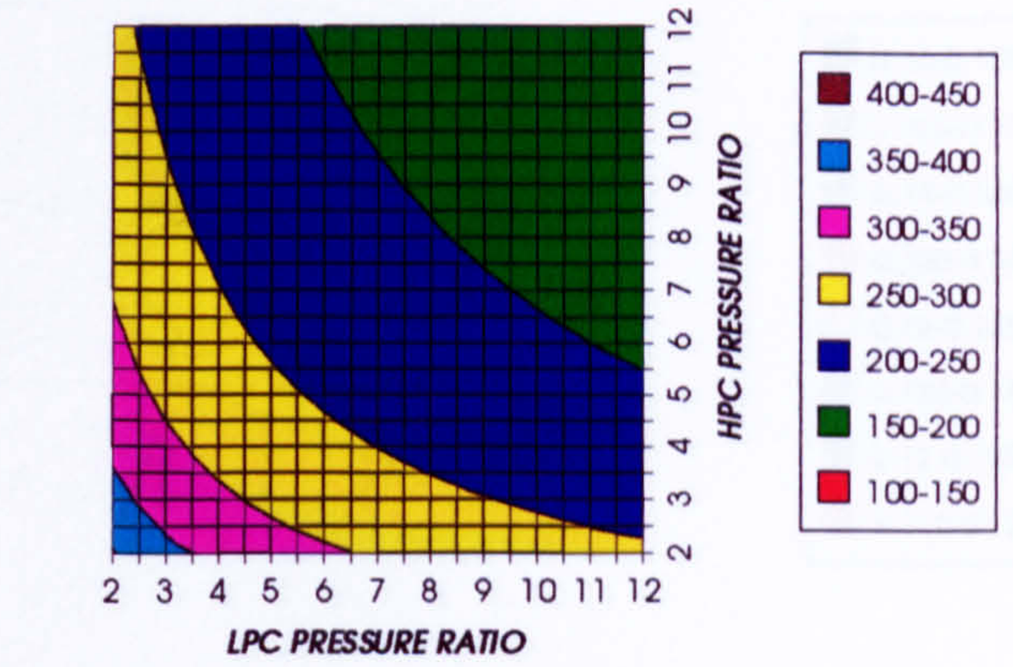

Figure 32. Steam turbine specific power output

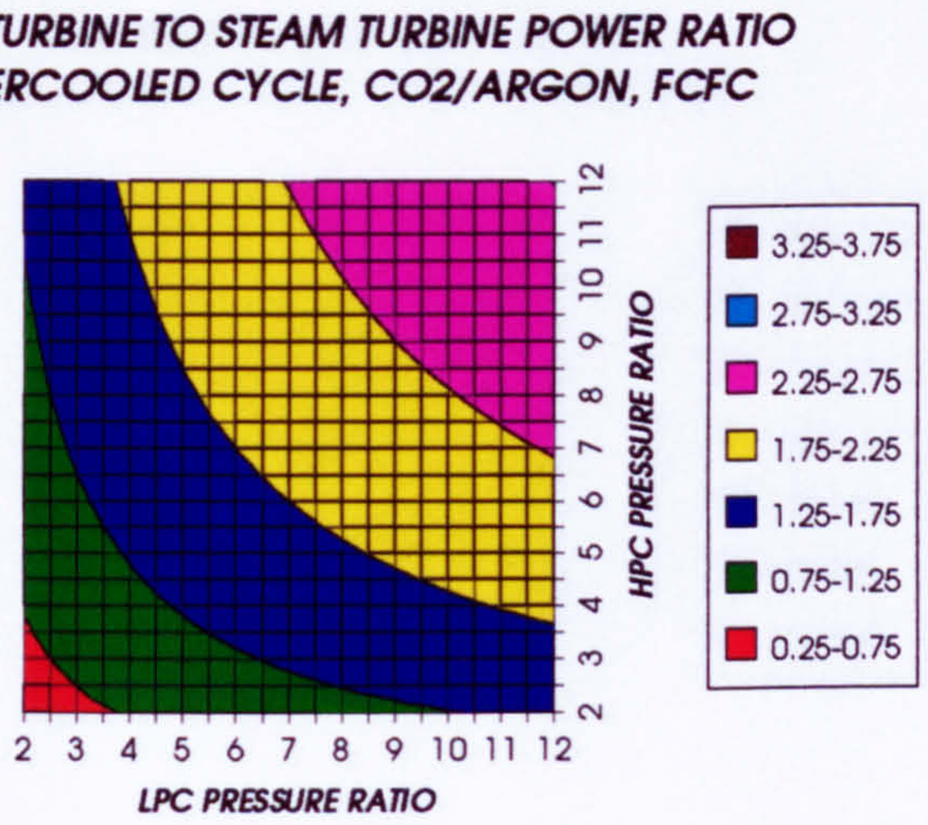

Figure 33. Gas turbine to steam turbine power ratio

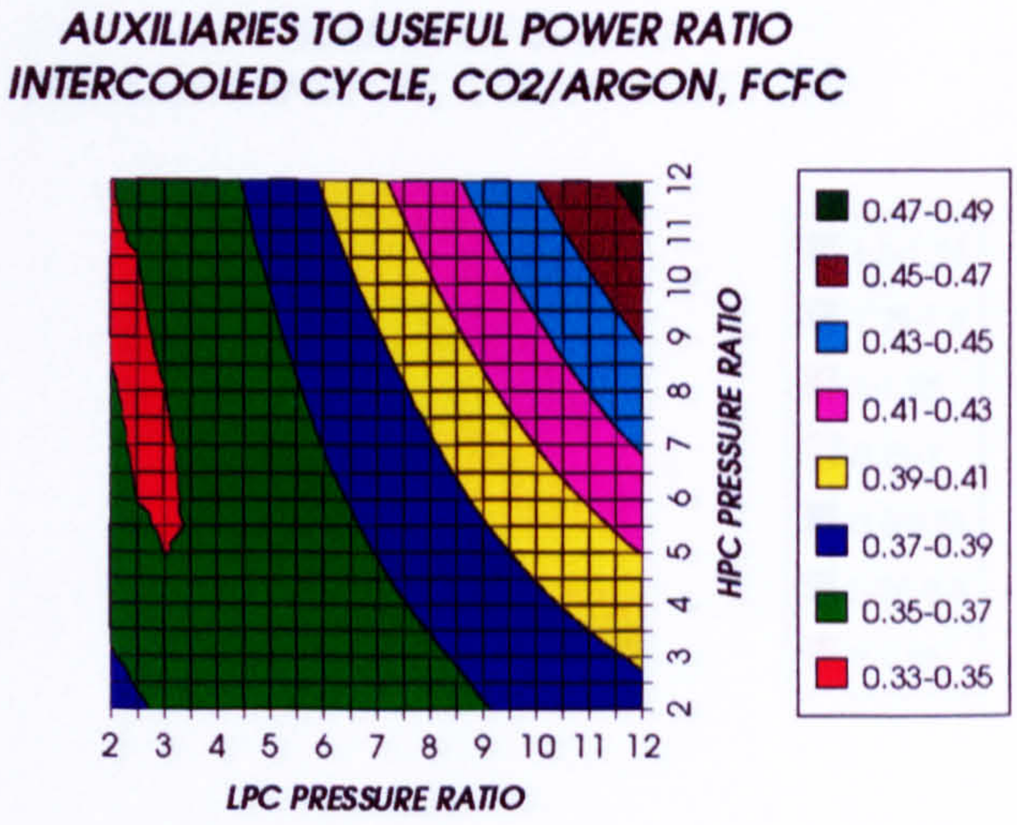

Figure 34. Auxiliary (CO2/Argon, O2 & Fuel) to usefuel power ratio

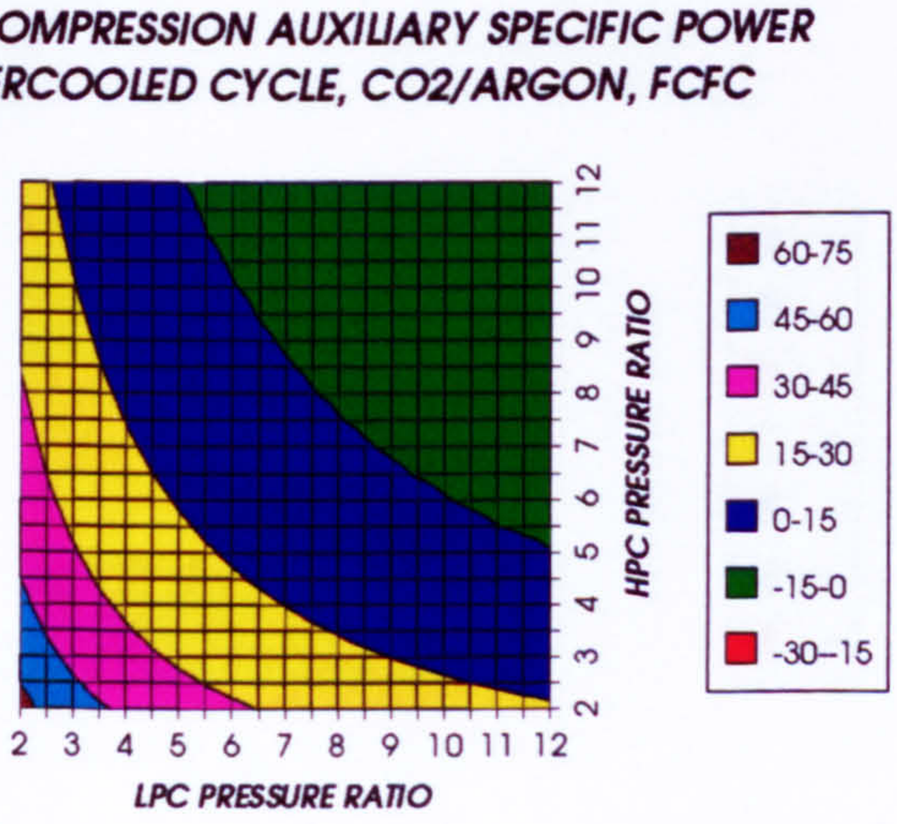

Figure 35. CO2/Argon compression specific power

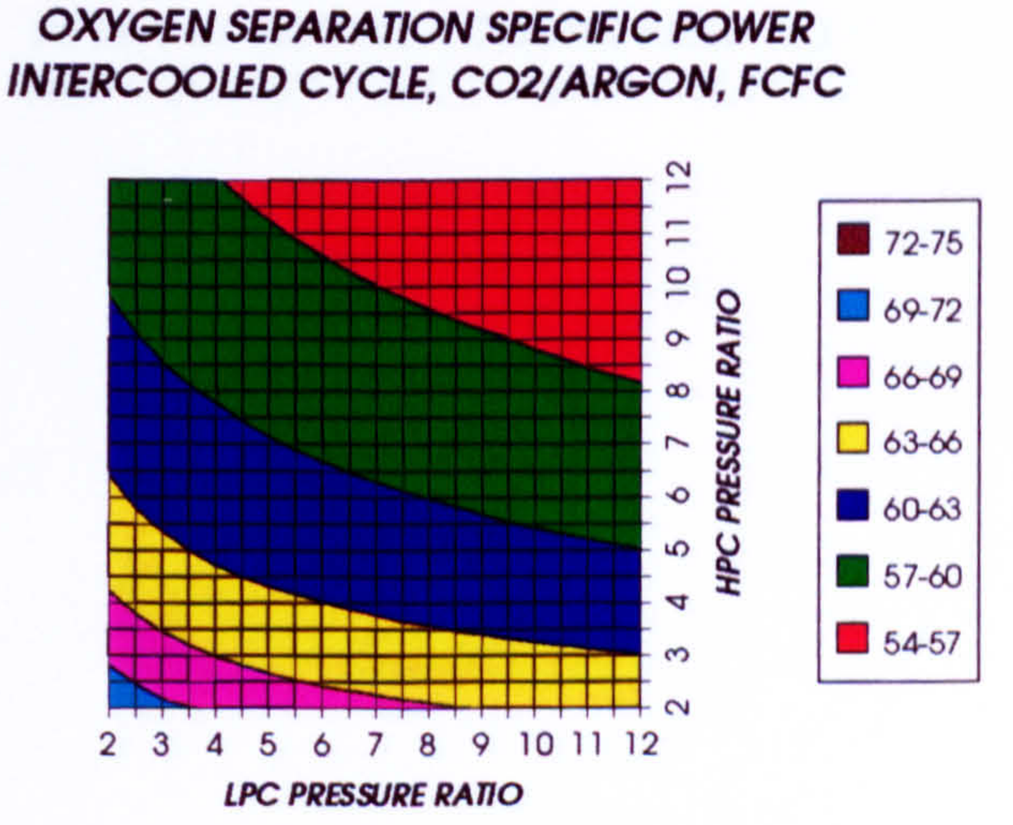

Figure 36. Oxygen separation specific power

COMPLETE PLANT (TET=1650 K)

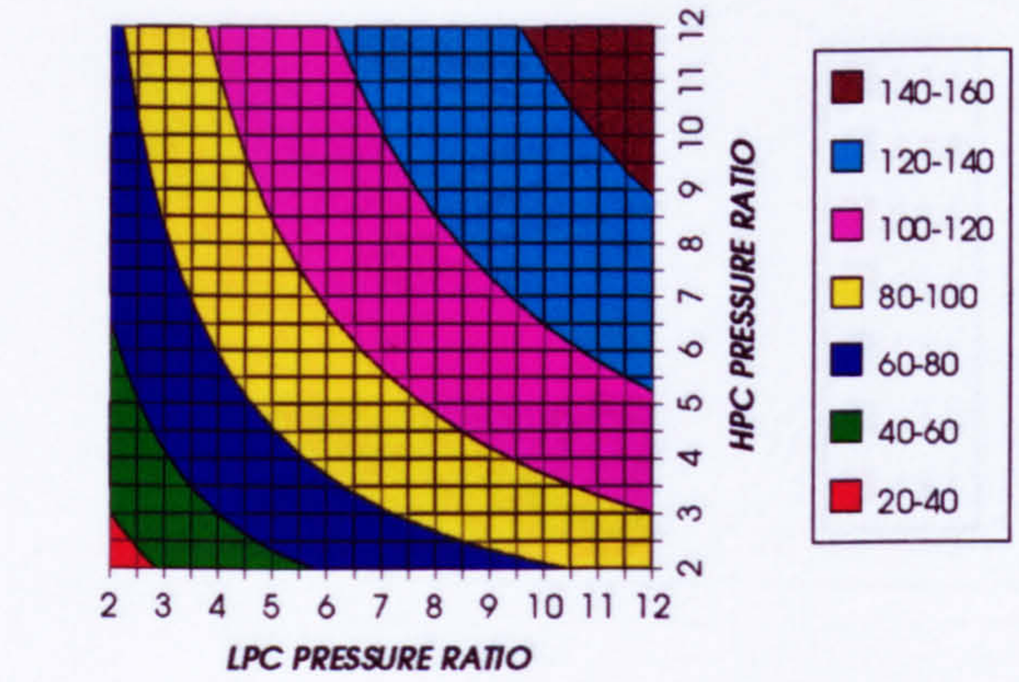

Figure 37. Fuel compression specific power

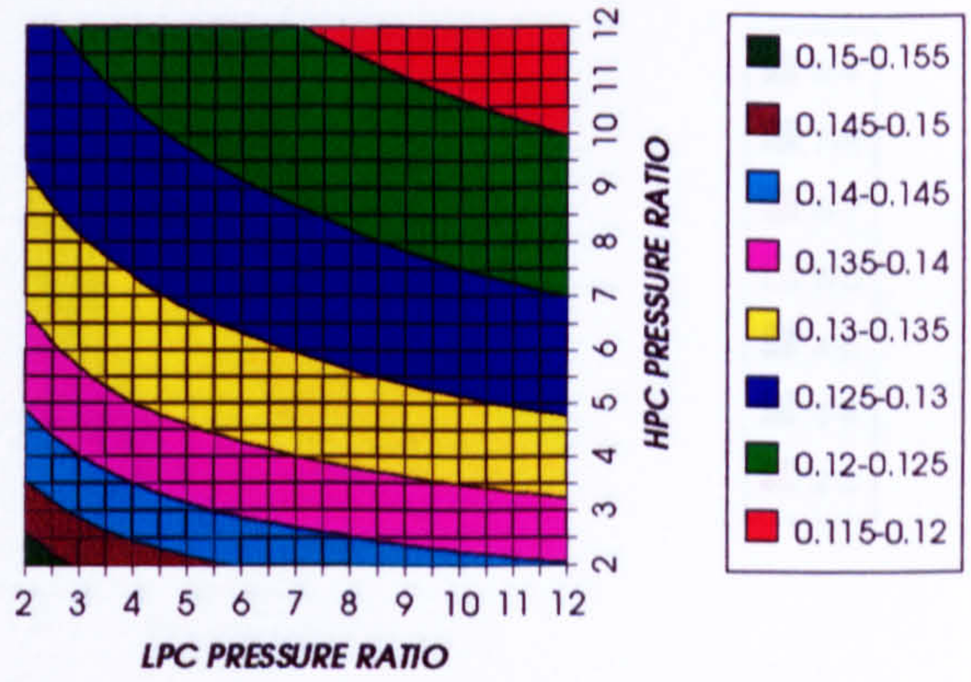

Figure 38. Fuel to compressor inlet mass flow ratio

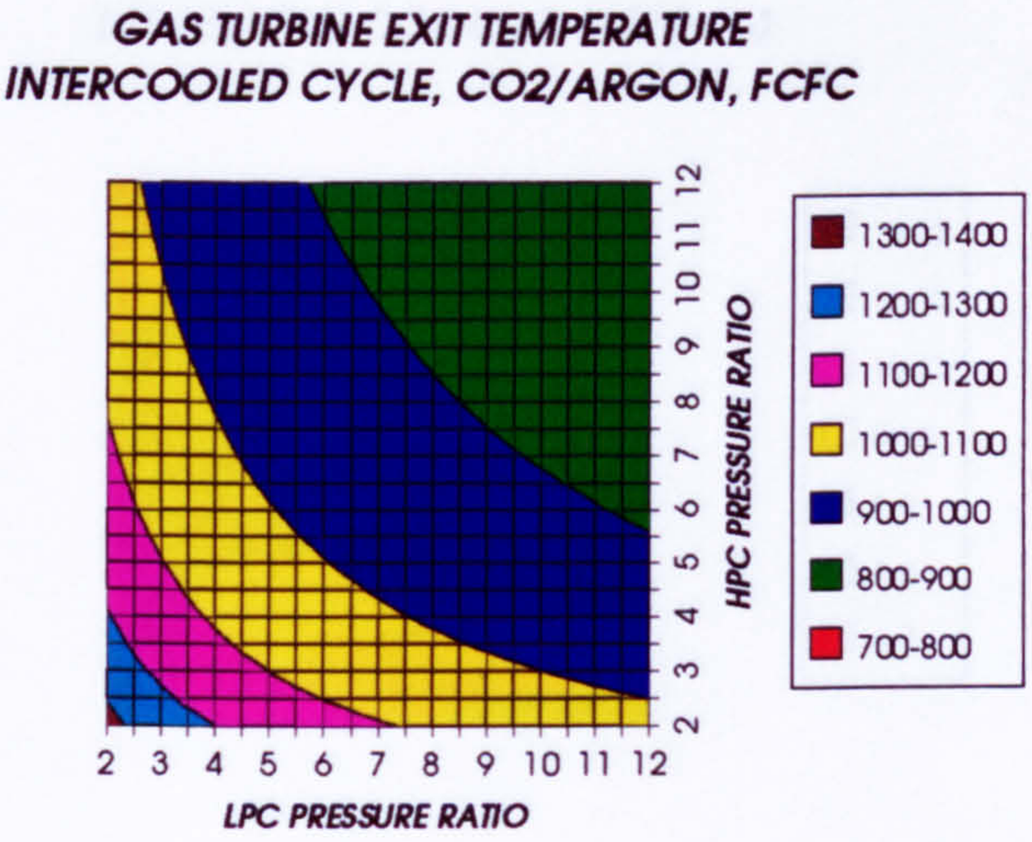

Figure 39. Gas turbine exit temperature

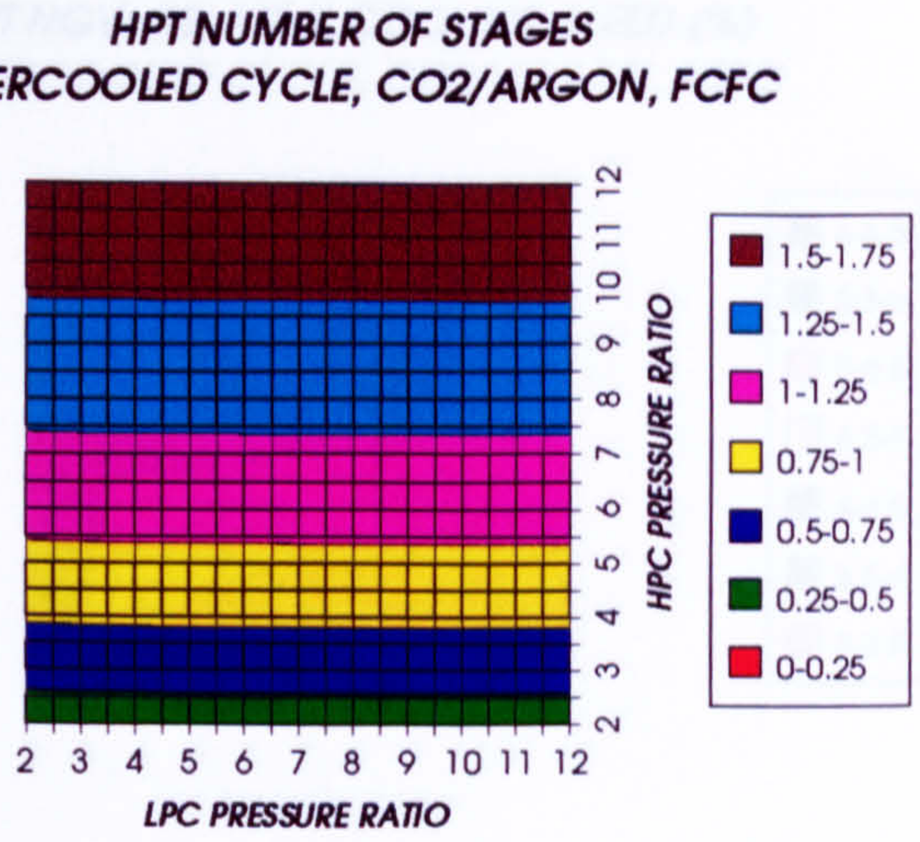

Figure 40. Number of HPT stages

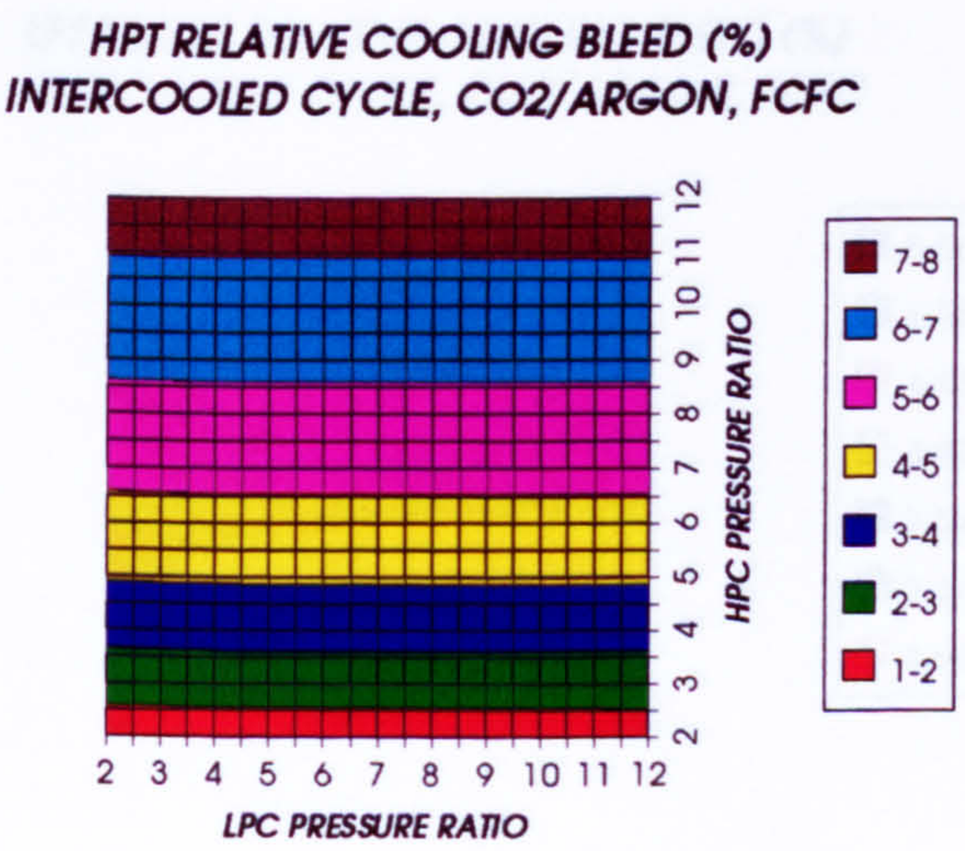

Figure 41. HPT cooling to compressor inlet mass flow ratio

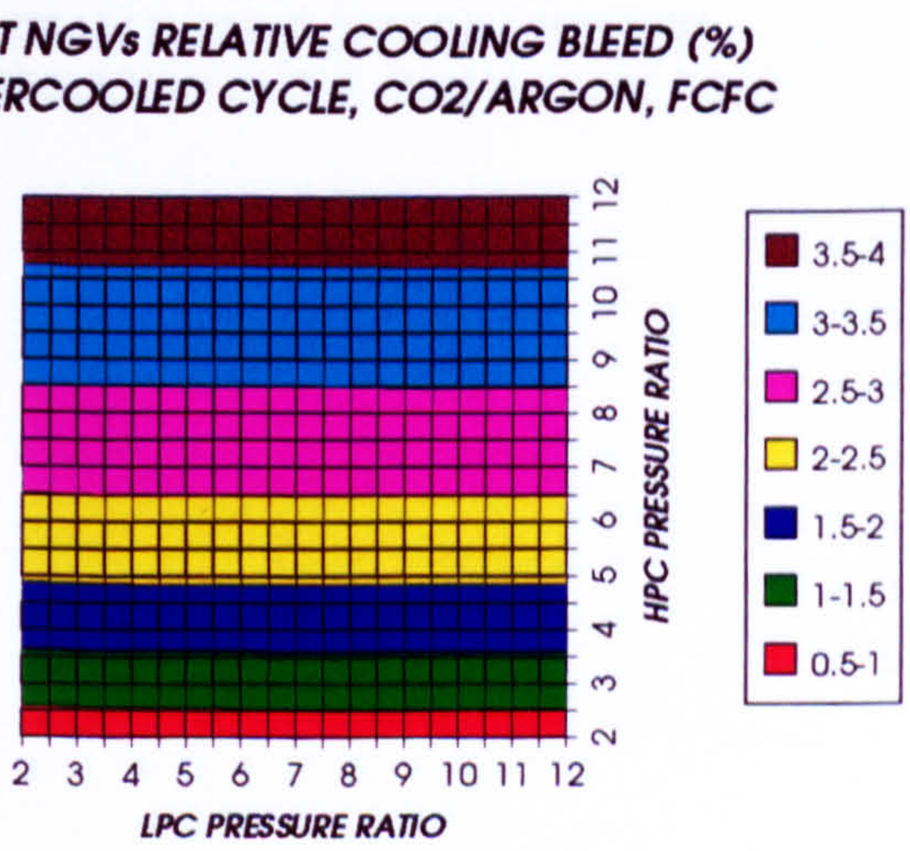

Figure 42. HPT NGVs cooling to compressor inlet mass flow ratio

COMPLETE PLANT (TET=1650 K)

HPT ROTOR RELATIVE COOLING BLEED (%)
INTERCOOLED CYCLE, CO2/ARGON, FCFC

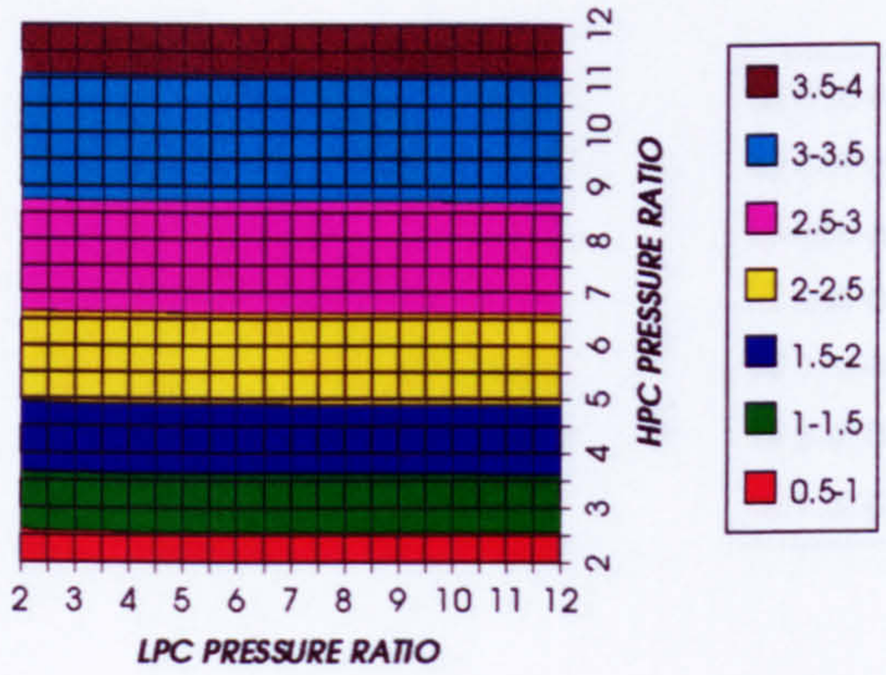

Figure 43. HPT rotor cooling to compressor inlet mass flow ratio

LPT NUMBER OF STAGES
INTERCOOLED CYCLE, CO2/ARGON, FCFC

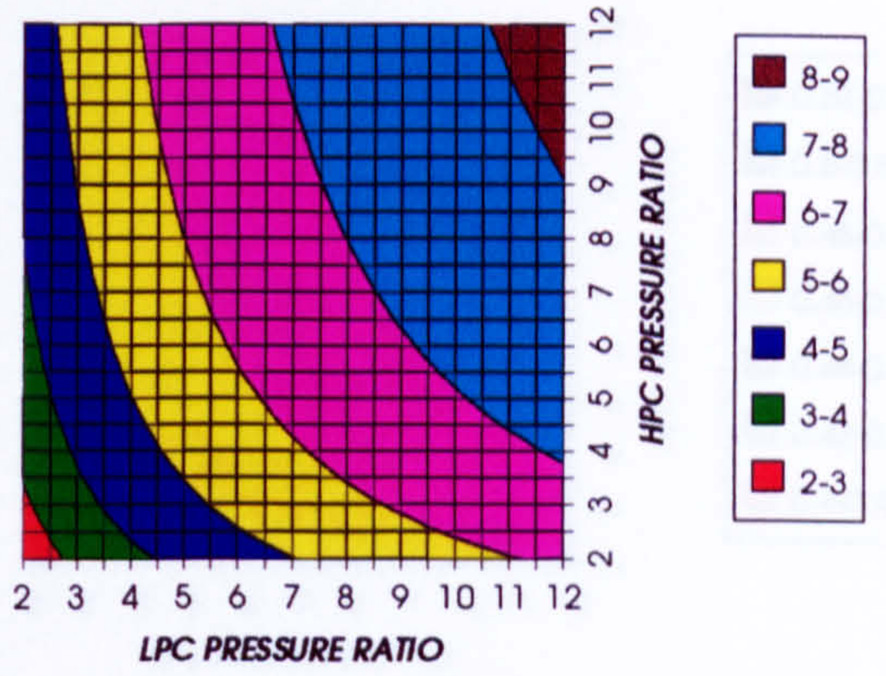

Figure 44. Number of LPT stages

LPT RELATIVE COOLING BLEED (%)
INTERCOOLED CYCLE, CO2/ARGON, FCFC

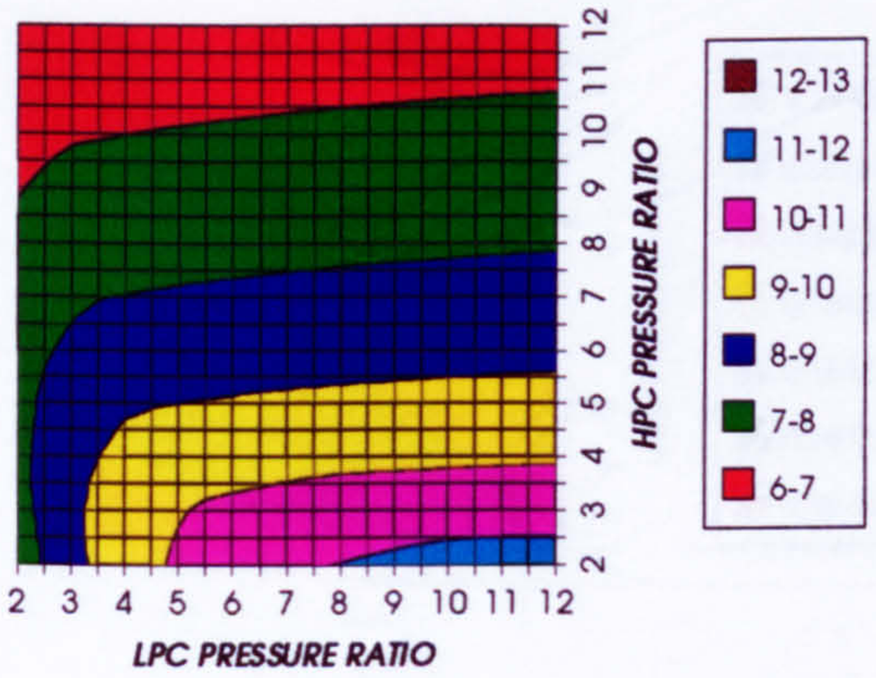

Figure 45. LPT cooling to compressor inlet mass flow ratio

LPT NGVs RELATIVE COOLING BLEED (%)
INTERCOOLED CYCLE, CO2/ARGON, FCFC

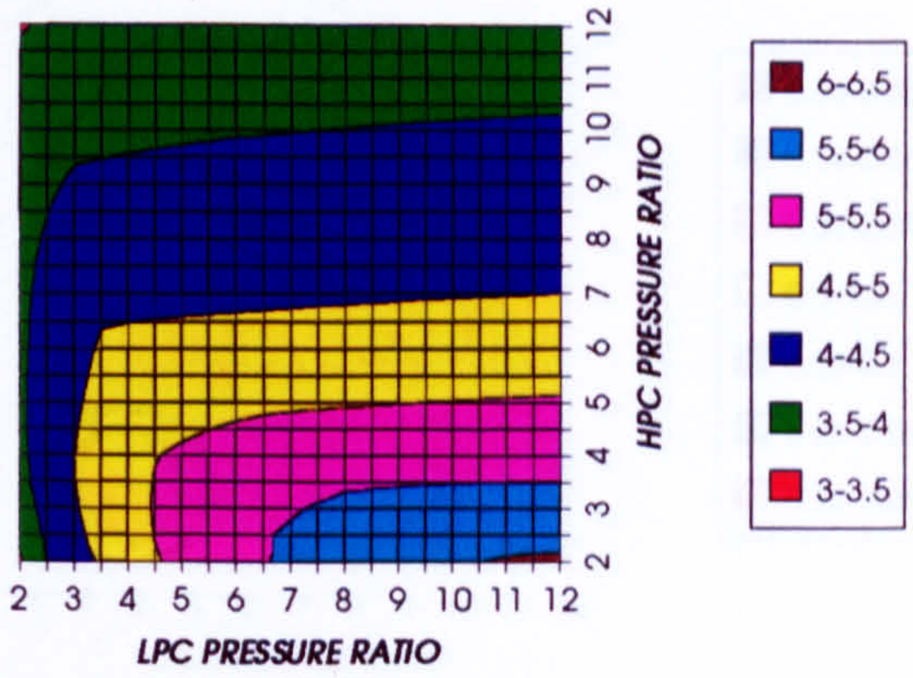

Figure 46. LPT NGVs cooling to compressor inlet mass flow ratio

LPT ROTOR RELATIVE COOLING BLEED (%)
INTERCOOLED CYCLE, CO2/ARGON, FCFC

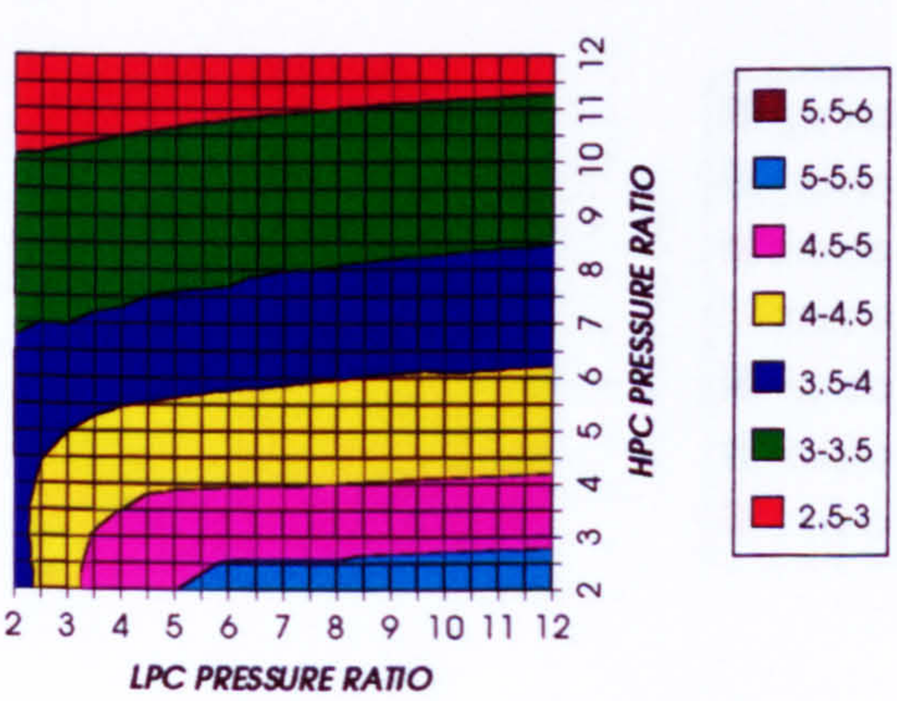

Figure 47. LPT rotor cooling to compressor inlet mass flow ratio

STEAM TURBINE OPTIMUM PRESSURE
INTERCOOLED CYCLE, CO2/ARGON, FCFC

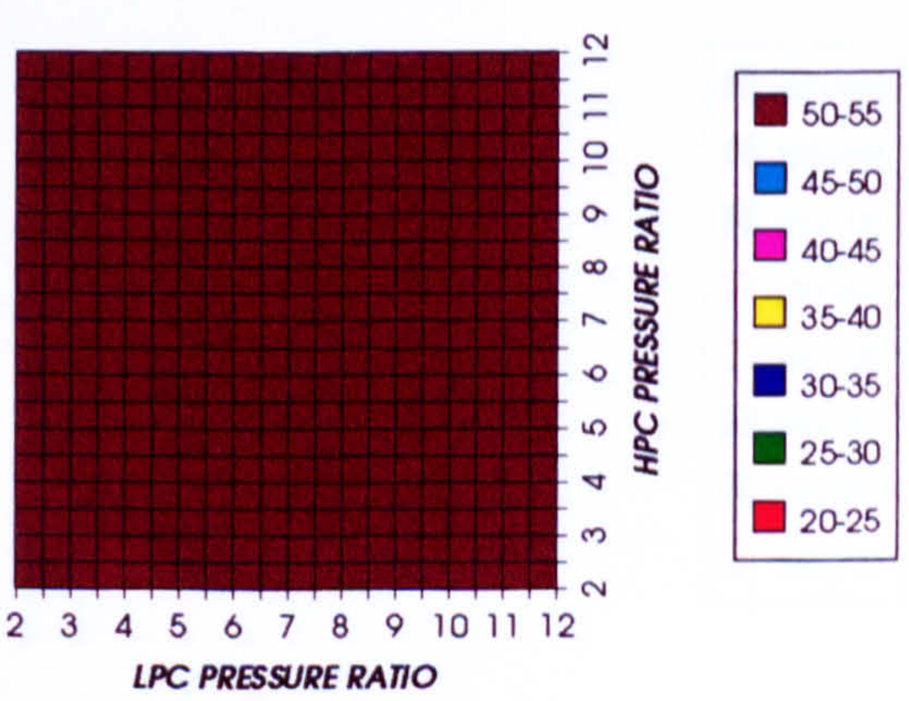

Figure 48. Steam turbine optimum pressures (maximum)

COMPLETE PLANT (TET=1650 K)

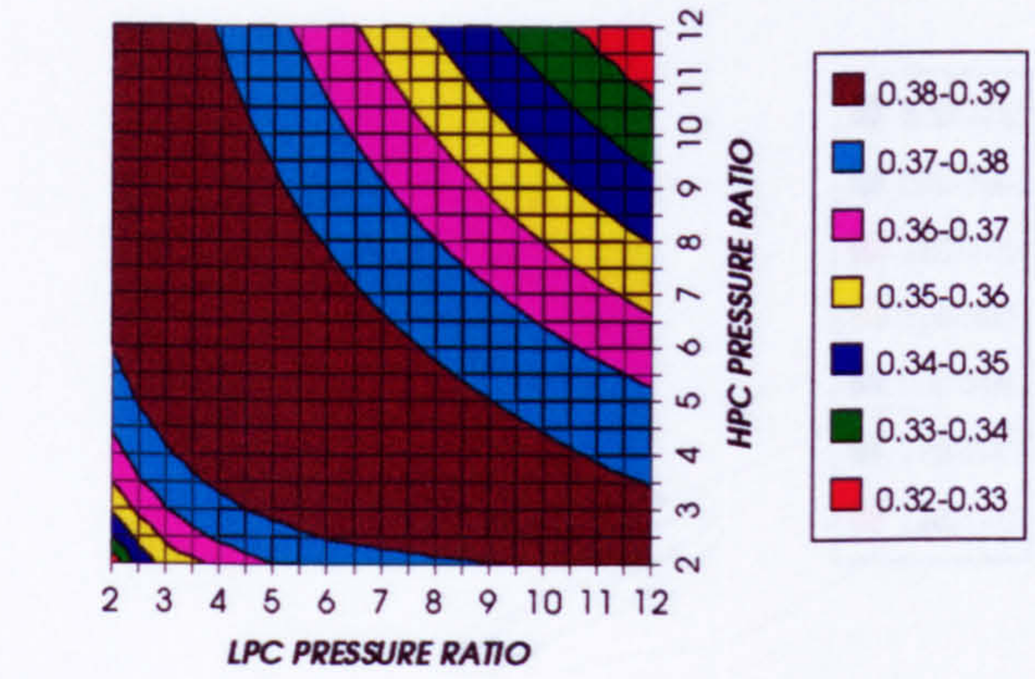

Figure 49. Combined cycle thermal efficiency

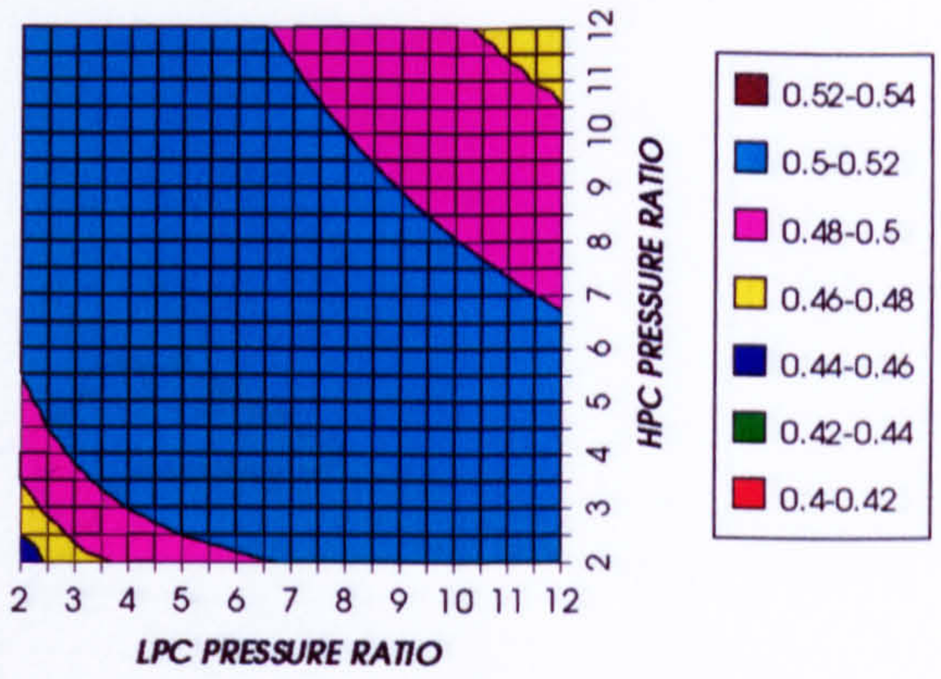

Figure 50. Combined cycle ideal thermal efficiency

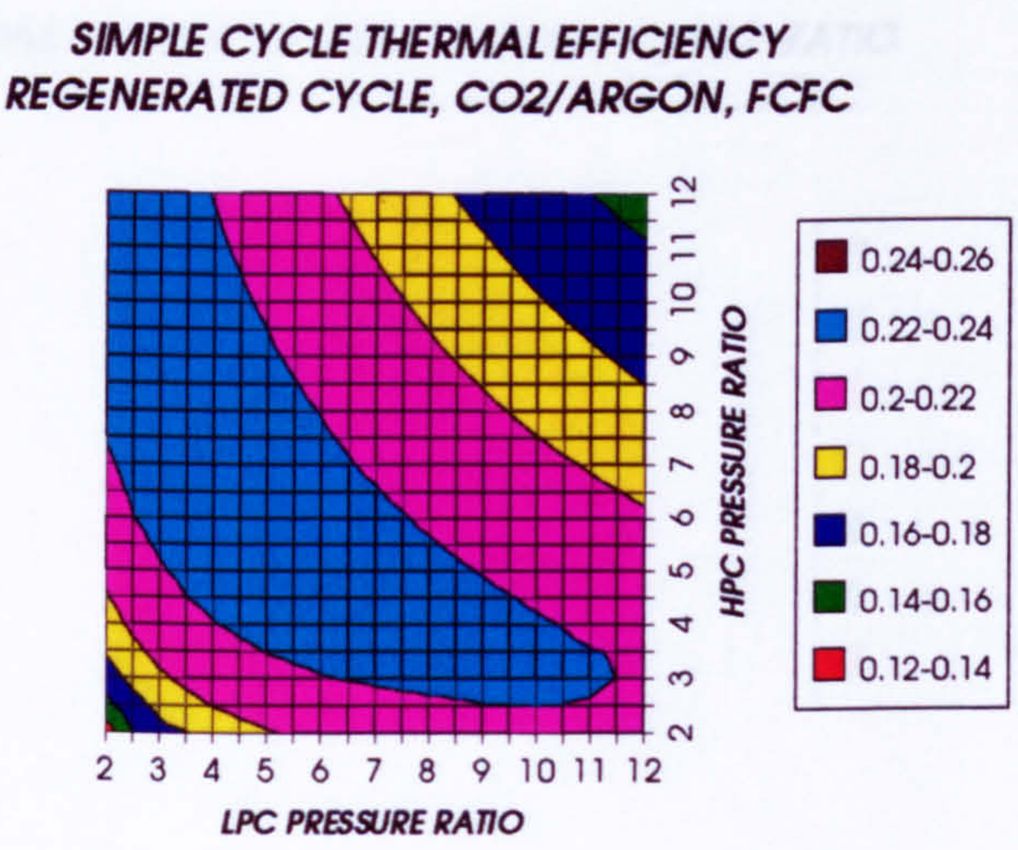

Figure 51. Simple cycle thermal efficiency

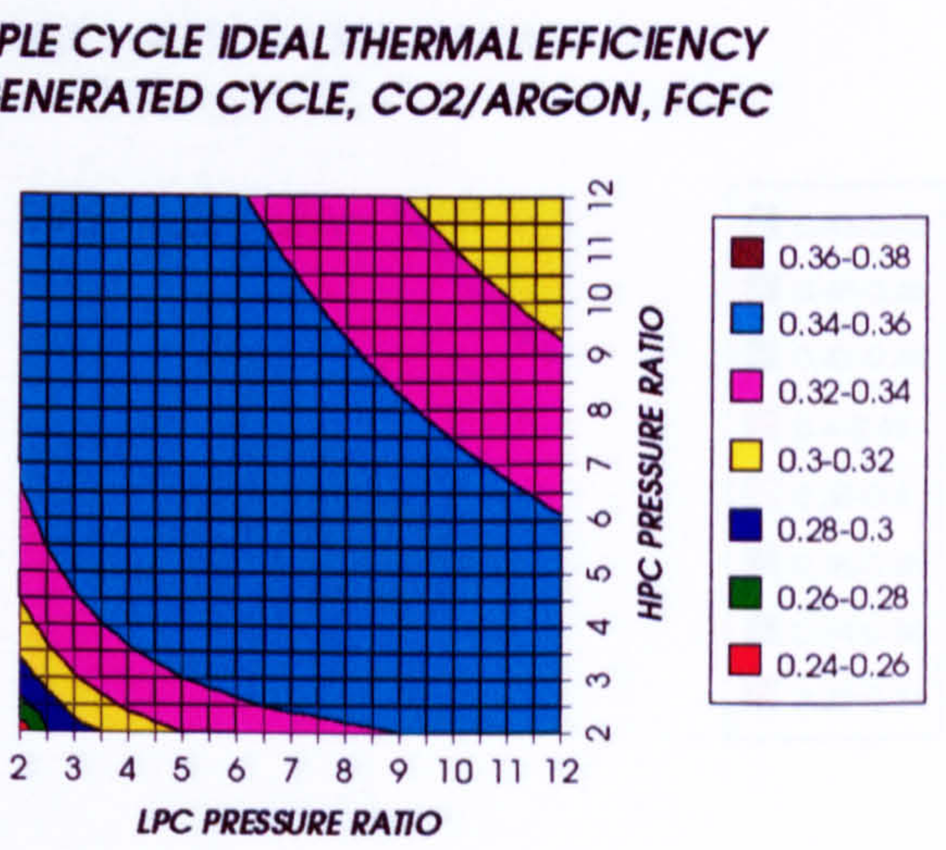

Figure 52. Simple cycle ideal thermal efficiency

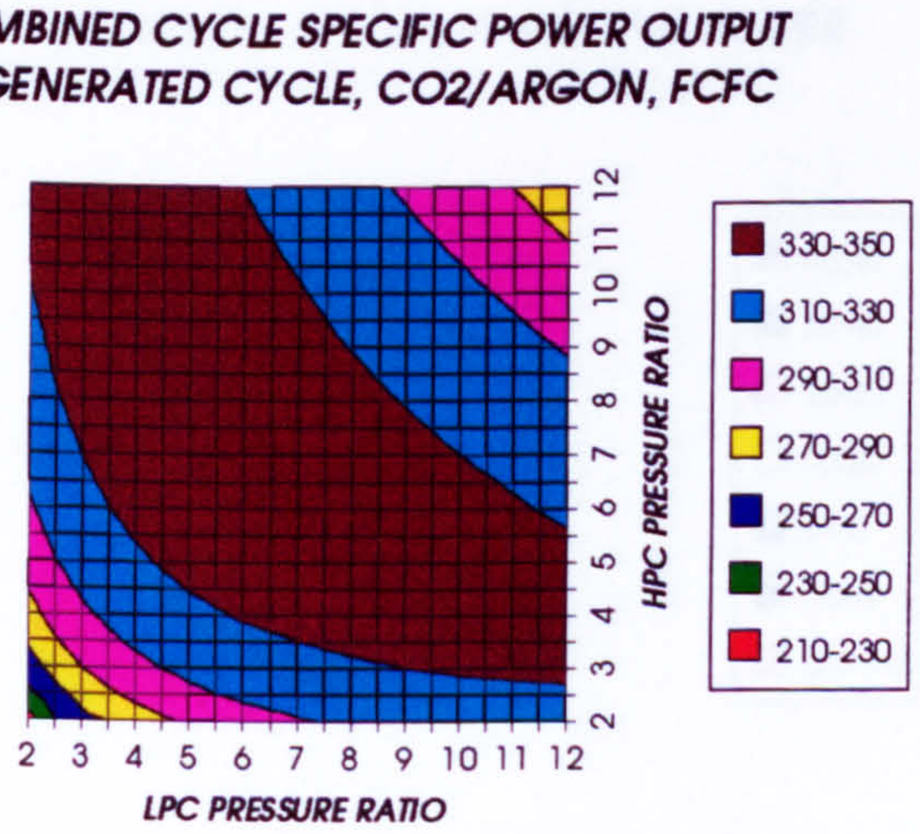

Figure 53. Combined cycle specific power output

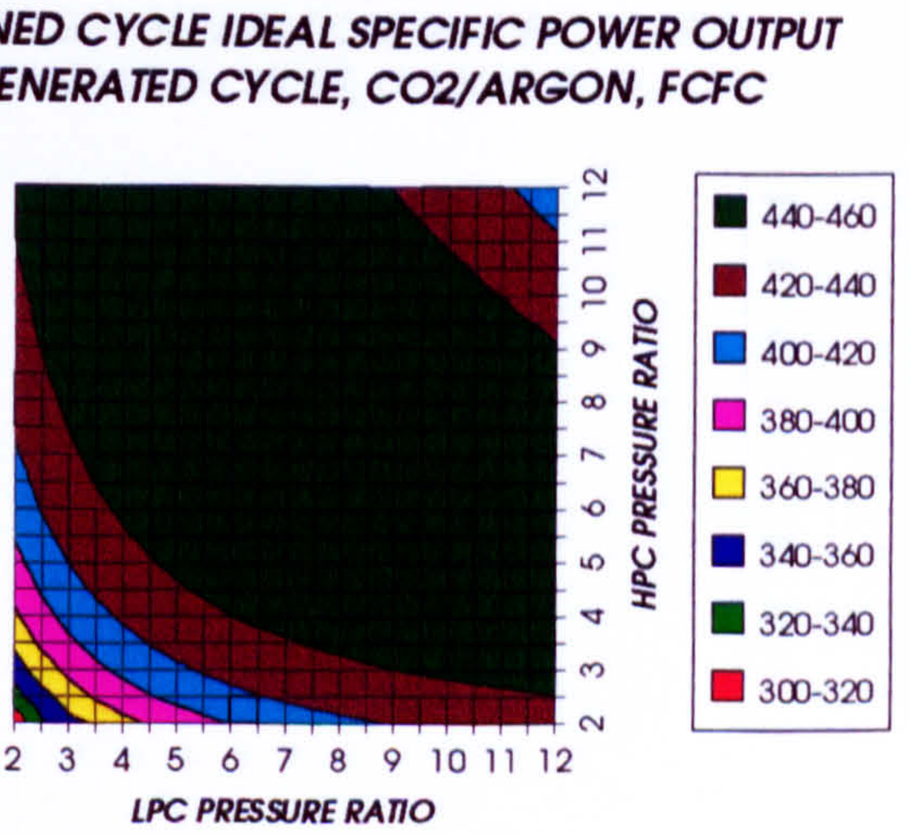

Figure54. Combined cycle ideal specific power output

COMPLETE PLANT (TET=1650 K)

GAS TURBINE SPECIFIC POWER OUTPUT REGENERATED CYCLE, CO2/ARGON, FCFC

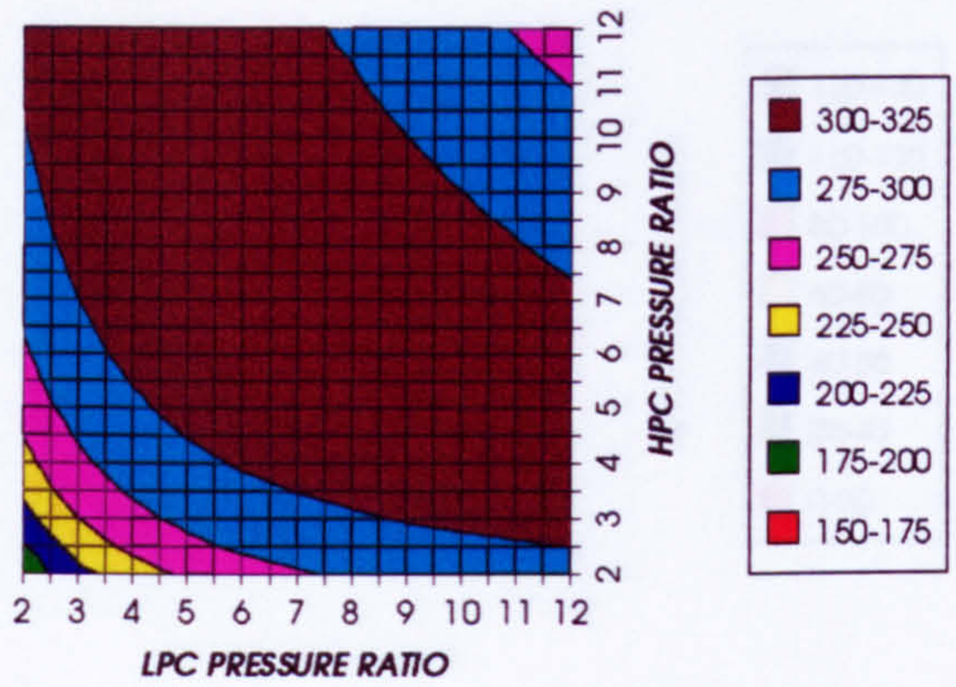

Figure 55. Gas turbine specific power output

STEAM TURBINE SPECIFIC POWER OUTPUT REGENERATED CYCLE, CO2/ARGON, FCFC

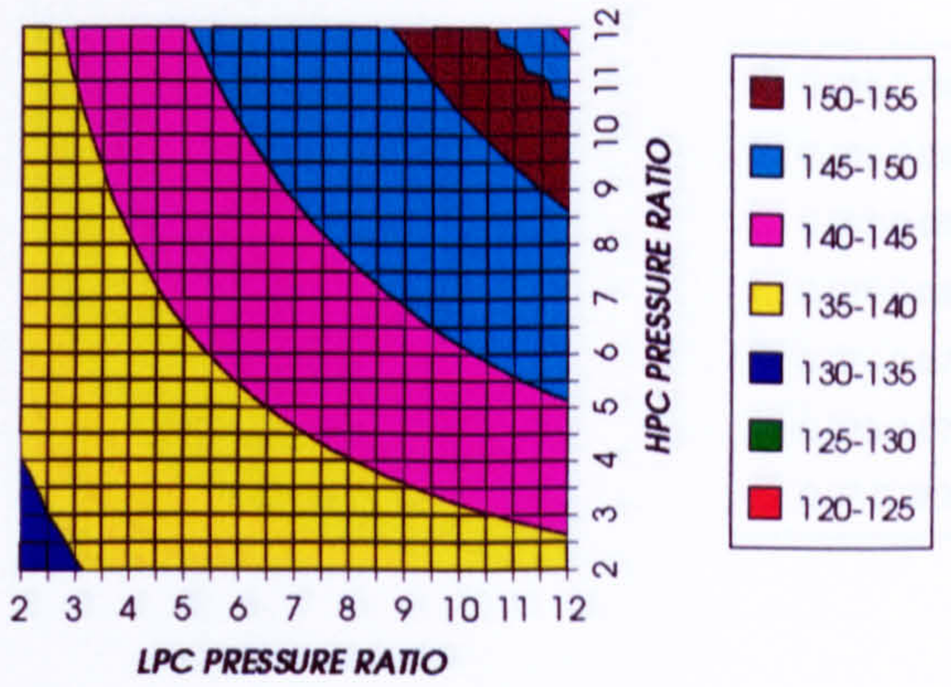

Figure 56. Steam turbine specific power output

GAS TURBINE TO STEAM TURBINE POWER RATIO REGENERATED CYCLE, CO2/ARGON, FCFC

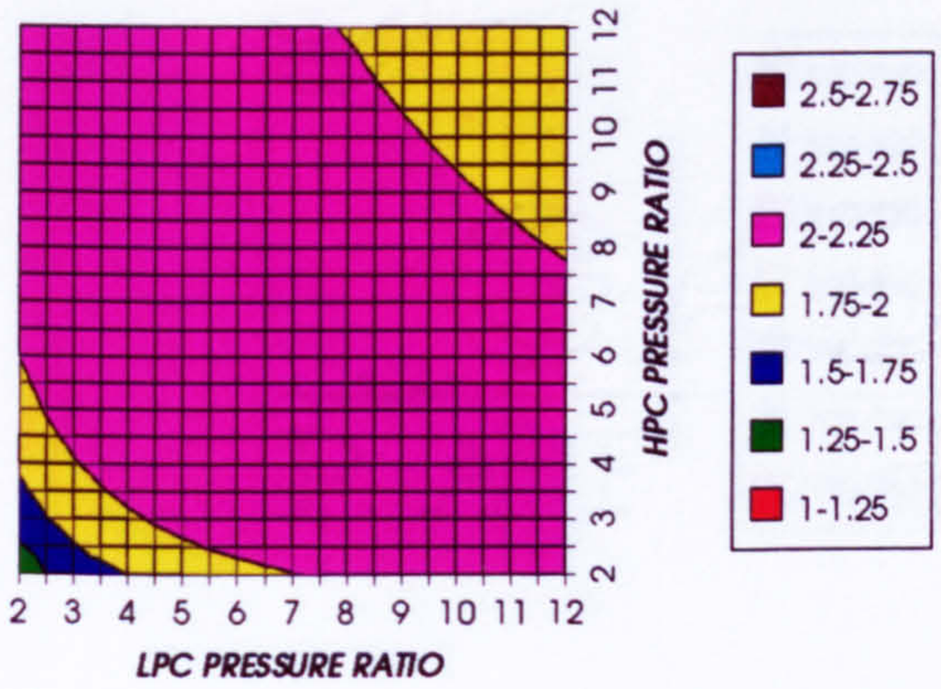

Figure 57. Gas turbine to steam turbine power ratio

AUXILIARIES TO USEFUL POWER RATIO REGENERATED CYCLE, CO2/ARGON, FCFC

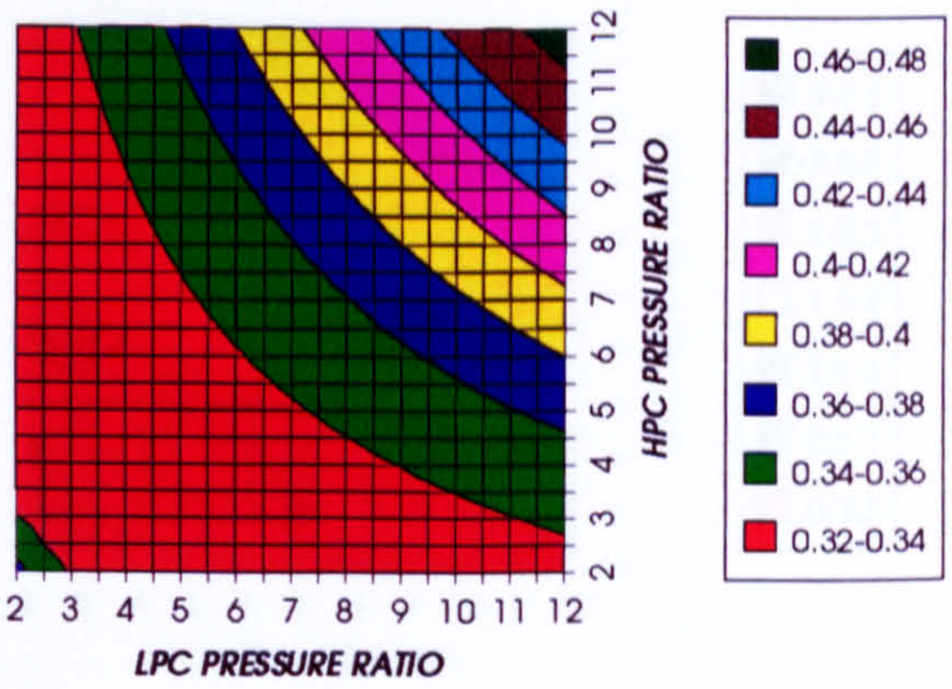

Figure 58. Auxiliary (CO2/Argon, O2 & Fuel) to usefuel power ratio

CO2 COMPRESSION AUXILIARY SPECIFIC POWER REGENERATED CYCLE, CO2/ARGON, FCFC

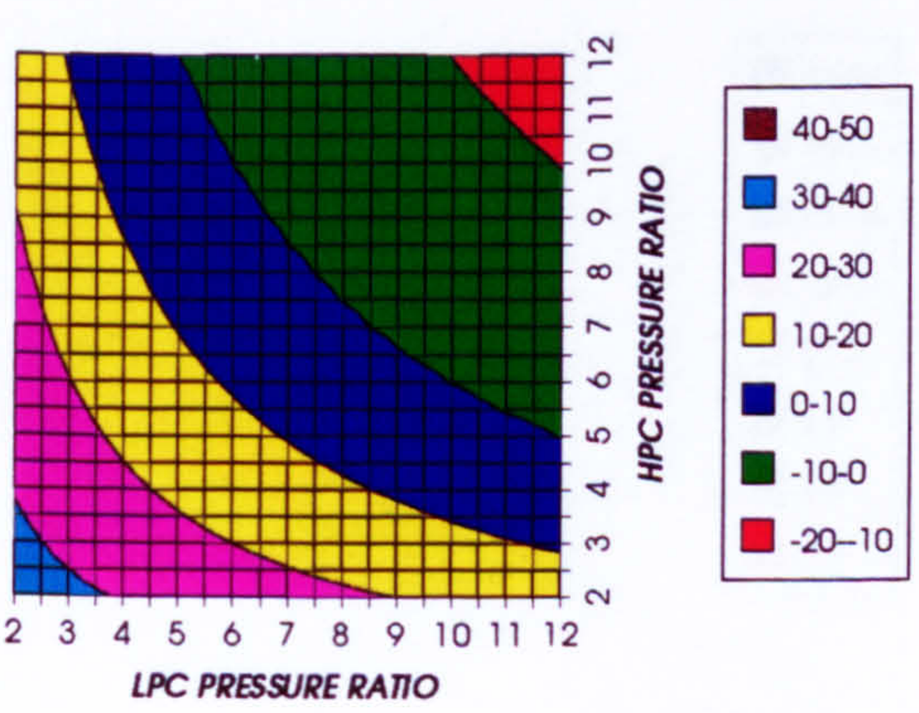

Figure 59. CO2/Argon compression specific power

OXYGEN SEPARATION SPECIFIC POWER REGENERATED CYCLE, CO2/ARGON, FCFC

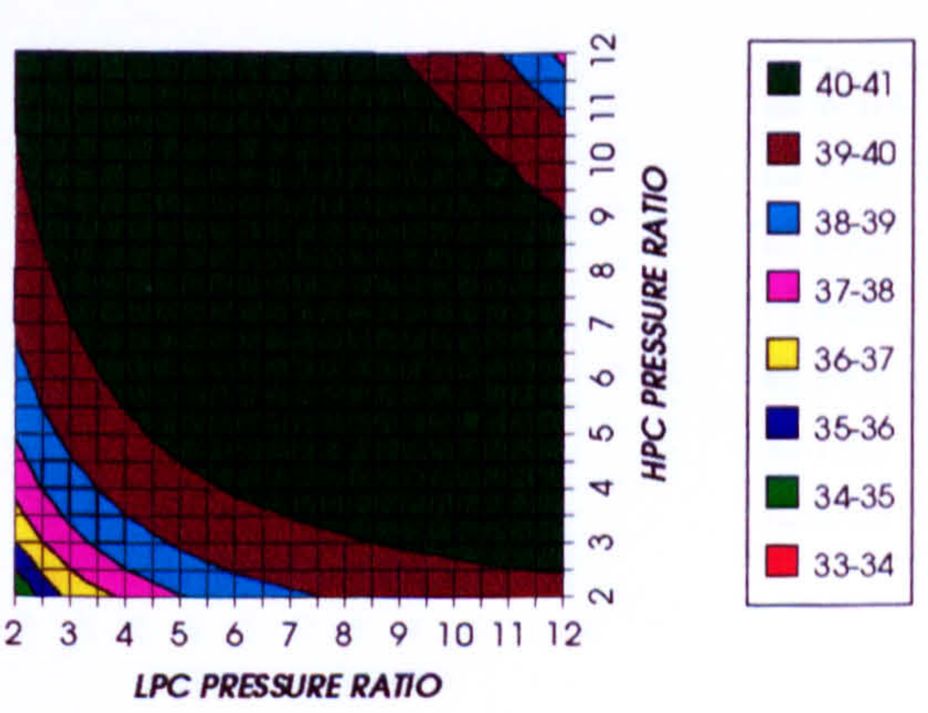

Figure 60. Oxygen separation specific power

COMPLETE PLANT (TET=1650 K)

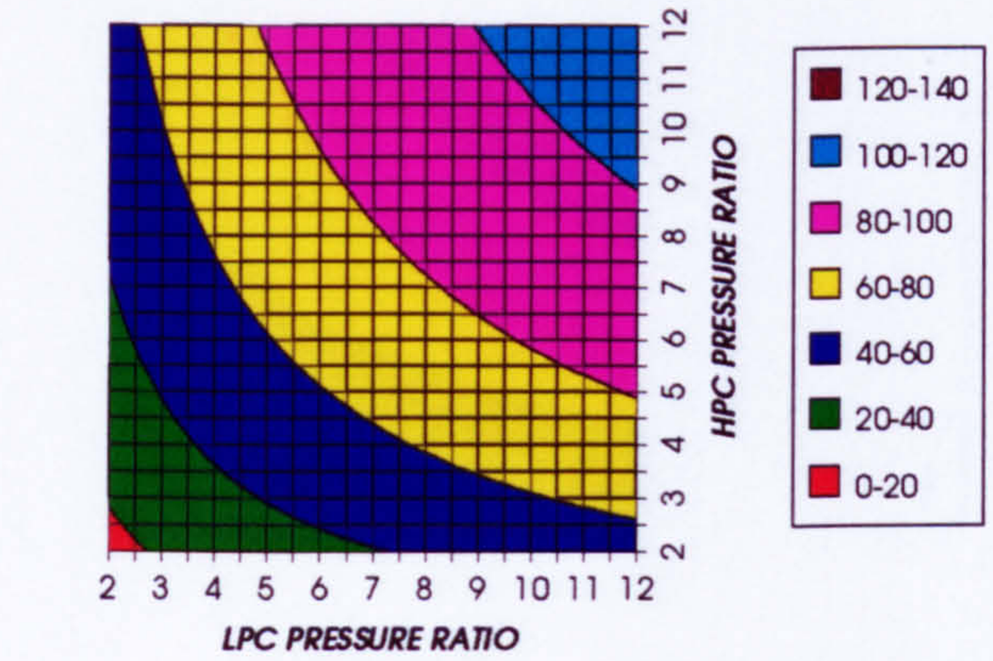

Figure 61. Fuel compression specific power

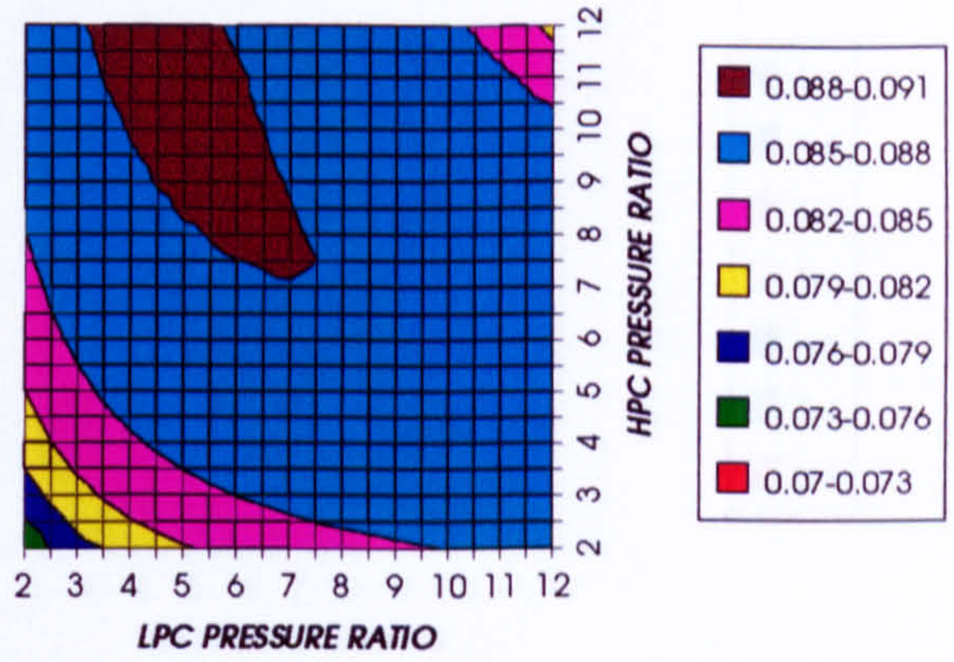

Figure 62 Fuel to compressor inlet mass flow ratio

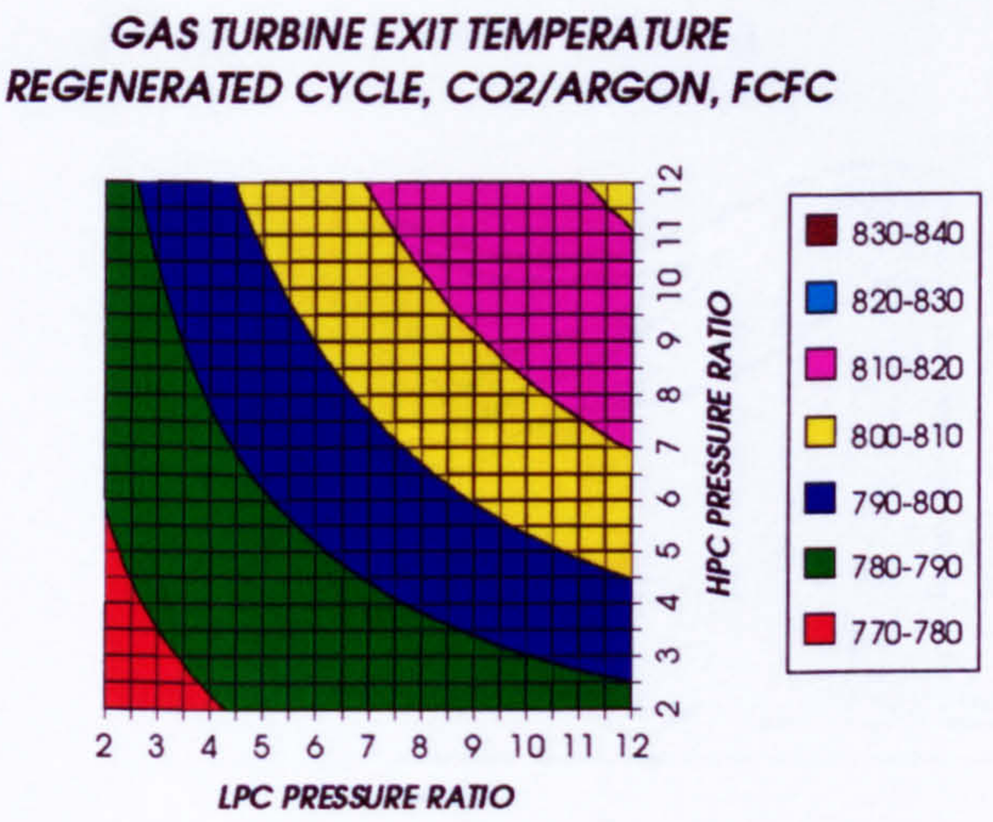

Figure 63. Gas turbine exit temperature

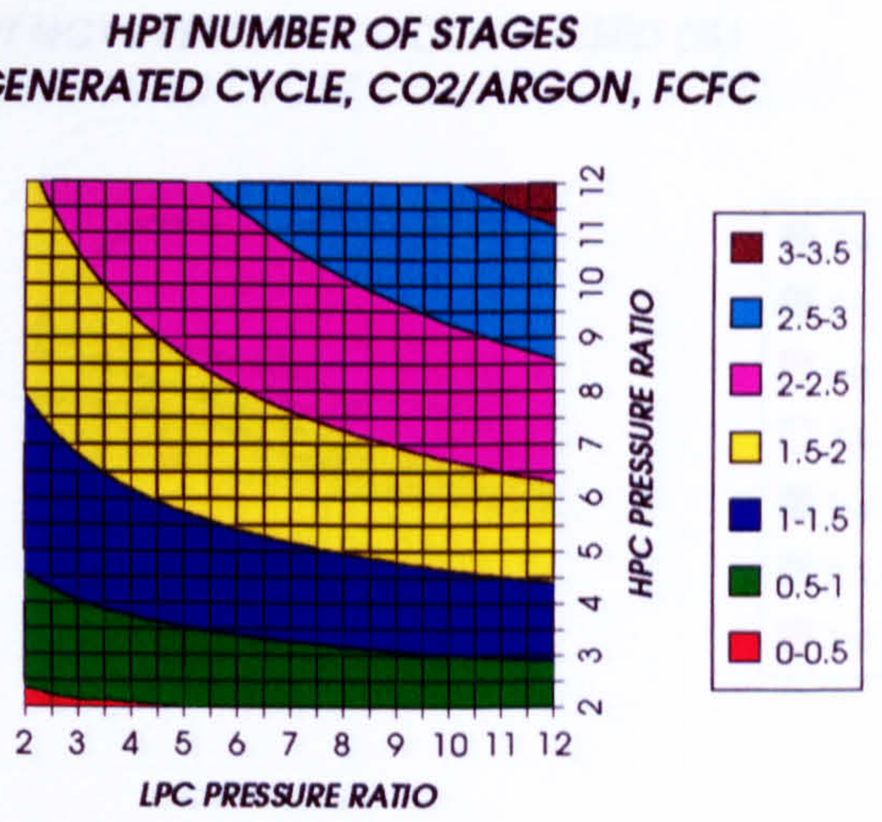

Figure 64. Number of HPT stages

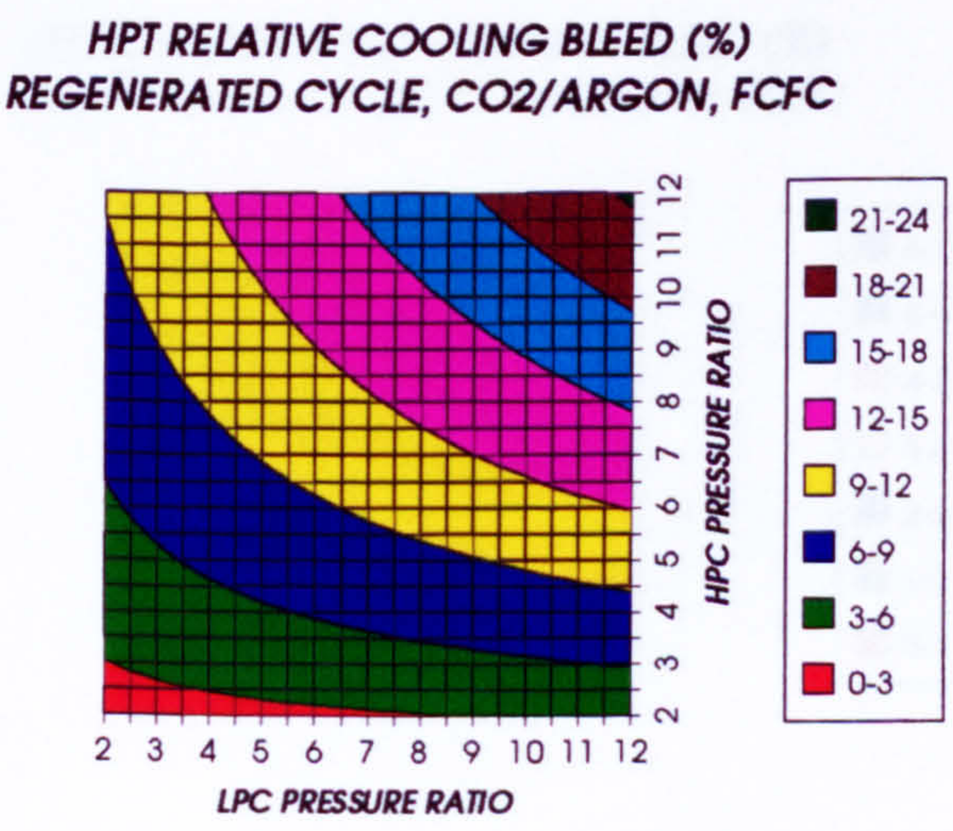

Figure 65. HPT cooling to compressor inlet mass flow ratio

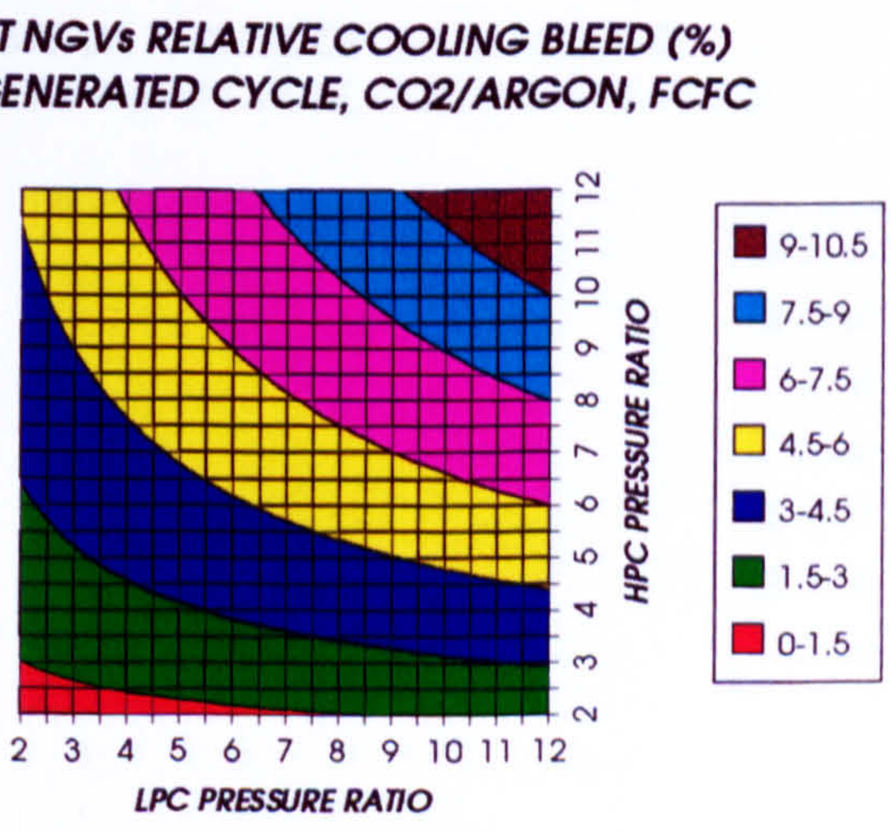

Figure 66. HPT NGVs cooling to compressor inlet mass flow ratio

COMPLETE PLANT (TET=1650 K)

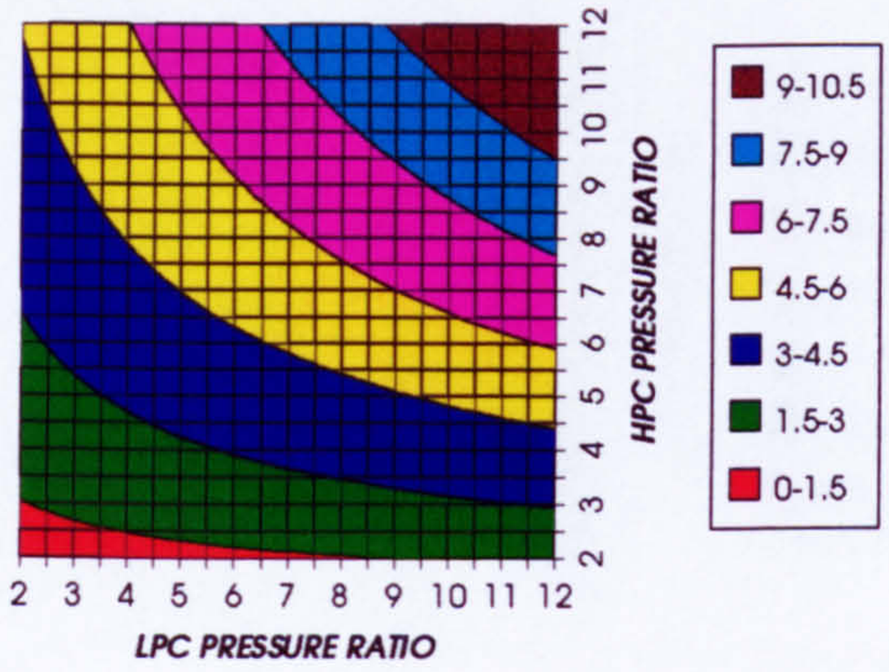

Figure 67. HPT rotor cooling to compressor inlet mass flow ratio

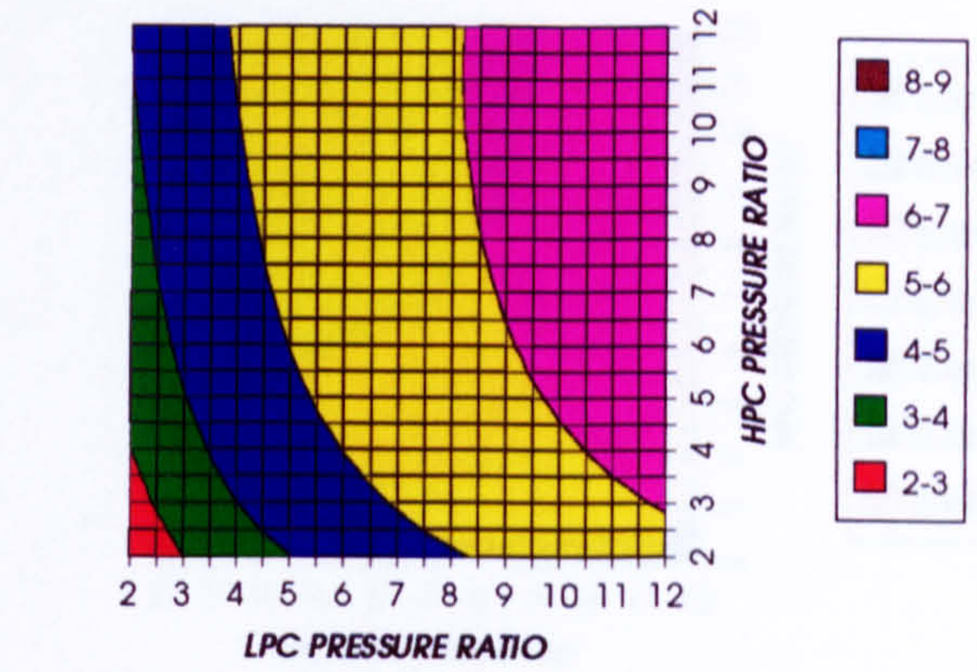

Figure 68. Number of LPT stages

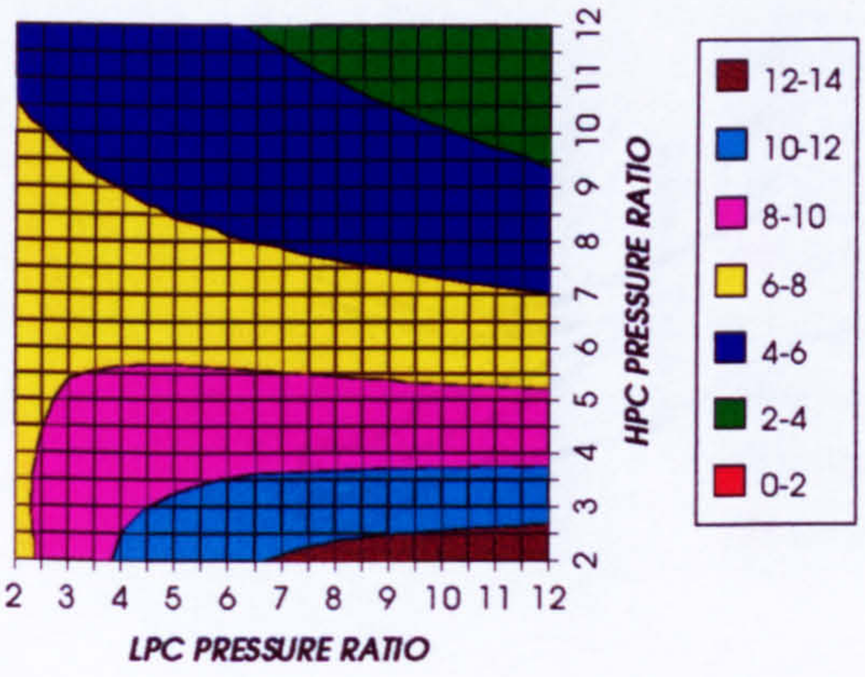

Figure 69. LPT cooling to compressor inlet mass flow ratio

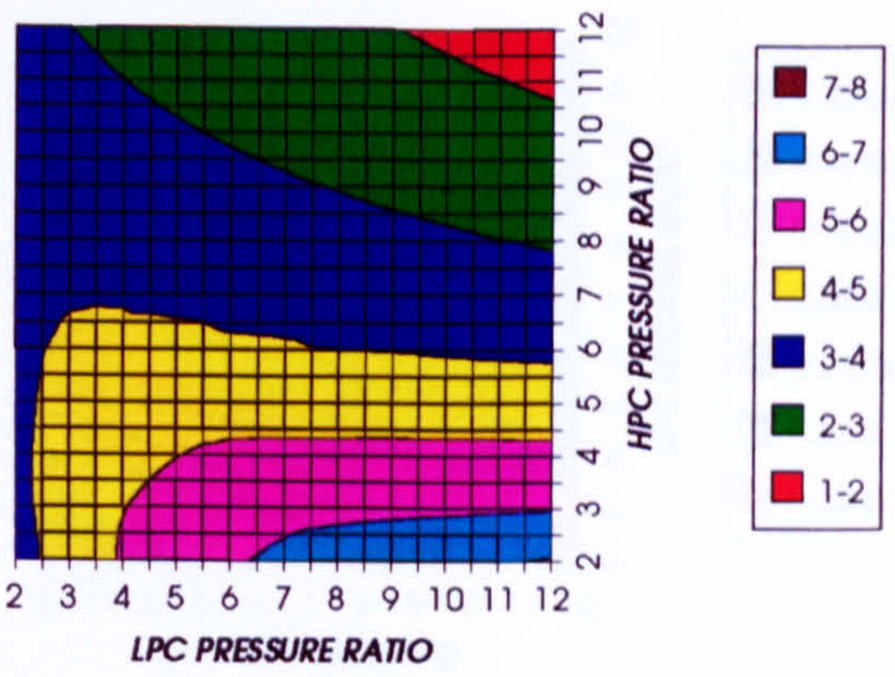

Figure 70. LPT NGVs cooling to compressor inlet mass flow ratio

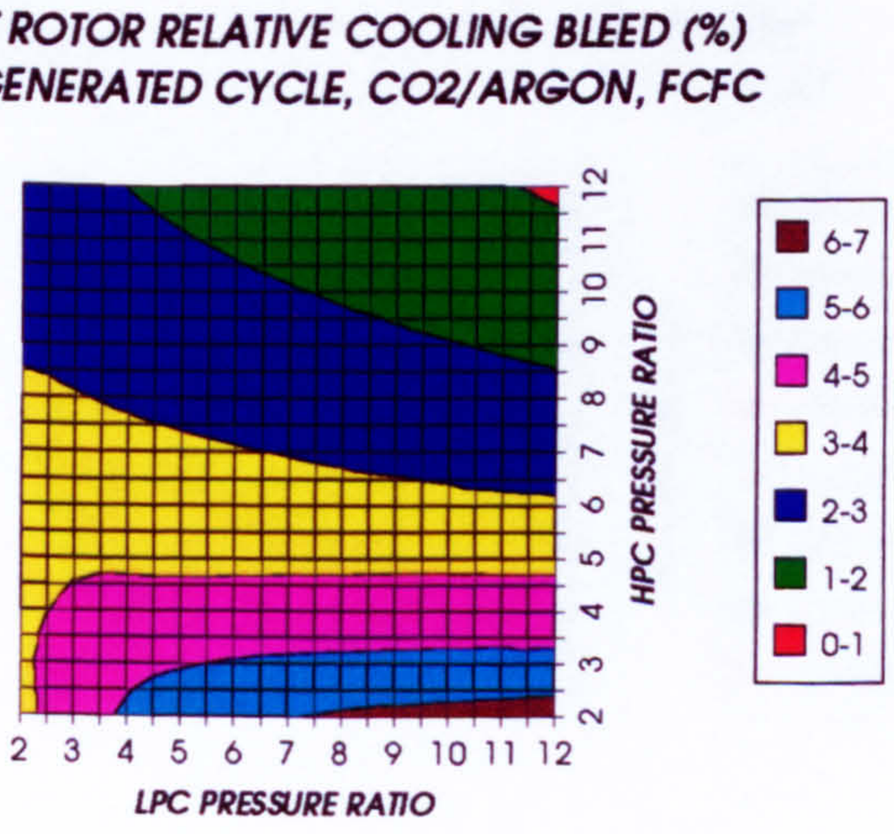

Figure 71. LPT rotor cooling to compressor inlet mass flow ratio

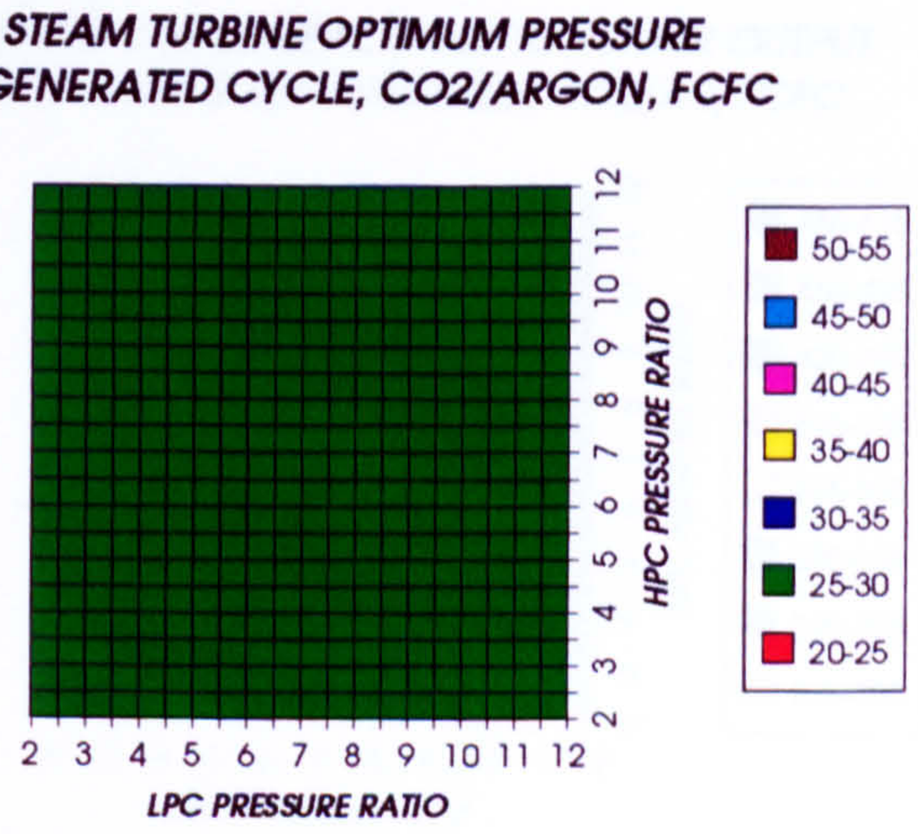

Figure 72. Steam turbine optimum pressures (maximum)

COMPLETE PLANT (TET=1650 K)

COMBINED CYCLE THERMAL EFFICIENCY INTERCOOLED & REGENERATED, CO2/AR, FCFC

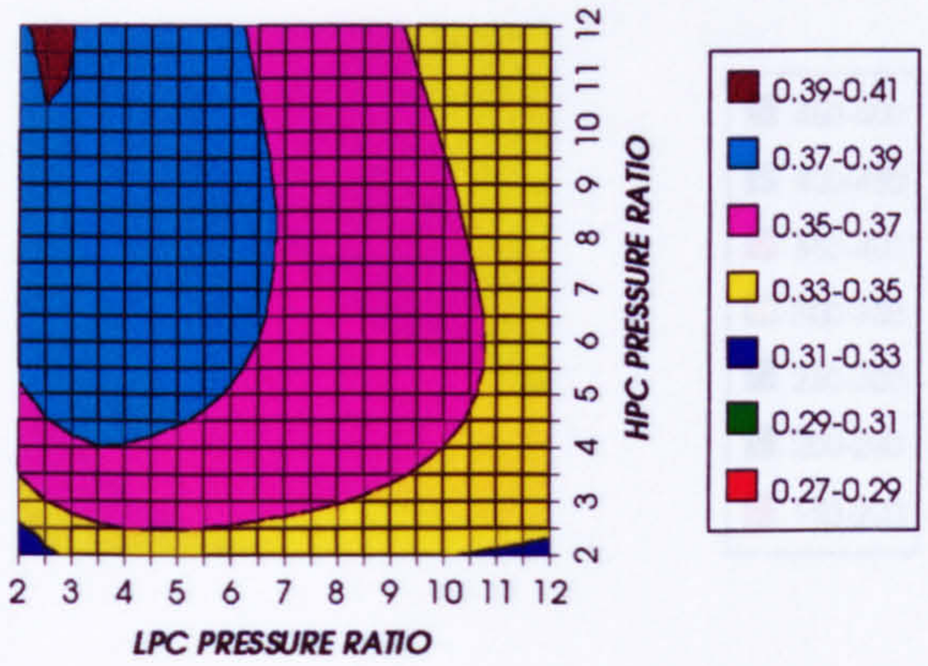

Figure 73. Combined cycle thermal efficiency

COMBINED CYCLE IDEAL THERMAL EFFICIENCY INTERCOOLED & REGENERATED, CO2/AR, FCFC

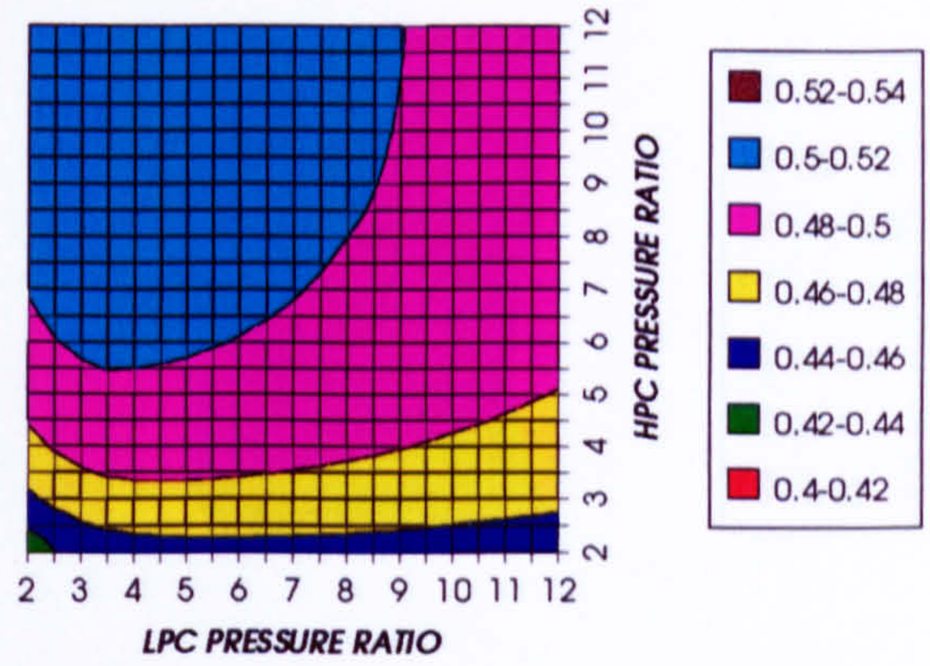

Figure 74. Combined cycle ideal thermal efficiency

SIMPLE CYCLE THERMAL EFFICIENCY INTERCOOLED & REGENERATED, CO2/AR, FCFC

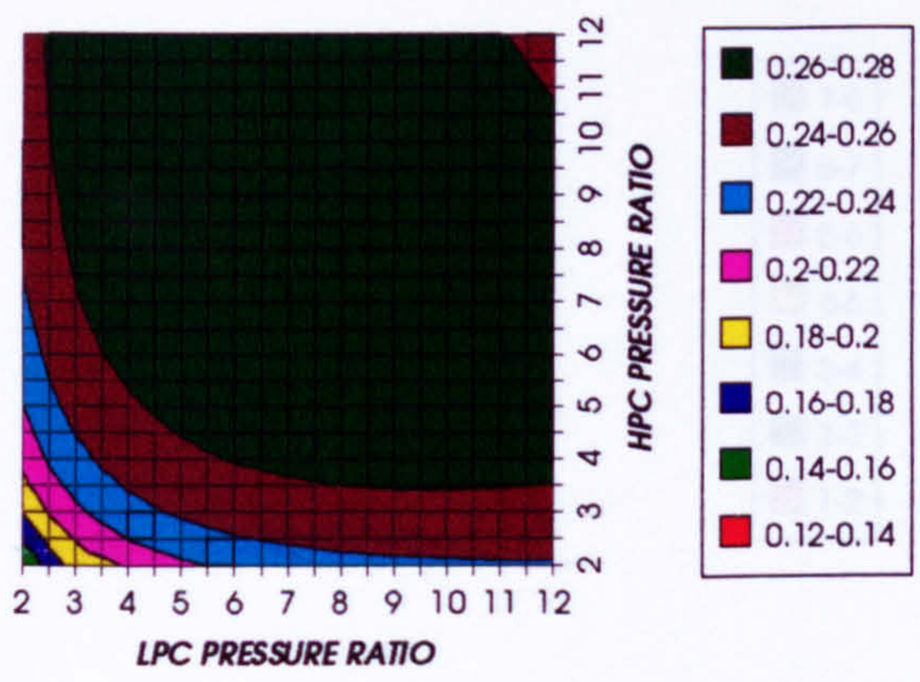

Figure 75. Simple cycle thermal efficiency

SIMPLE CYCLE IDEAL THERMAL EFFICIENCY INTERCOOLED & REGENERATED, CO2/AR, FCFC

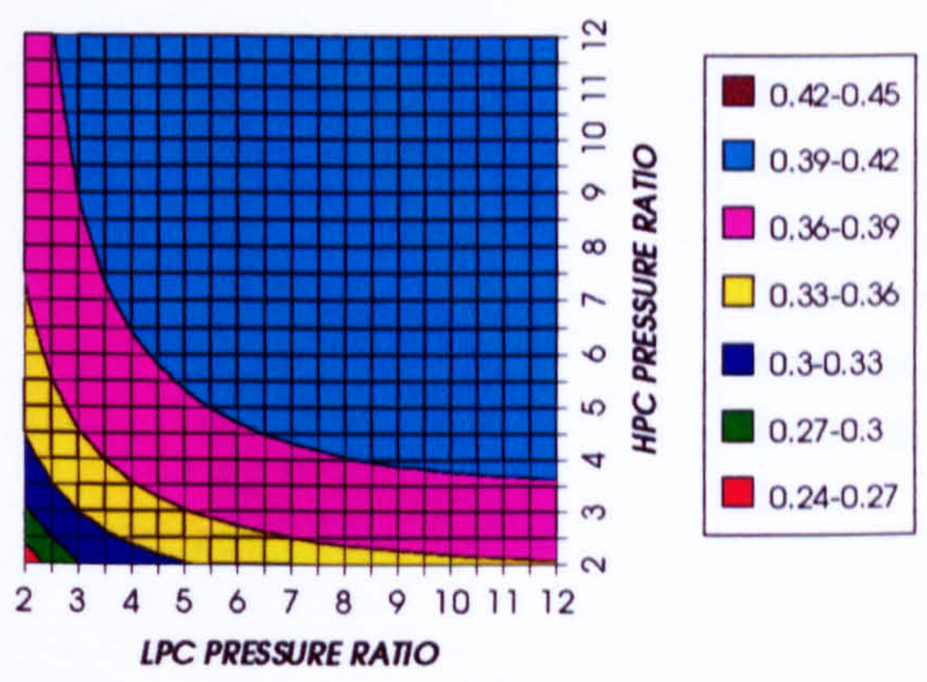

Figure 76. Simple cycle ideal thermal efficiency

COMBINED CYCLE SPECIFIC POWER OUTPUT INTERCOOLED & REGENERATED, CO2/AR, FCFC

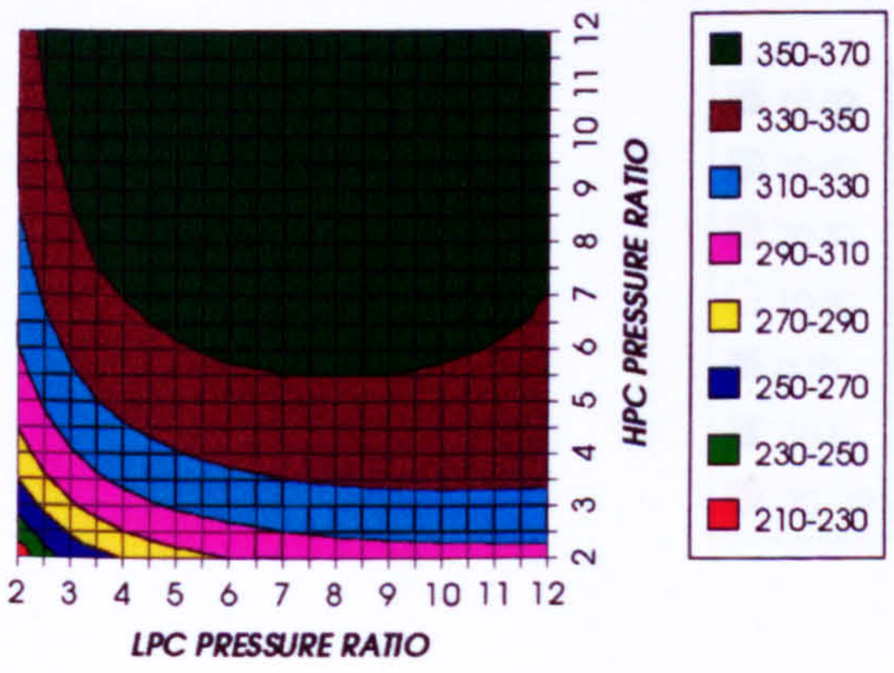

Figure 77. Combined cycle specific power output

COMBINED CYCLE IDEAL SPECIFIC POWER OUTPUT INTERCOOLED & REGENERATED, CO2/AR, FCFC

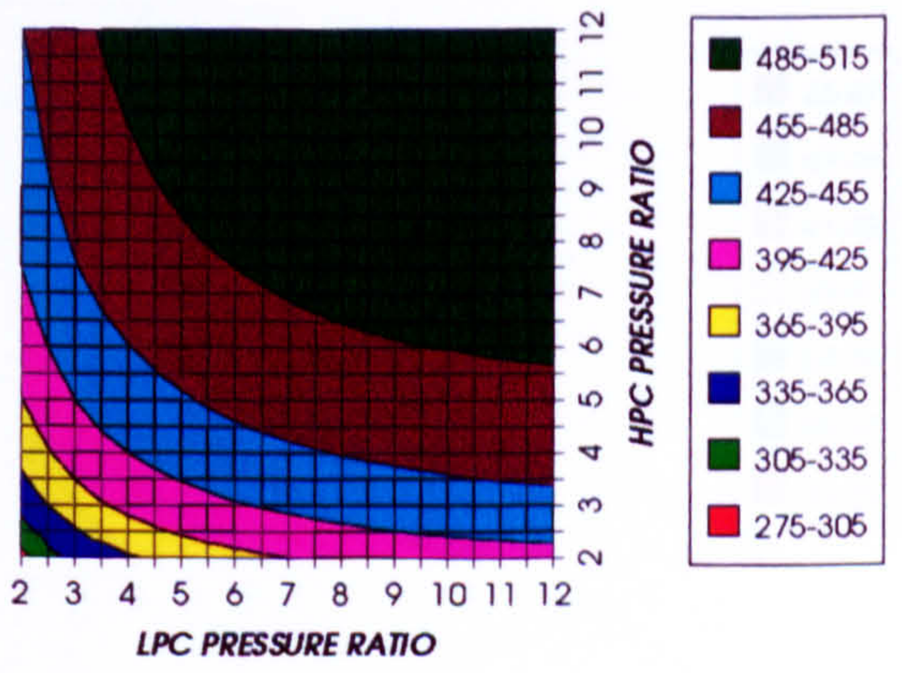

Figure78. Combined cycle ideal specific power output

COMPLETE PLANT (TET=1650 K)

GAS TURBINE SPECIFIC POWER OUTPUT
INTERCOOLED & REGENERATED, CO2/AR, FCFC

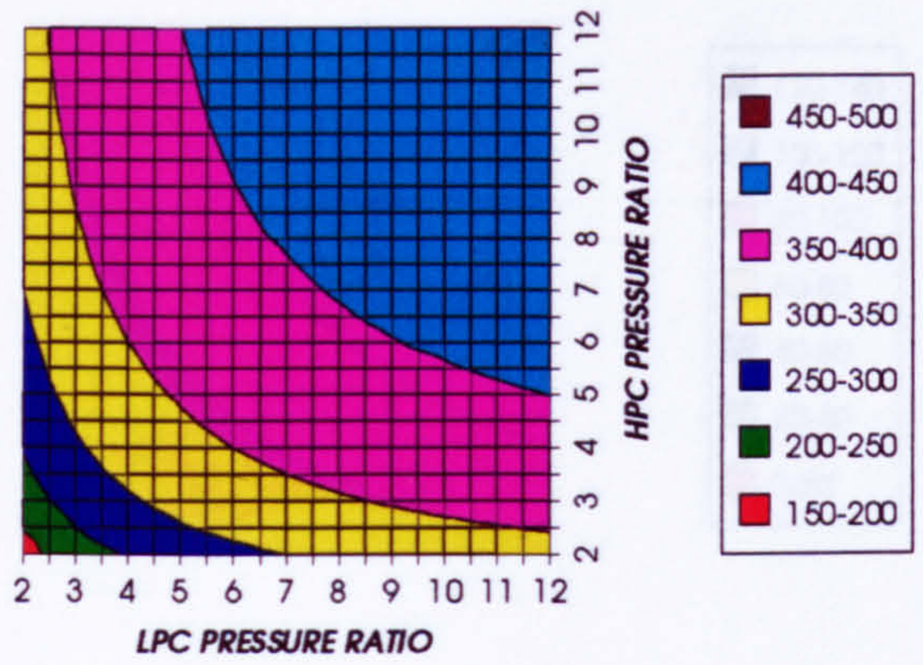

Figure 79. Gas turbine specific power output

STEAM TURBINE SPECIFIC POWER OUTPUT
INTERCOOLED & REGENERATED, CO2/AR, FCFC

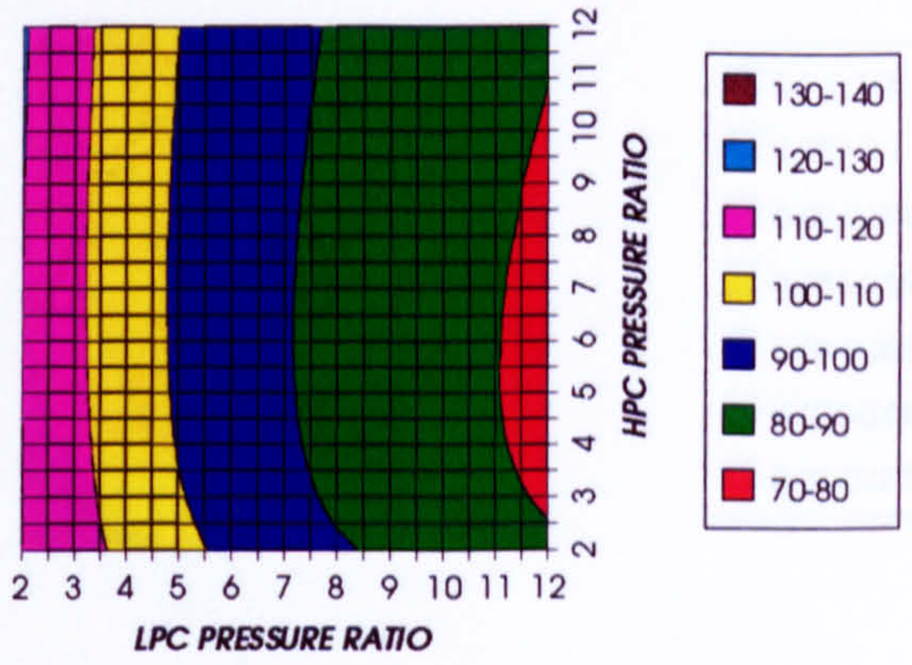

Figure 80. Steam turbine specific power output

GAS TURBINE TO STEAM TURBINE POWER RATIO
INTERCOOLED & REGENERATED, CO2/AR, FCFC

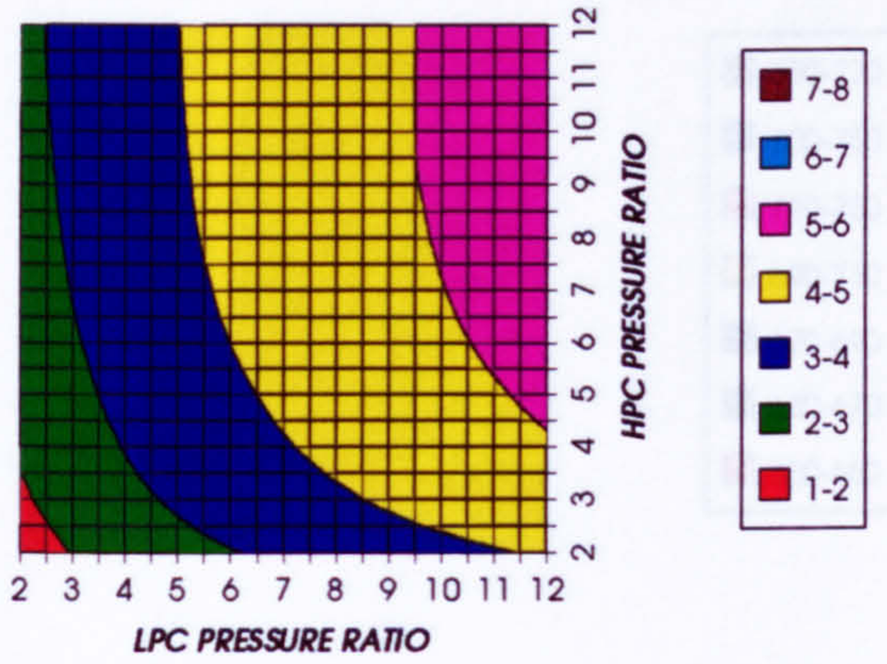

Figure 81. Gas turbine to steam turbine power ratio

AUXILIARIES TO USEFUL POWER RATIO
INTERCOOLED & REGENERATED, CO2/AR, FCFC

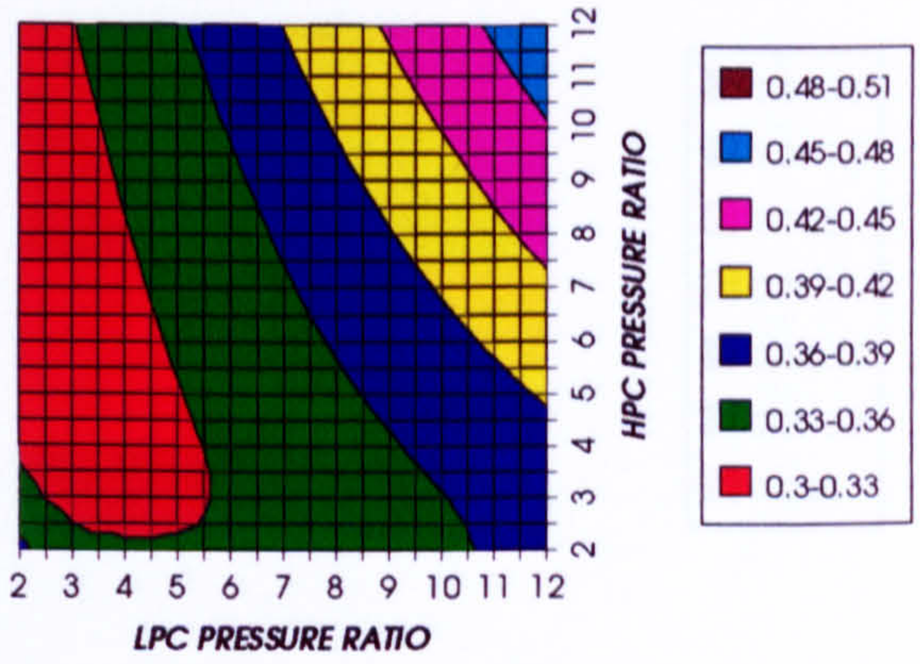

Figure 82. Auxiliary (CO2/Argon, O2 & Fuel) to usefuel power ratio

CO2 COMPRESSION AUXILIARY SPECIFIC POWER
INTERCOOLED & REGENERATED, CO2/AR, FCFC

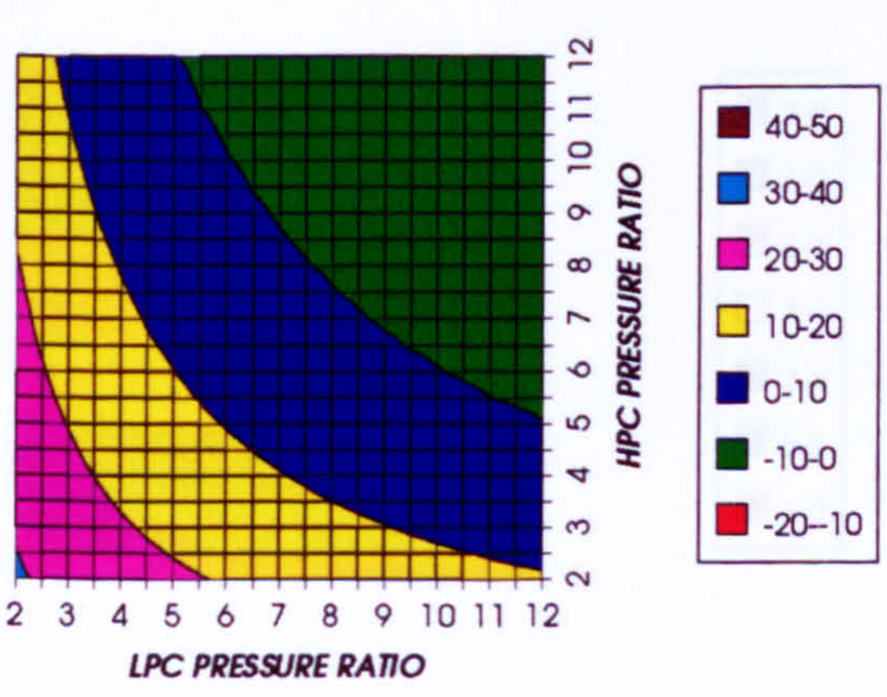

Figure 83. CO2/Argon compression specific power

OXYGEN SEPARATION SPECIFIC POWER
INTERCOOLED & REGENERATED, CO2/AR, FCFC

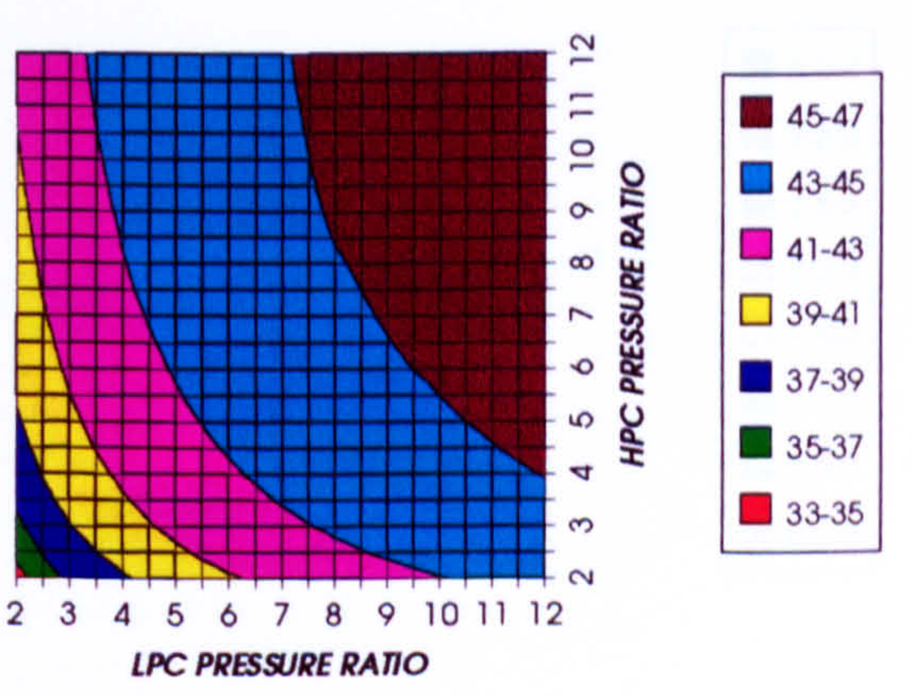

Figure 84. Oxygen separation specific power

FUEL COMPRESSION SPECIFIC POWER
INTERCOOLED & REGENERATED, CO2/AR, FCFC

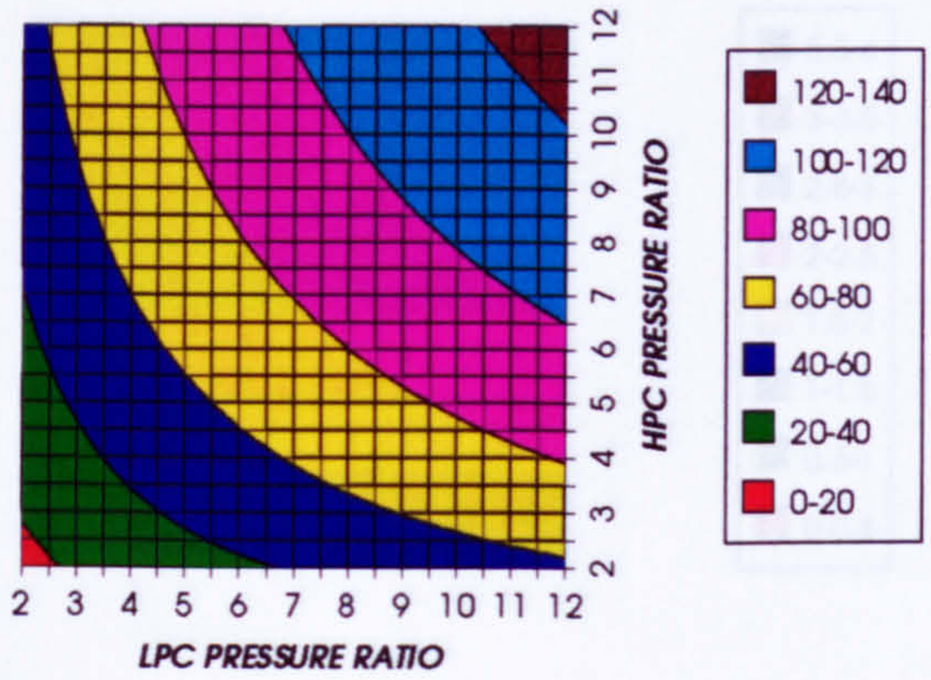

Figure 85. Fuel compression specific power

FUEL TO COMPRESSOR INLET MASS FLOW RATIO
INTERCOOLED & REGENERATED, CO2/AR, FCFC

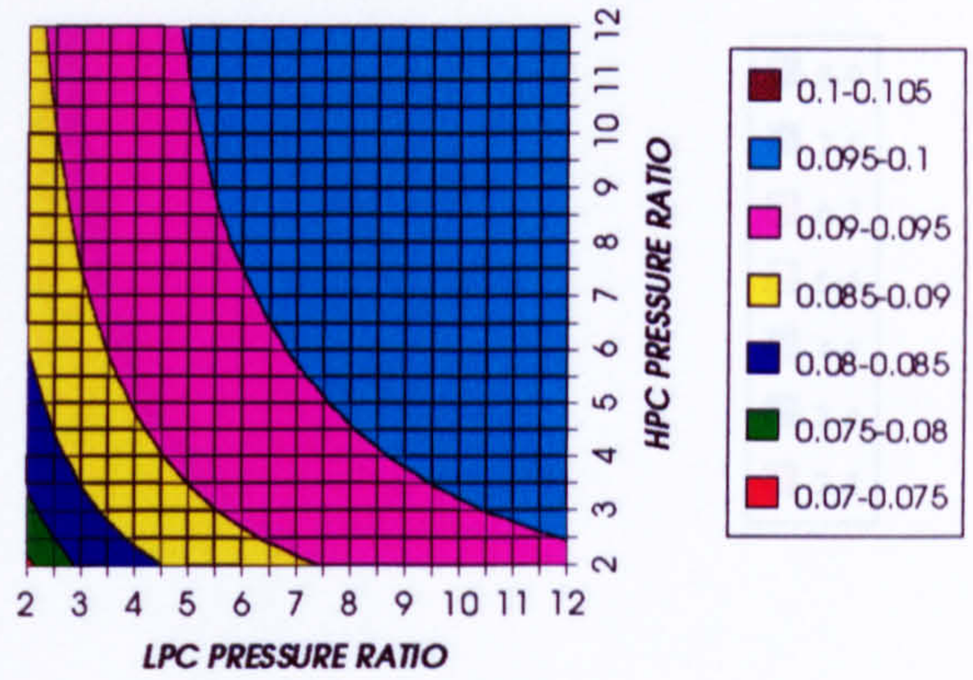

Figure 86. Fuel to compressor inlet mass flow ratio

GAS TURBINE EXIT TEMPERATURE
INTERCOOLED & REGENERATED, CO2/AR, FCFC

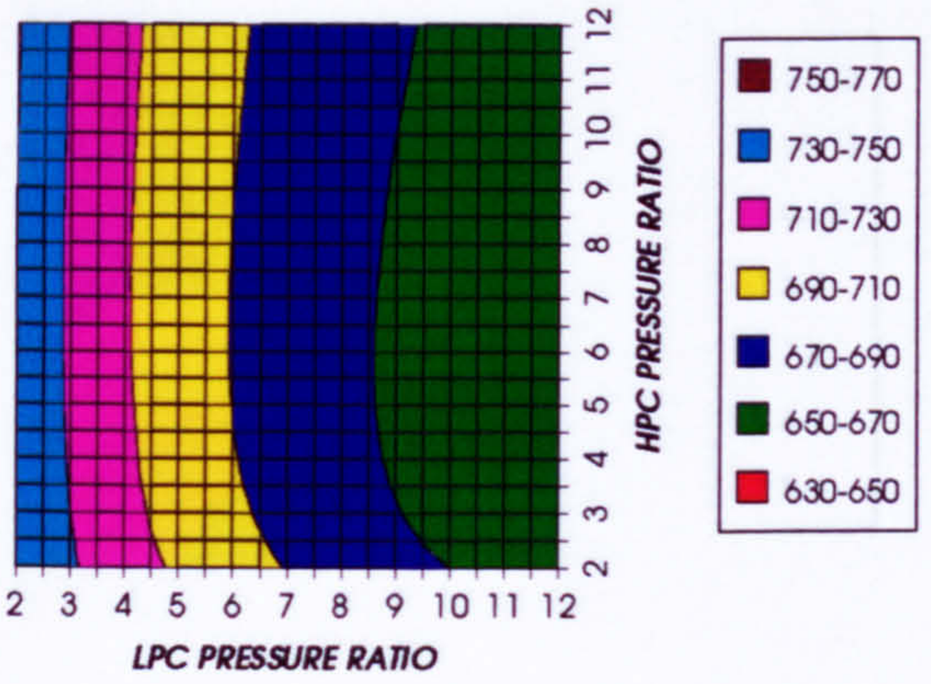

Figure 87. Gas turbine exit temperature

HPT NUMBER OF STAGES
INTERCOOLED & REGENERATED, CO2/AR, FCFC

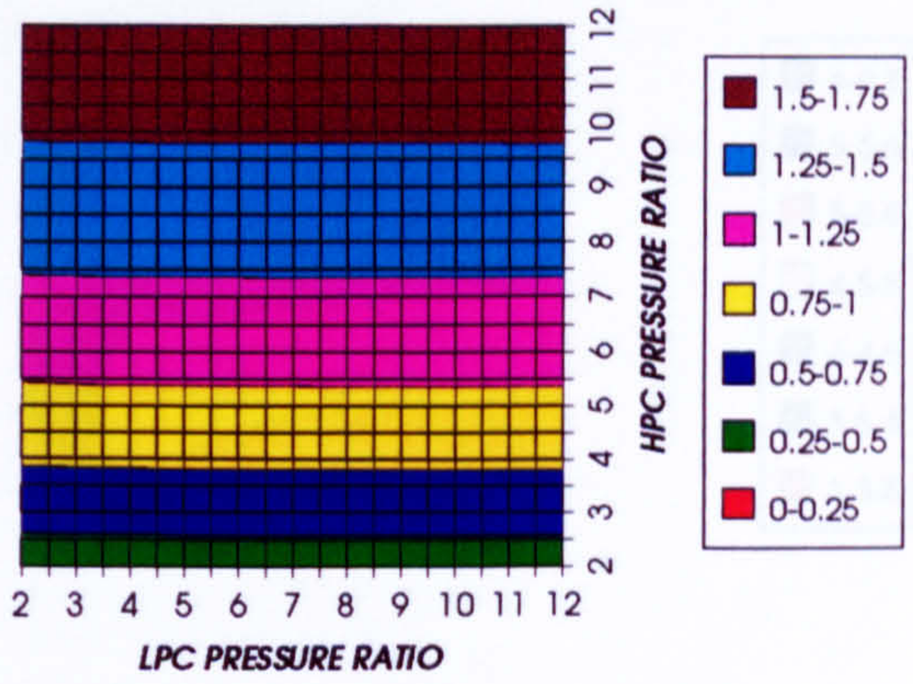

Figure 88. Number of HPT stages

HPT RELATIVE COOLING BLEED (%)
INTERCOOLED & REGENERATED, CO2/AR, FCFC

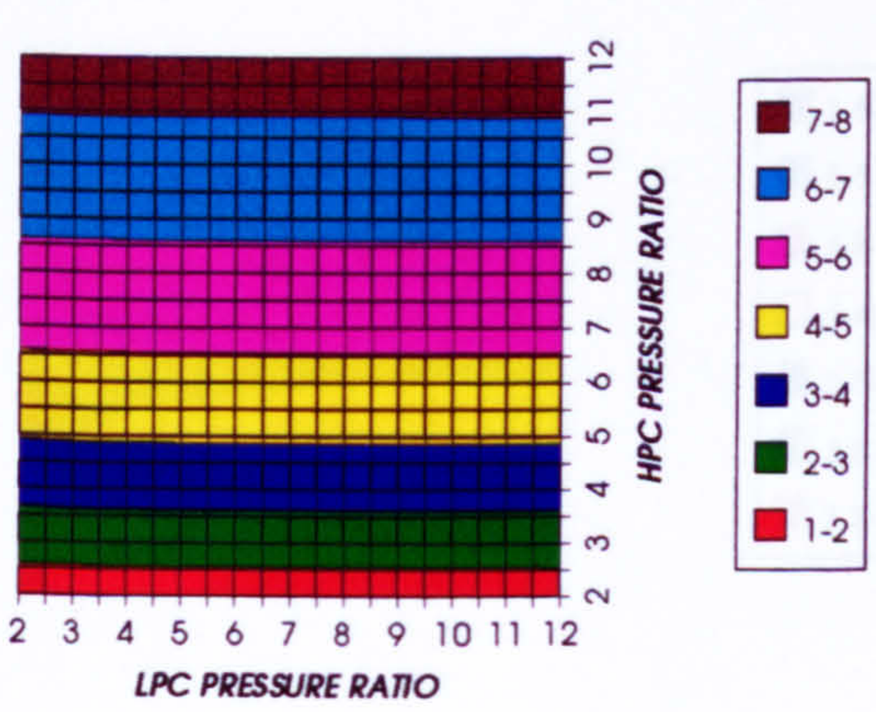

Figure 89. HPT cooling to compressor inlet mass flow ratio

HPT NGVs RELATIVE COOLING BLEED (%)
INTERCOOLED & REGENERATED, CO2/AR, FCFC

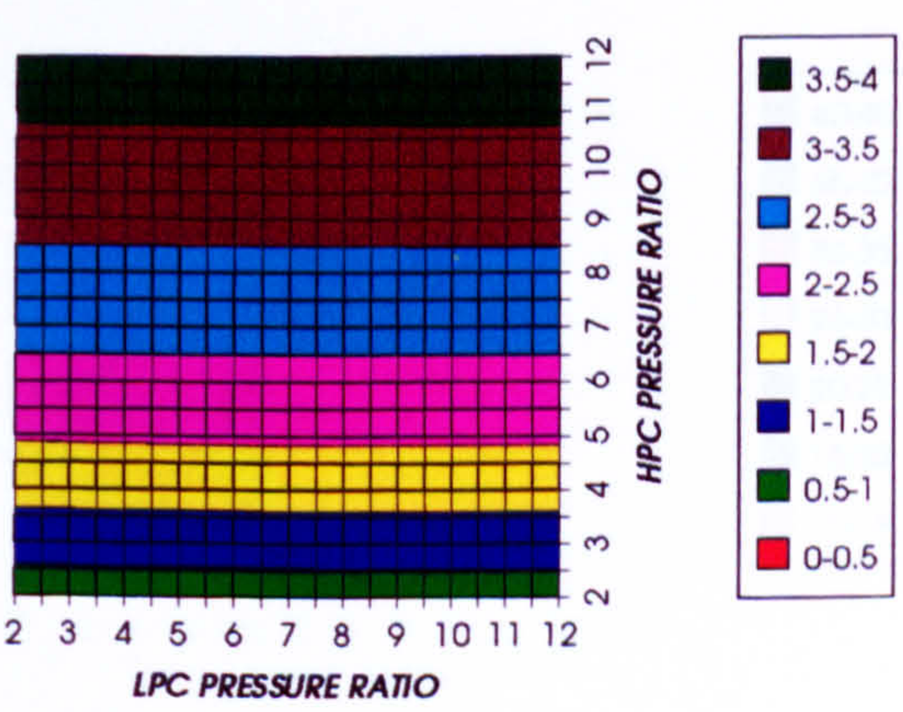

Figure 90. HPT NGVs cooling to compressor inlet mass flow ratio

HPT ROTOR RELATIVE COOLING BLEED (%)
INTERCOOLED & REGENERATED, CO2/AR, FCFC

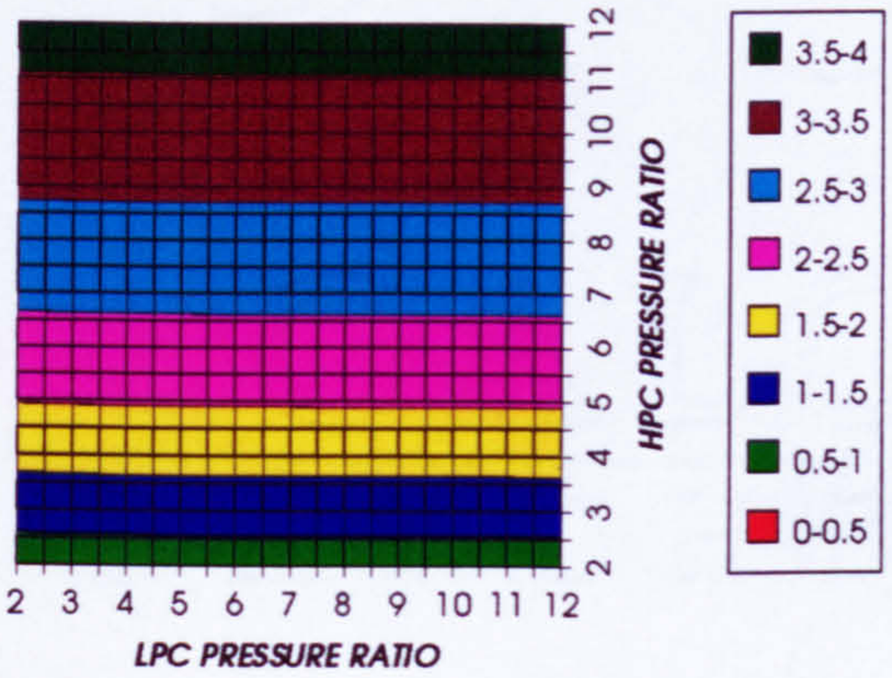

Figure 91. HPT rotor cooling to compressor inlet mass flow ratio

LPT NUMBER OF STAGES
INTERCOOLED & REGENERATED, CO2/AR, FCFC

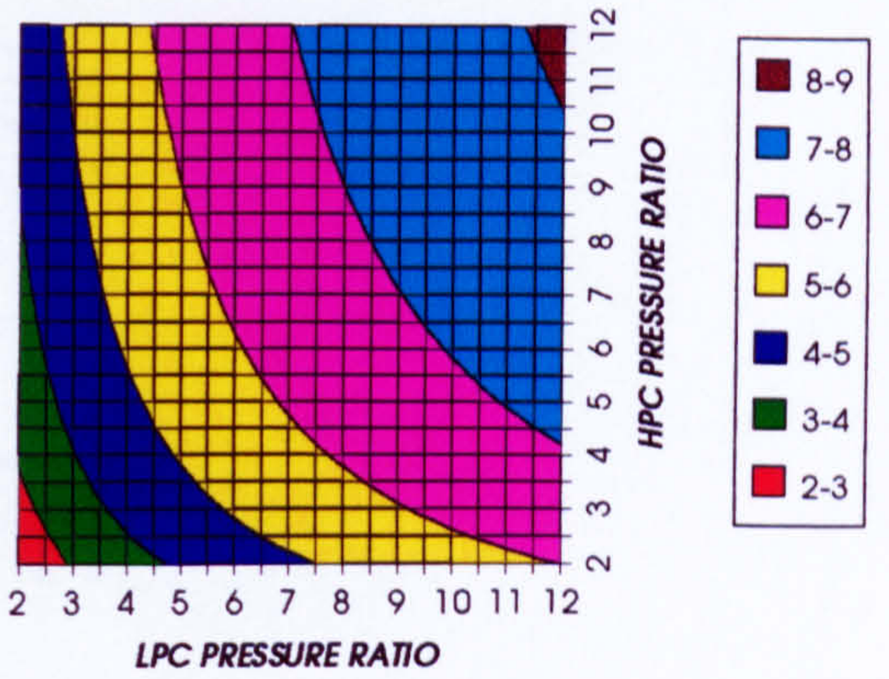

Figure 92. Number of LPT stages

LPT RELATIVE COOLING BLEED (%)
INTERCOOLED & REGENERATED, CO2/AR, FCFC

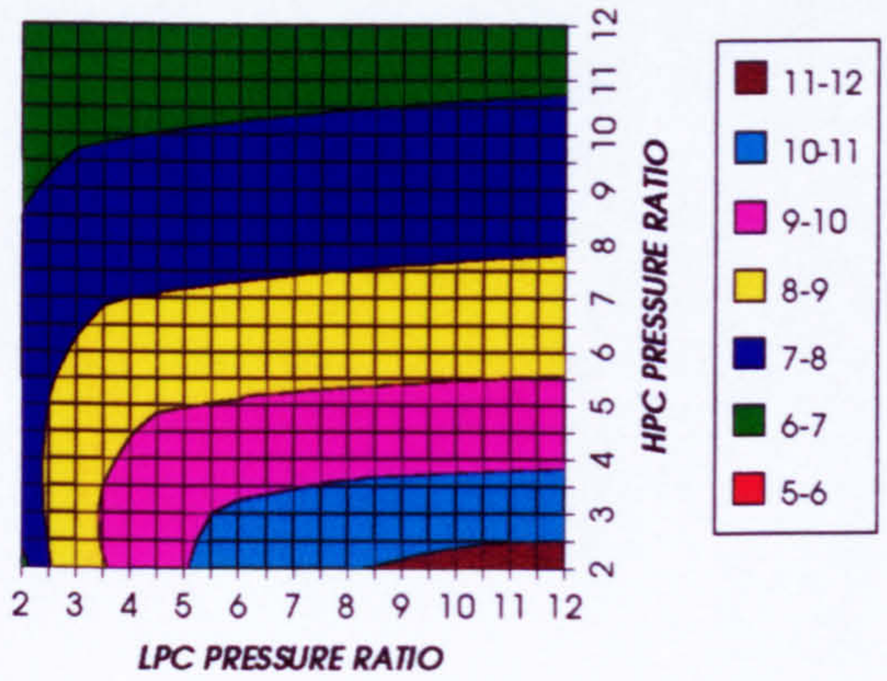

Figure 93. LPT cooling to compressor inlet mass flow ratio

LPT NGVs RELATIVE COOLING BLEED (%)
INTERCOOLED & REGENERATED, CO2/AR, FCFC

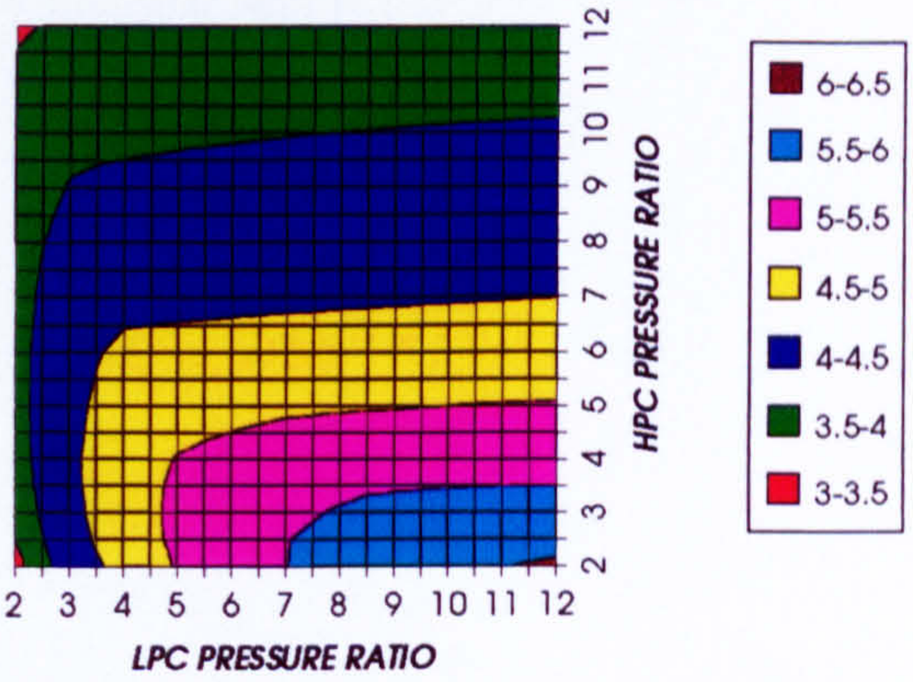

Figure 94. LPT NGVs cooling to compressor inlet mass flow ratio

LPT ROTOR RELATIVE COOLING BLEED (%)
INTERCOOLED & REGENERATED, CO2/AR, FCFC

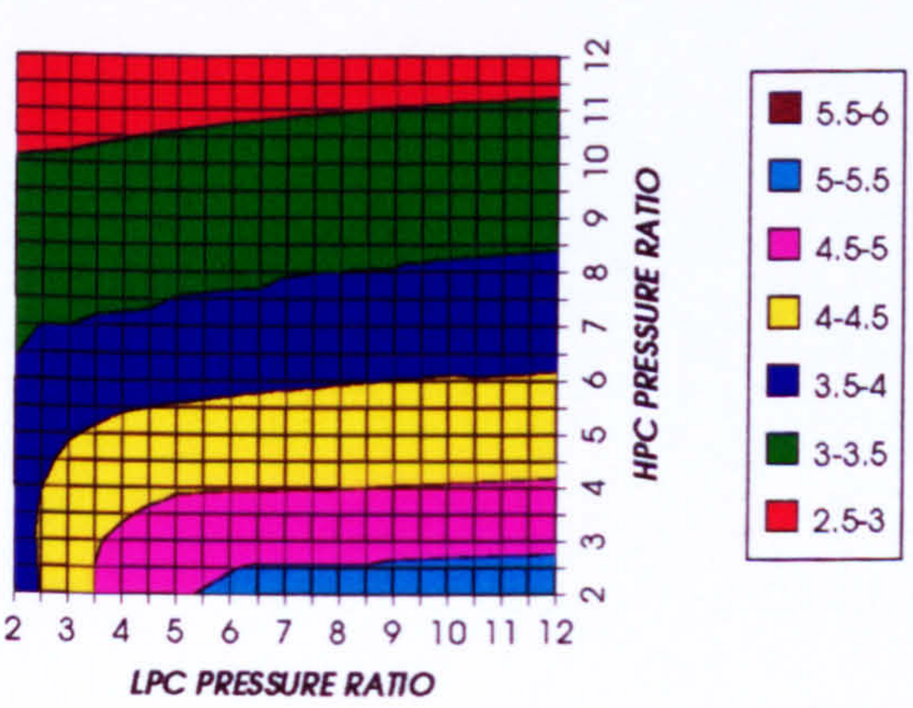

Figure 95. LPT rotor cooling to compressor inlet mass flow ratio

STEAM TURBINE OPTIMUM PRESSURE
INTERCOOLED & REGENERATED, CO2/AR, FCFC

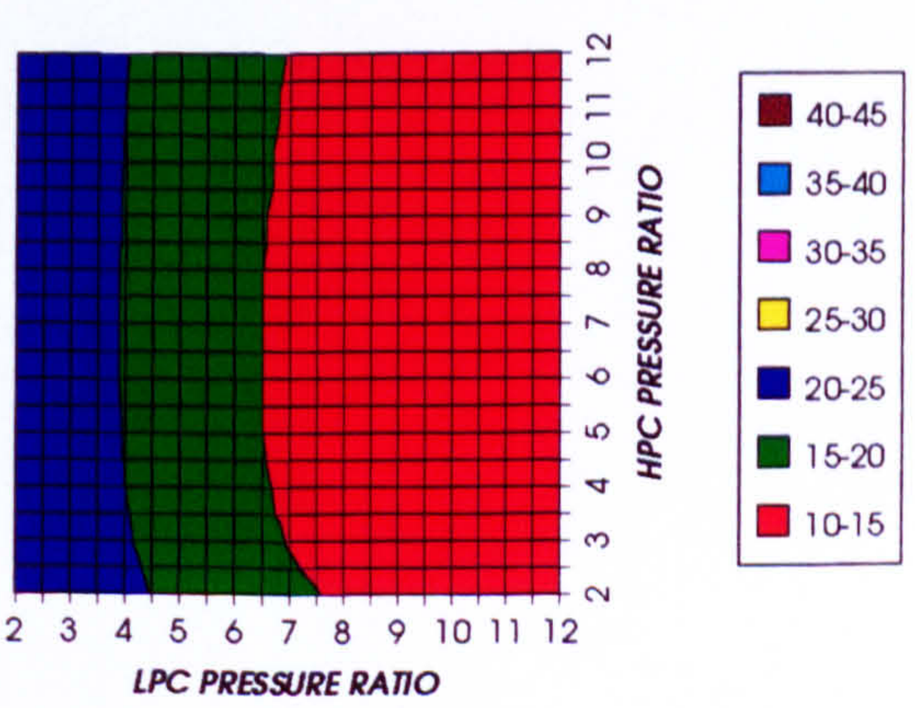

Figure 96. Steam turbine optimum pressures (maximum)

APPENDIX VI

COMPLETE PLANT PERFORMANCE WITH CRYOGENIC PRECOOLING (WORKING FLUID CO_2/ARGON, TET=1650 K)

COMPLETE PLANT WITH CRYOGENIC PRECOOLING (TET=1650 K)

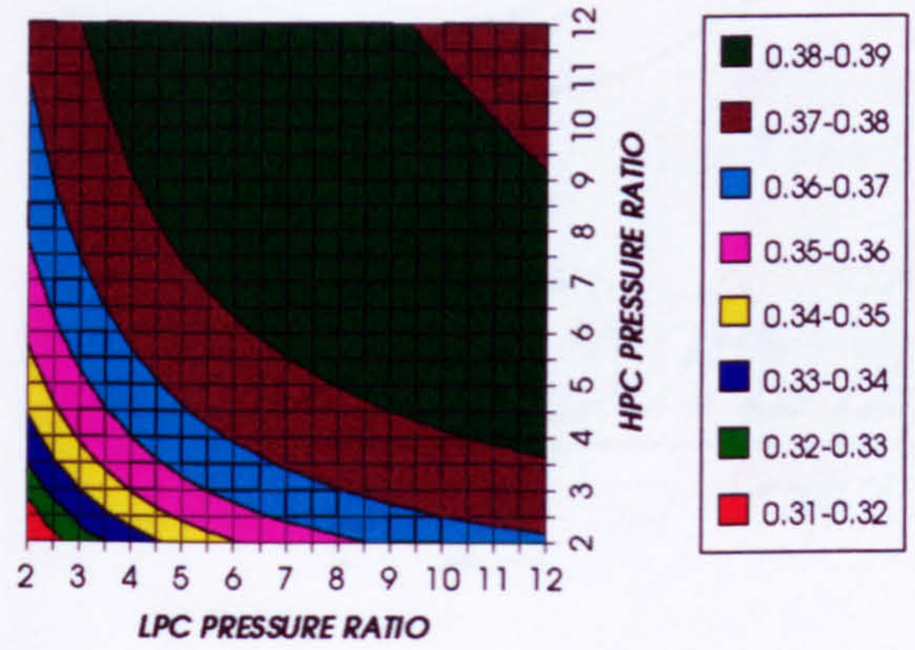

Figure 1. Combined cycle thermal efficiency

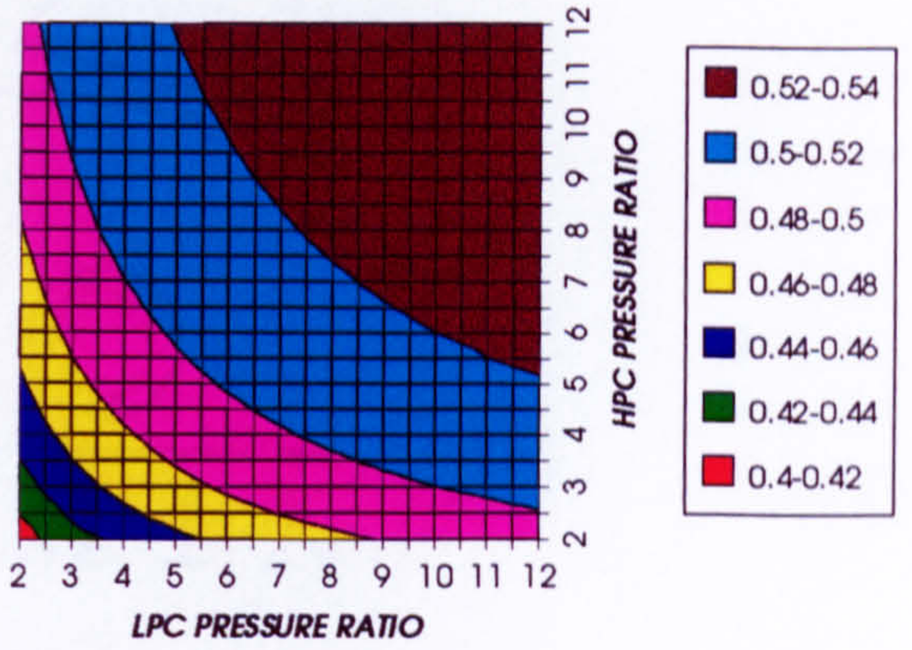

Figure 2. Combined cycle ideal thermal efficiency

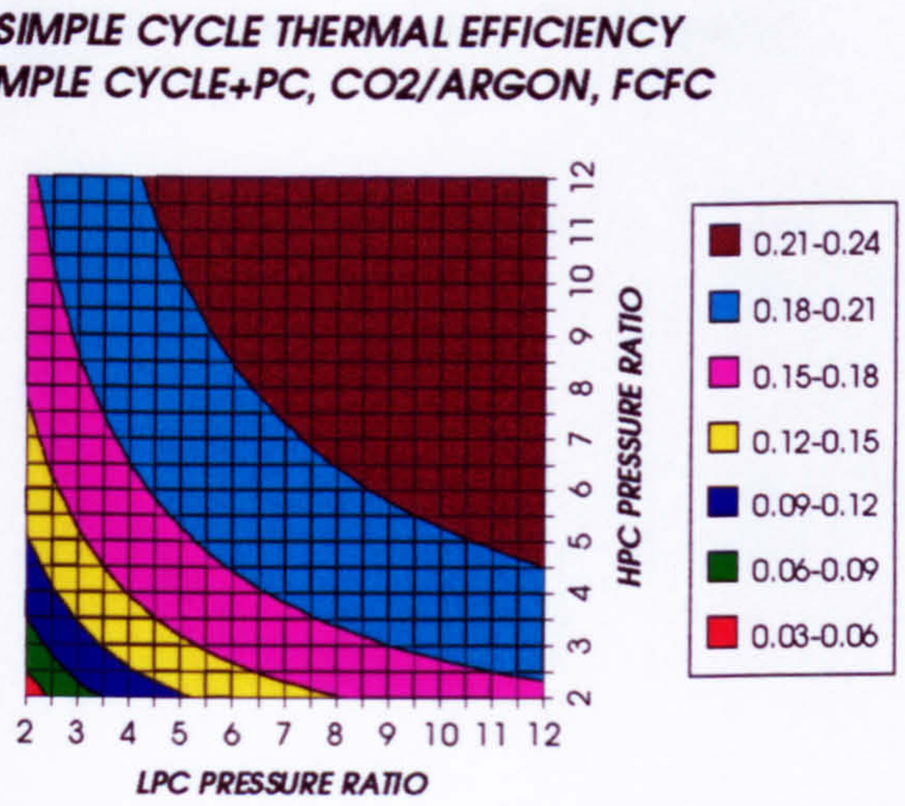

Figure 3. Simple cycle thermal efficiency

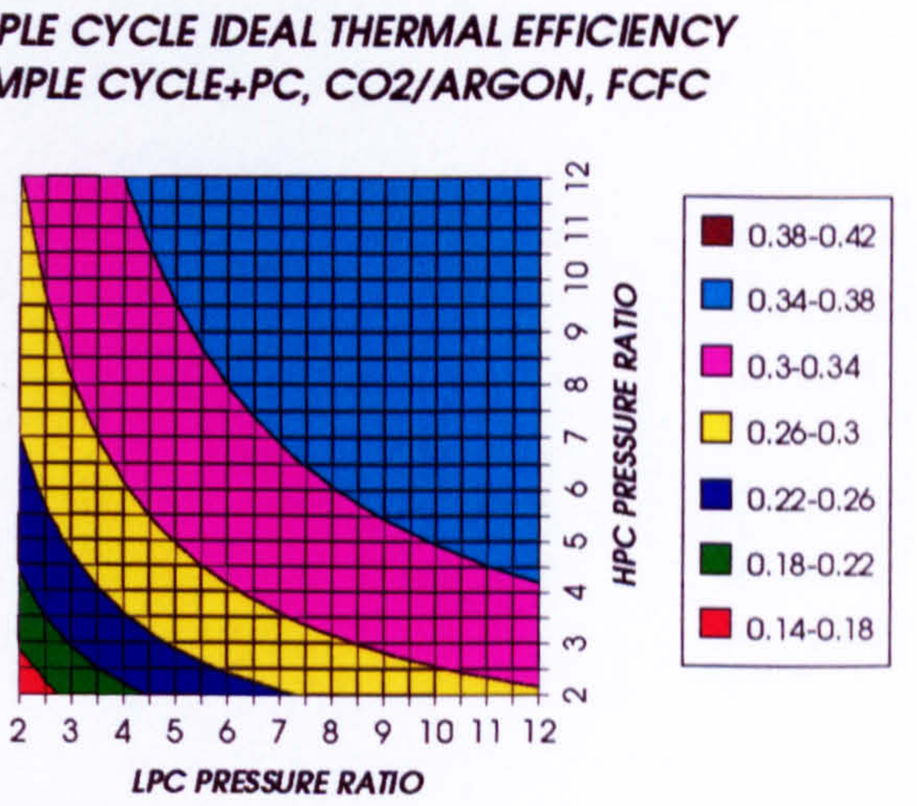

Figure 4. Simple cycle ideal thermal efficiency

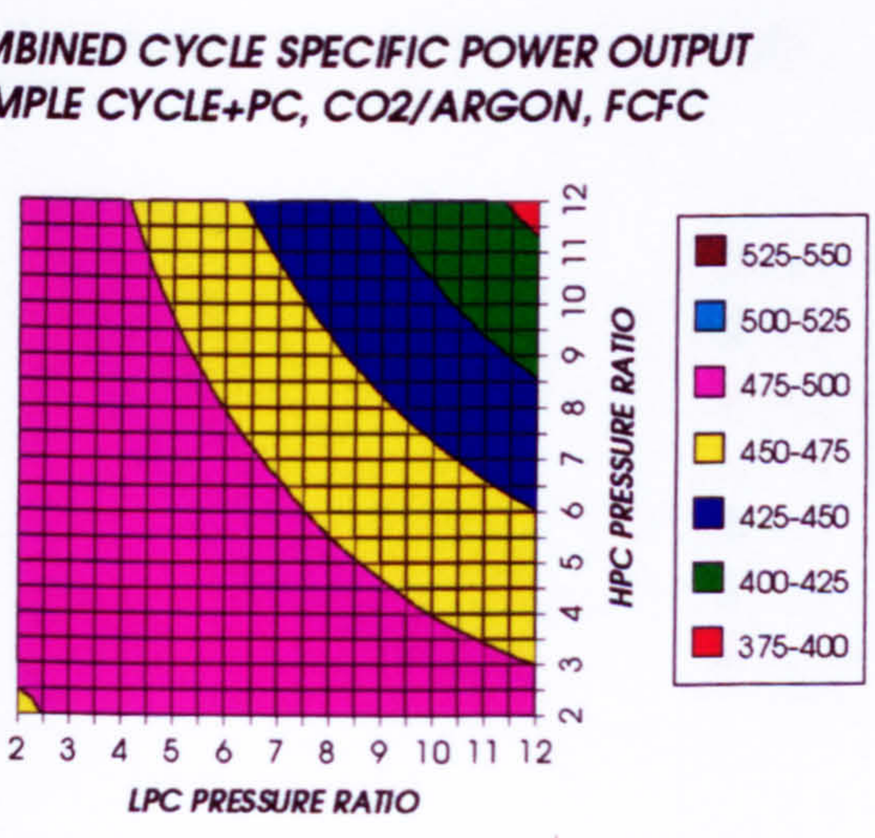

Figure 5. Combined cycle specific power output

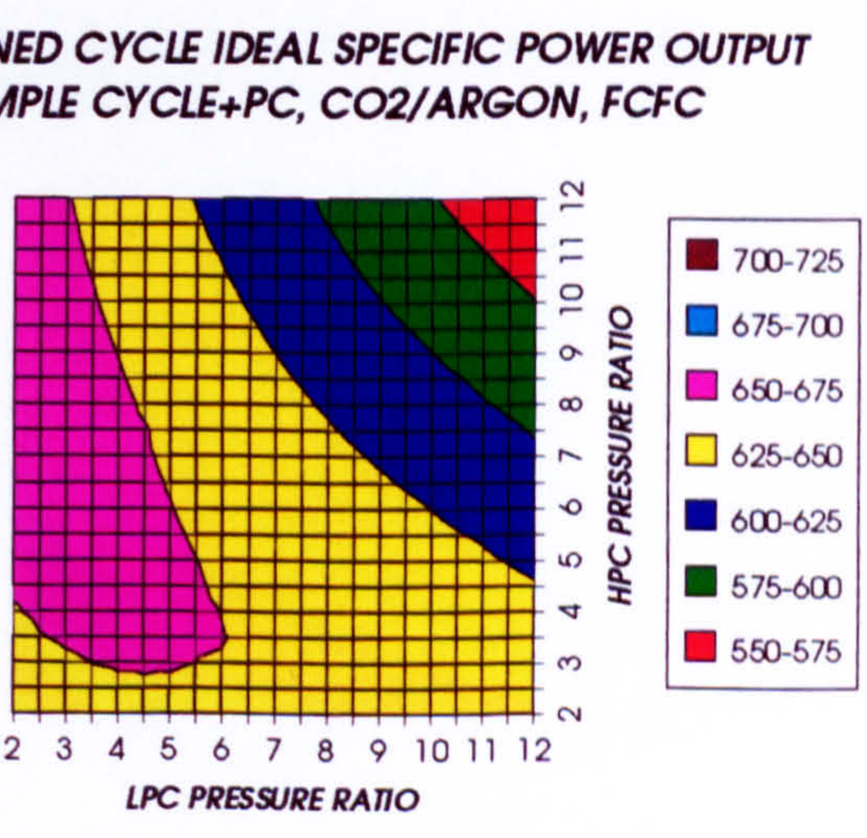

Figure 6. Combined cycle ideal specific power output

COMPLETE PLANT WITH CRYOGENIC PRECOOLING (TET=1650 K)

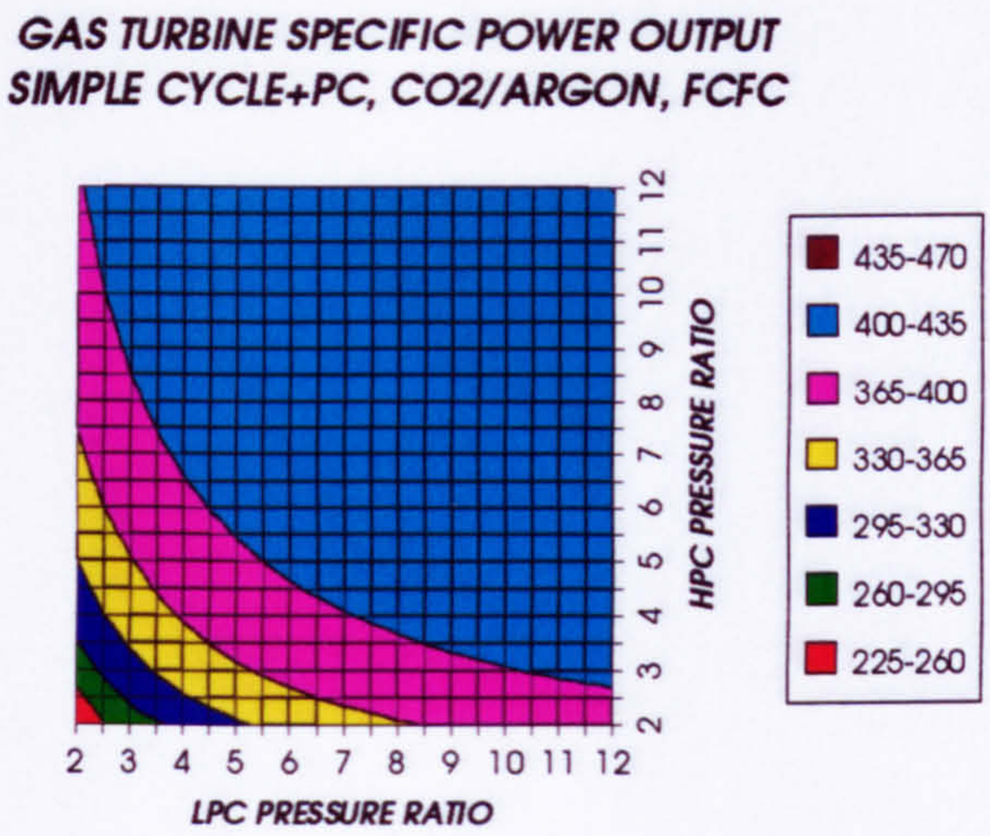

Figure 7. Gas turbine specific power output

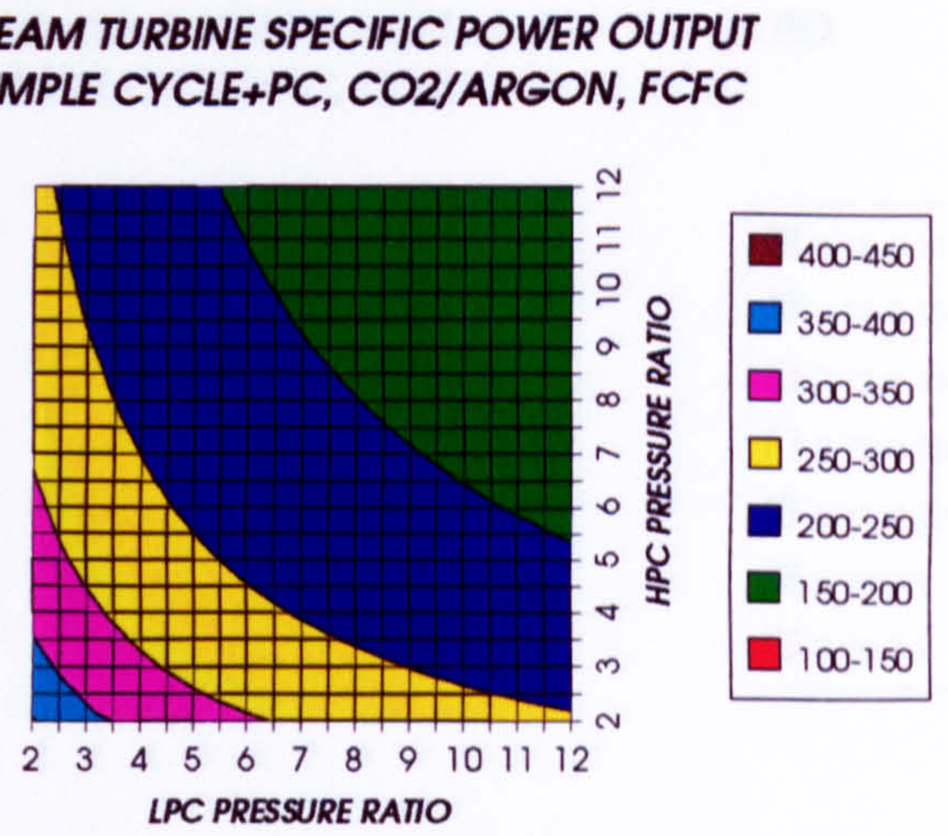

Figure 8. Steam turbine specific power output

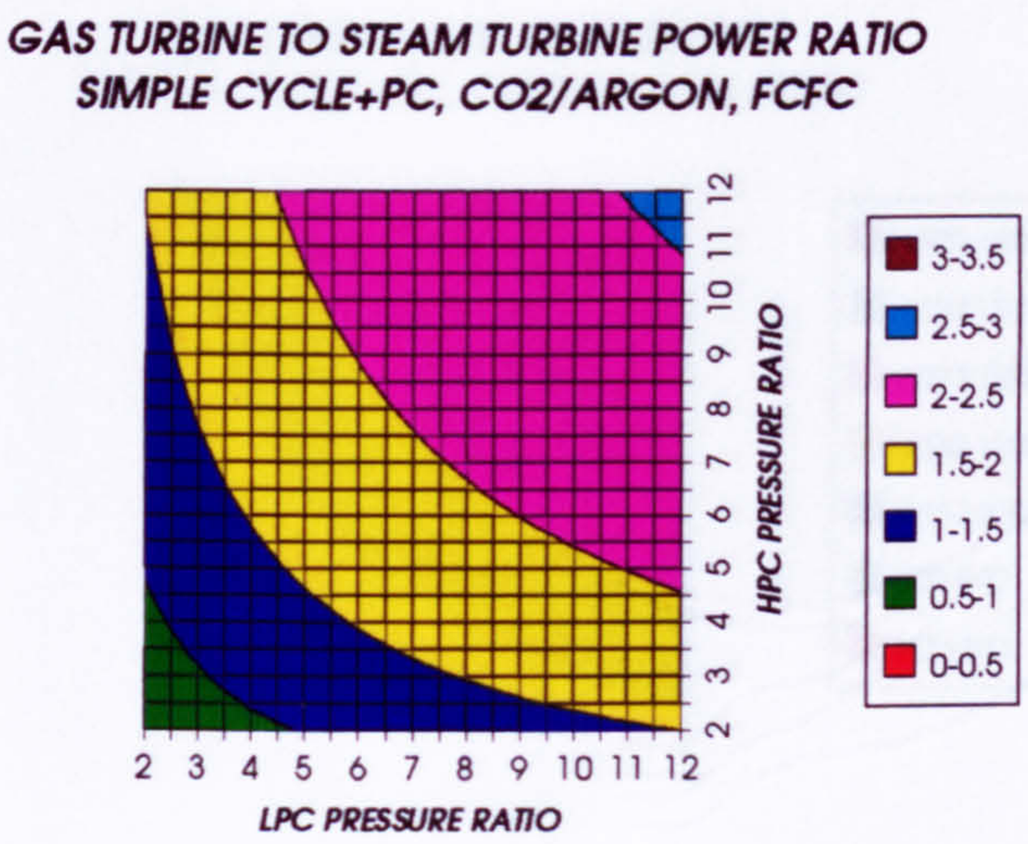

Figure 9. Gas turbine to steam turbine power ratio

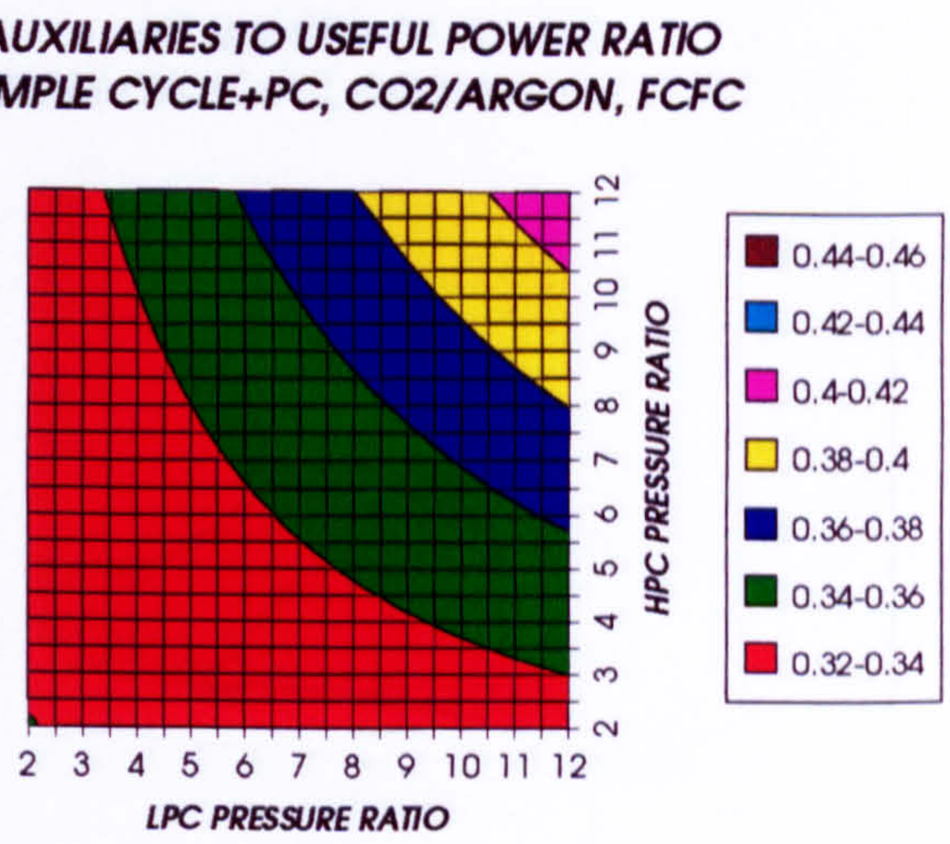

Figure 10. Auxiliary (CO2/Argon, O2 & Fuel) to usefuel power ratio

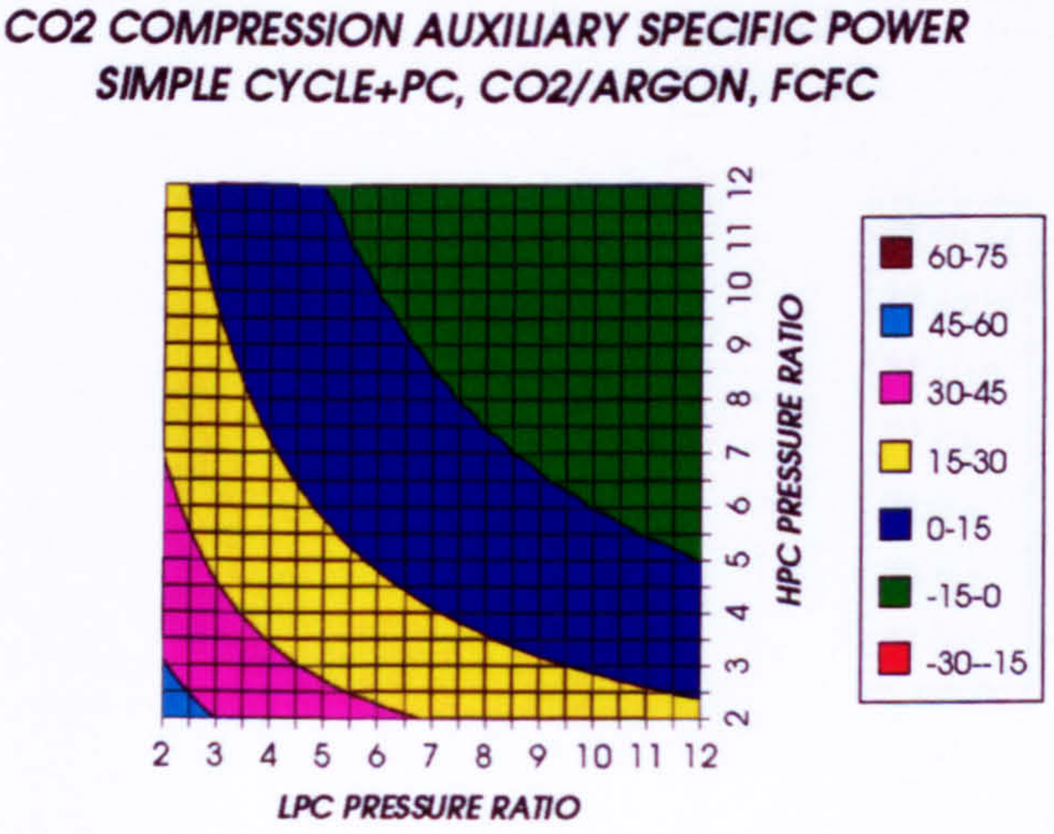

Figure 11. CO2/Argon compression specific power

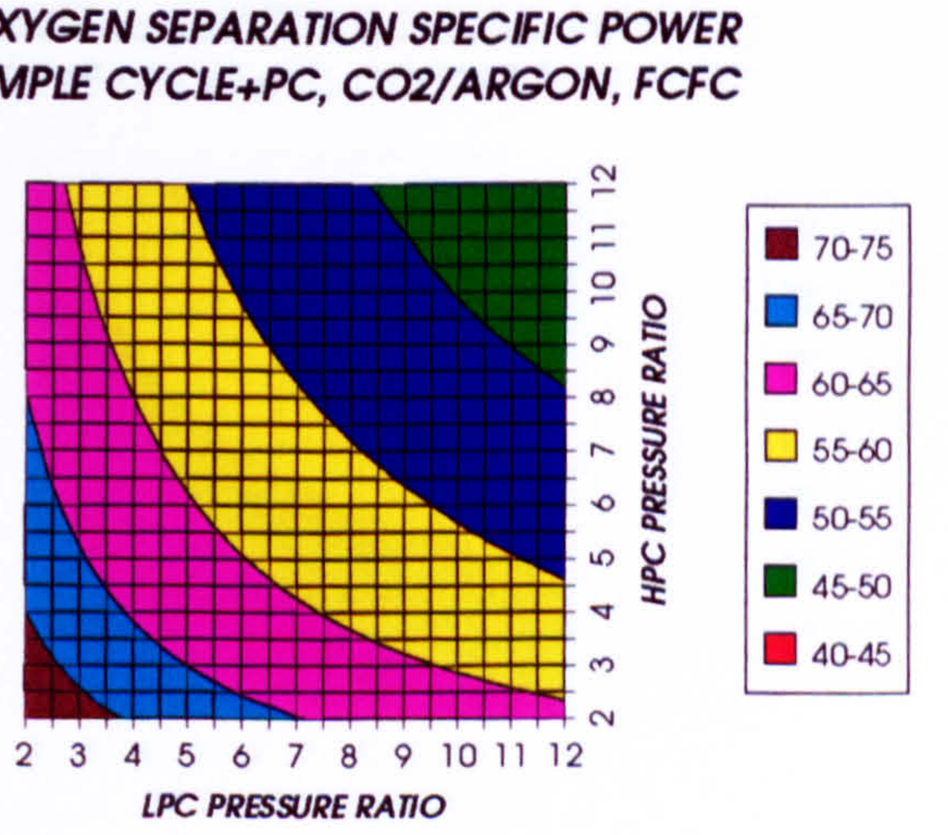

Figure 12. Oxygen separation specific power

COMPLETE PLANT WITH CRYOGENIC PRECOOLING (TET=1650 K)

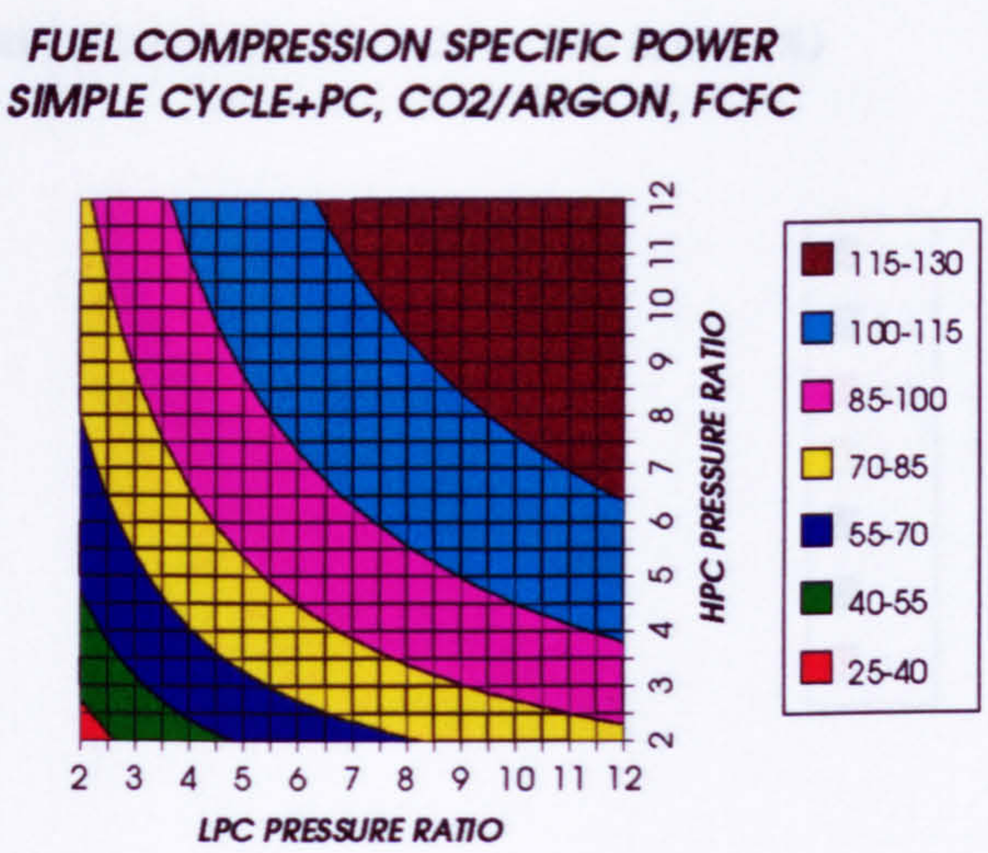

Figure 13. Fuel compressio specific power

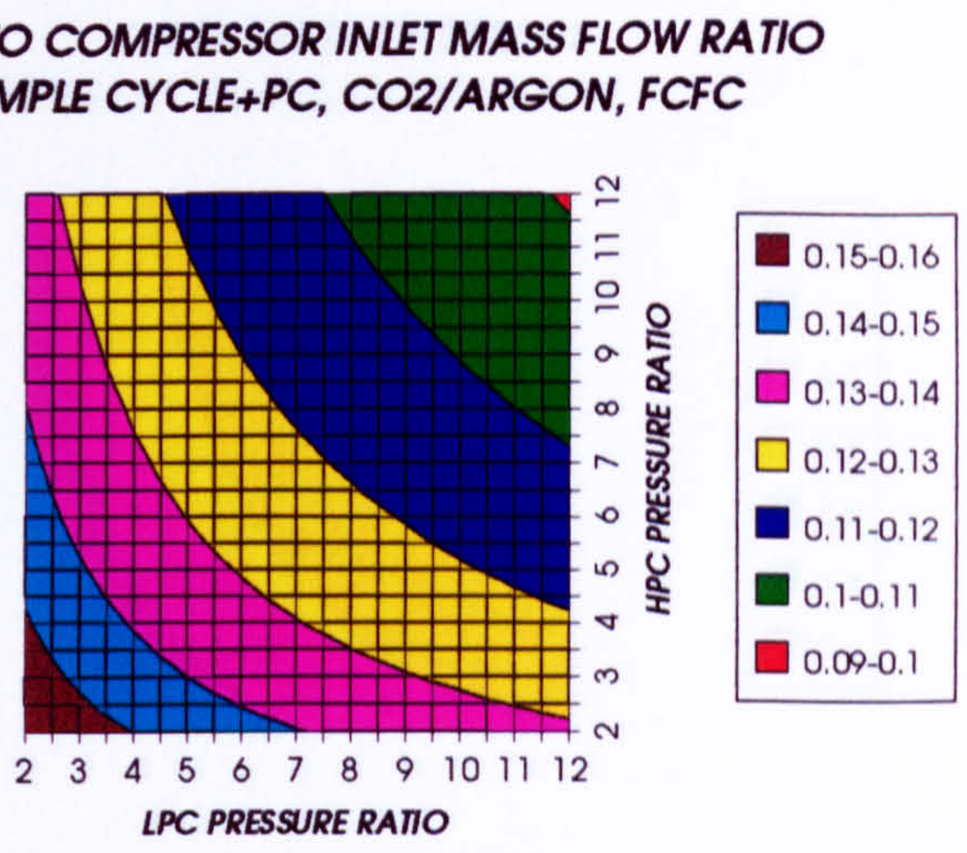

Figure 14. Fuel to compressor inlet mass flow ratio

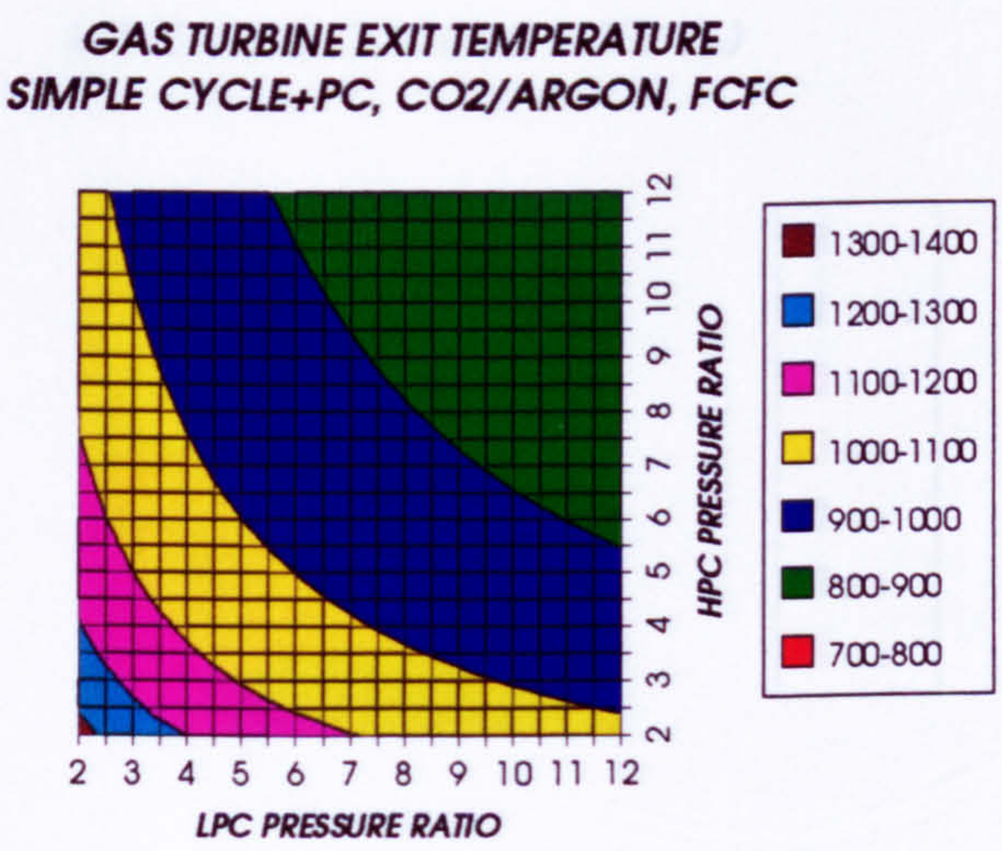

Figure 15. Gas turbine exit temperature

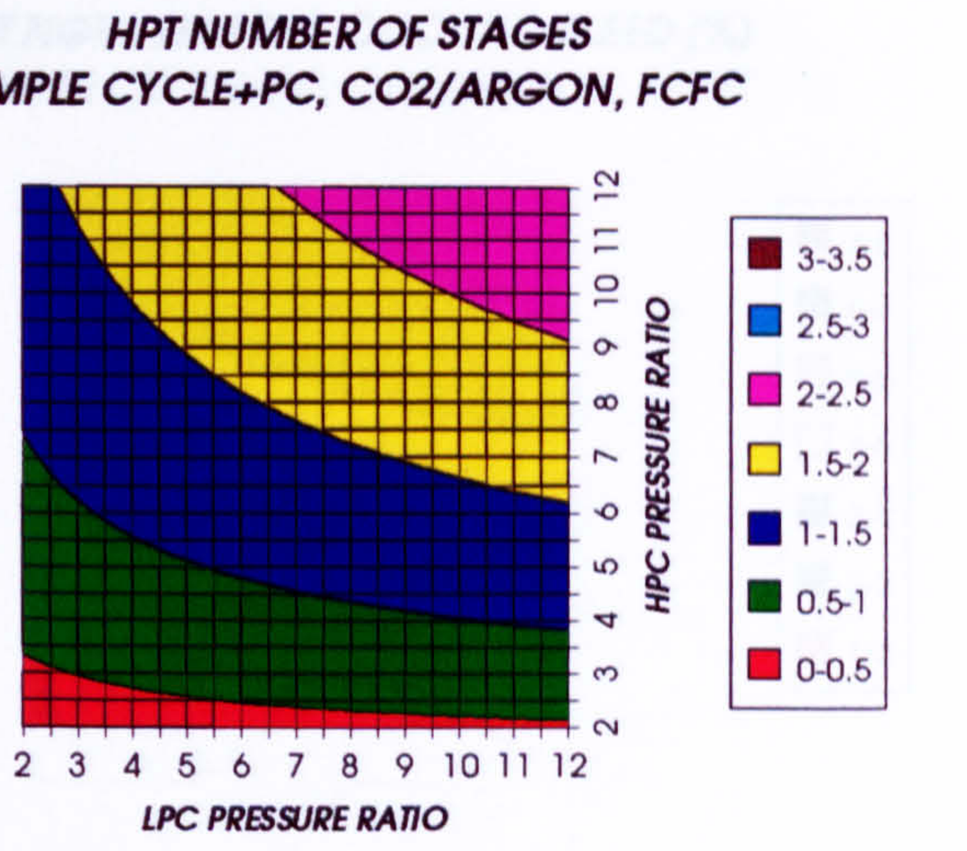

Figure 16. Number of HPT stages

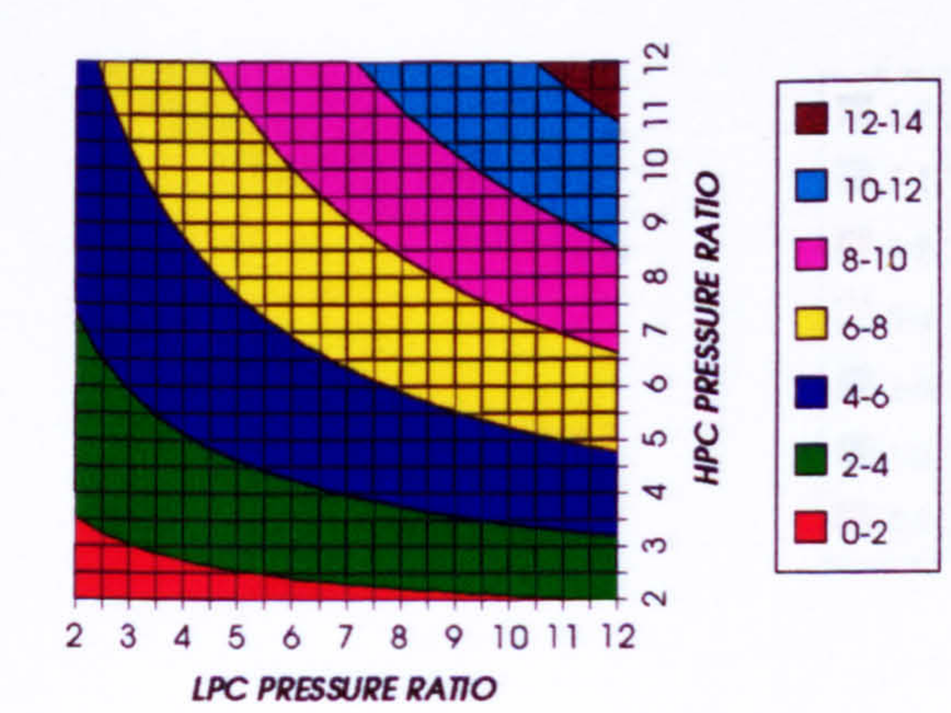

Figure 17. HPT cooling to compressor inlet mass flow ratio

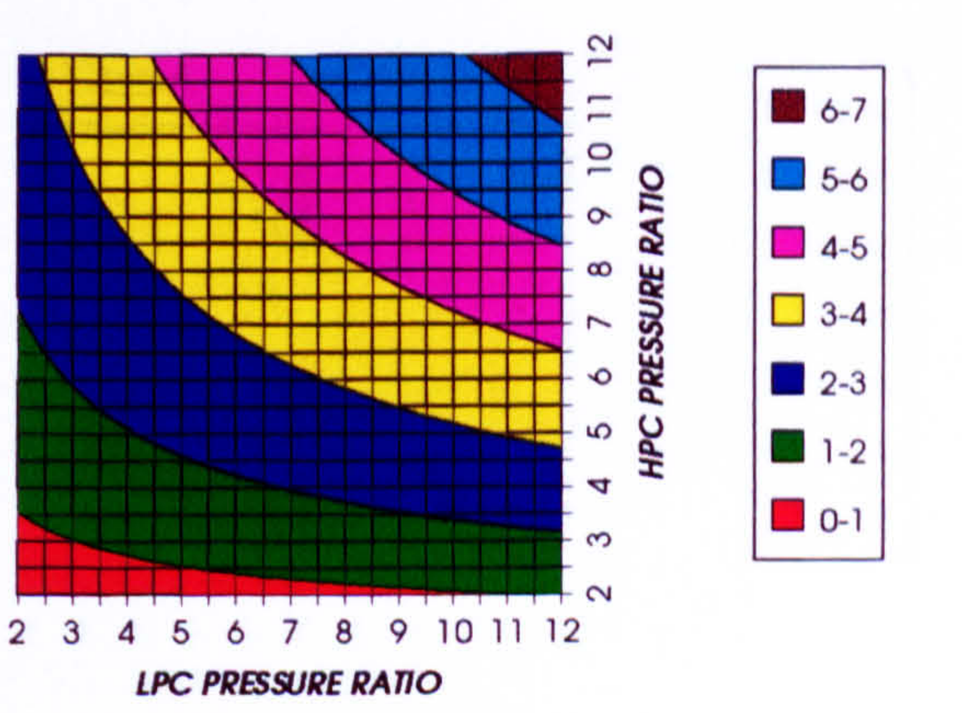

Figure 18. HPT NGVs cooling to compressor inlet mass flow ratio

COMPLETE PLANT WITH CRYOGENIC PRECOOLER (TET=1650 K)

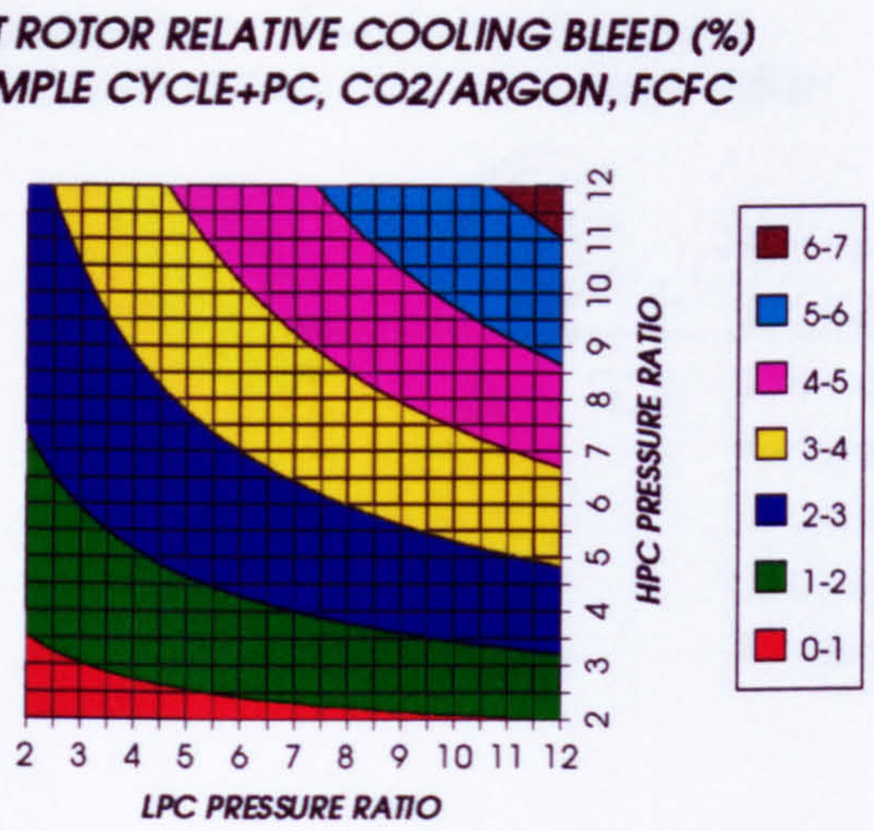

Figure 19. HPT rotor cooling to compressor inlet mass flow ratio

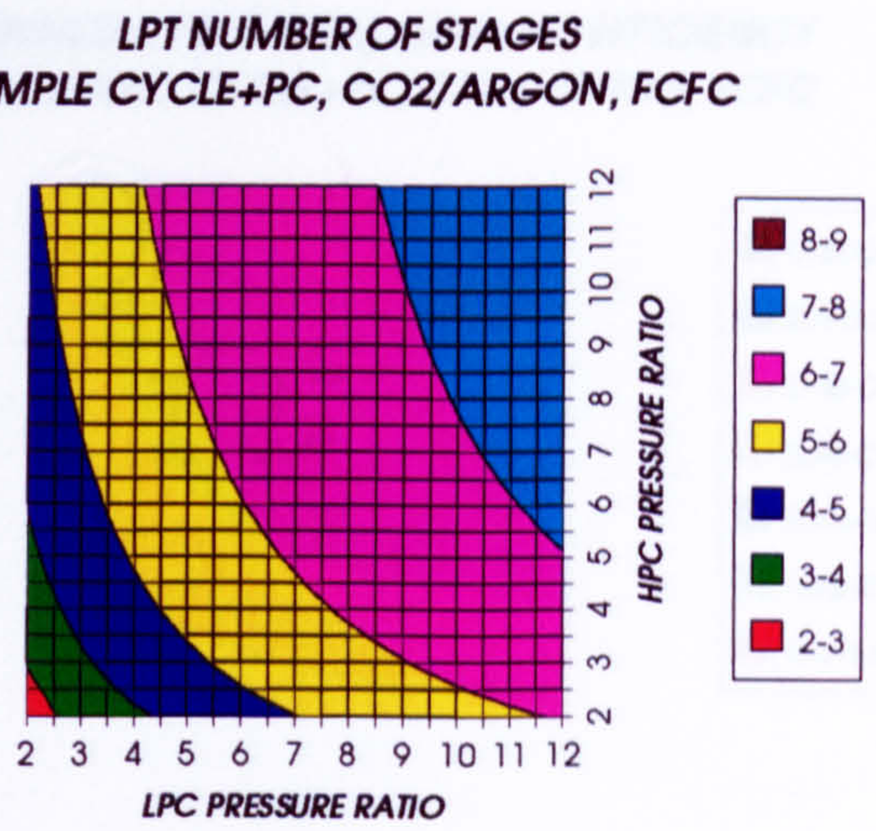

Figure 20. Number of LPT stageS

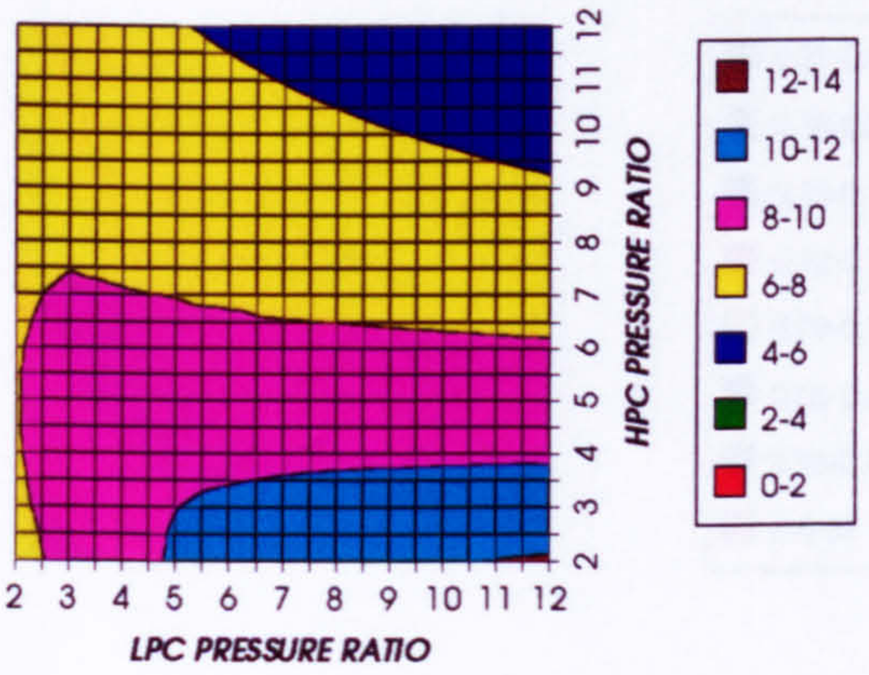

Figure 21. LPT cooling to compressor inlet mass flow ratio

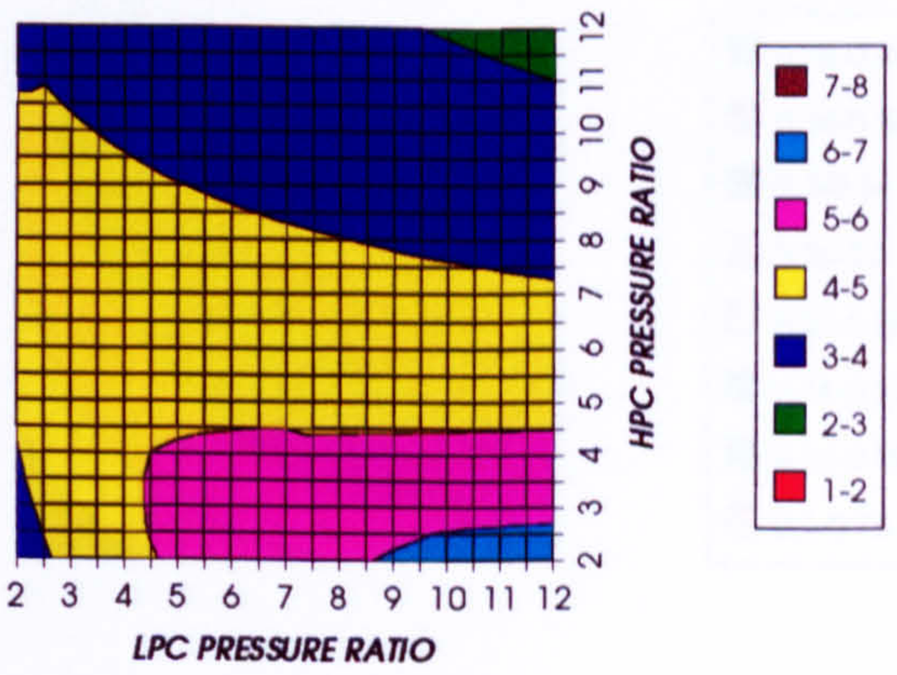

Figure 22. LPT NGVs cooling to compressor inlet mass flow ratio

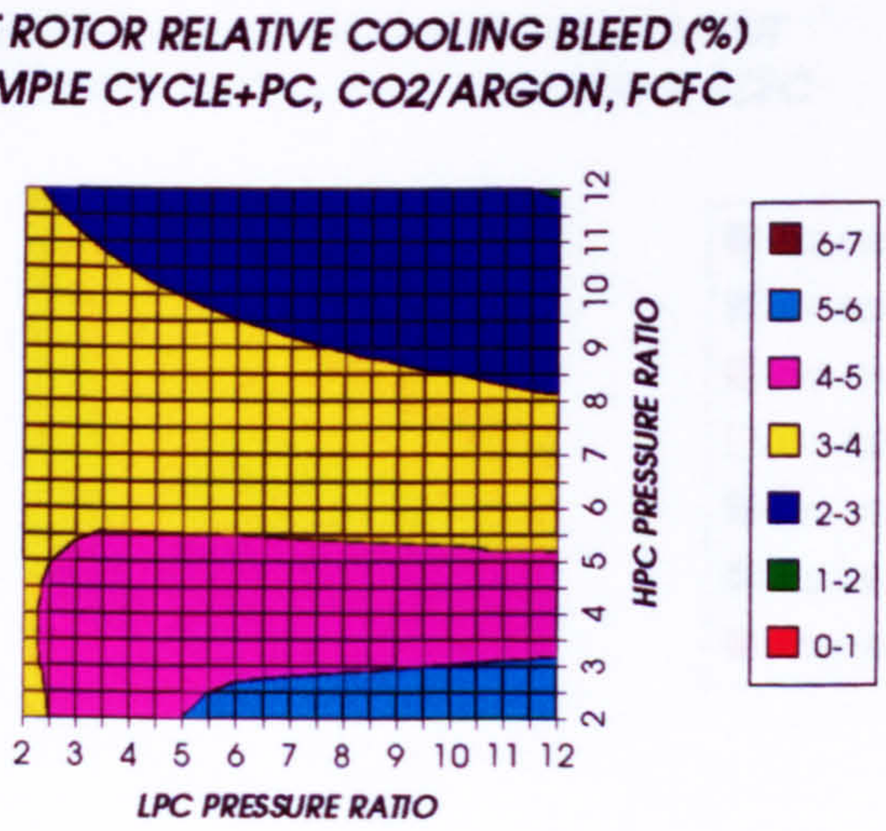

Figure 23. LPT rotor cooling to compressor inlet mass flow ratio

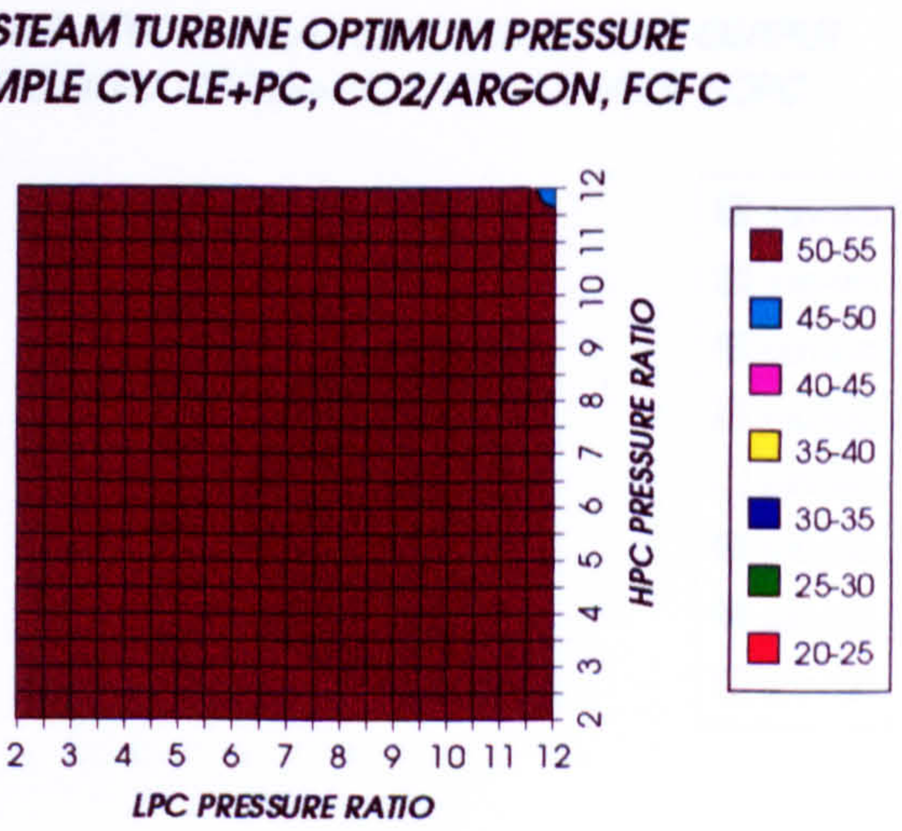

Figure 24. Steam turbine optimum pressures (bars)

COMPLETE PLANT WITH CRYOGENIC PRECOOLING (TET=1650 K)

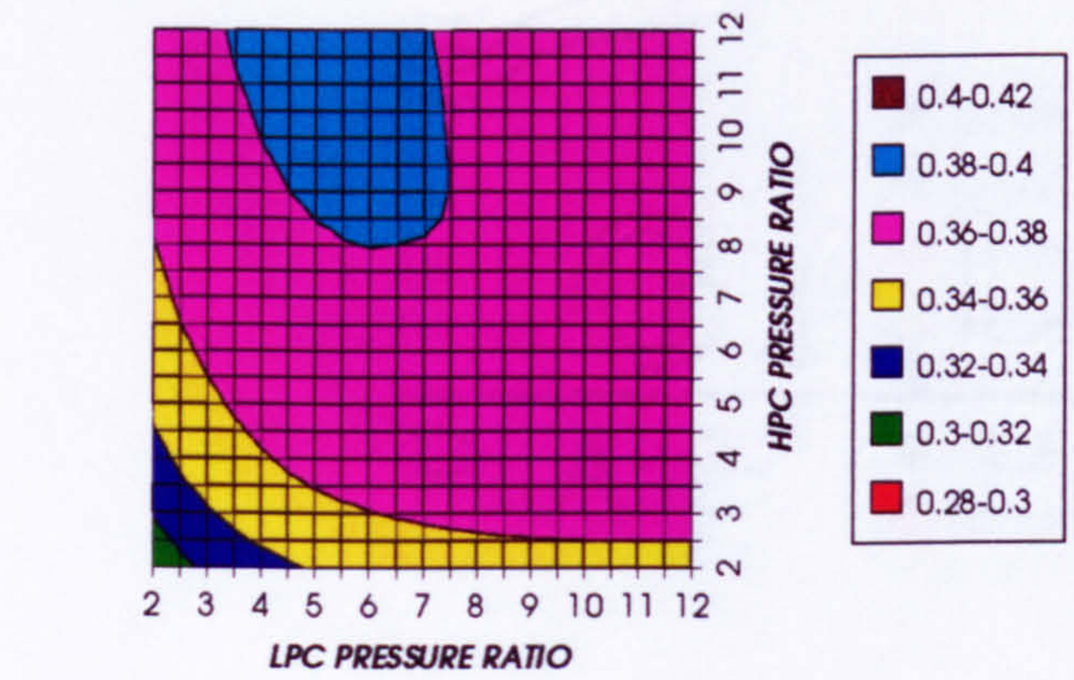

Figure 25. Combined cycle thermal efficiency

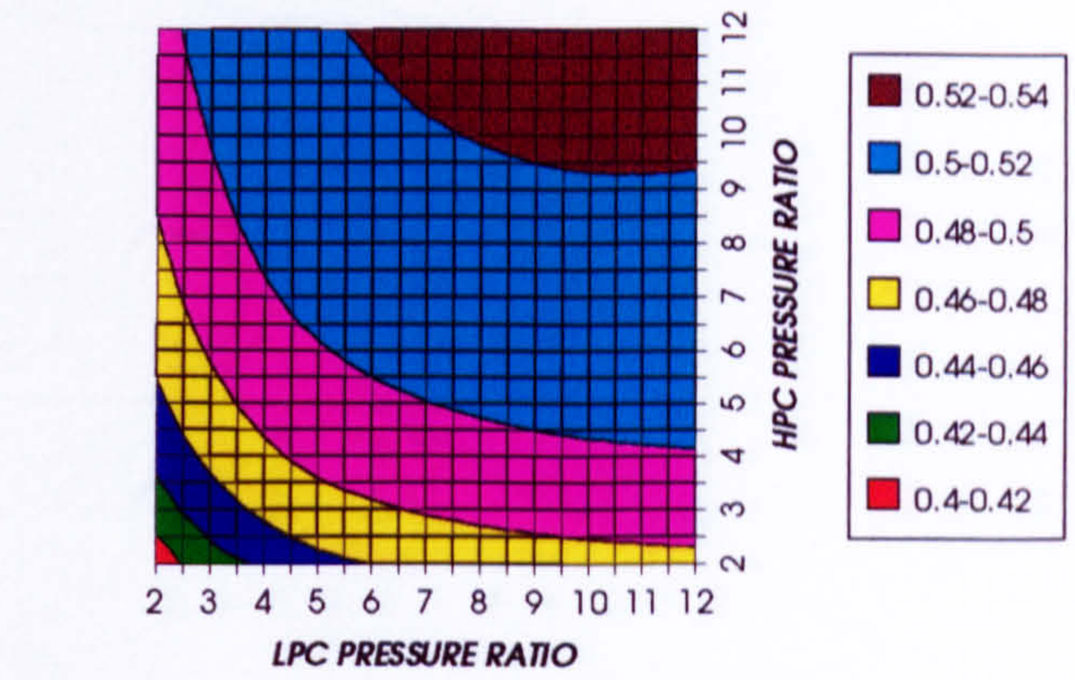

Figure 26. Combined cycle ideal thermal efficiency

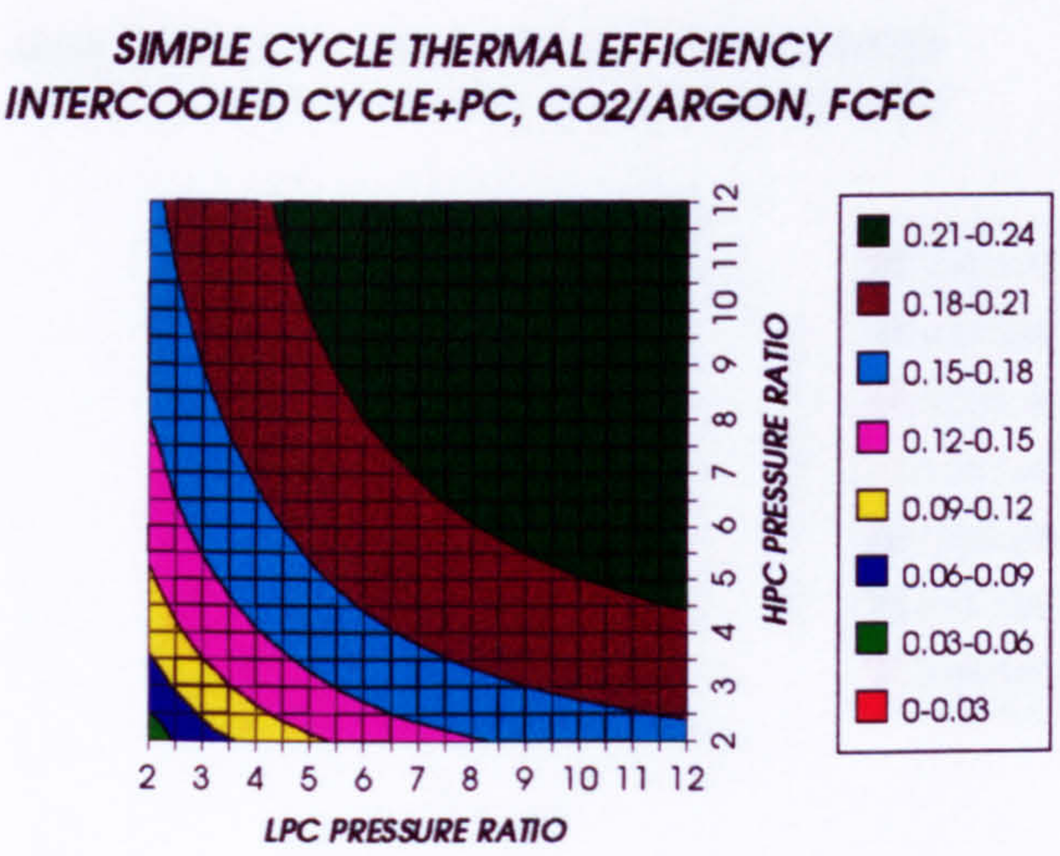

Figure 27. Simple cycle thermal efficiency

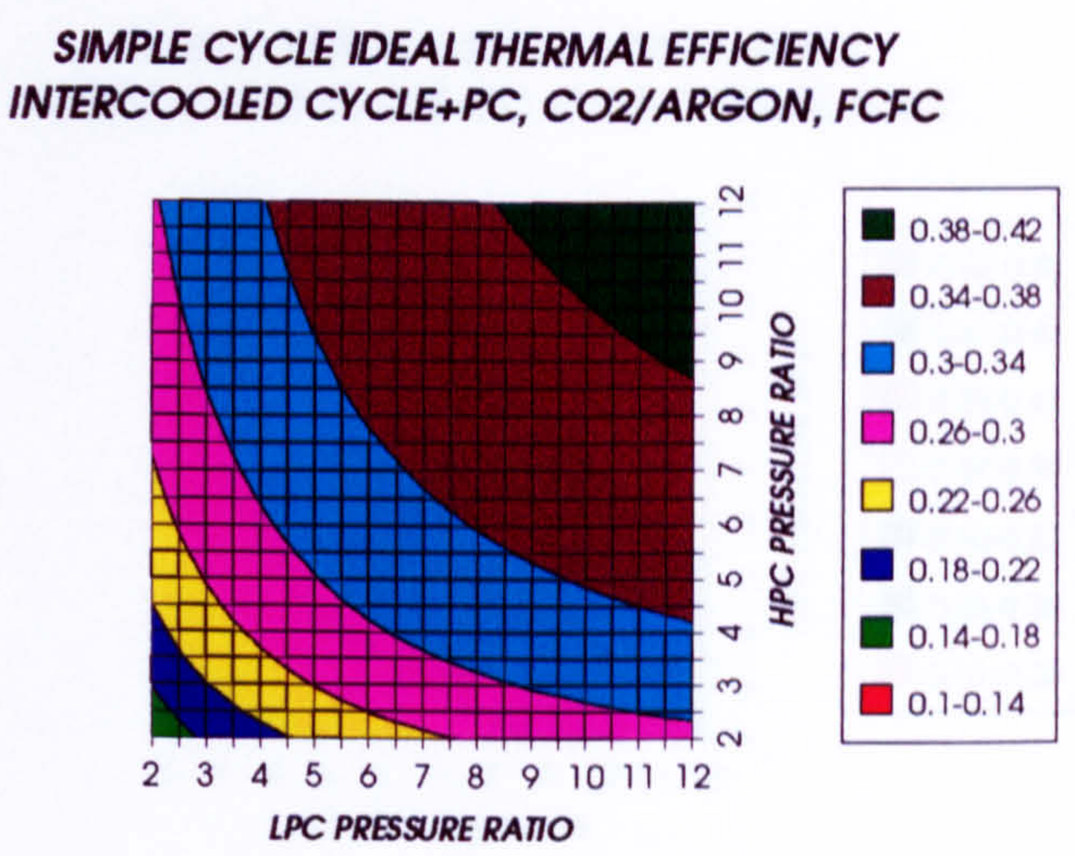

Figure 28. Simple cycle ideal thermal efficiency

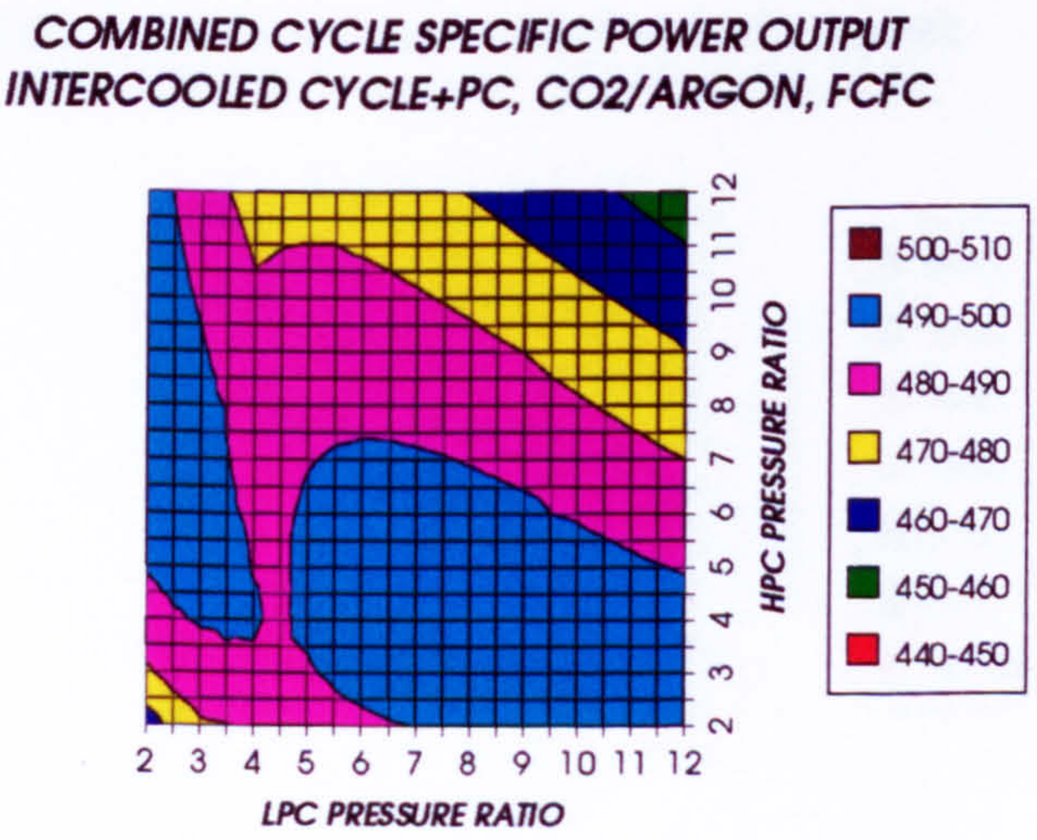

Figure 29. Combined cycle specific power output

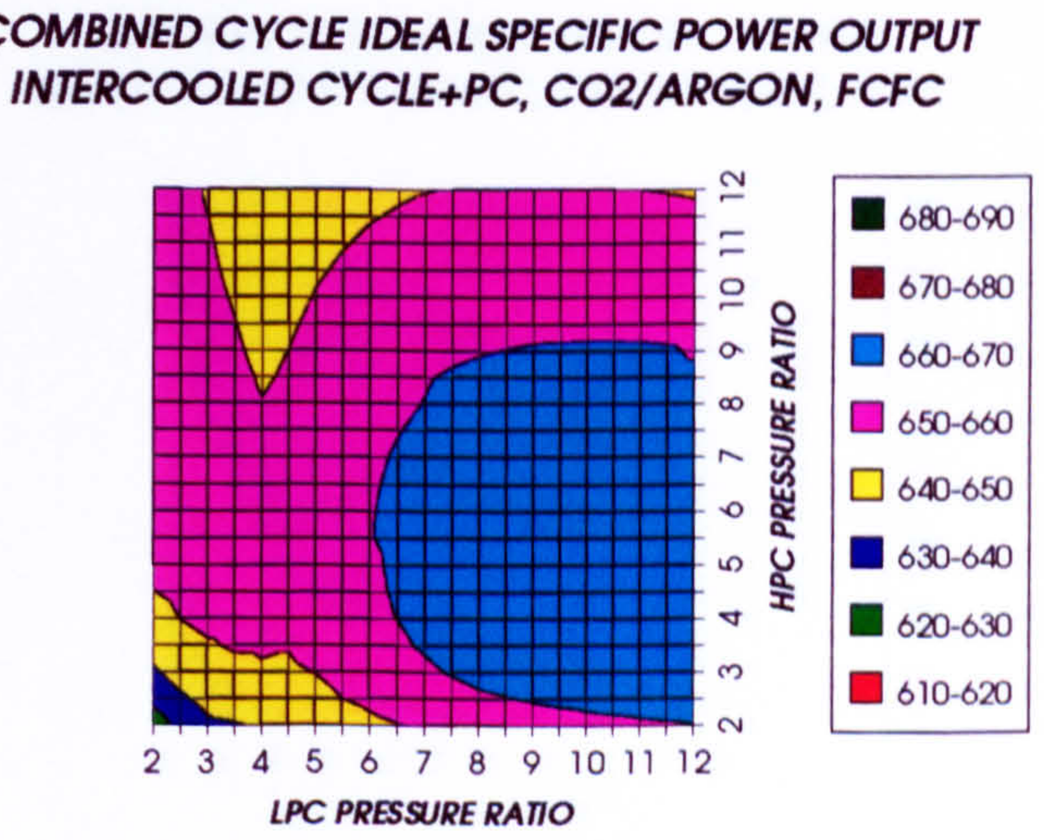

Figure 30. Combined cycle ideal specific power output

COMPLETE PLANT WITH CRYOGENIC PRECOOLING (TET=1650 K)

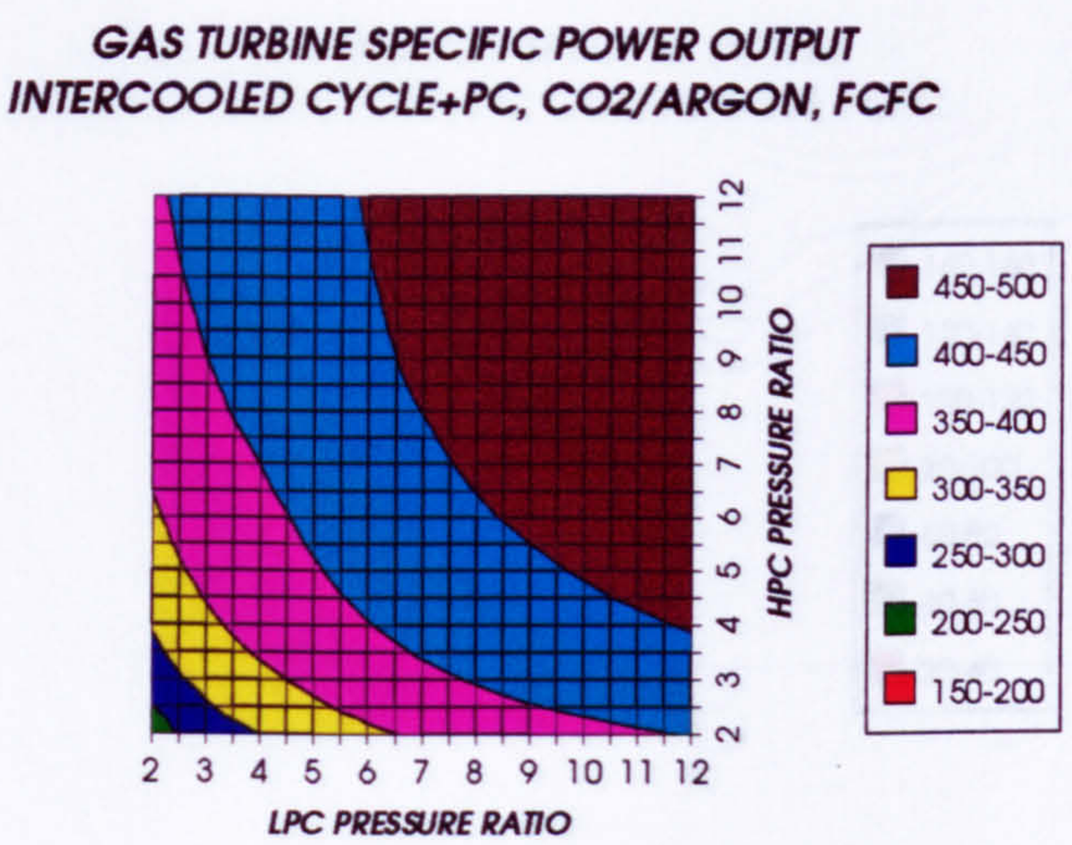

Figure 31. Gas turbine specific power output

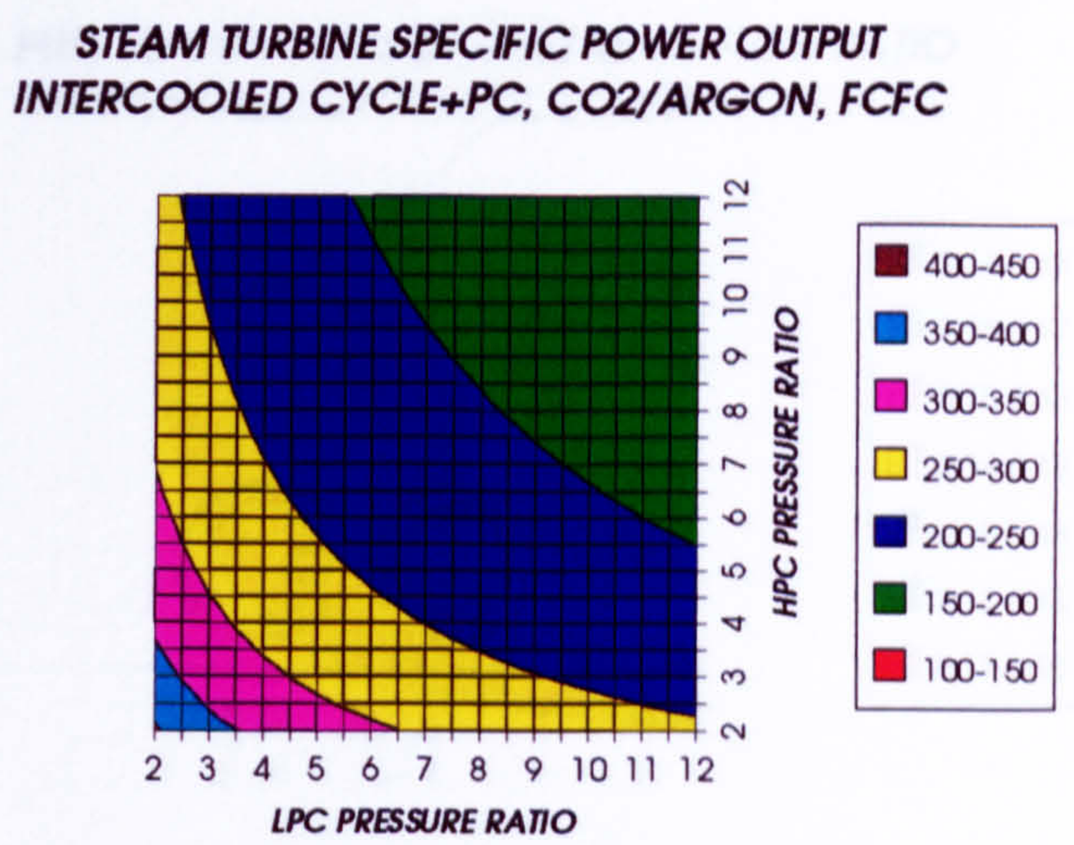

Figure 32. Steam turbine specific power output

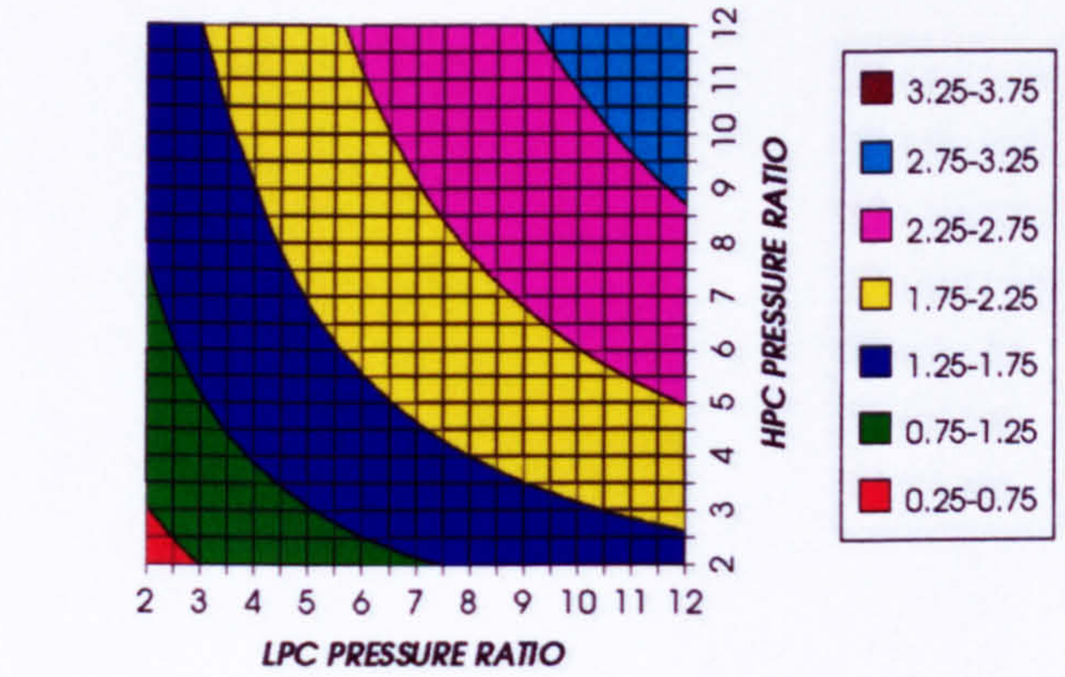

Figure 33. Gas turbine to steam turbine power ratio

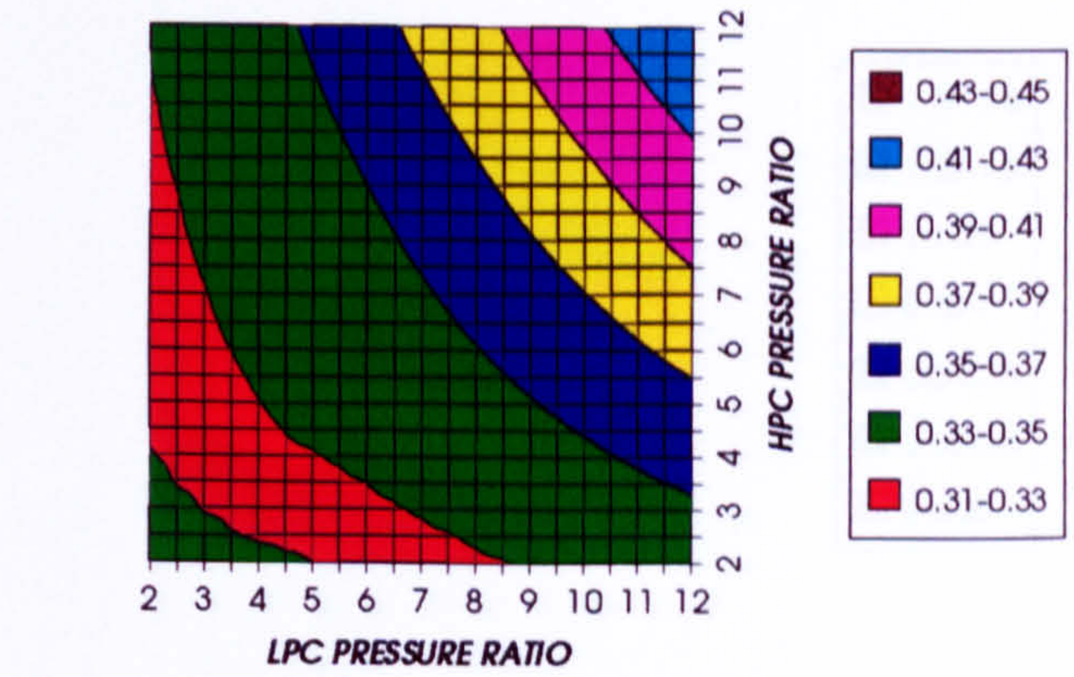

Figure 34. Auxiliary (CO2/Argon, O2 & Fuel) to usefuel power ratio

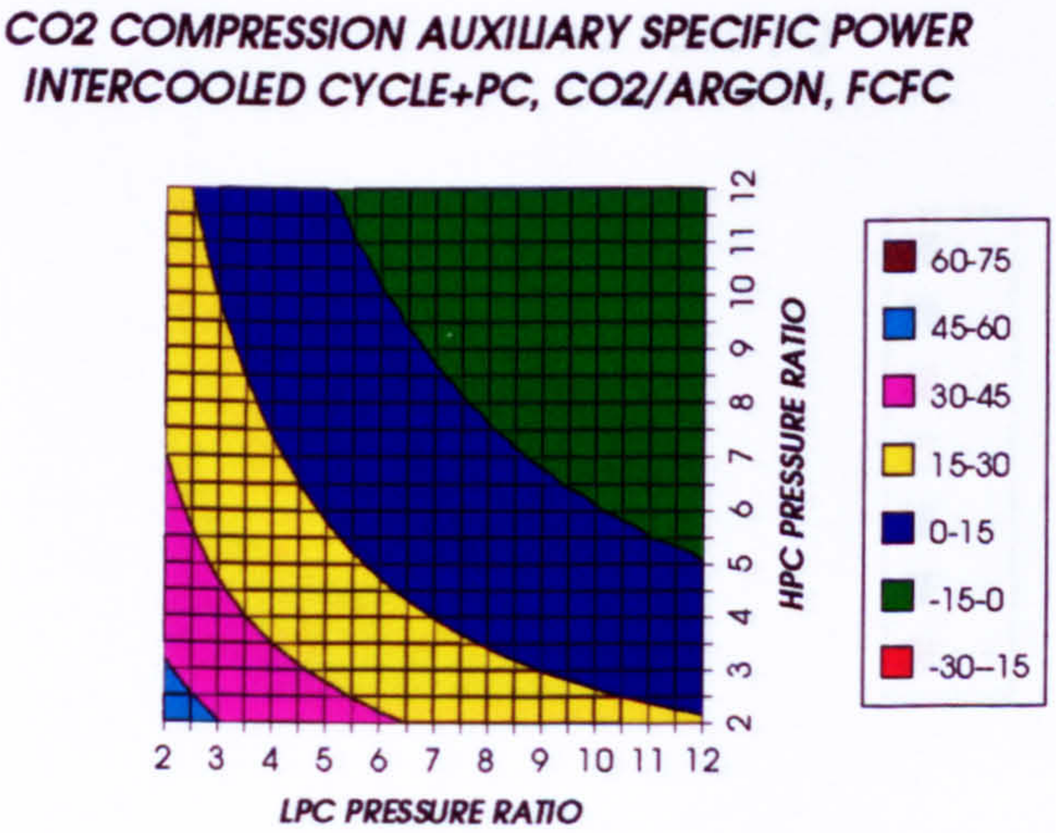

Figure 35. CO2/Argon compression specific power

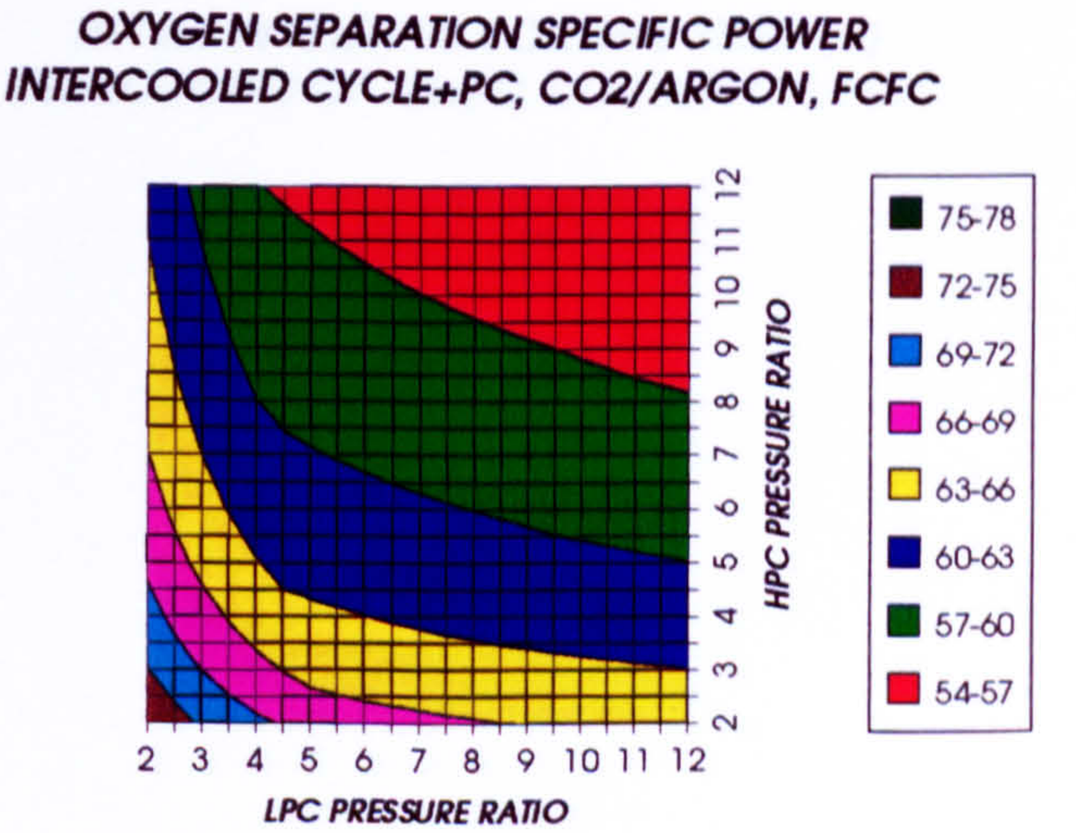

Figure 36. Oxygen separation specific power

COMPLETE PLANT WITH CRYOGENIC PRECOOLING (TET=1650 K)

FUEL COMPRESSION SPECIFIC POWER
INTERCOOLED CYCLE+PC, CO2/ARGON, FCFC

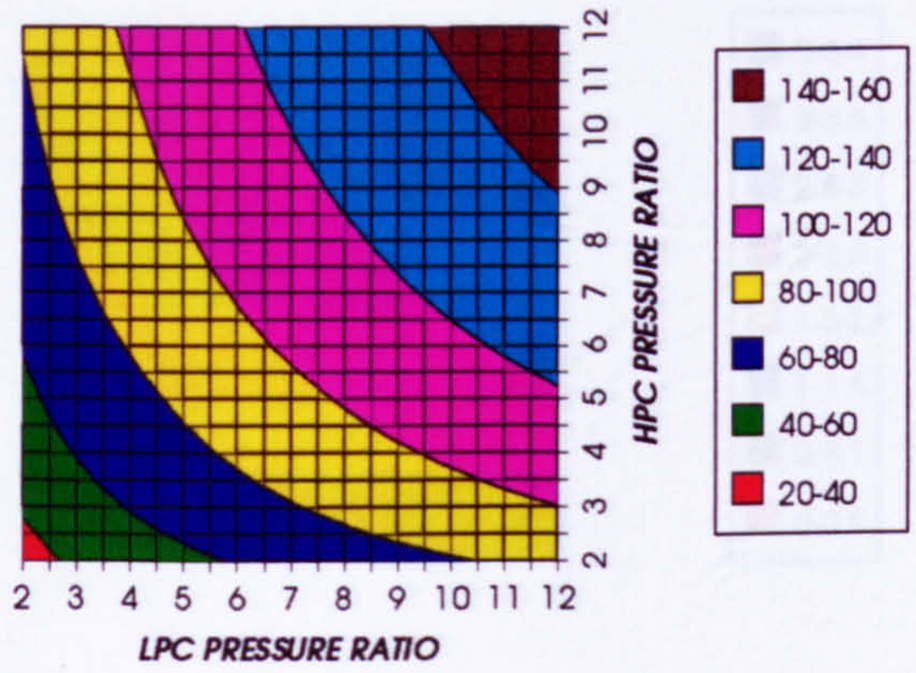

Figure 37. Fuel compression specific power

FUEL TO COMPRESSOR INLET MASS FLOW RATIO
INTERCOOLED CYCLE+PC, CO2/ARGON, FCFC

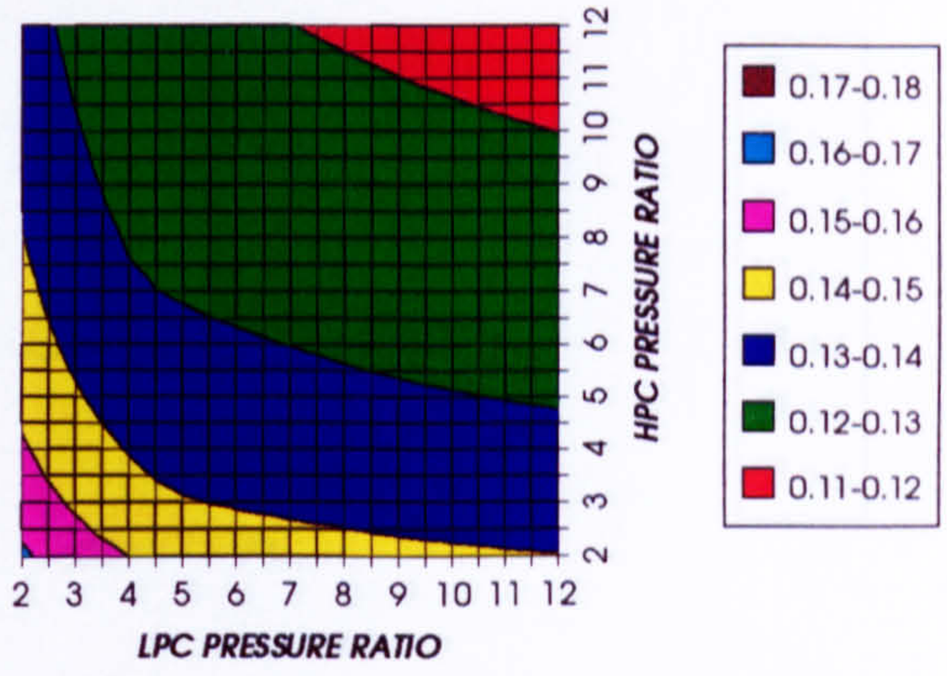

Figure 38. Fuel to compressor inlet mass flow ratio

GAS TURBINE EXIT TEMPERATURE
INTERCOOLED CYCLE+PC, CO2/ARGON, FCFC

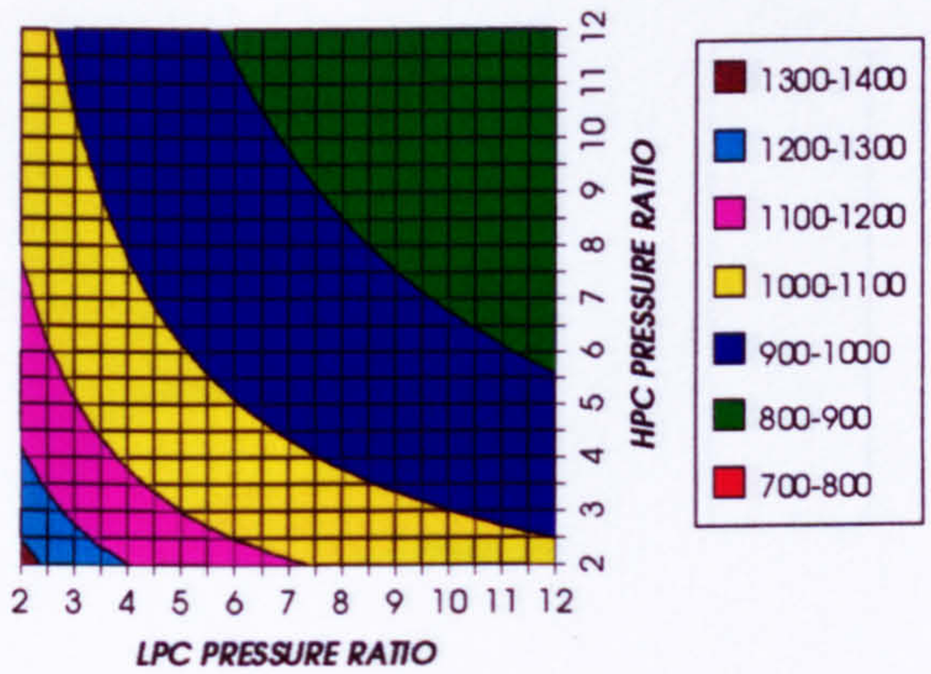

Figure 39. Gas turbine exit temperature

HPT NUMBER OF STAGES
INTERCOOLED CYCLE+PC, CO2/ARGON, FCFC

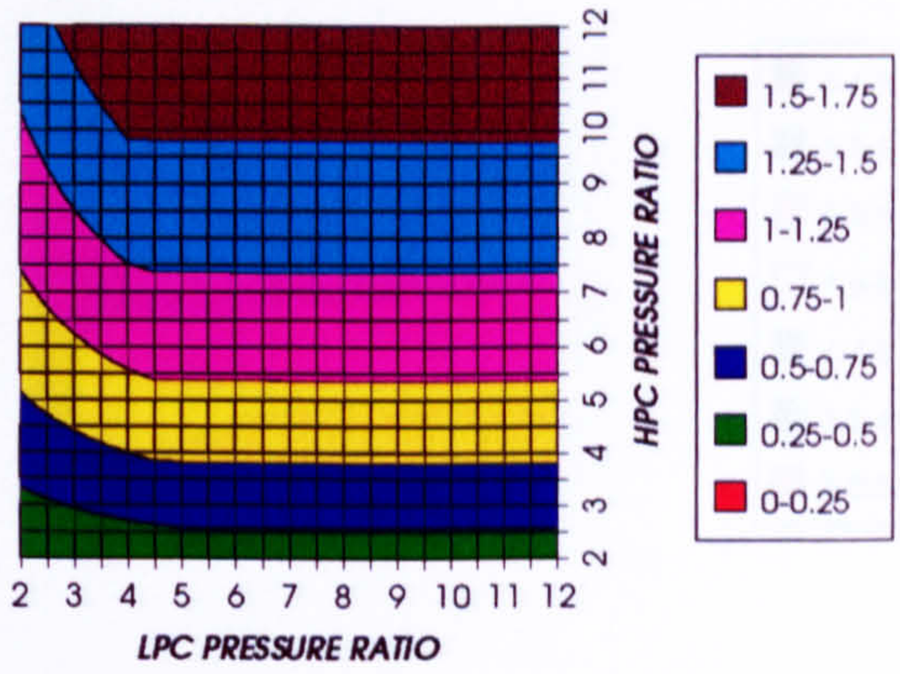

Figure 40. Number of HPT stages

HPT RELATIVE COOLING BLEED (%)
INTERCOOLED CYCLE+PC, CO2/ARGON, FCFC

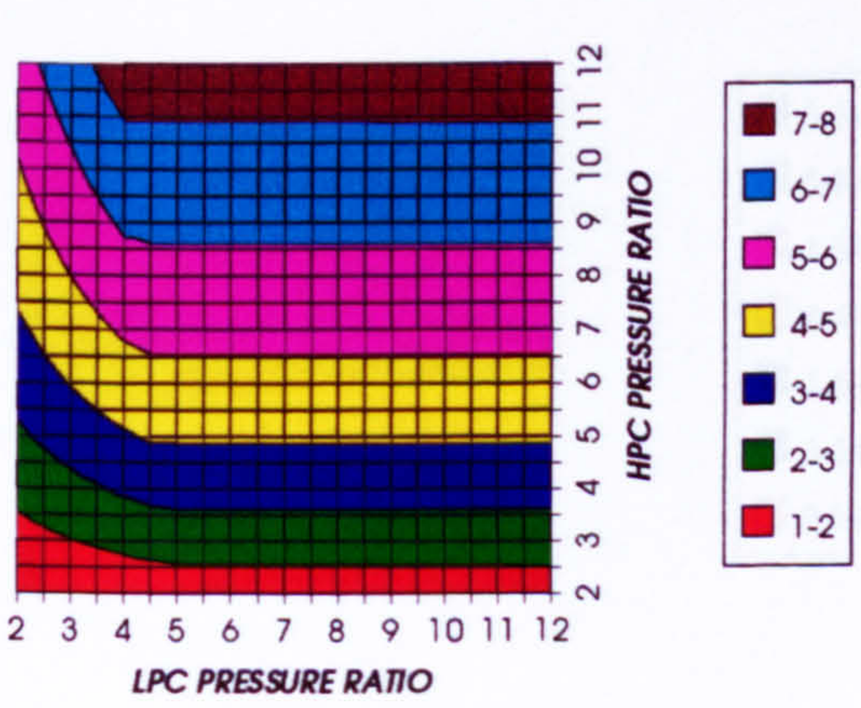

Figure 41. HPT cooling to compressor inlet mass flow ratio

HPT NGVs RELATIVE COOLING BLEED (%)
INTERCOOLED CYCLE+PC, CO2/ARGON, FCFC

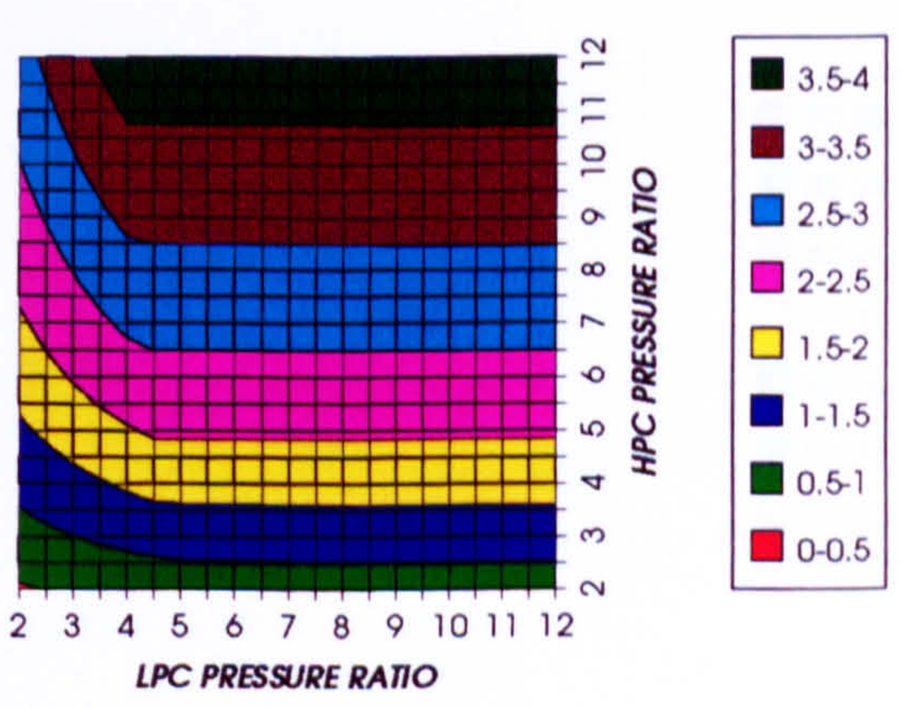

Figure 42. HPT NGVs cooling to compressor inlet mass flow ratio

COMPLETE PLANT WITH CRYOGENIC PRECOOLING (TET=1650 K)

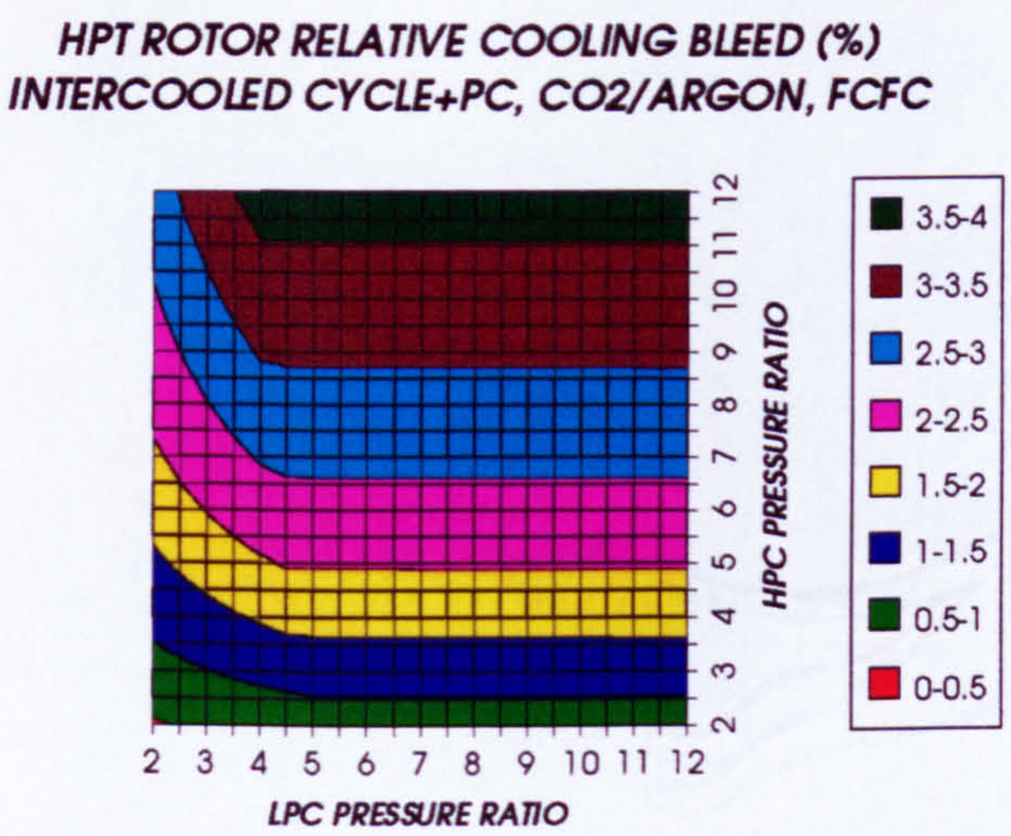

Figure 43. HPT rotor cooling to compressor inlet mass flow ratio

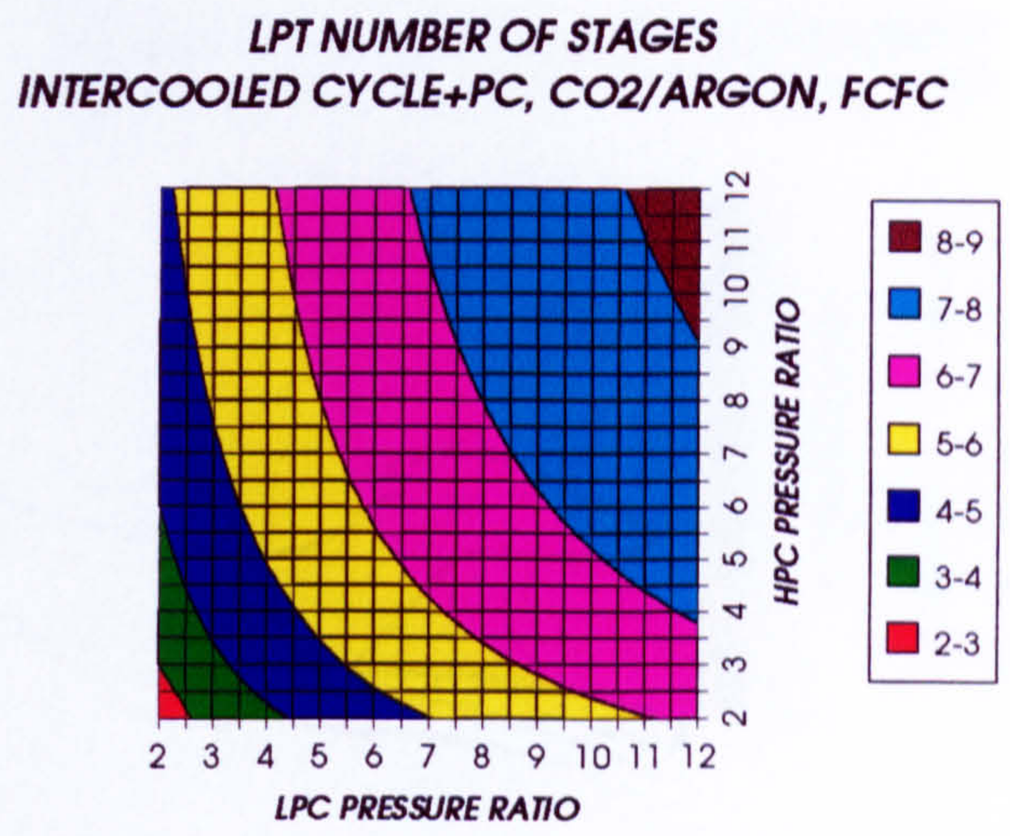

Figure 44. Number of LPT stages

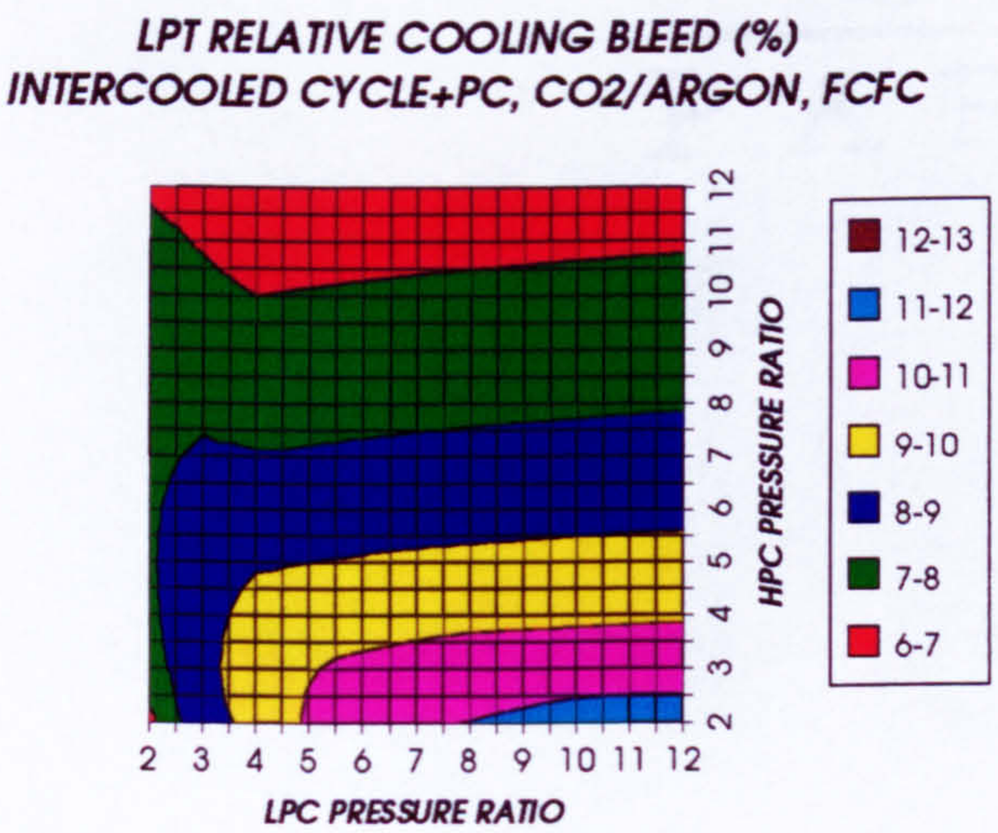

Figure 45. LPT cooling to compressor inlet mass flow ratio

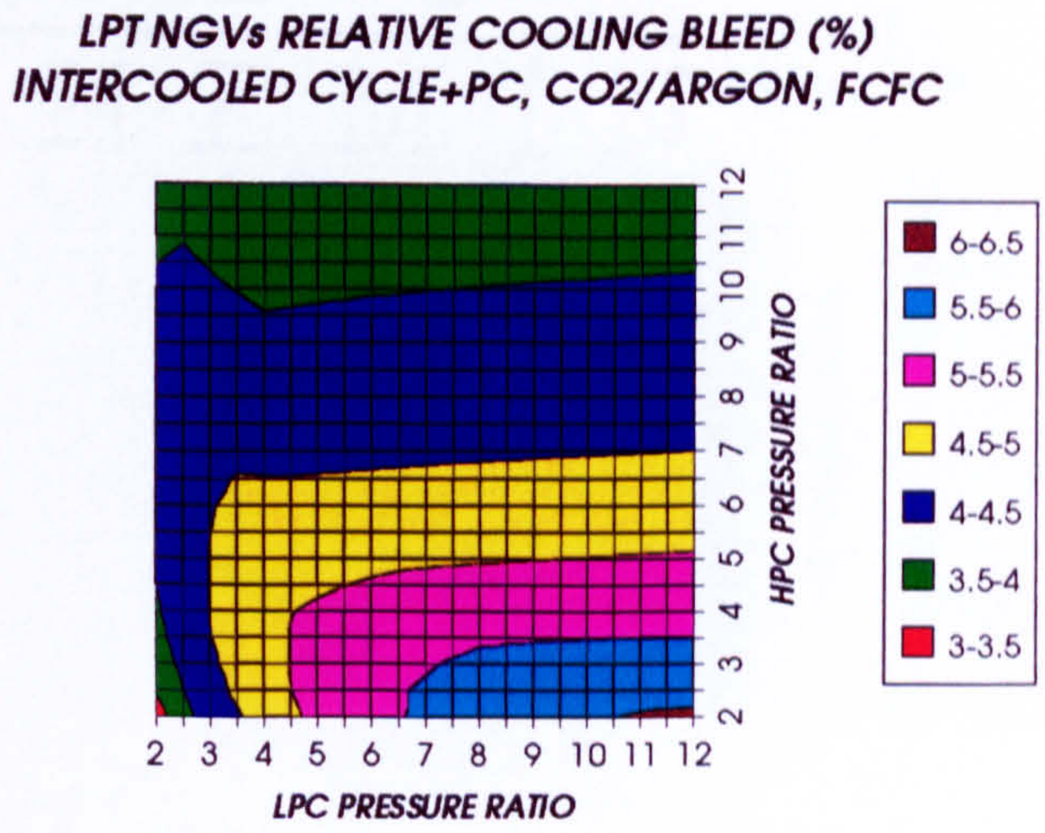

Figure 46. LPT NGVs cooling to compressor inlet mass flow ratio

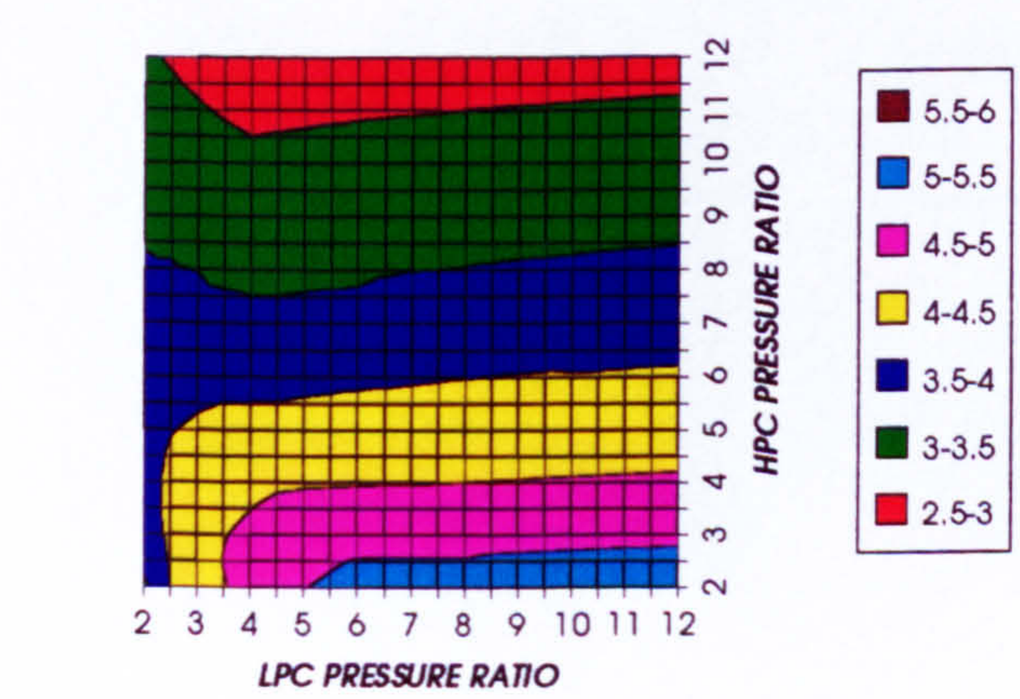

Figure 47. LPT rotor cooling to compressor inlet mass flow ratio

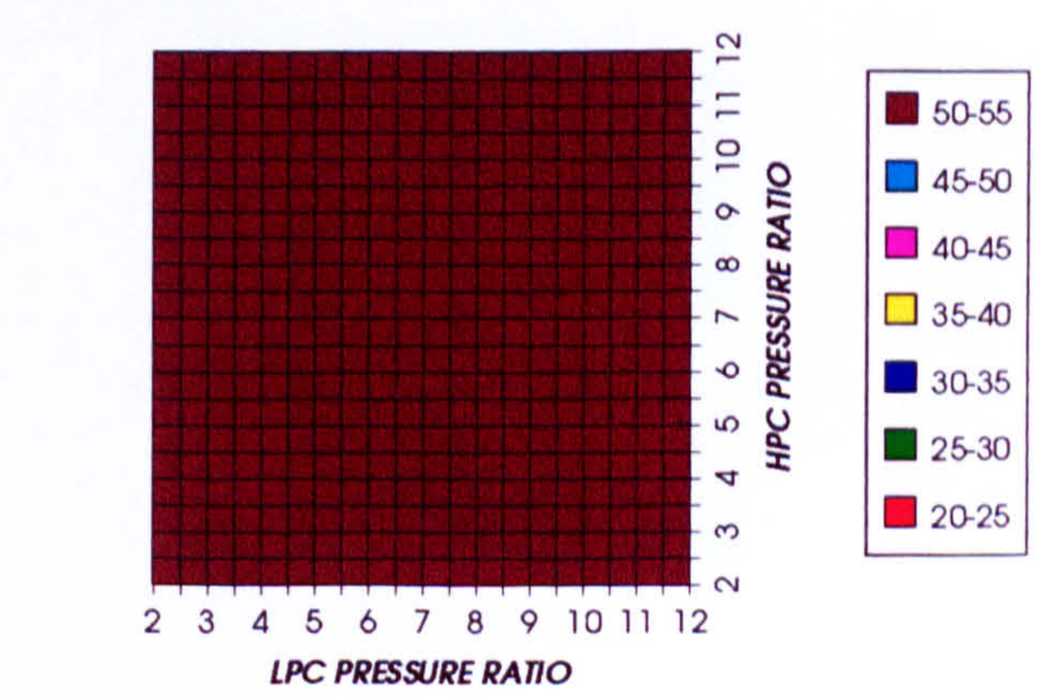

Figure 48. Steam turbine optimum pressures (maximum)

COMPLETE PLANT WITH CRYOGENIC PRECOOLING (TET=1650 K)

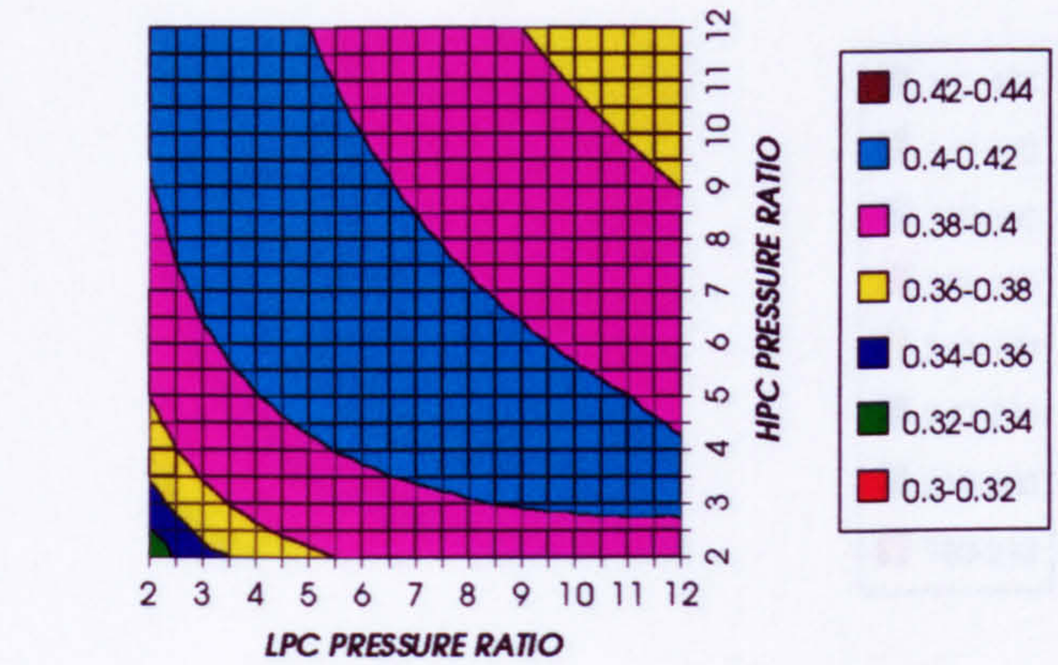

Figure 49. Combined cycle thermal efficiency

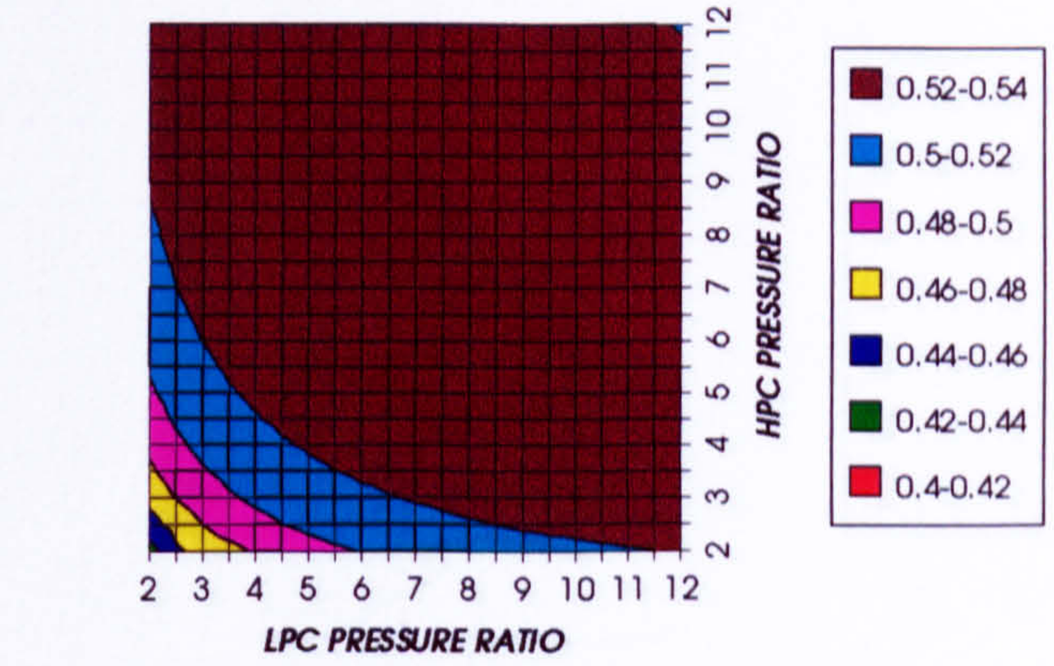

Figure 50. Combined cycle ideal thermal efficiency

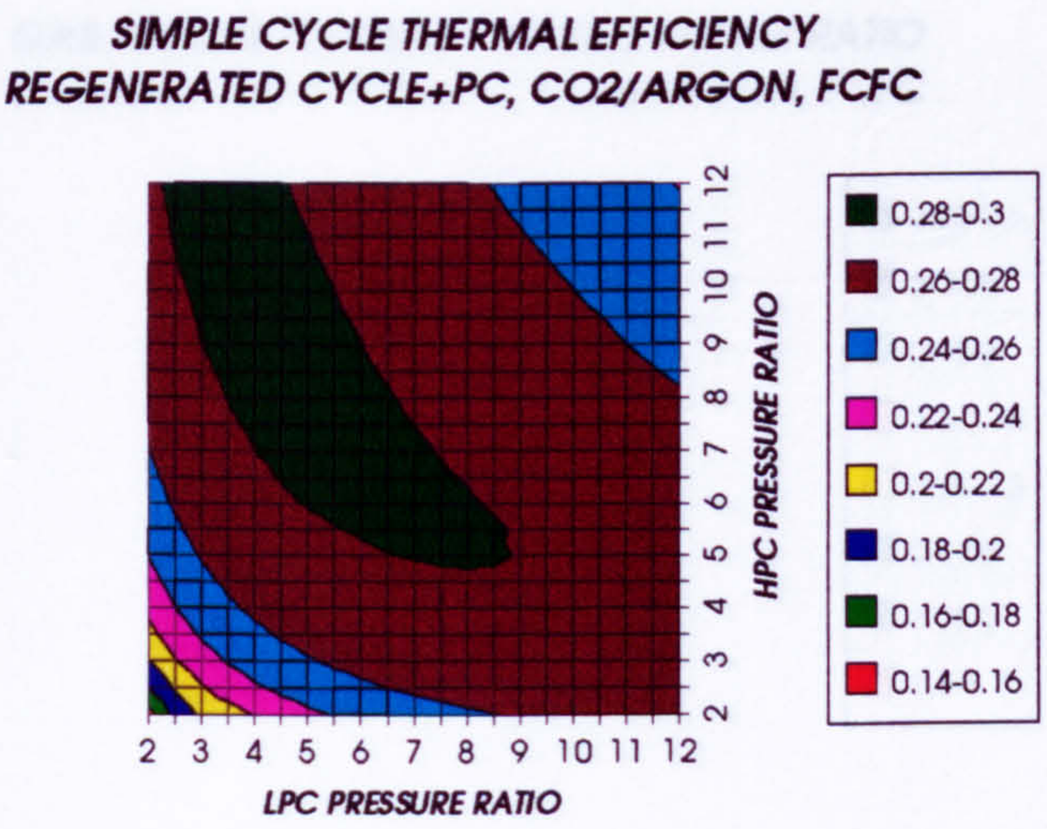

Figure 51. Simple cycle thermal efficiency

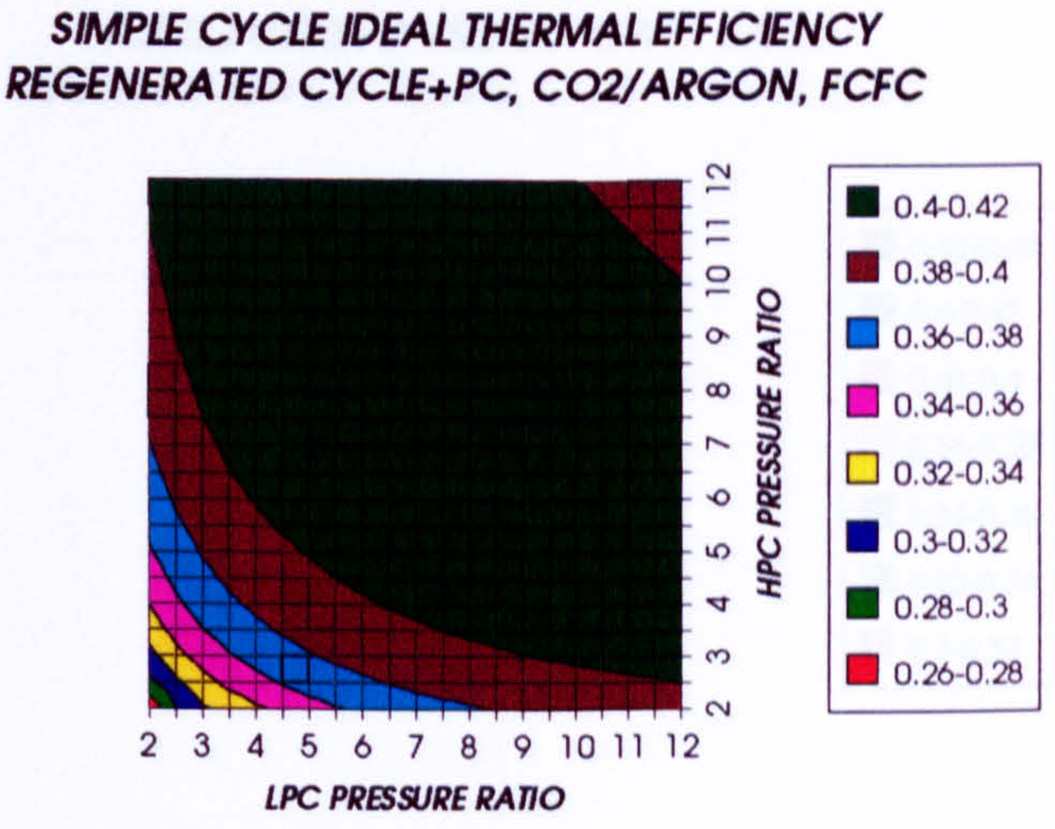

Figure 52. Simple cycle ideal thermal efficiency

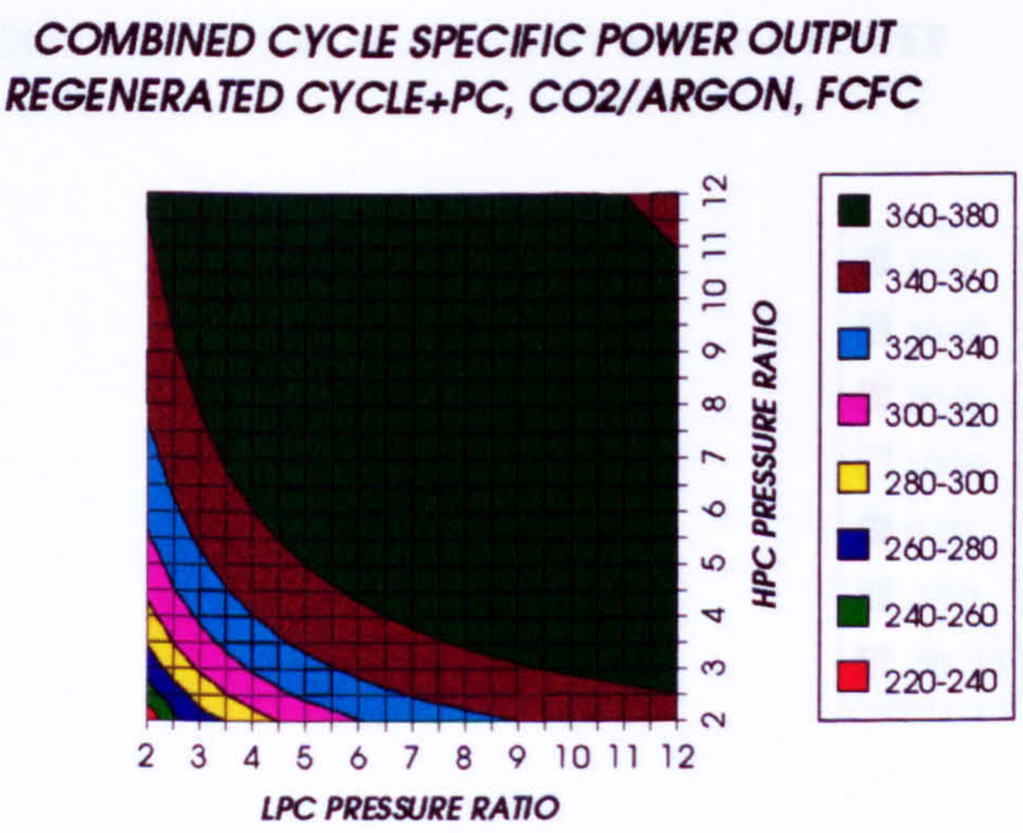

Figure 53. Combined cycle specific power output

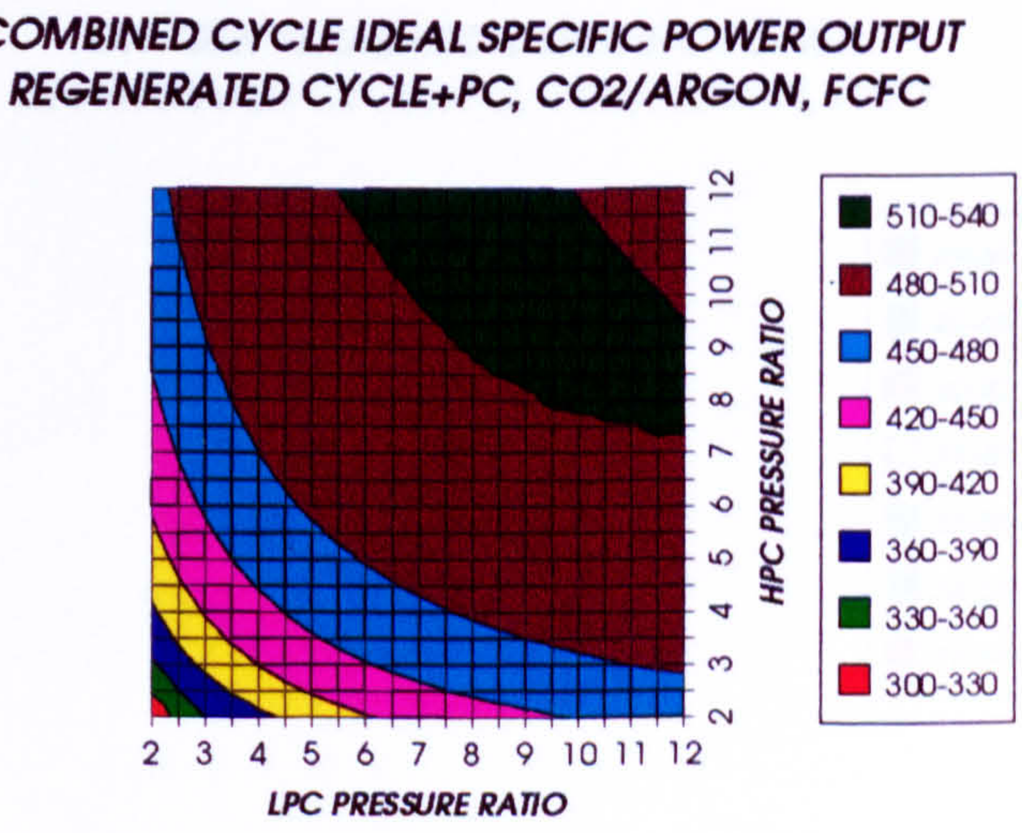

Figure54. Combined cycle ideal specific power output

COMPLETE PLANT WITH CRYOGENIC PRECOOLING (TET=1650 K)

GAS TURBINE SPECIFIC POWER OUTPUT REGENERATED CYCLE+PC, CO2/ARGON, FCFC

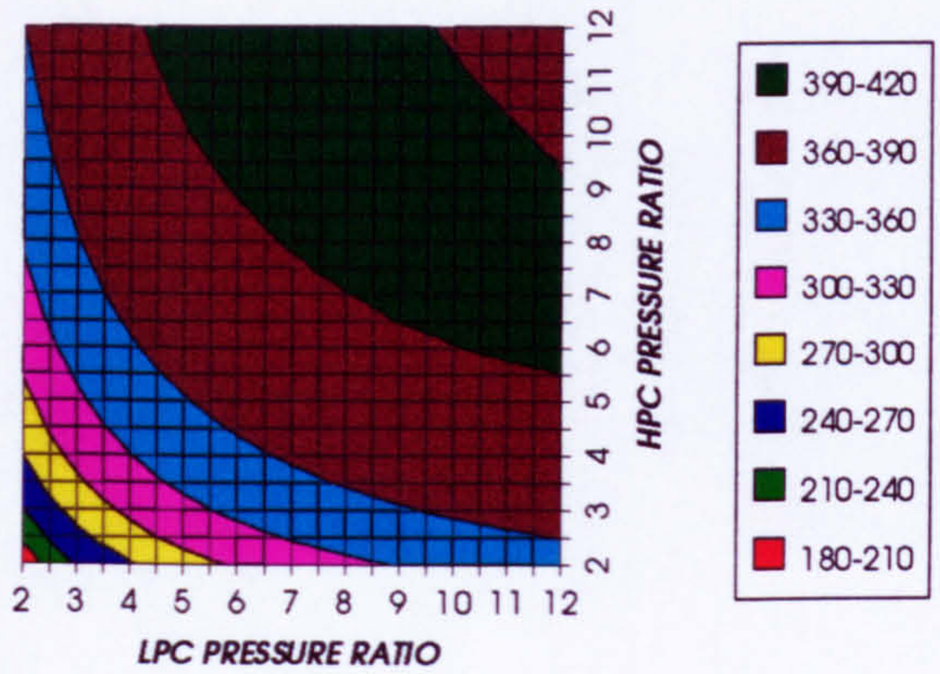

Figure 55. Gas turbine specific power output

STEAM TURBINE SPECIFIC POWER OUTPUT REGENERATED CYCLE+PC, CO2/ARGON, FCFC

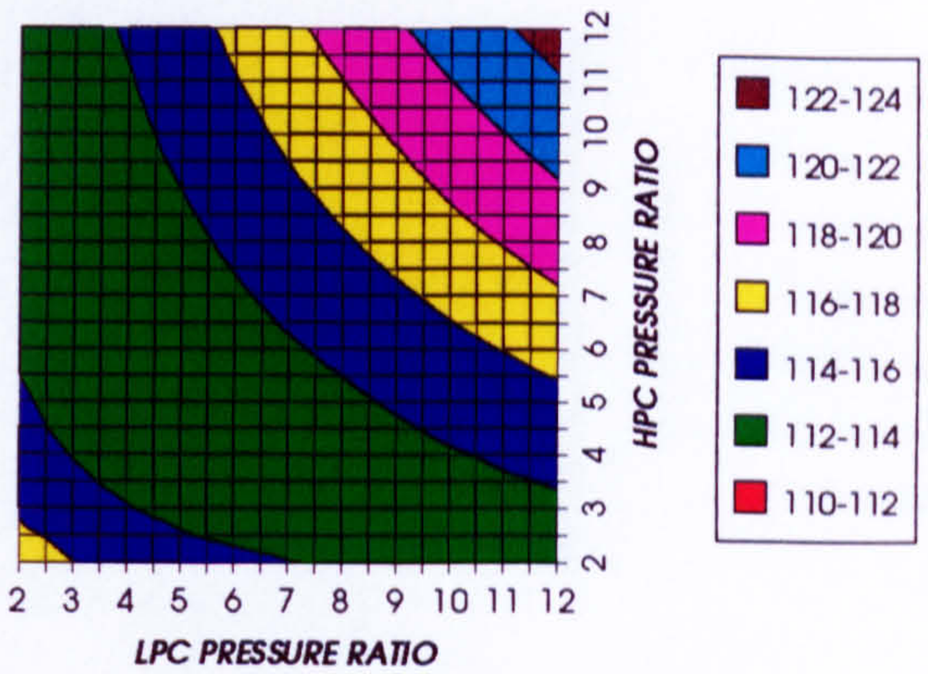

Figure 56. Steam turbine specific power output

GAS TURBINE TO STEAM TURBINE POWER RATIO REGENERATED CYCLE+PC, CO2/ARGON, FCFC

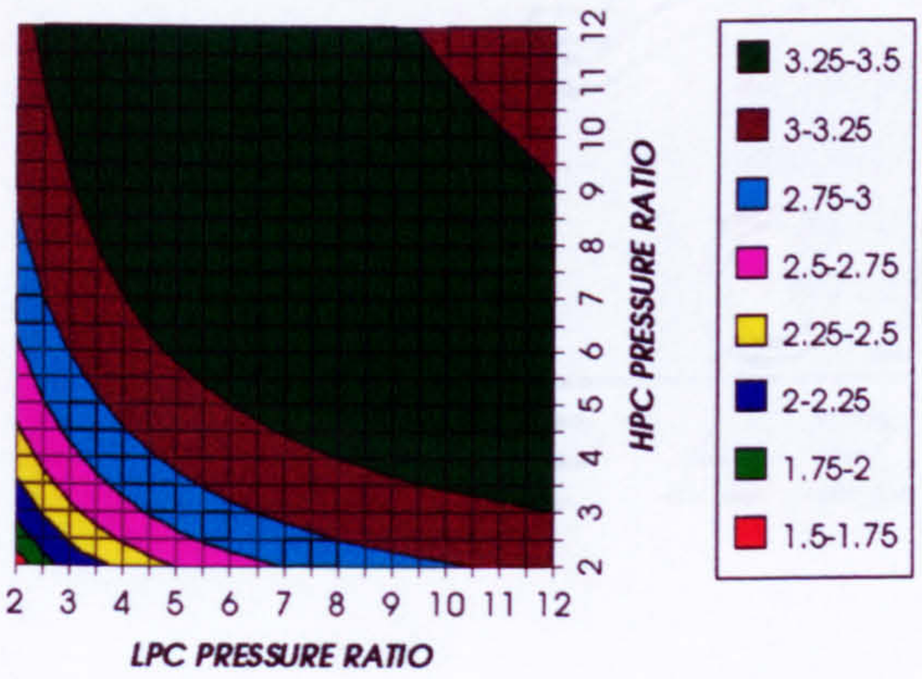

Figure 57. Gas turbine to steam turbine power ratio

AUXILIARIES TO USEFUL POWER RATIO REGENERATED CYCLE+PC, CO2/ARGON, FCFC

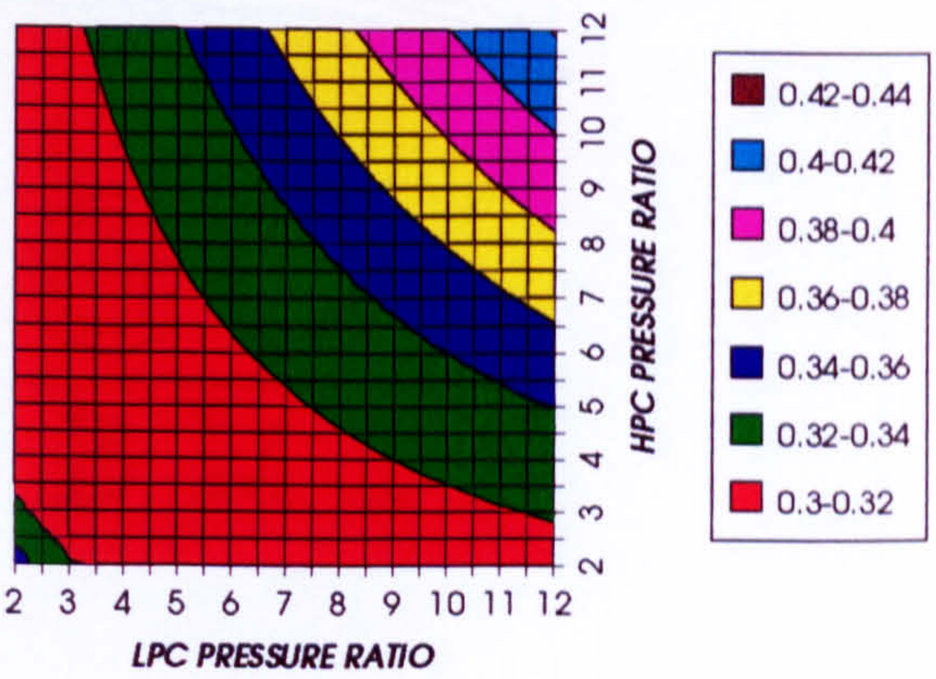

Figure 58. Auxiliary (CO2/Argon, O2 & Fuel) to usefuel power ratio

CO2 COMPRESSION AUXILIARY SPECIFIC POWER REGENERATED CYCLE+PC, CO2/ARGON, FCFC

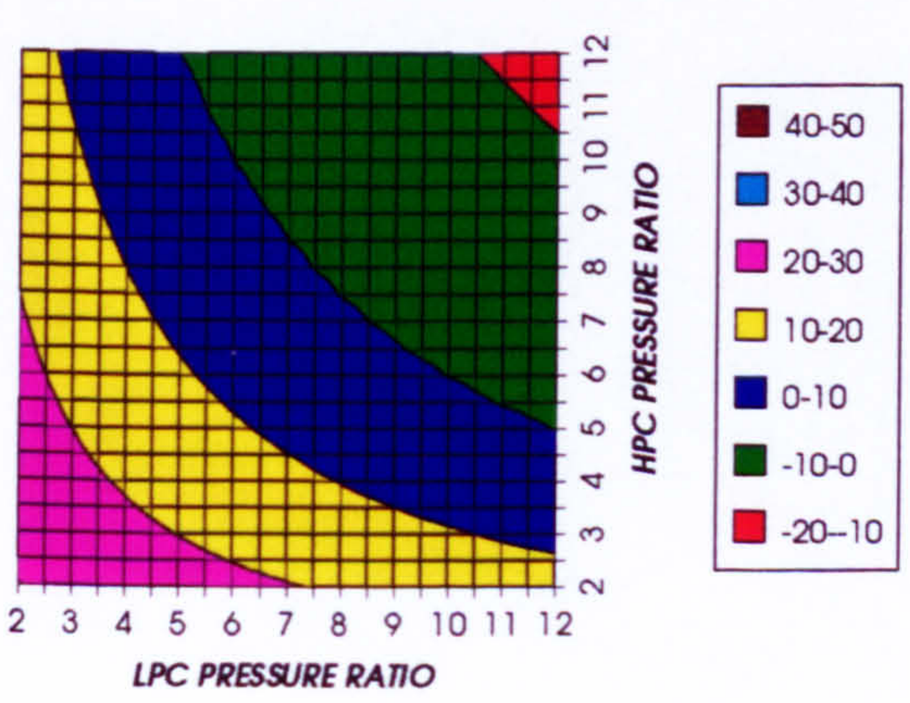

Figure 59. CO2/Argon compression specific power

OXYGEN SEPARATION SPECIFIC POWER REGENERATED CYCLE+PC, CO2/ARGON, FCFC

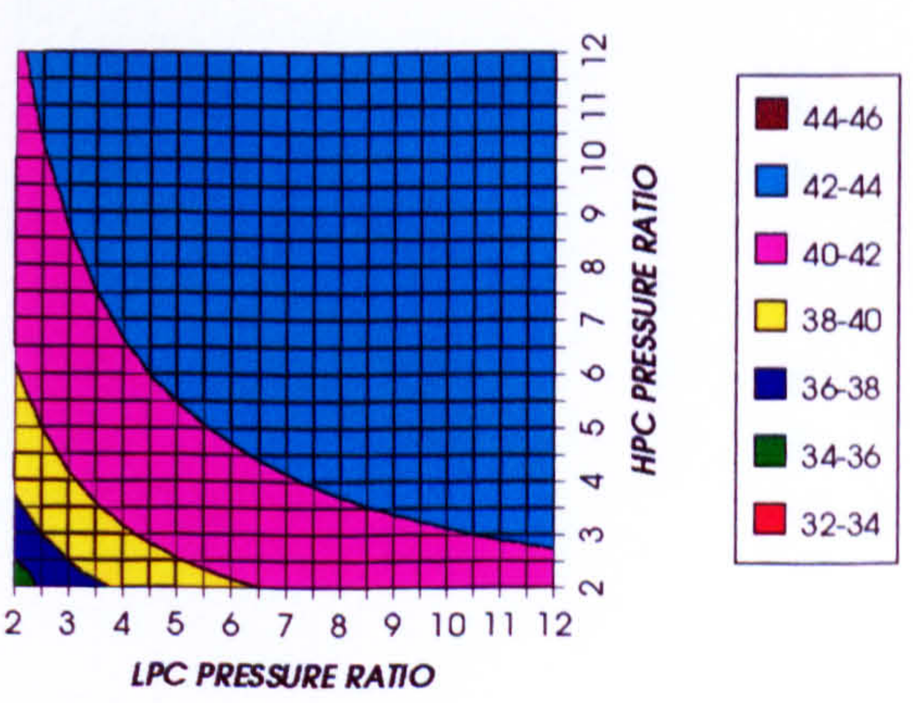

Figure 60. Oxygen separation specific power

COMPLETE PLANT WITH CRYOGENIC PRECOOLING (TET=1650 K)

FUEL COMPRESSION SPECIFIC POWER
REGENERATED CYCLE+PC, CO2/ARGON, FCFC

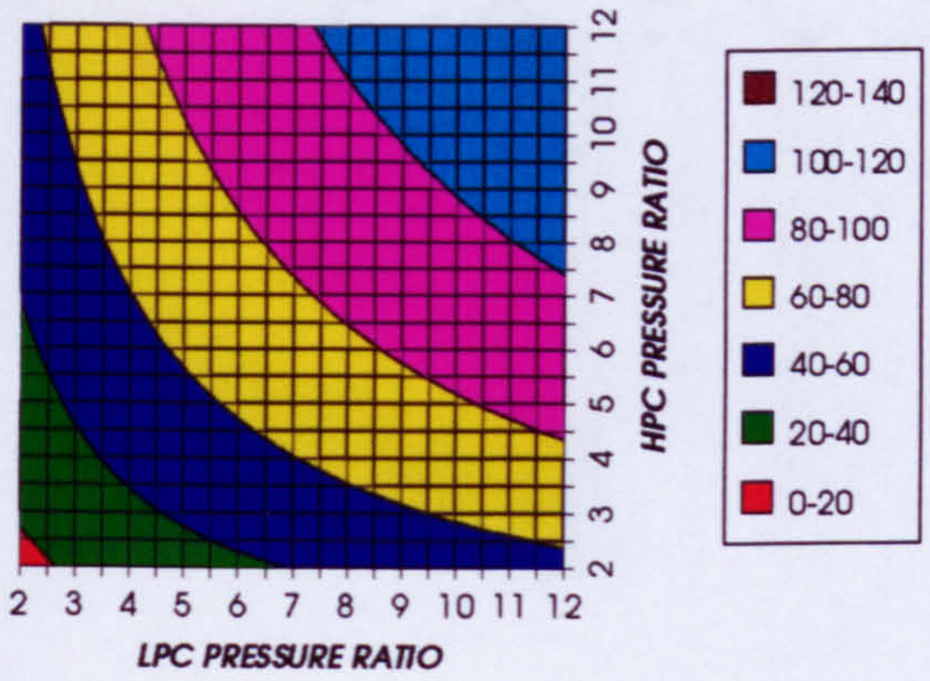

Figure 61. Fuel compression specific power

FUEL TO COMPRESSOR INLET MASS FLOW RATIO
REGENERATED CYCLE+PC, CO2/ARGON, FCFC

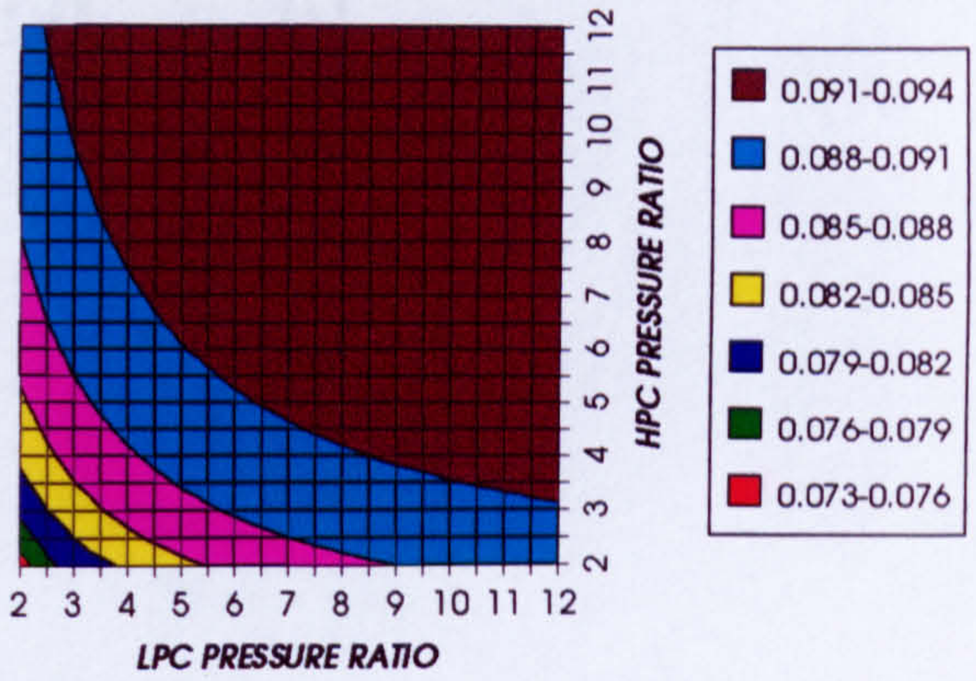

Figure 62. Fuel to compressor inlet mass flow ratio

GAS TURBINE EXIT TEMPERATURE
REGENERATED CYCLE+PC, CO2/ARGON, FCFC

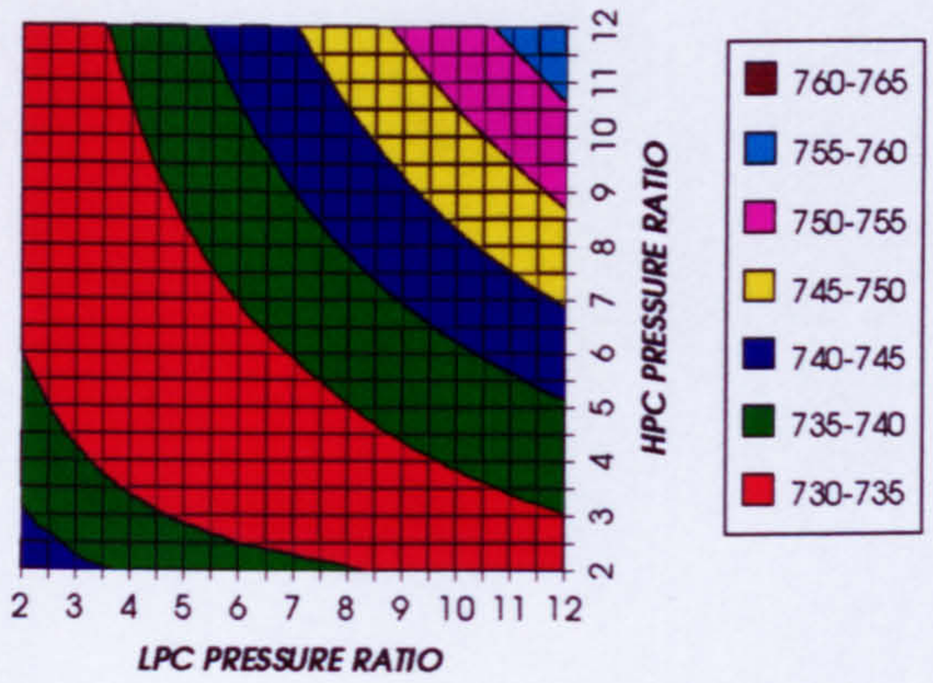

Figure 63. Gas turbine exit temperature

HPT NUMBER OF STAGES
REGENERATED CYCLE+PC, CO2/ARGON, FCFC

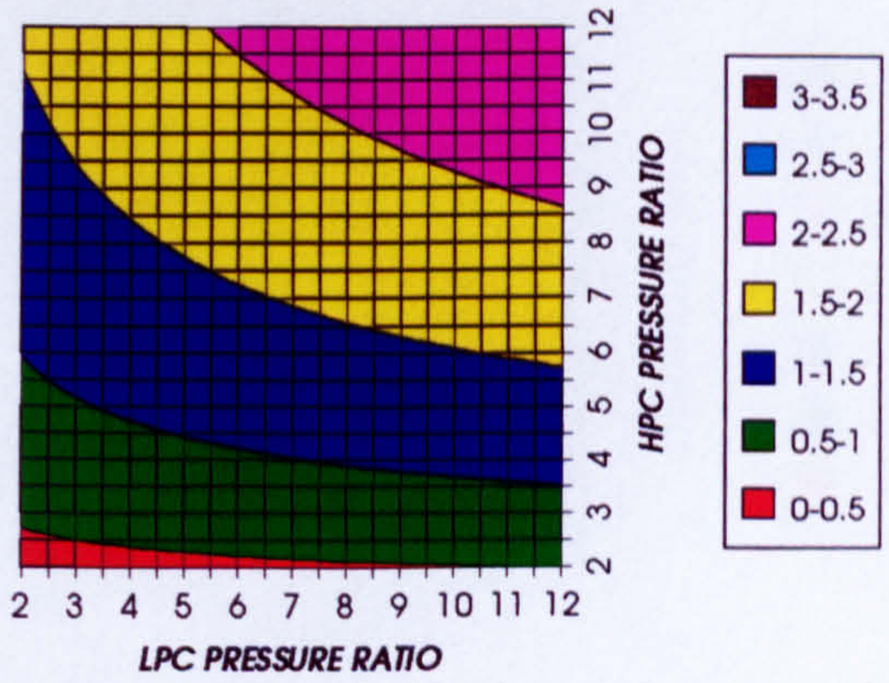

Figure 64. Number of HPT stages

HPT RELATIVE COOLING BLEED (%)
REGENERATED CYCLE+PC, CO2/ARGON, FCFC

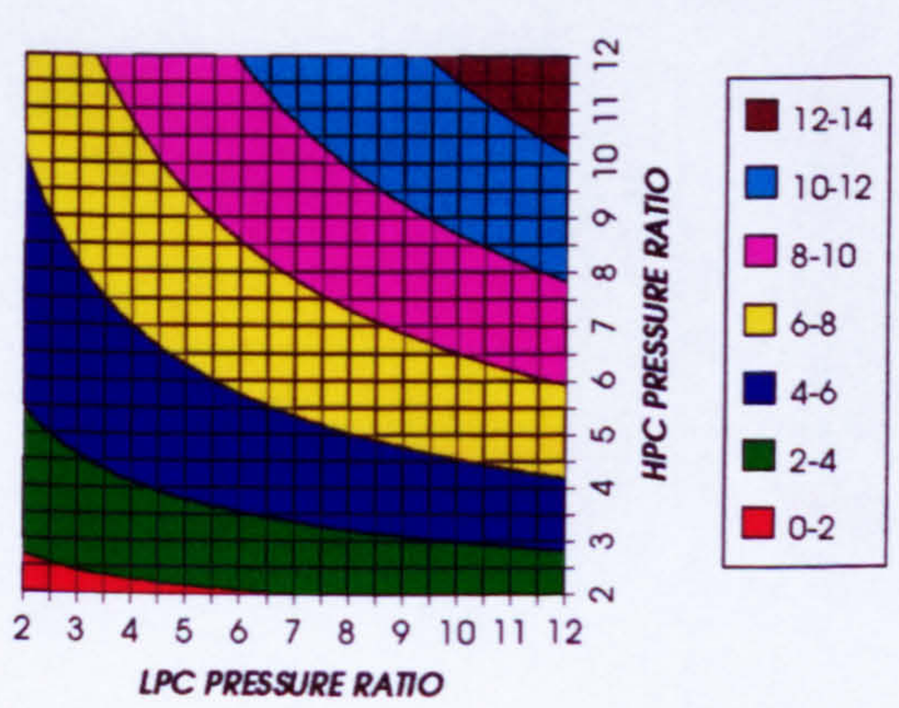

Figure 65. HPT cooling to compressor inlet mass flow ratio

HPT NGVs RELATIVE COOLING BLEED (%)
REGENERATED CYCLE+PC, CO2/ARGON, FCFC

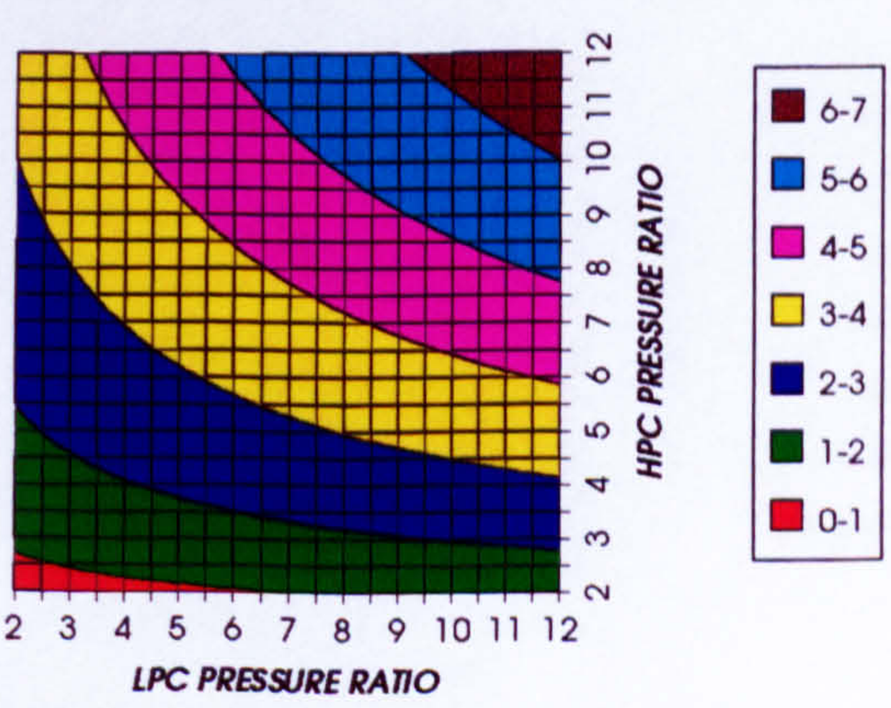

Figure 66. HPT NGVs cooling to compressor inlet mass flow ratio

COMPLETE PLANT WITH CRYOGENIC PRECOOLING (TET=1650 K)

HPT ROTOR RELATIVE COOLING BLEED (%)
REGENERATED CYCLE+PC, CO2/ARGON, FCFC

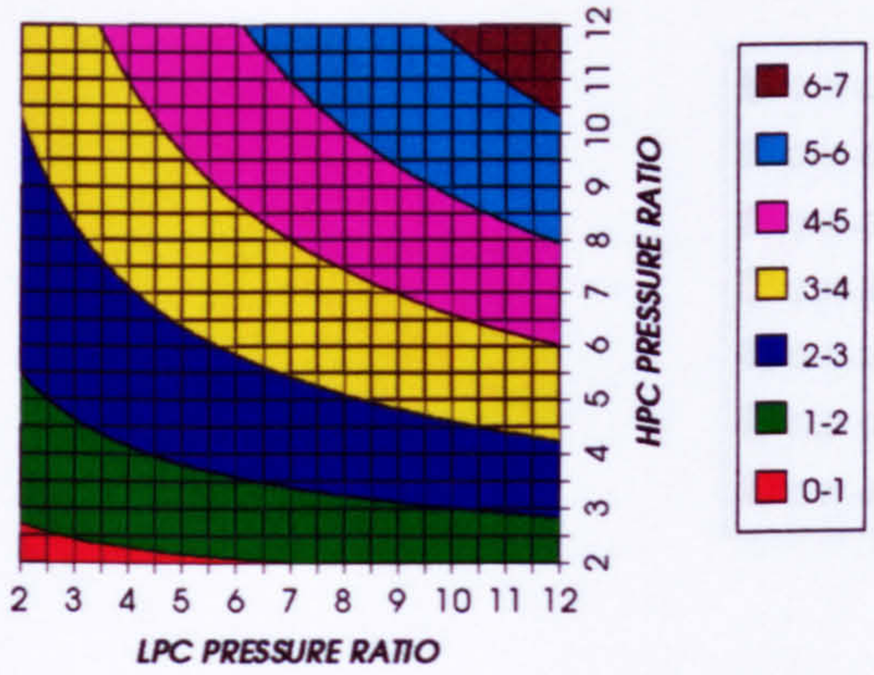

Figure 67. HPT rotor cooling to compressor inlet mass flow ratio

LPT NUMBER OF STAGES
REGENERATED CYCLE+PC, CO2/ARGON, FCFC

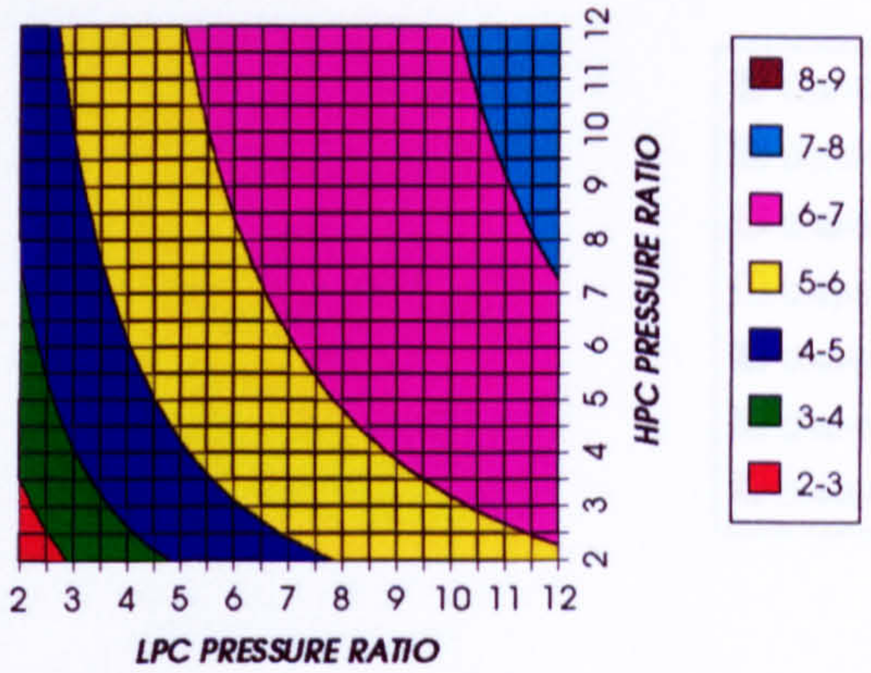

Figure 68. Number of LPT stages

LPT RELATIVE COOLING BLEED (%)
REGENERATED CYCLE+PC, CO2/ARGON, FCFC

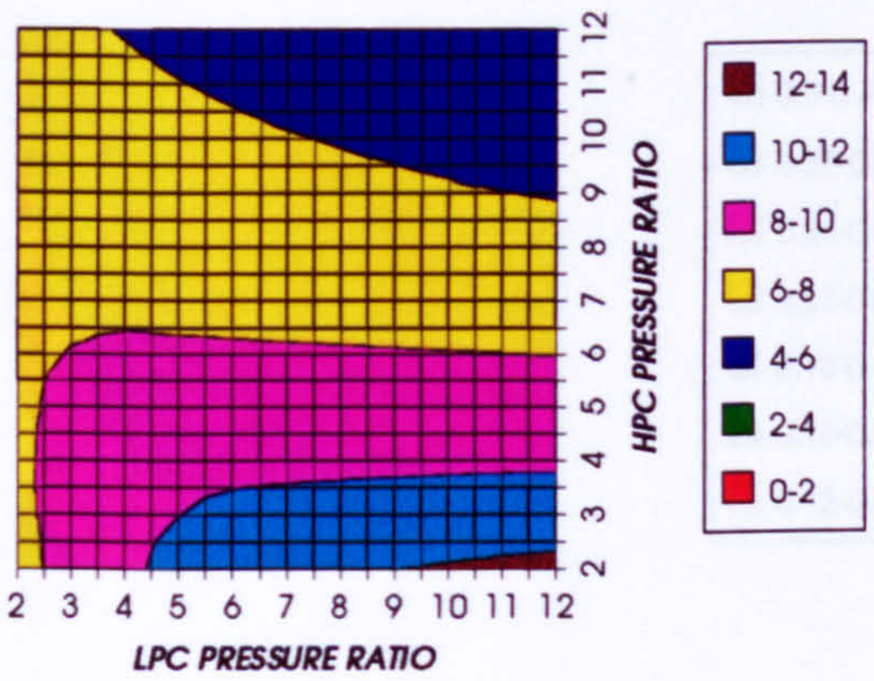

Figure 69. LPT cooling to compressor inlet mass flow ratio

LPT NGVs RELATIVE COOLING BLEED (%)
REGENERATED CYCLE+PC, CO2/ARGON, FCFC

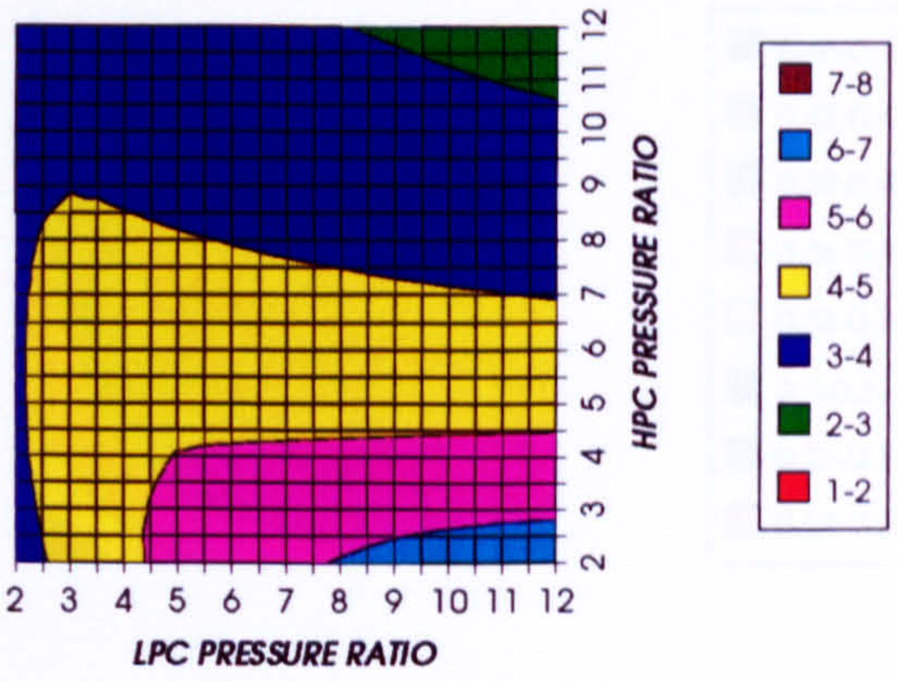

Figure 70. LPT NGVs cooling to compressor inlet mass flow ratio

LPT ROTOR RELATIVE COOLING BLEED (%)
REGENERATED CYCLE+PC, CO2/ARGON, FCFC

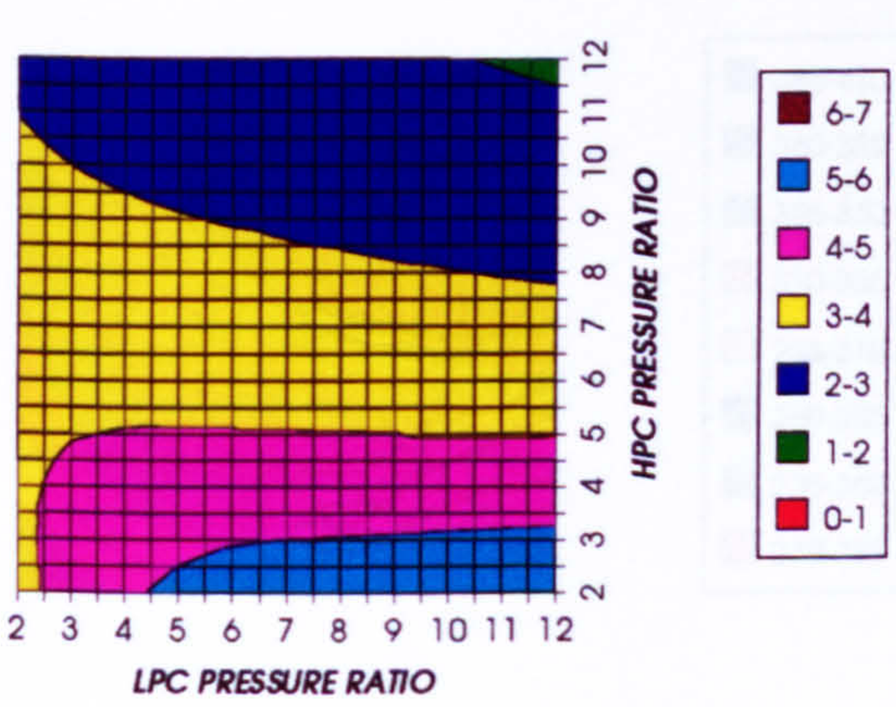

Figure 71. LPT rotor cooling to compressor inlet mass flow ratio

STEAM TURBINE OPTIMUM PRESSURE
REGENERATED CYCLE+PC, CO2/ARGON, FCFC

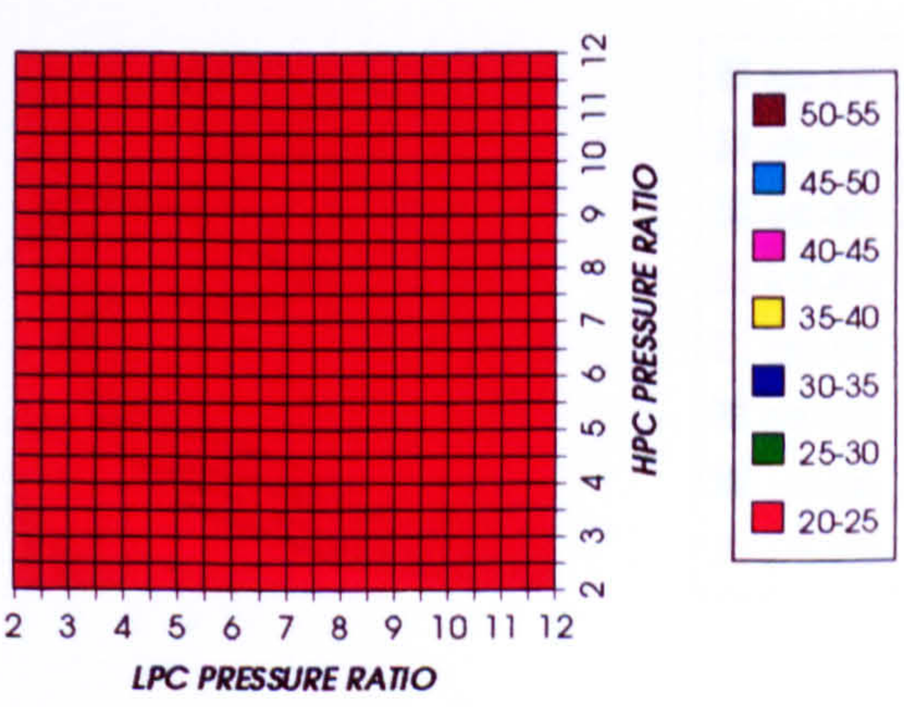

Figure 72. Steam turbine optimum pressures (maximum)

COMPLETE PLANT WITH CRYOGENIC PRECOOLING (TET=1650 K)

COMBINED CYCLE THERMAL EFFICIENCY
INTERCOOLED & REGENERATED+PC, CO2/AR, FCFC

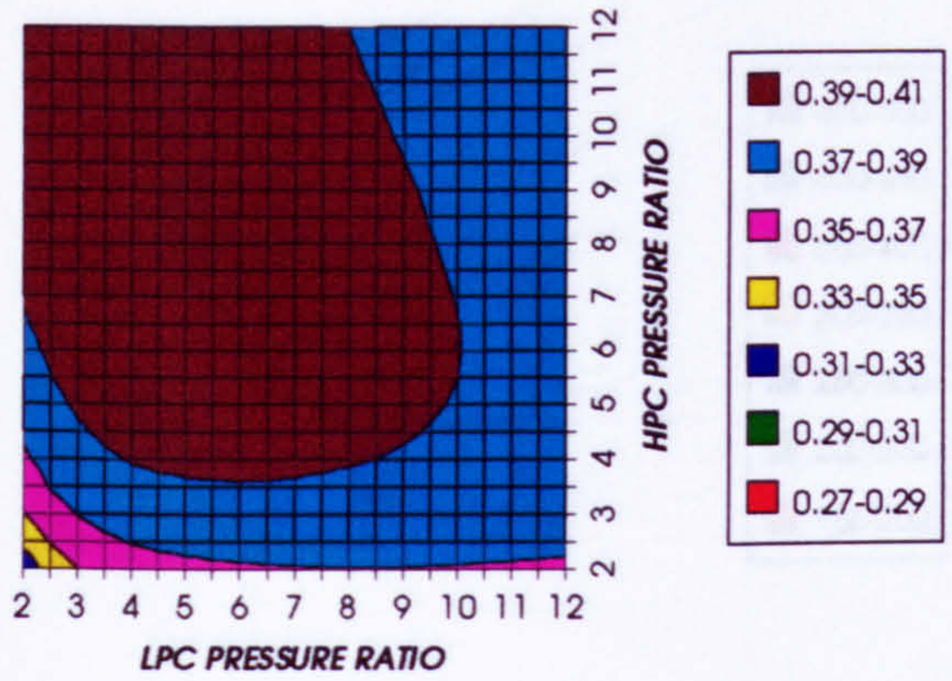

Figure 73. Combined cycle thermal efficiency

COMBINED CYCLE IDEAL THERMAL EFFICIENCY
INTERCOOLED & REGENERATED+PC, CO2/AR, FCFC

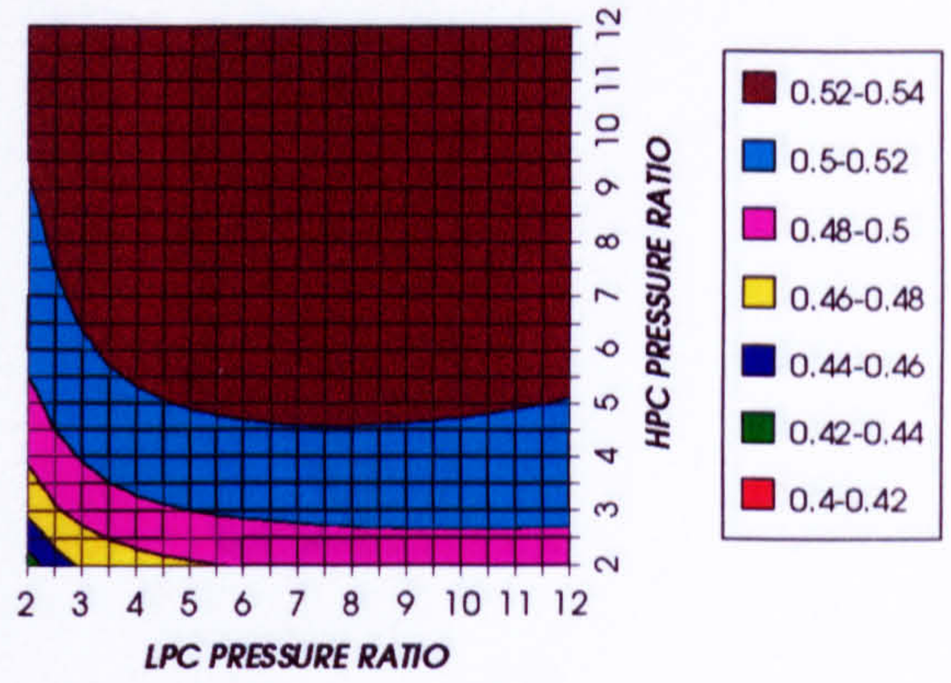

Figure 74. Combined cycle ideal thermal efficiency

SIMPLE CYCLE THERMAL EFFICIENCY
INTERCOOLED & REGENERATED+PC, CO2/AR, FCFC

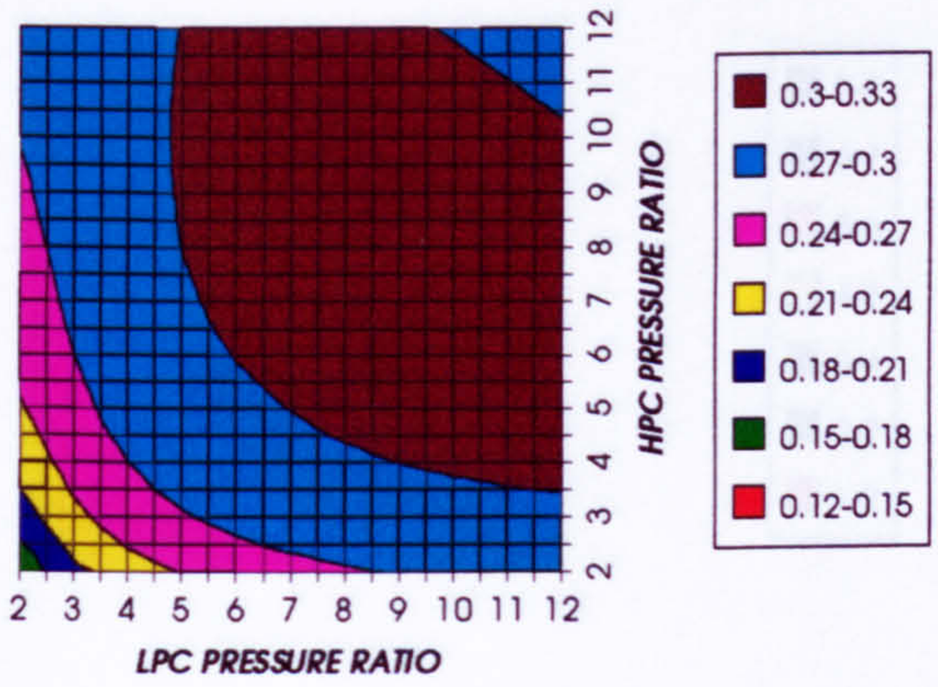

Figure 75. Simple cycle thermal efficiency

SIMPLE CYCLE IDEAL THERMAL EFFICIENCY
INTERCOOLED & REGENERATED+PC, CO2/AR, FCFC

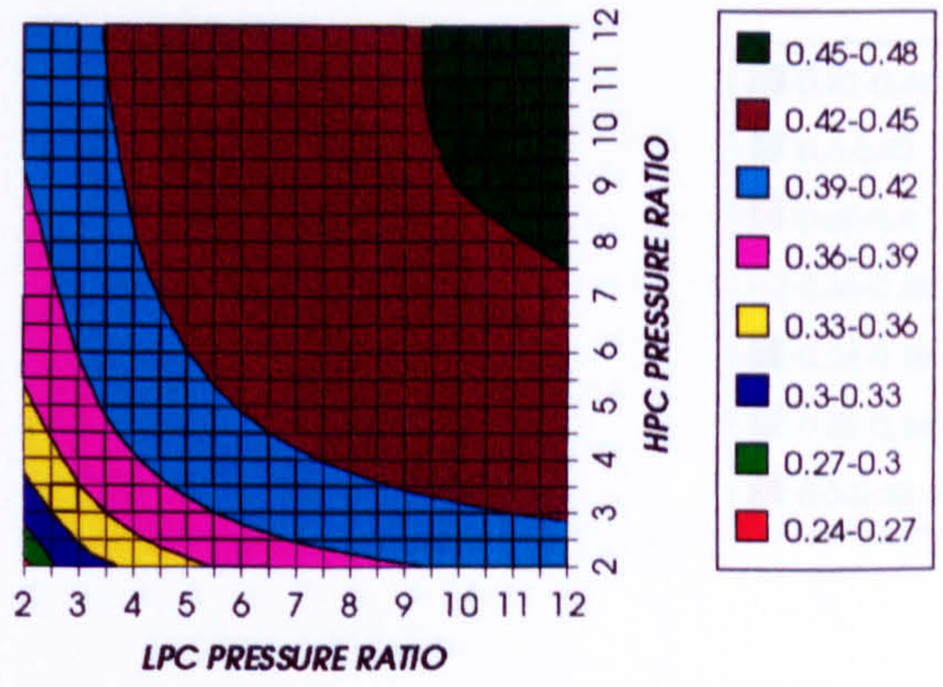

Figure 76. Simple cycle ideal thermal efficiency

COMBINED CYCLE SPECIFIC POWER OUTPUT
INTERCOOLED & REGENERATED+PC, CO2/AR, FCFC

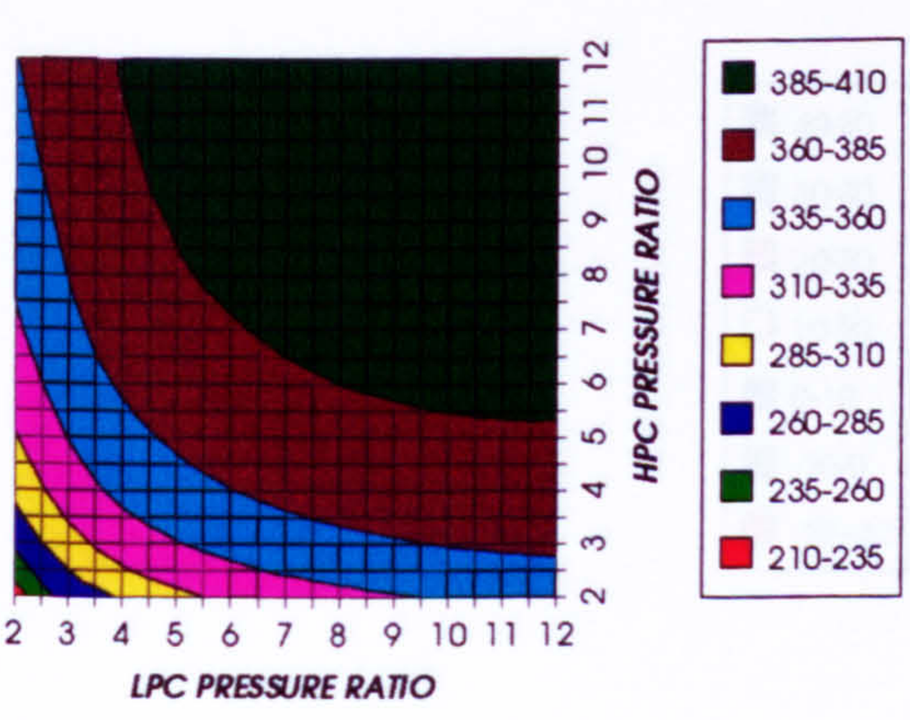

Figure 77. Combined cycle specific power output

COMBINED CYCLE IDEAL SPECIFIC POWER OUTPUT
INTERCOOLED & REGENERATED+PC, CO2/AR, FCFC

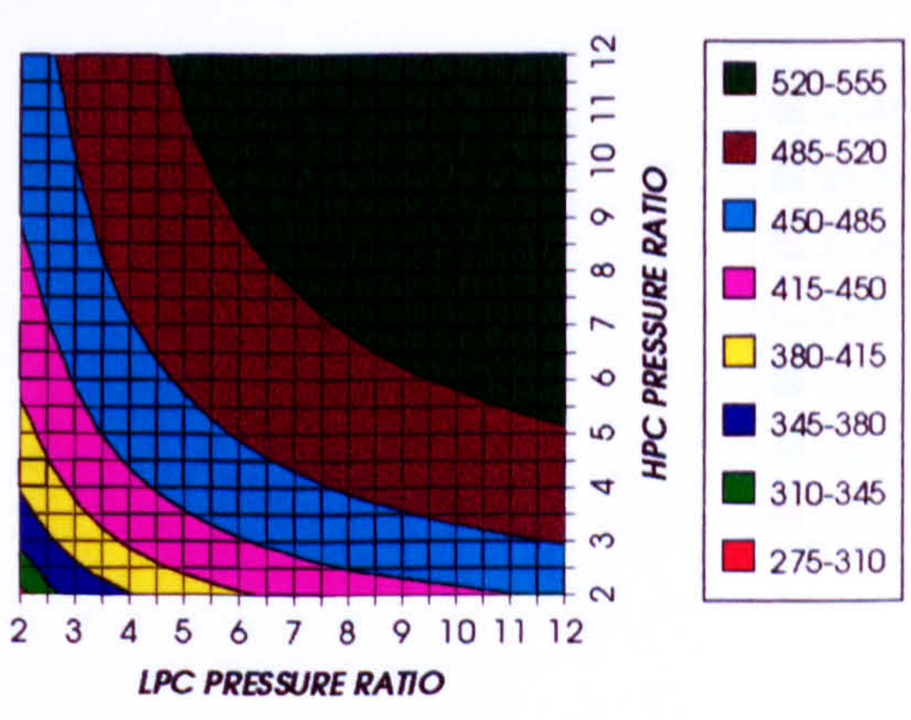

Figure78. Combined cycle ideal specific power output

COMPLETE PLANT WITH CRYOGENIC PRECOOLING (TET=1650 K)

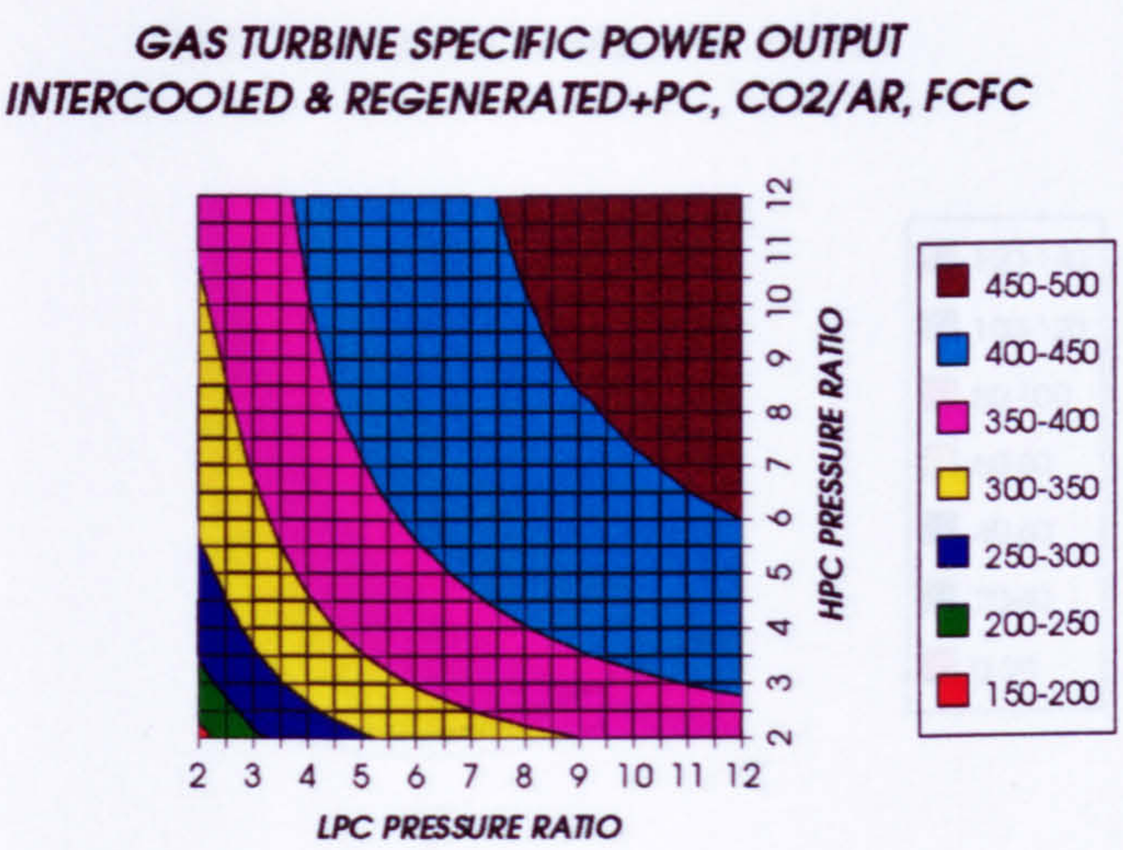

Figure 79. Gas turbine specific power output

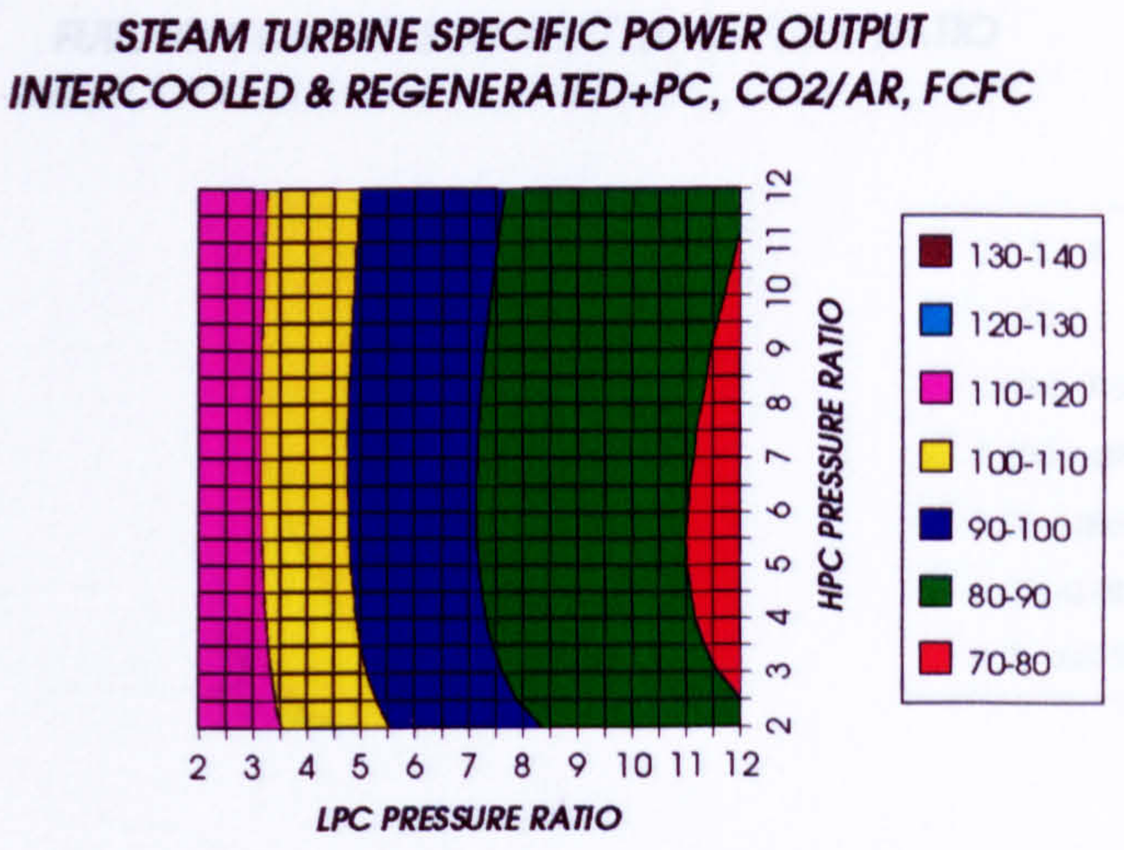

Figure 80. Steam turbine specific power output

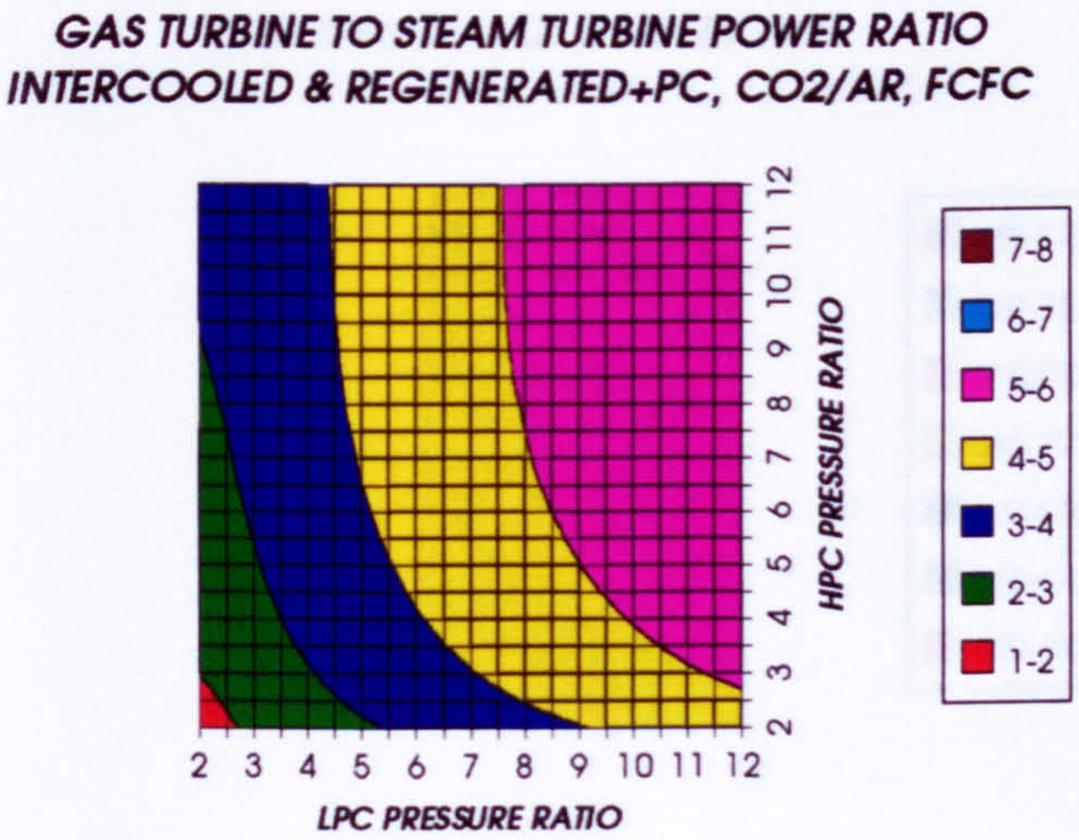

Figure 81. Gas turbine to steam turbine power ratio

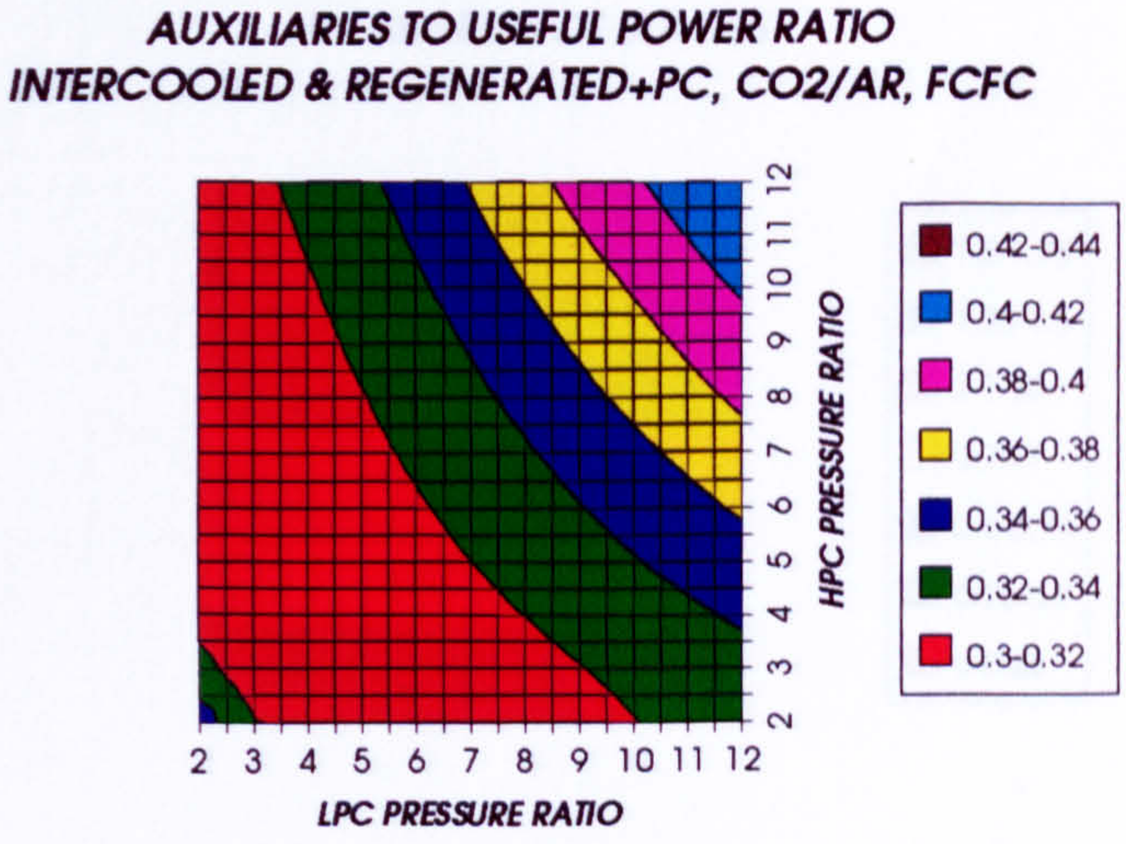

Figure 82. Auxiliary (CO2/Argon, O2 & Fuel) to usefuel power ratio

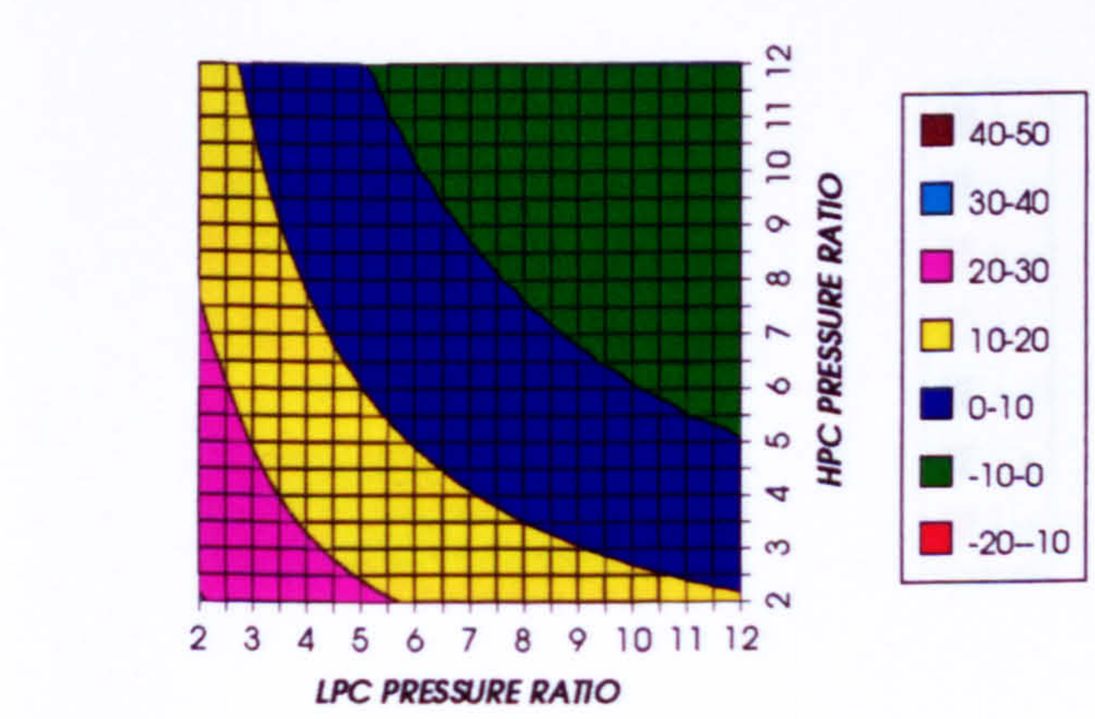

Figure 83. CO2/Argon compression specific power

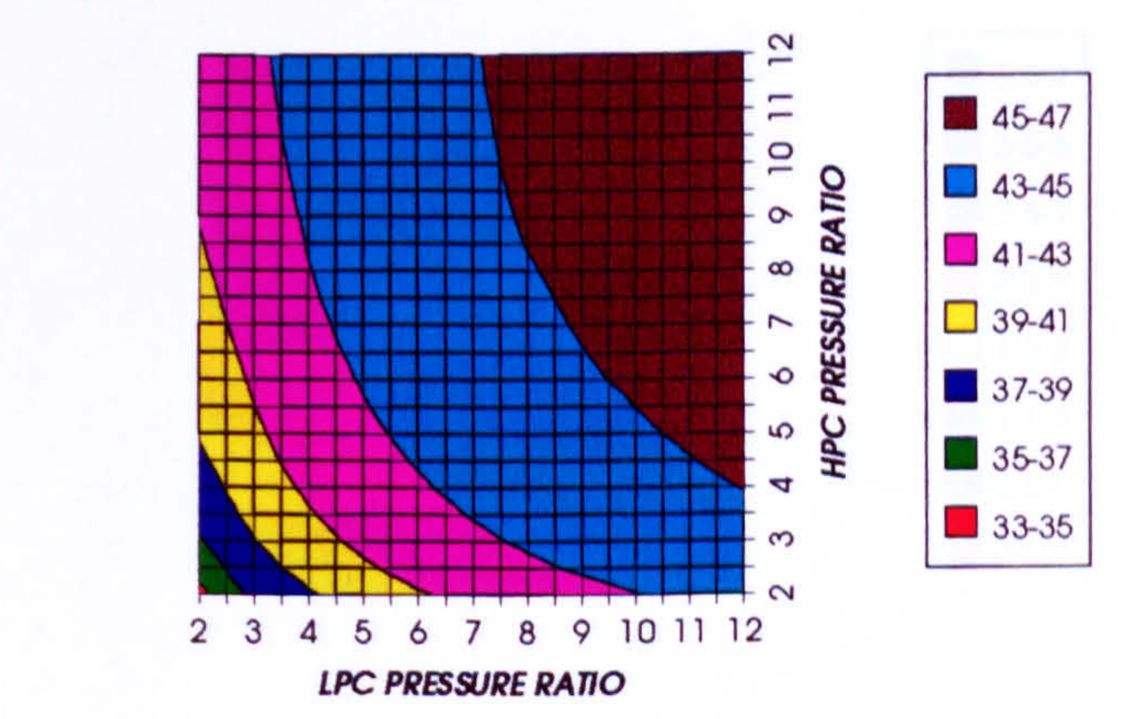

Figure 84. Oxygen separation specific power

COMPLETE PLANT WITH CRYOGENIC PRECOOLING (TET=1650 K)

FUEL COMPRESSION SPECIFIC POWER
INTERCOOLED & REGENERATED+PC, CO2/AR, FCFC

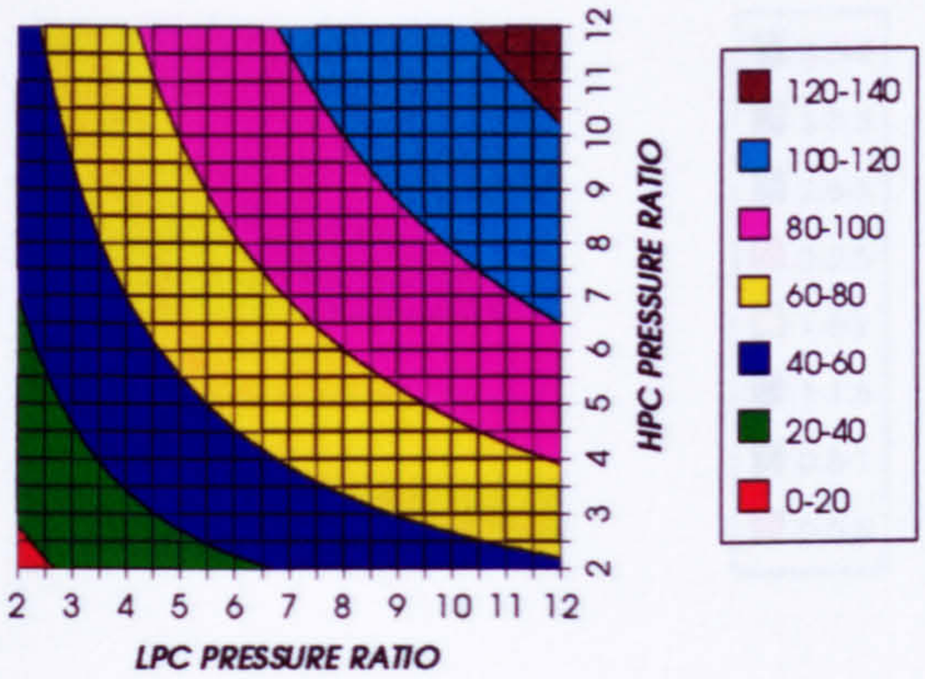

Figure 85. Fuel compression specific power

FUEL TO COMPRESSOR INLET MASS FLOW RATIO
INTERCOOLED & REGENERATED+PC, CO2/AR, FCFC

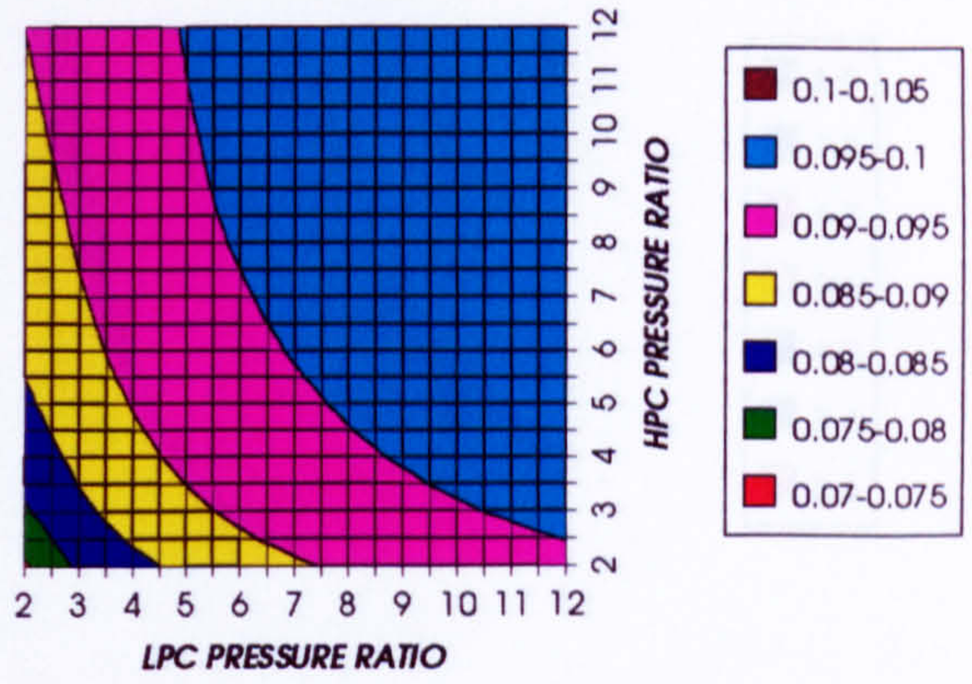

Figure 86. Fuel to compressor inlet mass flow ratio

GAS TURBINE EXIT TEMPERATURE
INTERCOOLED & REGENERATED+PC, CO2/AR, FCFC

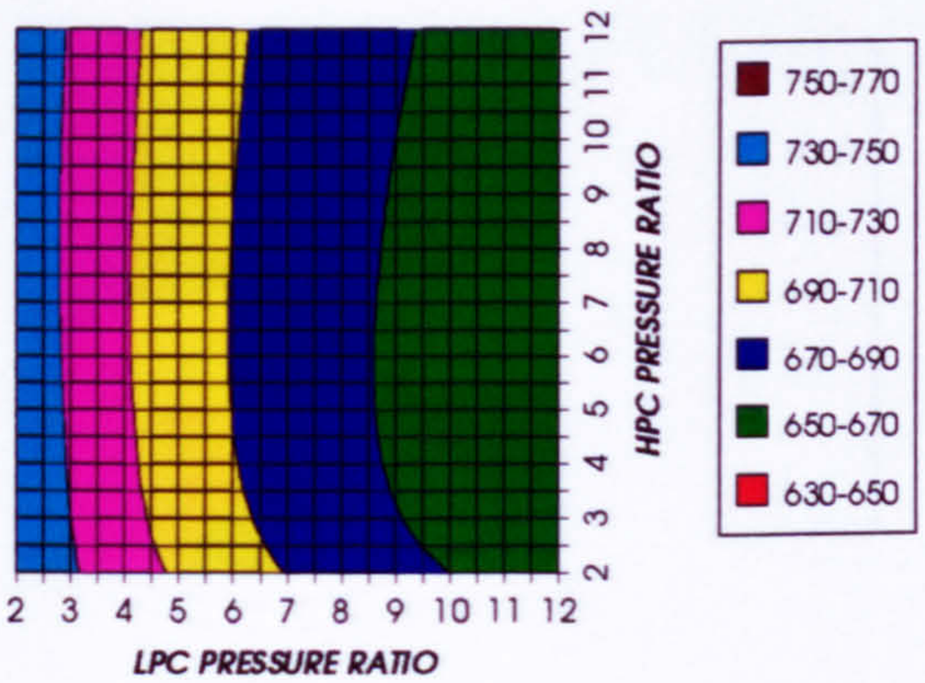

Figure 87. Gas turbine exit temperature (K)

HPT NUMBER OF STAGES
INTERCOOLED & REGENERATED+PC, CO2/AR, FCFC

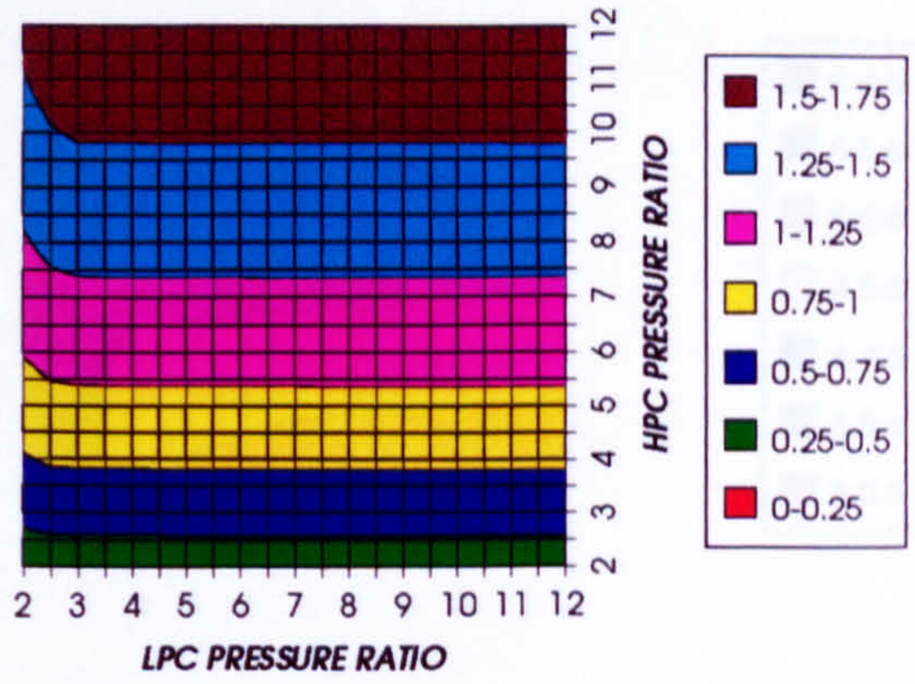

Figure 88. Number of HPT stages

HPT RELATIVE COOLING BLEED (%)
INTERCOOLED & REGENERATED+PC, CO2/AR, FCFC

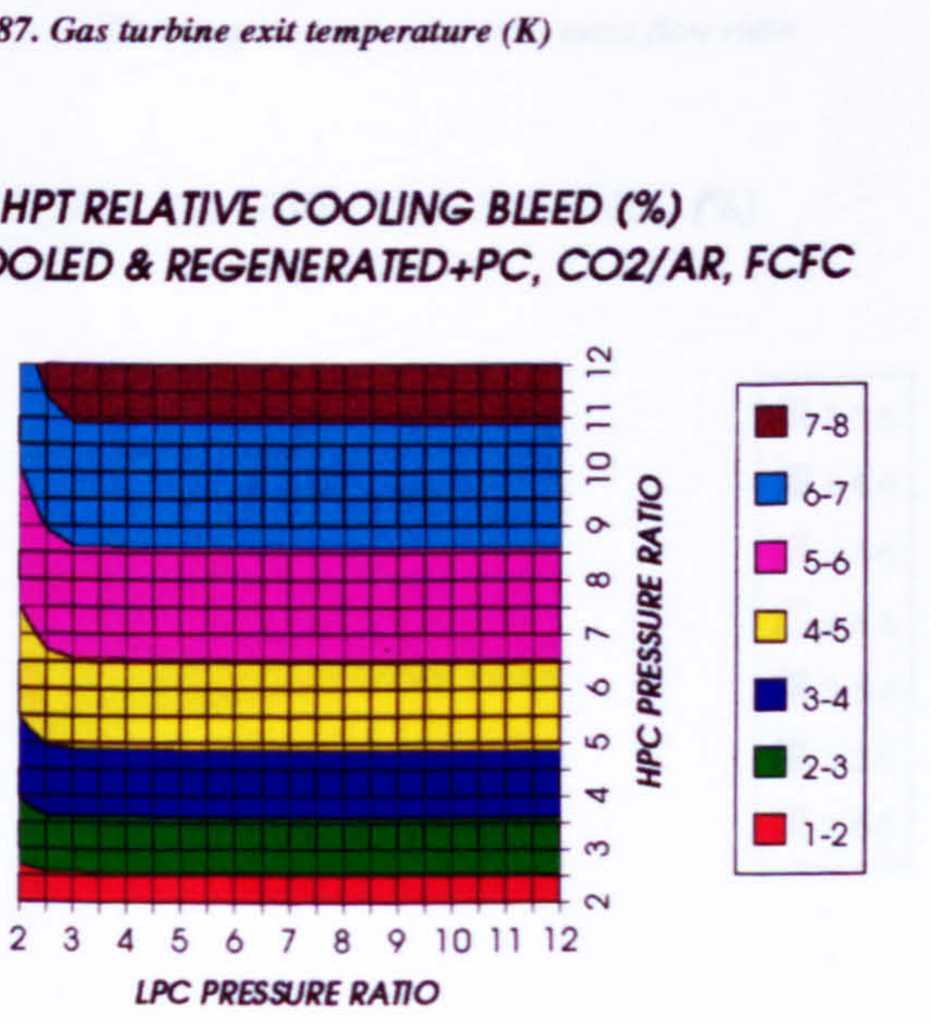

Figure 89. HPT cooling to compressor inlet mass flow ratio

HPT NGVs RELATIVE COOLING BLEED (%)
INTERCOOLED & REGENERATED+PC, CO2/AR, FCFC

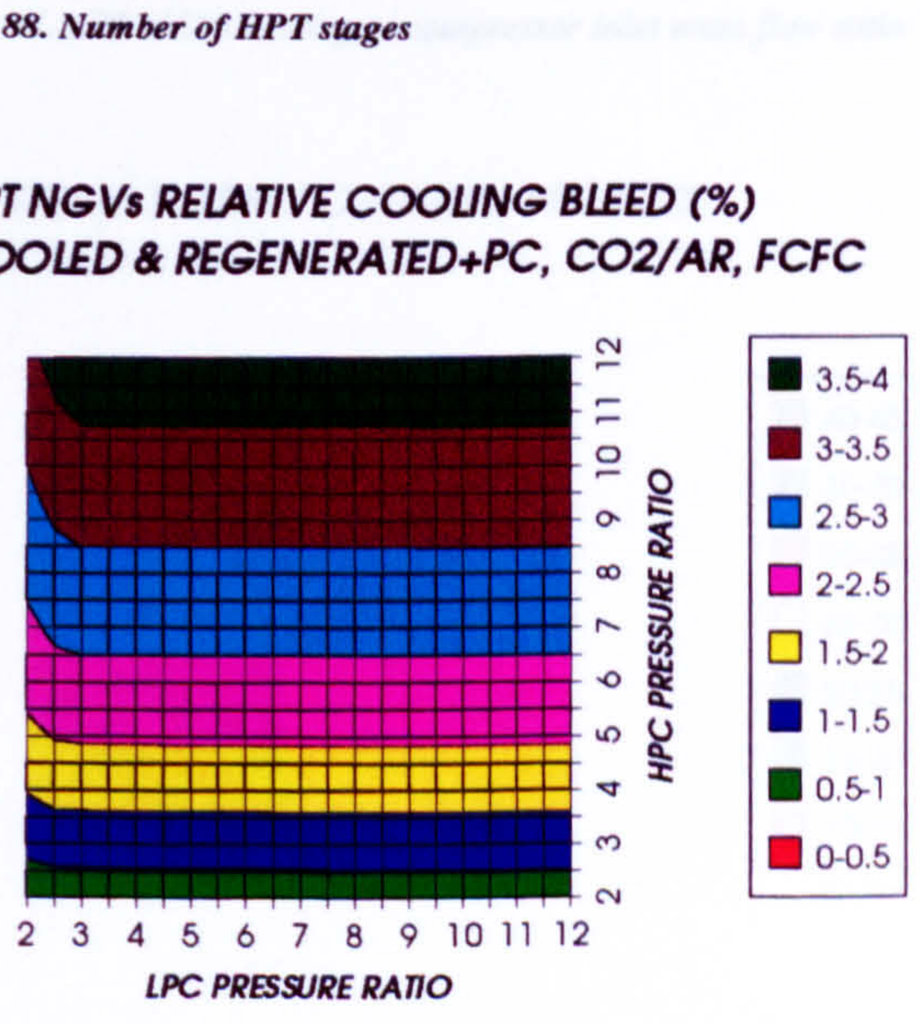

Figure 90. HPT NGVs cooling to compressor inlet mass flow ratio

COMPLETE PLANT WITH CRYOGENIC PRECOOLING (TET=1650 K)

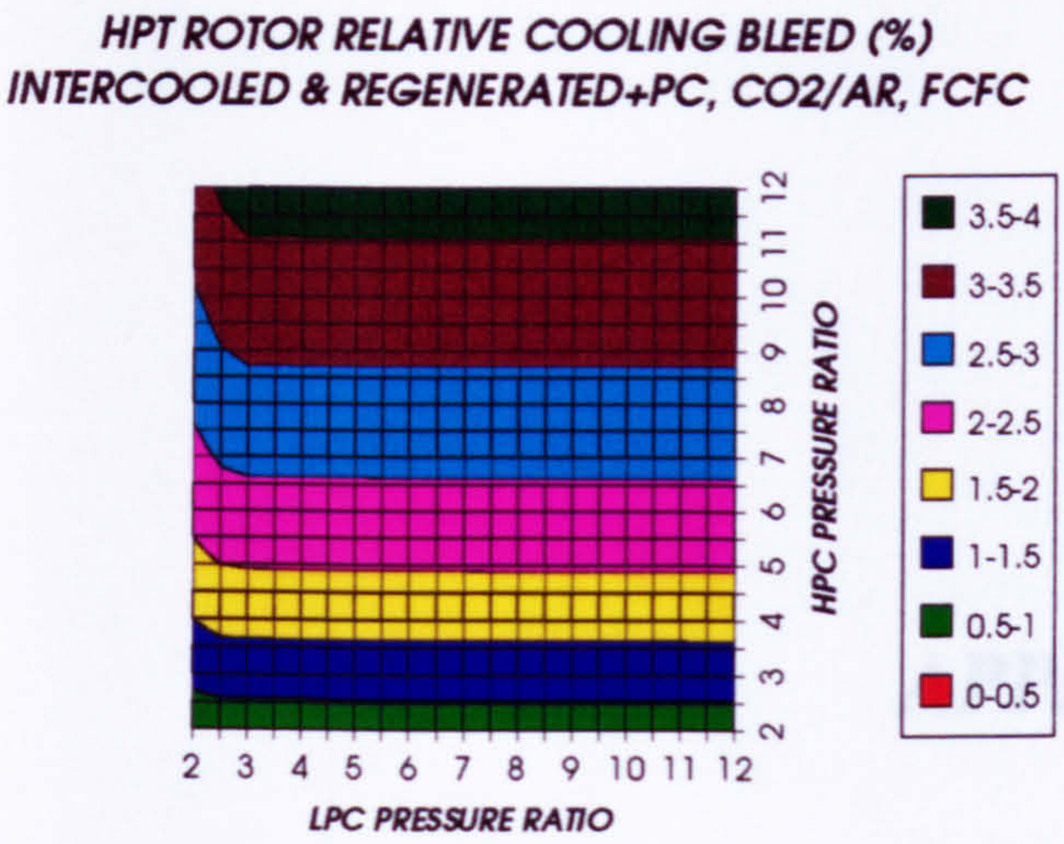

Figure 91. HPT rotor cooling to compressor inlet mass flow ratio

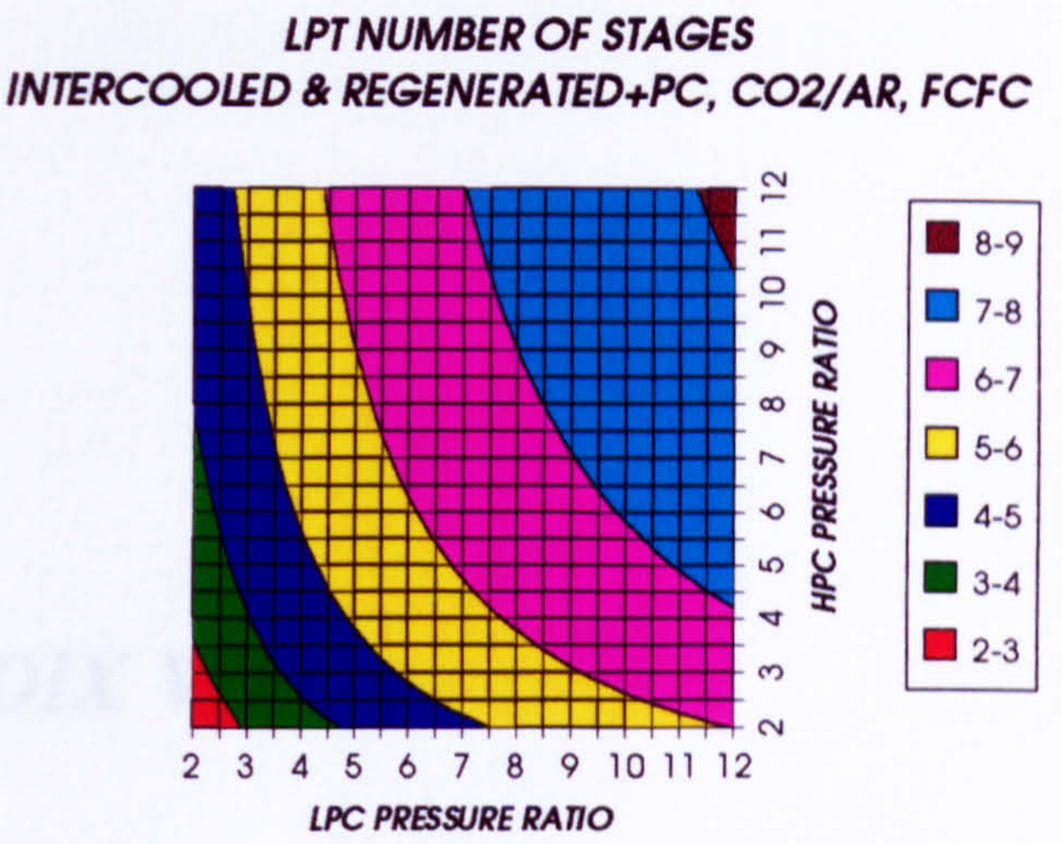

Figure 92. Number of LPT stages

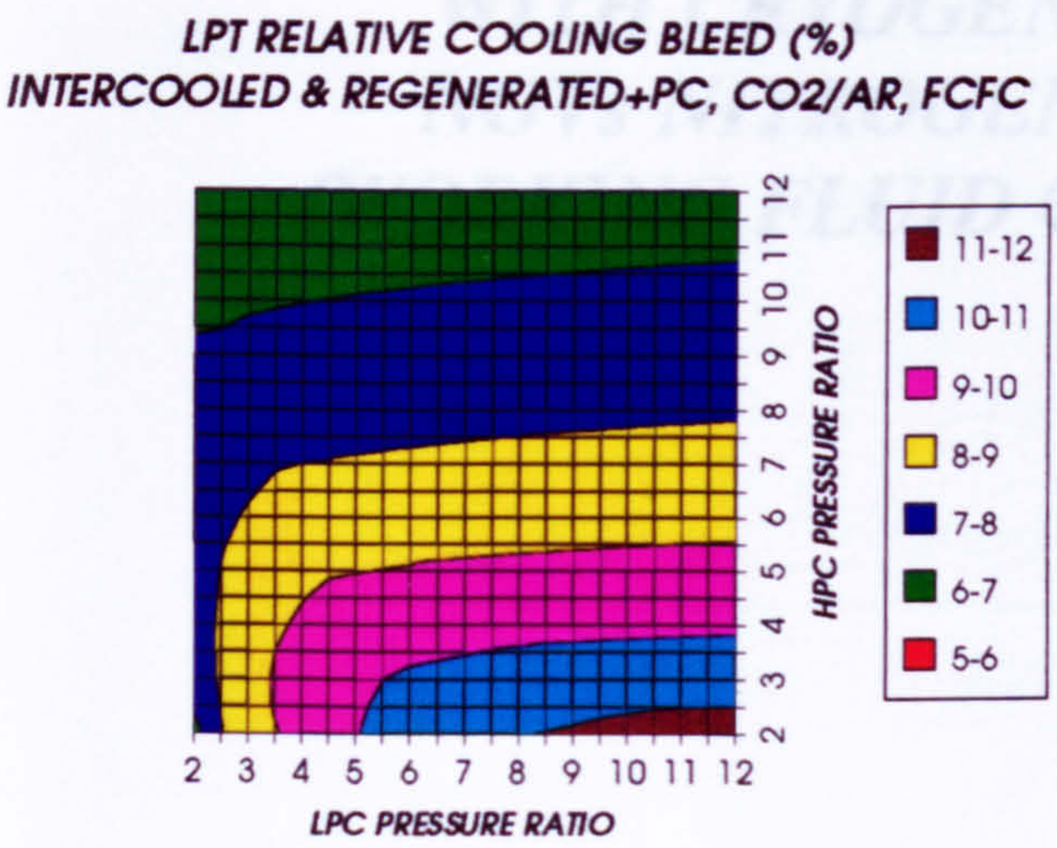

Figure 93. LPT cooling to compressor inlet mass flow ratio

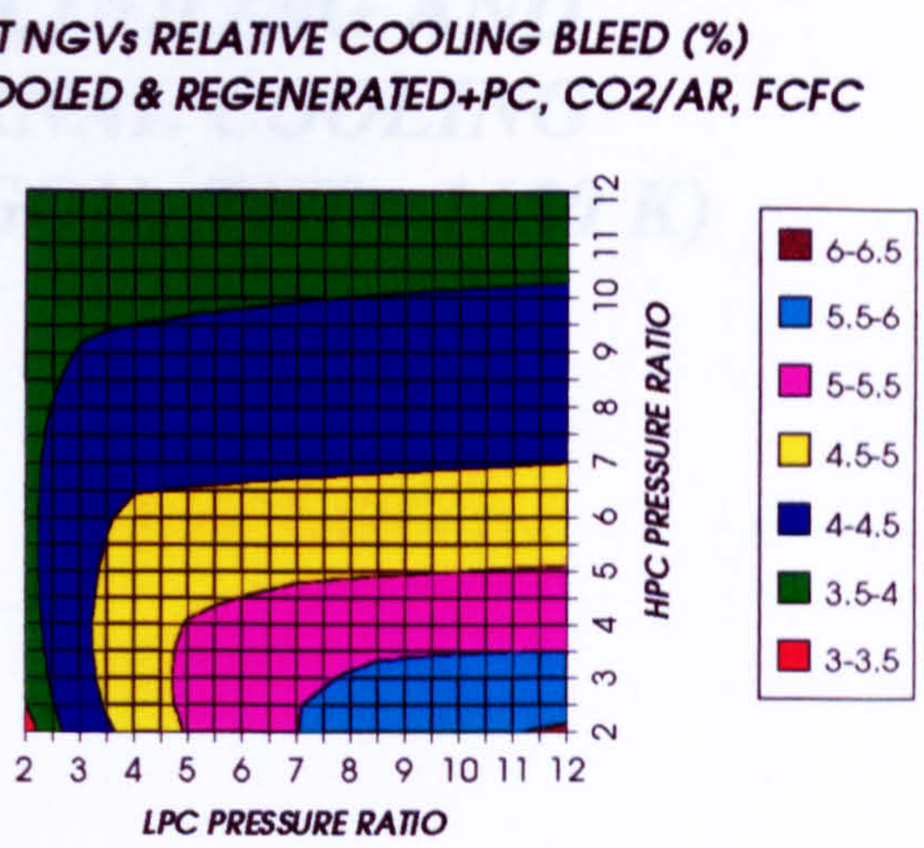

Figure 94. LPT NGVs cooling to compressor inlet mass flow ratio

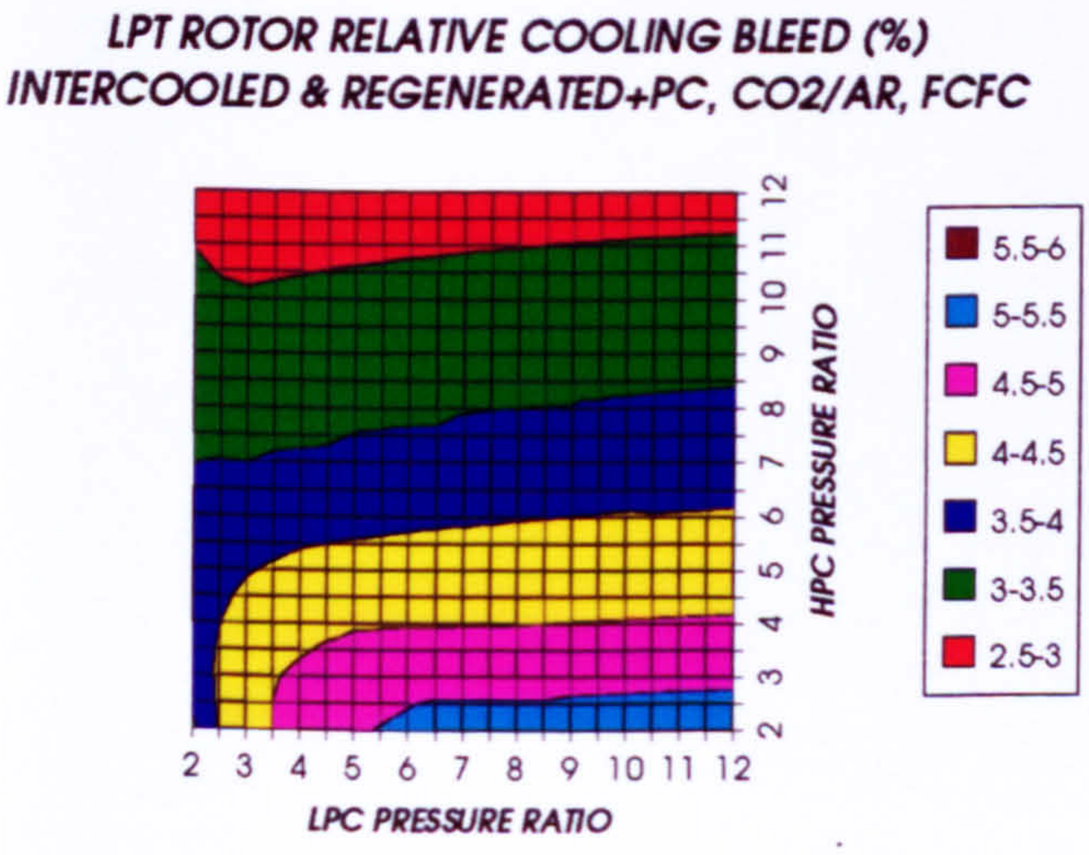

Figure 95. LPT rotor cooling to compressor inlet mass flow ratio

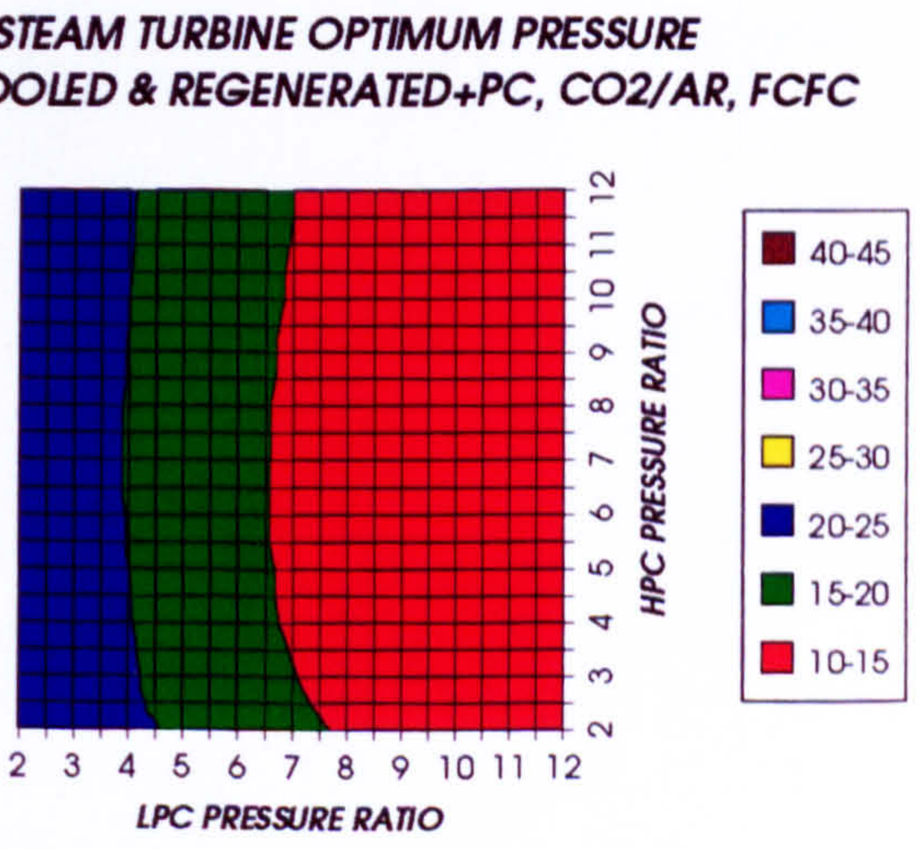

Figure 96. Steam turbine optimum pressures (maximum)

APPENDIX VII

COMPLETE PLANT PERFORMANCE WITH CRYOGENIC PRECOOLING AND NGVs NITROGEN INTERNAL COOLING (WORKING FLUID CO_2/ARGON, TET=1650 K)

COMPLETE PLANT WITH CRYOGENIC PRECOOLER & NGVs N_2 COOLING (TET=1650 K)

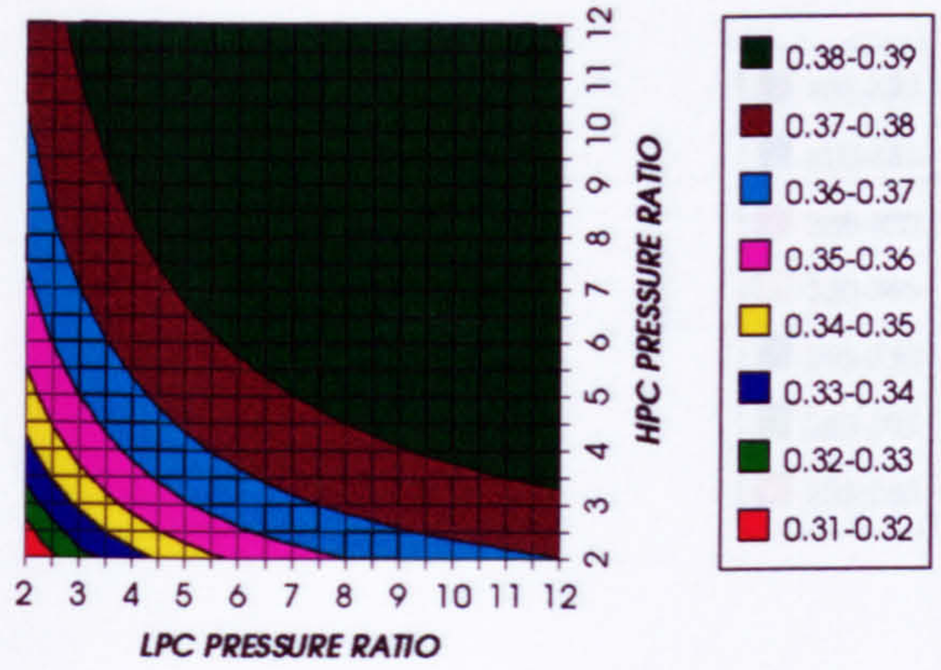

Figure 1. Combined cycle thermal efficiency

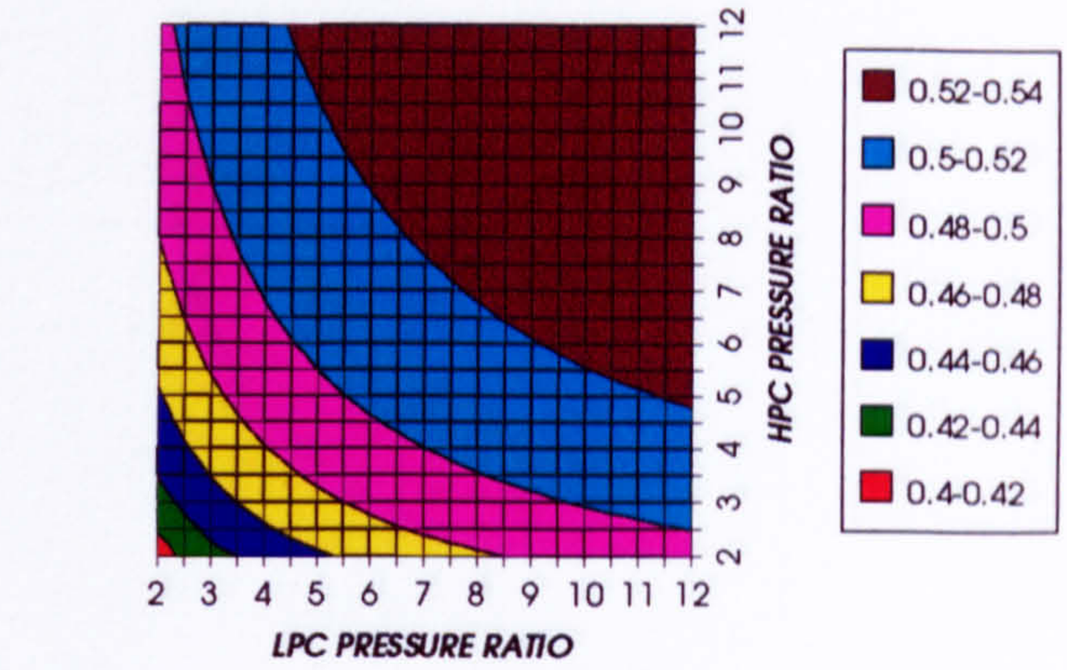

Figure 2. Combined cycle ideal thermal efficiency

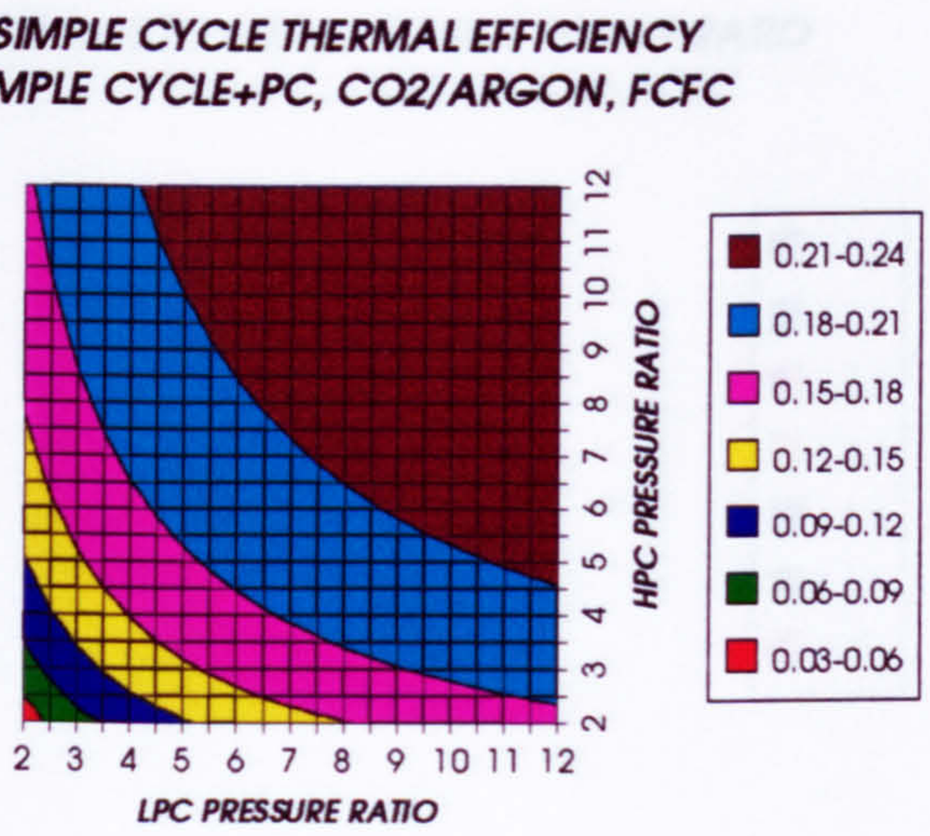

Figure 3. Simple cycle thermal efficiency

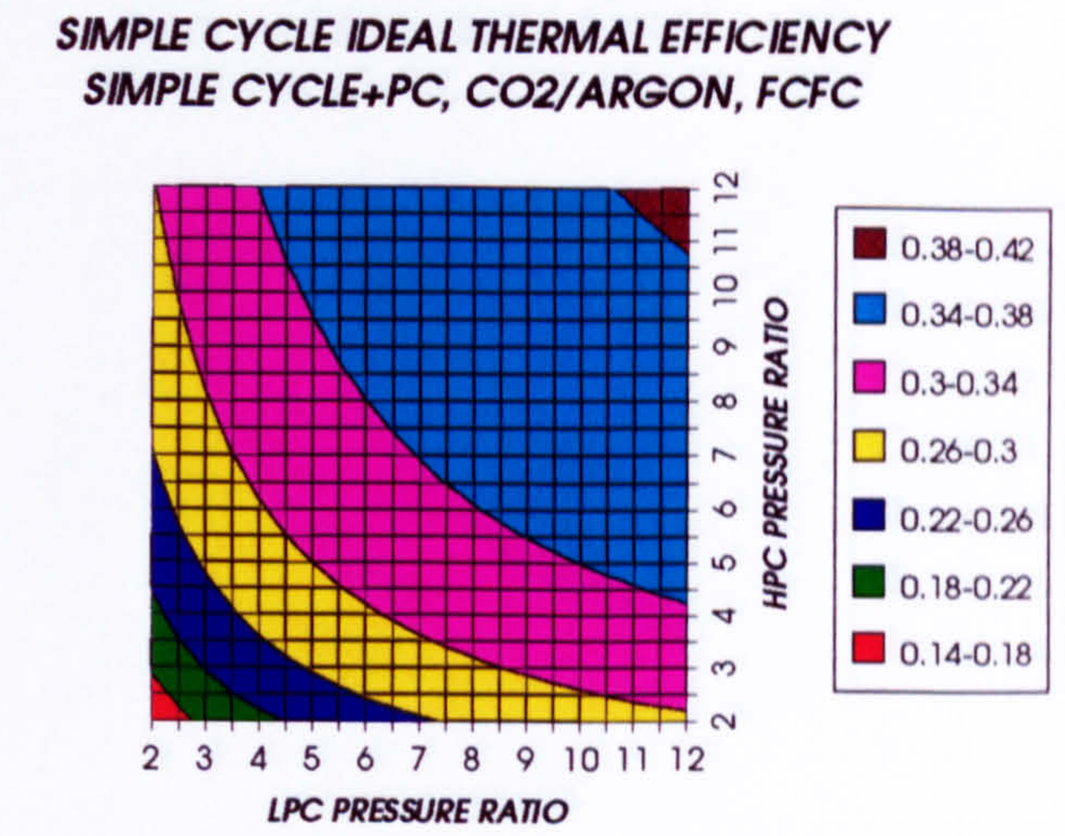

Figure 4. Simple cycle ideal thermal efficiency

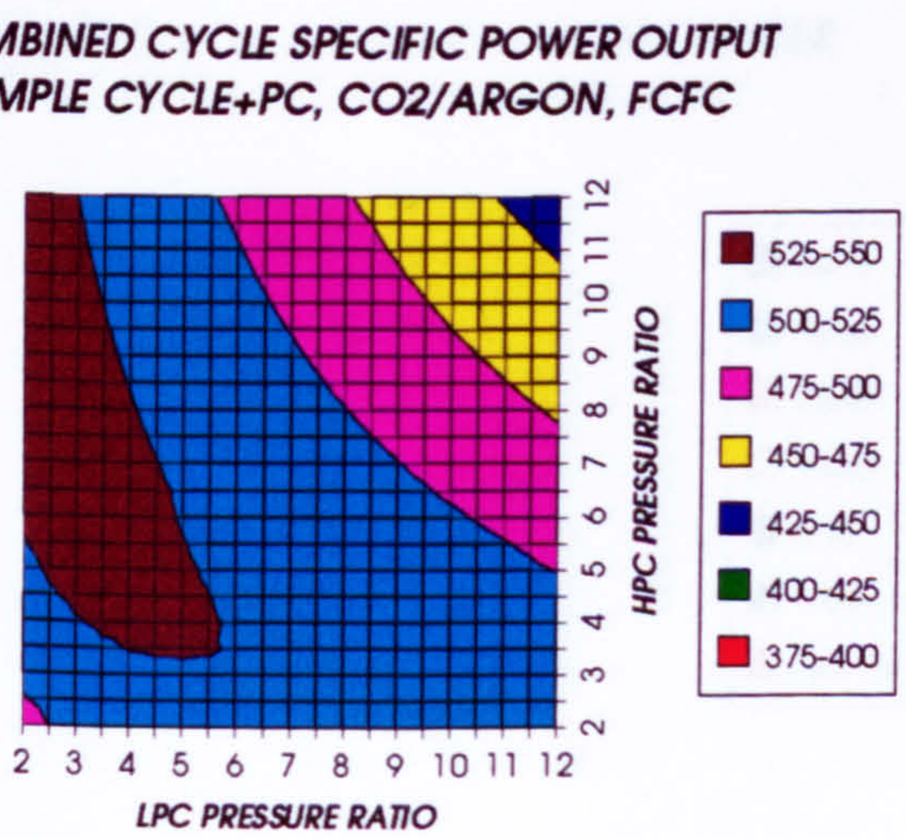

Figure 5. Combined cycle specific power output

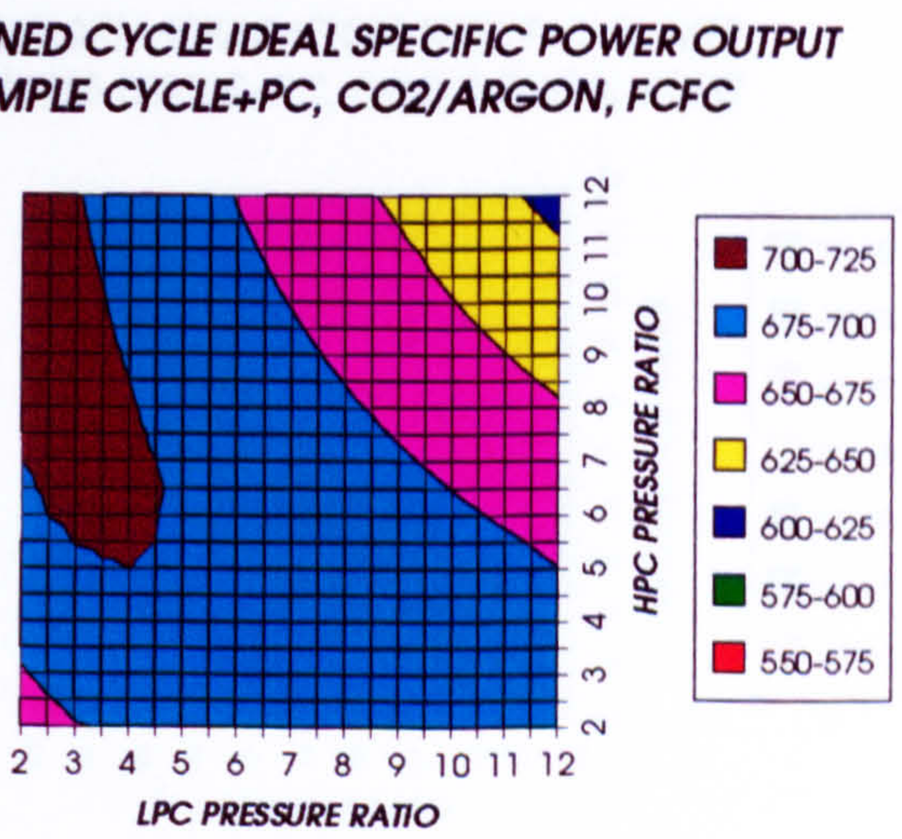

Figure 6. Combined cycle ideal specific power output

COMPLETE PLANT WITH CRYOGENIC PRECOOLER & NGVs N_2 COOLING (TET=1650 K)

GAS TURBINE SPECIFIC POWER OUTPUT
SIMPLE CYCLE+PC, CO2/ARGON, FCFC

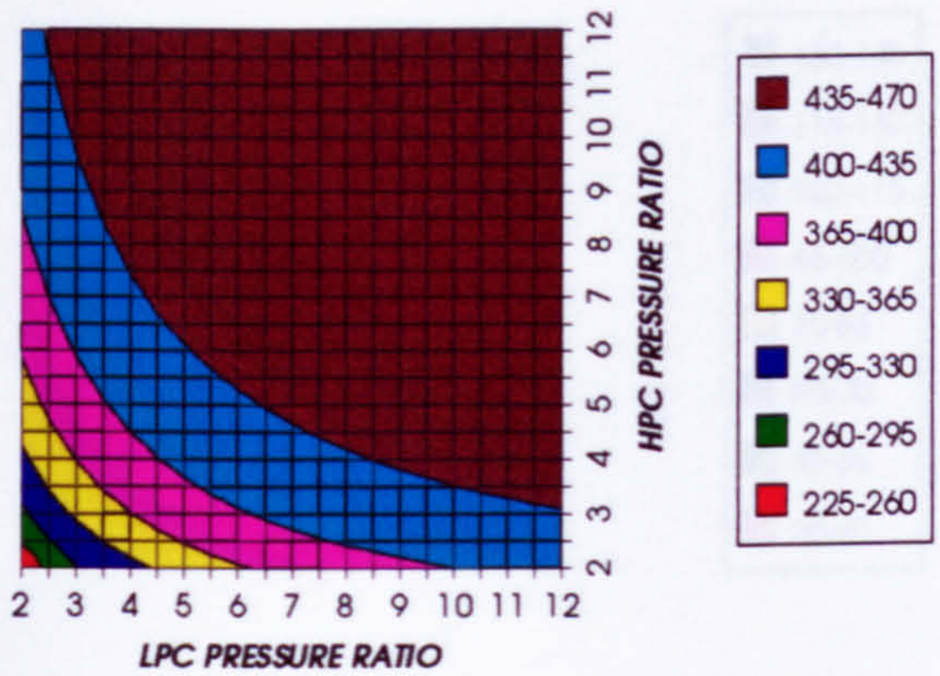

Figure 7. Gas turbine specific power output

STEAM TURBINE SPECIFIC POWER OUTPUT
SIMPLE CYCLE+PC, CO2/ARGON, FCFC

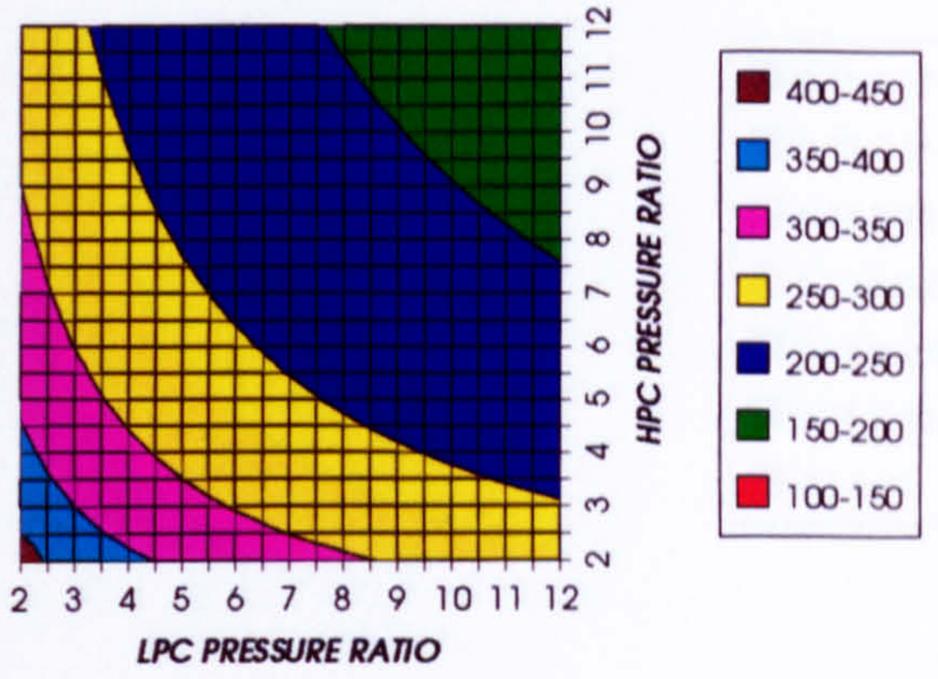

Figure 8. Steam turbine specific power output

GAS TURBINE TO STEAM TURBINE POWER RATIO
SIMPLE CYCLE+PC, CO2/ARGON, FCFC

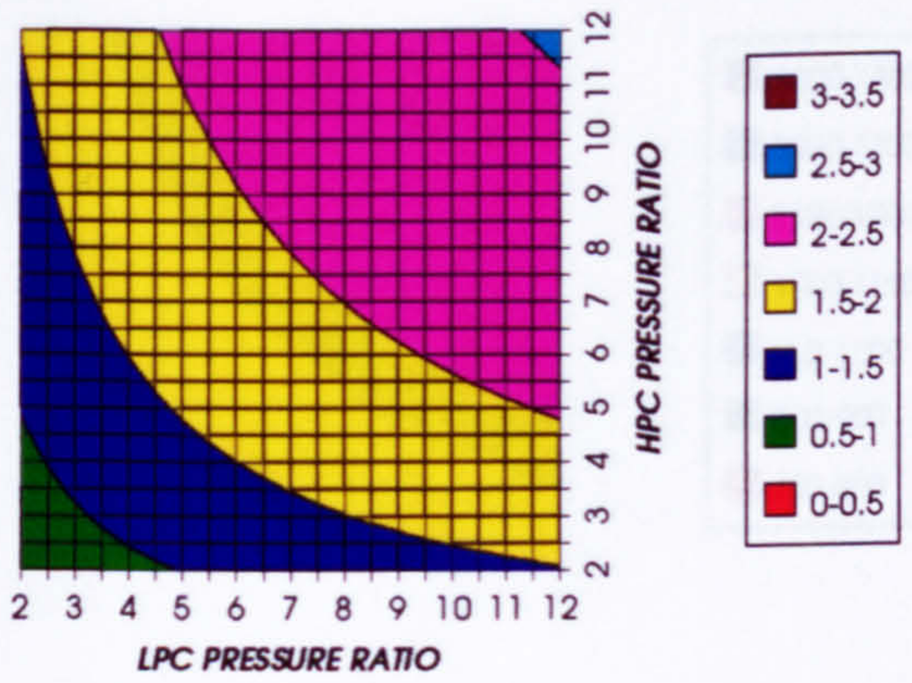

Figure 9. Gas turbine to steam turbine power ratio

AUXILIARIES TO USEFUL POWER RATIO
SIMPLE CYCLE+PC, CO2/ARGON, FCFC

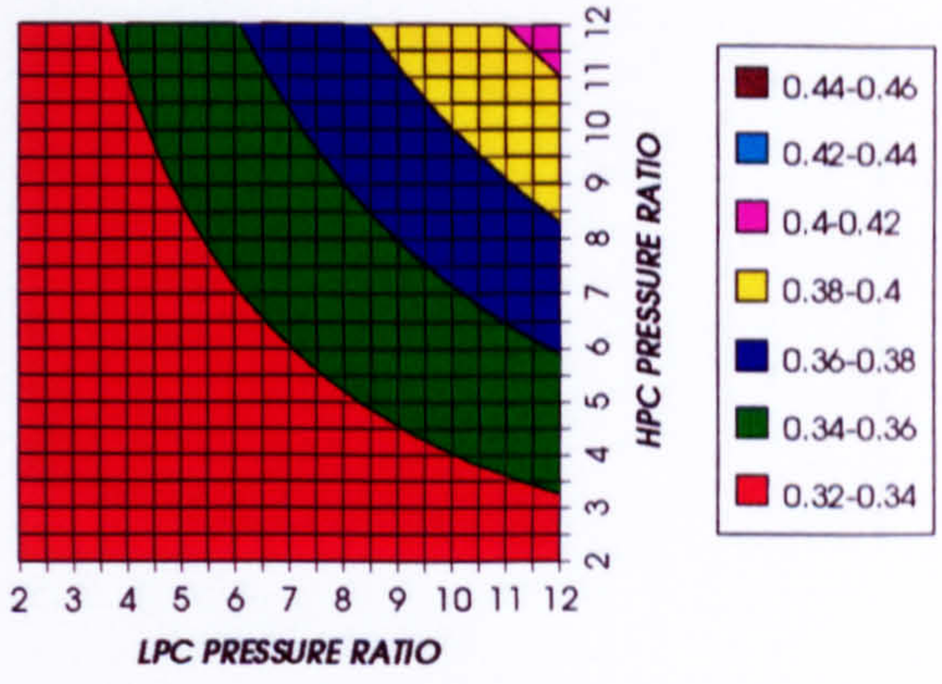

Figure 10. Auxiliary (CO2/Argon, O2 & Fuel) to usefuel power ratio

CO2 COMPRESSION AUXILIARY SPECIFIC POWER
SIMPLE CYCLE+PC, CO2/ARGON, FCFC

Figure 11. CO2/Argon compression specific power

OXYGEN SEPARATION SPECIFIC POWER
SIMPLE CYCLE+PC, CO2/ARGON, FCFC

Figure 12. Oxygen separation specific power

COMPLETE PLANT WITH CRYOGENIC PRECOOLER & NGVs N_2 COOLING (TET=1650 K))

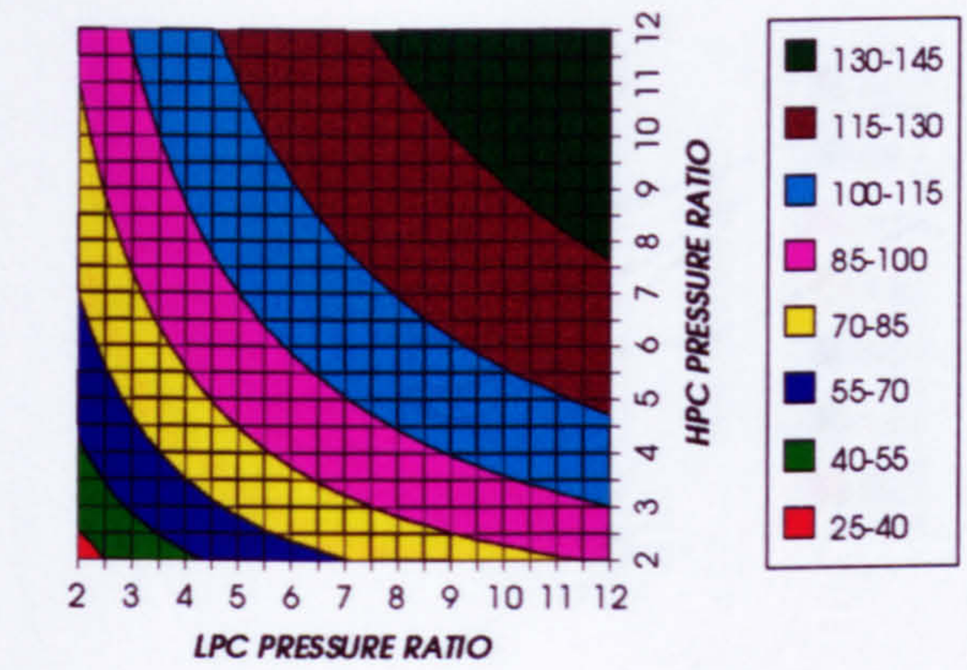

Figure 13. Fuel compression specific power

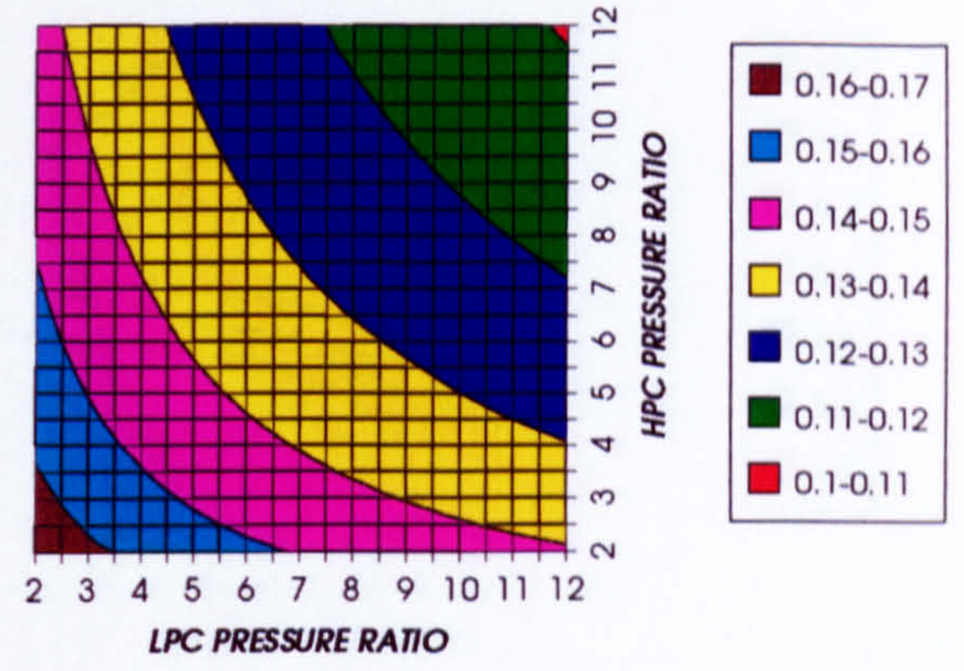

Figure 14. Fuel to compressor inlet mass flow ratio

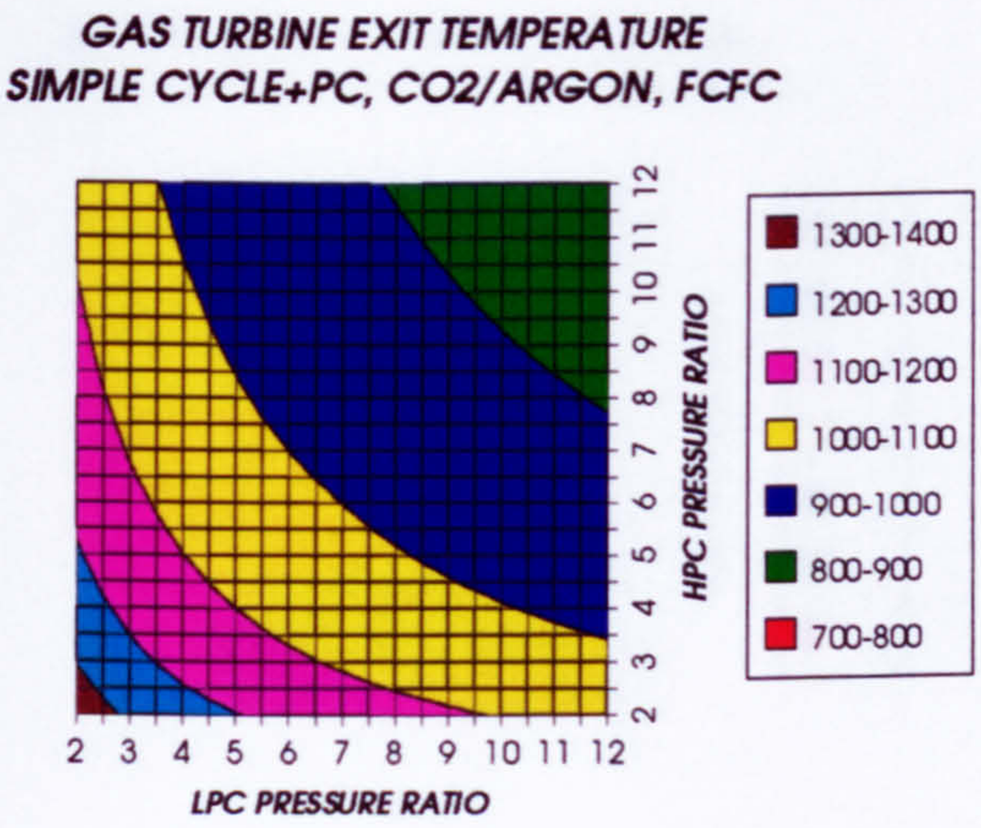

Figure 15. Gas turbine exit temperature (K)

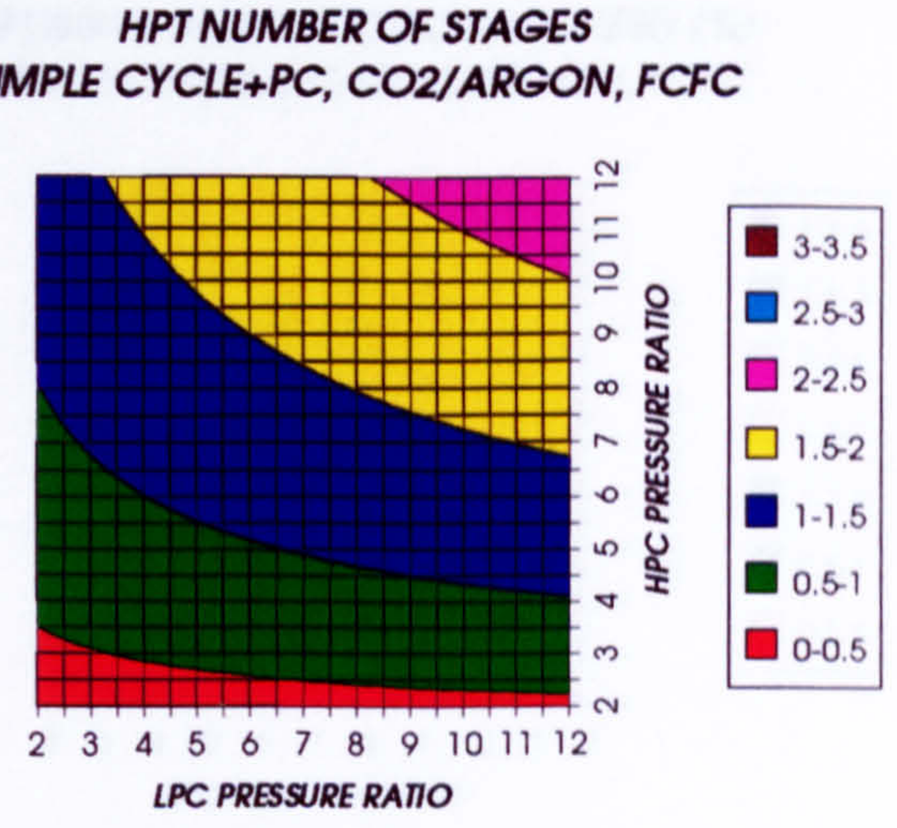

Figure 16. Number of HPT stages

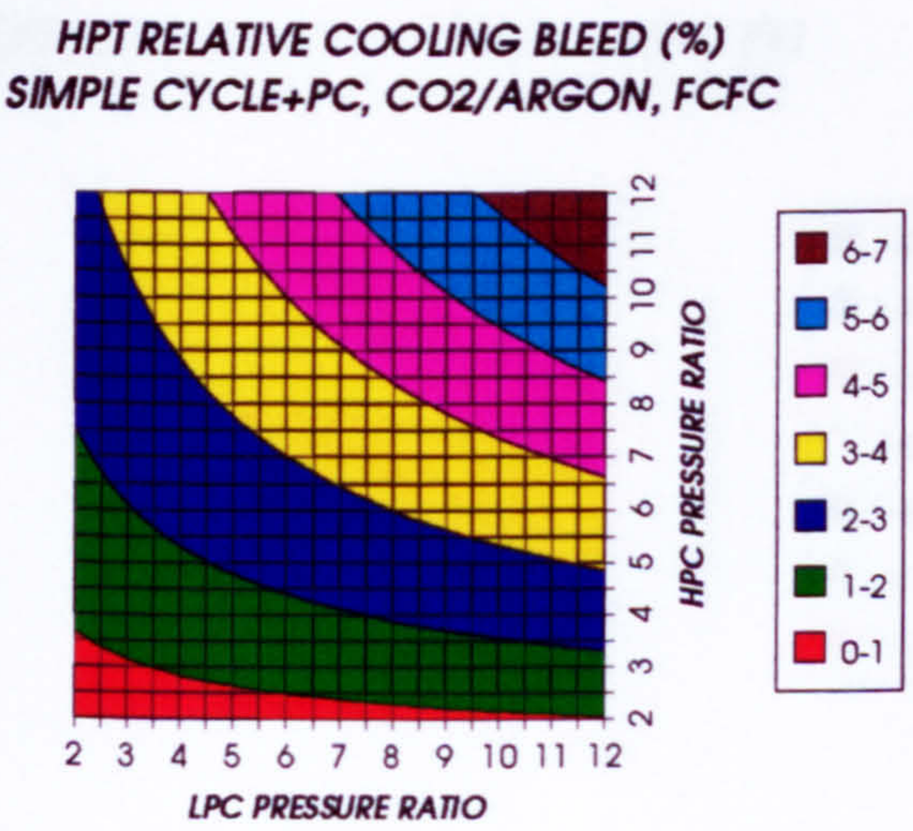

Figure 17. HPT cooling to compressor inlet mass flow ratio

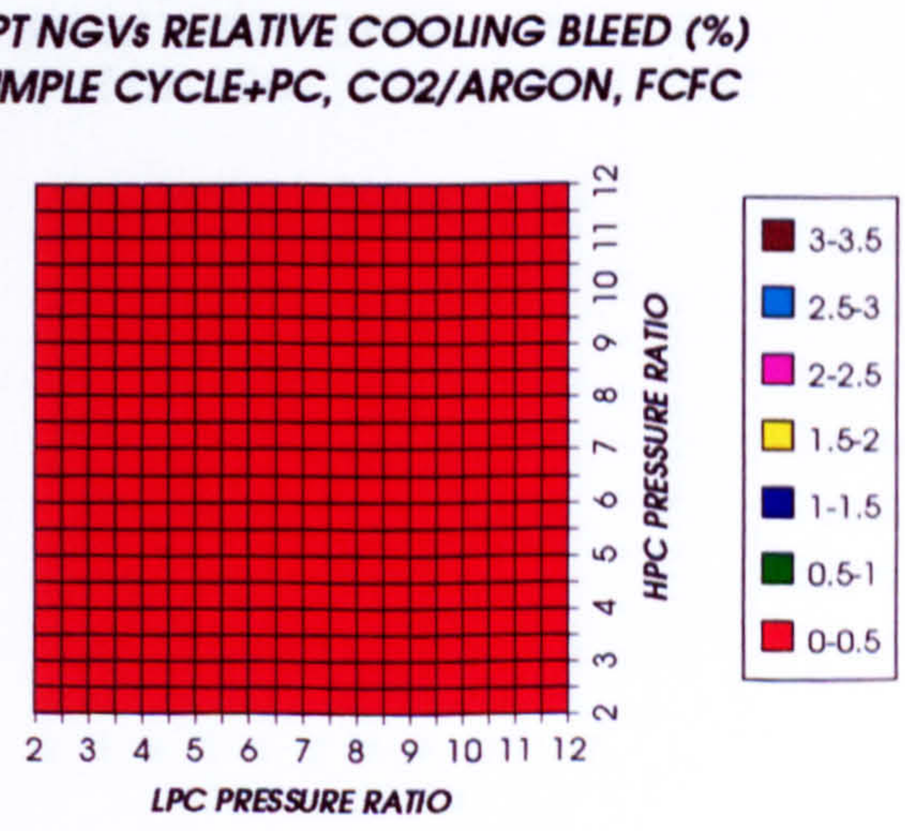

Figure 18. HPT NGVs cooling to compressor inlet mass flow ratio

COMPLETE PLANT WITH CRYOGENIC PRECOOLER & NGVs N_2 COOLING (TET=1650 K))

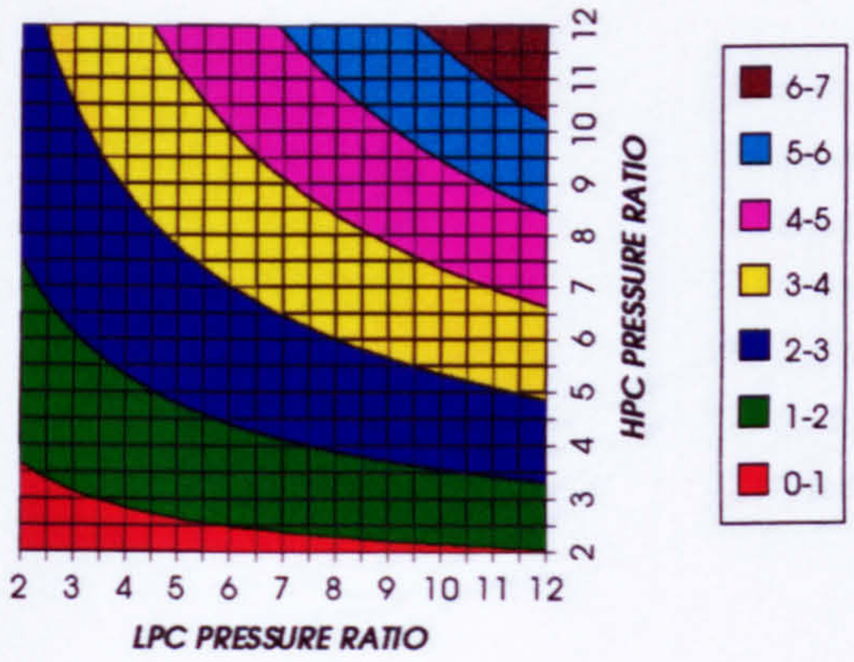

Figure 19. HPT rotor cooling to compressor inlet mass flow ratio

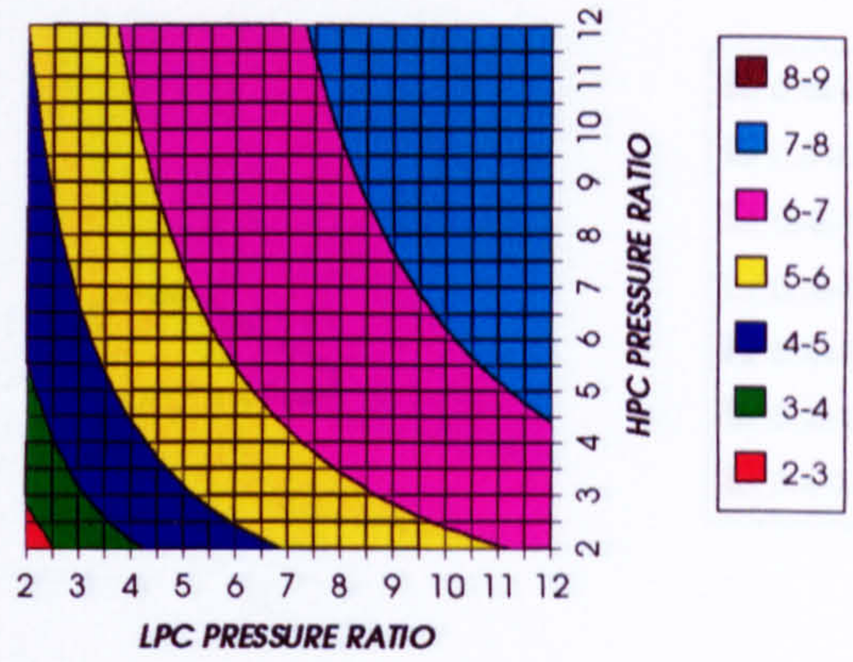

Figure 20. Number of LPT stages

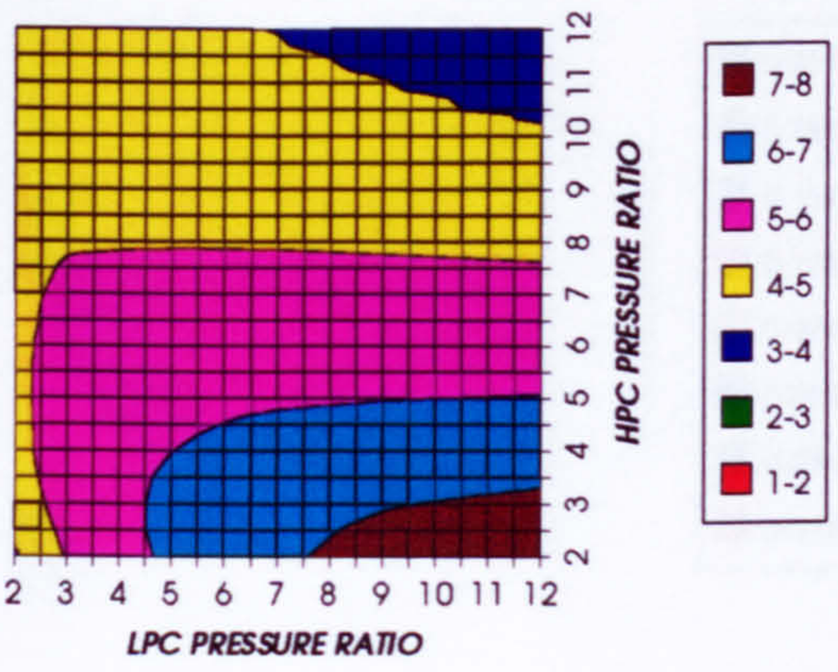

Figure 21. LPT cooling to compressor inlet mass flow ratio

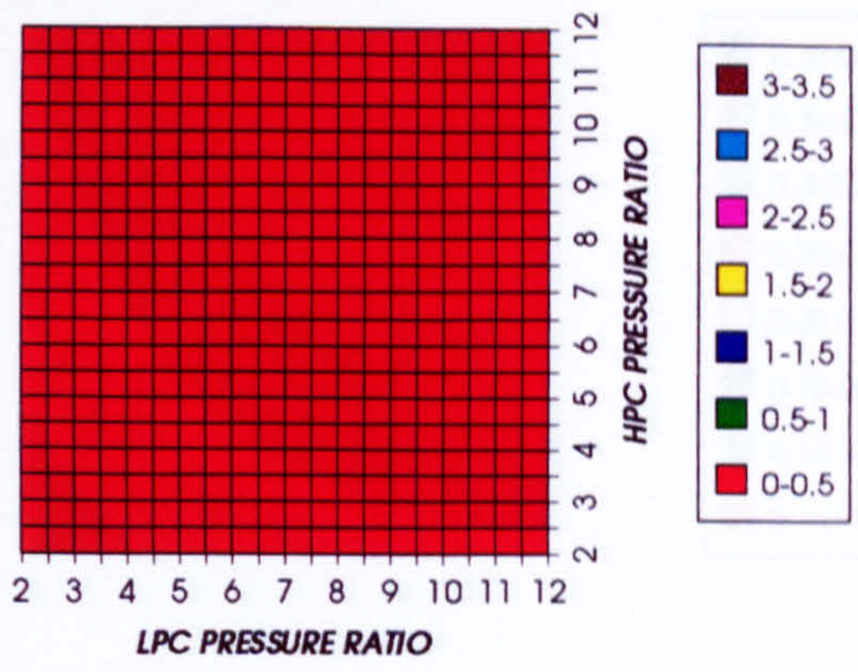

Figure 22. LPT NGVs cooling to compressor inlet mass flow ratio

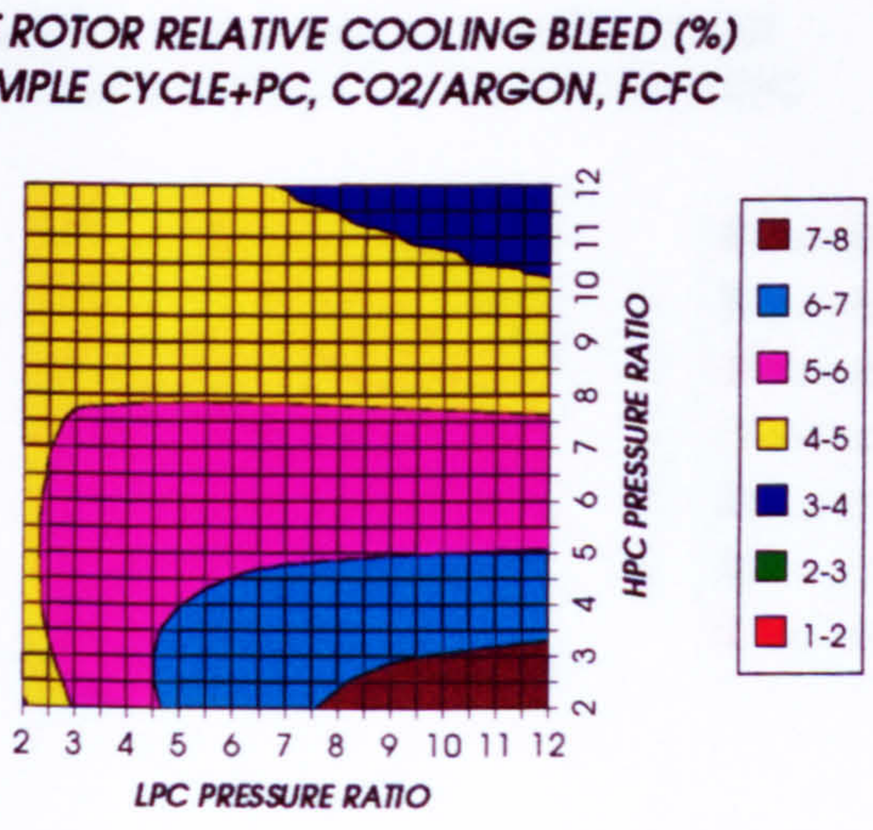

Figure 23. LPT rotor cooling to compressor inlet mass flow ratio

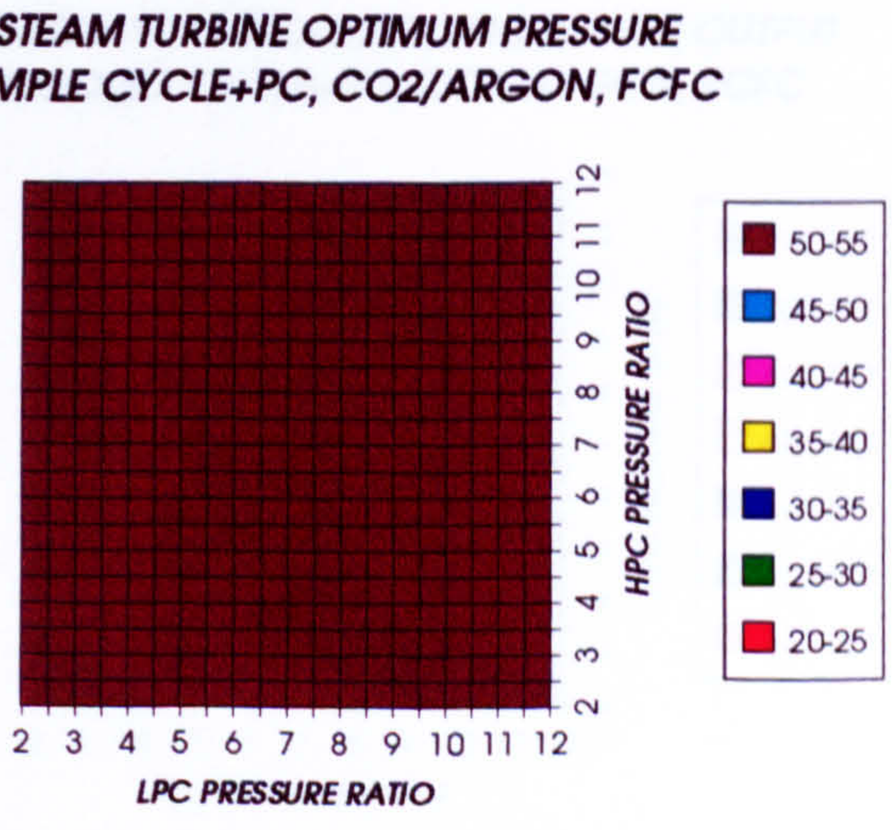

Figure 24. Steam turbine optimum pressures (maximum)

COMPLETE PLANT WITH CRYOGENIC PRECOOLER & NGVs N_2 COOLING (TET=1650 K)

COMBINED CYCLE THERMAL EFFICIENCY INTERCOOLED CYCLE+PC, CO2/ARGON, FCFC

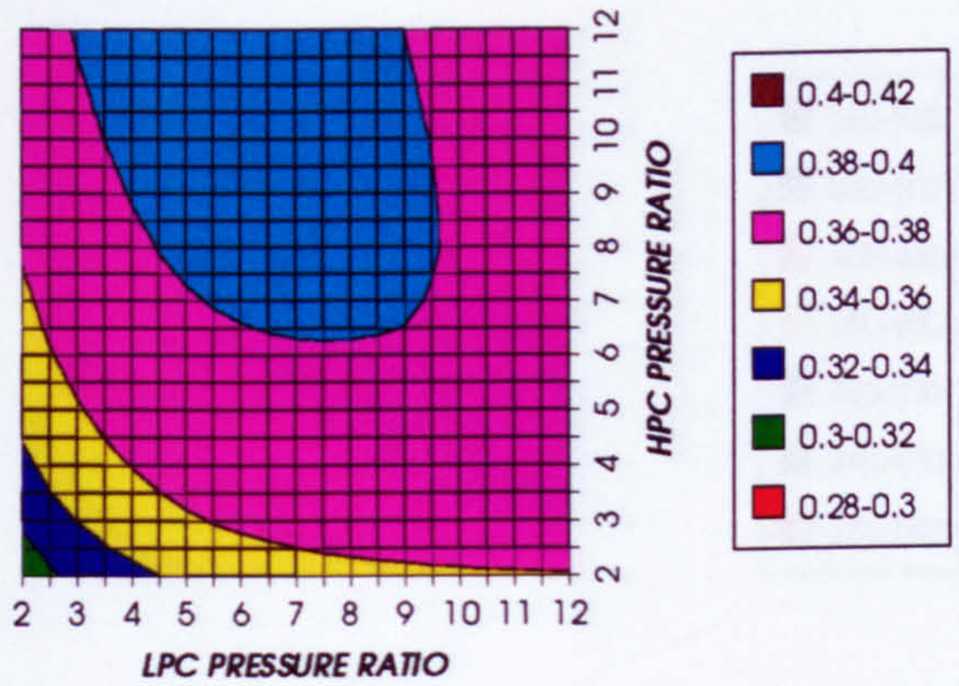

Figure 25. Combined cycle thermal efficiency

COMBINED CYCLE IDEAL THERMAL EFFICIENCY INTERCOOLED CYCLE+PC, CO2/ARGON, FCFC

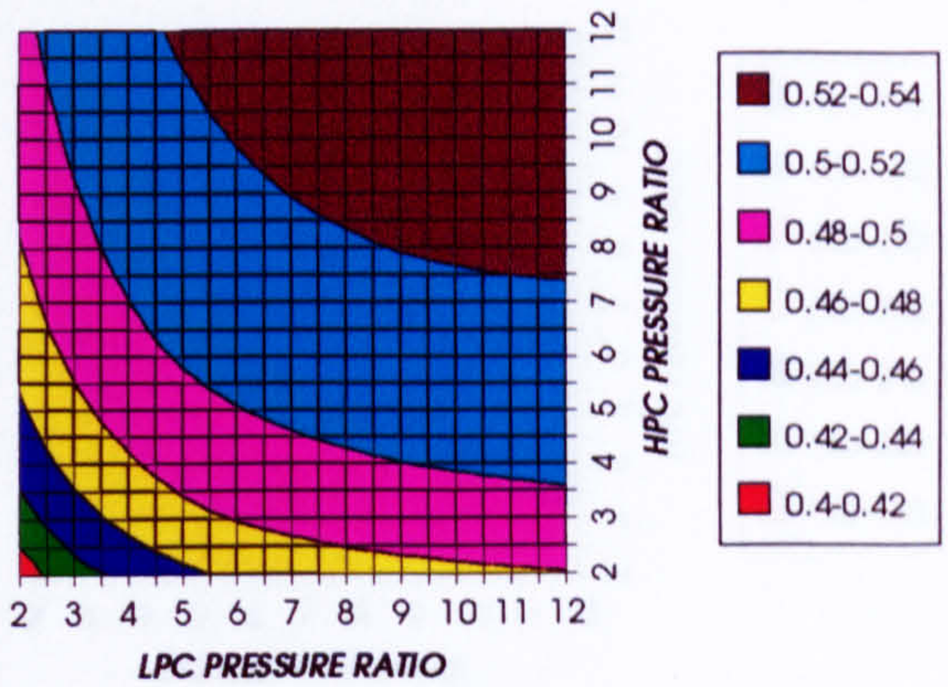

Figure 26. Combined cycle ideal thermal efficiency

SIMPLE CYCLE THERMAL EFFICIENCY INTERCOOLED CYCLE+PC, CO2/ARGON, FCFC

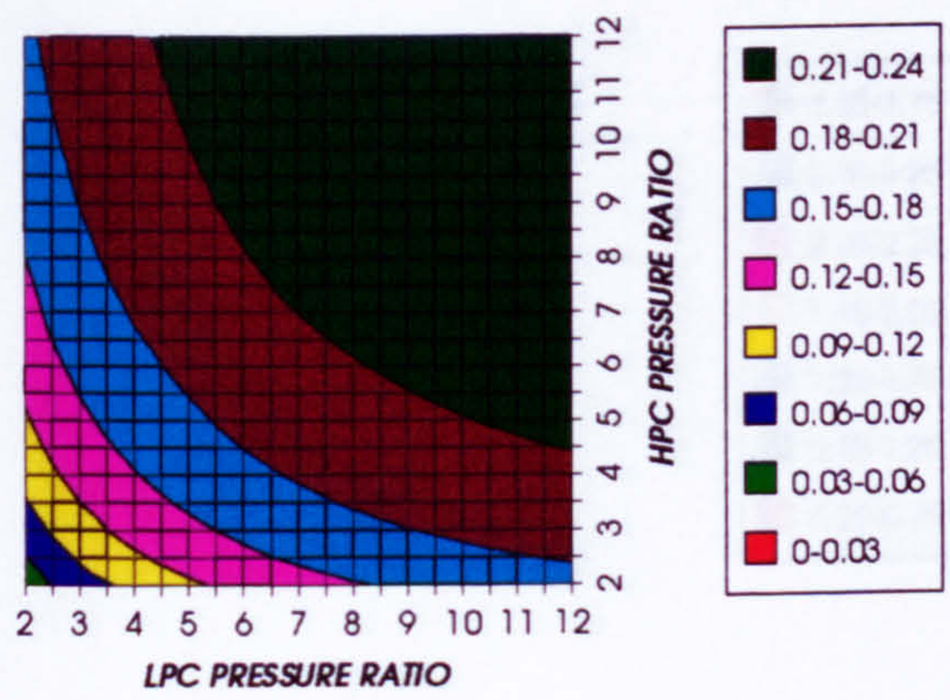

Figure 27. Simple cycle thermal efficiency

SIMPLE CYCLE IDEAL THERMAL EFFICIENCY INTERCOOLED CYCLE+PC, CO2/ARGON, FCFC

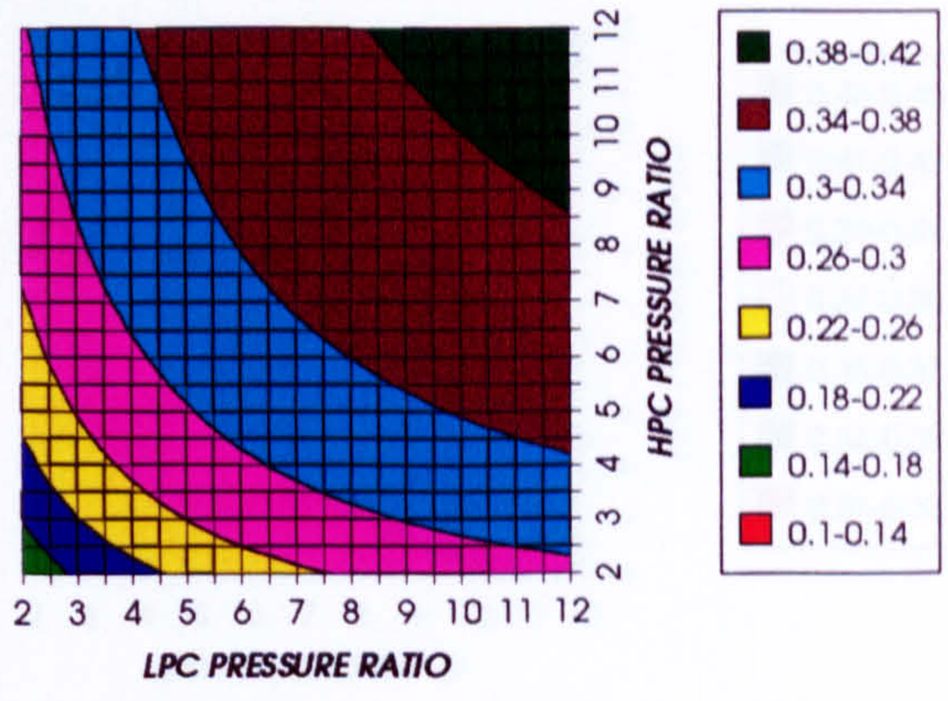

Figure 28. Simple cycle ideal thermal efficiency

COMBINED CYCLE SPECIFIC POWER OUTPUT INTERCOOLED CYCLE+PC, CO2/ARGON, FCFC

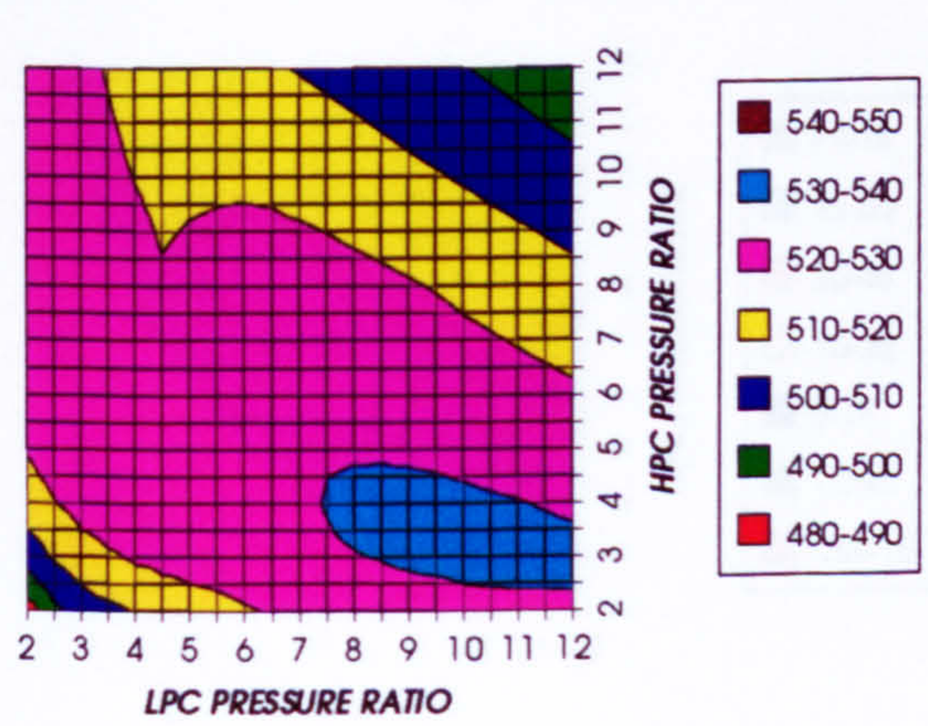

Figure 29. Combined cycle specific power output

COMBINED CYCLE IDEAL SPECIFIC POWER OUTPUT INTERCOOLED CYCLE+PC, CO2/ARGON, FCFC

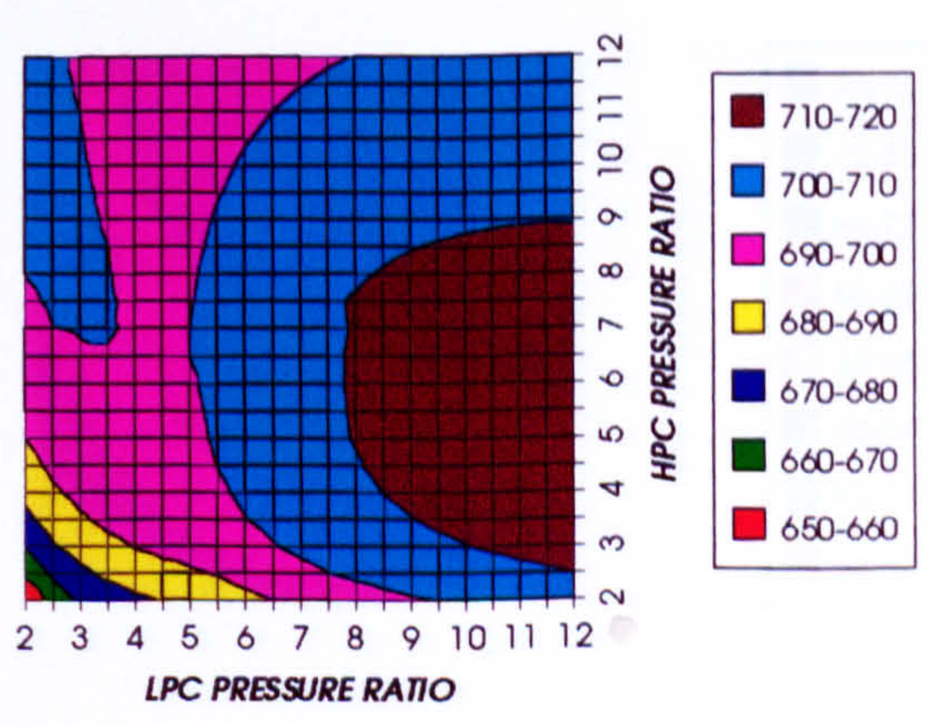

Figure 30. Combined cycle ideal specific power output

COMPLETE PLANT WITH CRYOGENIC PRECOOLER & NGVs N_2 COOLING (TET=1650 K)

GAS TURBINE SPECIFIC POWER OUTPUT
INTERCOOLED CYCLE+PC, CO2/ARGON, FCFC

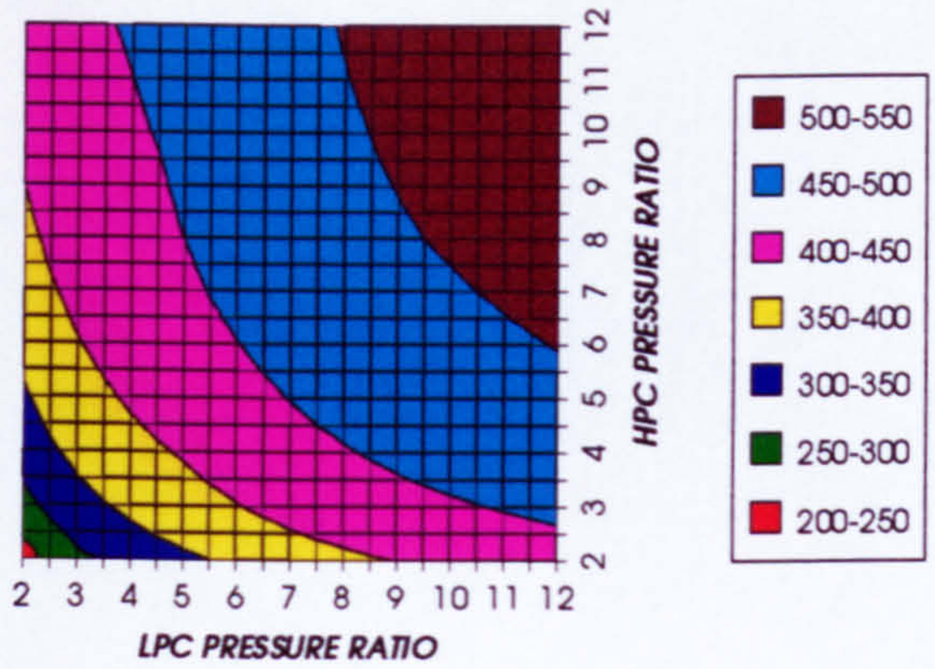

Figure 31. Gas turbine specific power output

STEAM TURBINE SPECIFIC POWER OUTPUT
INTERCOOLED CYCLE+PC, CO2/ARGON, FCFC

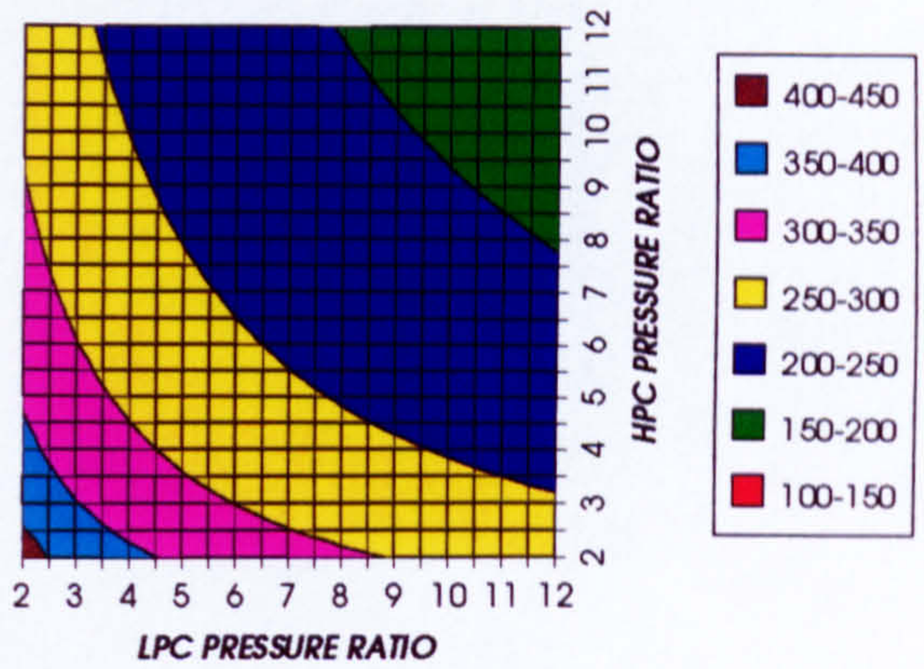

Figure 32. Steam turbine specific power output

GAS TURBINE TO STEAM TURBINE POWER RATIO
INTERCOOLED CYCLE+PC, CO2/ARGON, FCFC

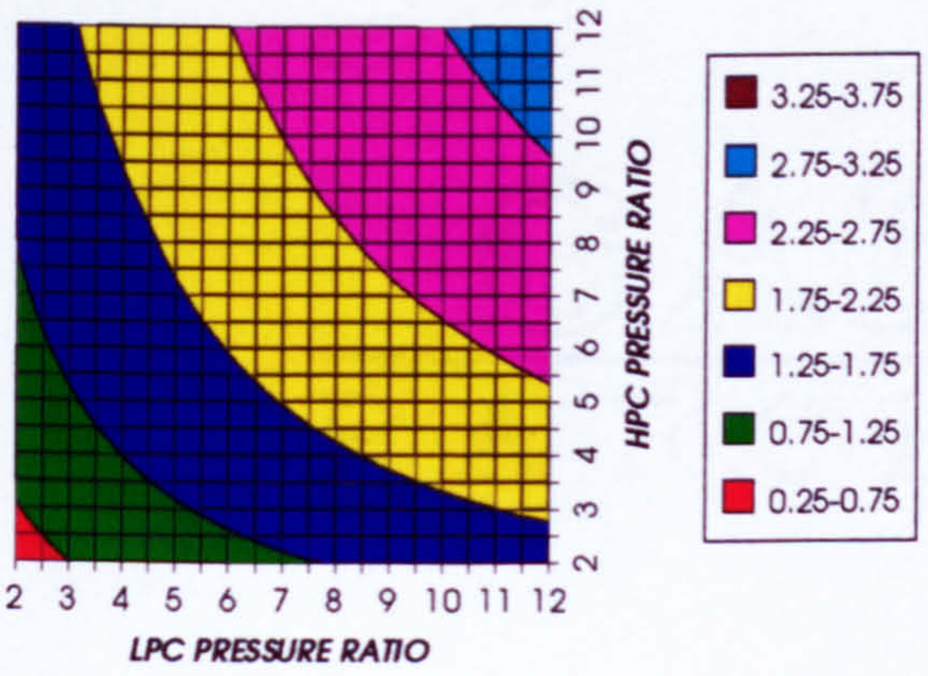

Figure 33. Gas turbine to steam turbine power ratio

AUXILIARIES TO USEFUL POWER RATIO
INTERCOOLED CYCLE+PC, CO2/ARGON, FCFC

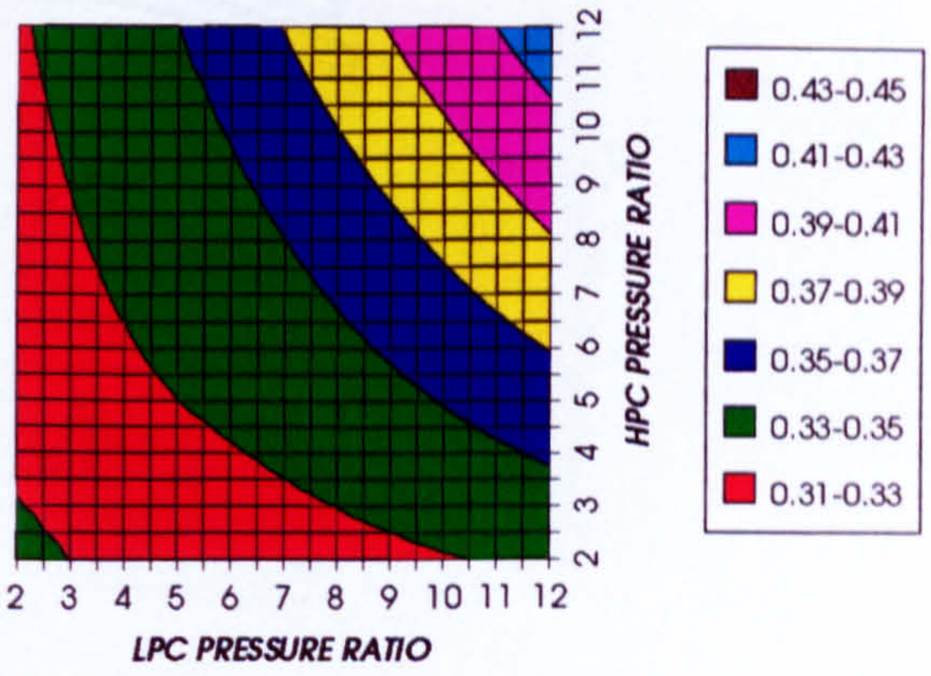

Figure 34. Auxiliary (CO2/Argon, O2 & Fuel) to usefuel power ratio

CO2 COMPRESSION AUXILIARY SPECIFIC POWER
INTERCOOLED CYCLE+PC, CO2/ARGON, FCFC

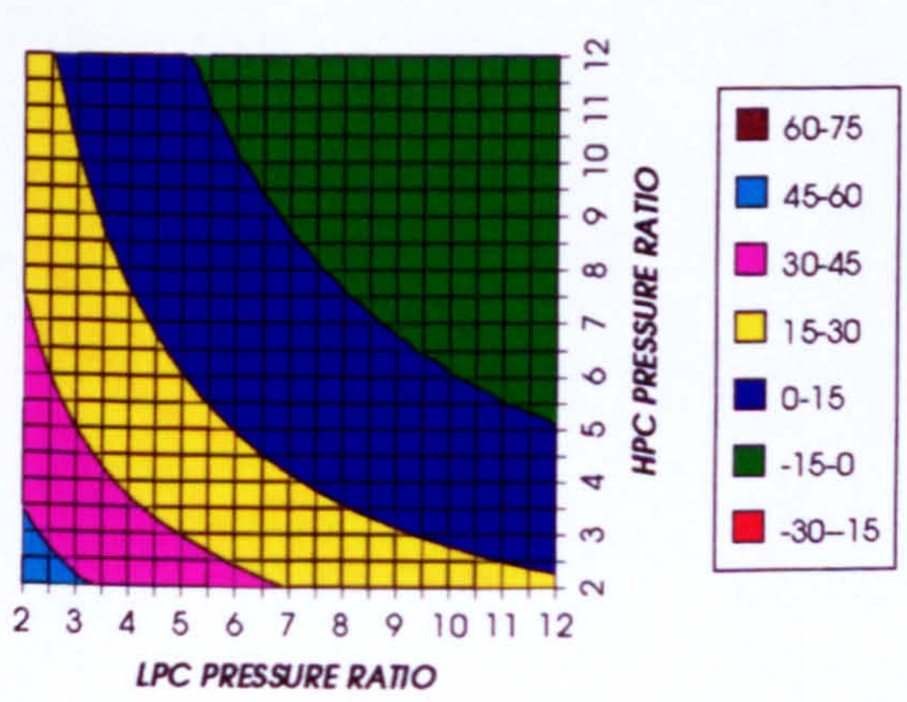

Figure 35. CO2/Argon compression specific power

OXYGEN SEPARATION SPECIFIC POWER
INTERCOOLED CYCLE+PC, CO2/ARGON, FCFC

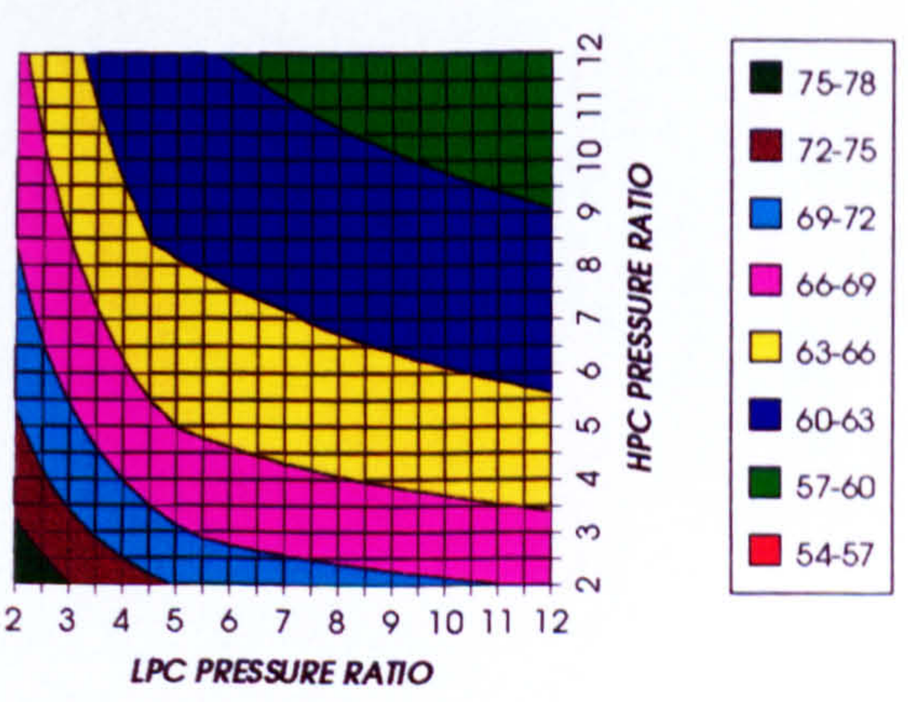

Figure 36. Oxygen separation specific power

COMPLETE PLANT WITH CRYOGENIC PRECOOLER & NGVs N_2 COOLING (TET=1650 K)

FUEL COMPRESSION SPECIFIC POWER
INTERCOOLED CYCLE+PC, CO2/ARGON, FCFC

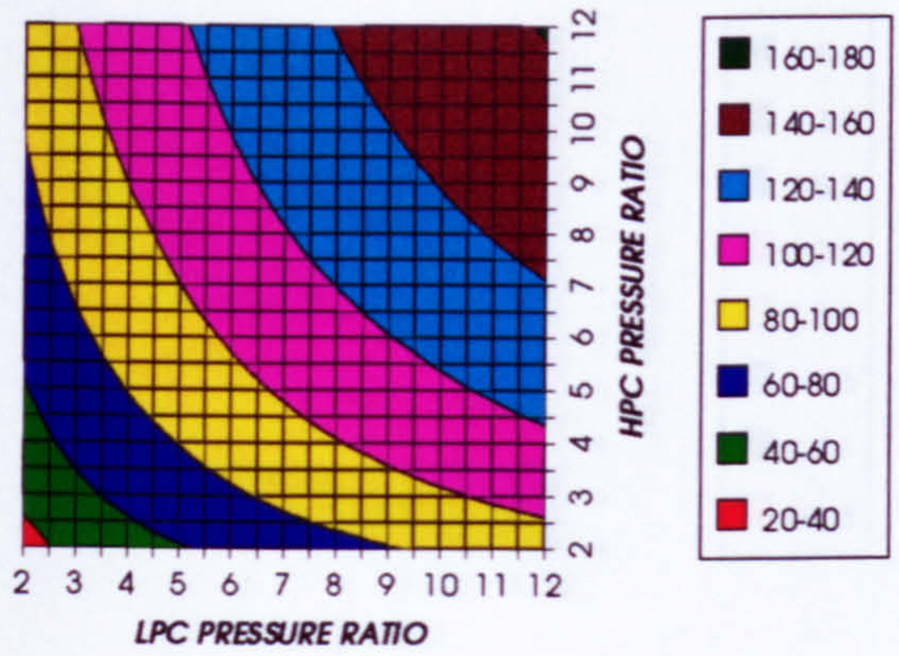

Figure 37. Fuel compression specific power

FUEL TO COMPRESSOR INLET MASS FLOW RATIO
INTERCOOLED CYCLE+PC, CO2/ARGON, FCFC

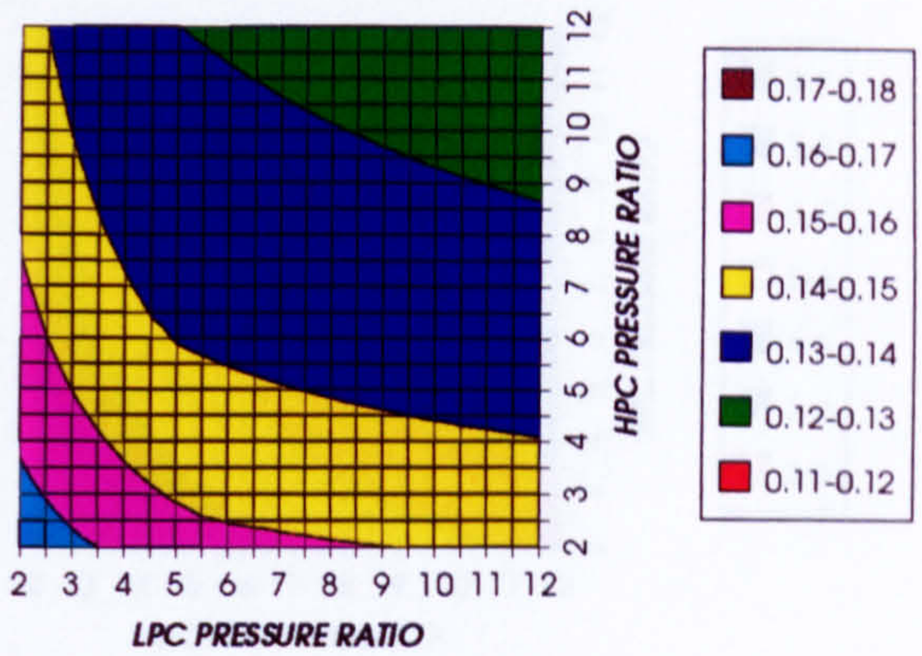

Figure 38. Fuel to compressor inlet mass flow ratio

GAS TURBINE EXIT TEMPERATURE
INTERCOOLED CYCLE+PC, CO2/ARGON, FCFC

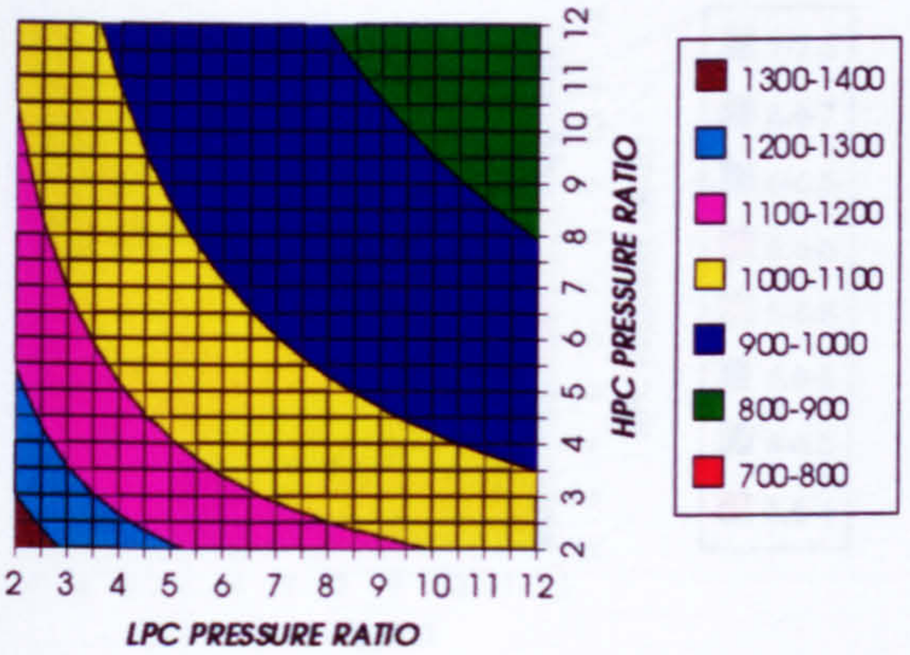

Figure 39. Gas turbine exit temperature

HPT NUMBER OF STAGES
INTERCOOLED CYCLE+PC, CO2/ARGON, FCFC

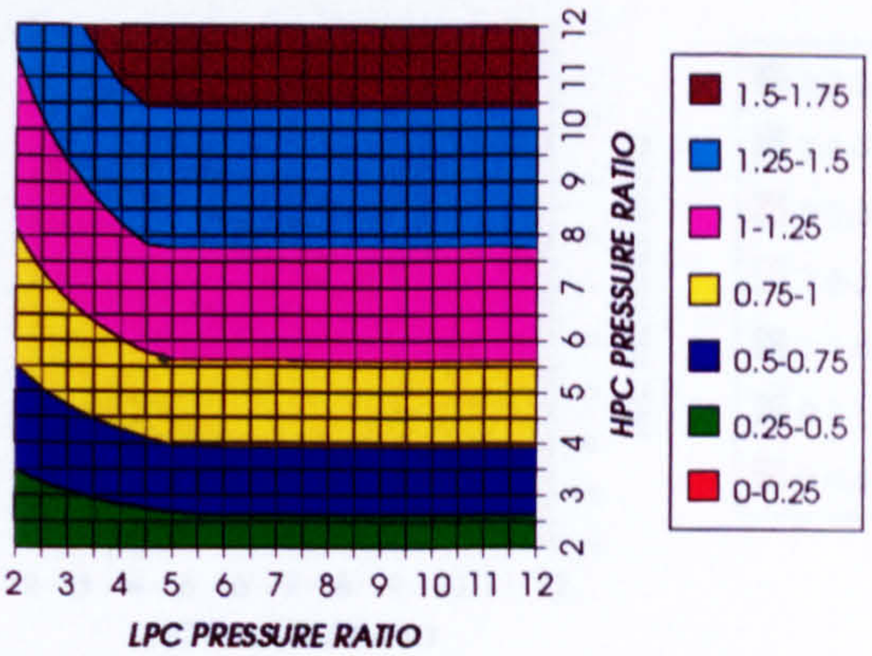

Figure 40. Number of HPT stages

HPT RELATIVE COOLING BLEED (%)
INTERCOOLED CYCLE+PC, CO2/ARGON, FCFC

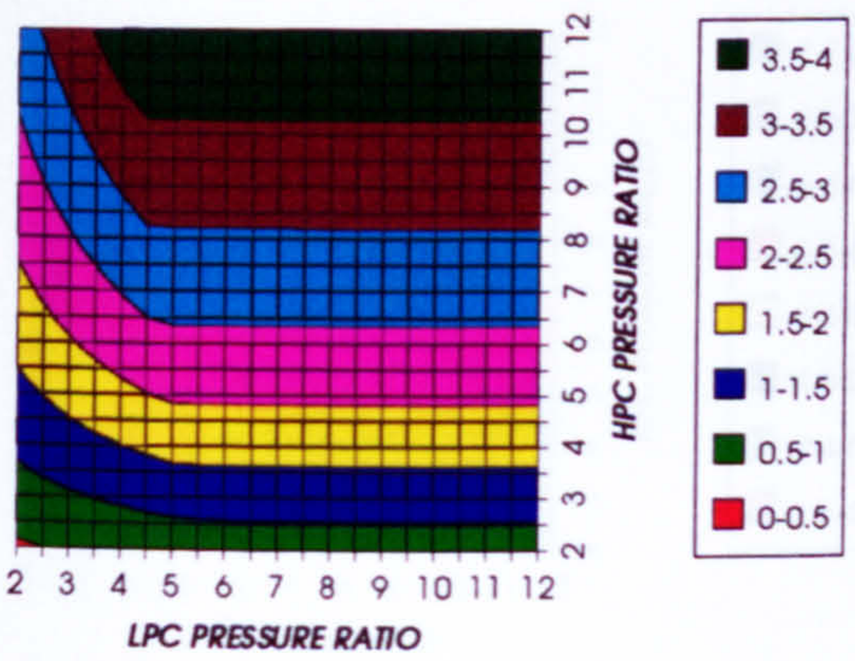

Figure 41. HPT cooling to compressor inlet mass flow ratio

HPT NGVs RELATIVE COOLING BLEED (%)
INTERCOOLED CYCLE+PC, CO2/ARGON, FCFC

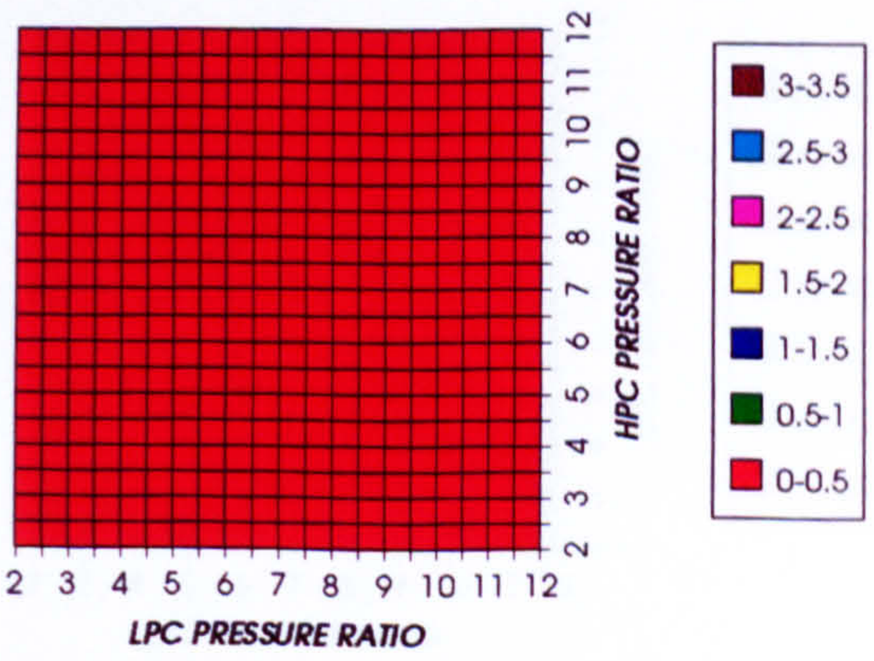

Figure 42. HPT NGVs cooling to compressor inlet mass flow ratio

COMPLETE PLANT WITH CRYOGENIC PRECOOLER & NGVs N_2 COOLING (TET=1650 K)

HPT ROTOR RELATIVE COOLING BLEED (%)
INTERCOOLED CYCLE+PC, CO2/ARGON, FCFC

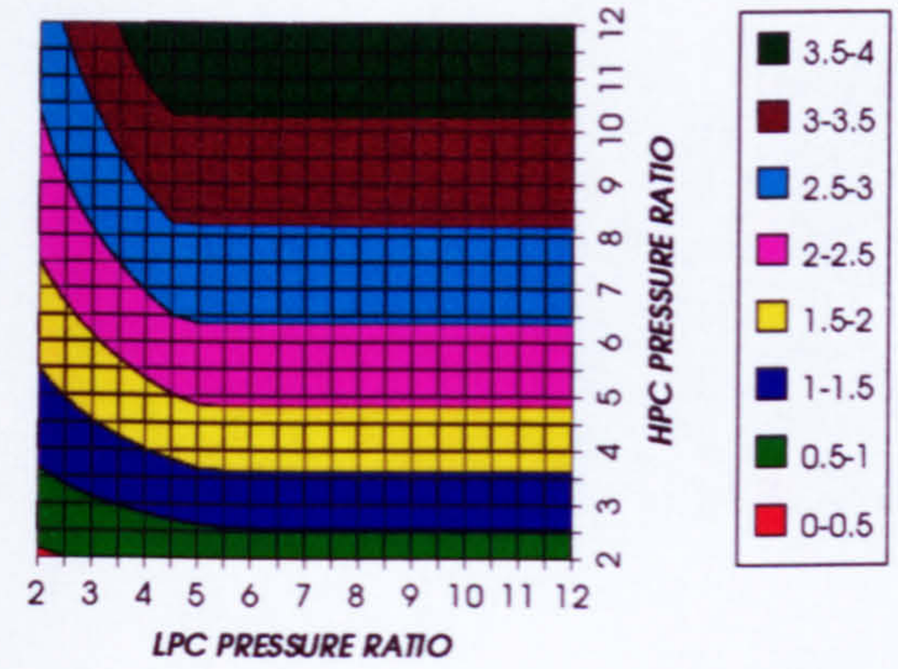

Figure 43. HPT rotor cooling to compressor inlet mass flow ratio

LPT NUMBER OF STAGES
INTERCOOLED CYCLE+PC, CO2/ARGON, FCFC

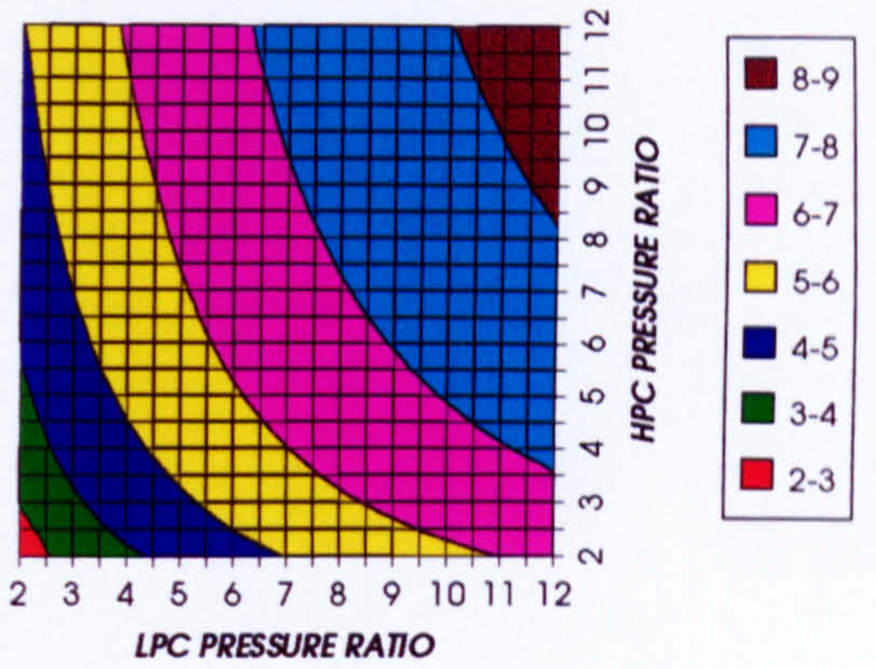

Figure 44. Number of LPT stages

LPT RELATIVE COOLING BLEED (%)
INTERCOOLED CYCLE+PC, CO2/ARGON, FCFC

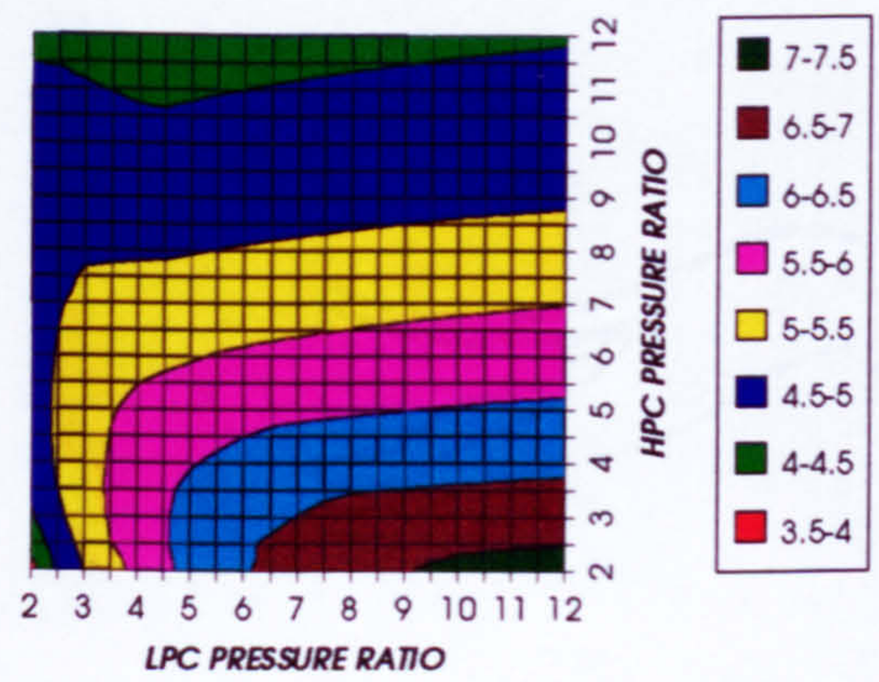

Figure 45. LPT cooling to compressor inlet mass flow ratio

LPT NGVs RELATIVE COOLING BLEED (%)
INTERCOOLED CYCLE+PC, CO2/ARGON, FCFC

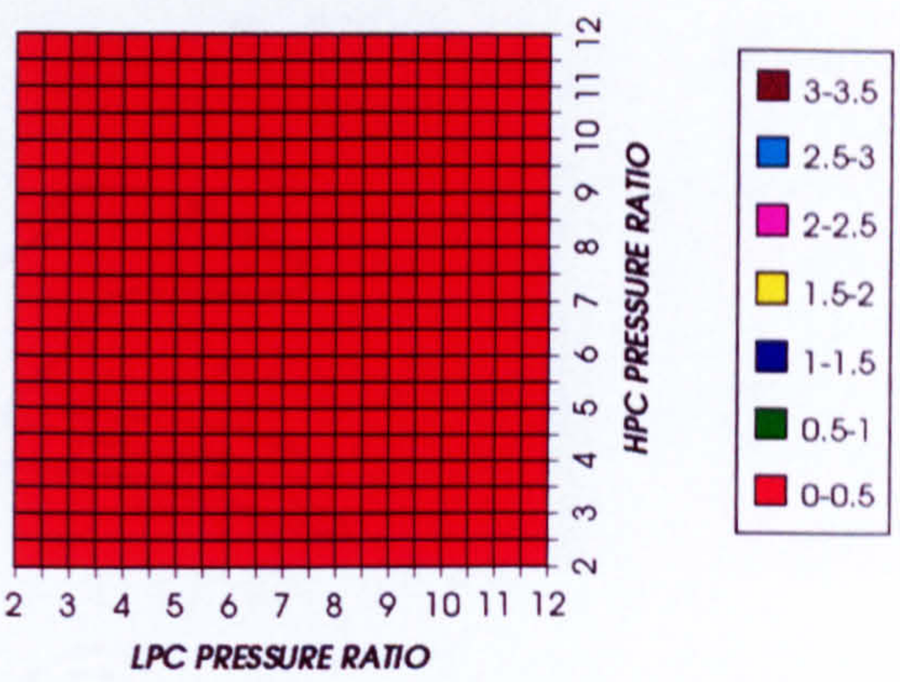

Figure 46. LPT NGVs cooling to compressor inlet mass flow ratio

LPT ROTOR RELATIVE COOLING BLEED (%)
INTERCOOLED CYCLE+PC, CO2/ARGON, FCFC

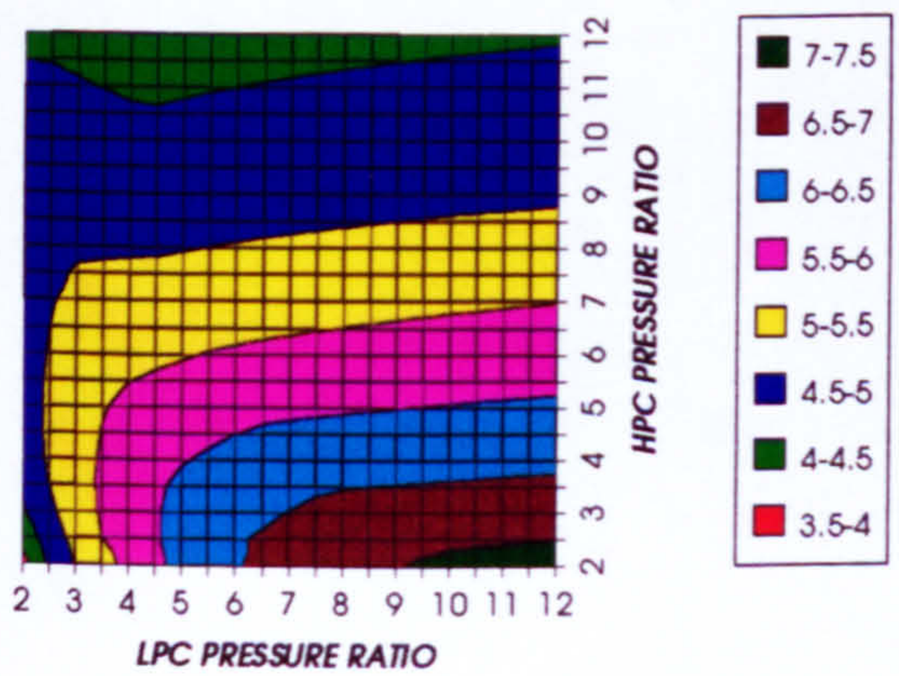

Figure 47. LPT rotor cooling to compressor inlet mass flow ratio

STEAM TURBINE OPTIMUM PRESSURE
INTERCOOLED CYCLE+PC, CO2/ARGON, FCFC

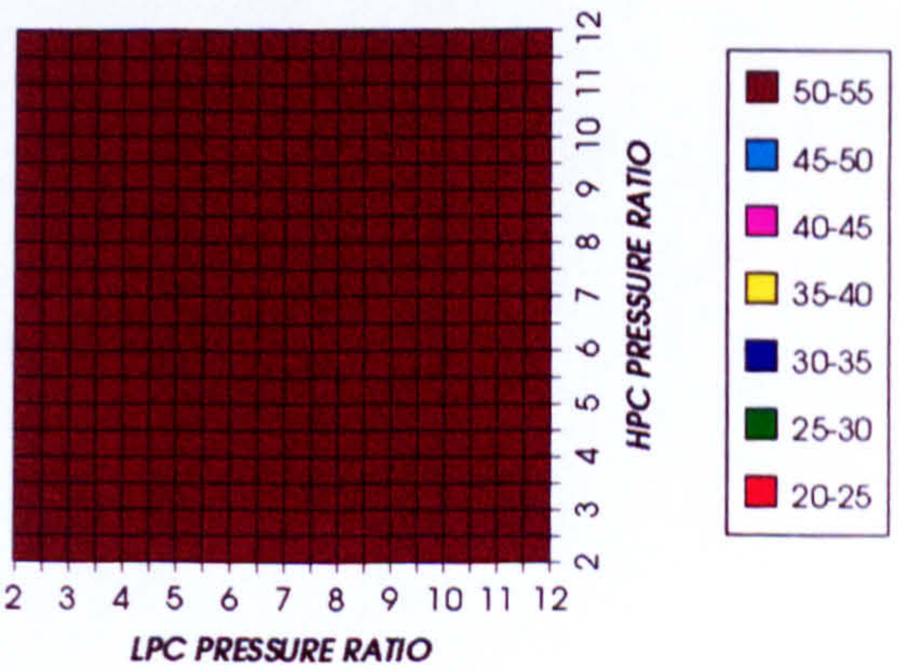

Figure 48. Steam turbine optimum pressures (maximum)

COMPLETE PLANT WITH CRYOGENIC PRECOOLER & NGVs N_2 COOLING (TET=1650 K)

COMBINED CYCLE THERMAL EFFICIENCY
REGENERATED CYCLE+PC, CO2/ARGON, FCFC

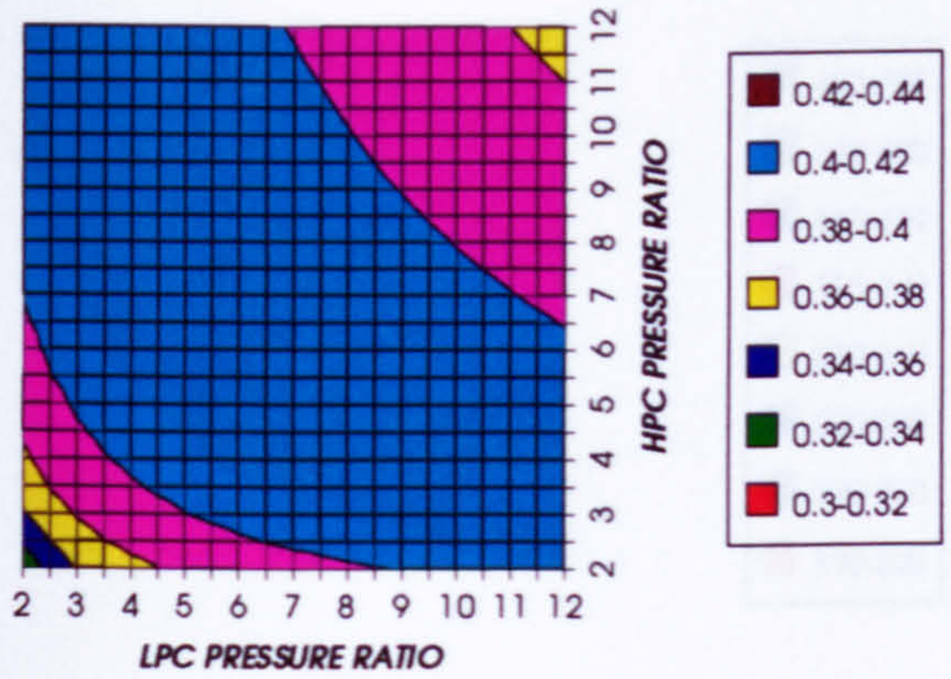

Figure 49. Combined cycle thermal efficiency

COMBINED CYCLE IDEAL THERMAL EFFICIENCY
REGENERATED CYCLE+PC, CO2/ARGON, FCFC

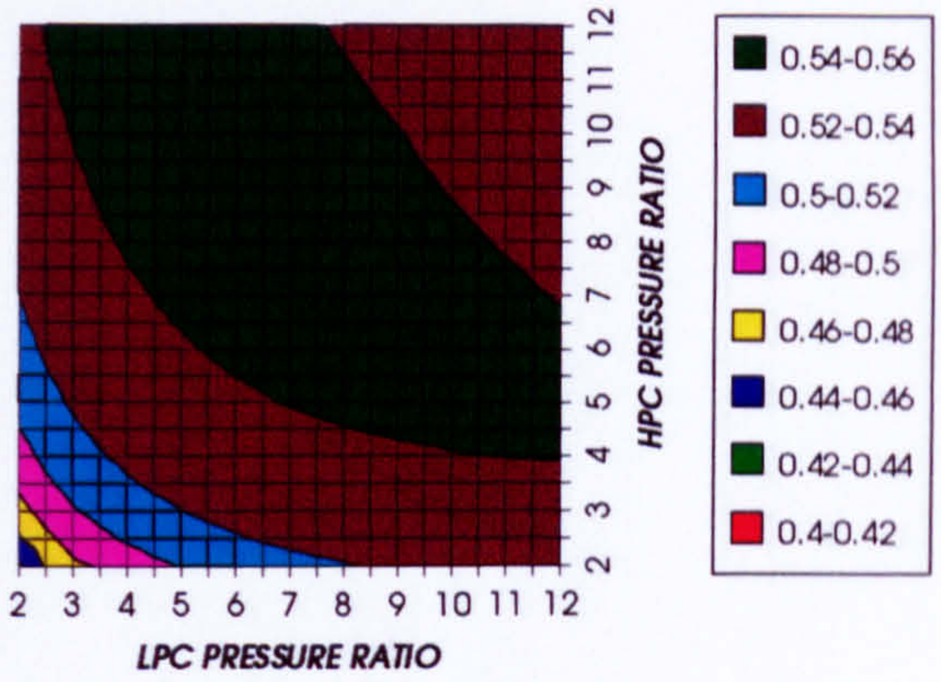

Figure 50. Combined cycle ideal thermal efficiency

SIMPLE CYCLE THERMAL EFFICIENCY
REGENERATED CYCLE+PC, CO2/ARGON, FCFC

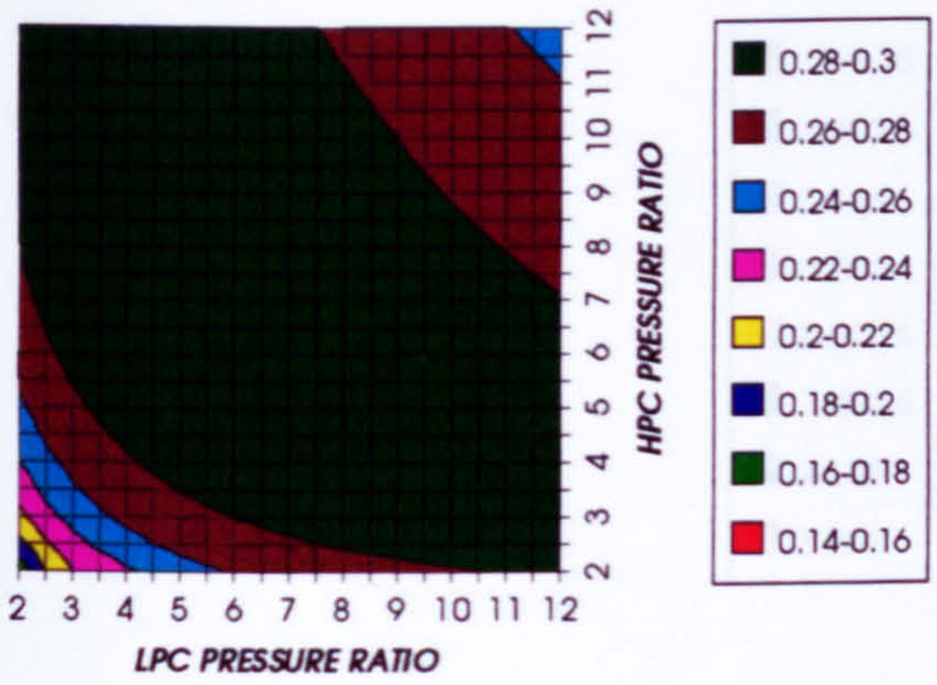

Figure 51. Simple cycle thermal efficiency

SIMPLE CYCLE IDEAL THERMAL EFFICIENCY
REGENERATED CYCLE+PC, CO2/ARGON, FCFC

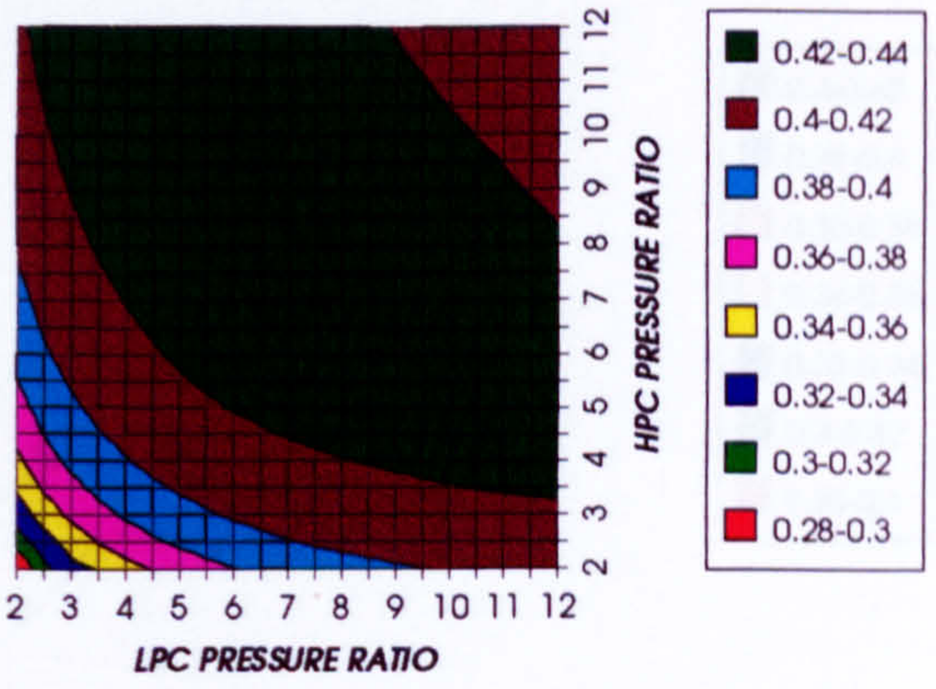

Figure 52. Simple cycle ideal thermal efficiency

COMBINED CYCLE SPECIFIC POWER OUTPUT
REGENERATED CYCLE+PC, CO2/ARGON, FCFC

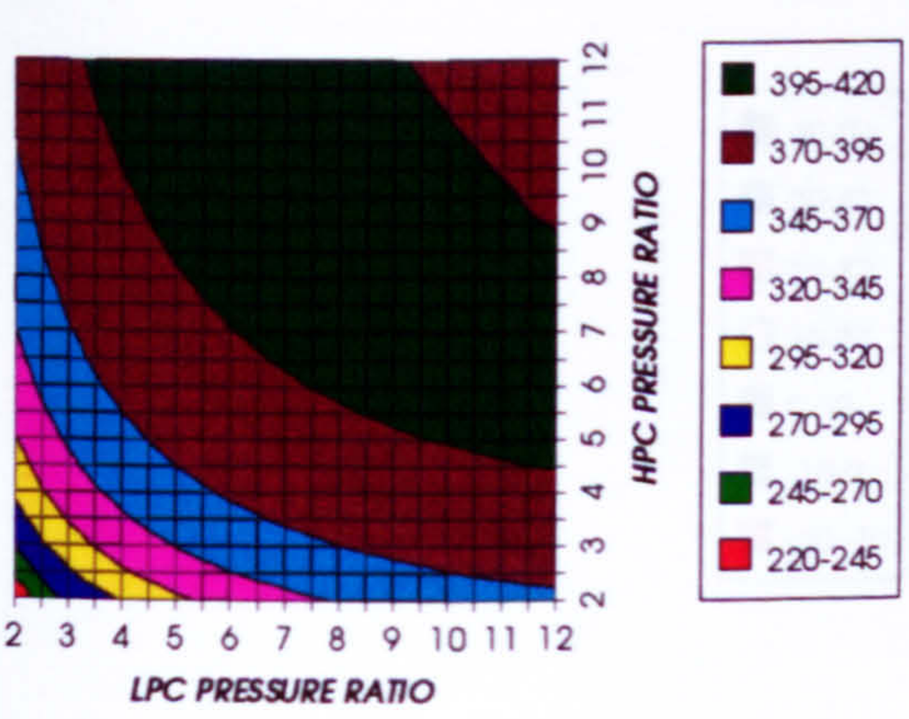

Figure 53. Combined cycle specific power output

COMBINED CYCLE IDEAL SPECIFIC POWER OUTPUT
REGENERATED CYCLE+PC, CO2/ARGON, FCFC

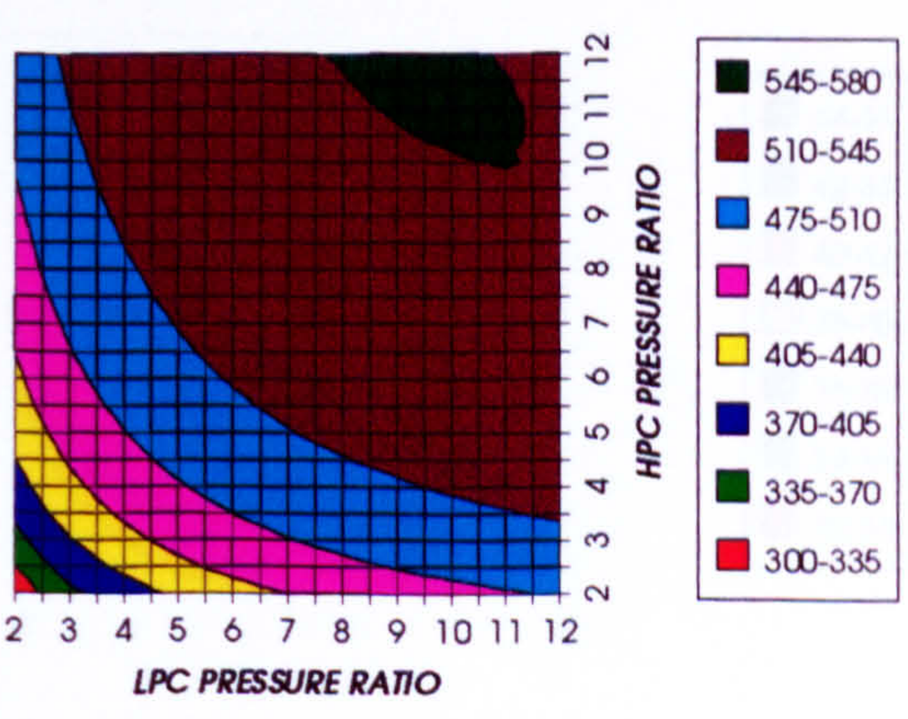

Figure54. Combined cycle ideal specific power output

COMPLETE PLANT WITH CRYOGENIC PRECOOLER & NGVs N_2 COOLING (TET=1650 K)

GAS TURBINE SPECIFIC POWER OUTPUT
REGENERATED CYCLE+PC, CO2/ARGON, FCFC

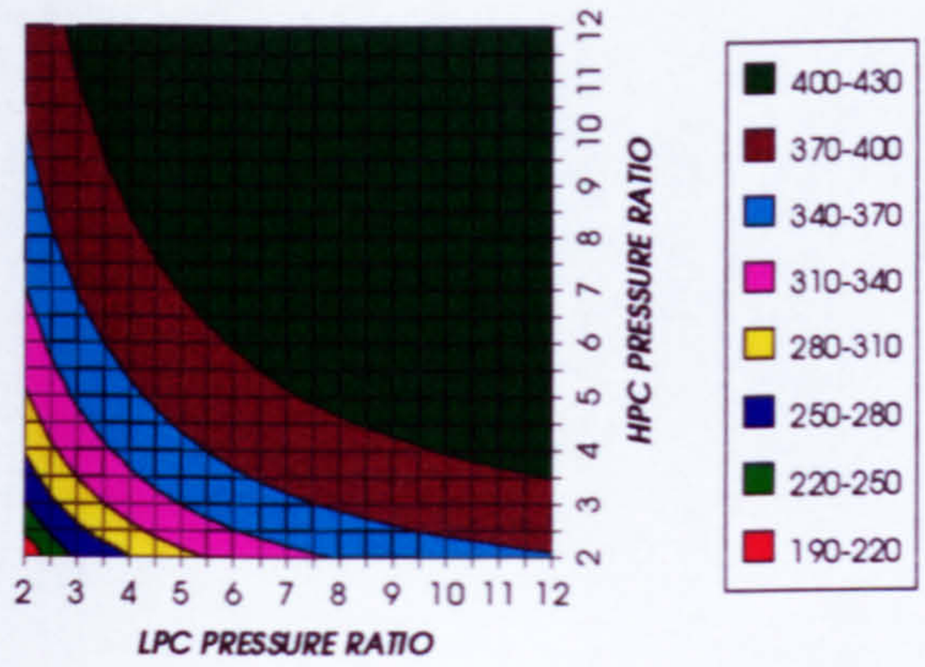

Figure 55. Gas turbine specific power output

STEAM TURBINE SPECIFIC POWER OUTPUT
REGENERATED CYCLE+PC, CO2/ARGON, FCFC

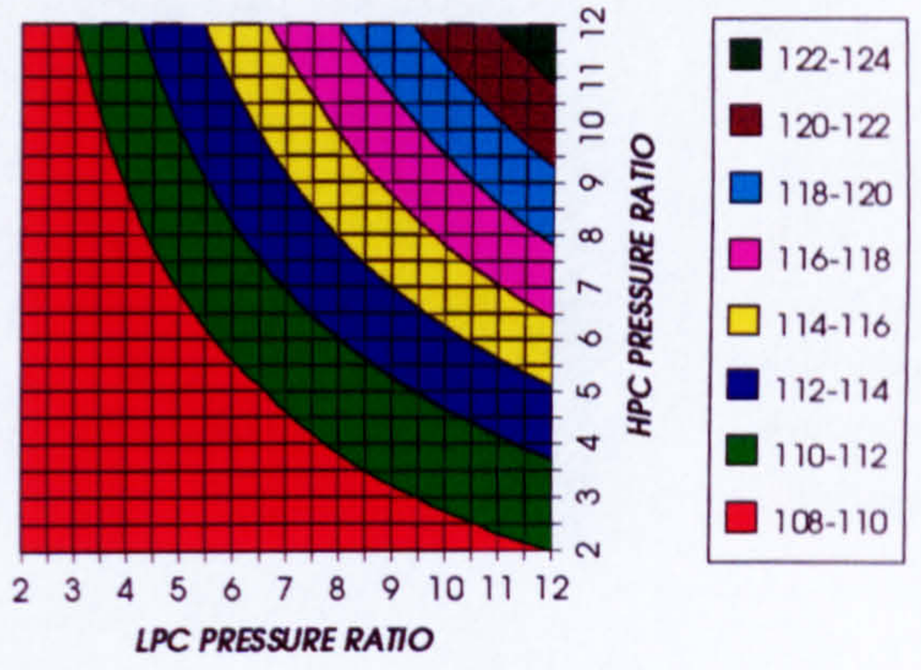

Figure 56. Steam turbine specific power output

GAS TURBINE TO STEAM TURBINE POWER RATIO
REGENERATED CYCLE+PC, CO2/ARGON, FCFC

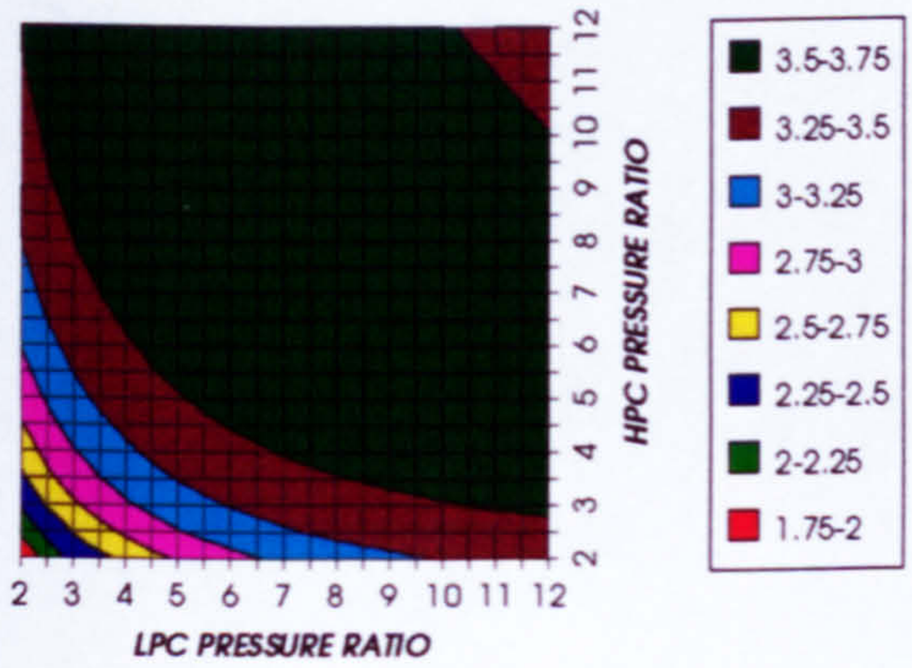

Figure 57. Gas turbine to steam turbine power ratio

AUXILIARIES TO USEFUL POWER RATIO
REGENERATED CYCLE+PC, CO2/ARGON, FCFC

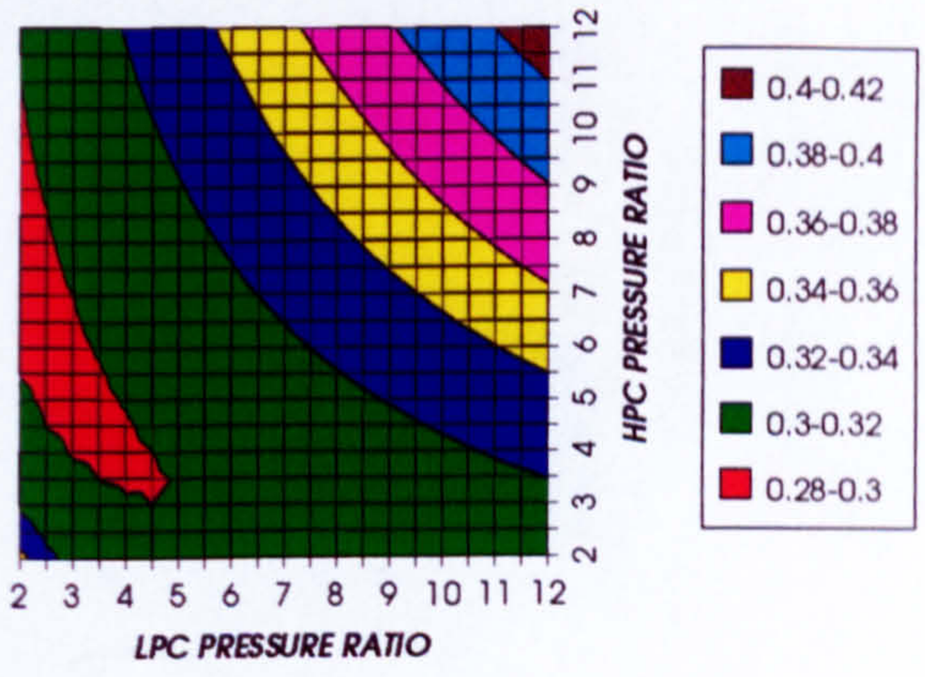

Figure 58. Auxiliary (CO2/Argon, O2 & Fuel) to usefuel power ratio

CO2 COMPRESSION AUXILIARY SPECIFIC POWER
REGENERATED CYCLE+PC, CO2/ARGON, FCFC

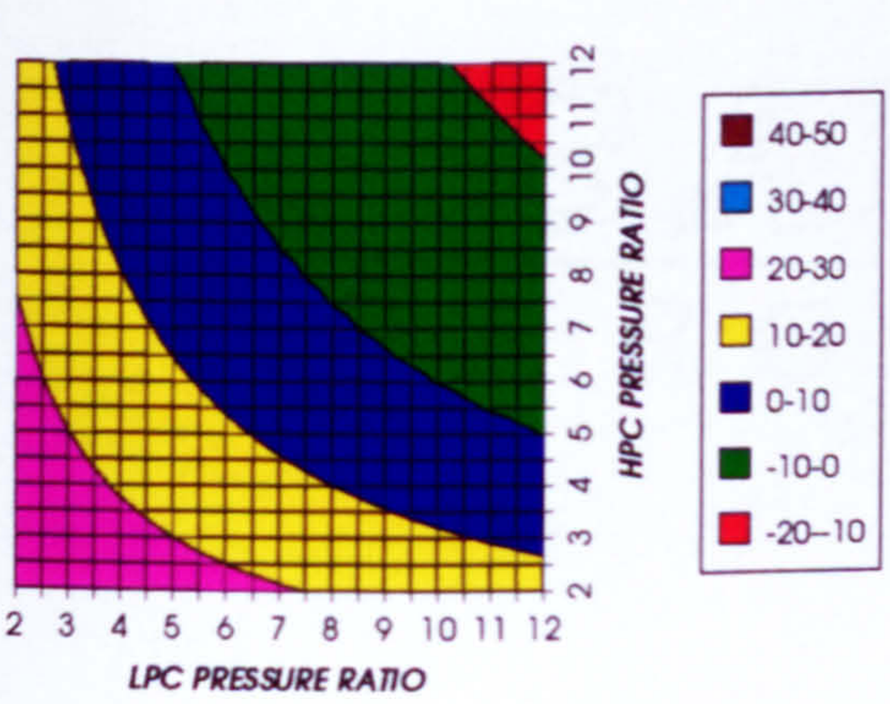

Figure 59. CO2/Argon compression specific power

OXYGEN SEPARATION SPECIFIC POWER
REGENERATED CYCLE+PC, CO2/ARGON, FCFC

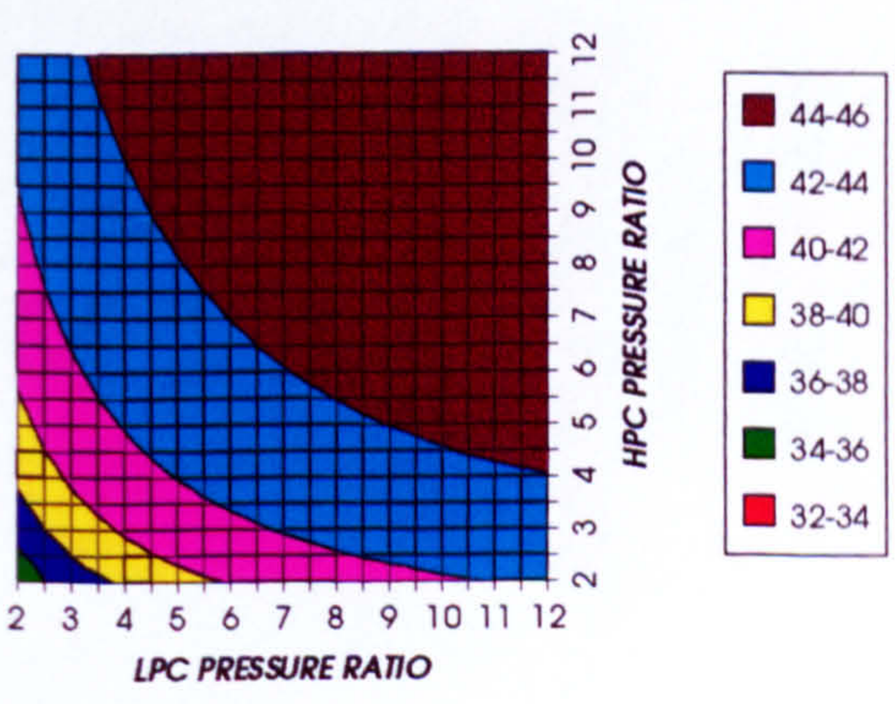

Figure 60. Oxygen separation specific power

COMPLETE PLANT WITH CRYOGENIC PRECOOLER & NGVs N_2 COOLING (TET=1650 K)

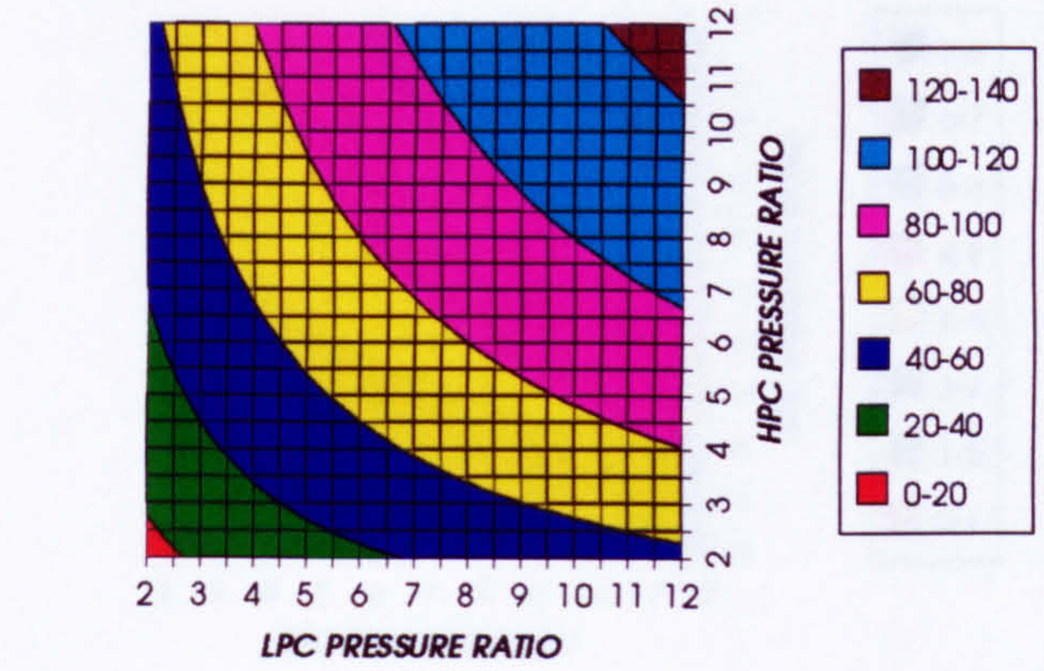

Figure 61. Fuel compression specific power

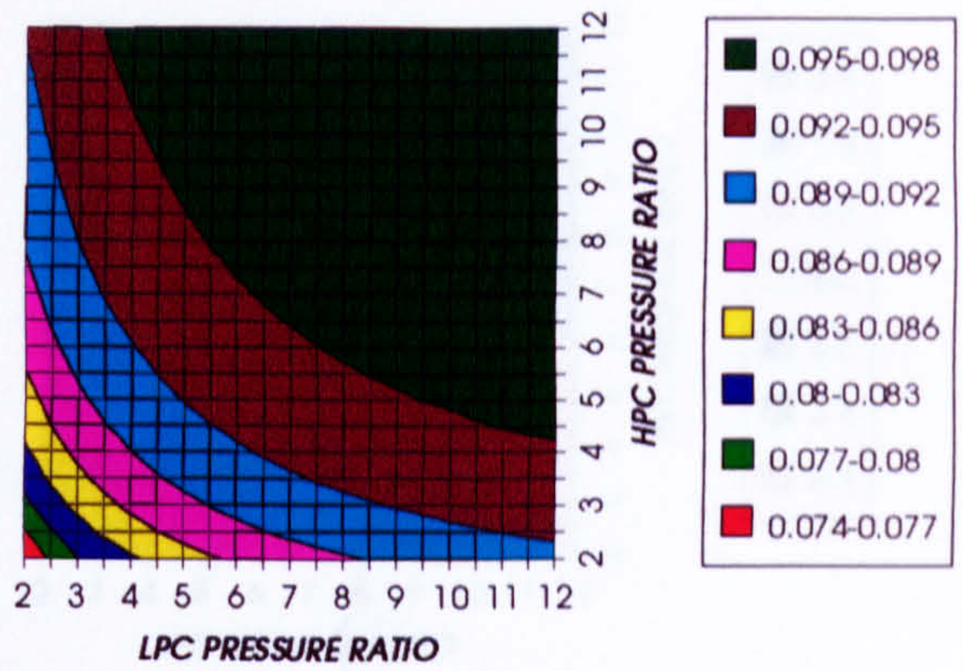

Figure 62. Fuel to compressor inlet mass flow ratio

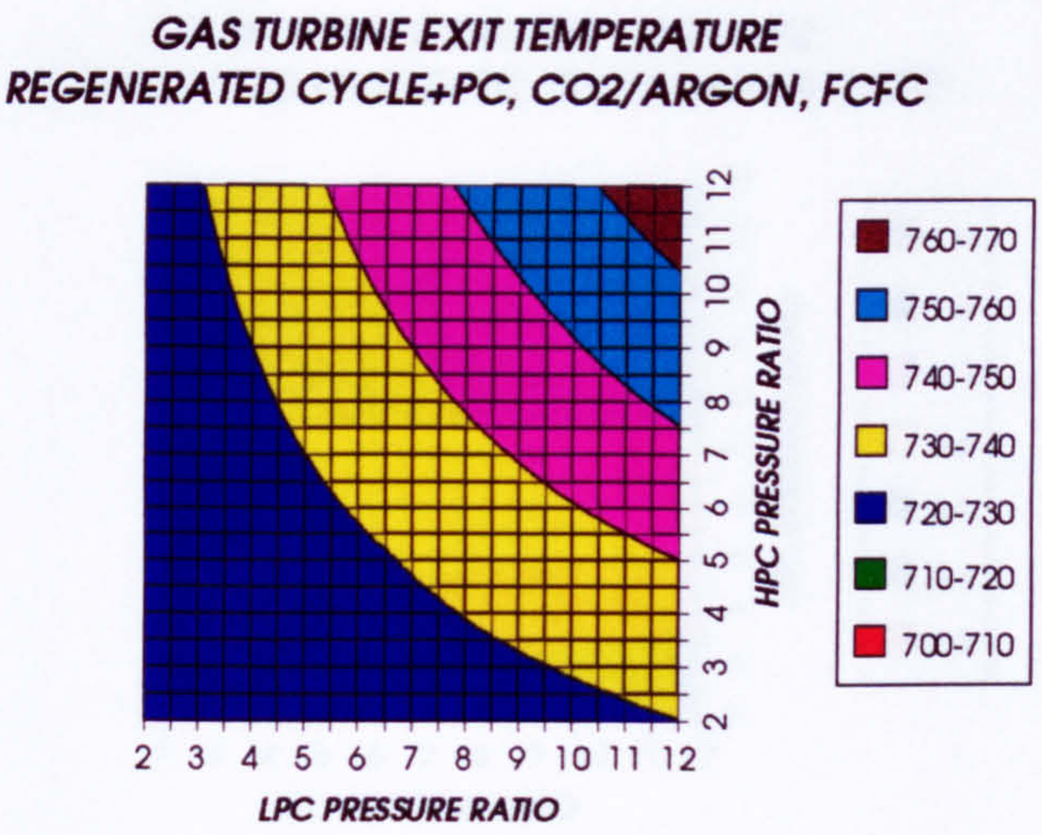

Figure 63. Gas turbine exit temperature

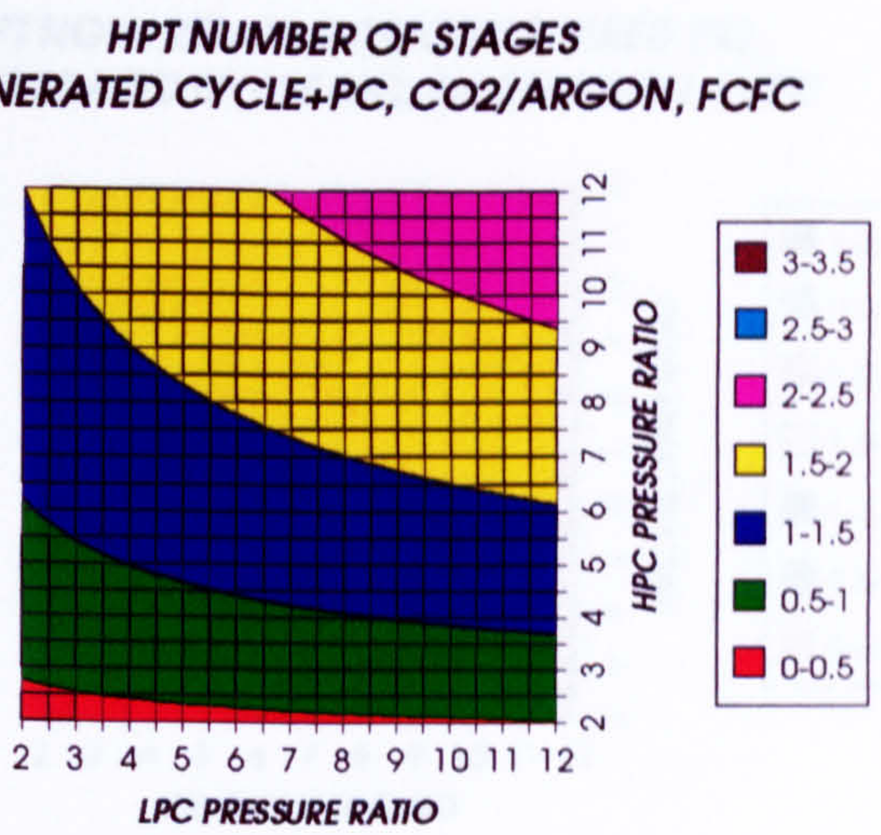

Figure 64. Number of HPT stages

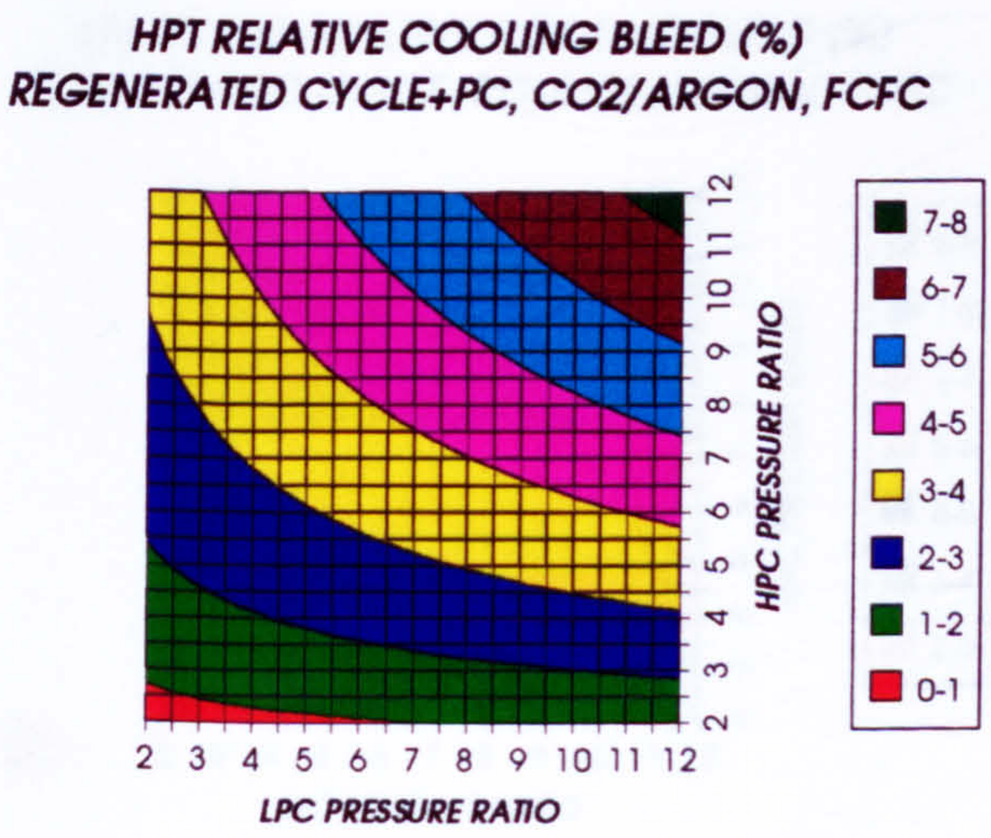

Figure 65. HPT cooling to compressor inlet mass flow ratio

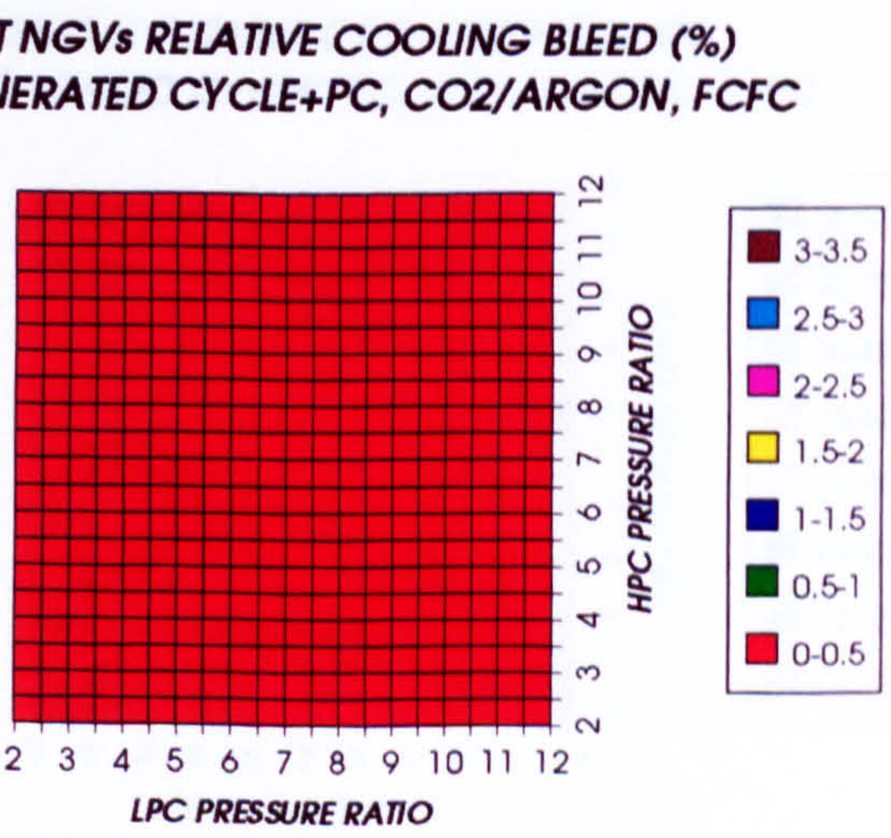

Figure 66. HPT NGVs cooling to compressor inlet mass flow ratio

COMPLETE PLANT WITH CRYOGENIC PRECOOLER & NGVs N_2 COOLING (TET=1650 K)

HPT ROTOR RELATIVE COOLING BLEED (%)
REGENERATED CYCLE+PC, CO2/ARGON, FCFC

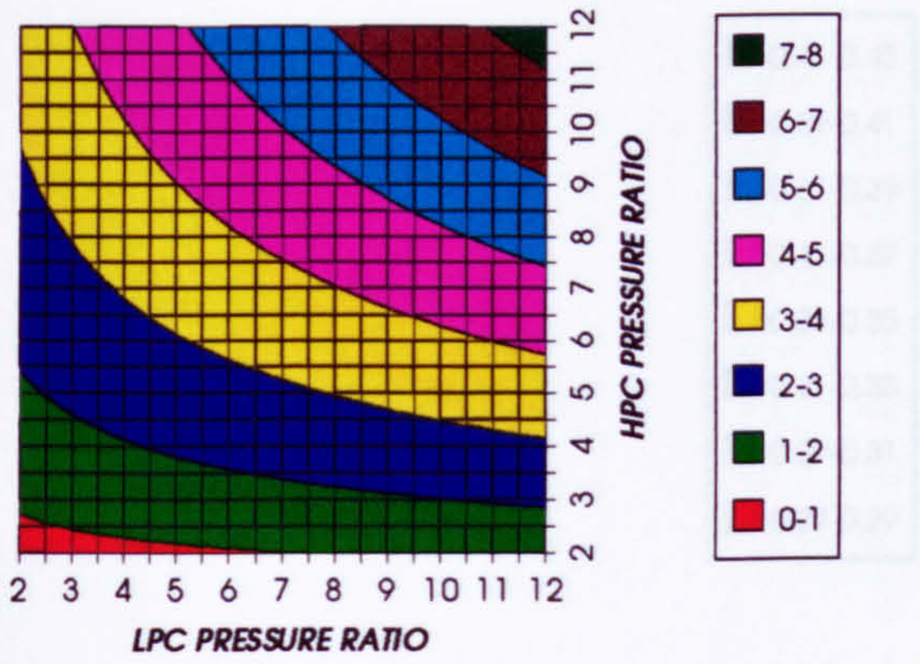

Figure 67. HPT rotor cooling to compressor inlet mass flow ratio

LPT NUMBER OF STAGES
REGENERATED CYCLE+PC, CO2/ARGON, FCFC

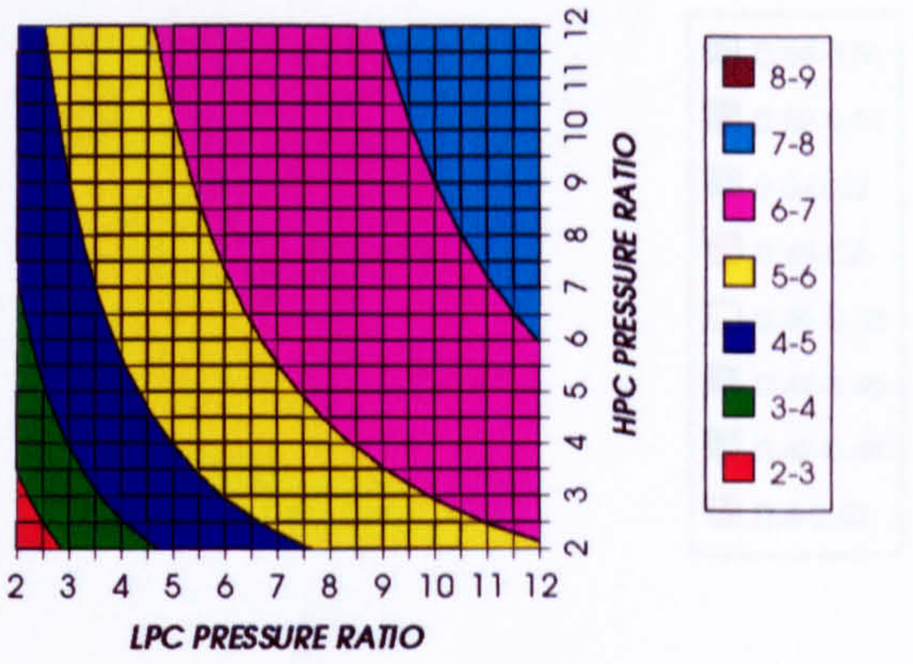

Figure 68. Number of LPT stage

LPT RELATIVE COOLING BLEED (%)
REGENERATED CYCLE+PC, CO2/ARGON, FCFC

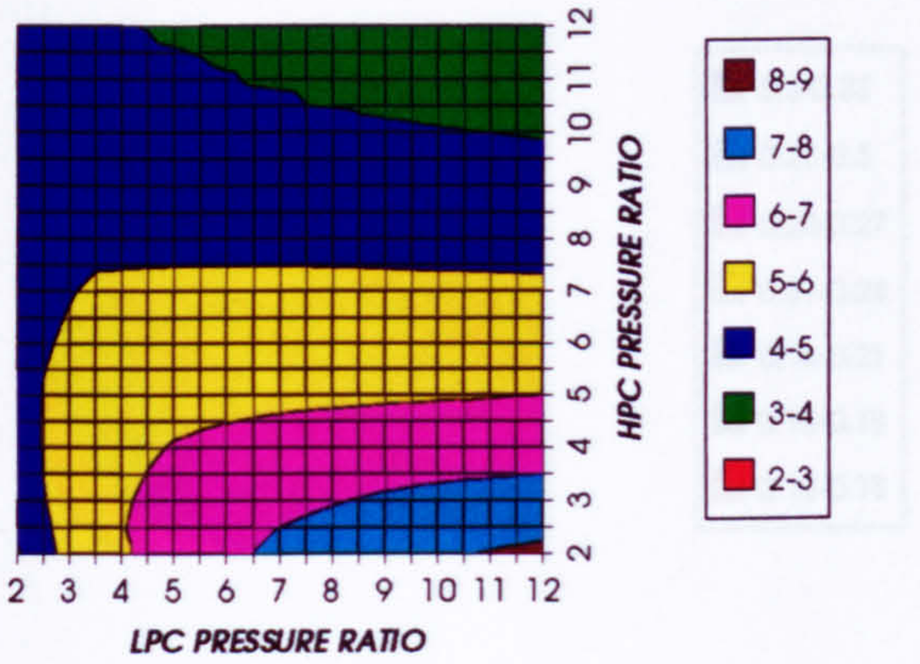

Figure 69. LPT cooling to compressor inlet mass flow ratio

LPT NGVs RELATIVE COOLING BLEED (%)
REGENERATED CYCLE+PC, CO2/ARGON, FCFC

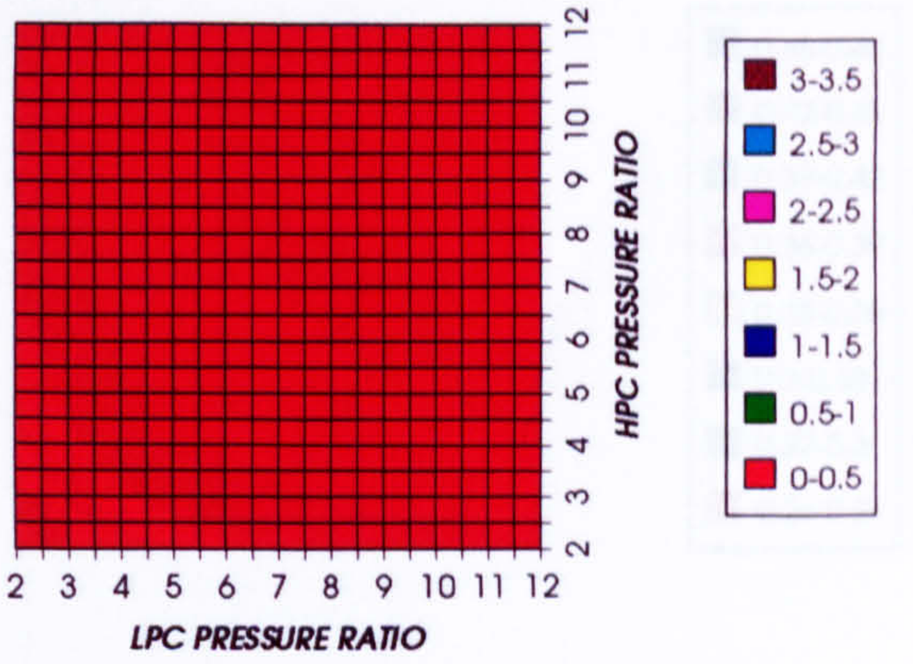

Figure 70. LPT NGVs cooling to compressor inlet mass flow ratio

LPT ROTOR RELATIVE COOLING BLEED (%)
REGENERATED CYCLE+PC, CO2/ARGON, FCFC

Figure 71. LPT rotor cooling to compressor inlet mass flow ratio

STEAM TURBINE OPTIMUM PRESSURE
REGENERATED CYCLE+PC, CO2/ARGON, FCFC

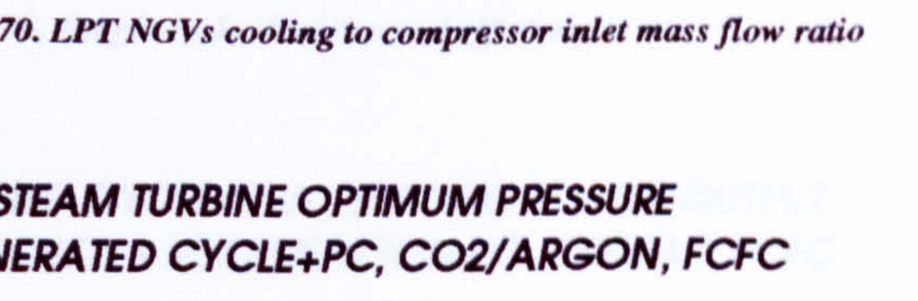

Figure 72. Steam turbine optimum pressures (maximum)

COMPLETE PLANT WITH CRYOGENIC PRECOOLER & NGVs N_2 COOLING (TET=1650 K)

COMBINED CYCLE THERMAL EFFICIENCY
INTERCOOLED & REGENERATED+PC, CO2/AR, FCFC

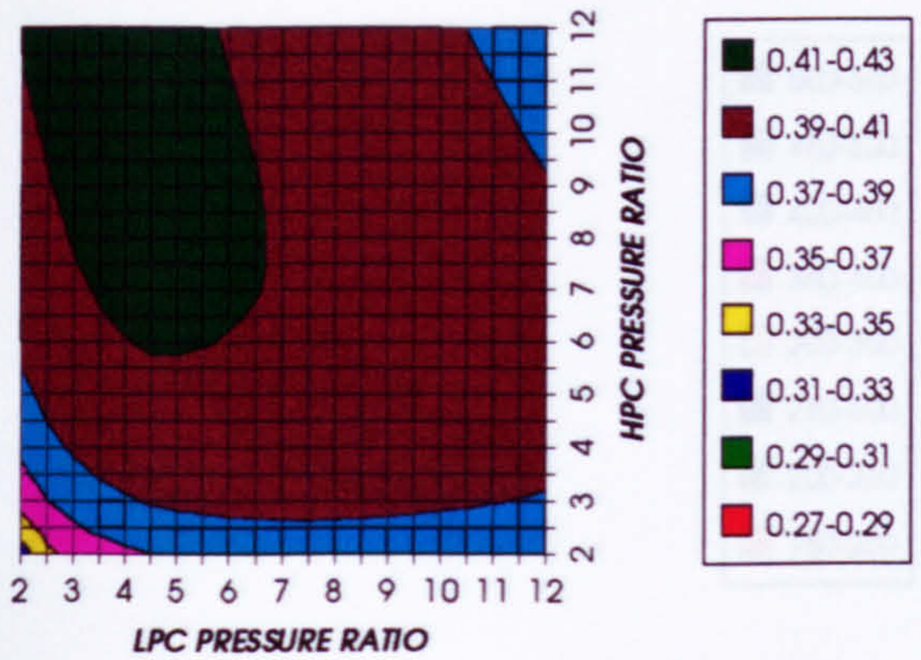

Figure 73. Combined cycle thermal efficiency

COMBINED CYCLE IDEAL THERMAL EFFICIENCY
INTERCOOLED & REGENERATED+PC, CO2/AR, FCFC

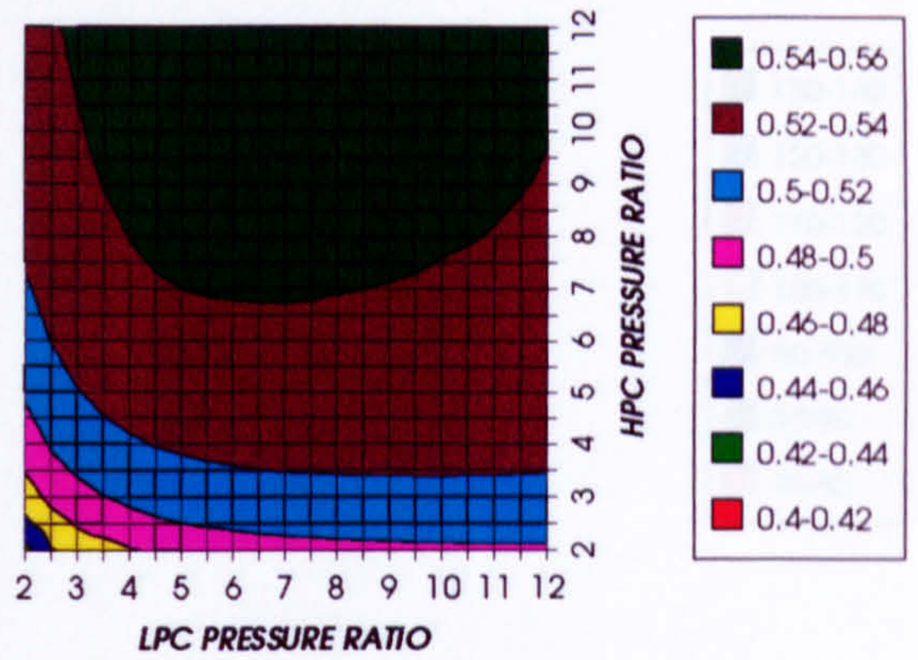

Figure 74. Combined cycle ideal thermal efficiency

SIMPLE CYCLE THERMAL EFFICIENCY
INTERCOOLED & REGENERATED+PC, CO2/AR, FCFC

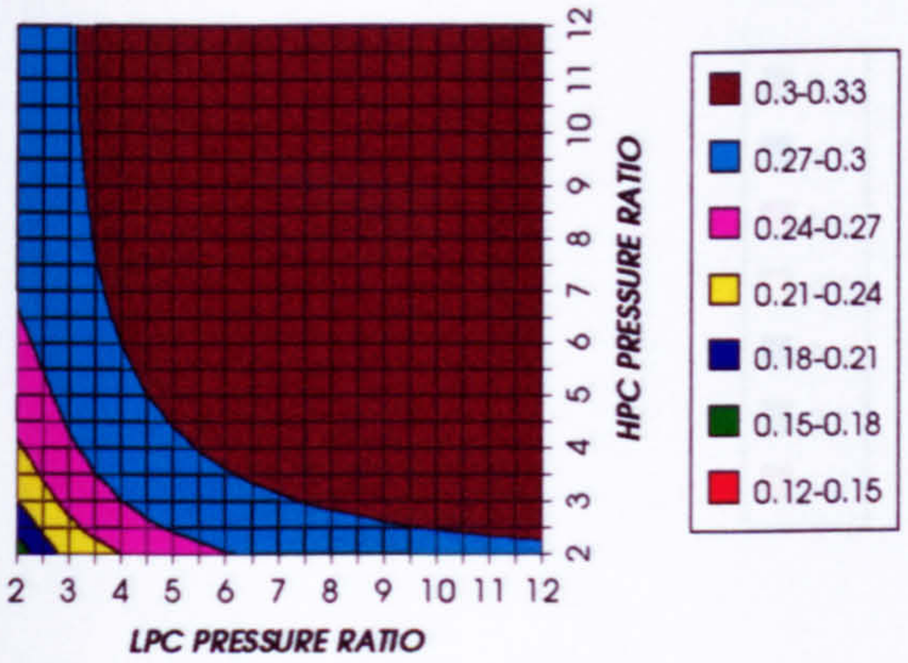

Figure 75. Simple cycle thermal efficiency

SIMPLE CYCLE IDEAL THERMAL EFFICIENCY
INTERCOOLED & REGENERATED+PC, CO2/AR, FCFC

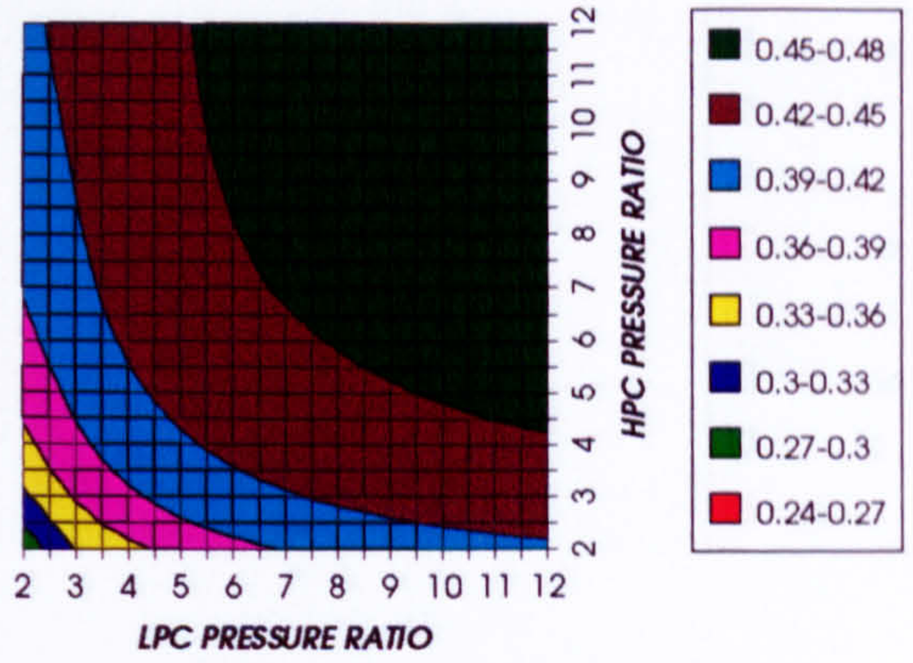

Figure 76. Simple cycle ideal thermal efficiency

COMBINED CYCLE SPECIFIC POWER OUTPUT
INTERCOOLED & REGENERATED+PC, CO2/AR, FCFC

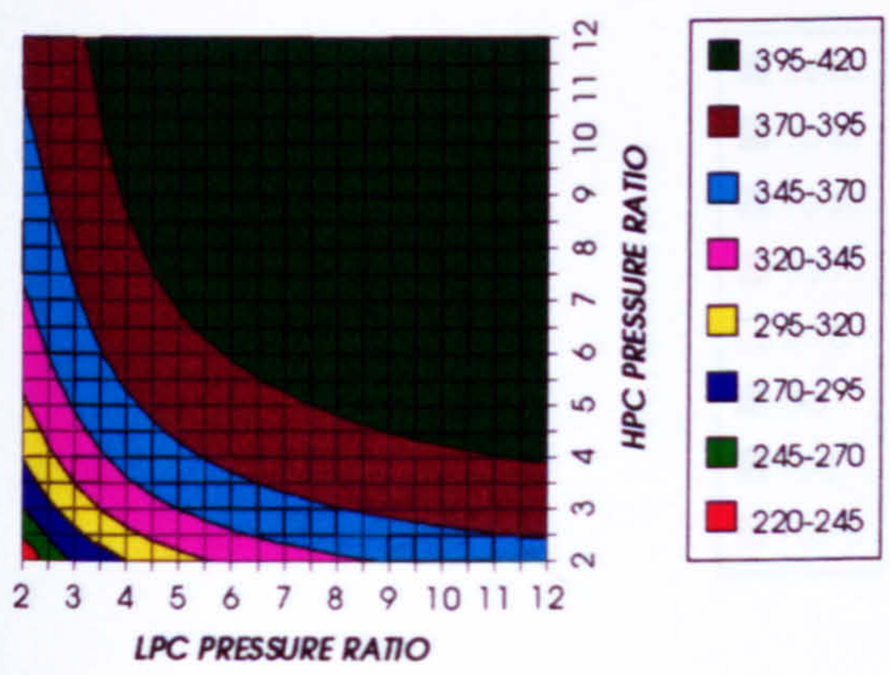

Figure 77. Combined cycle specific power output

COMBINED CYCLE IDEAL SPECIFIC POWER OUTPUT
INTERCOOLED & REGENERATED+PC, CO2/AR, FCFC

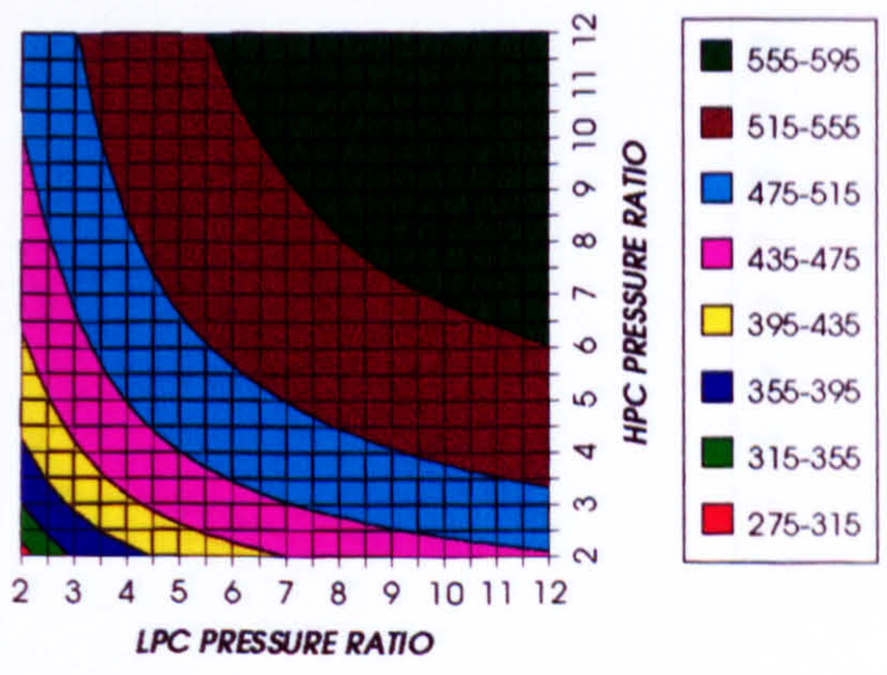

Figure78. Combined cycle ideal specific power output

COMPLETE PLANT WITH CRYOGENIC PRECOOLER & NGVs N_2 COOLING (TET=1650 K)

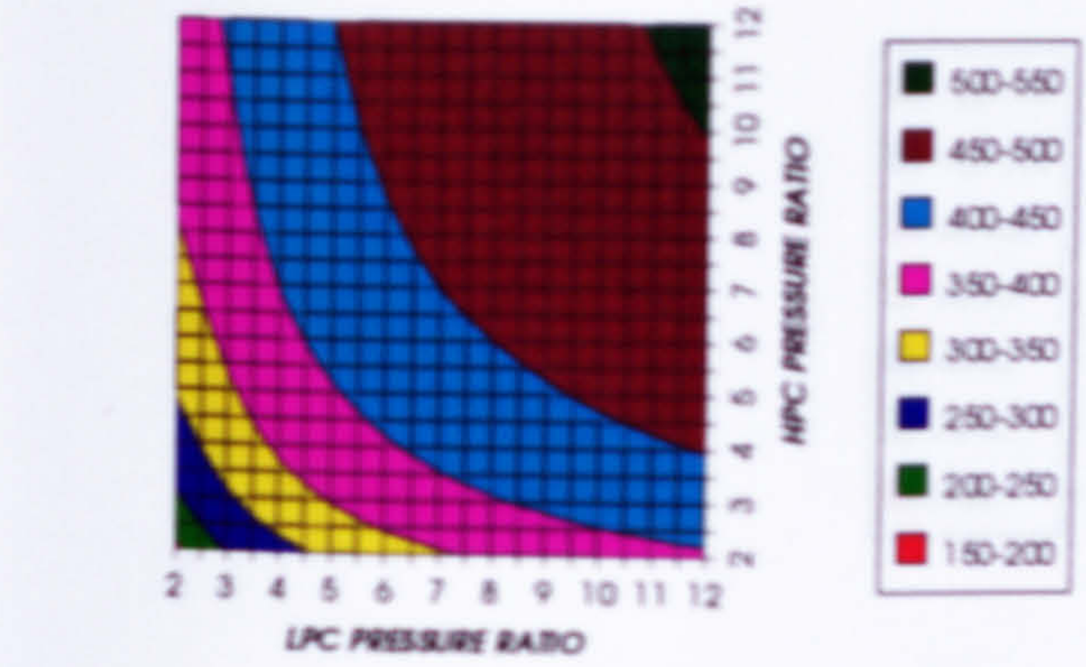

Figure 79. Gas turbine specific power output

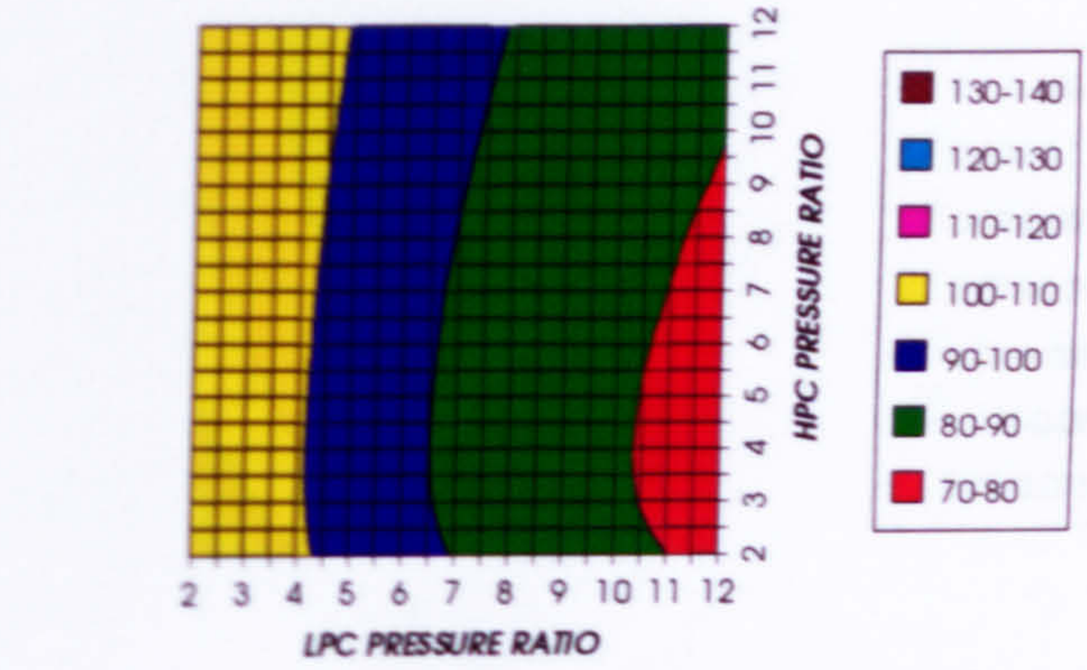

Figure 80. Steam turbine specific power output

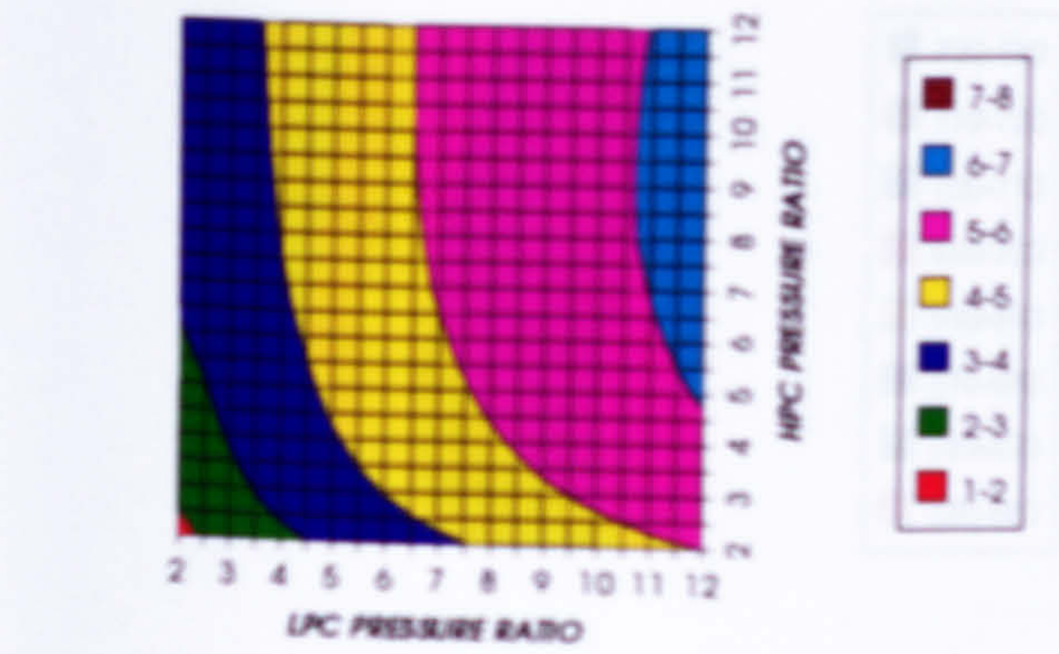

Figure 81. Gas turbine to steam turbine power ratio

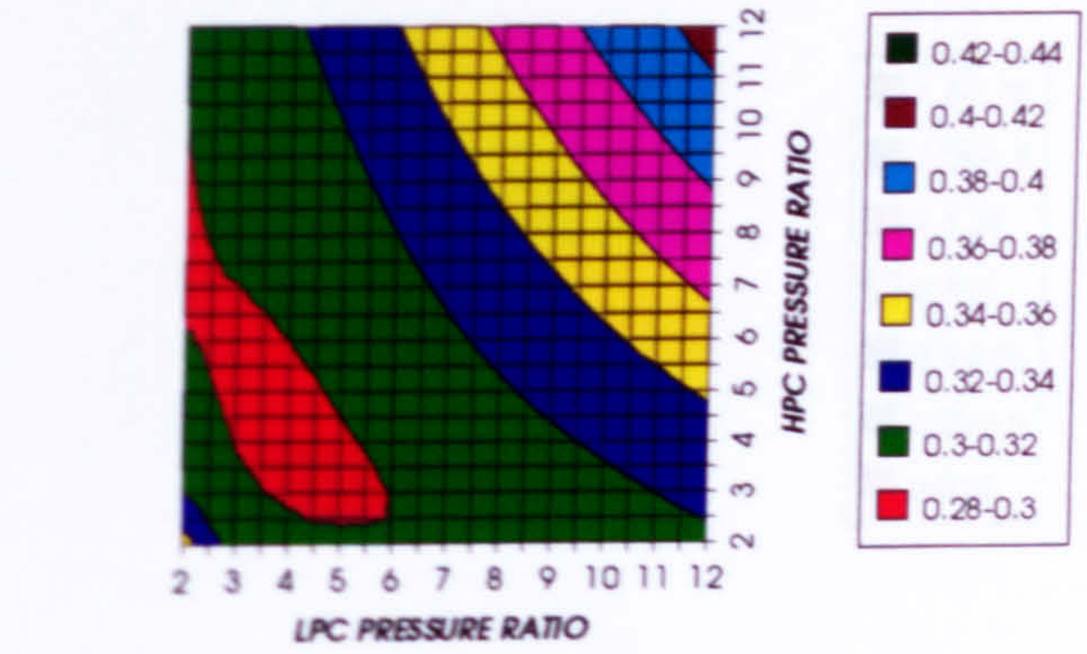

Figure 82. Auxiliary (CO2/Argon, O2 & Fuel) to usefuel power ratio

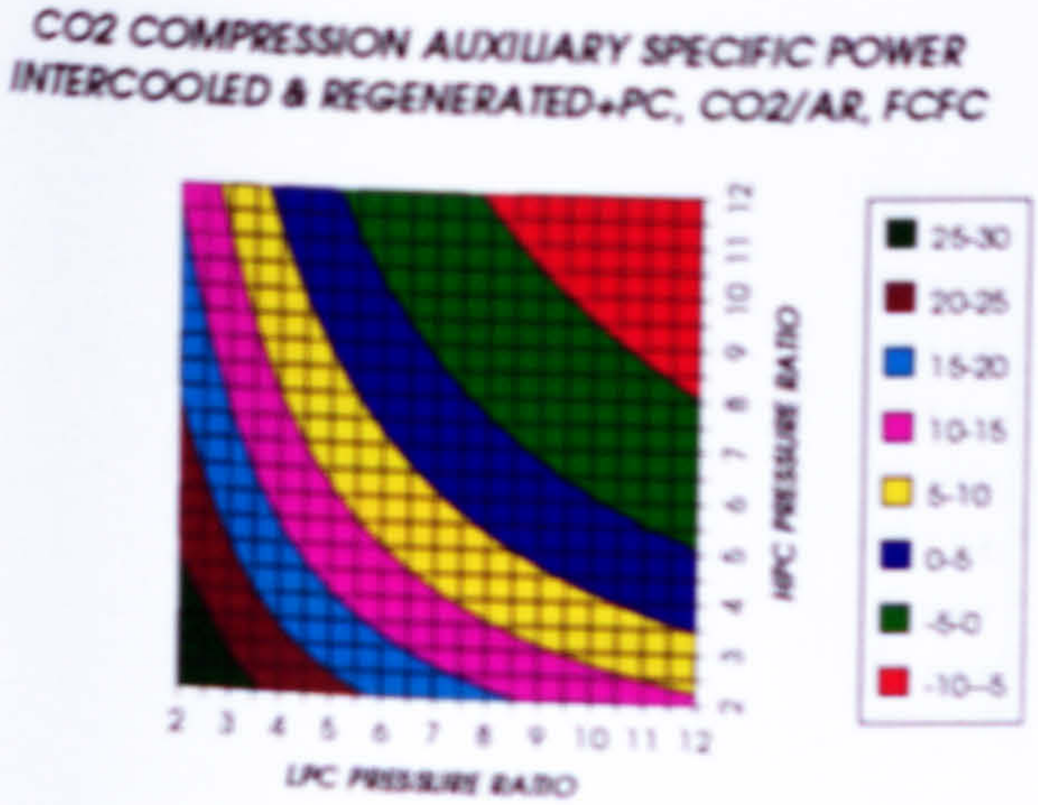

Figure 83. CO2/Argon compression specific power

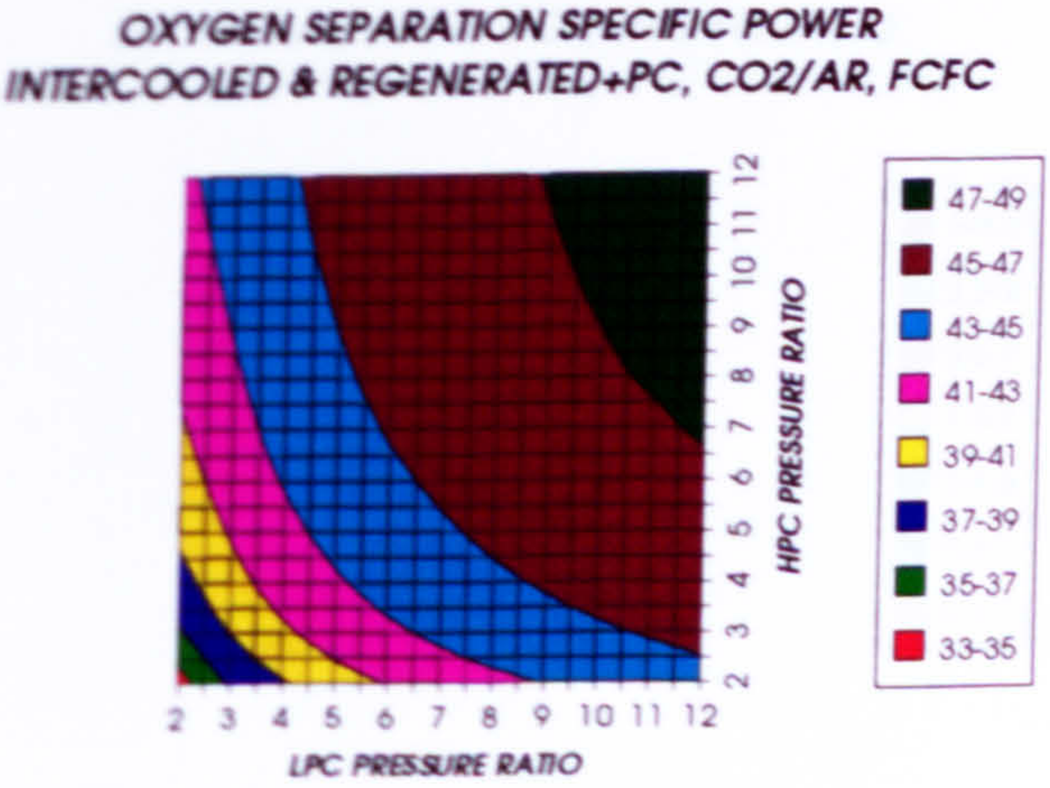

Figure 84. Oxygen separation specific power

COMPLETE PLANT WITH CRYOGENIC PRECOOLER & NGVs N_2 COOLING (TET=1650 K)

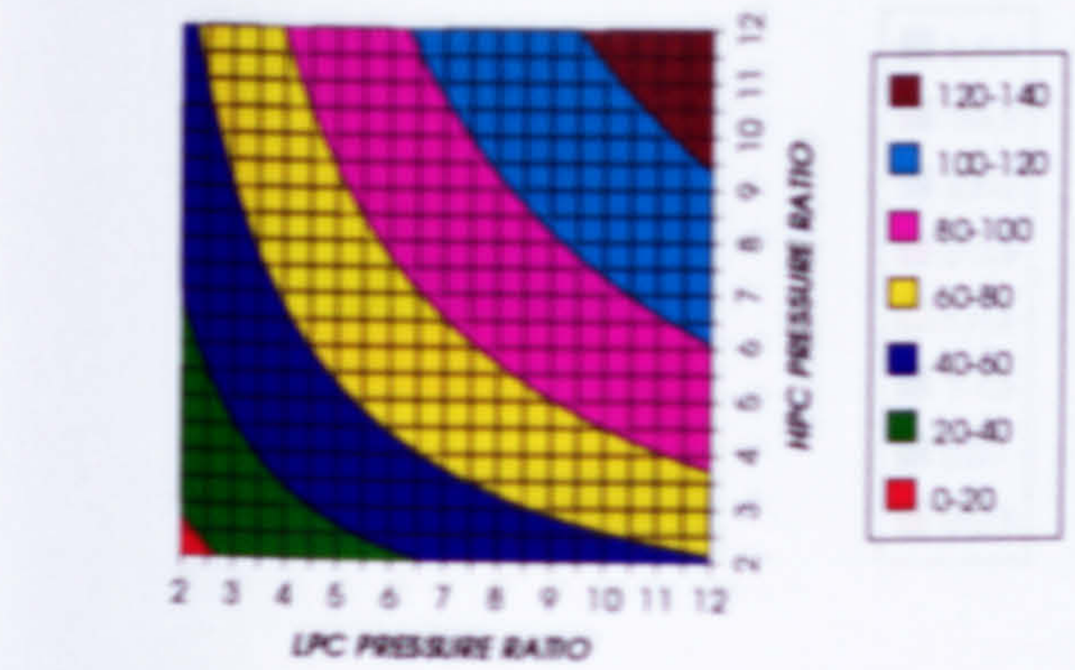

Figure 85. Fuel compression specific power

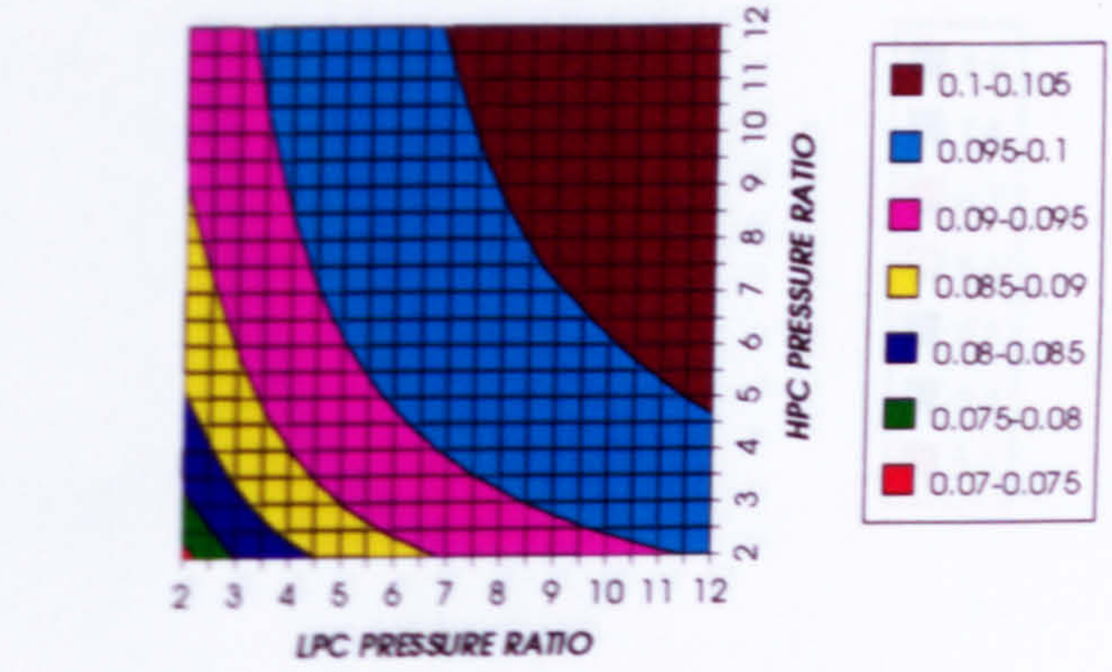

Figure 86. Fuel to compressor inlet mass flow ratio

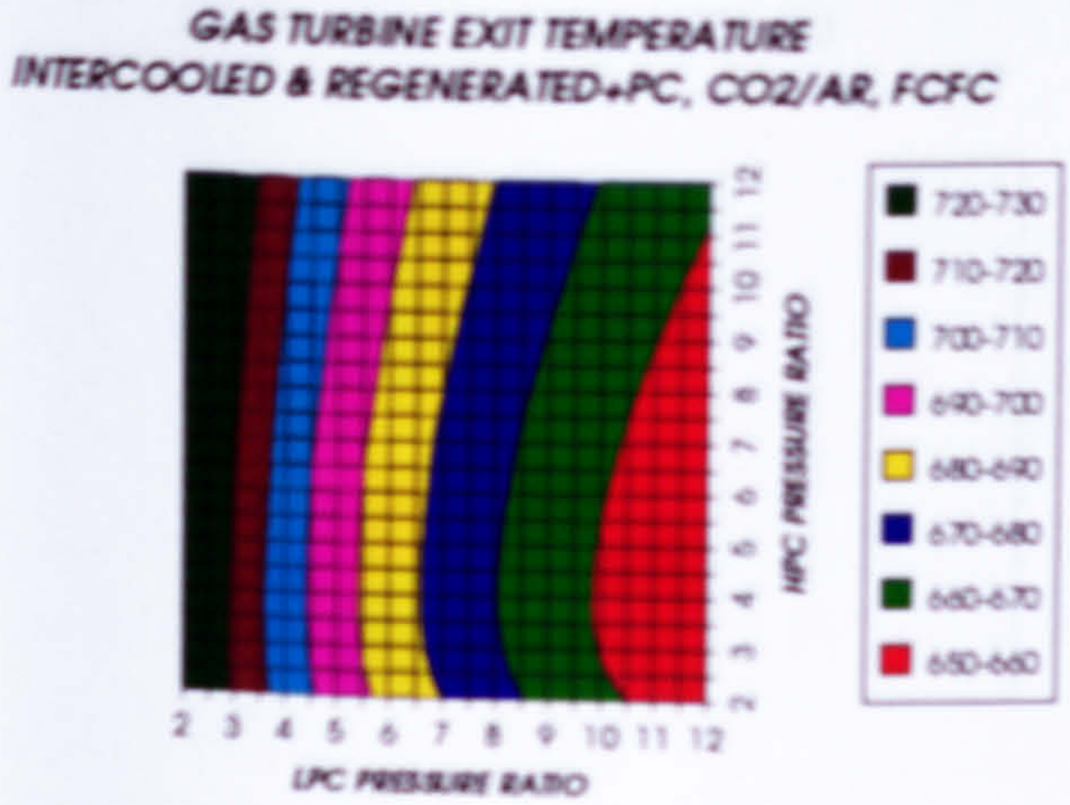

Figure 87. Gas turbine exit temperature

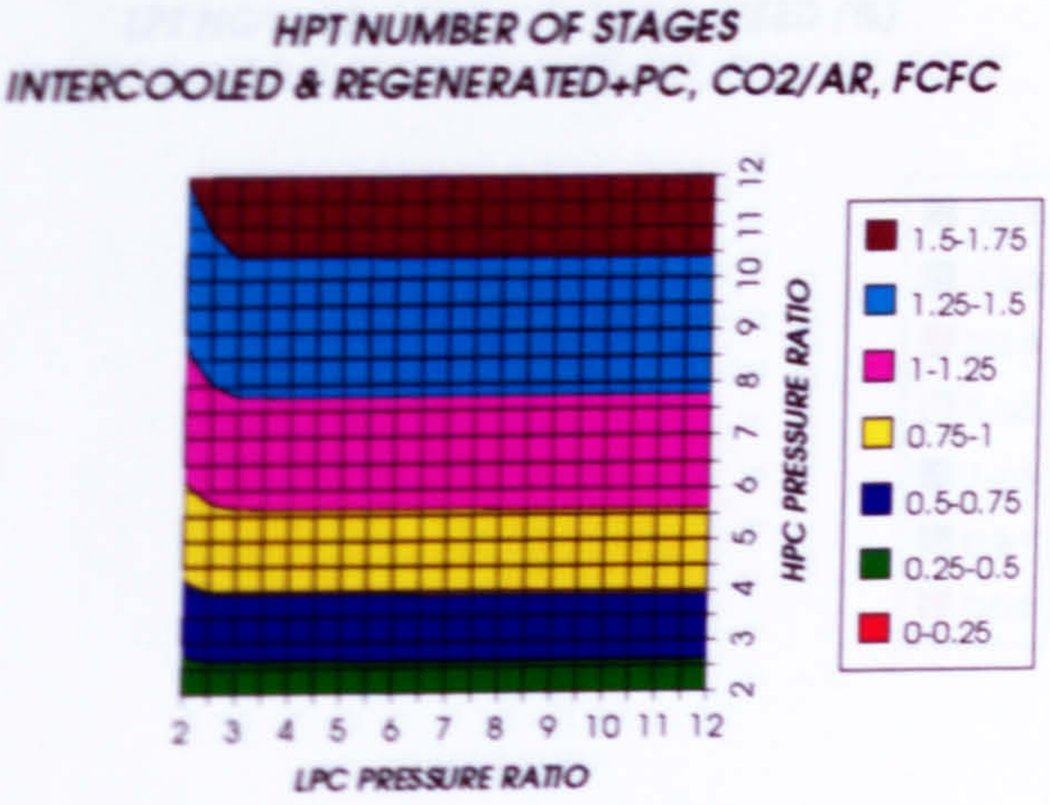

Figure 88. Number of HPT stages

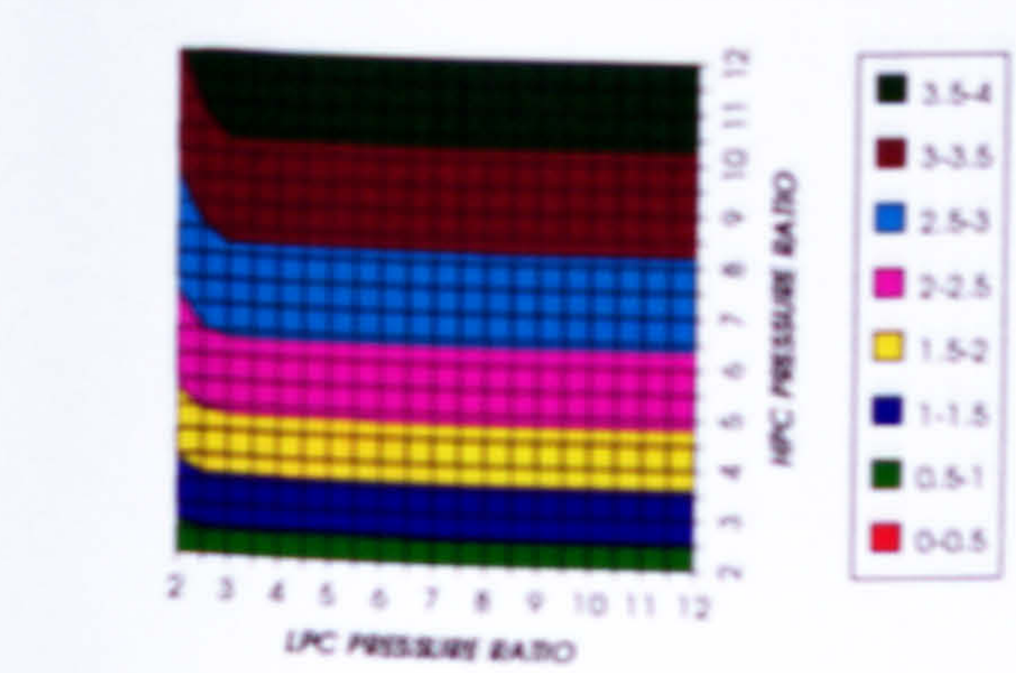

Figure 89. HPT cooling to compressor inlet mass flow ratio

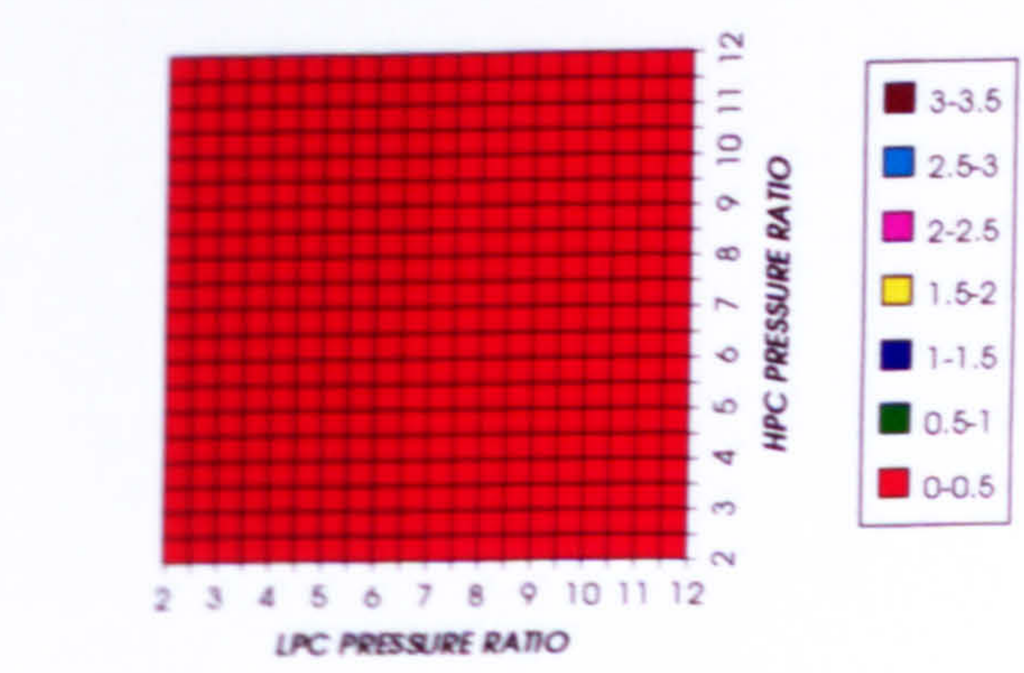

Figure 90. HPT NGVs cooling to compressor inlet mass flow ratio

COMPLETE PLANT WITH CRYOGENIC PRECOOLER & NGVs N_2 COOLING (TET=1650 K)

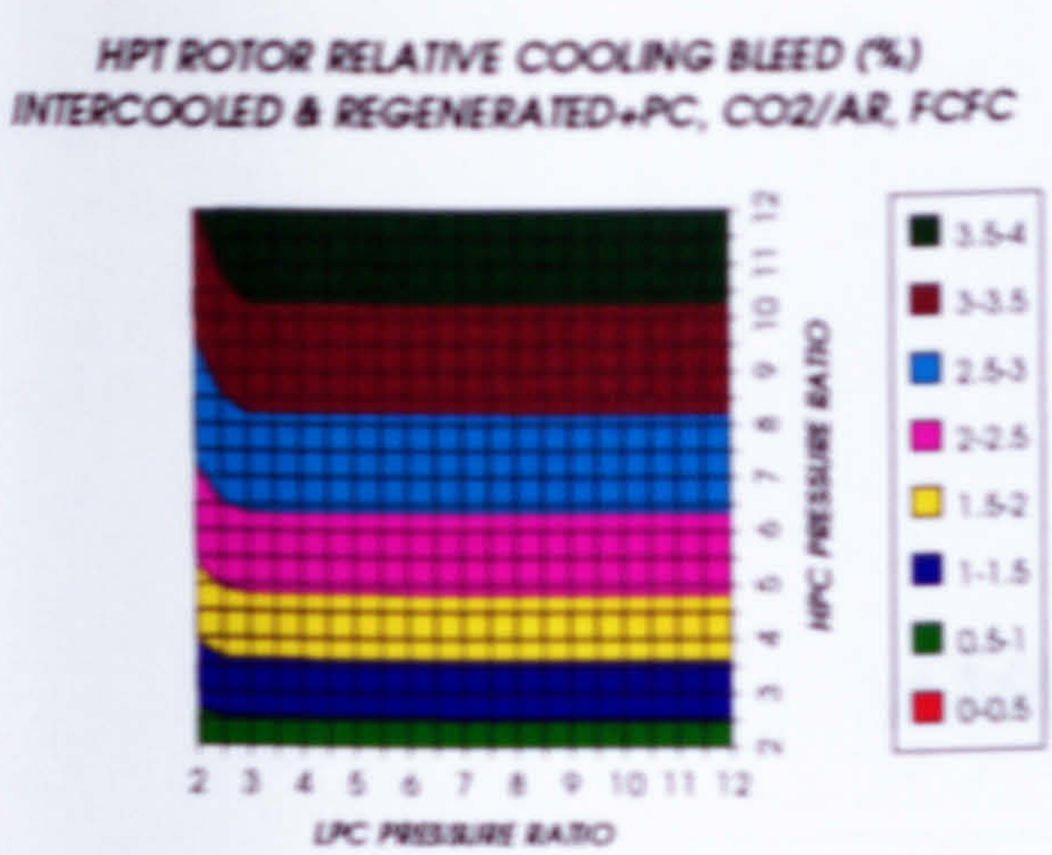

Figure 91. HPT rotor cooling to compressor inlet mass flow ratio

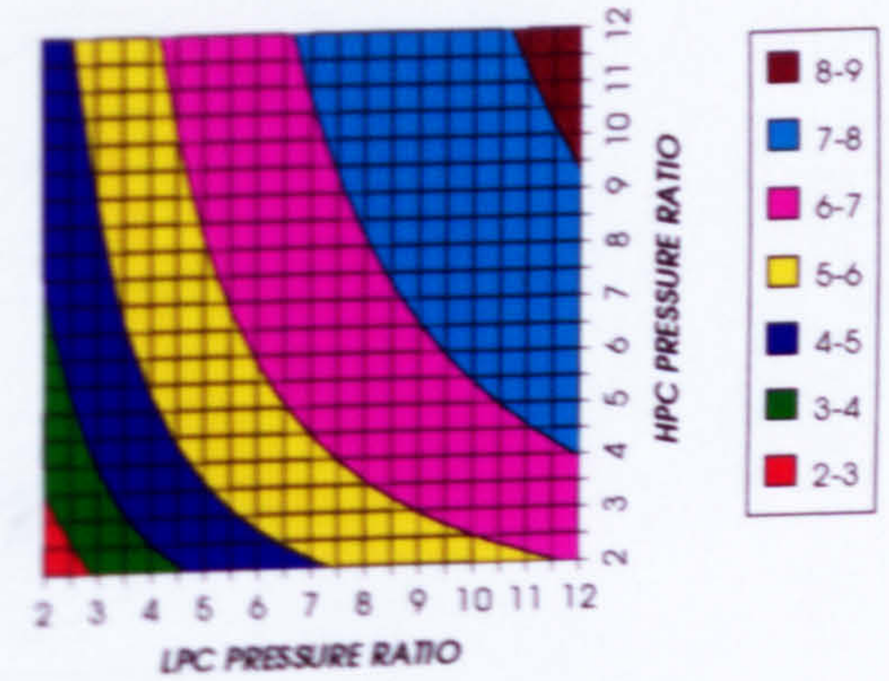

Figure 92. Number of LPT stages

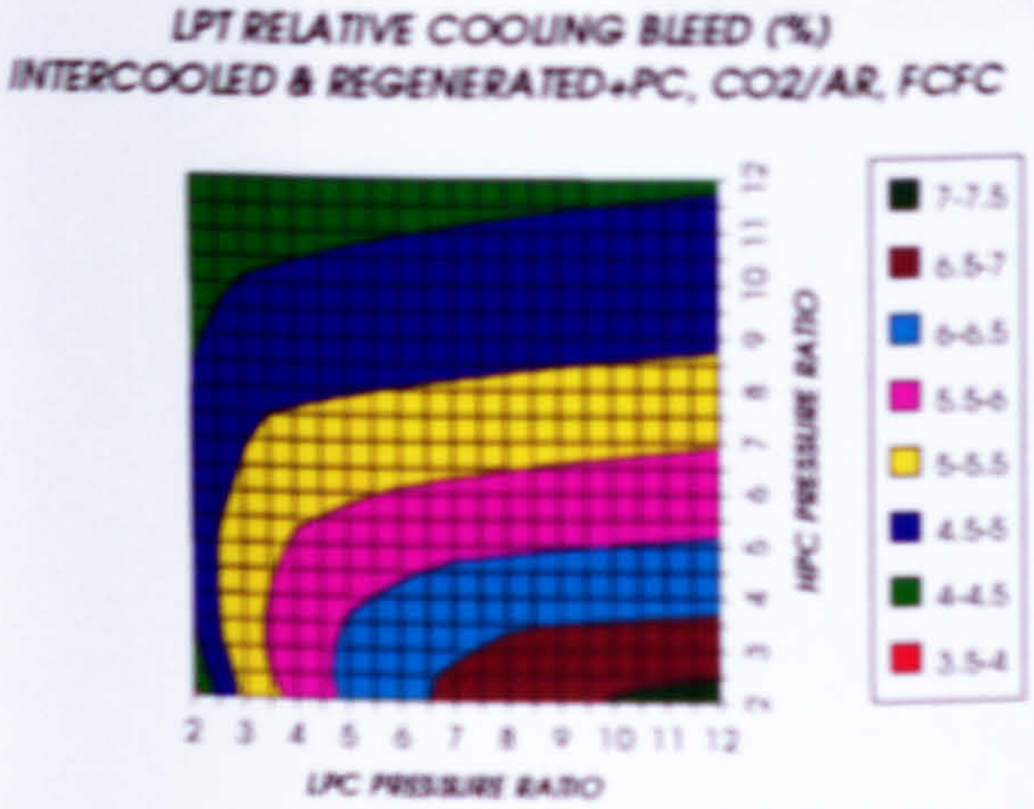

Figure 93. LPT cooling to compressor inlet mass flow ratio

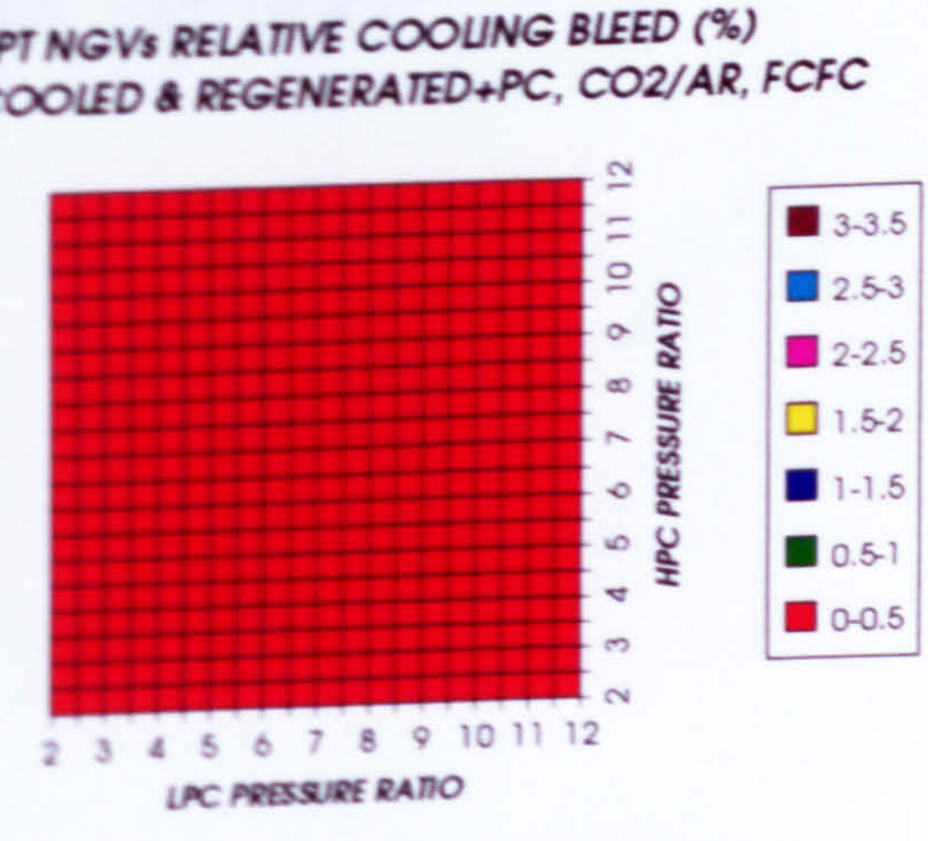

Figure 94. LPT NGVs cooling to compressor inlet mass flow ratio

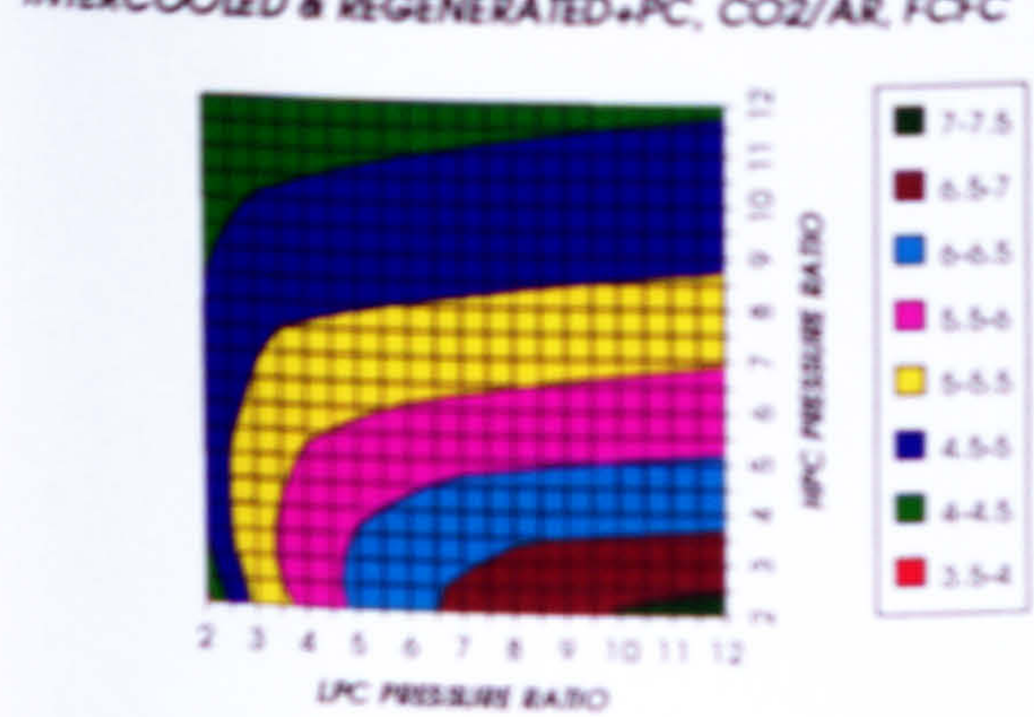

Figure 95. LPT rotor cooling to compressor inlet mass flow ratio

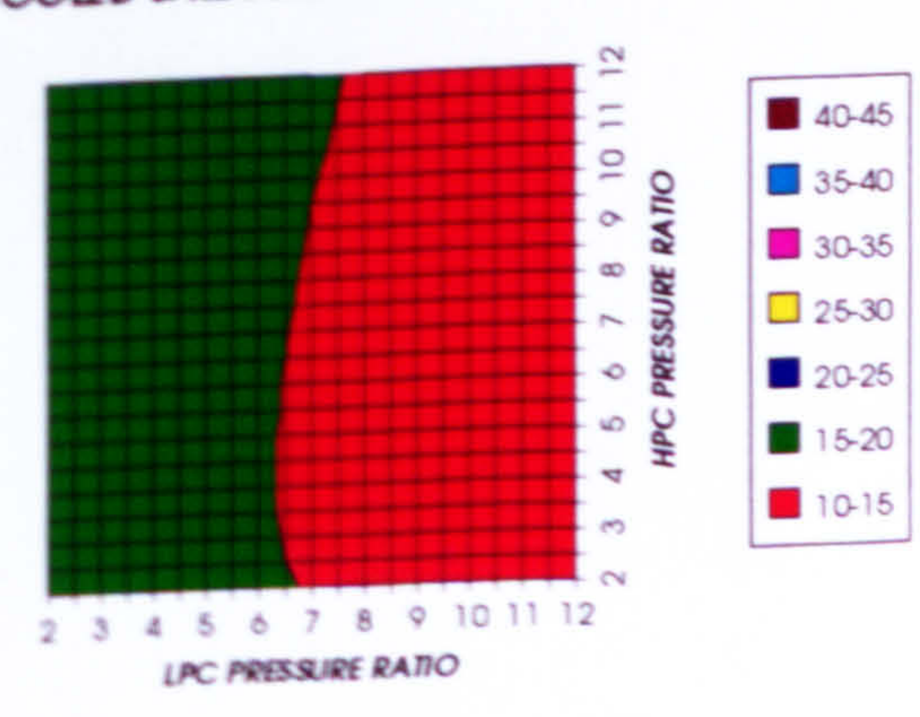

Figure 96. Steam turbine optimum pressures (maximum)

APPENDIX VIII

EFFECT OF CHANGING THE WORKING FLUID (ONE SPOOL - ONE SHAFT)

EFFECT OF CHANGING THE WORKING FLUID (1 SPOOL - 1 SHAFT)

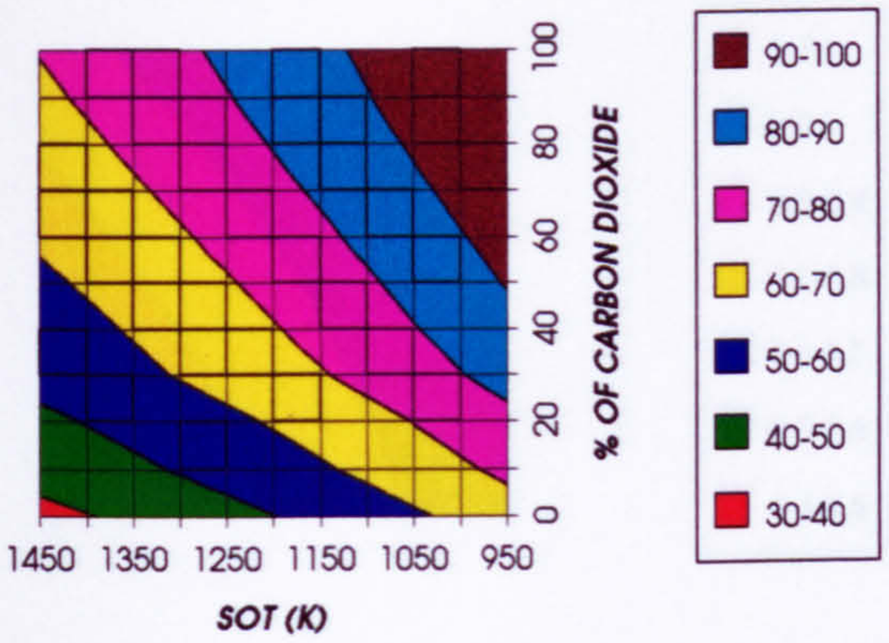

Figure 1. HP compressor surge margin (%)
1 spool -1 shaft configuration

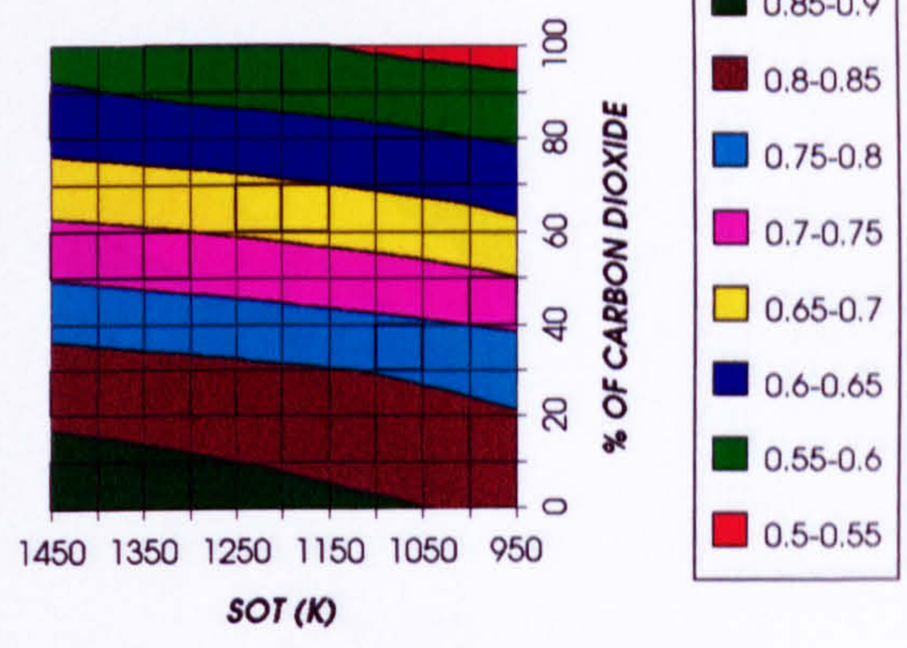

Figure 2. HP compressor adiabatic efficiency
1 spool -1 shaft configuration

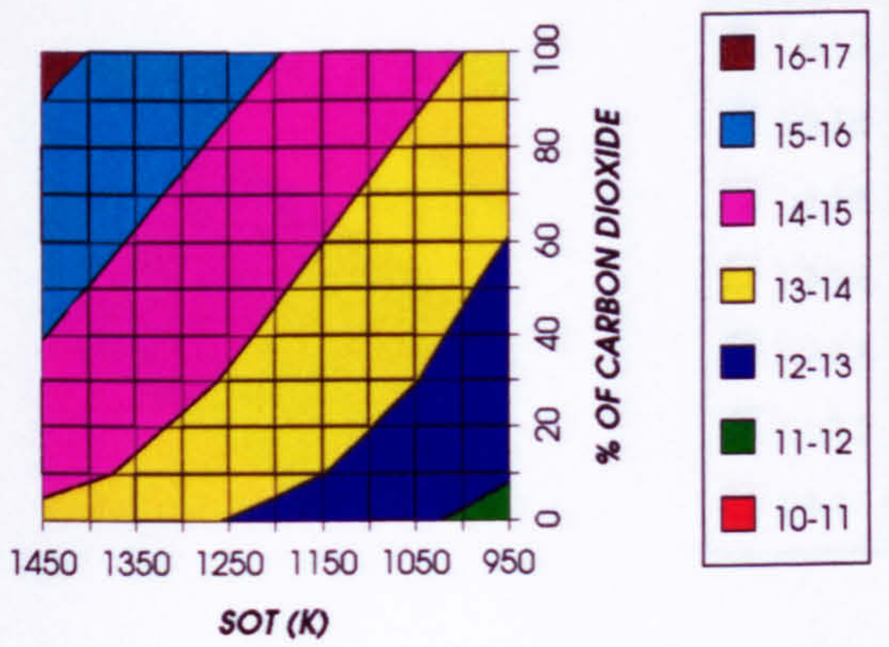

Figure 3. HP compressor pressure ratio
1 spool -1 shaft configuration

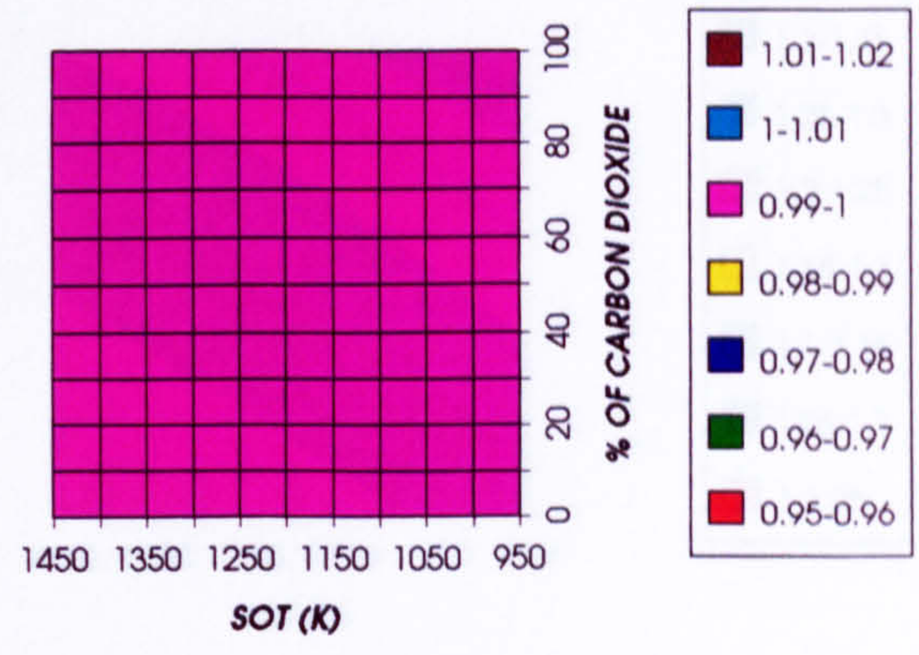

Figure 4. HP shaft speed (relative to design)
1 spool -1 shaft configuration

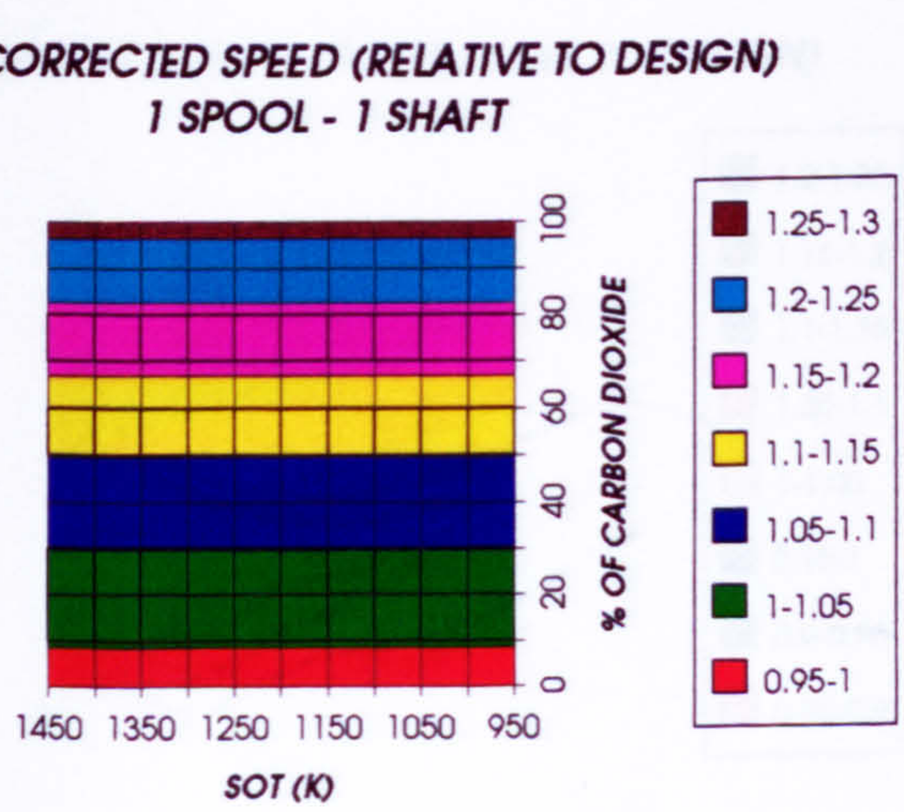

Figure 5. HP compressor corrected speed (relative to design)
1 spool -1 shaft configuration

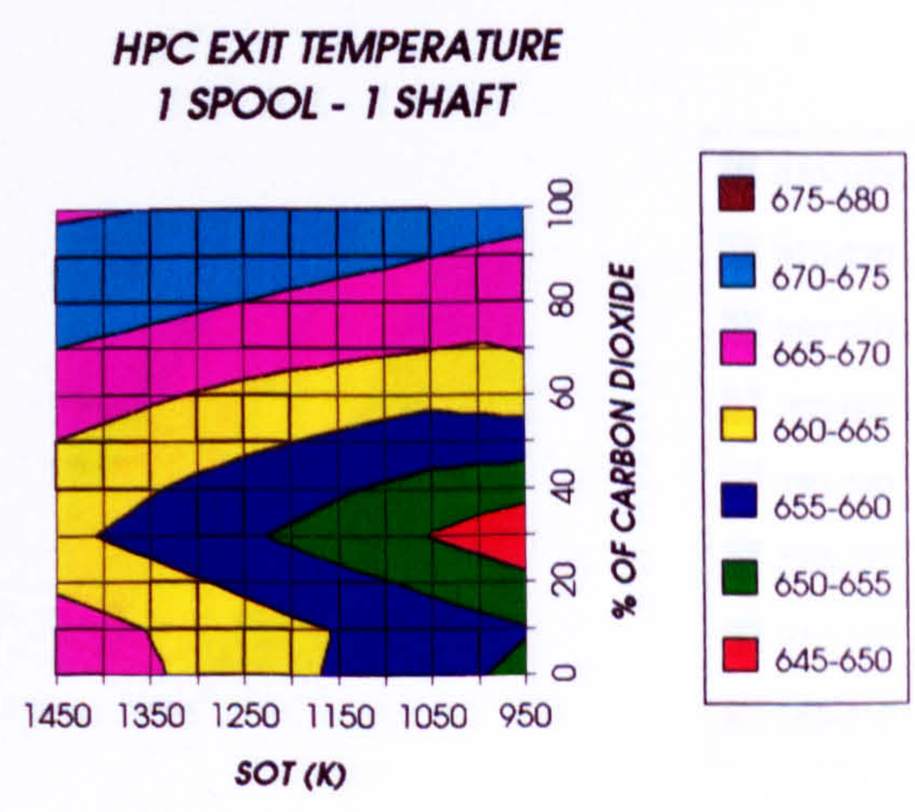

Figure 6. HP compressor exit temperature (K)
1 spool -1 shaft configuration

EFFECT OF CHANGING THE WORKING FLUID (1 SPOOL - 1 SHAFT)

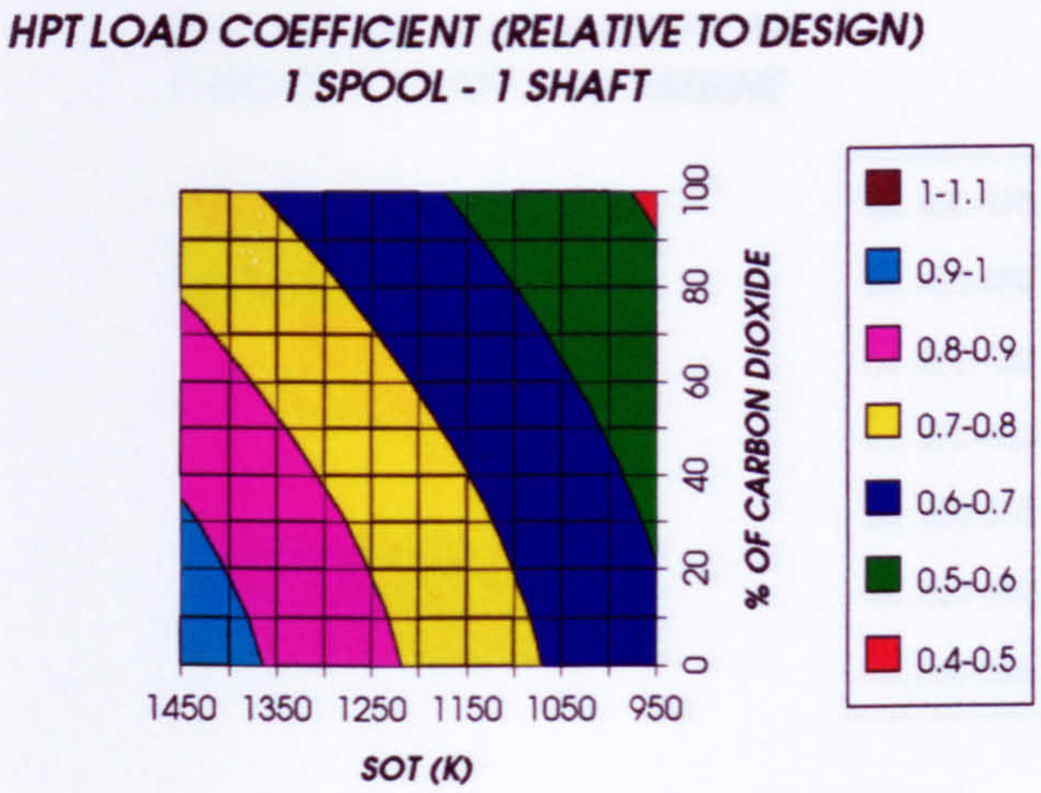

Figure 7. HP turbine load coefficient (relative to design) 1 spool -1 shaft configuration

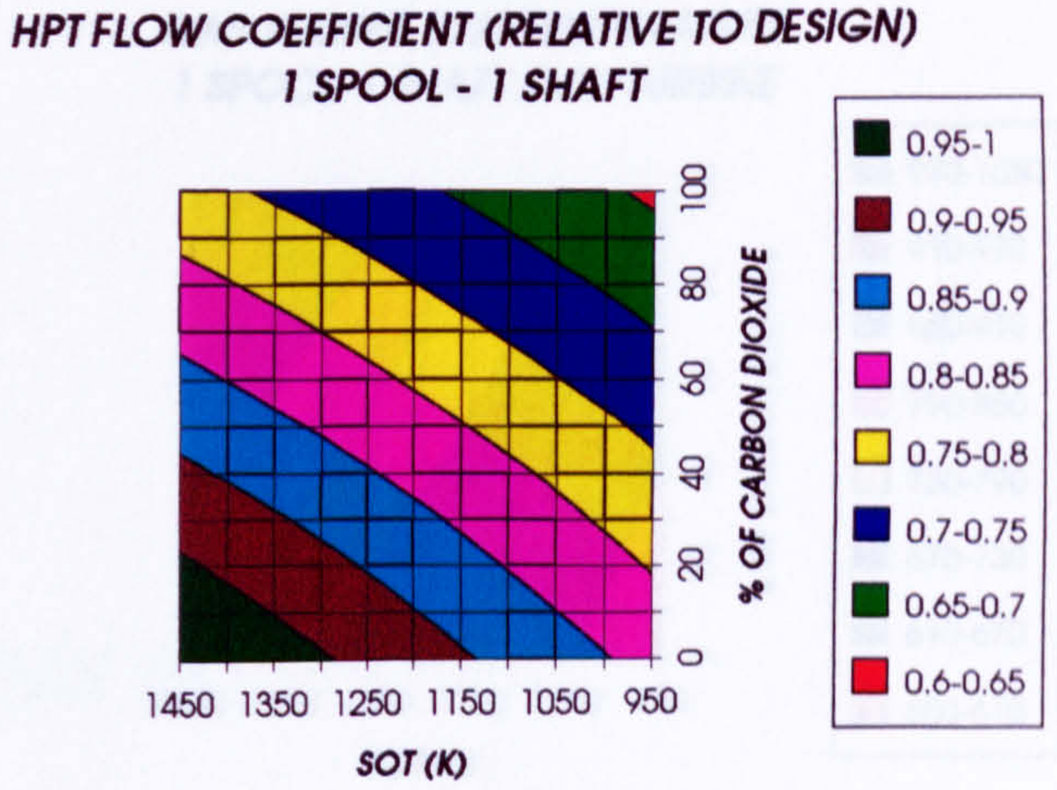

Figure 8. HP turbine flow coefficient (relative to design) 1 spool -1 shaft configuration

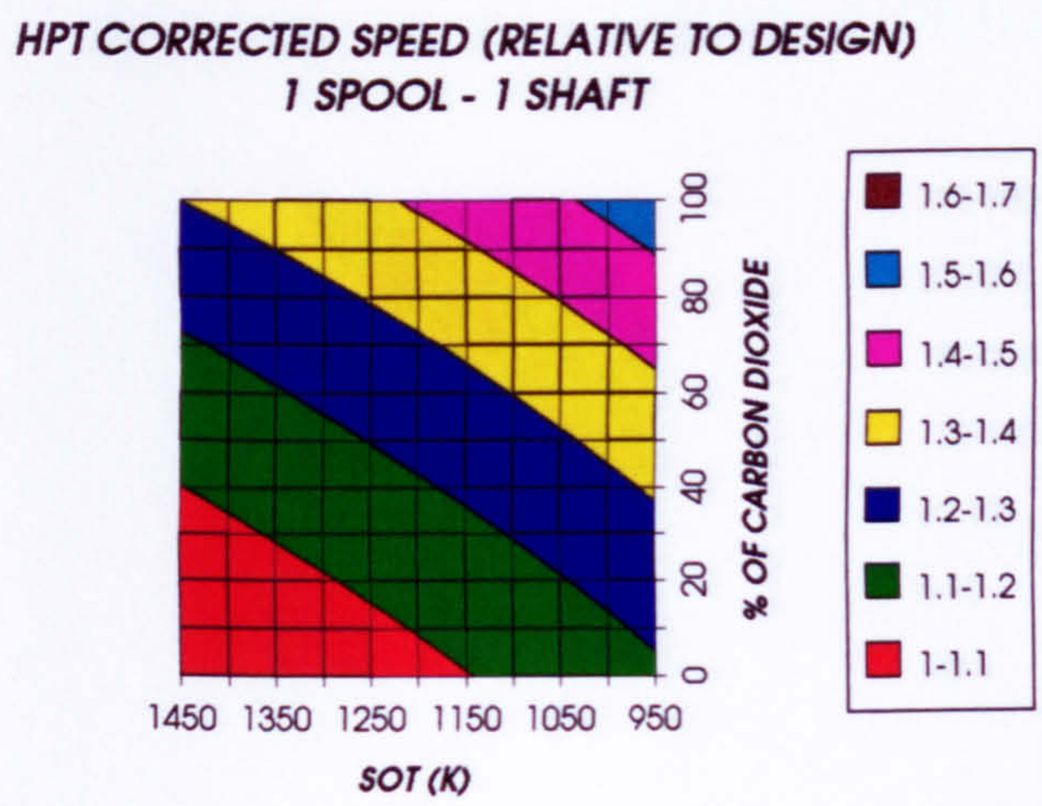

Figure 9. HP turbine corrected speed (relative to design) 1 spool -1 shaft configuration

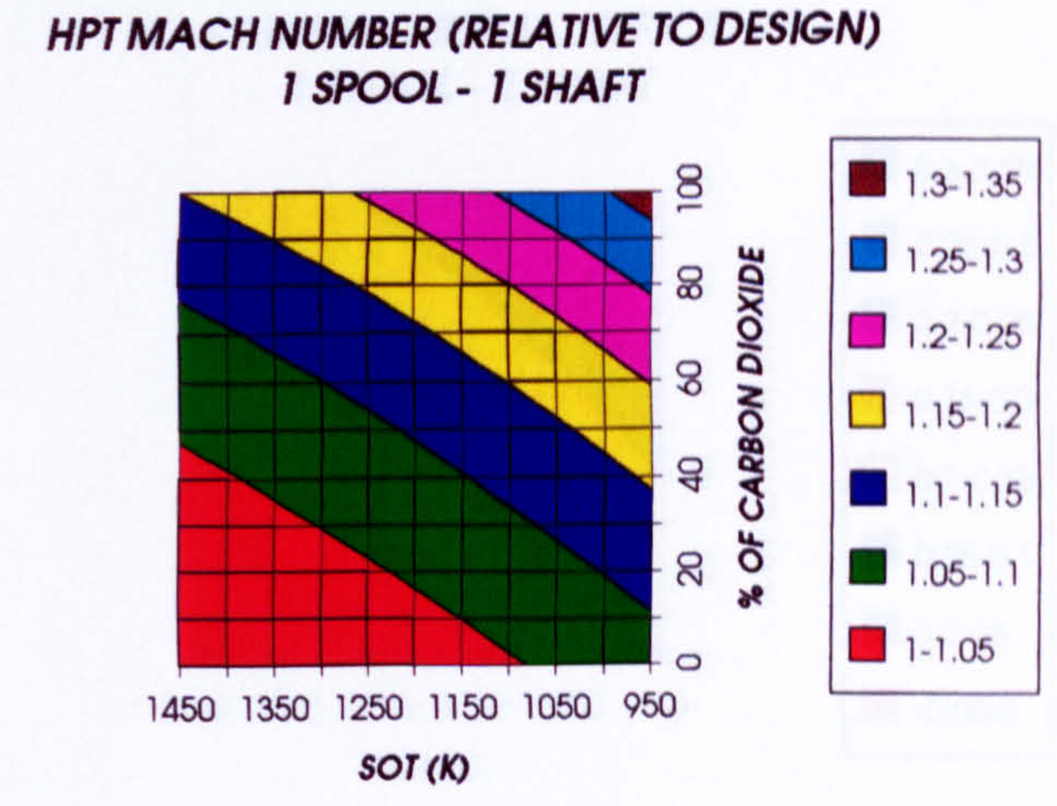

Figure 10. HP turbine Mach number (relative to design) 1 spool -1 shaft configuration

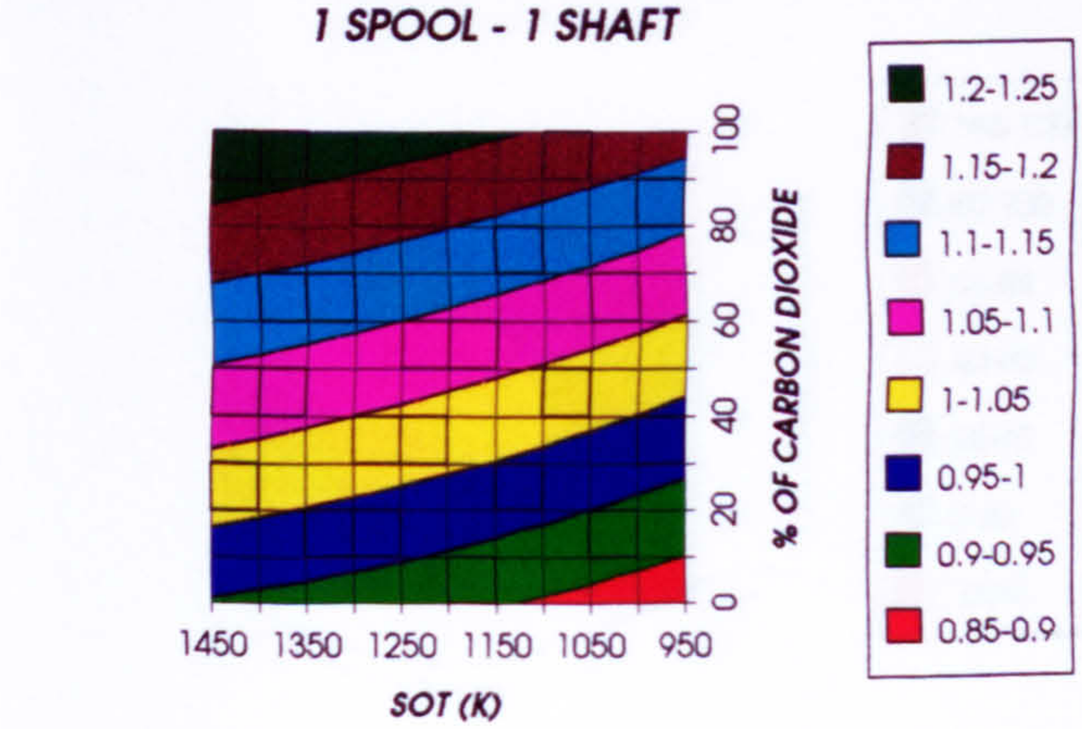

Figure 11. HP turbine corrected enthalpy (relative to design) 1 spool -1 shaft configuration

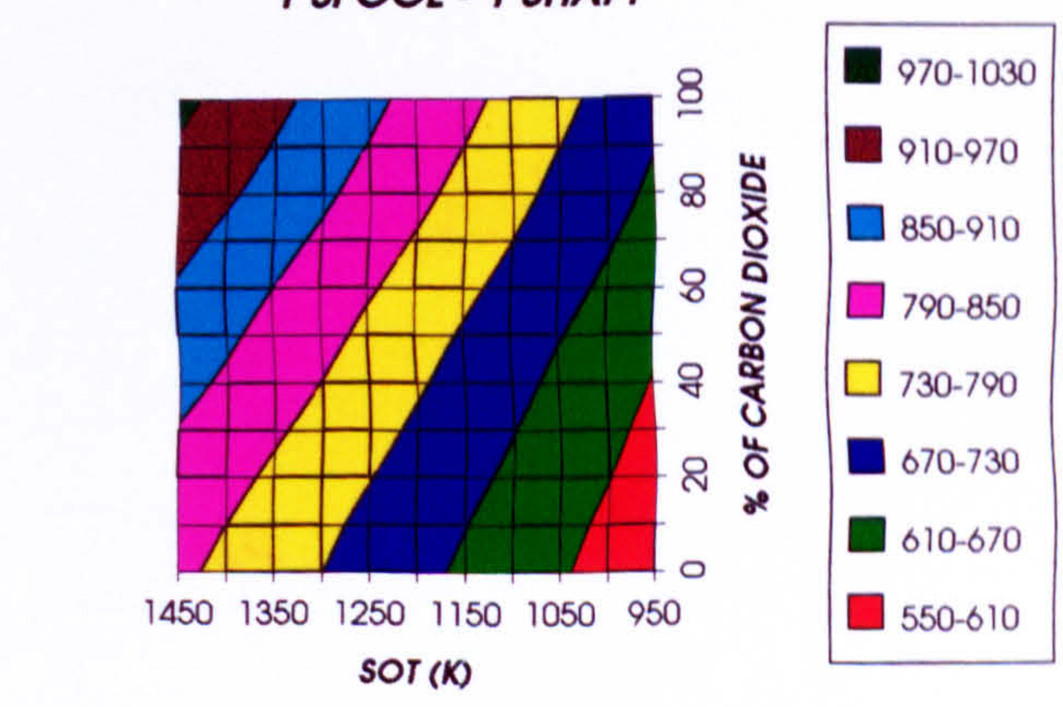

Figure 12. HP turbine exit temperature (K) 1 spool -1 shaft configuration

EFFECT OF CHANGING THE WORKING FLUID (1 SPOOL - 1 SHAFT)

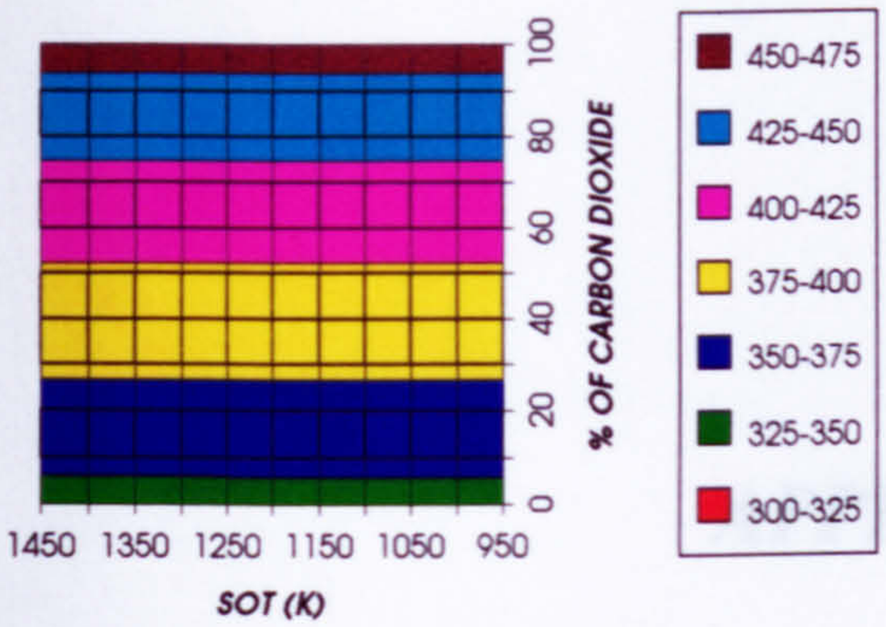

Figure 13. Gas turbine inlet mass flow (kg/s)
1 spool -1 shaft configuration

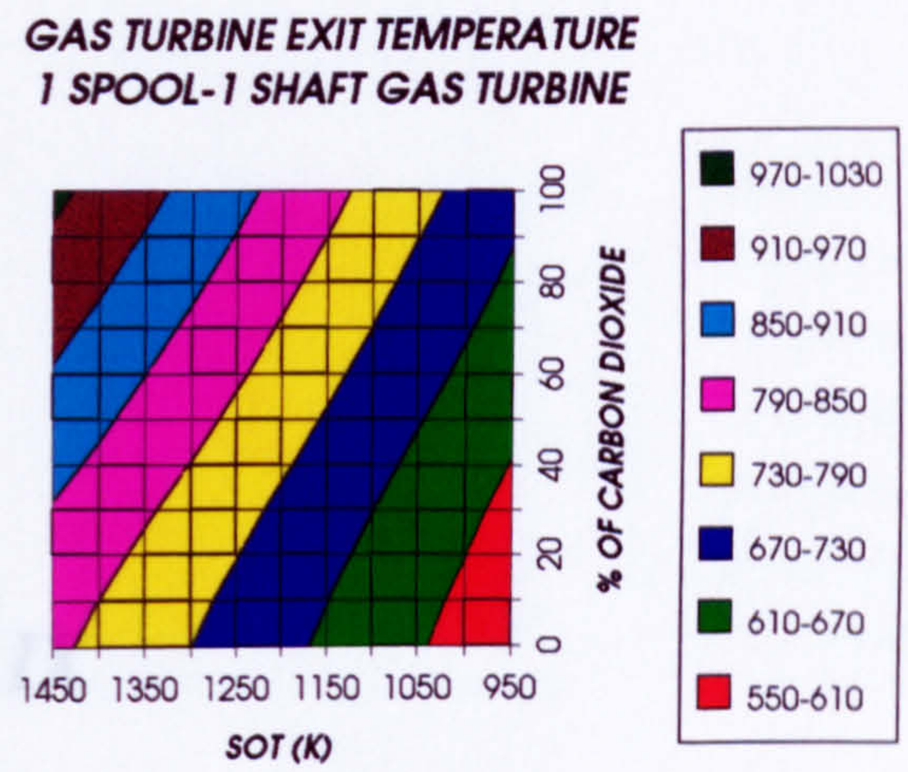

Figure 14. Gas turbine exit temperature (K)
1 spool -1 shaft configuration

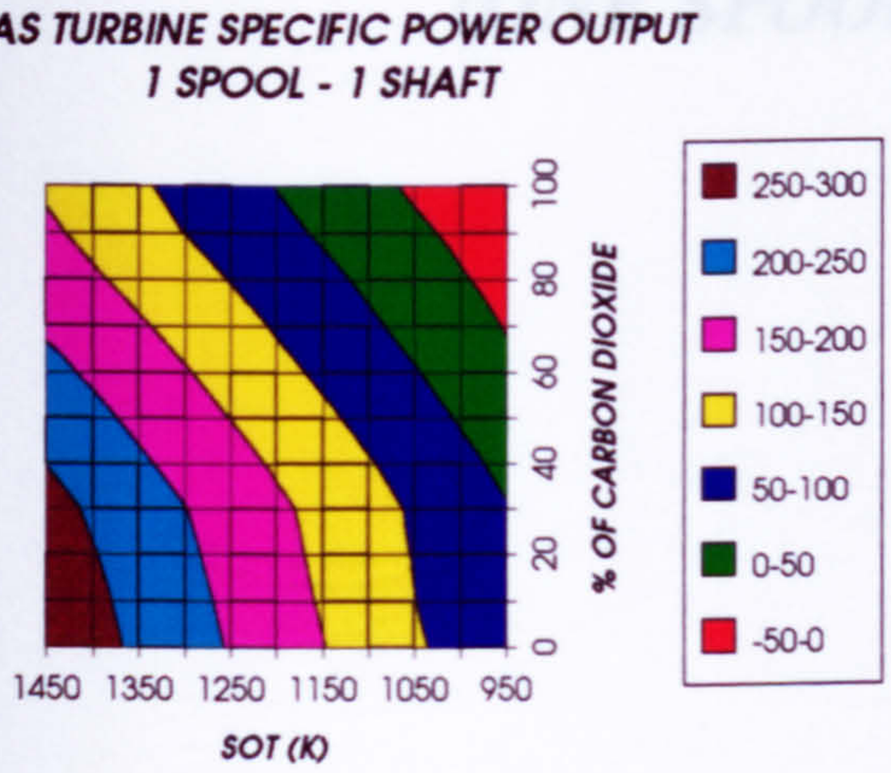

Figure 15. Gas turbine specific power output (kW/kg/s)
1 spool -1 shaft configuration

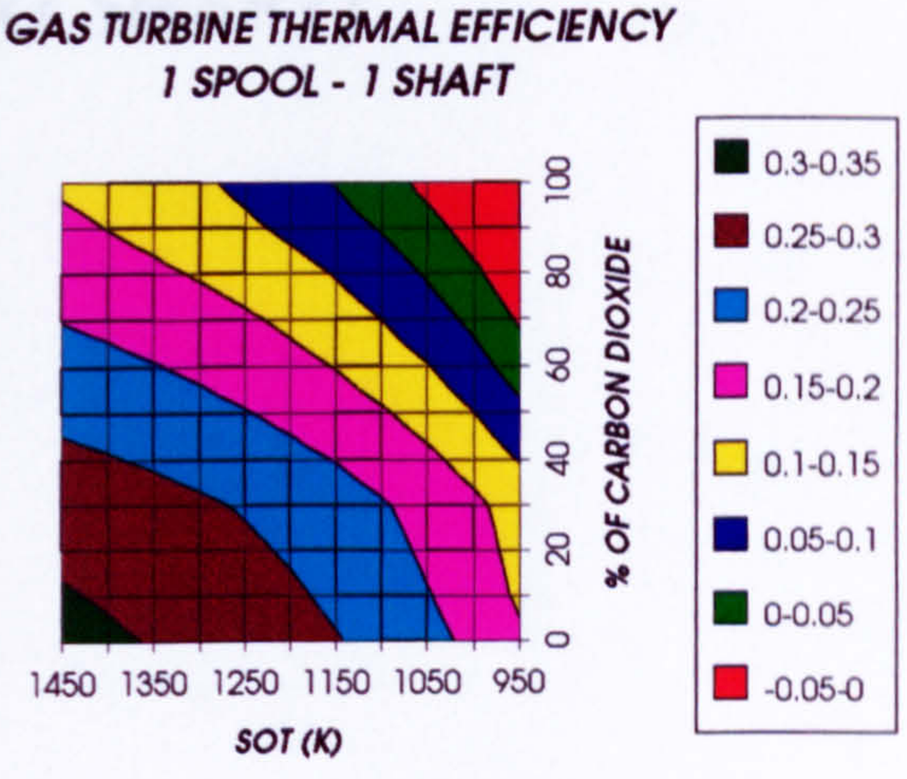

Figure 16. Gas turbine thermal efficiency
1 spool -1 shaft configuration

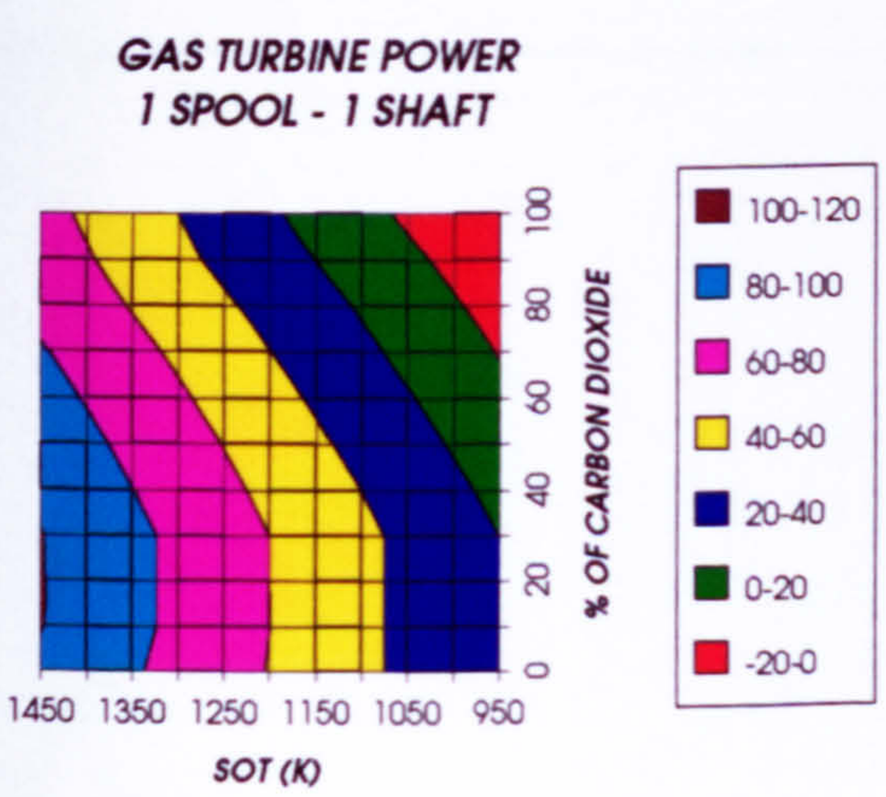

Figure 17. Gas turbine power (MW)
1 spool -1 shaft configuration

APPENDIX IX

EFFECT OF CHANGING THE WORKING FLUID (ONE SPOOL - TWO SHAFT)

EFFECT OF CHANGING THE WORKING FLUID (1 SPOOL - 2 SHAFT)

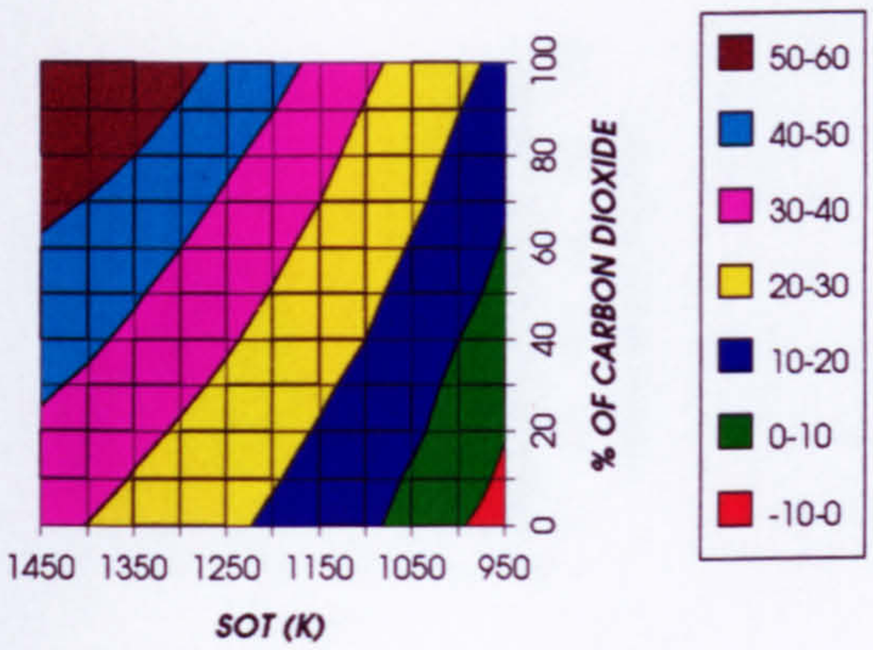

Figure 1. HP compressor surge margin (%)
1 spool -2 shaft configuration

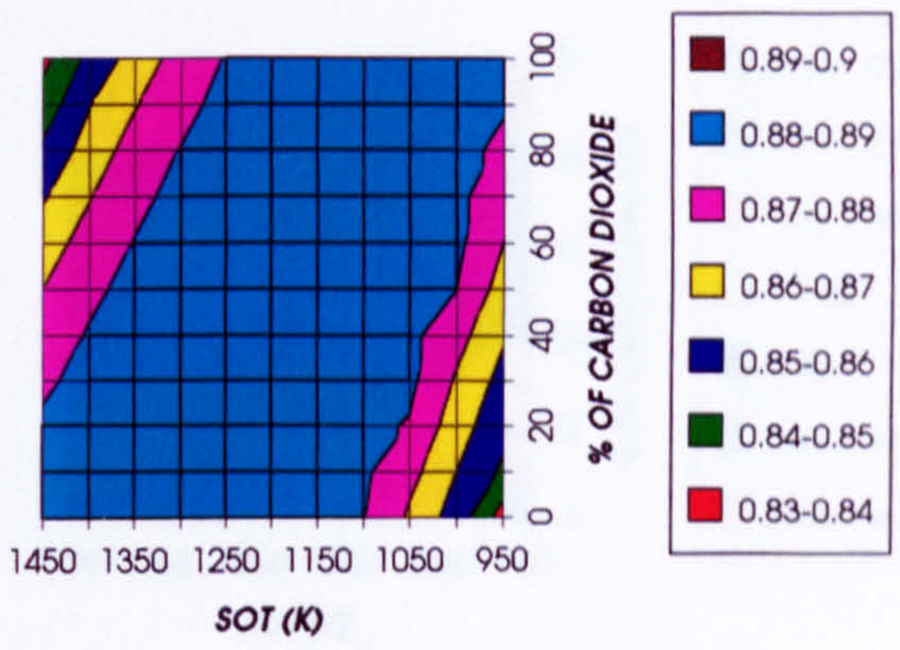

Figure 2. HP compressor adiabatic efficiency
1 spool -2 shaft configuration

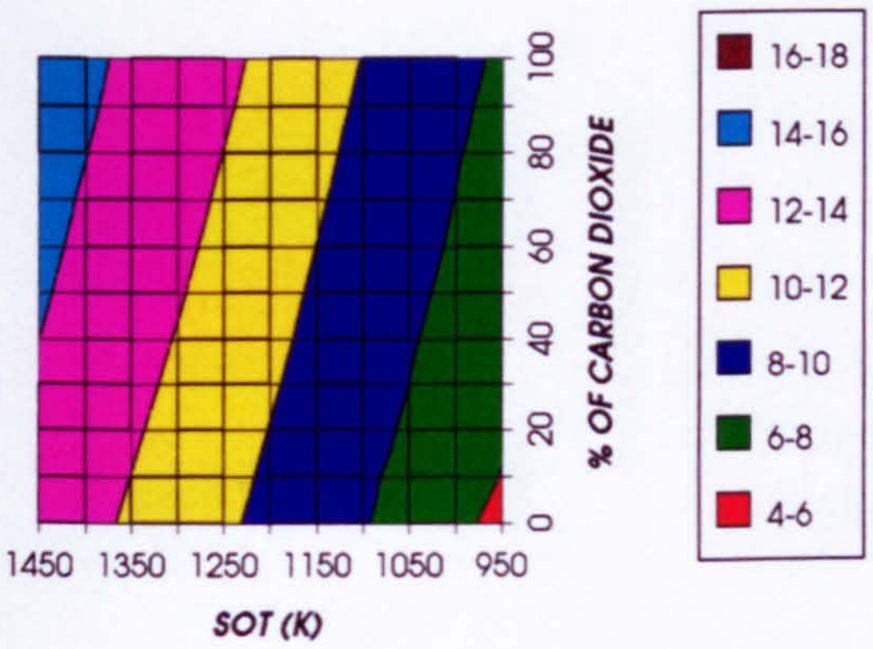

Figure 3. HP compressor pressure ratio
1 spool -2 shaft configuration

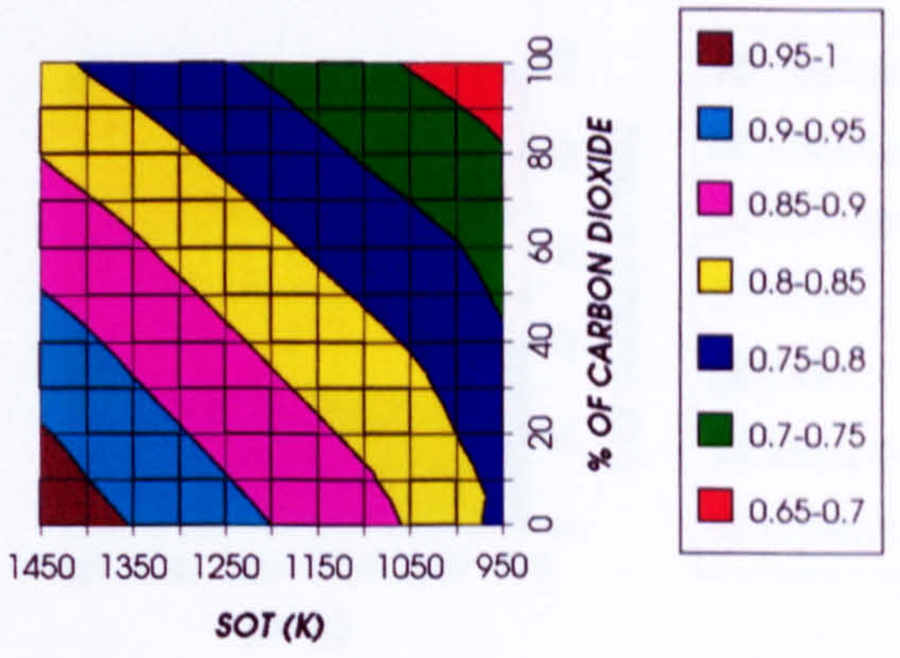

Figure 4. HP shaft speed (relative to design)
1 spool -2 shaft configuration

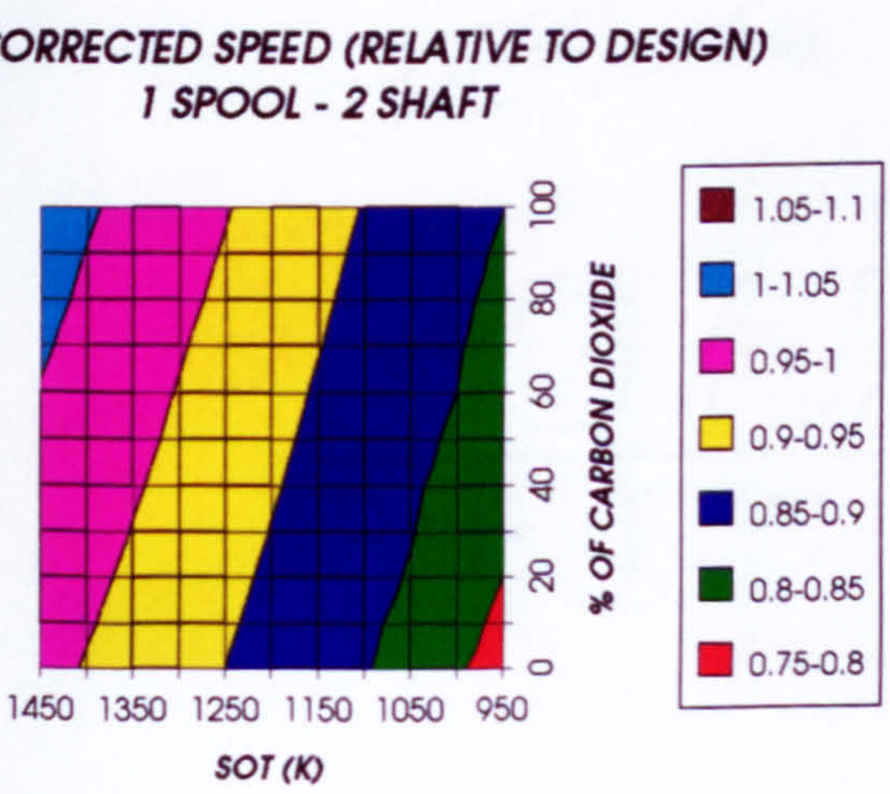

Figure 5. HP compressor corrected speed (relative to design)
1 spool -2 shaft configuration

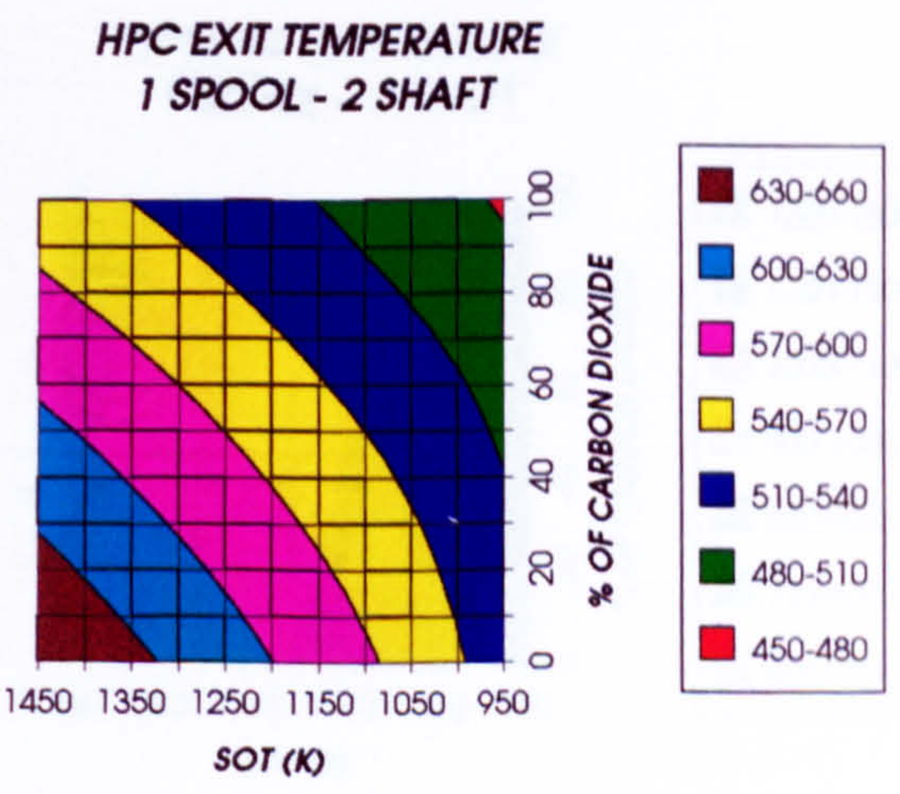

Figure 6. HP compressor exit temperature (K)
1 spool -2 shaft configuration

EFFECT OF CHANGING THE WORKING FLUID (1 SPOOL - 2 SHAFT)

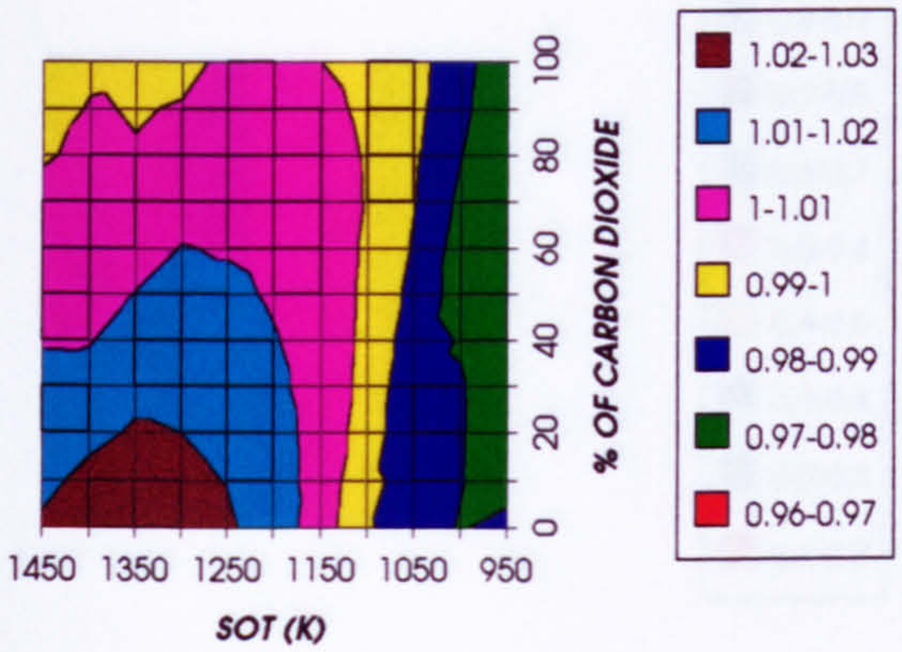

Figure 7. HP turbine load coefficient (relative to design) 1 spool -2 shaft configuration

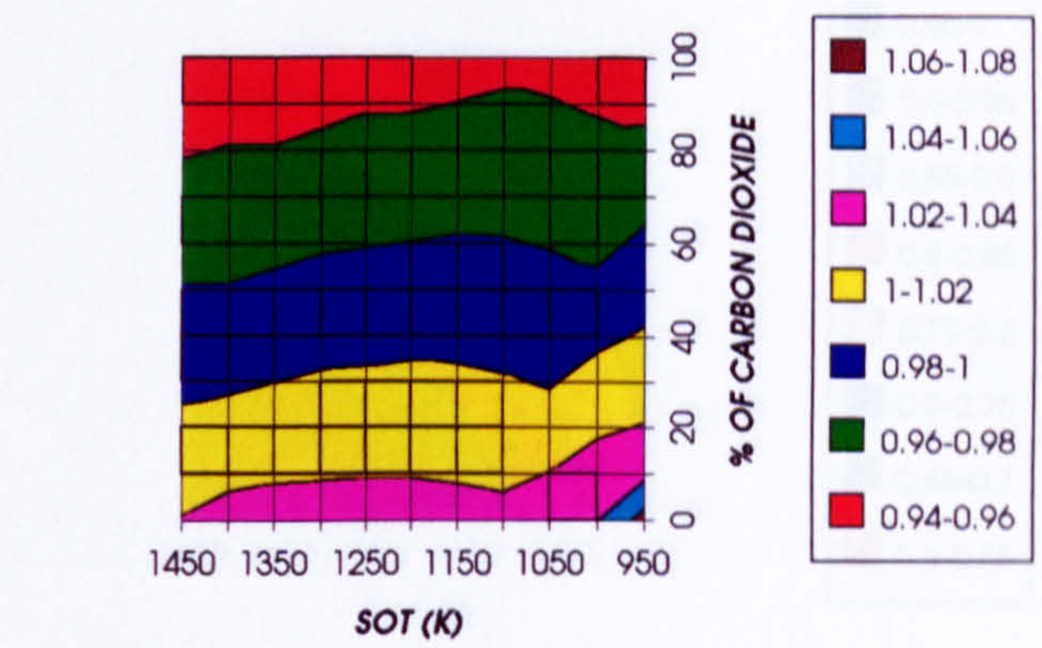

Figure 8. HP turbine flow coefficient (relative to design) 1 spool -2 shaft configuration

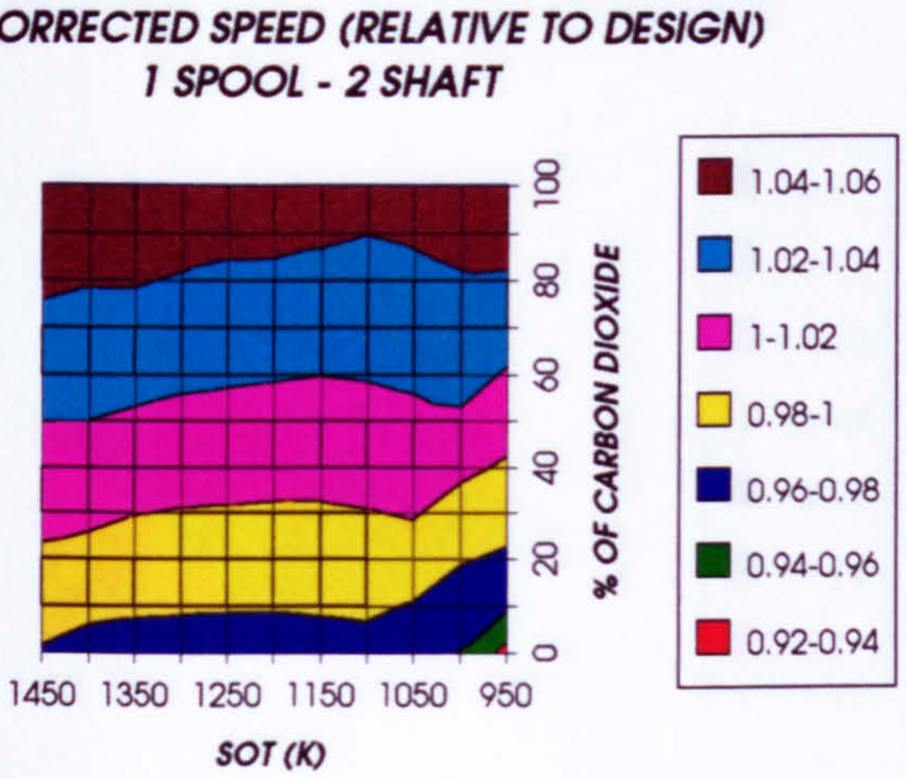

Figure 9. HP turbine corrected speed (relative to design) 1 spool -2 shaft configuration

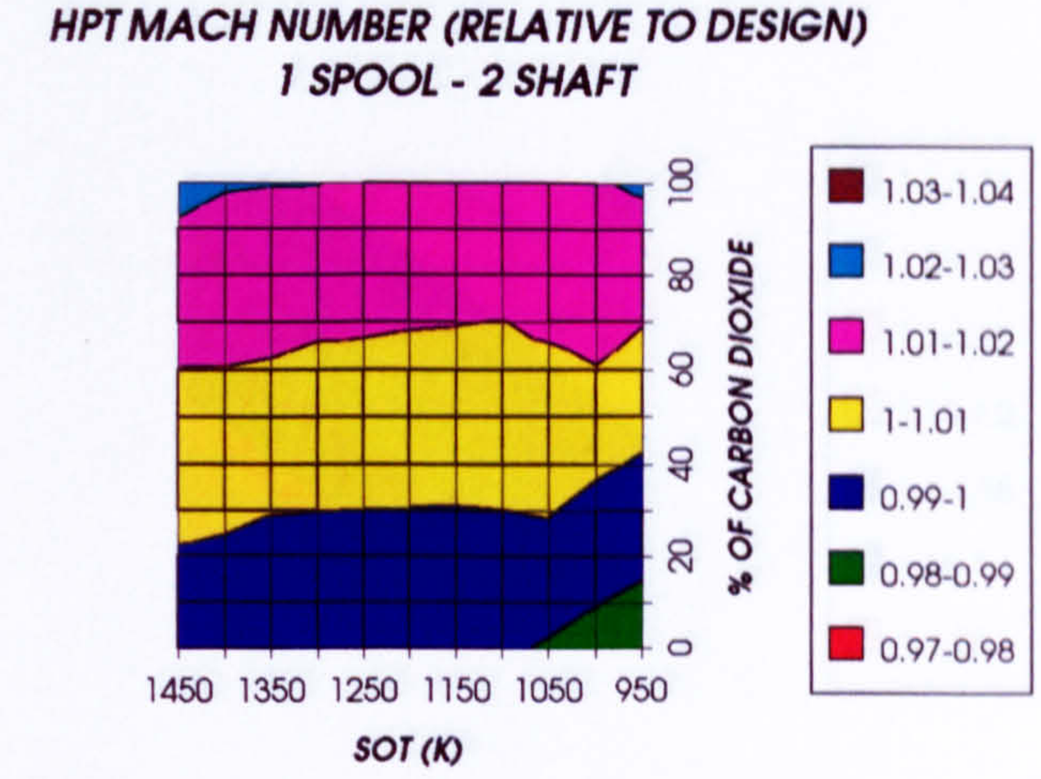

Figure 10. HP turbine Mach number (relative to design) 1 spool -2 shaft configuration

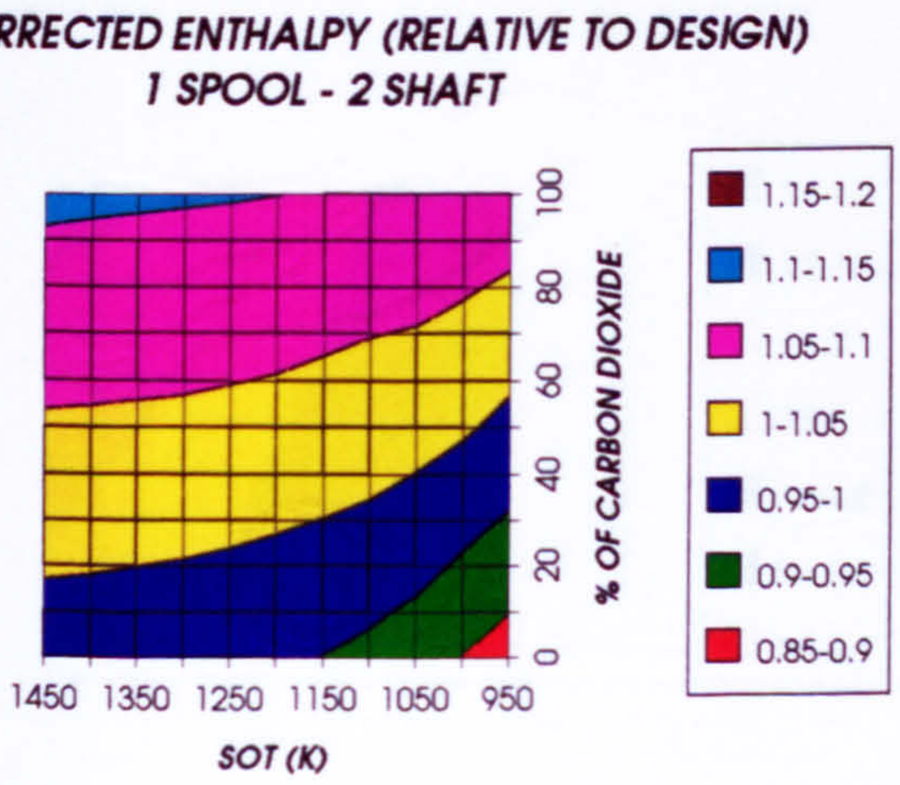

Figure 11. HP turbine corrected enthalpy (relative to design) 1 spool -2 shaft configuration

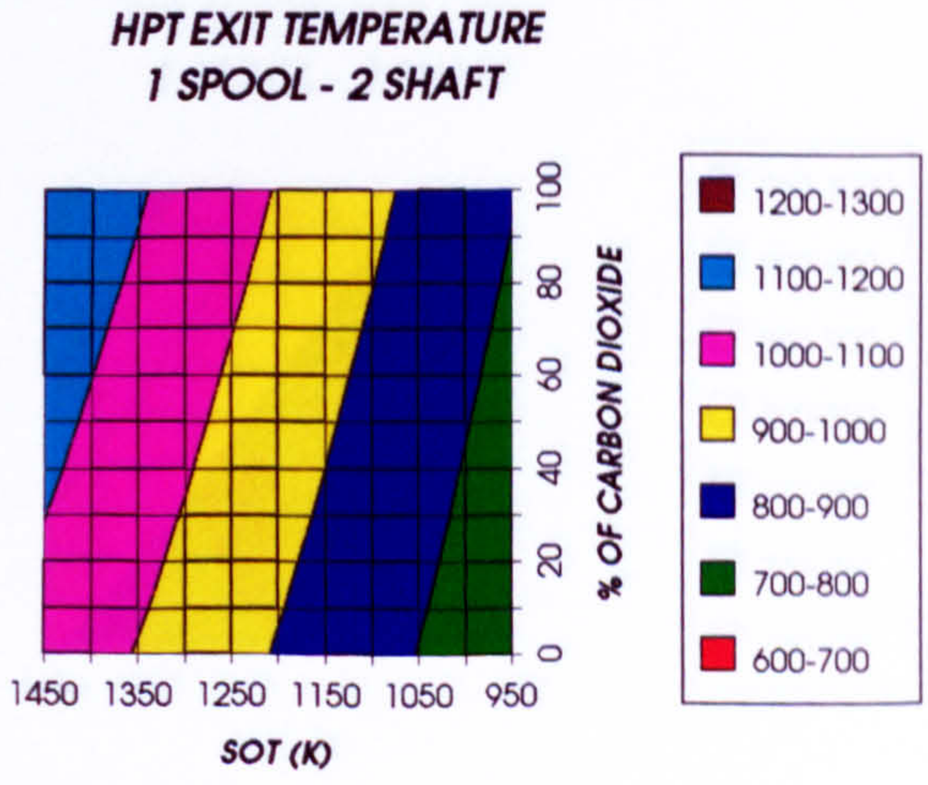

Figure 12. HP turbine exit temperature (K) 1 spool -2 shaft configuration

EFFECT OF CHANGING THE WORKING FLUID (1 SPOOL - 2 SHAFT)

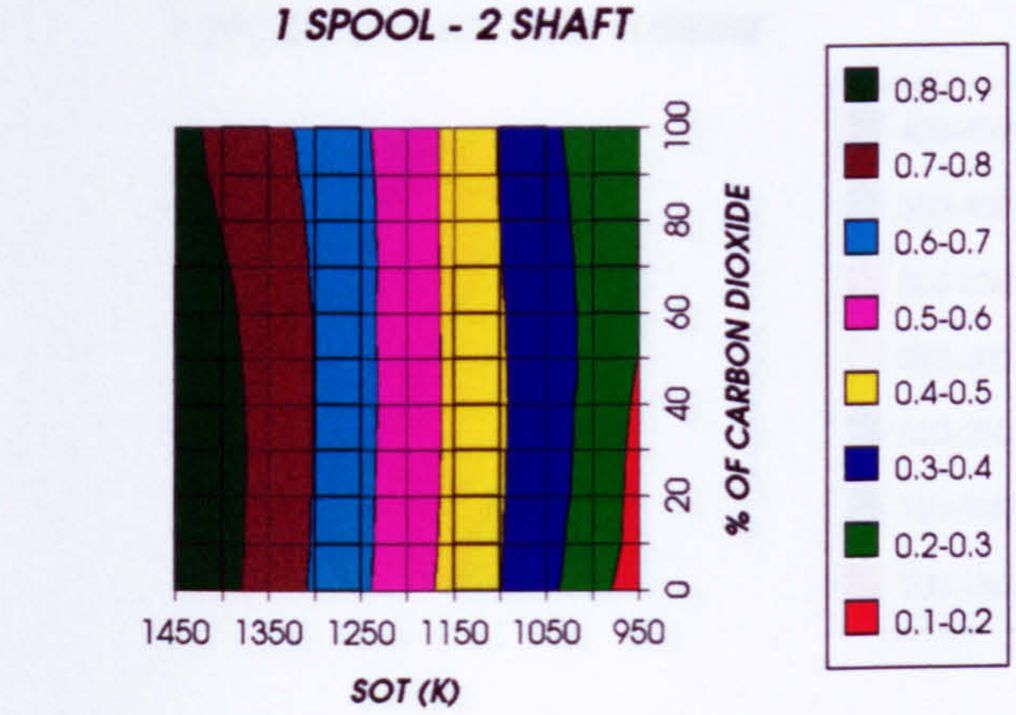

Figure 13 FP turbine load coefficient (relative to design)
1 spool -2 shaft configuration

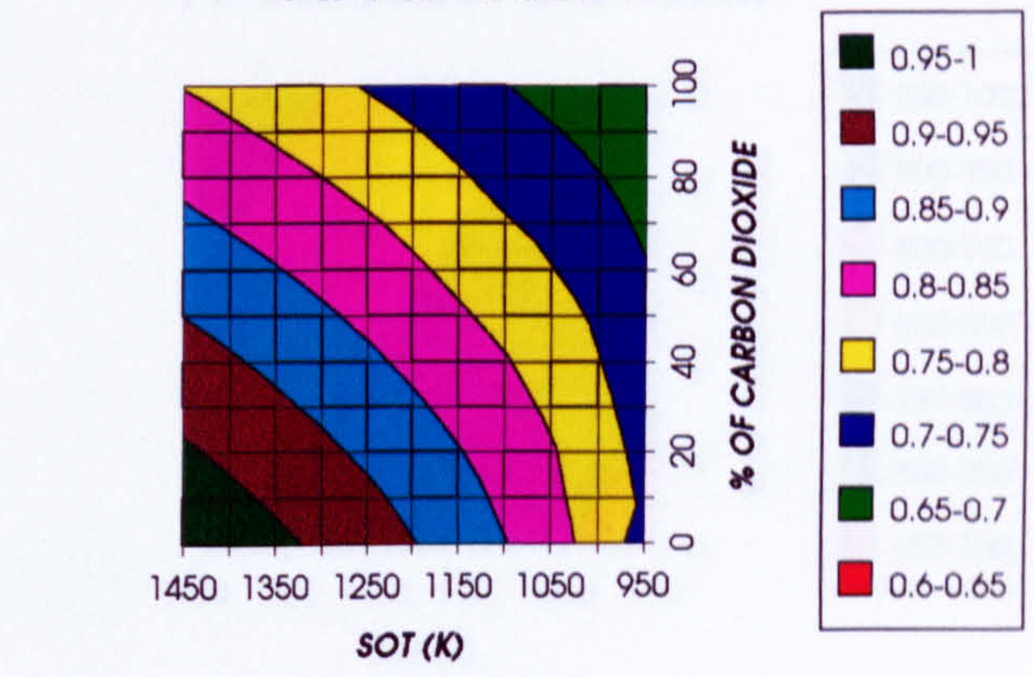

Figure 14. FP turbine flow coefficient (relative to design)
1 spool -2 shaft configuration

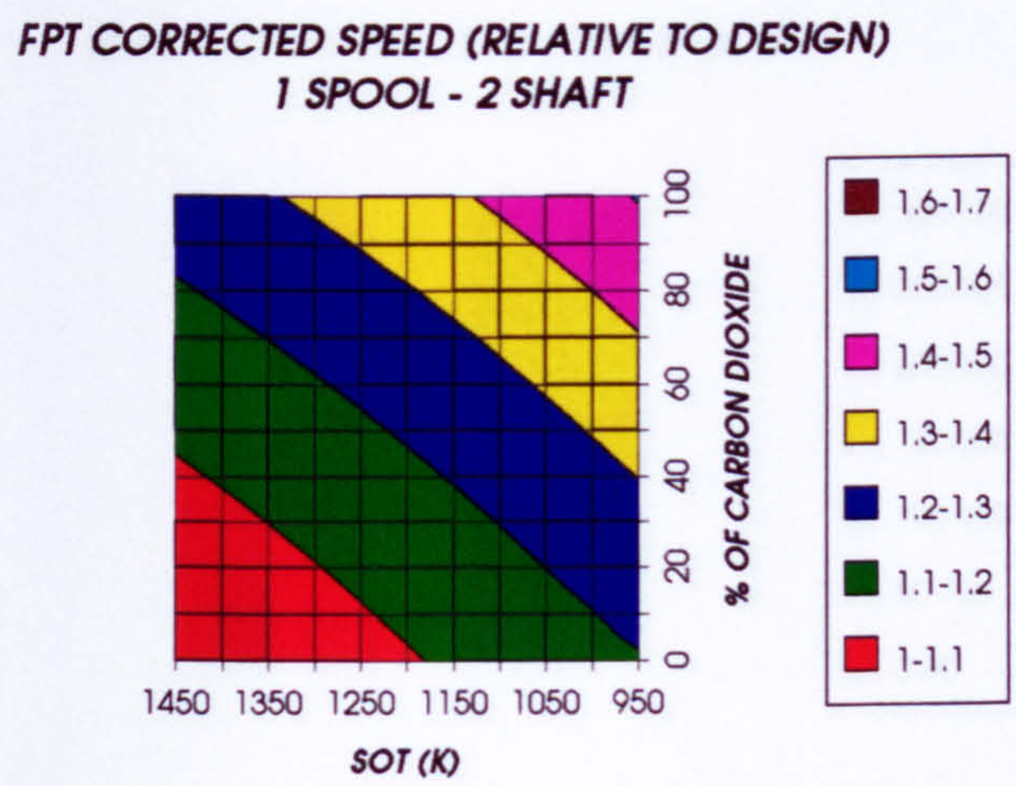

Figure 15. FP turbine corrected speed (relative to design)
1 spool -2 shaft configuration

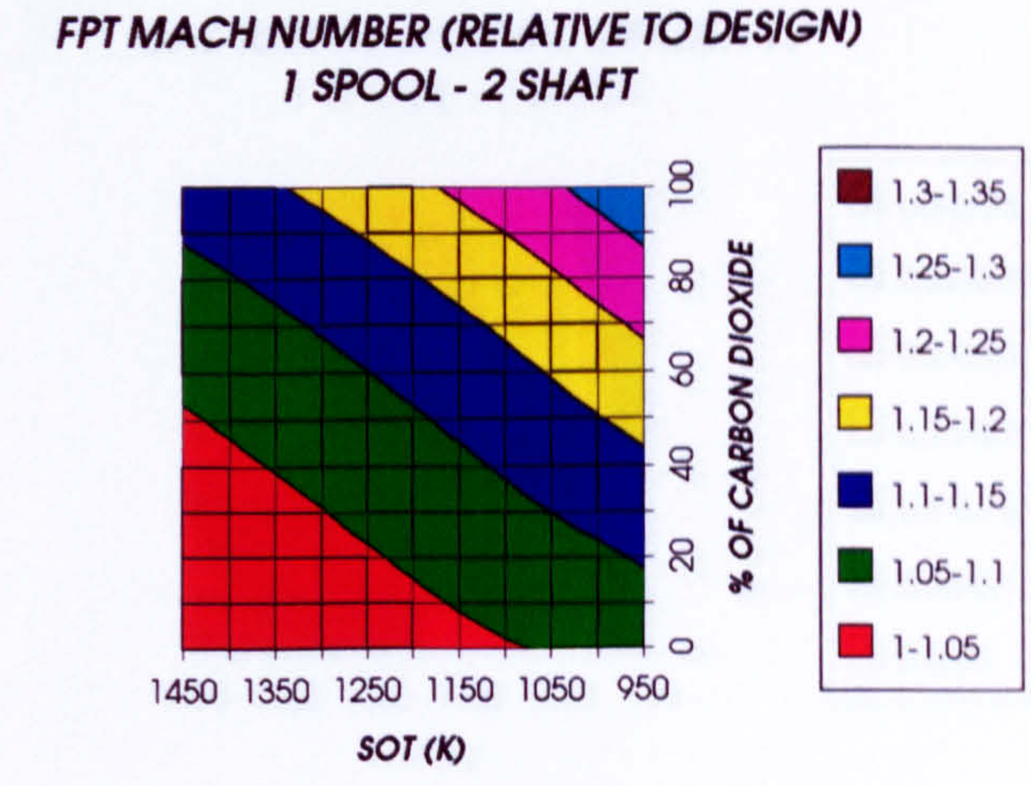

Figure 16. FP turbine Mach number (relative to design)
1 spool -2 shaft configuration

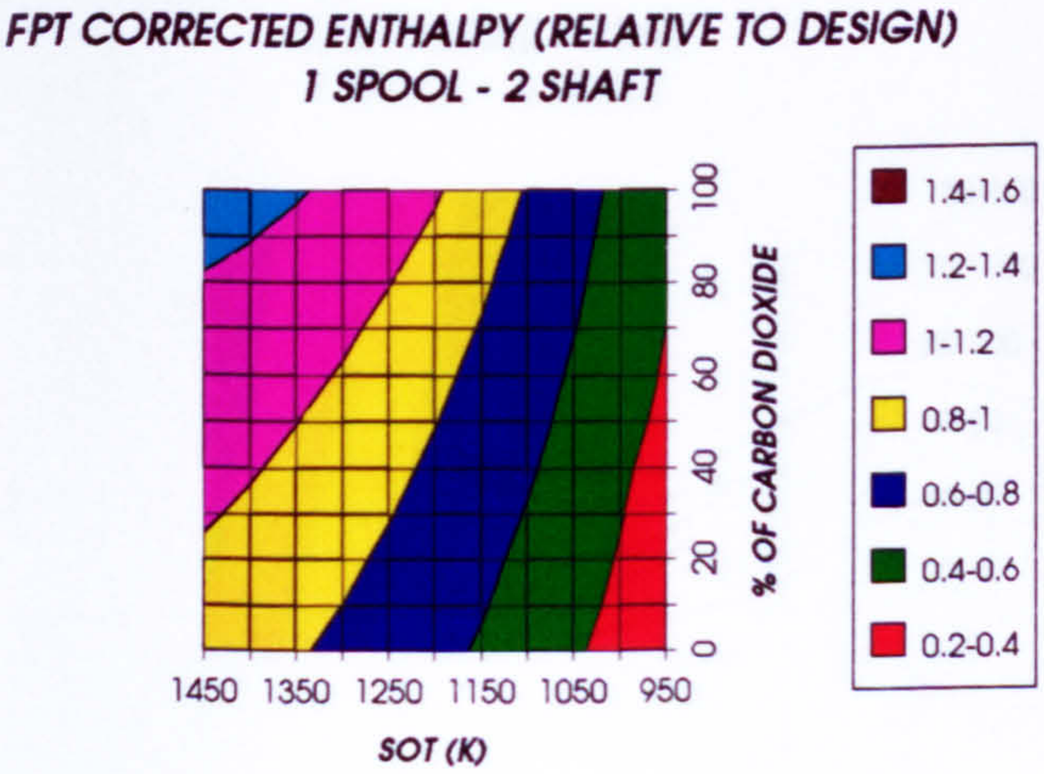

Figure 17. FP turbine corrected enthalpy (relative to design)
1 spool -2 shaft configuration

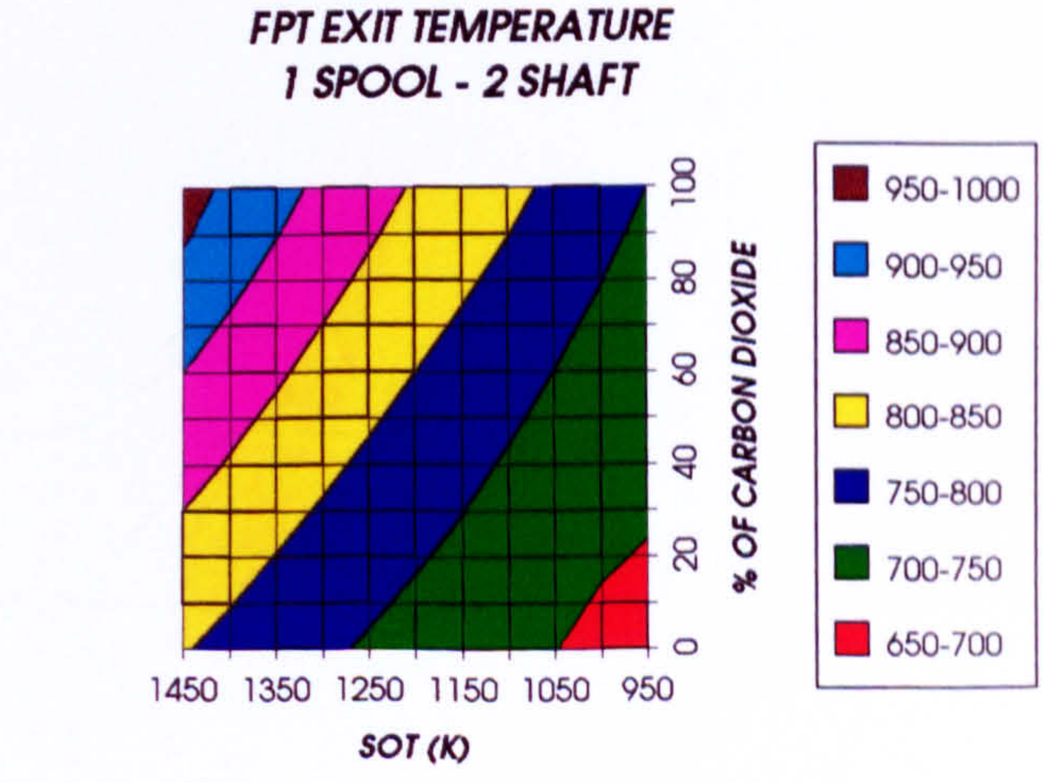

Figure 18. FP turbine exit temperature (K)
1 spool -2 shaft configuration

EFFECT OF CHANGING THE WORKING FLUID (1 SPOOL - 2 SHAFT)

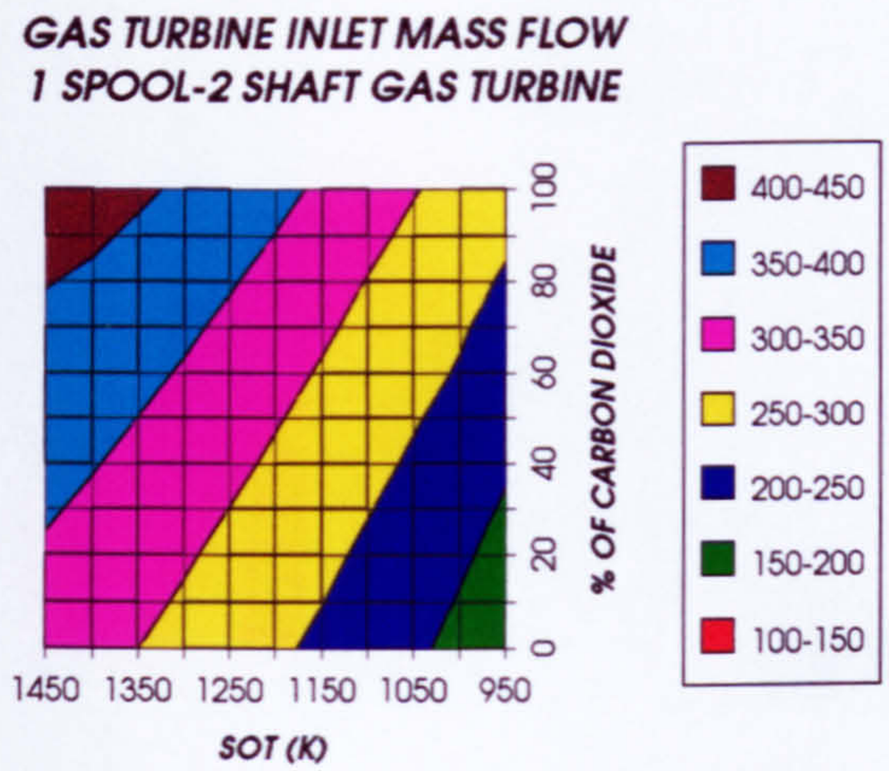

Figure 19. Gas turbine inlet mass flow (kg/s)
1 spool -2 shaft configuration

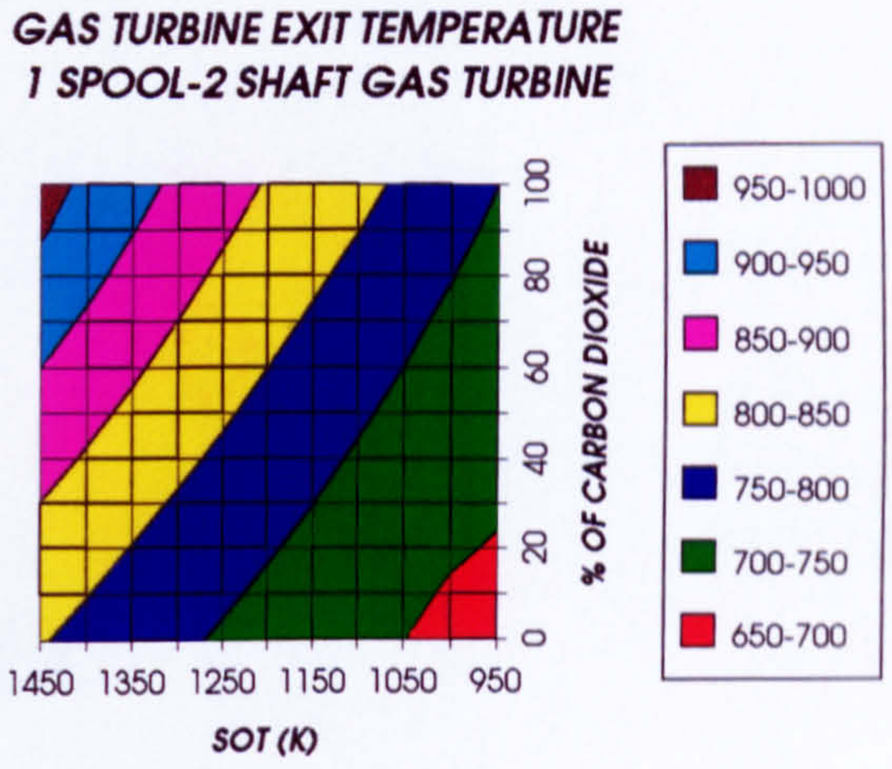

Figure 20. Gas turbine exit temperature (K)
1 spool -2 shaft configuration

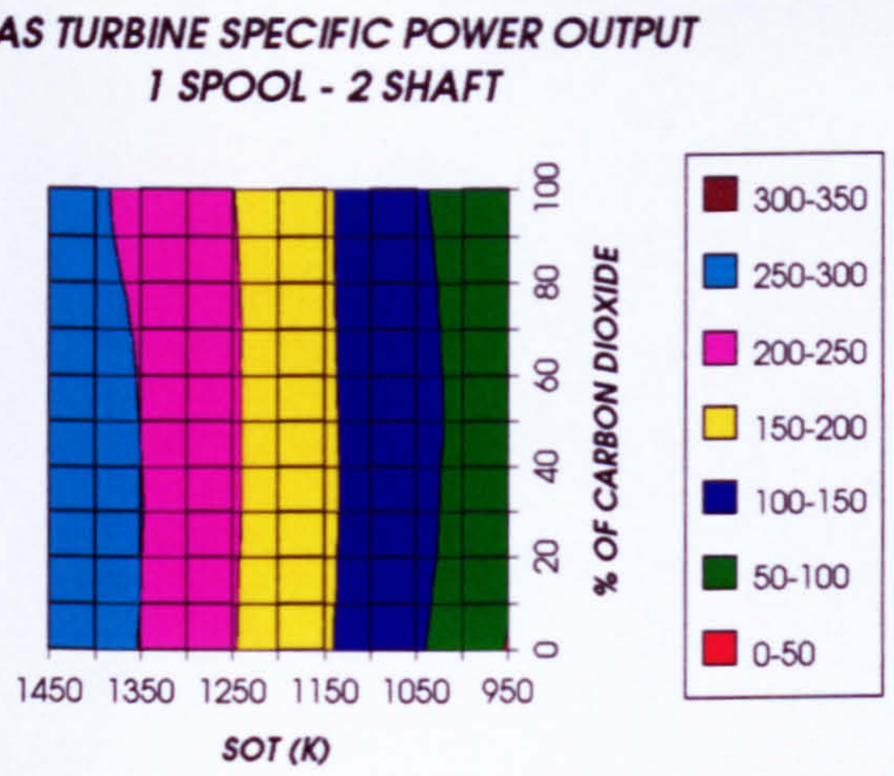

Figure 21. Gas turbine specific power output (kW/kg/s)
1 spool -2 shaft configuration

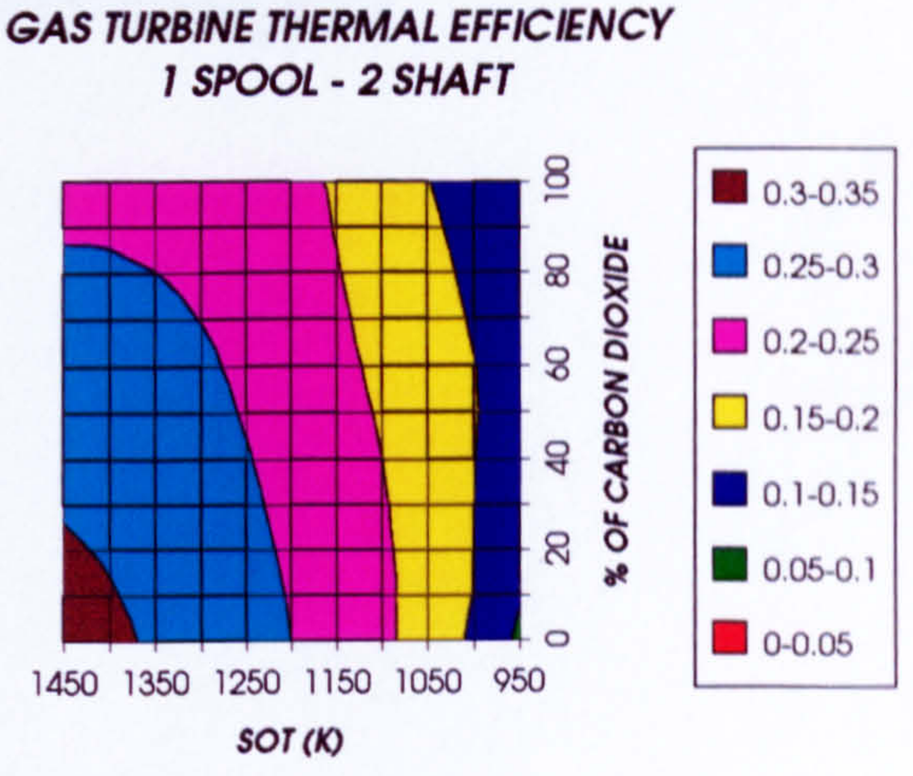

Figure 22. Gas turbine thermal efficiency
1 spool -2 shaft configuration

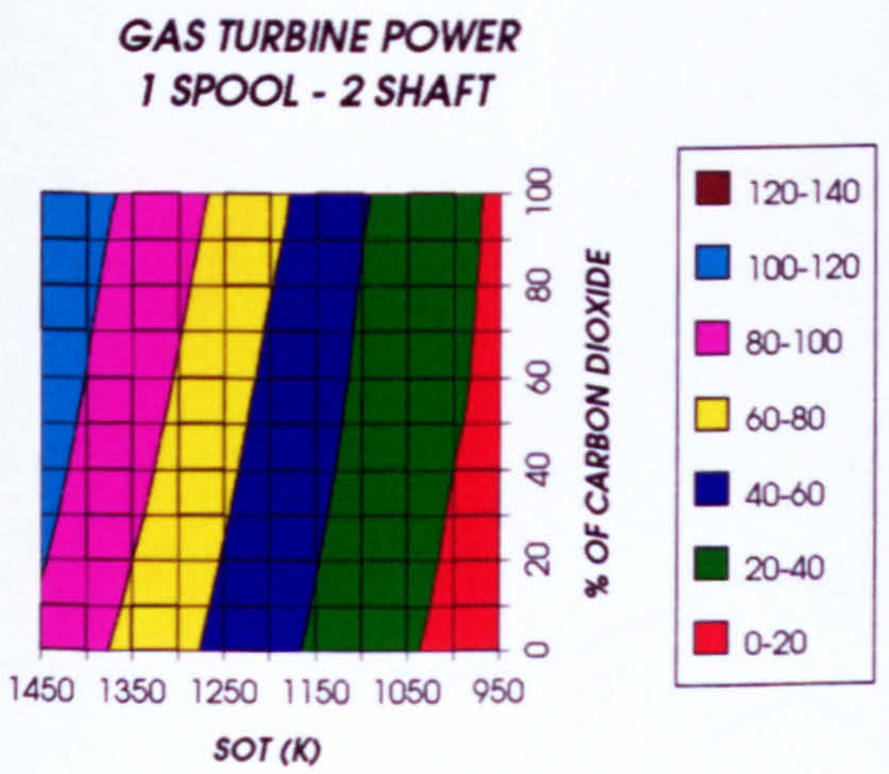

Figure 23. Gas turbine power (MW)
1 spool -2 shaft configuration

APPENDIX X

EFFECT OF CHANGING THE WORKING FLUID (TWO SPOOL - TWO SHAFT)

EFFECT OF CHANGING THE WORKING FLUID (2 SPOOL - 2 SHAFT)

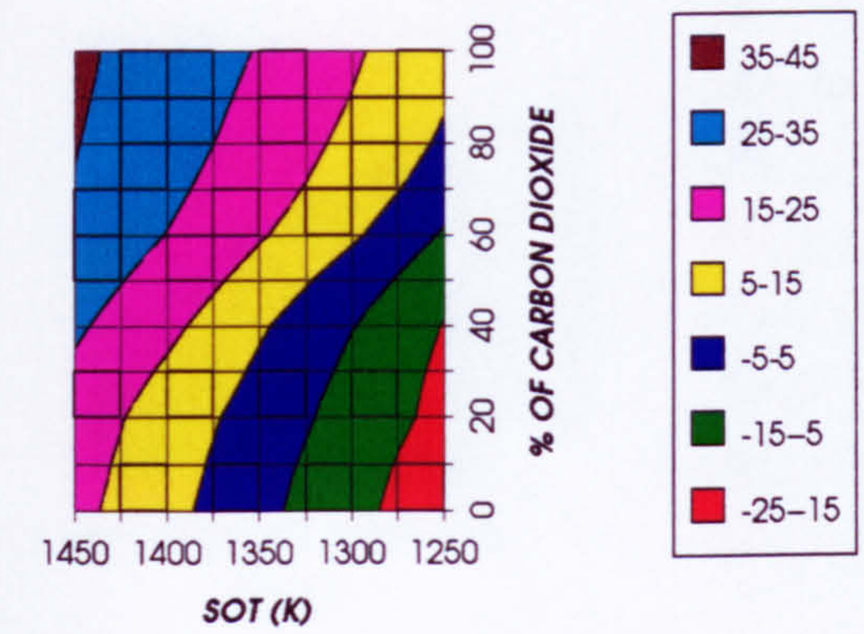

Figure 1. LP compressor surge margin (%) 2 spool -2 shaft configuration

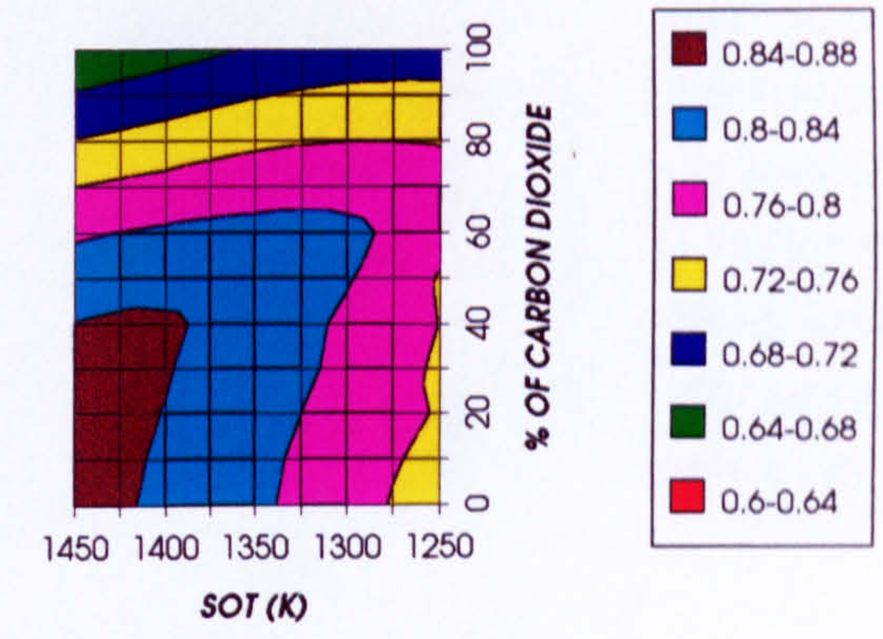

Figure 2. LP compressor adiabatic efficiency 2 spool -2 shaft configuration

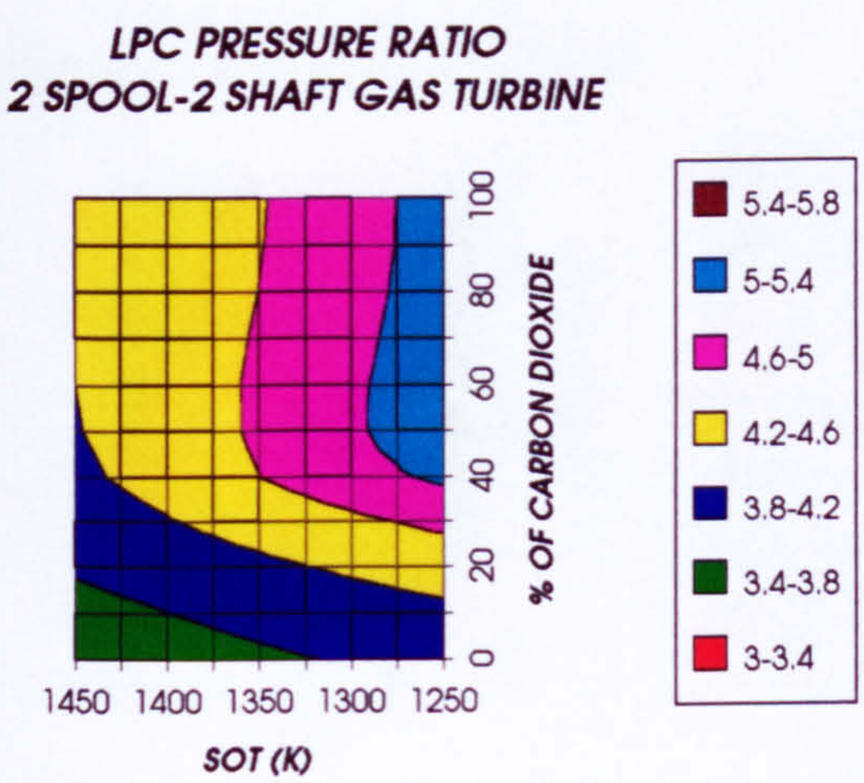

Figure 3. LP compressor pressure ratio 2 spool -2 shaft configuration

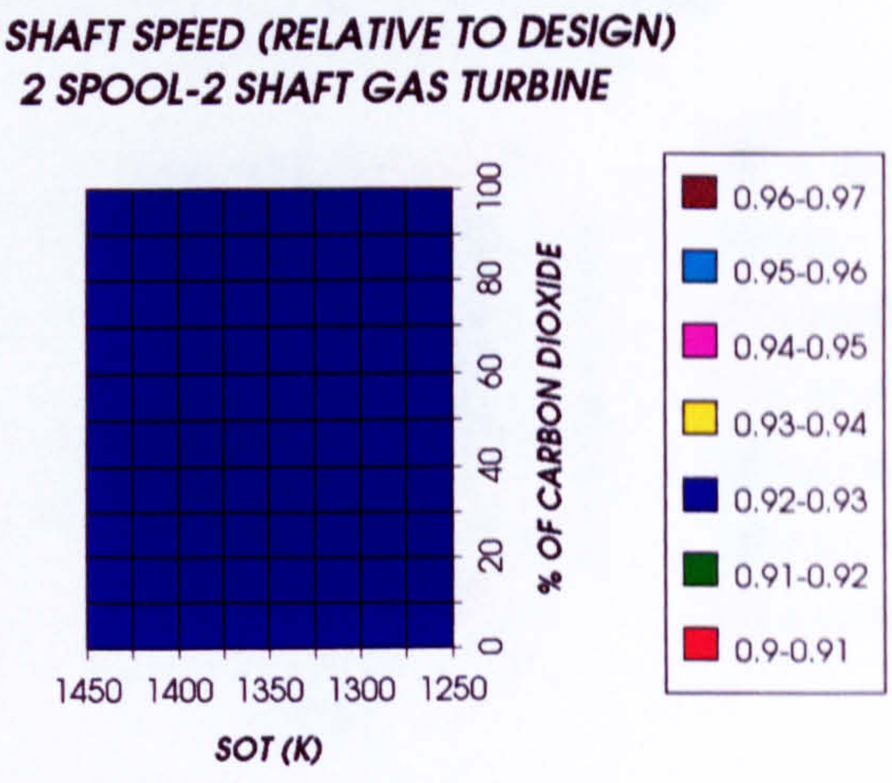

Figure 4. LP shaft speed (relative to design) 2 spool -2 shaft configuration

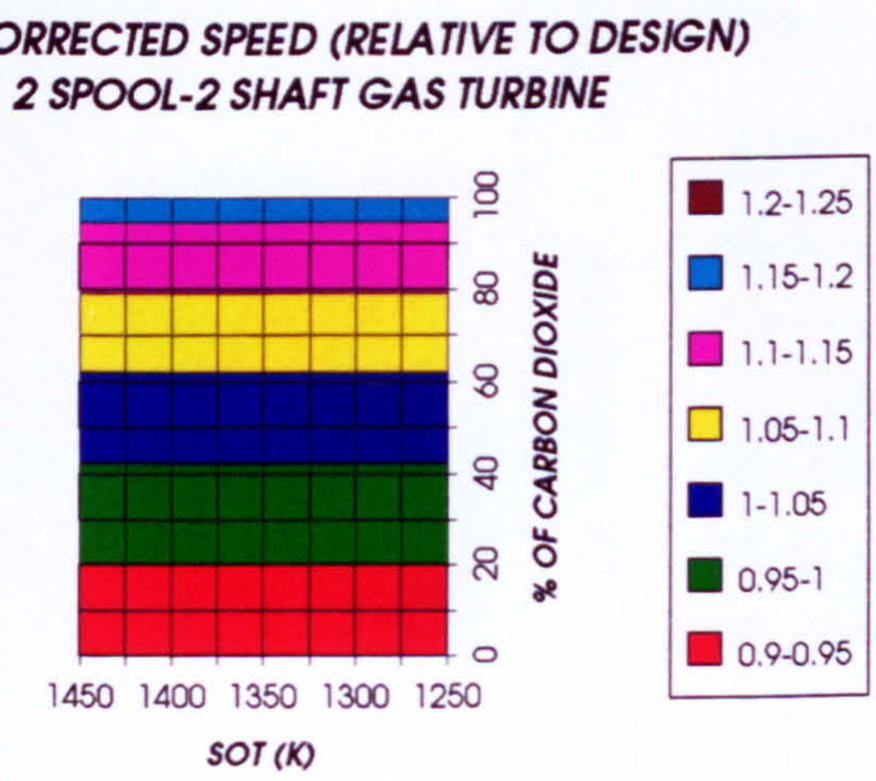

Figure 5. LP compressor corrected speed (relative to design) 2 spool -2 shaft configuration

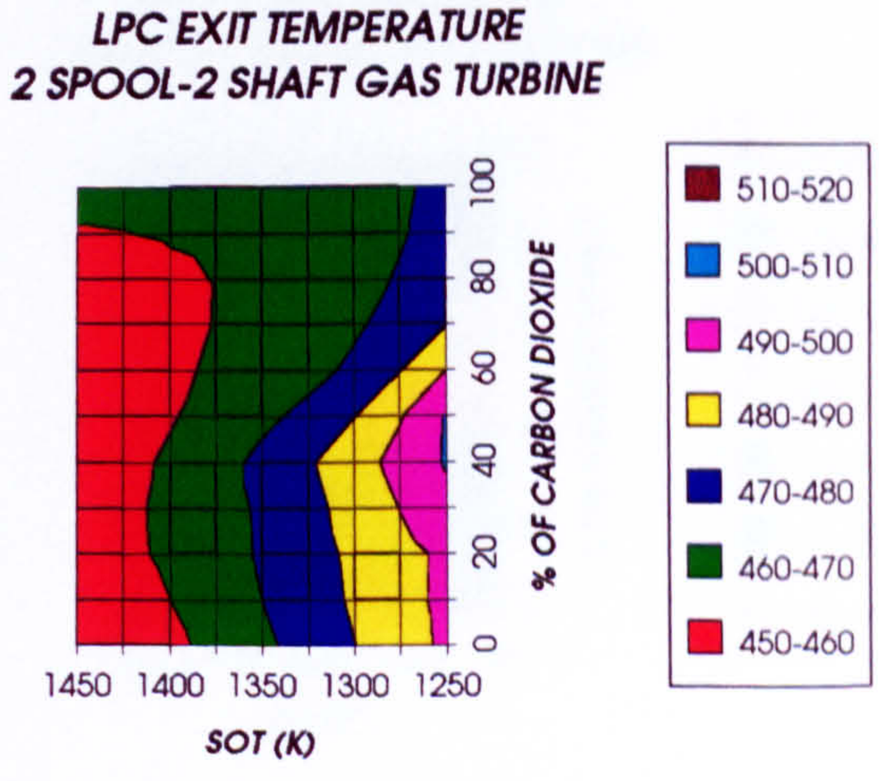

Figure 6. LP compressor exit temperature (K) 2 spool -2 shaft configuration

EFFECT OF CHANGING THE WORKING FLUID (2 SPOOL - 2 SHAFT)

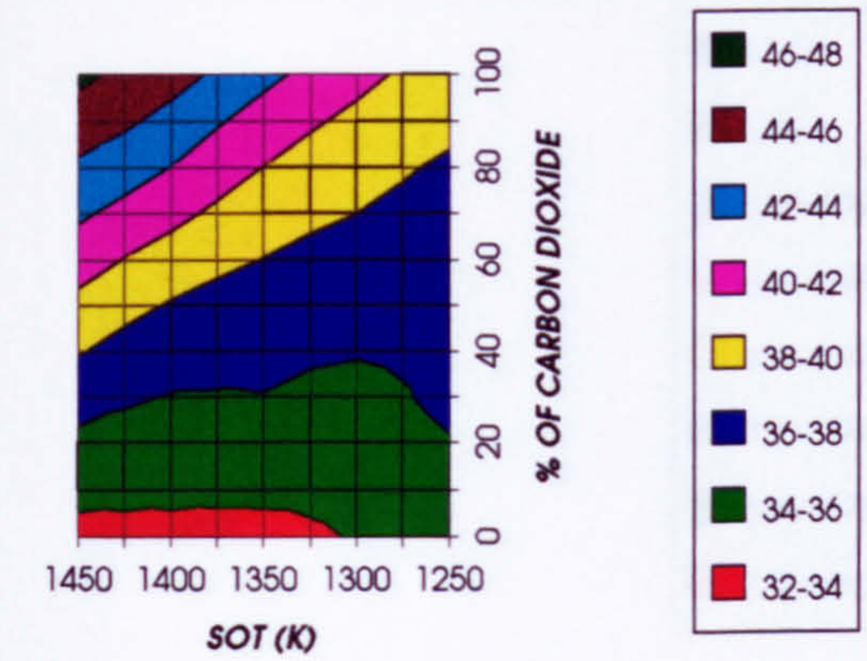

Figure 7. HP compressor surge margin (%)
2 spool -2 shaft configuration

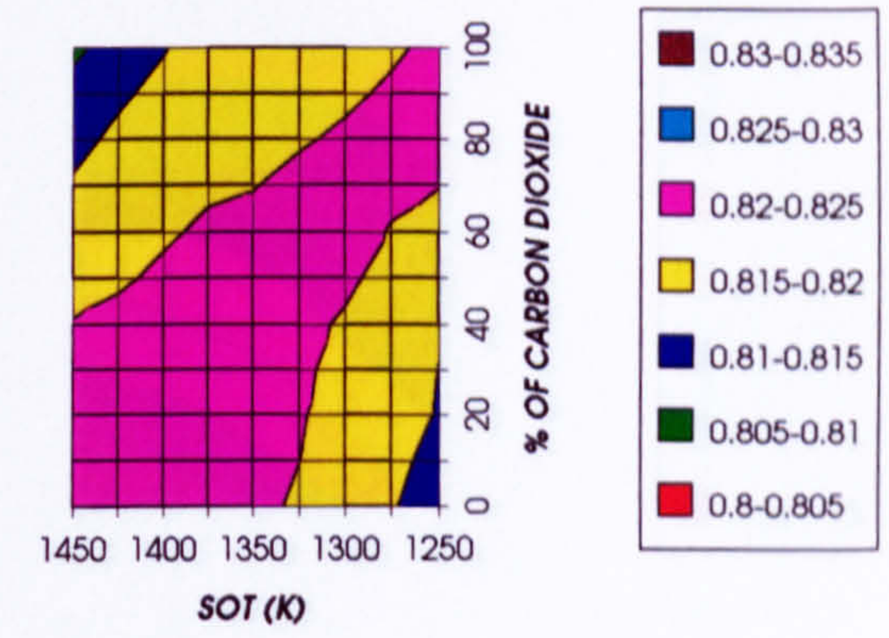

Figure 8. HP compressor adiabatic efficiency
2 spool -2 shaft configuration

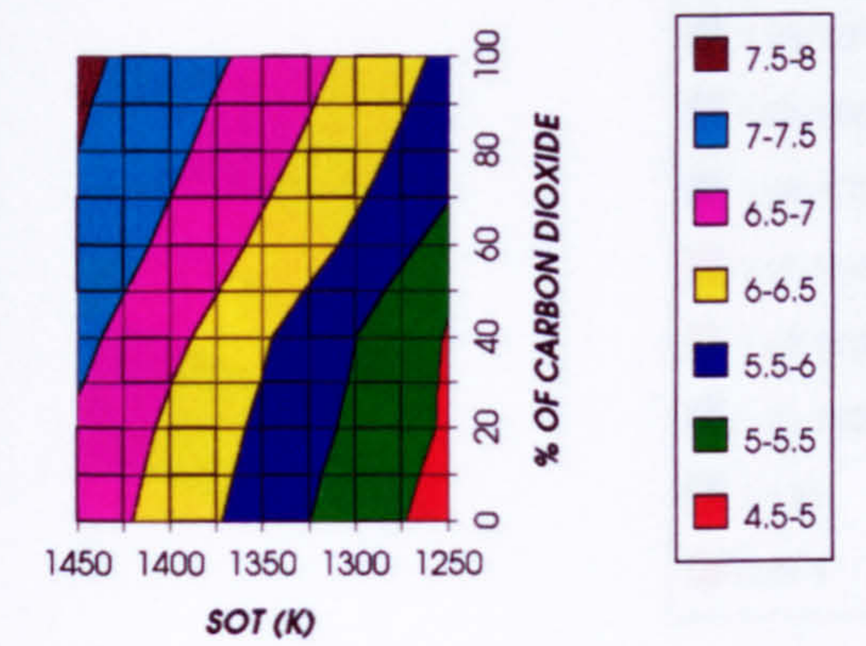

Figure 9. HP compressor pressure ratio
2 spool -2 shaft configuration

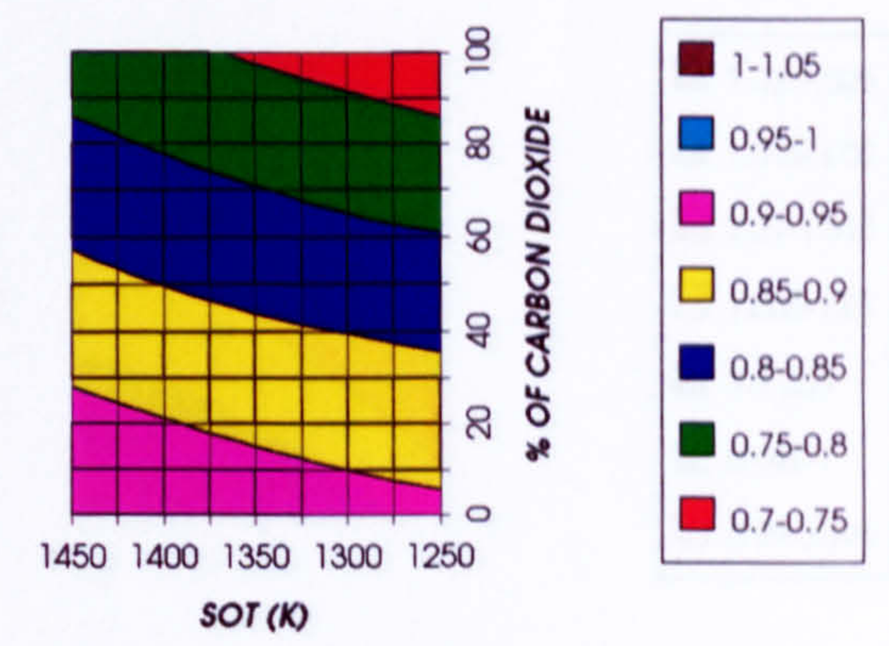

Figure 10. HP shaft speed (relative to design)
2 spool -2 shaft configuration

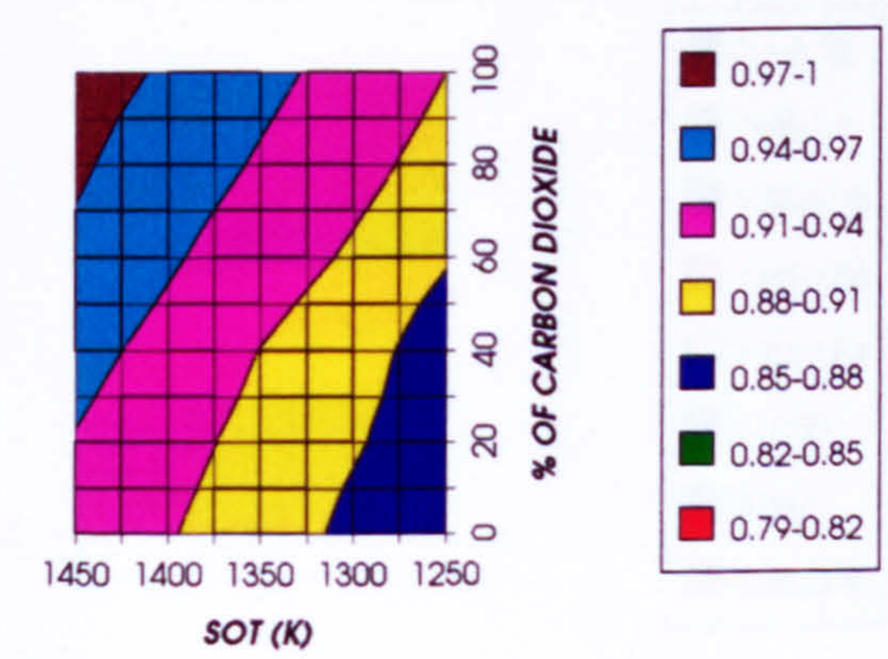

Figure 11. HP compressor corrected speed (relative to design)
2 spool -2 shaft configuration

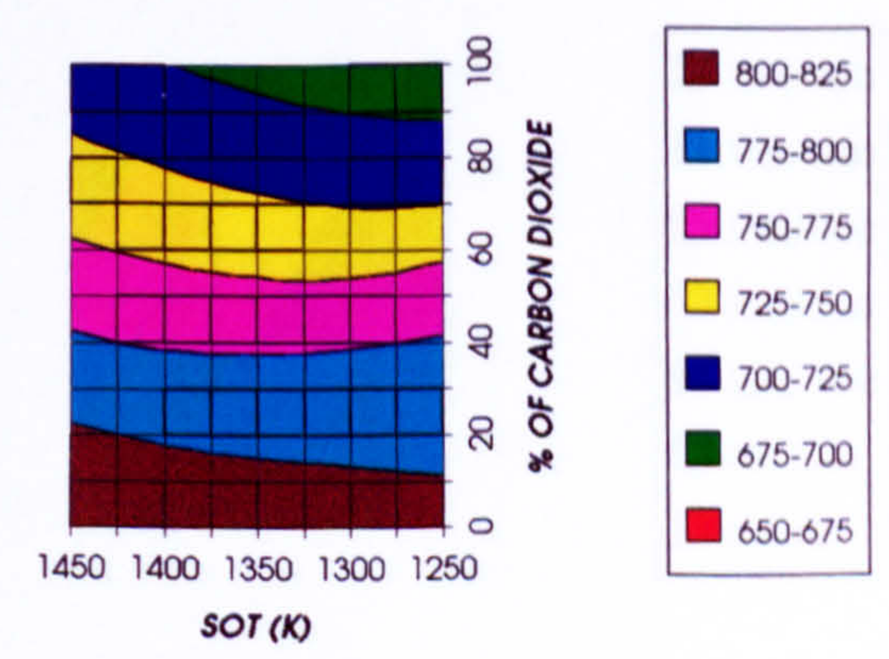

Figure 12. HP compressor exit temperature (K)
2 spool -2 shaft configuration

EFFECT OF CHANGING THE WORKING FLUID (2 SPOOL - 2 SHAFT)

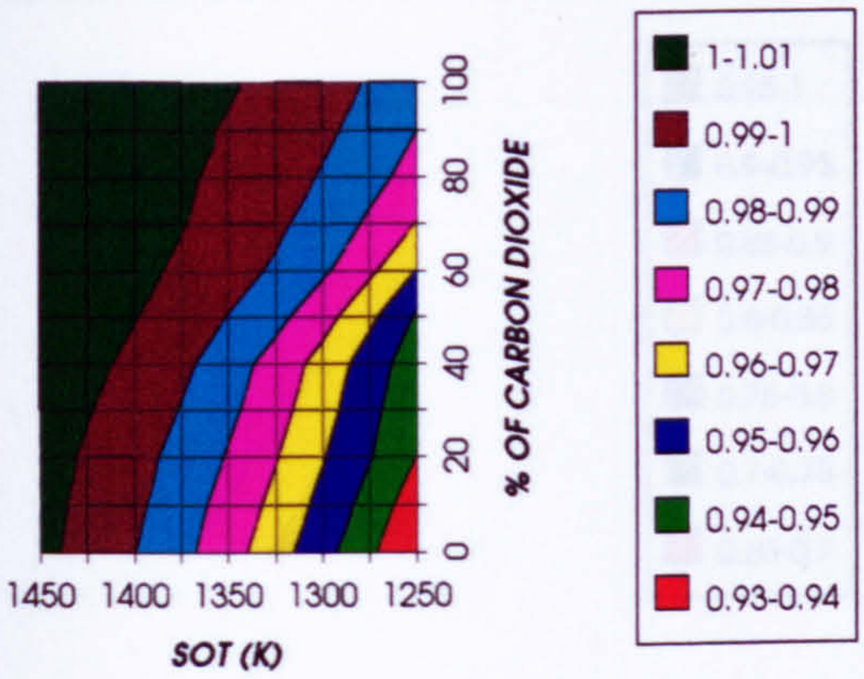

Figure 13. HP turbine load coefficient (relative to design) 2 spool -2 shaft configuration

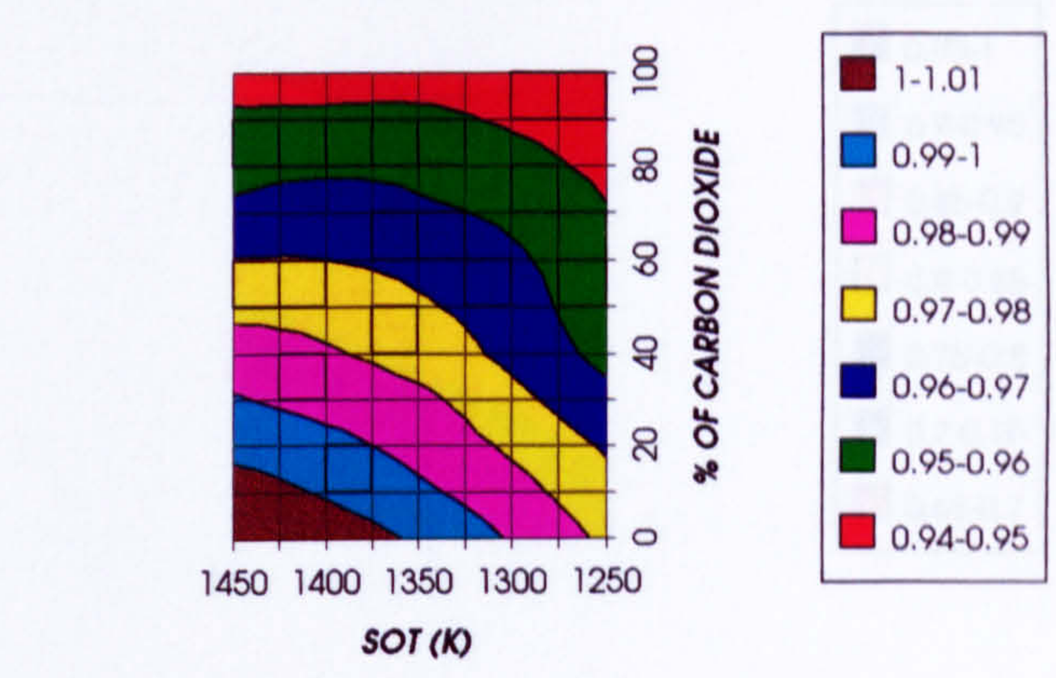

Figure 14. HP turbine flow coefficient (relative to design) 2 spool -2 shaft configuration

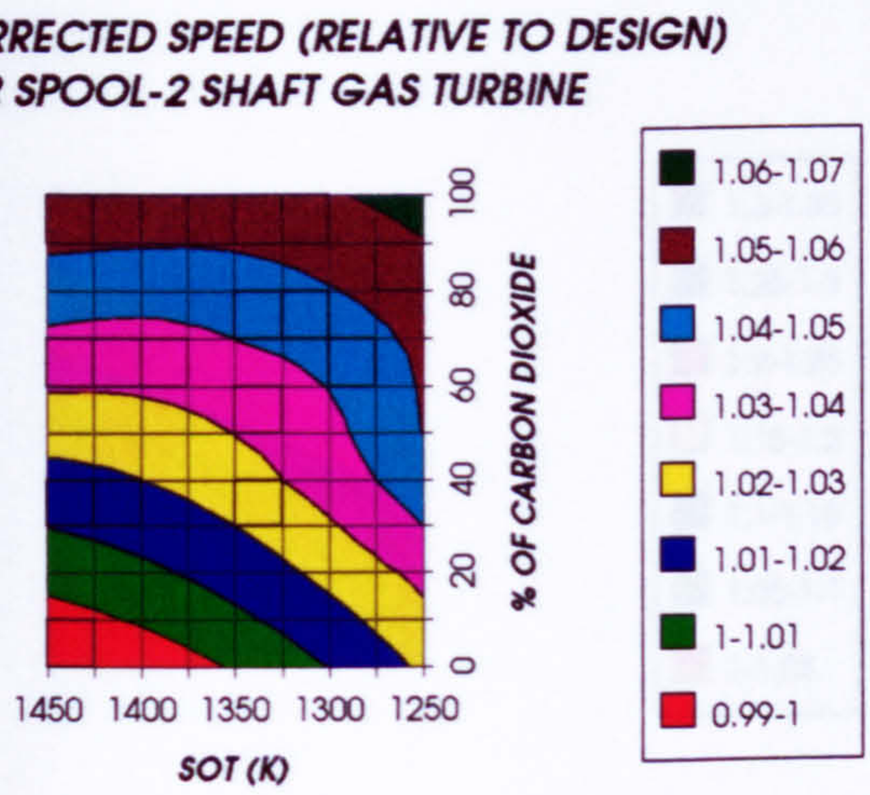

Figure 15. HP turbine corrected speed (relative to design) 2 spool -2 shaft configuration

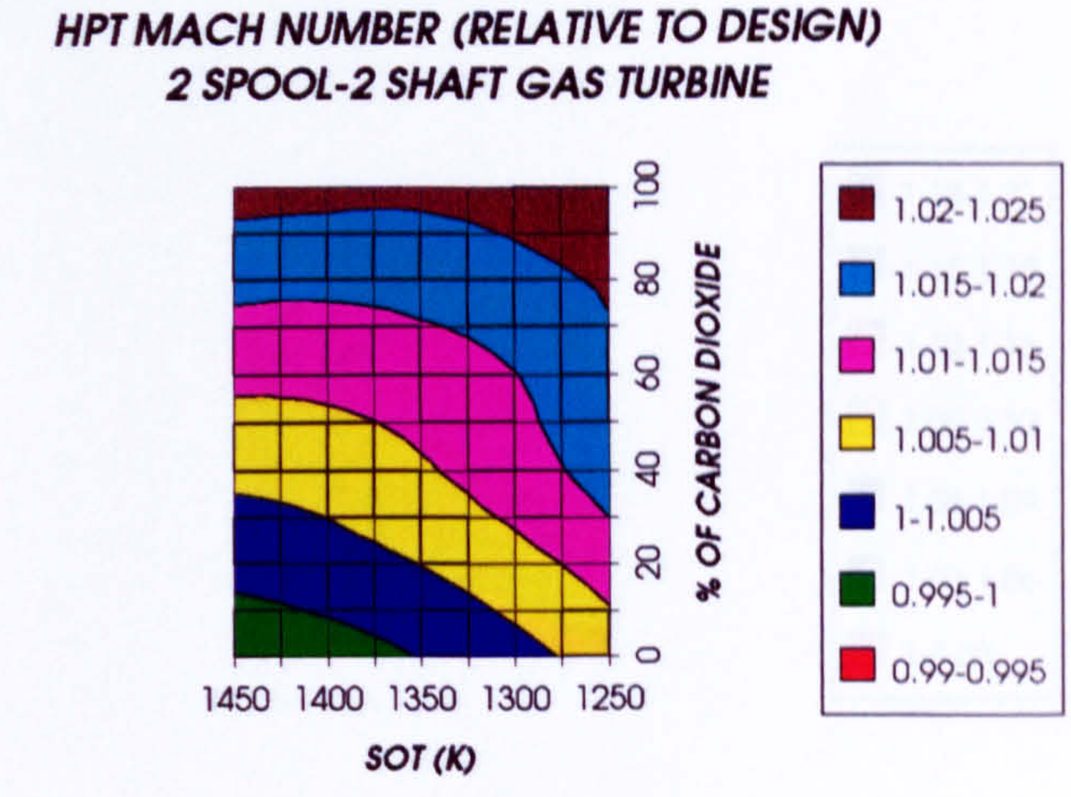

Figure 16. HP turbine Mach number (relative to design) 2 spool -2 shaft configuration

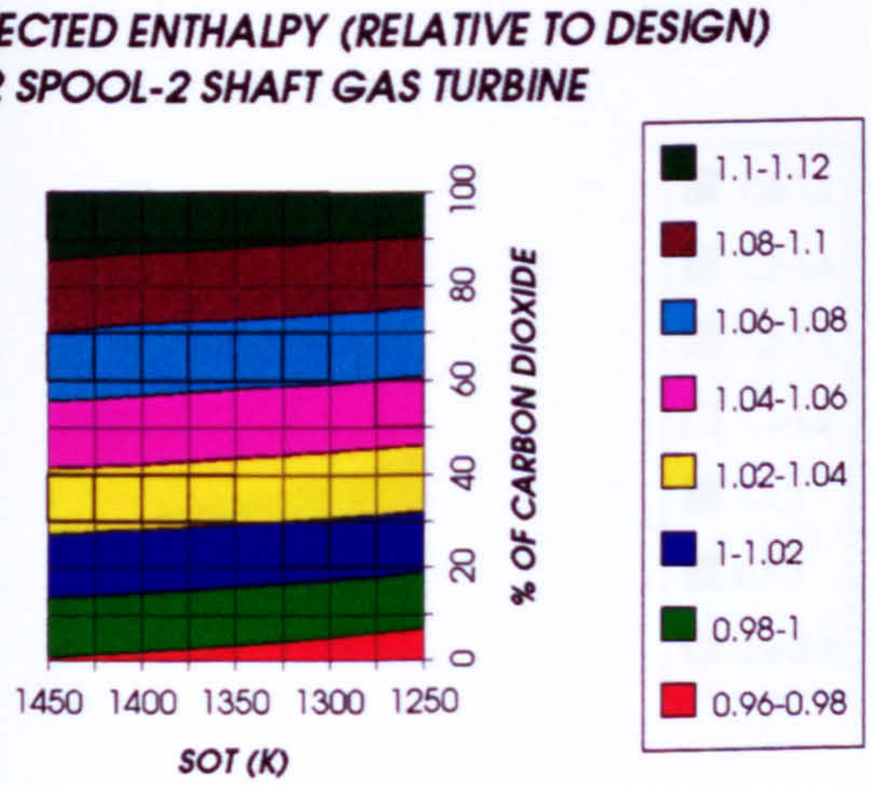

Figure 17. HP turbine corrected enthalpy (relative to design) 2 spool -2 shaft configuration

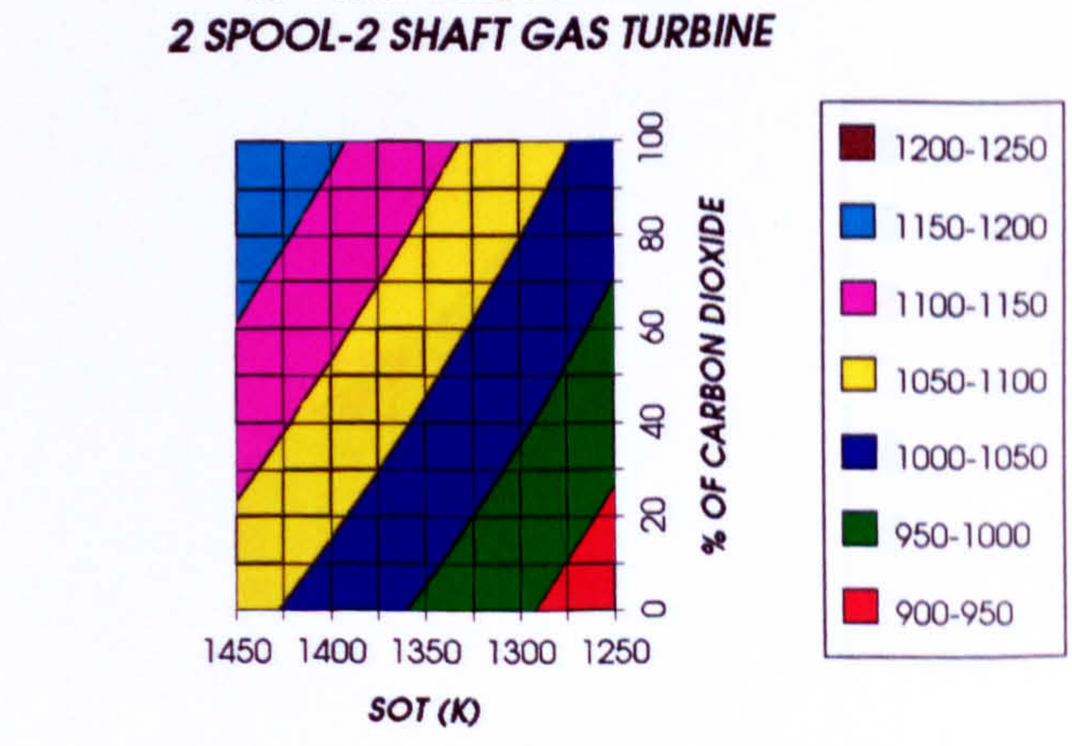

Figure 18. HP turbine exit temperature (K) 2 spool -2 shaft configuration

EFFECT OF CHANGING THE WORKING FLUID (2 SPOOL - 2 SHAFT)

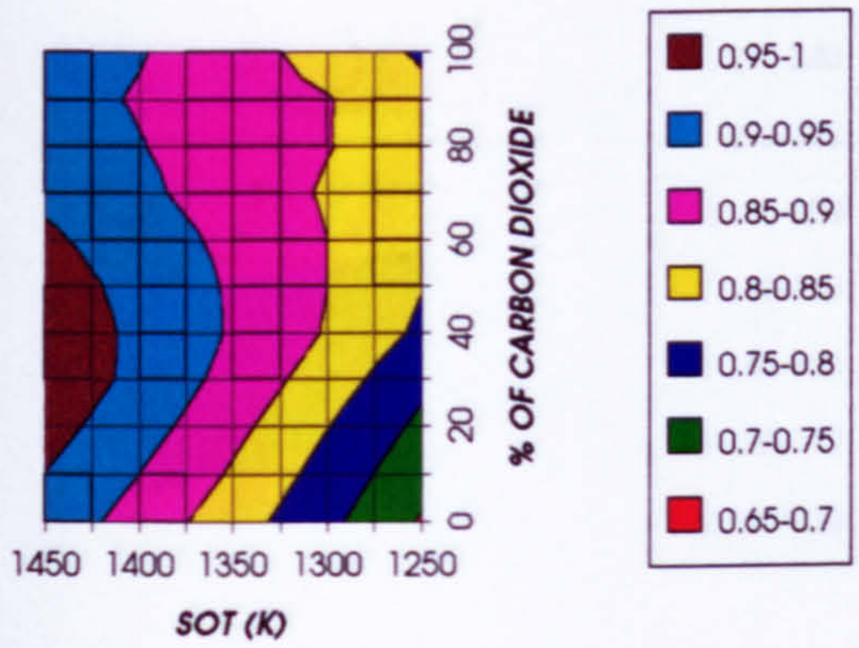

Figure 19. LP turbine load coefficient (relative to design) 2 spool -2 shaft configuration

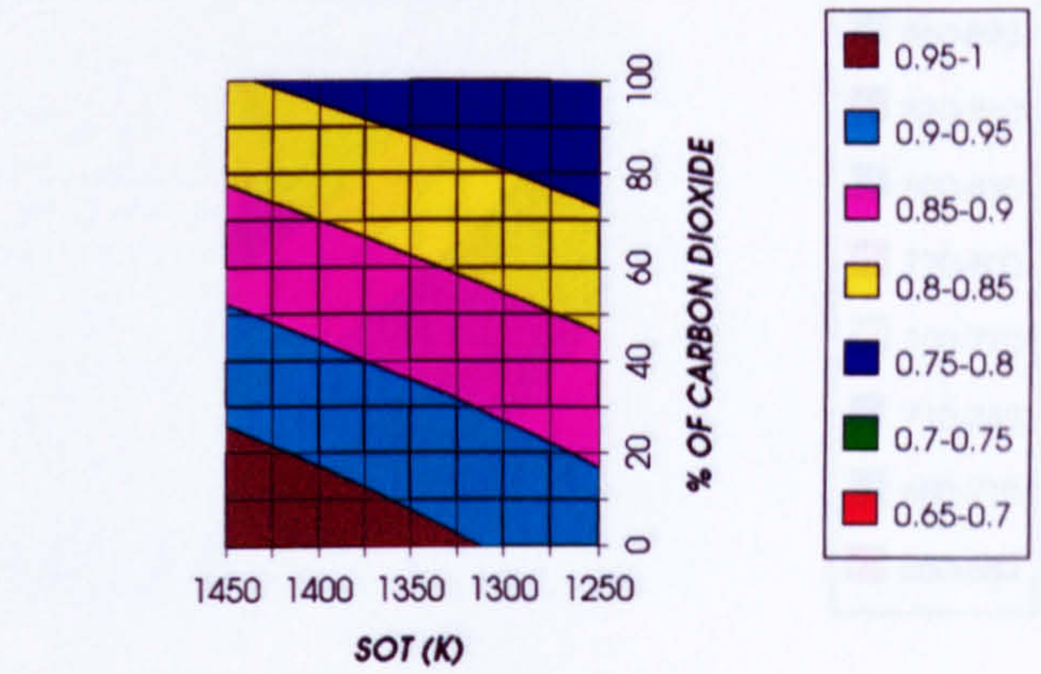

Figure 20. LP turbine flow coefficient (relative to design) 2 spool -2 shaft configuration

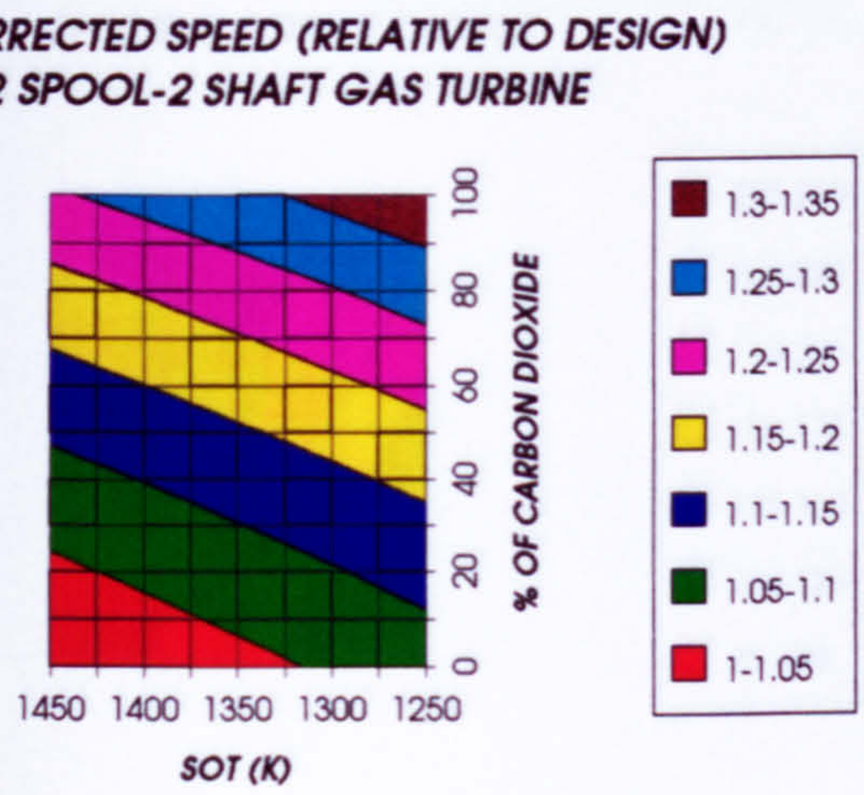

Figure 21. LP turbine corrected speed (relative to design) 2 spool -2 shaft configuration

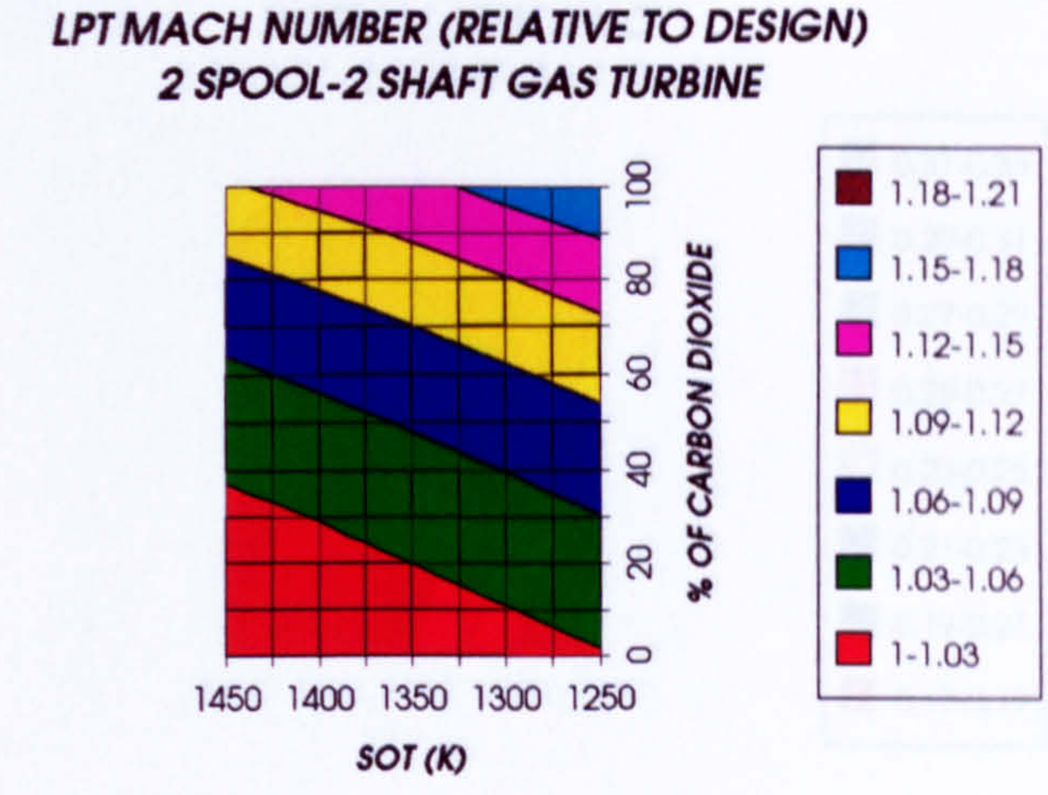

Figure 22. LP turbine Mach number (relative to design) 2 spool -2 shaft configuration

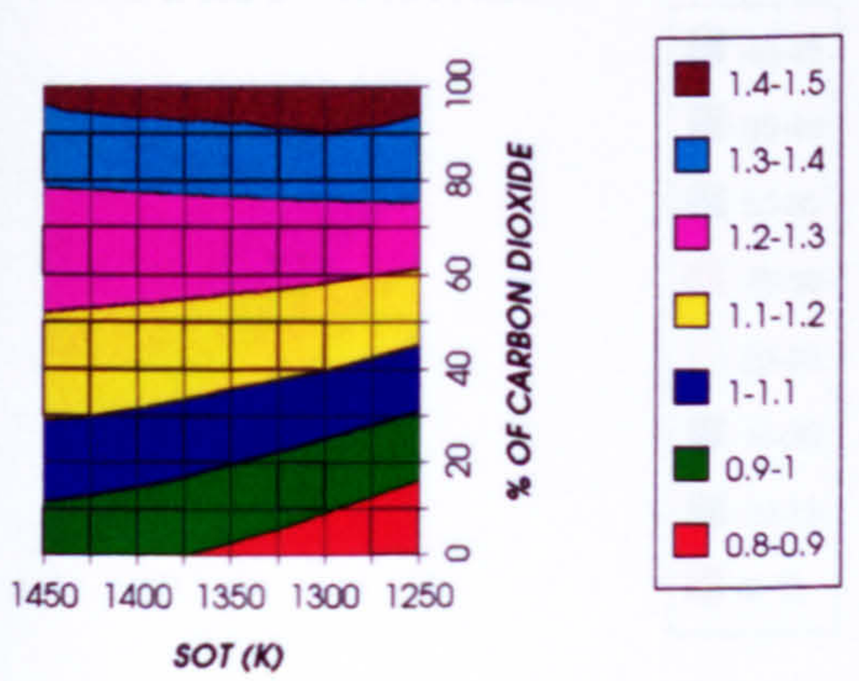

Figure 23. LP turbine corrected enthalpy (relative to design) 2 spool -2 shaft configuration

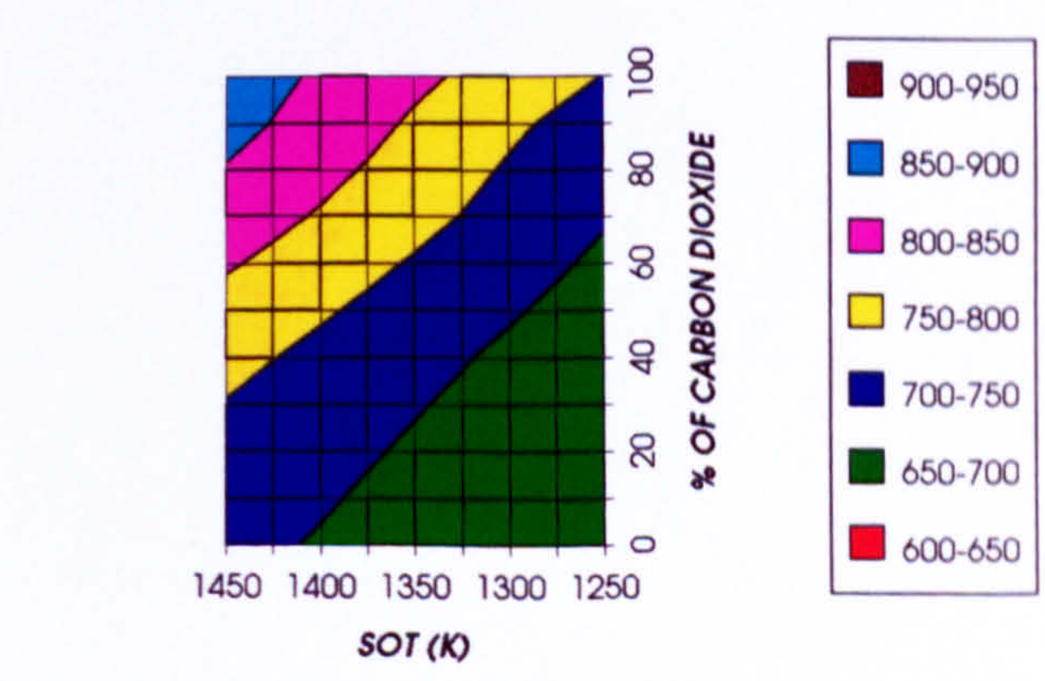

Figure 24. LP turbine exit temperature (K) 2 spool -2 shaft configuration

EFFECT OF CHANGING THE WORKING FLUID (2 SPOOL - 2 SHAFT)

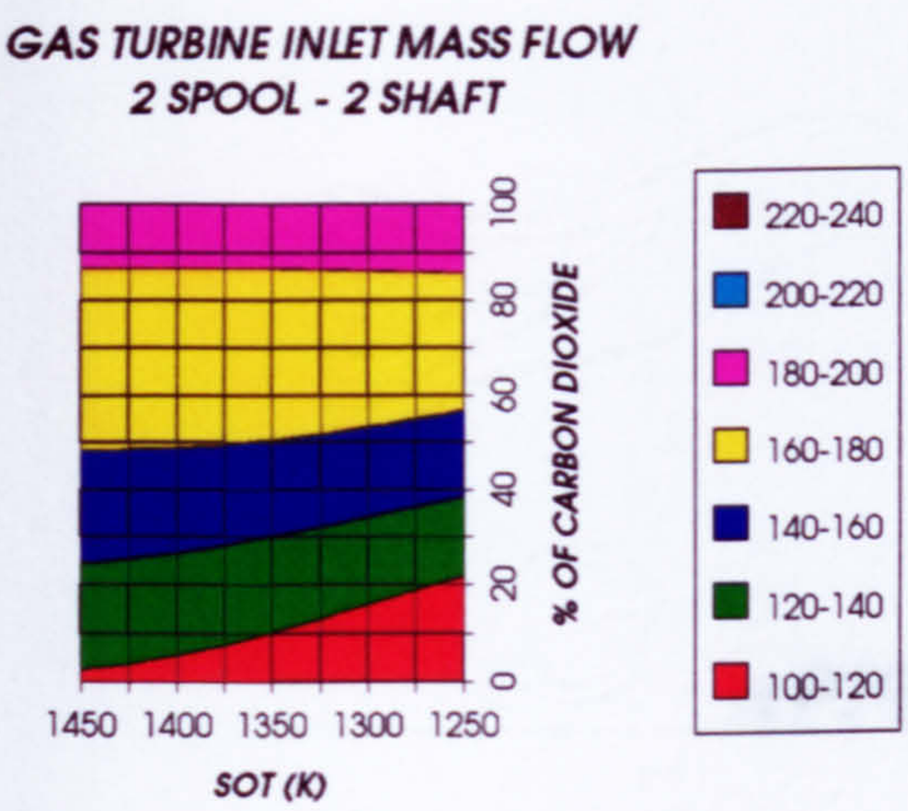

Figure 25. Gas turbine inlet mass flow (kg/s)
2 spool -2 shaft configuration

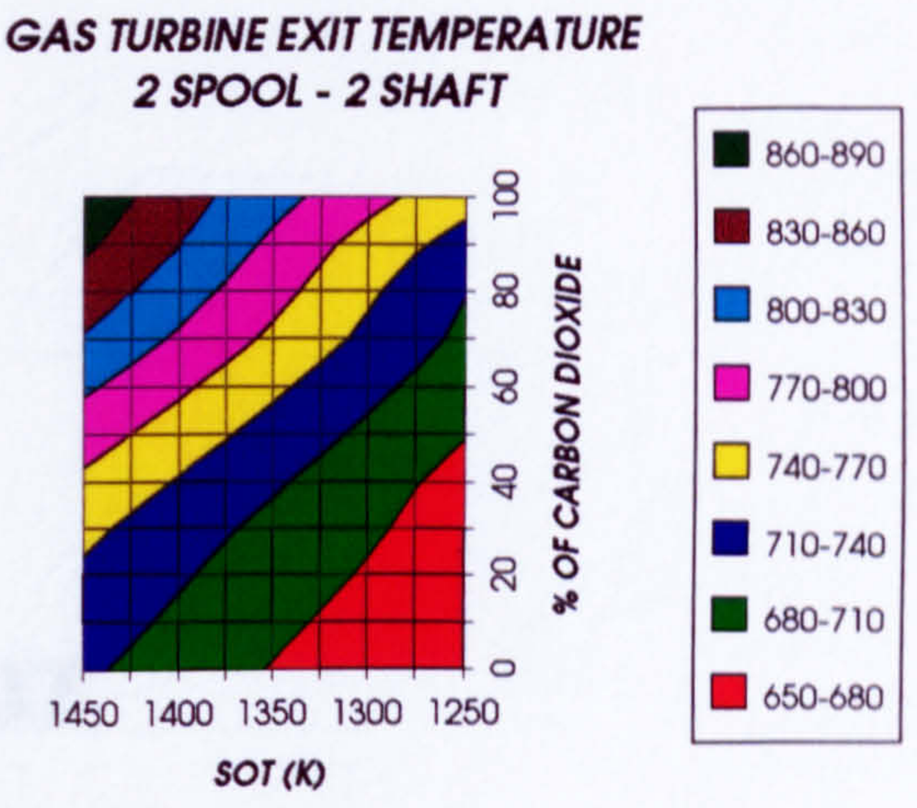

Figure 26. Gas turbine exit temperature (K)
2 spool -2 shaft configuration

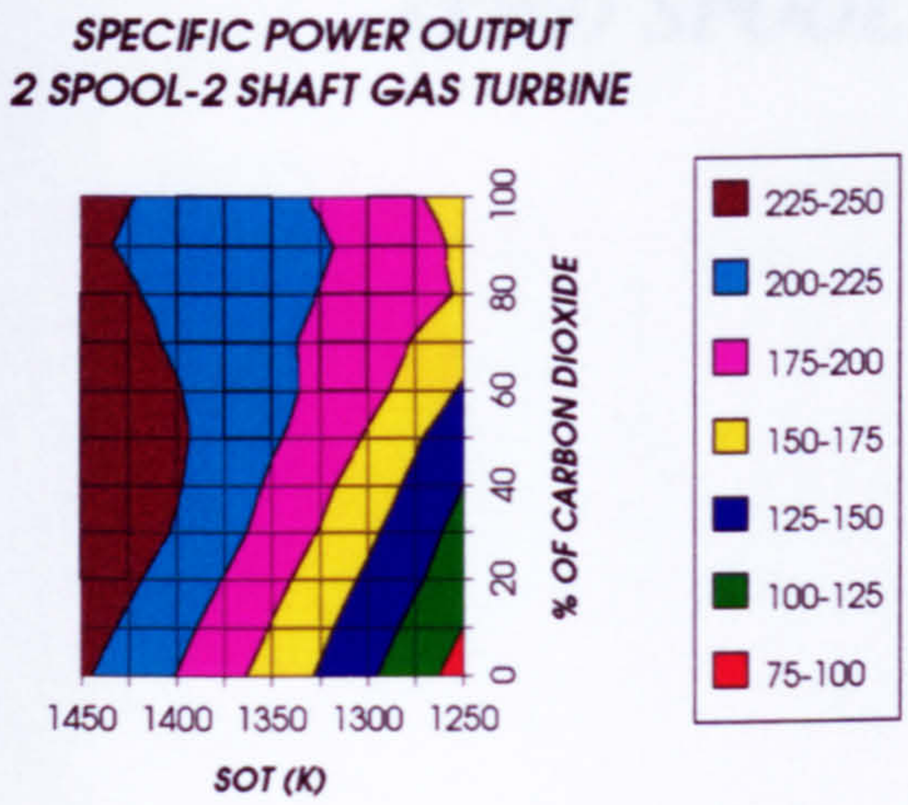

Figure 27. Gas turbine specific power output (kW/kg/s)
2 spool -2 shaft configuration

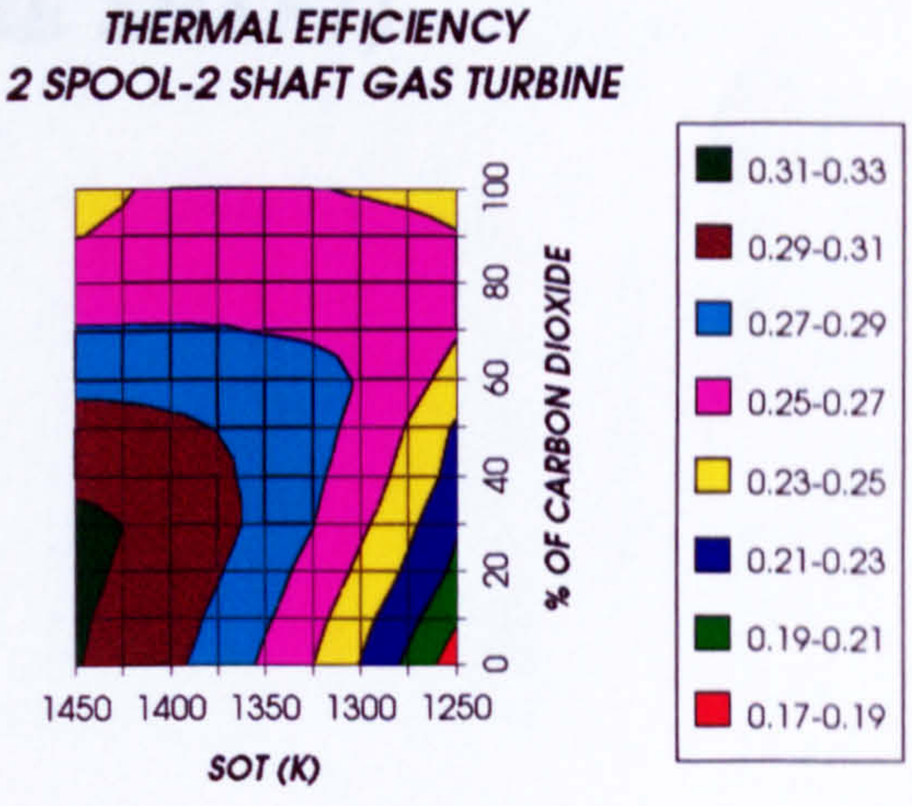

Figure 28. Gas turbine thermal efficiency
2 spool -2 shaft configuration

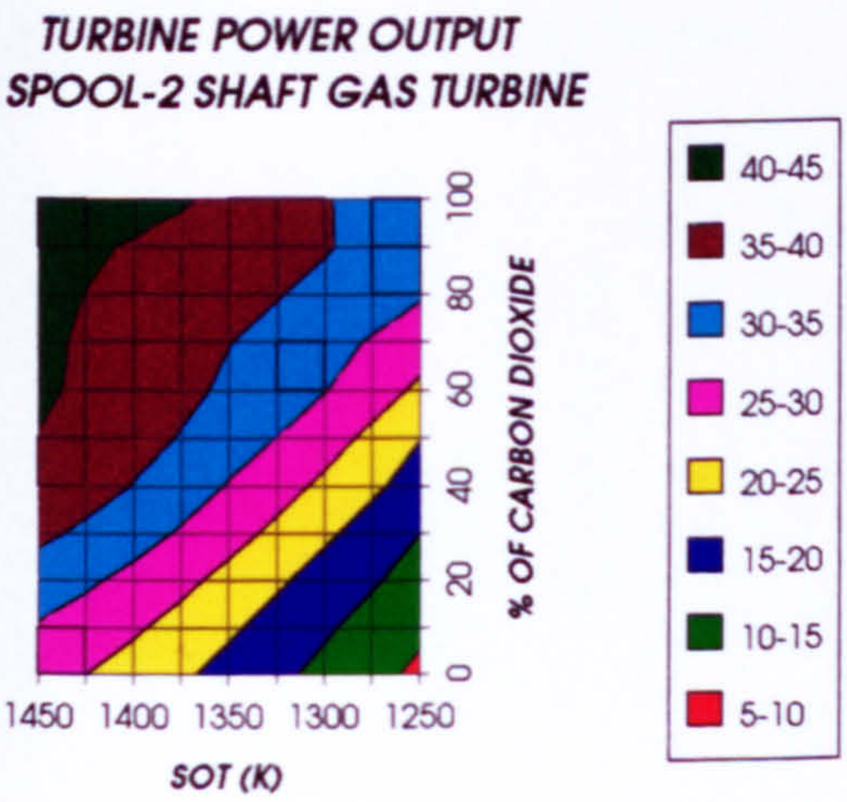

Figure 29. Gas turbine power (MW)
2 spool -2 shaft configuration

APPENDIX XI

EFFECT OF CHANGING THE WORKING FLUID (TWO SPOOL - THREE SHAFT)

EFFECT OF CHANGING THE WORKING FLUID (2 SPOOL - 3 SHAFT)

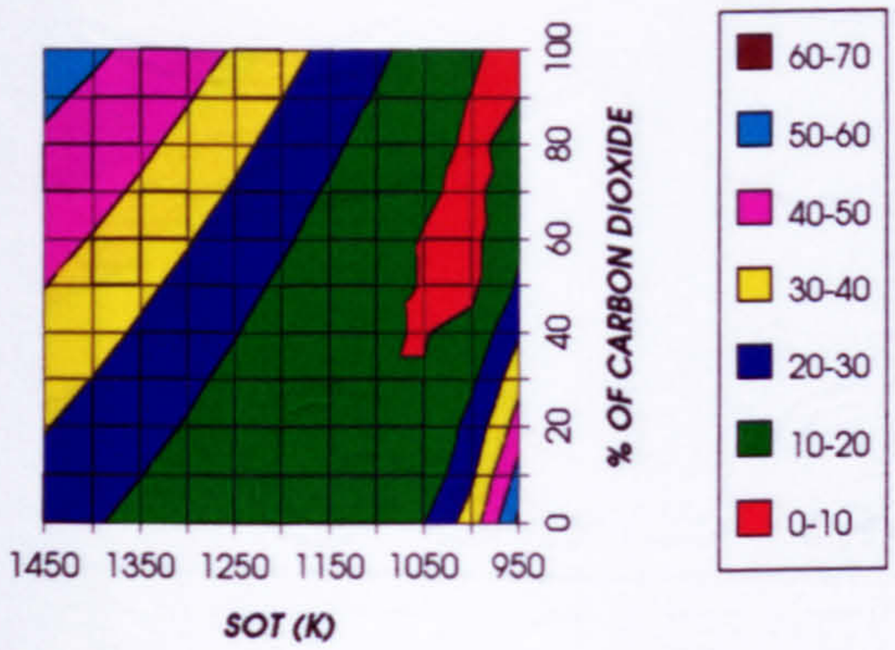

Figure 1. LP compressor surge margin (%)
2 spool -3 shaft configuration

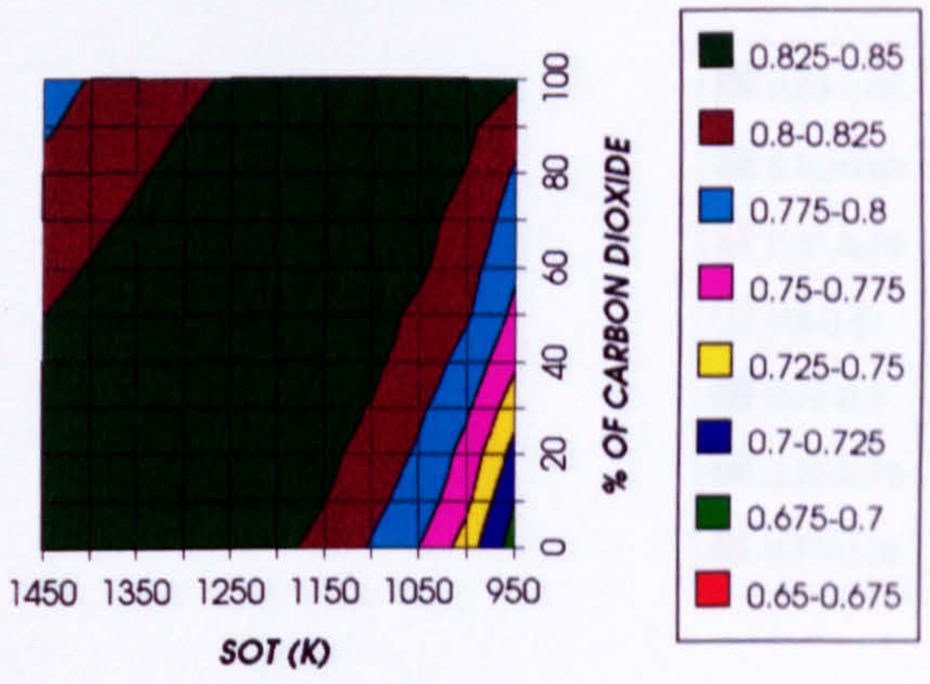

Figure 2. LP compressor adiabatic efficiency
2 spool -3 shaft configuration

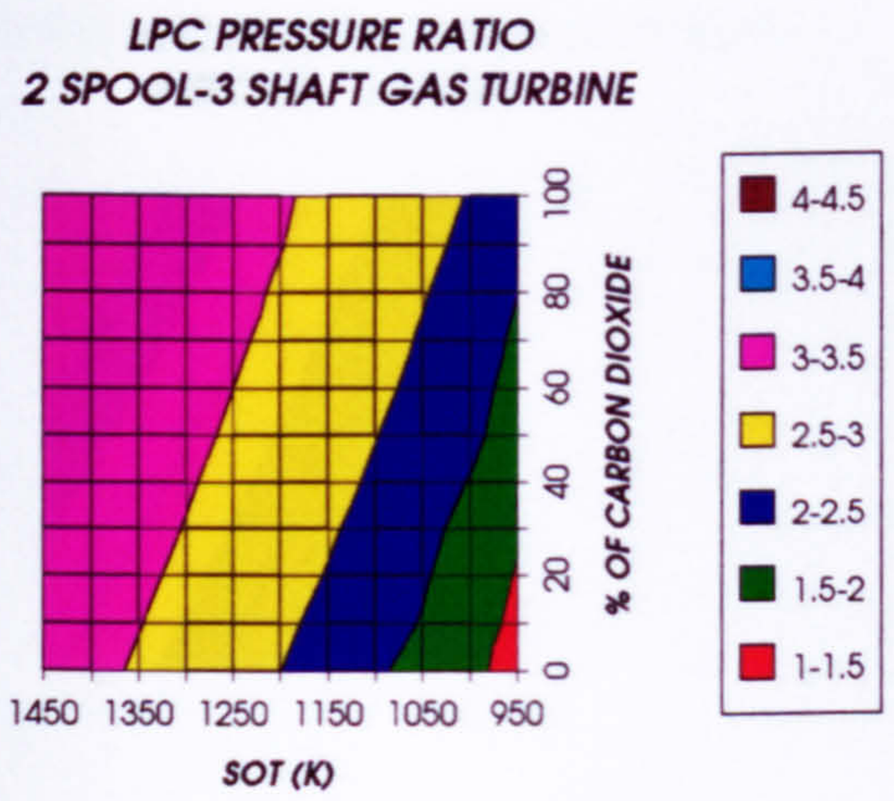

Figure 3. LP compressor pressure ratio
2 spool -3 shaft configuration

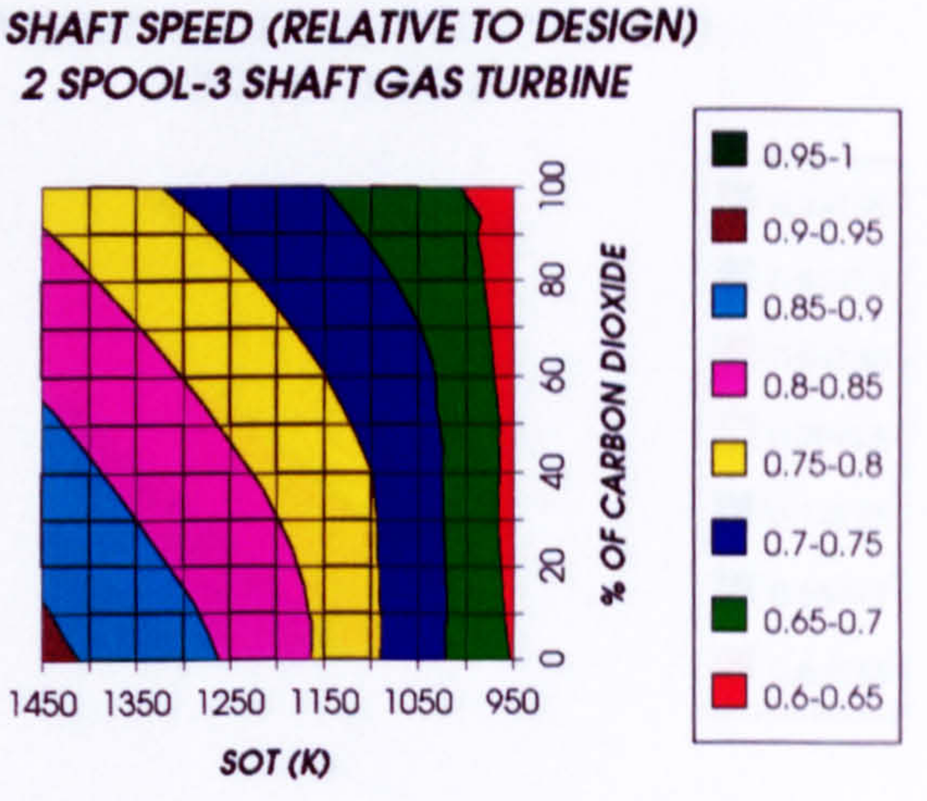

Figure 4. LP shaft speed (relative to design)
2 spool -3 shaft configuration

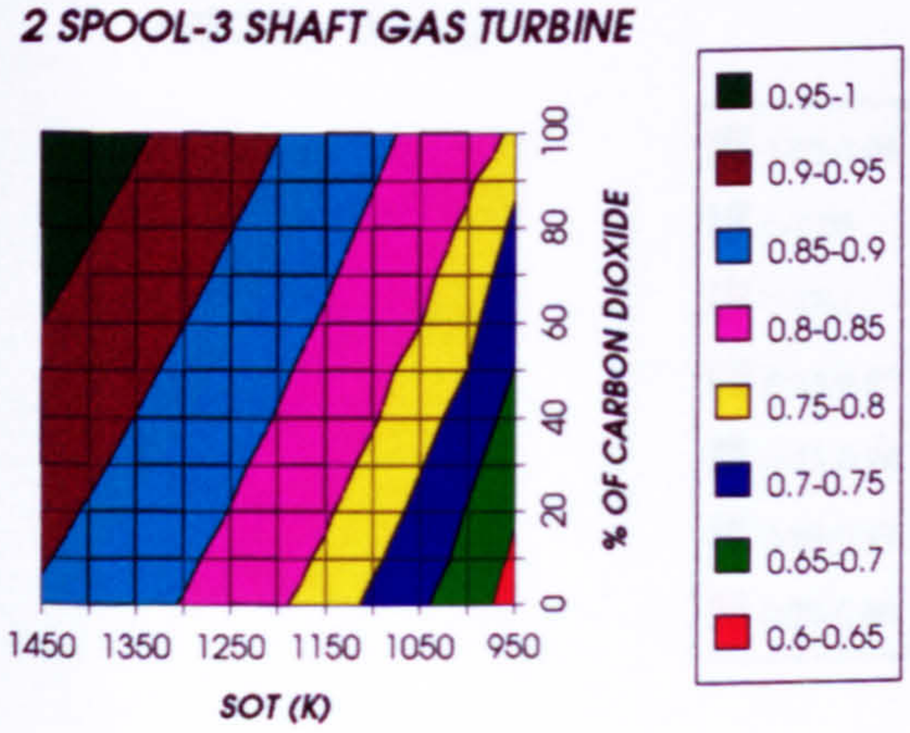

Figure 5. LP compressor corrected speed (relative to design)
2 spool -3 shaft configuration

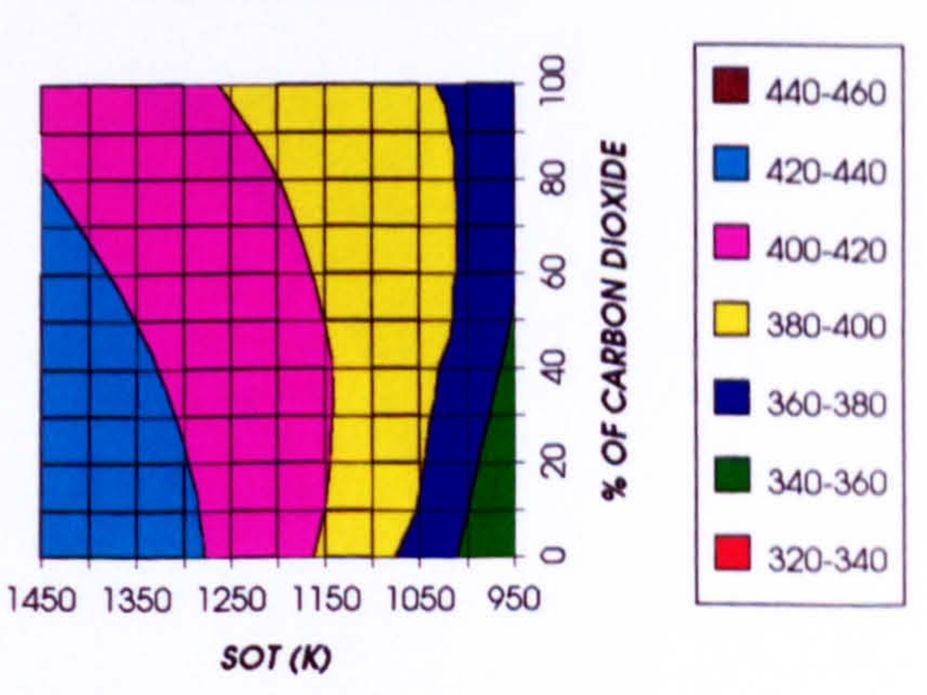

Figure 6. LP compressor exit temperature (K)
2 spool -3 shaft configuration

EFFECT OF CHANGING THE WORKING FLUID (2 SPOOL - 3 SHAFT)

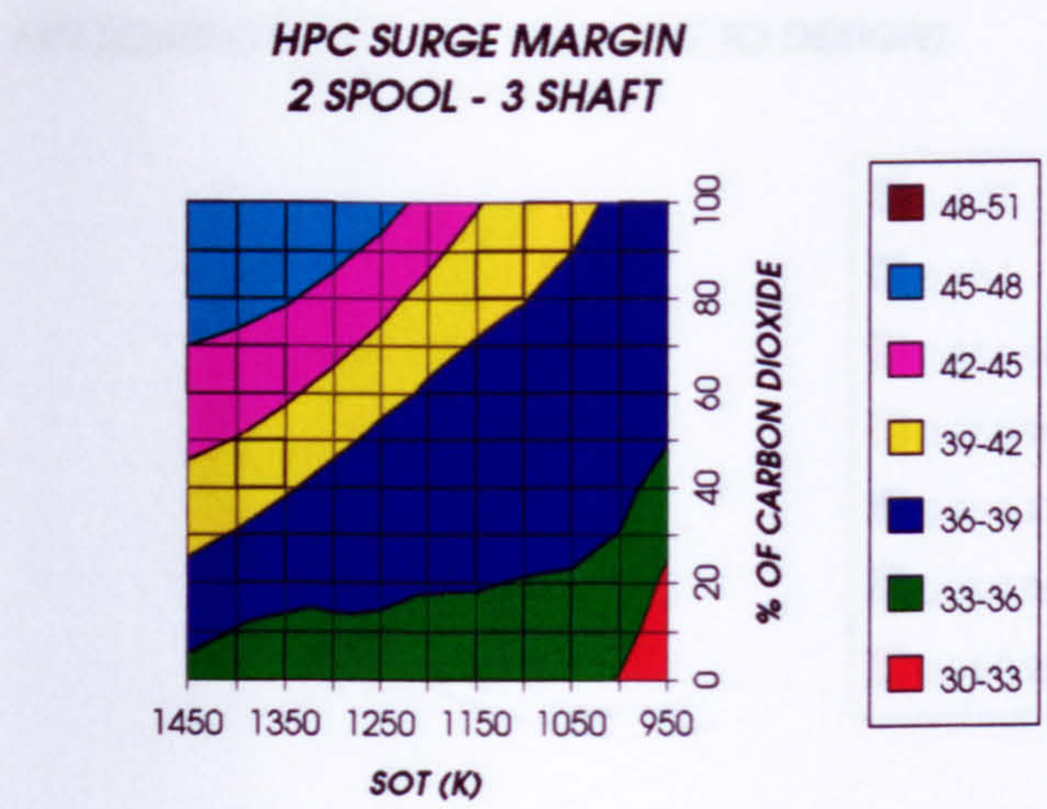

Figure 7. HP compressor surge margin (%)
2 spool -3 shaft configuration

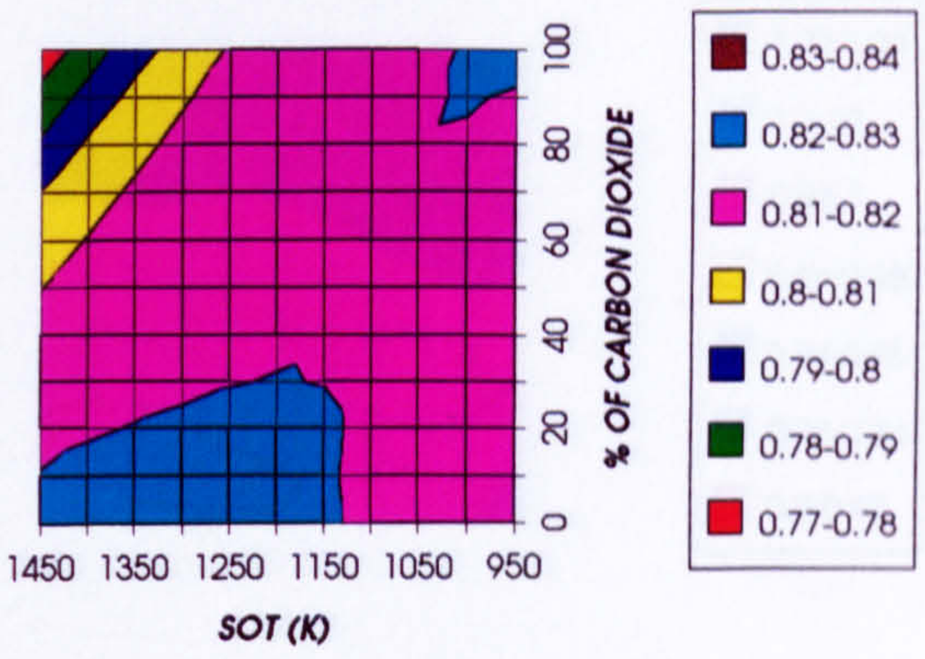

Figure 8. HP compressor adiabatic efficiency
2 spool -3 shaft configuration

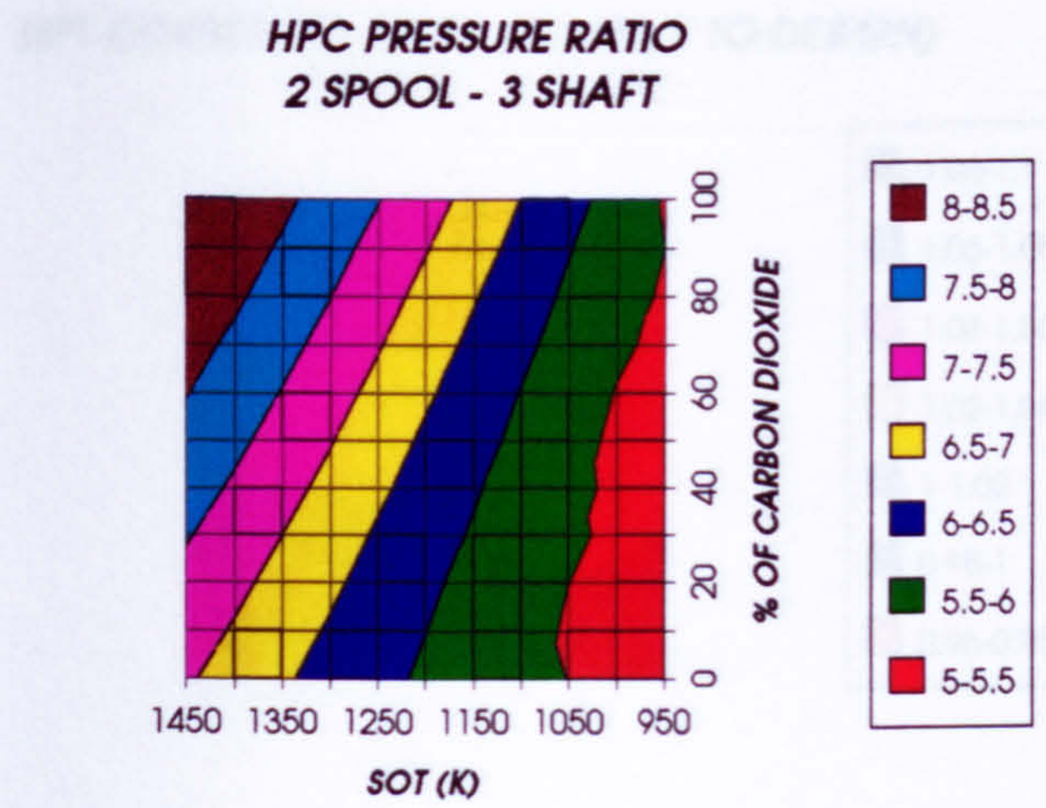

Figure 9. HP compressor pressure ratio
2 spool -3 shaft configuration

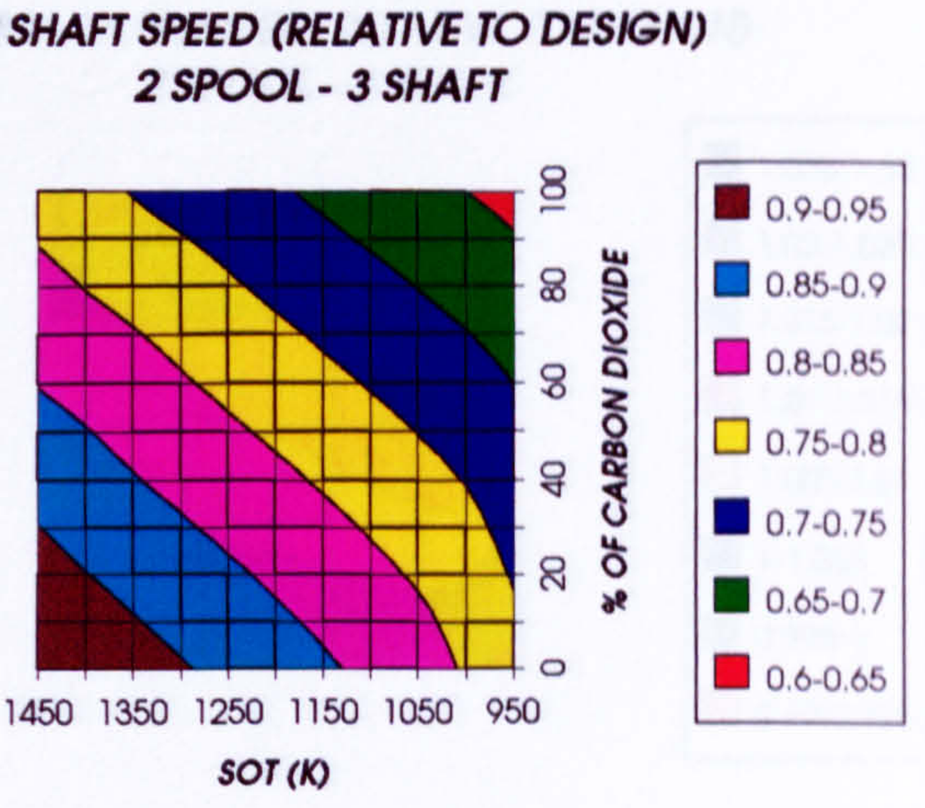

Figure 10. HP shaft speed (relative to design)
2 spool -3 shaft configuration

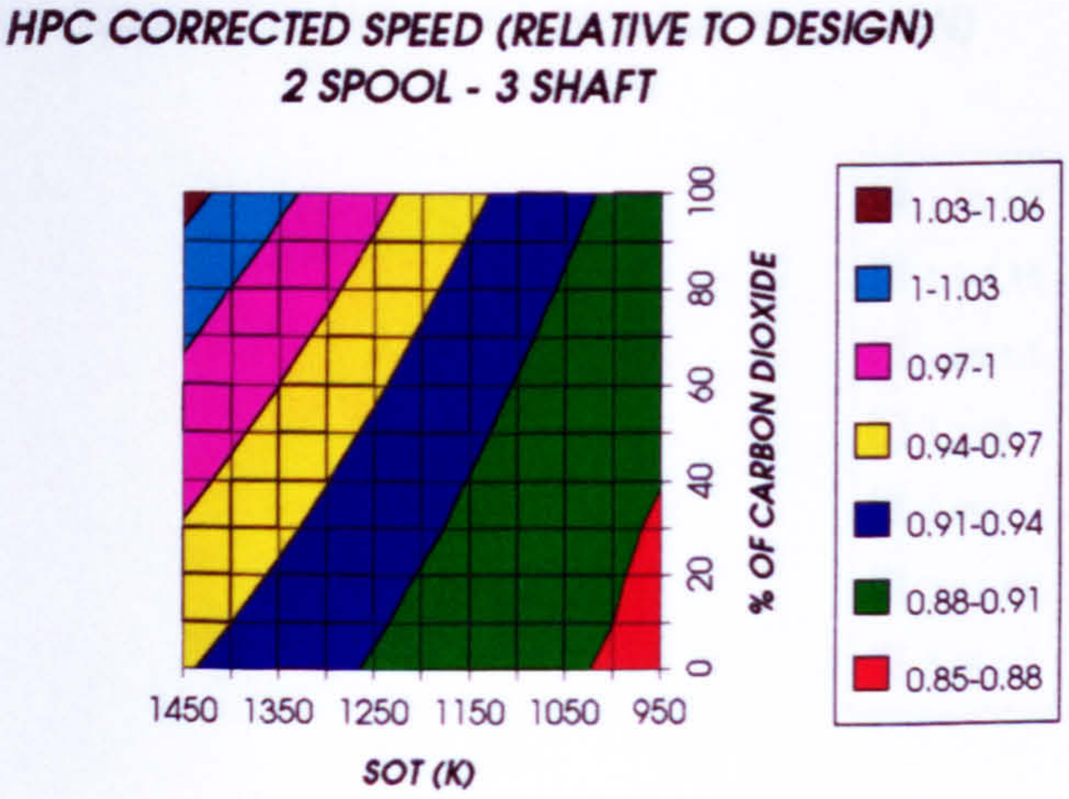

Figure 11. HP compressor corrected speed (relative to design)
2 spool -3 shaft configuration

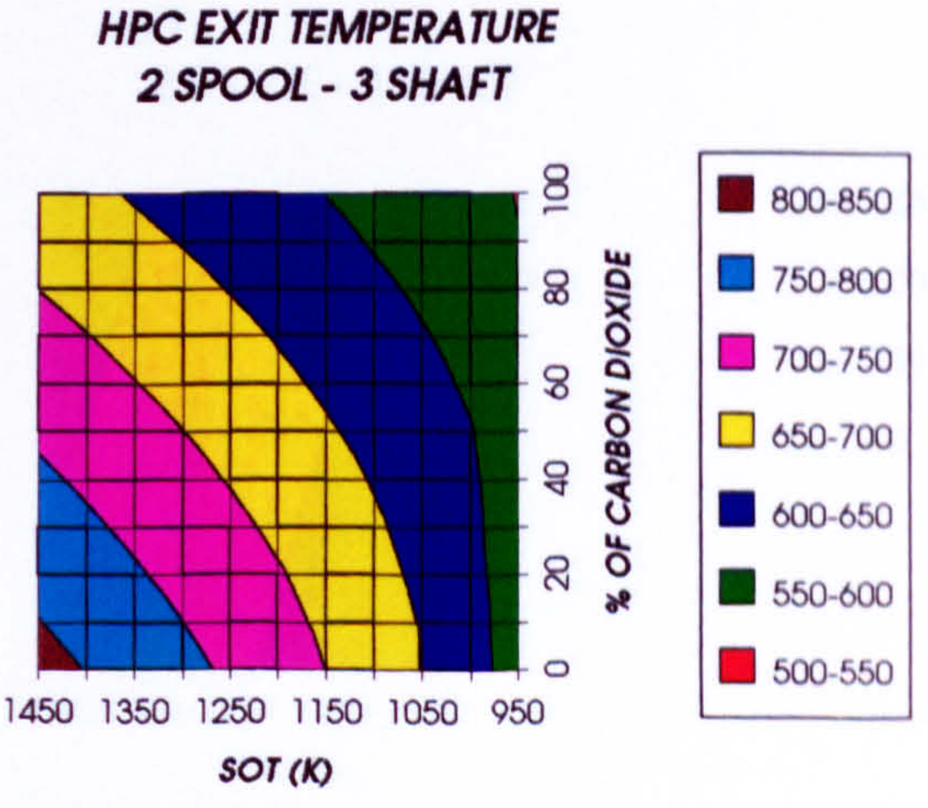

Figure 12. HP compressor exit temperature (K)
2 spool -3 shaft configuration

EFFECT OF CHANGING THE WORKING FLUID (2 SPOOL - 3 SHAFT)

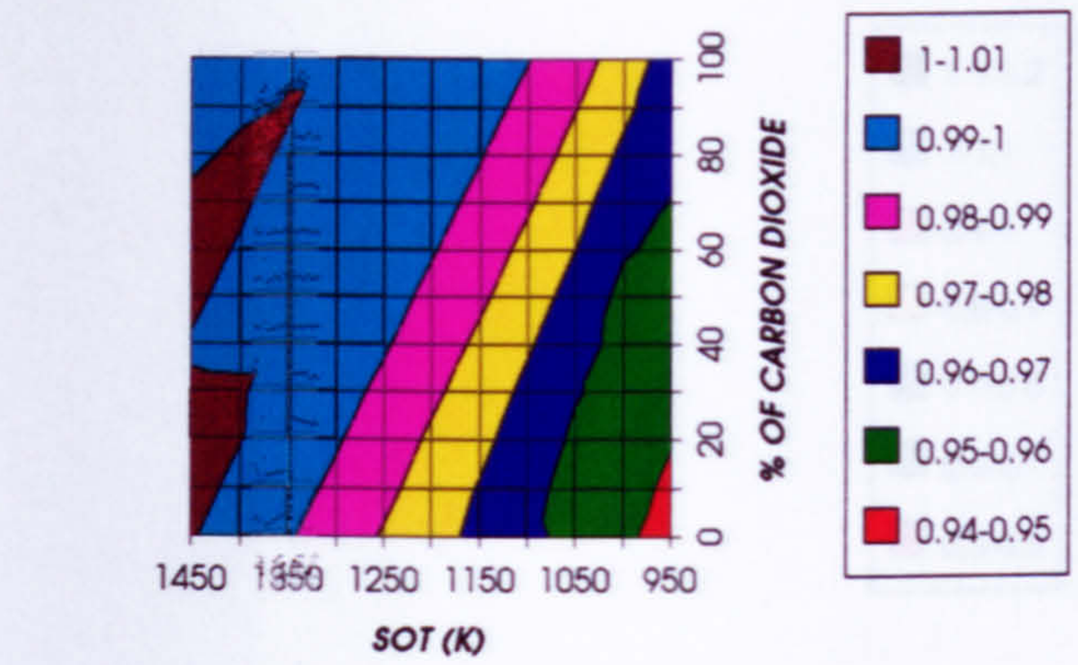

Figure 13. HP turbine load coefficient (relative to design) 2 spool -3 shaft configuration

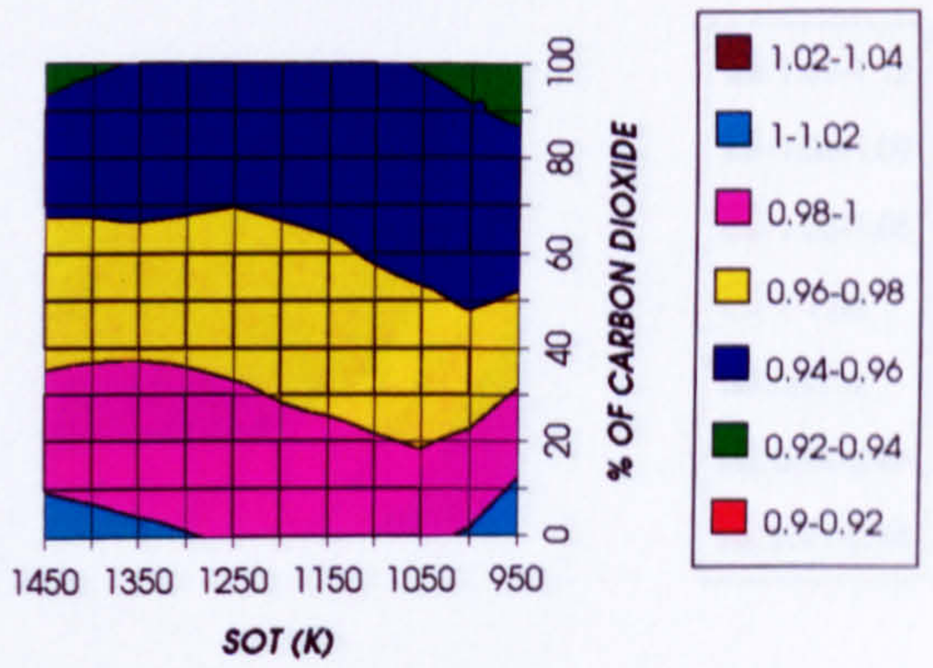

Figure 14. HP turbine flow coefficient (relative to design) 2 spool -3 shaft configuration

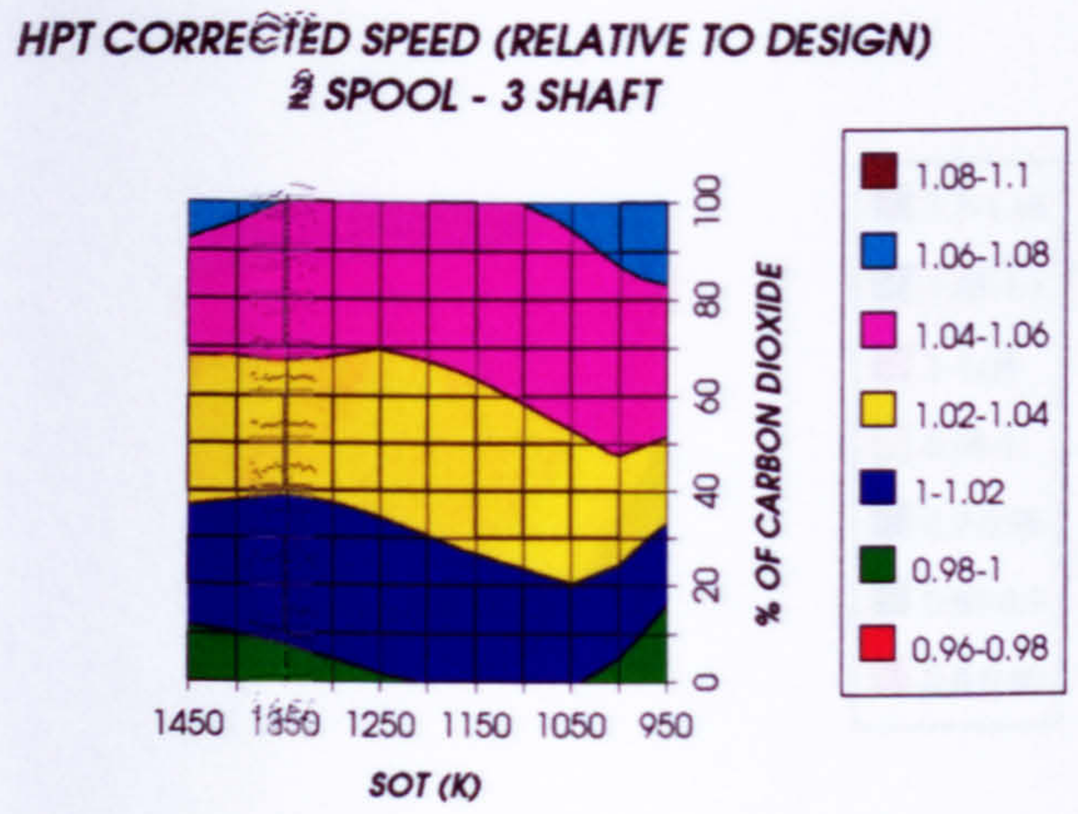

Figure 15. HP turbine corrected speed (relative to design) 2 spool -3 shaft configuration

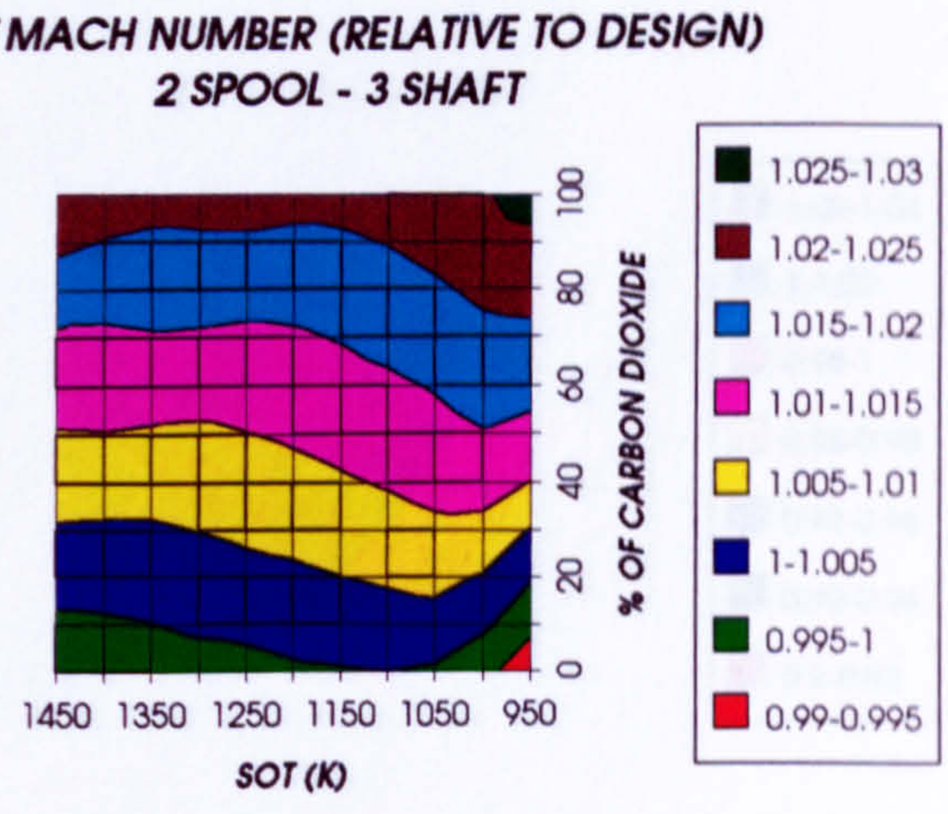

Figure 16. HP turbine Mach number (relative to design) 2 spool -3 shaft configuration

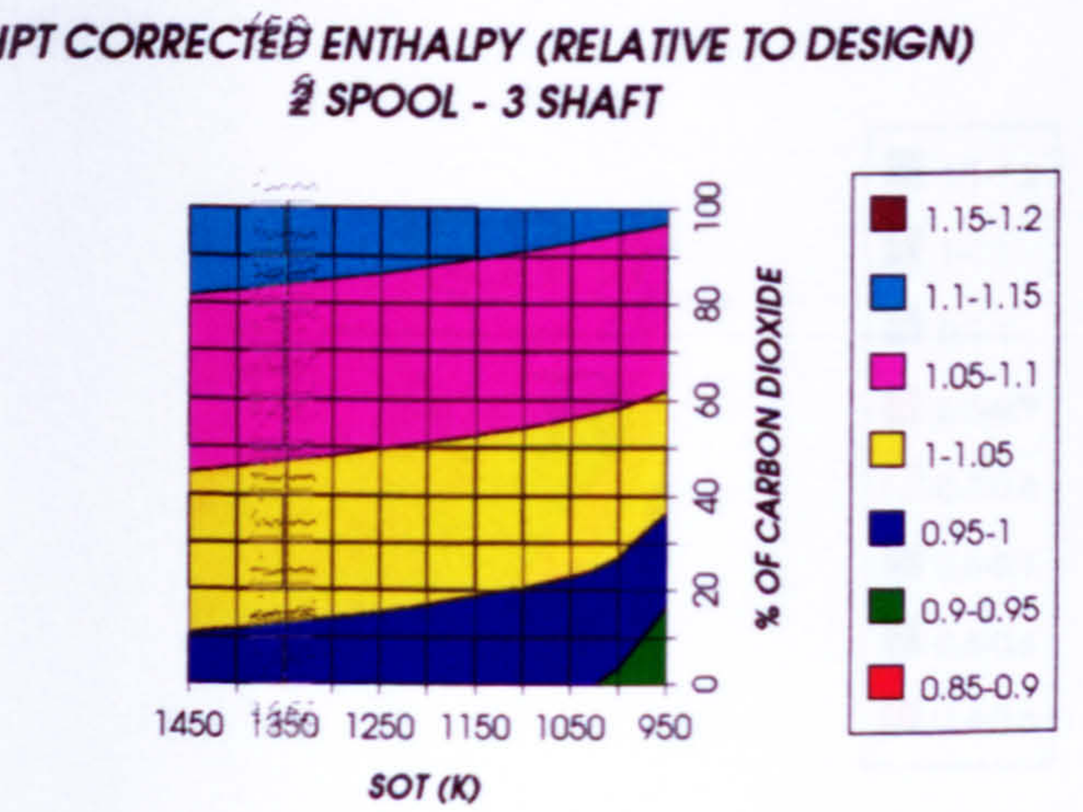

Figure 17. HP turbine corrected enthalpy (relative to design) 2 spool -3 shaft configuration

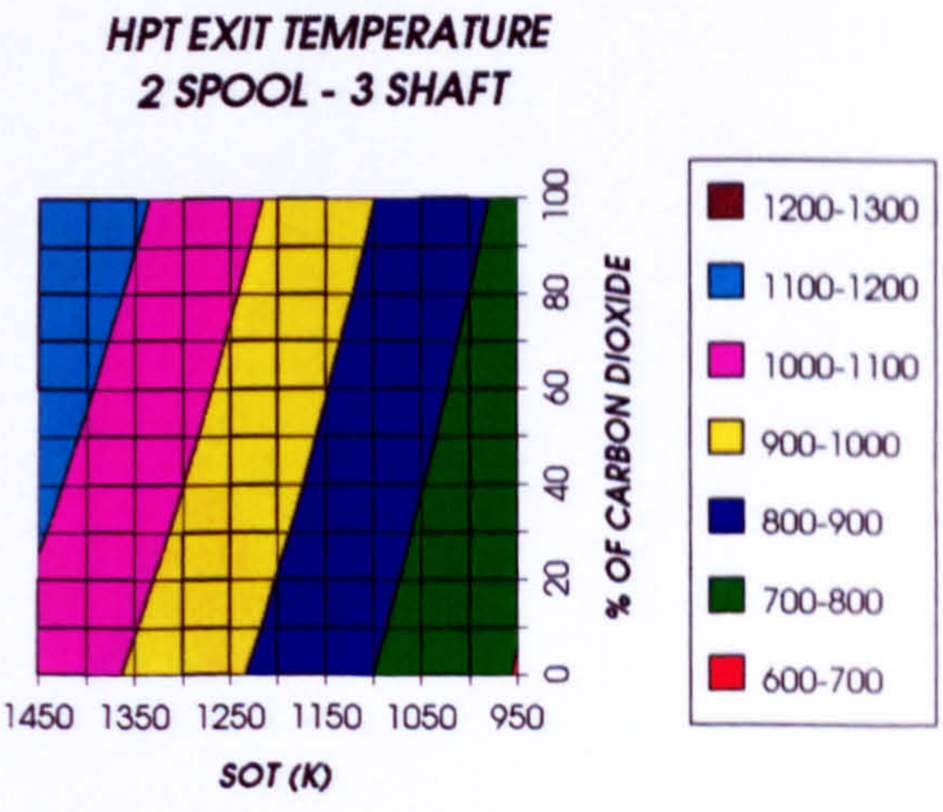

Figure 18. HP turbine exit temperature (K) 2 spool -3 shaft configuration

EFFECT OF CHANGING THE WORKING FLUID (2 SPOOL - 3 SHAFT)

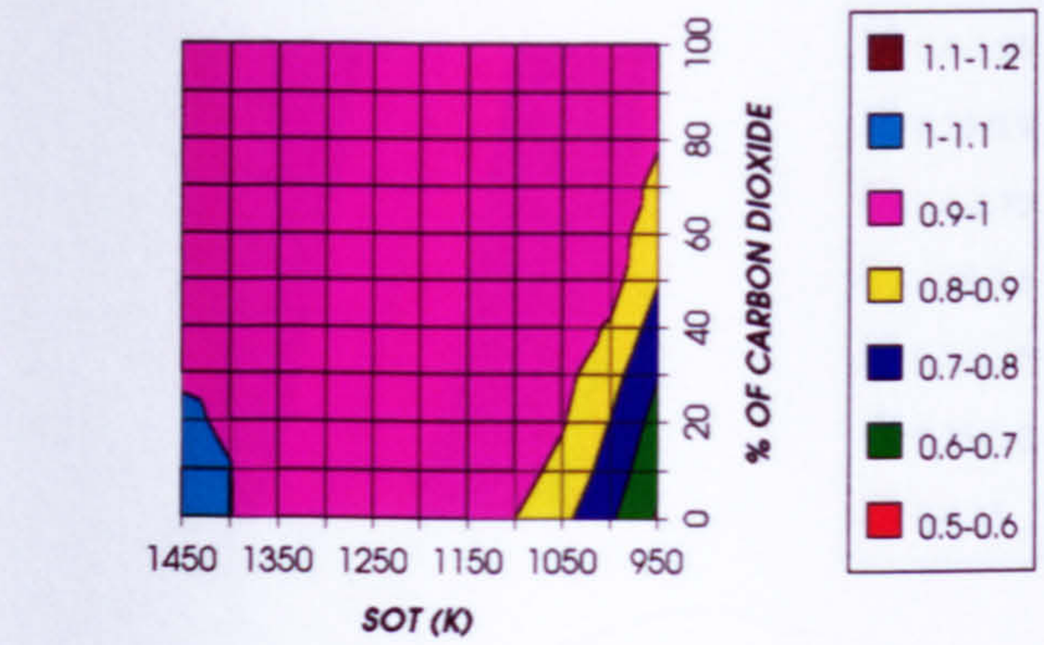

Figure 19. LP turbine load coefficient (relative to design) 2 spool -3 shaft configuration

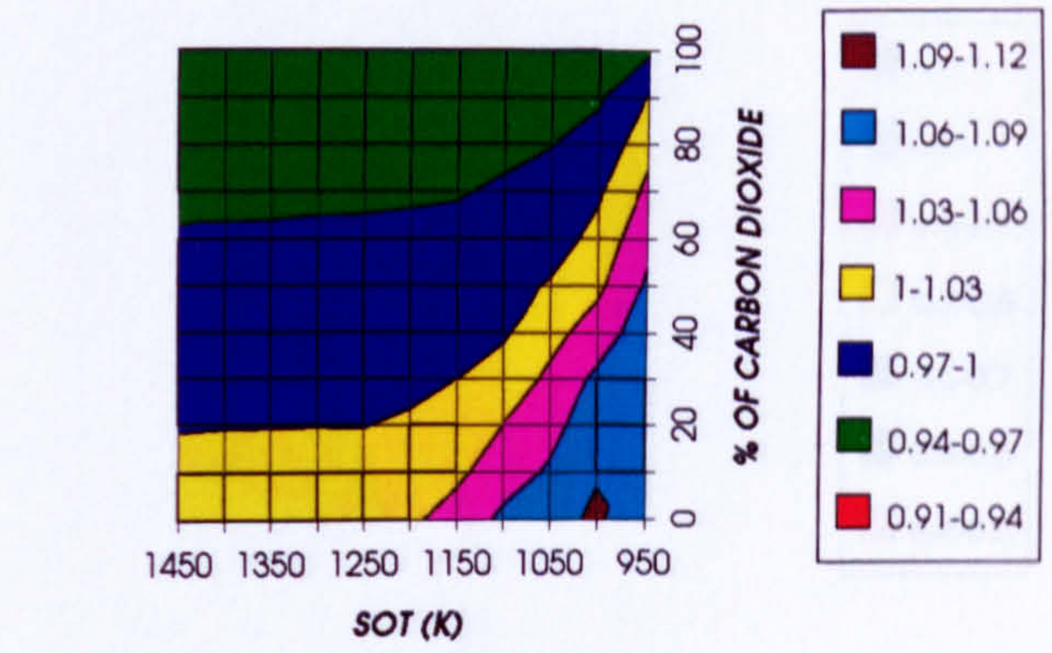

Figure 20. LP turbine flow coefficient (relative to design) 2 spool -3 shaft configuration

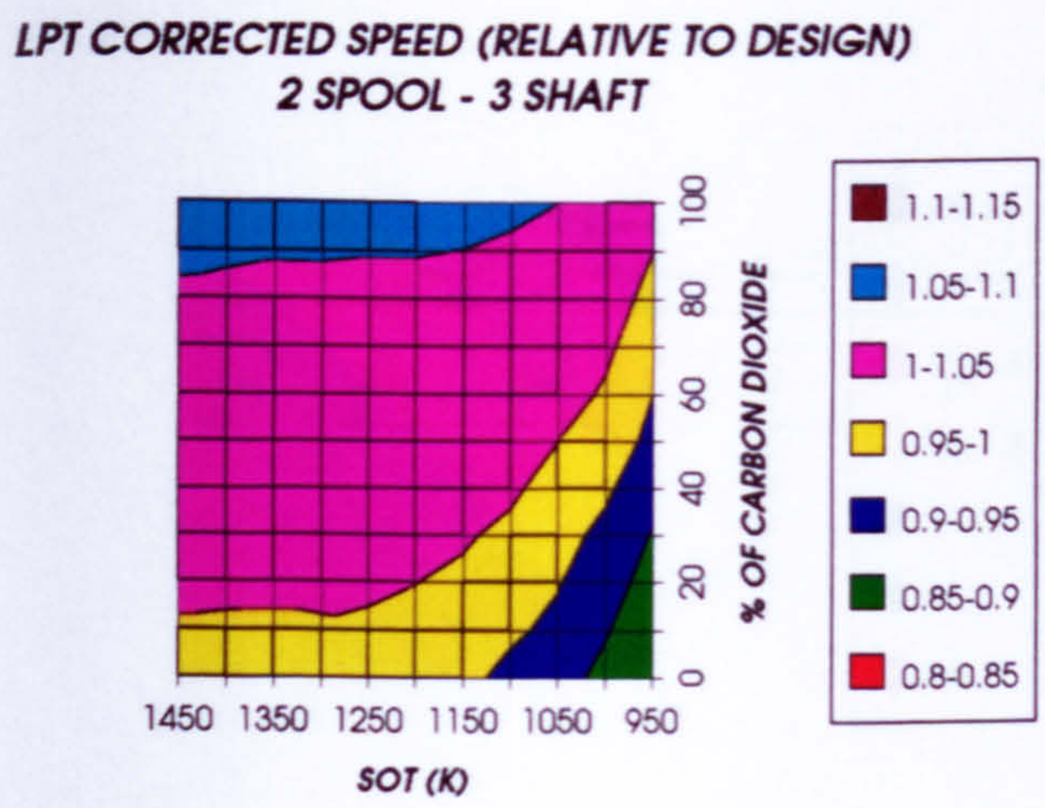

Figure 21. LP turbine corrected speed (relative to design) 2 spool -3 shaft configuration

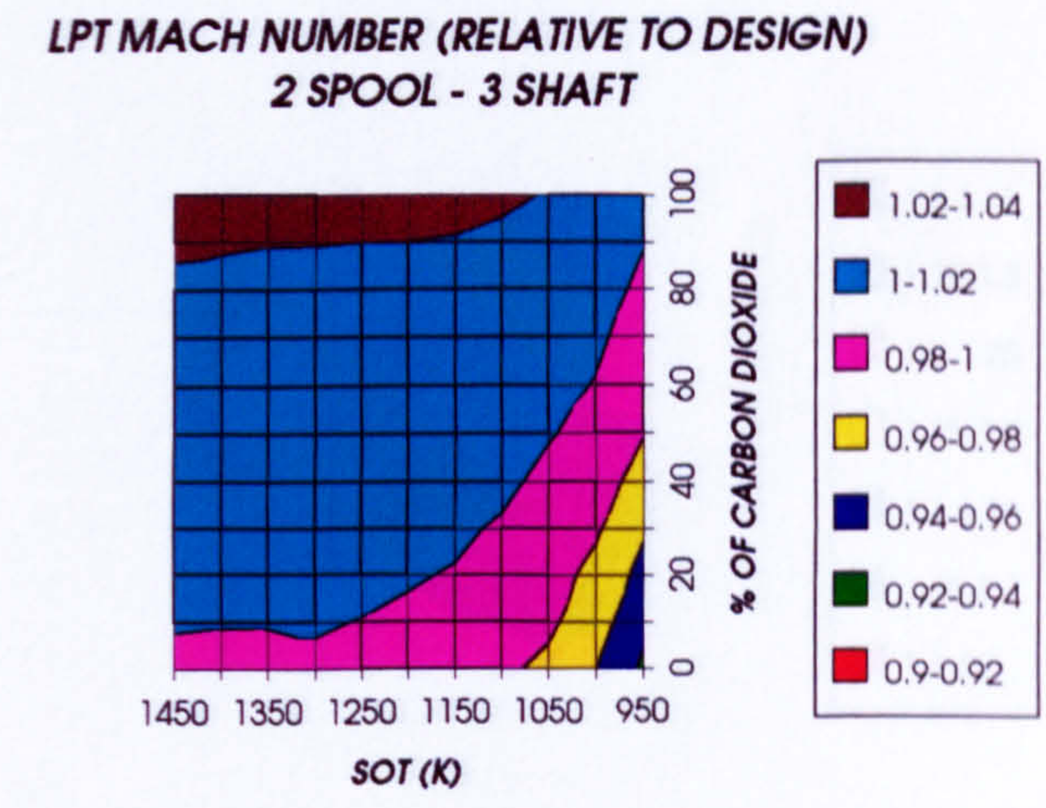

Figure 22. LP turbine Mach number (relative to design) 2 spool -3 shaft configuration

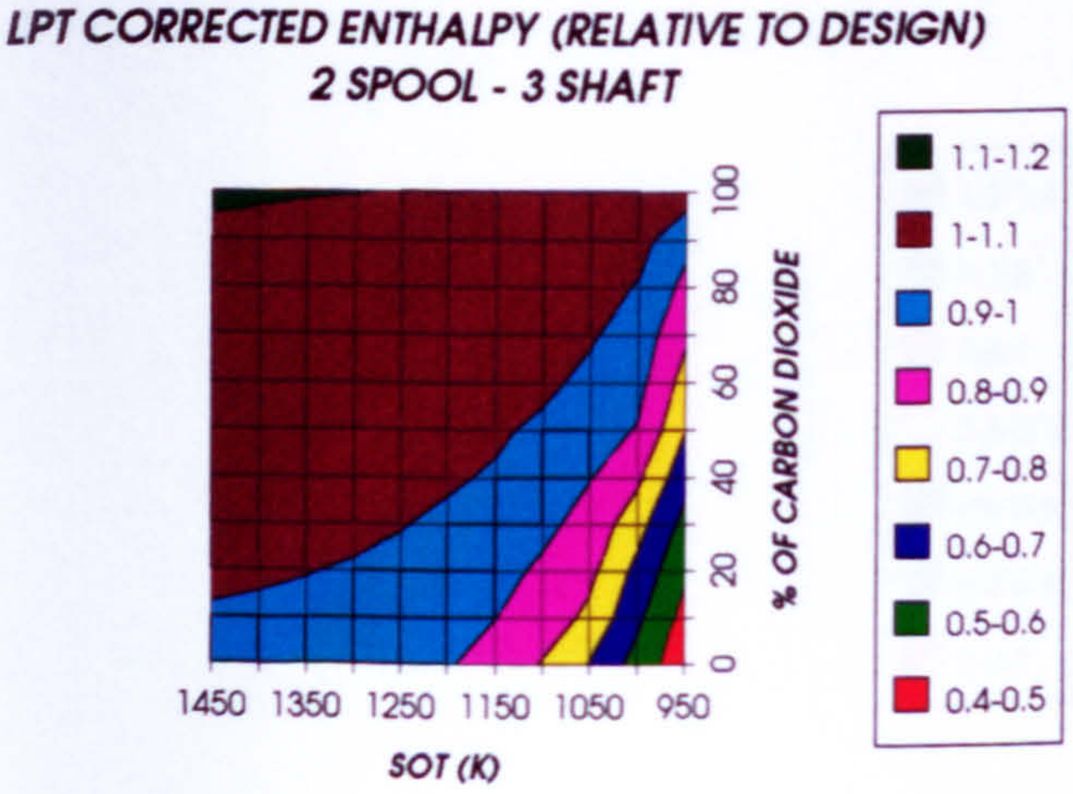

Figure 23. LP turbine corrected enthalpy (relative to design) 2 spool -3 shaft configuration

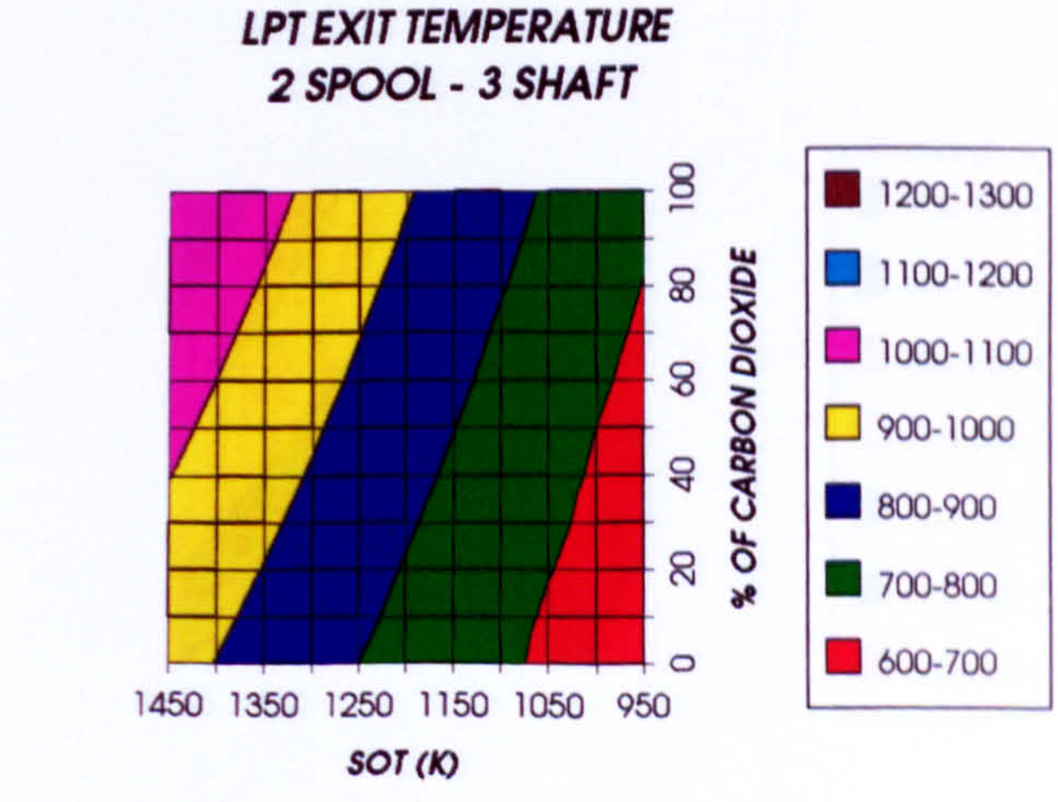

Figure 24. LP turbine exit temperature (K) 2 spool -3 shaft configuration

EFFECT OF CHANGING THE WORKING FLUID (2 SPOOL - 3 SHAFT)

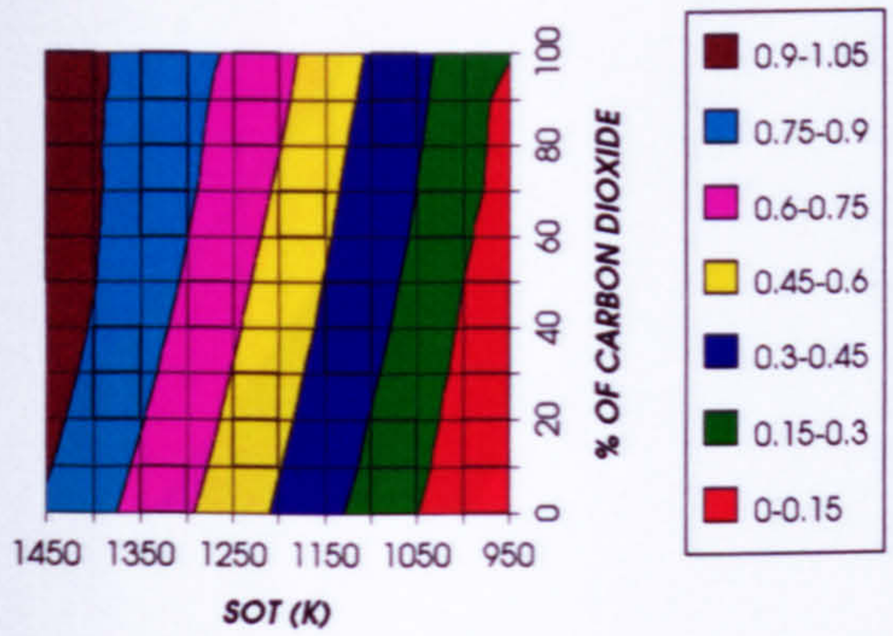

Figure 25. FP turbine load coefficient (relative to design) 2 spool -3 shaft configuration

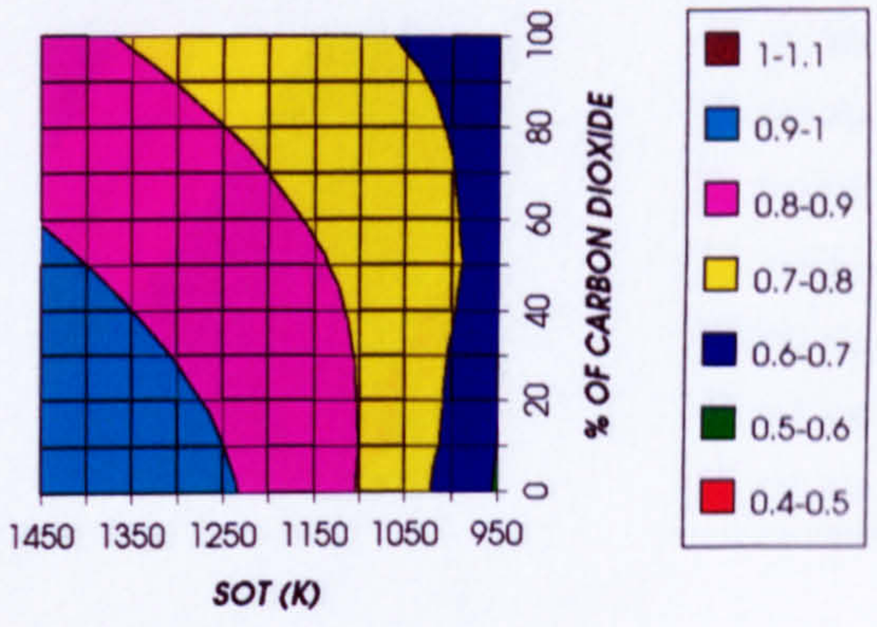

Figure 26. FP turbine flow coefficient (relative to design) 2 spool -3 shaft configuration

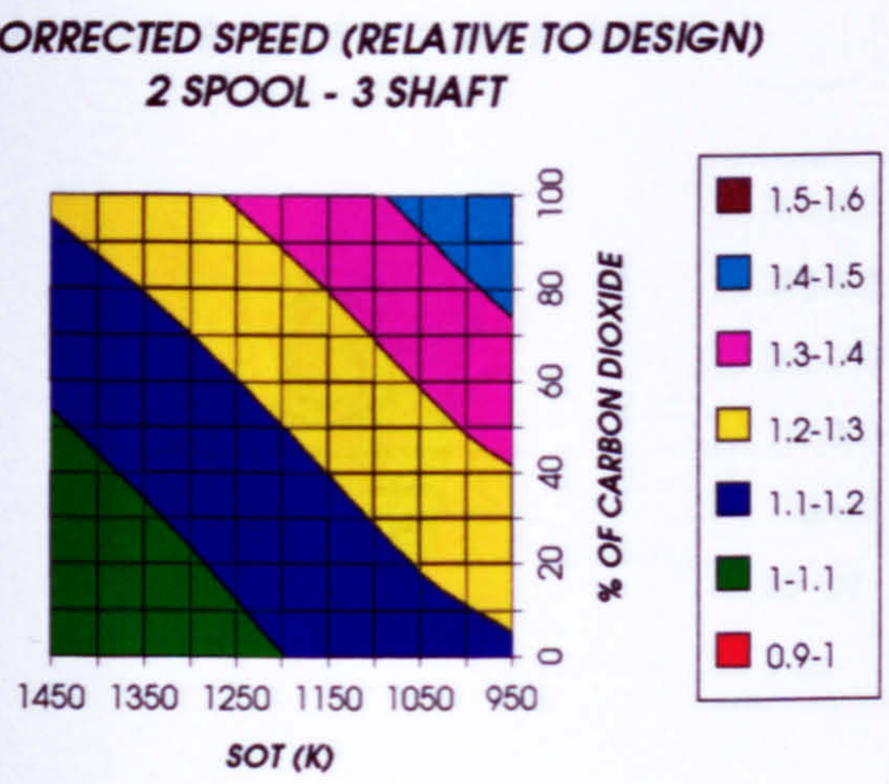

Figure 27. FP turbine corrected speed (relative to design) 2 spool -3 shaft configuration

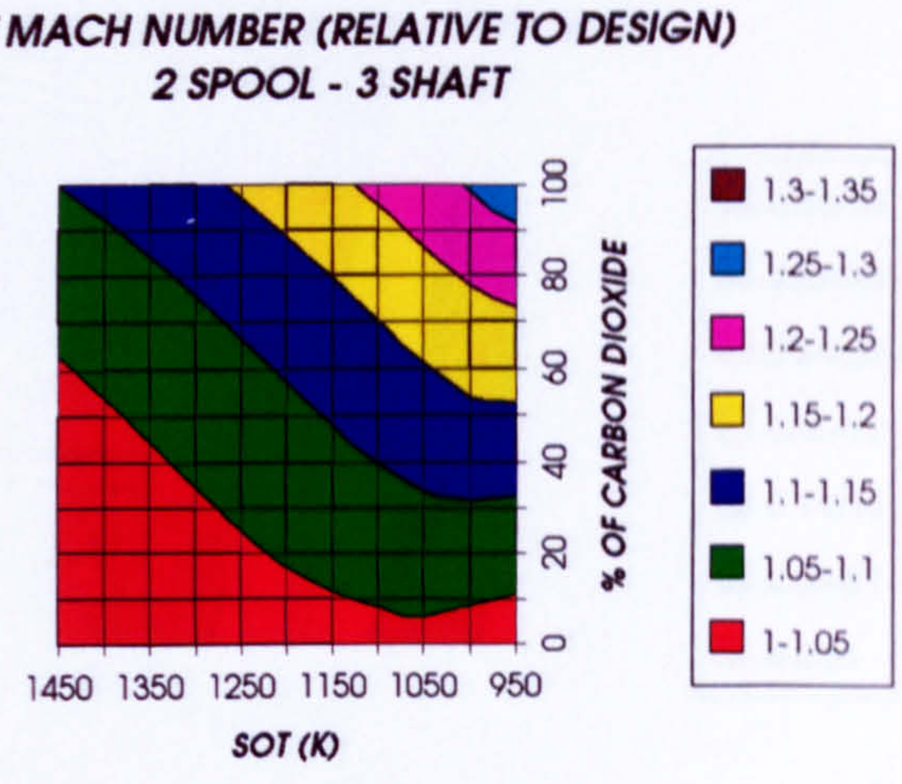

Figure 28. FP turbine Mach number (relative to design) 2 spool -3 shaft configuration

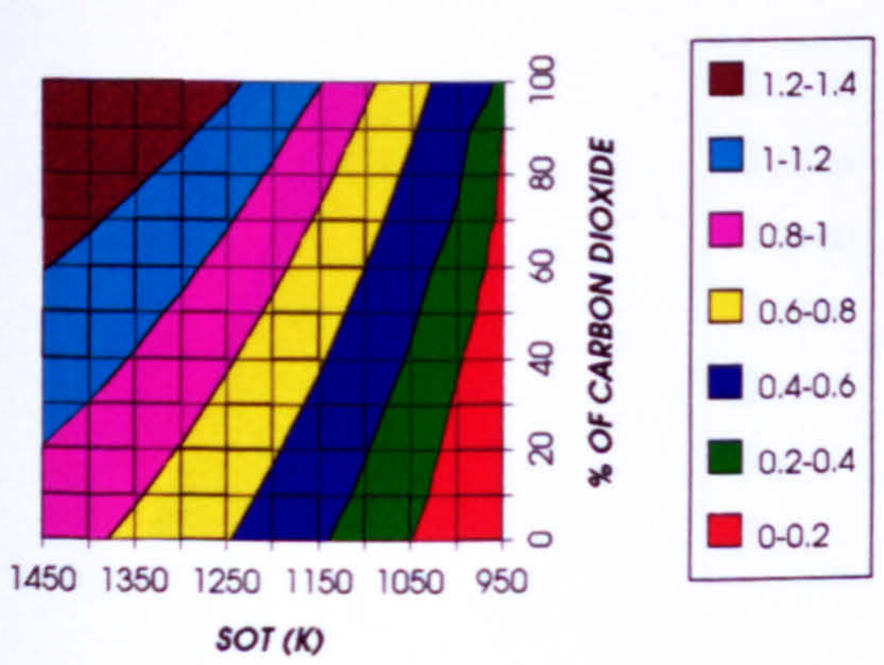

Figure 29. FP turbine corrected enthalpy (relative to design) 2 spool -3 shaft configuration

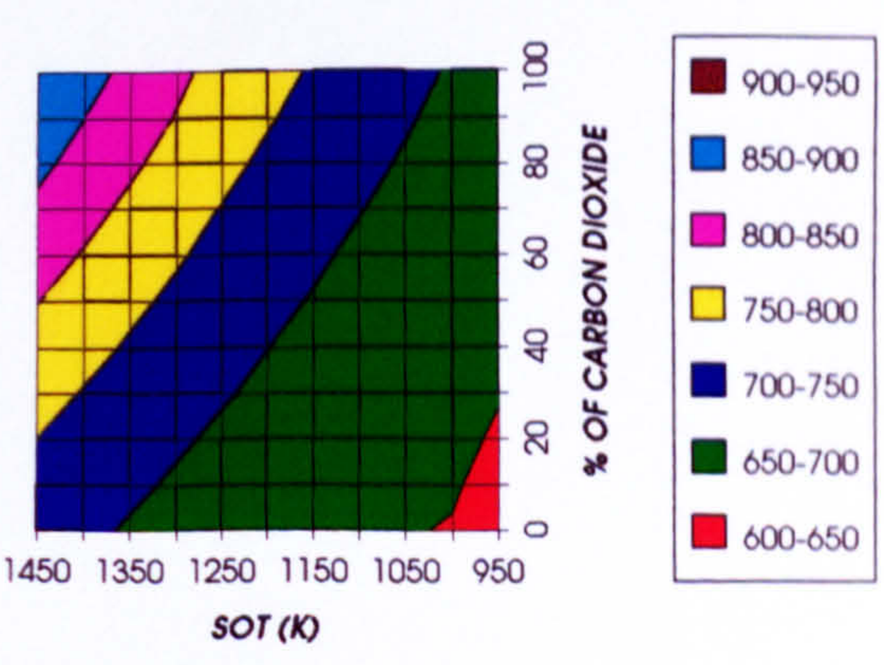

Figure 30. FP turbine exit temperature (K) 2 spool -3 shaft configuration

EFFECT OF CHANGING THE WORKING FLUID (2 SPOOL - 3 SHAFT)

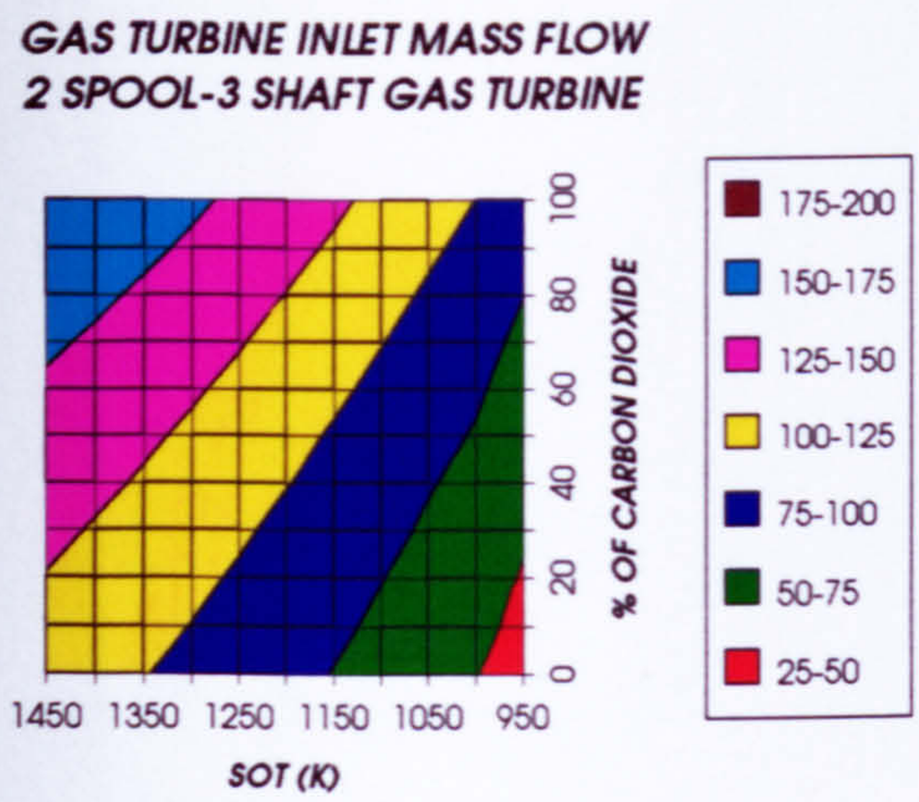

Figure 31. Gas turbine inlet mass flow (kg/s)
2 spool -3 shaft configuration

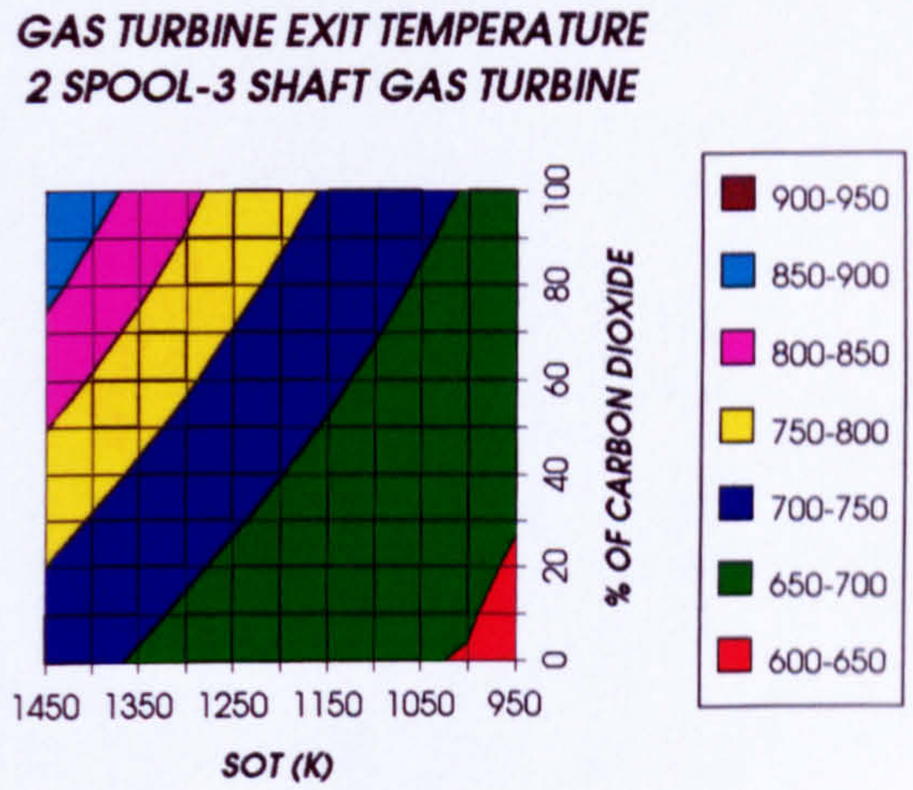

Figure 32. Gas turbine exit temperature (K)
2 spool -3 shaft configuration

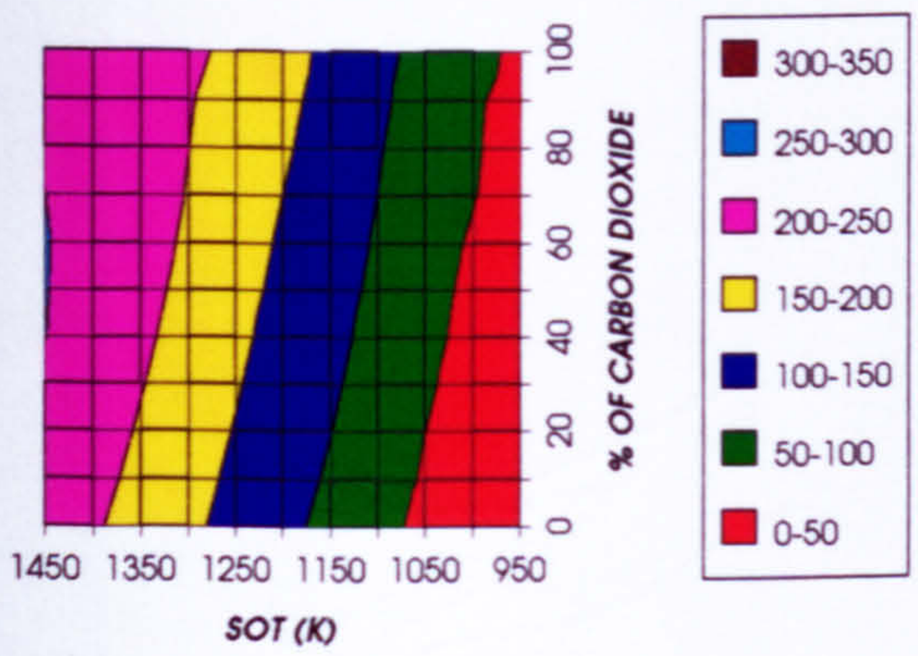

Figure 33. Gas turbine specific power output (kW/kg/s)
2 spool -3 shaft configuration

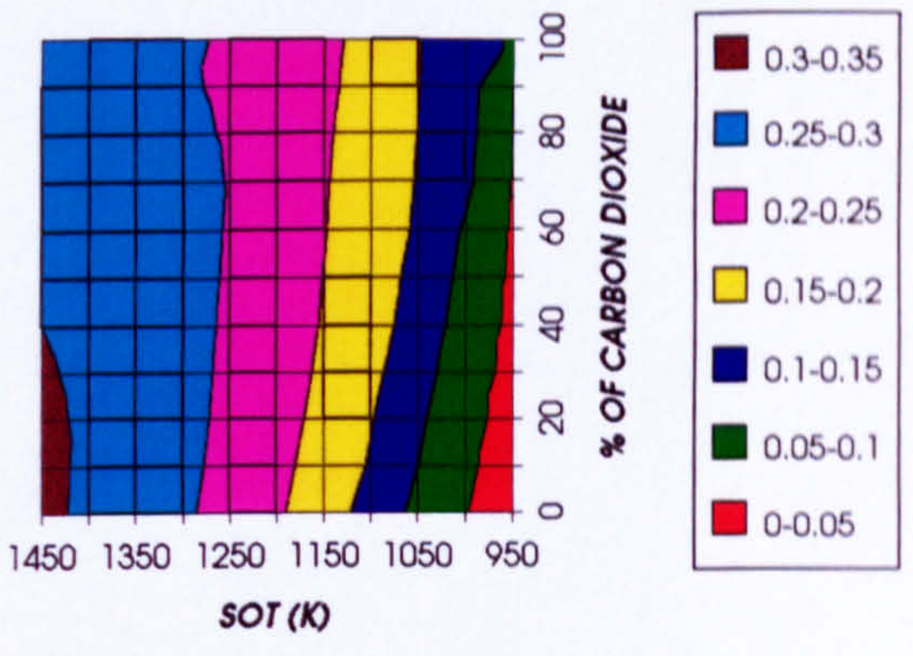

Figure 34. Gas turbine thermal efficiency
2 spool -3 shaft configuration

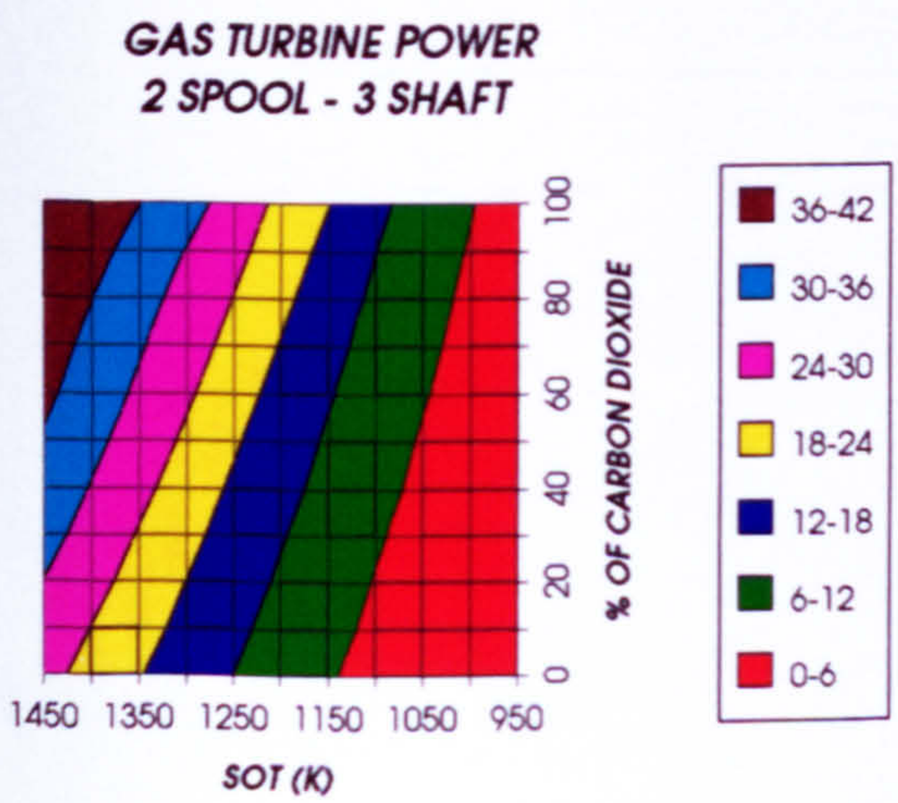

Figure 35. Gas turbine power (MW)
2 spool -3 shaft configuration